



Italian National Agency for New Technologies,  
Energy and Sustainable Economic Development

# GENERATION IV LEAD COOLED FAST REACTOR STATO ATTUALE DELLA TECNOLOGIA E PROSPETTIVE DI SVILUPPO

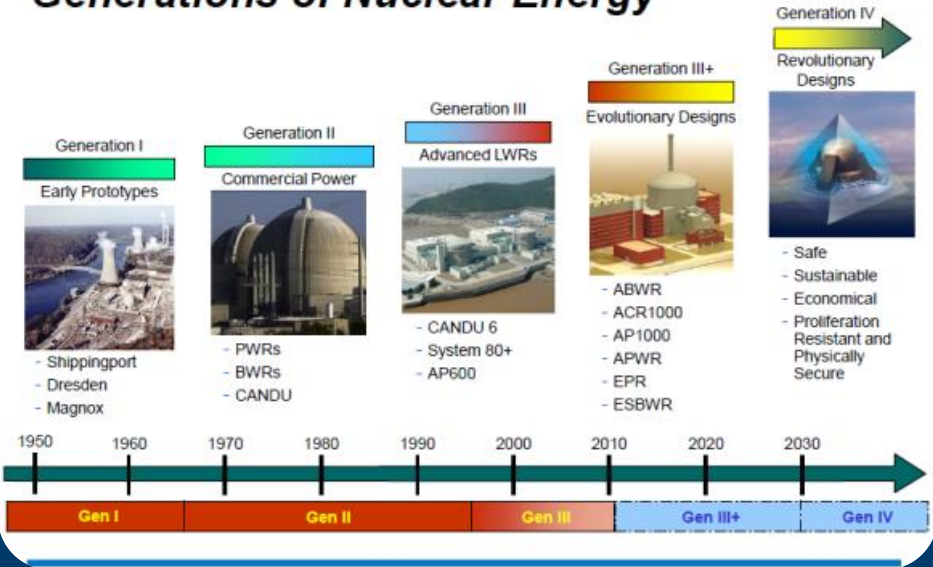
WORKSHOP TEMATICO ACCORDO DI PROGRAMMA MISE – ENEA  
PAR2017 – PROGETTO B.3. LP2

*DIAEE Università di Roma "La Sapienza", 14-15 giugno, 2018*

**Mariano Tarantino, Responsabile Divisione Ingegneria Sperimentale  
Dipartimento Fusione e Tecnologie per la Sicurezza Nucleare**



# Generations of Nuclear Energy



# GEN-IV LFR Development Strategies & Perspectives

# Outline



- ❑ **Why Nuclear?!**
- ❑ **Why Fast Reactor?!**
- ❑ **Why Lead-cooled Fast Reactor?**
- ❑ **Italian Contribution**
- ❑ **International Context**
- ❑ **Final Remarks**

# Energy Demand

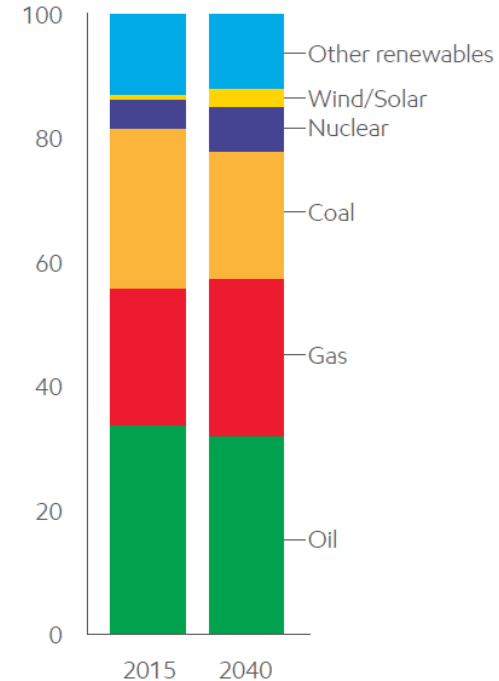


- ➔ **Oil** remains the world's primary energy source through 2040, meeting about one-third of demand
- ➔ **Natural gas** grows the most of any energy type, reaching a quarter of all demand
- ➔ **Coal** remains important in parts of the world, but loses significant share as the world transitions toward energy sources with lower emissions
- ➔ **Nuclear and renewables** see strong growth, contributing close to 40 percent of incremental energy supplies to meet demand growth

Source: **Exxon Mobil Energy Outlook 2017**

## Global energy mix evolves

Share of primary energy



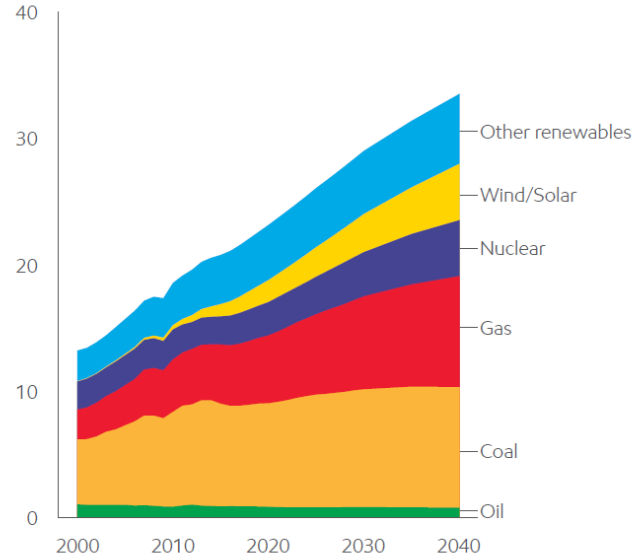
# Electricity Demand



- ➔ World shifts to **less carbon-intensive energy for electricity generation**, led by gas, renewables (wind, solar) and **nuclear**
- ➔ **Coal provides less** than 30 percent of world's electricity in 2040, versus about 40 percent in 2015
- ➔ **Wind and solar electricity supplies grow about 360 percent**, approaching 15 percent of global electricity by 2040
- ➔ Renewables growth supported by policies to **reduce CO2 emissions**

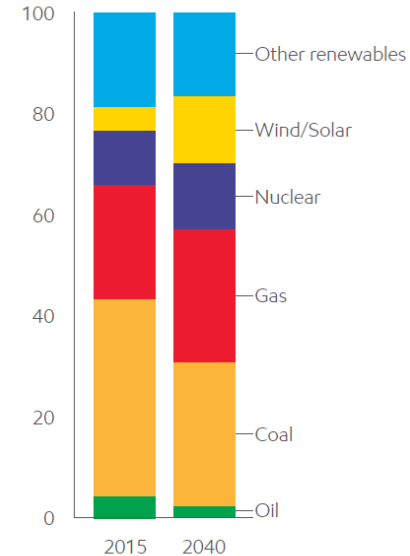
Electricity supplies reflect diverse sources

Thousand TWh (net delivered)



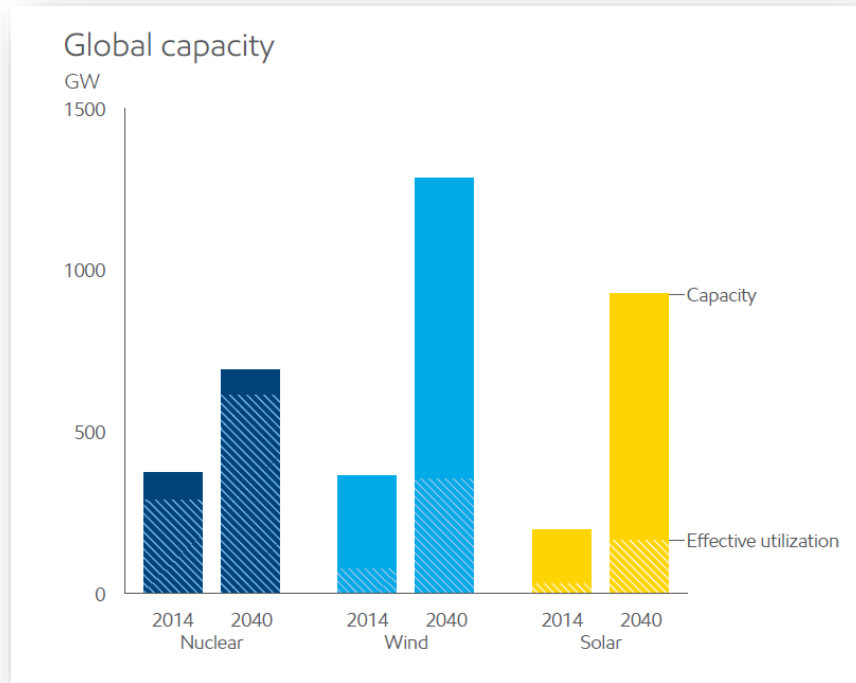
Electricity supply mix shifts

Percent share TWh (net delivered)



Source: Exxon Mobil Energy Outlook 2017

# Electricity Generation & Nuclear Role



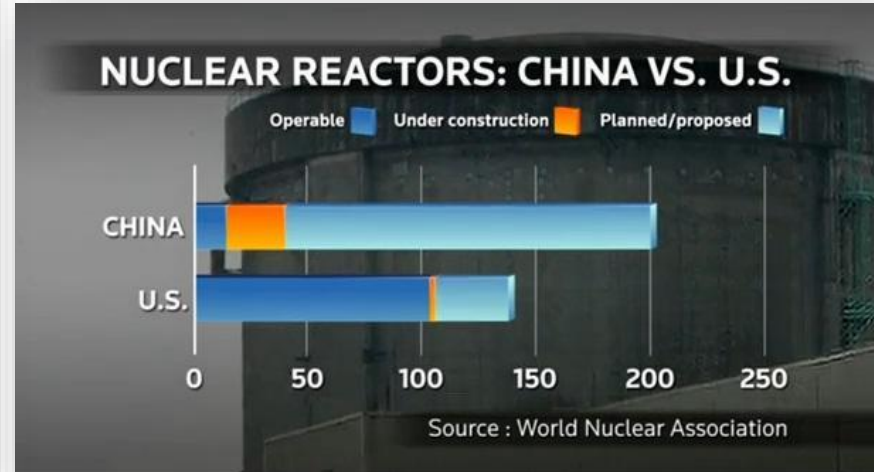
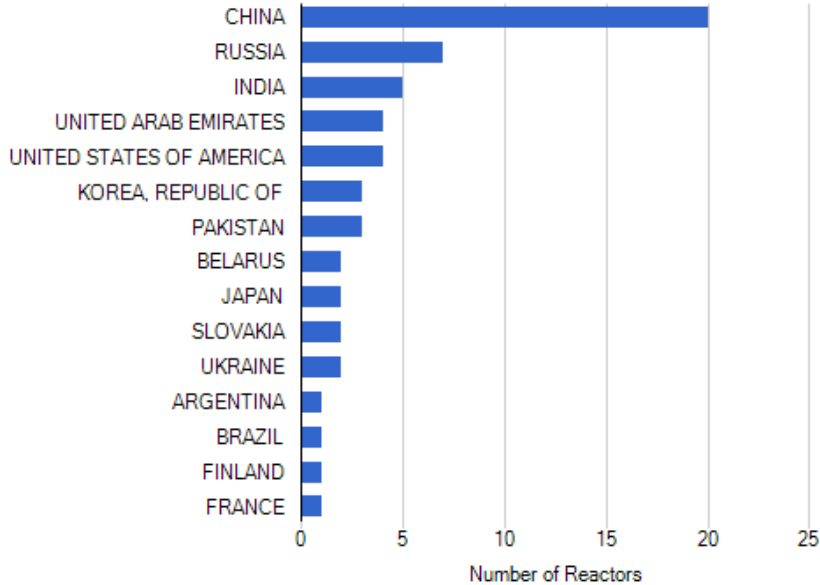
- ➔ Global nuclear, wind, solar all see big capacity additions
- ➔ **Nuclear capacity to grow 85% 2014-2020, led by China**
- ➔ **Intermittency limits the utilization of wind, solar capacity**
- ➔ Globally, less than 30% of wind capacity is utilized; solar less than 20%
- ➔ **Wind, solar provide less electricity in 2040 than nuclear despite 3 times the capacity**

Source: Exxon Mobil Energy Outlook 2017

# Electricity Generation & Nuclear Role

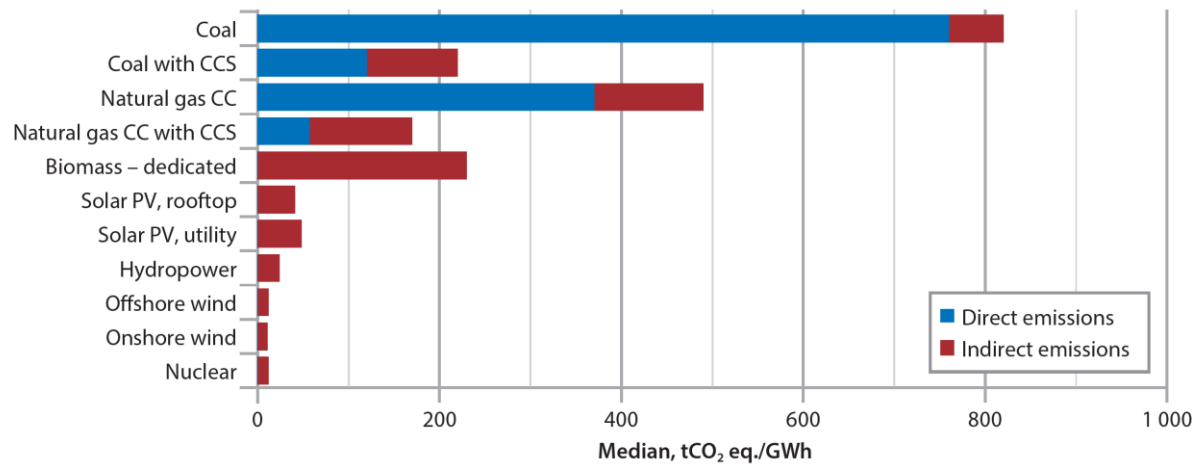


Total Number of Reactors: 60



Source: IAEA – Power Reactor Information System

# Electricity Generation & Nuclear Role



Note: Lifecycle emissions from dedicated energy crops are relatively high due to the N<sub>2</sub>O emissions from agricultural soils. N<sub>2</sub>O has a global warming factor that is 298 times that of CO<sub>2</sub> (IPCC [2014], Chapter 11, p. 880).

CC = combined cycle; CCS = carbon capture and storage; GWh = Gigawatt-hour.

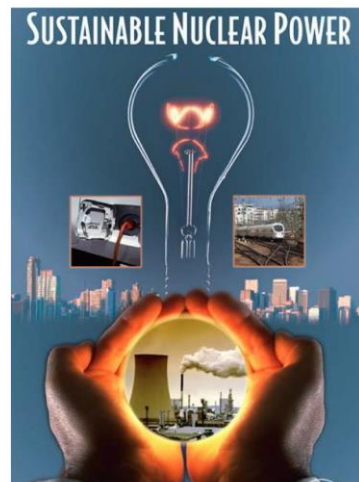
- ➔ Nuclear energy produced **11% of global electricity supply in 2013**.
- ➔ This corresponds to 18% of electricity supply in OECD countries and slightly more than 4% in non-OECD countries.
- ➔ **Nuclear is the largest low-carbon source of electricity in OECD countries**. Its share in non-OECD countries is still low but is expected to rise substantially in coming years.

Source: **IPCC (Intergovernmental Panel on Climate Change), 2014**

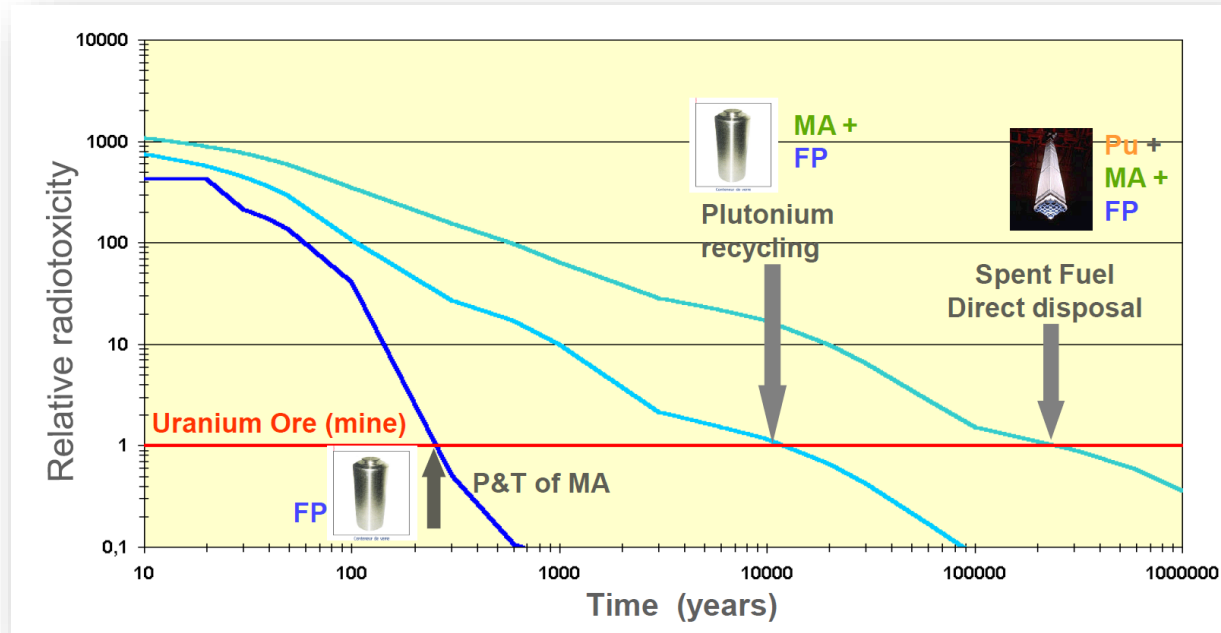


# Nuclear Open Issues

- ➔ Nuclear Energy  
good but not good enough
- ➔ Improvement Safety
- ➔ Waste  
Too much of it  
Too long lived
- ➔ Economy  
Once through strata  
uses less than 0,5% of the fuel



# Waste Minimization & Economy



Recycle of all actinides in spent LWR fuel in fast reactors provides a significant **reduction in the time required for radiotoxicity to decrease to that of the original natural uranium ore used for the LWR fuel** (i.e., man-made impact is eliminated). From **250,000 years down to about 400 years** with 0.1% actinide loss to wastes

**Severe Nuclear Accidents.** During the historically short period several low probability NPP accidents occurred with significant radioactivity release into environment and considerable economical losses



**Three Mile Island-2  
(PWR)  
1979**



**Chernobyl-4  
(RBMK)  
1986**



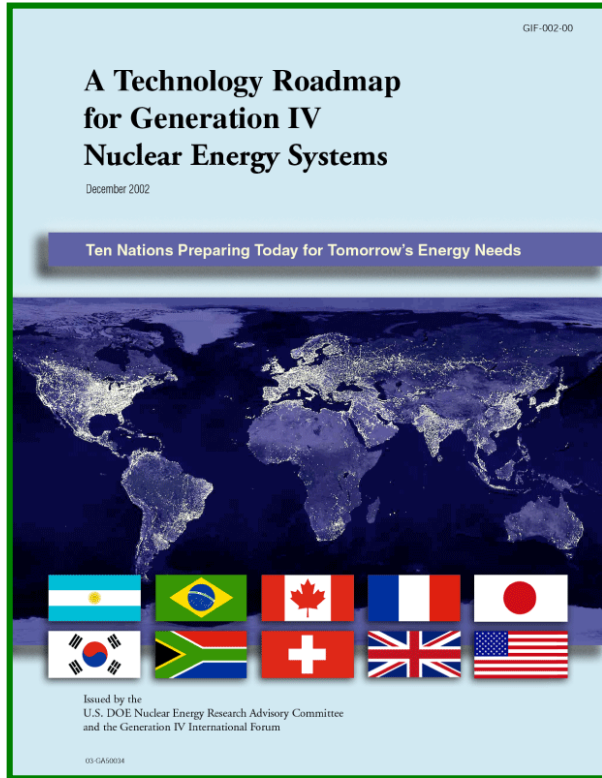
**Fukushima-1  
(BWR)  
2011**

**The initial events for these accidents are of extremely low probability**

**technical failure**

**human error**

**extreme external impact**



The path from current nuclear systems to Generation IV systems is described in a 2002 Roadmap Report entitled “**A technology Roadmap for Generation IV Nuclear Energy Systems**” which:

**defines challenging technology goals** for Generation IV nuclear energy systems in four areas:

- ✓ **sustainability,**
- ✓ **economics,**
- ✓ **safety and reliability, and**
- ✓ **proliferation resistance and physical protection.**

**identifies six systems** known as Generation IV to enhance the future role of nuclear energy;

**defines and plans the necessary R&D**

| <i>Generation IV Systems</i>                                | <i>Acronym</i> |
|---|----------------|
| Gas-Cooled <b>F</b> ast <b>R</b> eactor                     | <b>GFR</b>     |
| Lead-Cooled <b>F</b> ast <b>R</b> eactor                    | <b>LFR</b>     |
| Molten <b>S</b> alt <b>R</b> eactor                         | <b>MSR</b>     |
| Sodium-Cooled <b>F</b> ast <b>R</b> eactor                  | <b>SFR</b>     |
| Super <b>c</b> ritical <b>W</b> ater-Cooled <b>R</b> eactor | <b>SCWR</b>    |
| Very-High- <b>T</b> emperature <b>R</b> eactor              | <b>VHTR</b>    |

Because the capability of fast reactors **to meet the sustainability goal and hence to re-position nuclear energy from the present transition-energy role into an inexhaustible source of clean energy**

- ❖ three out of the six systems selected by GIF (GFR, LFR and SFR) are fast reactors and
- ❖ for two systems (MSR and SCWR) studies have been carried out recently to explore the possibility of them to become fast reactors.

# Lead cooled Fast Reactor



- ➔ For heavy liquid metal coolants (lead-bismuth alloy, lead) **the stored thermal potential energy cannot be converted into kinetic energy.**
- ➔ There is **no significant release of energy and hydrogen in an events of coolant contacting with air, water, structural materials.**
- ➔ There is **no loss of core cooling in an event of tightness failure in the gas system of the primary circuit.**
- ➔ The way to improve the NPP safety and economic performance is to implement reactor facilities with **the lowest stored potential energy**, where the inherent self-protection and passive safety properties are used to the maximal extent.

# Lead cooled Fast Reactor



## Main advantages and main drawbacks of Lead

| <i>Atomic mass</i> | <i>Absorption cross-section</i> | <i>Boiling Point (°C)</i> | <i>Chemical Reactivity (w/Air and Water)</i> | <i>Risk of Hydrogen formation</i> | <i>Heat transfer properties</i> | <i>Retention of fission products</i> | <i>Density (Kg/m<sup>3</sup>) @400°C</i> | <i>Melting Point (°C)</i> | <i>Opacity</i> | <i>Compatibility with structural materials</i> |
|--------------------|---------------------------------|---------------------------|--|-----------------------------------|---------------------------------|--------------------------------------|--|---------------------------|----------------|--|
| <b>207</b>         | <b>Low</b>                      | <b>1737</b>               | <b>Inert</b>                                 | <b>No</b>                         | <b>Good</b>                     | <b>High</b>                          | <b>10580</b><br><b>10580</b>             | <b>327</b>                | <b>Yes</b>     | <b>Corrosive</b>                               |

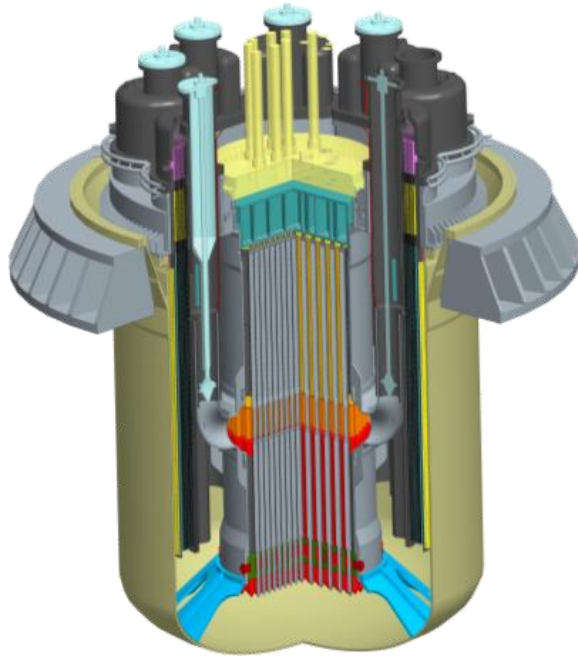
## *A comprehensive R&D program is necessary because of:*

- The use of a **new coolant and associated technology**, properties, neutronic characteristics, and compatibility with structural materials of the primary system and of the core.
- Innovations which require validation programs of **new components and systems** (the SG and its integration inside the reactor vessel, the extended stem fuel element, the dip coolers of the safety-related DHR system, pump, OCS, ...)
- The use of advanced fuels (*at least in a further stage*).



- ❑ The **industrial interest on LFR technology increased worldwide**, thanks to the enhanced safety and sustainability performances, the potential for economic competitiveness and the unique flexibility in terms of plant size and potential applications.
- ❑ In the European context, the attractive features of the LFR technology are being considered for the industrial deployment of a **lead-cooled Small Modular Reactors (SMR), able to achieve commercial maturity in a short-term**. It will offer a more advanced **alternative to current generation reactors facing retirement between 2035-2040**, while progressively achieving top-scoring performances in economics, safety, sustainability and proliferation resistance in line with the Generation-IV objectives.
- ❑ The **ALFRED Project** is framed as a priority to address the challenges of the European Union energy policy. **Italian industries, research centers and academia** have invested in developing and promoting the Project. The ALFRED implementation in Romania will represent an opportunity for the Italian system and is worth support towards the decision makers and European level.

# Italian Contribution: ALFRED



**Advanced**, since integrating innovation-intensive solutions in nuclear technology

**Lead**, because of its intrinsic properties as primary coolant to achieve superior safety

**Fast**, for the full exploitation of fuel energy and the reduction of long-term radiotoxicity

**Reactor**, as a representative training system for industry, utilities and safety authorities

**European**, because conceived and developed by a pan-European collaboration of experts

**Demonstrator**, to prove the viability LFR for a safe, clean, economic, and sustainable nuclear energy source



## **Framework Agreement (AdP)**

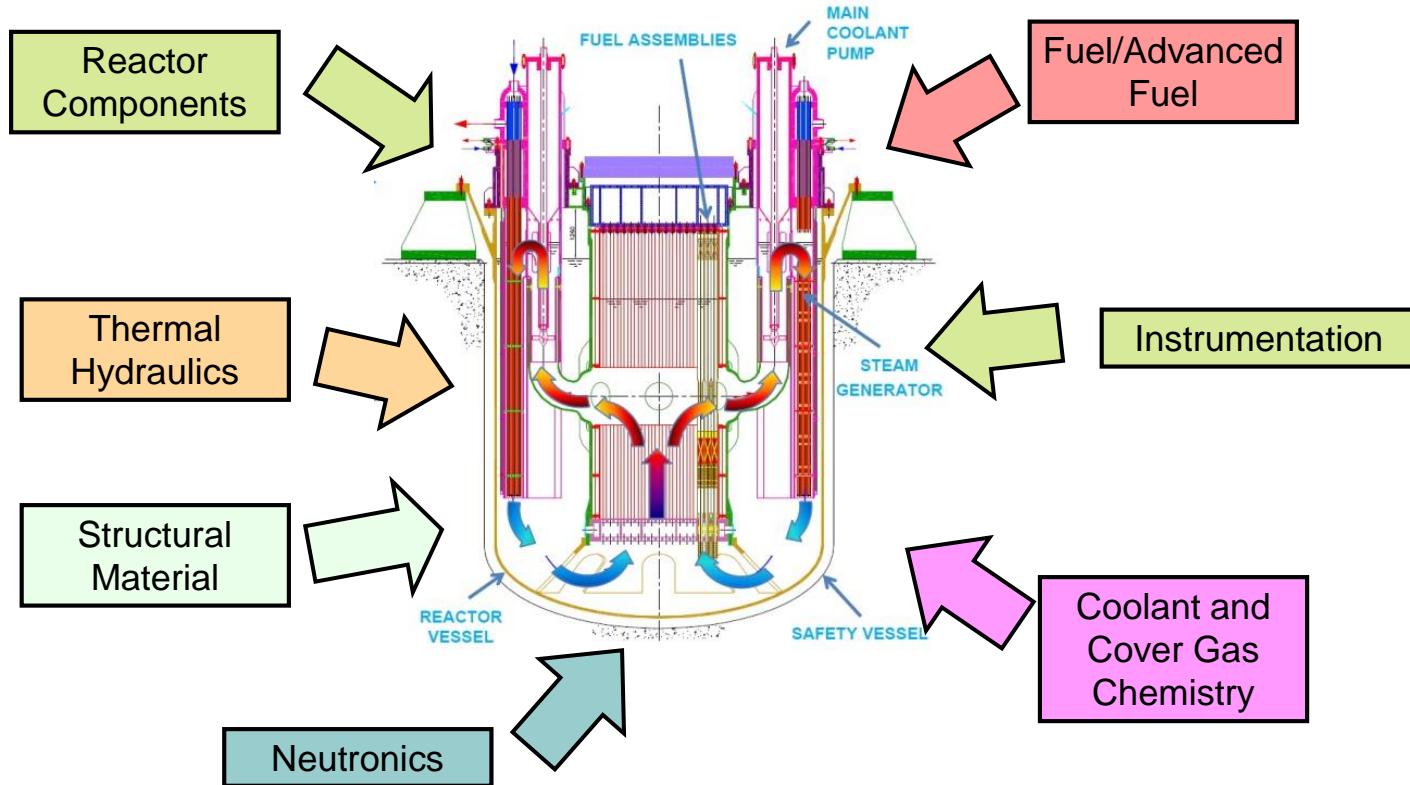
**between the Italian Ministry for Economic Development (MiSE) and ENEA.**

### **Project B.3. → Nuclear Fission**

#### **LP2 “International Collaboration on Gen-IV Nuclear Systems”**

- Design and Safety Analysis**
- Structural Materials and Coolant Chemistry**
- Thermalfluidynamic & Innovative Components**

# Towards Lead-cooled Fast Reactors

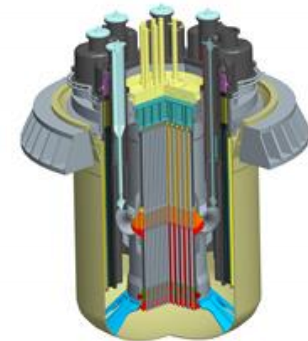


# Towards Lead-cooled Fast Reactors



|                     | TRL | TRL Function                           | Generic Definition   | Phase             |
|---------------------|-----|--|--|-------------------|
| achieved            | 1   | Technology Down-Selection              | •Basic principles definition   | Screening         |
|                     | 2   |  | •Technology concepts and applications definition                           |                   |
| Ongoing             | 3   | Final Process Selections & integration | •Demonstration of critical function<br>•Proof of concept                   | Pre-qualification |
|                     | 4   |  | •Lab-scale component validation  |                   |
|                     | 5   |  | •Component validation in a relevant environment                            | Qualification     |
| Further Development | 6   | Full-scale integrated testing          | •System/subsystem model or prototype demonstration in relevant environment |                   |
|                     | 7   |  | •System prototype demonstration in prototypic environment                  |                   |
|                     | 8   | Full-scale demo                        | •Actual system completed and qualified through test and demonstration      |                   |
|                     | 9   |  | •Actual system proven through successful operations                        |                   |

**DEMO  
is needed!**



**ALFRED**

## SNETP → Sustainable Nuclear Energy Technological Platform

To ensure the long-term sustainability of nuclear energy, **Gen IV Fast Neutron Reactors should be available for deployment by 2040** or even earlier. Therefore an ambitious yet realistic R&D and demonstration programme is to be put in place.

## ESNII → European Sustainable Nuclear Industrial Initiative

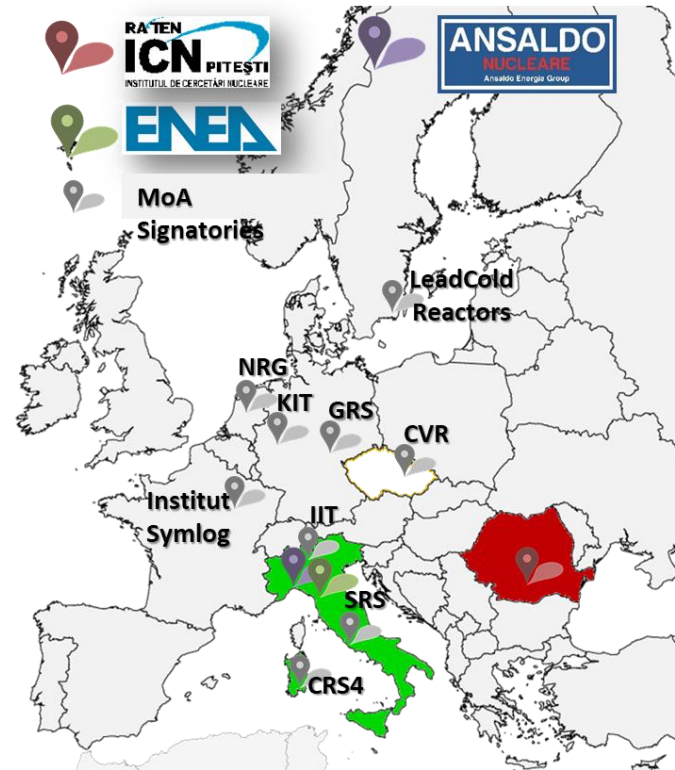
ESNII addresses the need for **demonstration of Generation IV Fast Neutron Reactor technologies**, together with supporting research infrastructures, fuel facilities and R&D work.

## SRIA → Strategic Research and Innovative Agenda (2013)

The **main objective of Europe** is to maintain the leadership in fast spectrum reactor technologies that will **excel in safety** and will be able to achieve a more **sustainable development of nuclear energy**.

“.....Lead Fast Reactor technology has significantly extended its technological base and can be considered as the shorter-term alternative technology (to SFR), whereas the Gas Fast reactor technology has to be considered as a longer-term alternative option.

- **FALCON** Consortium Agreement established in **2013** to bring LFR technology to **industrial maturity**.
- **Infrastructures** in Mioveni platform:
  - European “**Lead School**” for E&T and dissemination services,
  - **CoE on HLM** equipped with unique facilities,
  - **ALFRED** playing the role of ETDR of the LFR technology
- New members sharing the **objective** of a rapid deployment of an LFR demonstrator, interested in the R&D supporting **infrastructure** and in the **ALFRED** industrial outcomes are **welcome to join**.



# Final Remarks

- Nuclear will play still an important roles in the next years.
- Nuclear energy technology is among the **most reliable and safer technologies**. Nevertheless a in improvement is required about:
  - **Safety**
  - **Waste**
  - **Economy**
- Gen-IV reactors have been conceived to match these goals. Among the others, **Lead cooled Fast Reactors** seems to be the most promising! (but R&D needs are not negligible...)
- In this context the **Italian contribution is significant worldwide**. ENEA and its industrial partners led the technology development.
- International Context is positive (everyday more!!)



Mariano Tarantino  
mariano.tarantino@enea.it



1101 0110 1100  
0101 0010 1101  
0001 0110 1110  
1101 0010 1101  
1111 1010 0000





# DEMO-LFR ALFRED: Technical Overview

Michele Frignani  
Project Engineer – Nuclear Technologies and Safety  
Member of Expert Board, FALCON Consortium



Cosa vorremmo fare...



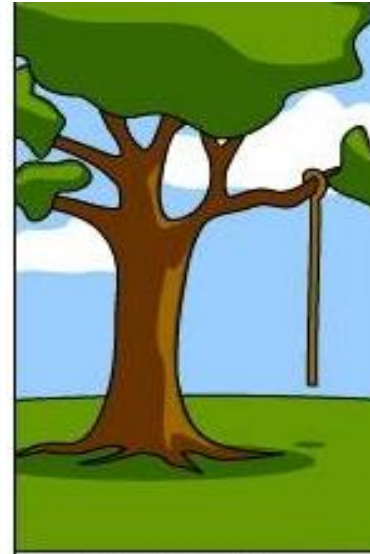
Cosa promettiamo ...



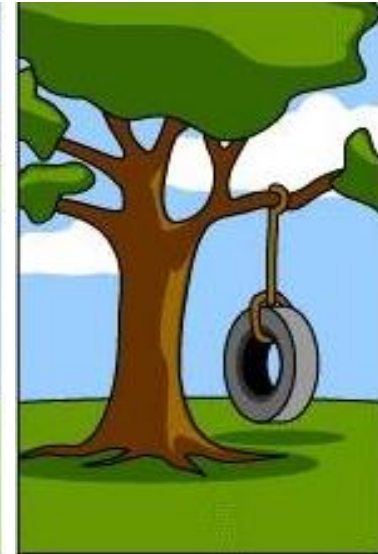
Cosa rischiamo di fare...



Cosa abbiamo...



Cosa dovremmo fare...



Cosa vorremmo fare...



Cosa promettiamo...



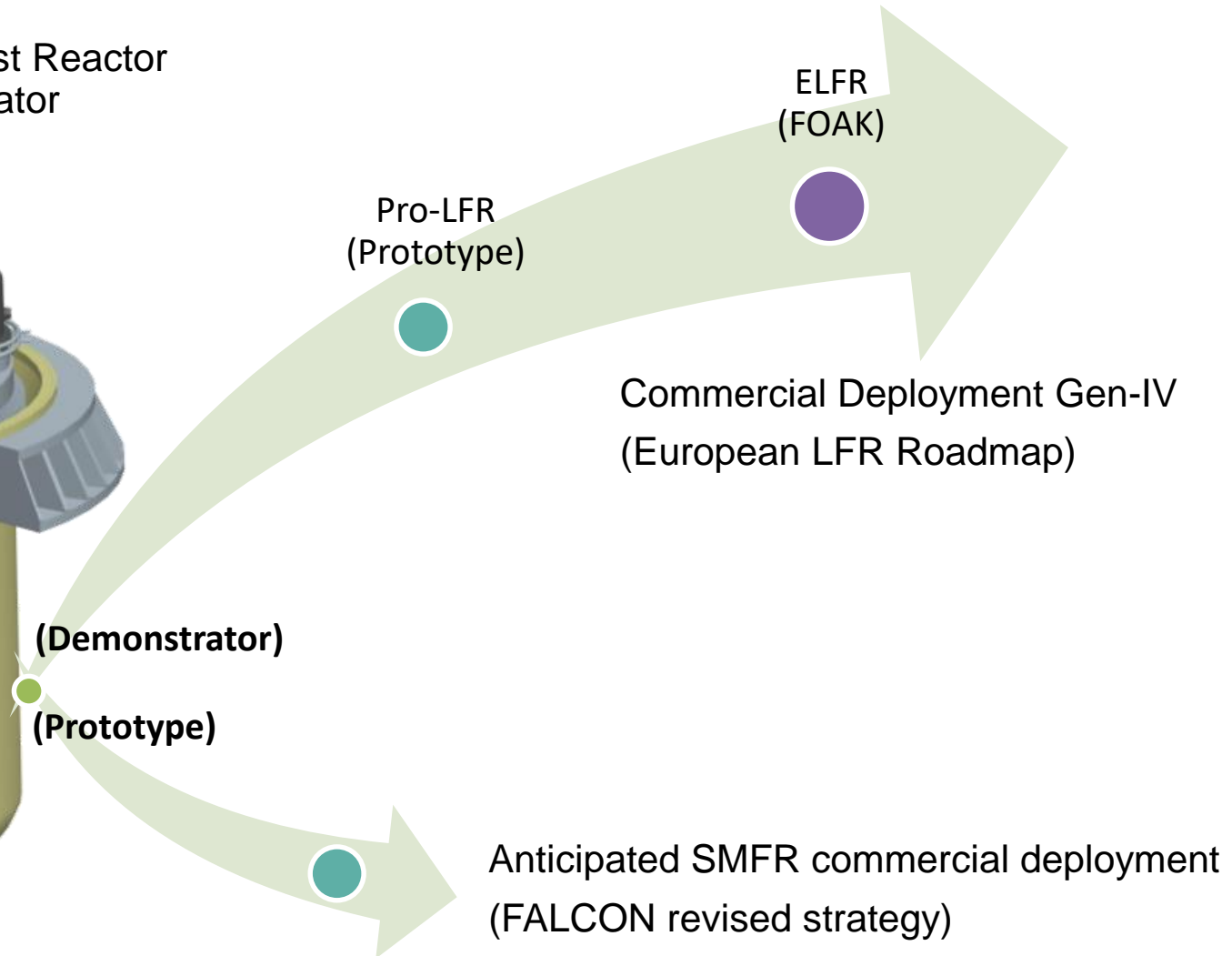
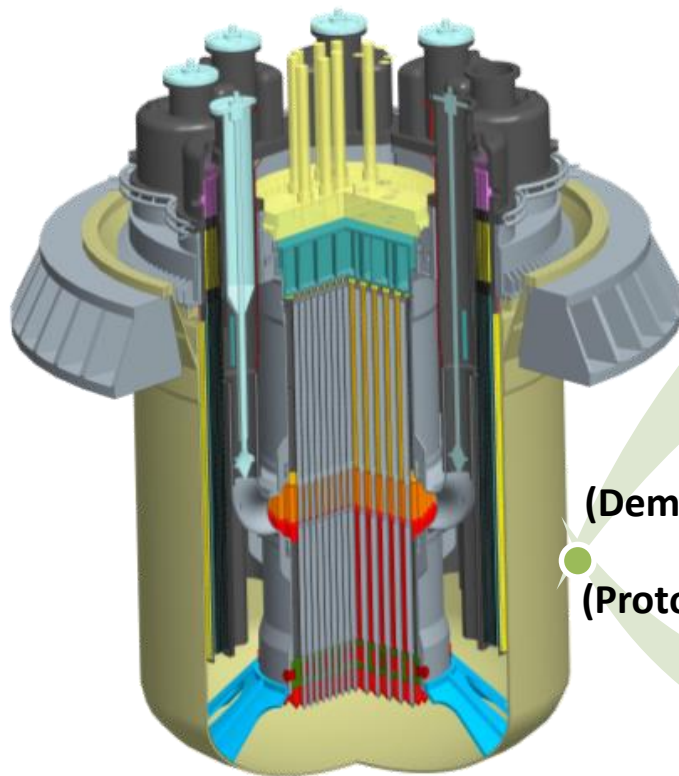
Cosa dovremmo fare...



|                                       | FOAK  | ALFRED<br>(n <sup>th</sup> stage) | ALFRED<br>(1 <sup>st</sup> stage) |
|---------------------------------------|---|-----------------------------------|-----------------------------------|
| POWER (MWth)                          | 600   | 300                               | 100                               |
| POWER (MWe)                           | 250   | 125                               | 40                                |
| DELTA – T (°C)                        | 120 (400-520)                                   | 120 (400-520)                     | 40 (390-430)                      |
| Dia. INNER VESSEL (m)                 | 4   | 3                                 |                                   |
| Dia. MAIN VESSEL (m)                  | 9 (investigation to decrease)                   | 8                                 |                                   |
| Height VESSEL (m)                     | 10 (investigation to decrease)                  | 10 (investigation to decrease)    |                                   |
| Volume/Power<br>(m <sup>3</sup> /MWe) | 2,5   | 4                                 | 12                                |
| FUEL                                  | MOX<br>(or UO <sub>2</sub> - 19.75% enrichment) | MOX                               | MOX                               |
| CLADDING                              | 15-15 Ti + PLD coating                          | 15-15 Ti +<br>PLD coating         | 15-15 Ti                          |
| FUEL ASSEMBLIES                       | Hex, wrap, grid, orifice, diagrid, stem         |                                   |                                   |
| PRIMARY PUMP                          | Mechanical, hot leg                             |                                   |                                   |
| STEAM GENERATOR                       | Once through                                    |                                   |                                   |

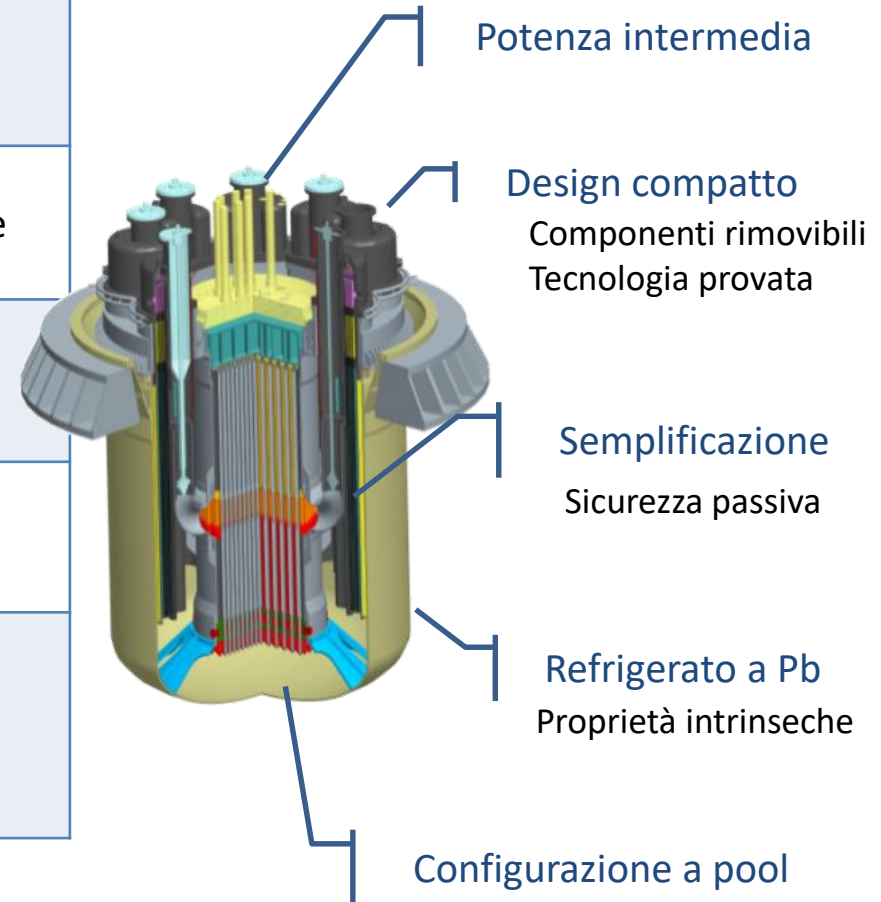
# Dimostratore, Prototipo o entrambi

**ALFRED**  
Advanced Lead-cooled Fast Reactor  
European Demonstrator



Anticipated SMFR commercial deployment  
(FALCON revised strategy)

| Area             | Approccio per affrontare la problematica con il dimostratore  |
|------------------|---|
| <b>Design</b>    | Focalizzato sugli obiettivi di breve termine<br>R&D in parallelo per trarre il lungo termine                              |
| <b>Safety</b>    | Potenza ragionevole per dare evidenza della sicurezza della tecnologia e risolvere le incertezze facendo leva sui margini |
| <b>Licensing</b> | Mezzo per migliorare il regulatory framework da utilizzare per il licensing di reattori commerciali                       |
| <b>Operation</b> | Maturare esperienza operativa<br>Commissioning e operazione a stadi   |
| <b>Financing</b> | Ridurre il tempo necessario per la commercializzazione<br>Rinforzare le sinergie e le opportunità tra pubblico e privato  |





# A volte occorre fermarsi e reindirizzare

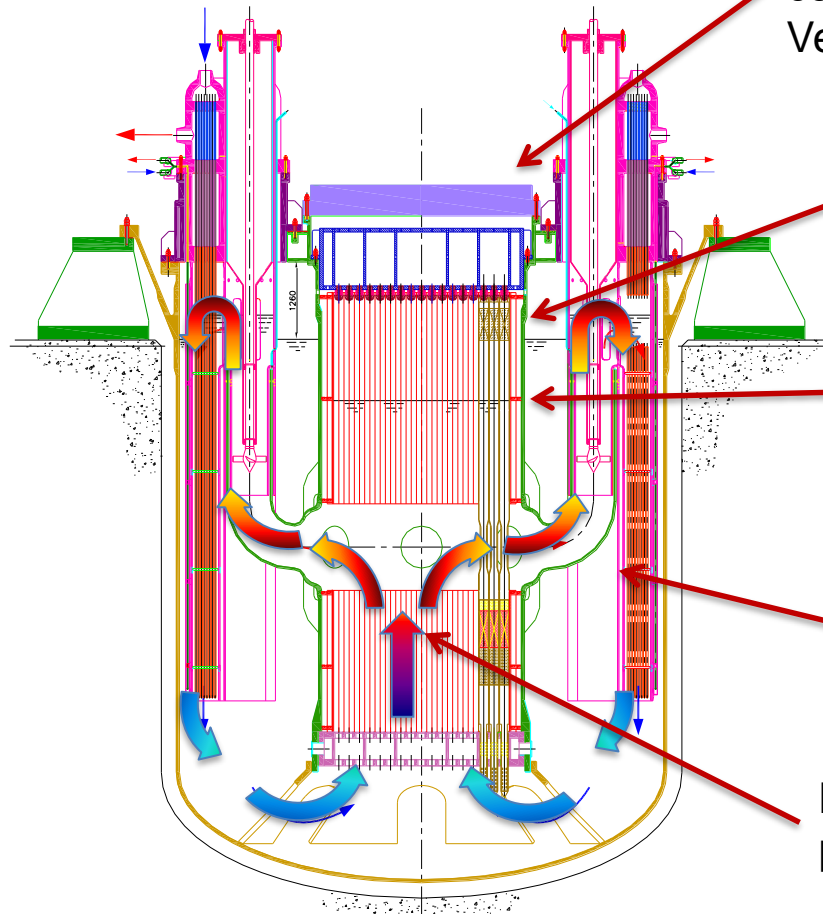
Cosa  
rischiamo di fare...



Cosa  
abbiamo...



Configurazione ampiamente analizzata mediante analisi di sicurezza mirate a mostrarne la robustezza



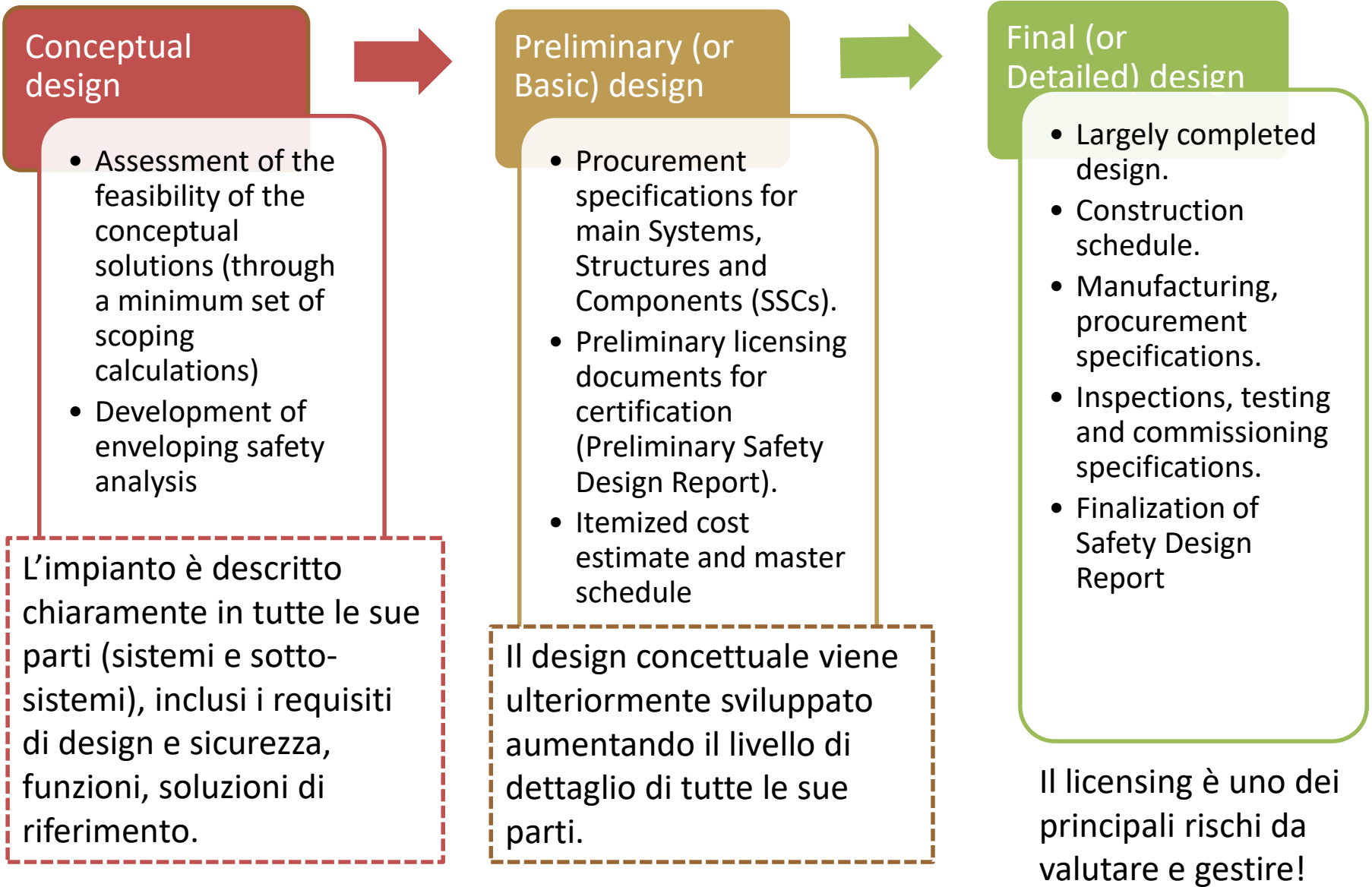
**Reattore a pool:** design compatto, principali componenti integrati all'interno del Reactor Vessel

**Configurazione del Reactor Coolant System:** flow-path semplificato ed ottimizzato per la circolazione naturale

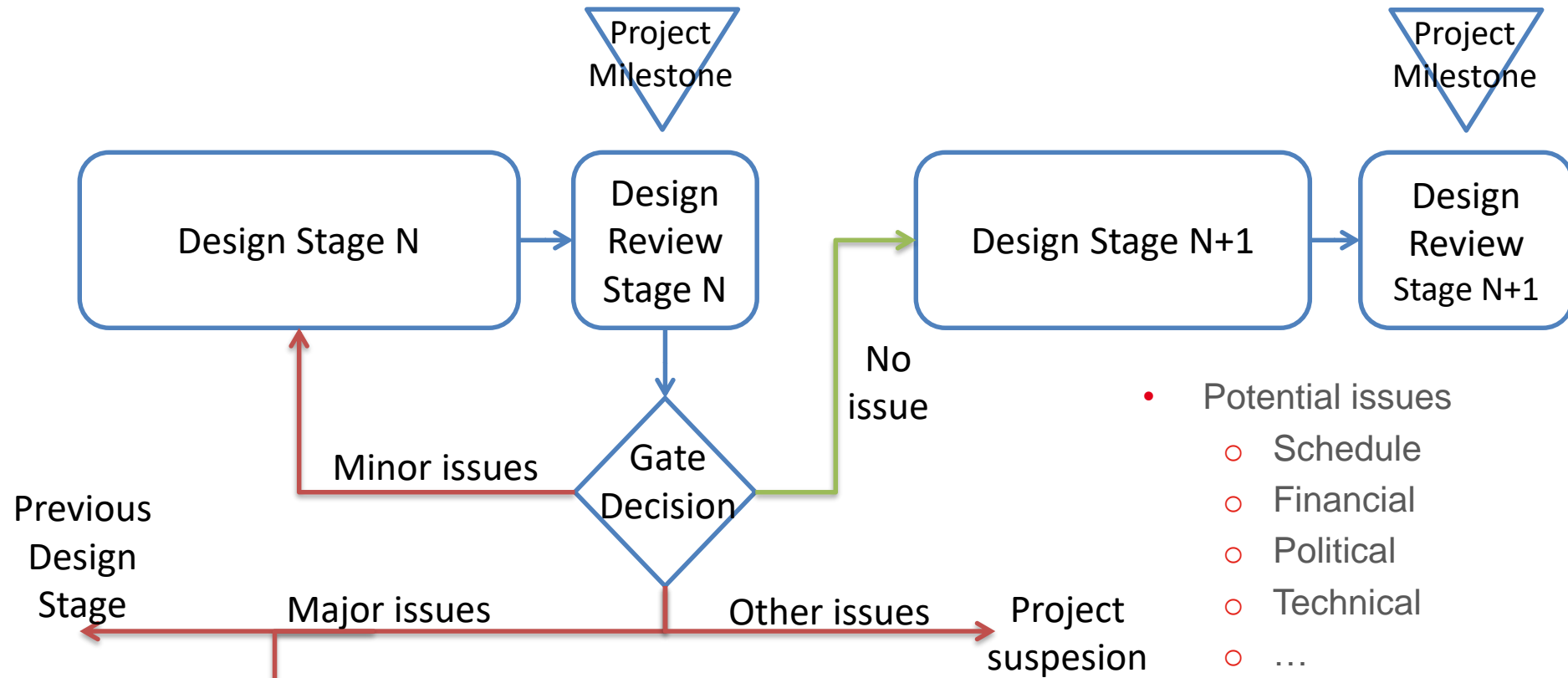
**Temperatura del refrigerante:** temperatura media uscita nocciolo compatibile con i materiali strutturali

**Componenti principali:** pompe primarie e generatori di vapore integrati con funzione di DHR

**Nocciolo:** basato sulla esperienza pregressa per quanto possibile



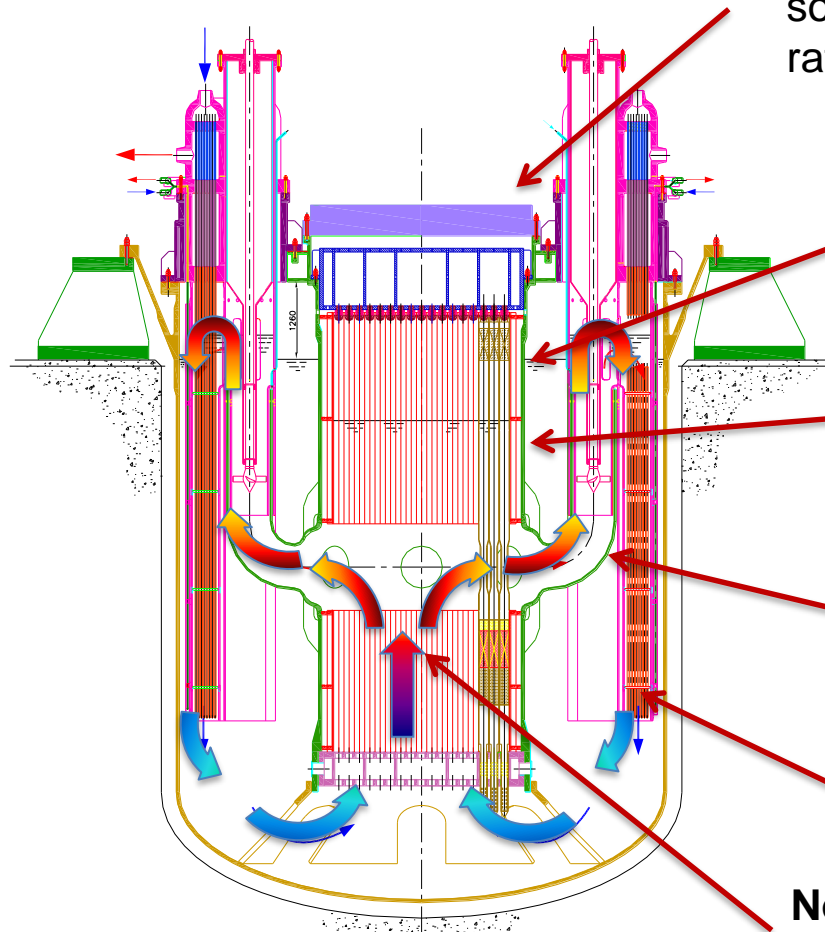
# Quando passare da design concettuale a preliminare



- Finalità di un approccio a stadi: riduzione del rischio associato al progetto nel progressivo miglioramento del livello di dettaglio dei sistemi ingegnerizzati.
- Principale ragione: i costi per l'eliminazione di inconsistenze o errori nel design aumentato drammaticamente con il livello di dettaglio raggiunto nella progettazione dei sistemi.

# Revisione del design di ALFRED

Sistema a pool fortemente integrato per definizione: sono necessari compromessi non esistendo una buona soluzione di per sé



**Refueling:** fuel assembly da movimentare sotto il pelo libero del piombo per assicurare il raffreddamento passivo in caso di incidente

**Configurazione del Reactor Coolant System:** afflitta da rischi termo-idraulici tipici dei reattori veloci

**Temperatura del refrigerante:** incompatibile con il cladding hot-spot comprese le incertezze

**Componenti principali:** affetti da vulnus di fabbricabilità, ispezionabilità, performance

**DHR:** sistema non sufficientemente diversificato

**Nocciolo:** da ottimizzare ed equipaggiare con un canale caldo per la qualifica di stadi futuri

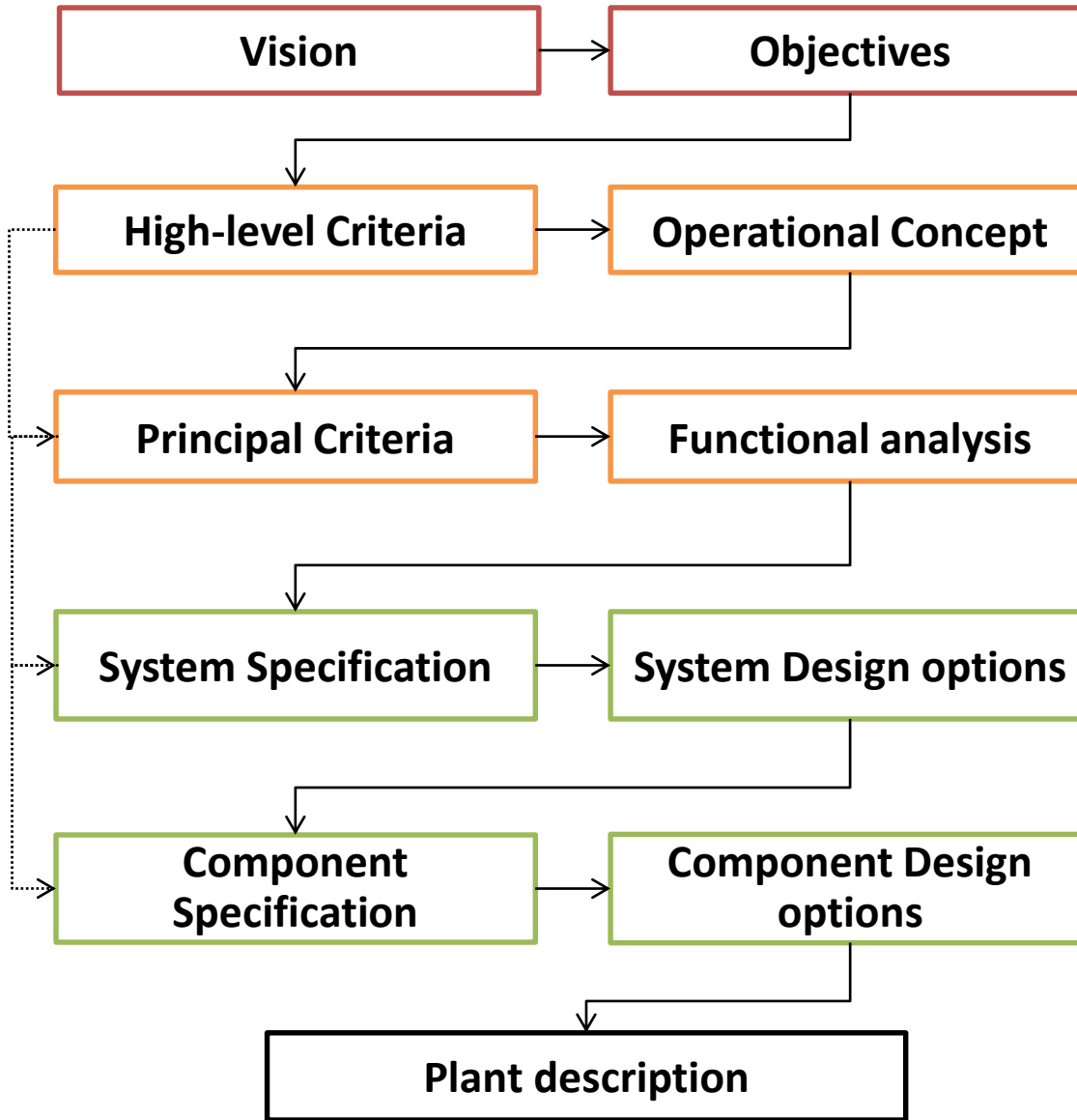
# Valorizzare il progresso pensando al futuro

Cosa  
abbiamo...



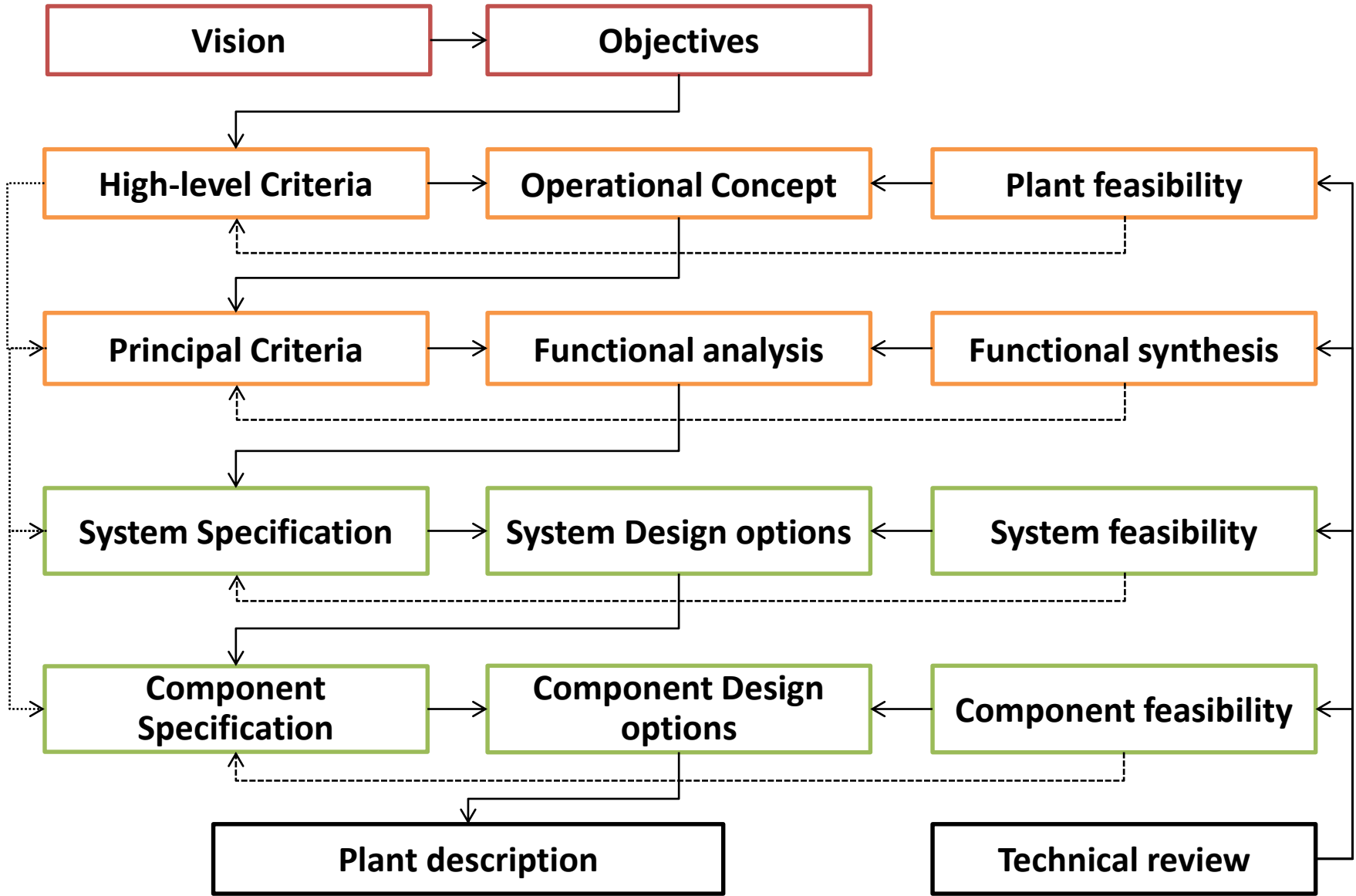
Cosa  
dovremmo fare...





- Deve fornire una **dimostrazione** robusta della operazione in **sicurezza** di un LFR in ogni condizione
- Deve consentire un **licensing** in accordo con **standard internazionali**, facendo leva sulle caratteristiche di dimostratore (**elevati margini**, sistemi di sicurezza)
- Deve permettere la **verifica** dei principali parametri progettuali, consentendo di **acquisire esperienza** per **ridurre le incertezze** per futuri LFR
- Deve garantire l'**estrapolabilità** del concetto (principali componenti) su **scala industriale**
- Deve fornire la possibilità di **testare** nuovi combustibili, materiali e componenti
- Deve consentire di supportare la **dimostrazione di sicurezza e sostenibilità** per futuri LFR commerciali
- Deve permettere il **training** di personale di organizzazioni interessate





Inner Vessel reso estraibile

Refueling strategy

Stratificazione termica e gas  
 entrainment eliminati con nuova  
 configurazione termo-idraulica

Separazione dei  
 componenti  
 (qualifica  
 meccanica,  
 standardizzazione)

Funzioni di  
 sicurezza delle  
 strutture interne  
 separate

Ottimizzazione ed  
 ingegnerizzazione  
 del core

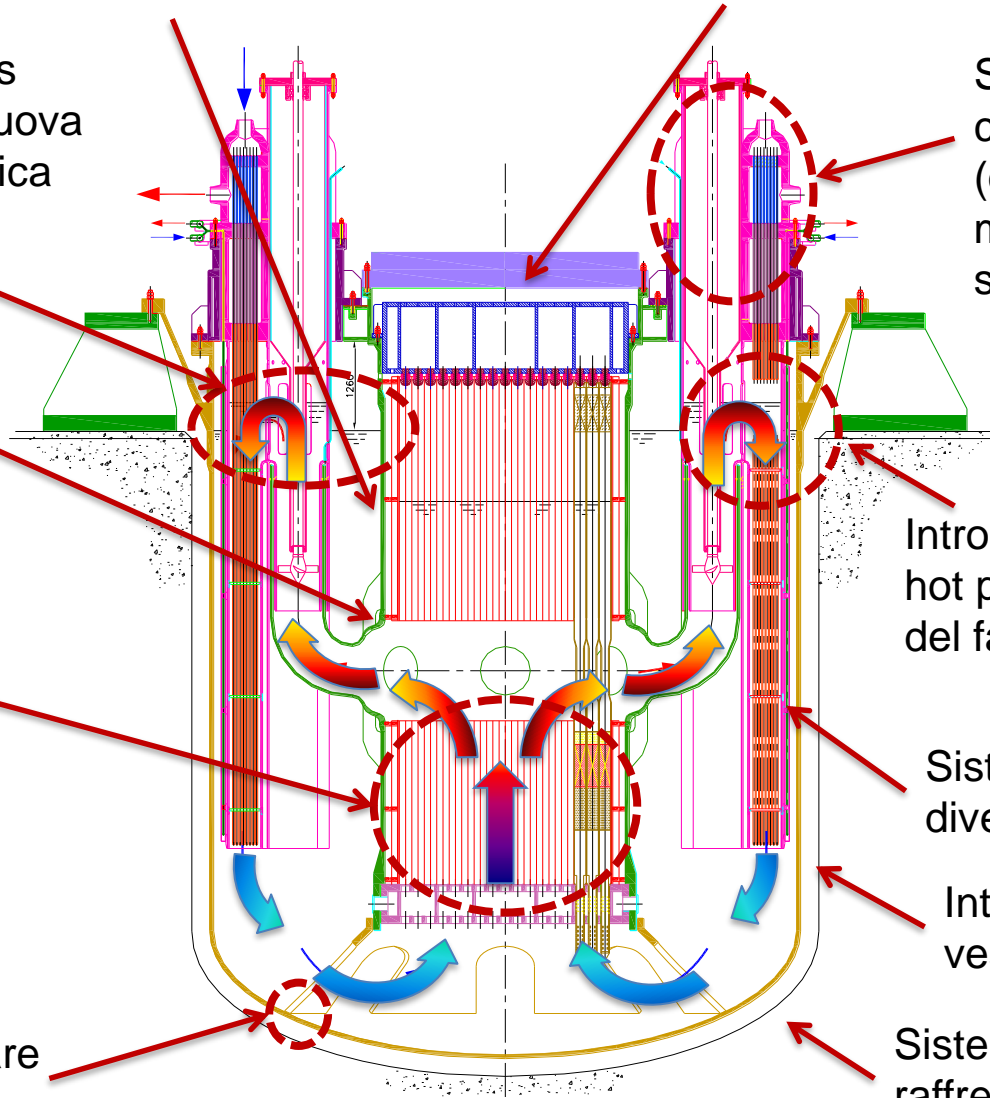
Introduzione di una  
 hot pool (bagnabilità  
 del fascio tubiero)

Sistemi DHR  
 diversificati

Introdotta un safety  
 vessel

Radial restraint  
 ripensato per evitare  
 ispezioni

Sistema passivo di  
 raffreddamento della  
 cavity

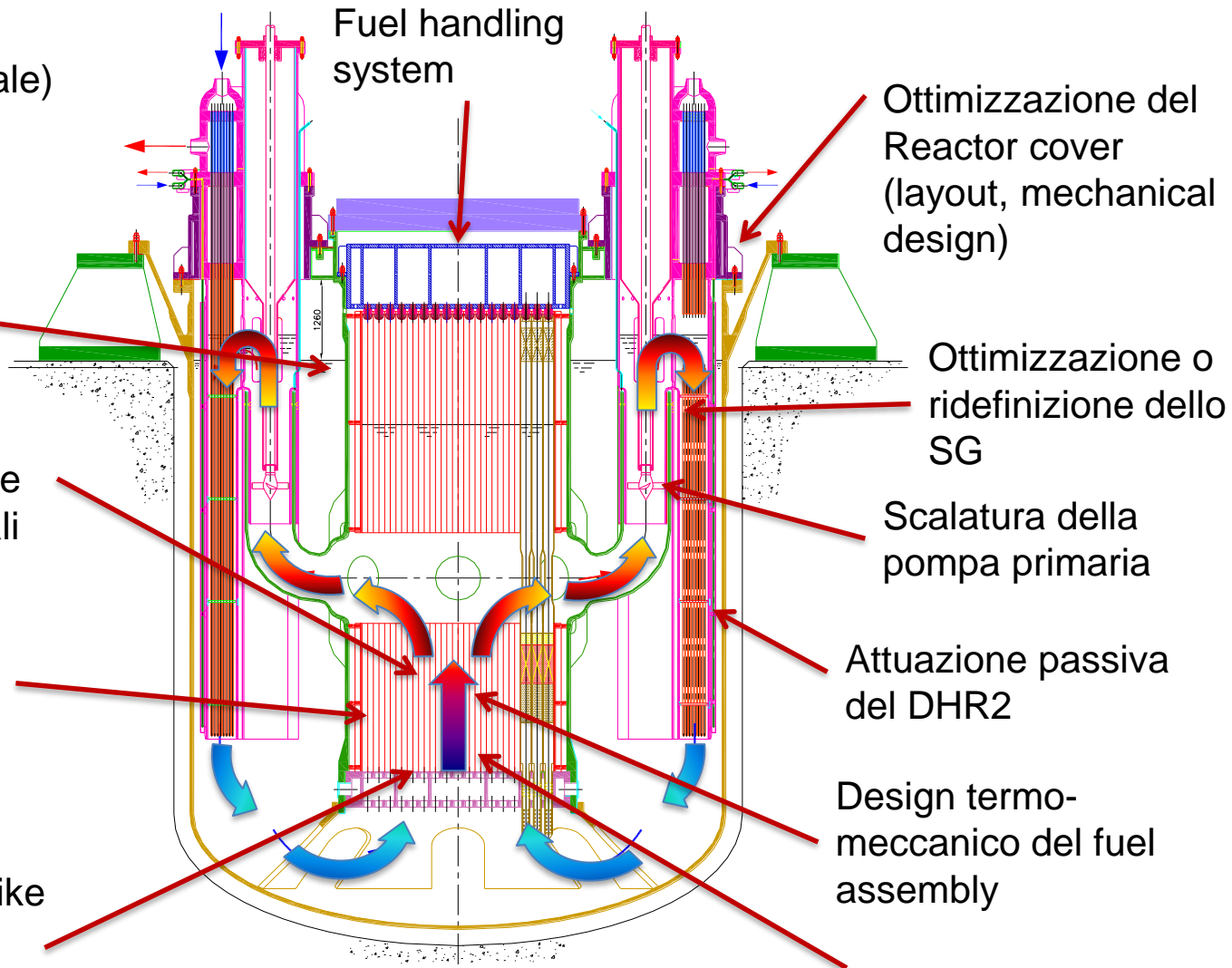


Analisi termoidrauliche di sistema (circolazione naturale)  
 Analisi CFD (thermal striping, gas entrainment, free level fluctuation,...)

Condizioni operative (massima temperatura) e compatibilità coi materiali

Introduzione di un sistema di spegnimento passivo

Ottimizzazione dello spike del fuel assembly



Ottimizzazione del Reactor cover (layout, mechanical design)

Ottimizzazione o ridefinizione dello SG

Scalatura della pompa primaria

Attuazione passiva del DHR2

Design termo-meccanico del fuel assembly

Qualifica del fuel assembly (grid spaced)

## Stages of operation:

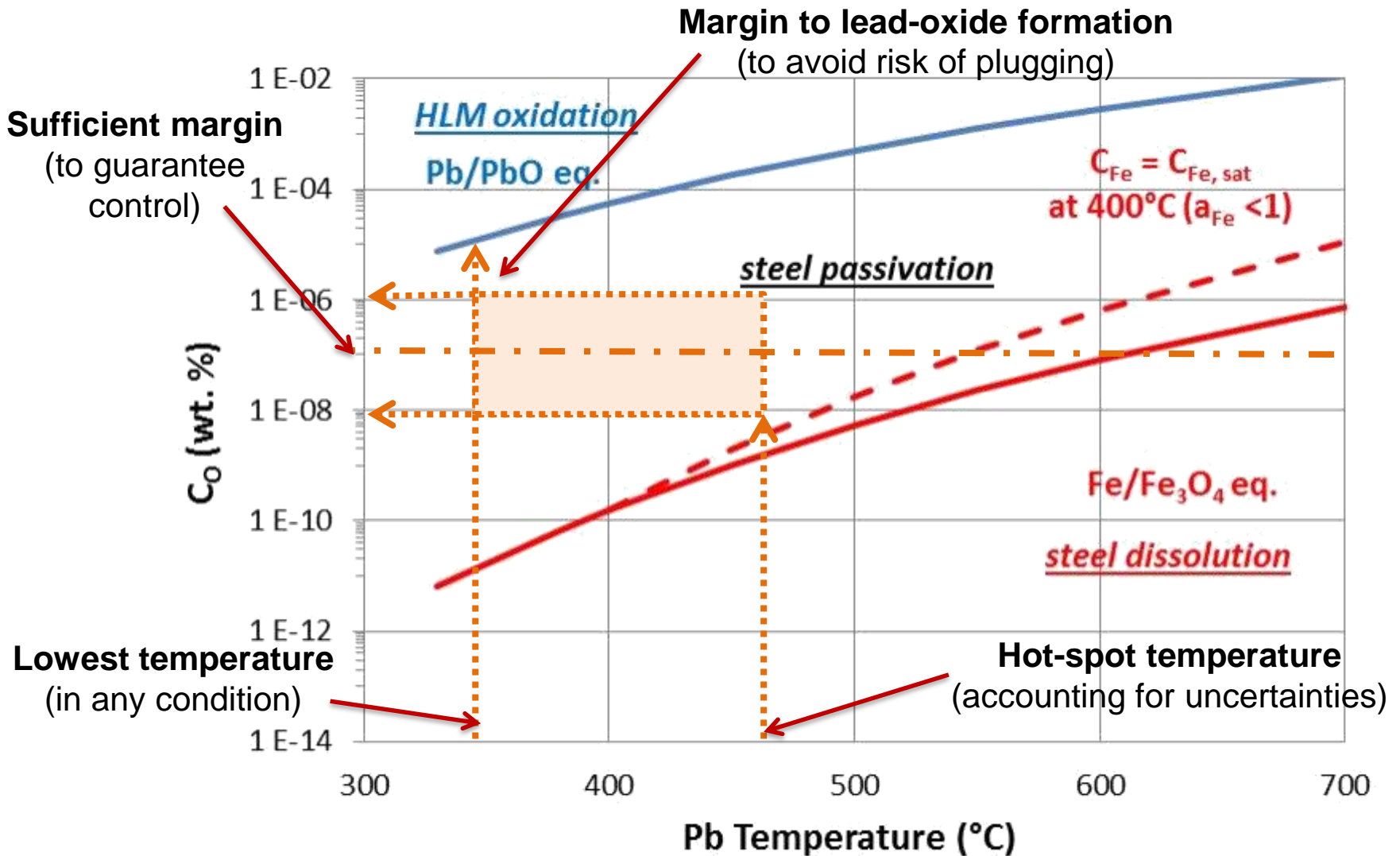
- 1<sup>st</sup> – Qualification of PLD coating
- 2<sup>nd</sup> – Operation with PLD coated FAs
- Final – Operation at reference temperature for commercial reactor

|                    | Thermal power (MW) | Core inlet temperature (°C) | Core outlet temperature (°C) | Temperature variation (°C) | Mass flow rate @avg. Temp. (kg/s) | Volum. flow rate (m <sup>3</sup> /s) |
|--------------------|--------------------|-----------------------------|------------------------------|----------------------------|-----------------------------------|--------------------------------------|
| ALFRED - LEADER    | 300                | 400                         | 480                          | 80                         | 25177,2                           | 2,4                                  |
| ALFRED - 1st stage | 101                | 390                         | 430                          | 40                         | 16845,7                           | 1,6                                  |
| ALFRED - 2nd stage | 201                | 400                         | 480                          | 80                         | 16845,7                           | 1,6                                  |
| ALFRED - Final     | 300                | 400                         | 520                          | 120                        | 16845,7                           | 1,6                                  |

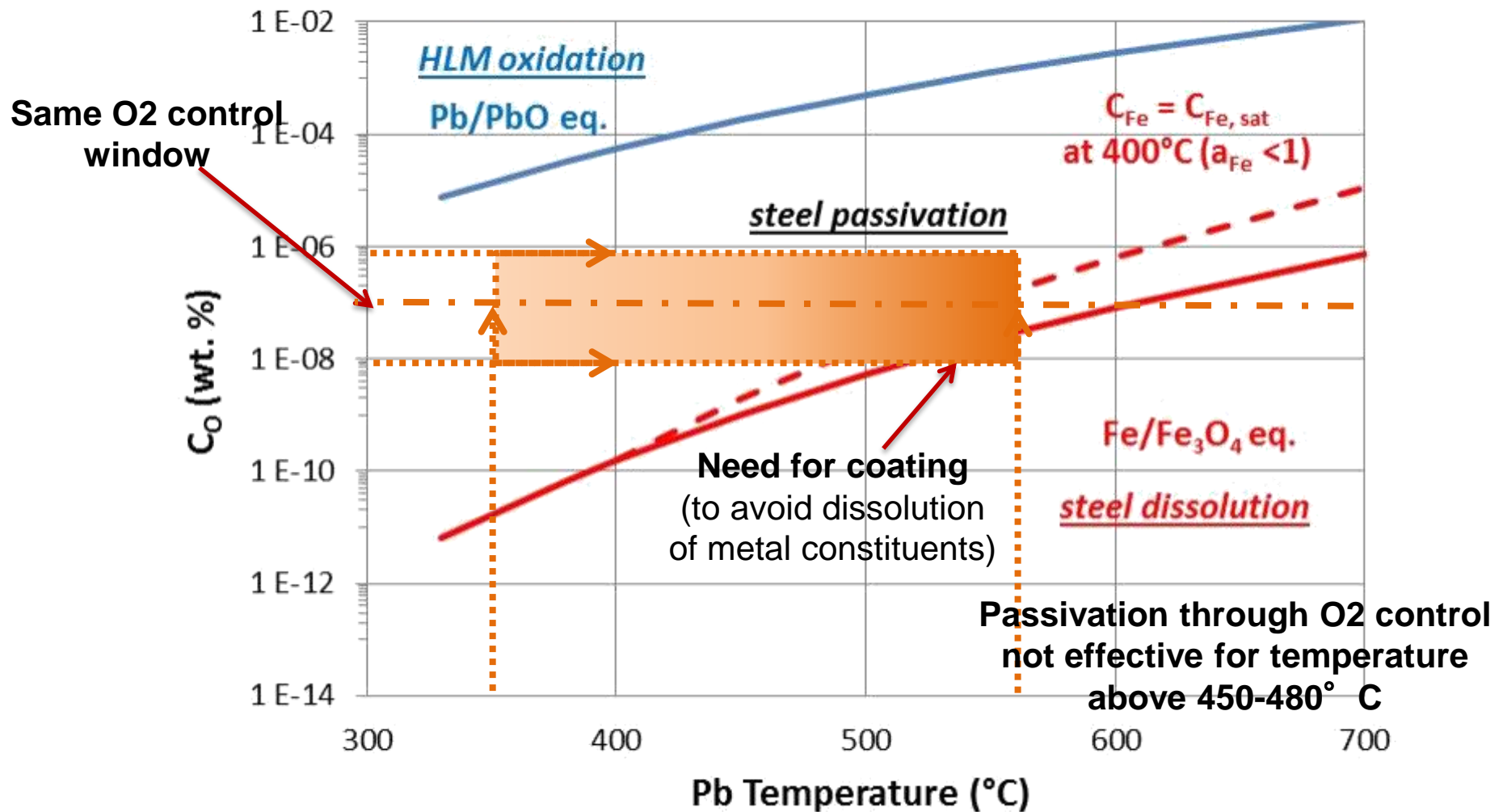
Lead density: ~10500 kg/m<sup>3</sup>

Lead specific heat capacity: ~150 J/kgK

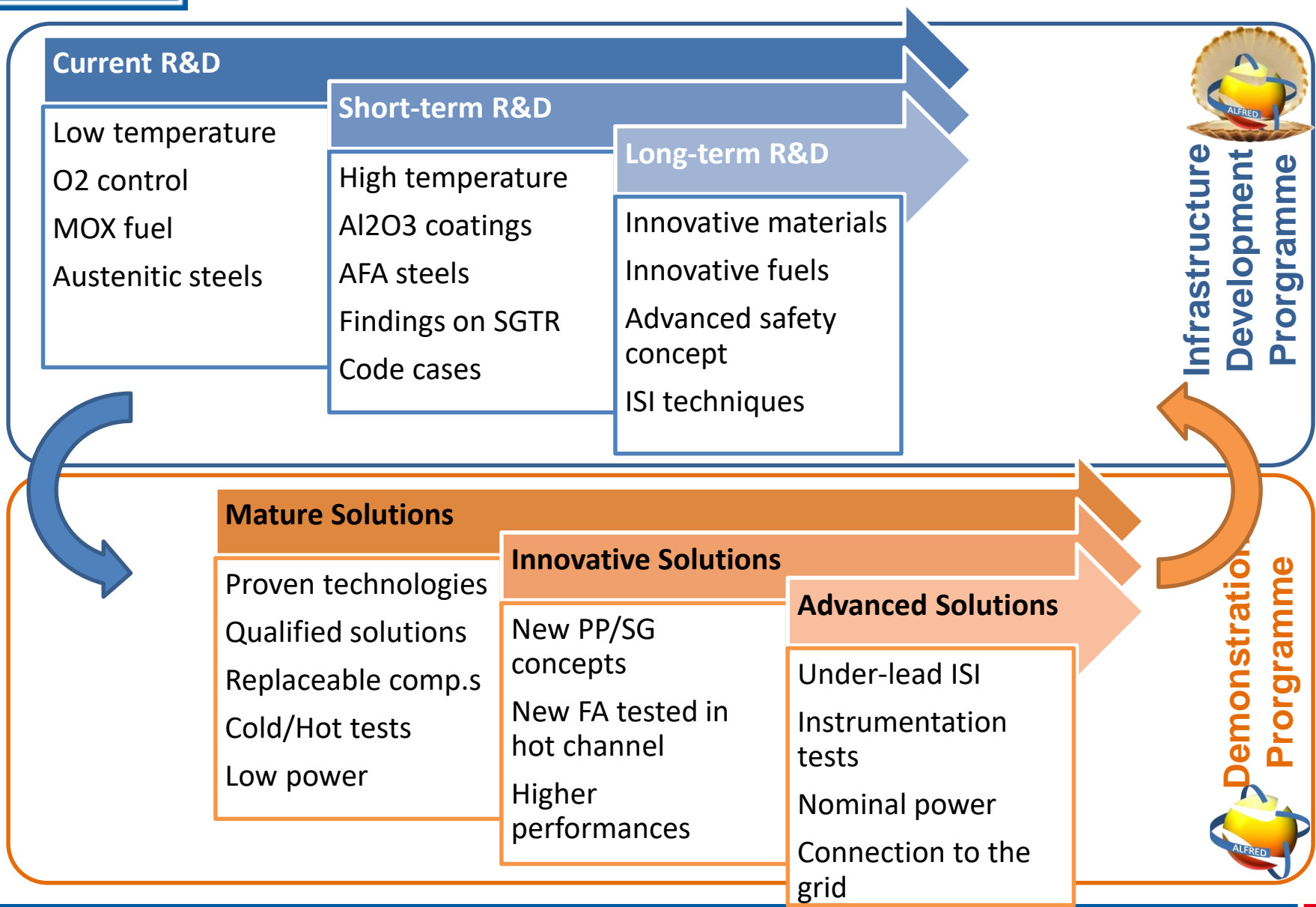
# Impact of temperature (1st stage)



# Impact of temperature (final stage)



- Strategia per lo **short-term**
  - Definire un design consistente ed un piano sistematico di R&D
  - Adeguare la potenza del reattore per mantenere ridotte dimensioni
  - Concentrarsi su materiali esistenti e colmare i gap
  - Esercizio del dimostratore a bassa temperatura
  - Utilizzare il dimostratore stesso per qualificare nuovi materiali
  
- Strategia di **lungo termine**
  - Perseverare sulla qualifica di materiali innovativi e coating
  - Migliorare le prestazioni nel lungo termine
  - Integrare soluzioni ottimizzate grazie alla flessibilità del dimostratore







- ESNII Executive Board – 21 Marzo, 2018:
  - Riconosce gli avanzamenti del progetto
  - Riconosce la maggiore maturità raggiunta
  - Sostiene la richiesta FALCON di un maggiore supporto

**Il progetto ALFRED è ora incluso nella  
“fast track” dei dimostratori Europei**





- **FALCON** è stato rinnovato nel Novembre 2017
- **Obiettivi principali:**
  - Impegno della Romania a investire in ALFRED come **Major Project** per il Paese
  - **Finalizzazione** del **feasibility study** di ALFRED come dimostratore LFR,
  - Inizio della **costruzione** di **infrastrutture di ricerca** e di un **Centro di Eccellenza**.
- **Full-members:**
  - Ansaldo Nucleare,
  - ENEA,
  - RATEN-ICN
- **Supporting organizations:** in fase di definizione





## Governance, Management and Financing

- Nuovo Consortium Agreement (nuovi obiettivi e regole)
- Identificazione di potenziali supporting organizations
- Azioni informative a livello Nazionale ed Europeo



## Research, Development and Qualification

- Identificazione di infrastrutture di ricerca chiave e priorità
- Studi di fattibilità e stima dei costi
- Costruzione di facility attingendo a fondi infrastrutturali



## Safety, Siting and Licensing

- Dialogo con CNCAN iniziato nel 2017
- Draft del Licensing Basis Documents
- Nuove investigazioni per il sito e consultazioni pubbliche



## Engineering, Procurement and Construction

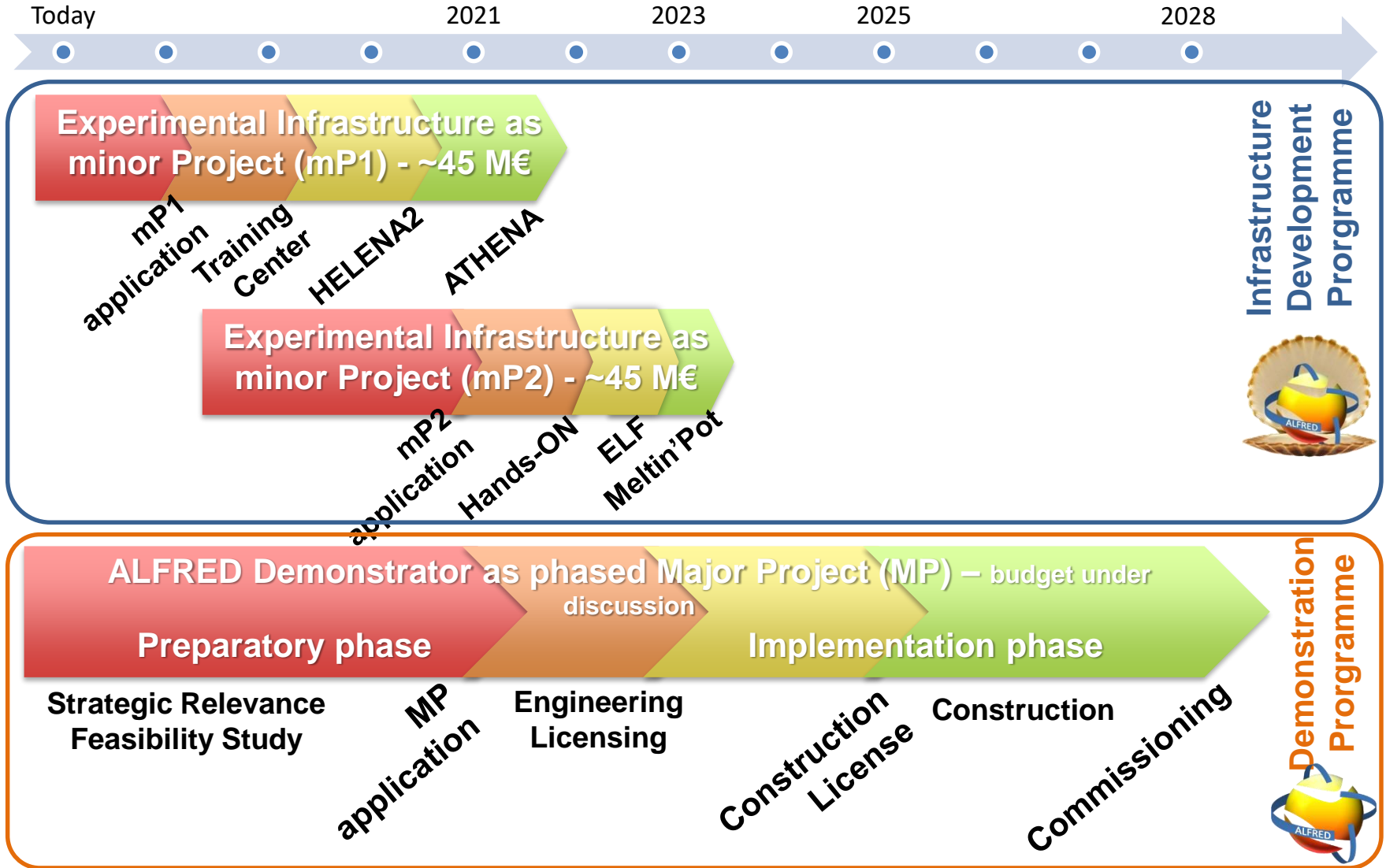
- Review tecnica di ALFRED e selezione delle opzioni di design
- Nuovo approccio per l'aumento progressivo di temperatura
- Identificazione di soluzioni tecniche più robuste



## Human resources, Education and Training

- Education program che copra moduli su GenIV and LFR
- CESINA partnership tra istituti del mondo E&T e R&D
- Mobilità e training di ricercatori ICN

# Multi-annual Funding Scheme (under discussion)



**CIRCE** – large pool, assisted/force circ., int. test  
**LIFUS5** – small pool, stagnant, lead-water int. (high p)  
**HELENA1** – loop, forced circ., bundle exp.  
**LECOR** – loop, forced circ., corrosion exp.  
**NACIE-UP** – loop, nat. circ., bundle exp.  
**PLACE** – large plant, controlled env., comp. cleaning  
**RACHEL** – 10 capsules, stagnant, chemistry exp.  
**TAPIRO** – 0-pwr reactor, propagation and calibration  
**SOLIDX** – small vessel, stagnant, freez/melt exp.  
**BID1** – small pool, stagnant/mixed, O2 control exp.

**HELENA2** – loop, forced circ., full-scale FA qual.  
**ATHENA** – large pool, forced circ., comp. qual., SGTR  
**ChemLab** – capsules/loop, stagant/flowing, chem ctrl  
**ELF** – large pool, forced circ., integral and endurance  
**Hands-ON** – vessel with core mock-up, handling sys  
**Meltin'Pot** – vessels and loop, fuel/coolant int.  
**Lead School** – E&T facilities, supercomp., conf. center



Viability



Preparation



Construction



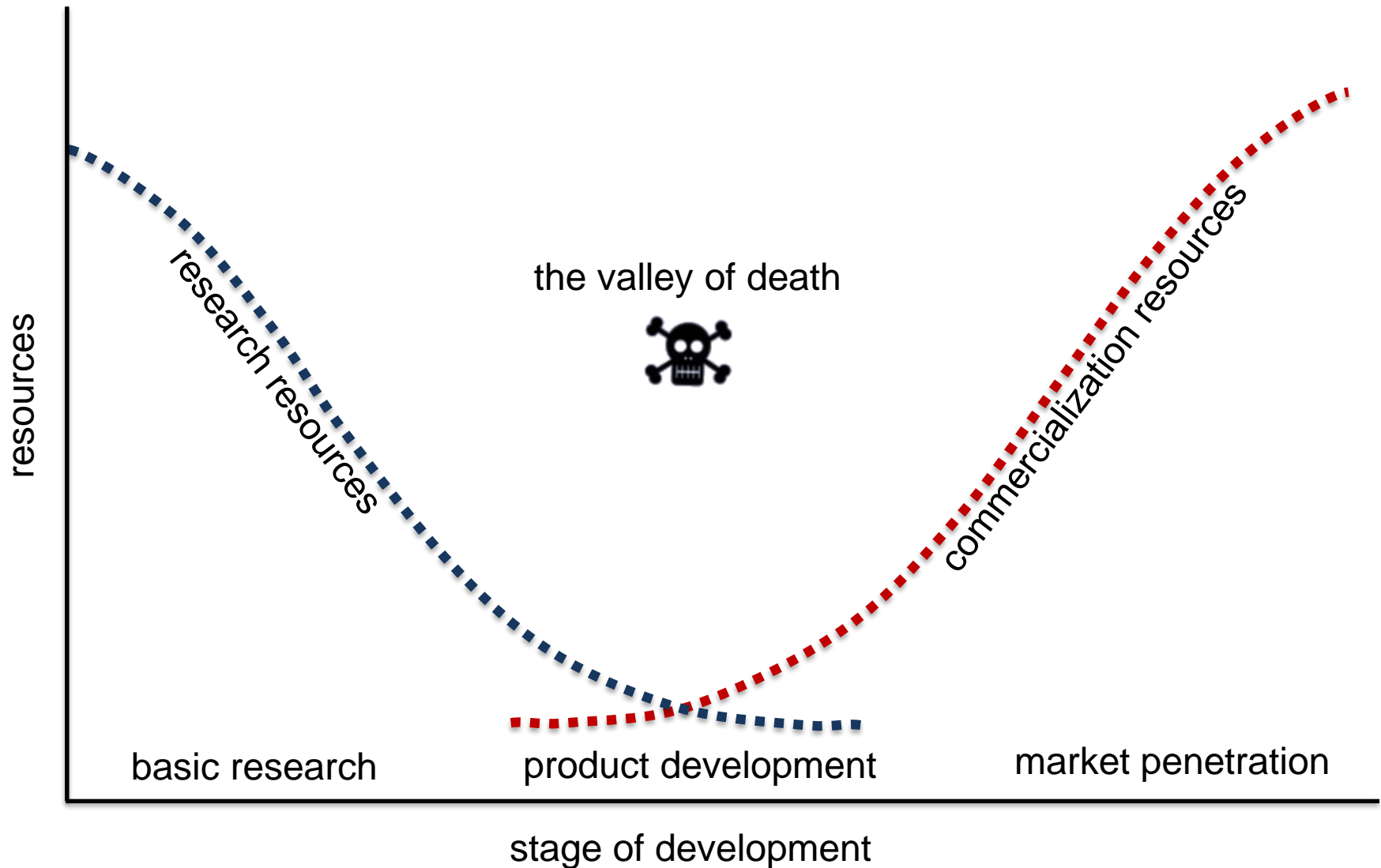
Commissioning

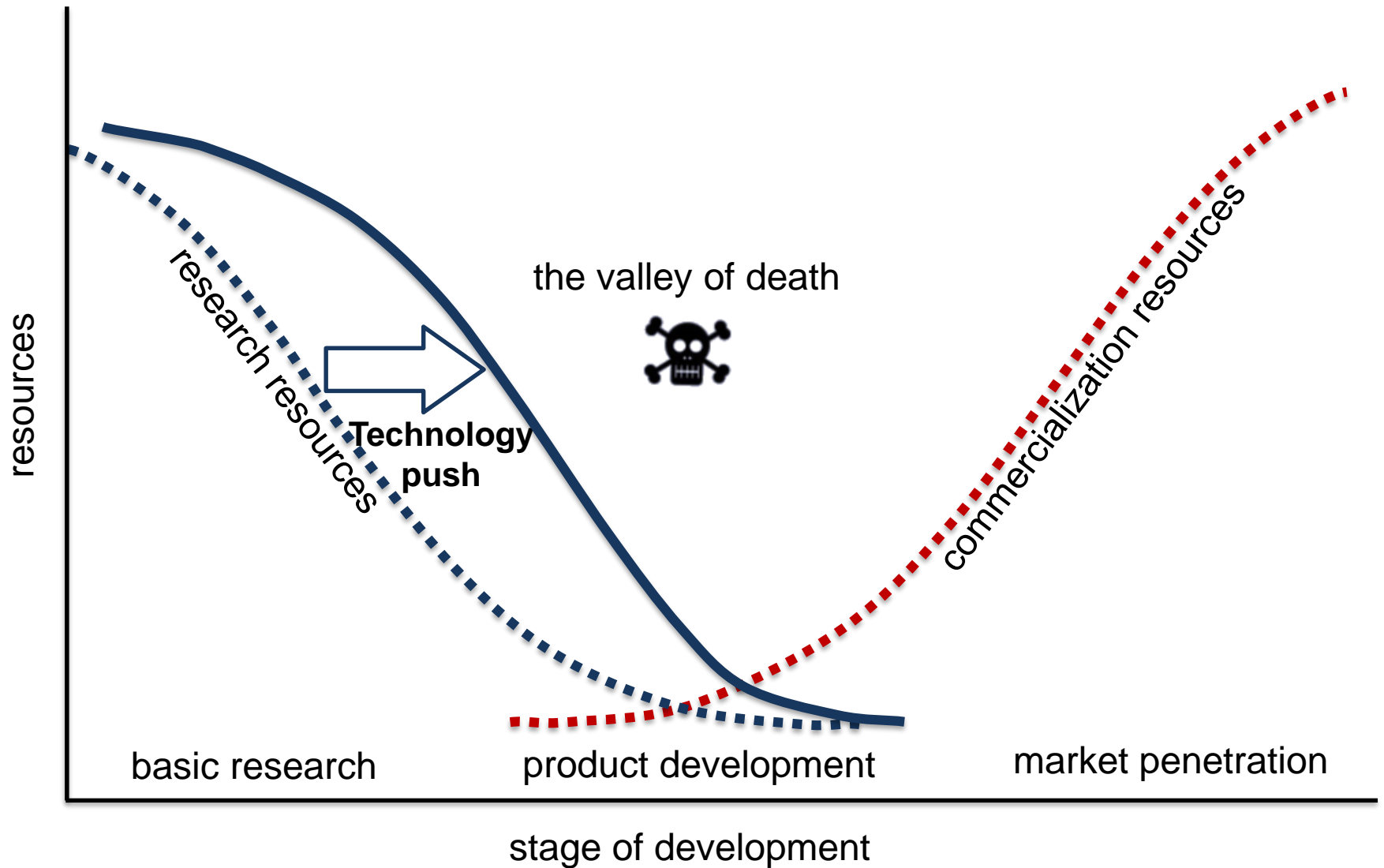


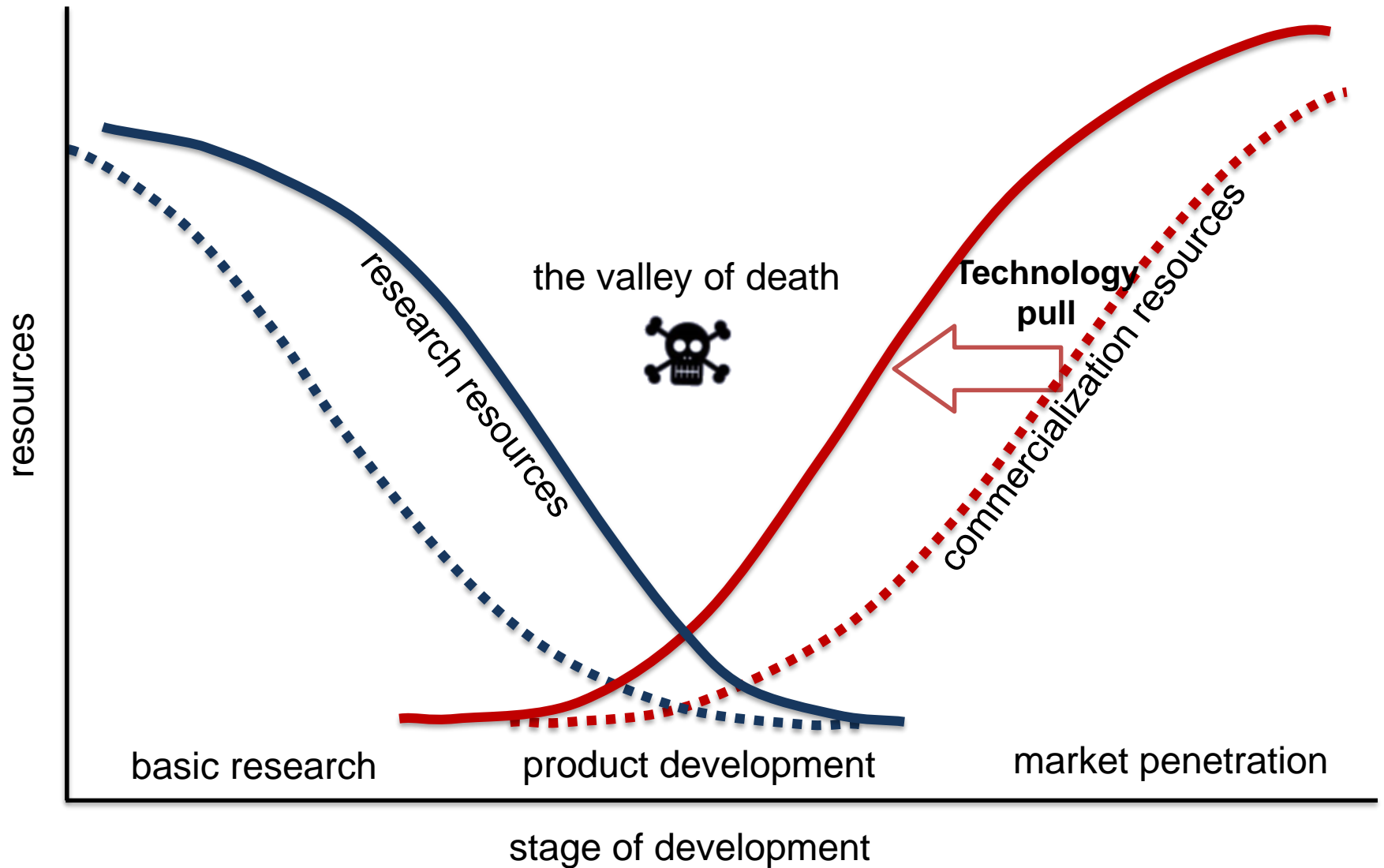
Operation

## 9 Obiettivi scientifici

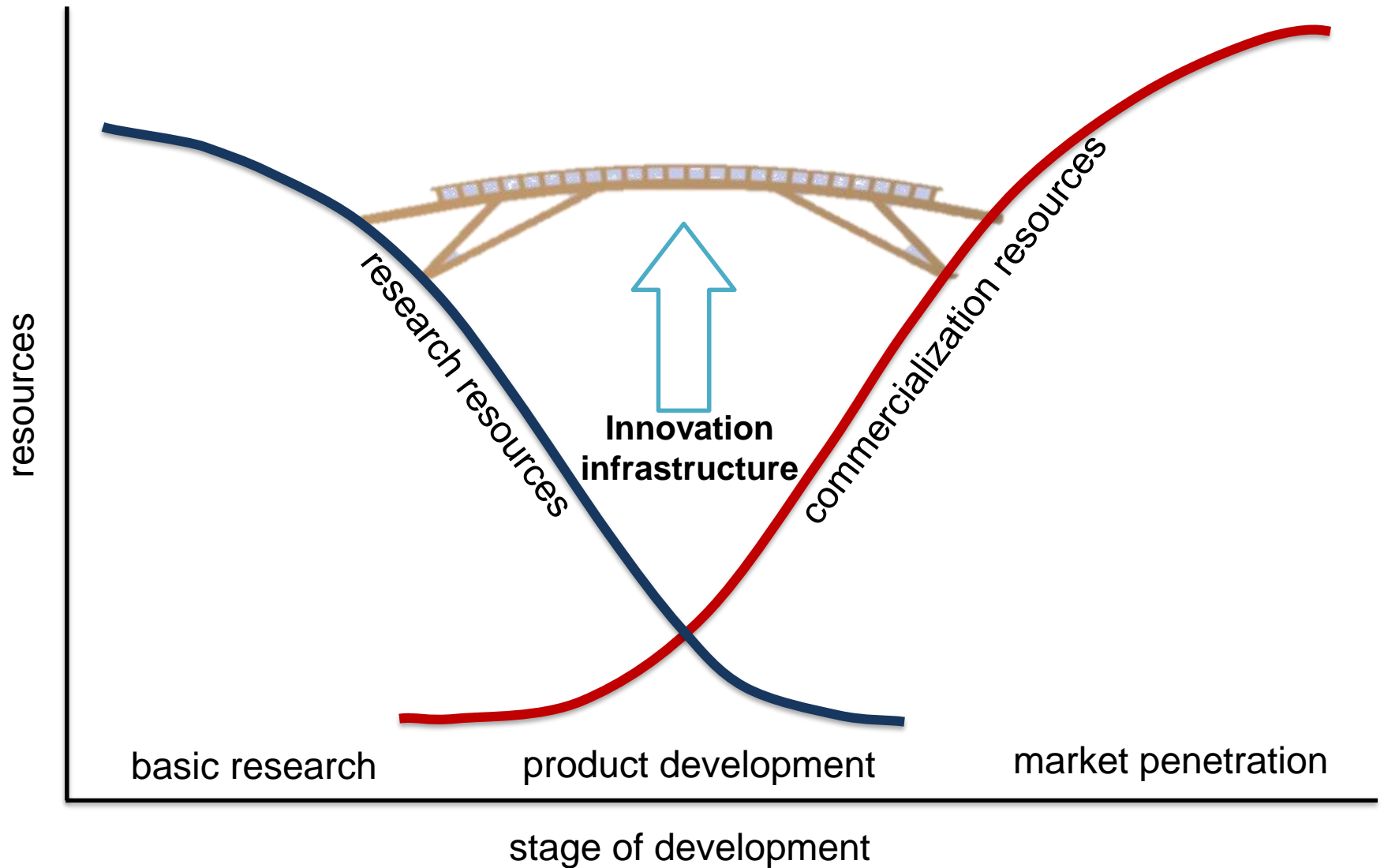
- **Material** science for qualified solutions
- **HLMs** physical-chemical properties
- HLMs as coolants in **practical applications**
- **Solutions and provisions** to exploit HLMs
- **Characterization** of concepts
- **Qualification** of prototypical SSCs
- **Integral tests** for NESs
- **Viability** of LFR concept
- **Safe and sustainable** operation of future LFRs









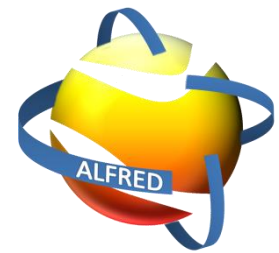


- Temi di interesse trasversale
  - Strumentazione e logica di controllo
  - Strategia di confinamento
  - Gestione degli incidenti severi (difficili da escludere per un dimostratore)
  - Strategie di ispezione, manutenzione, refueling
  - Analisi termo-idrauliche di performance e di sicurezza
  - Analisi CFD delle fenomenologie termo-idrauliche
- Piano sistematico di R&D
  - Test per colmare i gap dei codes & standards applicabili
  - Perseverare sulla qualifica di materiali innovativi e coating
  - Qualifica di componenti prototipici
  - Sviluppo di nuovi codici per assistere la progettazione
  - Verifica e validazione di codici di calcolo



Grazie per l'attenzione

sustainable  
pan-European  
**ALFRED**  
technology  
unique  
future  
excellent  
open  
secure  
safe  
science  
acceptable  
innovative



[www.alfred-reactor.eu](http://www.alfred-reactor.eu)



Italian National Agency for New Technologies,  
Energy and Sustainable Economic Development

# [1-1] Development of best estimate numerical tools for LFR design and safety analysis

*WORKSHOP TEMATICO – AdP MISE – ENEA, PAR2017 –B.3 - LP2*

*DIAEE- Università di Roma "La Sapienza" - San Pietro in Vincoli, Via Eudossiana 18, Roma*

*14 Giugno 2018*

**Alessandro Del Nevo – ENEA FSN-ING-PAN**



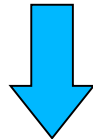
# Introductory remarks



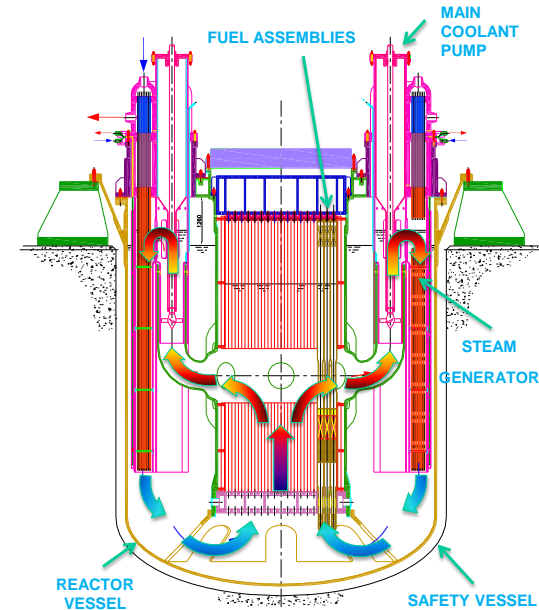
## AdP PAR LP2 (>2012)

*Collaborative activity between ENEA-CIRTEN carried out (also) in synergy with EC H2020 Project and Research International Activity (e.g. NEA, IAEA)*

- ❑ A.2 Progettazione nocciolo
- ❑ A.3 Analisi di sicurezza
- ❑ C. Termoidraulica (parzialmente)



**Development and validation of codes and multi-physics models for the design and the safety analysis of Gen. IV fast reactors**



- *Power: 300 MWth (125 MWe)*
- *Prim. cycle: Molten Lead 400-480 °C*
- *Sec. cycle: Water/superheated steam: 335-450 °C*

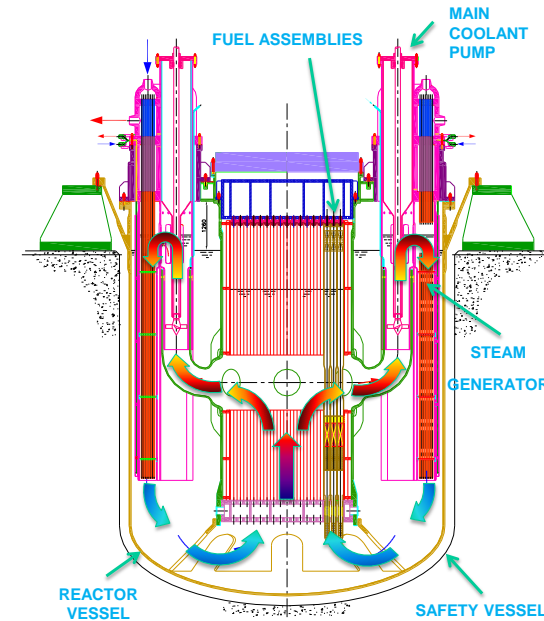
# Strategic objectives of the Task



The Task “*sviluppo e convalida di codici e modelli multi-fisica per progetto e analisi di sicurezza di reattori veloci di IV generazione*” has the following objectives

1. **Collaborazione** tra ENEA-CIRTEN. Attività condotte (anche) in **sinergia con progetti EC e attività di ricerca internazionali (e.g. NEA, IAEA)**
2. **Continuità**. Le attività tecniche dovrebbero essere condotte in continuità con quanto svolto fino ad oggi  
→ rendere gradualmente **l'attività coordinata e finalizzata**  
→ **no brusche discontinuità** che possano penalizzare know-how acquisiti ed investimenti delle istituzioni coinvolte
3. **Coinvolgimento**. ENEA/Università CIRTEN coinvolte su un **unico progetto dove ognuno contribuisce per l'obiettivo comune**

## Progetto di riferimento



# Strategic objectives of the Task and involved Institutions



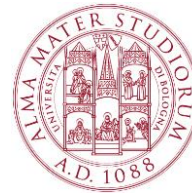
4. **R&D e qualità.** Attività **orientata allo sviluppo di strumenti di calcolo, integrazione degli stessi, identificazione delle aree di utilizzo e documentazione, validazione ed applicazione. Risultati tangibili.**
5. **ENEA stakeholder** delle attività a supporto delle attività di R&D in corso e della progettazione ed implementazione delle campagne sperimentali al CR Brasimone



*CIRTEN - CONSORZIO INTERUNIVERSITARIO  
PER LA RICERCA TECNOLOGICA NUCLEARE*



**POLITECNICO**  
MILANO 1863



UNIVERSITÀ DI PISA

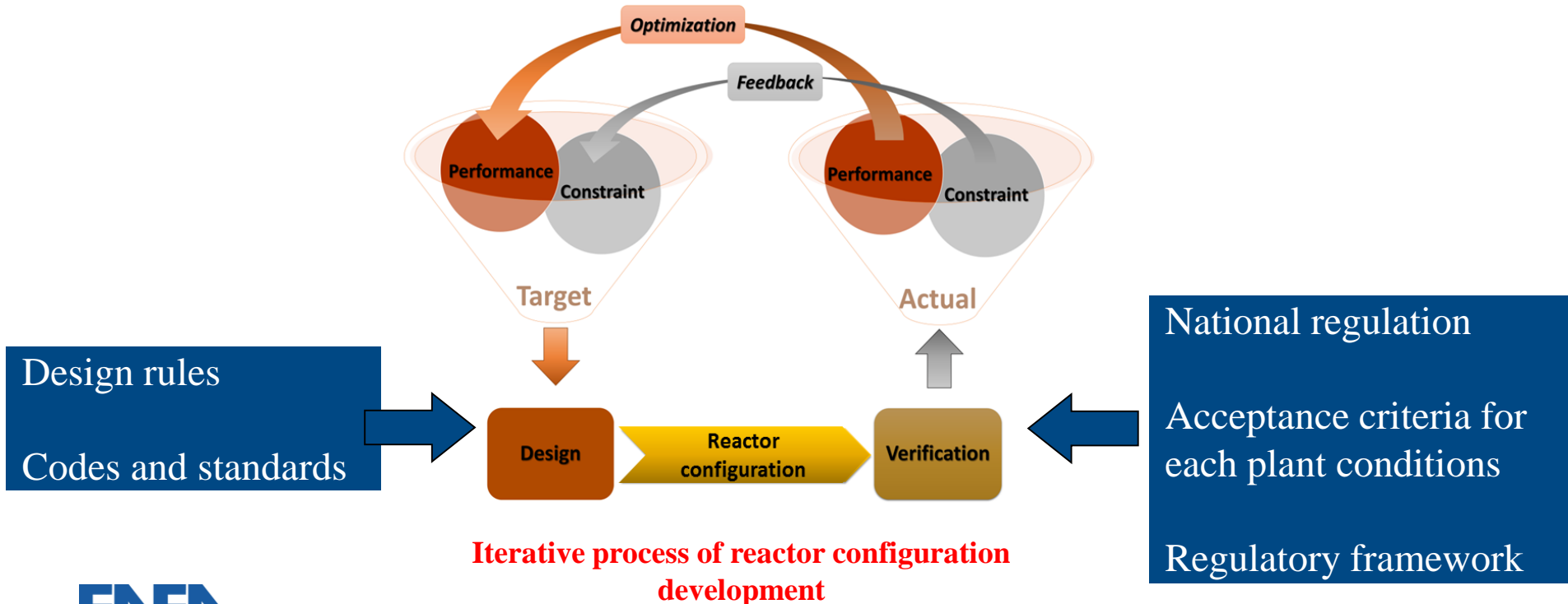


**SAPIENZA**  
UNIVERSITÀ DI ROMA





# Design and safety analysis framework



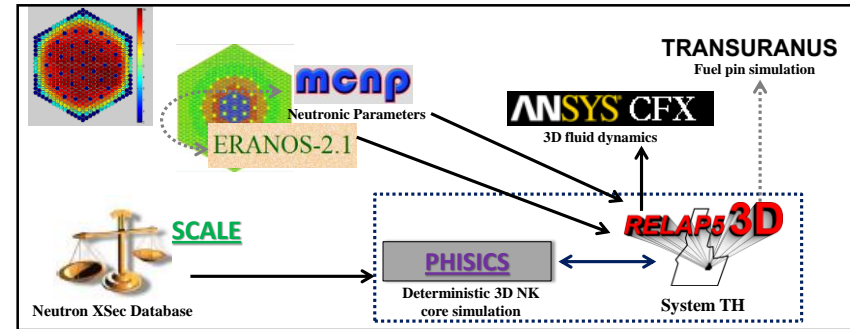
# Specific Objectives of the Task



The objective is to make available numerical tools for supporting the design and the DSA of the LFR

- ❑ Developing and validating new tools
- ❑ Extending the capability and the area of application of existing codes and their validation
- ❑ Setting-up chain of codes and interfaces
- ❑ Developing code coupling techniques

| Reactor    |                                     | Encompassed aspect |    |    |   |   |
|------------|-------------------------------------|--------------------|----|----|---|---|
|            |                                     | N                  | TH | TM | C | E |
| Sub-system | Core system                         | ×                  | ×  | ×  |   |   |
|            | Primary system                      |                    | ×  | ×  |   |   |
|            | Auxiliary and Ancillary systems     |                    | ×  | ×  | × |   |
|            | Instrumentation and control systems |                    |    |    |   | × |
|            | Reactor (integration)               | ×                  | ×  | ×  | × | × |



**Sample chain of codes set up in the framework of IAEA EBR-II benchmark**

**Aspects encompassed in the design and verification of main reactor sub-systems**

# Computer codes: the relevance of the qualification



## ❑ Employed computer codes

- range from specialized reactor physics codes to coupled codes
- provide “Best Estimate” predictions
- Require demonstration of qualification

## ❑ The level of qualification

- depends by the availability of experimental data or NPP data, and the extent of independent assessment → *Experimental data are fundamental for supporting the development and demonstrating the reliability of computer codes in simulating the behavior of an NPP during a postulated accident scenario: in general, this is a regulatory requirement*
- is strictly related to the user → *The user always has the responsibility of the appropriate use of such codes.*

# Computer codes: the relevance of the qualification



## Identified categories of codes

- Core physics codes
- Component specific or phenomenon specific codes
  - Fuel behaviour codes
  - Sub-channel codes
  - Porous media codes
  - Containment analysis codes, with features for the transport of radioactive materials
  - Atmospheric dispersion and dose codes
- Structural analysis codes
- System thermo-hydraulic codes
- CFD
- Coupled codes

*Validation and verification are essential steps in qualifying any computational method and are the primary means of assessing the accuracy of computational simulations*

# Overview of the R&D efforts in AdP2015-2017



|                         | Core Physics     |                 |                     |          |        |           | Component specific or phenomenon specific |                      |        |           |        |                                   | System |                             |           |               |          |        |  |  |
|-------------------------|------------------|-----------------|---------------------|----------|--------|-----------|---|----------------------|--------|-----------|--------|-----------------------------------|--------|-----------------------------|-----------|---------------|----------|--------|--|--|
|                         | X-sec generation | Reactor Physics | Burn-up Calculation | 3D NK    | 3D NK  | Shielding | FPC                                       | TH lumped parameters | CFD    |           |        | Fission product dispersion & dose | TM     | Material molecular dynamics | SYS-TH    | SYS-TH        | SYS-TH   | SA     |  |  |
| <i>pellet</i>           | SERPENT          | SERPENT         | SERPENT             |          |        |           | Transuranus                               |                      |        |           |        |                                   |        |                             |           |               |          |        |  |  |
| <i>gap</i>              |                  |                 |                     |          |        |           |   |                      |        |           |        |                                   |        |                             |           |               |          |        |  |  |
| <i>cladding</i>         |                  |                 |                     |          |        |           |   |                      |        |           |        |                                   |        |                             |           |               |          |        |  |  |
| <i>subchannel</i>       |                  |                 |                     |          |        |           |   |                      |        |           |        |                                   |        |                             |           |               |          |        |  |  |
| <i>fuel assembly</i>    |                  |                 |                     |          |        |           | 1-2                                       |                      |        |           |        |                                   |        |                             |           |               |          |        |  |  |
| <i>core</i>             |                  |                 |                     | FRENETIC | SIMMER |           |   | FRENETIC             | COMSOL | FEM-LCORE | FLUENT |                                   |        |                             | RELAP5-3D | RELAP5/Mod3.3 | CATHARE2 | SIMMER |  |  |
| <i>coolant</i>          |                  |                 |                     |          |        |           |   |                      |        |           |        | SIMMER                            |        | CALPHAD                     |           |               |          |        |  |  |
| <i>primary system</i>   |                  |                 |                     |          |        |           |   |                      |        |           |        |                                   |        |                             |           |               |          |        |  |  |
| <i>secondary system</i> |                  |                 |                     |          |        |           |   |                      |        |           |        |                                   |        |                             |           |               |          |        |  |  |
| <i>containemnt</i>      |                  |                 |                     |          |        |           |   |                      |        |           |        |                                   |        |                             |           |               |          |        |  |  |
| <i>I&amp;C</i>          |                  |                 |                     |          |        |           |   |                      |        |           |        |                                   |        |                             |           |               |          |        |  |  |
| <i>site</i>             |                  |                 |                     |          |        |           |   |                      |        |           |        |                                   |        |                             |           |               |          |        |  |  |

Design and Licensing

Design (including safety analysis)

Code Coupling  $\longleftrightarrow$

Chain of Code  $\cdots\cdots\rightarrow$

Uncertainty



# Fuel Performance Code [1-2]



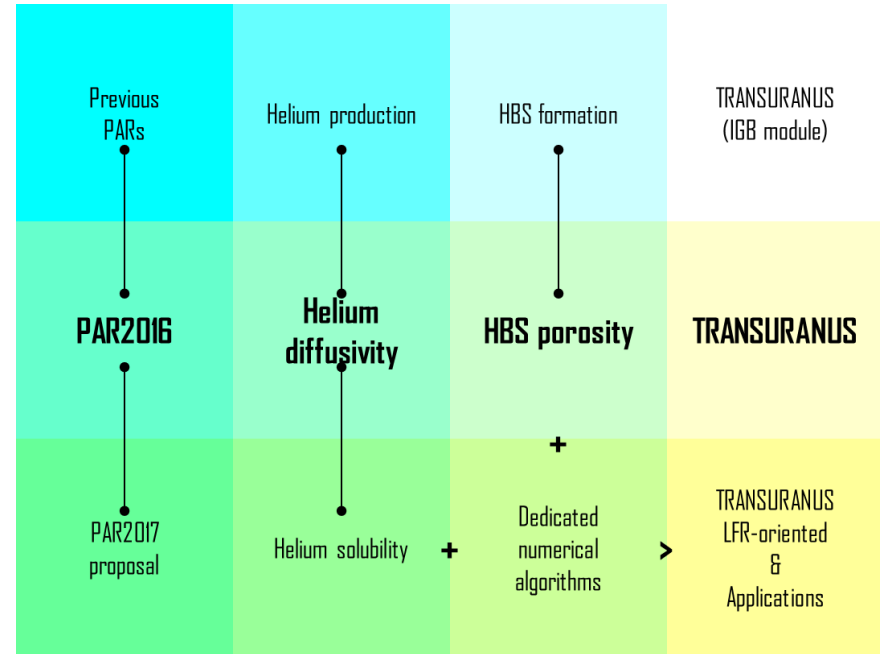
Development/assessment of models describing the inert gas behavior in the fuel for application to the TRANSURANUS fuel pin thermo-mechanical code

## Main Results

1. Development of new **correlations for Helium diffusivity**
2. Development of a new **model for High Burn-up Structure porosity evolution**

## Future developments

- Development of new **correlations for Helium solubility**
- Development of **dedicated numerical algorithms**
- Fuel rod integral analysis in support of design of FRs using the improved version of TRANSURANUS fuel pin thermo-mechanical code



Improvements of TRANSURANUS code models in AdP PAR-2016

# Overview of the R&D efforts in AdP2015-2017



|                                    | Core Physics     |                 |                     |          |        |           | Component specific or phenomenon specific |                      |             |           |        |                                   | System  |                             |           |               |          |        |  |  |  |
|------------------------------------|------------------|-----------------|---------------------|----------|--------|-----------|---|----------------------|-------------|-----------|--------|-----------------------------------|---------|-----------------------------|-----------|---------------|----------|--------|--|--|--|
|                                    | X-sec generation | Reactor Physics | Burn-up Calculation | 3D NK    | 3D NK  | Shielding | FPC                                       | TH lumped parameters | CFD         |           |        | Fission product dispersion & dose | TM      | Material molecular dynamics | SYS-TH    | SYS-TH        | SYS-TH   | SA     |  |  |  |
| <i>pellet</i>                      | SERPENT          | SERPENT         | SERPENT             |          |        |           |   |                      |             |           |        |                                   |         |                             |           |               |          |        |  |  |  |
| <i>gap</i>                         |                  |                 |                     |          |        |           |   |                      | Transuranus |           |        |                                   |         |                             |           |               |          |        |  |  |  |
| <i>cladding</i>                    |                  |                 |                     |          |        |           |   |                      |             |           |        |                                   |         |                             |           |               |          |        |  |  |  |
| <i>subchannel</i>                  |                  |                 |                     |          |        |           |   |                      |             |           |        |                                   |         |                             |           |               |          |        |  |  |  |
| <i>fuel assembly</i>               |                  |                 |                     |          |        |           |   |                      |             |           |        |                                   |         |                             |           |               |          |        |  |  |  |
| <i>core</i>                        |                  |                 |                     | FRENETIC | SIMMER |           |   | FRENETIC             | COMSOL      | FEM-LCORE | FLUENT |                                   |         | 1-3                         | RELAP5-3D | RELAP5/Mod3.3 | CATHARE2 | SIMMER |  |  |  |
| <i>coolant</i>                     |                  |                 |                     |          |        |           |   |                      |             |           |        | SIMMER                            | CALPHAD |                             |           |               |          |        |  |  |  |
| <i>primary system</i>              |                  |                 |                     |          |        |           |   |                      |             |           |        |                                   |         |                             |           |               |          |        |  |  |  |
| <i>secondary system</i>            |                  |                 |                     |          |        |           |   |                      |             |           |        |                                   |         |                             |           |               |          |        |  |  |  |
| <i>containemnt</i>                 |                  |                 |                     |          |        |           |   |                      |             |           |        |                                   |         |                             |           |               |          |        |  |  |  |
| <i>I&amp;C</i>                     |                  |                 |                     |          |        |           |   |                      |             |           |        |                                   |         |                             |           |               |          |        |  |  |  |
| <i>site</i>                        |                  |                 |                     |          |        |           |   |                      |             |           |        |                                   |         |                             |           |               |          |        |  |  |  |
| Design and Licensing               |                  |                 |                     |          |        |           |   |                      |             |           |        |                                   |         |                             |           |               |          |        |  |  |  |
| Design (including safety analysis) |                  |                 |                     |          |        |           |   |                      |             |           |        |                                   |         |                             |           |               |          |        |  |  |  |
| Code Coupling                      | ↔                |                 |                     |          |        |           |   |                      |             |           |        |                                   |         |                             |           |               |          |        |  |  |  |
| Chain of Code                      | ⋯→               |                 |                     |          |        |           |   |                      |             |           |        |                                   |         |                             |           |               |          |        |  |  |  |
| Uncertainty                        |                  |                 |                     |          |        |           |   |                      |             |           |        |                                   |         |                             |           |               |          |        |  |  |  |

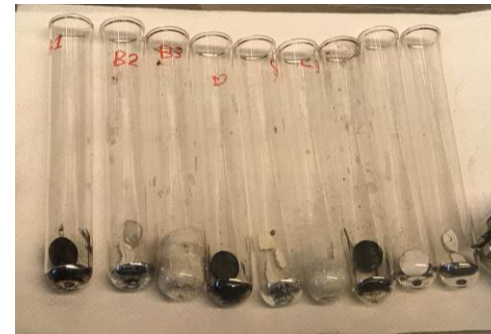
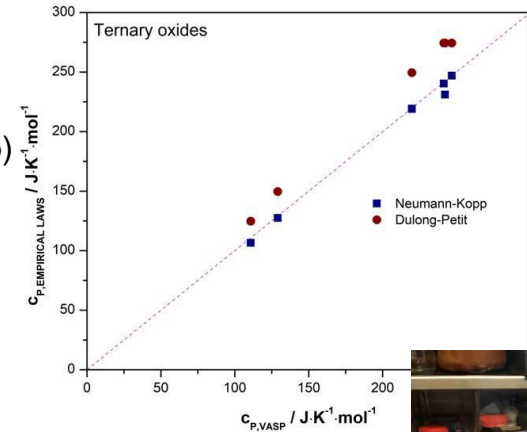
## Fuel-coolant chemical interactions

### Computational activities:

- ❖ Evaluation of thermodynamic properties for ternary oxides (An/FPs – O – Pb) by DFT approach
- ❖ Investigations on computational thermodynamics by CALPHAD method

### Experimental activities

- ❖ Interaction studies on different oxide-Pb systems:
  - Preliminary characterization of reagents by XRD, DSC and EDX
  - Preparation of pellets of SrO, ZrO<sub>2</sub>, La<sub>2</sub>O<sub>3</sub> and CeO<sub>2</sub>
  - Thermal treatment at 500-550°C under argon atmosphere
  - Reaction time of 3-7 hours
- ❖ Post-treatment characterization:
  - Identification of new phases by XRD on powder or pellet
  - Thermal analyses on powder by DSC
  - ICP-MS measurements of Pb
  - Investigations on pellet cross section by SEM-EDS
    - Sample preparation under evaluation





# Overview of the R&D efforts in AdP2015-2017



|                         | Core Physics     |                 |                     |          |        |           | Component specific or phenomenon specific |                      |           |        |  |                                   | System |                             |           |               |          |        |
|-------------------------|------------------|-----------------|---------------------|----------|--------|-----------|---|----------------------|-----------|--------|--|-----------------------------------|--------|-----------------------------|-----------|---------------|----------|--------|
|                         | X-sec generation | Reactor Physics | Burn-up Calculation | 3D NK    | 3D NK  | Shielding | FPC                                       | TH lumped parameters | CFD       |        |  | Fission product dispersion & dose | TM     | Material molecular dynamics | SYS-TH    | SYS-TH        | SYS-TH   | SA     |
| <i>pellet</i>           | SERPENT          | SERPENT         | SERPENT             |          |        |           | Transuranus                               |                      |           |        |  |                                   |        |                             | RELAP5-3D | RELAP5/Mod3.3 | CATHARE2 | SIMMER |
| <i>gap</i>              |                  |                 |                     |          |        |           |   |                      |           |        |  |                                   |        |                             |           |               |          |        |
| <i>cladding</i>         |                  |                 |                     |          |        |           |   |                      |           |        |  |                                   |        |                             |           |               |          |        |
| <i>subchannel</i>       |                  |                 |                     |          |        |           |   |                      |           |        |  |                                   |        |                             |           |               |          |        |
| <i>fuel assembly</i>    |                  |                 |                     |          |        |           |   |                      |           |        |  |                                   |        |                             |           |               |          |        |
| <i>core</i>             |                  |                 |                     | FRENETIC | SIMMER |           | FRENETIC                                  | COMSOL               | FEM-LCORE | FLUENT |  |                                   |        |                             |           |               |          |        |
| <i>coolant</i>          |                  |                 |                     |          |        |           |   |                      |           |        |  | SIMMER                            |        | CALPHAD                     |           |               |          |        |
| <i>primary system</i>   |                  |                 |                     |          |        |           |   |                      |           |        |  |                                   |        |                             |           |               |          |        |
| <i>secondary system</i> |                  |                 |                     |          |        |           |   |                      |           |        |  |                                   |        |                             |           |               |          |        |
| <i>containment</i>      |                  |                 |                     |          |        |           |   |                      |           |        |  |                                   |        |                             |           |               |          |        |
| <i>I&amp;C</i>          |                  |                 |                     |          |        |           |   |                      |           |        |  |                                   |        |                             |           |               |          |        |
| <i>site</i>             |                  |                 |                     |          |        |           |   |                      |           |        |  |                                   |        |                             |           |               |          |        |

|                                    |    |
|------------------------------------|----|
| Design and Licensing               |    |
| Design (including safety analysis) |    |
| Code Coupling                      | ↔  |
| Chain of Code                      | ⋯→ |
| Uncertainty                        |    |

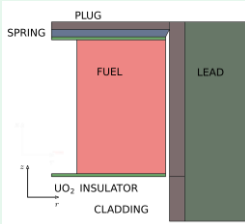
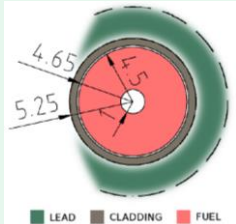
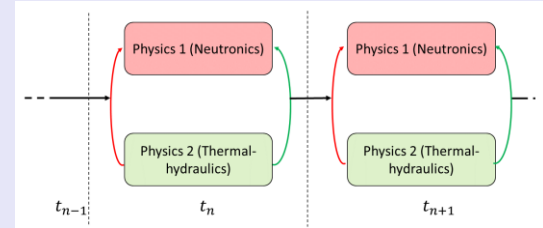
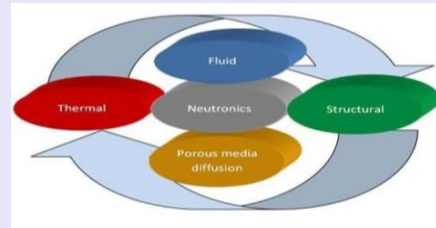
# Multi-physics code for LFR [1-4]



Implicit multi-physics approach for studying the LFR single-channel (average conditions)

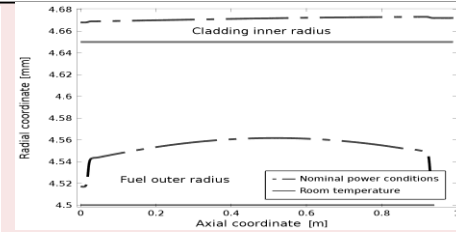
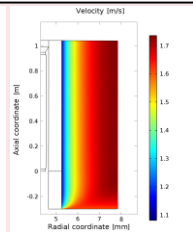
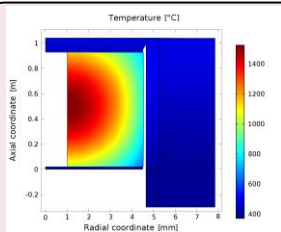
**Multiphysics** for:

- . **Deeper** physics insight
- . **Better** reactor paramter **evaluation**
- . **Verification** of operational constraint
- . **Combined analysis** with system codes



## LFR single-channel test – COMSOL tool

| Physics            | Modelling approach            |
|--------------------|-------------------------------|
| Neutronics         | Multi-group neutron diffusion |
| Thermal-hydraulics | CFD                           |
| Mechanics          | Linear elasticity             |



## Results and conclusion

- . **Good representation** of physical phenomena occurring in the reactor
- . **Evaluation** of coupling approaches
- . Near-term efforts on **OpenFOAM**



# Overview of the R&D efforts in AdP2015-2017



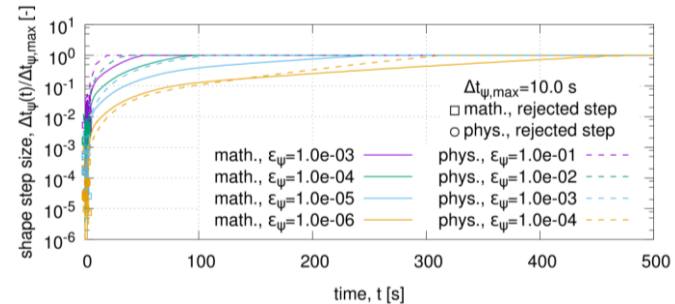
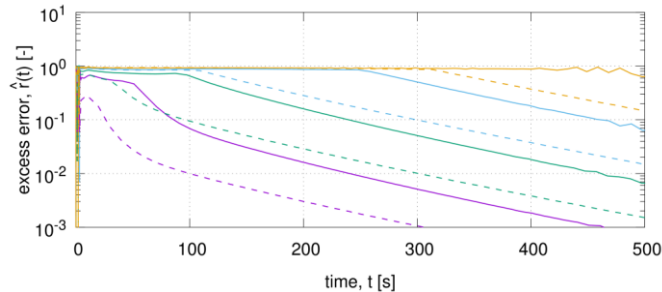
|                         | Core Physics     |                 |                     |       |        |           | Component specific or phenomenon specific |                      |        |           |        |                                   | System  |                             |               |          |        |    |
|-------------------------|------------------|-----------------|---------------------|-------|--------|-----------|---|----------------------|--------|-----------|--------|-----------------------------------|---------|-----------------------------|---------------|----------|--------|----|
|                         | X-sec generation | Reactor Physics | Burn-up Calculation | 3D NK | 3D NK  | Shielding | FPC                                       | TH lumped parameters | CFD    |           |        | Fission product dispersion & dose | TM      | Material molecular dynamics | SYS-TH        | SYS-TH   | SYS-TH | SA |
| <i>pellet</i>           | SERPENT          | SERPENT         | SERPENT             | 1-5   | SIMMER |           | Transuranus                               | 1-5                  | COMSOL | FEM-LCORE | FLUENT | SIMMER                            | CALPHAD | RELAP5-3D                   | RELAP5/Mod3.3 | CATHARE2 | SIMMER |    |
| <i>gap</i>              |                  |                 |                     |       |        |           |   |                      |        |           |        |                                   |         |                             |               |          |        |    |
| <i>cladding</i>         |                  |                 |                     |       |        |           |   |                      |        |           |        |                                   |         |                             |               |          |        |    |
| <i>subchannel</i>       |                  |                 |                     |       |        |           |   |                      |        |           |        |                                   |         |                             |               |          |        |    |
| <i>fuel assembly</i>    |                  |                 |                     |       |        |           |   |                      |        |           |        |                                   |         |                             |               |          |        |    |
| <i>core</i>             |                  |                 |                     |       |        |           |   |                      |        |           |        |                                   |         |                             |               |          |        |    |
| <i>coolant</i>          |                  |                 |                     |       |        |           |   |                      |        |           |        |                                   |         |                             |               |          |        |    |
| <i>primary system</i>   |                  |                 |                     |       |        |           |   |                      |        |           |        |                                   |         |                             |               |          |        |    |
| <i>secondary system</i> |                  |                 |                     |       |        |           |   |                      |        |           |        |                                   |         |                             |               |          |        |    |
| <i>containment</i>      |                  |                 |                     |       |        |           |   |                      |        |           |        |                                   |         |                             |               |          |        |    |
| <i>I&amp;C</i>          |                  |                 |                     |       |        |           |   |                      |        |           |        |                                   |         |                             |               |          |        |    |
| <i>site</i>             |                  |                 |                     |       |        |           |   |                      |        |           |        |                                   |         |                             |               |          |        |    |

|                                    |    |
|------------------------------------|----|
| Design and Licensing               |    |
| Design (including safety analysis) |    |
| Code Coupling                      | ↔  |
| Chain of Code                      | ⋯→ |
| Uncertainty                        |    |

## R&D on FRENETIC quasi-static time step adaptiveness

- ❑ **Approach:** to monitor and to control the variation of the local error of the shape during the integration algorithm.
- ❑ Step size relation 
$$\frac{\Delta t_{\psi,n}}{\Delta t_{\psi,n-1}} = \left( \frac{1}{\hat{r}_n} \right)^{1/(q+1)}$$
- ❑ Excess local error estimated according to an appropriate definition



- Excess error: in absence of artificial limitations, maintained close to unity
- Time step: expansion or contraction as appropriate for the current conditions of the transient

# Overview of the R&D efforts in AdP2015-2017



|                                    | Core Physics     |                 |                     |       |       |           | Component specific or phenomenon specific |                      |        |  |  |                                   | System  |                             |        |        |        |    |  |  |  |  |
|------------------------------------|------------------|-----------------|---------------------|-------|-------|-----------|---|----------------------|--------|--|--|-----------------------------------|---------|-----------------------------|--------|--------|--------|----|--|--|--|--|
|                                    | X-sec generation | Reactor Physics | Burn-up Calculation | 3D NK | 3D NK | Shielding | FPC                                       | TH lumped parameters | CFD    |  |  | Fission product dispersion & dose | TM      | Material molecular dynamics | SYS-TH | SYS-TH | SYS-TH | SA |  |  |  |  |
| <i>pellet</i>                      | SERPENT          | SERPENT         | SERPENT             |       |       |           | Transuranus                               |                      |        |  |  |                                   |         |                             |        |        |        |    |  |  |  |  |
| <i>gap</i>                         |                  |                 |                     |       |       |           |   |                      |        |  |  |                                   |         |                             |        |        |        |    |  |  |  |  |
| <i>cladding</i>                    |                  |                 |                     |       |       |           |   |                      |        |  |  |                                   |         |                             |        |        |        |    |  |  |  |  |
| <i>subchannel</i>                  |                  |                 |                     |       |       |           |   |                      |        |  |  |                                   |         |                             |        |        |        |    |  |  |  |  |
| <i>fuel assembly</i>               |                  |                 |                     |       |       |           |   |                      |        |  |  |                                   |         |                             |        |        |        |    |  |  |  |  |
| <i>core</i>                        |                  |                 |                     |       |       |           |   | FRENETIC             | SIMMER |  |  | FRENETIC                          | COMSOL  | FEM-LCORE                   | FLUENT | 1-6    |        |    |  |  |  |  |
| <i>coolant</i>                     |                  |                 |                     |       |       |           |   |                      |        |  |  | SIMMER                            | CALPHAD |                             |        |        |        |    |  |  |  |  |
| <i>primary system</i>              |                  |                 |                     |       |       |           |   |                      |        |  |  |                                   |         |                             |        |        |        |    |  |  |  |  |
| <i>secondary system</i>            |                  |                 |                     |       |       |           |   |                      |        |  |  |                                   |         |                             |        |        |        |    |  |  |  |  |
| <i>containment</i>                 |                  |                 |                     |       |       |           |   |                      |        |  |  |                                   |         |                             |        |        |        |    |  |  |  |  |
| <i>I&amp;C</i>                     |                  |                 |                     |       |       |           |   |                      |        |  |  |                                   |         |                             |        |        |        |    |  |  |  |  |
| <i>site</i>                        |                  |                 |                     |       |       |           |   |                      |        |  |  |                                   |         |                             |        |        |        |    |  |  |  |  |
| Design and Licensing               |                  |                 |                     |       |       |           |   |                      |        |  |  |                                   |         |                             |        |        |        |    |  |  |  |  |
| Design (including safety analysis) |                  |                 |                     |       |       |           |   |                      |        |  |  |                                   |         |                             |        |        |        |    |  |  |  |  |
| Code Coupling                      | ↔                |                 |                     |       |       |           |   |                      |        |  |  |                                   |         |                             |        |        |        |    |  |  |  |  |
| Chain of Code                      | ⋯→               |                 |                     |       |       |           |   |                      |        |  |  |                                   |         |                             |        |        |        |    |  |  |  |  |
| Uncertainty                        |                  |                 |                     |       |       |           |   |                      |        |  |  |                                   |         |                             |        |        |        |    |  |  |  |  |

# SYS/TH – CFD code coupling [1-6]



## RELAP5/Mod3.3 – Fluent coupling codes to CIRCE-HERO

**RELAP5 domain:** 2 pipes for water side + inner tube solid structure

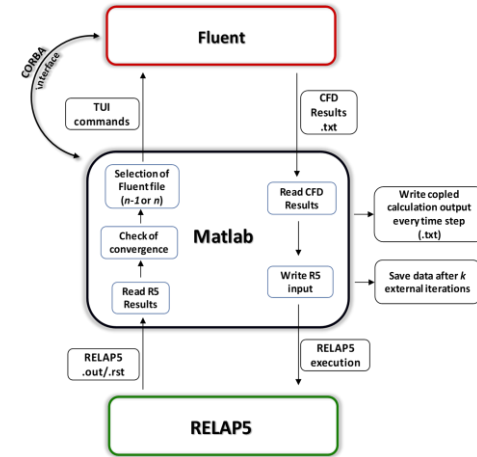
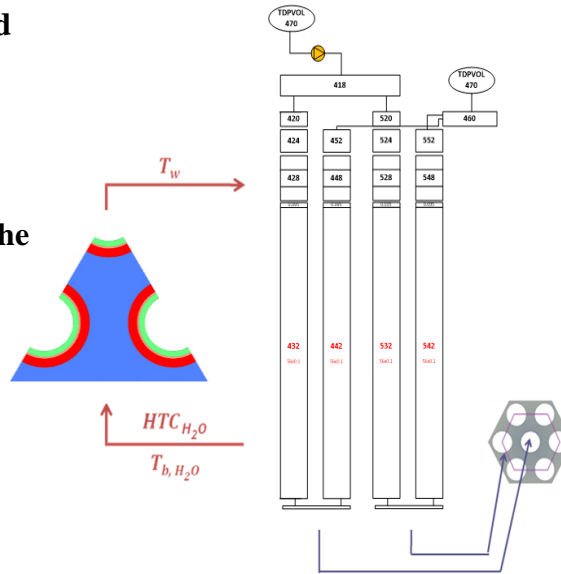
- one representative of central tube
- one representative of 6 external tubes

**CFD domain:** LBE side + annulus solid structures (1/6 of the transversal section)

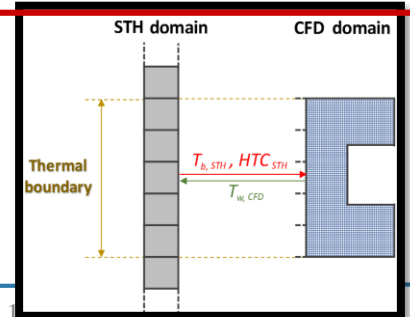
- In **blue** the LBE domain
- In **red** the AISI304 tube in contact with LBE
- In **green** the AISI304 tube in contact with H<sub>2</sub>O
- In **orange** the AISI316 powder in between the tubes

Data are exchanged at the interface of water tubes

The wall temperature (calculated by the CFD code) is given to the STH code as BC, the STH code gives to the CFD code the bulk temperature and the heat transfer coefficient (calculated in the STH side)



Coupling logic managed by Matlab software

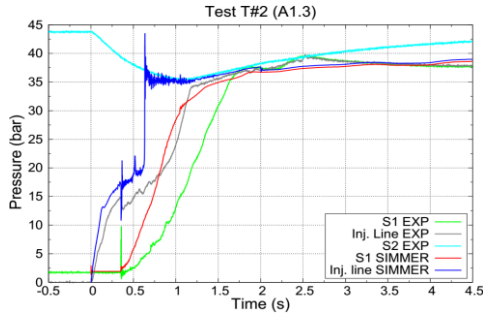


# SIMMER-III code validation [1-6]

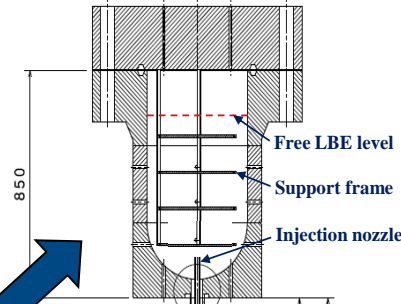
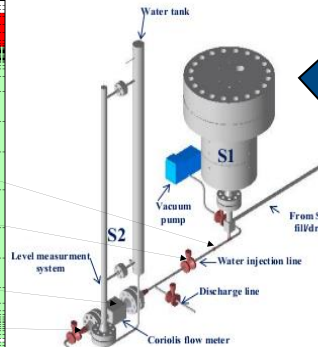
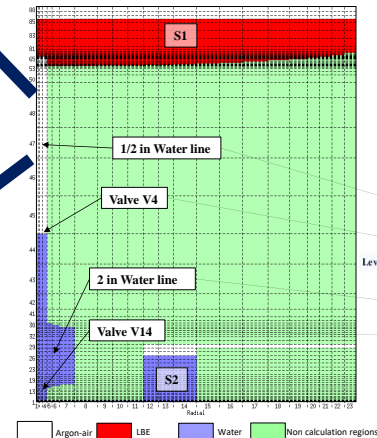


## SIMMER-III validation on LIFUS5/Mod2 data

## LIFUS5/Mod2 S1 interaction vessel



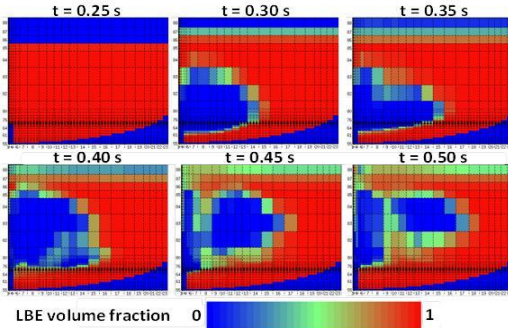
## SIMMER-III model



## LIFUS5/Mod2 facility

## LIFUS5/Mod2 injector cap

## SIMMER-III results: pressure trends



## SIMMER-III results: Steam bubble formation



# Overview of the R&D efforts in AdP2015-2017



|                         | Core Physics     |                 |                     |        |       |           | Component specific or phenomenon specific |                      |        |        |  |                                   | System |                             |           |               |          |        |
|-------------------------|------------------|-----------------|---------------------|--------|-------|-----------|---|----------------------|--------|--------|--|-----------------------------------|--------|-----------------------------|-----------|---------------|----------|--------|
|                         | X-sec generation | Reactor Physics | Burn-up Calculation | 3D NK  | 3D NK | Shielding | FPC                                       | TH lumped parameters | CFD    |        |  | Fission product dispersion & dose | TM     | Material molecular dynamics | SYS-TH    | SYS-TH        | SYS-TH   | SA     |
| <i>pellet</i>           | SERPENT          | SERPENT         | SERPENT             |        |       |           | Transuranus                               |                      |        |        |  |                                   |        |                             | RELAP5-3D | RELAP5/Mod3.3 | CATHARE2 | SIMMER |
| <i>gap</i>              |                  |                 |                     |        |       |           |   |                      |        |        |  |                                   |        |                             |           |               |          |        |
| <i>cladding</i>         |                  |                 |                     |        |       |           |   |                      |        |        |  |                                   |        |                             |           |               |          |        |
| <i>subchannel</i>       |                  |                 |                     |        |       |           |   |                      |        |        |  |                                   |        |                             |           |               |          |        |
| <i>fuel assembly</i>    |                  |                 |                     |        |       |           |   |                      |        |        |  |                                   |        |                             |           |               |          |        |
| <i>core</i>             |                  |                 | FRENETIC            | SIMMER |       | FRENETIC  | COMSOL                                    | FEM-LCORE            | FLUENT |        |  |                                   |        |                             |           |               |          |        |
| <i>coolant</i>          |                  |                 |                     |        |       |           |   |                      |        | SIMMER |  | CALPHAD                           |        |                             |           |               |          |        |
| <i>primary system</i>   |                  |                 |                     |        |       |           |   |                      |        |        |  |                                   |        |                             |           |               |          |        |
| <i>secondary system</i> |                  |                 |                     |        |       |           |   |                      |        |        |  |                                   |        |                             |           |               |          |        |
| <i>containment</i>      |                  |                 |                     |        |       |           |   |                      |        |        |  |                                   |        |                             |           |               |          |        |
| <i>I&amp;C</i>          |                  |                 |                     |        |       |           |   |                      |        |        |  |                                   |        |                             |           |               |          |        |
| <i>site</i>             |                  |                 |                     |        |       |           |   |                      |        |        |  |                                   |        |                             |           |               |          |        |

|                                    |    |
|------------------------------------|----|
| Design and Licensing               |    |
| Design (including safety analysis) |    |
| Code Coupling                      | ↔  |
| Chain of Code                      | ⋯→ |
| Uncertainty                        |    |



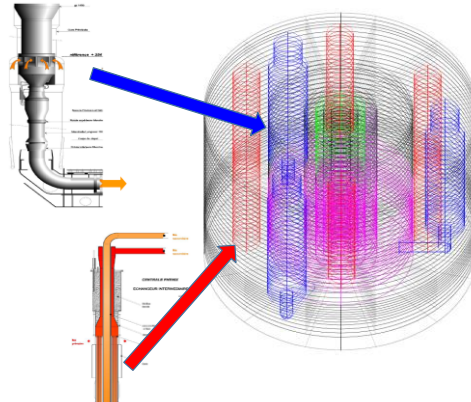
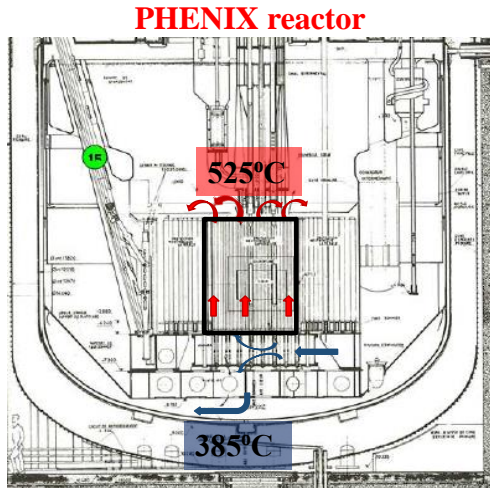
# REALP5-3D independent assessment [1-7]



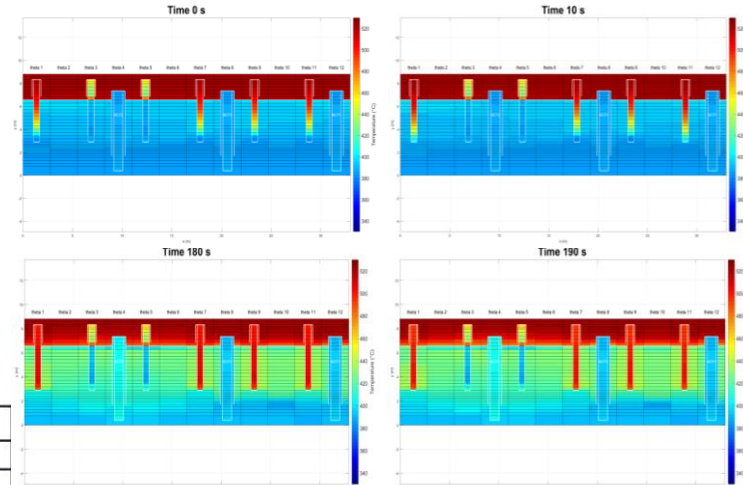
## APPLICATION OF RELAP3D ON PHENIX EXPERIMENTAL TEST

- Framework. Application of SYS-TH to Gen. IV reactors. Synergy with H2020 SESAME Project
- Objectives. 1) Assessment of RELAP5, 2) Application of RELAP5 to nuclear reactor scale test, 3) Enhancing the experience of using SYS-TH to LM FR, 4) Mastering the code limitations and developing modelling approaches, 5) Availability of numerical tool for supporting design and safety analysis, 6) Developing reliable approaches for SYS analysis of new gen. FR systems, including coupling

### 3D model of PHENIX reactor by RELAP5-3D



| # | QUANTITY                         | Value |
|---|----------------------------------|-------|
| 1 | # of HYDR volumes                | 7492  |
| 2 | # of HYDR junctions              | 12419 |
| 3 | # of HEAT structures             | 8100  |
| 4 | # of HEAT structures mesh points | 45054 |



**RELAP5-3D results: pool temperature distribution**

# Overview of the R&D efforts in AdP2015-2017



|                                    | Core Physics     |                 |                     |          |        |           | Component specific or phenomenon specific |                      |        |           |        |                                   | System |                             |           |               |          |        |  |  |  |  |
|------------------------------------|------------------|-----------------|---------------------|----------|--------|-----------|---|----------------------|--------|-----------|--------|-----------------------------------|--------|-----------------------------|-----------|---------------|----------|--------|--|--|--|--|
|                                    | X-sec generation | Reactor Physics | Burn-up Calculation | 3D NK    | 3D NK  | Shielding | FPC                                       | TH lumped parameters | CFD    |           |        | Fission product dispersion & dose | TM     | Material molecular dynamics | SYS-TH    | SYS-TH        | SYS-TH   | SA     |  |  |  |  |
| <i>pellet</i>                      | SERPENT          | SERPENT         | SERPENT             |          |        |           | Transuranus                               |                      |        |           |        |                                   |        |                             |           |               |          |        |  |  |  |  |
| <i>gap</i>                         |                  |                 |                     |          |        |           |   |                      |        |           |        |                                   |        |                             |           |               |          |        |  |  |  |  |
| <i>cladding</i>                    |                  |                 |                     |          |        |           |   |                      |        |           |        |                                   |        |                             |           |               |          |        |  |  |  |  |
| <i>subchannel</i>                  |                  |                 |                     |          |        |           |   |                      |        |           |        |                                   |        |                             |           |               |          |        |  |  |  |  |
| <i>fuel assembly</i>               |                  |                 |                     |          |        |           |   |                      |        |           |        |                                   |        |                             |           |               |          |        |  |  |  |  |
| <i>core</i>                        |                  |                 |                     | FRENETIC | SIMMER |           |   | FRENETIC             | COMSOL | FEM-LCORE | FLUENT |                                   |        |                             | RELAP5-3D | RELAP5/Mod3.3 | CATHARE2 | SIMMER |  |  |  |  |
| <i>coolant</i>                     |                  |                 |                     |          |        |           |   |                      |        |           |        | SIMMER                            |        | CALPHAD                     |           |               |          |        |  |  |  |  |
| <i>primary system</i>              |                  |                 |                     |          |        |           |   |                      |        |           |        |                                   |        |                             |           |               |          |        |  |  |  |  |
| <i>secondary system</i>            |                  |                 |                     |          |        |           |   |                      |        |           |        |                                   |        |                             |           |               |          |        |  |  |  |  |
| <i>containment</i>                 |                  |                 |                     |          |        |           |   |                      |        |           |        |                                   |        |                             |           |               |          |        |  |  |  |  |
| <i>I&amp;C</i>                     |                  |                 |                     |          |        |           |   |                      |        |           |        |                                   |        |                             |           |               |          |        |  |  |  |  |
| <i>site</i>                        |                  |                 |                     |          |        |           |   |                      |        |           |        |                                   |        |                             |           |               |          |        |  |  |  |  |
| Design and Licensing               |                  |                 |                     |          |        |           |   |                      |        |           |        |                                   |        |                             |           |               |          |        |  |  |  |  |
| Design (including safety analysis) |                  |                 |                     |          |        |           |   |                      |        |           |        |                                   |        |                             |           |               |          |        |  |  |  |  |
| Code Coupling                      | ↔                |                 |                     |          |        |           |   |                      |        |           |        |                                   |        |                             |           |               |          |        |  |  |  |  |
| Chain of Code                      | ⋯→               |                 |                     |          |        |           |   |                      |        |           |        |                                   |        |                             |           |               |          |        |  |  |  |  |
| Uncertainty                        |                  |                 |                     |          |        |           |   |                      |        |           |        |                                   |        |                             |           |               |          |        |  |  |  |  |

1-8



# Overview of the R&D efforts in AdP2015-2017



|                         | Core Physics     |                 |                     |        |       |           | Component specific or phenomenon specific |                      |        |  |        |                                   | System |                             |           |               |          |        |
|-------------------------|------------------|-----------------|---------------------|--------|-------|-----------|---|----------------------|--------|--|--------|-----------------------------------|--------|-----------------------------|-----------|---------------|----------|--------|
|                         | X-sec generation | Reactor Physics | Burn-up Calculation | 3D NK  | 3D NK | Shielding | FPC                                       | TH lumped parameters | CFD    |  |        | Fission product dispersion & dose | TM     | Material molecular dynamics | SYS-TH    | SYS-TH        | SYS-TH   | SA     |
| <i>pellet</i>           | SERPENT          | SERPENT         | SERPENT             |        |       |           | Transuranus                               |                      |        |  |        |                                   |        |                             | RELAP5-3D | RELAP5/Mod3.3 | CATHARE2 | SIMMER |
| <i>gap</i>              |                  |                 |                     |        |       |           |   |                      |        |  |        |                                   |        |                             |           |               |          |        |
| <i>cladding</i>         |                  |                 |                     |        |       |           |   |                      |        |  |        |                                   |        |                             |           |               |          |        |
| <i>subchannel</i>       |                  |                 |                     |        |       |           |   |                      |        |  |        |                                   |        |                             |           |               |          |        |
| <i>fuel assembly</i>    |                  |                 |                     |        |       |           |   |                      |        |  |        |                                   |        |                             |           |               |          |        |
| <i>core</i>             |                  |                 | FRENETIC            | SIMMER |       | FRENETIC  | COMSOL                                    | FEM-LCORE            | FLUENT |  |        |                                   |        |                             |           |               |          |        |
| <i>coolant</i>          |                  |                 |                     |        |       |           |   |                      |        |  | SIMMER | CALPHAD                           |        |                             |           |               |          |        |
| <i>primary system</i>   |                  |                 |                     |        |       |           |   |                      |        |  |        |                                   |        |                             |           |               |          |        |
| <i>secondary system</i> |                  |                 |                     |        |       |           |   |                      |        |  |        |                                   |        |                             |           |               |          |        |
| <i>containment</i>      |                  |                 |                     |        |       |           |   |                      |        |  |        |                                   |        |                             |           |               |          |        |
| <i>I&amp;C</i>          |                  |                 |                     |        |       |           |   |                      |        |  |        |                                   |        |                             |           |               |          |        |
| <i>site</i>             |                  |                 |                     |        |       |           |   |                      |        |  |        |                                   |        |                             |           |               |          |        |

Design and Licensing

Design (including safety analysis)

Code Coupling ↔

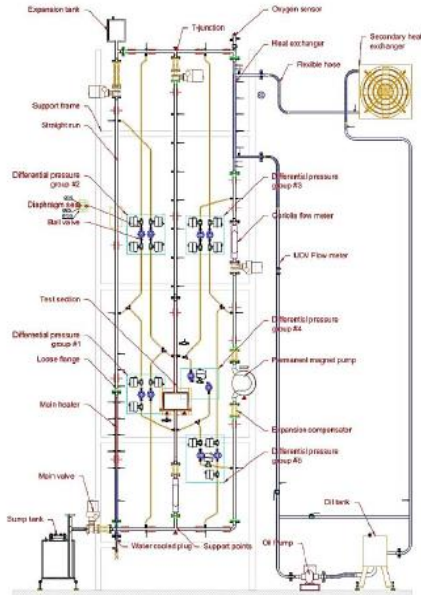
Chain of Code .....>

Uncertainty

# SYS/TH – CFD code coupling [1-9]

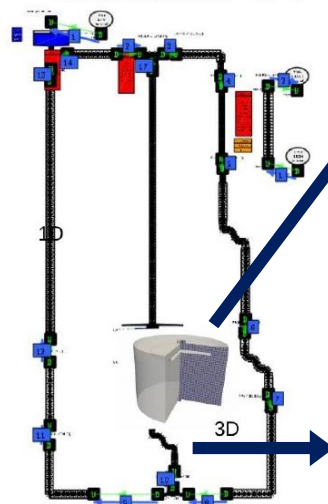


## Validation of FEM-LCORE/CATHARE coupled code by TALL-3D experimental tests

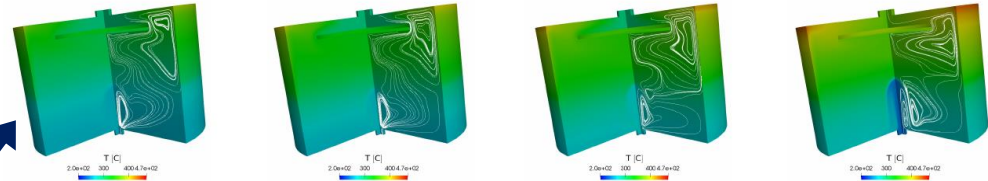


Tall-3D facility

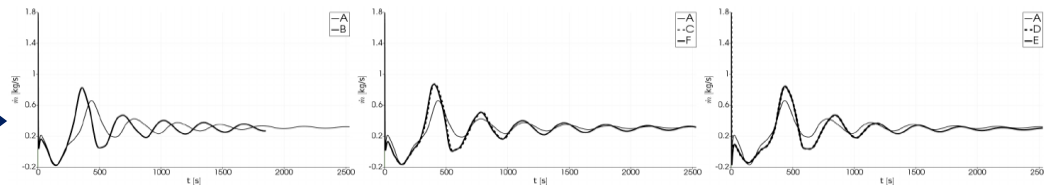
Cathare nodalization + 3D CFI



Model of Tall-3D by CATHARE2 / FEM-LCORE coupled code



Sample CFD T prediction in 3D test section



Sample mass flow rate predictions

Alessandro Del Nevo  
Alessandro.delnevo@enea.it



1101 0110 1100  
0101 0010 1101  
0001 0110 1110  
1101 0010 1101  
1111 1010 0000



POLITECNICO DI MILANO  
B 18



**POLITECNICO  
MILANO 1863**

Workshop Tematico, Accordo di Programma MiSE-ENEA, PAR2017, Progetto B.3 - LP2 (Roma, 14-15 giugno 2018)

## **Development / Assessment of models describing the inert gas behaviour in the fuel for application to the TRANSURANUS fuel pin thermo-mechanical code**

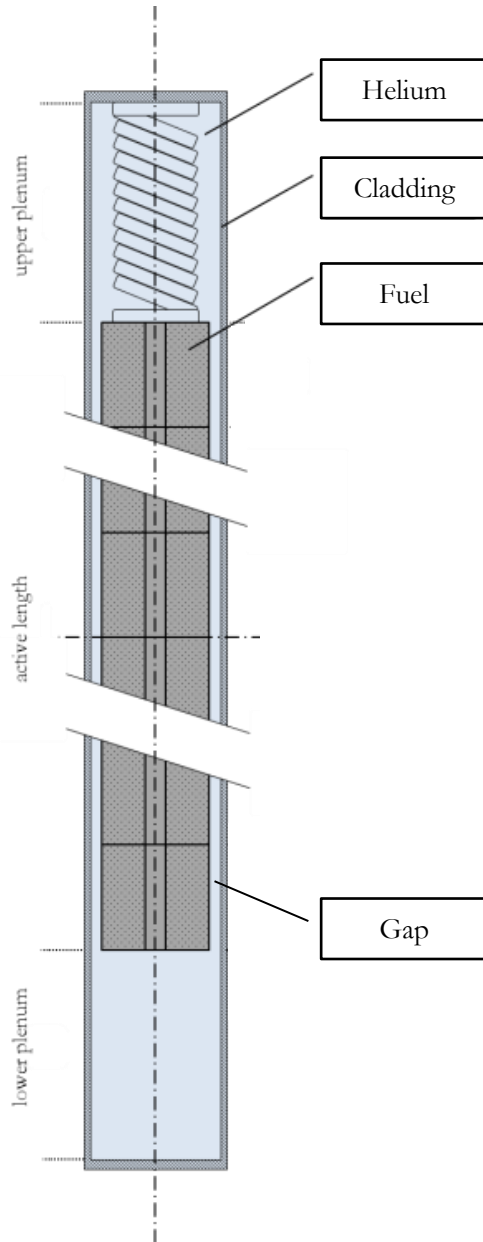
Lelio Luzzi, Tommaso Barani, Luana Cognini, Davide Pizzocri

*Politecnico di Milano, Energy Department  
CeSNEF-Nuclear Engineering Division*



**N**uclear  
**NR**actors  
**G**roup

# Fuel pin for LMFR



- Nuclear fuel pin (LMFR) is made of a stack of MOX fuel pellets wrapped in steel cladding (BOTH IMPORTANT!)
- Its performance is fundamental for **safe operation** of the reactor (and for **design & licensing** as well)



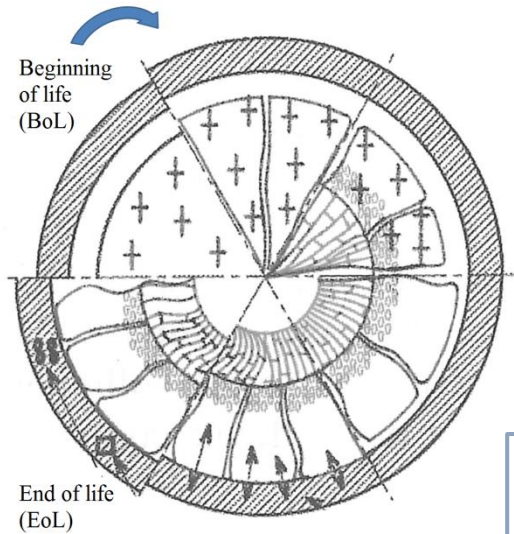
- Need of **fuel performance codes (FPCs)** and Integral Irradiation Experiments to assess the fuel pin thermo-mechanical behaviour ( $\bar{\sigma}$ ,  $\bar{\epsilon}$ ,  $\bar{u}$ , and T)



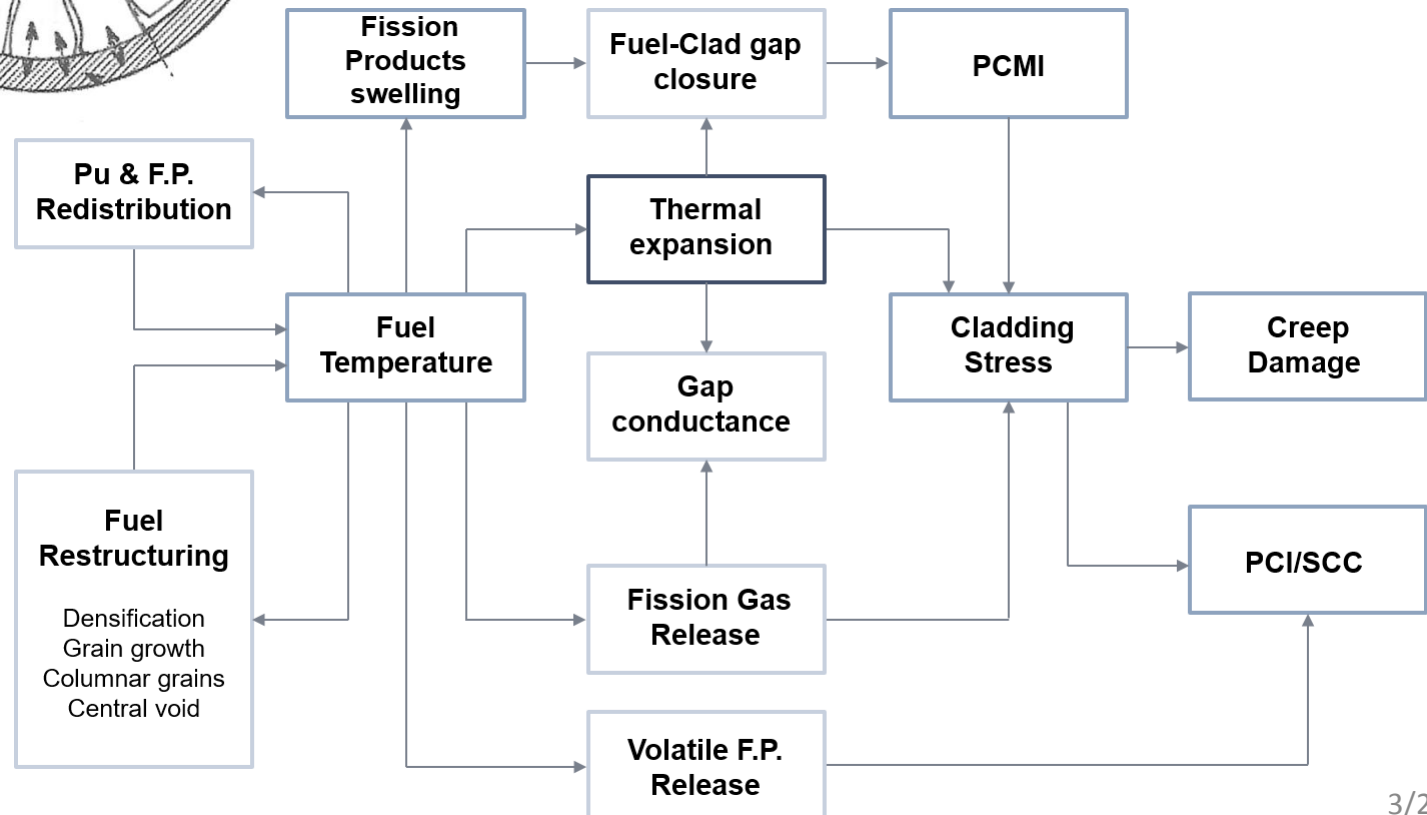
- Focus on fuel (**gaseous swelling & fission gas release**), and cladding materials as well



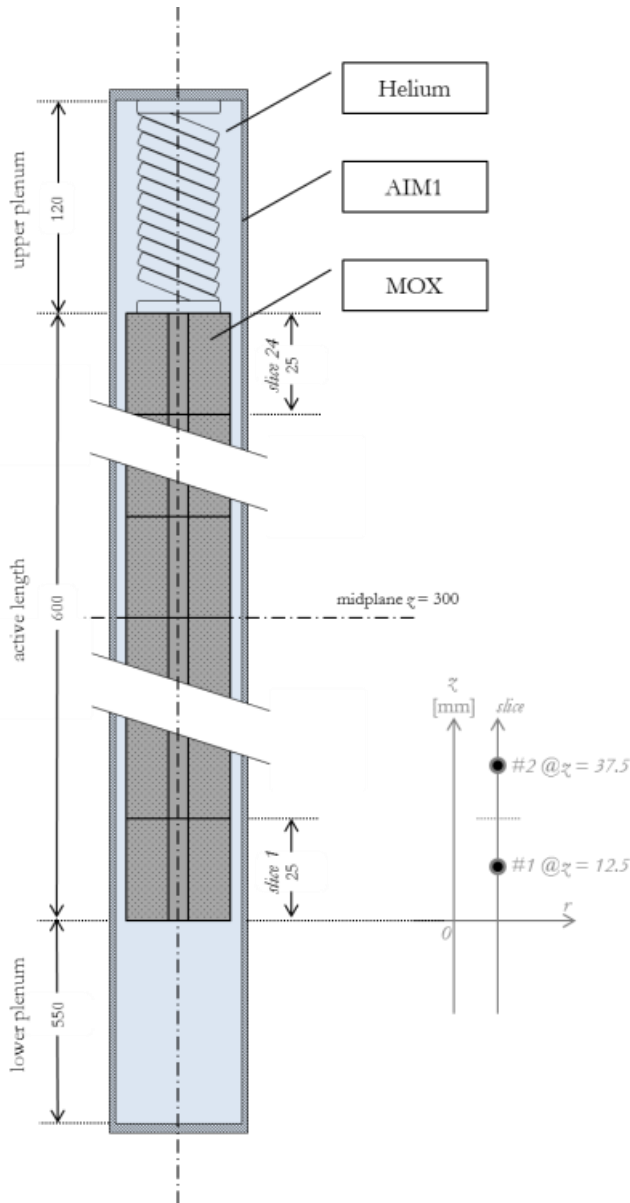
# LMFR fuel pin behaviour



Interrelationship of multiple physical phenomena featured by *different time and space scales* concerning both fuel and cladding as a "coupled system"



# TRANSURANUS code



- Thermo-mechanical code for analysing integral fuel pin behaviour under irradiation
- Developed at JRC-Karlsruhe, and extensively validated for LWRs (design & licensing)
- Fuel pin axial and radial discretization with  $1\frac{1}{2}$ -D solution of thermo-mechanics ( $\bar{\sigma}$ ,  $\bar{\epsilon}$ ,  $\bar{u}$ , and  $T$ )
- Mathematical/numerical frame into which models for the fuel pin performance of other types of reactors (Na, LBE, Pb) can be easily incorporated



v1m3j12

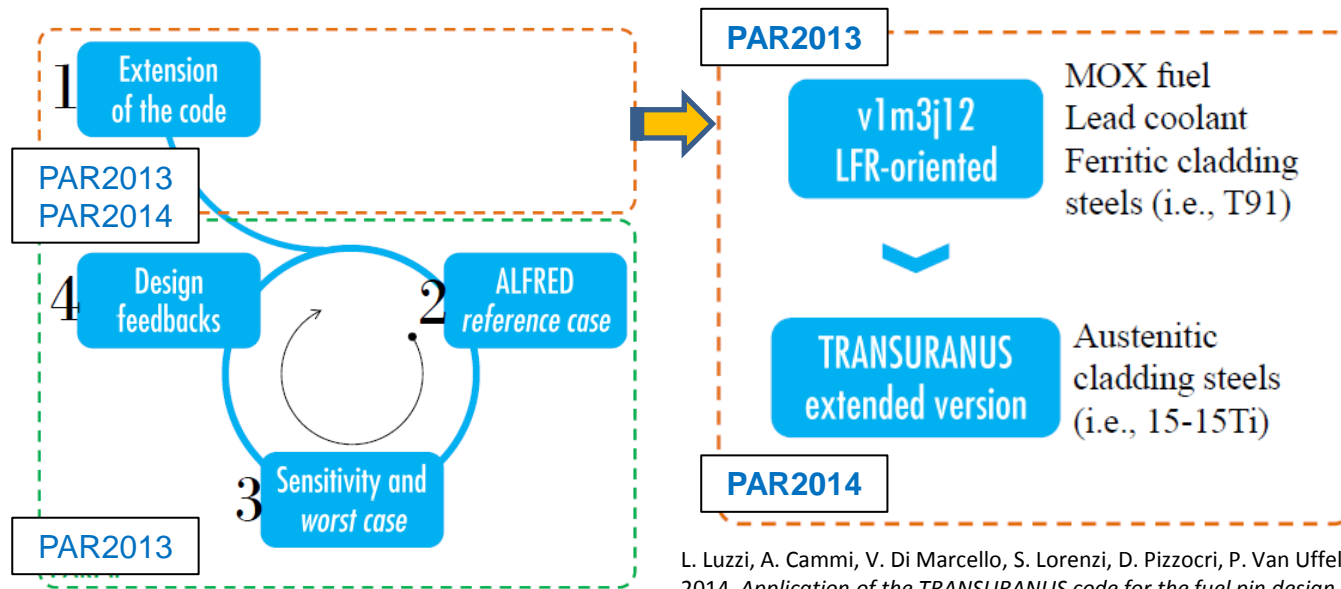


LFR-oriented

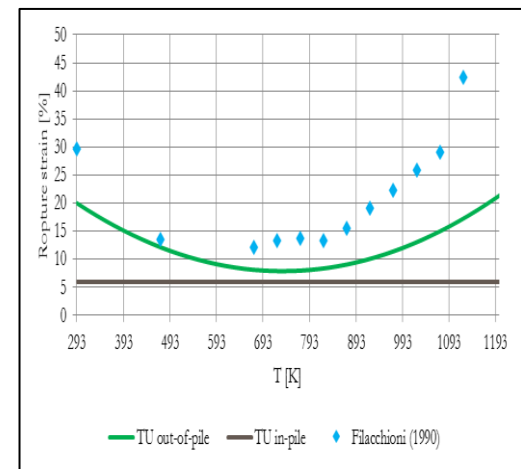
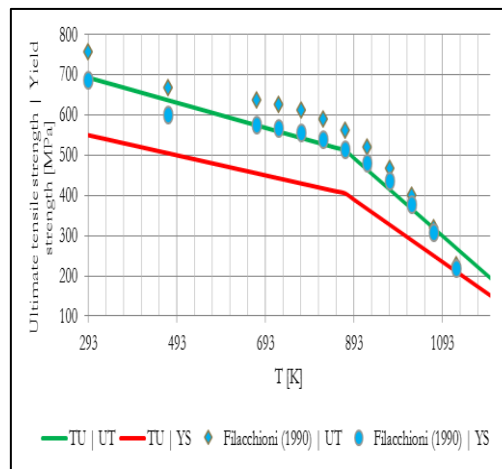
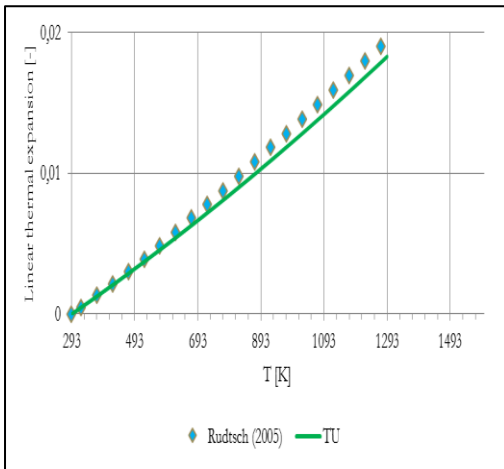


POLITECNICO  
MILANO 1863

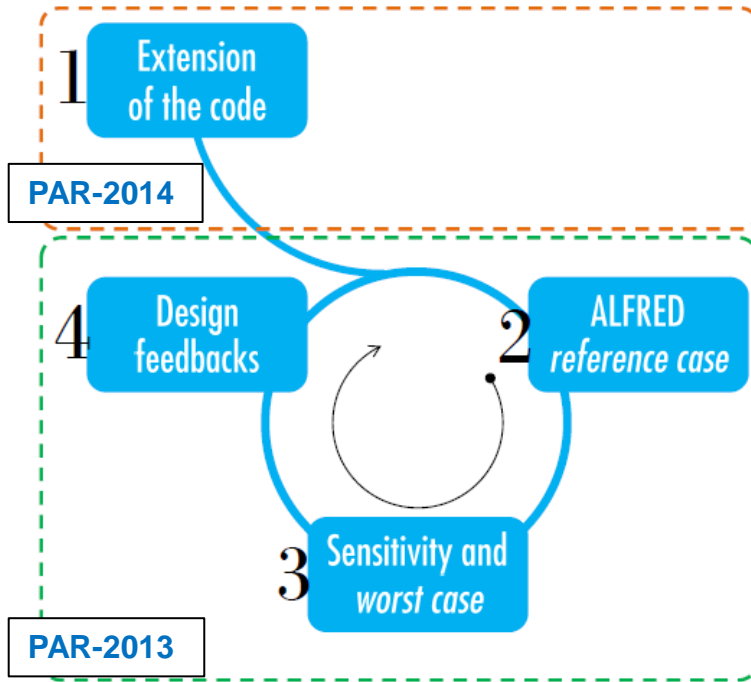
# Strategy (Fuel + Cladding models → FPC → IFPE)



L. Luzzi, A. Cammi, V. Di Marcello, S. Lorenzi, D. Pizzocri, P. Van Uffelen, 2014. *Application of the TRANSURANUS code for the fuel pin design process of the ALFRED reactor*. Nuclear Engineering and Design, 277, 173–187.



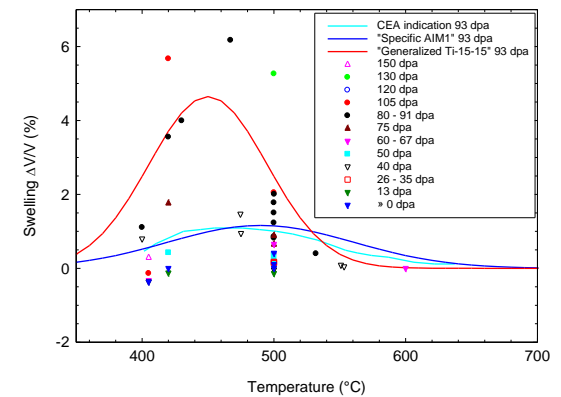
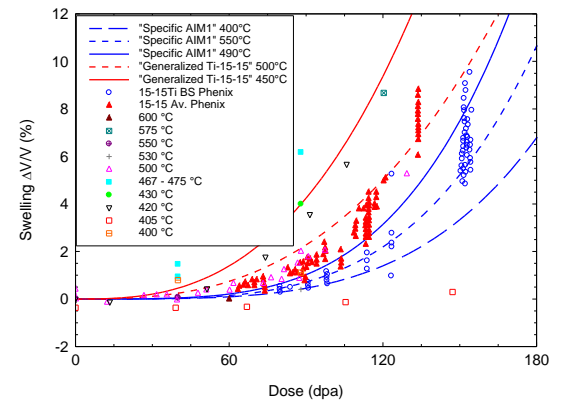
# Previous activities (PAR-2013&2014)



Critical overview of 15-15Ti physical and mechanical properties

- Cladding swelling
- Cladding creep (*ad hoc* P & LMP – CDF)

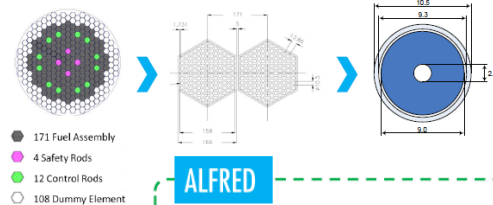
## Cladding swelling



PAR-2013

TRANSURANUS application to the ALFRED reactor

Fuel pin performance integrated in the conceptual design phase

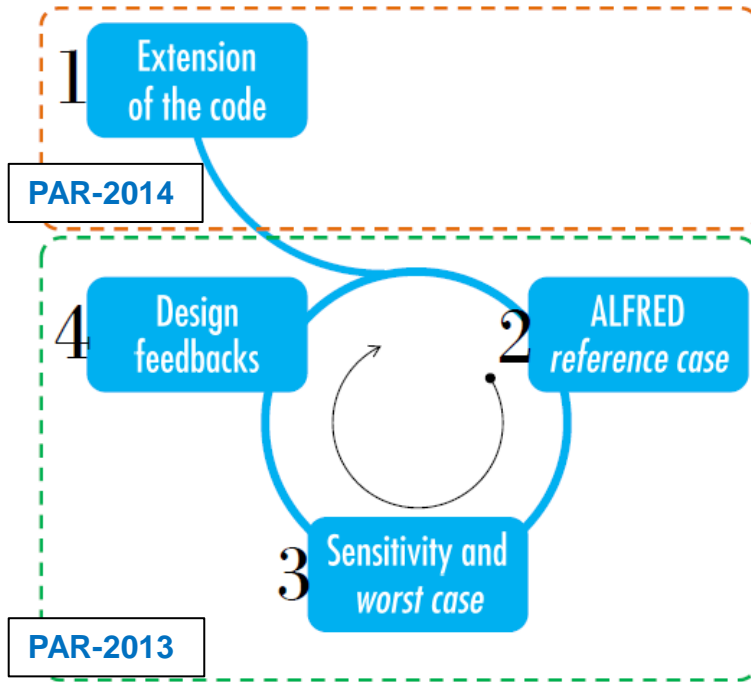


Fuel – MOX  
Cladding – 1.4970m  
Coolant – Pb

Only operative conditions have been considered: safety analysis to be performed

To reduce FCMI, neutronic design should be changed, optimizing core radial peak factor and/or core refueling scheme

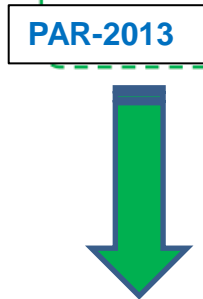
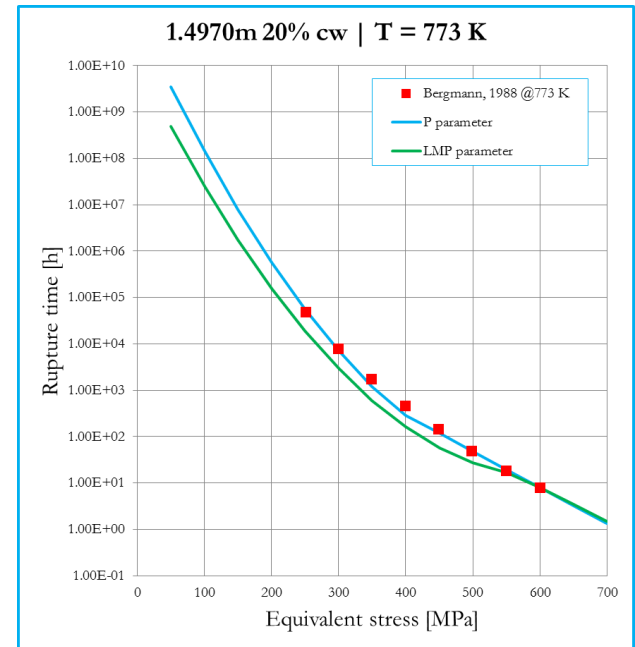
# Previous activities (PAR-2013&2014)



Critical overview of 15-15Ti physical and mechanical properties

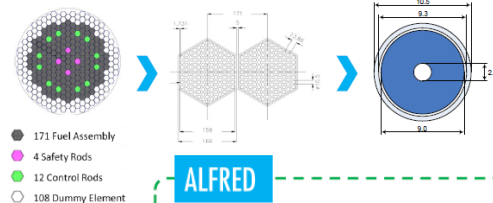
- Cladding swelling
- Cladding creep (*ad hoc* P & LMP – CDF)

## Cladding creep



TRANSURANUS application to the ALFRED reactor

Fuel pin performance integrated in the conceptual design phase



Fuel – MOX  
 Cladding – 1.4970m  
 Coolant – Pb

**ALFRED**

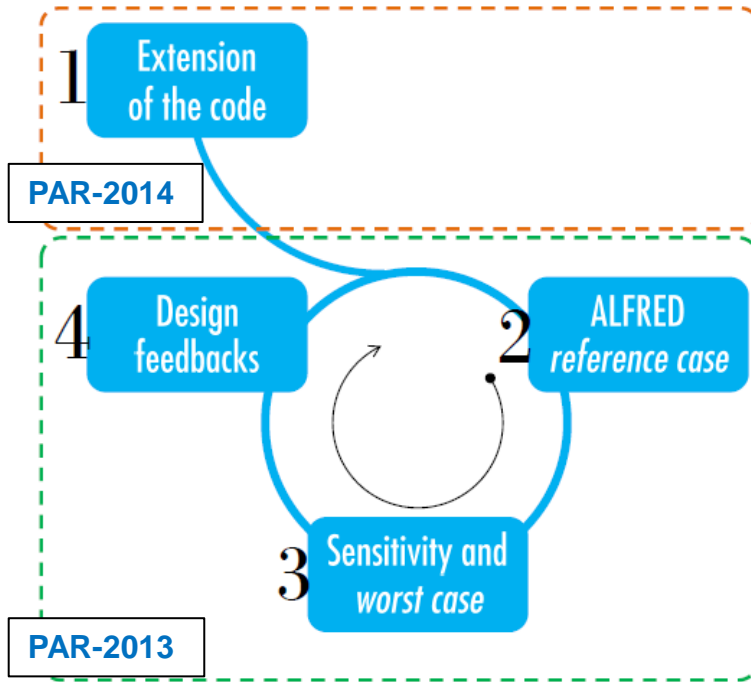
Only operative conditions have been considered: safety analysis to be performed

To reduce FCMI, neutronic design should be changed, optimizing core radial peak factor and/or core refueling scheme

$$LMP = T(C + \text{Log } t_R)$$

$$P \equiv T(C + \text{Log } \frac{t_R}{T})$$

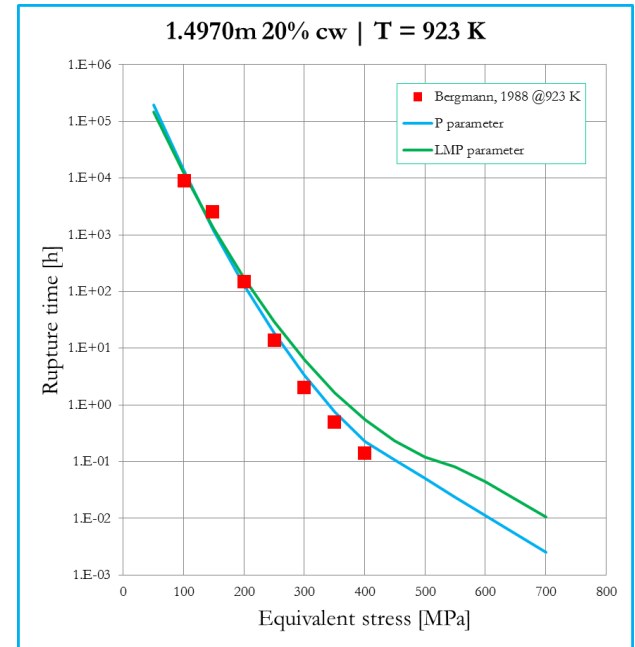
# Previous activities (PAR-2013&2014)



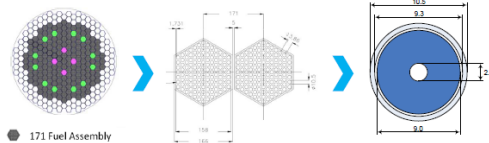
Critical overview of 15-15Ti physical and mechanical properties

- . Cladding swelling
- . Cladding creep (*ad hoc* P & LMP – CDF)

## Cladding creep



PAR-2013



Fuel – MOX  
Cladding – 1.4970m  
Coolant – Pb

### ALFRED

Only operative conditions have been considered: safety analysis to be performed

To reduce FCMI, neutronic design should be changed, optimizing core radial peak factor and/or core refueling scheme

TRANSURANUS application to the ALFRED reactor

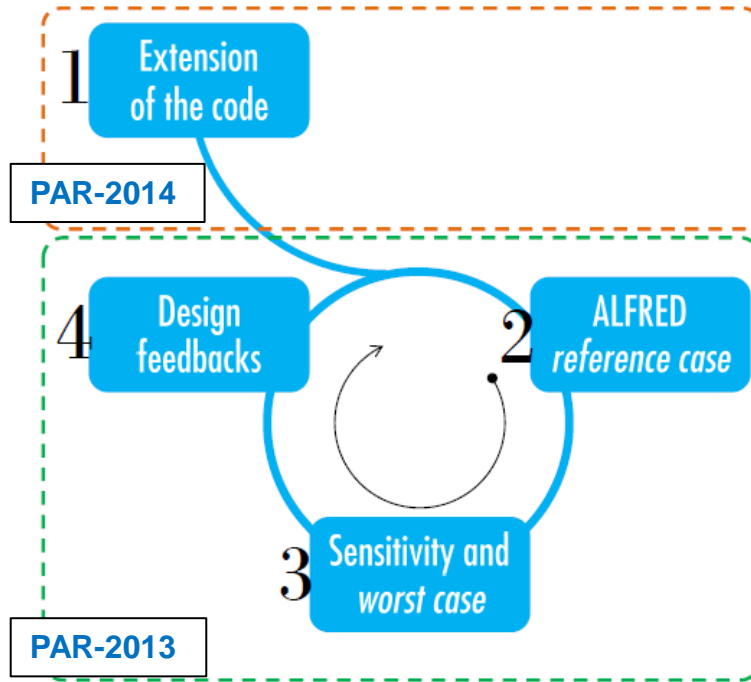
Fuel pin performance integrated in the conceptual design phase

$$LMP = T(C + \text{Log } t_R)$$



$$P \equiv T(C + \text{Log } \frac{t_R}{T})$$

# Previous activities (PAR-2013&2014) + future ...



- . Critical overview of 15-15Ti physical and mechanical properties
- . Cladding swelling
- . Cladding creep (*ad hoc* P & LMP – CDF)

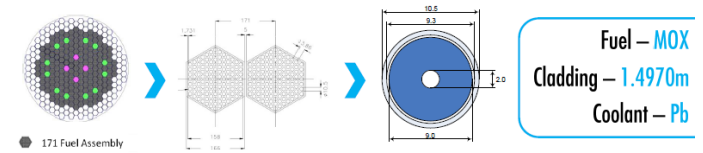
## Open issues and further developments

- . Coating selection and in-reactor qualification is still an open technological issue
- . More detailed **cladding swelling modelling** (e.g., stress dependence and coupling with creep)
- . PCMI
- . Chemical interaction
- . JOG formation
- . Cesium migration
- . Availability of in-pile data for various properties/phenomena of the cladding will be welcome



**TRANSURANUS application to the ALFRED reactor**

Fuel pin performance integrated in the **conceptual design phase**



**ALFRED**

Only operative conditions have been considered: safety analysis to be performed

To reduce FCMI, neutronic design should be changed, optimizing core radial peak factor and/or core refueling scheme

L. Luzzi, A. Cammi, V. Di Marcello, S. Lorenzi, D. Pizzocri, P. Van Uffelen, 2014. *Application of the TRANSURANUS code for the fuel pin design process of the ALFRED reactor*. Nuclear Engineering and Design, 277, 173–187.

# Extension of the code, Fuel

**Problem.** Need to improve the modelling of inert gas behaviour (IGB) in transient conditions, within fuel pin performance codes (TRANSURANUS)

- IGB modelling is fundamental for **performance & safety** (post-Fukushima) analysis of fuel pins
- IGB can represent a limiting life factor for their permanence in reactor, thus limiting the **economic** gain related to the safe operation of the fuel at extended burn-up

-  EERA-JPNM Project  
JOINT PROGRAMME ON NUCLEAR MATERIALS
- COMBATFUEL & **INSPYRE** (EC)
- ENEN+ Project (EC)
- Several **previous PARs**



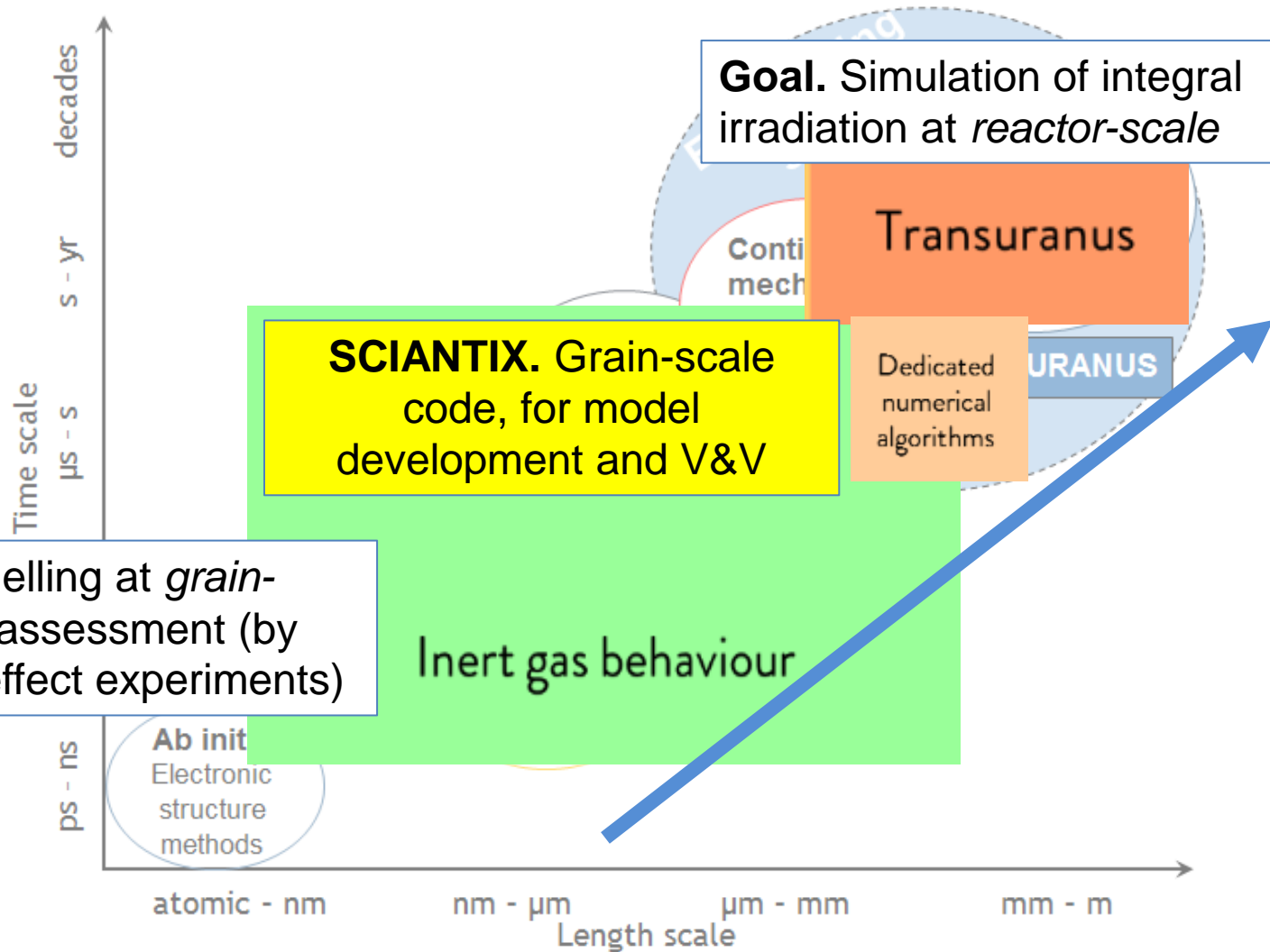


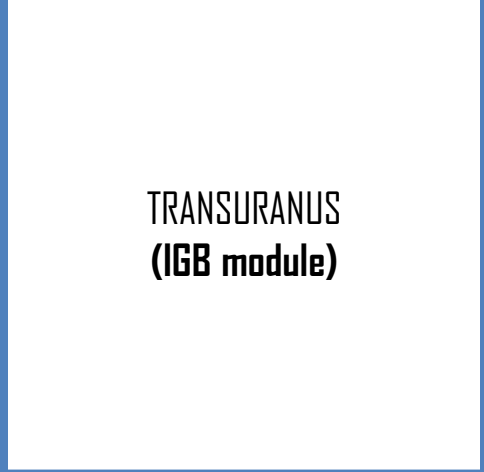
# State of the art

Modelling of inert gas behaviour is currently available in fuel performance codes (FPCs), but has **several critical limitations in transients** (and in DBAs)

- Majority of current models are **correlation-based**
  - Modelling of several phenomena is neglected
  - Generally assumed that FGR is 100% (extreme approximation for LFRs, *may be* reasonable for high temperature SFRs)
1. Intra-granular trapping and resolution are assumed in equilibrium and lumped in an *effective diffusion coefficient* ( $D_{\text{eff}}$ )
  2. Currently used algorithms for intra-granular gas diffusion can handle only simplified equations
  3. The description of helium behaviour is oversimplified
  4. Present models for IGB in the high burn-up structure (HBS) are oversimplified, usually assuming quasi-stationary conditions

# Inert gas behaviour: A multi-scale problem





**TRANSURANUS  
(IGB module)**

**Previous PARs  
on oxide fuels**



**PAR2016**

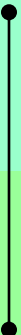


**PAR2017**

**Helium production**



**Helium diffusivity**



**Helium solubility**

**+**

**HBS formation**



**HBS porosity**

**+**

**Dedicated  
numerical  
algorithms**

**>**

**TRANSURANUS**

**TRANSURANUS  
LFR-oriented  
&  
Applications**

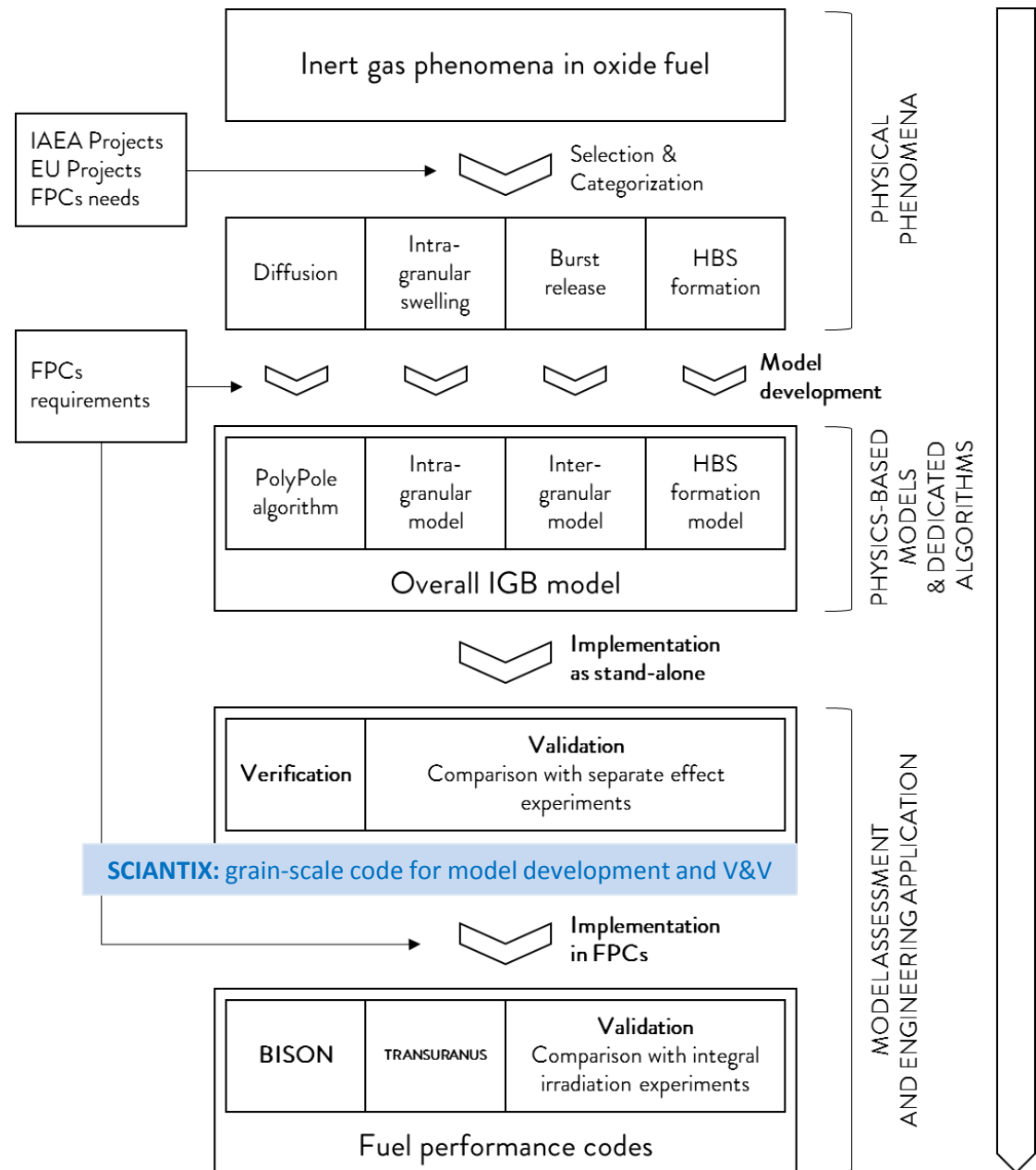
# Physics-based IGB module

- **Giovanni Pastore**

*Modelling of Fission Gas Swelling and Release in Oxide Nuclear Fuel and Application to the TRANSURANUS Code*  
**PhD thesis**, Politecnico di Milano, 2012.

- **Davide Pizzocri**

*Modelling and assessment of inert gas behaviour in UO<sub>2</sub> nuclear fuel for transient analysis*  
**PhD thesis**, Politecnico di Milano, 2018.



Previous PARs  
on **oxide fuels**

Helium production

HBS formation

TRANSURANUS  
(IGB module)

PAR2016

Helium diffusivity

HBS porosity

TRANSURANUS

PAR2017

Helium solubility

+

Dedicated  
numerical  
algorithms

>

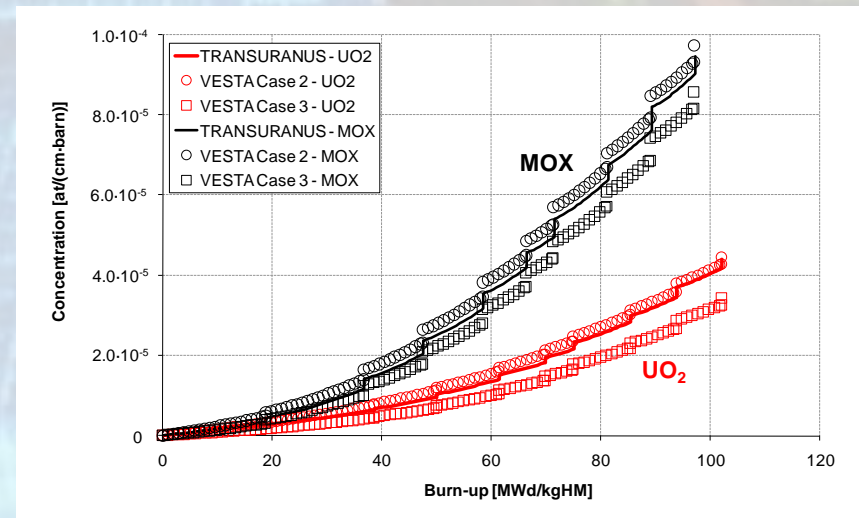
TRANSURANUS  
LFR-oriented  
&  
Applications

# The importance of being Helium

## Helium behaviour

is fundamental to assess the fuel performance

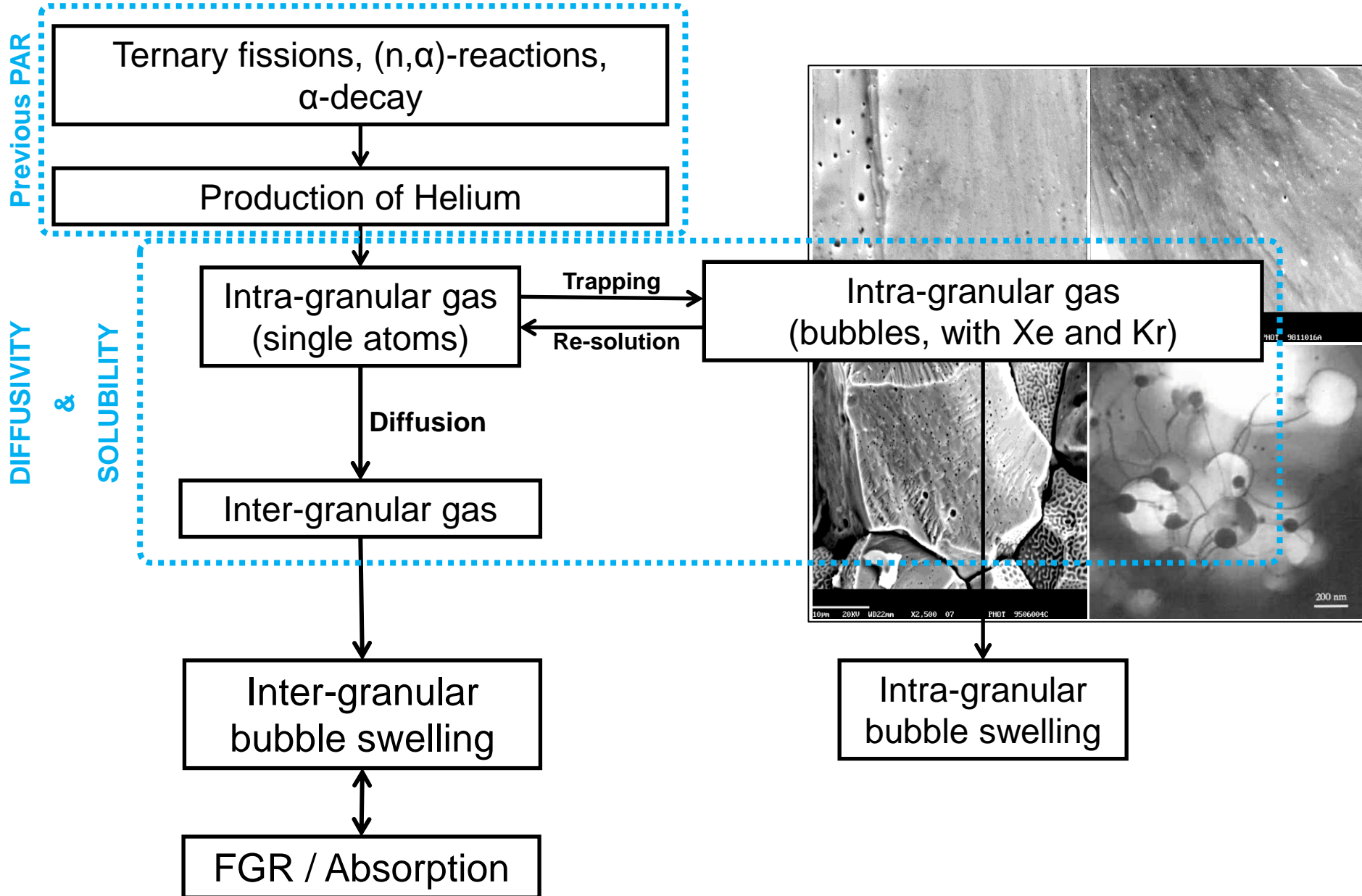
- **In-pile conditions**, especially
  - at high burnup
  - employing MOX fuel
  - employing MA-bearing fuel



P. Botazzoli, L. Luzzi, S. Brémier, A. Schubert, P. Van Uffelen, C.T. Walker, W. Haeck, W. Goll, 2011. *Extension and Validation of the TRANSURANUS Burn-up Model for Helium Production in High Burn-up LWR Fuels*. Journal of Nuclear Materials, 419(1-3), 329–338.

- **In storage conditions**, due the continuous production from  $\alpha$ -emitters

# Helium behaviour (intra- and inter-granular)



# Modelling Helium behaviour in FPCs

$$\begin{cases} \frac{\partial c_{He}}{\partial t} = D_{He} \nabla^2 c_{He} - \beta_{He} (c_{He} - C_{s,pig}) + \alpha_{He} m_{He} + S_{He} \\ \frac{\partial m_{He}}{\partial t} = \beta_{He} (c_{He} - C_{s,pig}) - \alpha_{He} m_{He} \end{cases}$$

$c_{He}$  - He dissolved in matrix  
 $m_{He}$  - He present in bubbles  
 $\alpha_{He}$  - thermal re-solution rate  
 $\beta_{He}$  - trapping rate

Helium diffusivity

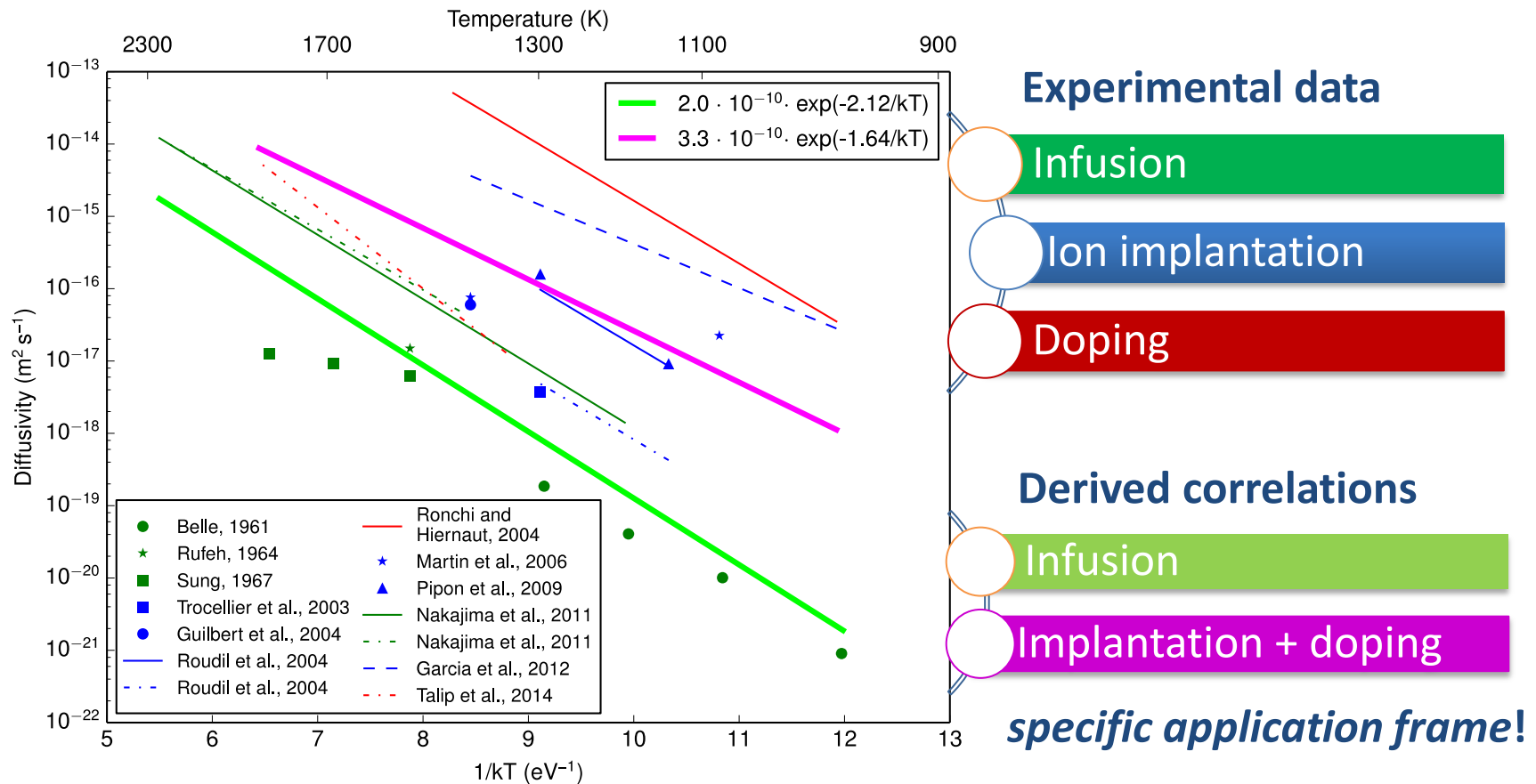
Helium solubility

Helium production

- Model including the **mechanistic** description of helium behaviour in oxide fuels
- Definition of the model parameters is the first fundamental step
- Dedicated algorithms required in FPCs (PDEs to be solved in each mesh point...)



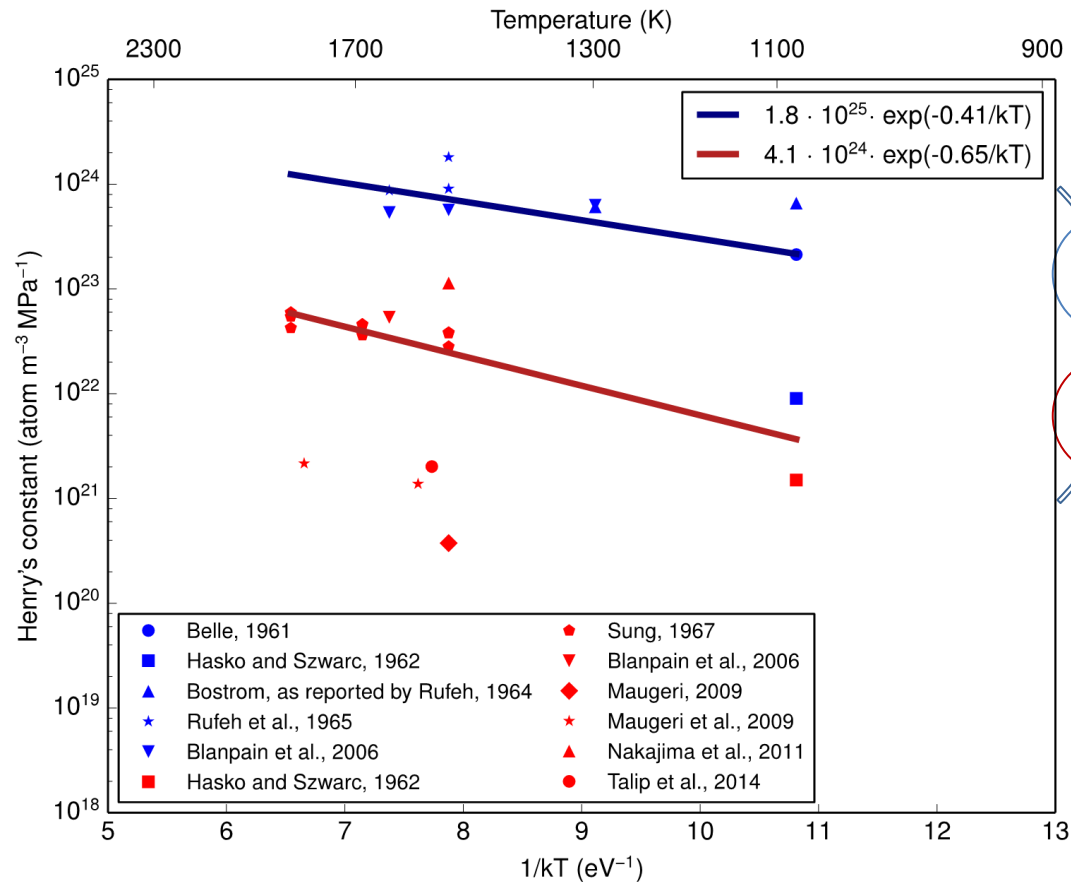
# Helium diffusivity (part of PAR2016)



| Data                        | Log $D_0$ ( $\text{m}^2 \text{s}^{-1}$ ) | Q (eV)            | Range (K) | $R^2$             |
|-----------------------------|--|-------------------|-----------|-------------------|
| Infusion                    | -9.7 (-11, -8.4)                         | 2.12 (1.77, 2.56) | 968–2110  | 0.93              |
| Ion implantation and doping | -9.5 (-13, -5.8)                         | 1.64 (0.74, 2.56) | 973–1800  | 0.52 <sup>b</sup> |

<sup>b</sup> This value of  $R^2$  does not seem fully satisfactory. Nevertheless, we still choose to report this fit since it includes all the data available in the literature. Further refinement of this correlation is of major interest, once more data will become available.

# Helium solubility (part of PAR2017)



Experimental data & derived correlations

Powder

Single crystal

| Data           | Log A (at m <sup>-3</sup> MPa <sup>-1</sup> ) | B (eV)            | Range (K) | R <sup>2</sup> |
|----------------|---|-------------------|-----------|----------------|
| Powder         | 25.25 (23.91,26.6)                            | 0.41 (0.75, 0.06) | 1073–1773 | 0.83           |
| Single crystal | 24.61 (23.41, 25.82)                          | 0.65 (1.01, 0.28) | 1073–1773 | 0.83           |

# Numerical algorithms (part of PAR2015)

## PolyPole-1

MULTI-SCALE !

SotA. *Effective diffusion*  
SotA. URGAS and FORMAS

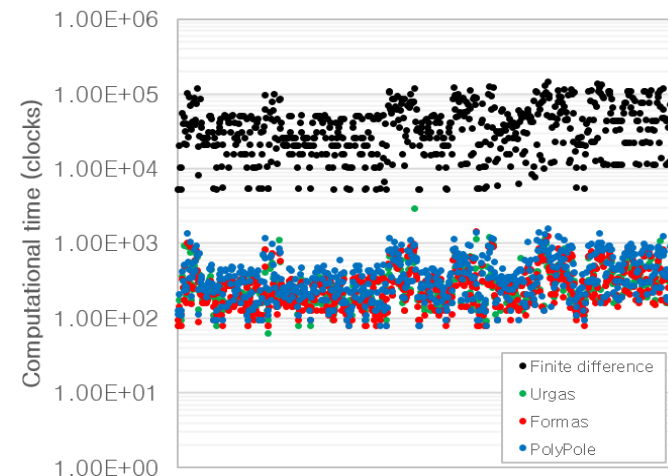
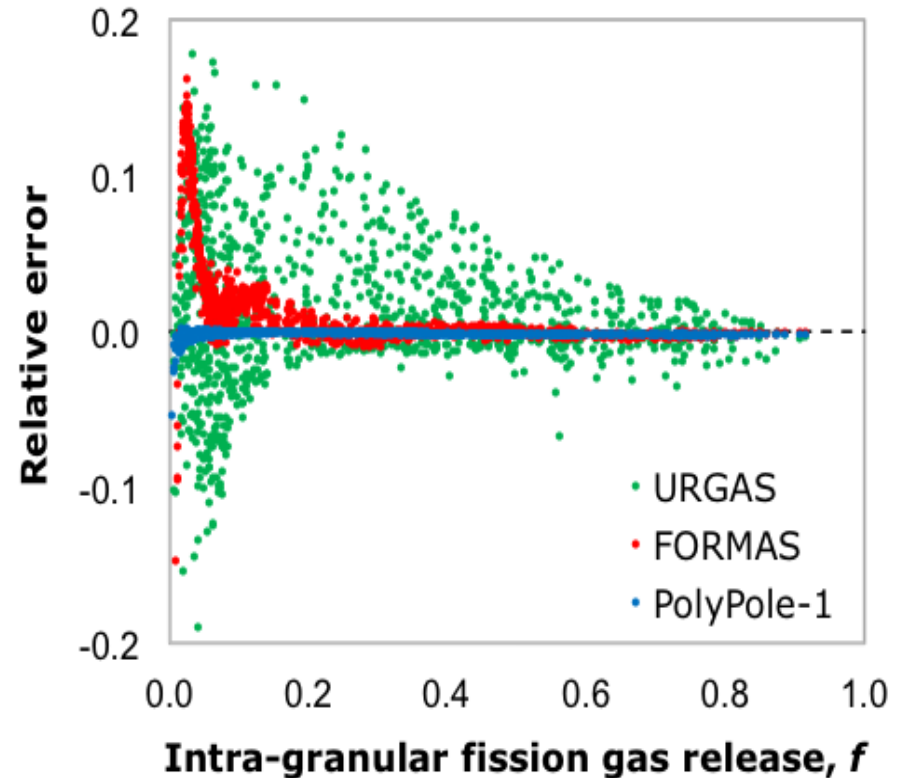
$$\frac{\partial c_t}{\partial t} = \beta + \mathbf{D}_{\text{eff}} \nabla^2 c_t$$

In FPC time-steps,  $\mathbf{D}_{\text{eff}}$   
can vary order of magnitudes !

Based on **modal expansion** in  
space and including corrective  
polynomial factors to **account for**  
**the time dependency of the**  
**parameters**

Assessed against reference algorithm  
Released OpenSource

D. Pizzocri, C. Rabiti, L. Luzzi, T. Barani, P. Van Uffelen, G. Pastore, 2016.  
*PolyPole-1: An accurate numerical algorithm for intra-granular fission gas release.* Journal of Nuclear Materials, 478, 333–342.



# Numerical algorithms (part of PAR2017)

## PolyPole-2

$$\frac{\partial}{\partial t} \bar{c} = \bar{\beta} + \bar{D}\bar{c} + \bar{S}\bar{c}$$

**SotA. Not available**

Allows considering all the physical time-scales of the system, overcoming the *effective diffusion* hypothesis

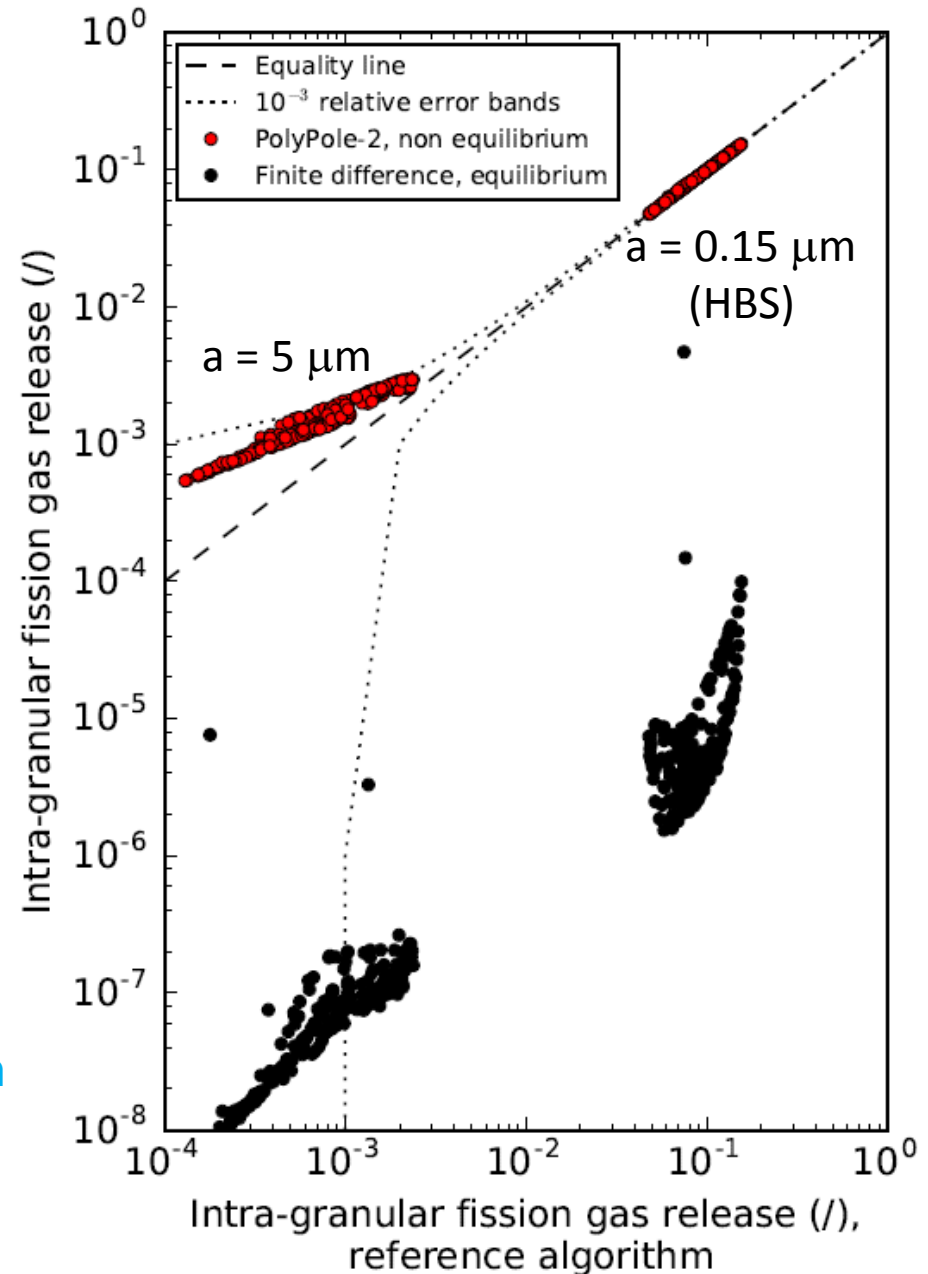
→ **Fundamental in fast transients !**

Identical numerical scheme of PolyPole-1

Numerical experiment with randomly generated transients

Assessed against reference algorithm

G. Pastore, D. Pizzocri, C. Rabiti, T. Barani, P. Van Uffelen, L. Luzzi, 2017. *An effective numerical algorithm for intra-granular fission gas release during non-equilibrium trapping and resolution*. Submitted to Journal of Nuclear Materials.



# Conclusions (PAR2017) and future steps

1. Development of new **correlations for Helium diffusivity and solubility**
  - Accounting for all available data
  - Greatly reducing calculation uncertainties
  - Clarified scope of application

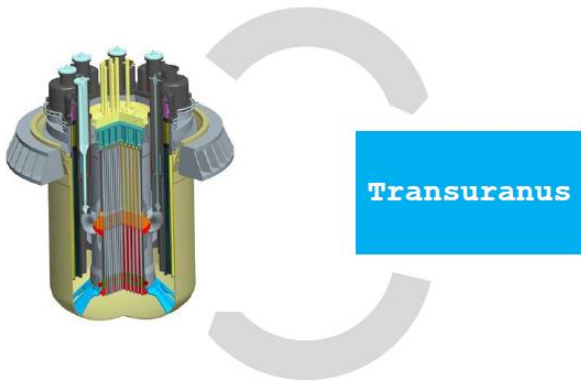
**NEXT: Assessment of Helium model in TRANSURANUS**

2. Development of new **dedicated numerical algorithms** (PolyPole-1, PolyPole-2)
  - Superior accuracy with respect to SotA
  - Similar computational effort
  - Allowing for the treatment of multiple PDEs (fundamental for **Helium**)

**NEXT: Implementation in TRANSURANUS** (coupled with **SCIANTIX** *mesoscale* module)

**NEXT: Keep going the activity of extending TRANSURANUS (both fuel and cladding) towards LFR-oriented version, as more data/knowledge (e.g., HBS, restructuring and Pu redistribution, FP chemistry, intra-granular bubble coarsening) **become available...****

**NEXT: Fuel rod integral analysis in support of design of LFRs using the improved version of TRANSURANUS** (assessed against Integral Irradiation Experiments, e.g., SUPERFACT, RAPSODIE-I, NESTOR-3 ----> Task Force of INSPYRE H2020 Project)



## MORE IN PERSPECTIVE ...

*Starting multi-physics coupling of FPCs (TRANSURANUS, Bison) with neutronics & thermal-hydraulics for LFR conditions*

Development of a **well-structured module** able to provide TRANSURANUS with accurate information from the reactor scale, typically the initial and boundary conditions for the fuel rod thermo-mechanical analysis:

- Modelling of the neutronics and thermal-hydraulics reactor conditions typical of Gen-IV LFRs, in normal, transient and annealing/storage conditions.
- Creation of initial and boundary conditions needed by TRANSURANUS, starting from the multi-physics and high-fidelity simulations, for normal, transient and annealing/storage conditions.
- Evaluation of reactor dynamics and feedback effects during transient conditions with a specific focus on the safety-related key parameters and their influence on the TRANSURANUS modelling and simulation capabilities.
- Assessment of the burn-up model of TRANSURANUS with MOX (and more in perspective with MA-bearing fuels) against Monte Carlo simulations.
- Development of ad-hoc coupling scheme among **SERPENT**, **OpenFOAM / RELAP** and **TRANSURANUS** to provide an accurate multi-physics modelling approach that can serve as reference solution for the evaluation of TRANSURANUS outcomes.

# Publications (---> PAR2013÷2017)

1. P. Van Uffelen, P. Botazzoli, L. Luzzi, S. Bremier, A. Schubert, P. Raison, R. Eloirdi, M.A. Barker - *An experimental study of grain growth in mixed oxide samples with various microstructures and plutonium concentrations* - **Journal of Nuclear Materials**, 434, 287-290, **2013**.
2. G. Pastore, L. Luzzi, V. Di Marcello, P. Van Uffelen - *Physics-based modelling of fission gas swelling and release in UO<sub>2</sub> applied to integral fuel rod analysis* - **Nuclear Engineering and Design**, 256, 75-86, **2013**.
3. V. Di Marcello, S. Lorenzi, L. Luzzi, D. Pizzocri - *Improvements of the Transuranus Code for Lead-Cooled Fast Reactor Analysis: ALFRED Reactor Fuel Rod* - Proceedings of the International Workshop "Towards Nuclear Fuel Modelling in the Various Reactor Types across Europe", Karlsruhe, Germany, June 10-11, 2013.
4. L. Luzzi, A. Cammi, V. Di Marcello, S. Lorenzi, D. Pizzocri, P. Van Uffelen - *Application of the TRANSURANUS code for the fuel pin design process of the ALFRED reactor* - **Nuclear Engineering and Design**, 277, 173-187, **2014**.
5. G. Pastore, D. Pizzocri, J.D. Hales, S.R. Novascone, D.M. Perez, B.W. Spencer, R.L. Williamson, P. Van Uffelen, L. Luzzi - *Modelling of Transient Fission Gas Behaviour in Oxide Fuel and Application to the BISON Code* - Proceedings of the Enlarged Halden Programme Group (EHPG) Meeting, Session F7, Paper 4, Røros, Norway, September 7-12, 2014.
6. D. Pizzocri, S. Lorenzi, L. Luzzi - *Extension of the TRANSURANUS code to the 15-15Ti austenitic steels for the fuel pin performance analysis of Gen-IV Liquid Metal-cooled Fast Reactors* - CESNEF-IN-03-2015 Technical Report, pp. 1-68, Department of Energy, Nuclear Engineering Division, Politecnico di Milano, March 2015.
7. D. Pizzocri, T. Barani, E. Bruschi, L. Luzzi, P. Van Uffelen - *Development and validation of a transient fission gas release model for TRANSURANUS* - Proceedings of the International Workshop "Towards Nuclear Fuel Modelling in the Various Reactor Types across Europe", Karlsruhe, Germany, June 8-9, 2015.
8. D. Pizzocri, G. Pastore, T. Barani, E. Bruschi, L. Luzzi, P. Van Uffelen - *Modelling of Burst Release in Oxide Fuel and Application to the Transuranus Code* - Proceedings of the 11th International Conference on WWER Fuel Performance, Modelling and Experimental Support, Vol. I, pp. 311-320, Golden Sands Resort, Bulgaria, September 26 - October 3, 2015.
9. D. Pizzocri, G. Pastore, T. Barani, S. Lorenzi, L. Luzzi - *An efficient energy remainder criterion for intra-granular diffusion calculations: Improving the PolyPole-1 algorithm* - The Nuclear Materials Conference (NuMat 2016), Montpellier, France, November 7-10, 2016.
10. D. Pizzocri, F. Cappia, V.V. Rondinella, P. Van Uffelen - *Preliminary model for the fission gas behaviour in the high burnup structure (HBS)* - JRC Technical Report, JRC-Karlsruhe, 2016.
11. D. Pizzocri, C. Rabiti, L. Luzzi, T. Barani, P. Van Uffelen, G. Pastore - *PolyPole-1: An accurate numerical algorithm for intra-granular fission gas release* - **Journal of Nuclear Materials**, 478, 333-342, **2016**.

12. F. Cappia, D. Pizzocri, A. Schubert, P. Van Uffelen, G. Paperini, D. Pellottiero, R. Macià-Juan, V.V. Rondinella - *Critical assessment of the pore size distribution in the rim region of high burnup UO<sub>2</sub> fuel* - **Journal of Nuclear Materials**, 480, 138-149, **2016**.
13. D. Pizzocri, F. Cappia, L. Luzzi, G. Pastore, V.V. Rondinella, P. Van Uffelen - *A semi-empirical model for the formation and depletion of the high burnup structure in UO<sub>2</sub>* - **Journal of Nuclear Materials**, 487, 23-29, **2017**.
14. T. Barani, E. Bruschi, D. Pizzocri, G. Pastore, P. Van Uffelen, R.L. Williamson, L. Luzzi - *Analysis of transient fission gas behaviour in oxide fuel using BISON and TRANSURANUS* - **Journal of Nuclear Materials**, 486, 96-110, **2017**.
15. P. Van Uffelen, A. Schubert, J. van de Laar, W. Li, C. Gyori, R. Dubourg, T. Pavlov, F. Cappia, L. Cognini, T. Barani, D. Pizzocri, G. Pastore, L. Luzzi - *Current meso-scale modelling developments for TRANSURANUS* - NEA Workshop: Advanced Fuel Modelling for Safety and Performance Enhancement, Paris, France, March 7-9, 2017.
16. D. Pizzocri, F. Cappia, L. Luzzi, V.V. Rondinella, P. Van Uffelen - *Modelling of high burnup structure in fuel performance codes: formation and porosity evolution* - Proceedings of the International Workshop "Towards Nuclear Fuel Modelling in the Various Reactor Types Across Europe", Lappeenranta, Finland, June 15-16, 2017.
17. T. Barani, L. Cognini, D. Pizzocri, A. Schubert, L. Luzzi, P. Van Uffelen - *Modelling and assessment of helium intra-granular behaviour in oxide fuels* - Proceedings of the International Workshop "Towards Nuclear Fuel Modelling in the Various Reactor Types Across Europe", Lappeenranta, Finland, June 15-16, 2017.
18. L. Luzzi, D. Pizzocri, T. Barani - *Physically-based inert gas behaviour modelling for fuel performance codes* - Proceedings of the Second Workshop on Research into Nuclear Fuel and Cladding in Europe (NuFuel), Lecco, Italy, September 4-6, 2017.
19. L. Luzzi, L. Cognini, D. Pizzocri, T. Barani, G., Pastore, A. Schubert, T. Wiss, P. Van Uffelen - *Helium diffusivity in oxide nuclear fuel: Critical data analysis and new correlations* - **Nuclear Engineering and Design**, 330, 265-271, **2018**.
20. G. Pastore, T. Barani, D. Pizzocri, A. Magni, L. Luzzi - *Modeling Fission Gas Release and Bubble Evolution in UO<sub>2</sub> for Engineering Fuel Rod Analysis* - Proceedings of the International Conference on Reactor Fuel Performance (Top Fuel 2018), Paper A0240, Prague, Czech Republic, September 30 - October 4, 2018.
21. L. Cognini, D. Pizzocri, T. Barani, P. Van Uffelen, A. Schubert, T. Wiss, L. Luzzi - *Helium solubility in oxide nuclear fuel: Critical review and derivation of new correlations for Henry's constant* - **Nuclear Engineering and Design**, **2018** (submitted).
22. G. Pastore, D. Pizzocri, C. Rabiti, T. Barani, P. Van Uffelen, L. Luzzi - *An effective numerical algorithm for intra-granular fission gas release during non-equilibrium trapping and resolution* - **Journal of Nuclear Materials**, **2018** (accepted).

***Thank you for your kind attention***



WORKSHOP TEMATICO  
**LFR-GEN IV: STATO ATTUALE DELLA TECNOLOGIA E  
PROSPETTIVE DI SVILUPPO**

ADP ENEA-MSE (PAR2017-LP2)



# **POLIMI contribution**

## **Chemical issues within the development of Lead-cooled Fast Reactors**

E. Macerata, M. Mariani, M. Giola

14-15 June, 2018, Roma



**POLITECNICO  
MILANO 1863**

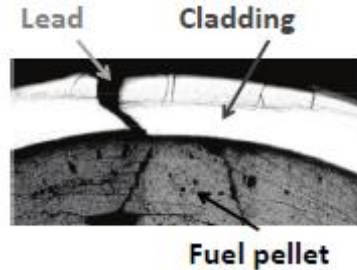


Agenzia nazionale per le nuove tecnologie,  
l'energia e lo sviluppo economico sostenibile

- Chemical issue in LFRs
  - Fuel-coolant chemical interaction
  - System features
  - Approach
- Computational studies
- Experimental activities

## Fuel-coolant chemical interaction

Cladding failure event



under nominal operation

in accidental conditions

## What influences do chemical effects have?

- Fuel material properties and behaviour
  - Thermal conductivity
  - Melting point
  - Swelling
- Cladding material properties and behaviour
  - Chemical composition of the gas: corrosion and oxidation of cladding
- Release of radionuclides from fuel
  - Different volatility and solubilities of the species

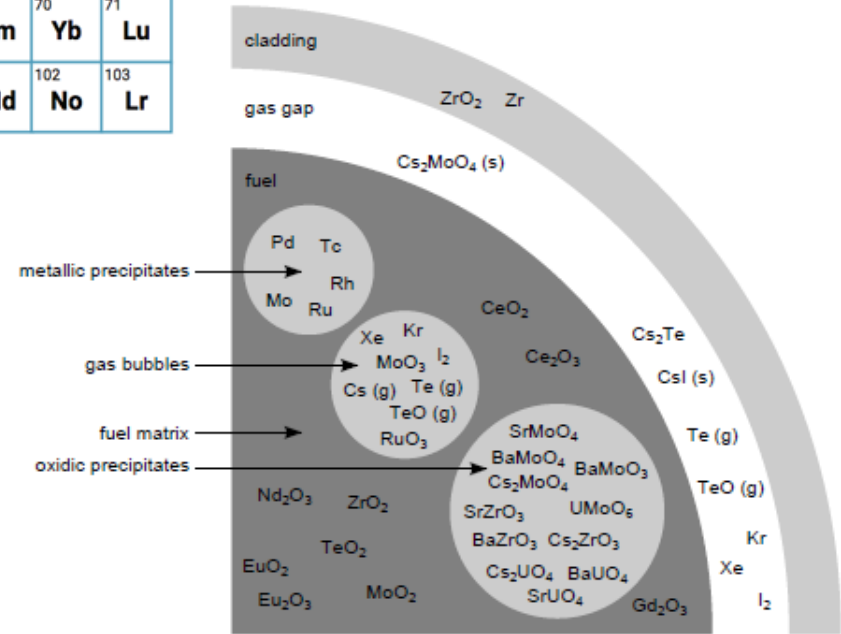
|   |          |          |           |           |           |           |           |           |           |           |           |           |           |           |           |           |           |            |  |  |  |  |  |  |  |  |  |  |  |  |  |  |  |  |  |          |          |          |          |          |          |          |          |          |          |          |          |          |          |          |          |         |          |          |          |          |          |          |          |           |           |           |           |
|---|----------|----------|-----------|-----------|-----------|-----------|-----------|-----------|-----------|-----------|-----------|-----------|-----------|-----------|-----------|-----------|-----------|------------|--|--|--|--|--|--|--|--|--|--|--|--|--|--|--|--|--|----------|----------|----------|----------|----------|----------|----------|----------|----------|----------|----------|----------|----------|----------|----------|----------|---------|----------|----------|----------|----------|----------|----------|----------|-----------|-----------|-----------|-----------|
| 1<br>H  |          |          |           |           |           |           |           |           |           |           |           |           |           |           |           |           | 2<br>He   |            |  |  |  |  |  |  |  |  |  |  |  |  |  |  |  |  |  |          |          |          |          |          |          |          |          |          |          |          |          |          |          |          |          |         |          |          |          |          |          |          |          |           |           |           |           |
| 3<br>Li   | 4<br>Be  |          |           |           |           |           |           |           |           |           |           | 5<br>B    | 6<br>C    | 7<br>N    | 8<br>O    | 9<br>F    | 10<br>Ne  |            |  |  |  |  |  |  |  |  |  |  |  |  |  |  |  |  |  |          |          |          |          |          |          |          |          |          |          |          |          |          |          |          |          |         |          |          |          |          |          |          |          |           |           |           |           |
| 11<br>Na  | 12<br>Mg |          |           |           |           |           |           |           |           |           |           | 13<br>Al  | 14<br>Si  | 15<br>P   | 16<br>S   | 17<br>Cl  | 18<br>Ar  |            |  |  |  |  |  |  |  |  |  |  |  |  |  |  |  |  |  |          |          |          |          |          |          |          |          |          |          |          |          |          |          |          |          |         |          |          |          |          |          |          |          |           |           |           |           |
| 19<br>K   | 20<br>Ca | 21<br>Sc | 22<br>Ti  | 23<br>V   | 24<br>Cr  | 25<br>Mn  | 26<br>Fe  | 27<br>Co  | 28<br>Ni  | 29<br>Cu  | 30<br>Zn  | 31<br>Ga  | 32<br>Ge  | 33<br>As  | 34<br>Se  | 35<br>Br  | 36<br>Kr  |            |  |  |  |  |  |  |  |  |  |  |  |  |  |  |  |  |  |          |          |          |          |          |          |          |          |          |          |          |          |          |          |          |          |         |          |          |          |          |          |          |          |           |           |           |           |
| 37<br>Rb  | 38<br>Sr | 39<br>Y  | 40<br>Zr  | 41<br>Nb  | 42<br>Mo  | 43<br>Tc  | 44<br>Ru  | 45<br>Rh  | 46<br>Pd  | 47<br>Ag  | 48<br>Cd  | 49<br>In  | 50<br>Sn  | 51<br>Sb  | 52<br>Te  | 53<br>I   | 54<br>Xe  |            |  |  |  |  |  |  |  |  |  |  |  |  |  |  |  |  |  |          |          |          |          |          |          |          |          |          |          |          |          |          |          |          |          |         |          |          |          |          |          |          |          |           |           |           |           |
| 55<br>Cs  | 56<br>Ba | 57<br>La | 72<br>Hf  | 73<br>Ta  | 74<br>W   | 75<br>Re  | 76<br>Os  | 77<br>Ir  | 78<br>Pt  | 79<br>Au  | 80<br>Hg  | 81<br>Tl  | 82<br>Pb  | 83<br>Bi  | 84<br>Po  | 85<br>At  | 86<br>Rn  |            |  |  |  |  |  |  |  |  |  |  |  |  |  |  |  |  |  |          |          |          |          |          |          |          |          |          |          |          |          |          |          |          |          |         |          |          |          |          |          |          |          |           |           |           |           |
| 87<br>Fr  | 88<br>Ra | 89<br>Ac | 104<br>Rf | 105<br>Db | 106<br>Sg | 107<br>Bh | 108<br>Hs | 109<br>Mt | 110<br>Ds | 111<br>Rg | 112<br>Cn | 113<br>Nh | 114<br>Fl | 115<br>Mc | 116<br>Lv | 117<br>Ts | 118<br>Og |            |  |  |  |  |  |  |  |  |  |  |  |  |  |  |  |  |  |          |          |          |          |          |          |          |          |          |          |          |          |          |          |          |          |         |          |          |          |          |          |          |          |           |           |           |           |
| <table border="1"> <tr> <td>119<br/>Uue</td> <td colspan="17"></td> </tr> <tr> <td>58<br/>Ce</td> <td>59<br/>Pr</td> <td>60<br/>Nd</td> <td>61<br/>Pm</td> <td>62<br/>Sm</td> <td>63<br/>Eu</td> <td>64<br/>Gd</td> <td>65<br/>Tb</td> <td>66<br/>Dy</td> <td>67<br/>Ho</td> <td>68<br/>Er</td> <td>69<br/>Tm</td> <td>70<br/>Yb</td> <td>71<br/>Lu</td> </tr> <tr> <td>90<br/>Th</td> <td>91<br/>Pa</td> <td>92<br/>U</td> <td>93<br/>Np</td> <td>94<br/>Pu</td> <td>95<br/>Am</td> <td>96<br/>Cm</td> <td>97<br/>Bk</td> <td>98<br/>Cf</td> <td>99<br/>Es</td> <td>100<br/>Fm</td> <td>101<br/>Md</td> <td>102<br/>No</td> <td>103<br/>Lr</td> </tr> </table> |          |          |           |           |           |           |           |           |           |           |           |           |           |           |           |           |           | 119<br>Uue |  |  |  |  |  |  |  |  |  |  |  |  |  |  |  |  |  | 58<br>Ce | 59<br>Pr | 60<br>Nd | 61<br>Pm | 62<br>Sm | 63<br>Eu | 64<br>Gd | 65<br>Tb | 66<br>Dy | 67<br>Ho | 68<br>Er | 69<br>Tm | 70<br>Yb | 71<br>Lu | 90<br>Th | 91<br>Pa | 92<br>U | 93<br>Np | 94<br>Pu | 95<br>Am | 96<br>Cm | 97<br>Bk | 98<br>Cf | 99<br>Es | 100<br>Fm | 101<br>Md | 102<br>No | 103<br>Lr |
| 119<br>Uue  |          |          |           |           |           |           |           |           |           |           |           |           |           |           |           |           |           |            |  |  |  |  |  |  |  |  |  |  |  |  |  |  |  |  |  |          |          |          |          |          |          |          |          |          |          |          |          |          |          |          |          |         |          |          |          |          |          |          |          |           |           |           |           |
| 58<br>Ce  | 59<br>Pr | 60<br>Nd | 61<br>Pm  | 62<br>Sm  | 63<br>Eu  | 64<br>Gd  | 65<br>Tb  | 66<br>Dy  | 67<br>Ho  | 68<br>Er  | 69<br>Tm  | 70<br>Yb  | 71<br>Lu  |           |           |           |           |            |  |  |  |  |  |  |  |  |  |  |  |  |  |  |  |  |  |          |          |          |          |          |          |          |          |          |          |          |          |          |          |          |          |         |          |          |          |          |          |          |          |           |           |           |           |
| 90<br>Th  | 91<br>Pa | 92<br>U  | 93<br>Np  | 94<br>Pu  | 95<br>Am  | 96<br>Cm  | 97<br>Bk  | 98<br>Cf  | 99<br>Es  | 100<br>Fm | 101<br>Md | 102<br>No | 103<br>Lr |           |           |           |           |            |  |  |  |  |  |  |  |  |  |  |  |  |  |  |  |  |  |          |          |          |          |          |          |          |          |          |          |          |          |          |          |          |          |         |          |          |          |          |          |          |          |           |           |           |           |

**VOLATILE FISSION PRODUCTS**

**METALLIC PRECIPITATES AS ALLOYS**

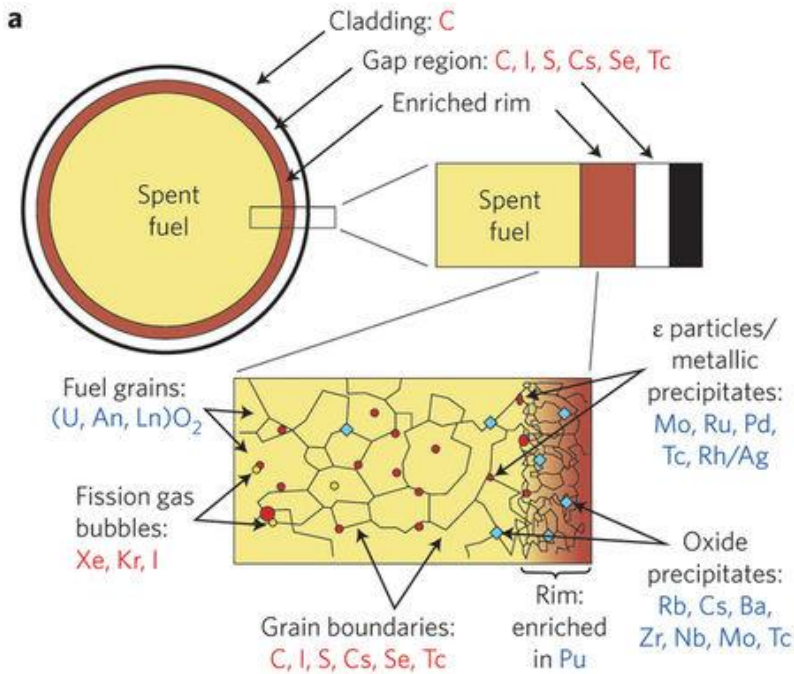
**OXIDES DISSOLVED IN THE FUEL MATRIX**

**CERAMIC PRECIPITATES AS OXIDES**

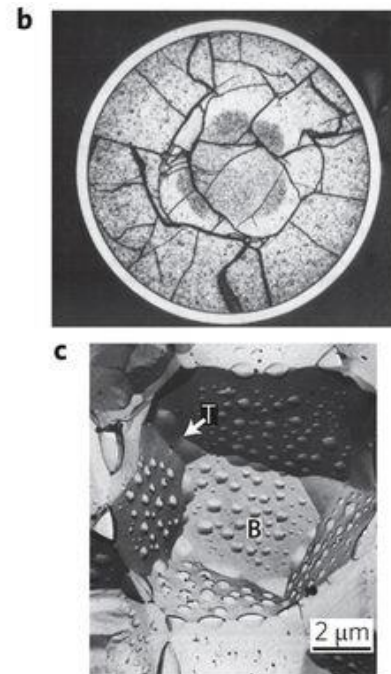


## IRRADIATED FUEL

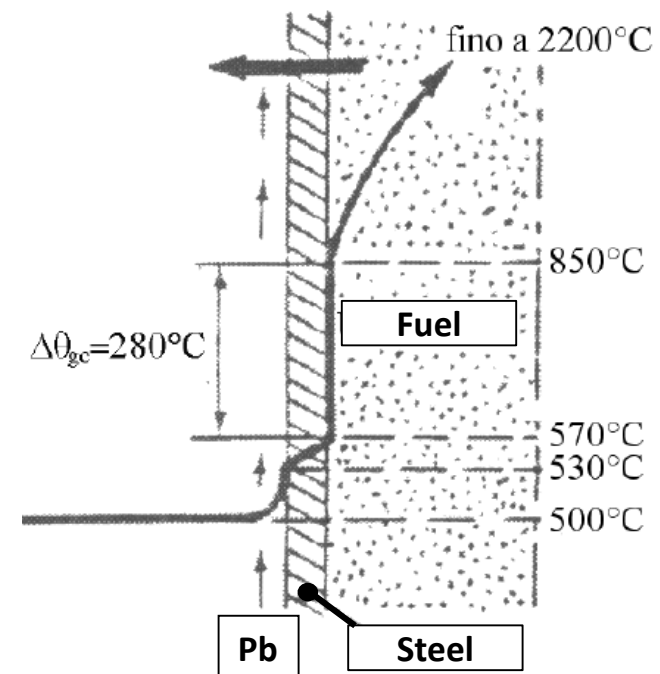
### COMPOSITION



### MIGRATION PHENOMENA/ RELEASE MECHANISMS



### TEMPERATURE GRADIENT



Fuel-coolant = multi-component and multi-phase system

## INPUT

mole of components  
temperature  
pressure



Minimization of Gibbs free energy of the system



## OUTPUT

System composition at thermodynamic equilibrium  
at T and p



Thermodynamic Database

Thermochemical properties



Phase diagrams



Experimental phase diagrams  
Semi-empirical methods  
DFT-GGA simulations



Implementation of  
**Thermochemical Database**  
of interest for LFR

## Thermodynamic simulation by **CALPHAD** method

- based on minimization of the Gibbs free energy of the system under specific assumptions
- enable the modeling of thermochemical properties and phase diagrams
- by using experimental or calculated data
- enable to study multi-phase and multi-component systems by extrapolation of the description of the lower component subsystems
- Software: old free source codes, a number of commercial software packages (FactSage, Thermo-Calc), recent development of free CALPHAD software (OpenCalphad)
- Database: specific commercial databases in continuous development in order to improve accuracy and reliability

Hickel et al., *Phys. Status Solidi B* **251**, 1, 9-13 (2014)

Kattern et al., *Tecnol. Metal. Mater. Miner.*, 13, 3-15 (2016)

Kattern et al., *Calphad*, 24, 55-94 (2000)

## Thermodynamic simulation by CALPHAD

### Methodology

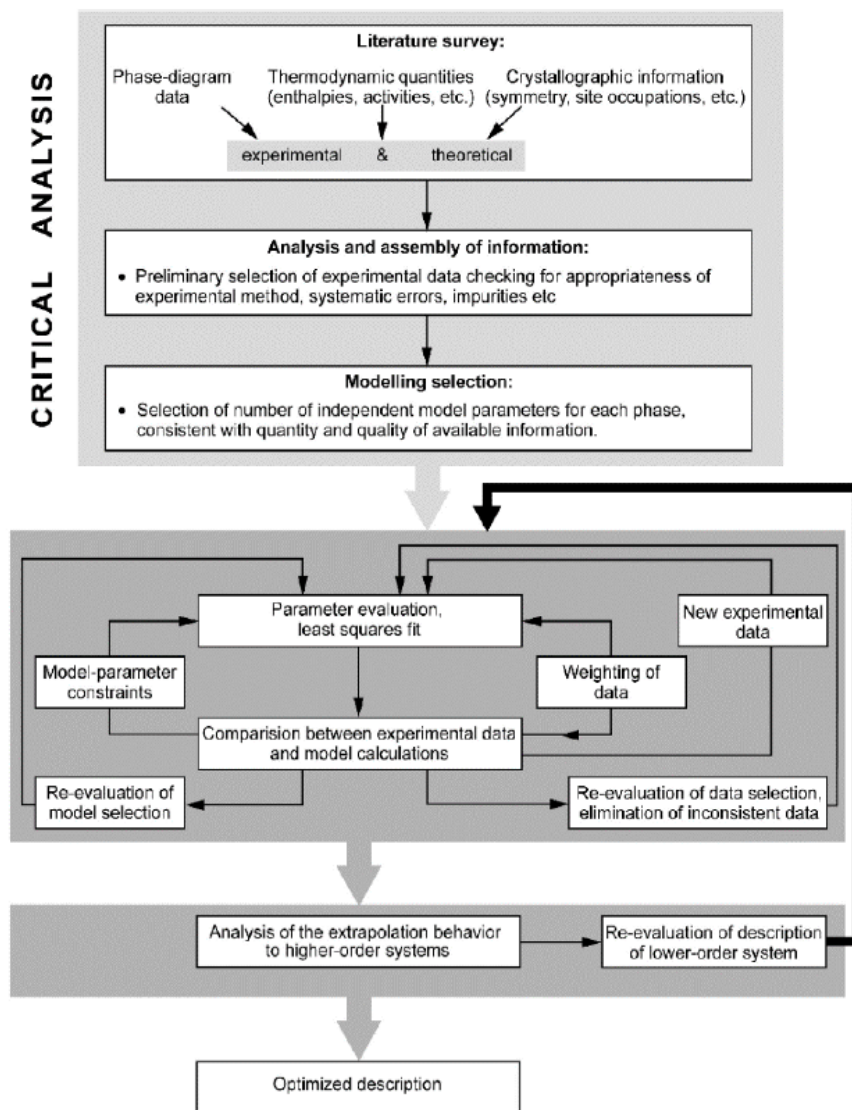
Application to:



La-Pb-O and U-Pb-O systems

by using:

- the data estimated by DFT-GGA approach
- experimental binary phase diagrams





## Integrating thermodynamic calculations in multi-physics codes for nuclear applications

**Thermodynamic calculations** provide, directly or indirectly, material properties, boundary conditions and source terms



**Multi-physics simulations** predict nuclear fuel behavior to support performance and safety analysis

### Some examples...

Report NEA/NSC/R/(2015)5

Loukusa et al., JNM 481 (2016) 101-110

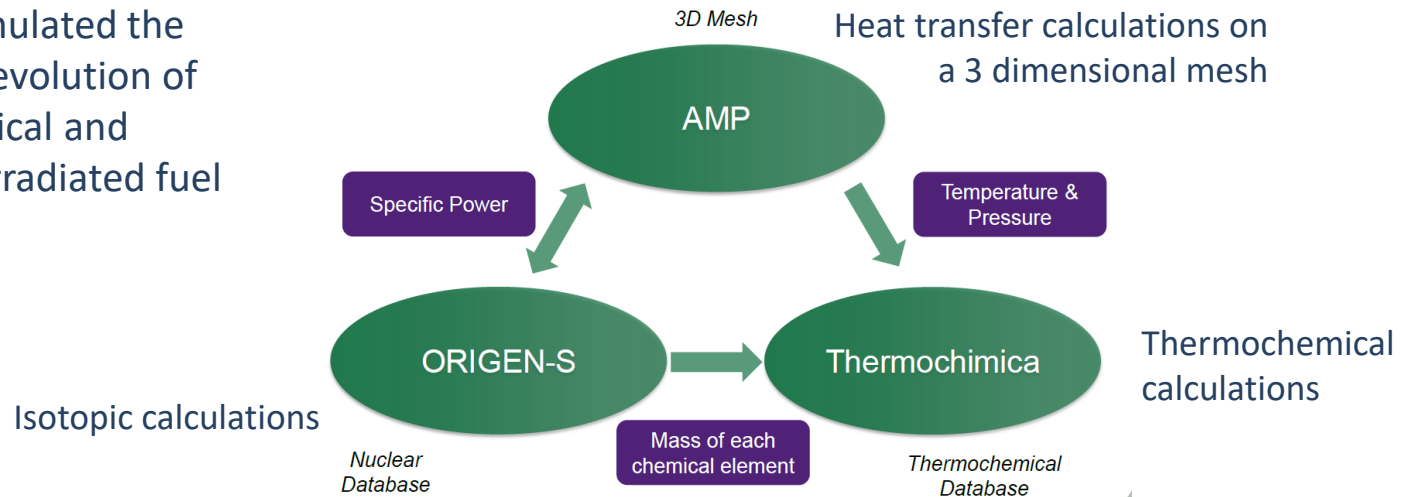
Piro et al., JNM 441 (2013) 240-251

Baurens et al., JNM 452 (2014) 578-594

In 1995



In 2013, *Piro et al.* simulated the temporal and spatial evolution of coupled thermochemical and nuclear reactions of irradiated fuel



- Able to predict oxygen chemical potential including fission products and minor phases formed;
- Able to predict chemical potentials of all the system components;
- Able to predict the formation of new phases in the fuel;
- Incorporation of chemical effects on the fuel surface with cladding.

In 2014, *Baurens et al.* studied the phenomena behind iodine stress corrosion cracking

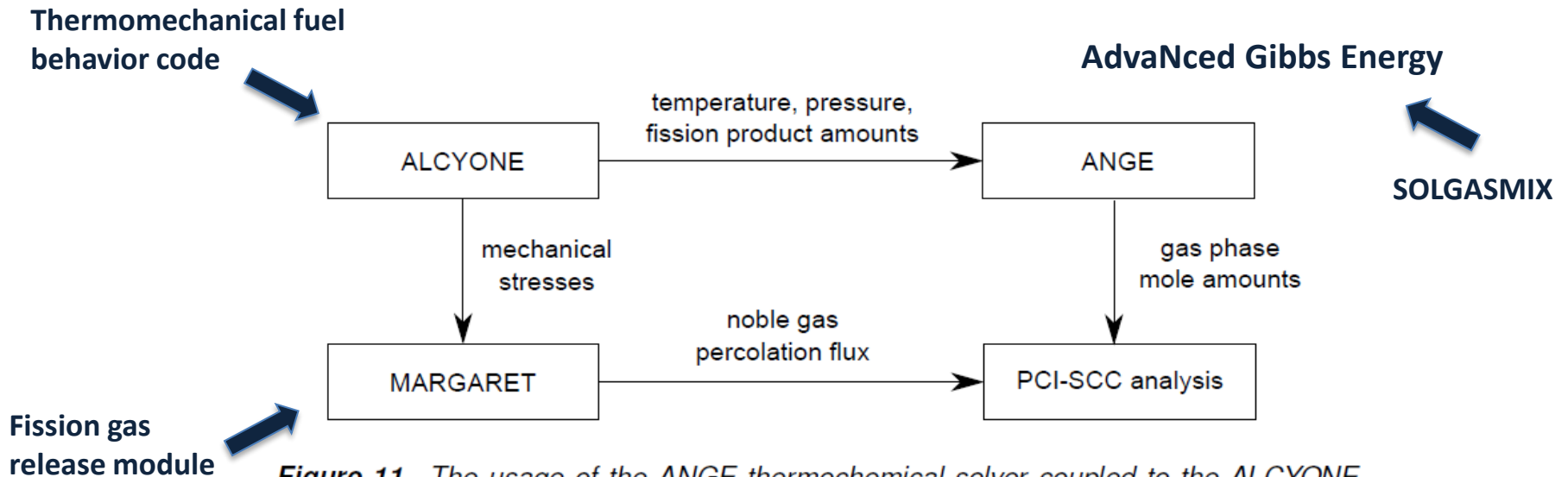


**Figure 11.** The usage of the ANGE thermochemical solver coupled to the ALCYONE fuel performance code in stress corrosion cracking studies [11]. Note that there is no feedback from ANGE to ALCYONE.

Next activity...

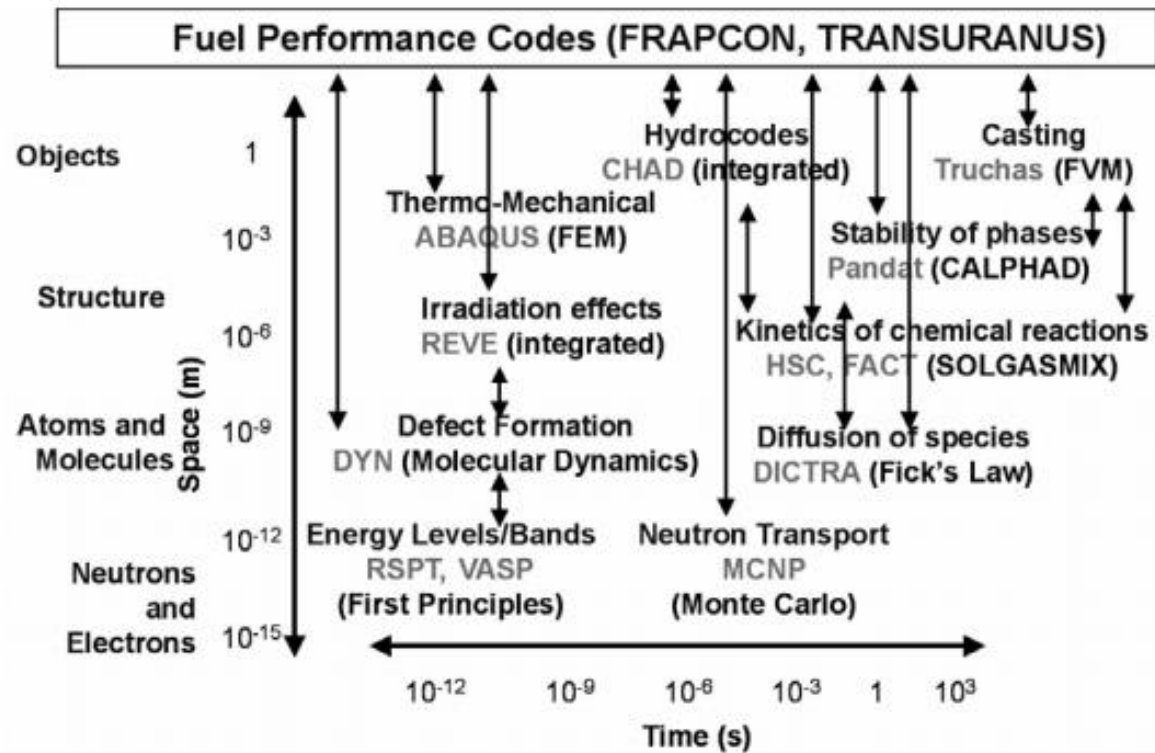


Figure 2. Space and time scales involved in simulating phenomena relevant for nuclear materials (black). The methods are shown in parenthesis. Several software packages (gray) are used to illustrate the type of simulation. [M. Stan, T. Amer. Nucl. Soc, 91 (2004) 131]

## AIMS:

- To observe a possible reactivity between Pb and an element/compound simulating the irradiated fuel
- To identify the new products formed
- To evaluate possible solubilities in Pb

## SELECTED SYSTEMS:

- Metallic elements
- SrO, CeO<sub>2</sub>, La<sub>2</sub>O<sub>3</sub>
- Fe<sub>2</sub>O<sub>3</sub>
- Pb as powder or wire

## EXPERIMENTS

- Preliminary investigations
- Reactivity experiments

High reactivity of Pb and metals  
in presence of air



Glove box with inert atmosphere  
(Ar with a O content < 0.1 ppm)

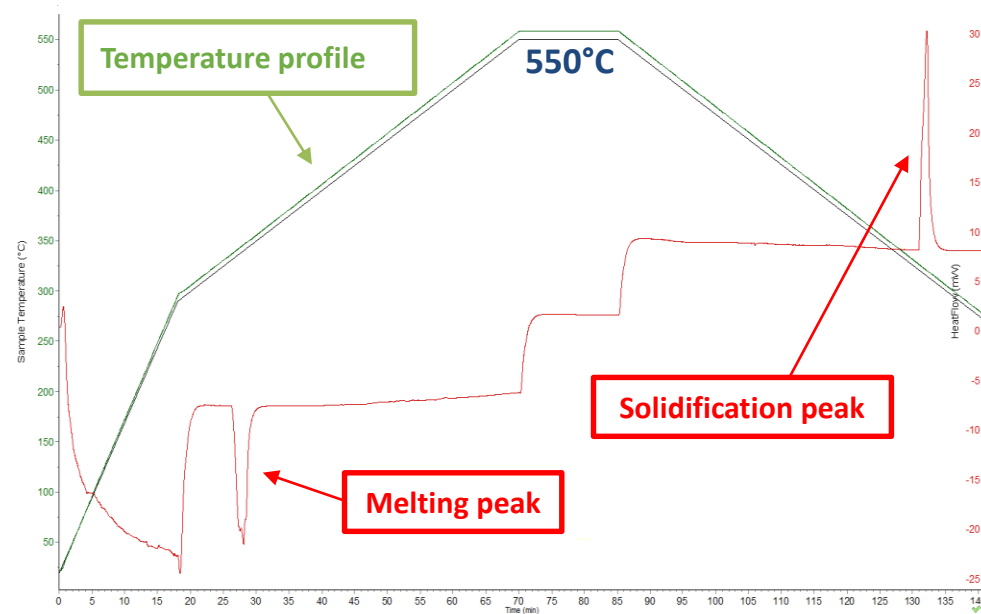
## PRELIMINARY EXPERIMENTS BY DIFFERENTIAL SCANNING CALORIMETRY

- Check of pure reagents
- First check of a possible reactivity between lead and oxide powder
  - Pieces of Pb and oxide powders are placed in the DSC crucible
  - The T profile is set through the software
  - Melting and enthalpy values are compared with the reference ones



### RESULTS

|   | Lead Melting Temperature [°C] | Lead Melting Enthalpy [J/g] |
|---|-------------------------------|-----------------------------|
| <b>Reference Pb</b>                     | 327.4 ± 0.1                   | 23.0 ± 2.6                  |
| <b>Pb</b>                               | 327.3 ± 0.1                   | 21.6 ± 1.9                  |
| <b>Pb - La<sub>2</sub>O<sub>3</sub></b> | 327.9 ± 0.1                   | 21.5 ± 2.1                  |
| <b>Pb - Fe<sub>2</sub>O<sub>3</sub></b> | 327.0 ± 0.1                   | 21.5 ± 1.8                  |
| <b>Pb - CeO<sub>2</sub></b>             | 327.2 ± 0.1                   | 21.5 ± 1.9                  |
| <b>Pb - SrO</b>                         | 327.9 ± 0.1                   | 21.7 ± 2.1                  |



**No interaction between oxide powders and Pb**

## REACTIVITY EXPERIMENTS

### MATERIALS:

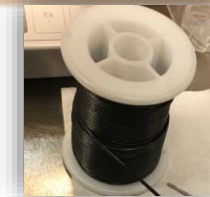
$\text{CeO}_2$ ,  $\text{Fe}_2\text{O}_3$ ,  $\text{La}_2\text{O}_3$ ,  $\text{SrO}$  in powder or pellet  
Pb (99.9%) in wire

### PELLET PREPARATION:

Pressure = 100 bar  
Inert atmosphere (Ar)

### THERMAL TREATMENT:

Temperature range: 500-550-750°C  
Reaction time: 2-6 hours  
Inert atmosphere (Ar)  
In glass or Pyrex test tubes

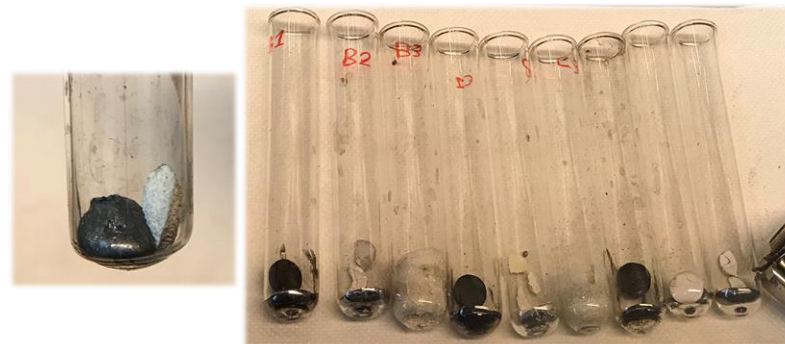


## THERMAL TREATMENT IN FURNACE

|    | Pellet (1 g)                   | Pb [g] | T [°C] | t [min] | pellet setup |
|----|--------------------------------|--------|--------|---------|--------------|
| A1 | -                              | 2.5    | 500    | 310     | air          |
| A2 | La <sub>2</sub> O <sub>3</sub> | 2.3    | 500    | 310     | air          |
| A3 | Fe <sub>2</sub> O <sub>3</sub> | 2.5    | 500    | 310     | air          |
| B1 | Fe <sub>2</sub> O <sub>3</sub> | 4      | 500    | 210     | air          |
| B2 | La <sub>2</sub> O <sub>3</sub> | 4.3    | 500    | 210     | air          |
| B3 | SrO                            | 4.2    | 500    | 210     | air          |
| C1 | Fe <sub>2</sub> O <sub>3</sub> | 4.5    | 550    | 290     | argon        |
| C2 | CeO <sub>2</sub>               | 4.7    | 550    | 290     | argon        |
| C3 | SrO                            | 4.3    | 550    | 290     | argon        |
| D1 | Fe <sub>2</sub> O <sub>3</sub> | 4.6    | 550    | 345     | argon        |
| D2 | La <sub>2</sub> O <sub>3</sub> | 4.5    | 550    | 345     | argon        |
| D3 | La <sub>2</sub> O <sub>3</sub> | 4.2    | 550    | 345     | argon        |
| E1 | Fe <sub>2</sub> O <sub>3</sub> | 4.4    | 750    | 300     | argon        |
| E2 | La <sub>2</sub> O <sub>3</sub> | 4.3    | 750    | 300     | argon        |
| E3 | CeO <sub>2</sub>               | 4.5    | 750    | 300     | argon        |
| F1 | La <sub>2</sub> O <sub>3</sub> | 4.9    | 550    | 290     | argon        |
| F2 | SrO                            | 4.8    | 550    | 290     | argon        |
| G1 | CeO <sub>2</sub>               | 4.9    | 750    | 290     | argon        |
| G2 | Fe <sub>2</sub> O <sub>3</sub> | 4.8    | 750    | 290     | argon        |

Optimization of sample preparation has been needed.

## FIRST MACROSCOPIC OBSERVATIONS



Temperature = 500-550 °C

| Pellet                         | Floats over Pb | Change in shape | Change in colour |
|--------------------------------|----------------|-----------------|------------------|
| CeO <sub>2</sub>               | ✓              | ✗               | ✗                |
| Fe <sub>2</sub> O <sub>3</sub> | ✓              | ✗               | ✓                |
| La <sub>2</sub> O <sub>3</sub> | ✓              | ✗               | ✗                |
| SrO                            | ✗              | ✓               | ✗                |

Temperature = 750 °C

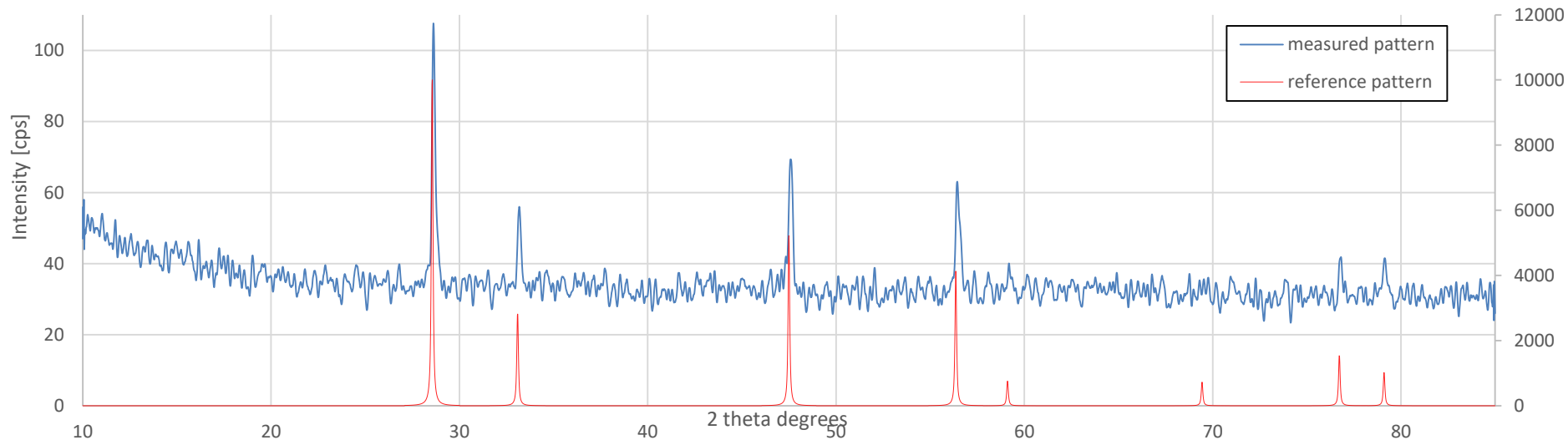
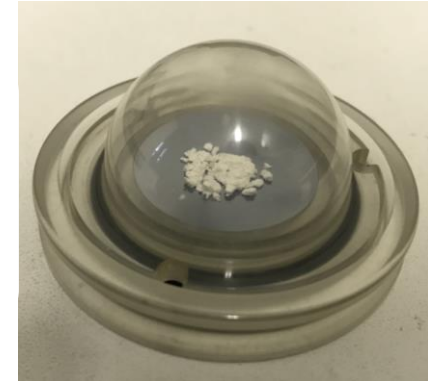
Same behaviour at higher temperature.

Lead vapours are not detected.



## CHARACTERIZATION BY X-RAY DIFFRACTION

- Check of pure reagents
- The contact surface between lead and oxide pellet is scratched
- The powder is placed in the sample holder with the dome
- The measured pattern is compared with a reference pattern



## CHARACTERIZATION BY SEM-EDX

- The contact surface between lead and oxide pellet is scratched
- The powder is placed in the sample holder (in vacuum) and opened inside the SEM
- The image is sent to EDX for the elemental analysis

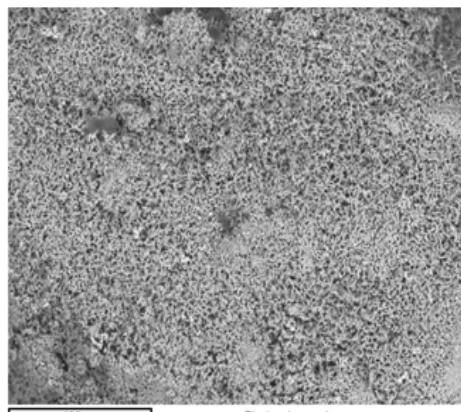
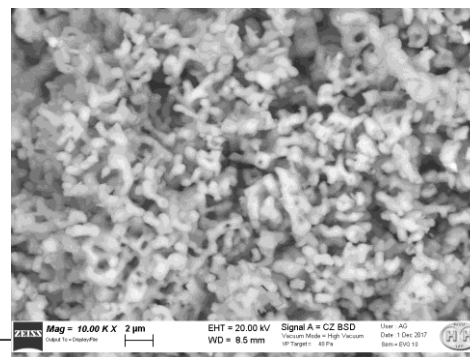
Spectrum processing :  
Peak possibly omitted : 0.257 keV

Processing option : All elements analyzed (Normalised)  
Number of iterations = 3

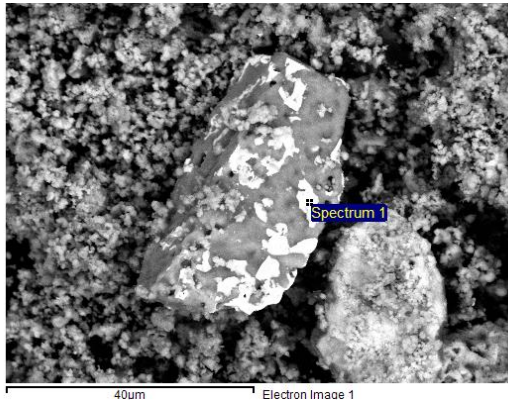
Standard :  
O SiO2 1-Jun-1999 12:00 AM  
Sr SrF2 1-Jun-1999 12:00 AM

| Element | App   | Intensity | Weight % | Weight % | Atomic % |
|---------|-------|-----------|----------|----------|----------|
|         | Conc. | Corrn.    |          | Sigma    |          |
| OK      | 31.24 | 0.5107    | 25.66    | 0.37     | 65.41    |
| Sr L    | 173.6 | 0.9802    | 74.34    | 0.37     | 34.59    |
|         | 7     |           |          |          |          |
| Totals  |       |           | 100.00   |          |          |

Sample: SrO tq  
Type: Default  
ID:



## CHARACTERIZATION RESULTS



### XRD ANALYSES

| Sample                  | Check on pristine powders | After the experiment  |
|-------------------------|---------------------------|-----------------------|
| $\text{CeO}_2$          | Cerianite                 | Cerianite             |
| $\text{Fe}_2\text{O}_3$ | Hematite                  | Maghemite             |
| $\text{La}_2\text{O}_3$ | Lanthanum (III) oxide     | Lanthanum (III) oxide |
| $\text{SrO}$            | Strontium (II) oxide      | Strontium (II) oxide  |

### SEM-EDX ANALYSES

| Compound                | Pristine powders                         | After the experiment  |
|-------------------------|--|---|
| $\text{CeO}_2$          | Ce, O                                    | Ce, O<br>Impurities (< 1%)  |
| $\text{Fe}_2\text{O}_3$ | Fe, O<br>Impurities (Ca, Ba, S, Si > 1%) | Fe, O<br>Impurities (Ca, Ba, S, Si > 1%)<br>Pb adherent on Ba and S |
| $\text{La}_2\text{O}_3$ | La, O                                    | La, O   |
| $\text{SrO}$            | Sr, O                                    | Sr, O   |

- No interaction compounds at the pellet surface are found
- The only change is in the iron oxide structure from  $\alpha\text{-Fe}_2\text{O}_3$  to  $\gamma\text{-Fe}_2\text{O}_3$

## INTERACTION STUDIES:

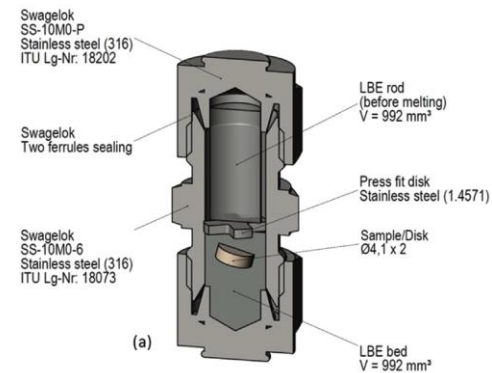
- Evaluation of solubility in liquid Pb by ICP-MS measurements
- Longer reaction time and  $T > 750^{\circ}\text{C}$
- Study a different setup for liquid-liquid interaction

### a) Sample container

Vigier et al., *Journal of Nuclear Materials*, 467 (2015), 840-847.

### b) Inert atmosphere

Gas purifier to reach lower O content ( $< 1$  ppb) in a small volume



- Metallic fission products
- Preparation of Pb intermetallics to obtain missing thermodynamic data by experiments
- Further investigations on pellet cross section
  - Sample preparation under evaluation



## Computational studies

- Investigations of U-Pb-O and La-Pb-O systems by CALPHAD approach by exploiting data previously estimated by DFT-GGA approach;
- Go deepen in the integration of the thermochemical simulations with multi-physics codes;

E. Macerata, *Studies on fuel-coolant chemical interaction in Lead-cooled Fast Reactors at Politecnico di Milano*, oral talk, CHERNE 2018 – 14° Workshop on European Collaboration on Radiological and Nuclear Engineering and Radiation Protection, 29/5-01/06/2018, Macugnaga (VB), Italy

## Experimental studies

- Reactivity experiments at higher temperatures;
- Development of a new experimental set up.

M. Cerini, O. Benes, K.Popa, E. Macerata, J.-C. Griveau, E. Colineau, M. Mariani, R.J.M. Konings, *Thermodynamic properties of  $Pb_3U_{11}O_{36}$* , submitted to J. Nucl. Mater.





**POLITECNICO**  
MILANO 1863



**POLITECNICO DI MILANO**

Workshop Tematico AdP MiSE – ENEA, PAR2017 – Progetto B.3 - LP2

Roma, 14<sup>th</sup> June, 2018

# LFR Multiphysics Model Development: OpenFoam – Serpent codes coupling

Antonio Cammi, Stefano Lorenzi



# Activity overview

**LP2:** Development and benchmark of codes and multiphysics model for Generation-IV Fast Reactor design and safety analysis

**PoliMi activity** Development of a LFR multiphysics model for

- i) design support
- ii) code verification (e.g., FRENETIC – collaboration with PoliTo)

## PAR 2016

Single channel LFR. Main physical phenomena – and their couplings – considered. Evaluation of the modelling approach and how to couple them.



## PAR 2017

Monte Carlo – CFD coupling for a better accuracy in neutronics modelling (relevant for design support).



...



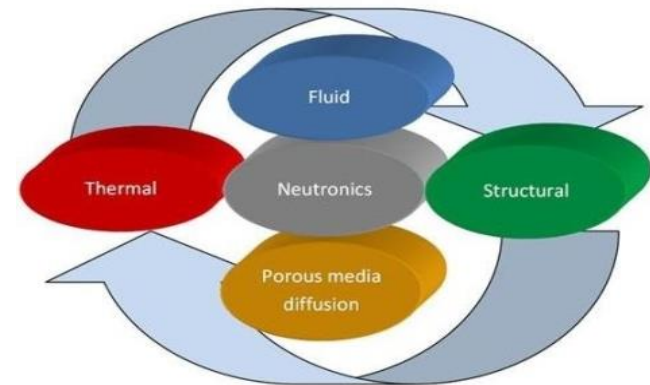
## PAR 2017

- . **Monte Carlo – CFD coupling** for a better accuracy in neutronics modelling (relevant for design support)
- . Starting **collaboration with PoliTo** (S. Dulla, P. Ravetto, L. Savoldi, R. Zanino) for interaction/comparison with FRENETIC
- . SERPENT code for Monte Carlo calculation and OpenFOAM for CFD analysis
  - **SERPENT** continuous energy Monte Carlo code with constant group capabilities
  - **OpenFOAM open source library** for numerical simulation with FV method. Flexible (obj-or programming), users can customize, extend and implement complex physical model
  - Multiphysics interface already present
- . **Neutronics** code provided with **realistic temperature profile** (improvement in reactivity and power outcomes)
- . **CFD** code provided with **realistic volumetric fission power distribution** (improvement in temperature profile)

# Motivation and background

**Multiphysics:** the study of the mutual interaction of different physical phenomena

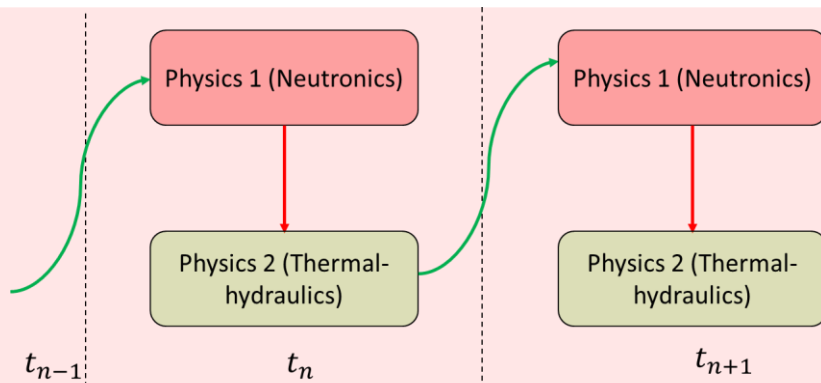
- . Fluid dynamics
- . Heat Transfer
- . Neutronics
- . Chemistry
- . Mechanics
- . BoP



Purpose of multi-physics code:

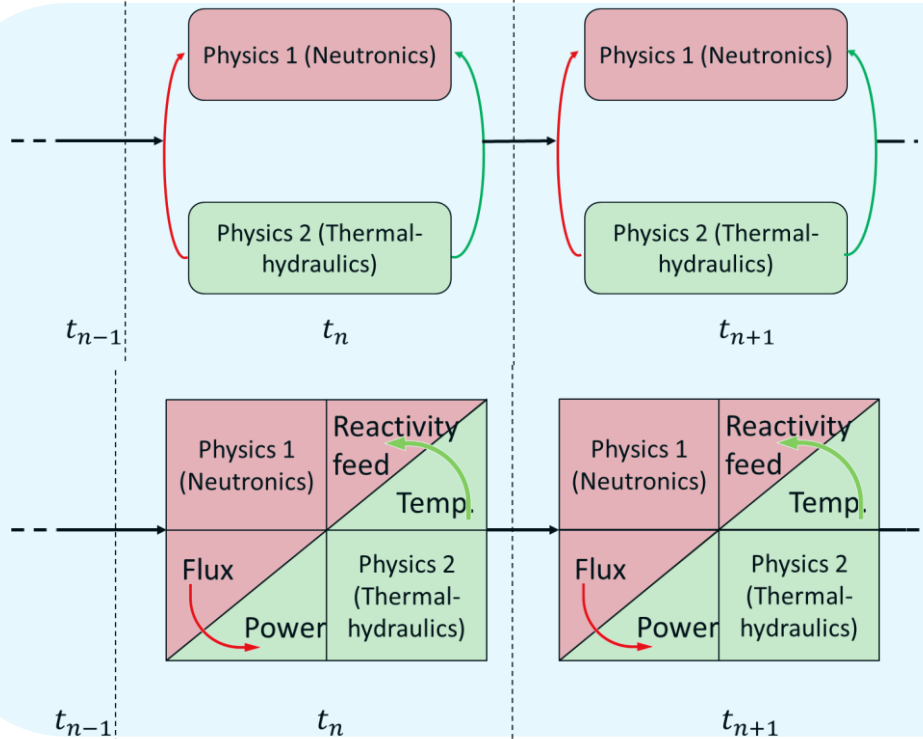
- . **deeper insight** about the complex physical phenomena occurring in the reactor system (and their mutual interactions)
- . allows **evaluating** a wide set of core parameters (e.g., temperature field, velocity field, and neutron fluxes) with a unique simulation tool
- . valuable for core designing, when **verifying** the satisfaction of the operational constraints
- . **combined analysis** with system codes (not replacing)

# Multiphysics modelling



## Explicit coupling:

- . Operator splitting approach
- . OK if coupling among physics is weak otherwise low accuracy in resolving multiphysics nonlinearities



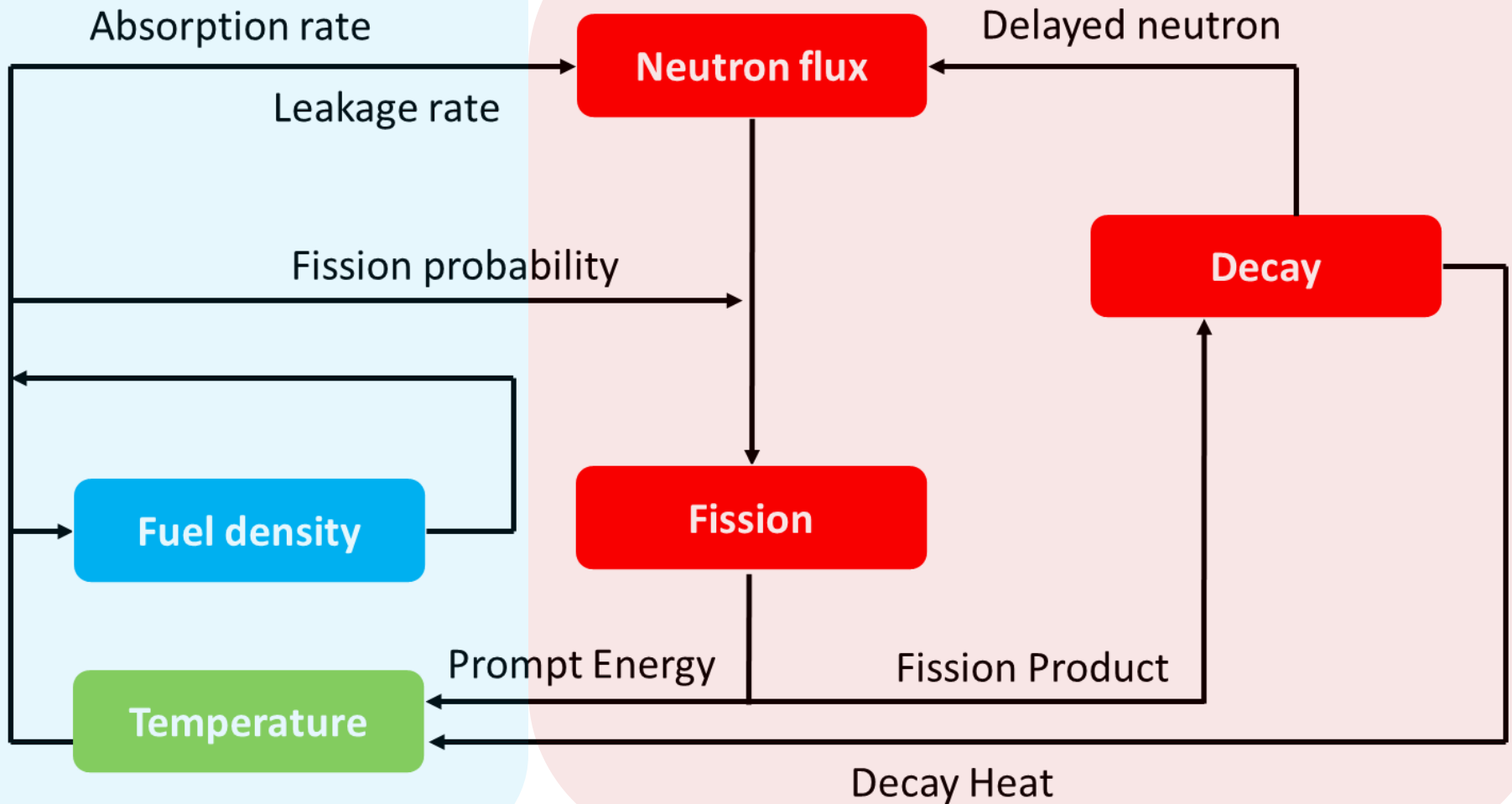
## Implicit coupling:

- . Iterative (Picard iteration) or monolithic approach (Jacobian-Free Newton Krylov)
- . Highest level of accuracy but also strong computational burden

# Neutronics – Thermal hydraulics coupling

## Thermal hydraulics

## Neutronics



# Neutronics – Thermal hydraulics coupling

## Thermal hydraulics (CFD)

$$\frac{\partial T}{\partial t} =$$

$$= -\nabla(\mathbf{u}T) +$$

$$+\nabla \cdot \frac{k}{\rho C_p} \nabla T + \frac{E_f}{\rho C_p} \Sigma_f \phi$$

## Neutronics (Monte Carlo)

$$(\mathbf{L} - \mathbf{S}) \phi = \frac{1}{k_{eff}} \mathbf{F} \phi$$

# Neutronics – Thermal hydraulics coupling

## Thermal hydraulics (CFD)

$$\frac{\partial T}{\partial t} =$$

$$= -\nabla(\mathbf{u}T) +$$

$$+\nabla \cdot \frac{k}{\rho C_p} \nabla T + \frac{E_f}{\rho C_p} \Sigma_f \phi$$

## Neutronics (Monte Carlo)

$$(\mathbf{L}(T) - \mathbf{S}(T)) \phi = \frac{1}{k_{eff}} \mathbf{F}(T) \phi$$

# Neutronics – Thermal hydraulics coupling

Thermal hydraulics

$$T = \mathcal{T}(q)$$

CFD  
(OpenFOAM code)

Neutronics

$$q = \mathcal{N}(T)$$

Monte Carlo  
(Serpent code)

$T, \rho$

$q$

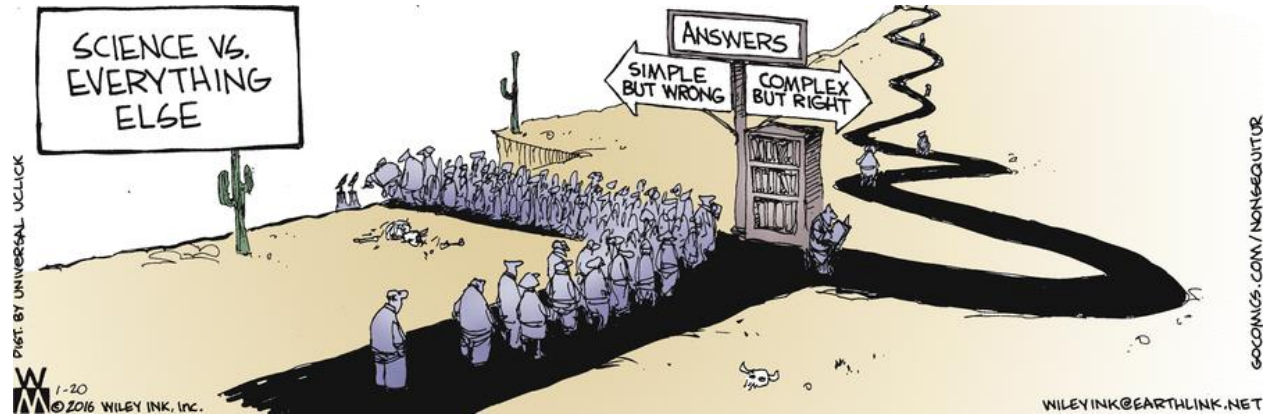
$$q = \mathcal{N}(\mathcal{T}(q)) = G(q)$$

The steady-state power distribution  $q$  is the fixed point of the coupled problem

$$q_{n+1} = G(q_n)$$

# Neutronics – Thermal hydraulics coupling

Easy (and wrong) way:  
use the brute force



Can the numerical (not the physical) coupling be unstable?

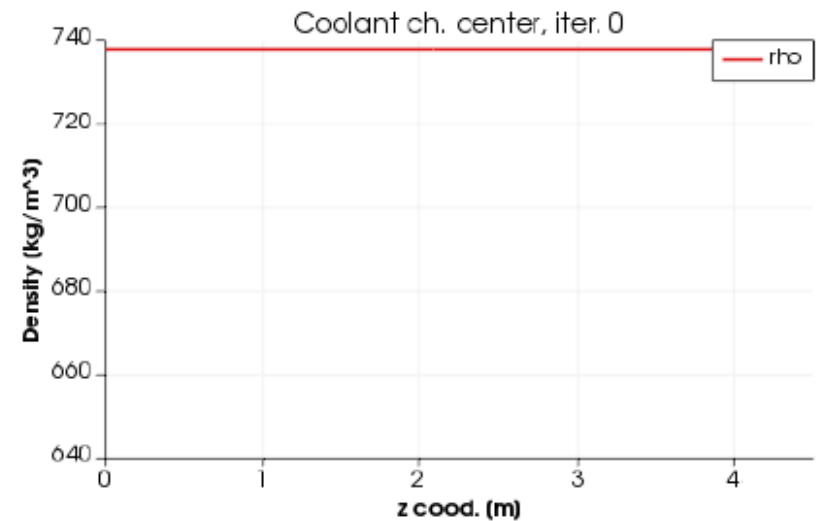
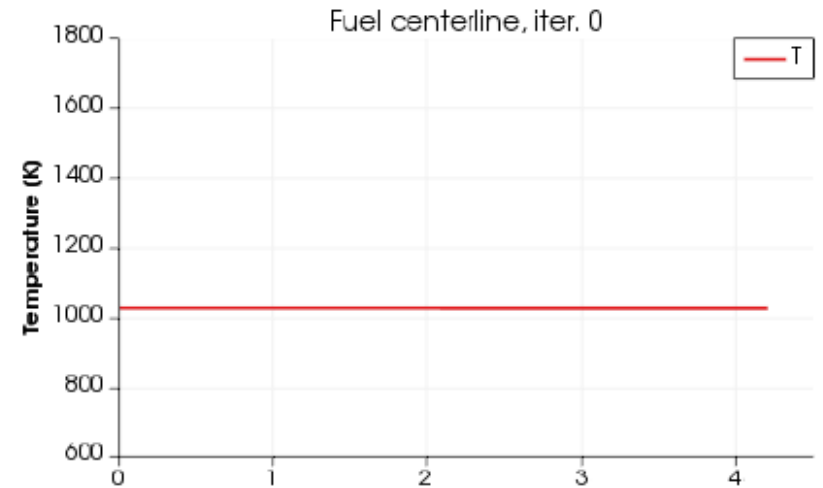
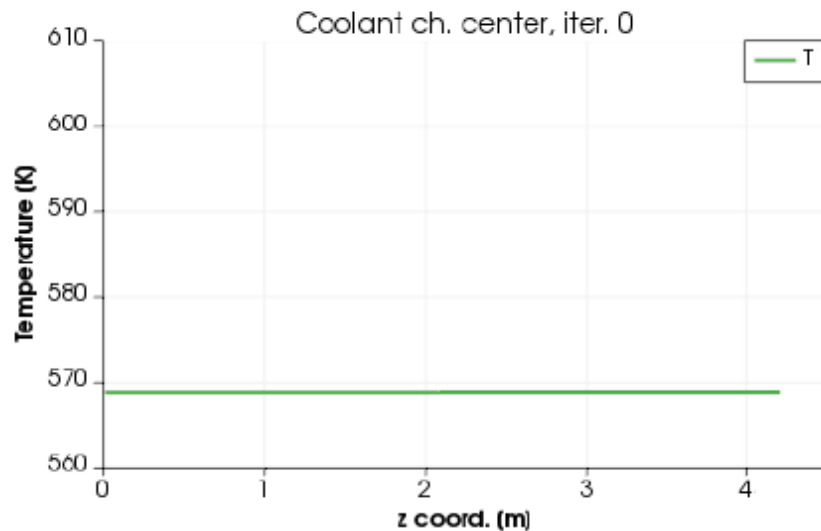
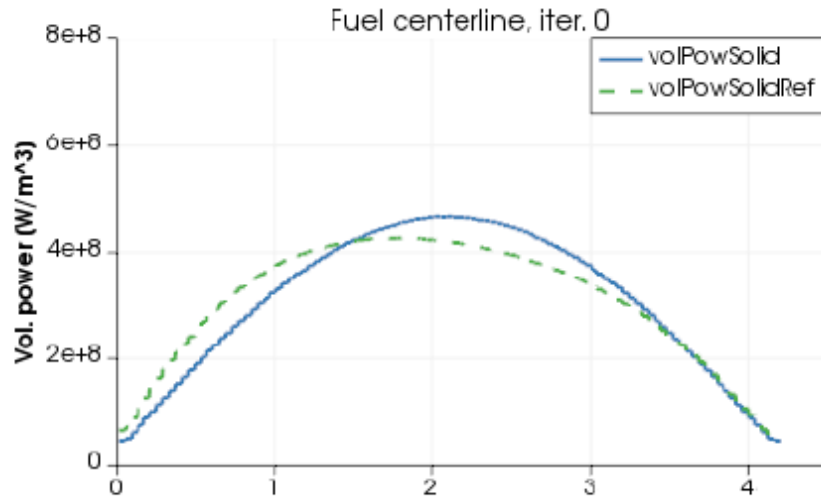
$$J_{i,j} = \frac{\partial G_i}{\partial q_j} \quad \rho(J) < 1 \quad \text{Stability condition}$$

Is numerical stability a problem for typical nuclear reactor problem?



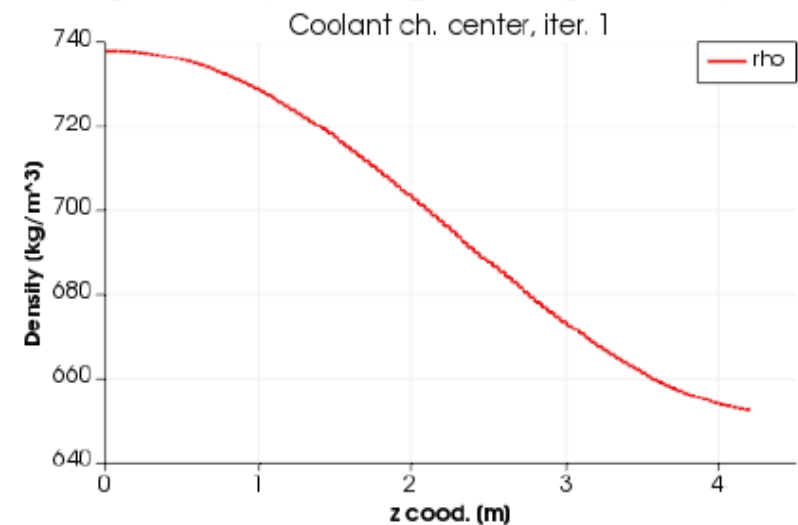
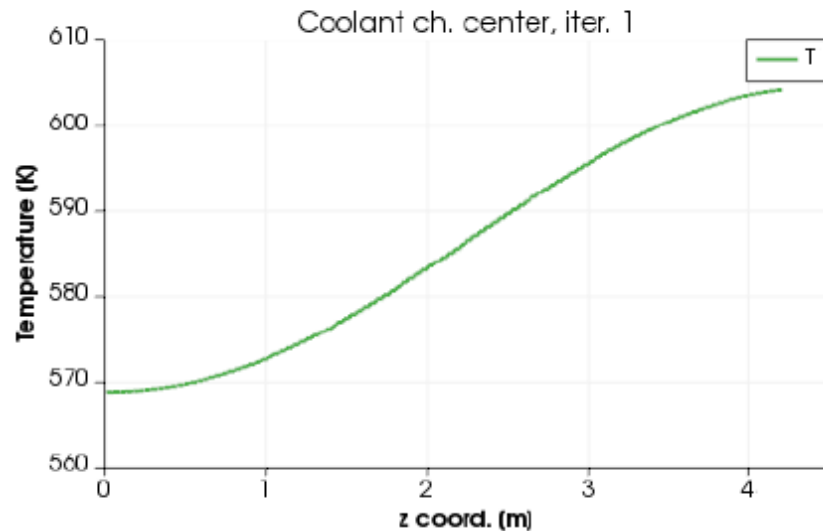
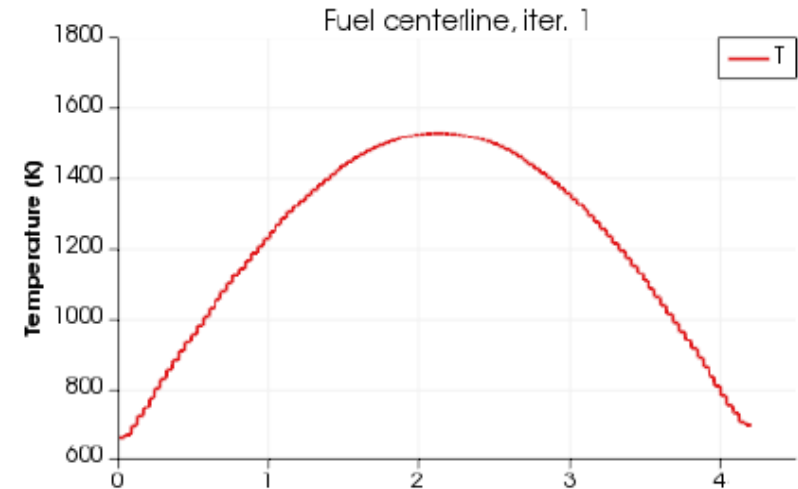
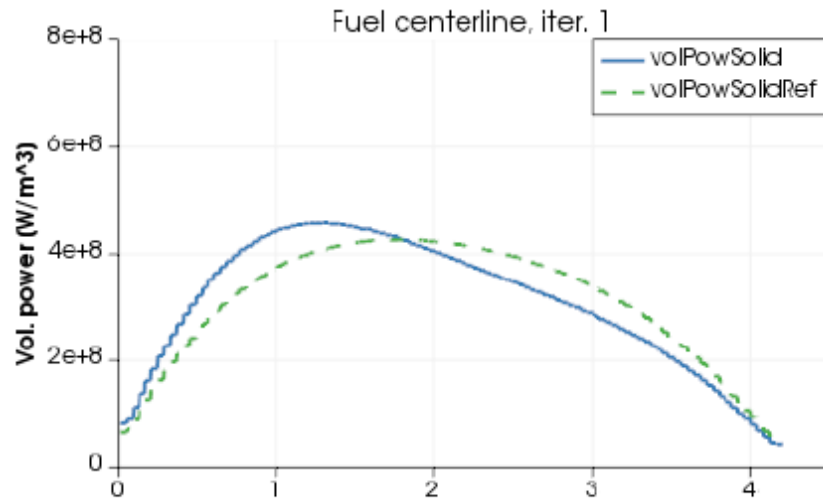
# Neutronics – Thermal hydraulics coupling

## EPR case – Iteration 0



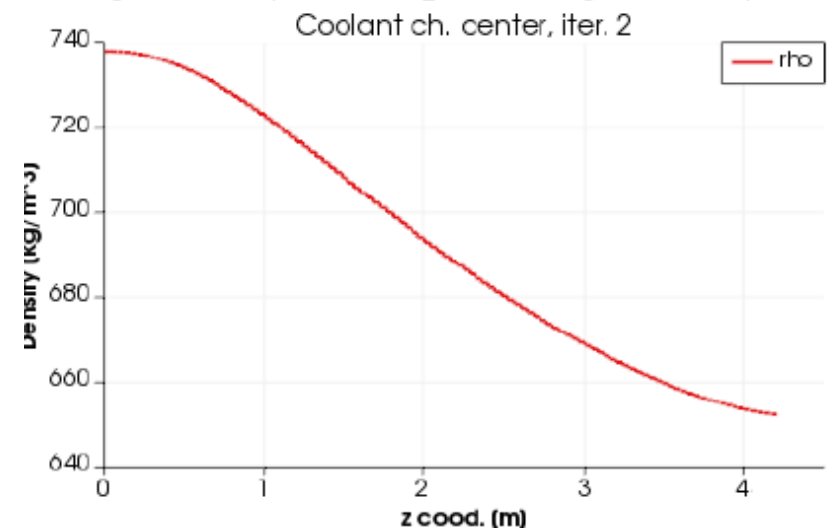
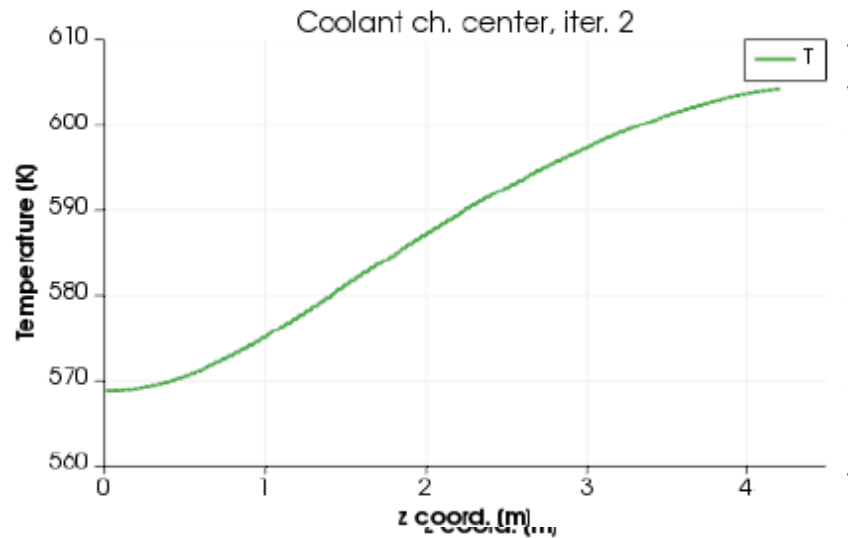
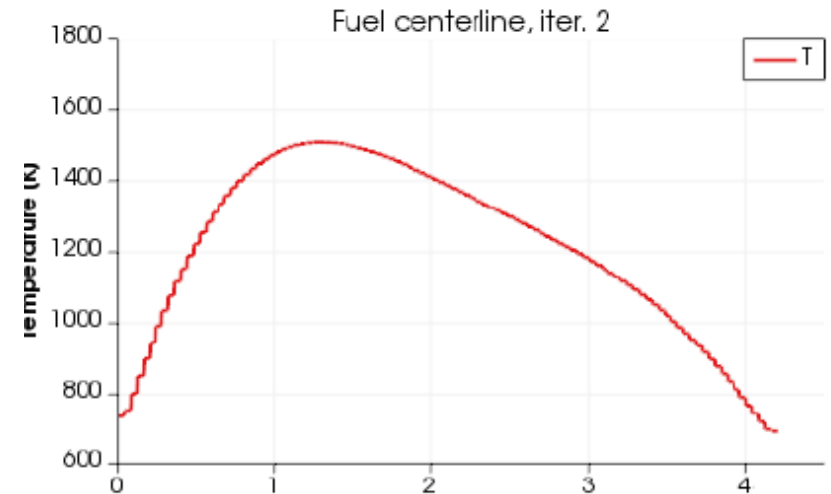
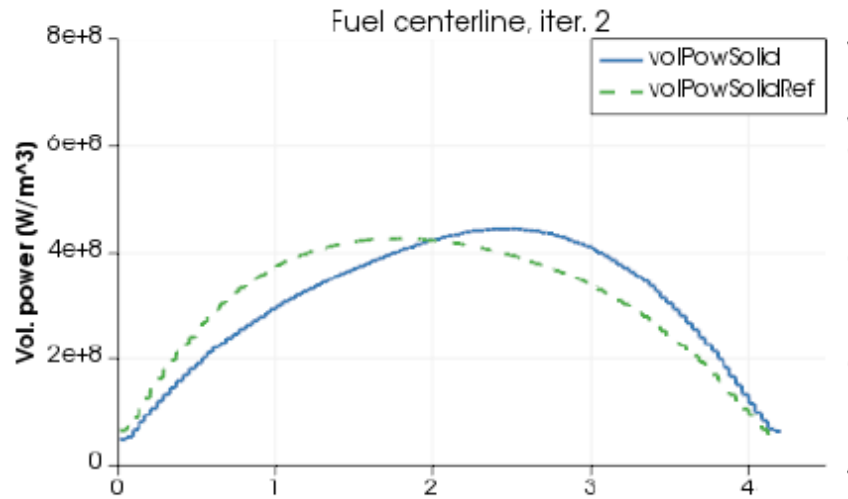
# Neutronics – Thermal hydraulics coupling

## EPR case – Iteration 1



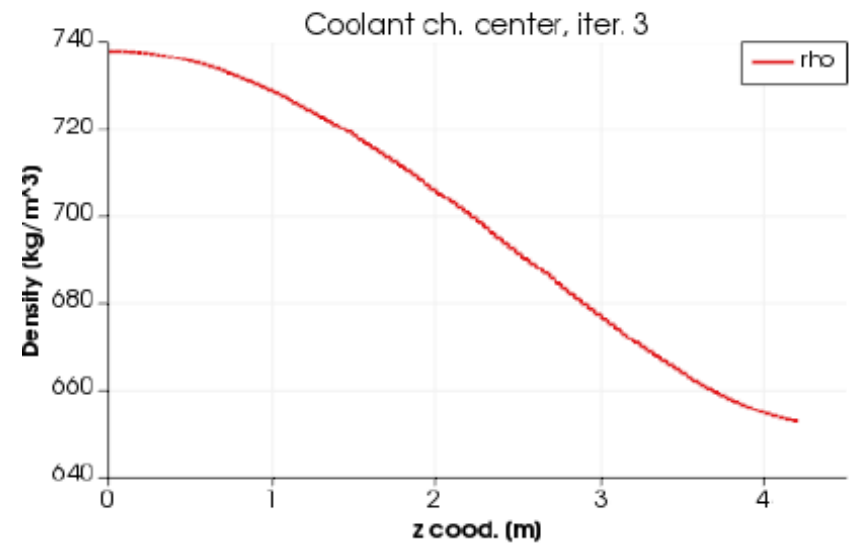
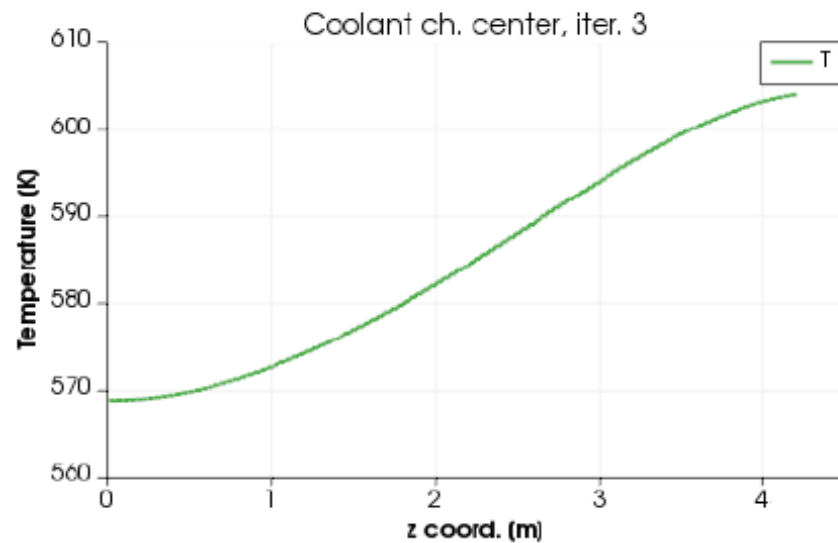
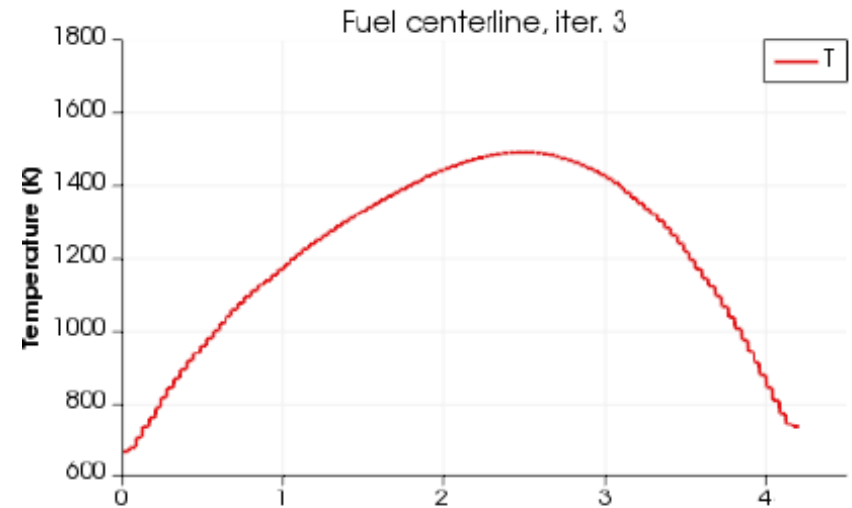
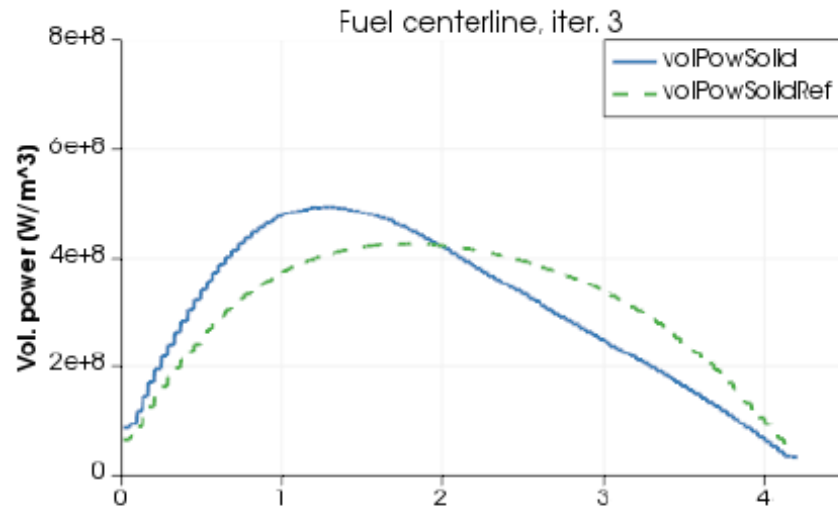
# Neutronics – Thermal hydraulics coupling

## EPR case – Iteration 2



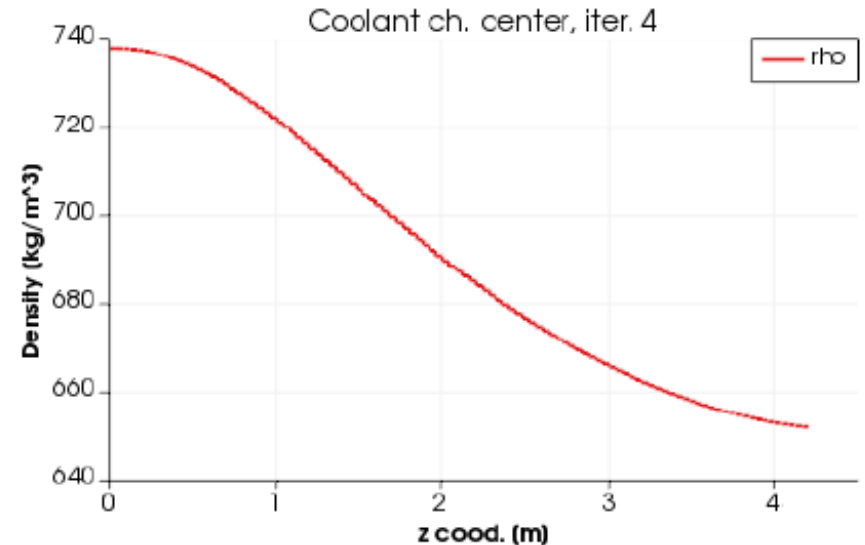
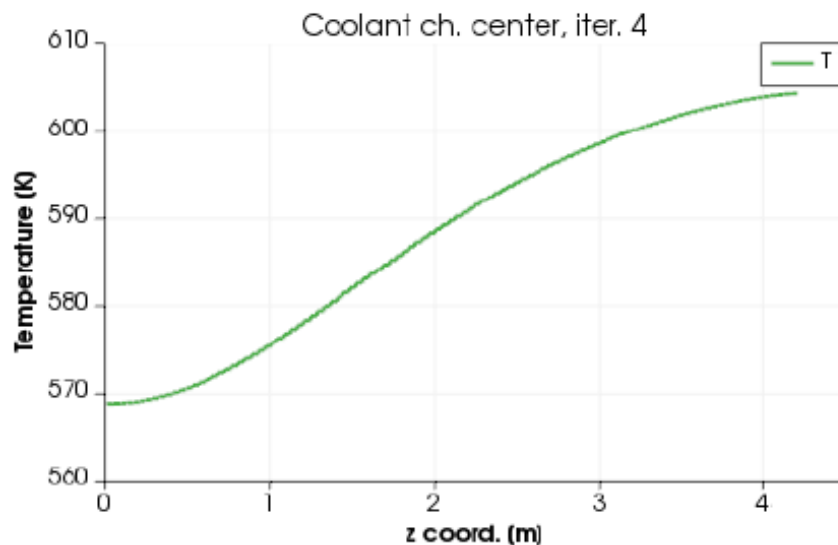
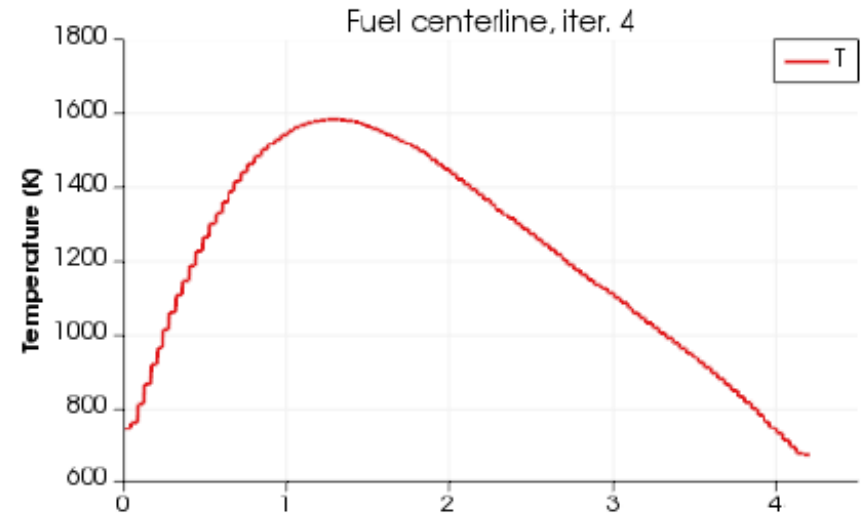
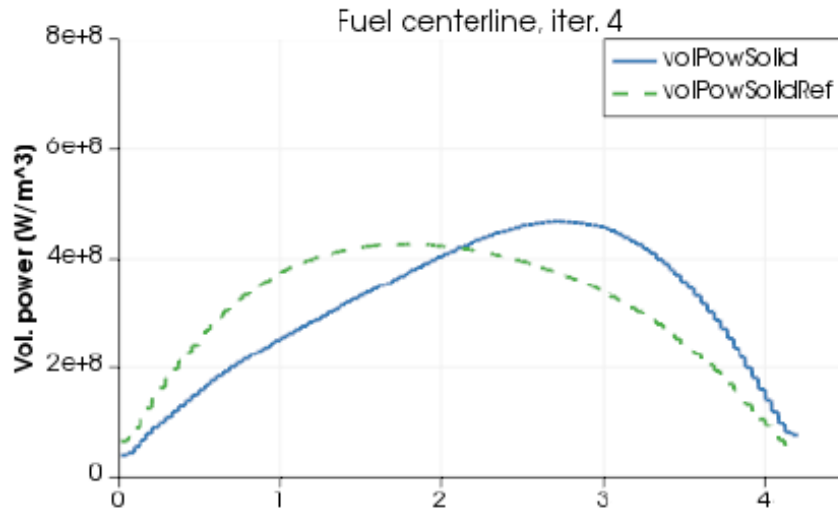
# Neutronics – Thermal hydraulics coupling

## EPR case – Iteration 3



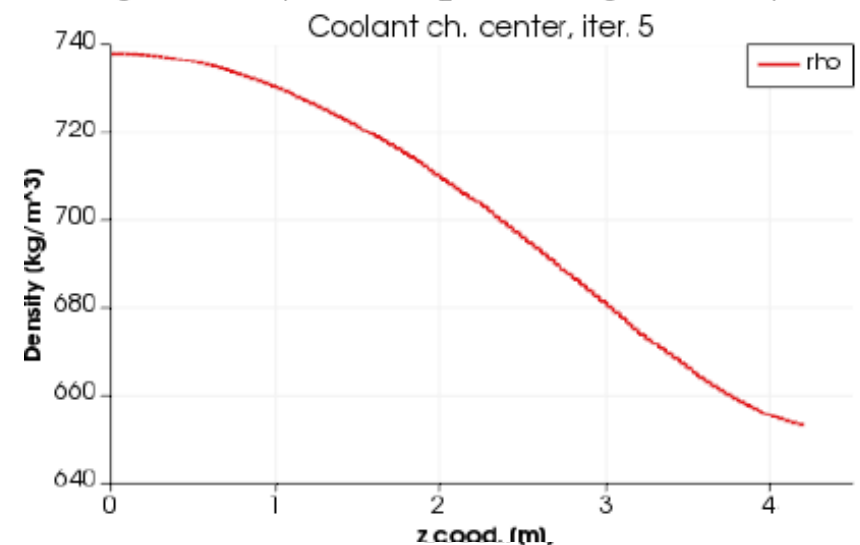
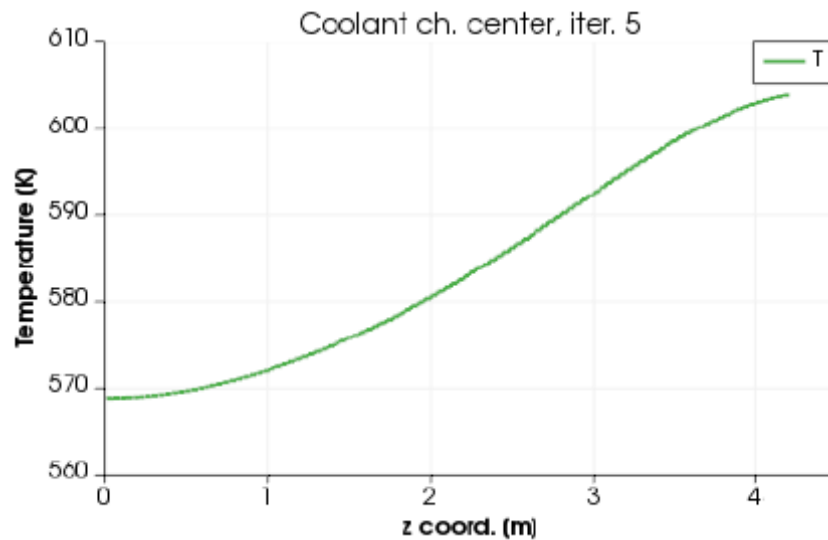
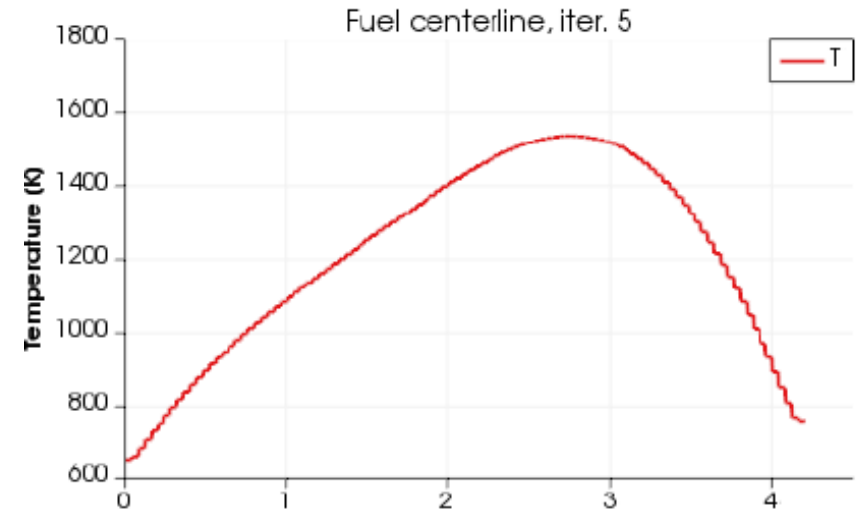
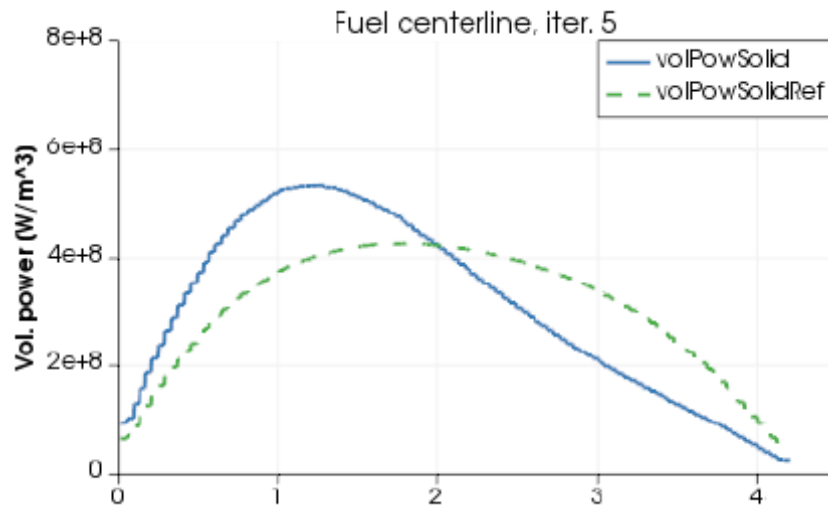
# Neutronics – Thermal hydraulics coupling

## EPR case – Iteration 4



# Neutronics – Thermal hydraulics coupling

## EPR case – Iteration 5



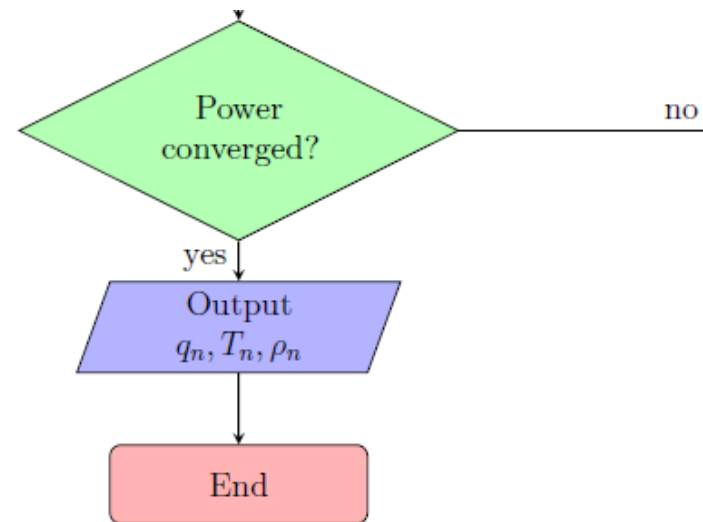
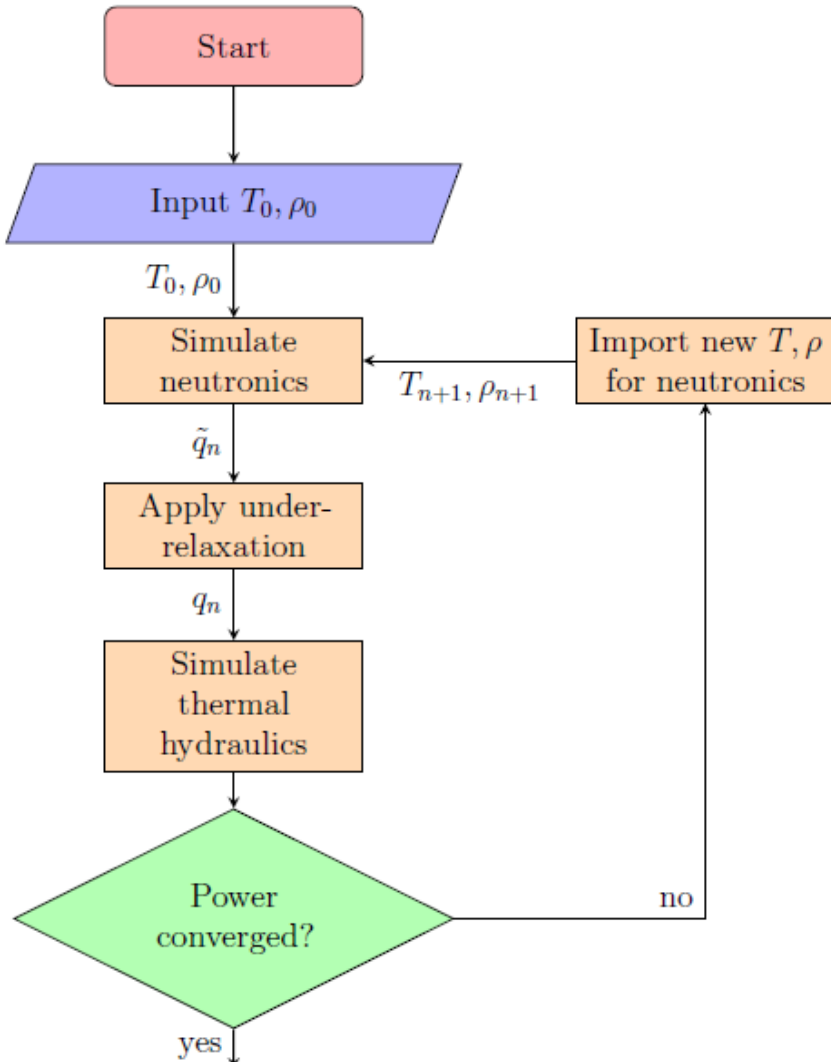
# Under relaxation techniques

Constant under relaxation factor

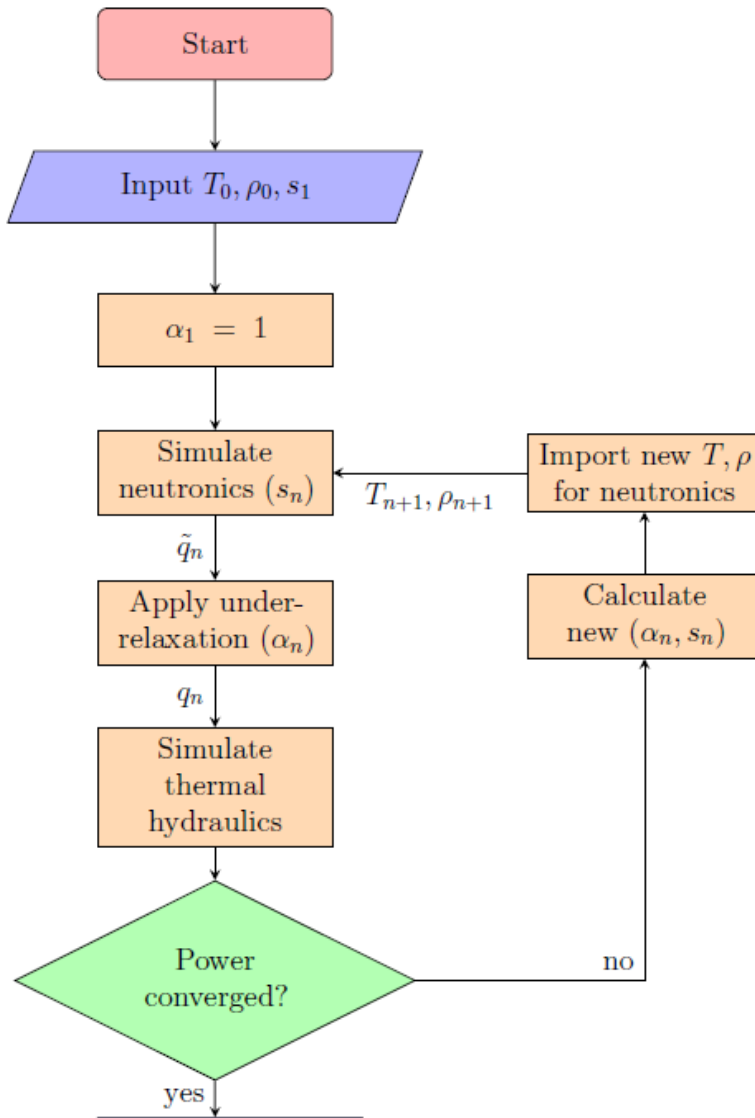
$$q^{(n+1)} = \alpha G(q^{(n)}) + (1 - \alpha)q^{(n)}, \quad 0 \leq \alpha \leq 1$$

Convergence criterion

$$\beta = \frac{\int_V |q_{n+1} - q_n| dV}{\int_V |q_n| dV} = \frac{\|q_{n+1} - q_n\|_{L^1}}{\|q_n\|_{L^1}}$$



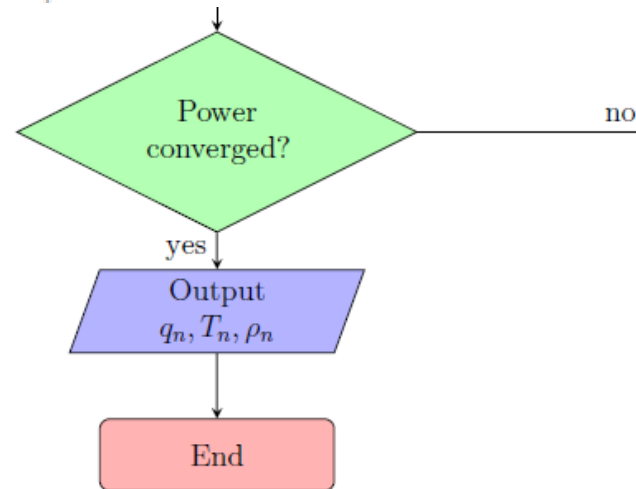
# Underrelaxation techniques



Stochastic approximation algorithm (Dufek, Gudowski)

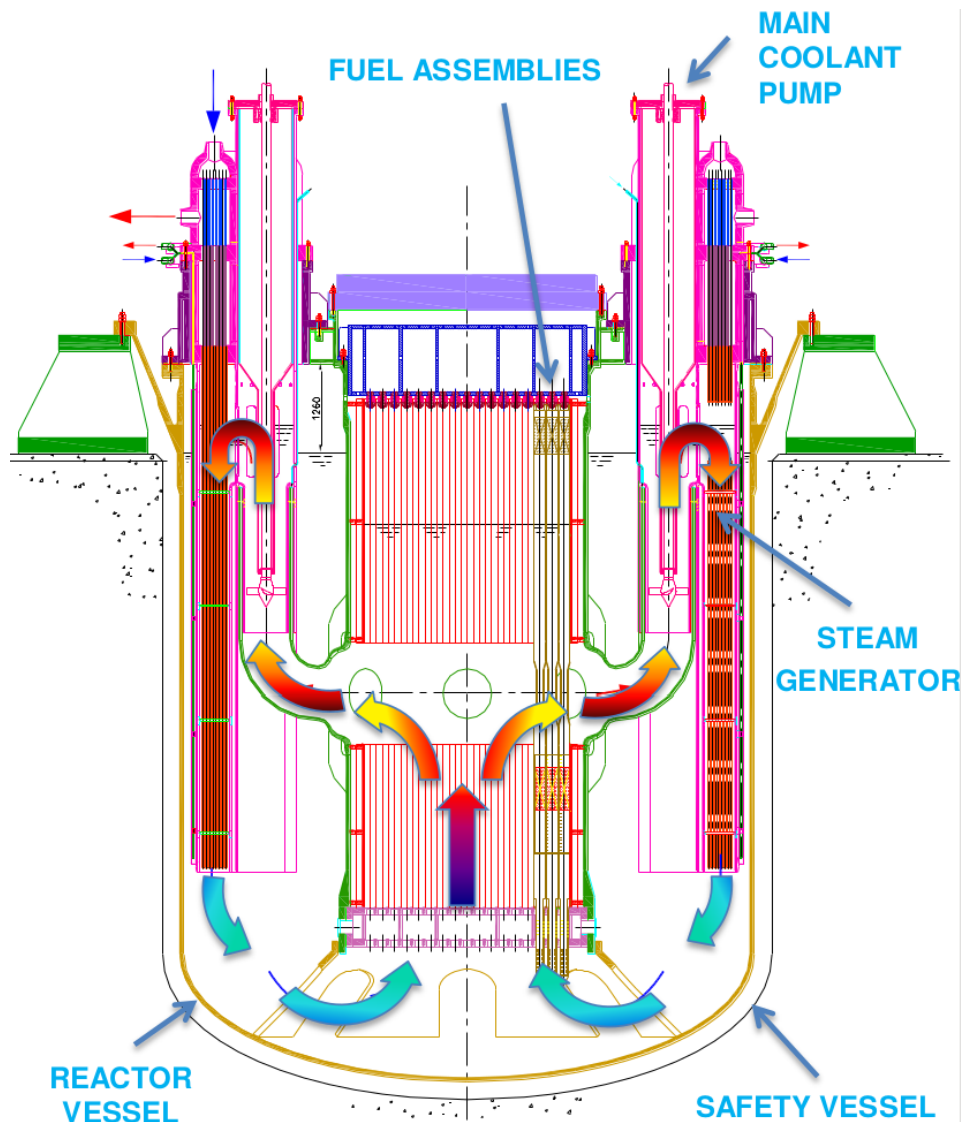
$$q^{(n+1)} = \alpha G(q^{(n)}) + (1 - \alpha)q^{(n)}, \quad 0 \leq \alpha \leq 1$$

$$\begin{cases} \alpha_n = \frac{s_n}{\sum_{i=1}^n s_i} \\ s_n = \frac{s_1 + \sqrt{s_1^2 + 4s_1 \sum_{i=1}^{n-1} s_i}}{2} \end{cases}$$





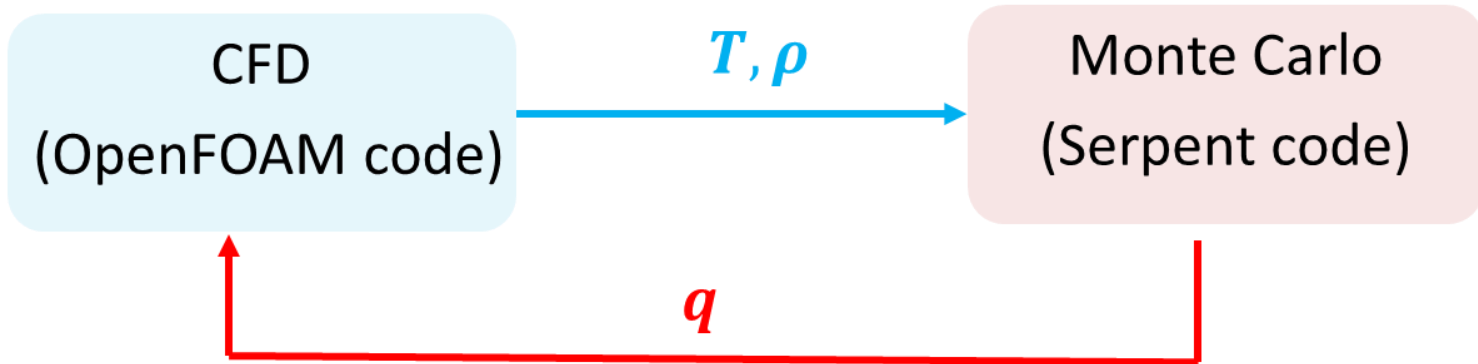
# Application to ALFRED reactor



- . Advanced Lead Fast Reactor European Demonstrator
- . 300 MW<sub>th</sub>
- . Pool reactor – 8 loops
- . Hexagonal FA
- . MOX fuel

# Application to ALFRED reactor

## PAR 2017 Monte Carlo – CFD coupling for ALFRED reactor

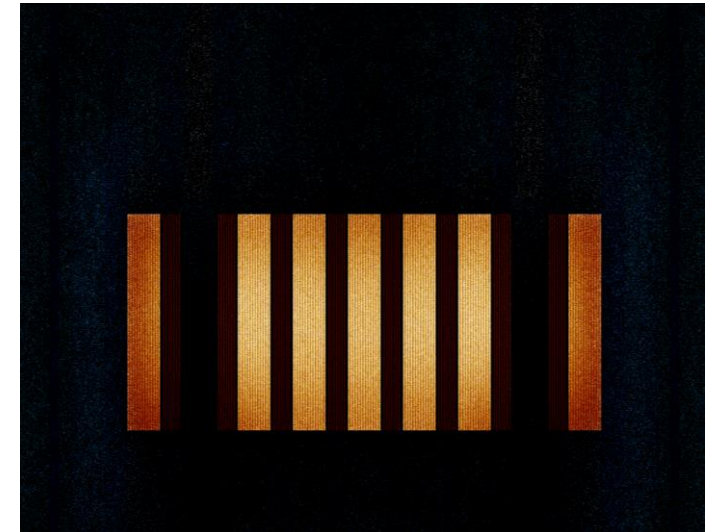
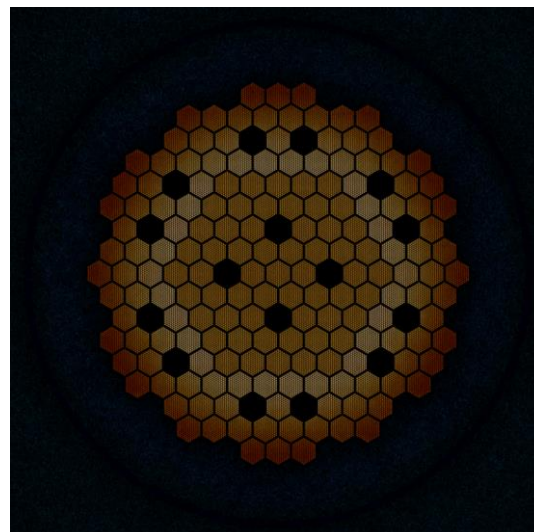
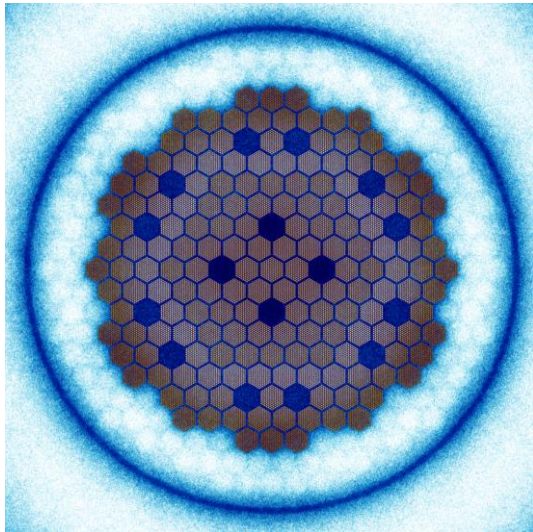
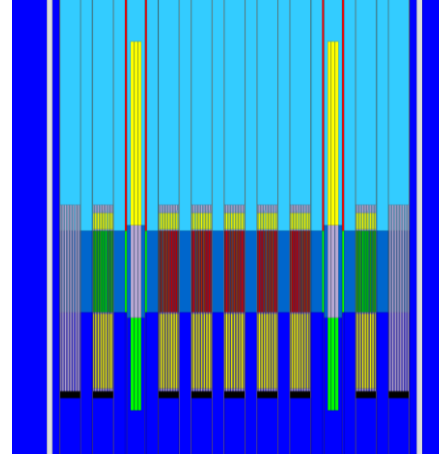
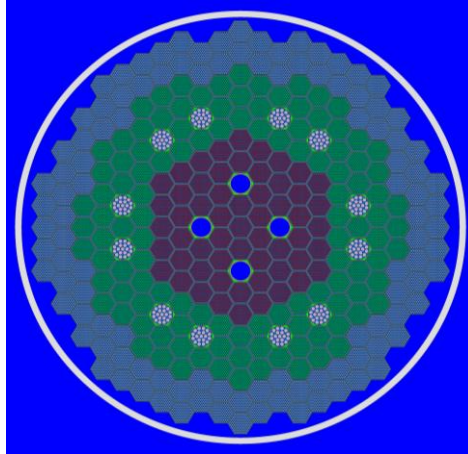


### Development step:

- 1) Creation of a full core Serpent model of ALFRED
- 2) Creation of a CFD model for the FA of ALFRED
  - a) 1/12 of FA (done)
  - b) Entire FA (ongoing collaboration with PoliTo)
- 3) Coupling between the two models
  - a) 1/12 of FA (done)
  - b) Entire FA (ongoing collaboration with PoliTo)

# Full core Serpent model

Monte Carlo model of the ALFRED reactor



# Full core Serpent model

| Parameter                                | SERPENT | ERANOS <sup>1</sup> | MCNPX <sup>1</sup> |
|--|---------|---------------------|--------------------|
| Max power in FA (MW)                     | 2.25    | 2.42                | 2.21               |
| Total worth of 12 CRs (pcm)              | -8511   | -9100               | -8500              |
| Total worth of 4 SRs (pcm)               | -2957   | -3700               | -3300              |
| Effective delayed neutron fraction (pcm) | 336     | 336                 | -                  |

| Parameter   | SERPENT | Uncertainty ( $\sigma$ ) | ERANOS <sup>1</sup> |
|---|---------|--------------------------|---------------------|
| Doppler constant (pcm)                                    | -580    | 18.219                   | -555                |
| Lead expansion coefficient (pcm/K) 1 <sup>st</sup> method | -0.282  | 0.113                    | -0.271              |
| Lead expansion coefficient (pcm/K) 2 <sup>nd</sup> method | -0.302  | 0.019                    | -0.271              |
| Axial fuel expansion (pcm/K)                              | -0.153  | 0.006                    | -0.148              |
| Axial cladding expansion (pcm/K)                          | 0.044   | 0.006                    | 0.037               |
| Grid expansion (pcm/K)                                    | -0.766  | 0.007                    | -0.762              |
| Axial wrapper expansion (pcm/K)                           | 0.036   | 0.006                    | 0.022               |

<sup>1</sup> Grasso, G., Petrovich, C., Mattioli, D., Artioli, C., Sciora, P., Gugiu, D., Bandini, G., Bubelis, E., Mikityuk, K., 2014. The core design of ALFRED, a demonstrator for the European lead-cooled reactors. Nuclear Engineering and Design 278, 287-301.



## Conjugate Heat Transfer multi region model

Fluid (Lead) |  $k - \varepsilon$  model

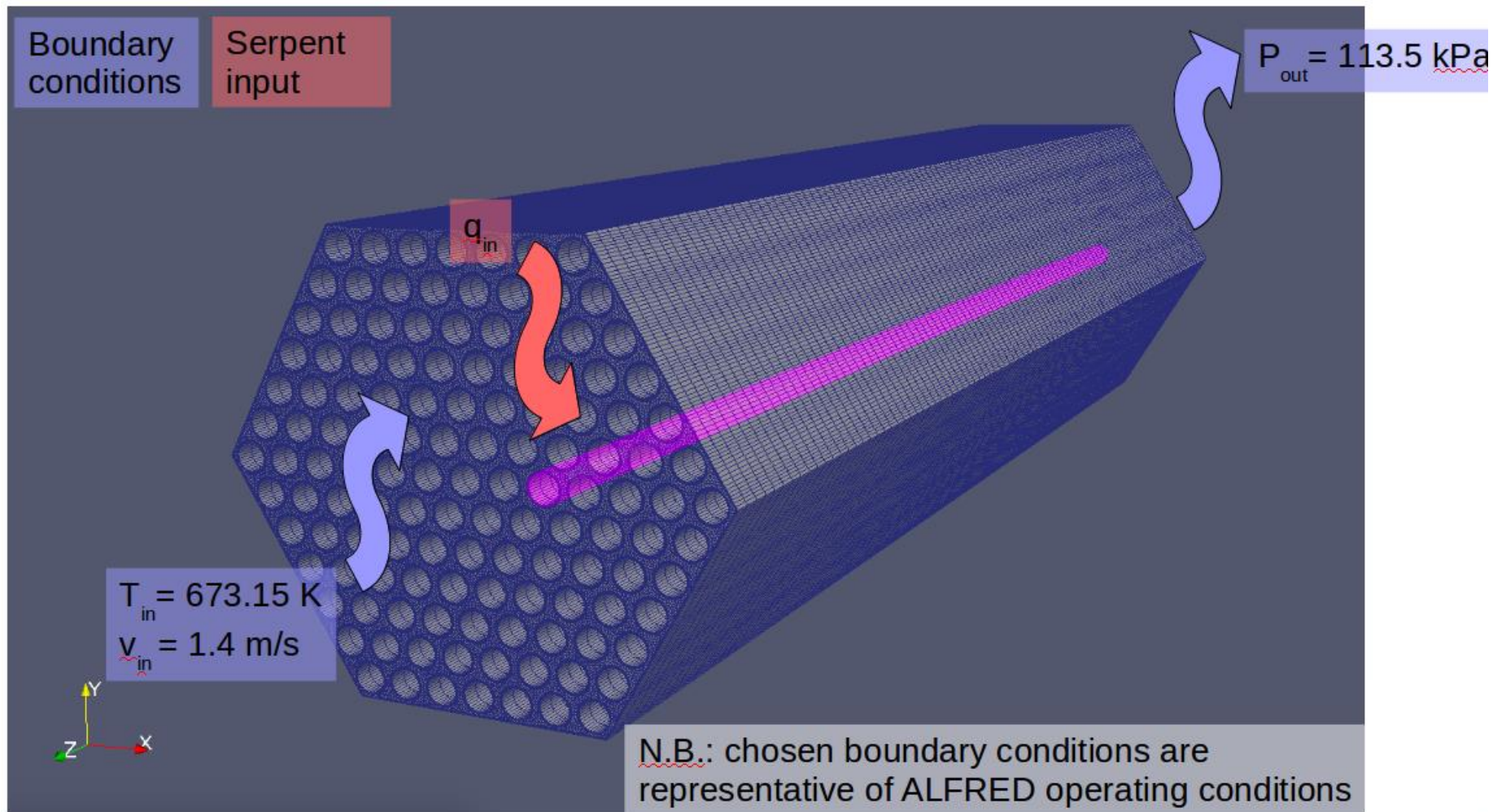
$$\begin{cases} \mathbf{u}_t + (\mathbf{u} \cdot \nabla)\mathbf{u} = \nabla \cdot \left[ -p\mathbf{I} + (\nu + \nu_t)(\nabla\mathbf{u} + (\nabla\mathbf{u})^T) - \frac{2}{3}k\mathbf{I} \right] \\ \nabla \cdot \mathbf{u} = 0 \\ \frac{\partial k}{\partial t} + (\mathbf{u} \cdot \nabla)k = \nabla \cdot \left[ \left( \nu + \frac{\nu_T}{\sigma_k} \right) \nabla k \right] - \varepsilon + P \\ \frac{\partial \varepsilon}{\partial t} + (\mathbf{u} \cdot \nabla)\varepsilon = \nabla \cdot \left[ \left( \nu + \frac{\nu_T}{\sigma_\varepsilon} \right) \nabla \varepsilon \right] - C_{2\varepsilon} \frac{\varepsilon^2}{k} \nu_T + 2C_{1\varepsilon} \frac{\varepsilon}{k} \nu_T P \end{cases}$$

Solid (Fuel) | Heat conduction

$$\rho_F C_{p,F} \frac{\partial T_f}{\partial t} = \nabla \cdot (K_F \nabla T) + Q_f + Q_{decay}$$

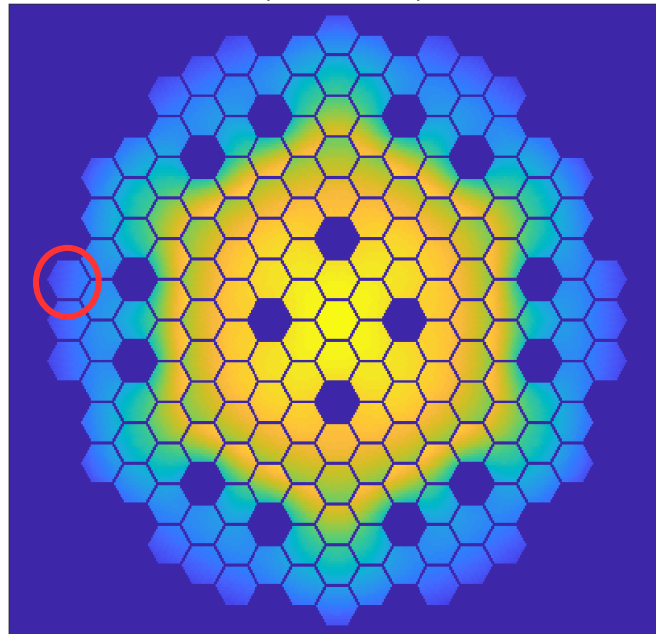
# CFD OpenFoam model for ALFRED

ALFRED FA – CFD analysis (collaboration with PoliTo, E. Guadagni MSc thesis and G. F Nallo PhD activity)



# CFD OpenFoam model for ALFRED

ALFRED FA – CFD analysis (collaboration with PoliTo, E. Guadagni MSc thesis and G. F Nallo PhD activity)



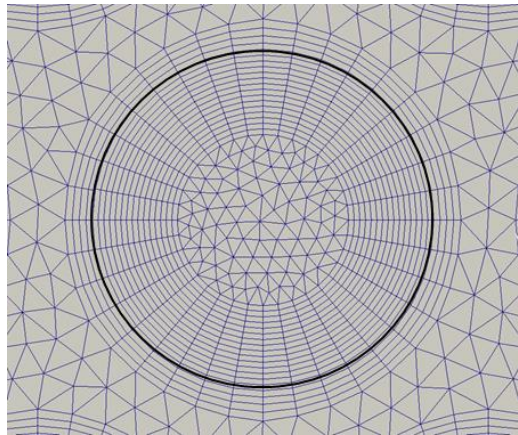
One specific FA, placed near the border of the reactor, was chosen for the CFD calculations due to its strongly asymmetric power distribution, evaluated with a preliminary Serpent neutronic simulation (one way coupling)



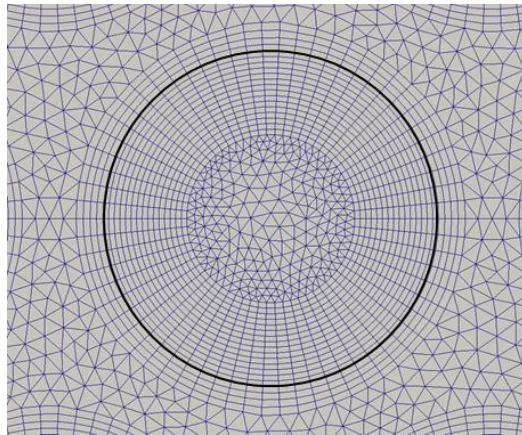
# CFD OpenFoam model for ALFRED

**ALFRED FA – CFD analysis (collaboration with PoliTo, E. Guadagni MSc thesis and G. F Nallo PhD activity)**

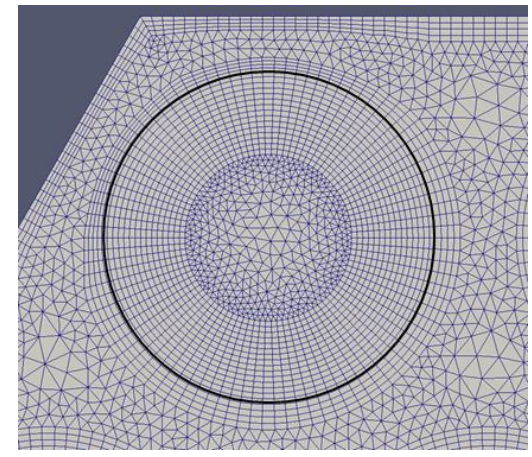
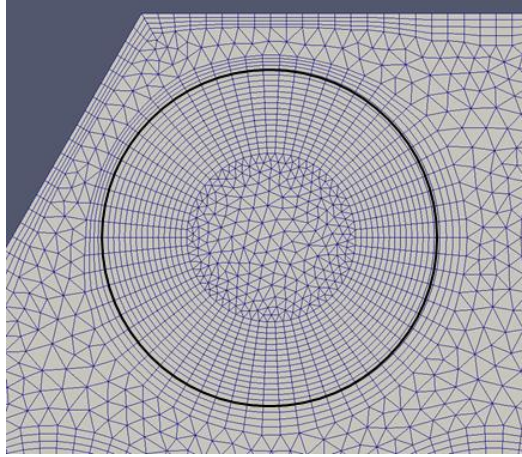
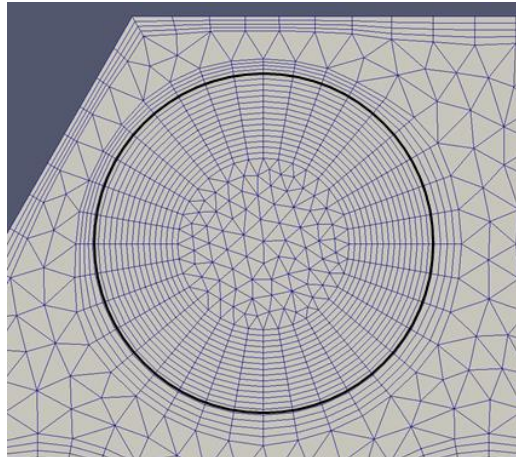
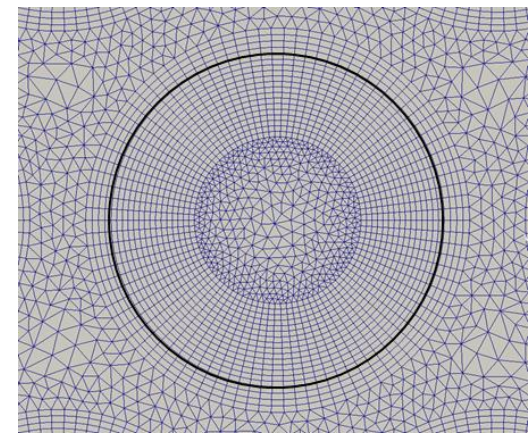
Mesh #1 (coarsest)



Mesh #2 (medium)

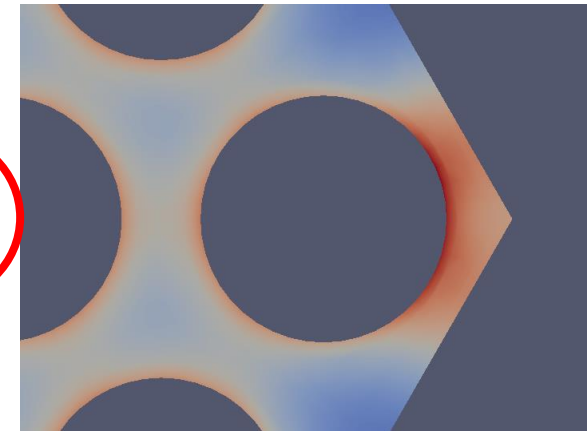
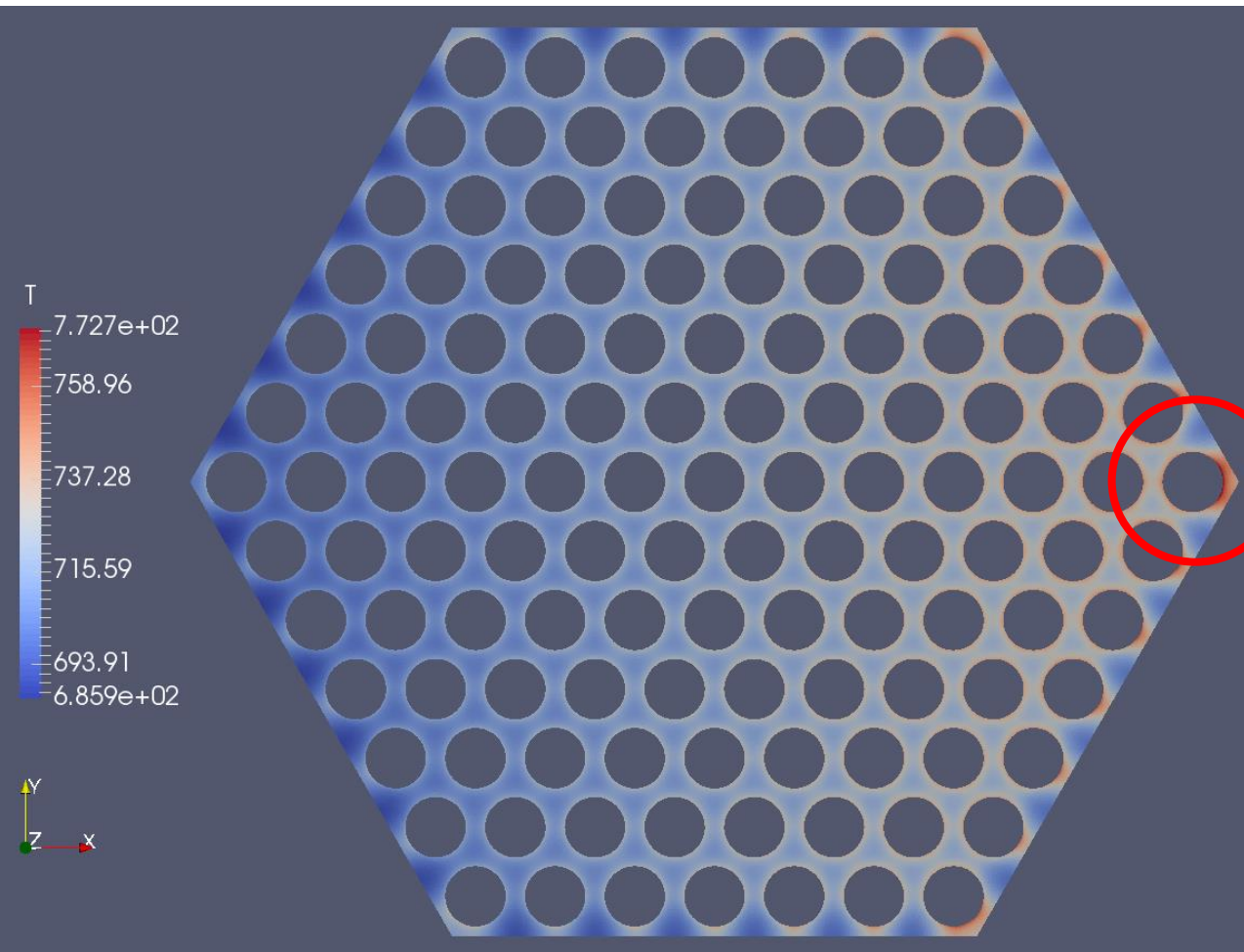


Mesh #3 (finest)



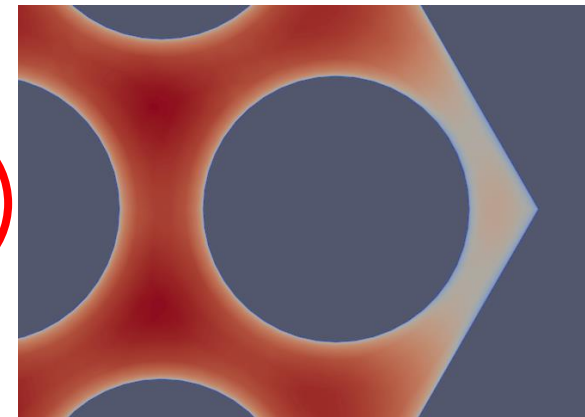
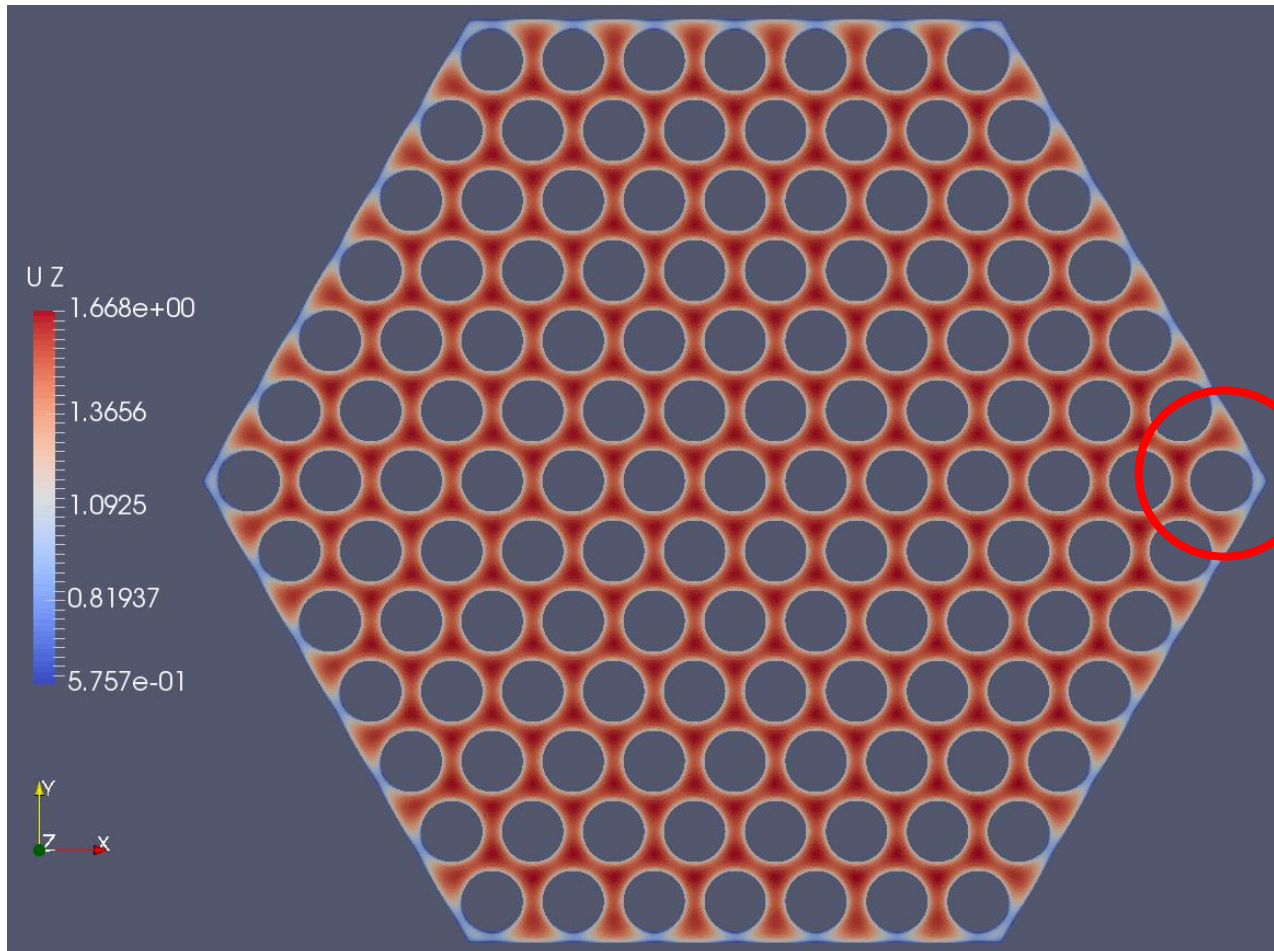
# CFD OpenFoam model for ALFRED

ALFRED FA – CFD analysis (collaboration with PoliTo, E. Guadagni MSc thesis and G. F Nallo PhD activity)



# CFD OpenFoam model for ALFRED

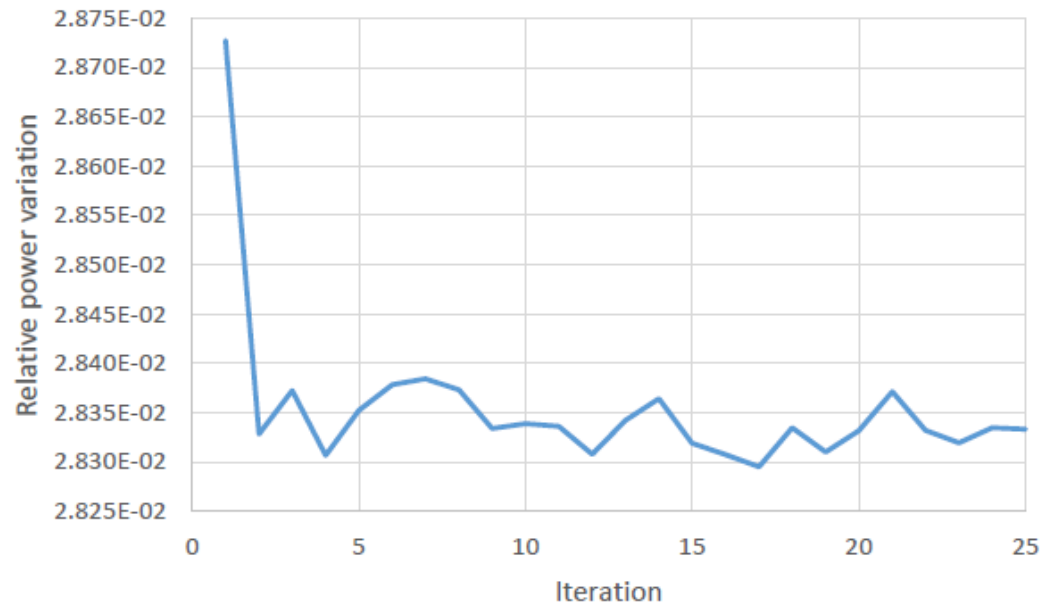
ALFRED FA – CFD analysis (collaboration with PoliTo, E. Guadagni MSc thesis and G. F Nallo PhD activity)



# Monte Carlo – CFD coupling

## ALFRED 1/12 central FA – Monte Carlo - CFD coupling

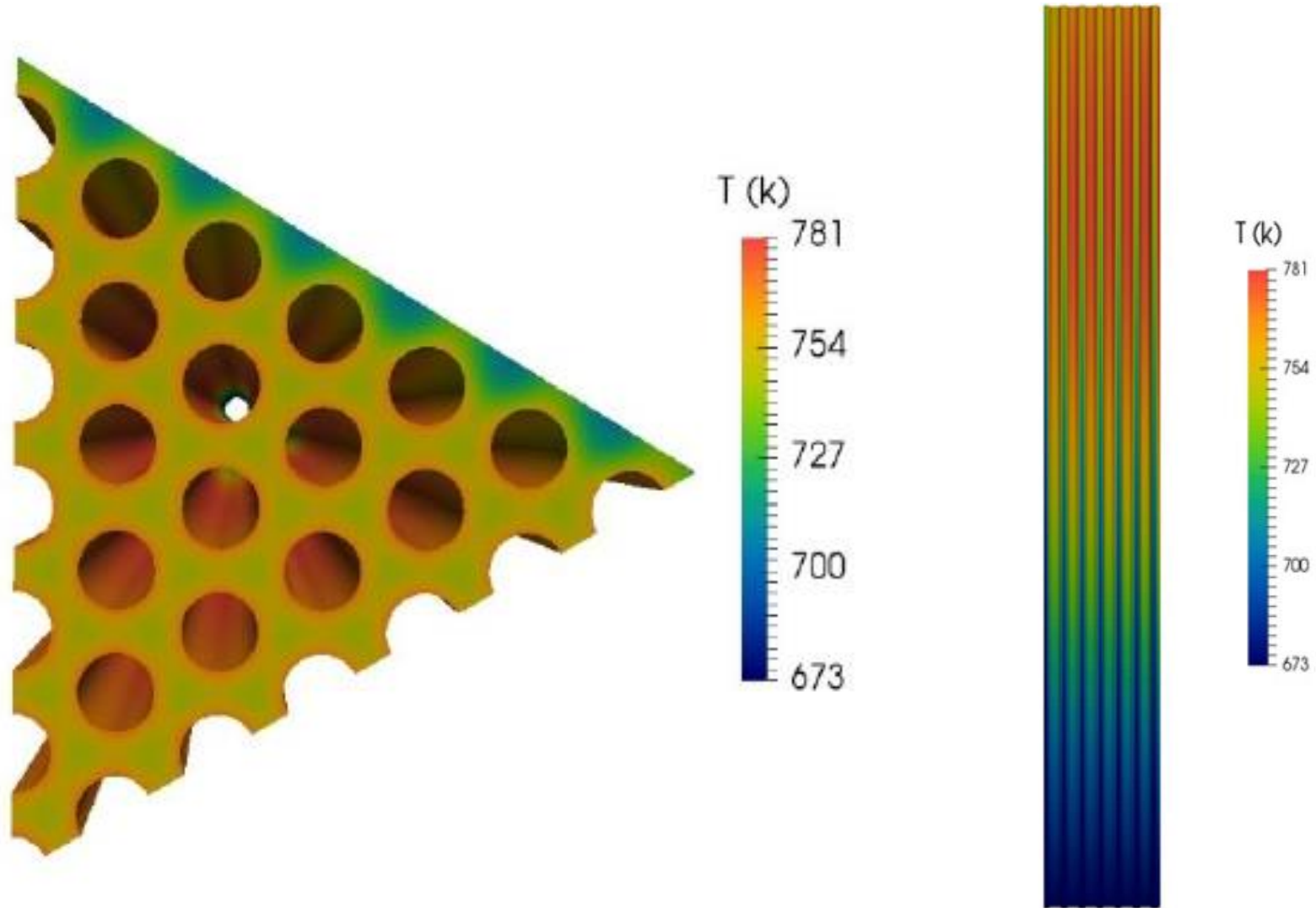
- . Serpent/OF coupling managed by an **external proxy file**
- . The simulation starts with a Serpent run to obtain the volumetric power distribution, which is then **translated into the OpenFOAM input file**
- . Temperature and density for fuel and coolant are calculated by OpenFOAM and they are passed to the next Serpent run using the **multi-physics interface**



- . The procedure iterates **until convergence is reached** (constant under relaxation factor and stochastic approximation algorithm available)

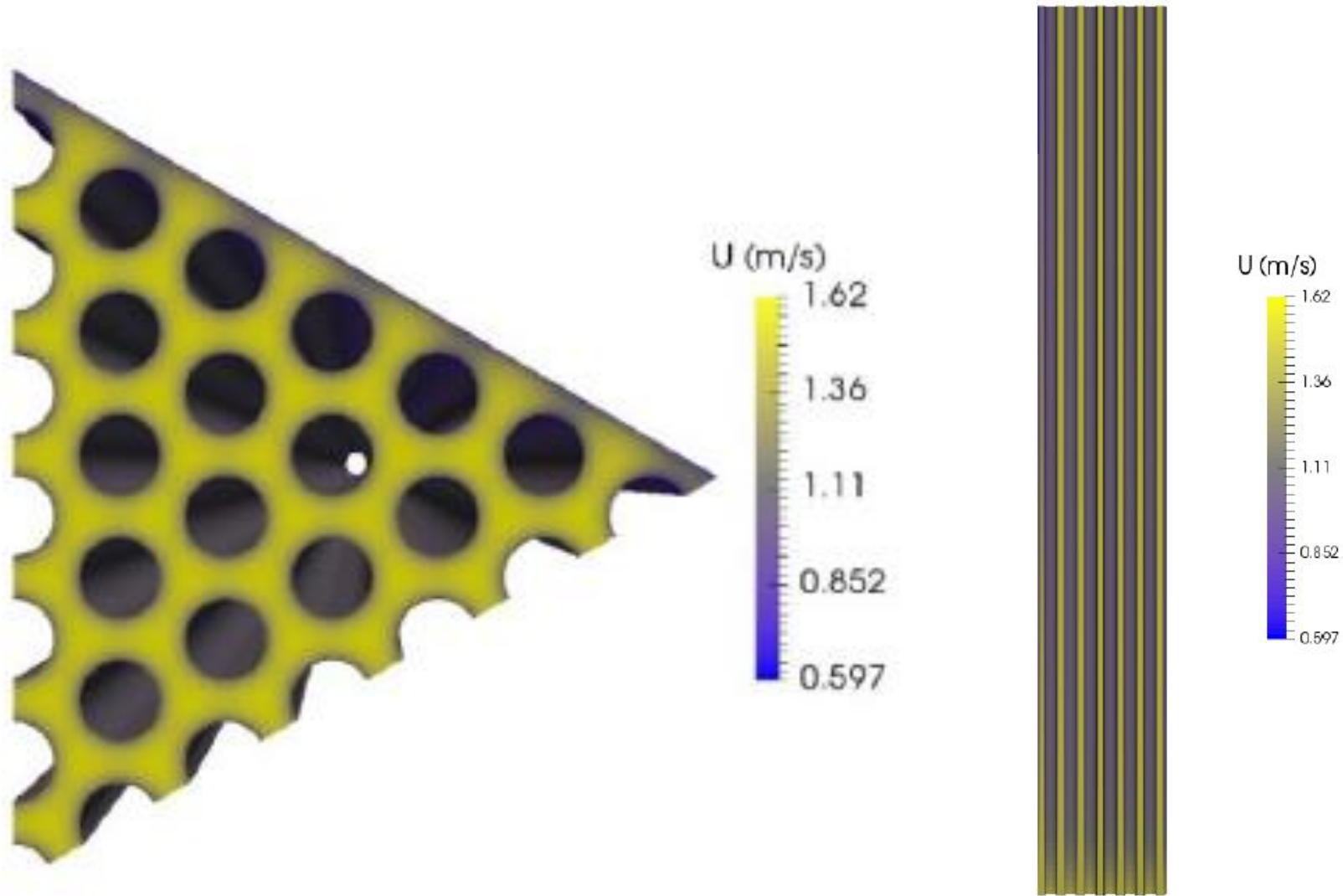
# Monte Carlo – CFD coupling

## ALFRED 1/12 central FA – Monte Carlo - CFD coupling



# Monte Carlo – CFD coupling

## ALFRED 1/12 central FA – Monte Carlo - CFD coupling



# Conclusions and future developments

## Ongoing activities

- . Finalization of coupling with entire FA
- . Analysis of the impact of the neutronics - thermal hydraulics coupling (difference between one way and two ways coupling)

## Conclusions and future developments

- . The activity is the step forward for the development of a multi-physics code for lead-cooled fast reactor aimed at supporting both the design choice and the verification of other numerical tools
- . Monte Carlo – CFD coupling for a better accuracy in neutronics modelling (relevant for design support) for ALFRED reactor
- . Near-term efforts focus on efficient use of the available computational resources (i.e., parallelization, optimization) and easy modification of the modelling description with OpenFOAM to develop a multi-physics platform



PoliMi is glad to announce the **International Seminar on Nuclear Reactor Core Thermal Hydraulics Analysis**

**Lecco, August 29 - 31**

Forum on the nuclear reactor core and fuel assembly thermal hydraulics analysis, by professionals for young professionals and students

**Organizer:** Prof. H. Ninokata

**TPC:** E. Baglietto, N. Toderas, E. Merzari, BW. Yang, F. Roelofs, Y. Hassan, H-M Prasser

<https://www.eko.polimi.it/index.php/rectha/rectha>



# Opener – Milano, September 3 – 7, 2018



PoliMi and Milano  
Multiphysics are glad to  
announce the first  
summer school on  
**OpenFOAM for  
multiphysics modeling of  
Nuclear Reactors**  
**Milano, September 3 - 7**

The students will be guided through a full multi-physics modeling (front lectures and tutorial) of a nuclear reactor, how to tailor the available OpenFOAM CFD solvers to the needs of nuclear reactor analysis, how to create new solvers for neutronics, and how to couple OpenFOAM to a Monte Carlo code like Serpent.

<https://www.eventbrite.it/e/opener-openfoam-for-multiphysics-modeling-of-nuclear-reactors-registration-42198523921>



*Thank you for attention*



**POLITECNICO  
MILANO 1863**



**Nuclear  
NR  
Reactors  
Group**



*ALFRED Design Analysis  
by FRENETIC code*

**FRENETIC benchmark activity  
based on comparison to coupled  
Serpent/OpenFoam simulations  
for the ALFRED design**

G.F. Nallo<sup>1</sup>, E. Guadagni<sup>1,2</sup>, S. Dulla<sup>1</sup>, N. Abrate<sup>1</sup>,  
P. Ravetto<sup>1</sup>, L. Savoldi<sup>1</sup>, R. Zanino<sup>1</sup>,  
S. Lorenzi<sup>2</sup>, A. Cammi<sup>2</sup>

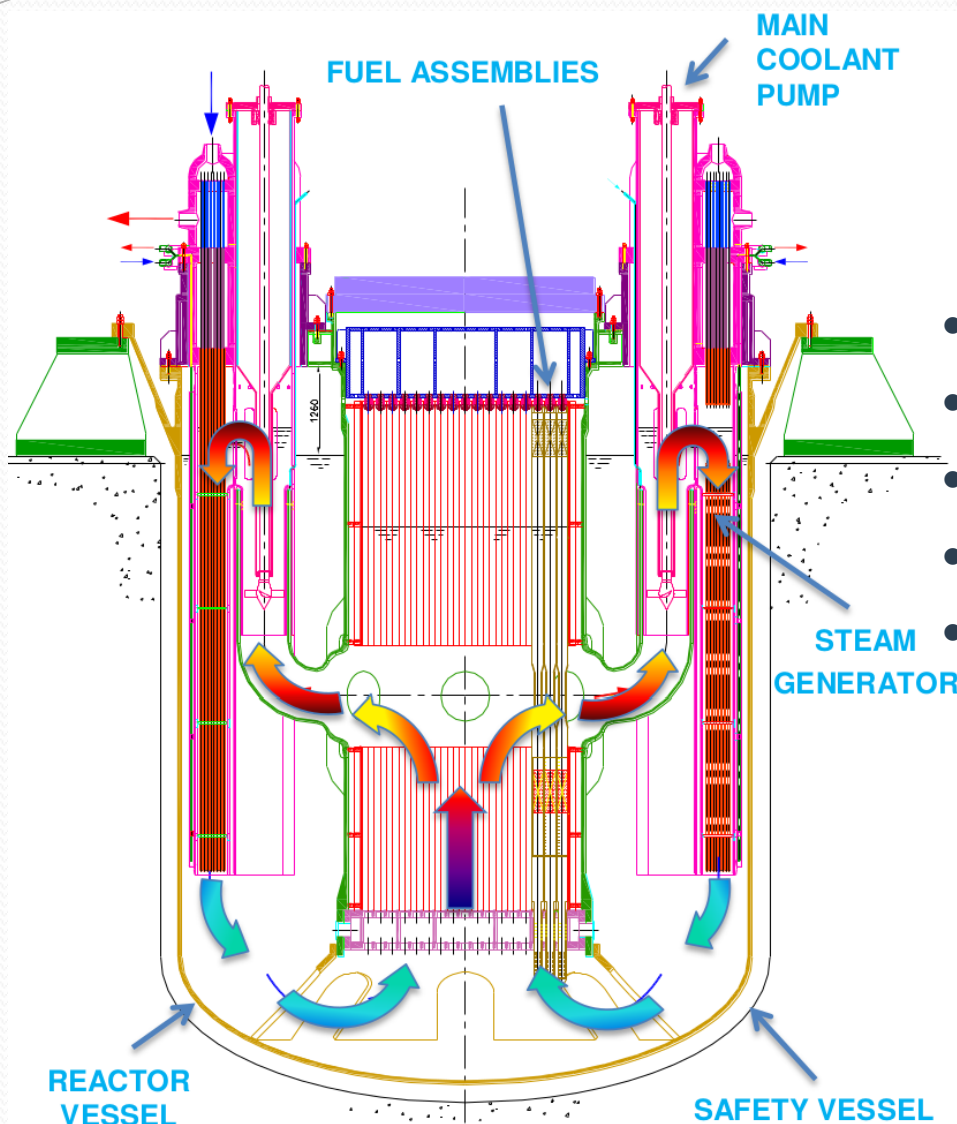
<sup>1</sup>*Politecnico di Torino, Italy*

<sup>2</sup>*Politecnico di Milano, Italy*

# Outline

- The ALFRED design
- The FRENETIC code
  - Neutronic module
  - Thermal-hydraulic module
  - Coupling strategy and feedback
- FRENETIC - Serpent/OpenFoam interaction
  - Use of FRENETIC to upgrade the Serpent code calculation
  - Use of FRENETIC to provide BC to OpenFoam
  - Comparison of FRENETIC and Serpent/OpenFoam results
- Conclusions and perspectives

# The ALFRED design

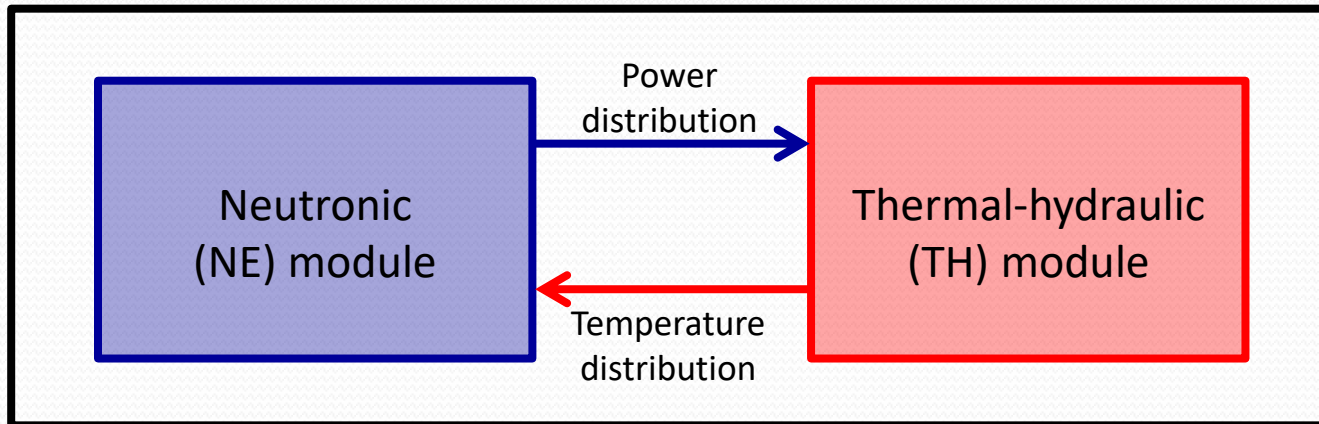


- 300 MWth LFR
- Forced/natural circulation
- MOX fuel
- Hexagonal Fuel Assemblies (FA)
- Two different enrichment zones

A. Alemberti, ALFRED presentation,  
*Education Training Seminar on Fast Reactors  
 Science and Technology at ITESM Campus  
 Santa Fe, Mexico City, 2015*

# FRENETIC

- **Fast REactor NEutronics/Thermal-hydraulICS** code for full-core coupled analyses of fast reactors with liquid-metal coolant [R. Bonifetto et al., Nucl. Eng. Des., 2013]

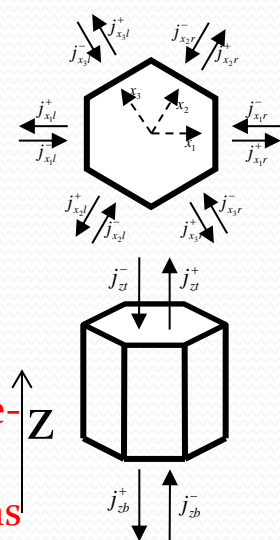


- **Principal objective:** computationally efficient, multiphysics analyses suitable for design and safety studies
- **Preliminary validation** of coupled code on EBR-II experimental data [D. Caron et al., Int. J. Energy Res., 2016]

# FRENETIC-NE module

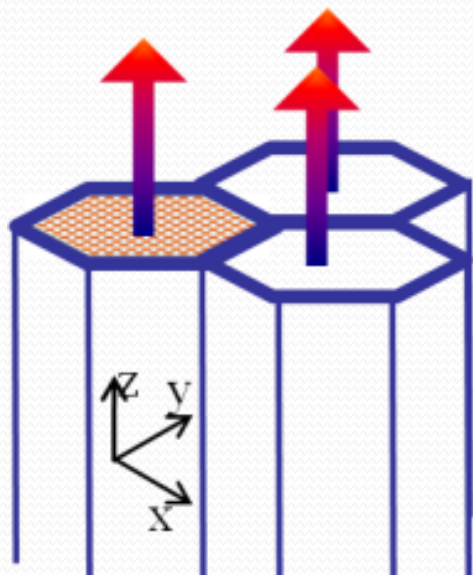
- Physical model
  - Multigroup neutron diffusion theory with delayed neutron precursors

$$\left\{ \begin{aligned} \frac{1}{v_g} \frac{\partial}{\partial t} \phi_g(\mathbf{r}, t) &= \nabla \cdot \underline{D_g(\mathbf{r}, t)} \nabla \phi_g(\mathbf{r}, t) - \underline{\Sigma_g(\mathbf{r}, t)} \phi_g(\mathbf{r}, t) + \sum_{g'=1}^G \underline{\Sigma_{gg'}(\mathbf{r}, t)} \phi_{g'}(\mathbf{r}, t) \\ &+ (1 - \beta) \chi_g(\mathbf{r}) \sum_{g'=1}^G \underline{\nu \Sigma_{fg'}(\mathbf{r}, t)} \phi_{g'}(\mathbf{r}, t) + \sum_{i=1}^R \chi_{gi}(\mathbf{r}) \lambda_i c_i(\mathbf{r}, t) + S_g(\mathbf{r}, t), \quad g = 1, \dots, G, \\ \frac{\partial}{\partial t} c_i(\mathbf{r}, t) &= \beta_i \sum_{g'=1}^G \underline{\nu \Sigma_{fg'}(\mathbf{r}, t)} \phi_{g'}(\mathbf{r}, t) - \lambda_i c_i(\mathbf{r}, t), \quad i = 1, \dots, R, \end{aligned} \right.$$



- Decay and photon heat (with photon transport) [D. Caron et al., PHYSOR, 2016]
- Space discretization: polynomial nodal method [D. Caron et al., ICENES, 2013]
- Time discretization: point-kinetic, direct and quasi-static methods [D. Caron et al., Ann. Nuc. Energy, 2015]

# FRENETIC-TH module (1)



**IN EACH fuel assembly:**

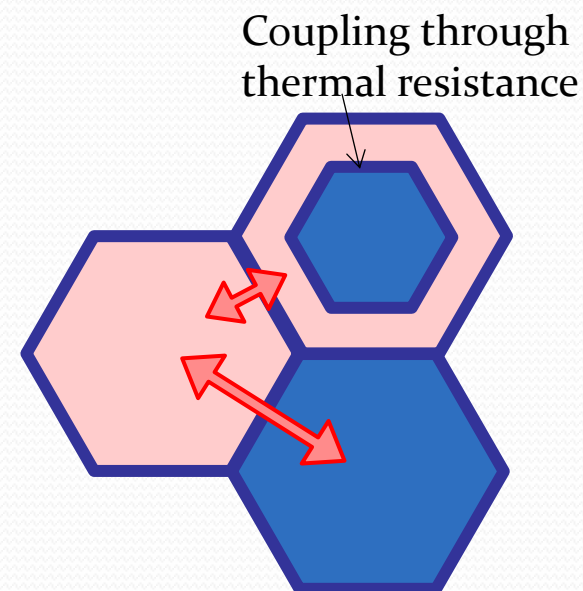
**Coolant:** 1D axial model (mass, momentum, and energy eqs.) along each closed assembly ( $z$ ), for 1+ regions in each hexagonal fuel assembly (FA)

- **Single FA (1D) validation** against experimental data from CIRCE facility @ ENEA Brasimone (**Pb-Bi eutectic**) [R. Zanino et al., Trans. Am. Nucl. Soc., 2012]

**Pins:** 1D radial model, locally coupled to coolant

**BETWEEN HAs:** (weak) 2D inter-assembly thermal coupling ( $xy$ )

- Steady-state **benchmark** against RELAP5-3D© in a simplified EBR-II geometry (Na) [R. Zanino et al., Trans. Am. Nucl. Soc., 2013]
- Preliminary **validation** against EBR-II data (Na) [R. Zanino et al., Proc. ATH, 2014]

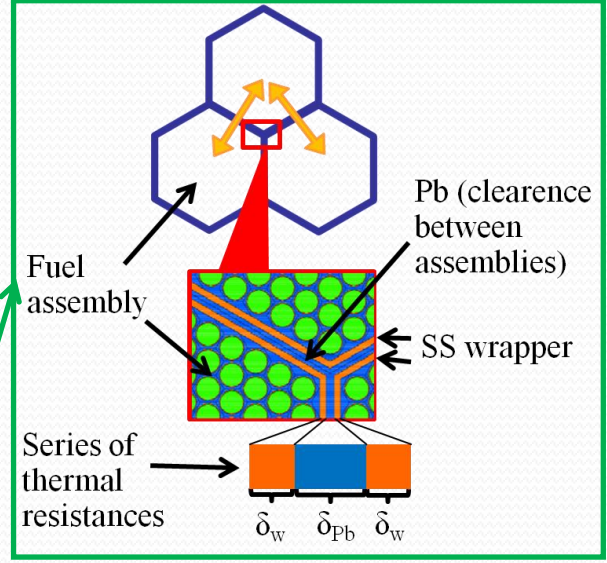




# FRENETIC-TH module (2)

**Coolant:** compressible flow with buoyancy (1D, axial)

$$\left[ \begin{aligned} \frac{\partial v}{\partial t} + v \frac{\partial v}{\partial z} + \frac{1}{\rho} \frac{\partial p}{\partial z} &= -Fv - g \cos \beta && \text{Used to compute coolant-pin heat transfer} \\ \frac{\partial p}{\partial t} + \rho c_s^2 \frac{\partial v}{\partial z} + v \frac{\partial p}{\partial z} - \Phi \frac{\partial}{\partial z} \left( k \frac{\partial T}{\partial z} \right) &= \Phi \left[ \frac{\Pi_{fuel} H}{A} (T_{fuel,s} - T) + v \rho F \right] \\ \rho c_v \frac{\partial T}{\partial t} + \rho c_v v \frac{\partial T}{\partial z} + \rho c_v \Phi T \frac{\partial v}{\partial z} - \frac{\partial}{\partial z} \left( k \frac{\partial T}{\partial z} \right) &= \\ &= \frac{\Pi_{fuel} H}{A} (T_{fuel,s} - T) + v \rho F + \sum_{i=1}^6 \frac{\Pi_{hex} h_i}{A} (T_i - T) && \text{Inter-channel coupling} \end{aligned} \right.$$



**Pin:** thermal conduction (1D, axial or radial to be chosen)

$$\left[ \rho_{fuel} c_{fuel} \frac{\partial T_{fuel}}{\partial t} - \frac{\partial}{\partial z} \left( k_{fuel} \frac{\partial T_{fuel}}{\partial z} \right) = \frac{\Pi_{fuel} H}{A_{fuel}} (T - T_{fuel,s}) + \frac{q_{fuel}^{lin}}{A_{fuel}} \right]$$

Neutronics-dependent heat source term

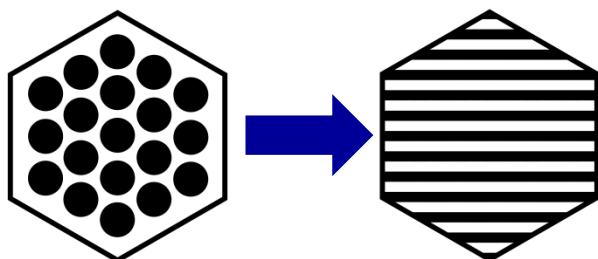
Friction term  $F = 2f \frac{|v_x|}{D_h}$

Gruneisen parameter  $\Phi = \left( \frac{\rho}{T} \frac{\partial T}{\partial \rho} \right)_s$

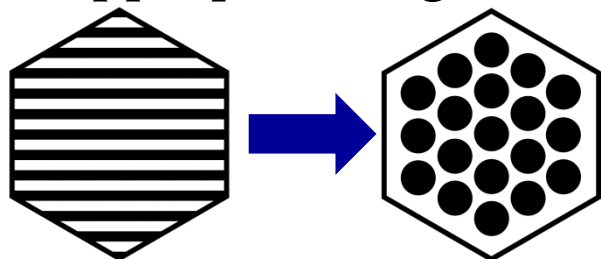
- 2D+1D heat exchange model**
- **1D:** advection + diffusion in each FA
  - **2D:** simplified «slab» inter-FA heat exchange

# Coupling strategy

- Spatial coupling procedure:
  - TH  $\rightarrow$  NE: fuel and coolant average temperatures attributed to entire node

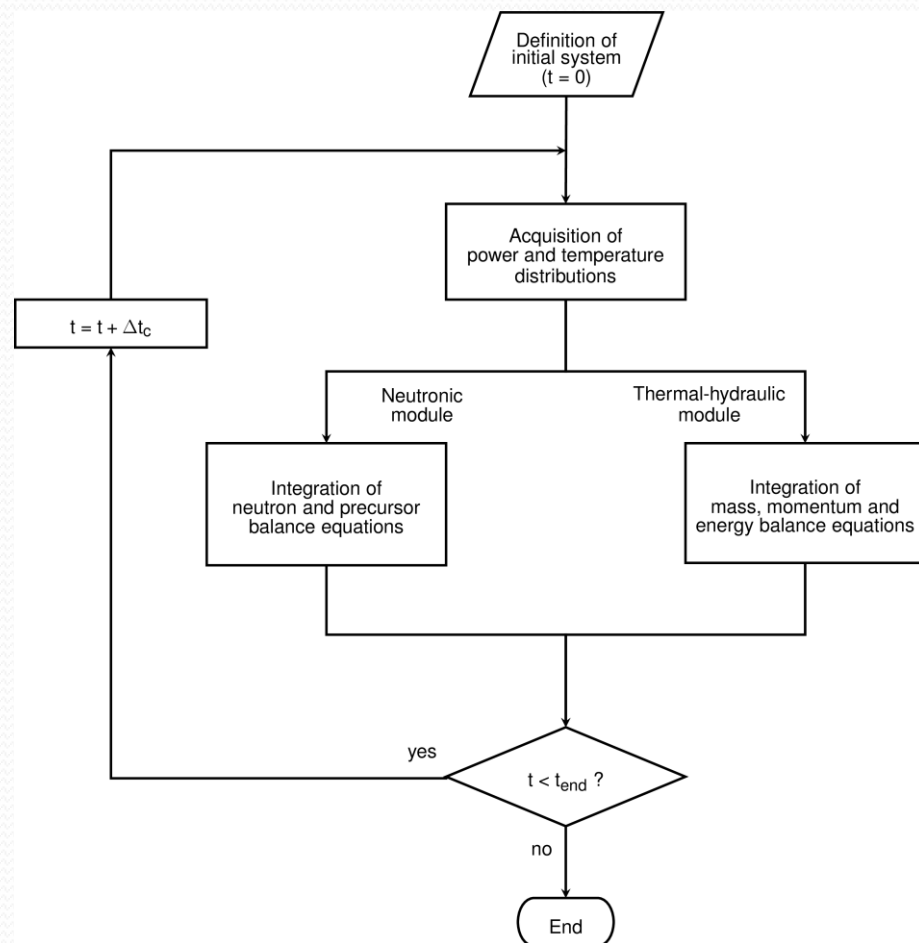


- NE  $\rightarrow$  TH: node-averaged power localised in appropriate region



- Averaging or interpolation on mesh as necessary

- Temporal coupling algorithm accounts for different time scales



# Coupling feedback

- TH module
  - neutronic effects accounted for directly by time- and position-dependent heat source term
- NE module
  - thermal effects accounted for indirectly by dependence of macroscopic cross sections on fuel and coolant temperatures
  - linear feedback model:

$$\Sigma(T_f, T_c) = \Sigma(T_{f0}, T_{c0}) + \left( \frac{\partial \Sigma}{\partial T_f} \right)_{T_c} (T_f - T_{f0}) + \left( \frac{\partial \Sigma}{\partial T_c} \right)_{T_f} (T_c - T_{c0})$$

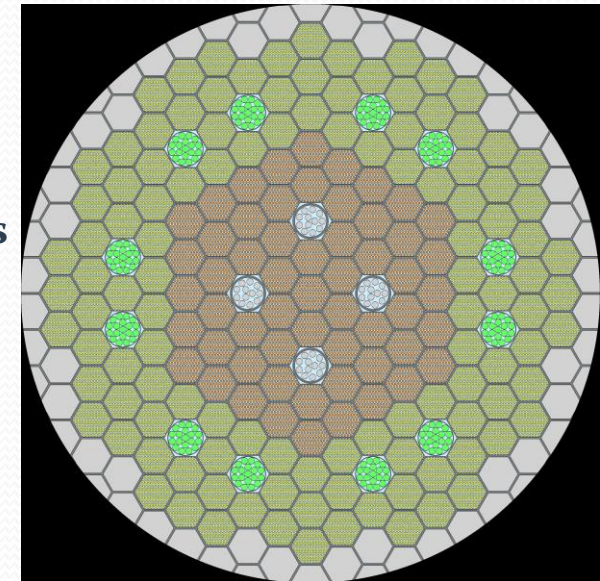
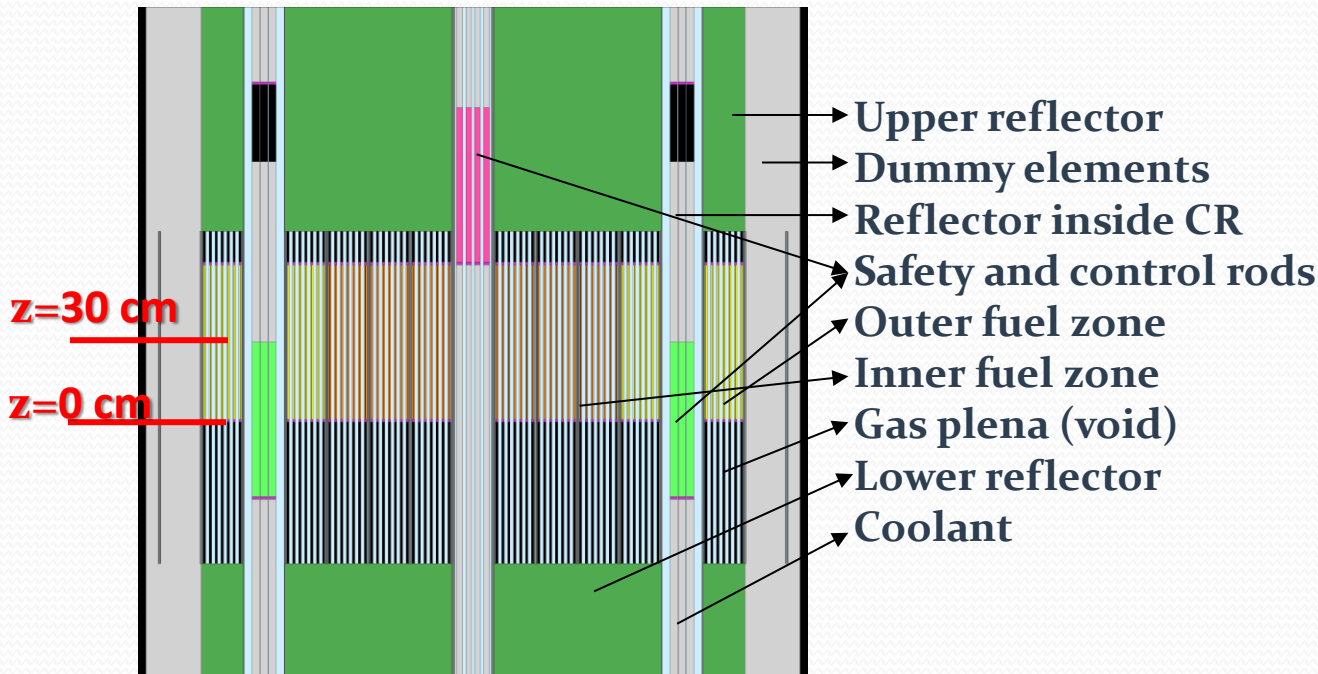
- tabular lookup model: bivariate linear interpolation

# Serpent/OpenFoam

- It is not a competition !
  - Different physical modelling for both NE and TH
  - Different domain of application → with FRENETIC, we are looking at the full-core
- Interest in
  - Exploiting the more detailed information provided by Monte Carlo and CFD to improve FRENETIC modelization
  - Use the full-core results available with FRENETIC to «improve» the CFD simulation of the single FA

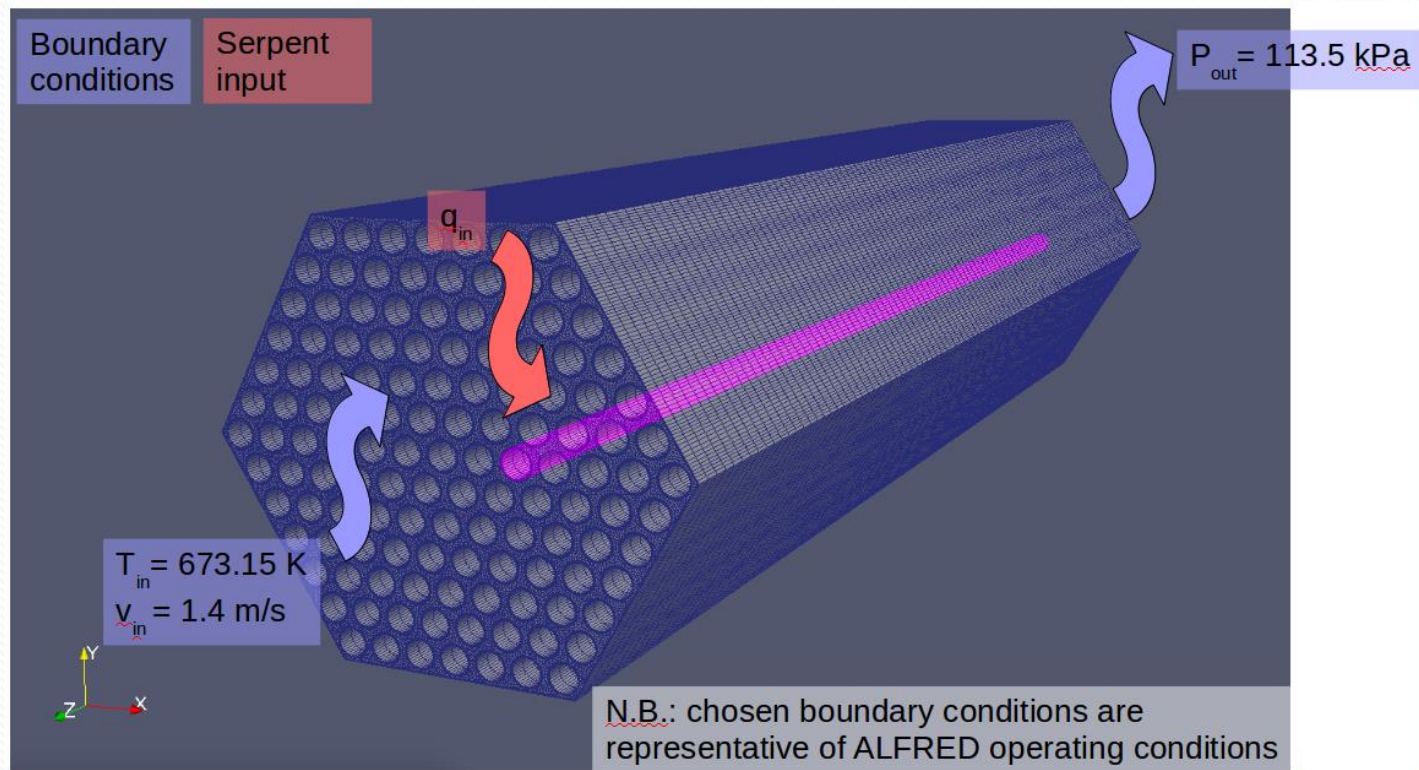
# Serpent simulation

- Full-core  $k_{\text{eff}}$  calculation
- Material and geometrical data from G. Grasso, et al., The core design of ALFRED, a demonstrator for the European lead-cooled reactors, Nuclear Engineering and Design 278, 2014
- Nuclear data depend on temperature

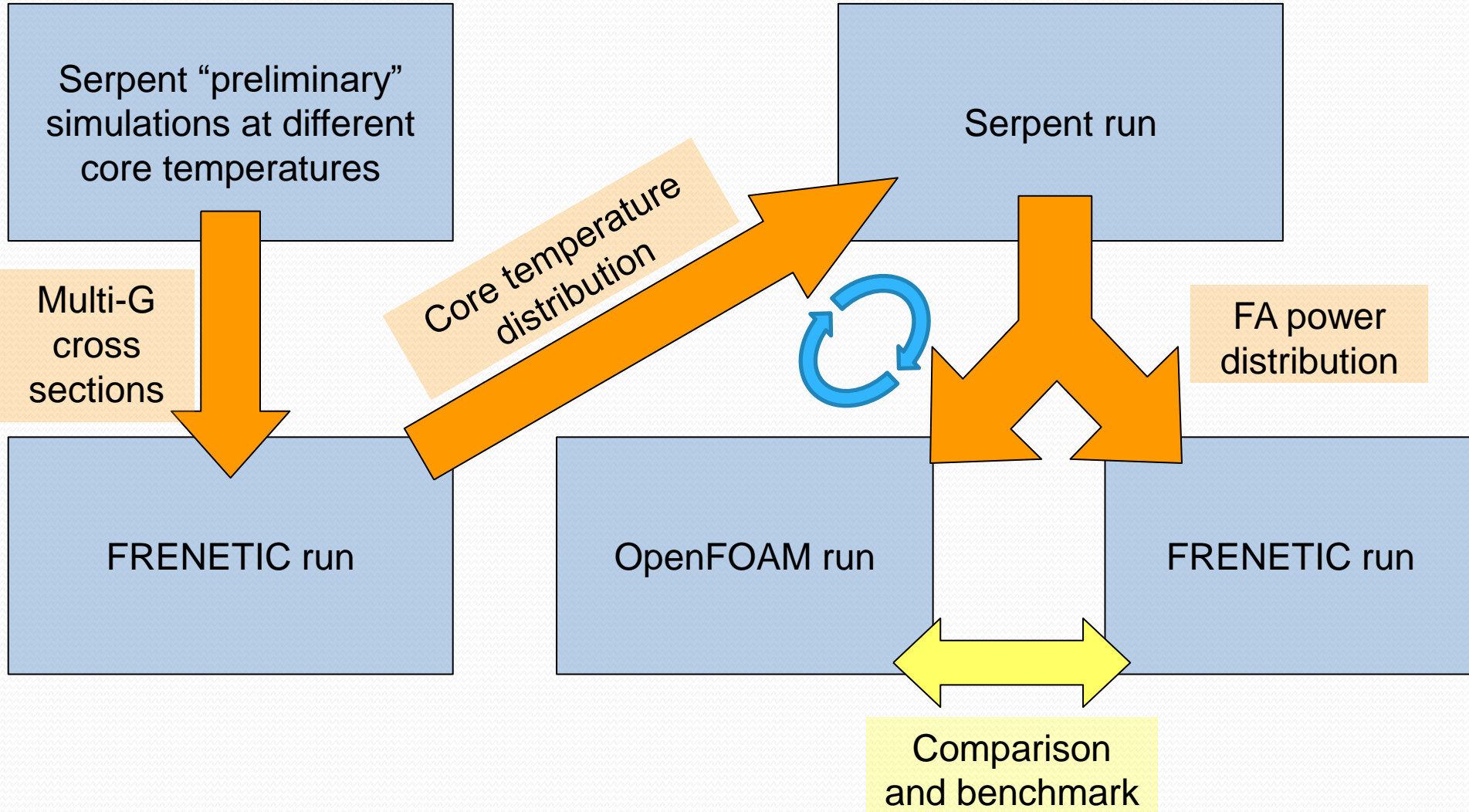


# OpenFoam simulation

- On a single FA
- Info on power source from Serpent (thus depending on the location in the core)
- BC ?



# General calculation scheme



## cross section generation

- FRENETIC requires homogenized, few-groups cross sections, which are generated by Serpent runs (four, in our case) at different temperatures

|                   | $T_{fuel} (K)$ | $T_{coolant} (K)$ |
|-------------------|----------------|-------------------|
| $T_{fuel} (K)$    | 673            | 1073              |
| $T_{coolant} (K)$ | 673            | 1073              |

| Group | Upper energy (MeV) |
|-------|--------------------|
| 1     | 19.64              |
| 2     | 1.3534             |
| 3     | 0.18316            |
| 4     | 0.067379           |
| 5     | 0.00091188         |

$$\Sigma(T_f, T_c) = \Sigma(T_{f,0}, T_{c,0}) + \left( \frac{\partial \Sigma}{\partial T_f} \right)_{T_c} (T_f - T_{f,0}) + \left( \frac{\partial \Sigma}{\partial T_c} \right)_{T_f} (T_c - T_{c,0})$$

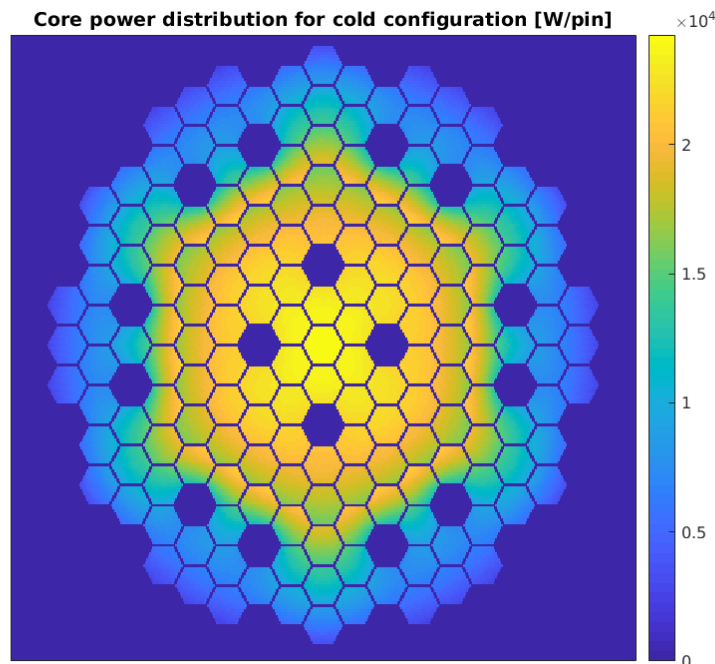
- The output of FRENETIC, i.e. the full core temperature distribution, is then fed to Serpent to perform the NE simulation with “improved” temperature information



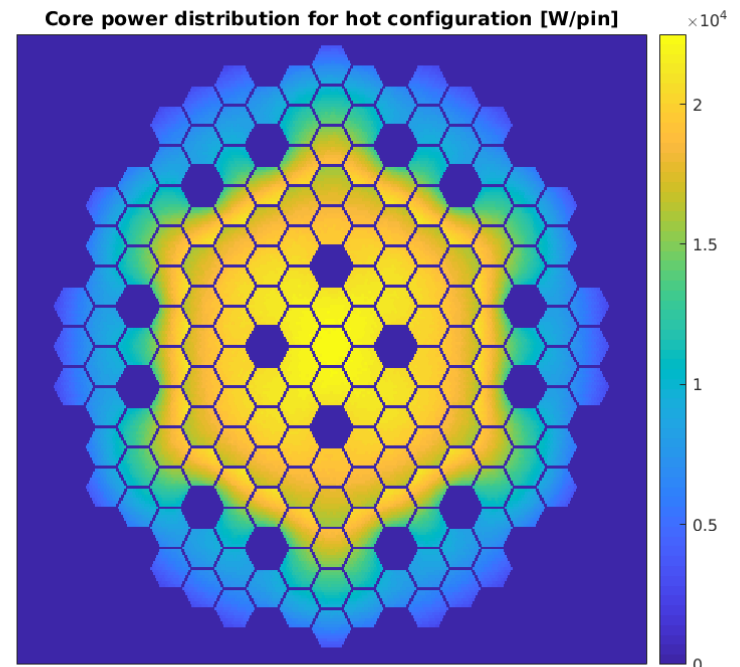
# Serpent results (1)

- Comparison of Serpent core keff calculations at
  - 673 K («cold») →  $k_{\text{eff}}=1.01027 \pm 3e-5$
  - 1073 K («hot») →  $k_{\text{eff}}=1.00772 \pm 3e-5$
- Power distribution, affected by temperature feedbacks

**cold**

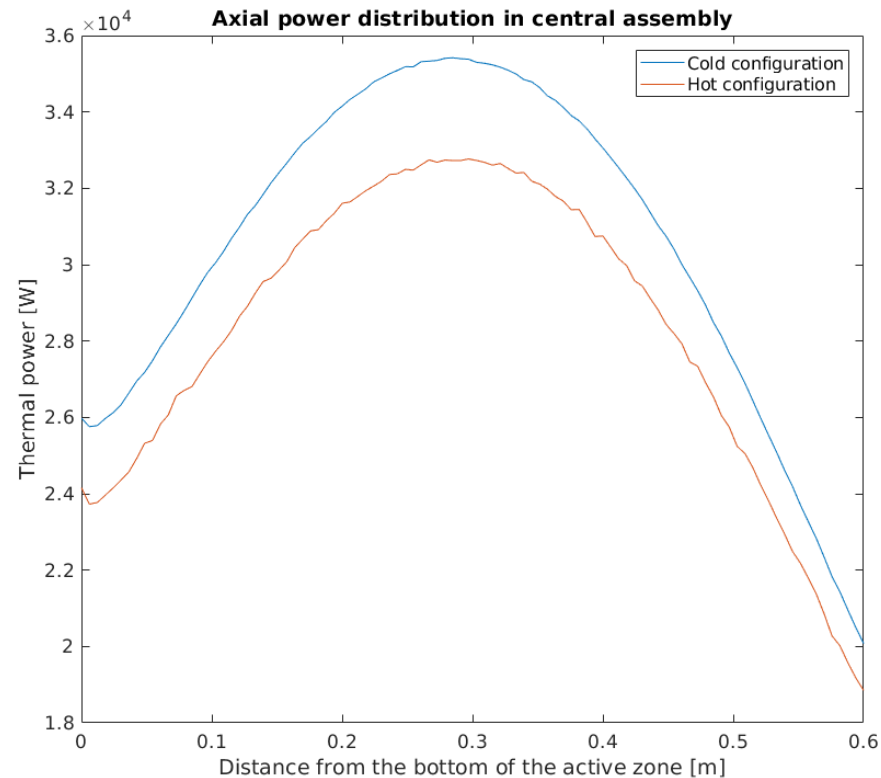
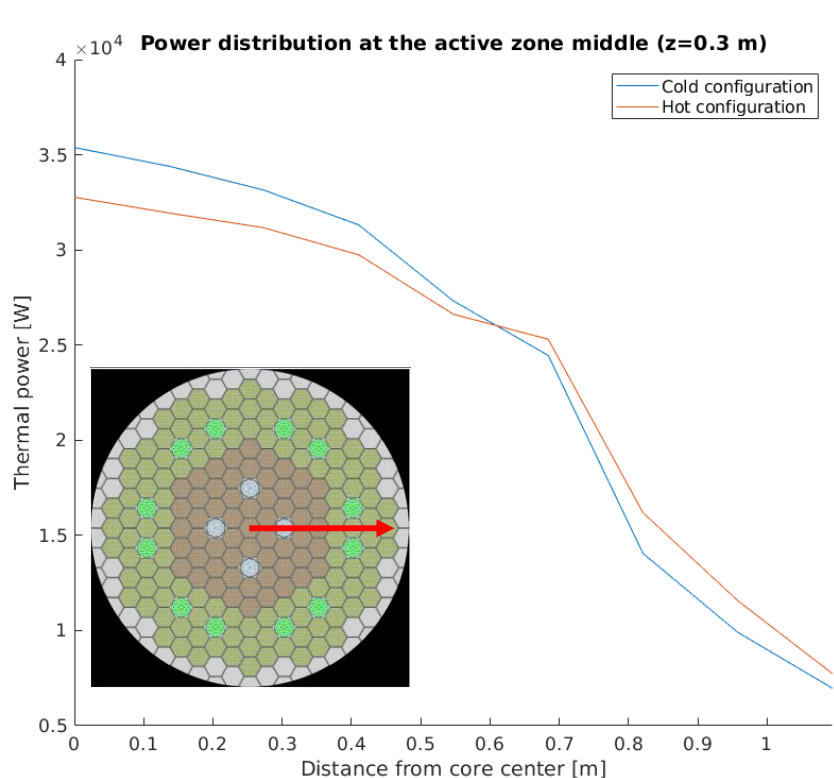


**hot**



# Serpent results (2)

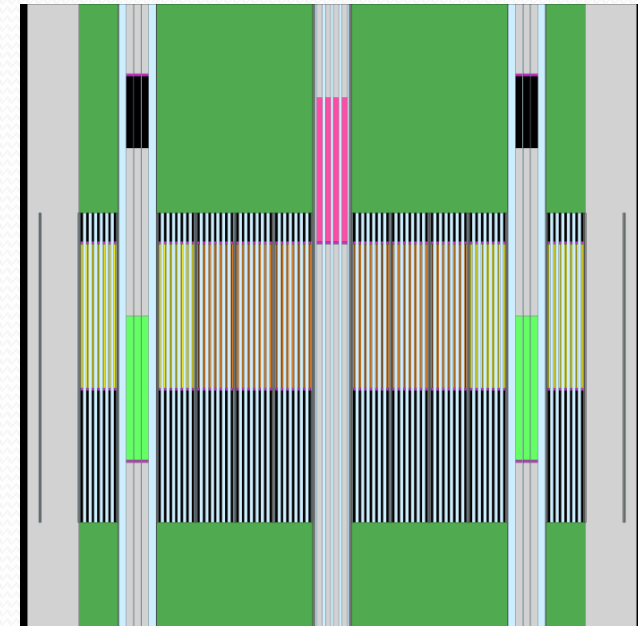
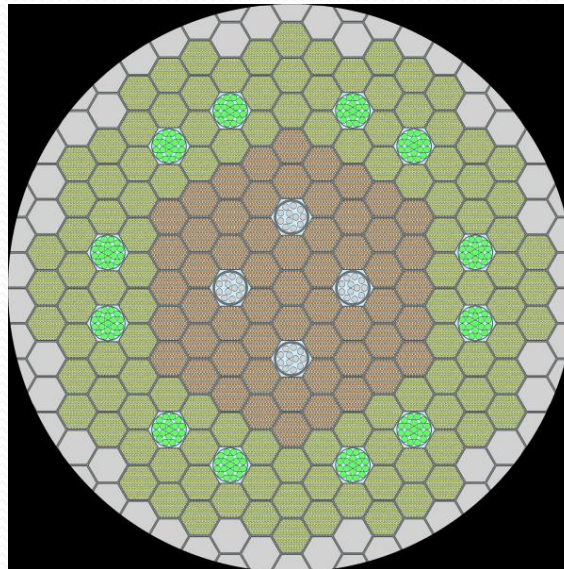
- Radial and axial profiles (power distribution flattening)



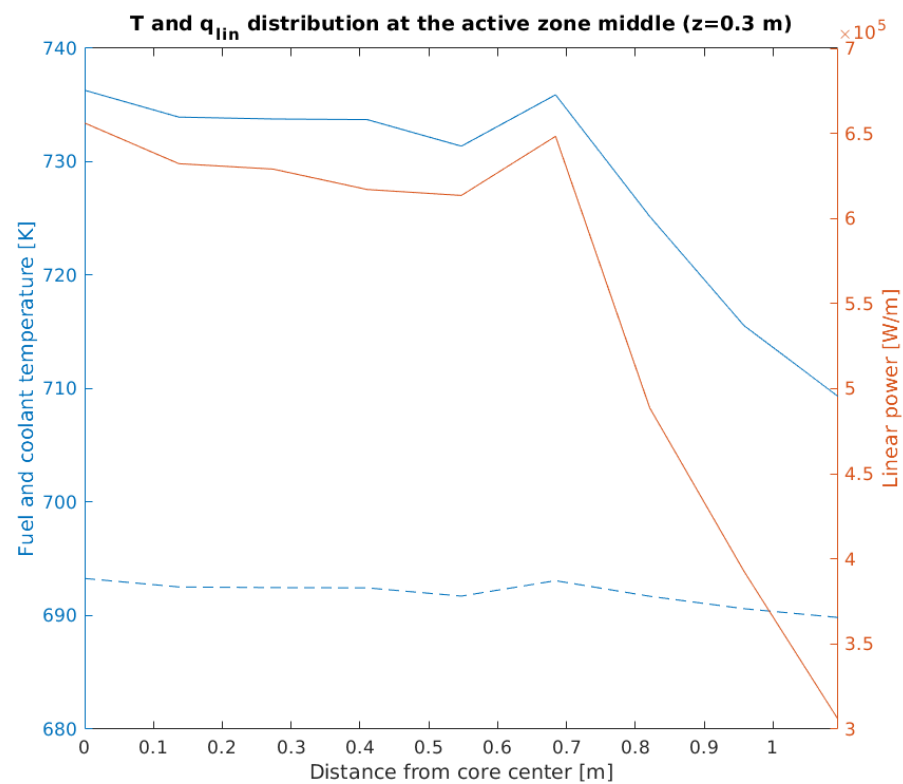
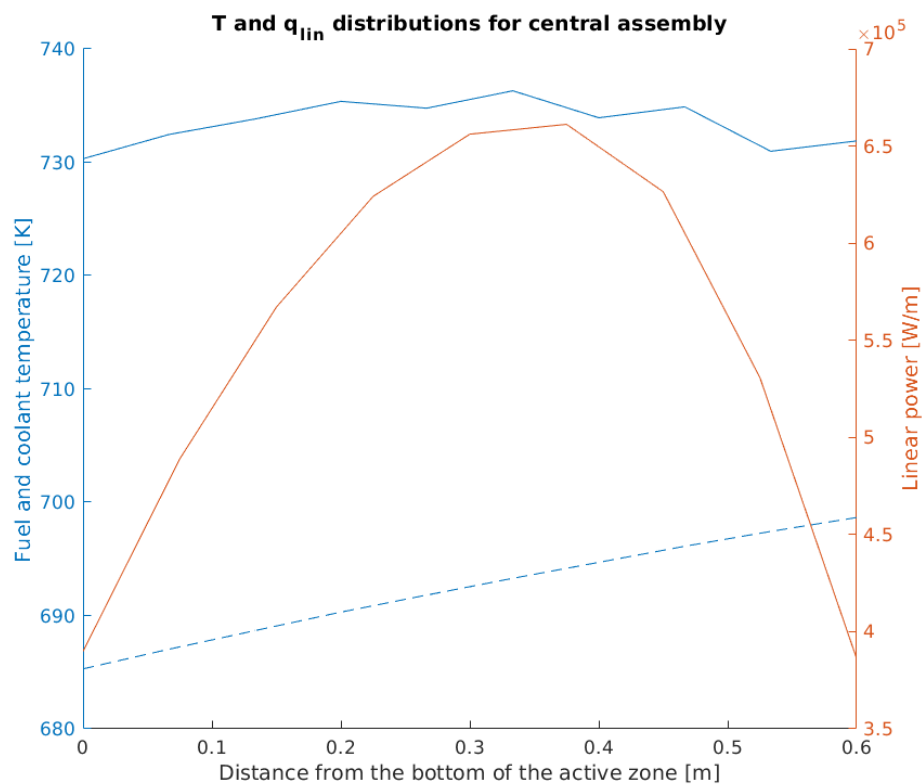
- **Next step:** Serpent run with representative temperature of the core at full power → FRENETIC run

# FRENETIC run (1)

- Coupled NE-TH run on full-core level to reach equilibrium (free evolution transient)
- Cross section homogenized at the fuel assembly level
- Focus on the core domain (consistently with the FRENETIC modelling capabilities)

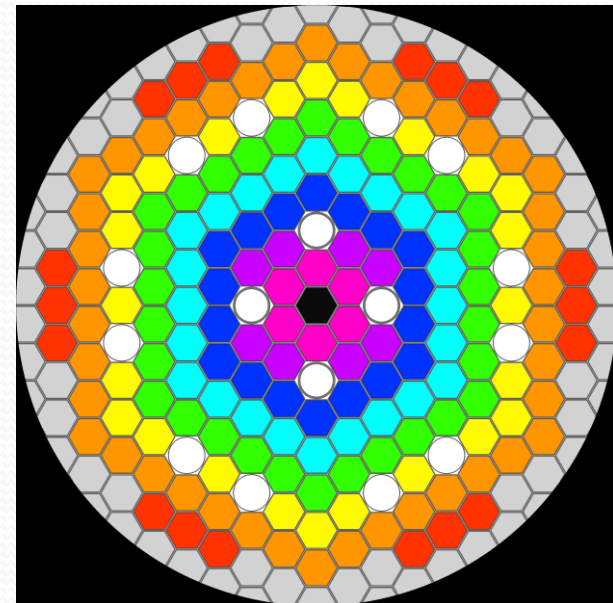


# FRENETIC run (2)



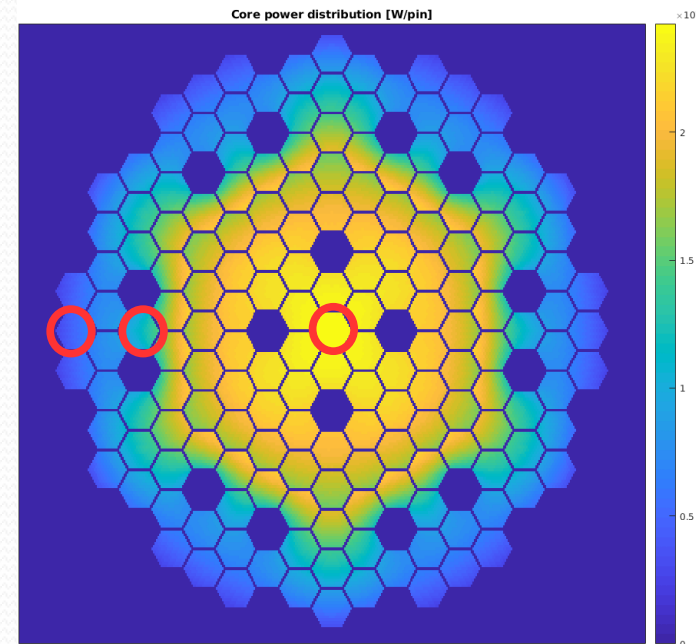
# «Upgraded» Serpent run

- Temperature distribution from FRENETIC
  - T for both fuel and coolant
  - Value at the FA level for different axial positions
  - If transferred directly into Serpent, memory issues arise ...
- Solution:
  - Definition of concentric regions
  - T associated to each region
  - Axial distribution preserved
- Serpent run ... in progress



# Work in progress

- Comparison of «upgraded» Serpent run with FRENETIC in terms of power distribution
  - Assessment of the quality of FRENETIC modelling w.r.t. reference Monte Carlo in the same thermal conditions
- OpenFoam calculation of the single FA with
  - «improved» boundary condition provided by FRENETIC (heat flux)
  - Power distribution representative of different regions in the core (from «upgraded» Serpent)



# Work in progress

- Comparison of OpenFoam results with FRENETIC on the single FA
  - Evaluation of the relevance of specific TH effects that FRENETIC may not be able to reproduce
  - Improvement of the current correlations and averaging processes currently existing in FRENETIC, based on CFD results

# Conclusions and perspectives

- The activity is part of a fruitful collaboration between PoliTO and PoliMI in the frame of the POLY<sup>2</sup>NUC program
- The work is still in progress and results are progressively produced and analyzed (both steps take time ...)
- The resulting upgraded models will be applied to the analysis of the forthcoming upgraded ALFRED design





**UNIVERSITY OF PISA**

**Dipartimento di Ingegneria Civile e Industriale (DICI)**

**HLM-Water Interaction**

**& SIMMER-RELAP5 code coupling development**

**N. Forgione**

# Introduction

- The interaction between two fluids, of which one is less volatile and at higher temperature than the other one, results in the production of high pressure vapour.

Thus, this is one of the most important concerns for safety issues of:

- Lead and Sodium cooled reactors belonging to “Generation IV” systems
- ADS where both core and target are cooled by LBE
- In HLM reactors, the heavy liquid metal might come into contact with the water flowing in the steam generator because of an accidental Steam Generator Tube Rupture (SGTR).

→ CCI

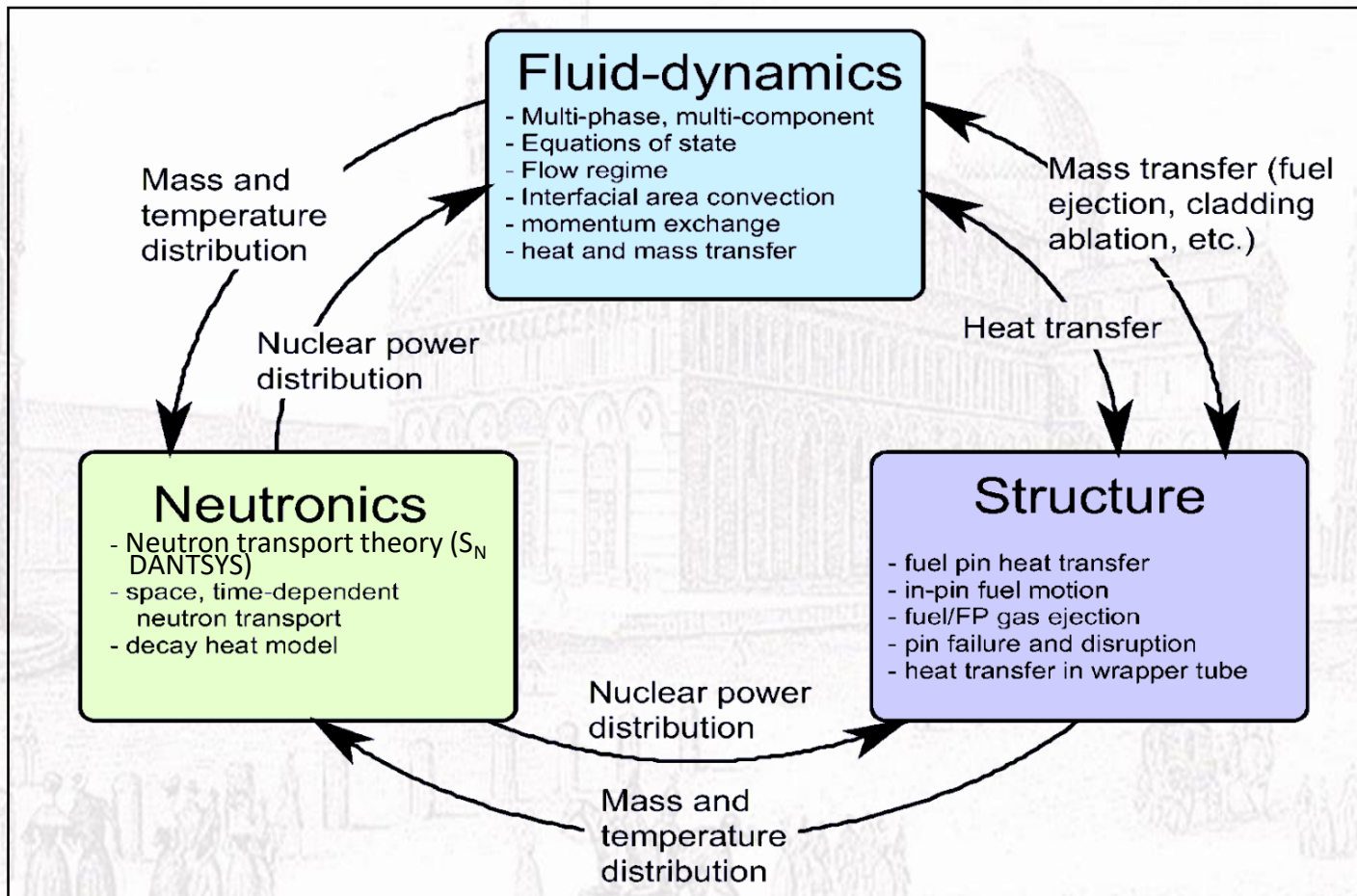
- In sodium cooled reactors a loss of coolant accident can increase the core temperature up to the fuel and steel melting, leading this mixture to interact with the surrounding coolant.

→ FCI

- One of the crucial issue is represented by the evaluation of the energy released in such interactions, in order to have indications of the potential loads and the resulting damage on reactor structures.

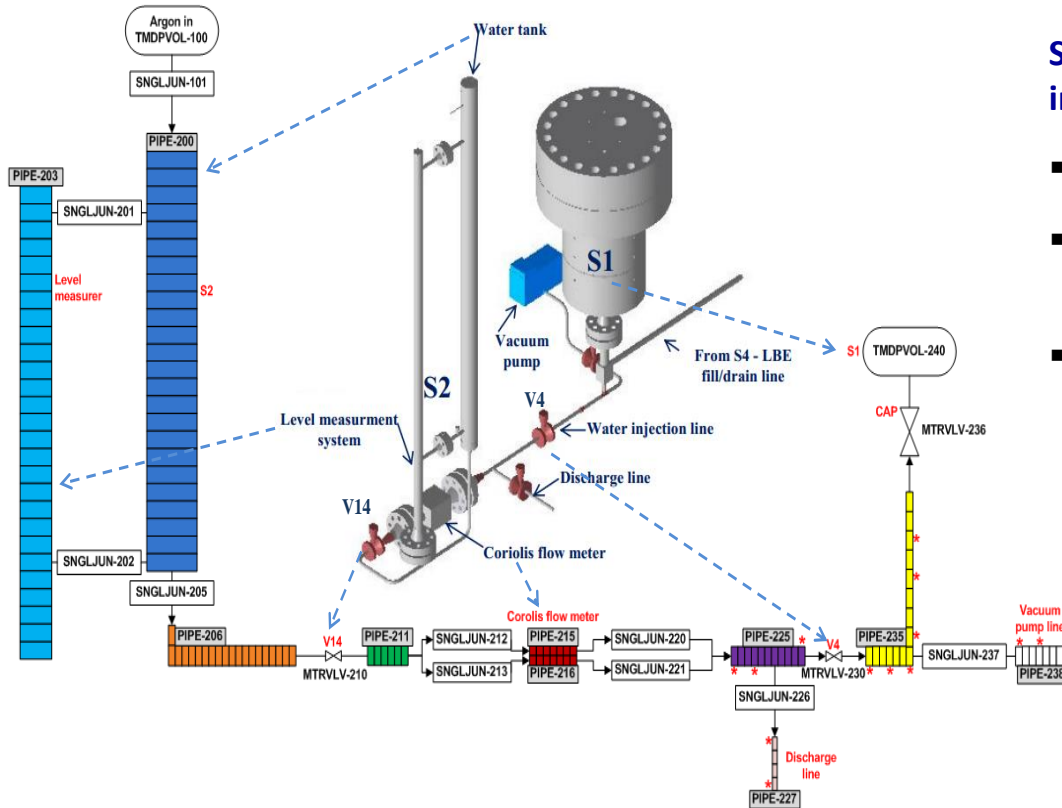
# SIMMER III Features

SIMMER III, jointly developed by JAEA (Japan), KIT (Germany), IRSN & CEA (France), is a 2D axysymmetric, three velocity-field, multi-component, multiphase, Eulerian fluid-dynamics code coupled with neutron kinetics model. It can deal with safety analysis problems in advanced fast reactors.



# THINS experimental campaign and SIMMER III validation LIFUS5/Mod2 injection line analysis

## Test A1.2\_2



Sensitivity analysis by RELAP5/MOD3.3 of the water injection line for characterizing:

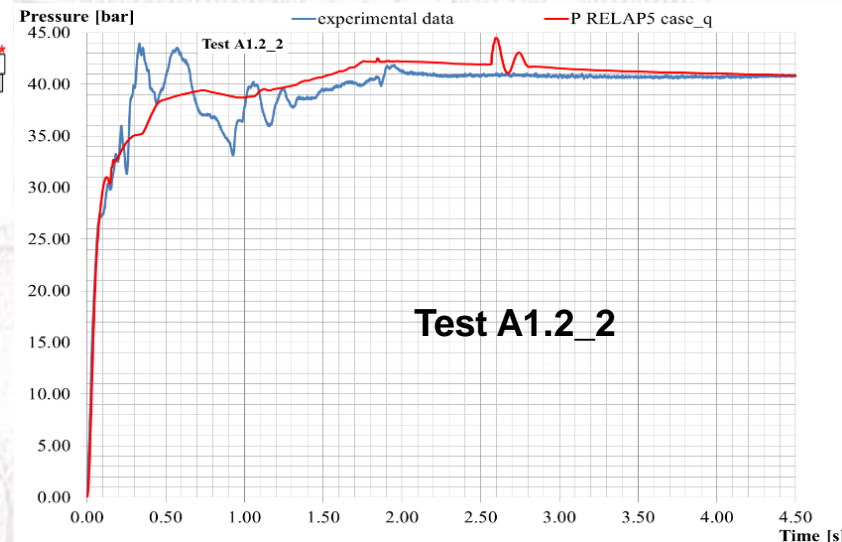
- Valves (V4, V14) opening/closing time  $\rightarrow 0.25$  s
- Valves (V4, V14) and Coriolis energy loss coefficient  $K \rightarrow 7$
- Coriolis tubes area  $\rightarrow 4.53e-5$  m<sup>2</sup>

$$T_{H_2O} = 240^\circ\text{C}$$

$$T_{LBE} = 400^\circ\text{C}$$

$$P_{H_2O} = 40 \text{ bar}$$

$$V_{Ar} / V_{LBE} = 30\%$$

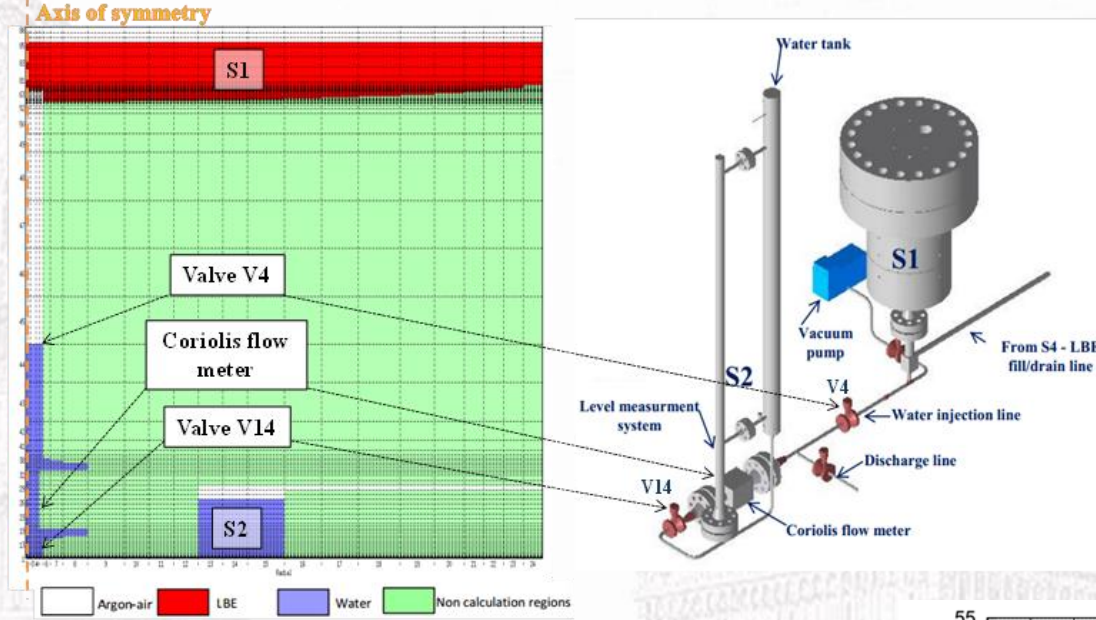


- RELAP5/Mod3.3 was able to predict pressure time trend in the injection line
- Pressure evolution in the injection line is a key parameter for evaluating water/LBE interaction  $\rightarrow$  S1 pressurization
- Post-test analysis of THINS tests (done by SIMMER III) could be significantly improved by SIMMER-RELAP5 coupling



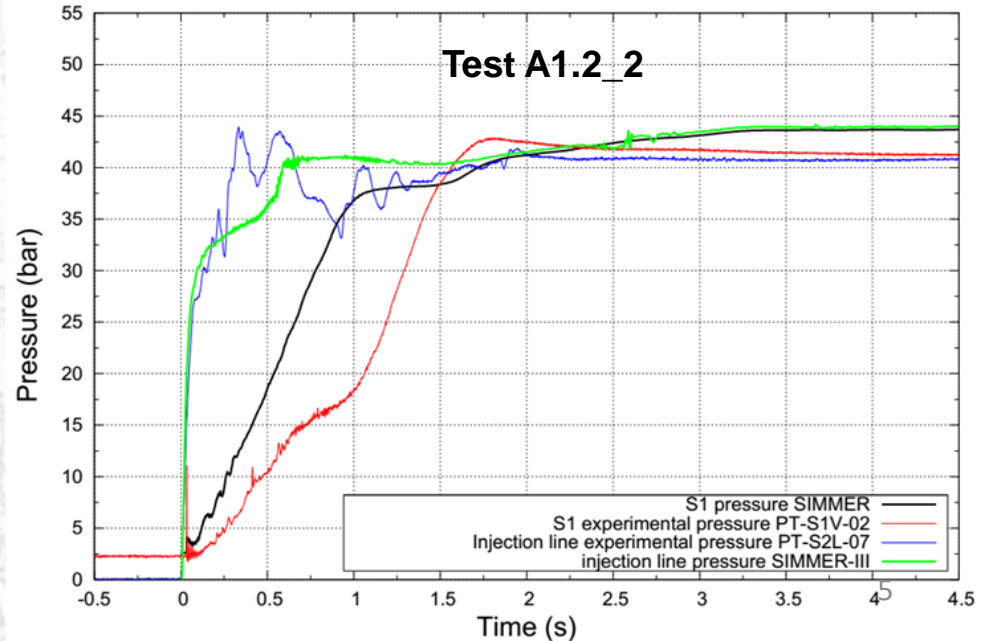
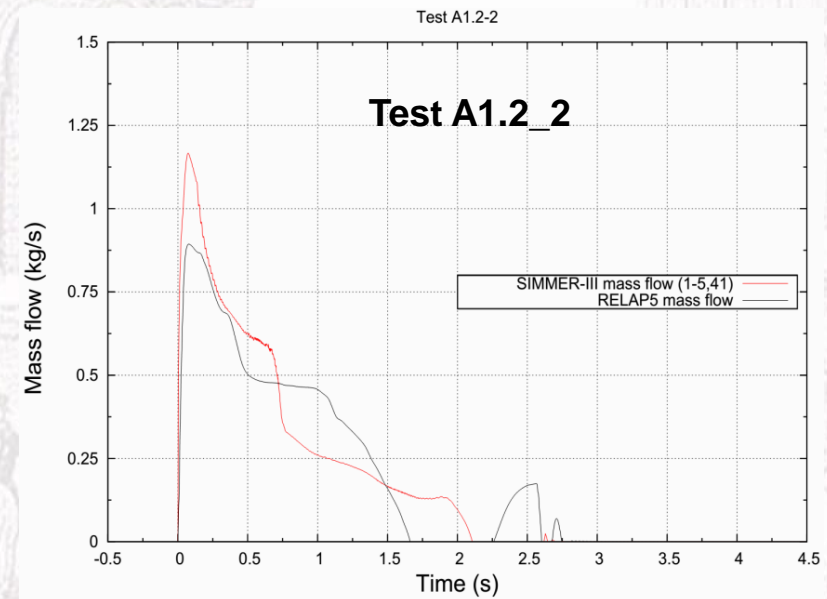
# THINS experimental campaign and SIMMER III validation

## LIFUS5/Mod2 injection line analysis



SIMMER III calculation with injection line parameters based on RELAP5/Mod3.3 sensitivity

- SIMMER III has improved the prediction of injection line pressurization
- Mass flow rate computed by SIMMER III is qualitatively analogous to that on compute by RELAP5/Mod3.3





# Goals & Tasks for the AdP 2017 Activity

---

## Main aim

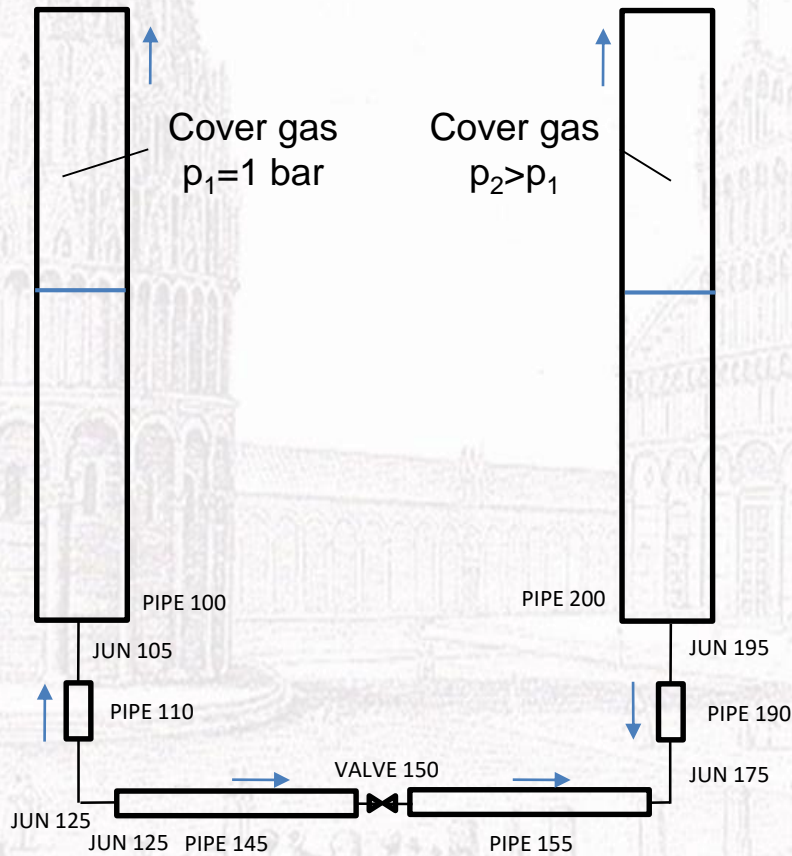
- Set up a coupling tool capable to reproduce part of a TH system, in which 2D/3D phenomena occur, with SIMMER code and the remaining part of the system with RELAP5 code.

## UNIFI activities foreseen inside AdP2017

- Set up of SIMMER-RELAP5 coupled tool and application to a simple configuration quite similar to the LIFUS5 test section.
- Development of SIMMER III model of LIFUS5/Mod3 facility.
- Development of RELAP5 nodalization of the LIFUS5/Mod3 facility.
- Preliminary application of the coupled tool to LIFUS5/Mod3 facility.

# Manometer flow oscillation problem

The geometry of the problem, used as preliminary verification of the coupling technique, consists of two tanks partially filled with water at different pressure ( $p_2 > p_1$ ).



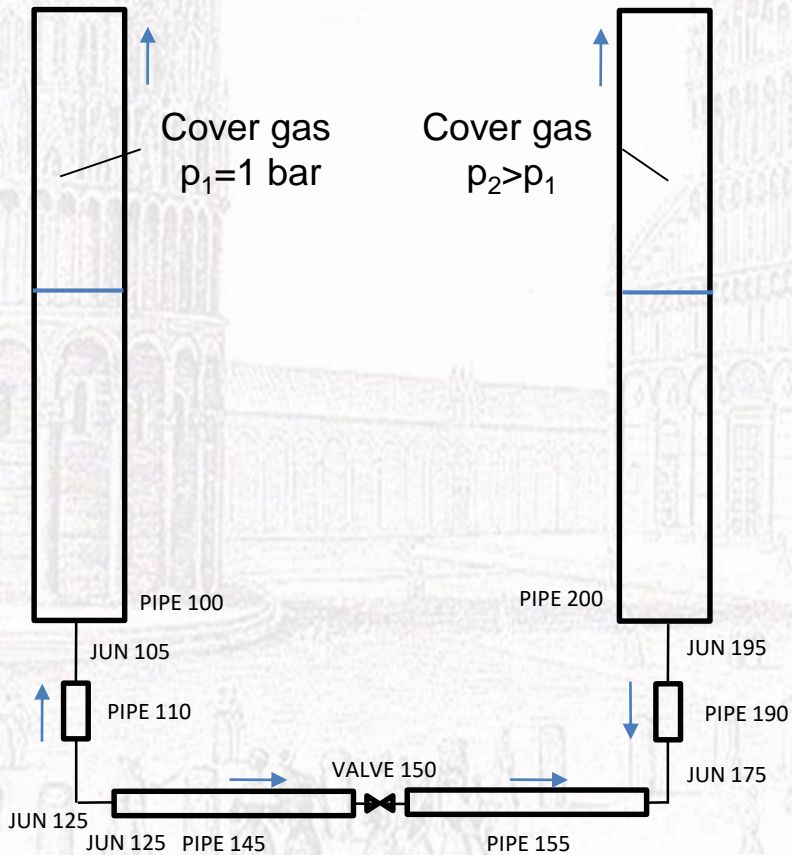
- Pipe 200 is the “High pressure tank”, and Pipe 100 is the “Low pressure tank”.
- Pipes 190, 155, 145, and 110 are the “Injection line”.
- Valve 150 isolates the two zones at different pressure. It opens in 0.01 s, 2.1 s after the beginning of each calculation.
- Pressure drop coefficients across junctions 105, 150, 175 and 195 set to 1.

| Pipe     | Dimensions                      |
|----------|---------------------------------|
| 100, 200 | H = 1 m, D = 0.5 m, 20 cells    |
| 110, 190 | H = 0.1 m, D = 0.05 m, 10 cells |
| 145, 155 | H = 2.5 m, D = 0.05 m, 10 cells |

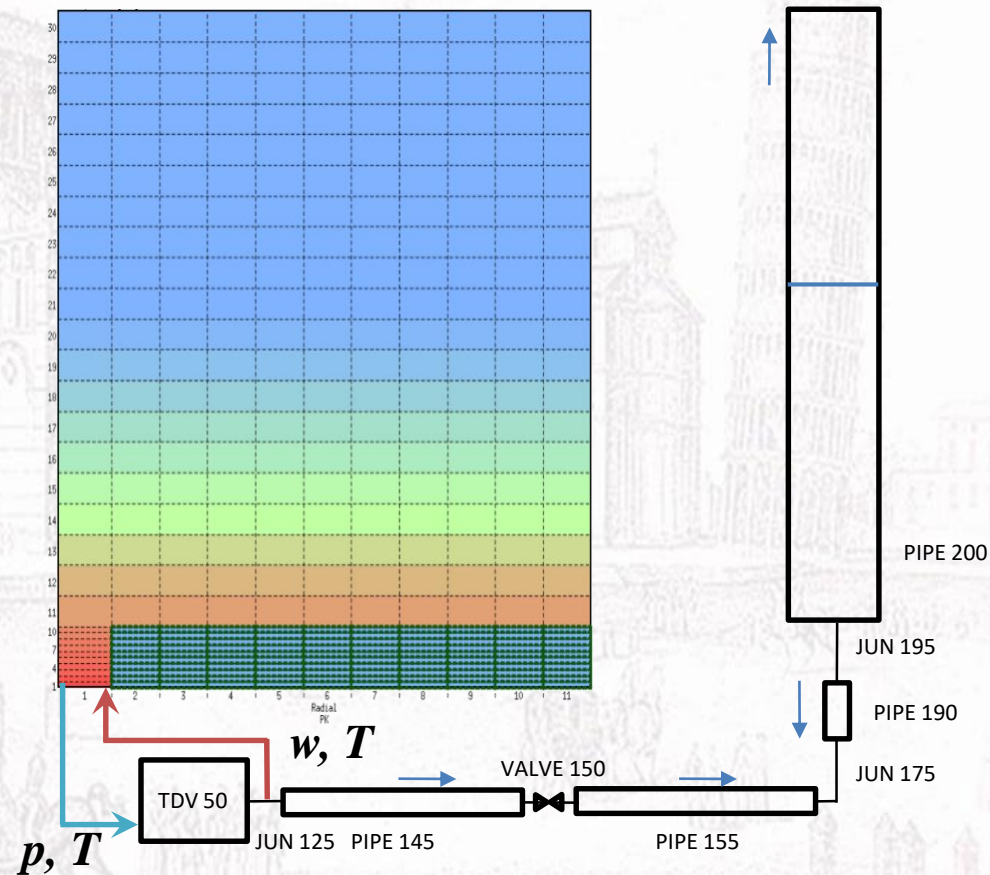
# Manometer flow oscillation problem

When possible, for the different test cases of the validation matrix, a comparison between the standalone (RELAP5) and the coupled calculation has been performed.

## RELAP5 STANDALONE



## SIMMER-RELAP5 COUPLED

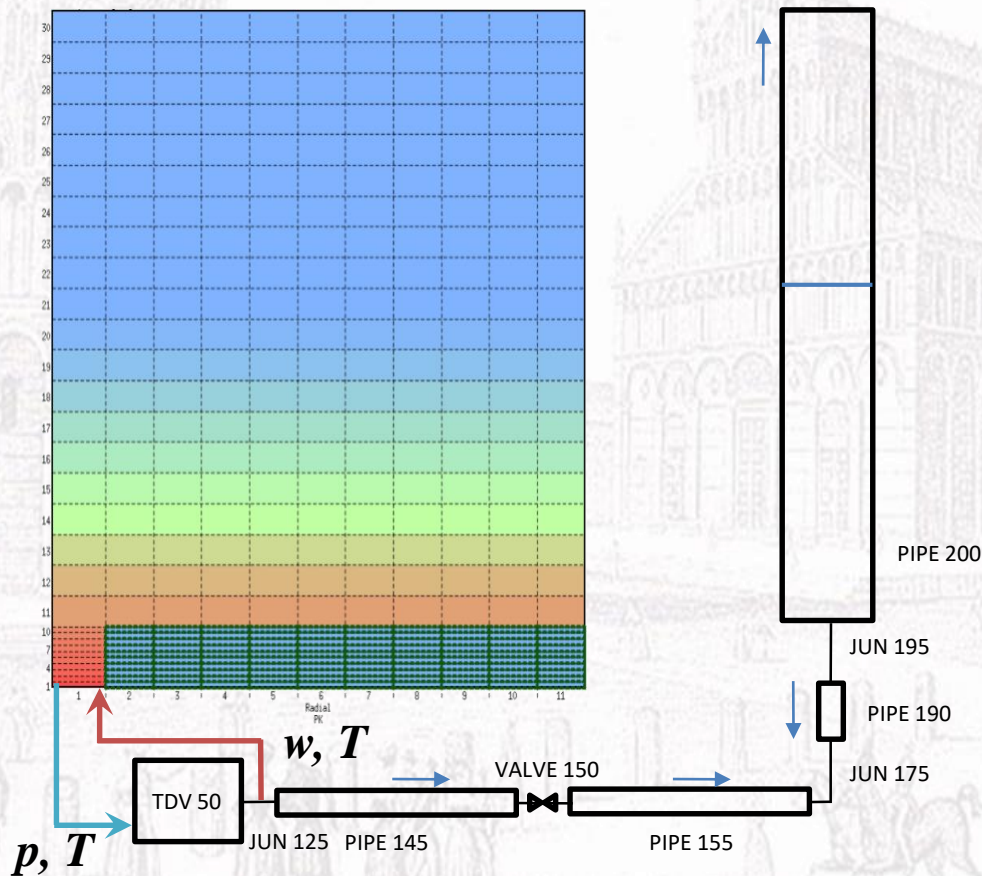




# Manometer flow oscillation problem

Low pressure tank (Pipe 100) and the Pipe 110 were replaced by a SIMMER III axial-symmetric domain discretized by 20 vertical cells and 11 radial cells.

Concentrated pressure drop coefficients ( $K = 0.05$ ) are set-up on the cells reproducing the Pipe 110 to account for the distributed pressure drops which are not automatically evaluated by SIMMER III code.

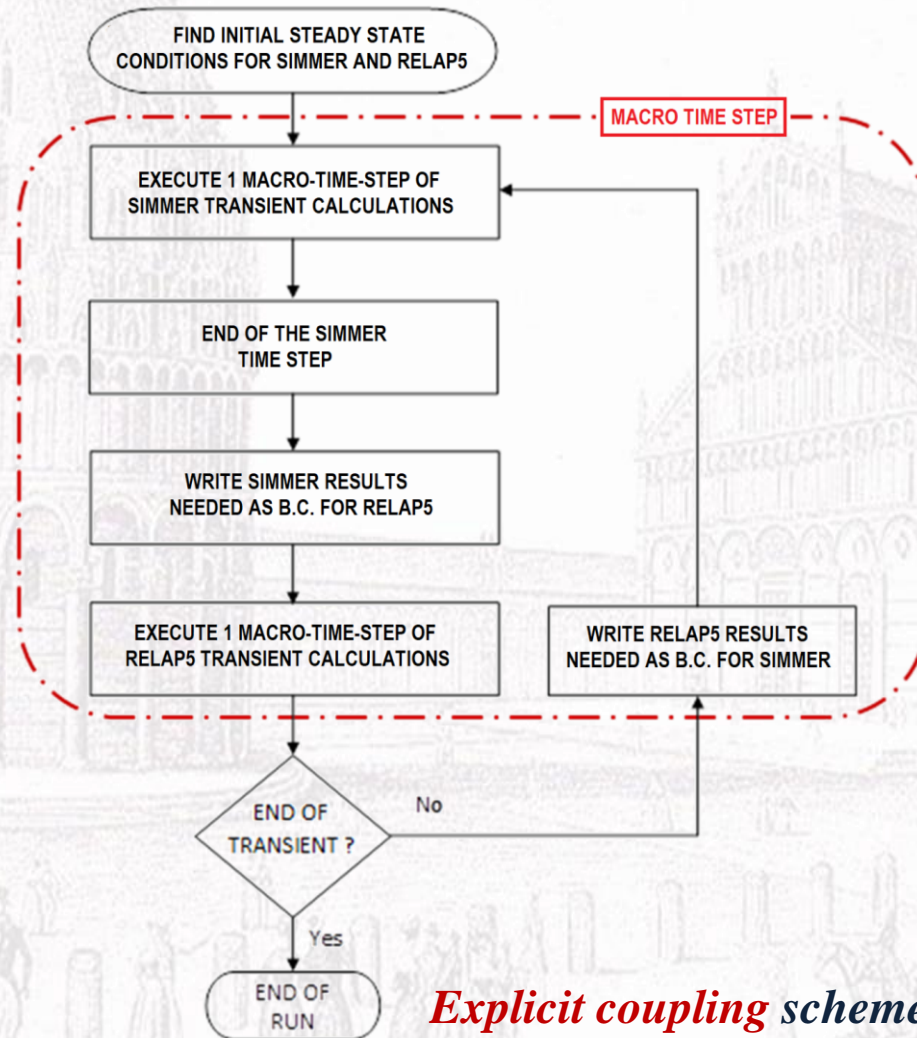


## Management of macro time-step:

- 1) A SIMMER III run is performed imposing as b.c. the fluid velocity and temperature through junction 125 (RELAP5).
- 2) The pressure and the temperature of inlet section (cell (1,1)) obtained at the end of the SIMMER III run are then given back to RELAP5 as b.c..
- 3) According to this new b.c., the RELAP5 code calculates a new fluid velocity and temperature across junction 125.
- 4) The macro time-step is over, and the coupling moves to the evaluation of the next macro time-step.

# Manometer flow oscillation problem

## Coupling Numerical Scheme



*Explicit coupling scheme*

- Execution of the SIMMER III and of the RELAP5/Mod3.3 code is **operated by** an appropriate **MATLAB** script.
- **MATLAB** algorithm implemented **to receive** b.c. data from SIMMER, and to **send** b.c. data to RELAP5, and vice versa.
- **Domain decomposition** (non overlapping) coupling approach.
- **“Two way”** coupling calculation.
- **SIMMER III** code is the **master** code.
- **RELAP5** code is the **slave** code.
- Both the codes work on the **Linux** operating system.
- The **RELAP5** version is that **modified at UNIPI** to take into account for the properties of the liquid metals.

# Manometer flow oscillation problem

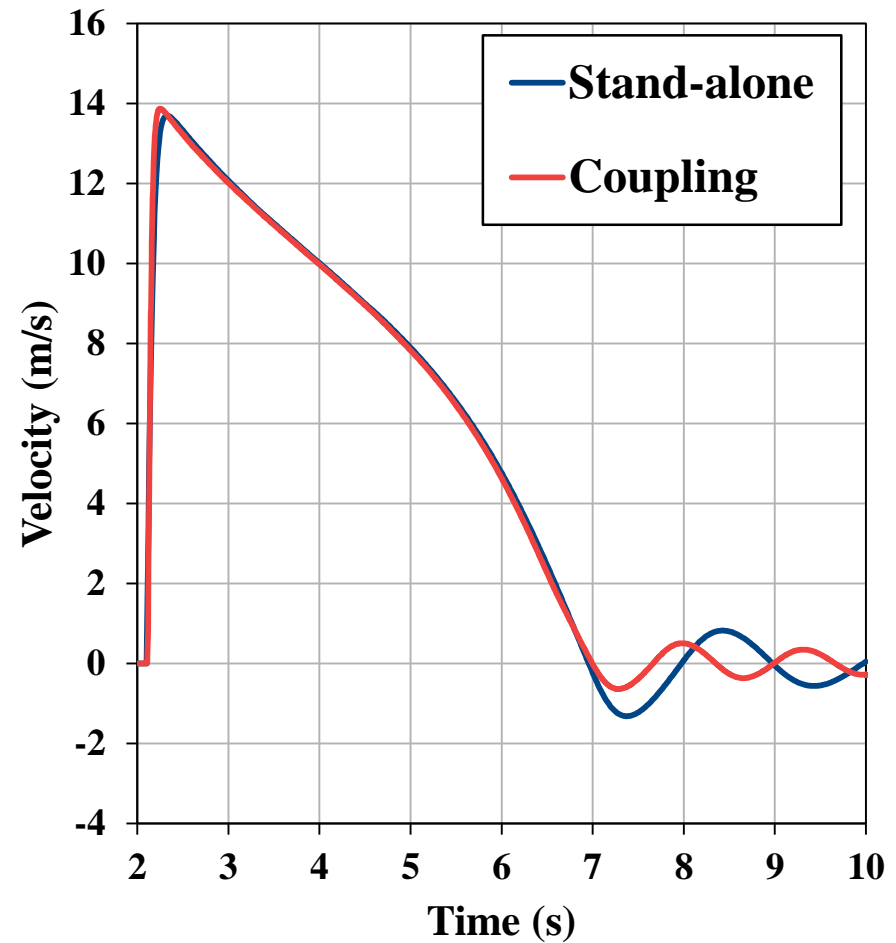
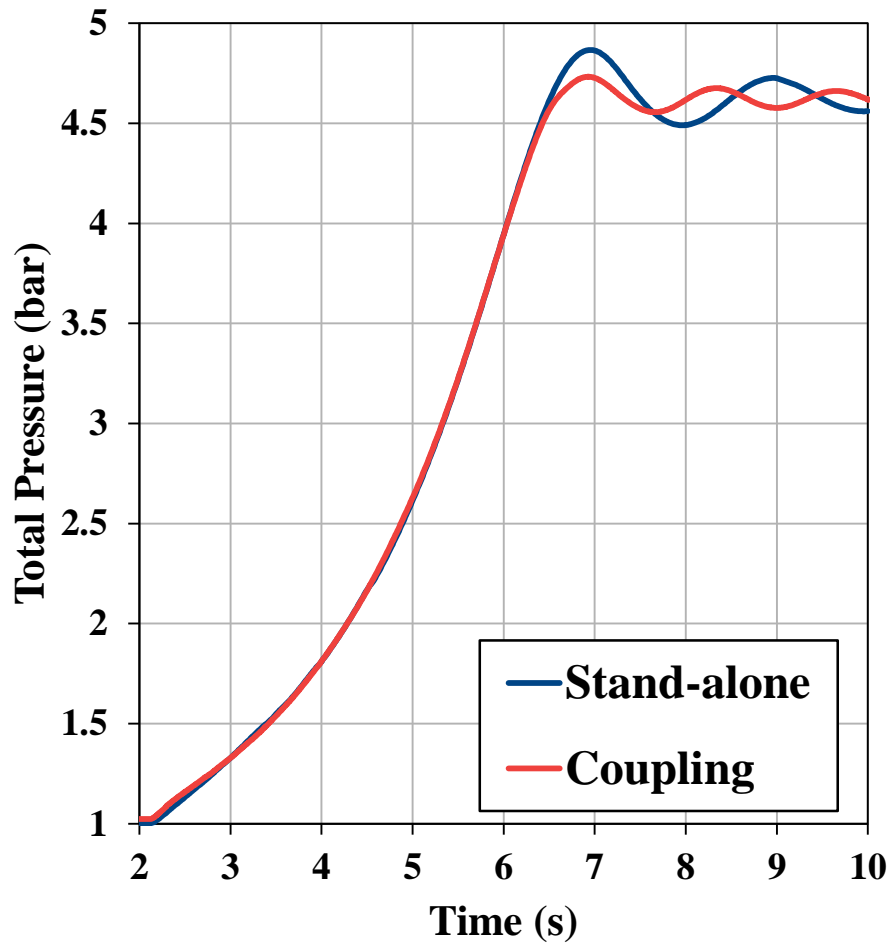
A **matrix of test cases** was initially set-up to check the stability and the capabilities of the coupling tools.

| Test case  | Init. Cond.<br>(RELAP5) | Init. Cond.<br>(SIMMER III) |
|--|-------------------------|-----------------------------|
| 1. Tanks at different initial pressure   | 10 bar / 20°C           | 1 bar / 20°C                |
| 2. High pressure tank kept at 10 bar during the transient                              | 10 bar / 20°C           | 1 bar / 20°C                |
| 3. High pressure tank kept at 10 bar with different water temperature in the two tanks | 10 bar / 80°C / 0.5 m   | 1 bar / 20°C / 0.5 m        |
| 4. High pressure tank kept at 50 bar   | 50 bar / 20°C / 0.95 m  | 1 bar / 20°C / 0.25 m       |
| 5. High pressure tank kept at 100 bar  | 100 bar / 20°C / 0.95 m | 1 bar / 20°C / 0.25 m       |

**The matrix is still under development. New test cases can be added.**

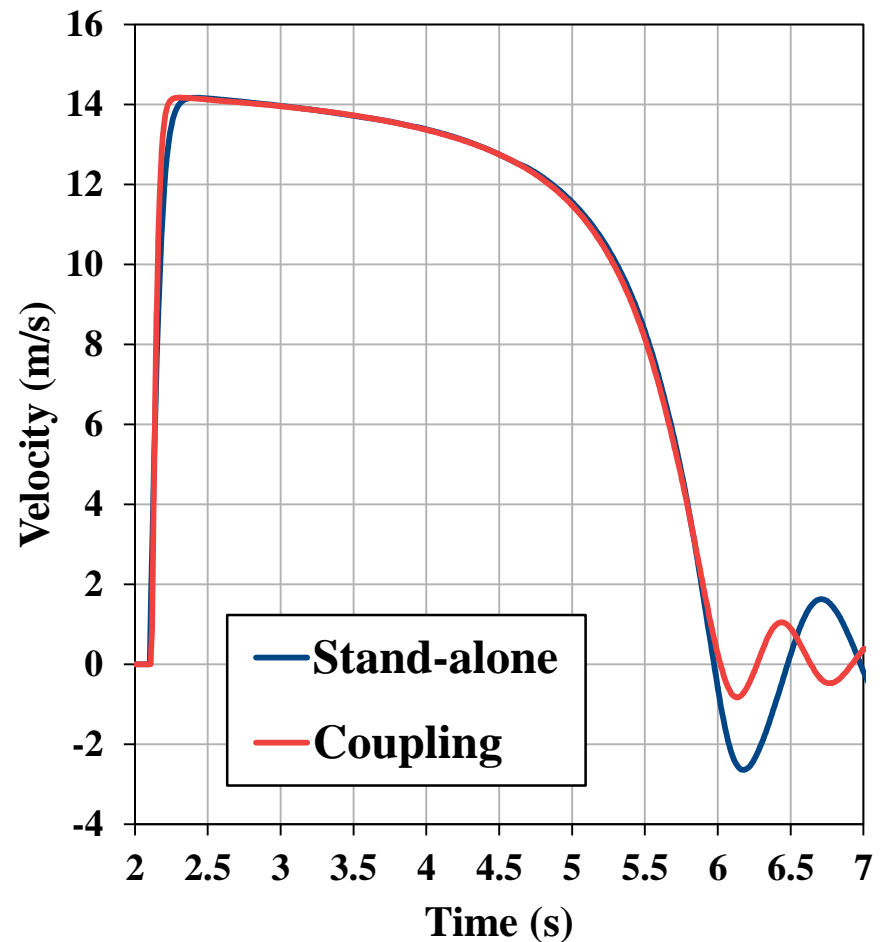
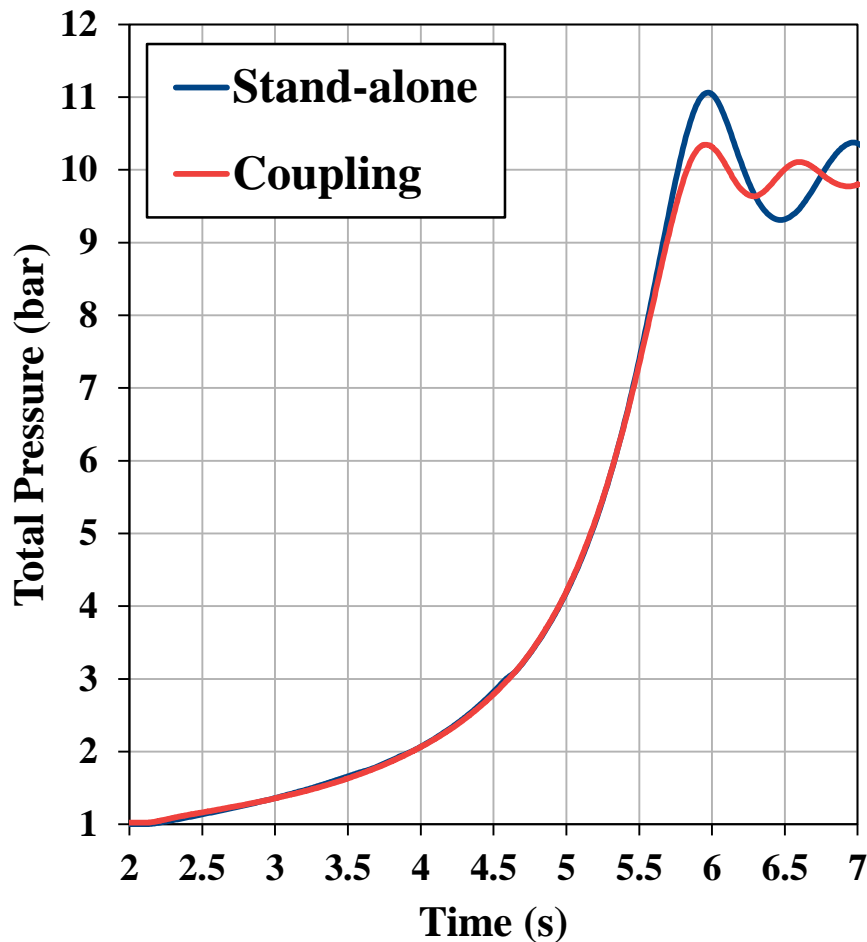
## Case 1: "Tanks at different pressure"

The tanks are initially at different pressure. The valve isolating the two sides of the system opens (at 2.1 s) and the transient start.



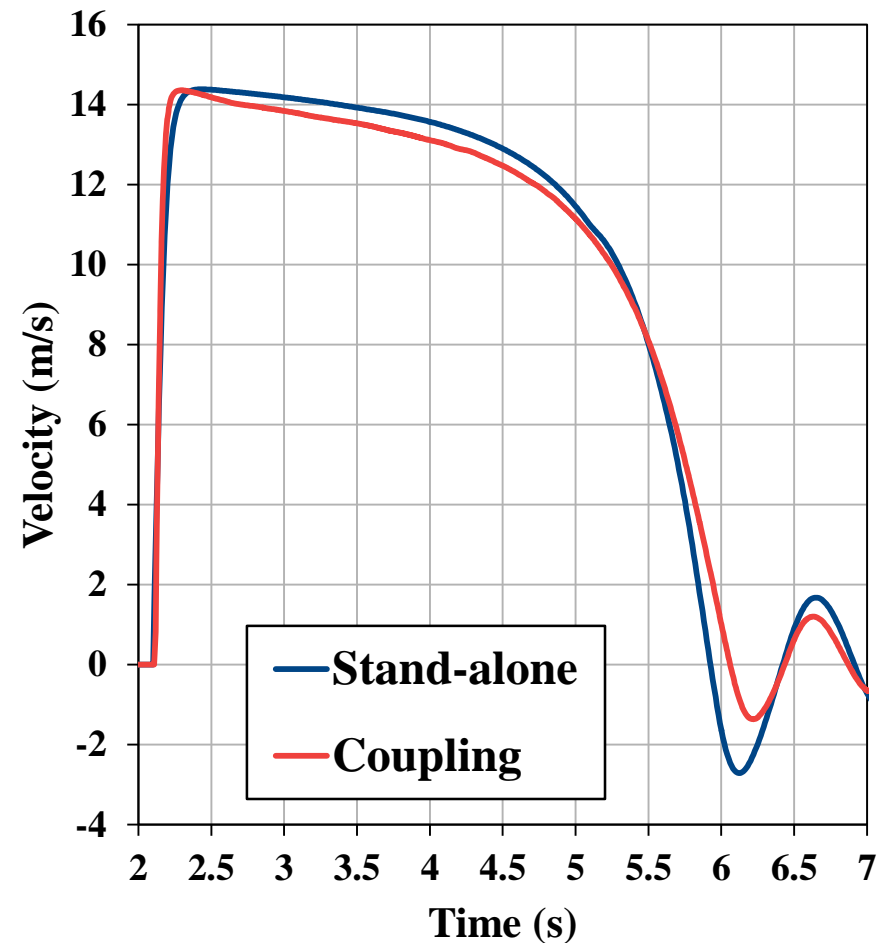
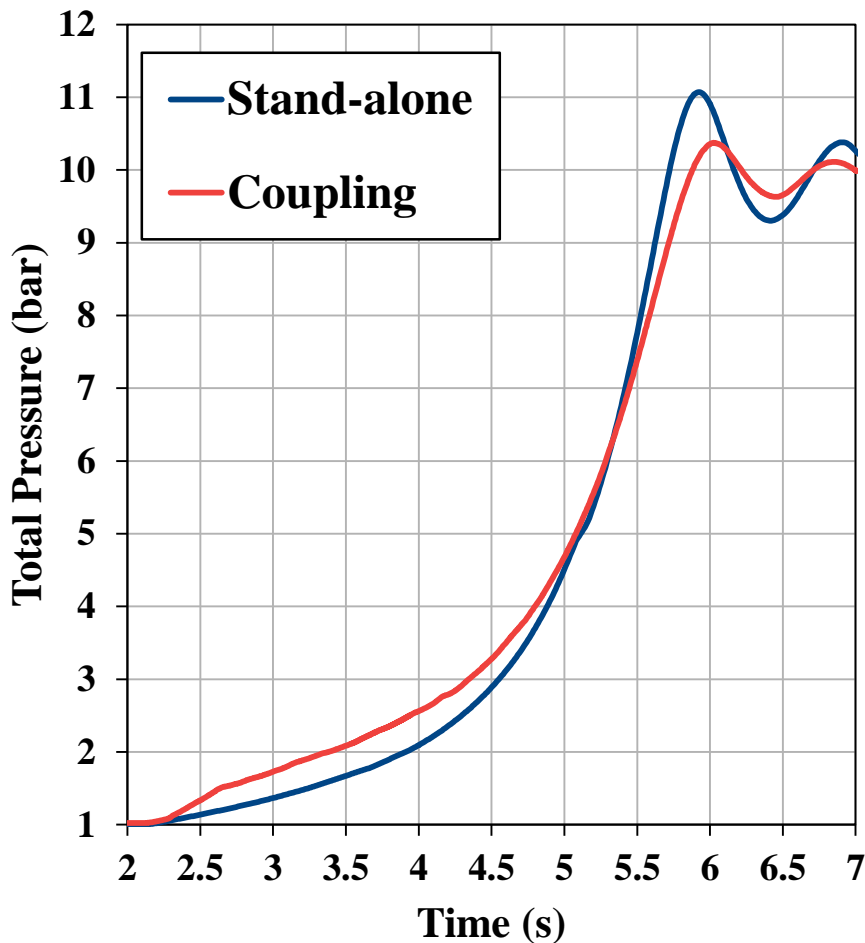
## Case 2: “High pressure tank kept at 10 bar”

The 2 tanks are initially at different pressure, and the “High Pressure” tank is kept at 10 bar. Initial water level and temperature identical in both tanks.



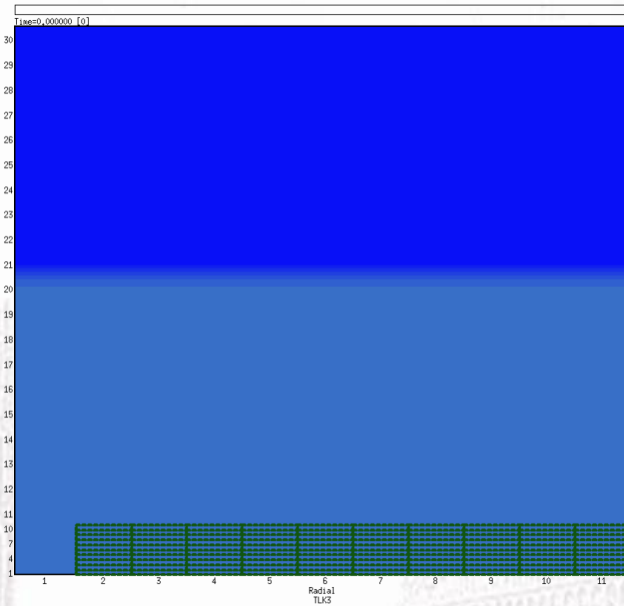
## Case 3: “High pressure tank kept at 10 bar with different water temperature in the two tanks”

The 2 tanks are initially at different pressure, and the “High Pressure” tank is kept at 10 bar. Initial water level identical in both tanks, and water temperatures set to 80°C in the “High Pressure” tank and 20°C in the “Low Pressure” tank.



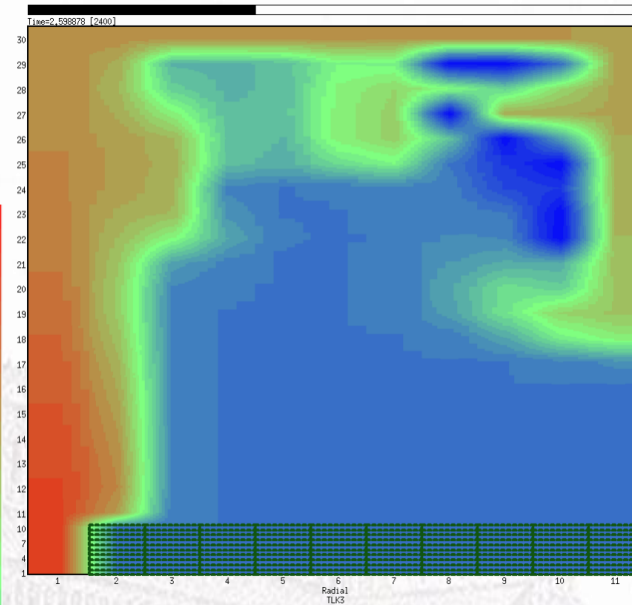
# Case 4: "High pressure tank kept at 10 bar with different water temperature in the two tanks"

$t = 0\text{ s}$

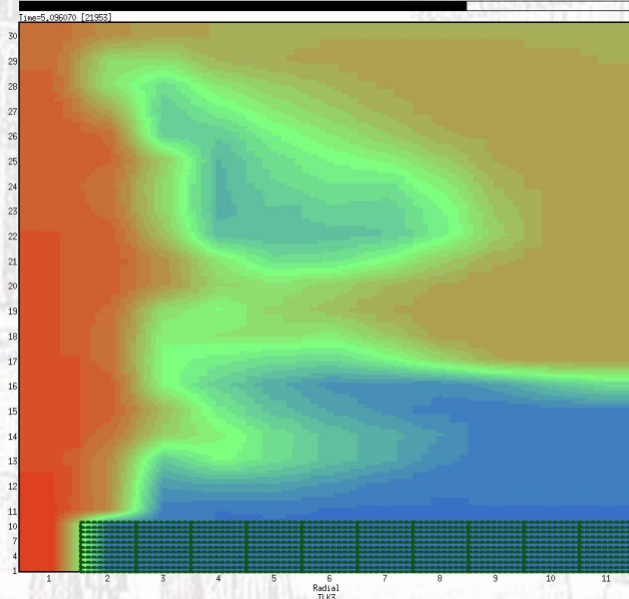


90 °C

$t = 2.6\text{ s}$

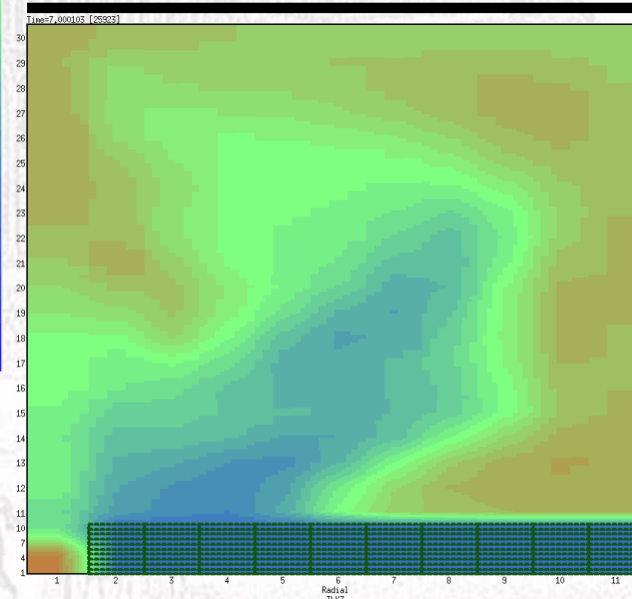


$t = 5.1\text{ s}$



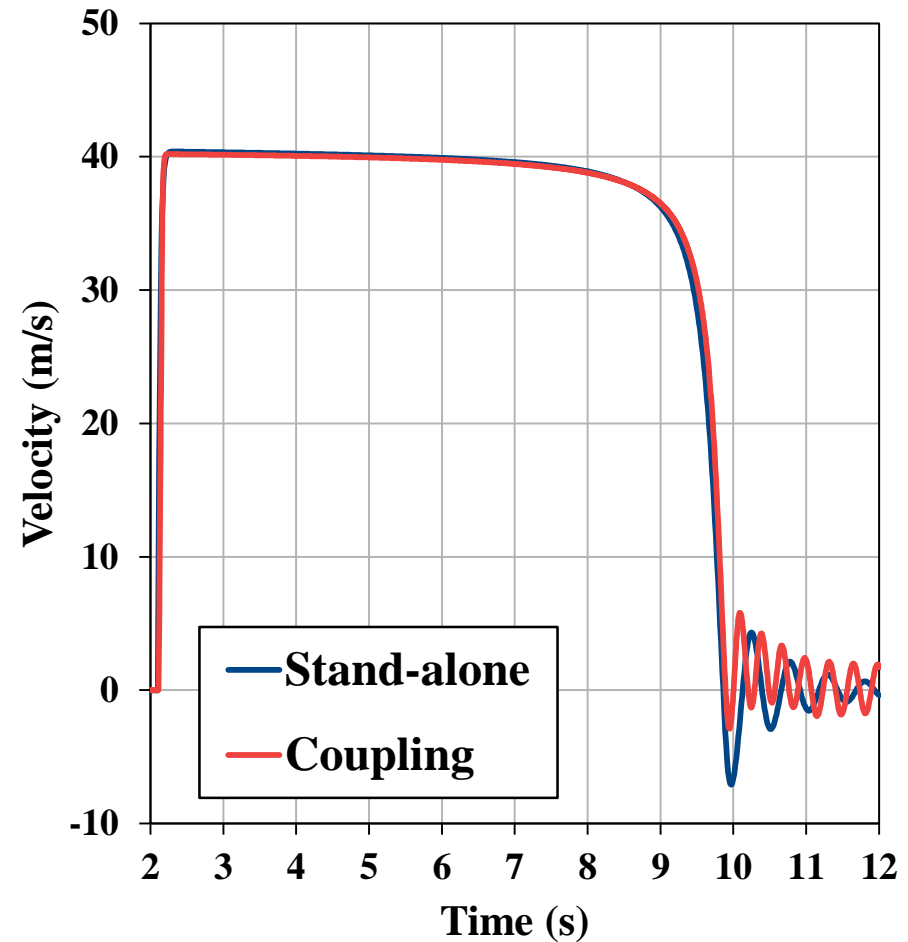
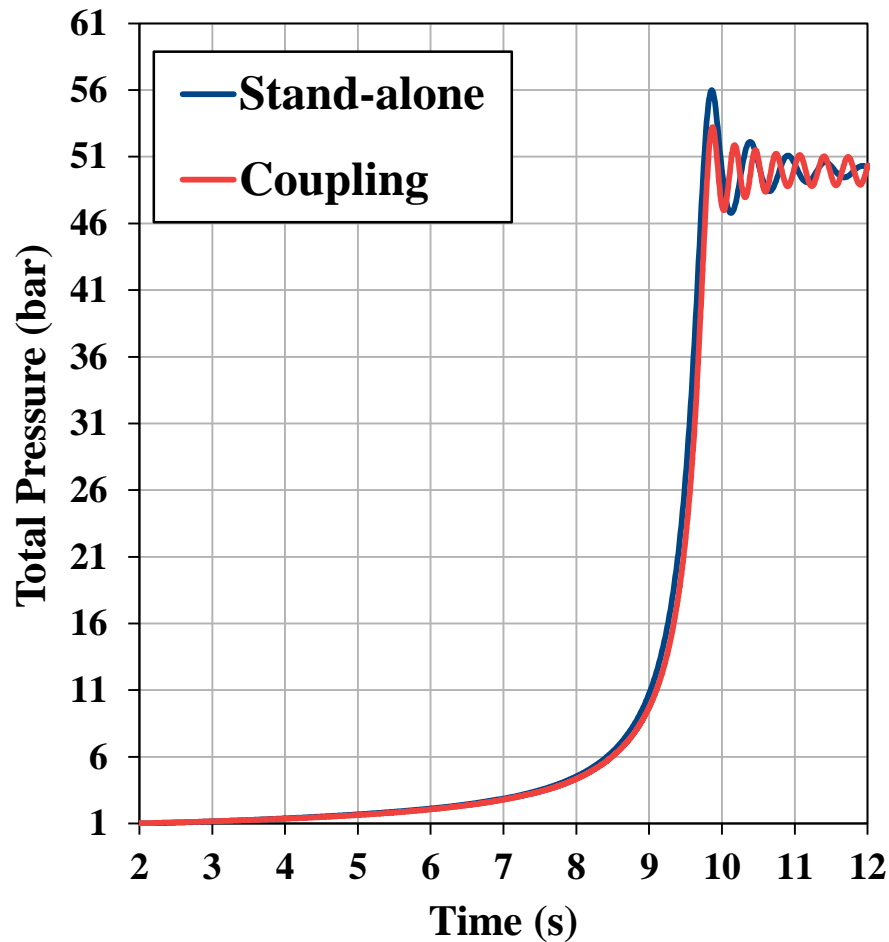
0 °C

$t = 7\text{ s}$



## Case 4: “High pressure tank kept at 50 bar”

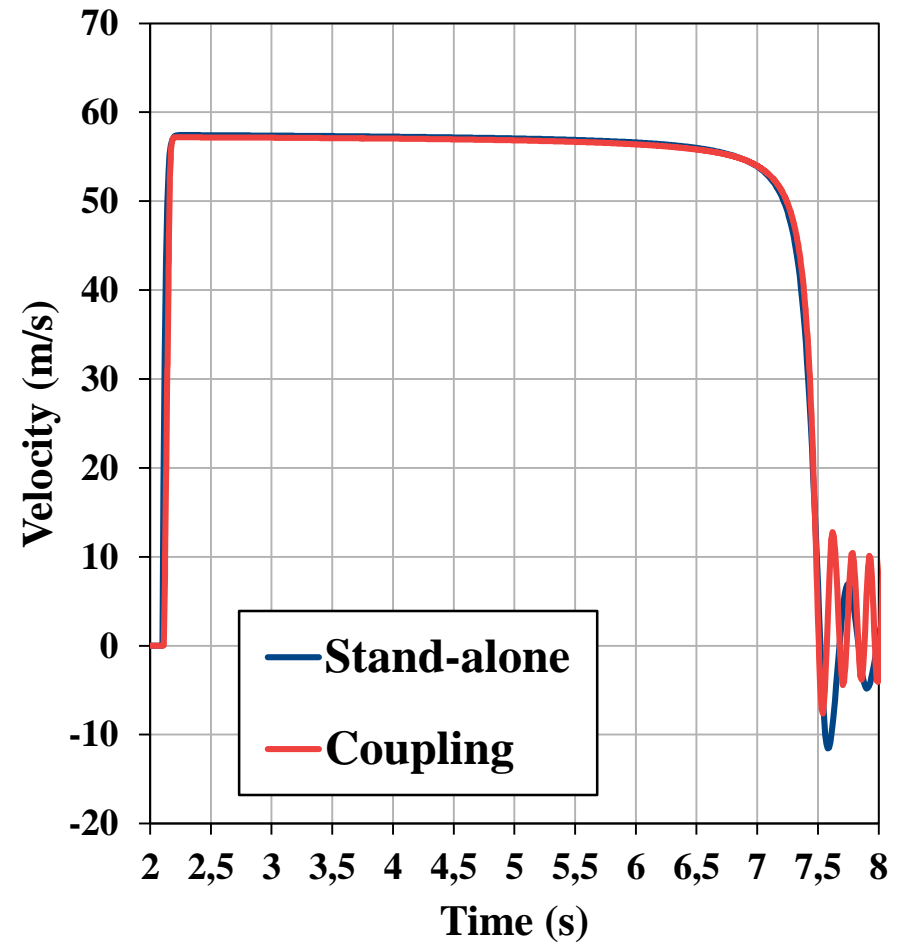
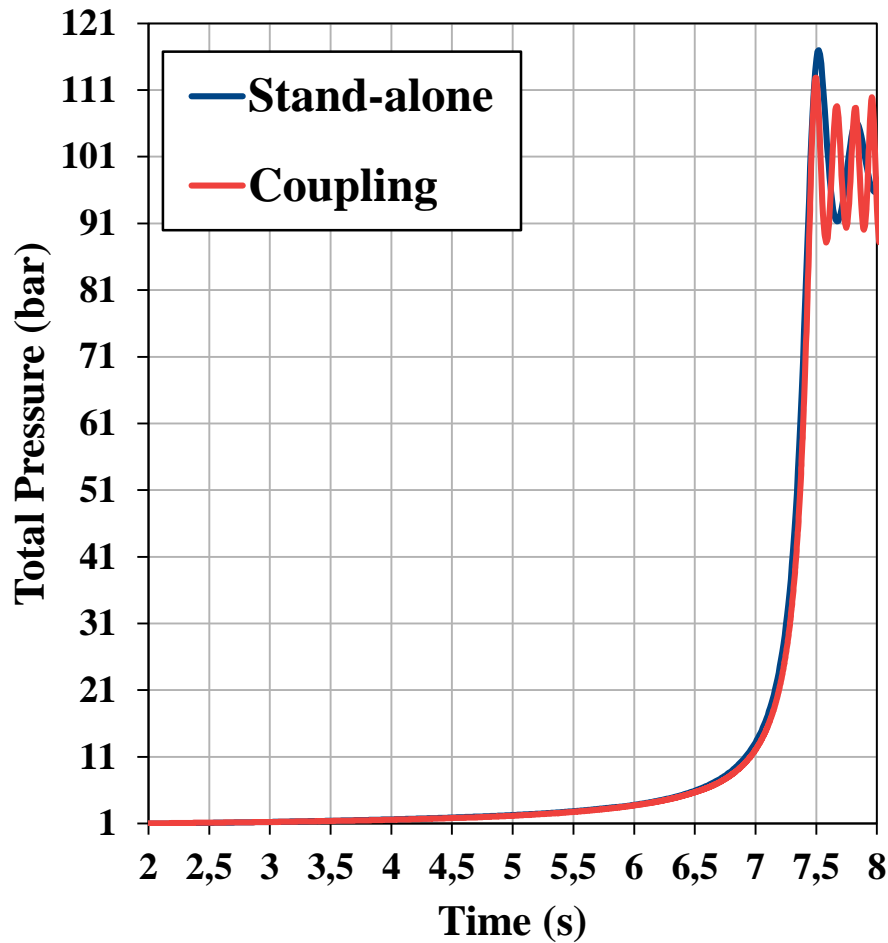
The tanks are initially at different pressure, the “High Pressure” tank is kept at 50 bar, and to avoid the gas flow between the two tanks the “Injection line” diameter was reduced to 0.025 m (0.05 m in the previous cases).





## Case 5: “High pressure tank kept at 100 bar”

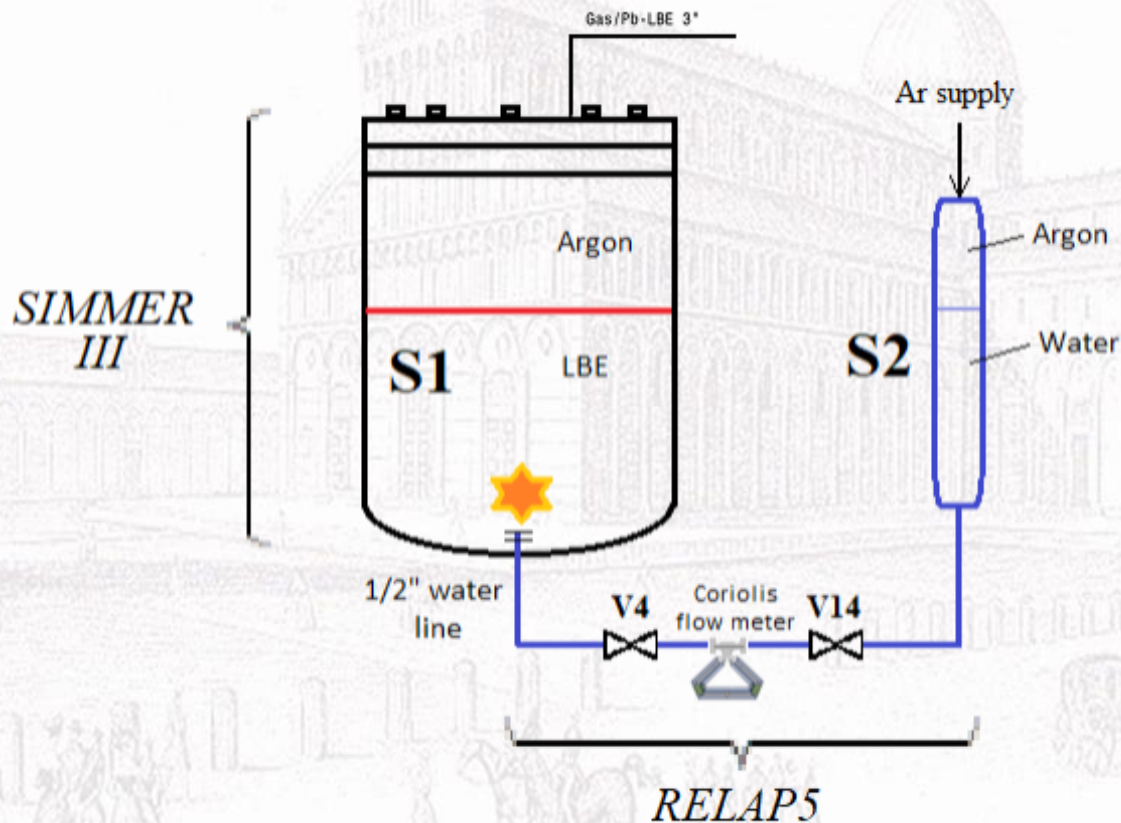
The tanks are initially at different pressure, the “High Pressure” tank is kept at 100 bar, and to avoid the gas flow between the two tanks the “Injection line” diameter was reduced to 0.025 m (0.05 m in the previous cases).



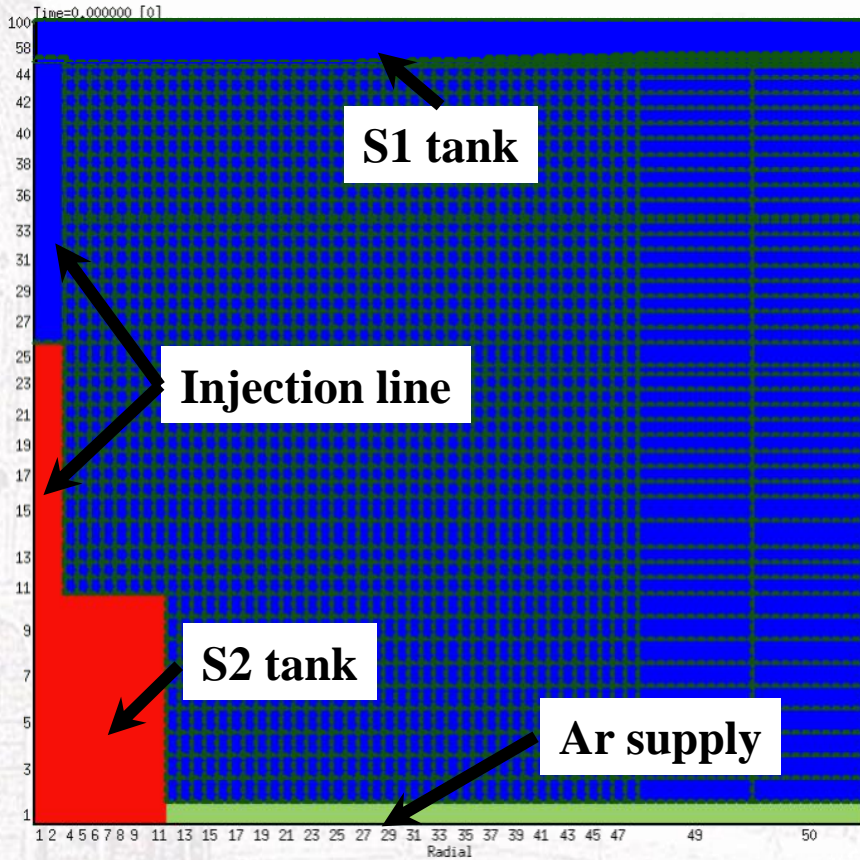
# SIMMER-RELAP5 coupled codes applied to LIFUS5/Mod3

Two-way coupling with “non-overlapping” strategy, i.e. the overall domain is divided into two regions modelled using the SIMMER III and RELAP5 codes:

- RELAP5 applied to simulate the S2 vessel and the injection line;
- SIMMER III code to simulate the Water/LBE interaction in the S2 vessel.



# SIMMER-RELAP5 coupled codes applied to LIFUS5/Mod3



- The facility is almost assembled and the tests are expected soon.
- Only preliminary input decks have been created and tested.

➤ **Short term:** have the SIMMER III and RELAP5 input decks ready for the end of June/mid of July.



# Conclusions

- Previous research activities performed byt UNIPI, in collaboration with ENEA, inside the EU Projects THINS (LIFUS 5 facility) and SEARCH (MYRRHA reactor), highlighted **possible improvements in performed analyses with a coupling between SIMMER and RELAP5 codes.**
- **Improvements and validation activities of the SIMMER and RELAP5 codes** have been carried out in order to study in depth phenomenological aspects of interest for accidents scenario in HLM reactors and fusion reactors.
- The developed coupling tool SIMMER-RELAP5, applied to a **manometer flow oscillation problem**, represent a first step of the activity that UNIPI must perform inside PAR2017.
- The future activity to be performed inside PAR2017 will consist in:
  - **improvement of the coupling tool implementing a semi-implicit numerical scheme** to enhance the stability of the calculations;
  - **application of the developed coupling tool to the LIFUS5/Mod3 facility** in support of the pre-test analysis.

# WORKSHOP TEMATICO: GEN IV LEAD COOLED FAST REACTOR

Stato attuale della tecnologia e prospettive di sviluppo  
ADP MiSE-ENEA (PAR2017-LP2)

*Aula 8 - Dipartimento di Ingegneria Astronautica, Elettrica ed Energetica  
Università di Roma "La Sapienza"  
San Pietro in Vincoli, Via Eudossiana 18  
14-15 Giugno 2018*



SAPIENZA  
UNIVERSITÀ DI ROMA



## Phenix Asymmetrical Test Simulation by 3D STH code

Fabio Giannetti [Sapienza]

Vincenzo Narcisi [Sapienza]

Andrea Subioli [Sapienza]

Gianfranco Caruso [Sapienza]

Alessandro Del Nevo [ENEA]

# CONTENTS

- Introduction
- Objectives of the activity
- Outline of PHENIX reactor
- RELAP5-3D<sup>®</sup> nodalization
- “Dissymmetric test” description
- Blind results and comparison with experimental data
- Preliminary TH-NK coupled model and results
- Summary and follow-up

# INTRODUCTION

- ❑ PHENIX End Of Life Tests performed in 2009 after the 56<sup>th</sup> irradiation cycle
- ❑ 2 tests were performed in thermal-hydraulics area
  - *a natural convection test* and
  - a dissymmetrical configuration test
    - this has been selected as a benchmark transient
    - synergy with H2020 SESAME project

# OBJECTIVES OF THE ACTIVITY

- ❑ to compare best-estimate TH-SYS code calculations to experimental data, thus to validate RELAP5-3D© system code in simulating FR designs
- ❑ to assess the reliability of SYS-TH multiD components in modeling transient in LM pool FR
- ❑ to identify and, as far as possible, to quantify the code limitations and the source of uncertainties in simulating postulated accidents occurring in liquid metal FR designs
- ❑ to improve the understanding of the TH processes and phenomena observed in dissymmetrical test
- ❑ to improve the understanding of FR neutronics, TH and SYS analysis



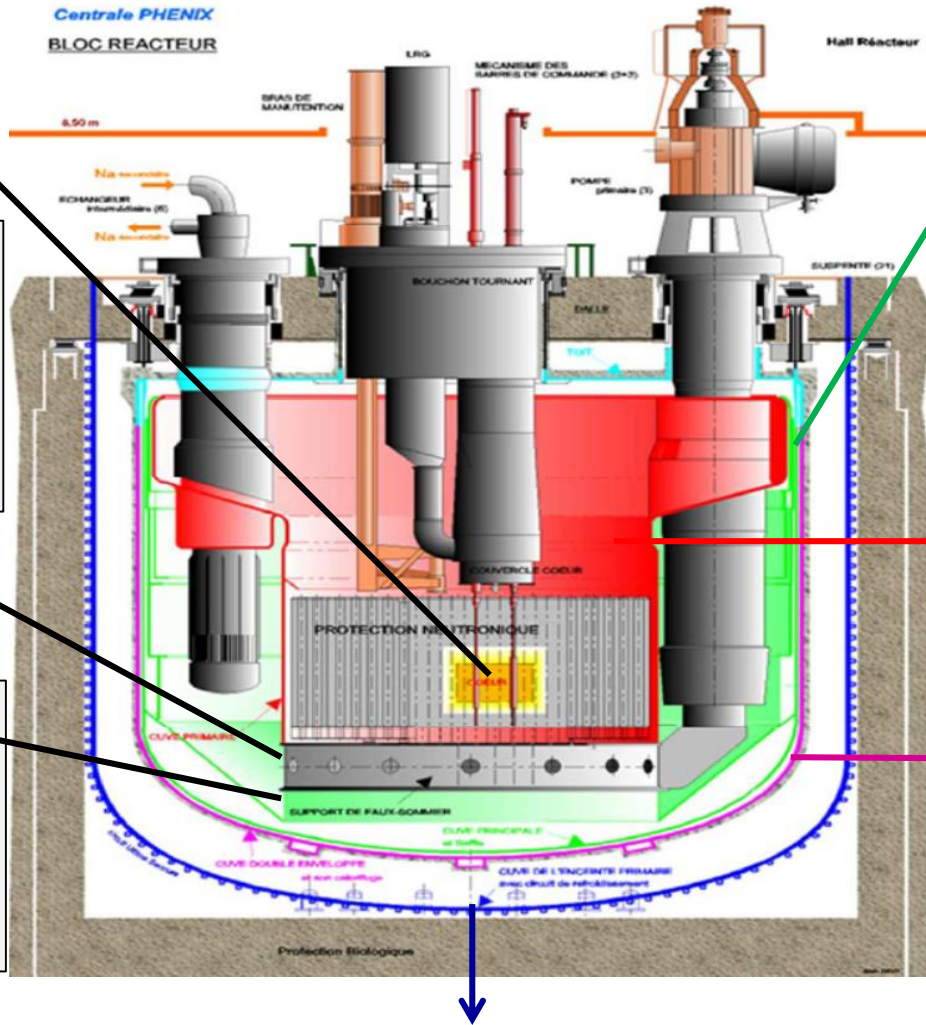
# PHENIX

Centrale PHENIX  
BLOC REACTEUR

CORE

**Diagrid** is connected to primary pumps. It has the function of positioning, supporting and supplying sodium to core SA

**Strongback** has the function of supporting the core and it carries about the 10% of operating flow to the vessel cooling system.



**Main vessel**

Diameter = 11.8 m  
Na inventory = 800 tons  
Attached to the upper slab by 21 suspension hangers  
Cooled in the upper zone by a vessel cooling system

**Inner vessel** separates the pool in two regions: hot and cold.

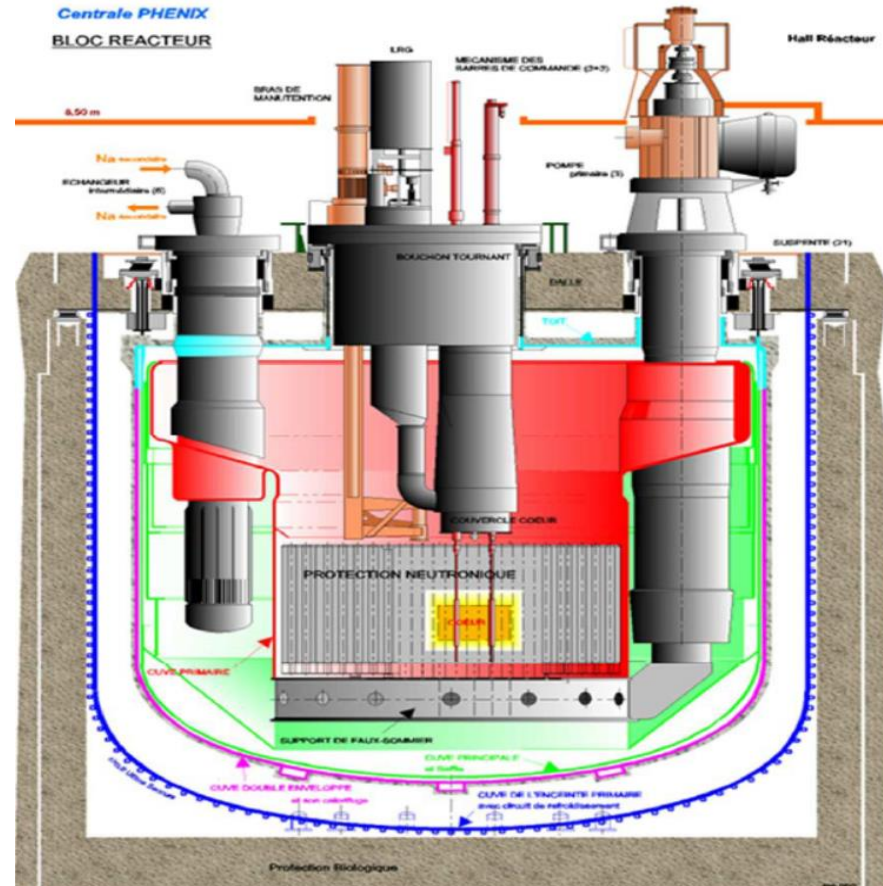
**Double- envelope vessel** is welded to the upper region of the main vessel and it has the function of containing any possible sodium leaks.

**Primary containment vessel** is welded to the slab's underside, and attached to the reactor pit. It has to retain radioactive release of postulated severe accident. It carries the final emergency cooling system which is designed to keeping the reactor concrete at ambient temperature, and to ensure the decay heat removal

# Nodalization description

## PHENIX nodalization man features:

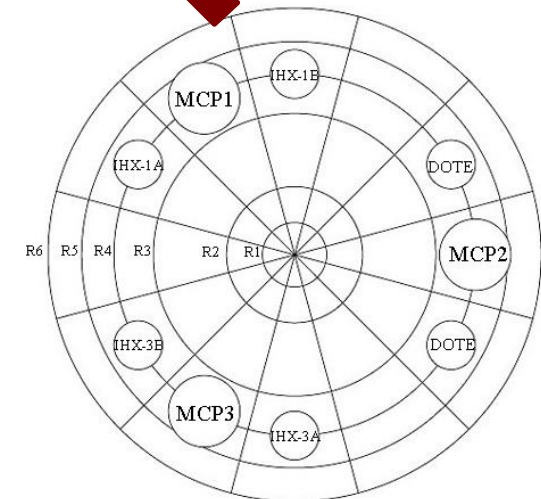
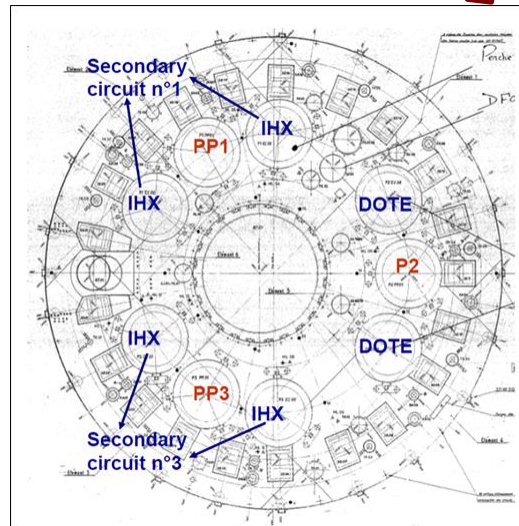
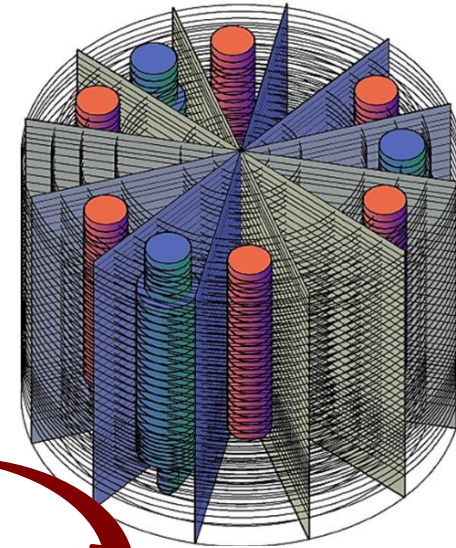
- ❑ MULTID component + 1D components for 3D nodalization; 1D components for bidimensional nodalization
- ❑ Relevant elevations of PHENIX are maintained in the nodalization, with minor ( $< \sim 5$  cm) exceptions due to modeling constraints (e.g. IHX bottom)
- ❑ WESTINGHOUSE heat transfer correlation in bundle regions, Seban –Shimazaki everywhere
- ❑ Wire wrapped fuel bundle friction losses modeled with Cheng and Todreas



# PHENIX: 3D Thermal-hydraulic model

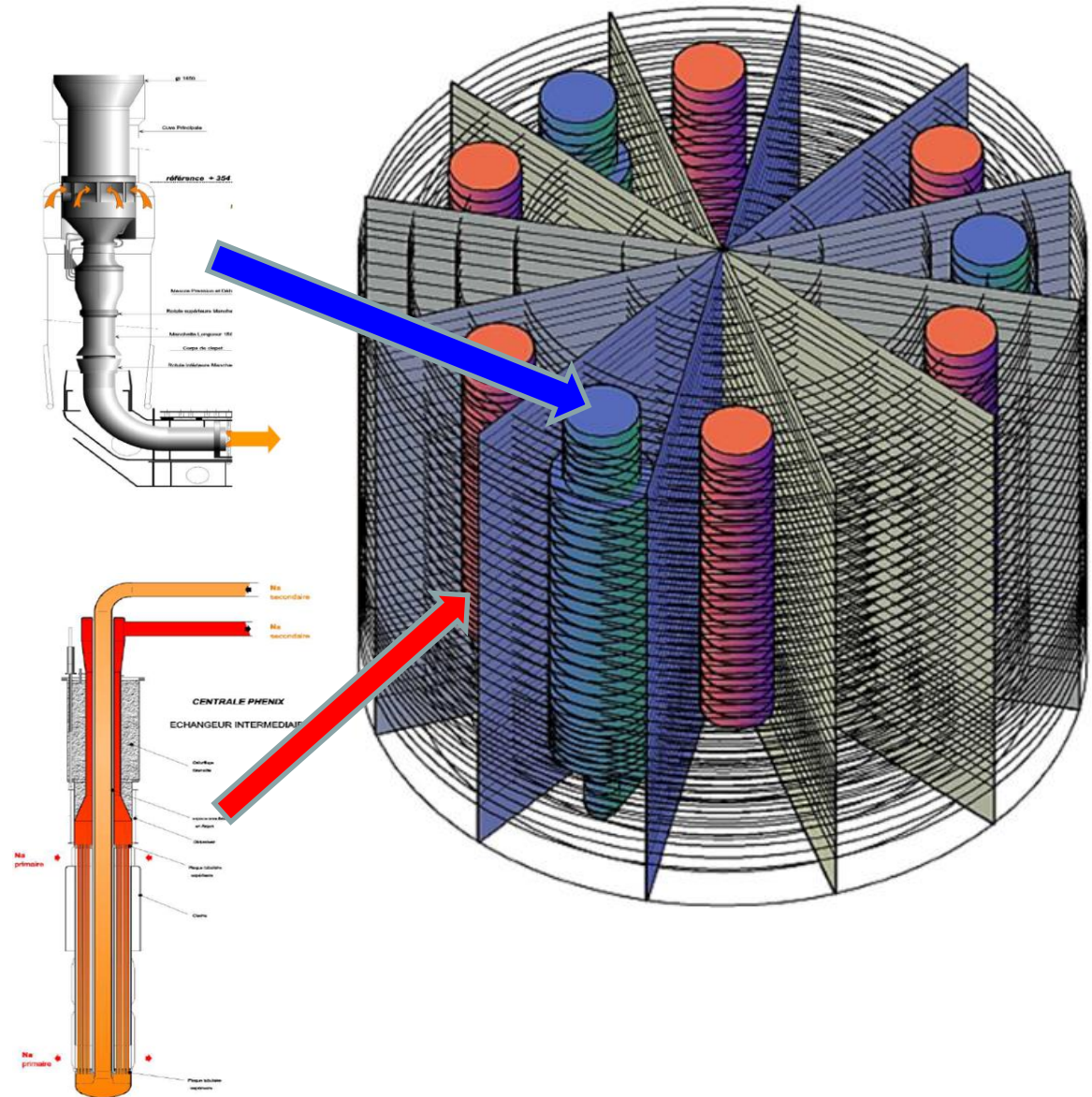
- Sliced approach applied in all systems
- FA orifice setup on the basis of mass flow rates and overall DP
- K-loss coeff. in junct. evaluated or estimated on the basis of geometries
- Roughness is set  $3.2 \text{ E-}5\text{m}$  with the exception of the core region where is set  $1 \text{ E-}6$

| QUANTITY                         | Value        |
|----------------------------------|--------------|
| # of HYDR volumes                | <b>6940</b>  |
| # of HYDR junctions              | <b>11840</b> |
| # of HEAT structures             | <b>6888</b>  |
| # of HEAT structures mesh points | <b>40170</b> |



# 3D pool model

- Layout of MCP conduits and IHXs modeled according with the real configuration ( $\theta$ ,  $z$ )
- Porosity factors are used to model the geometry and the flow paths
- MULTID dimension 6x12x35
- MULTID models:
  - Diagrid
  - Core bypass
  - Hot pool
  - Cold pool



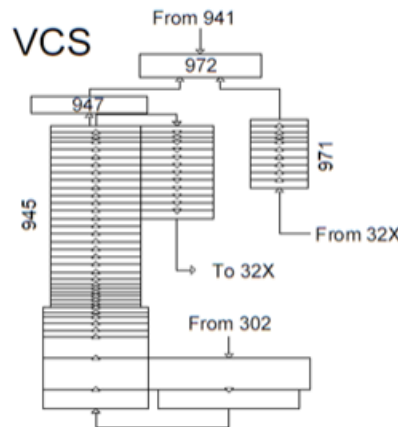
# 1D Nodalization description

## VCS, STRONGBACK, COLD/HOT POOL LEVEL

- Vessel cooling system and strongback are modeled with one PIPE, connected upstream with the diagrid, on the top with the gas plenum (972), and downstream with the corresponding regions of cold pool.
- Annular region representing the coldpool level is modeled with one PIPE connected downstream with the corresponding regions of cold pool.
- Level of the hot pool is represented with BRANCH component connected downstream with the upper levels of hot pool

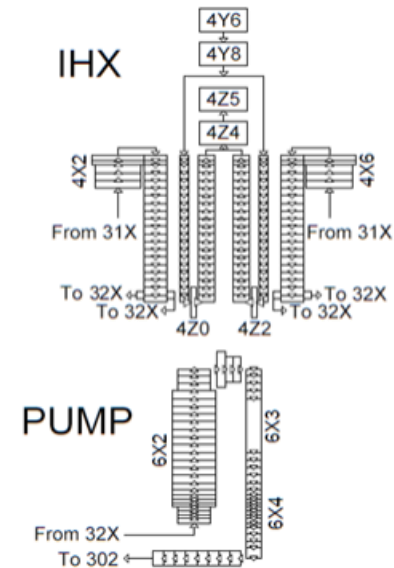
## PUMPS

- Annular inlet is simulated with an ascending pipe connected with the cold pool.
- Pump is modeled with PUMP component setting up the homologous curve using PHENIX reference data.
- Discharge is modelled with a descending pipe which leads the primary coolant to the diagrid.

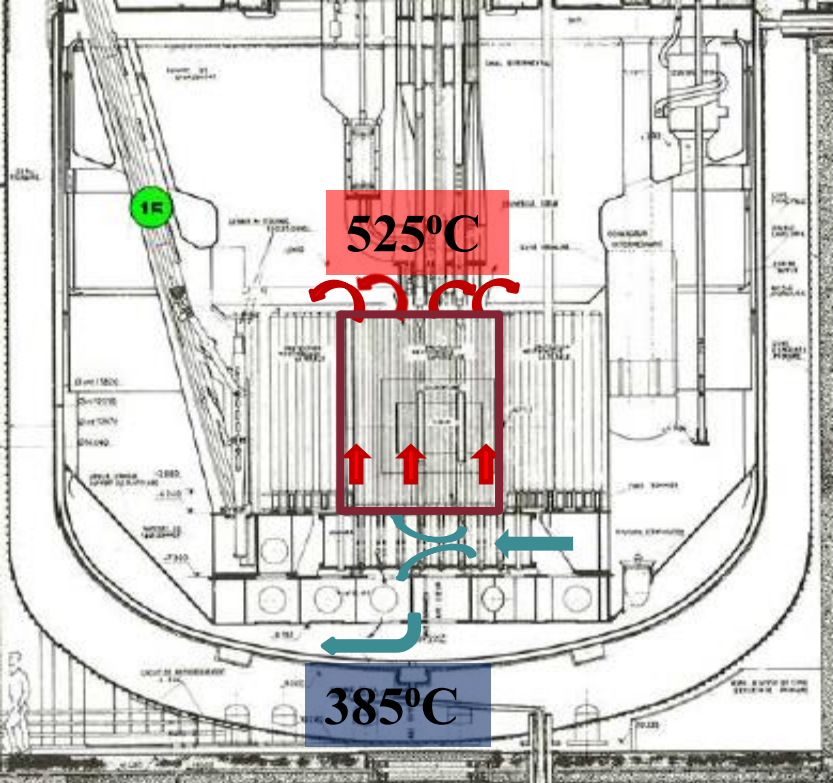


## IHX

- primary sides are modeled separately with PIPE components connected upstream and downstream with the correspondent region of hot pool and cold pool.
- secondary sides are modeled separately with pipe components from an inlet and outlet collectors (dummy) and fed with imposed boundary conditions



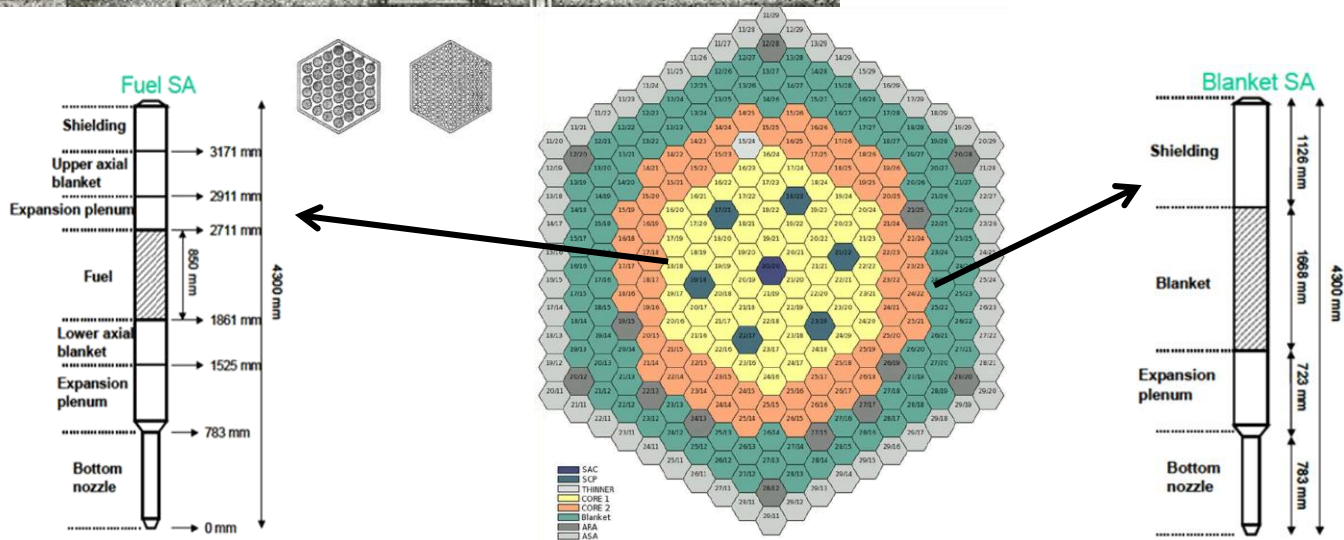
# CORE



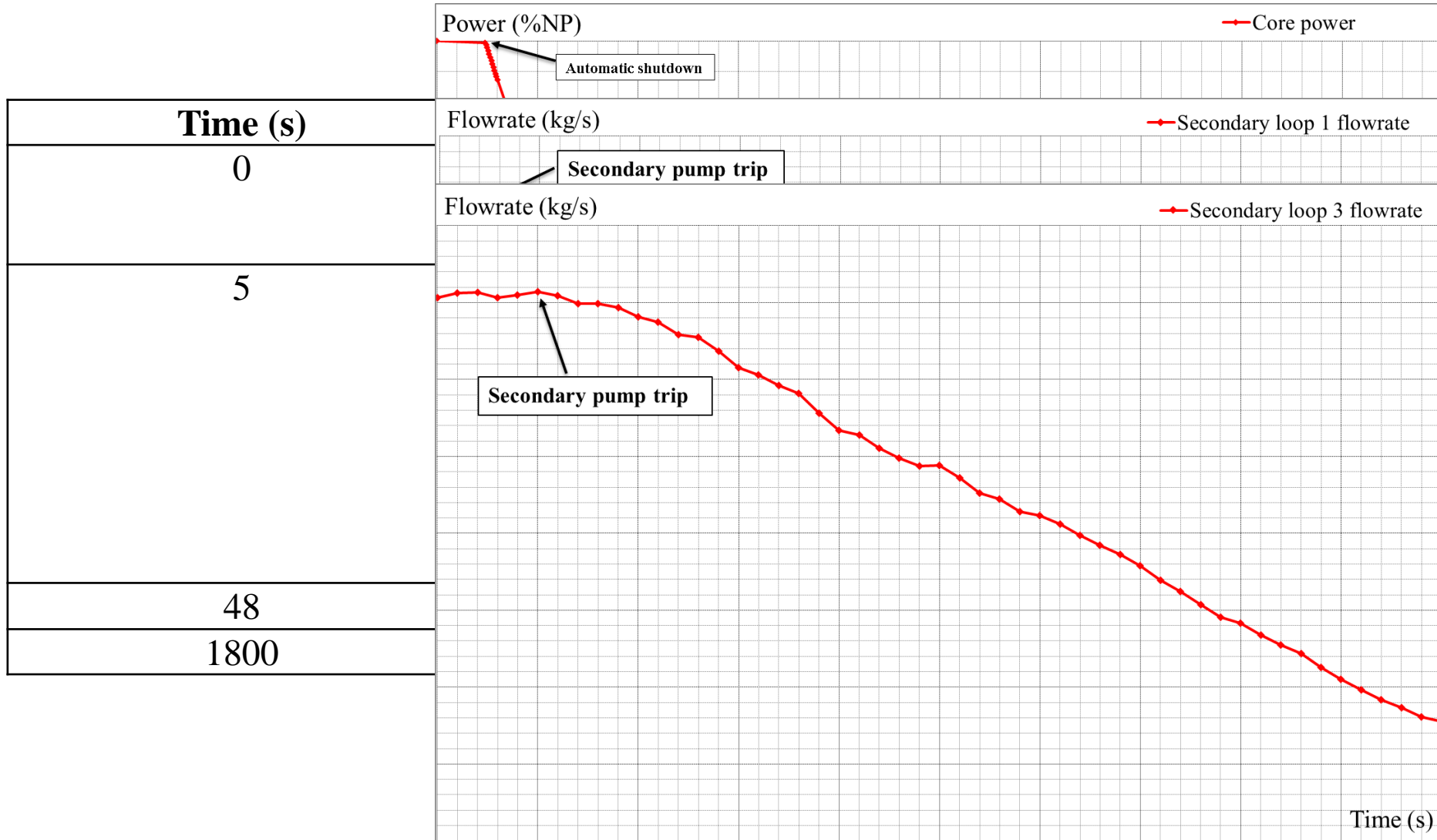
| zone              | Power [MWth] | Flow rate [kg/s] |
|-------------------|--------------|------------------|
| Inner core        | 180.9        | 861              |
| Outer core        | 143.1        | 779              |
| Blanket zone      | 24.1         | 226              |
| Control rods zone | 0.7          | 14               |
| Steel zone        | 1.2          | 62               |
| Storage zone      | 1.7          | 46               |
| <b>Total</b>      | <b>351.7</b> | <b>1988</b>      |

The Phénix core is composed by:

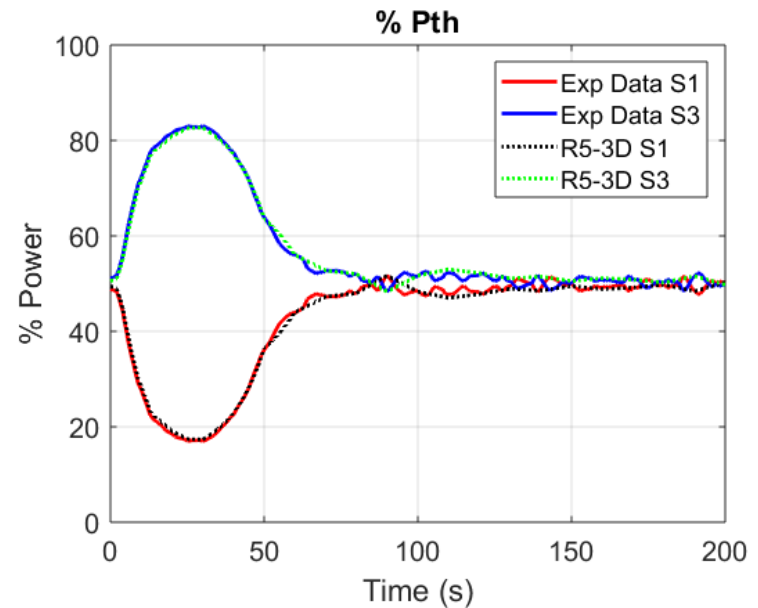
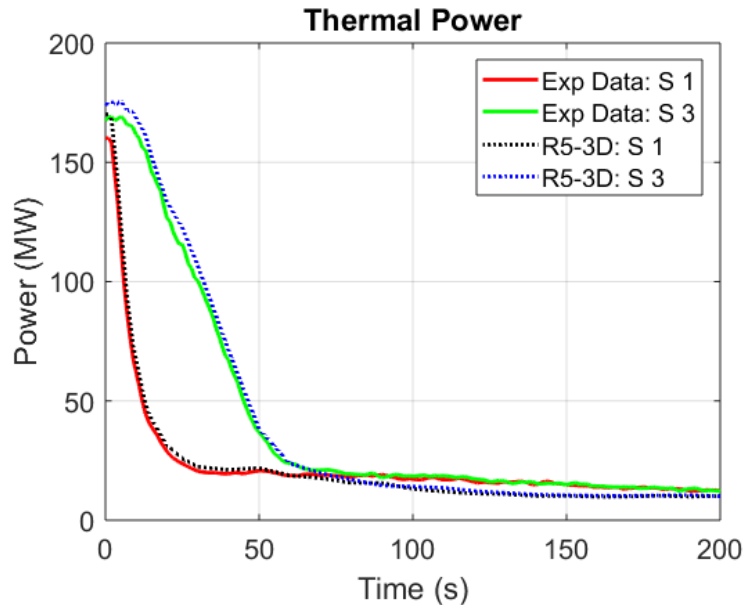
- 54 SA for the inner core zone
- 56 SA for the outer core zone
- 86 SA for the blanket zone
- 6 Control Rods (CRs) SA
- 1 Safety Rod (SR) SA
- 212 steel reflector SA
- 765  $B_4C$  shielding SA
- 297 steel shielding SA



# Asymmetrical test description



# PHENIX: main results



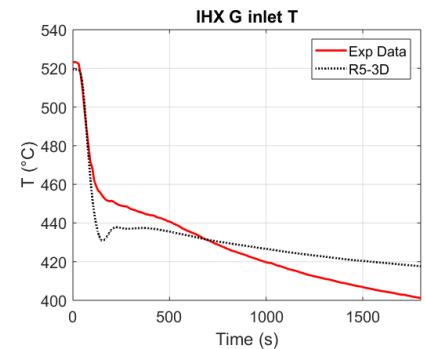
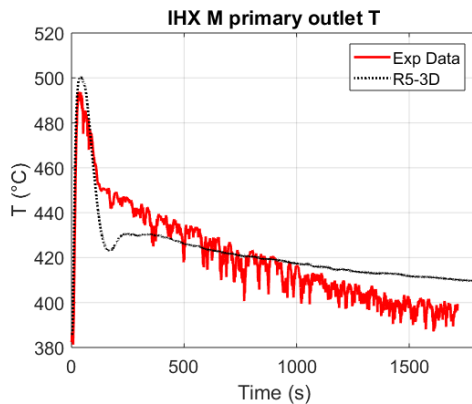
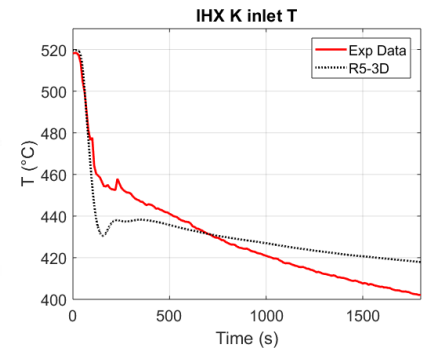
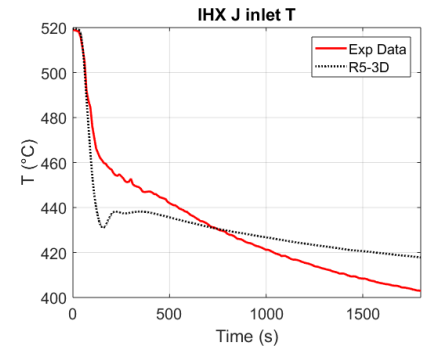
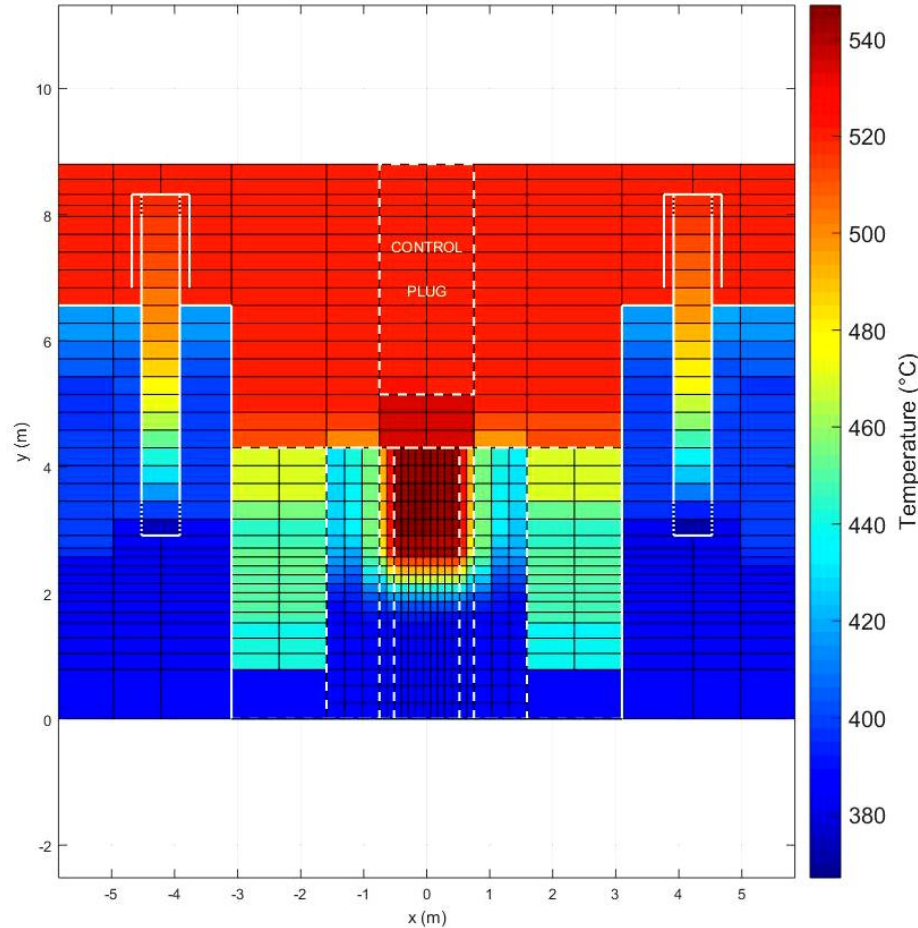
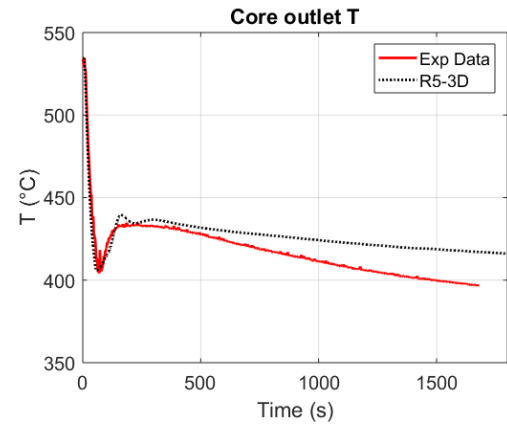
## Main results:

- At the beginning of the test, the secondary mass flow rate of the LOOP 1 decreases, causing the fast reduction of the thermal power removed by the IHX-1A and the IHX-1B.
- Thermal power removed by the LOOP 1 (IHX-1A + IHX-1B) and the LOOP 3 (IHX-3A + IHX-3B) in the first 200 s of the transient shows the delay of the power reduction of the LOOP 3, due to the delay time of the LOOP 3 trip

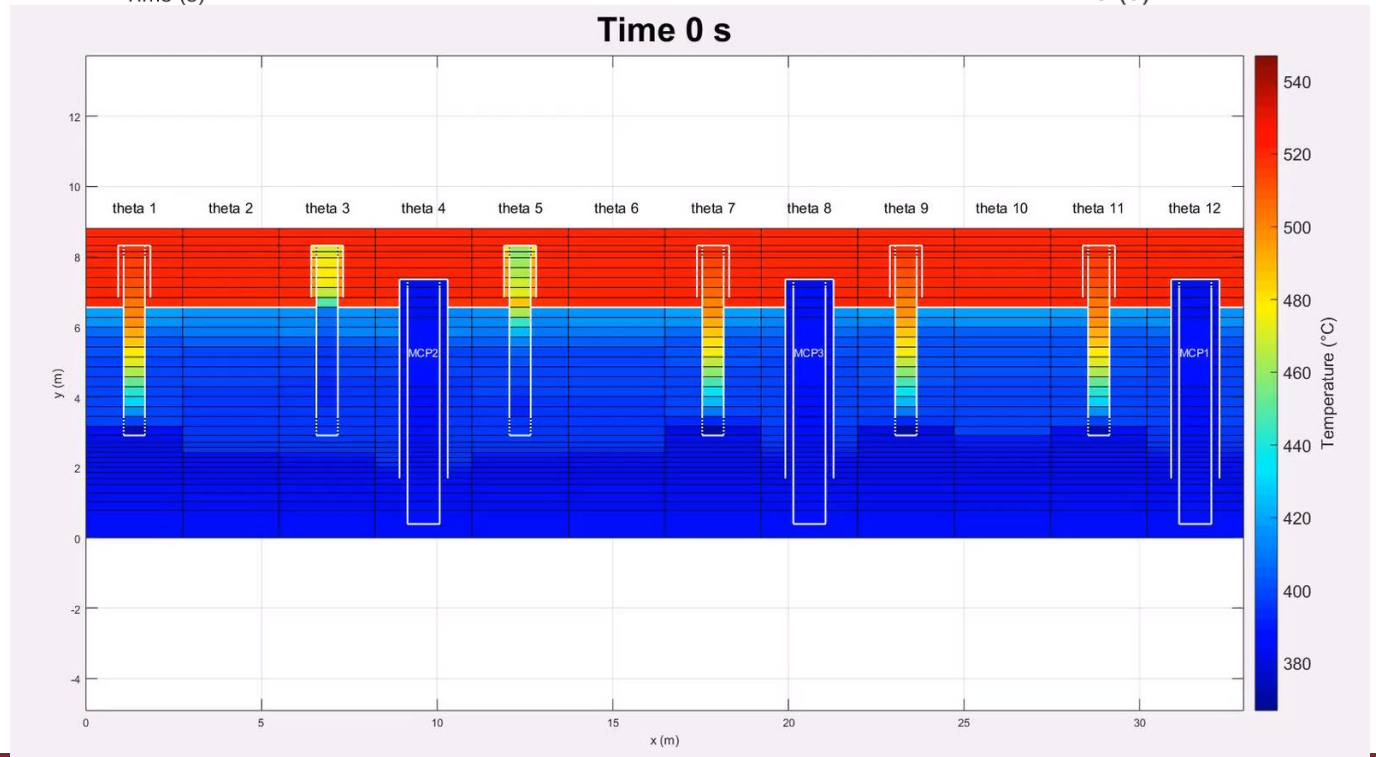
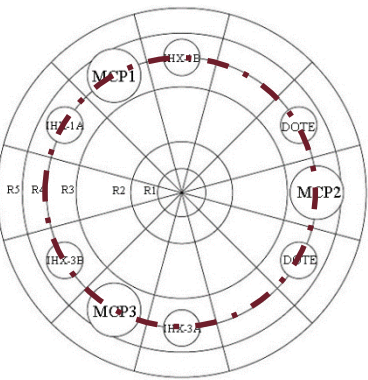
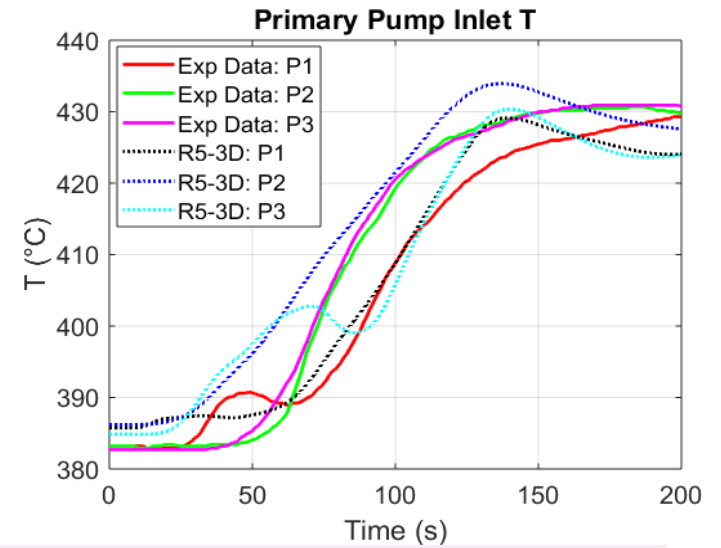
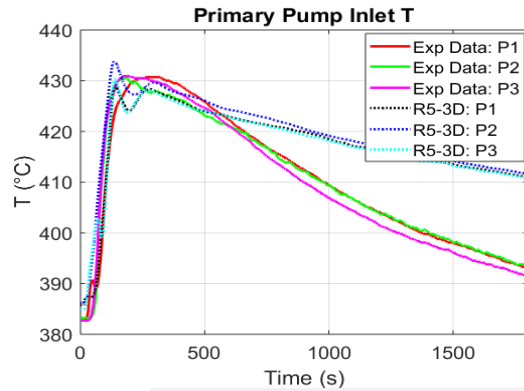


# PHENIX: main results

Time 0 s

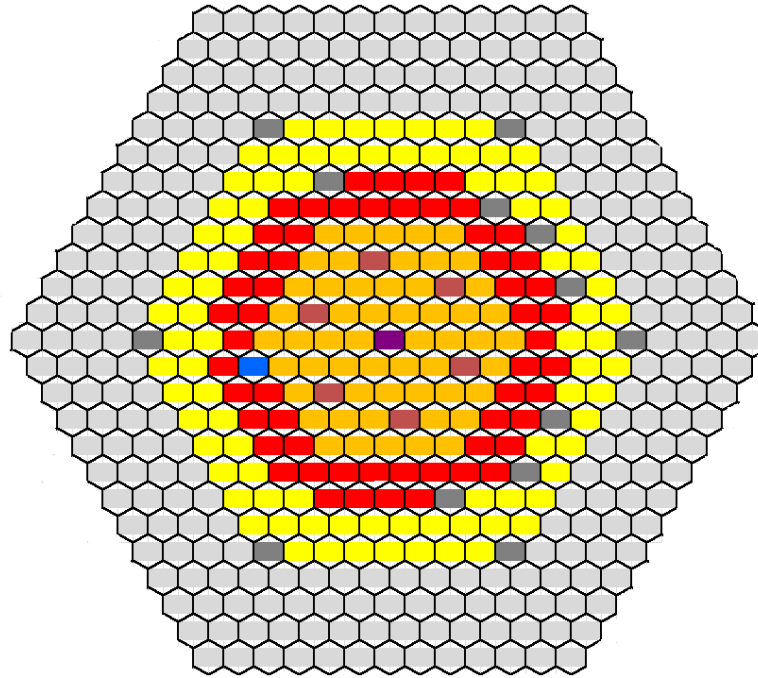
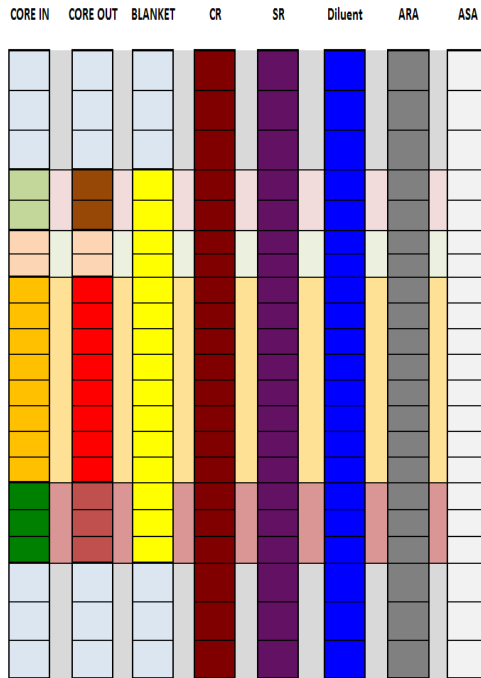


# PHENIX: main results



# PHENIX TH-NK COUPLED MODEL

# Model: Phénix Core Nodalization for PHISICS

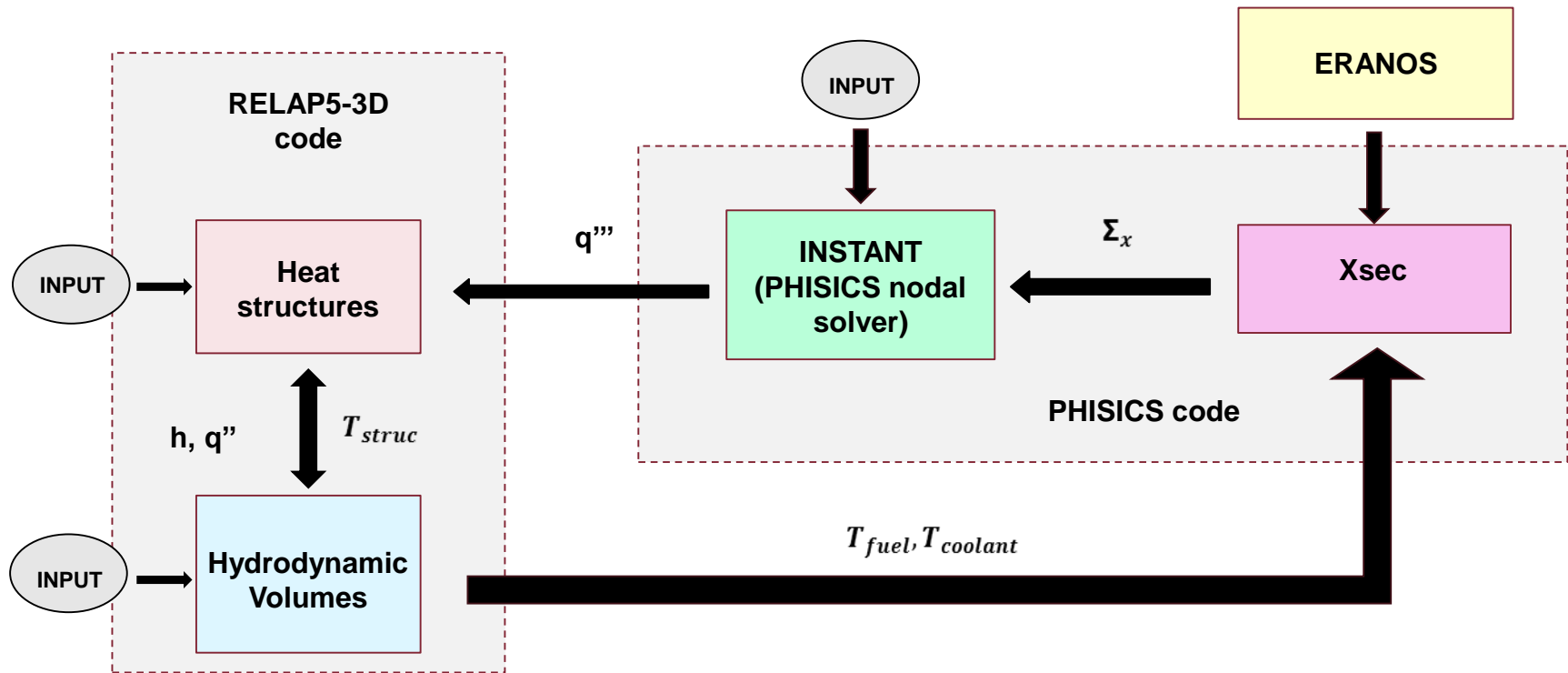


|   |         |    |                 |
|---|---------|----|-----------------|
| 1 | LAB 1   | 8  | CR              |
| 2 | LAB 2   | 9  | SR              |
| 3 | UAB 1   | 10 | Plenum Na       |
| 4 | UAB 2   | 11 | ARA             |
| 5 | Blanket | 12 | ASA             |
| 6 | CORE 1  | 13 | Axial shielding |
| 7 | CORE 2  | 14 | Diluent         |

|   |             |
|---|-------------|
| <b>Number of kinetic meshes</b>           | <b>21</b>   |
| <b>Zone Figures</b>                       | <b>17</b>   |
| <b>Composition Figures</b>                | <b>6</b>    |
| <b>Compositions</b>                       | <b>14</b>   |
| <b>Numero of rings</b>                    | <b>12</b>   |
| <b>Number of kinetic nodes in a plane</b> | <b>469</b>  |
| <b>Total number of kinetic nodes</b>      | <b>9849</b> |
| <b>Neutron groups</b>                     | <b>33</b>   |

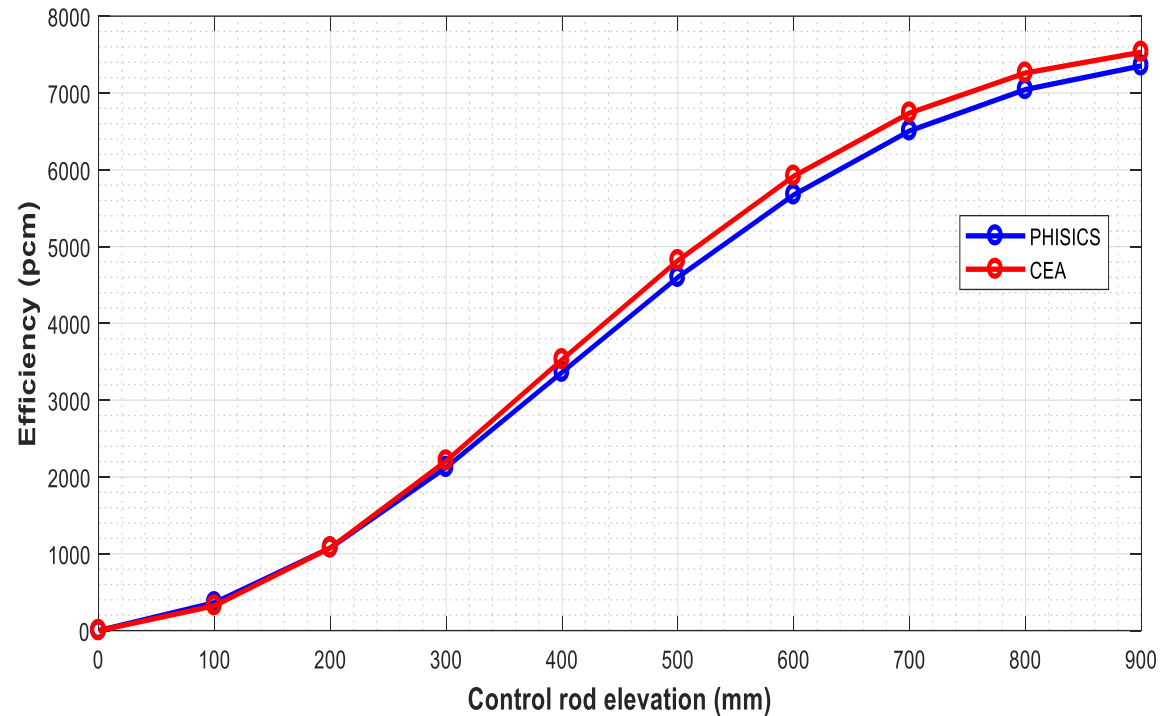
# RELAP5-3D/PHISICS Coupled Codes

- RELAP5-3D provides PHISICS with the **thermal-hydraulic parameters**
- They are used by PHISICS in order to interpolate the **macroscopic cross sections**
- PHISICS calculates **power distributions** that contribute to the change of the thermal-hydraulic parameters (RELAP5-3D feedback on power)



# Results: Control Rod Calibration Curve

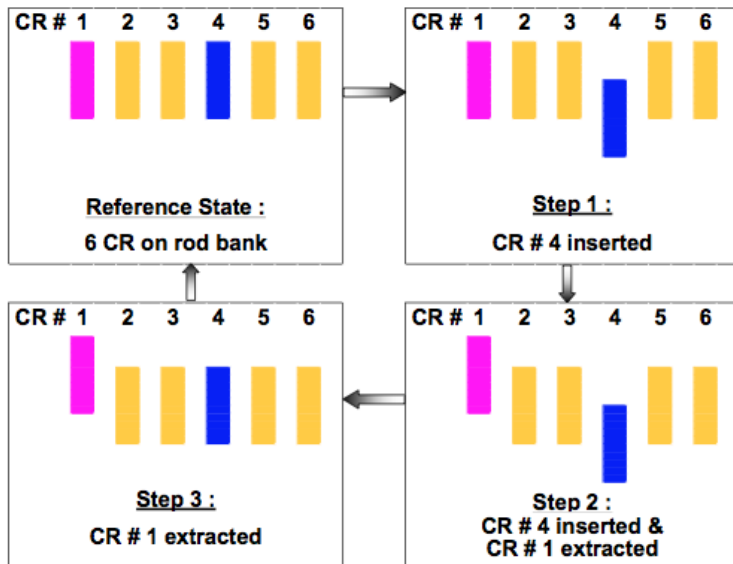
| Control rod positions (mm) | $K_{eff}$ | $\rho$ (pcm) | Efficiency (pcm) |
|----------------------------|-----------|--------------|------------------|
| 900                        | 1.02568   | 2504         | 7352             |
| 800                        | 1.02245   | 2196         | 7044             |
| 700                        | 1.01686   | 1658         | 6506             |
| 600                        | 1.00831   | 824          | 5673             |
| 500                        | 0.99752   | -248         | 4599             |
| 400                        | 0.98537   | -1485        | 3364             |
| 300                        | 0.97349   | -2723        | 2125             |
| 200                        | 0.96365   | -3772        | 1077             |
| 100                        | 0.95708   | -4485        | 364              |
| 0                          | 0.95376   | -4848        | 0.00             |



- The control rod worth calculated by CEA is 7531 pcm.
- The control rod worth calculated by PHISICS is 7352 pcm (about -2.4 % of difference if compared with CEA).

# Control rod shift test: Tested Configurations

Three configurations have been studied during the test. CR n° 1 and CR n° 4 were progressively offset in relation to each other, while maintaining constant the total power.



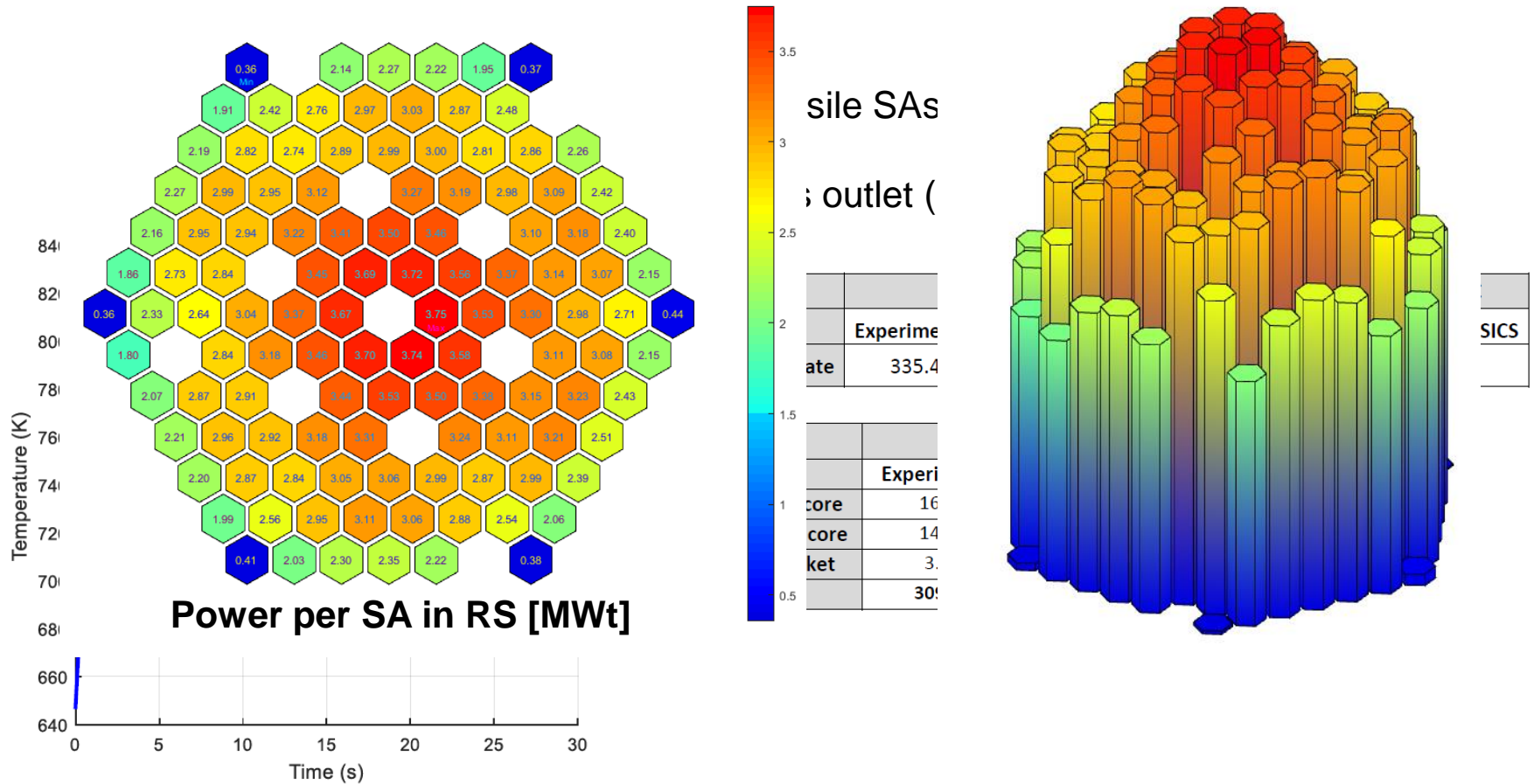
|                 | Control rod position (mm) |                  |                  |                  |                  |                  | Power (MW) |
|-----------------|---------------------------|------------------|------------------|------------------|------------------|------------------|------------|
|                 | 19/18<br>CR n° 1          | 22/17<br>CR n° 2 | 23/19<br>CR n° 3 | 21/22<br>CR n° 4 | 17/21<br>CR n° 5 | 18/23<br>CR n° 6 |            |
| Reference State | 558.3                     | 557.4            | 558              | 557.4            | 557.4            | 557.6            | 335.4      |
| Step 1          | 608.5                     | 608.6            | 606.6            | 340.8            | 608.5            | 607.8            | 337        |
| Step 2          | 848.4                     | 567.7            | 571              | 340.6            | 566.3            | 573.5            | 338.7      |
| Step 3          | 848.4                     | 523.6            | 523.4            | 523.4            | 523.5            | 523.5            | 336.3      |
| Final State     | 559.6                     | 558.7            | 558.7            | 559.4            | 559.5            | 559.4            | 335.2      |

- Control rod positions take into account core/vessel/control rod differential dilatations
- The origin of Z-axis is 5 mm below the fissile core

# Results: Power distributions in RS (1/2)

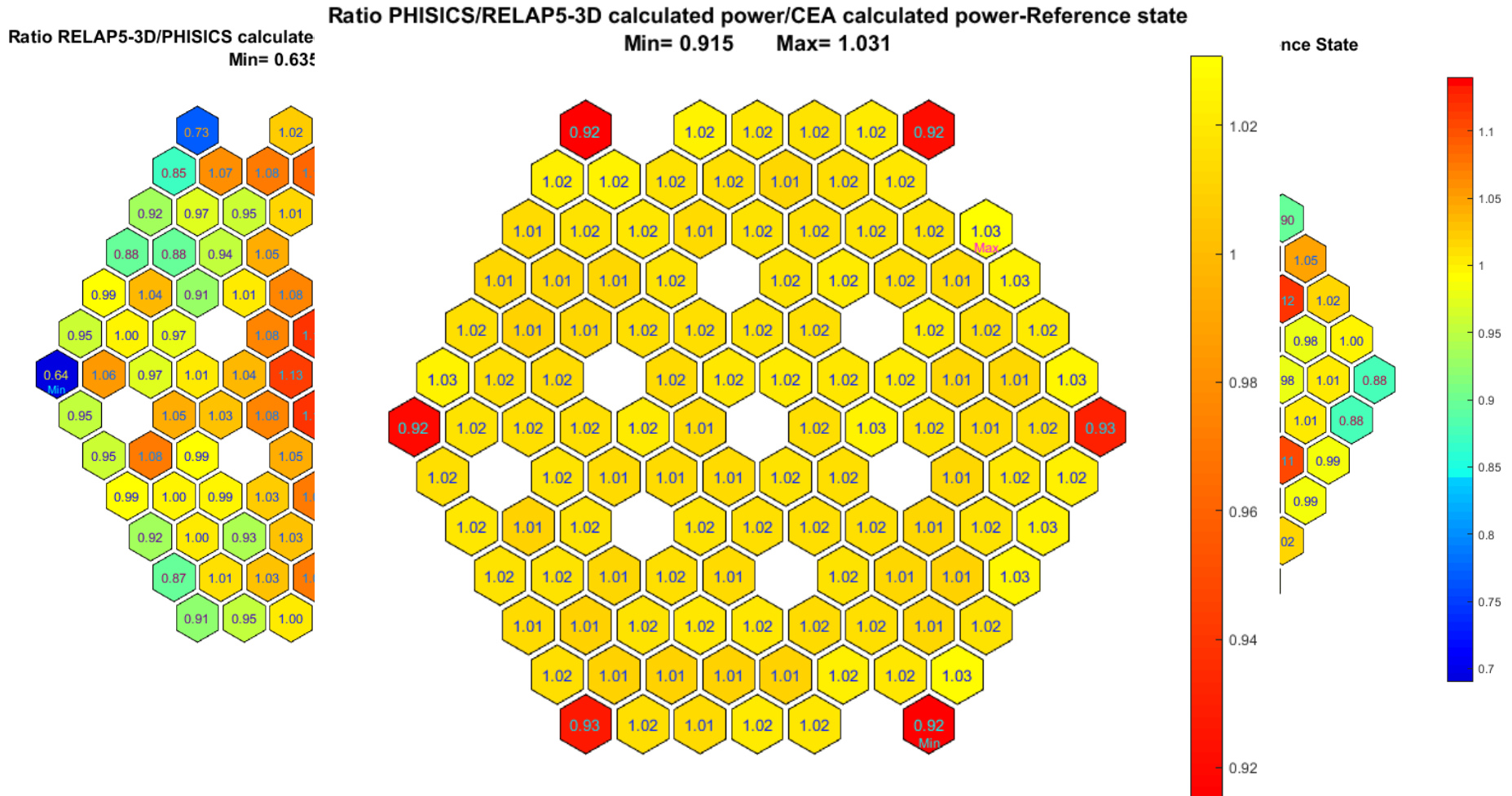
## Approximations:

➤ Approximation of using an average core description (an average Burnup has been

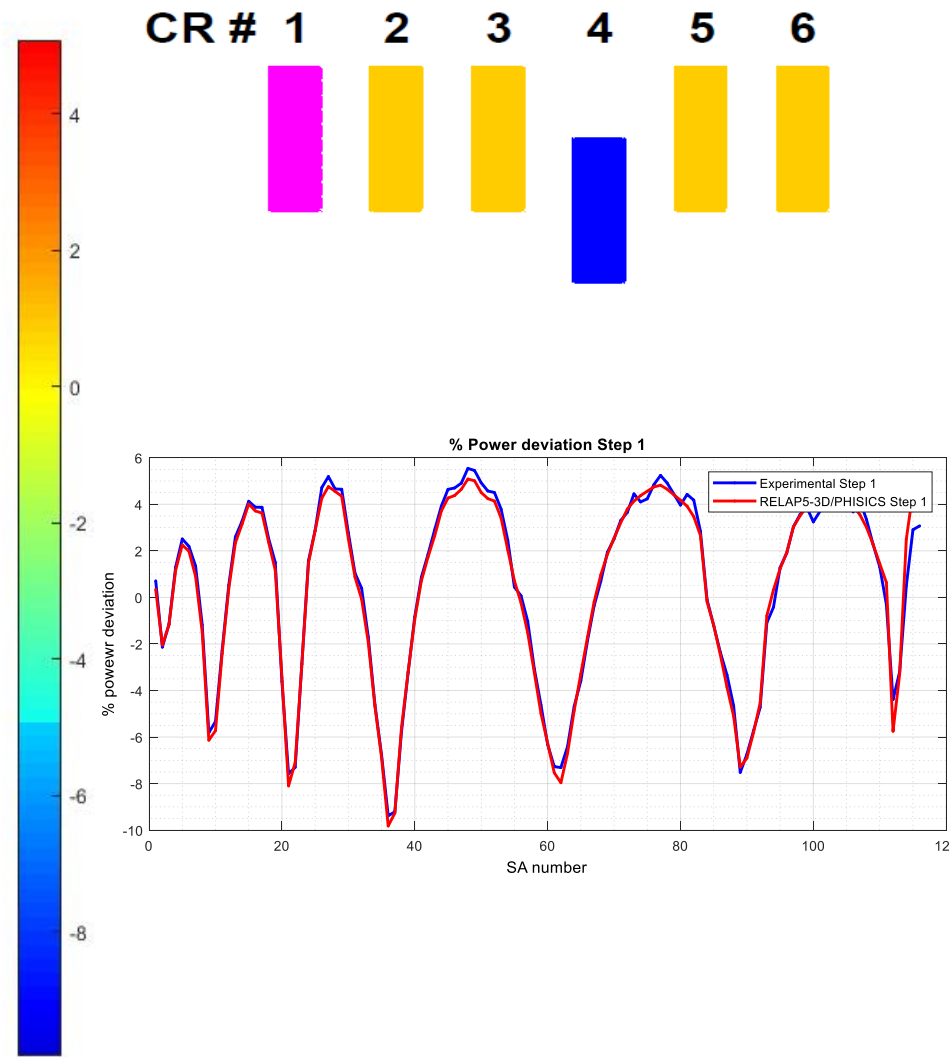
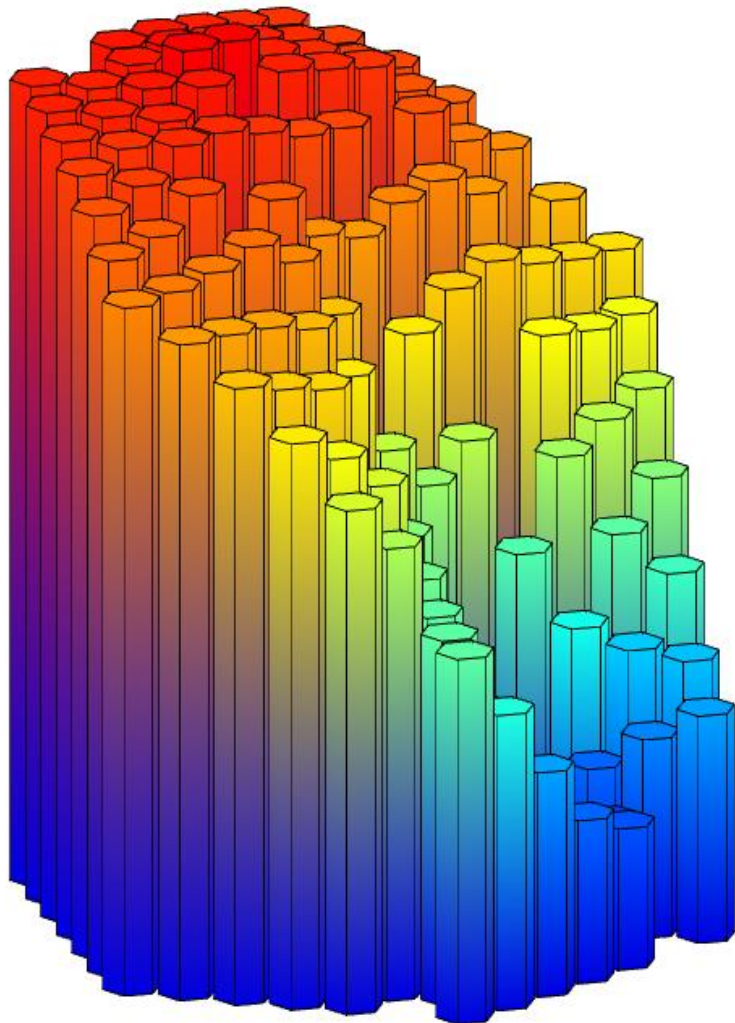




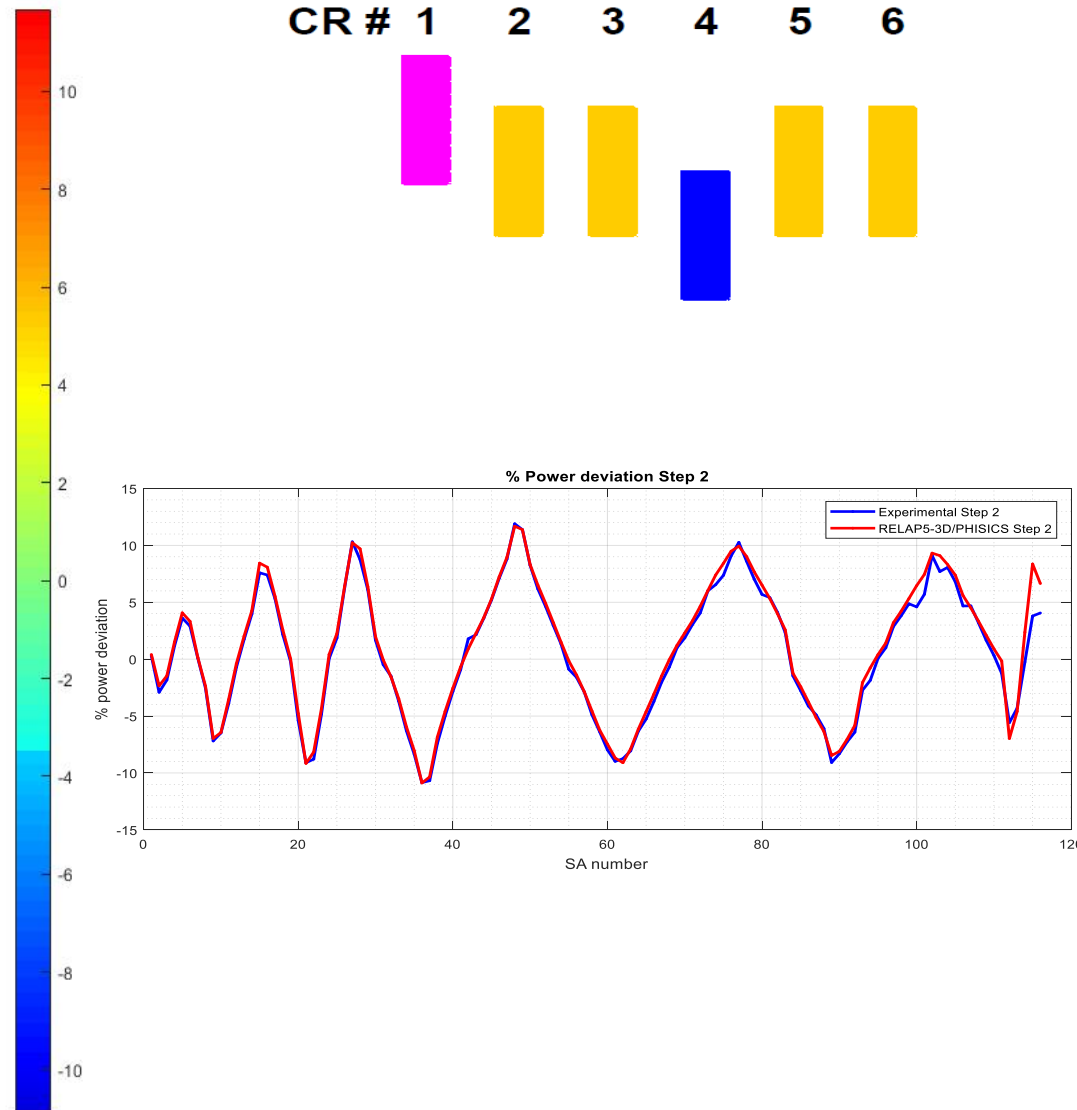
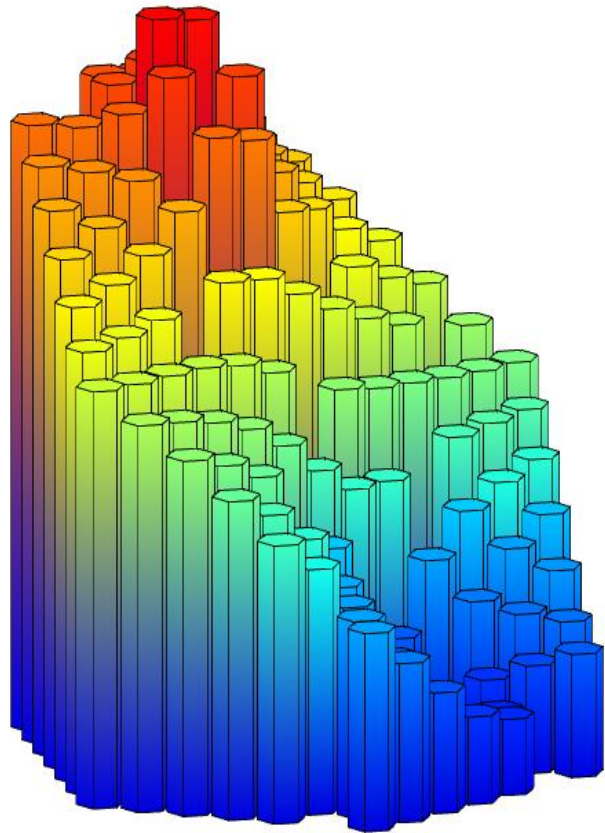
# Results: Power distributions in RS (2/2)



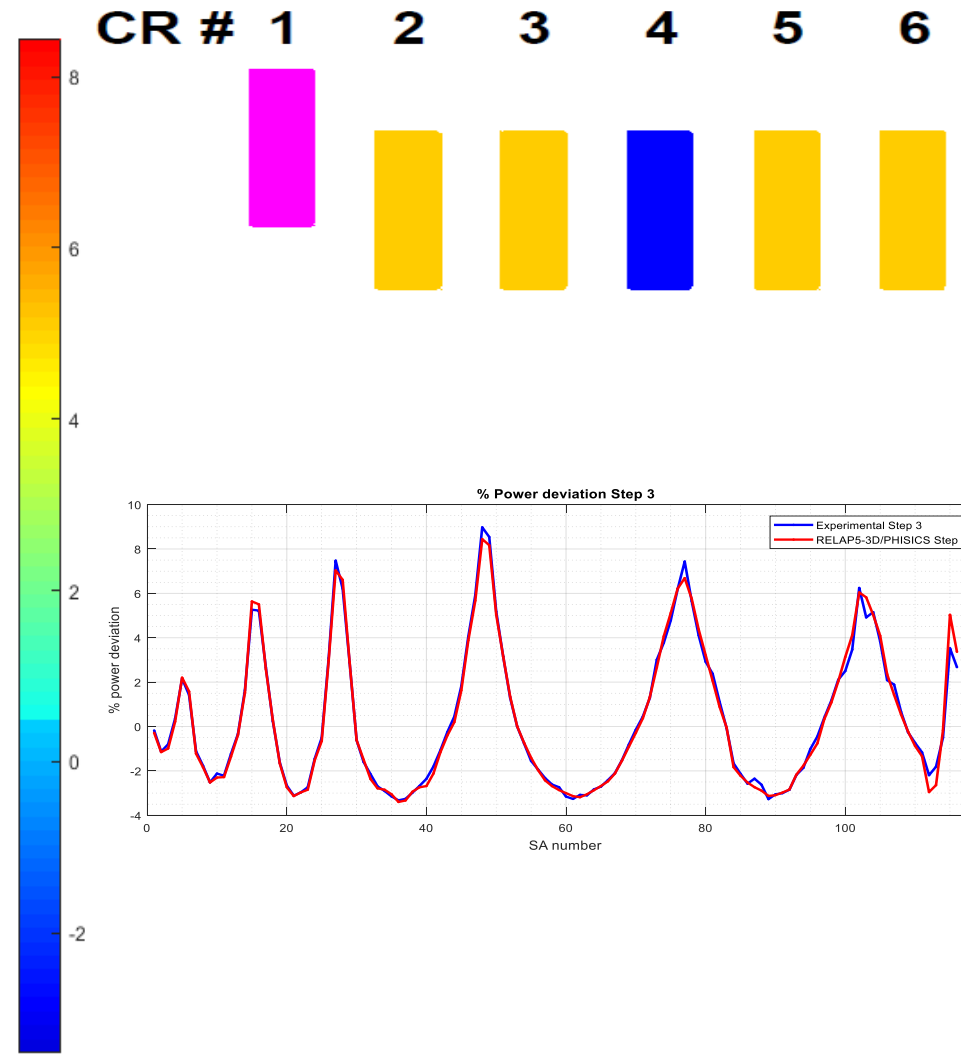
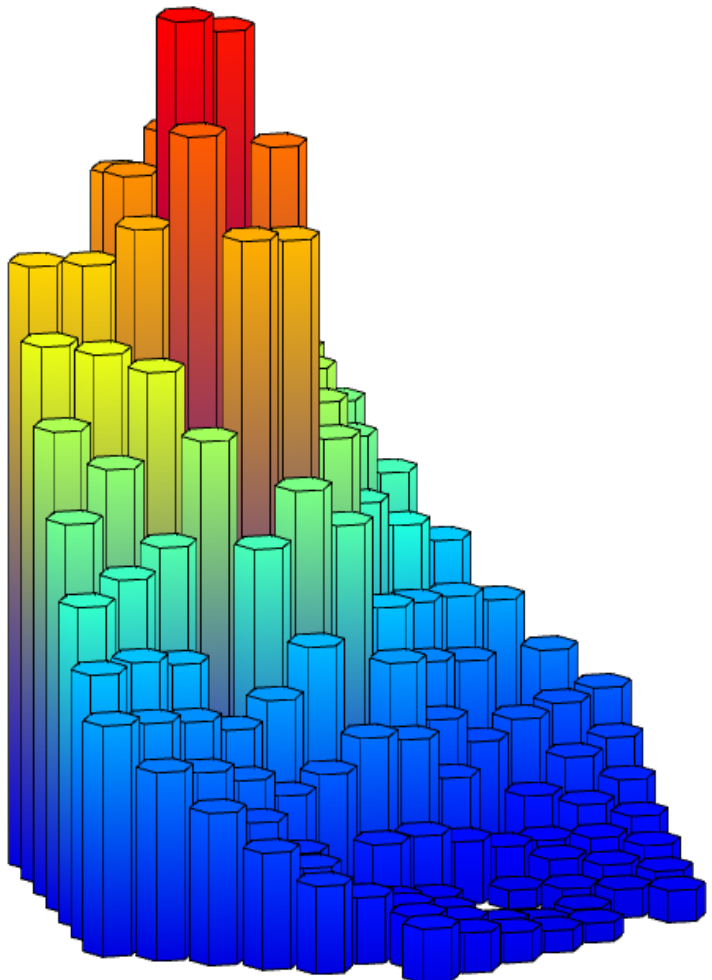
# Results: Power deviations [%] - Step 1



# Results: Power deviations [%] - Step 2



# Results: Power deviations [%] - Step 3



## Conclusive remarks and follow up

- ❑ Nodalization of PHENIX by REALP5-3D<sup>©</sup> and PHISICS
  - Highly Detailed nodalization suitable for 3D NK coupling
  - PHISICS 3D NK model
  
- ❑ Following activities are in completed and documented in the PAR deliverable
  1. Blind calculation of the dissymmetrical configuration test
  2. Comparison of the blind results with the experimental data
  3. Post-test calculation and sensitivity study (in progress)
  4. Preliminary TH-NK results (next months)

# GENERATION IV

## Lead cooled Fast Reactor

Stato attuale della tecnologia e prospettive di sviluppo

Roma, 14-15 Giugno 2018



SAPIENZA  
UNIVERSITÀ DI ROMA

CIRCE-HERO Transient Simulation by 3D STH  
code

V. Narcisi, F. Giannetti, G. Caruso

# OUTLINE

## ➤ GOAL OF THE ACTIVITY

In synergy with **Horizon 2020 SESAME project**, the activity aims to perform pre-test simulations to provide the preliminary test-matrix for the realization of the validation benchmark

## ➤ OVERVIEW

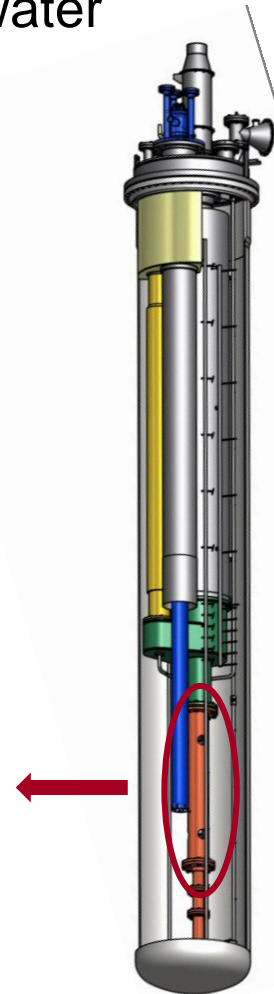
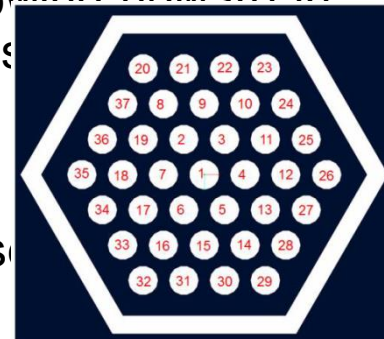
- CIRCE-HERO Test Section
- CIRCE-HERO: Thermal-Hydraulic model
- Model Validation
- Pre-Test Analysis
- Conclusions

# CIRCE-HERO Test Section

CIRColazione Eutettico – Heavy liquid metal-pRepressurized water cOoled tube

## Primary LBE Pool type facility

- ❖ Feeding conduit: placed in a hexagonal Main vessel.
- ❖ Fuel Pin Simulator (FPS): It corresponds to the heat source
- ❖ Riser: Outside diameter: 1200 mm, kW. Nominal and installed power of 800 kW. Active length of 1650 mm. A nozzle is installed in the lower section to allow the argon injection inside this pipe
- ❖ Separator: It allows the separation of the LBE, flowing downward, a power of about 25 kW, and a wall heat flux of 1 MW/m<sup>2</sup>, flowing upward in the gas expansion vessel. LBE inventory: 70 t. Range of temperature: 200-400° C
- ❖ SGBT: Lower core section, consists of 7 double wall bayonet tubes and two auxiliary tanks. The active length is 30 m.
- ❖ Pool: this is the volume between the test section and the main vessel. Storage tank

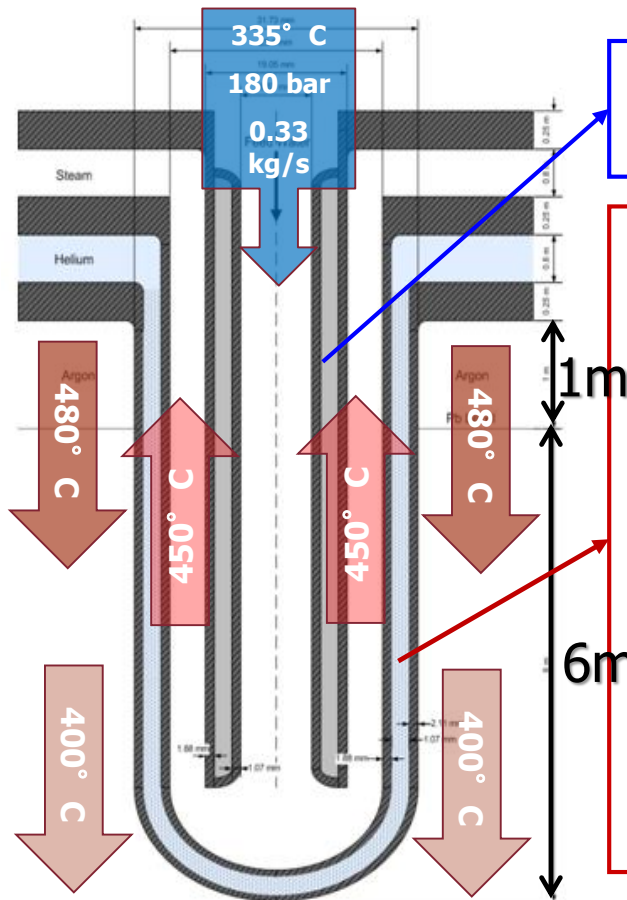


- LBE transfer tank



# CIRCE-HERO Test Section

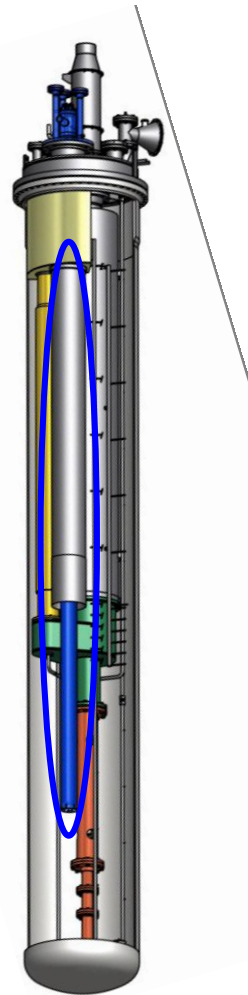
CIRColazione Eutettico – Heavy liquid metal-pRepressurized water cOoled tube



➤ Insulator layer in order to prevent the steam condensation

• To investigate a bundle of Gap pressurized with Helium and filled by high thermal conductivity powder to

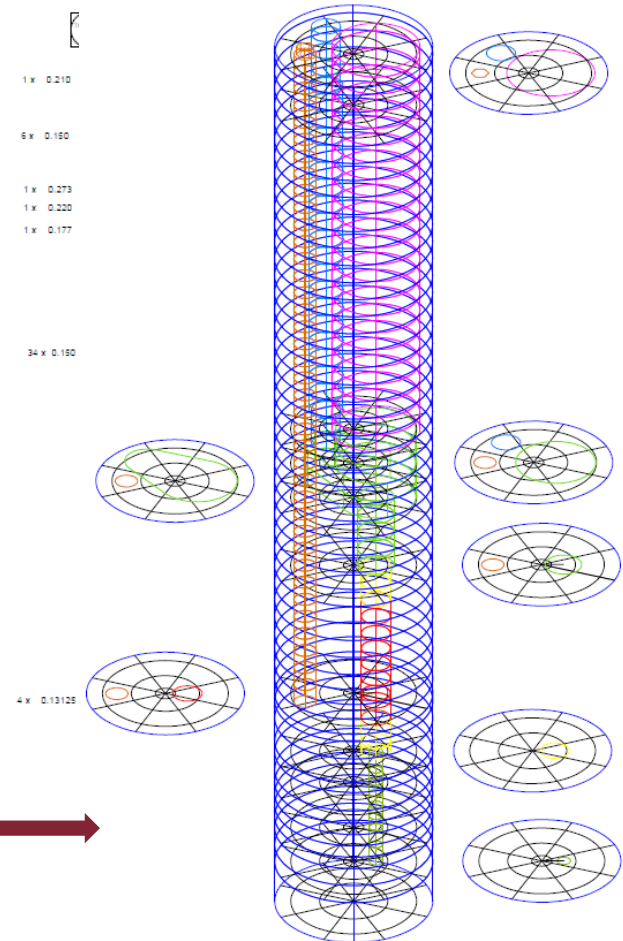
1. Avoid lead-water interaction in case of tube rupture (double physical separation).
2. Detect tube leakages thanks to monitoring the He pressure
3. Enhance the heat exchange capability thanks to the powder medium.



# CIRCE-HERO: Thermal-Hydraulic Model

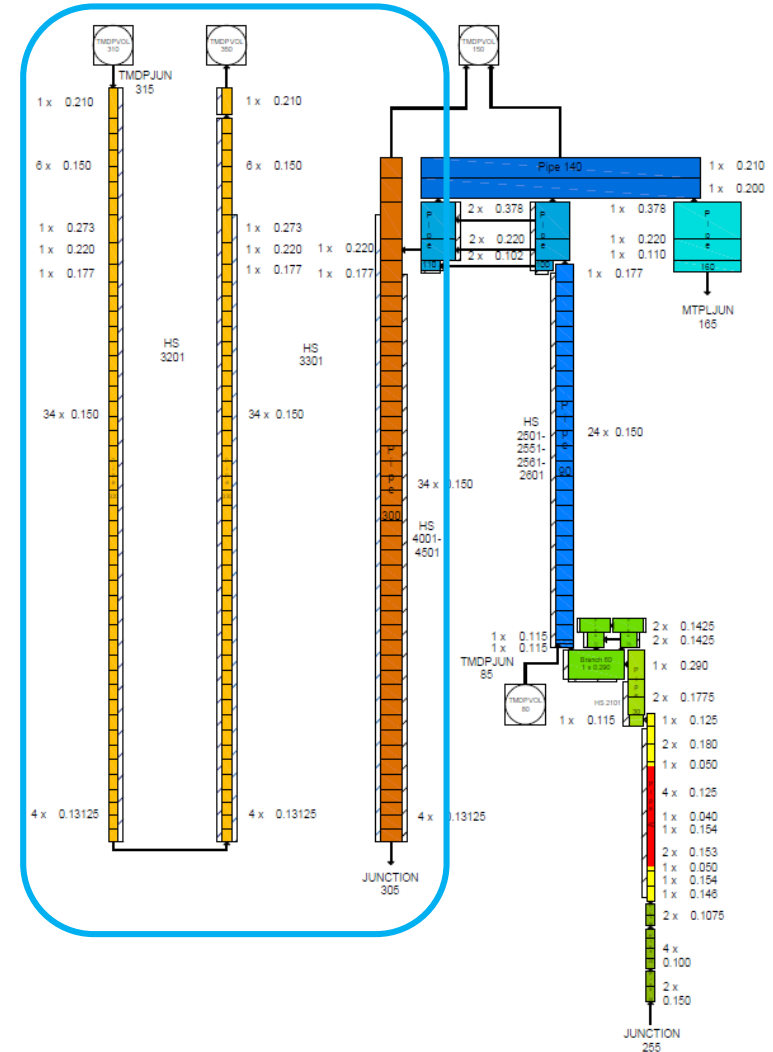
The validated thermal-hydraulic model of **CIRCE-ICE**, developed using **RELAP5-3D® ver. 4.3.4**, has been upgraded to reproduce the **HERO test section**

- **Region #1:**   
 The full **CIRCE-HERO** model
  - **Primary main flow path:** it is composed of the feeding conduit, FPS, fitting volume, riser, separator and the LBE side of the SGBT. At the bottom of the riser the Ar injection system is included
- **2942** hydrodynamic volumes
  - **SGBT** secondary side
- **7565** junctions
- **Region #2: CIRCE pool.** It consists of a **3D component** which reproduces the volume between the internals and the main vessel.
- **2153** heat transfer nodes



# CIRCE-HERO: Thermal-Hydraulic Model

- **LBE side:** a single equivalent tube composed of 43 volumes; 3 junctions connect the component to the separator, the upper plenum and the pool
- **Steam/water side:** 2 pipes for a total of 96 volumes
- 4 **heat structures** model thermal behavior of the unit:
  - HS 3201: 48 axial structures and 20 radial meshes (AISI 316 + insulator gap)
  - HS 3301: 41 axial structures and 31 radial meshes (AISI 316 + helium and high conductivity powder)
  - HS 4001 and 4501: 39 axial structure and 24 radial meshes
- **Calibrated factor** as the ratio between **Ushakov** and **Todreas&Kazimi** HTC correlation, in the range of the SG temperatures and assuming the predicted flow conditions: 1,02

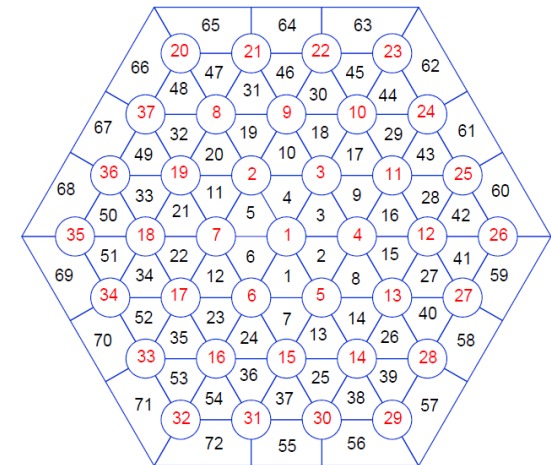
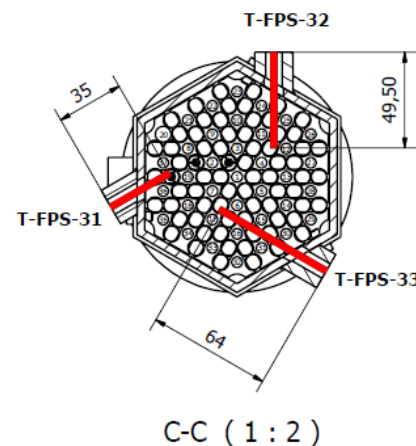
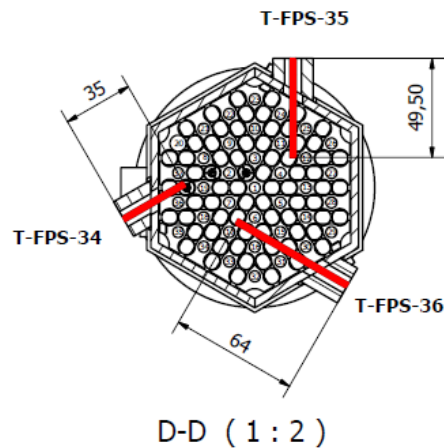
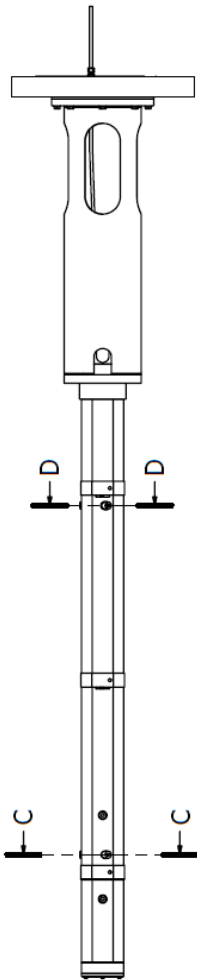


# CIRCE-HERO: Thermal-Hydraulic Model

The **FPS** is analyzed sub-channel by sub-channel: the model consists of **72 parallel pipes** (15 control volumes for each one), which simulates the sub-channels, **5760 heat structure active nodes** reproducing the thermal power supplied by the 37 pins, **1728 heat structure nodes** to models the heat dispersion through the hexagonal wrapper, **3456 heat nodes**, assuming a “fake” material with a negligible heat capacity and the LBE thermal conductivity, added to simulate the thermal conduction into the fluid and **1536 cross junctions**.

The unit is equipped with several TCs to measured the LBE temperature across the HS. The model is obtained to compare the temperature in the **exact position of the TCs**. The grids are simulated with pressure loss coefficients, dependent on the flow conditions and evaluated with **Rheme correlation**.

A calibrated multiplication factor is evaluated as the ratio between **Ushakov ( $p/d=1.8$ )** and **Todreas&Kazimi ( $p/d=1.4$ )** equal to 1,31 in order to better reproduce the HTC



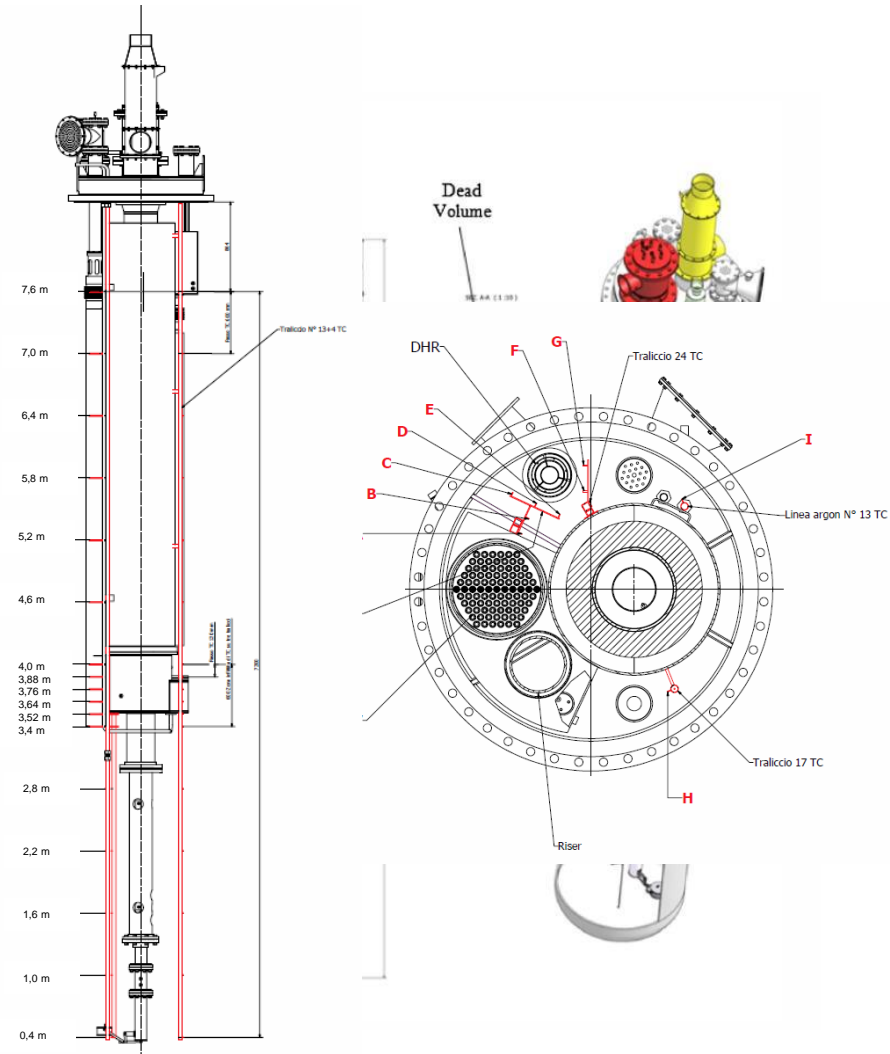
# Model validation

## ➤ CIRCE-ICE Test Facility:

- **Primary flow path:** ICE test section is the same of HERO campaign except for the presence of the **DHR system**, included inside the pool, and the **HX** that substitutes for the **SGBT**
- **HX:** water-cooled system
- **DHR:** air-cooled system

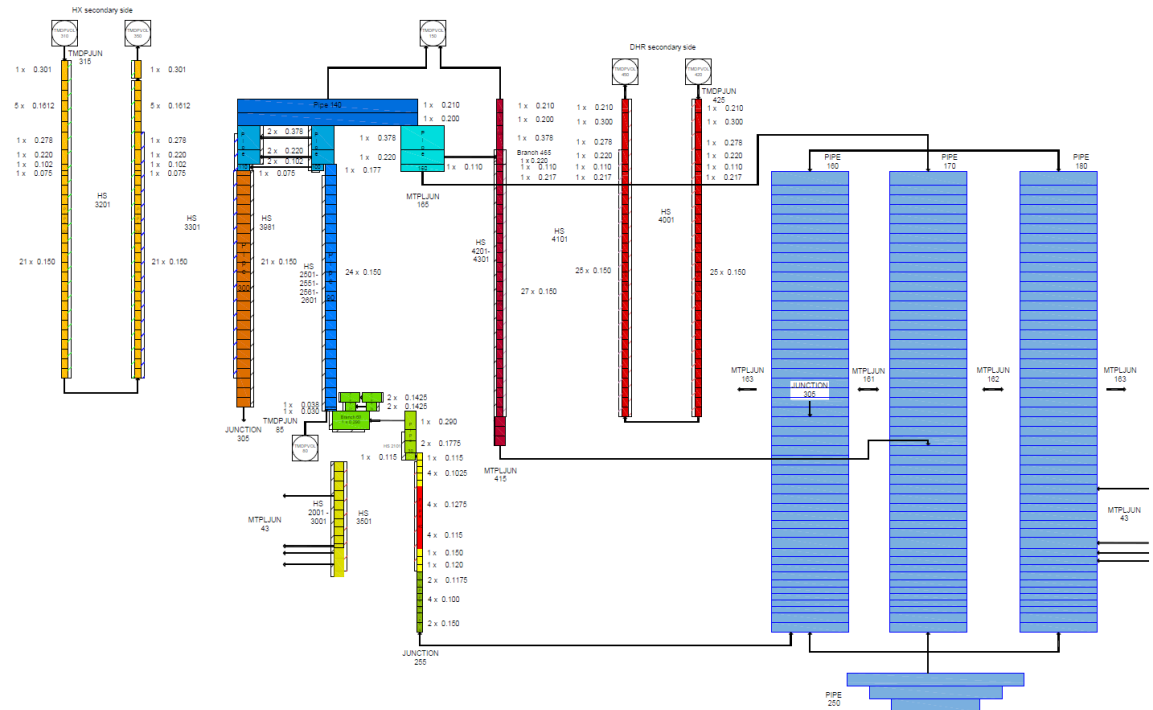
## ➤ Experimental campaign:

- To investigate **mixing convection** and **thermal stratification** phenomena in a pool type reactor
- To provide suitable experimental data to support the validation process of TH-SYS codes and CFD codes



# Model validation – 1D Nodalization scheme

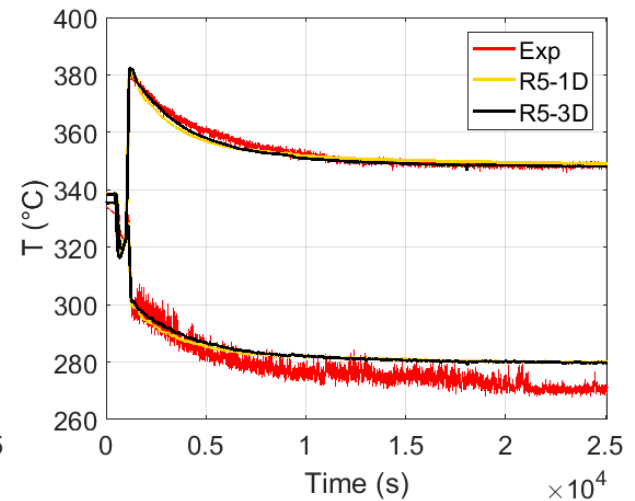
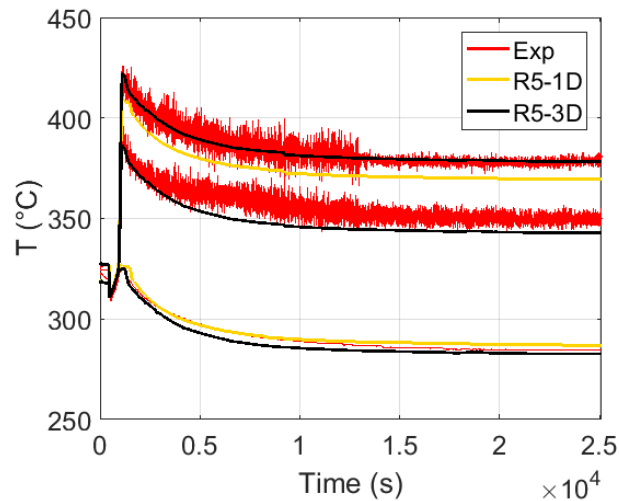
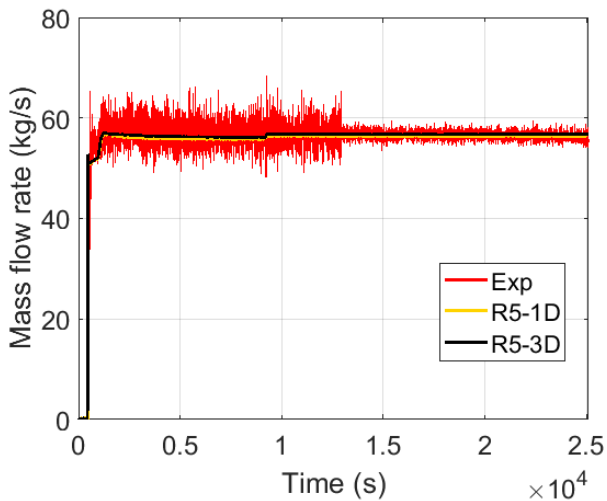
- ❖ **Primary Flow Path:** feeding conduit, FPS, fitting volume, riser, separator, HX, DHR
- ❖ **HX Secondary Side:** water cooling system
- ❖ **DHR Secondary Side:** air cooling system
- ❖ **Pool:** 3 parallel pipes which simulate the volume between the internals and the main vessel; 156 cross junctions to reproduce the mass transfer into the pool
- ❖ The thermal hydraulic model is consistent with the vertical sliced approach





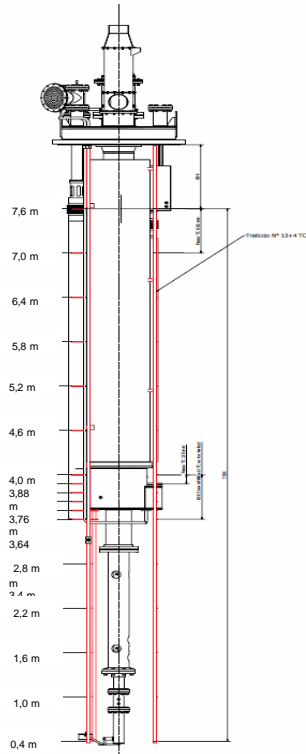
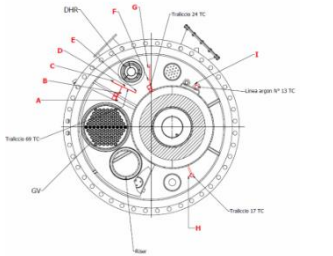
# Model validation

- ❖ The calculations were carried out using the most recent LBE thermo-physical properties correlation, recommended by NEA and implemented in RELAP5-3D
- ❖ The main results on the primary main flow path are comparable
- ❖ Both the calculations are in good agreement with experimental results

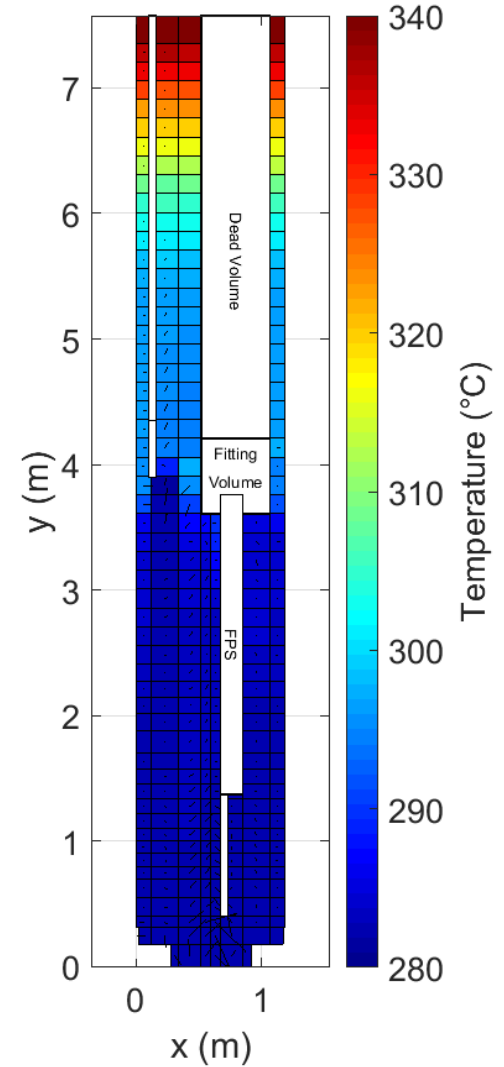
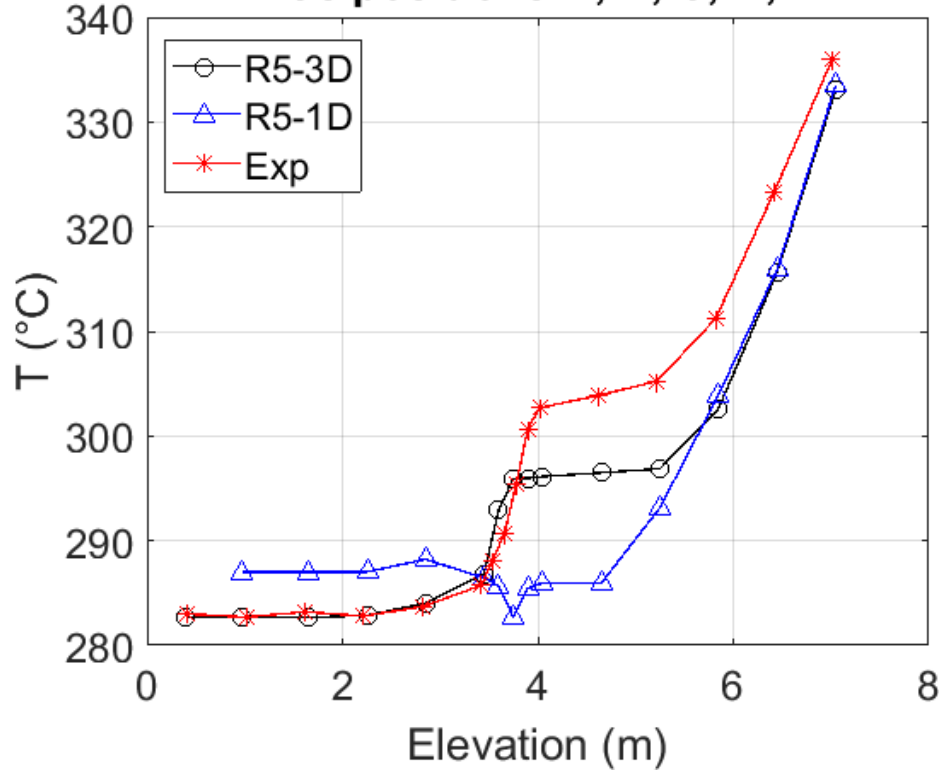




# Model validation



TCs positions A, B, C, D, E



# Pre-Test analysis

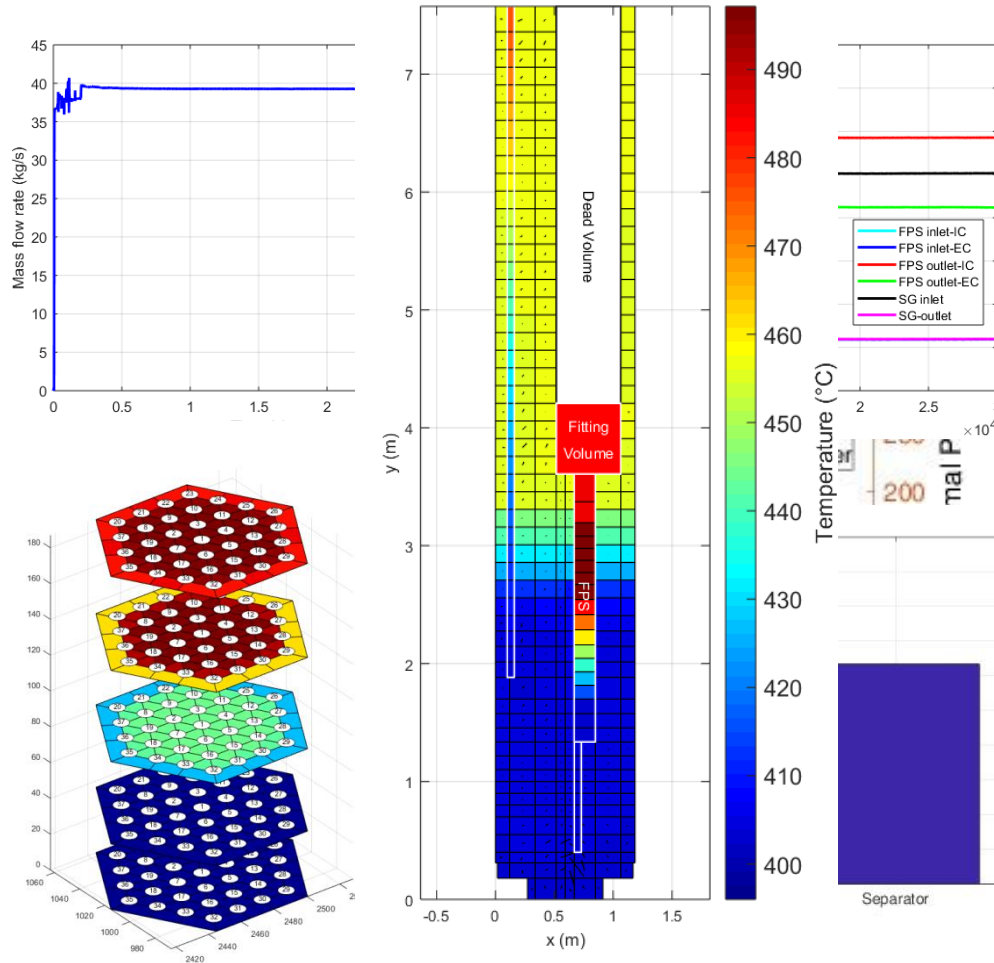
- **Phase 1:** assessment of **Steady State (SS) Full Power Conditions**, in order to determine initial conditions for transient
- **Phase 2:** transient simulations

## PHASE 1

For the identification of the initial conditions of the transient tests, 6 different SS conditions are analysed:

- **Case #1:** setting to achieve a constant temperature drop across the FPS equal to  $80^{\circ}\text{C}$  in the range of about  $400 - 480^{\circ}\text{C}$ , representative of the temperature drop across the **ALFRED core**; duration 30000 s, FPS power 450 kW, pool initial temperature  $396^{\circ}\text{C}$ , Ar mass flow rate 1,29 NI/s, feedwater mass flow rate 0.331 kg/s;
- **Case #2:** as **Case #1** except for the Ar mass flow rate: 2,35 NI/s. Case #2 has been set to achieve LBE mass flow rate across the SGBT section equal to 44,7 kg/s (representative of the scaled down **SG of ALFRED**);
- **Case #3, #4, #5, #6:** as **Case #1** except for the Ar mass flow rate: 2,24 NI/s, 2,13 NI/s, 1,85 NI/s, 1,79 NI/s.

# Pre-Test simulations: Full Power Conditions #1



|                            | Parameter                                   | Unit | Value |
|----------------------------|---|------|-------|
| <b>Boundary conditions</b> | Duration                                    | h    | > 8   |
|                            | FPS thermal power                           | kW   | 450   |
|                            | LBE average T inside the pool               | ° C  | 396   |
|                            | Ar mass flow rate                           | NI/s | 1.29  |
|                            | Steam pressure                              | bar  | 172   |
|                            | FW inlet T                                  | ° C  | 335   |
|                            | FW mass flow rate                           | kg/s | 0.33  |
| <b>Results</b>             | FPS LBE inlet T                             | ° C  | 403.8 |
|                            | FPS LBE average outlet T                    | ° C  | 486.8 |
|                            | HERO LBE inlet T                            | ° C  | 480.6 |
|                            | HERO LBE outlet T                           | ° C  | 403.9 |
|                            | LBE mass flow rate at inlet section of HERO | kg/s | 39.2  |
|                            | Power removed by HERO                       | kW   | 438   |
|                            | Steam max T                                 | ° C  | 398.9 |
| Steam velocity             | m/s   | 9    |       |

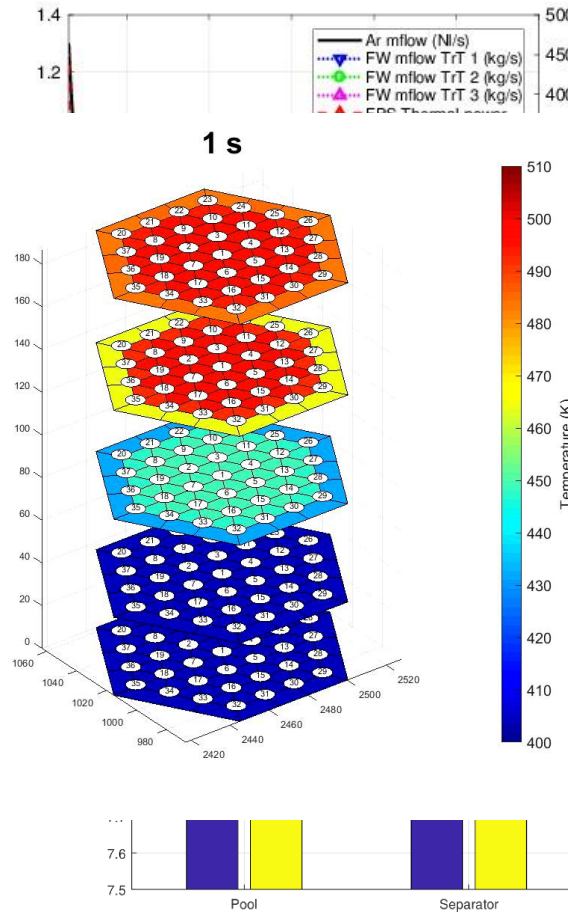
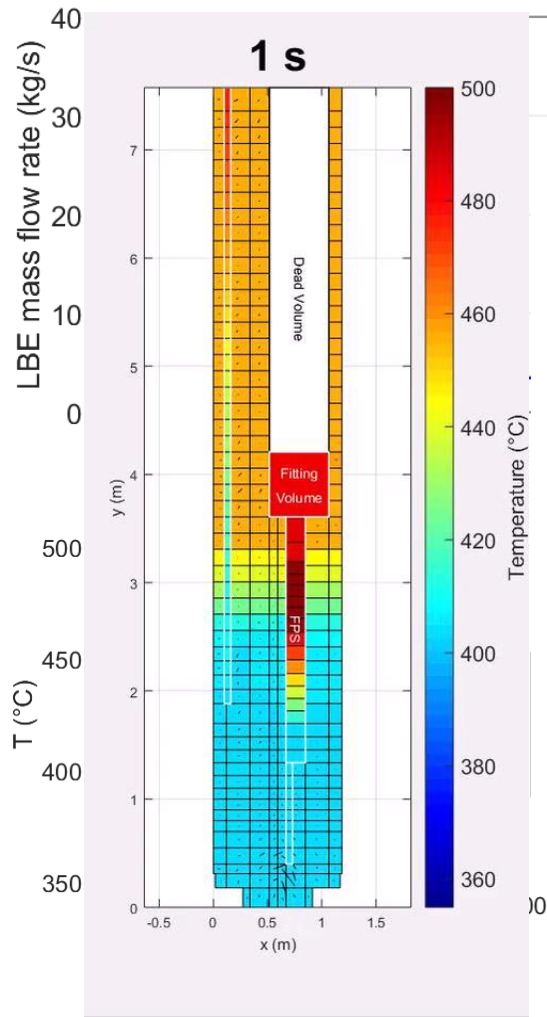
# Pre-Test analysis

## PHASE 2

The starting point for transient tests (TrT) is considered **Case #1**.

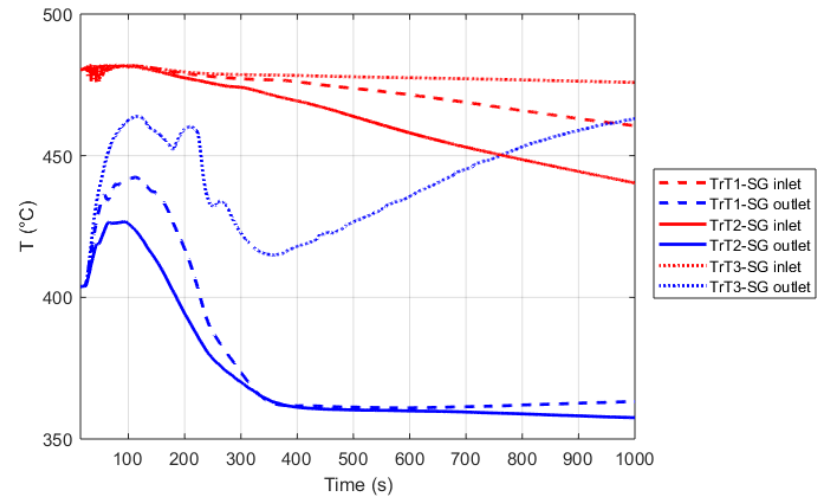
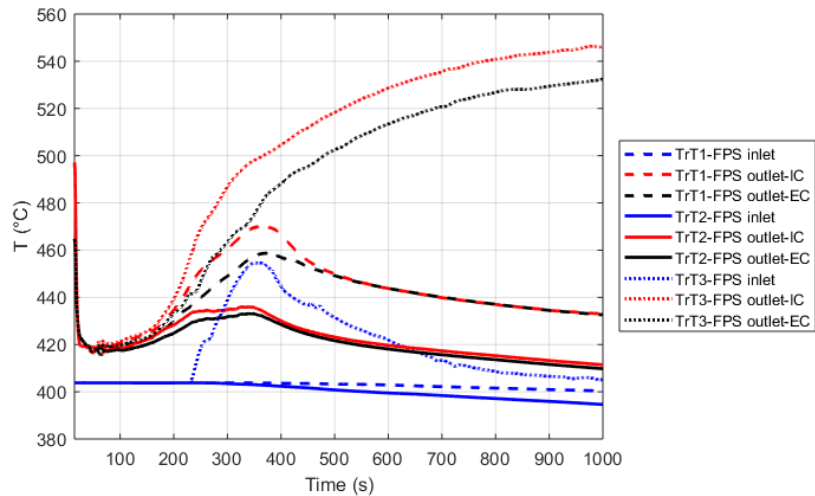
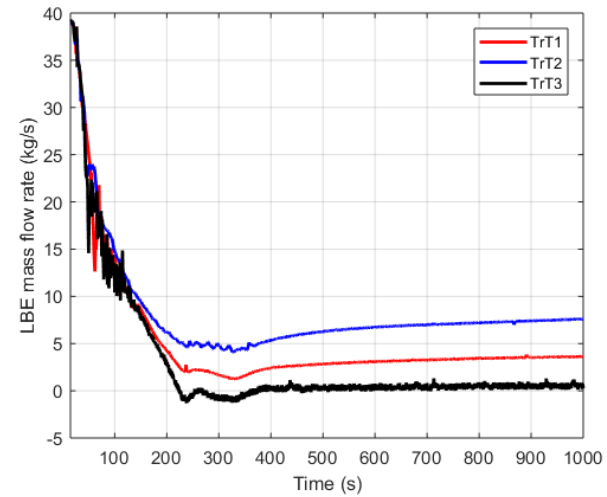
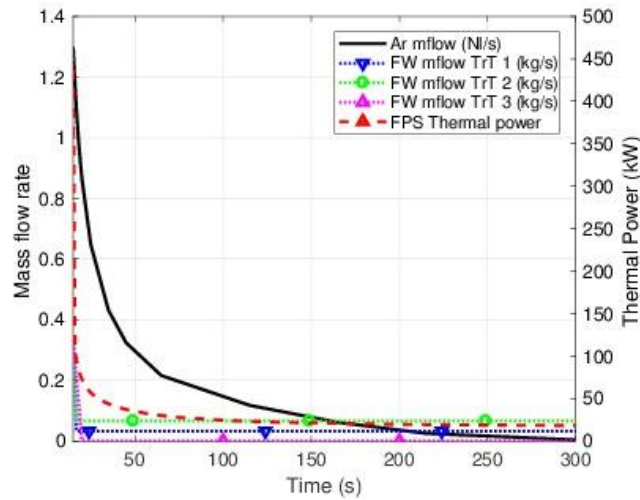
- **TrT #1:** it consists of a **protected loss of LBE pump**.
  - **FPS power** decreases down to the compensated decay heat value;
  - **Ar mass flow rate injection** decreases to 0 simulating presence of a pump flywheel;
  - **Feedwater mass flow rate** is set at 10% of nominal mass flow to simulate the activation of the DHR system;
- **TrT #2:** as **TrT #1** except for the feedwater mass flow rate, set to 20% of the nominal mass flow rate;
- **TrT #3:** as **TrT #1** except for the feedwater mass flow rate, which decreases to 0 in order to simulate a **loss of DHR function in hot conditions**.

# Transient Test #1: main results

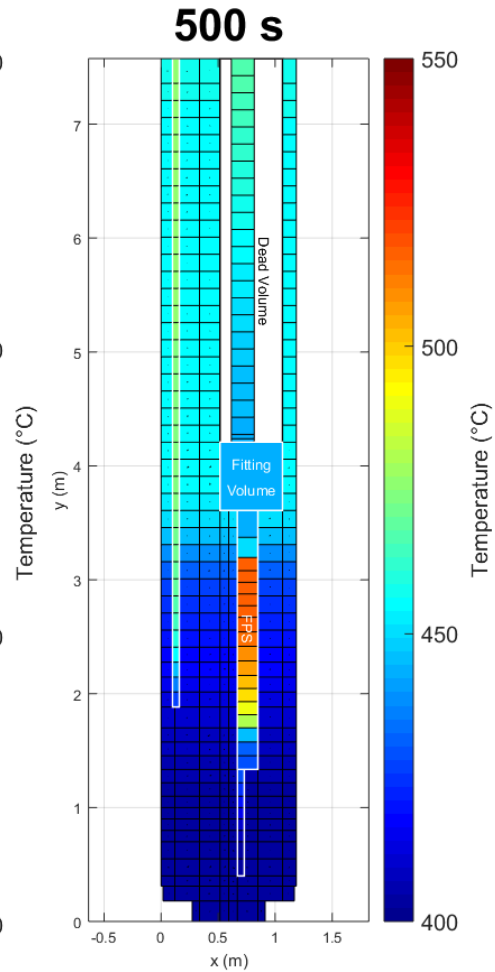
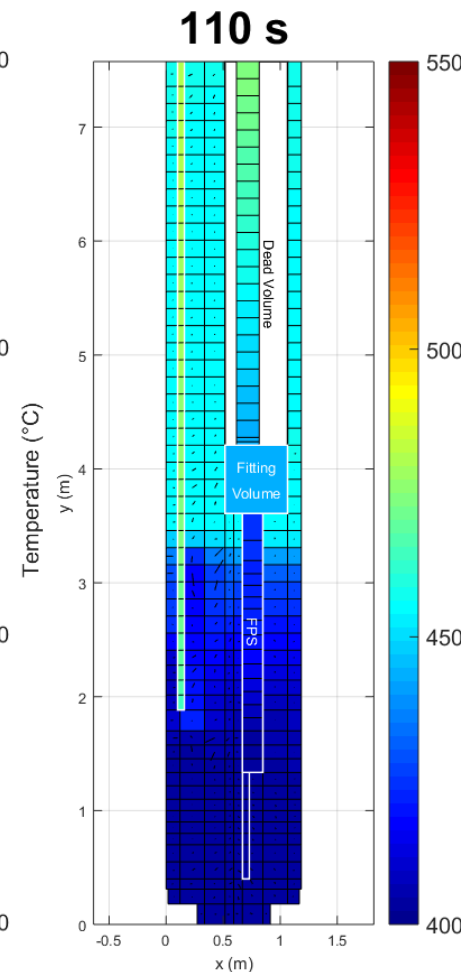
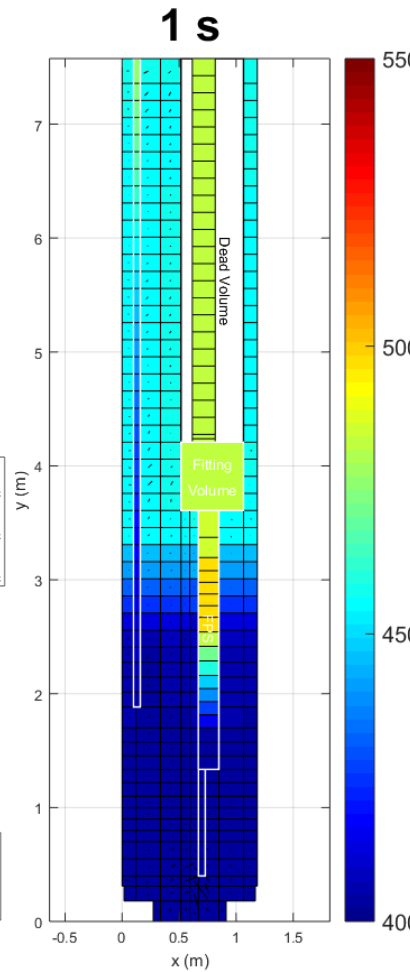
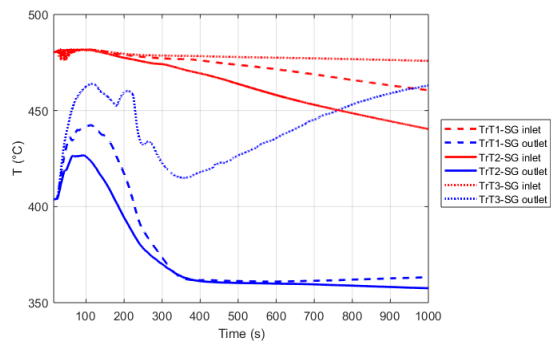
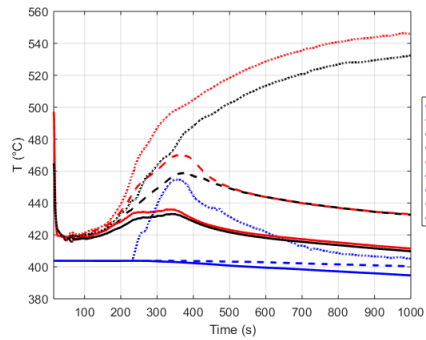
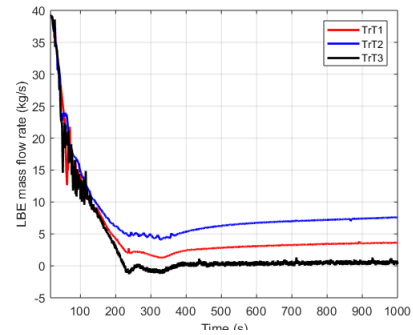


| Time (s) | Main event  |
|----------|---|
| 0        | Start of the transient sequence   |
| 80       | Minimum value of the LBE temperature at the outlet section of the FPS                           |
| 110      | Peak temperature at SG outlet section   |
| 340      | Minimum value of the LBE mass flow rate   |
| 350      | Peak temperature at the outlet section of the FPS and minimum temperature at the outlet of HERO |
| 1000     | End of the transient test   |

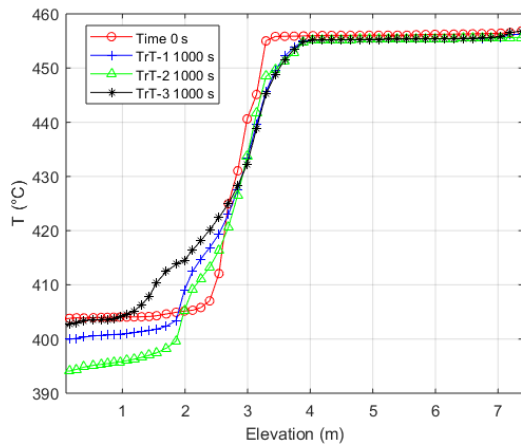
# Transient Test: compare #1 #2 #3



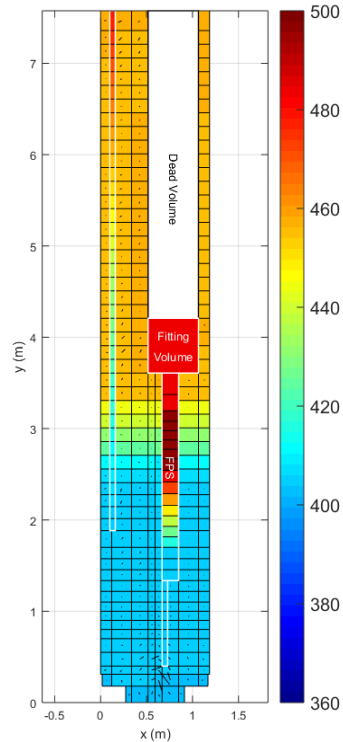
# Transient Test: compare #1 #2 #3



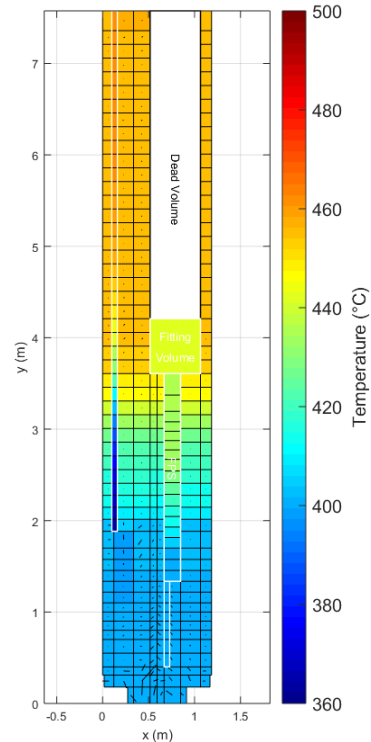
# Transient Test: compare #1 #2 #3



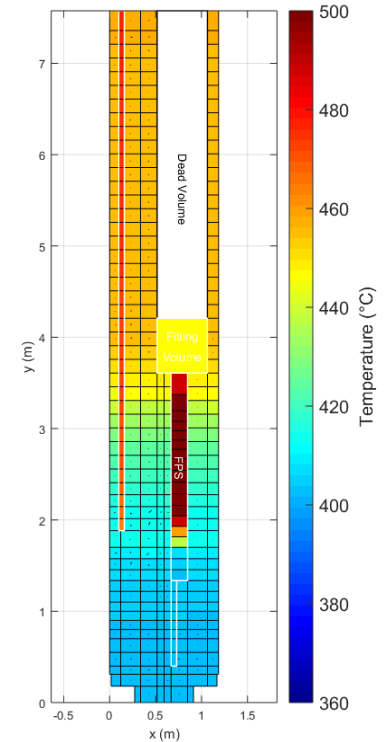
Time: 0 s



TrT1: 1000 s



Trt3: 1000 s





# CONCLUSIONS

- **CIRCE-HERO RELAP5-3D<sup>®</sup>** model has been developed and calibrated comparing **CIRCE-ICE** simulations results with experimental data
- **Sensitivity analysis** has been performed to determine the reference full power steady state conditions
- The transient test simulations have highlighted that **HERO test section** guarantees a sufficient natural circulation conditions to remove the decay heat in short term. When the feed-water mass flow rate is deactivated, the code predicts a **reverse flow** of the primary coolant. Further investigations are necessary in order to confirm that.
- The transient test 1 has been selected as the reference test for the validation benchmark

# THANKS FOR YOUR ATTENTION

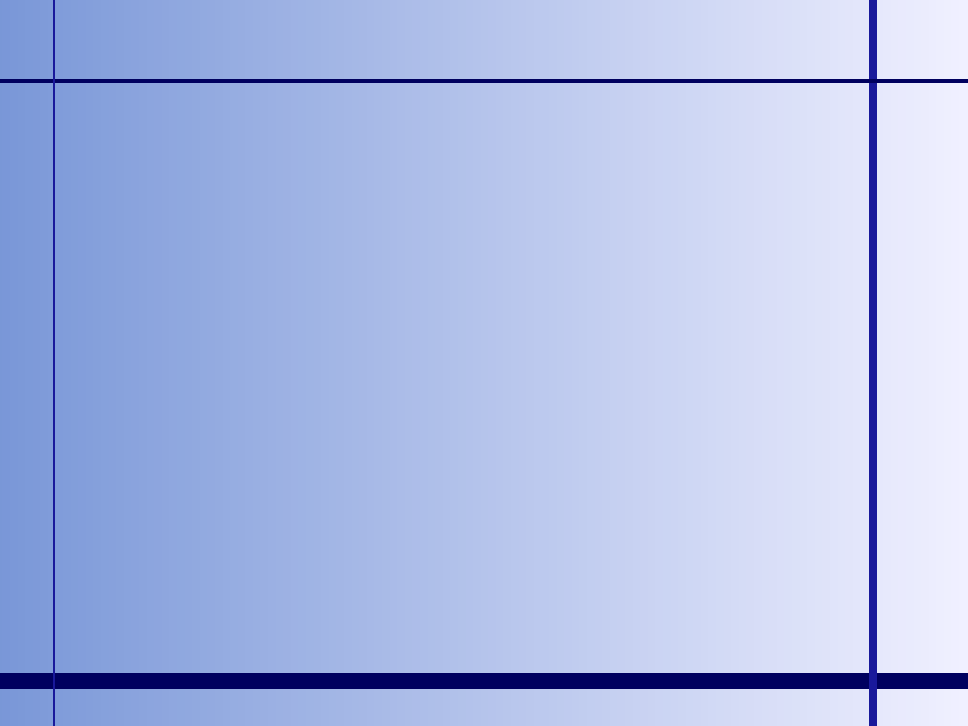
# OpenFoam-SALOME-FEMLCORE- CATHARE coupling development and validation against TALL-3D experimental data

**L. Chirco<sup>1</sup>, A. Chierici<sup>1</sup>, R. Da Vià<sup>1</sup>, S. Manservigi<sup>1</sup>**

Alma Mater Studiorum - Bologna<sup>1</sup>

**A. Cervone<sup>2</sup>**

Centro Ricerche ENEA - Bologna<sup>2</sup>



# Summary

1

- Multiphysics and Multiscale computational tools
- TALL-3D Facility and computational tests
- TALL-3D with In-house codes in platform (SALOME-CATHARE-FEMLCORE)
- TALL-3D with specialized nuclear CEA codes in platform (CATHARE- TRIOU)
- TALL-3D with open-source codes in platform (SALOME-OPENFOAM)
- Conclusions

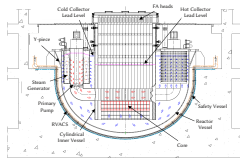
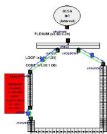
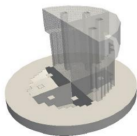


# Multiphysics and Multiscale computational tools

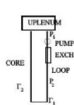


# LFR platform approach

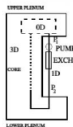
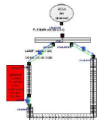
## Example 1 multi-scale defective mode approach



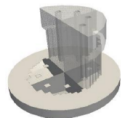
## Computational platform ENEA-UNIBO (LM experiment)



only 1D modules



1D+3D modules





# Multiphysics-Multiscale tools for LFR

## Computational platform (LFR)

IN-HOUSE CODES (FEMLCORE) → Developing, Research, Design

OPEN-SRC CODES (OPEN-FOAM) → Exchange, sharing data/results

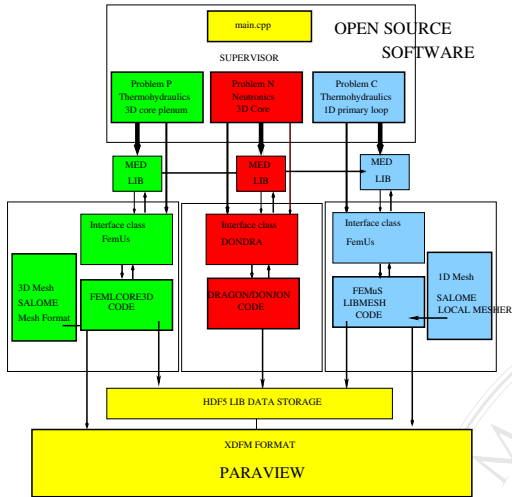
NUCLEAR TESTED CODES (CEA) → Verification, licensing

## Multi-scale Computational platform (LFR)

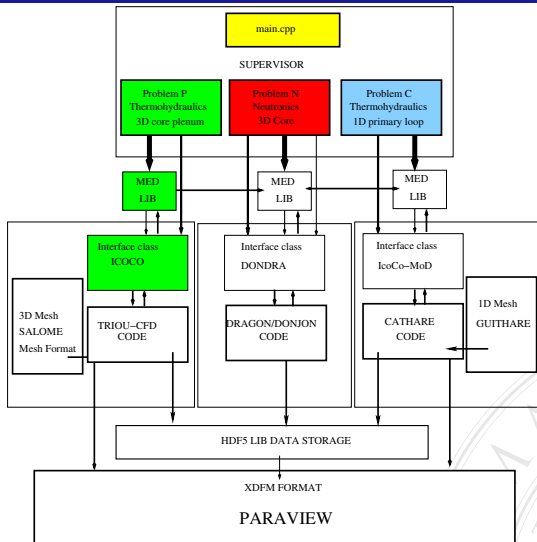
| Multi-physics               | space scale 1  | space scale 2                  |
|-----------------------------|--|--------------------------------|
| <b>Thermalhydraulics</b>    | <b>CFD-porous 3D</b>   | <b>system 1D</b>               |
| open-src<br>CEA-EDF         | TRIOCFD FEMLCORE OPENFOAM<br>MC/TRIOCFD (sourceforge)          | FEMuS OPENFOAM<br>CATHARE      |
| <b>Neutronics</b>           | <b>Transport</b>   | <b>group diffusion</b>         |
| open-src<br>CEA-EDF         | DRAGON (assembly)  | DONJON (core)<br>APOLLO2       |
| <b>Structural</b>           | <b>3D structural</b>   | <b>1D beam</b>                 |
| open-src<br>CEA-EDF         | Code_Aster FEMuS OPENFOAM<br>Code_Aster (CAELinux+sourceforge) | Code_Aster FEMuS<br>Code_Aster |
| <b>Two-phase</b>            | <b>interface</b>   | <b>two-fluid model</b>         |
| open-src<br>CEA-EDF         | TRIOCFD FEMuS OPENFOAM<br>TRIOU-CFD(sourceforge) NEPTUNE       | FEMuS (FEM)<br>CATHARE         |
| <b>uncertainty analysis</b> |  |                                |
| open-src<br>CEA-EDF         | URANIE<br>URANIE platform (sourceforge)                        | URANIE<br>URANIE platform      |

Multiphysics and multiscale platform (CEA-EDF) now almost

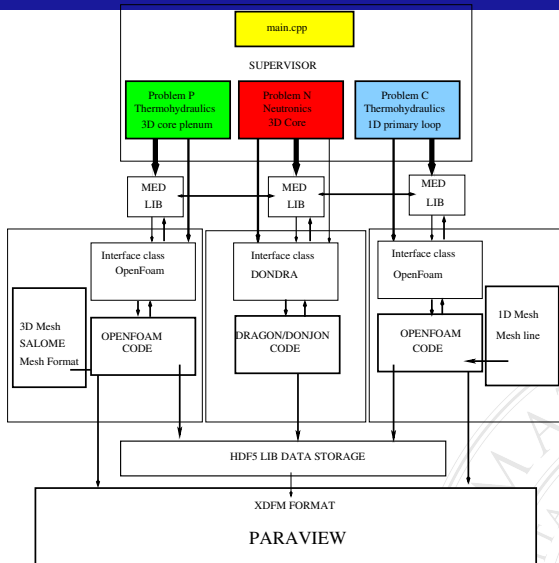
# In-house developing platform (research codes)



# CEA Developing platform (nuclear approved)



# OPEN-SRC Developing platform (OpenFOAM)



# SALOME platform

SALOME

SALOME opensource  $\longleftrightarrow$  CAD-MESH-VISUALIZATION



VISUALIZATION(PARAVIEW)

CAD(GEOM)

MES GEN(SMESH)

MESH GENERATION + SOLUTION VISUALIZATION (OPEN-SRC)

$\rightarrow$  MED libraries  $\rightarrow$  HDF5 data storage format

# SALOME-CEA platform

## SALOME-CEA codes

CATHARE → 1D nuclear thermal-hydraulics code → MED-HDF5

APOLLO2 → neutronics code → MED-HDF5 format

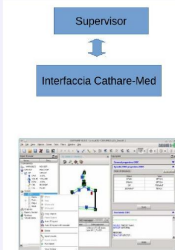
TRIOU → 3D -CFD code → MED-HDF5 format +mesh

NEPTUNE → 3D-CFD two-phase code → MED-HDF5 format +mesh

SATURNE → 3D -CFD code → MED-HDF5 format +mesh

## ICOCO interface

CATHARE interface ↔ SALOME



| return type                | function                           |
|----------------------------|------------------------------------|
|                            | start/stop program                 |
| local                      | initialize()                       |
| void                       | terminate()                        |
| void                       | setDataFile()                      |
|                            | interface time step                |
| double                     | presentTime() const;               |
| double                     | computeTimeStep() const;           |
| local                      | initTimeStep();                    |
| local                      | solveTimeStep();                   |
| void                       | validateTimeStep();                |
| local                      | isStationary() const;              |
| void                       | abortTimeStep();                   |
|                            | interface saving                   |
| void                       | save() const;                      |
| void                       | forget() const;                    |
| void                       | restart();                         |
|                            | interface FieldIO                  |
| vector< string >           | getInputFieldsNames() const;       |
| void                       | getInputFieldTemplate(....) const; |
| void                       | setInputField();                   |
| vector< string >           | getOutputFieldsNames() const;      |
| void                       | getOutputField();                  |
|                            | interface FieldIO                  |
| Problem_Cathare class only |                                    |
| double                     | getValue_Cathare (....)            |
| void                       | setValue_Cathare (....)            |

1D-SCALE (MAIN LOOP)

# SALOME ENEA-UNIBO in-house code platform

## In-house codes

FEMus → multi-scale, multi physics code → MED-HDF5

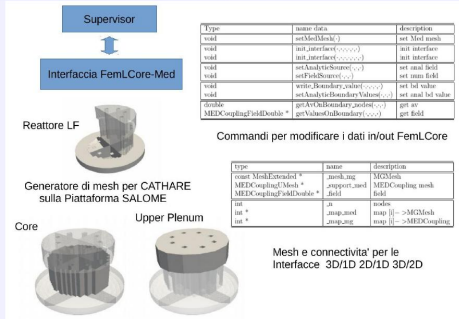
FEMLCORE-3D CFD → 3D -CFD code → MED-HDF5 format + mesh

FEMLCORE- 1D → 1D- thermal-hydraulics code → MED-HDF5

FEMLCORE- POROUS → 3D-CFD porous model code → MED-HDF5

## FEMus interface

### FEMLCORE interface ↔ SALOME



3D-SCALE (CFD and POROUS-CFD)

# OPEN-SOURCE SALOME platform

## OPEN-SOURCE codes

DRAGON-DONJON → neutronics code

TRIOU-CFD → 3D -CFD code

SATURNE → 3D -CFD code

OPENFOAM → multi purpose CFD code

## CODE interface

DRAGON-DONJON → DONJON interface → MED-HDF5

TRIOU-CFD → ICOCO interface → MED-HDF5 format +mesh

SATURNE → ICOCO interface → MED-HDF5 format +mesh

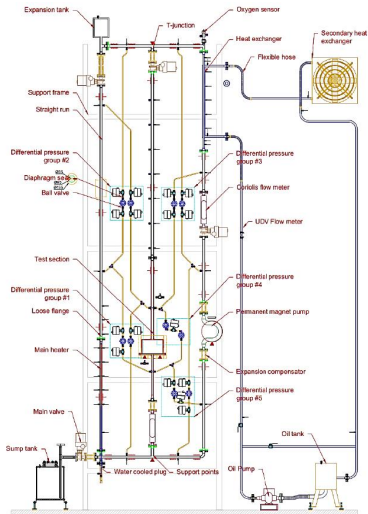
OPENFOAM → OPENFOAM interface → MED-HDF5 format +mesh

OPENFOAM interface is in working progress



# TALL-3D Facility and computational tests

# TALL-3D Facility



## Primary loop (LBE):

1D loops (3)

3d- Test section (1)

(MH) main heater (2)

(EPM) Electromagnetic Pump

(HX) Heat exchanger

## Secondary loop (oil):

Pump-Tank

Secondary HX

## Working conditions:

Pressure: 0.7MPa

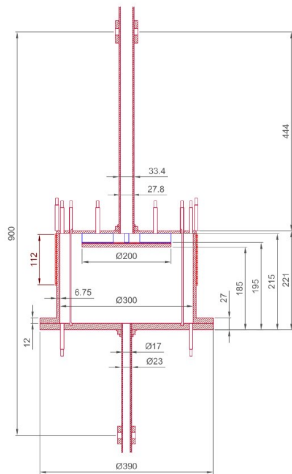
Temperature: 400-500°C

flow rate (LBE)= 5Kg/s; vel  
1.7m/s

heat removal=40 kW (10kw)

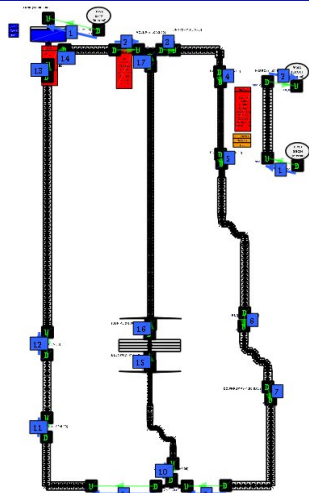
flow rate (oil)= 50 l/min;

# Defective coupling



3D domain

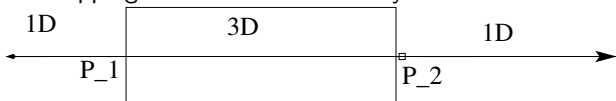
Overlapping and defective boundary conditions



1D domain

# Defective Approach

Overlapping and defective boundary conditions



## Inlet (3D) (P1)

1D value  $\rightarrow$  BC on 3D-equation

mass conservation balanced from the overlapping

## Inlet (1D)(P2)

3D value  $\rightarrow$  Source with Feed-back control (1D-equation)

$$Q = \gamma_1 (T_{3D} - T_{1D})$$

$$S = \gamma_2 (\Delta p_{3D} - \Delta p_{1D}) + \Delta p_0, \quad \gamma_2 = \text{inverse delay time}$$

TALL-3D with In-house  
codes in platform  
(SALOME-CATHARE-  
FEMLCORE)

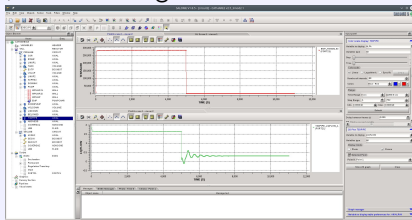
# SALOME-CATHARE-FEMLCORE

## Test: pump power off

1D circuit → CATHARE

3D circuit → FEMLCORE

Mesh, data exchange → MED-HDF5-SALOME



## Test computation

steady 1D circuit + steady 3D-CFD

time step → coupling 1D+3D

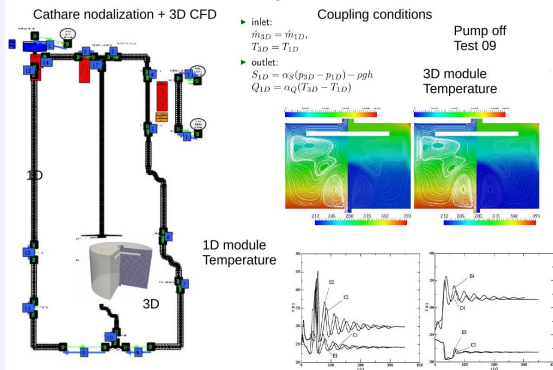
Pump failure

time step → coupling 1D+3D

# Defective coupling 3D-CFD + CATHARE 1D

## Defective coupling: overlapping mesh

### TALL-3D coupled simulation

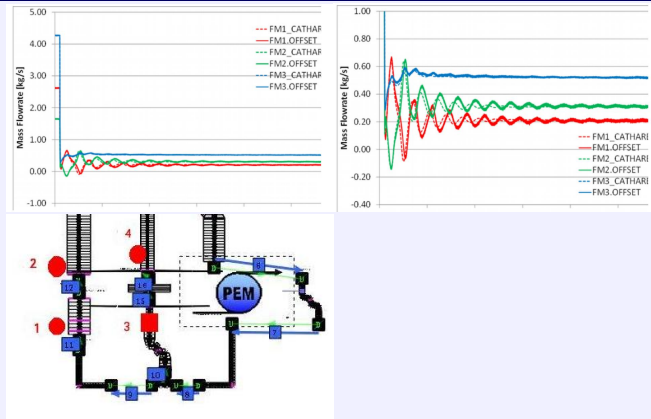


- inlet:  
 $\dot{m}_{3D} = \dot{m}_{1D}$   
 $T_{3D} = T_{1D}$
- outlet:  
 $S_{1D} =$   
 $\alpha_S(p_{3D} - p_{1D}) - \rho gh$   
 $Q_{1D} =$   
 $\alpha_Q(T_{3D} - T_{1D})$

Test 9: pump failure (Natural convection)// COUPLING  
FEMLCORE/OPENFOAM 3D + CATHARE 1D

# 1D-uncoupled CATHARE simulation

## Experimental and computed mass flow rate on different legs



Experimental and computed temperature at the thermocouple points on the left leg (FM1), on the right leg (FM2) and on central one (FM3).



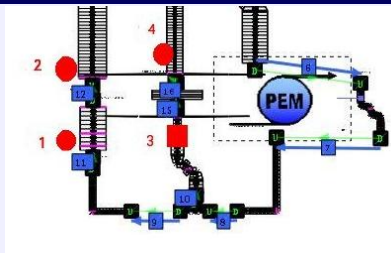
# 3D-1D coupling (FEMLCORE-CATHARE)

## Test numerical stabilization and turbulence models

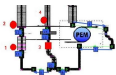
|                | A | B    | C                   | D                   | E                   | F                   |
|----------------|---|------|---------------------|---------------------|---------------------|---------------------|
| Stabilization  | - | SUPG | SUPG                | Upwind              | Upwind              | SUPG                |
| Dynamical Turb | - | -    | $\kappa$ - $\omega$ | $\kappa$ - $\omega$ | $\kappa$ - $\omega$ | $\kappa$ - $\omega$ |
| Thermal Turb   | - | -    | Const $Pr_t$        | Const $Pr_t$        | Kays $Pr_t$         | Kays $Pr_t$         |

Case A refers to Cathare standalone.

## Points of interest in the 1D overlapping mesh

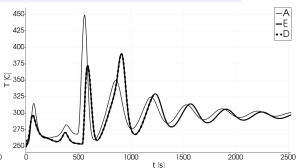
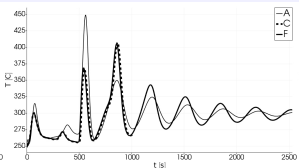
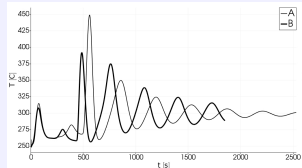


# Reference point (FEMLCORE-CATHARE)

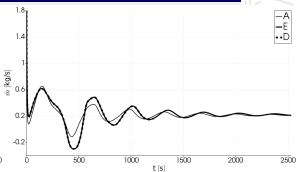
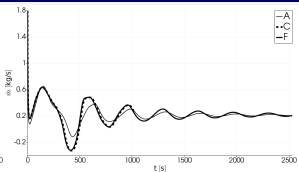
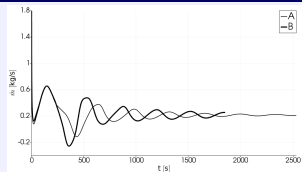


|                | A | B    | C            | D            | E           | F           |
|----------------|---|------|--------------|--------------|-------------|-------------|
| Stabilization  | - | SUPG | SUPG         | Upwind       | Upwind      | SUPG        |
| Dynamical Turb | - | -    | $k-\omega$   | $k-\omega$   | $k-\omega$  | $k-\omega$  |
| Thermal Turb   | - | -    | Const $Pr_t$ | Const $Pr_t$ | Kays $Pr_t$ | Kays $Pr_t$ |

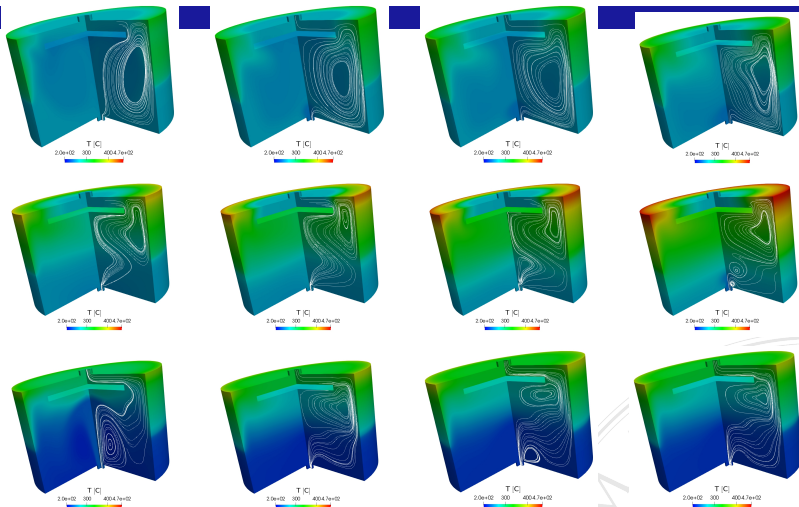
## Temperature. Reference point 2 (RESERVE4, leg 1)



## Mass flow . Reference point 2 (RESERVE4, leg 1)



# 3D coupling solution. Temperature



Temperature and streamline profiles over the 3D test component for  $t = 10 - 2000$  for  $k-\omega$  turbulence case and Kays turbulent Prandtl number model for heat exchange

TALL-3D with  
specialized nuclear  
CEA codes in platform  
(CATHARE- TRIOU)

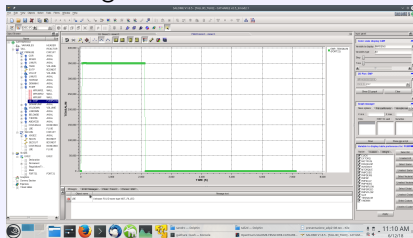
# SALOME-CATHARE-TRIOU (CEA platform)

## Test: pump power off

1D circuit → CATHARE

3D circuit → TRIOU-CFD

Mesh, data exchange → MED-HDF5-SALOME (ICOCO)



## Test computation

steady 1D circuit (0-2000s)+ steady 3D (2000-2100s)

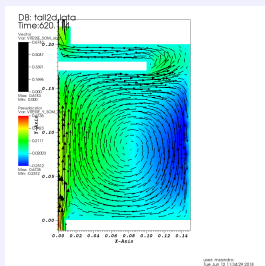
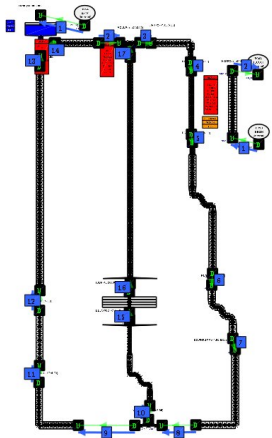
time step → coupling 1D+3D

Pump failure (> 2100s)

time step → coupling 1D+3D

# TRIOU-CFD(3D) + CATHARE 1D (CEA platform)

## Defective coupling: overlapping mesh



- inlet:

$$\dot{m}_{3D} = \dot{m}_{1D},$$
$$T_{3D} = T_{1D}$$

- outlet:

$$S_{1D} =$$
$$\alpha_S(p_{3D} - p_{1D})$$
$$Q_{1D} =$$
$$\alpha_Q(T_{3D} - T_{1D})$$

Test: pump failure (Natural convection)

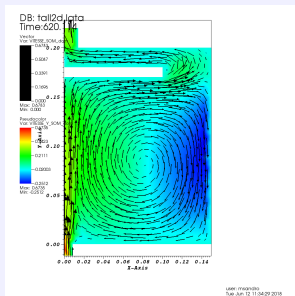
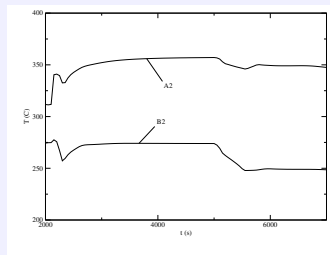
COUPLING TRIOU-CFD + CATHARE 1D → VISIT (VTK no HDF5)

# TRIOU-CFD + CATHARE 1D (CEA platform)

## Previous case

For the previous case → similar results

## Test case with high heat flux



Temperature before (B) and after (A)

Test with enhanced Natural convection +  $\kappa - \epsilon$  turbulent model)

COUPLING TRIOU-CFD + CATHARE 1D → VISIT (VTK no HDF5)

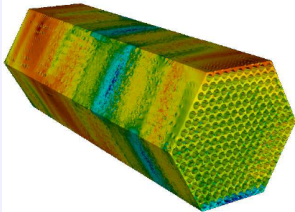
work in progress

TALL-3D with open-source  
codes in platform  
(SALOME-OPENFOAM)



# FEMLCORE-SALOME-CATHARE + OPENFOAM

OPENFOAM: taking advantage of other researcher expertise

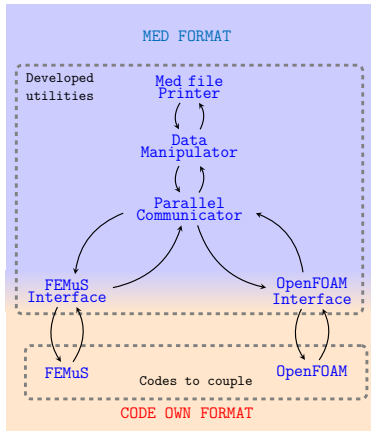


**Solver for:**

- DNS
- Incompressible Navier Stokes
- Heat Transfer
- Compressible Navier Stokes
- Turbulence models
- Combustion
- Multiphase flow
- Solid Mechanics
- Particle tracking

OPENFOAM released by OpenCFD Ltd  
Dynamical and thermal turbulence for liquid metals (KIT and VKI)

# Numerical code coupling

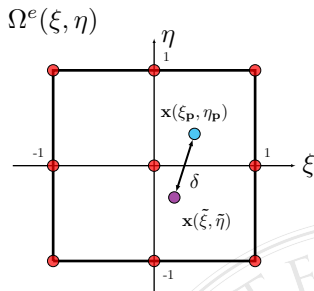
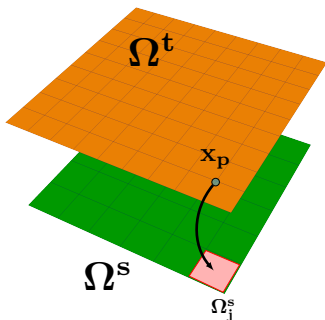


- OpenFoam Interface with MED-HDF5
  - Extract solution from code format to MED-format
  - Set a MED field in code solution
  - Set MED field as external field

# Numerical code coupling

## Projection of P2 fields

Data Manipulator class

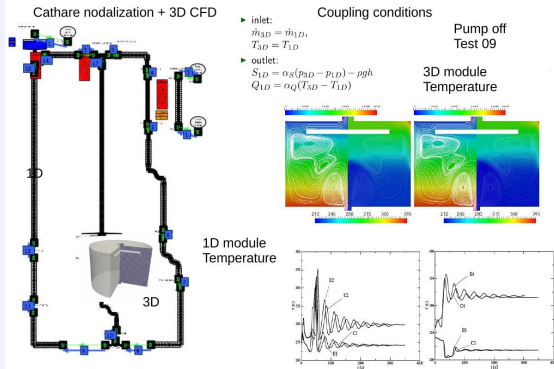


- $\xi_p : \min \left( \delta^2(\mathbf{x}_p, \tilde{\xi}) \right) \rightarrow \delta^2(\mathbf{x}_p, \tilde{\xi}) = \sum_{i=1}^{dim} \left( x_p^i - \sum_{l=1}^{n_n} x_l^i \phi_l(\tilde{\xi}) \right)^2$
- $\Psi^t(\mathbf{x}_p) = \sum_{l=1}^{n_n} \Psi^s(\mathbf{x}_l) \phi_l(\xi_p), \quad \mathbf{x}_l \in \Omega_j^s, \mathbf{x}_p \in \Omega_j^s$
- $\Psi^t = \mathbf{P}\Psi^s$

# Defective coupling 3D-CFD + CATHARE 1D

## Defective coupling: overlapping mesh

### TALL-3D coupled simulation

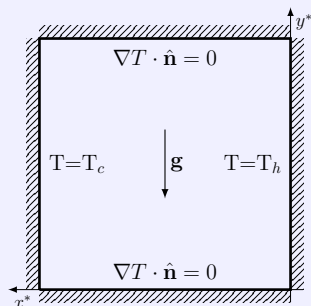


- inlet:  
 $\dot{m}_{3D} = \dot{m}_{1D}$   
 $T_{3D} = T_{1D}$
- outlet:  
 $S_{1D} =$   
 $\alpha_S(p_{3D} - p_{1D})$   
 $Q_{1D} =$   
 $\alpha_Q(T_{3D} - T_{1D})$

Test 9: pump failure (Natural convection)  
COUPLING OPENFOAM-FEMLCORE 3D + CATHARE 1D  
OPENFOAM → turbulence models

# Simulation settings: natural convection

## Geometry and Boundary conditions



- Squared cavity with side 0.1 m
- $\mathbf{u} = 0$  on all boundaries
- Thermal insulation on upper and lower boundaries
- Fixed temperature on left and right sides

| $\nu$ [m <sup>2</sup> /s] | $\alpha$ [m <sup>2</sup> /s] | $g$ [m/s <sup>2</sup> ] | $\beta$ [1/K] |
|---------------------------|------------------------------|-------------------------|---------------|
| 0.01                      | 0.002                        | 9.81                    | 10            |

- Simple and well studied case

# Simulation settings

## Simulated cases

### OpenFOAM

- $T_{OF}$  solver
- NS solver
- $\tilde{T}_{OF}$  source buoyancy

### FEMuS

- $T_{FM}$  solver
- NS solver
- $\tilde{T}_{FM}$  source buoyancy

## CASE

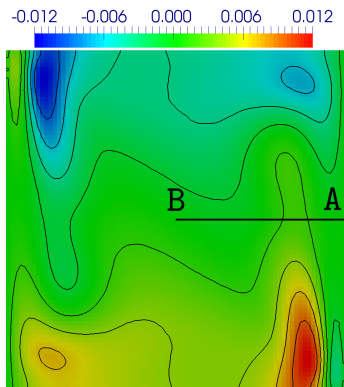
CASE A - OF:  $T_{OF} \rightarrow \tilde{T}_{OF}$  FEMuS:  $T_{FM} \rightarrow \tilde{T}_{FM}$

CASE B - FEMuS:  $T_{FM} \rightarrow \tilde{T}$ ,  $T_{FM} \rightarrow \tilde{T}_{OF}$

CASE C - OF:  $T_{OF} \rightarrow \tilde{T}_{OF}$ ,  $T_{OF} \rightarrow \tilde{T}_{FM}$

# Coupling Case A

$$T_{of}^* - T_{fe}^*$$



$$\square T^* = (T - T_c)/(T_h - T_c)$$

$$\square v^* = v * L/\alpha$$

---

| $v_{max}^*$ on A - B |       |          |
|----------------------|-------|----------|
| Grid size            | FEMuS | OpenFOAM |
| 20×20                | 73.51 | 67.99    |
| 40×40                | 73.48 | 73.93    |
| 80×80                | 73.48 | 73.98    |

---

|           |       |
|-----------|-------|
| Reference | 70.63 |
|-----------|-------|

---

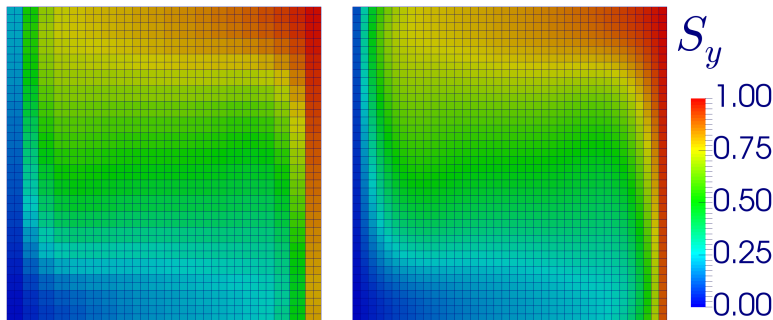
$\square$  OpenFOAM T higher near hot wall and smaller near cold wall

# Coupling Case B

□ FEMuS 20x20, OpenFOAM 40x40

B1

B2

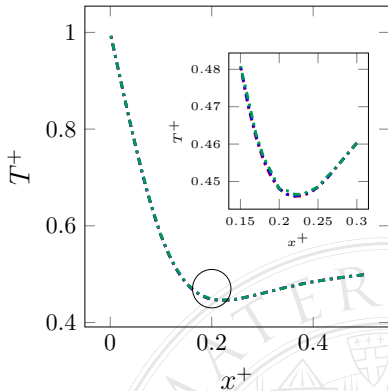
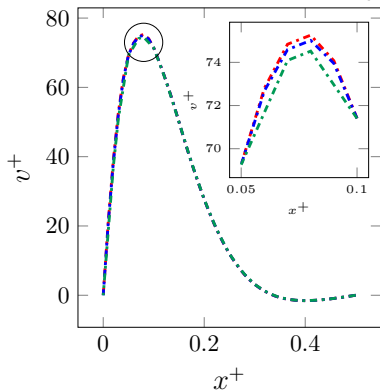


| $v_{max}^*$ on A-B | FEMuS | OpenFOAM A | OpenFOAM B1 | OpenFOAM B2 |
|--------------------|-------|------------|-------------|-------------|
|                    | 73.51 | 73.93      | 75,76       | 73,24       |



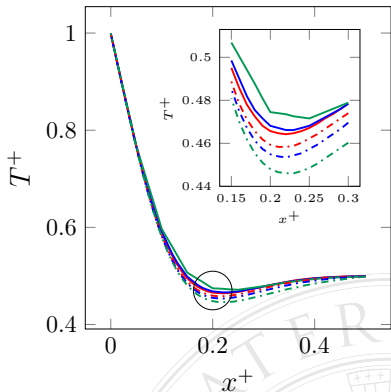
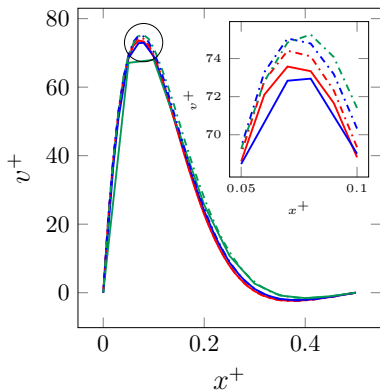
# Coupling Case C

□ FEMuS 20x20, 40x40, 80x80, OpenFOAM 20x20



| $v_{max}^*$ on A-B | FEMuS 20 | FEMuS 40 | FEMuS 80 |
|--------------------|----------|----------|----------|
|                    | 74,52    | 75       | 75,25    |

# Coupling Case C



- OpenFOAM domain discretization: 20x20, 40x40, 80x80
- FEMuS domain discretization: 80x80
- OpenFOAM solution: solid line, FEMuS solution: dashed

# Conclusions

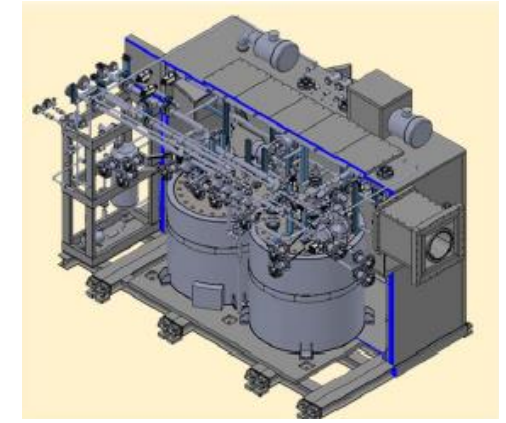
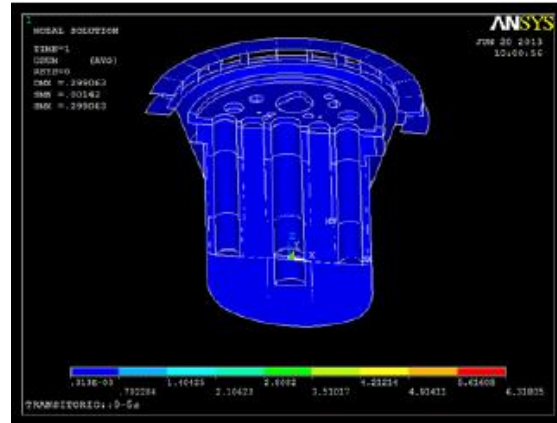
# Conclusions

## Working

- We are working on the TRIOU CFD-CATHARE-SALOME coupling interface (all nuclear tested codes)
- We are working on OPENFOAM-SALOME coupling interface
- We are working on CEA nuclear codes + open-source codes + in-house codes on SALOME platform

## TALL-3D experiment

- Comparison with old and new experimental results

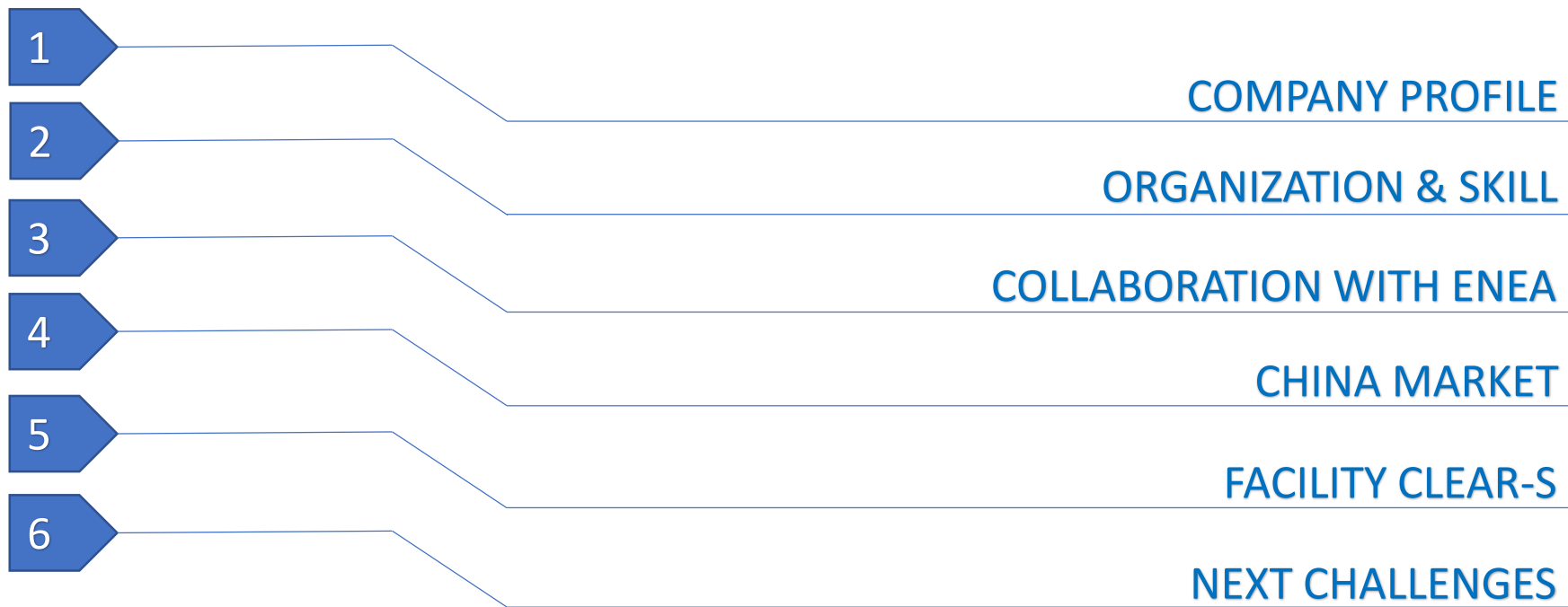


S.R.S. Servizi di Ricerche e Sviluppo S.r.l.

SRS PRESENTATION

ULISSE PASQUALI  
14.06.2018

# Summary



# Summary

1

## COMPANY PROFILE



# 1.COMPANY PROFILE

## S.R.S. Servizi di Ricerche e Sviluppo S.r.l.:

- is a SME with a 40-years experience in the field of design and engineering of processes, plants and machineries in several technological sectors mainly in the Nuclear sector
- Offers multidisciplinary engineering services in the design of equipment, systems and civil structures and provides services related to decommissioning activities of nuclear installations and Nuclear Waste Management
- Supplies, “as turn-key “, components and systems for nuclear application, including complete complex experimental facilities useful to test innovative components, as well as demonstration of component/plant behavior in any operational and accidental condition
- Belongs to SRS GROUP, which is a cluster of Companies whose characterizing feature is the capability in tackling new and complex engineering problems, always finding a solution, looking at cost effectiveness and at time scheduling





2

## ORGANIZATION & SKILL



## 2.ORGANIZATION & SKILL

The engineering production capacity of the company is over 70,000 h/year, achieved mainly through internal resources.

SRS has the availability of high skilled external staff able to immediately operative, thank to a proven network of cooperation with the other companies of SRS GROUP and with specialized companies, supported by specific cooperation agreements.

The whole staff (including external staff) is about 100 unit (more than **175,000 h/year**).

The technical structure include **five technical areas or divisions**. Each area has a technical responsible with a managing role coordinating the project activities.

The technical areas are:

- Nuclear;
- Mechanical;
- Civil;
- Electrical, automation and Instrumentation;
- Process and Chemical.



## 2. ORGANIZATION & SKILL

### NUCLEAR DIVISION

S.R.S. capabilities deal with all aspects of nuclear safety and radiological protection for nuclear installations, in particular:

- Nuclear installation safety analysis, including:
  - Identification and selection of initiating events;
  - Probabilistic, deterministic and hybrid safety assessments;
  - Calculation of doses and radiological impact on workers and population;
- Criticality and burn-up calculations; fuel loading strategies;
- Reliability analysis of reactivity control systems, power distribution calculation in sub-critical and critical systems, reactivity coefficients calculation;
- Radiation shielding analysis and design;
- Evaluation of radiation doses to exposed individuals and population;
- Evaluation of integral radiation doses to materials;
- Fluid-dynamic and thermal-hydraulic calculations, intransient and steady state conditions, in support to core and system design, in operational and accident scenarios.

The analysis are carried out according to international and national standards and rules, namely ANS, ANSI, ASME, IEEE, DOE, NUREG, SMACNA, ISO, IAEA, ICRP, CEI IERC, UNI and UNI EN.



## 2. ORGANIZATION & SKILL

### MECHANICAL DIVISION

S.R.S. capabilities includes:

- Process definition, concept analysis and feasibility studies;
- Design of complex mechanical systems, as nuclear systems (primary circuit components, reactor auxiliary systems, nuclear and non-nuclear), heating, ventilation, and air conditioning systems, liquid/solid/gaseous waste treatment facilities, fire-control systems and mechanical systems in general as per international industrial standards and nuclear safety rules; (AMSE, ANSI, API, IEEE, IAEA, EUR, DIN, UNI EN, ASME AG-1, ISO, NUREG, etc.)
- Structural analysis as per Italian regulations (UNI, PED);
- Structural analysis as per US and international nuclear standards (ASME III, ANSI, ASME AG-1, NUREG, ANS);
- Non-linear structural analysis;
- Preparation of technical specifications, engineering analysis reports, project development time schedules and cost estimates;



## 2.ORGANIZATION & SKILL

### CIVIL DIVISION

S.R.S. capabilities includes:

- Architectural design;
- Reinforced concrete structural design;
- Steel structure design;
- Structural analysis as per Italian rules and regulations;
- Structural analysis as per US regulation (ACI) and nuclear standard;
- non-linear structural analysis, static and dynamic (time histories);
- Preparation of technical specifications engineering calculations reports, project development time schedules and cost estimates.

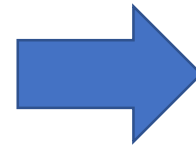
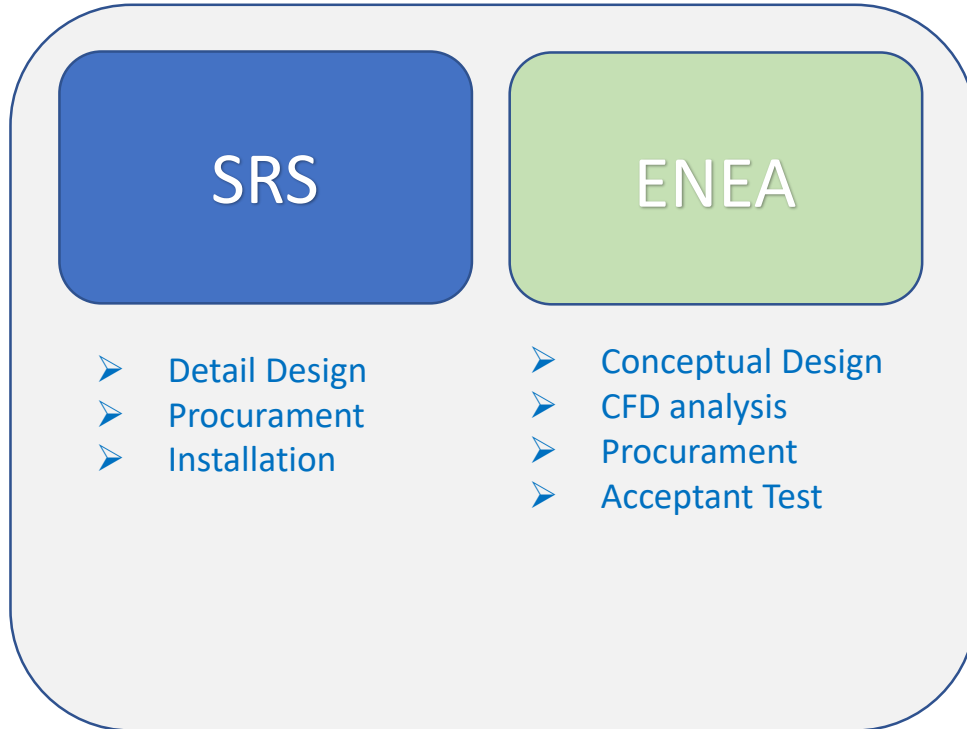


3

## COLLABORATION WITH ENEA



# 3. COLLABORATION WITH ENEA



- SIRIO Project (ALFRED)
- ELF Project (ALFRED)
- KYLIN-II (CHINA)
- CLEAR-S (CHINA)
- CLEAR-M1X (CHINA)



# 3. COLLABORATION WITH ENEA

## SIRIO PROJECT

### PARTNER:

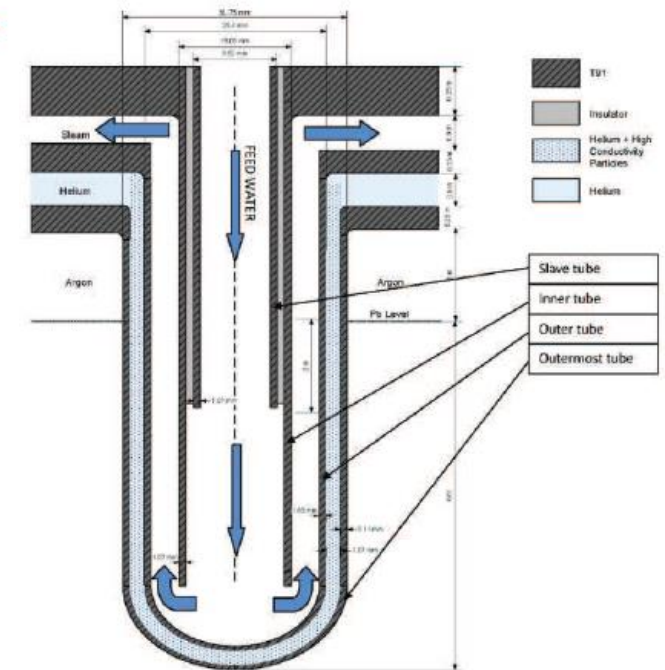
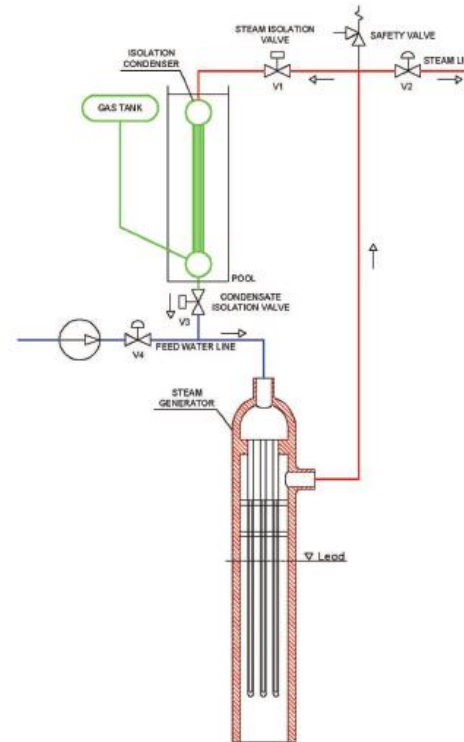
- SRS
- ENEA
- ANSALDO NUCLEARE
- SIET

### OBJECT:

The SIRIO project is an experimental facility which aim is to test the Decay Heat Removal System (DHRS) proposed by Ansaldo Nucleare within the project of the ALFRED Lead Fast Reactor.

The system mainly consists of:

- A steam generator (SG);
- An in-pool condenser (Isolation Condenser);
- A non-condensable tank;
- Piping system equipped with valves (On/Off and control)





# 3. COLLABORATION WITH ENEA

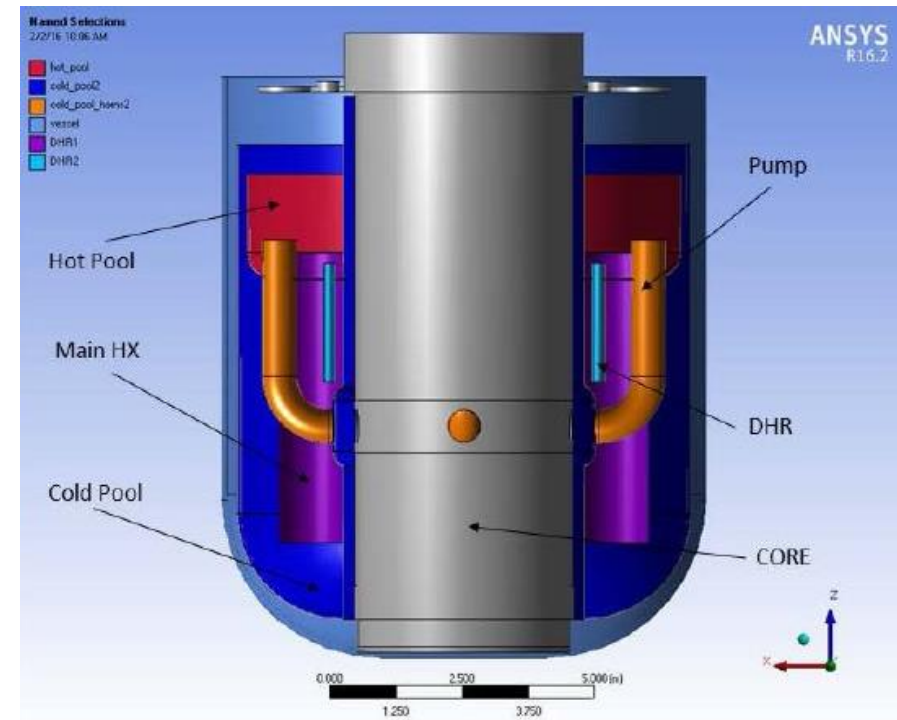
## ELF PROJECT

### PARTNER:

- SRS
- ENEA

### OBJECT:

The European Lead Fast facility (ELF) is conceived to investigate thermal hydraulic phenomena in a pool type configuration reproducing the main coolant flow path of the primary system of the ALFRED Reactor. The facility consists of a main vessel filled with molten pure lead as working fluid and hosting the Core Simulator (10 MW).



4

## CHINESE MARKET



## 4. CHINESE FACILITY

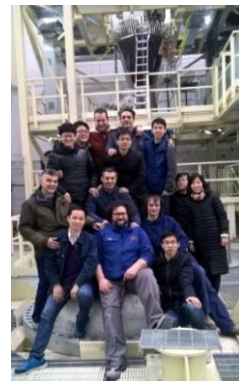
- Since 15 years ENEA Brasimone is promoting its wide experience in heavy metal experimental facility in the chinese market;
- This is a big chance for the italian company and SRS has put all its effort to support ENEA in this challenge;
- The chinese government is strongly interested in the **LEAd-based Reactor** and it is putting a lot of funds in different projects which support the design, licensing and construction of the nuclear reactor CLEAR-1.
- Walking this line, ENEA and SRS have been working together since 2012

### 2012-2014



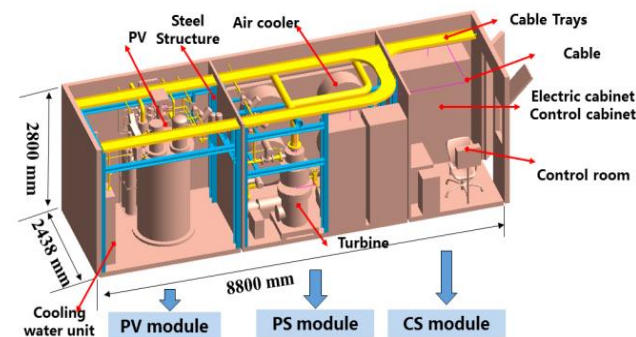
KYLIN-II (250 Kw)

### 2014-2017

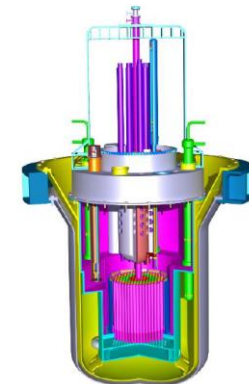


CLEAR-S (2,5 MW)

### 2018-on going



CLEAR-M1X (1,1 MW)



CLEAR-1 (10 MW)



5

## CLEAR-S FACILITY



# 5.CLEAR-S FACILITY

## CLEAR-S:

- LBE LOOP
  - 220 ton of LBE
  - $T=450\text{ }^{\circ}\text{C}$
- WATER LOOP
  - $T=300\text{ }^{\circ}\text{C}$
  - $P=120\text{ barg}$
- ELECTRICAL SYSTEM
  - Power 2,5 Mwe
- CONTROL SYSTEM
  - N.1500 I/O signals (TC,PT, etc)
- VENTILATION SYSTEM
  - Air flow  $60.000\text{ m}^3/\text{h}$
- CIVIL STRUCTURE
  - N.5 floor



# 5.CLEAR-S FACILITY

## DESIGN STEPS

### Conceptual design by ENEA:

- Conceptual P&I
- CFD analysis
- Components pre-design



### Detailed design by SRS:

- Pressurized components design
- Piping thermal-stress analysis
- Electrical system design
- Metallic structure design
- Control system software



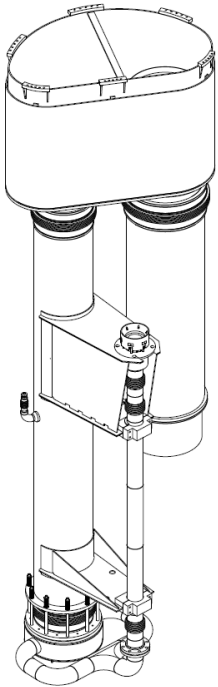
Assembly  
and test by  
SRS-ENEA



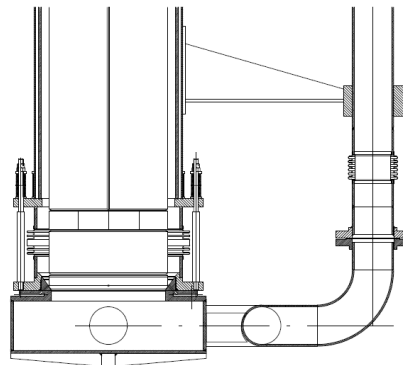
# 5.CLEAR-S FACILITY

## INTERNALS: DESIGN & REALIZATION

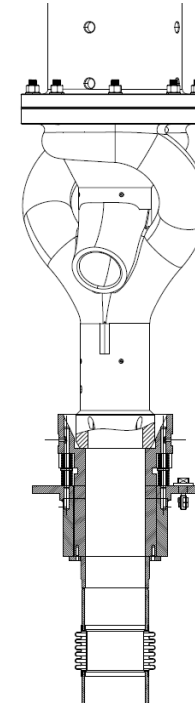
### ASSEMBLY



### Core Simulator coupling



### Pump coupling







# 5.CLEAR-S FACILITY

## CODE & STANDARDS

### PRESSURIZED VESSEL:

- Design according to ASME VIII DIV.1-2
- Certification according to PED

### PIPING:

- Design according to ANSI B31.1
- Certification according to PED

### METALLIC STRUCTURE:

- EUROCODE 0-1-3-8

### ELECTRICAL SYSTEM:

- IEC 61439-1/2



6

## NEXT CHALLENGES



# 6.NEXT CHALLENGES

## LEAD-BASED REACTORS



- CLEAR-M1X
- CLEAR-M
- CLEAR-1



- ALFRED
- FALCON



WORK IN  
PROGRESS...



THANK YOU





# WORKSHOP TEMATICO PAR 2017



GENERATION IV LEAD COOLED FAST REACTOR  
STATO ATTUALE DELLA TECNOLOGIA E PROSPETTIVE DI SVILUPPO

## **CIRCE-HERO experiment overview**

A. Pesetti

([alessio.pesetti@for.unipi.it](mailto:alessio.pesetti@for.unipi.it))

14-15 June 2018, Roma



# List of contents



- ❑ Introductory remarks & objectives
- ❑ CIRCE facility and HERO test section
- ❑ HERO Test Section
  - Primary system LBE
  - Secondary system H<sub>2</sub>O
  - Instrumentation
- ❑ CIRCE-HERO DACS
- ❑ CIRCE-HERO commissioning (heat losses tests)
- ❑ Experimental campaign Test Matrix
- ❑ Conclusive remarks

## RESEARCH MOTIVATION

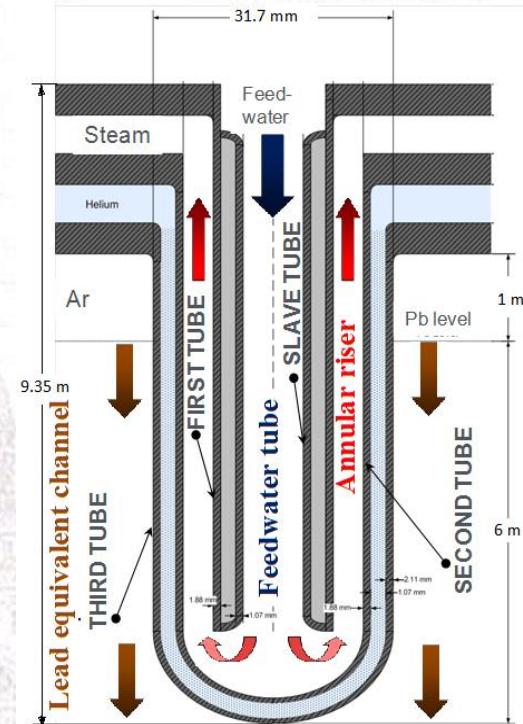
- **ALFRED** reactor design includes an innovative concept of Steam Generator, adopting double walled bayonet tubes (**SGBT**)
- Characterised by **two barriers** between primary and secondary coolant and a **leakage monitoring system** in between (He + high K powder @ ~10 bar)
- **R&D** is needed for characterising SGBT **performance** in steady-state and transient conditions

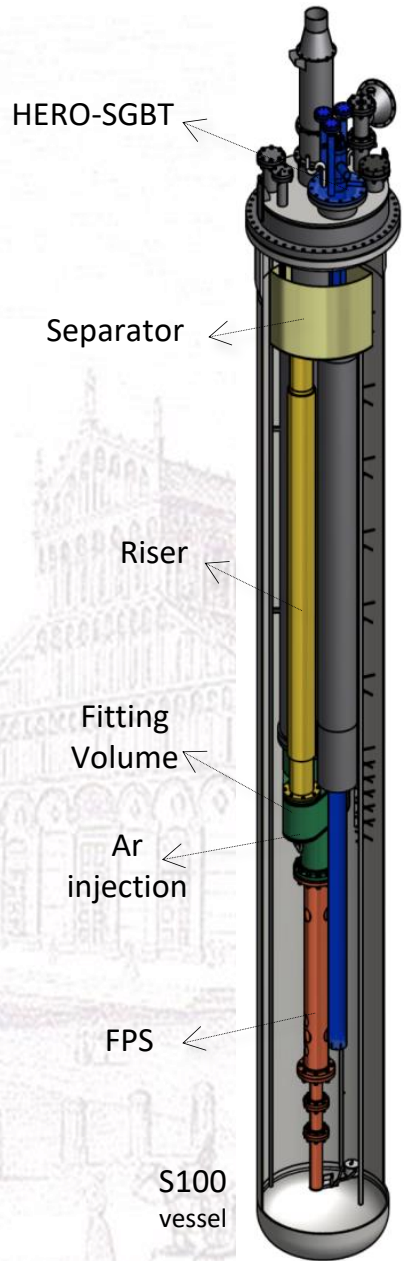
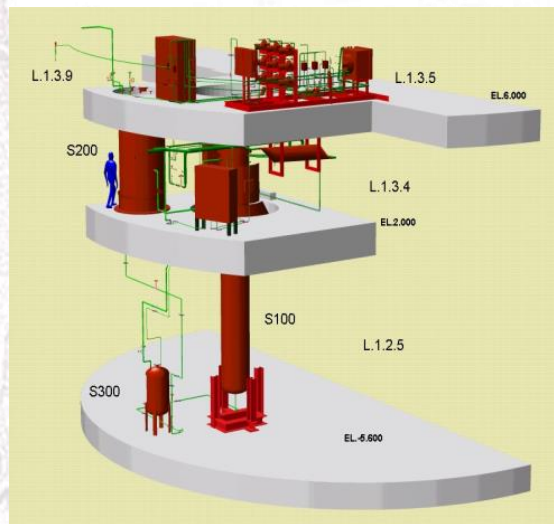
H<sub>2</sub>O inlet @ 335°C, steam outlet @ 450°C,  
180 bar, 0.047 kg/s

LBE @ 400÷480°C, 6.36 kg/s  
cover gas @ low pressure gauge

## MAIN ACTIVITIES and OBJECTIVES

- A **mock-up of 7 BTs** relevant for **ALFRED SG** was designed, assembled and implemented in **HERO** test section at ENEA CR Brasimone
- An **experimental campaign** of 3 forced to natural circulation transition will be carried out (1 run SESAME bench.)
- **Engineering** and **safety feedbacks** for designer and high quality data for **code validation/model development**





| CIRCE Parameters               | Value       |
|--------------------------------|-------------|
| Outside diameter [mm]          | 1200        |
| Wall thickness [mm]            | 15          |
| Material                       | AISI 316L   |
| Max LBE Inventory [kg]         | 90000       |
| Electrical Heating [kW]        | 47          |
| Temperature Range [°C]         | 200 to 500  |
| Operating Pressure [kPa]       | 15 (gauge)  |
| Design Pressure [kPa]          | 450 (gauge) |
| Argon Flow Rate [NI/s]         | 15          |
| Argon Injection Pressure [kPa] | 600 (gauge) |

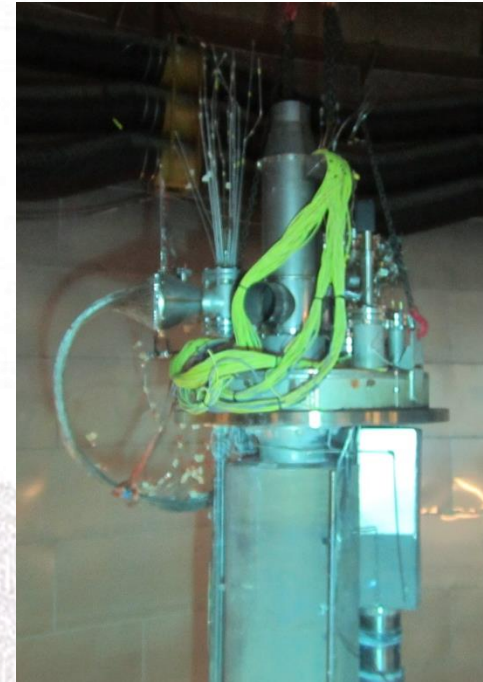


# HERO TS primary system

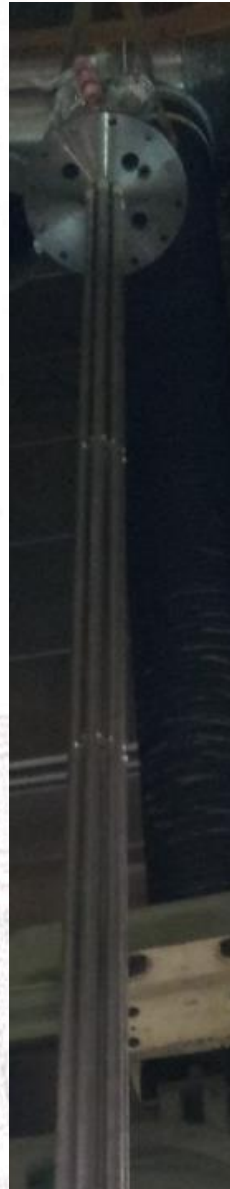
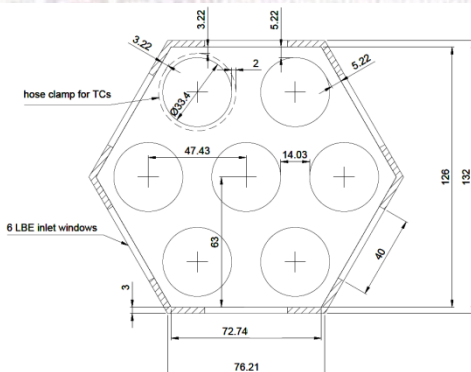
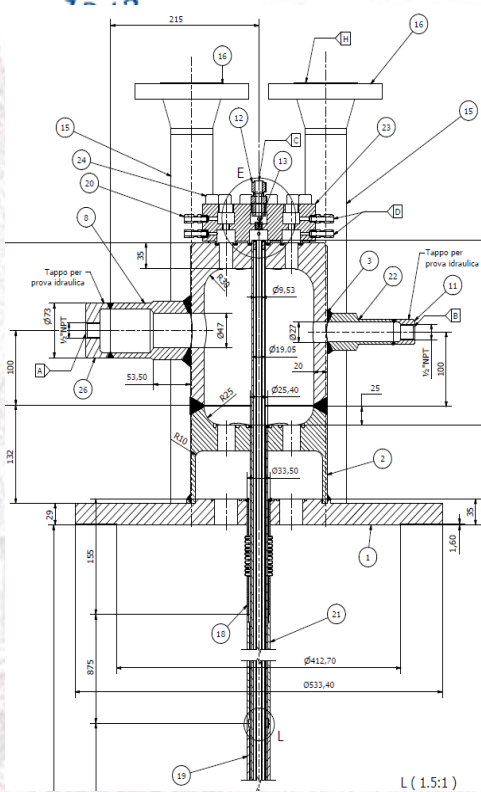


# HERO TS primary system

HERO TS implemented in CIRCE main vessel



## SGBT set in HERO TS

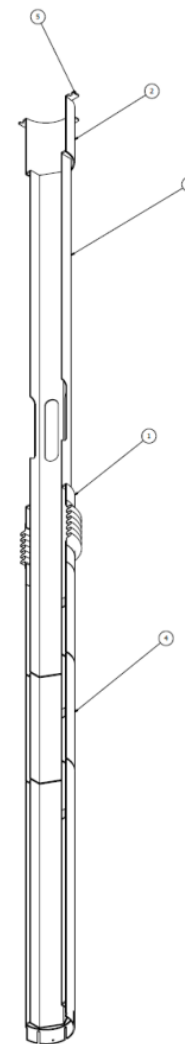


| Double-Walls BT                    | Inner diameter [mm] | Outer diameter [mm] | Thickness [mm] | Material        |
|------------------------------------|---------------------|---------------------|----------------|-----------------|
| Feed-water slave tube              | 7.09                | 9.53                | 1.22           | AISI-304        |
| Feed-water tube gap                | 9.53                | 15.75               | 3.11           | Slight vacuum   |
| First tube (feed-water outer tube) | 15.75               | 19.05               | 1.65           | AISI-304        |
| Annular riser gap                  | 19.05               | 21.18               | 1.07           | Water-steam     |
| Second tube                        | 21.18               | 25.40               | 2.11           | AISI-304        |
| Annular gap                        | 25.40               | 26.64               | 0.62           | AISI 316 powder |
| Third tube                         | 26.64               | 33.40               | 3.38           | AISI-304        |

|                       | Unit | Water-Steam side             | He side               | LBE side        |
|-----------------------|------|------------------------------|-----------------------|-----------------|
| Fluid                 | --   | Water – steam                | Helium                | LBE             |
| Circulation mechanism | --   | Axial pump + accumulator     | leakage accommodation | Gas enhanced    |
| Main components       | --   | bayonet tubes, steam chamber | Helium chamber        | SGBT unit shell |
| Bundle type and P/D   | -    | Triangular / 1.42            | --                    | Shell           |
| Inlet temp.           | °C   | 335                          | --                    | 480             |
| Mass flow             | kg/s | 0.330785                     | stagnant              | 44.573529       |
| Design pressure       | bar  | 180                          | 5.0                   | As CIRCE        |
| Operating pressure    | bar  | 172                          | 4.5                   | Hydraulic head  |
| Design temp.          | °C   | 432                          | 432                   | As CIRCE        |

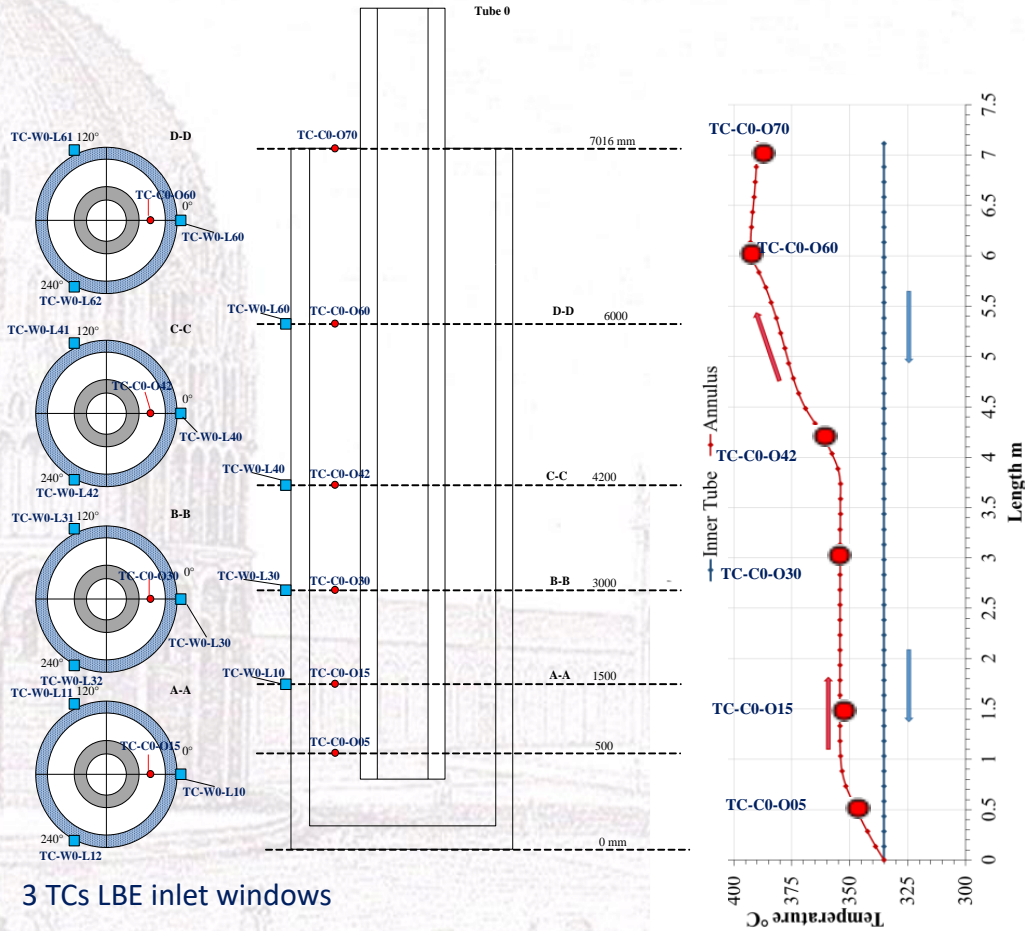
# HERO TS secondary system

## HERO SGBT details



## HERO SGBT instrumentation, 48 TCs

Central byonet tube



3 TCs LBE inlet windows

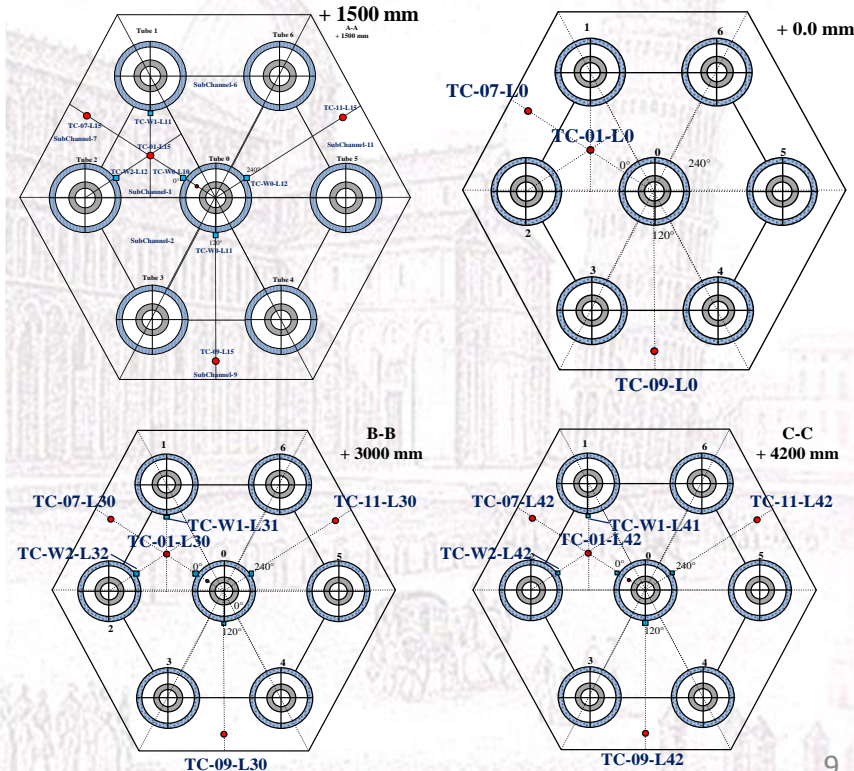
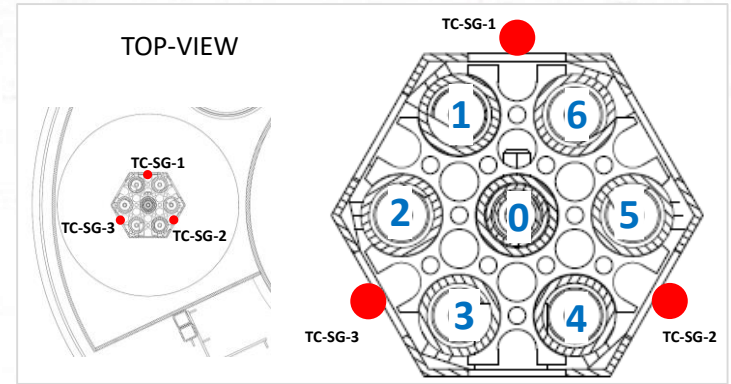
15 TCs LBE sub-channel

12 TCs LBE/outer surface central tube

6 TCs LBE/outer surface outer tube

5 TCs in annular steam gap T0

7 TCs steam outlet all tubes



FPS → **39** TCs ( N-type 0.5 mm,  $\pm 0.1^\circ\text{C}$ )

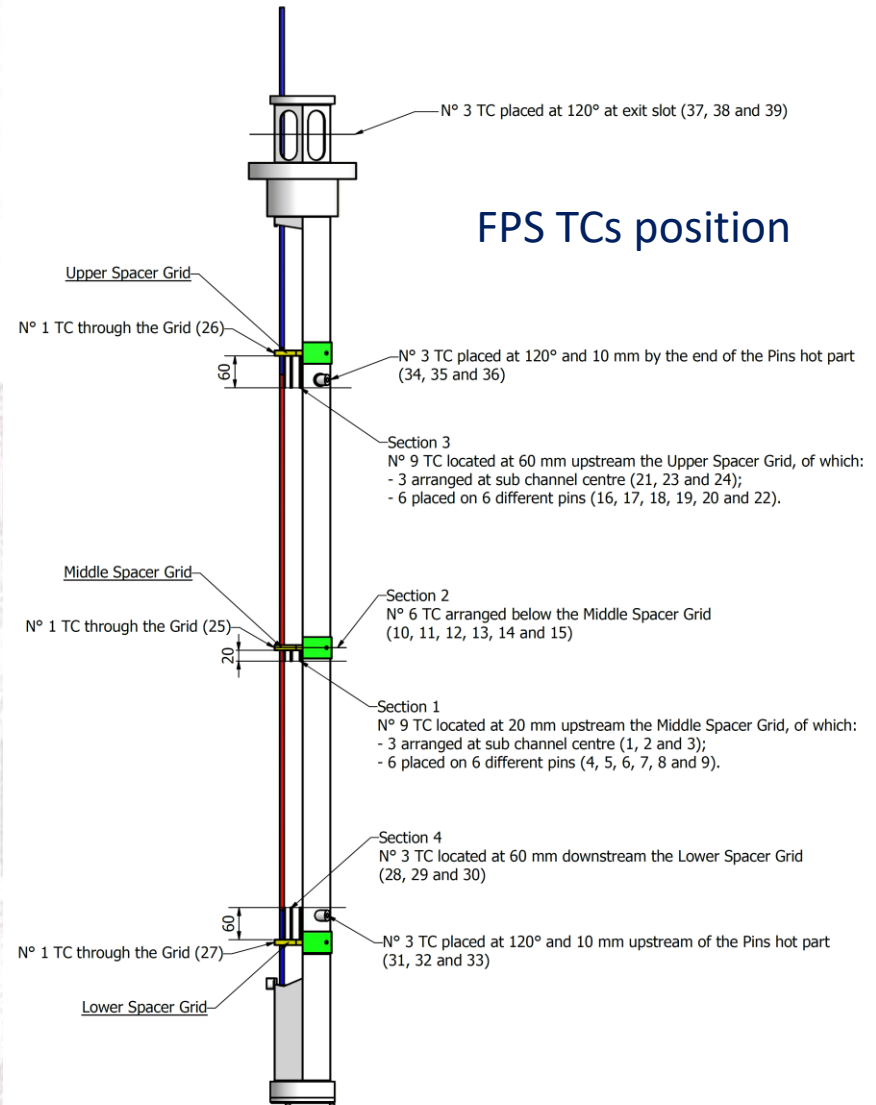
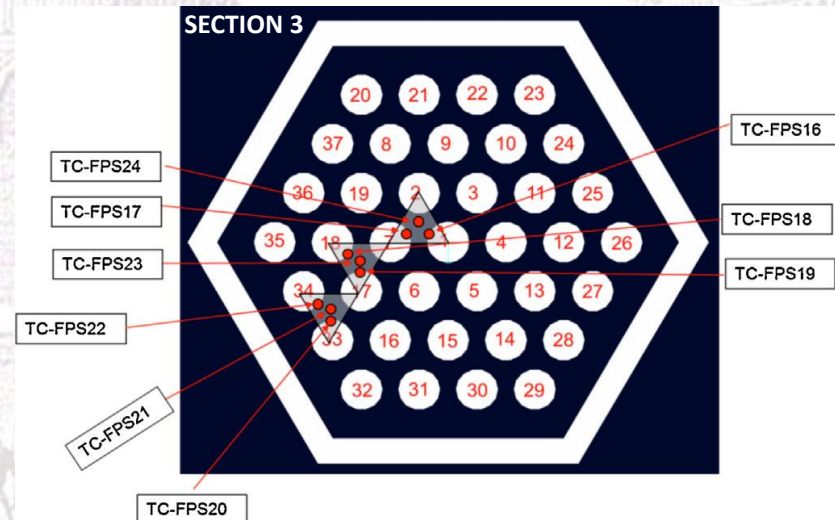
Fitting volume → **5** TCs ( N-type 3 mm,  $\pm 1^\circ\text{C}$ )

Riser → **6** TCs ( N-type 3 mm,  $\pm 1^\circ\text{C}$ )

Cover gas → **1** TCs

Heat Exchanger → **48** TCs

Pool → **122** TCs ( N-type 3 mm,  $\pm 1^\circ\text{C}$ )



FPS → **39** TCs ( N-type 0.5 mm,  $\pm 0.1^\circ\text{C}$ )

Fitting volume → **5** TCs ( N-type 3 mm,  $\pm 1^\circ\text{C}$ )

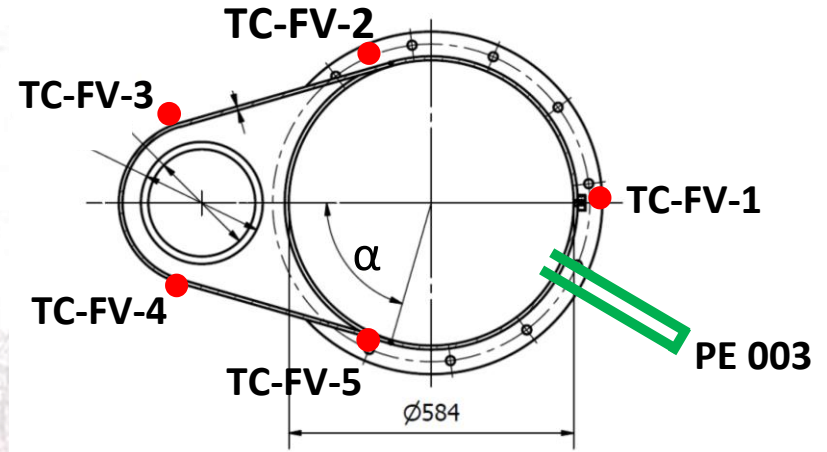
Riser → **6** TCs ( N-type 3 mm,  $\pm 1^\circ\text{C}$ )

Cover gas → **1** TCs

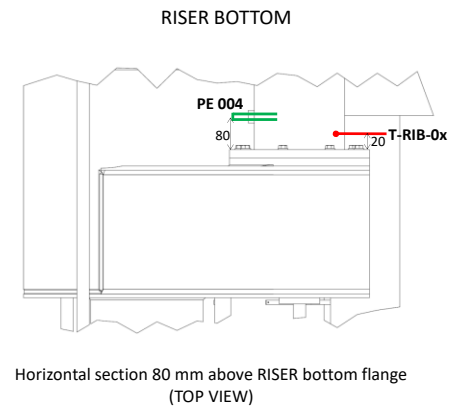
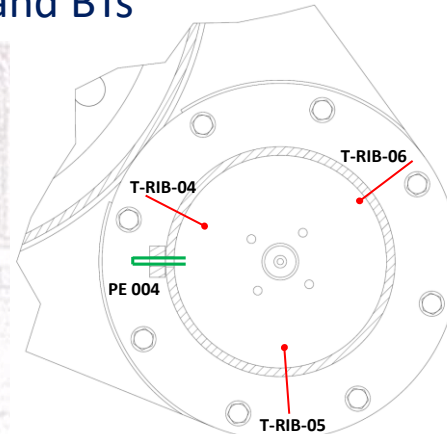
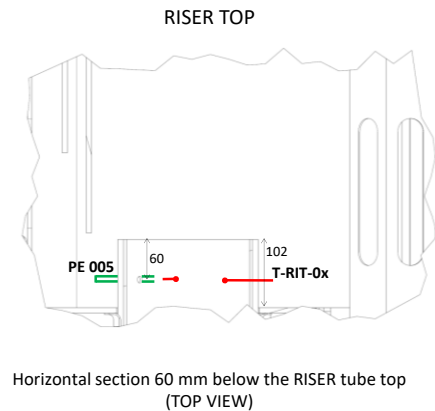
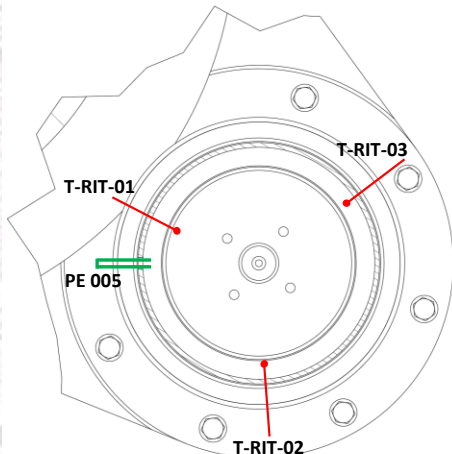
Heat Exchanger → **48** TCs

Pool → **122** TCs ( N-type 3 mm,  $\pm 1^\circ\text{C}$ )

## FITTING VOLUME



## RISER TCs and BTs



POOL MIXING and STRATIFICATION

CIRCE-ICE



CIRCE-HERO

pool mixing and stratification

FPS → **39** TCs ( N-type 0.5 mm, ± 0.1°C)

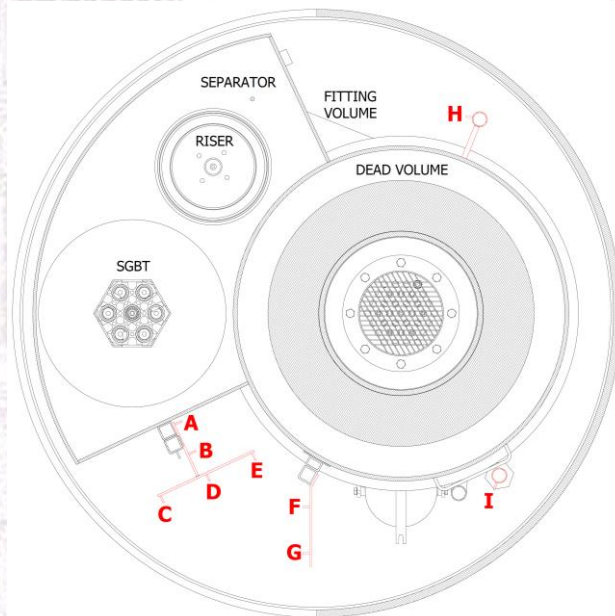
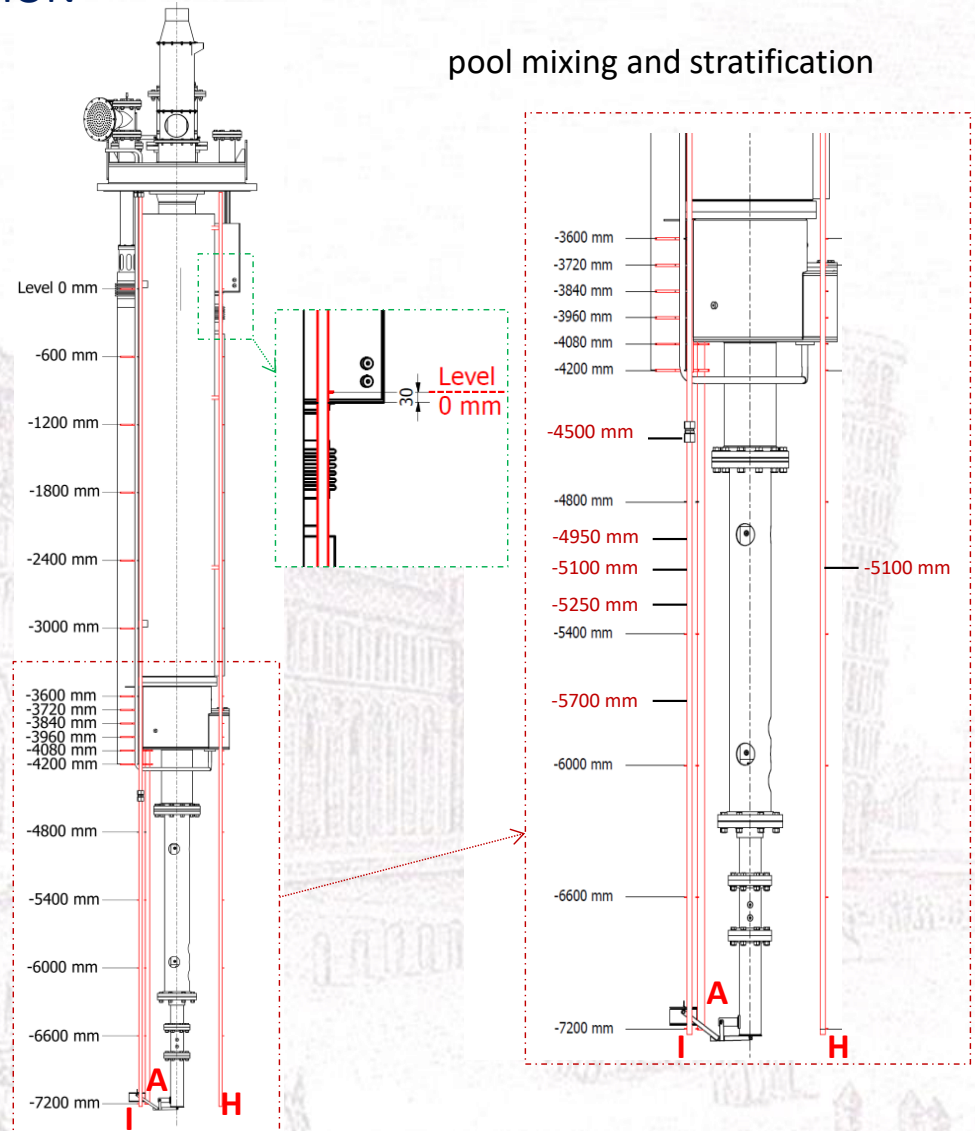
Fitting volume → **5** TCs ( N-type 3 mm, ± 1°C)

Riser → **6** TCs ( N-type 3 mm, ± 1°C)

Cover gas → **1** TCs

Heat Exchanger → **48** TCs

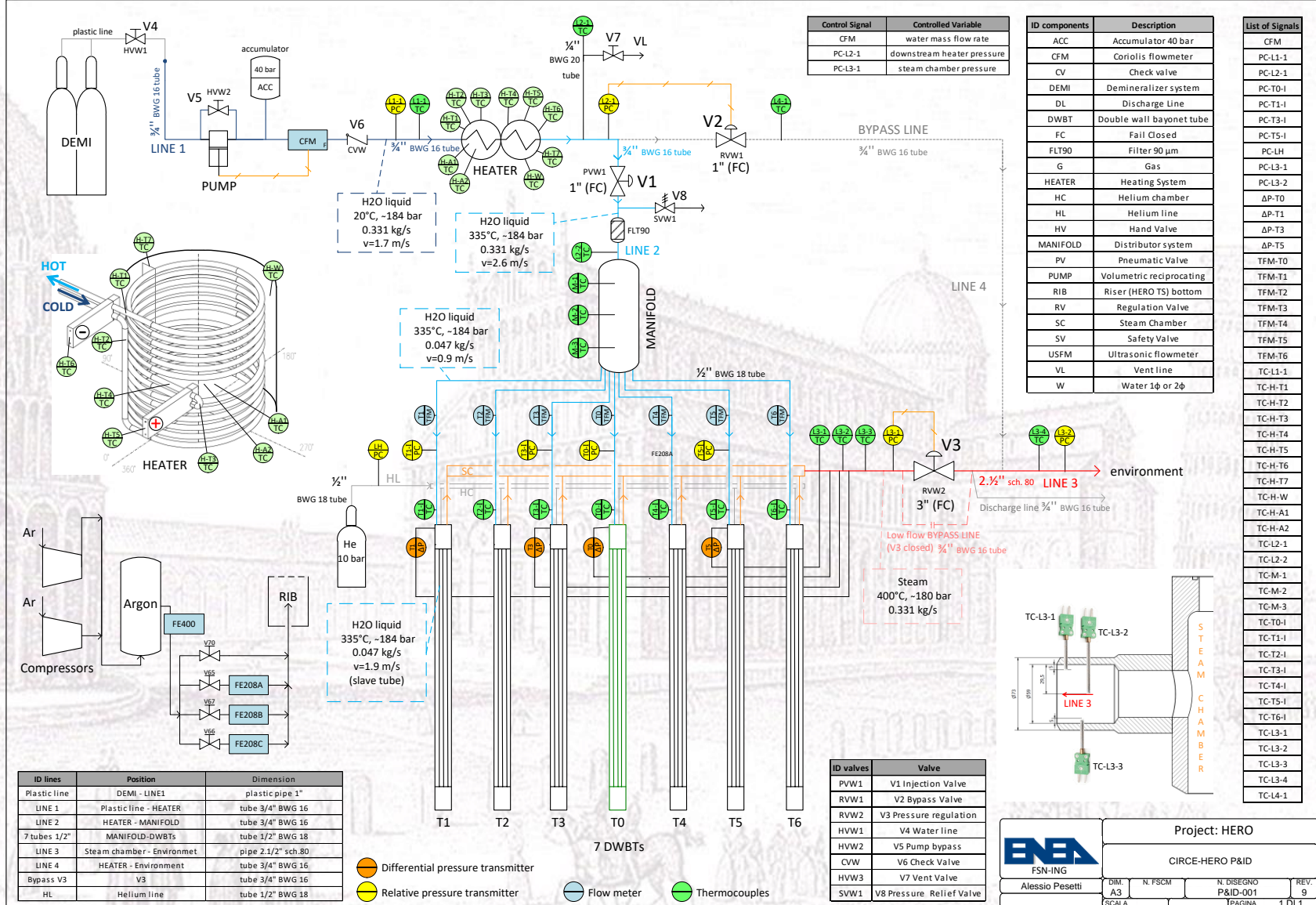
Pool → **122** TCs ( N-type 3 mm, ± 1°C)



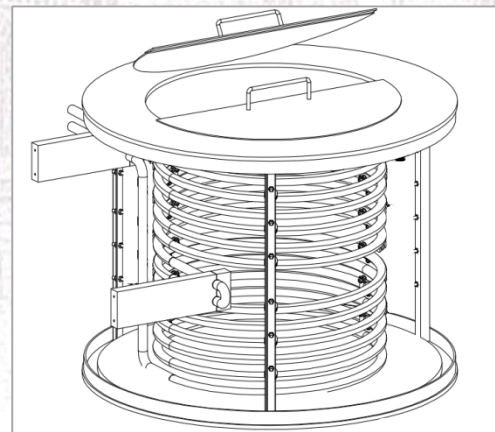
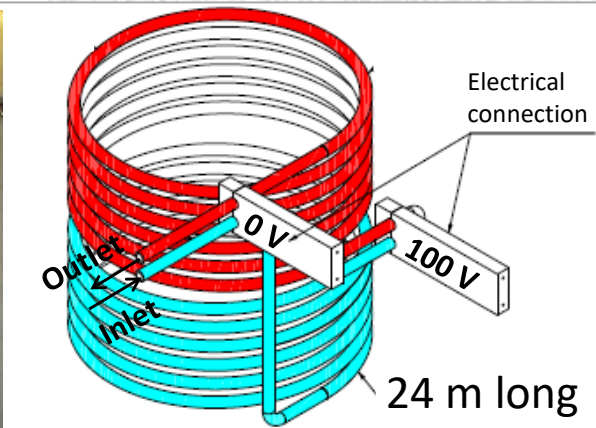


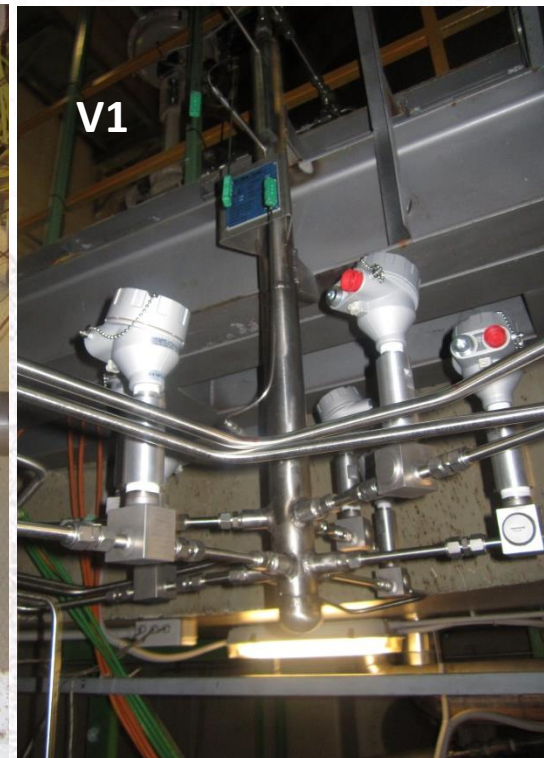
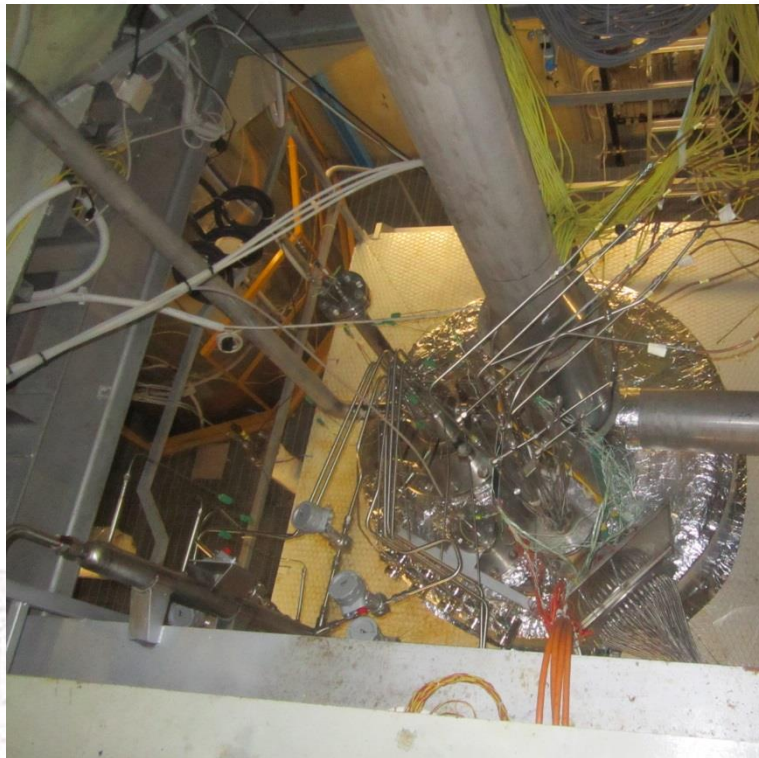


# CIRCE-HERO 2<sup>ary</sup> side components and instrumentation



## Heating system of the feed water

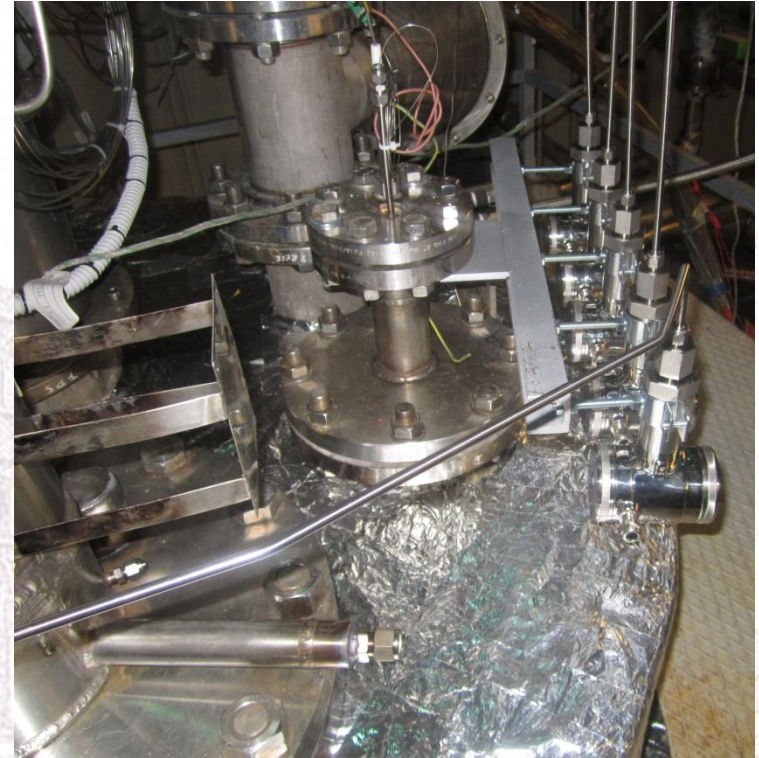
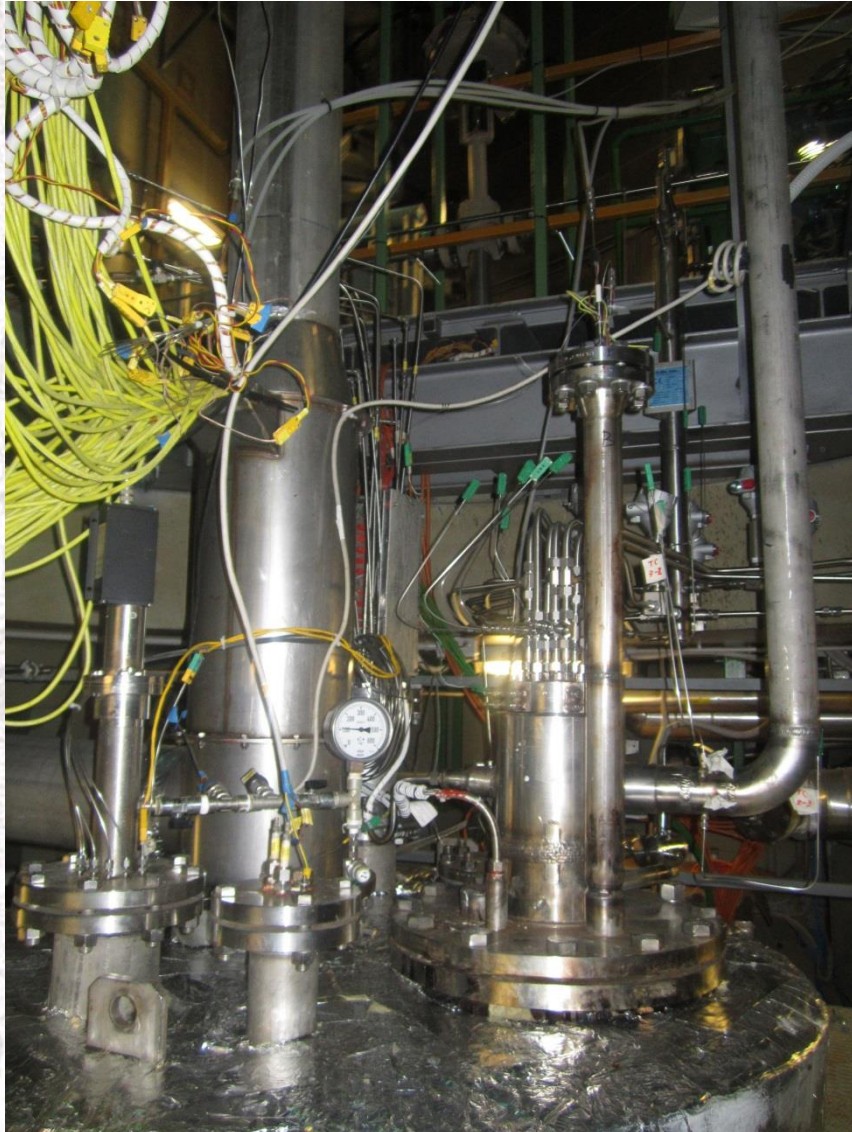




V1 isolation valve  
V2 bypass valve  
V3 regulation valve

CIRCE cover

Isolation valve V1  
Manifold  
7 turbin flow meter

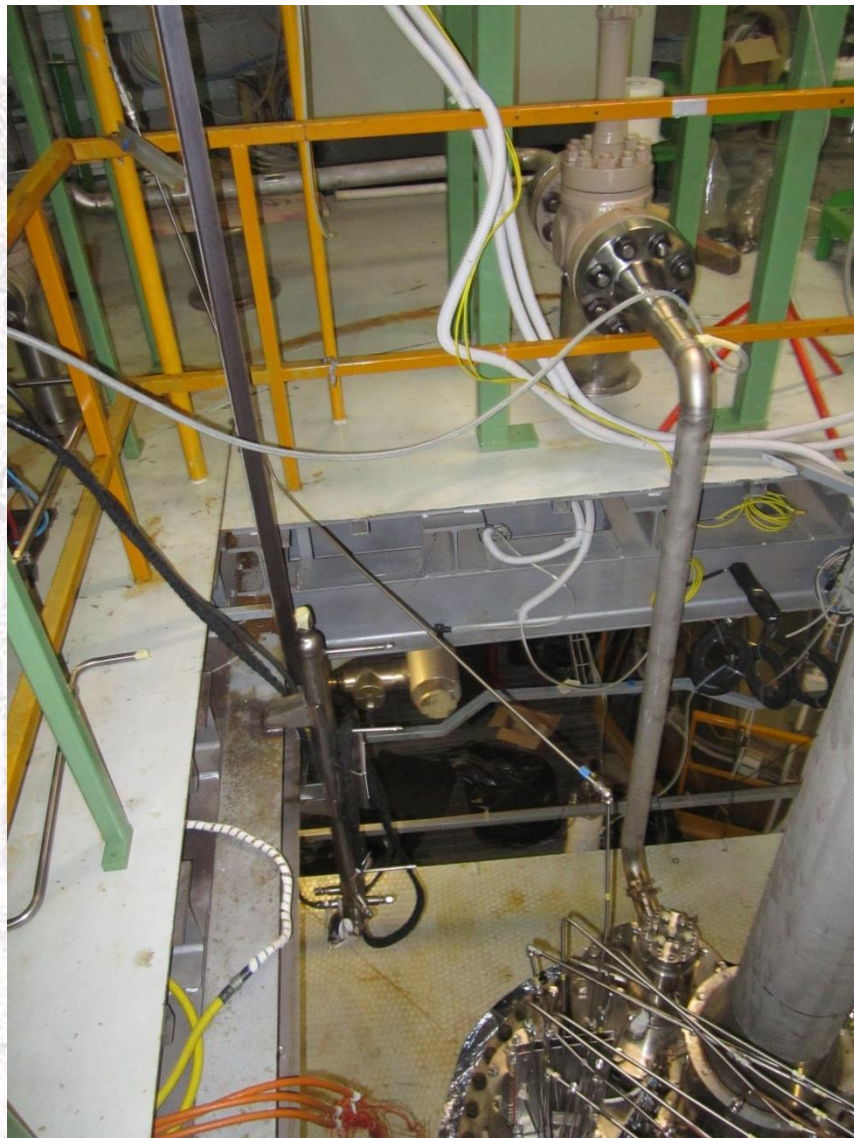


2 O<sub>2</sub> sensors

5 PTs

1 laser level measurement

# CIRCE-HERO 2<sup>ary</sup> side components



Software interface for the CIRCE-HERO DACS system. The interface includes a menu bar (File, Edit, Operate, Tools, Window, Help), a toolbar with icons for Description, Operations, Visualization, Communication, and File & Extra, and a main menu with tabs for Configurazione, Tracc. Elettrico, Sez. Prova HERO, Water, Tube 0, SG, FPS, AC/DC, PID, Stratification, ARGON, Carico/Scarico + Fughe, Real Trend, and Historian.

**MX100 Section:**

- 60 mm upstream the upper spacer grid
- Temperature sensors: T-FPS-24 (295), T-FPS-23 (295), T-FPS-22 (295), T-FPS-21 (295), T-FPS-20 (295), T-FPS-16 (295), T-FPS-18 (294), T-FPS-19 (295)
- MX100 STATUS: MX100 On-Line

**Protezioni di impianto (Plant Protections):**

- Bassa Portata Pb: Escase, DVen Raw < 100mBar
- Alta temp Code: Attiva, T-CL-1---7 > 180°
- Alta temp PIN: Attivo, T-FPS-16---22 > 600°

**Graphs:**

- Portata LBE(g/sec) vs Time (841650 to 842200): Shows a fluctuating signal around 4.4 g/sec (M(LBE,HS)).
- Temperature °C vs Time (840966 to 841989): Shows a stable temperature around 300°C.

**Bubble Tubes Section:**

- Pressure sensors: PE007 (266 mBar), PE005 (103 mBar), PE004 (3844 mBar), PE003 (4122 mBar), DP-Grid (241 mBar), DP-Ven (1 mBar), DP-Ven Raw (44 mBar), PE007-BT (278 mBar)
- DP-Lev: -6 mBar

**S100 Section:**

- Temperature sensors: SO2a (291 °C), SO2b (98 °C)
- Flow: Flussaggio (100 Set, 101 TImax Code, 20 Out %)
- Setpoint: 0.00 NI/s
- Temperature sensors: T-CL-7 (63), T-TS-07 (209), T-RT-01 (294), T-RT-02 (295), T-RT-03 (294), T-RB-04 (293), T-RB-05 (294), T-RB-06 (294), T-FPS-37 (293), T-FPS-38 (294), T-FPS-39 (294), T-FPS-34 (294), T-FPS-35 (294), T-FPS-36 (294), T-FPS-31 (294), T-FPS-32 (294), T-FPS-33 (294), T-CL-1 (101), T-CL-2 (89), T-CL-3 (92), T-CL-4 (66), T-CL-5 (69), T-CL-6 (67)
- Other sensors: RFB2, RFB1, LE001, LE002
- Temperature: Tpin (294) - Temperatura superficiale calcolata

**System Diagrams:**

- Left: Vertical cross-section of the bubble tubes assembly with various pressure and differential pressure sensors.
- Right: Detailed view of the S100 vessel showing internal components, flow paths, and temperature measurement points.

**Windows Taskbar:** Shows the system clock at 10:51 on 14/06.



# CIRCE-HERO DACS

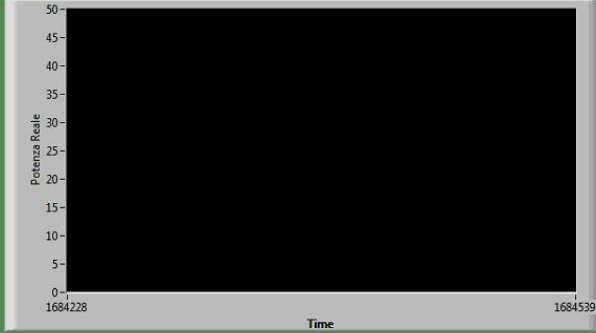


Licenza gratuita (solo per uso non commerciale)

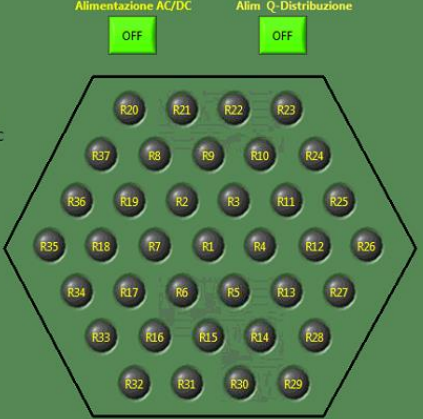
File Edit Operate Tools Window Help

Descrizione Operazioni Visualizza Comunica File & Extra

Configurazione Tracc. Elettrico Sez. Prova HERO Water Tube 0 SG FPS AC/DC PID Stratification ARGON Carico/Scarico + Fughe Real Trend Historiarmi



Apertura resistenze Spegnimento AC/DC



ACDC timing Fast Slow

Kw Richiesti: 0

Current Time: 14/06/2018 10:55:46

STOP RAMPA

1 Livello 2 Livelli Manuale

START

Setpoint Potenza (KW)

Pendenza Rampa (KW/sec)

R barretta 3.9 ohm

Comando AC/DC

P Barretta

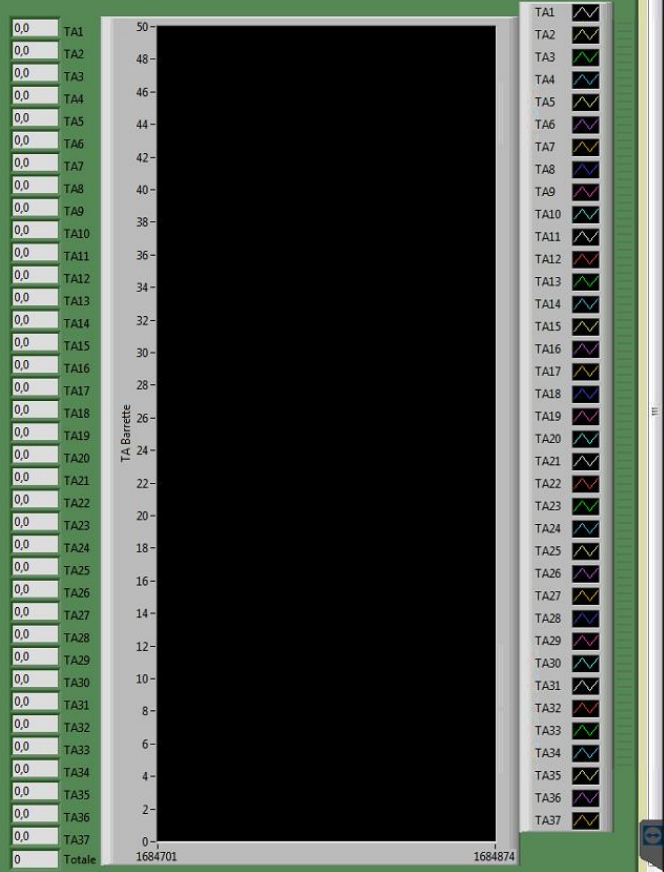
Tolleranza I

Inominale

min

- Q Distribuzione
- AC/DC on
- Allarme T ac/dc
- Allarme Fuse ac/dc

|       |       |       |                       |
|-------|-------|-------|-----------------------|
| RS 1  | RS 11 | RS 21 | RS 31                 |
| Reset | Reset | Reset | Reset                 |
| RS 2  | RS 12 | RS 22 | RS 32                 |
| Reset | Reset | Reset | Reset                 |
| RS 3  | RS 13 | RS 23 | RS 33                 |
| Reset | Reset | Reset | Reset                 |
| RS 4  | RS 14 | RS 24 | RS 34                 |
| Reset | Reset | Reset | Reset                 |
| RS 5  | RS 15 | RS 25 | RS 35                 |
| Reset | Reset | Reset | Reset                 |
| RS 6  | RS 16 | RS 26 | RS 36                 |
| Reset | Reset | Reset | Reset                 |
| RS 7  | RS 17 | RS 27 | RS 37                 |
| Reset | Reset | Reset | Reset                 |
| RS 8  | RS 18 | RS 28 |                       |
| Reset | Reset | Reset |                       |
| RS 9  | RS 19 | RS 29 |                       |
| Reset | Reset | Reset |                       |
| RS 10 | RS 20 | RS 30 |                       |
| Reset | Reset | Reset |                       |
|       |       |       | Inserzione Resistenze |
|       |       |       | Non Inserite          |

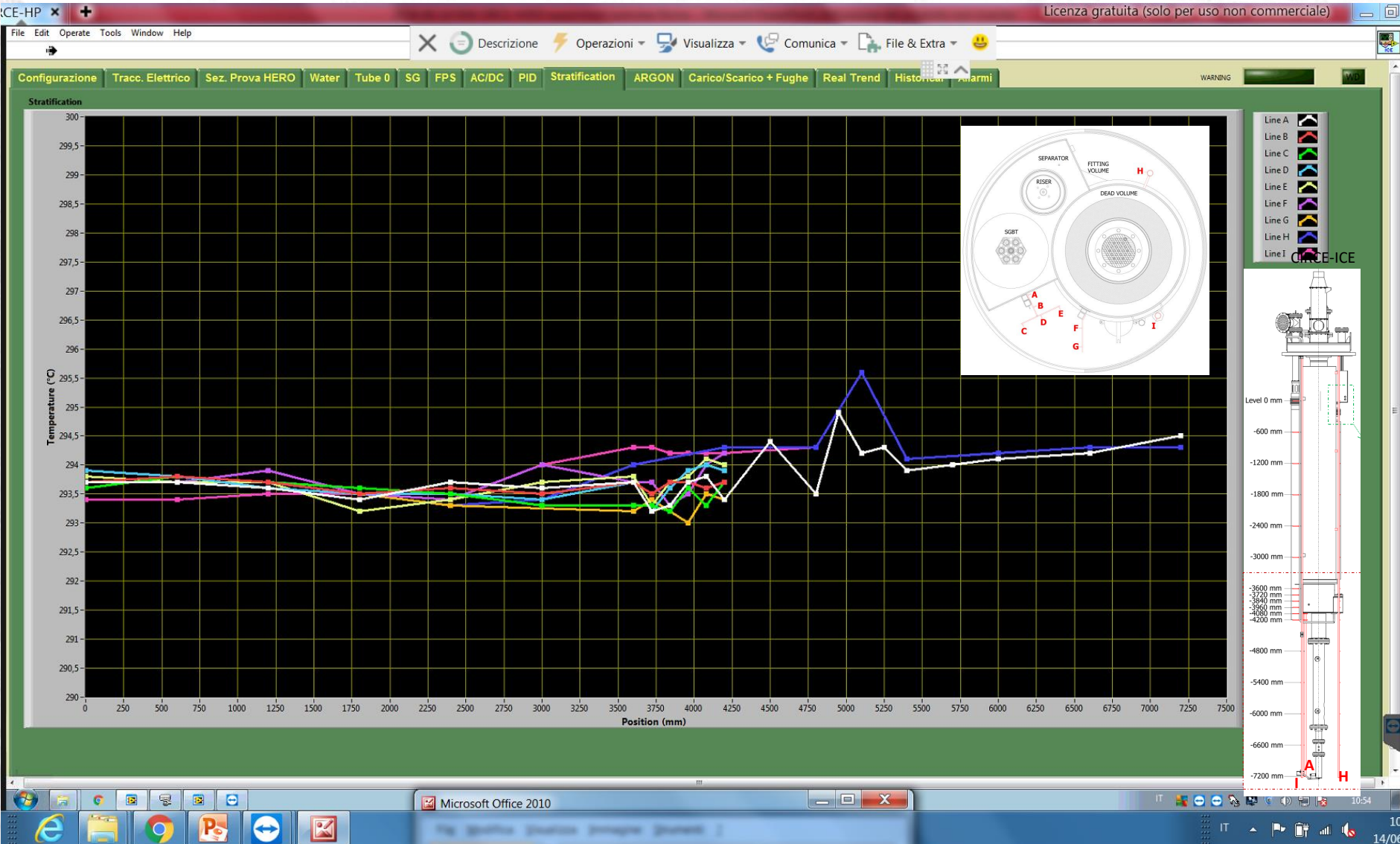


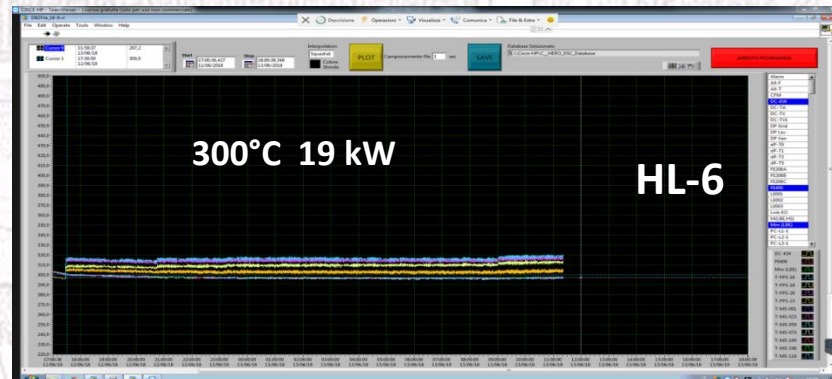
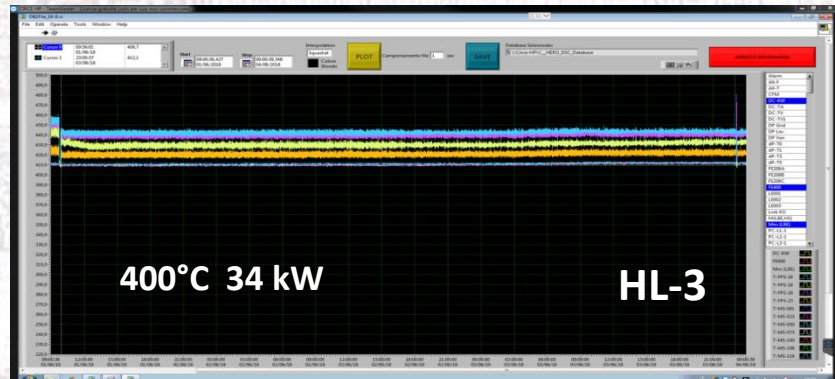
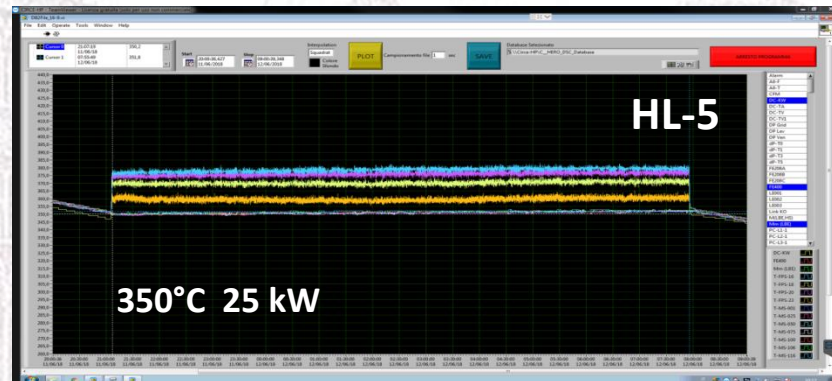
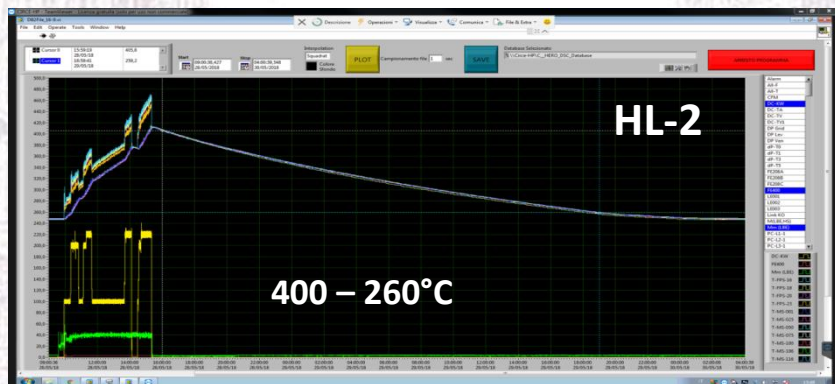
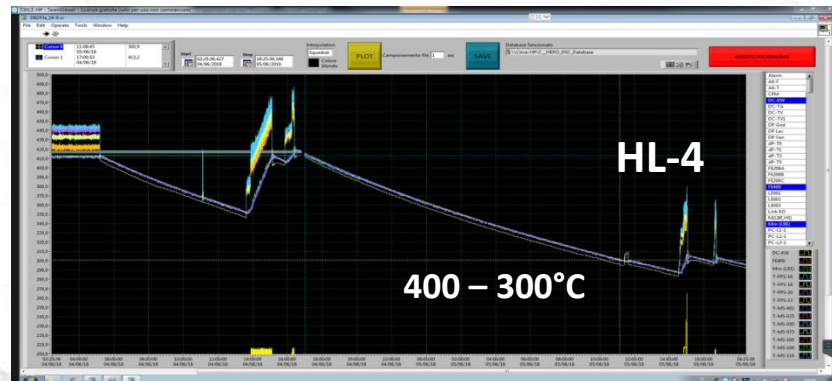
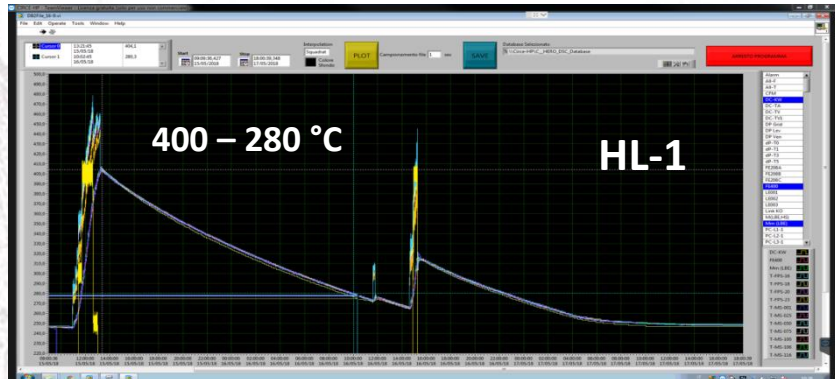






# CIRCE-HERO DACS







# CIRCE-HERO test matrix



- ❑ Steady state condition: H<sub>2</sub>O subcooled inlet @ 335°C – superheated steam outlet @ 400°C, 180 bar, 0.33 kg/s ; LBE @ 400÷480°C, 40 kg/s
  
- ❑ Transient test 1 PLOFA:
  - P) FPS power decreases by decay heat curve
  - LOFA) gas lift @ 0 in 10 sec
  - Feedwater kg/s at 10% after 10 sec (**DHR**)
  
- ❑ Transient test 2 PLOFA:
  - P) FPS power decreases by decay heat curve
  - LOFA) gas lift @ 0 in 10 sec
  - Feedwater kg/s at 0% after 10 sec (**without DHR**)
  
- ❑ Transient test 3 PLOFA:
  - P) FPS power decreases by decay heat curve
  - LOFA) gas lift decreases by table (**pump flywheel**)
  - Feedwater kg/s at 10% after 10 sec (**DHR**)



## Conclusive remarks



- A new HX with **7 double wall bayonet** tubes 1:1 scale of ALFRED SG tube was designed, assembled and implemented in **HERO TS** and **CIRCE** facility at ENEA CR Brasimone
- **Primary system** of the facility is completely assembled, the secondary side is almost completed (instrumentation and DACS)
- **Heat-losses** tests carried out
- Experimental campaign (**3 tests**) for SGBT characterization both in steady-state and transient conditions (enhanced to natural circulation) by next September



## Conclusive remarks



**THANK YOU  
FOR  
YOUR ATTENTION**

*Alessio Pesetti*

*[alessio.pesetti@for.unipi.it](mailto:alessio.pesetti@for.unipi.it)*

University of Pisa

Largo Lucio Lazzarino 2

56122 Pisa



SAPIENZA  
UNIVERSITÀ DI ROMA



Agenzia nazionale per le nuove tecnologie,  
l'energia e lo sviluppo economico sostenibile

# HERO NUMERICAL CHARACTERIZATION BY STH CODE

Pierdomenico Lorusso

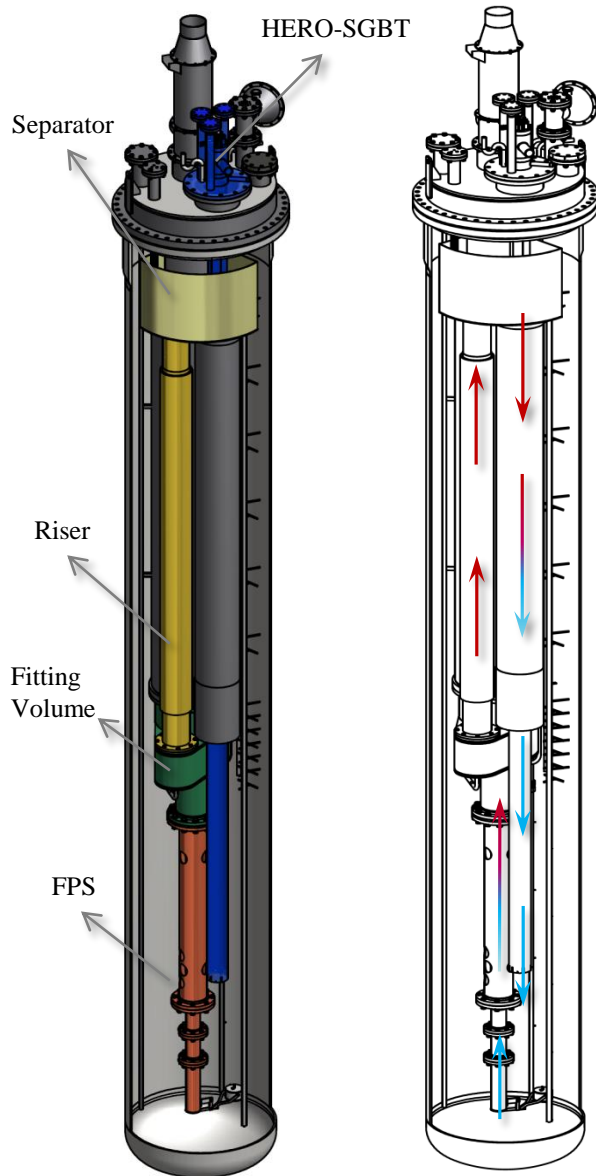
GENERATION IV LEAD COOLED FAST REACTOR  
STATO ATTUALE DELLA TECNOLOGIA E PROSPETTIVE DI SVILUPPO  
WORKSHOP TEMATICO ACCORDO DI PROGRAMMA MISE – ENEA  
PAR2017 – PROGETTO B.3 LP2  
*Università di Roma “La Sapienza”*  
14-15 Giugno 2018

# OUTLINE

- CIRCE-HERO Overview
- CIRCE-HERO Model
- Start-Up Procedure
- HERO Pre-Test Analysis
- Final Remarks



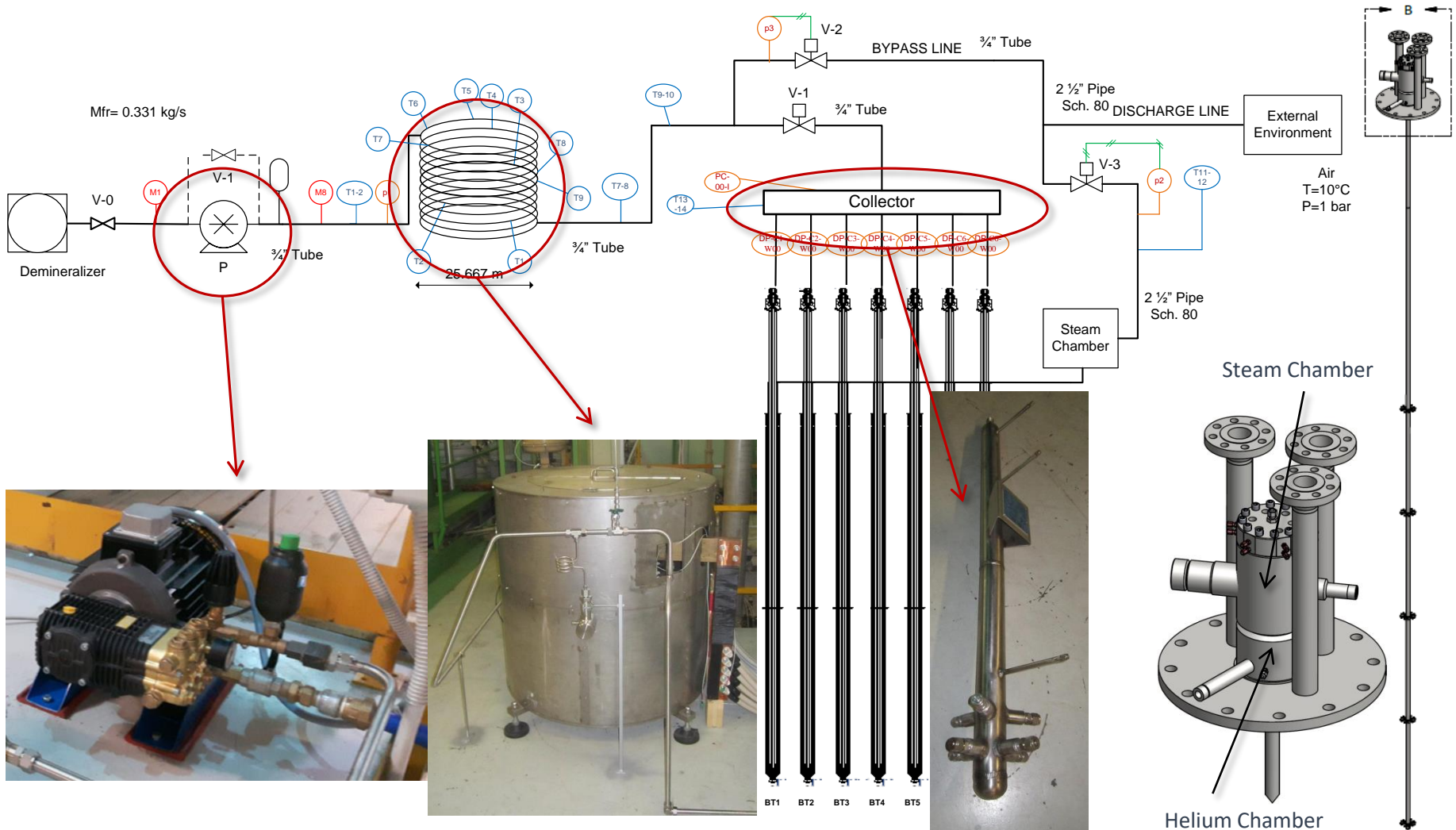
# CIRCE-HERO OVERVIEW



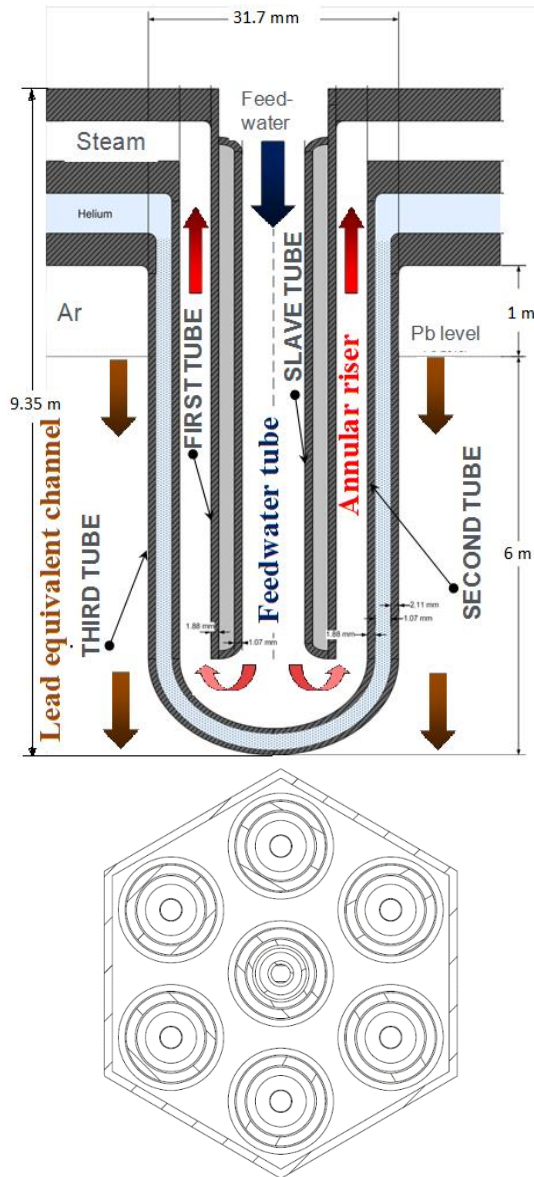
| CIRCE Parameters        | Value     | CIRCE Parameters               | Value       |
|-------------------------|-----------|--------------------------------|-------------|
| Outside diameter [mm]   | 1200      | Temperature Range [° C]        | 200 to 500  |
| Wall thickness [mm]     | 15        | Operating Pressure [kPa]       | 15 (gauge)  |
| Material                | AISI 316L | Design Pressure [kPa]          | 450 (gauge) |
| Max LBE Inventory [kg]  | 90000     | Argon Flow Rate [NI/s]         | 15          |
| Electrical Heating [kW] | 47        | Argon Injection Pressure [kPa] | 600 (gauge) |

# CIRCE-HERO OVERVIEW

The secondary loop is an once through loop fed by demineralized water. In working conditions the water is pressurized at 172 bar ( $T_{sat}$  353.25° C) at the SGBT outlet and preheated at 335° C at the inlet of the SGBT unit.



# CIRCE-HERO OVERVIEW

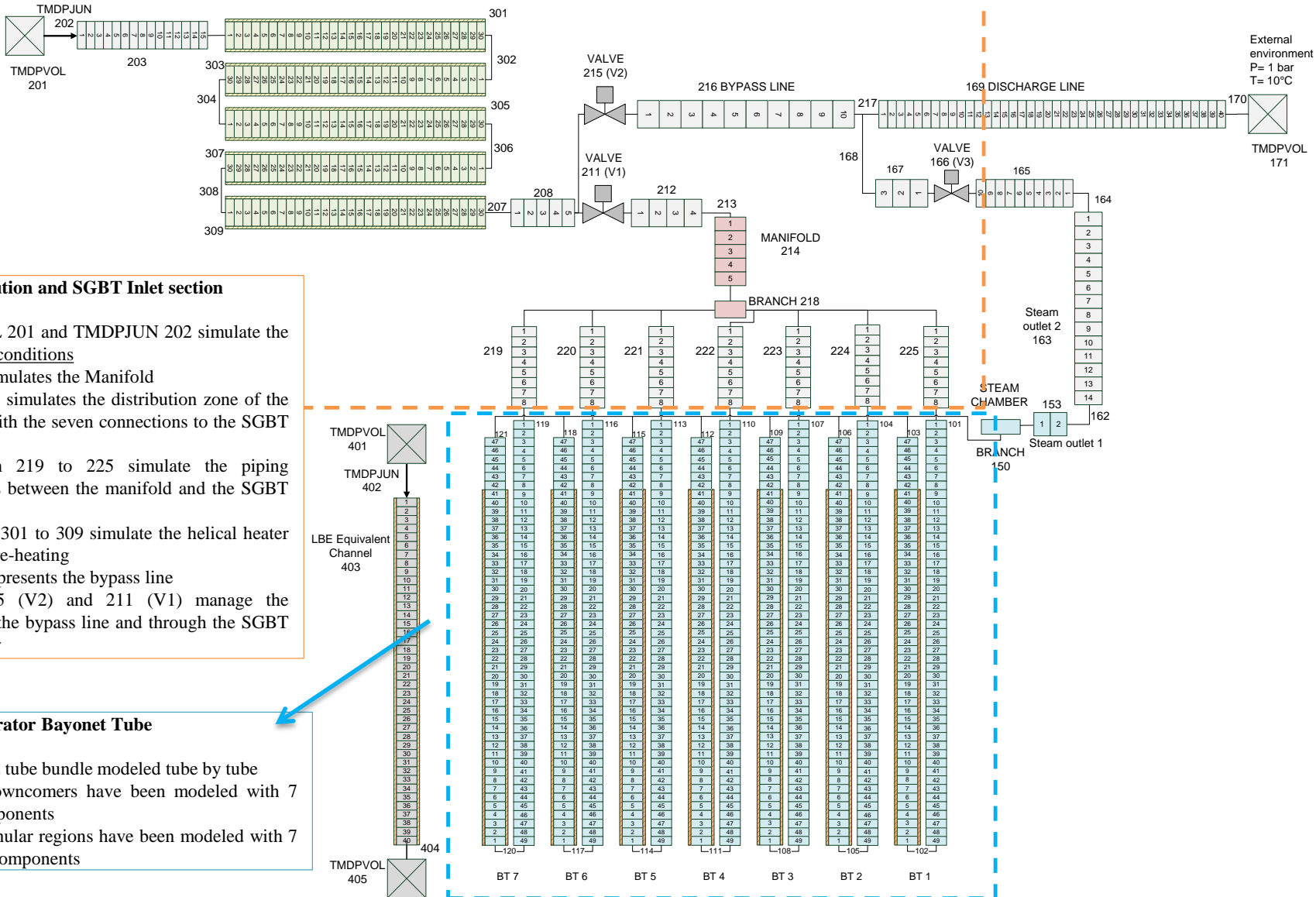


| Label                 | Inner diameter [mm] | Outer diameter [mm] | Thickness [mm] | Material --     |
|-----------------------|---------------------|---------------------|----------------|-----------------|
| Feed-water slave tube | 7.09                | 9.53                | 1.22           | AISI-304        |
| Feed-water tube gap   | 9.53                | 15.75               | 3.11           | Slight vacuum   |
| Feed-water outer tube | 15.75               | 19.05               | 1.65           | AISI-304        |
| Annular riser gap     | 19.05               | 21.18               | 1.07           | Water-steam     |
| Second tube           | 21.18               | 25.40               | 2.11           | AISI-304        |
| Annular gap           | 25.40               | 26.64               | 0.62           | AISI 316 powder |
| Third tube            | 26.64               | 33.40               | 3.38           | AISI-304        |

| Description           | Unit | Water-Steam side             | He side               | LBE side        |
|-----------------------|------|------------------------------|-----------------------|-----------------|
| Fluid                 | --   | Water – steam                | Helium                | LBE             |
| Circulation mechanism | --   | Axial pump + accumulator     | leakage accommodation | Gas enhanced    |
| Main components       | --   | bayonet tubes, steam chamber | Helium chamber        | SGBT unit shell |
| Bundle type and P/D   | -    | Triangular / 1.42            | --                    | Shell           |
| Inlet temp.           | ° C  | 335                          | --                    | 480             |
| Mass flow             | kg/s | 0.330785                     | stagnant              | 44.573529       |
| Design pressure       | bar  | 180                          | 5.0                   | As CIRCE        |
| Operating pressure    | bar  | 172                          | 4.5                   | Hydraulic head  |
| Design temp.          | ° C  | 432                          | 432                   | As CIRCE        |

# CIRCE-HERO MODEL

# RELAP5-3D<sup>®</sup> Model



## Water distribution and SGBT Inlet section

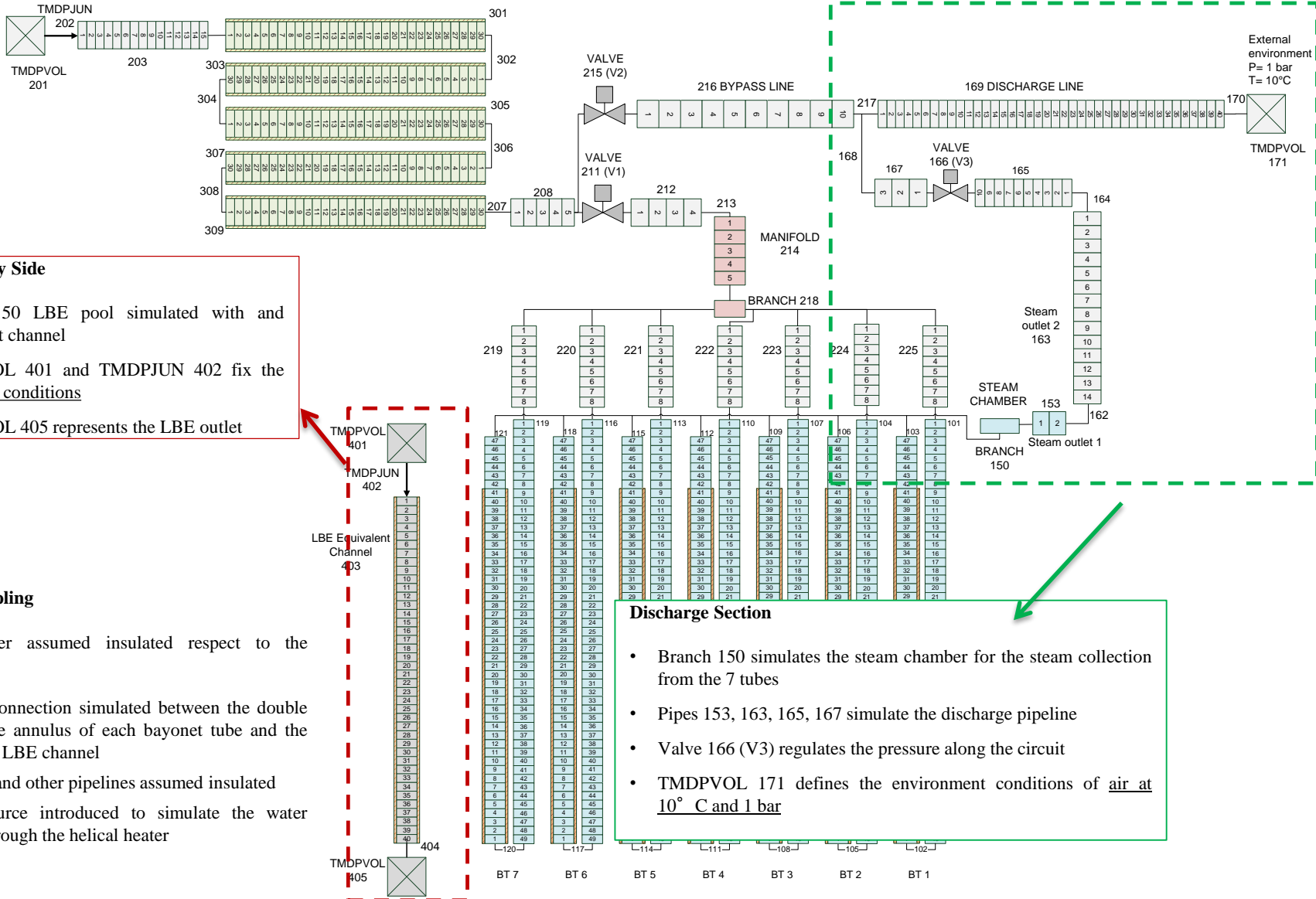
- TMDPVOL 201 and TMDPJUN 202 simulate the water inlet conditions
- Pipe 214 simulates the Manifold
- Branch 218 simulates the distribution zone of the manifold with the seven connections to the SGBT tubes
- Pipes from 219 to 225 simulate the piping connections between the manifold and the SGBT tubes
- Pipes from 301 to 309 simulate the helical heater for water pre-heating
- Pipe 216 represents the bypass line
- Valves 215 (V2) and 211 (V1) manage the passage in the bypass line and through the SGBT respectively

## Steam Generator Bayonet Tube

- 7 bayonet tube bundle modeled tube by tube
- The 7 downcomers have been modeled with 7 pipe components
- The 7 annular regions have been modeled with 7 annulus components

# CIRCE-HERO MODEL

# RELAP5-3D<sup>®</sup> Model



- LBE Primary Side**
- Branch 150 LBE pool simulated with and equivalent channel
  - TMDPVOL 401 and TMDPJUN 402 fix the LBE inlet conditions
  - TMDPVOL 405 represents the LBE outlet

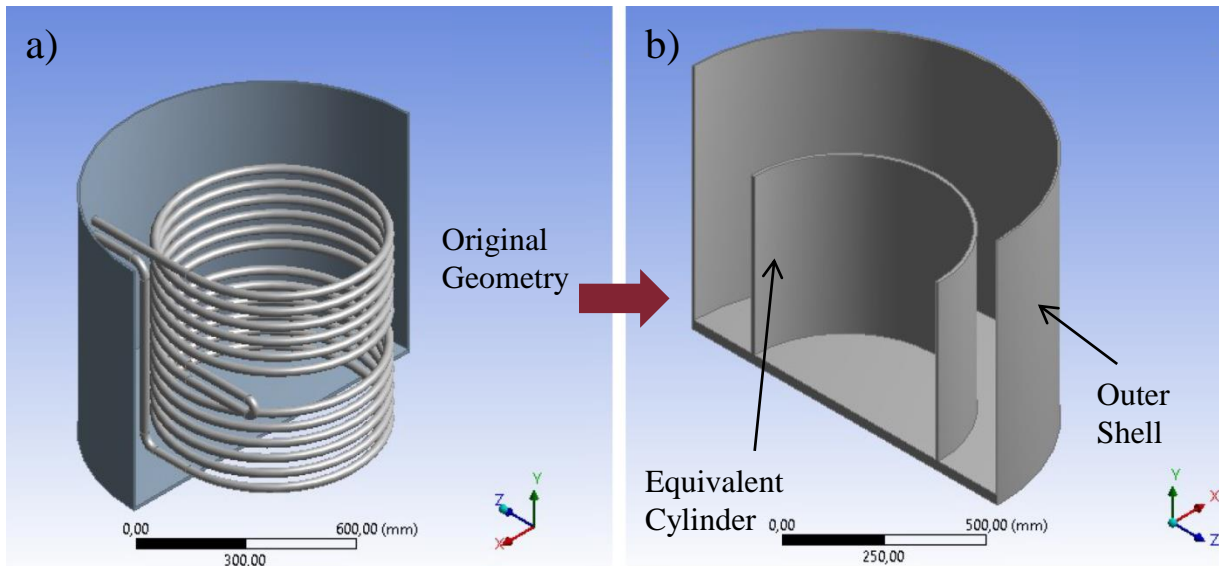
- Thermal coupling**
- Downcomer assumed insulated respect to the annulus
  - Thermal connection simulated between the double wall of the annulus of each bayonet tube and the equivalent LBE channel
  - Manifold and other pipelines assumed insulated
  - Power source introduced to simulate the water heating through the helical heater

- Discharge Section**
- Branch 150 simulates the steam chamber for the steam collection from the 7 tubes
  - Pipes 153, 163, 165, 167 simulate the discharge pipeline
  - Valve 166 (V3) regulates the pressure along the circuit
  - TMDPVOL 171 defines the environment conditions of air at 10° C and 1 bar

# CIRCE-HERO MODEL

## Pre-Heater Simulations

Analytical model with a simplified geometry for the evaluation of the heat transfer coefficient and the air temperature, coupled with RELAP5-3D simulations for an iterative calculation.



### Boundary Conditions

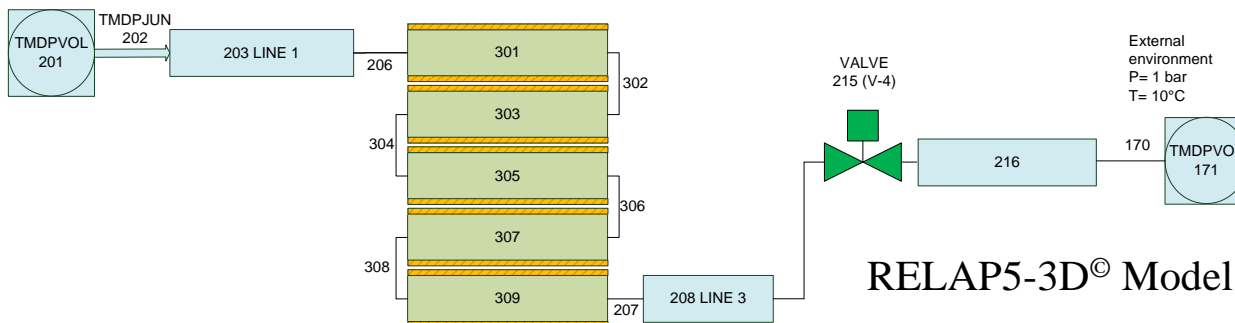
- Pressure: 180 bar
- $T_{\text{inlet h2o}}$ : 15° C
- H<sub>2</sub>O mfr: 0.331 kg/s

### Initial conditions

- $T_{\text{wall}}$ : 300° C
- $T_{\text{air}}$ : 20° C
- $\text{HTC}_{\text{ext, air}}$ : 7 W/(m<sup>2</sup>K)

### Outcomes

- ✓ Air Temperature inside the Shell
- ✓ Power Distribution  $f(R(T))$
- ✓ Wall Temperature

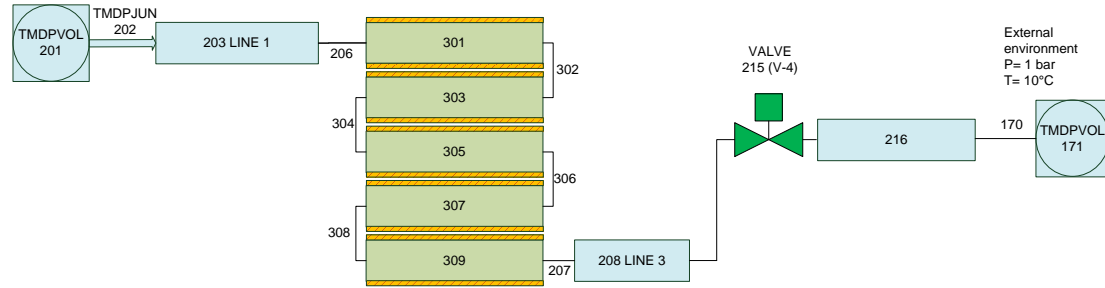


RELAP5-3D<sup>®</sup> Model

# CIRCE-HERO MODEL

## Pre-Heater Simulations

Analytical model with a simplified geometry for the evaluation of the heat transfer coefficient and the air temperature, coupled with RELAP5-3D simulations for an iterative calculation



$$Nu = \frac{hL_c}{k} = C(Gr_L Pr)^n = CRa_L^n$$

$$\overline{Nu}_{FP} = \left\{ 0.825 + \frac{0.387Ra_L^{\frac{1}{6}}}{\left[1 + (0.492/Pr)^{\frac{9}{16}}\right]^{\frac{8}{27}}} \right\}^2$$

**Boundary Conditions**

- Pressure: 180 bar
- T inlet h2o: 15° C
- H2o mfr: 0.331 kg/s

$$\frac{\overline{Nu}}{\overline{Nu}_{FP}} = 1 + B \left[ 32^{0.5} Gr_L^{-0.25} \left( \frac{L}{D} \right) \right]^C$$

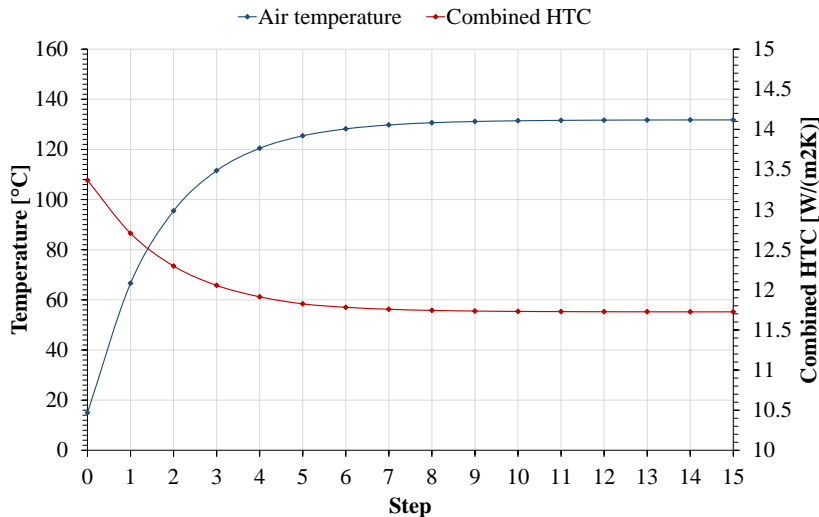
*Churchill and Chu- Cebeci correlation for cylinder*

### Initial conditions

- T<sub>wall</sub>: 300° C
- T<sub>air</sub>: 20° C
- HTC<sub>ext, air</sub>: 7 W/(m²K)

### Outcomes

- ✓ Air Temperature inside the Shell
- ✓ Power Distribution  $f(R(T))$
- ✓ Wall Temperature



| RUN #1 |            |                            |                             |                            |
|--------|------------|----------------------------|-----------------------------|----------------------------|
| Test   | Power [kW] | T <sub>out</sub> h2o [° C] | T <sub>max</sub> wall [° C] | T <sub>av</sub> wall [° C] |
| 1      | 485        | 334.55                     | 360.85                      | 216.94                     |
| 2      | 487.5      | 335.6                      | 361.97                      | 217.64                     |
| 3      | 490        | 336.65                     | 363.12                      | 218.36                     |
| 4      | 492.5      | 337.72                     | 364.25                      | 219.10                     |
| RUN #2 |            |                            |                             |                            |
| Test   | Power [kW] | T <sub>out</sub> h2o [° C] | T <sub>max</sub> wall [° C] | T <sub>av</sub> wall [° C] |
| 1      | 485        | 334.1                      | 360.15                      | 216.42                     |
| 2      | 487.5      | 335.4                      | 361.65                      | 217.315                    |
| 3      | 490        | 336.3                      | 362.81                      | 218.035                    |
| 4      | 492.5      | 337.36                     | 363.98                      | 218.77                     |
| RUN #3 |            |                            |                             |                            |
| Test   | Power [kW] | T <sub>out</sub> h2o [° C] | T <sub>max</sub> wall [° C] | T <sub>av</sub> wall [° C] |
| 1      | 485        | 334.1                      | 360.15                      | 216.4                      |
| 2      | 487.5      | 335.35                     | 361.64                      | 217.31                     |
| 3      | 490        | 336.27                     | 362.8                       | 218.03                     |
| 4      | 492.5      | 337.35                     | 363.95                      | 218.75                     |

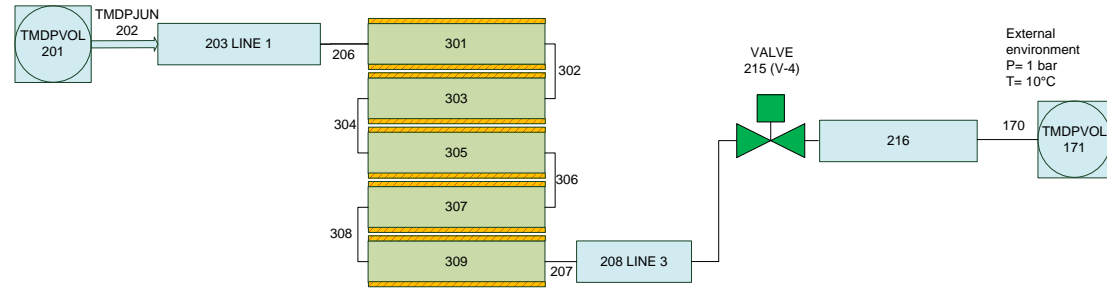
# CIRCE-HERO MODEL

## Pre-Heater Simulations

The thermal power produced by the Joule effect depends on the electrical resistivity, which is a function of the temperature. As the temperature changes along the pipe length, the resistivity changes too and, in consequence the power distribution is not uniform.

$$R(T) = \frac{\rho(T)l}{A} \quad \rho(T) = \rho_{20^{\circ}C} [1 + \alpha(T)(T - 20)]$$

$$\alpha(T) = \alpha_{20^{\circ}C} / [1 + T\alpha_{20^{\circ}C}]$$



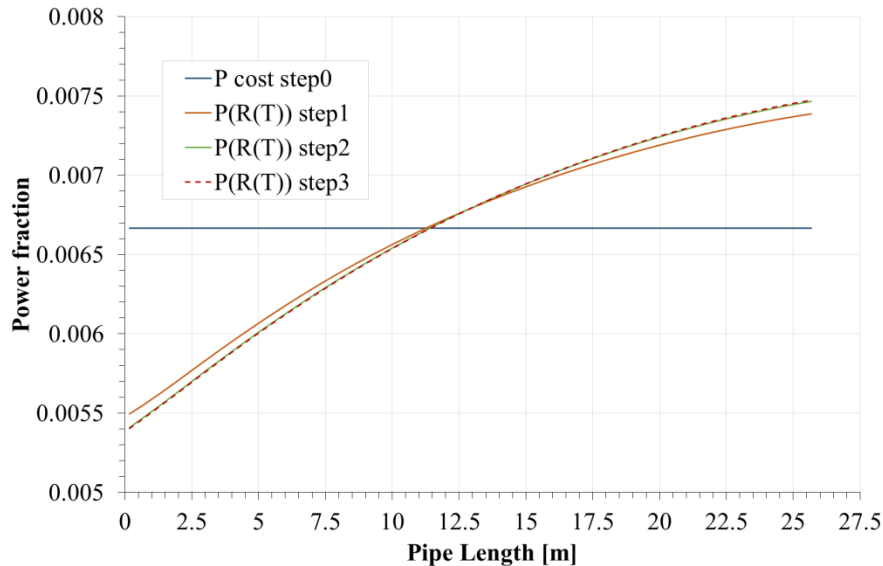
### Boundary Conditions

- Pressure: 180 bar
- T inlet h2o: 15° C
- H2o mfr: 0.331 kg/s

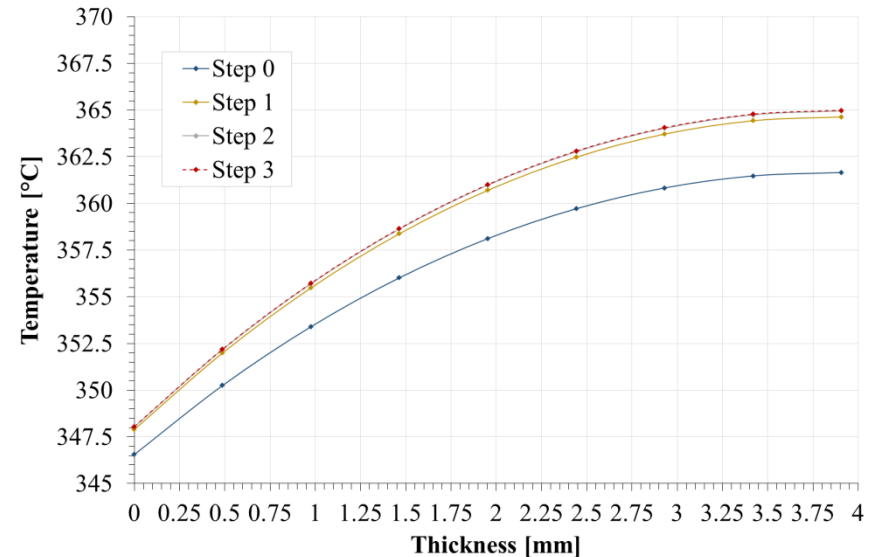
### Outcomes

- ✓ Air Temperature inside the Shell
- ✓ Power Distribution  $f(R(T))$
- ✓ Wall Temperature

**Power distribution**

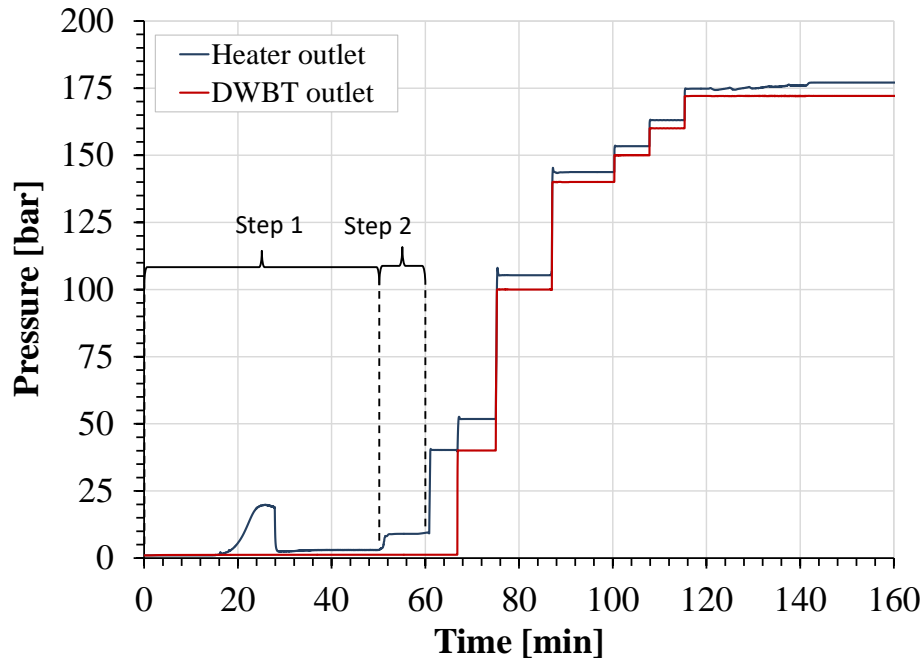


**Wall Temperature at Pre-heater outlet**





# CIRCE-HERO START-UP



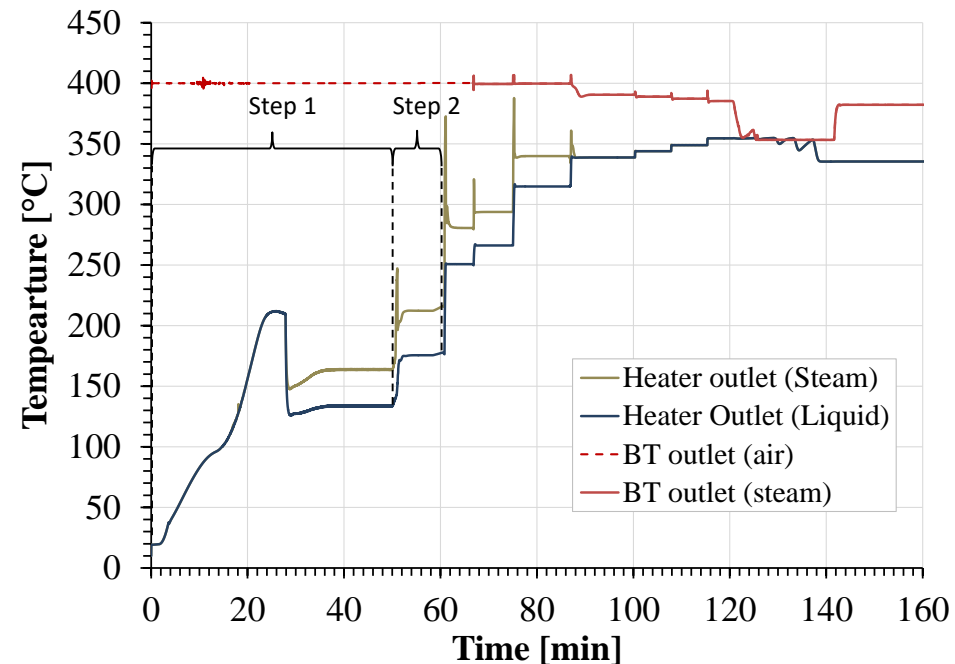
*Pressure peak up to ~20 bar due to the water vaporization along the heater, followed by a fast decrease when the steam produced reaches the discharge section*

## Step 2

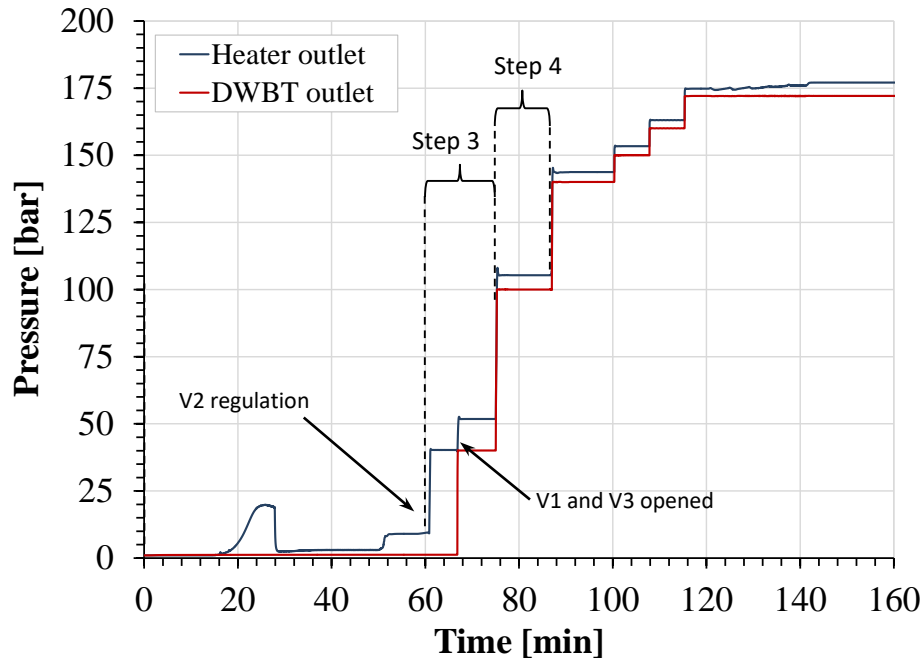
- The water mass flow rate is increased passing from  $\dot{m} = (1/10)\dot{m}_{nom}$  to  $\dot{m} = (1/3)\dot{m}_{nom}$ .
- Power is increased up to  $\approx 290$  kW for the complete vaporization.

## Step 1

- Feedwater line and heat exchanger are empty at the pressure of 1 bar, the water mass flow rate is zero and the pre-heater is switched off. The heat exchanger is bypassed by valves V1 and V3, valve V2 is opened.
- Injection of **water mass flow rate  $\dot{m} = 1/10$  of  $\dot{m}_{nom}$**  at  $10^\circ\text{C}$  and 1 bar.
- The pre-heater is switched on supplying a thermal power of  $\approx 90$  kW for the water vaporization.



# CIRCE-HERO START-UP



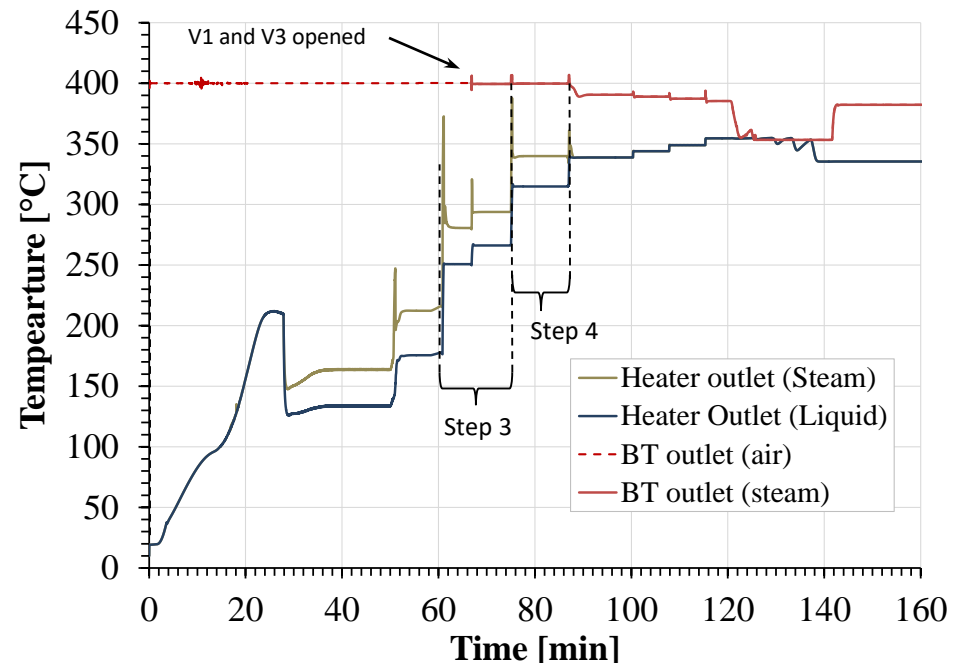
The steam injected at  $\sim 270^\circ\text{C}$  assures a low heat transfer coefficient, a very low fraction of thermal power removed from the LBE pool and a small difference in temperature between the double wall of the bayonet tubes.

## Step 4

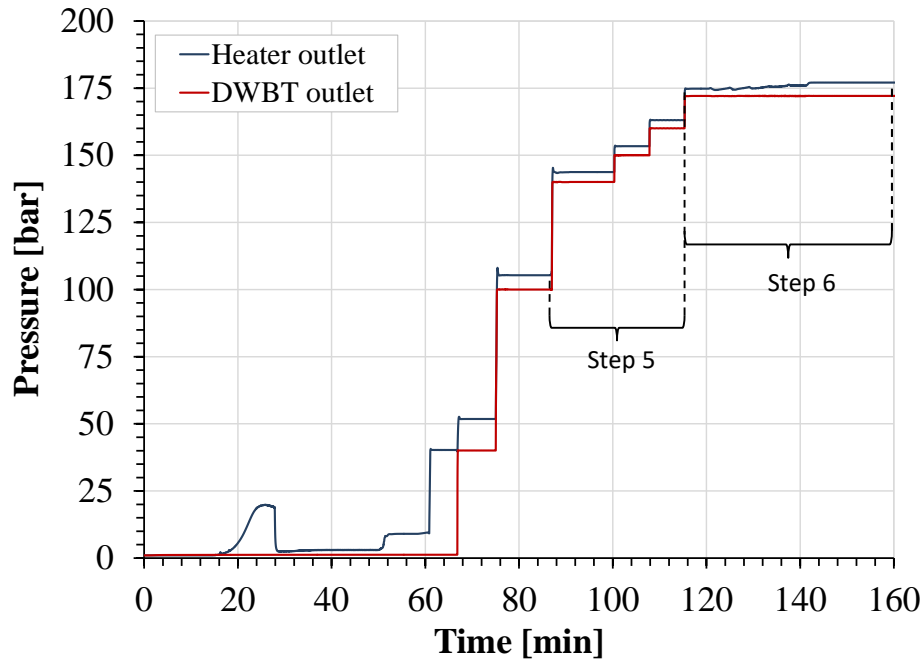
- The pressure is increased from 40 bar to 100 bar.
- At the end of the step 4, the water mass flow rate is increased from  $1/3$  of  $\dot{m}_{\text{nom}}$  to  $1/2$  of  $\dot{m}_{\text{nom}}$
- At the end of the step 4, the power passes from 311 kW to 335 kW.
- Production of mixture liquid/steam (mass fraction  $\approx 0.5$ )

## Step 3

- Valve V2 is regulated in order to **pressurize the feedwater line up to 40 bar**.
- The power of the pre-heater is increased up to  $\approx 311$  kW for the generation of superheated steam at  $270^\circ\text{C}$  at 40 bar.
- After the achievement of steady state conditions, **the valves V1 and V3 are opened** allowing the passage of the steam in the main pipeline and through the bayonet tubes; **the valve V2 is closed** avoiding the passage of the steam through the bypass. **Valve V3 is regulated in order to pressurize HERO SGBT at 40 bar**.



# CIRCE-HERO START-UP

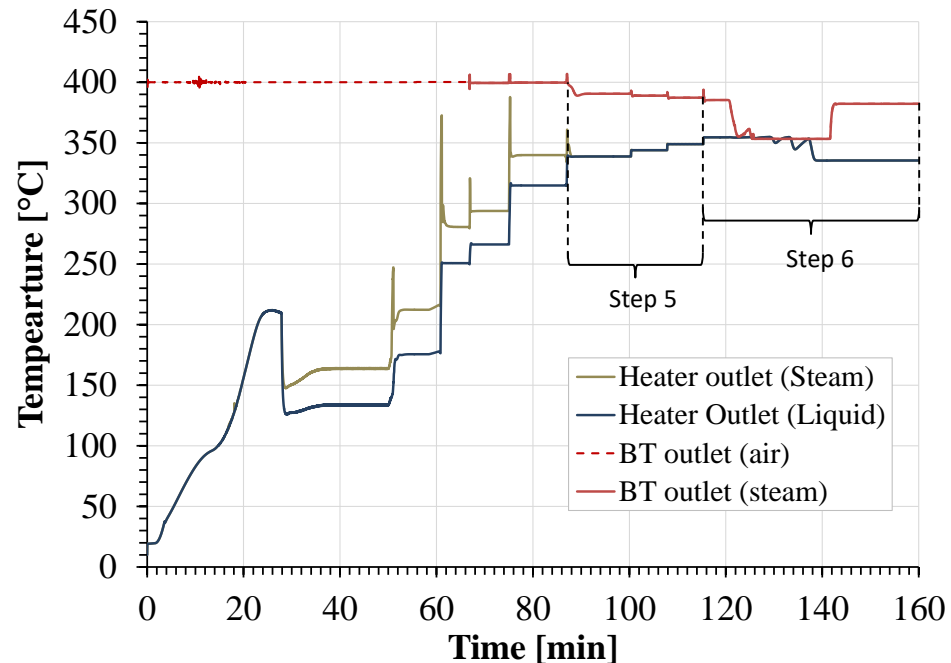


## Step 6

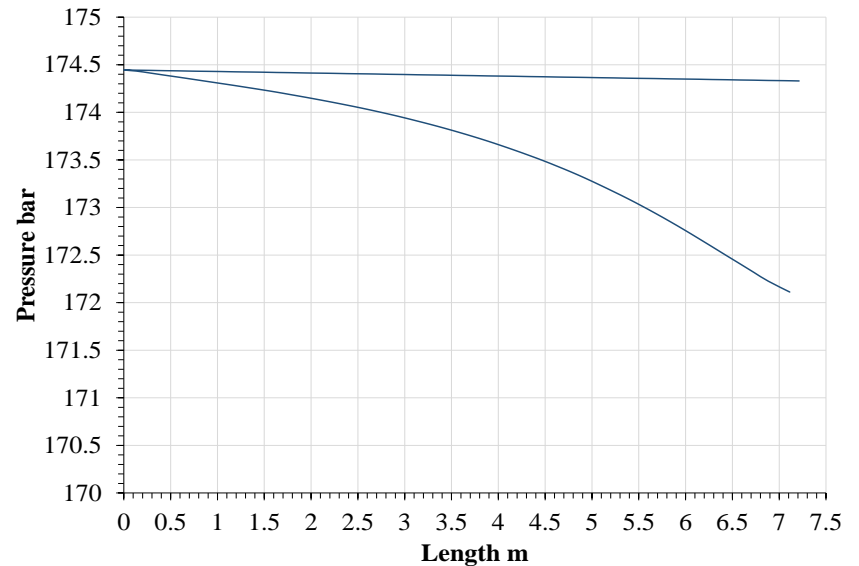
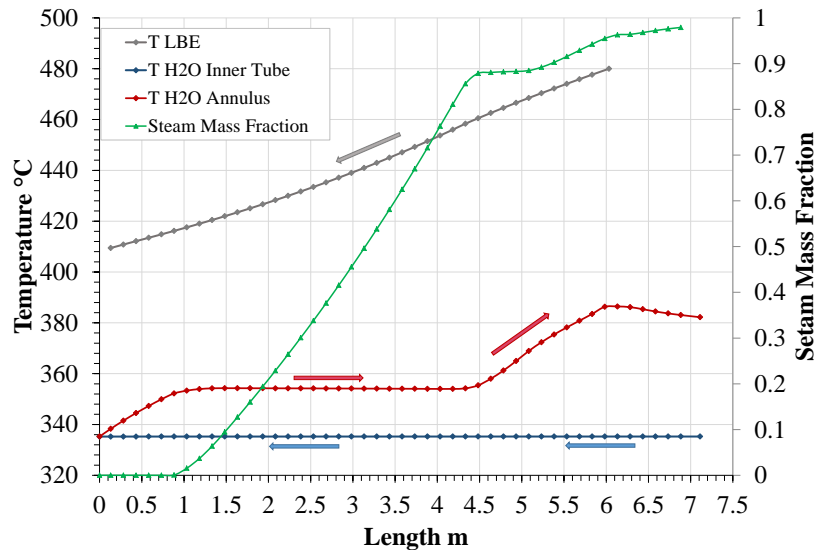
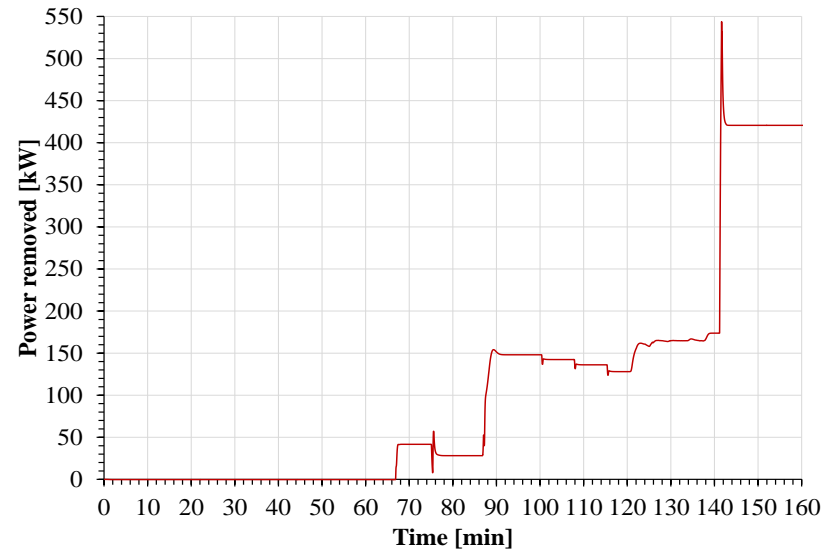
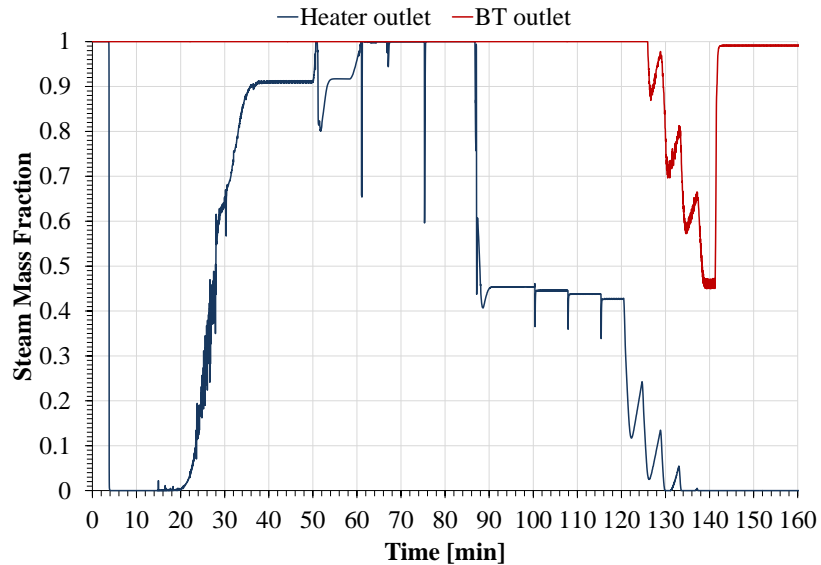
- Growth in several steps of water mass flow rate and pre-heating thermal power up to the working conditions of **0.331 kg/s** and **335° C**.
- At least, temperature growth on LBE side from **400° C** to **480° C**.

## Step 5

- The pipe line is pressurized from **100 bar to 140**, and then to **150, 160 up to 172 bar** after several steps. The other parameters remain constant.

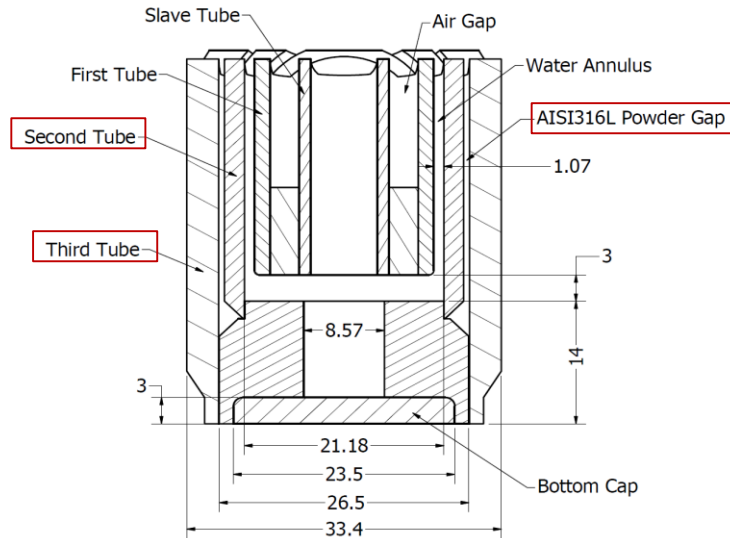


# CIRCE-HERO START-UP

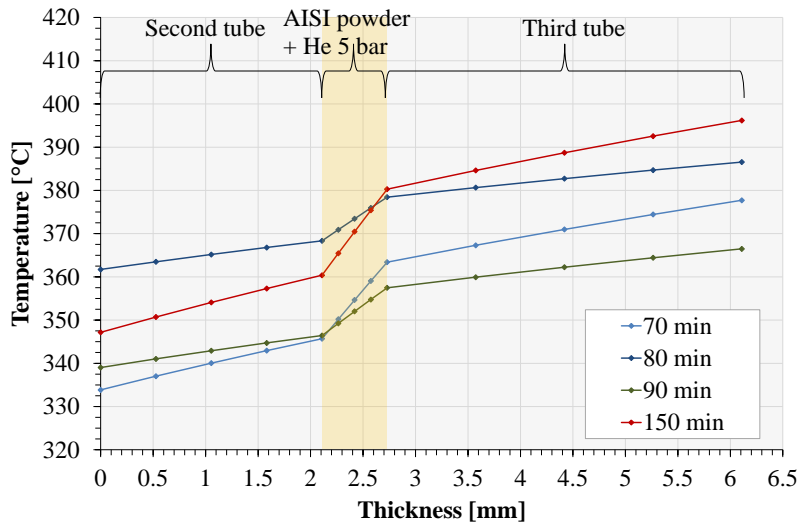


# CIRCE-HERO START-UP

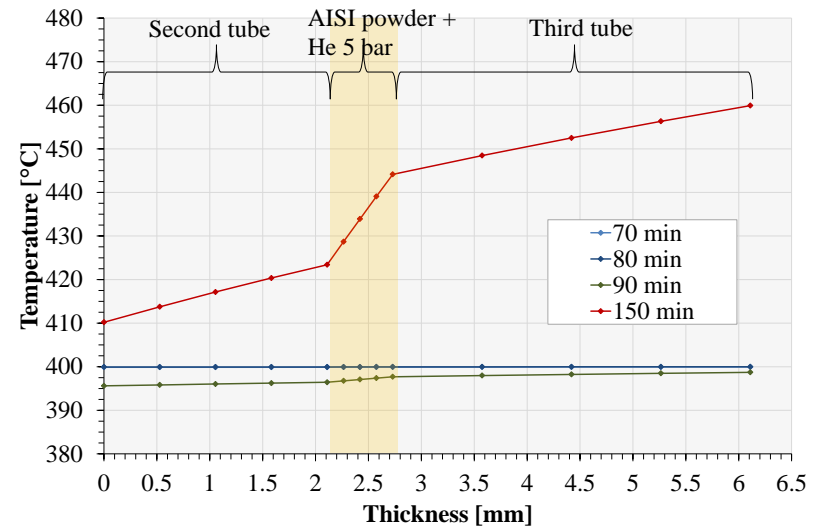
## Temperature Profiles



BT Radial temperature (bottom)



BT Radial temperature (top)



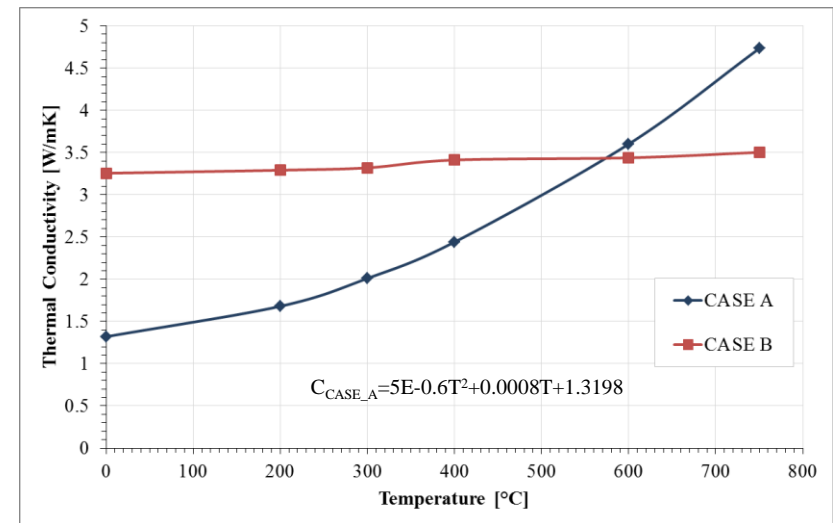
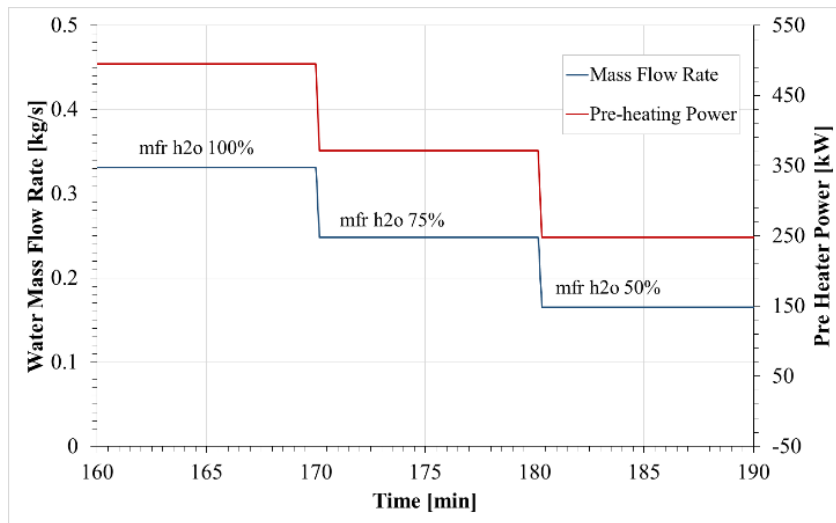
# HERO PRE-TEST ANALYSIS

Preliminary test analysis for the HERO SGBT thermal-hydraulic characterization

| Parameter             | Unit | CASE A      |             |             | CASE B      |             |             |
|-----------------------|------|-------------|-------------|-------------|-------------|-------------|-------------|
| Test #                | -    | RUN #1      | RUN #2      | RUN #3      | RUN #4      | RUN #5      | RUN #6      |
| LBE inlet temperature | ° C  | 480         | 480         | 480         | 480         | 480         | 480         |
| HERO outlet Pressure  | bar  | 172         | 172         | 172         | 172         | 172         | 172         |
| Water SGBT Tin        | ° C  | 335         | 335         | 335         | 335         | 335         | 335         |
| LBE mfr SS1           | kg/s | 37.5 (100%) | 39.2 (100%) | 44.7 (100%) | 37.5 (100%) | 39.2 (100%) | 44.7 (100%) |
| LBE mfr SS2           | kg/s | 28.1 (75%)  | 29.4 (75%)  | 33.5 (75%)  | 28.1 (75%)  | 29.4 (75%)  | 33.5 (75%)  |
| LBE mfr SS3           | kg/s | 18.7 (50%)  | 19.6 (50%)  | 22.3 (50%)  | 18.7 (50%)  | 19.6 (50%)  | 22.3 (50%)  |
| Water mfr SS1         | kg/s | 0.33 (100%) | 0.33 (100%) | 0.33 (100%) | 0.33 (100%) | 0.33 (100%) | 0.33 (100%) |
| Water mfr SS2         | kg/s | 0.25 (75%)  | 0.25 (75%)  | 0.25 (75%)  | 0.25 (75%)  | 0.25 (75%)  | 0.25 (75%)  |
| Water mfr SS3         | kg/s | 0.17 (50%)  | 0.17 (50%)  | 0.17 (50%)  | 0.17 (50%)  | 0.17 (50%)  | 0.17 (50%)  |

Two sets of tests based on different correlations of powder thermal conductivity

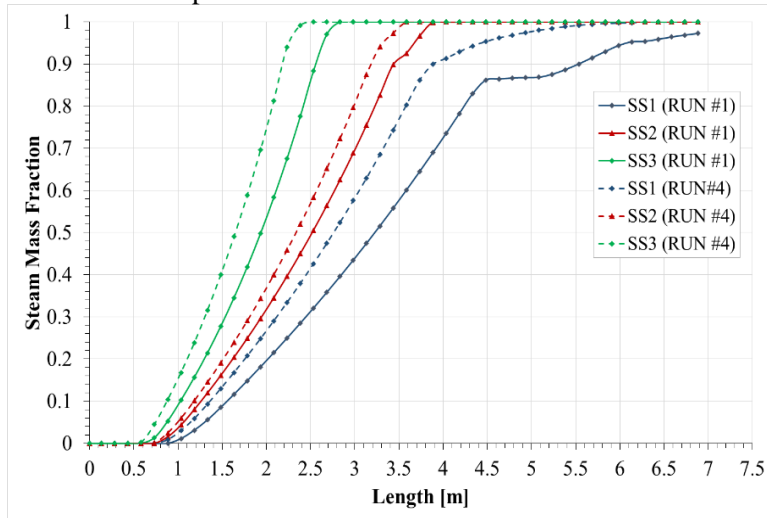
- **Case A:** based on TxP tests after powder thermal cycling under He at 4 bar\*
- **Case B:** based on experimental data of NACIE Heat Exchanger



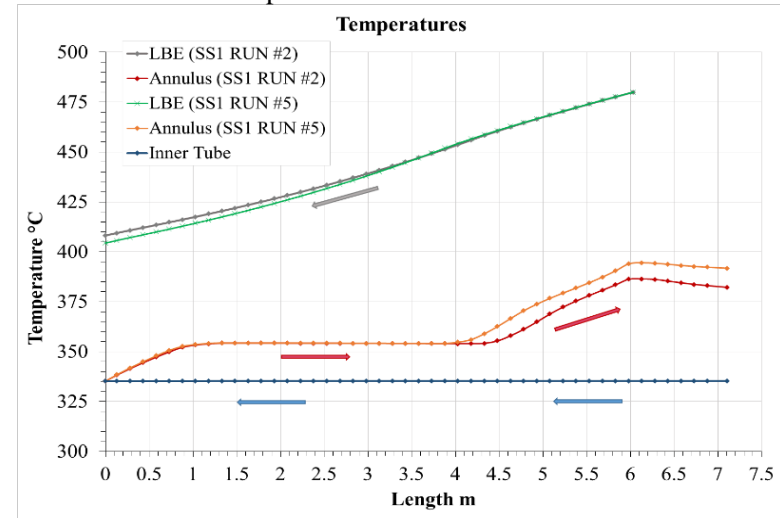
\*D. Rozzia et al., «Experimental Investigation on Powder Conductivity for the Application to Double Wall Bayonet Tube Bundle Steam Generator», 24<sup>th</sup> NENE Conference, 2015.

# HERO PRE-TEST ANALYSIS

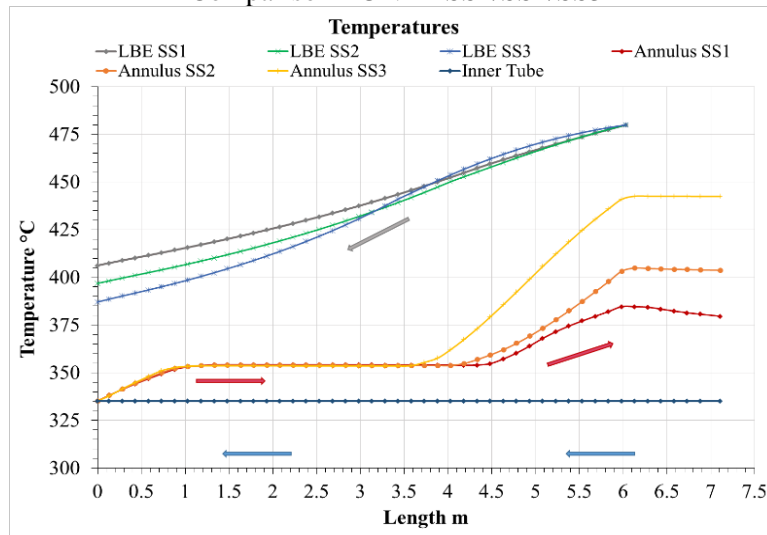
Comparison RUN #1/RUN #4 SS1/SS2/SS3



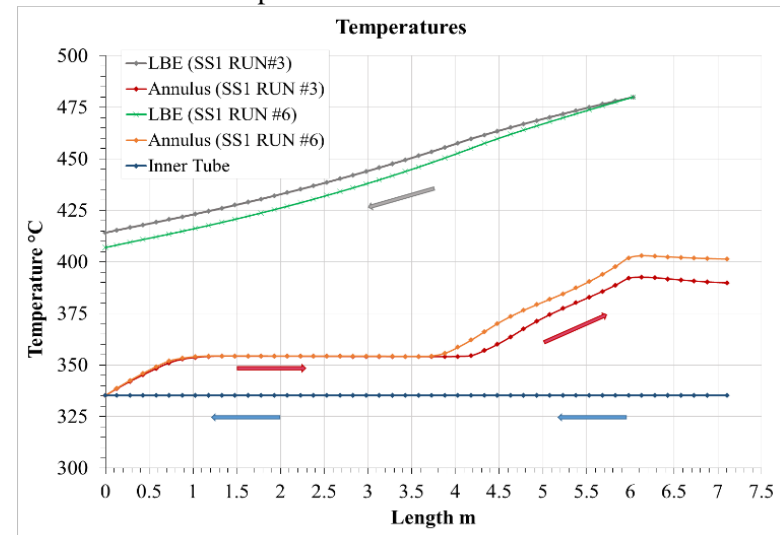
Comparison SS1 RUN #2/RUN#5



Comparison RUN #1 SS1/SS2/SS3

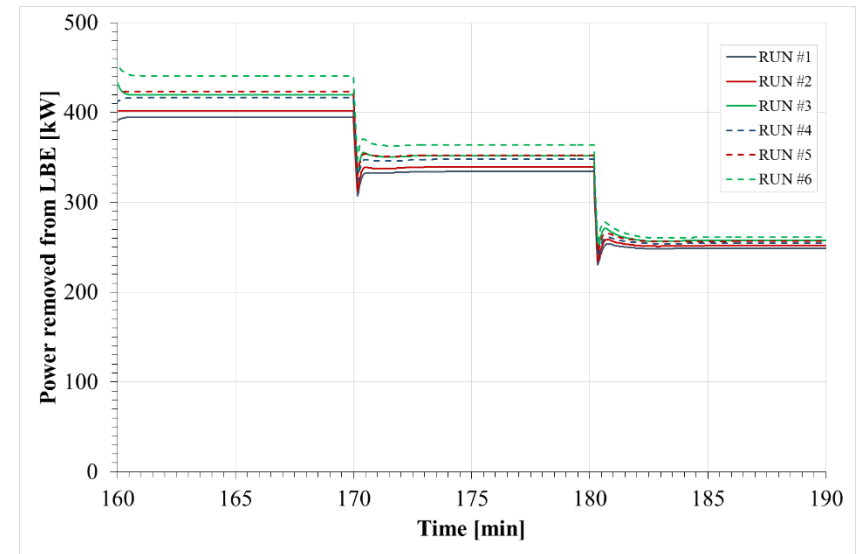
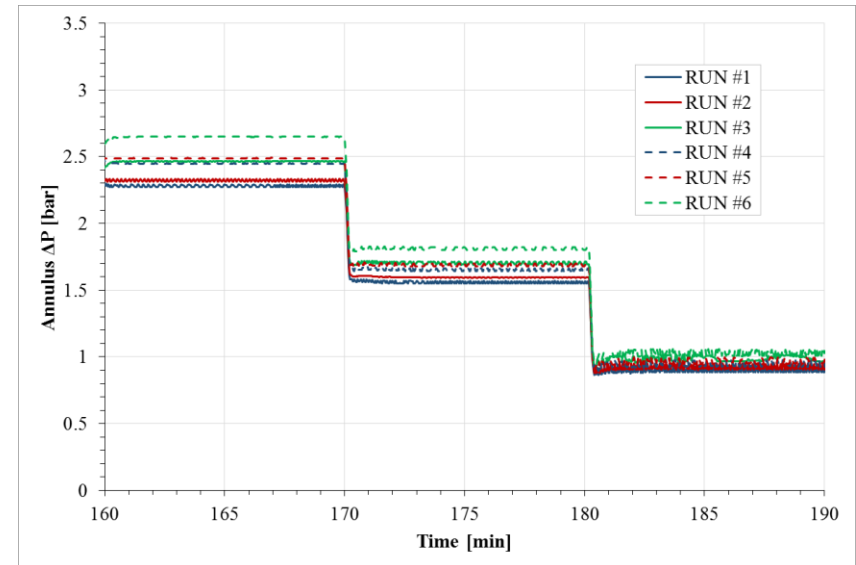


Comparison SS1 RUN #3/RUN#6



# HERO PRE-TEST ANALYSIS

|     | Parameter          | Unit         | CASE A |        |        | CASE B |        |        |
|-----|--------------------|--------------|--------|--------|--------|--------|--------|--------|
|     |                    |              | RUN #1 | RUN #2 | RUN #3 | RUN #4 | RUN #5 | RUN #6 |
| SS1 | LBE $\Delta T$     | $^{\circ}$ C | 73.7   | 71.8   | 65.7   | 77.8   | 75.6   | 69.0   |
|     | LBE $T_{out}$      | $^{\circ}$ C | 406.3  | 408.2  | 414.3  | 402.2  | 404.4  | 411.0  |
|     | Steam $T_{out}$    | $^{\circ}$ C | 379.6  | 382.2  | 389.8  | 388.6  | 391.8  | 401.3  |
|     | Power              | kW           | 394    | 402    | 419    | 416    | 423    | 441    |
|     | Annulus $\Delta P$ | bar          | 2.27   | 2.32   | 2.46   | 2.45   | 2.49   | 2.65   |
| SS2 | LBE $\Delta T$     | $^{\circ}$ C | 83.1   | 80.8   | 73.5   | 86.5   | 83.9   | 76.0   |
|     | LBE $T_{out}$      | $^{\circ}$ C | 396.9  | 399.2  | 406.5  | 393.5  | 396.1  | 404.0  |
|     | Steam $T_{out}$    | $^{\circ}$ C | 403.7  | 408.0  | 419.8  | 415.9  | 420.6  | 432.7  |
|     | Power              | kW           | 334    | 339    | 352    | 348    | 352    | 364    |
|     | Annulus $\Delta P$ | bar          | 1.55   | 1.60   | 1.69   | 1.65   | 1.68   | 1.80   |
| SS3 | LBE $\Delta T$     | $^{\circ}$ C | 92.9   | 89.8   | 80.7   | 94.8   | 91.5   | 81.8   |
|     | LBE $T_{out}$      | $^{\circ}$ C | 387.1  | 390.2  | 399.3  | 385.2  | 388.5  | 398.2  |
|     | Steam $T_{out}$    | $^{\circ}$ C | 442.4  | 446.9  | 457.2  | 451.6  | 455.4  | 463.55 |
|     | Power              | kW           | 249    | 252    | 257    | 254    | 256    | 261    |
|     | Annulus $\Delta P$ | bar          | 0.89   | 0.94   | 1.00   | 0.93   | 1.00   | 1.05   |





# CONCLUSIVE REMARKS AND FOLLOW UP

- ❑ Complete nodalization of the CIRCE HERO Secondary Loop
  
- ❑ Preliminary start-up procedure simulated
  
- ❑ High pressure characterization for HERO SGBT unit carried out
  - 3 LBE and h<sub>2</sub>o mfr; 100%, 75%, 50%
  - 2 Kpowder-He
  
- ❑ Activities planned in PAR-2018
  - Comparison of the pre-tests results with the experimental data
  - Post-test calculation and sensitivity study

**THANK YOU  
FOR  
YOUR ATTENTION**



Italian National Agency for New Technologies,  
Energy and Sustainable Economic Development



S.R.S. Servizi di Ricerche e Sviluppo S.r.l.



UNIVERSITÀ DI PISA

# Small Leakage Detection in LFR SG

Workshop Tematico: Gen. IV - LCFR  
ADP MiSE-ENEA (PAR2017-LP2)

*DIAEE – Università di Roma «La Sapienza»*

*14-15 Giugno 2018*

**M. Eboli, N. Forgone / UNIPI**

**A. Del Nevo / ENEA FSN-ING**

**D. Mazzi, F. Giannetti / SRS**



1101 0110 1100  
0101 0010 1101  
0001 0110 1110  
1101 0010 1101  
1111 1010 0000



# List of contents

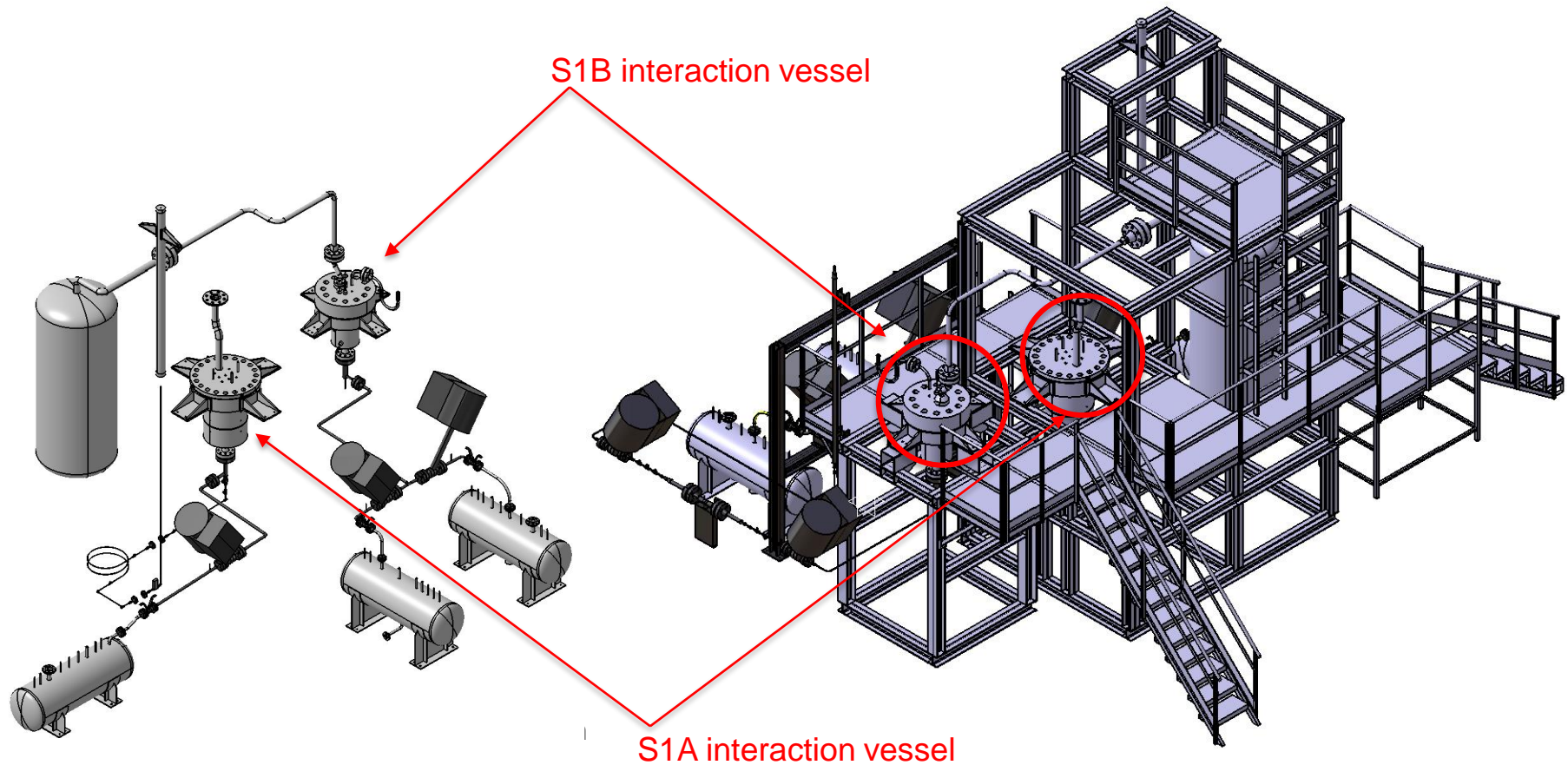
- ❑ Objectives
- ❑ Introduction to LIFUS5/Mod3
- ❑ Description of LIFUS5/Mod3 – Test Section Small Leak (S1A)
- ❑ Execution of the experiments – Test series C
- ❑ Summary and Follow-up

# Objectives

- The goal was to implement an experimental activity, supported by the numerical simulations, which **characterizes the leak rate and bubbles sizing through typical cracks** occurring in the pressurized tubes
  - Basic tests in LIFUS5/Mod3 facility have been carried out to correlate the flow rates of the leakage through selected cracks with signals detected by proper transducers
  - Different crack sizes and geometries have been analyzed, while the injection pressure and the temperature have been recorded
  - A detection system detected the bubbles migration through the free level

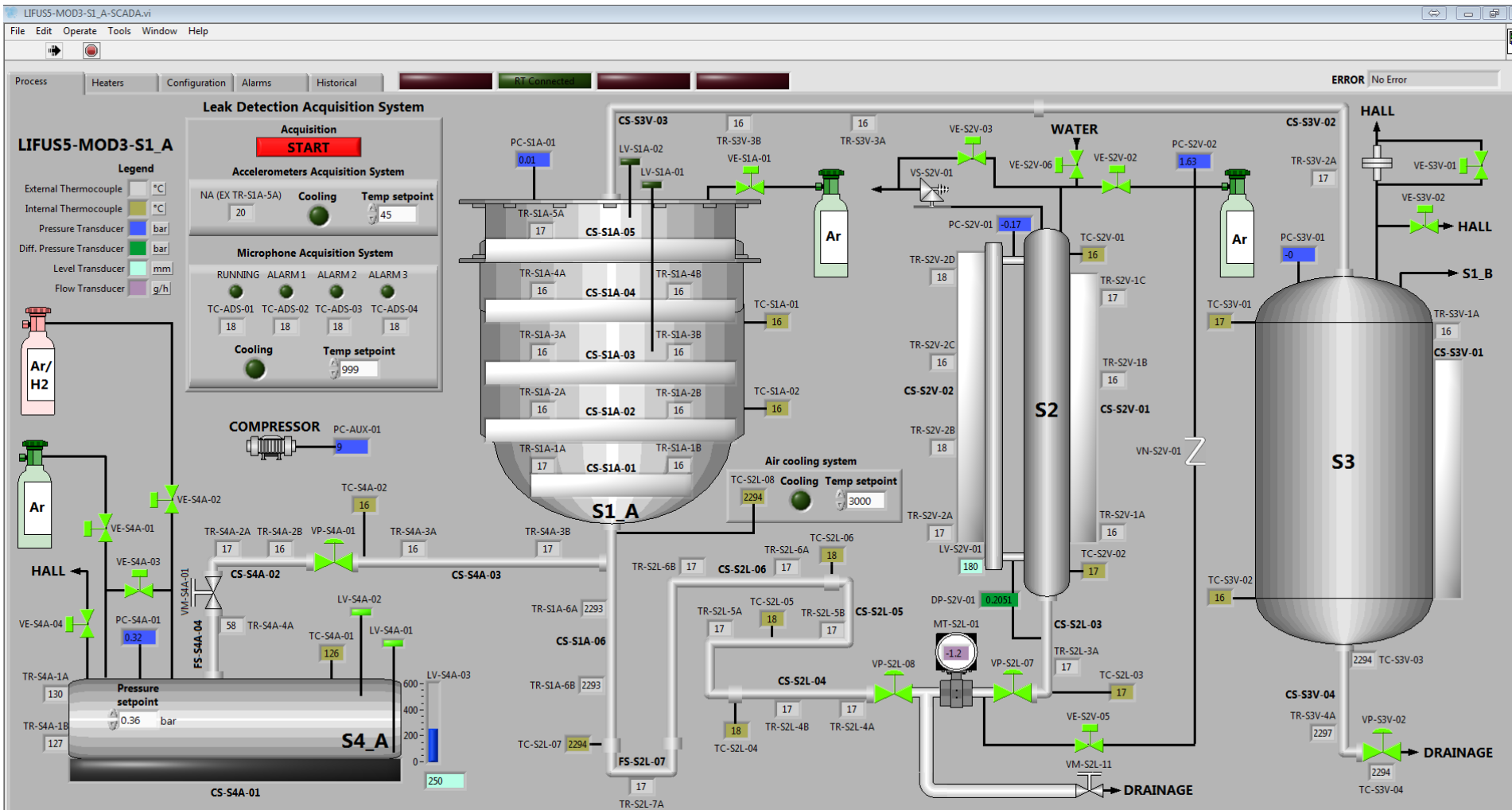
# Introduction to LIFUS5/Mod3

- LIFUS5/Mod3 (*the third refurbishment*) is a multi purpose facility:
  - experiments related the HLM (i.e. PbLi, LBE, Pb) and H<sub>2</sub>O interaction /reaction
    - ✓ S1A → Small Leak detection
    - ✓ S1B → Large break – BE code model development and validation



# LIFUS5/Mod3: Test Section Small Leak

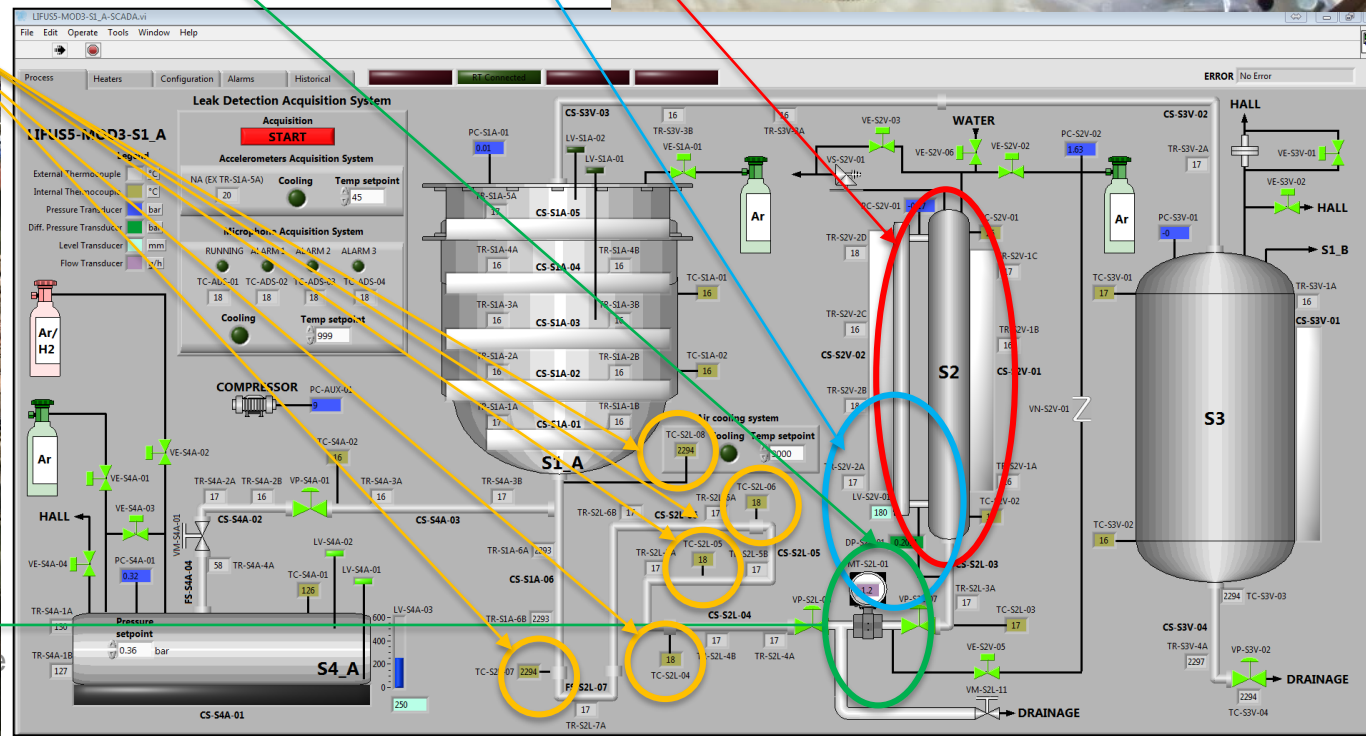
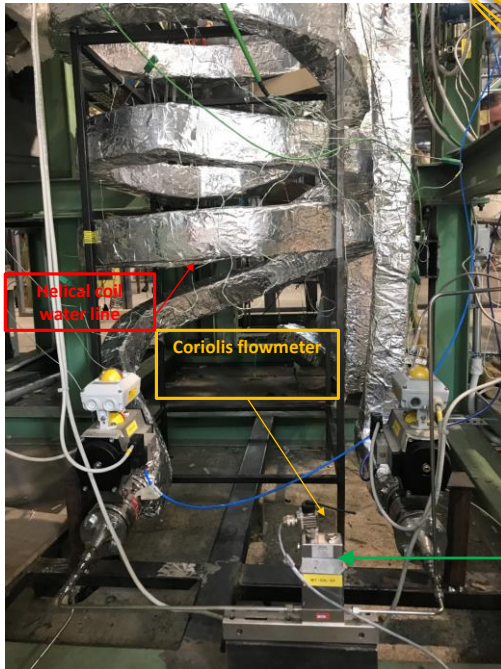
- LIFUS5/Mod3-S1A synoptic (control system and data recording based on NI / Labview)
  - Two additional PCs are in charge of the leak detection systems (NI and DAWESoft)



# LIFUS5/Mod3: Test Section Small Leak

Injection system acquisition (1 Hz)

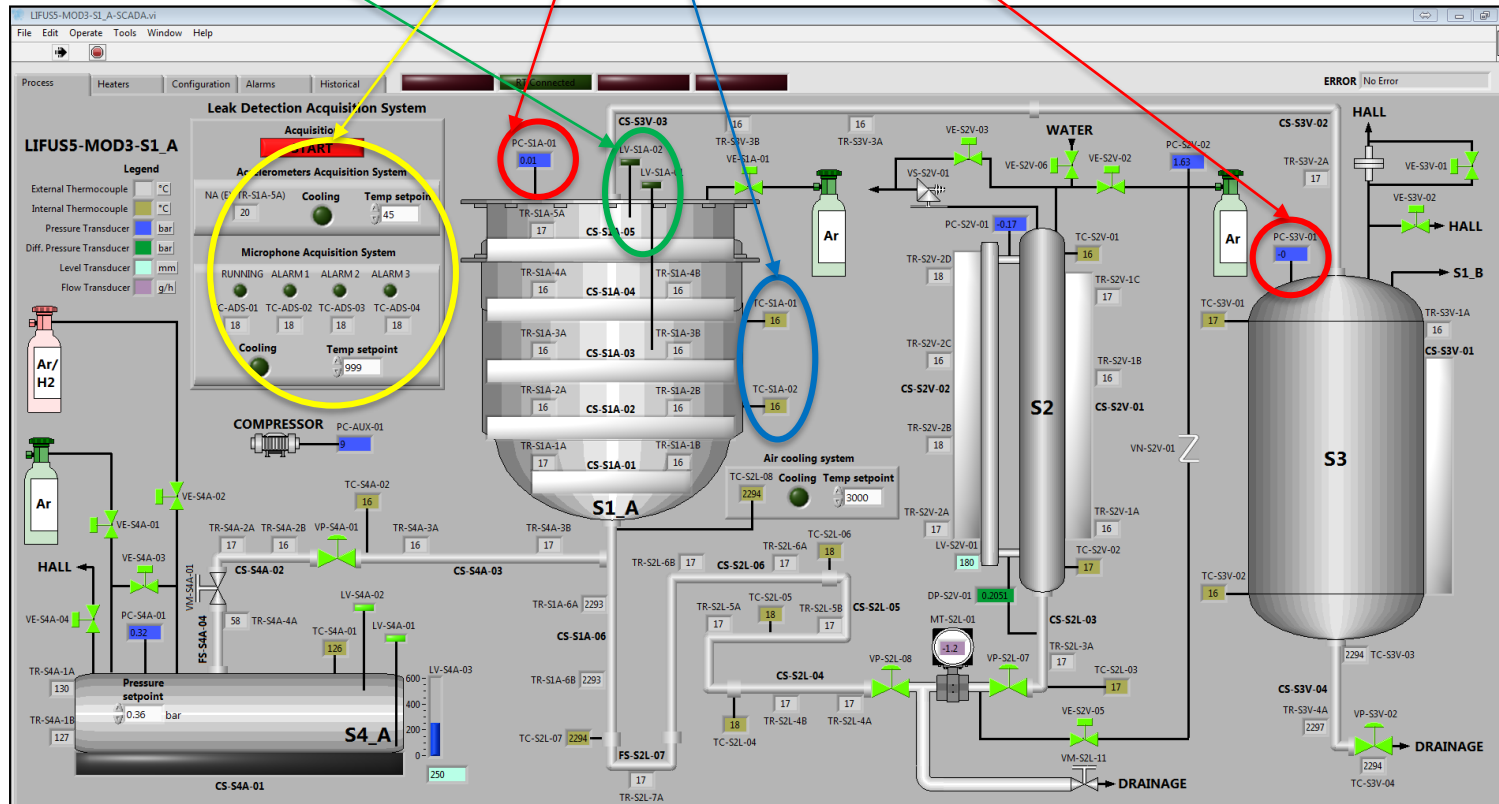
- ❑ S2V filled with “cold” water at 16 bar
- ❑ Mass of water injected monitored through
  - the level meter (resolution 5 mm)
  - DP meter (resolution < 1 mm)
  - Coriolis flow meter
  - 5 TC





# LIFUS5/Mod3: Test Section Small Leak

- ❑ S1A filled with LBE @ 1 bar - S3V connected
  - Absolute pressures in S1A and S3V
  - LBE temperature monitored by 2 TC
  - 2 Level ON/OFF
  - Small leak detection system



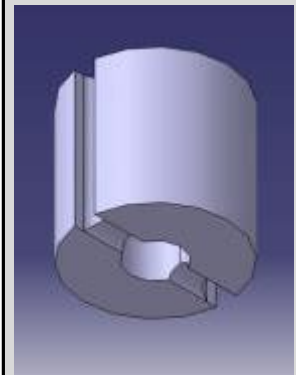
# LIFUS5/Mod3: Test Section Small Leak

## Primary detection system

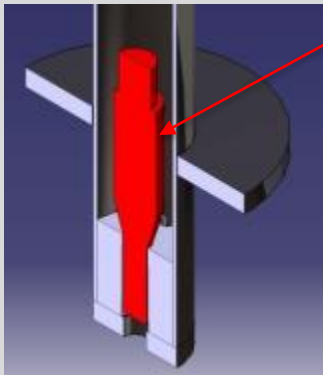
Acoustic Detection (**ADS**) with dedicated hardware and software (i.e. real time acquisition system)

- ❑ Acquisition at @ 20 kHz
- ❑ Data analysis on real time (8 channels)
- ❑ 5 microphones on the cover flange

ADS support and cooling system of Low T acoustic sensors



Ceramic support



AD support and cooling system

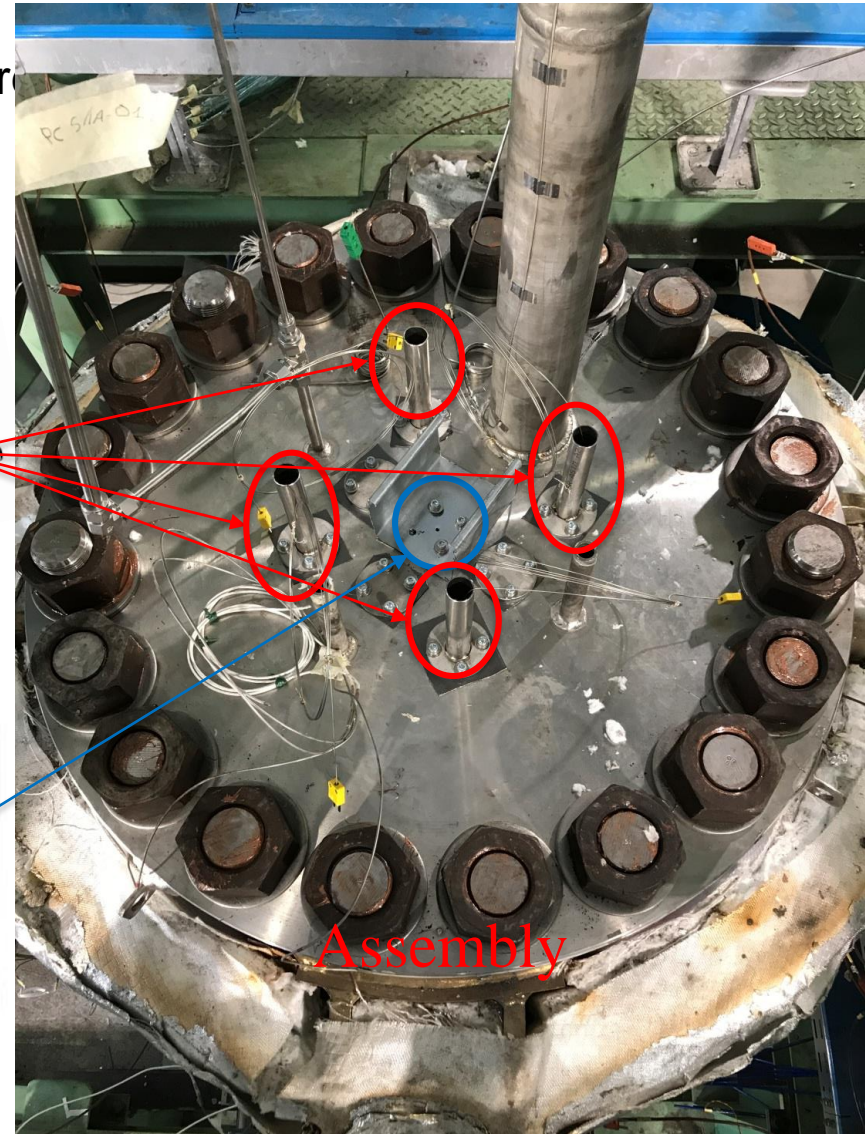
Temperature is monitored (TC) and Ar gas cooling thanks the lateral grooves in the ceramic support



#4 → Model 130E20  
(low temperature)



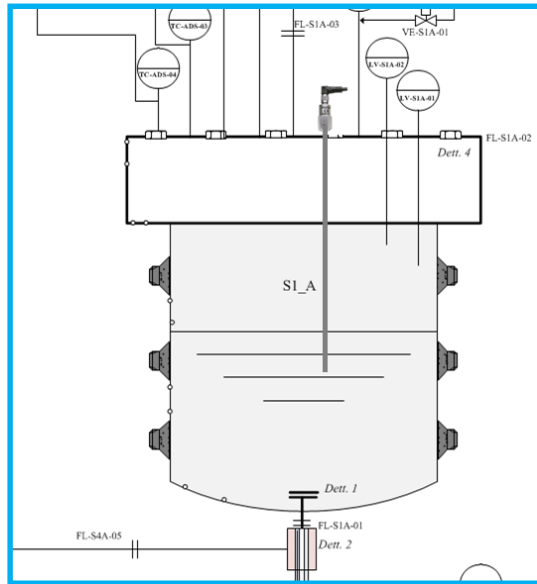
#1 → Model 377B26  
(high temperature)



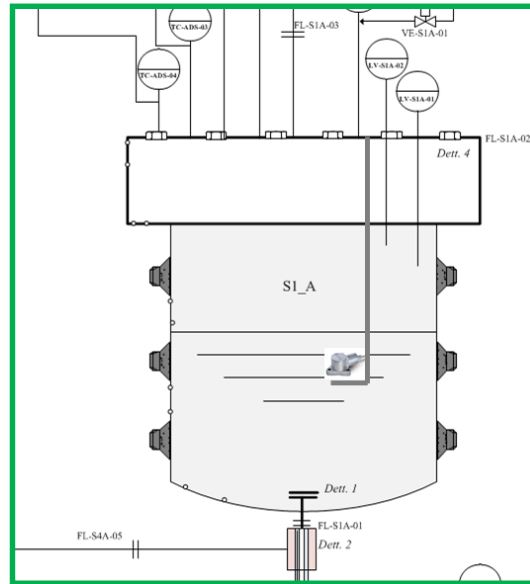
# LIFUS5/Mod3: Test Section Small Leak

## Alternative detection systems

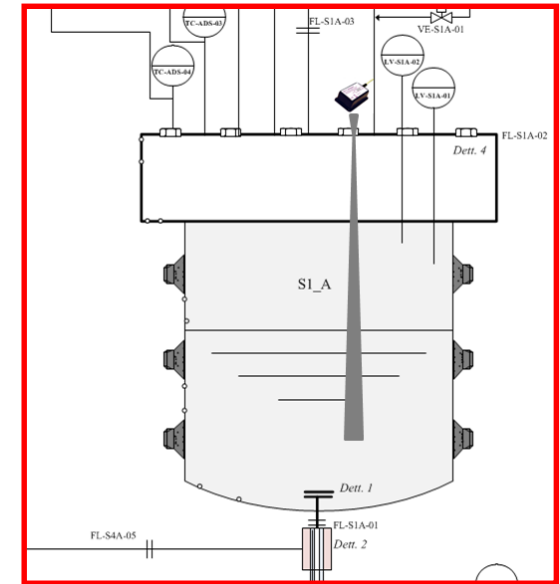
1. Inductive proximity sensor (i.e. High Sensitivity Accelerometer – **HSA**) installed outside the vessel
2. Accelerometer sensors installed inside the vessel (i.e. High Temperature Accelerometer – **HTA**) installed on a metallic support
3. Acoustic Emission (**AE**) sensor installed outside the vessel, measuring the high frequency signals



High Sensitivity Accelerometer – **HSA**



High Temperature Accelerometer – **HTA**



Acoustic Emission – **AE**

# LIFUS5/Mod3: Test Section Small Leak

## Alternative detection systems

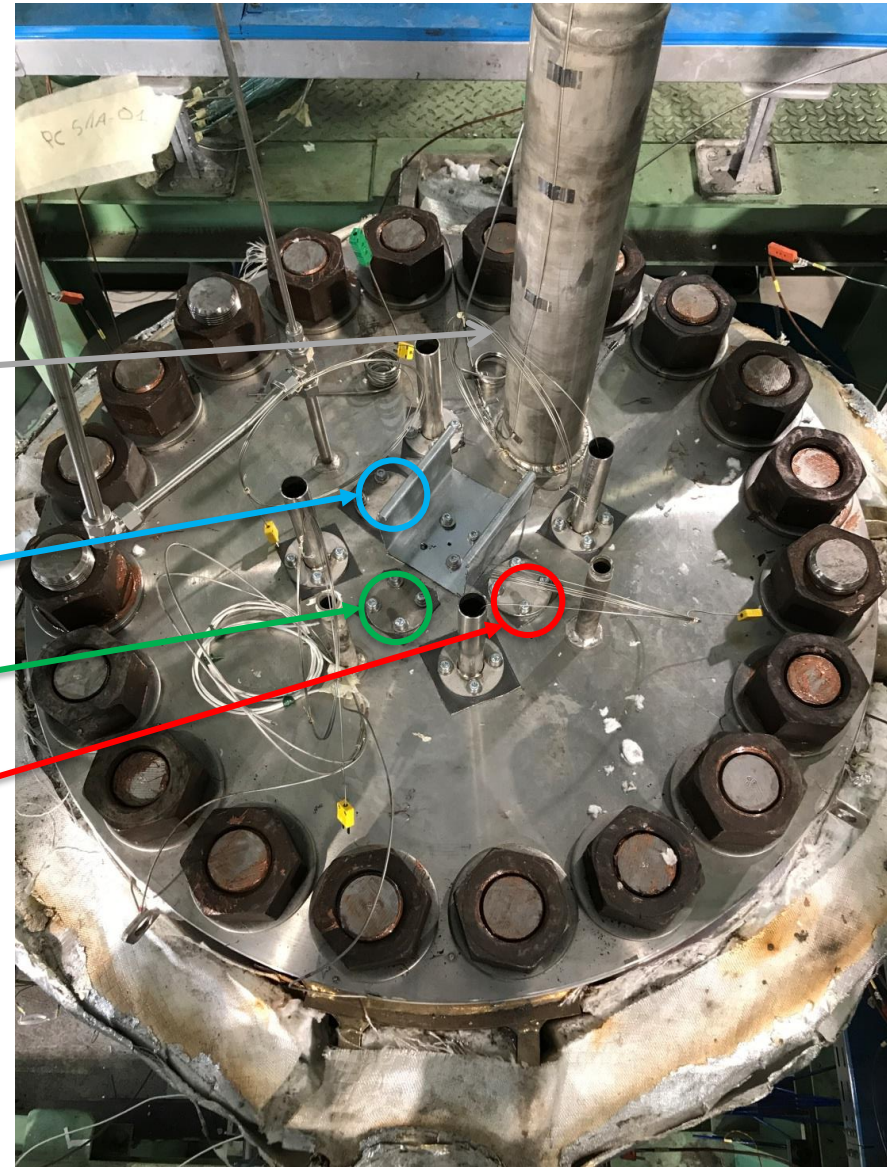
1. High Sensitivity Accelerometer – **HSA**
2. High Temperature Accelerometer – **HTA**
3. Acoustic Emission (**AE**)



HSA

HTA

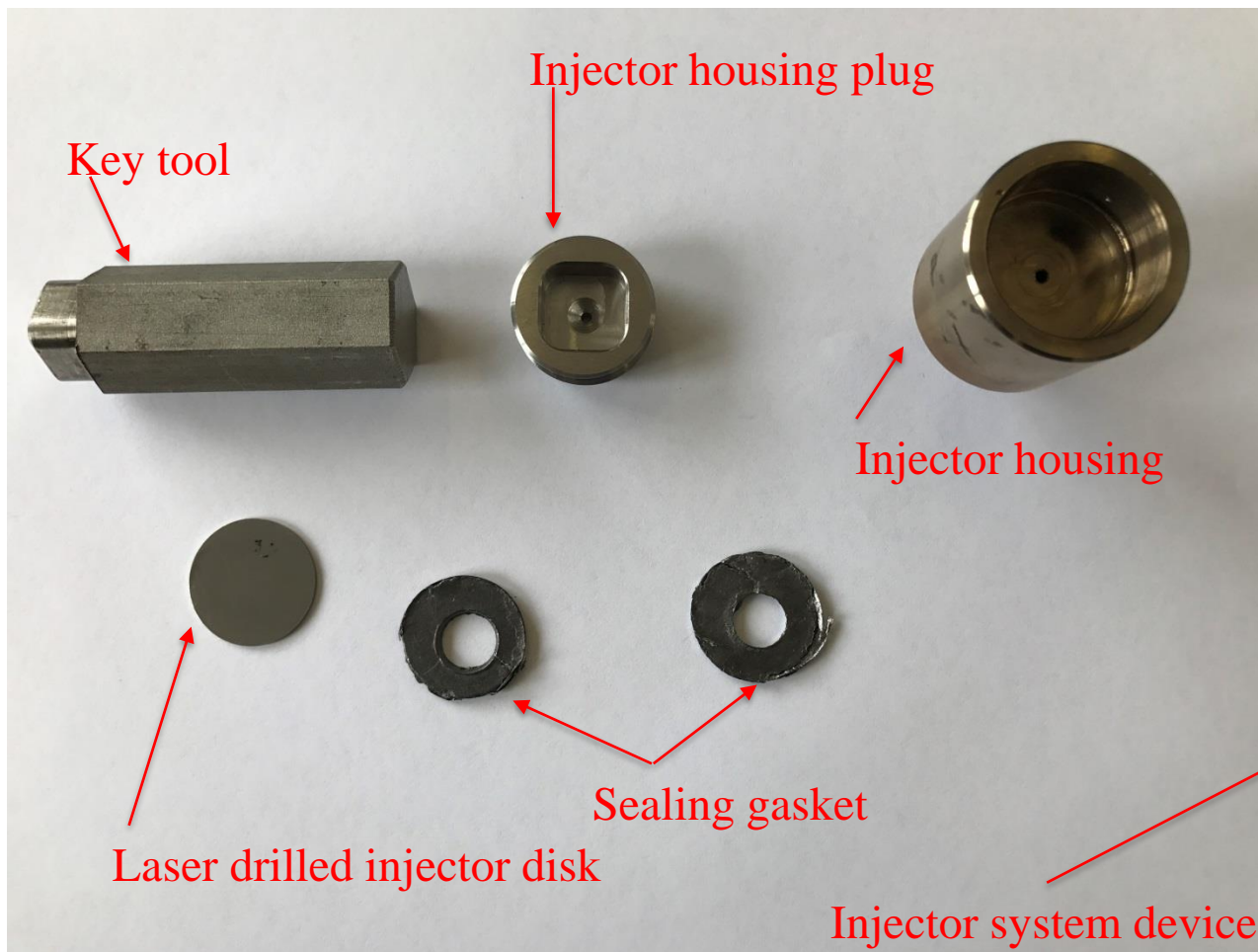
AE



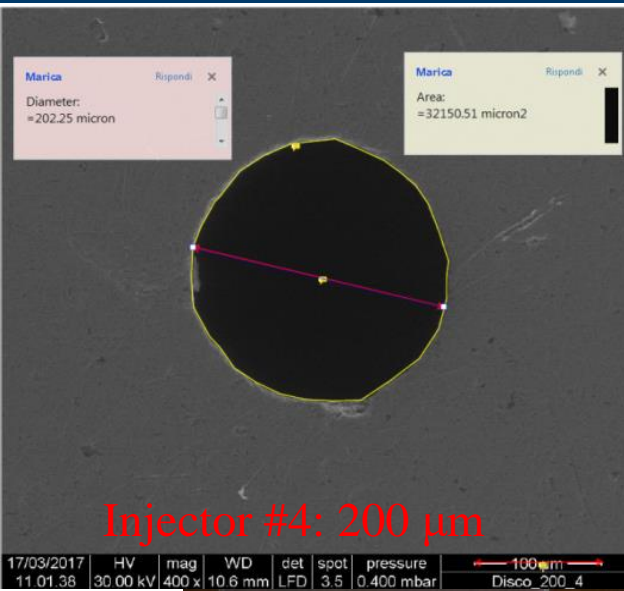
# LIFUS5/Mod3: Test Section Small Leak

- Injector disk hole design: nominal orifice diameters

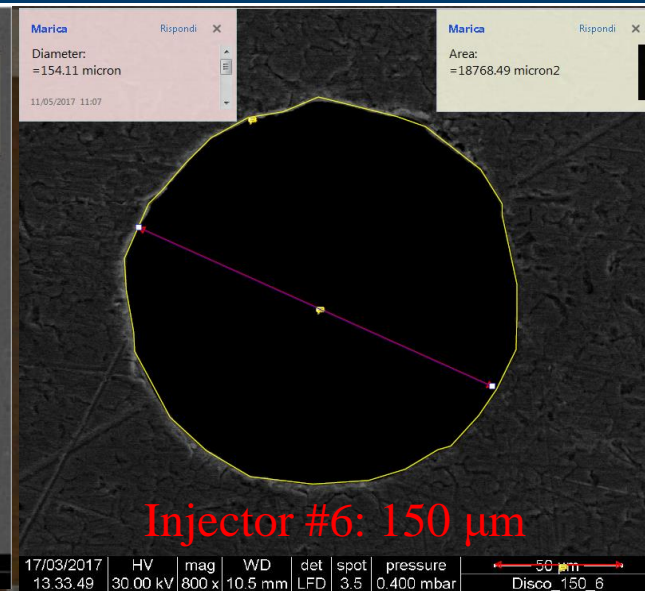
| Description           | #1    | #2    | #3    | #4    | #5    | #6    | #7   | #8   | #9   |
|-----------------------|-------|-------|-------|-------|-------|-------|------|------|------|
| Orifice diameter [mm] | 0.005 | 0.010 | 0.020 | 0.040 | 0.060 | 0.080 | 0.10 | 0.15 | 0.20 |



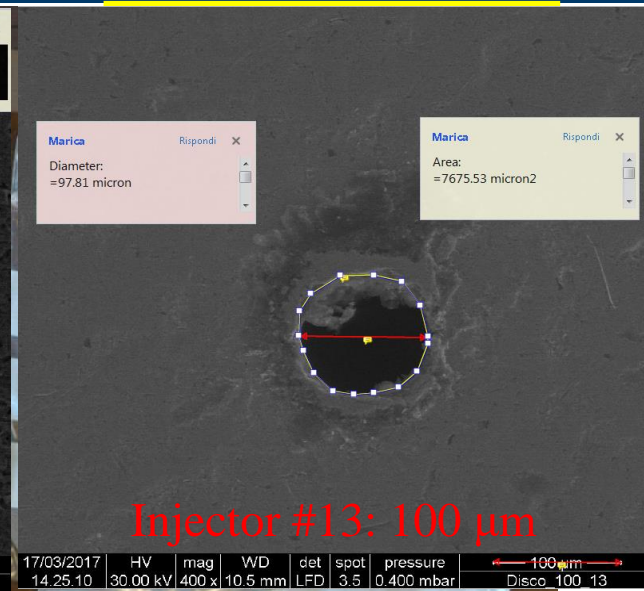
# LIFUS5/Mod3: Test Section Small Leak



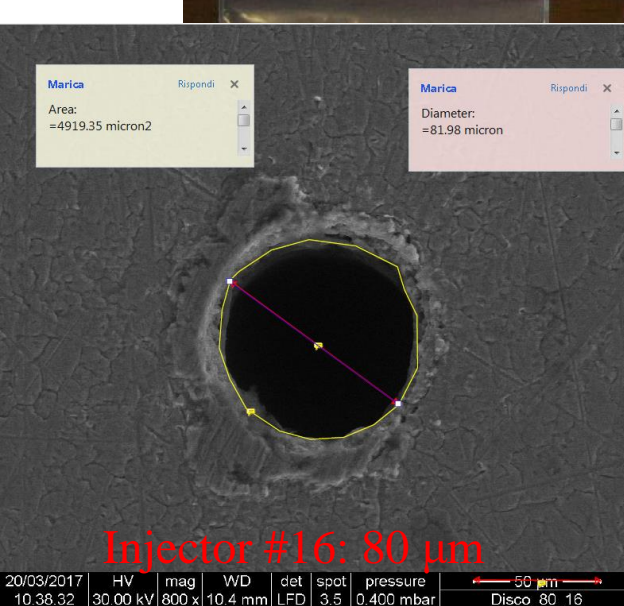
Injector #4: 200 µm



Injector #6: 150 µm



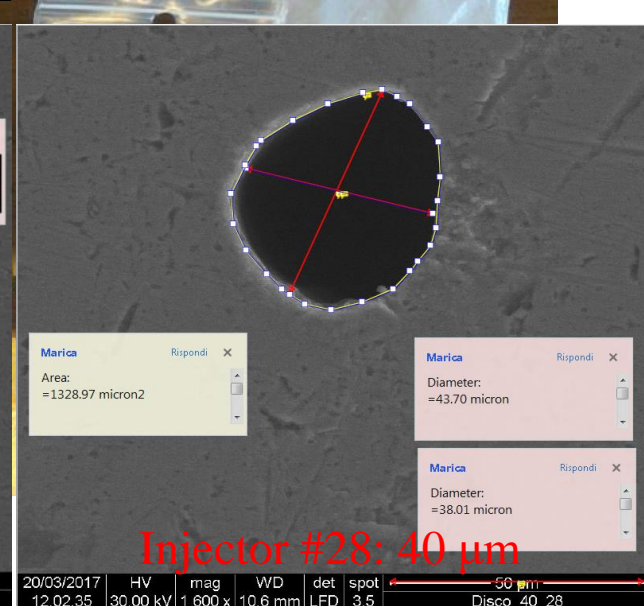
Injector #13: 100 µm



Injector #16: 80 µm














Injector #21: 60 µm

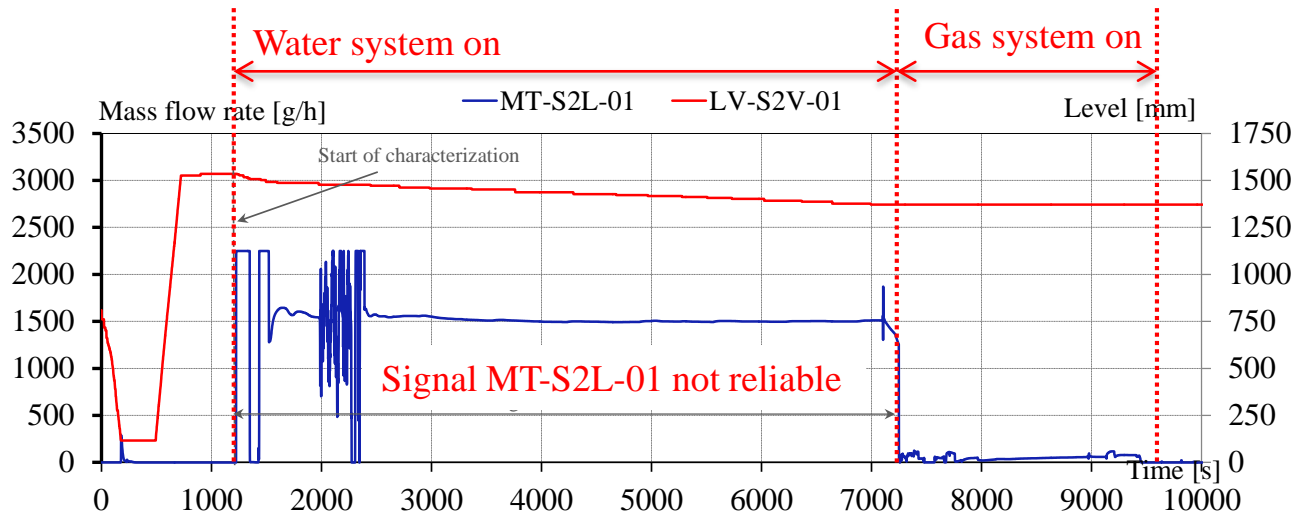


Injector #28: 40 µm

# Execution of experiments – Test series C

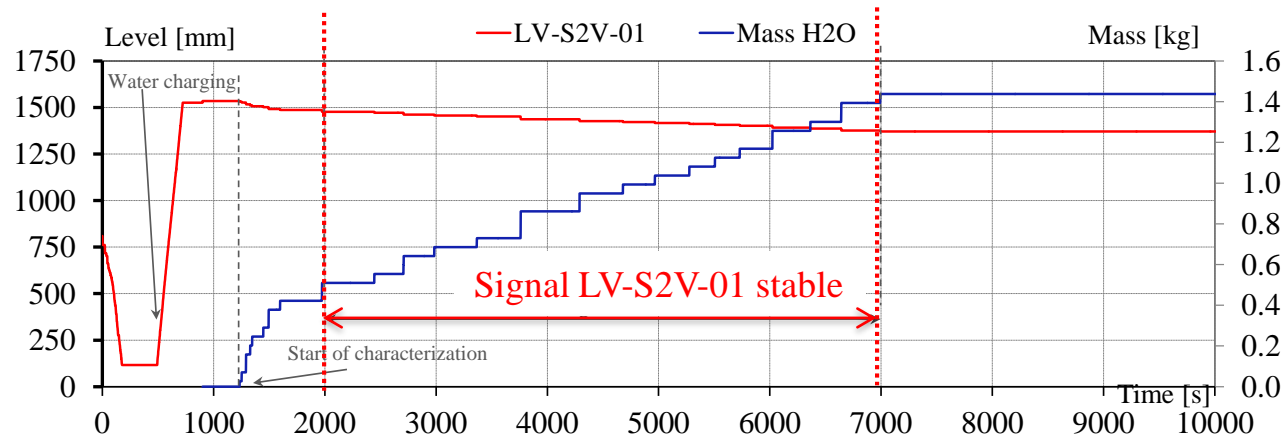
| Parameter   | TEST  |   |   |   |   |   |   |   |   |   |   |
|---|---|---|---|---|---|---|---|---|---|---|---|
|   | C1.1<br>(_60)   | C1.2<br>(_60)   | C1.3<br>(_60)   | C2.1<br>(_80)   | C2.2<br>(_80)   | C3.1<br>(_40)   | C3.2<br>(_40)   | C4.1<br>(_100)  | C4.2<br>(_100)  | C5.1<br>(_150)  | C6.1<br>(_200)  |
| Number of Test                                      | T#1   | T#7   | T#10  | T#2   | T#9   | T#3   | T#6   | T#4   | T#5   | T#8   | T#11  |
| Date of execution                                   | 06 Sep  | 19 Jan  | 8 Feb   | 13 Sep  | 2 Feb   | 20 Oct  | 15 Dec  | 10 Nov  | 22 Nov  | 26 Jan  | 6 Apr   |
| Number of laser-holed plate                         | 21  | 22  | 23  | 16  | 19  | 27  | 28  | 11  | 13  | 6   | 4   |
| Inj. orifice design diameter [ $\mu\text{m}$ ]      | 60  | 60  | 60  | 80  | 80  | 40  | 40  | 100   | 100   | 150   | 200   |
| Inj. orifice measured flow area [ $\mu\text{m}^2$ ] | 3188  | 3080  | 3257  | 4919  | 5508  | 1392  | 1329  | 8116  | 7676  | 18768   | 32151   |
| Acquisition time [hh:mm]                            | 06:15   | NA  | 09:00   | 11:22   | 5:00  | NA  | 5:29  | NA  | 7:29  | 5:59  | 3:00  |
| Leak detection system acquisition                   | All   | NA  | All   | All   | All   | NA  | *   | NA  | *   | All   | All   |
| LBE temperature TC-S4A-01 [ $^{\circ}\text{C}$ ]    | 203   | NA  | 226   | 209   | 226   | NA  | NI  | NA  | NI  | 226   | 246   |
| Water pressure PC-S2V-01 [bar]                      | 19.7  | NA  | 20.1  | 20.2  | 19.3  | NA  | NI  | NA  | NI  | 20.3  | 20.2  |
| Water temperature TC-S2L-08 [ $^{\circ}\text{C}$ ]  | 170   | NA  | 219   | 200   | 210   | NA  | NI  | NA  | NI  | 203   | 247   |
|   |  |  |  |  |  |  |  |  |  |  |  |

# Test C.1.1\_60 : Characterization prior-to-test



Preparation to Test  
C1.1\_60  
Injector #21 (60  $\mu$ m):  
Injection performance is  
characterized prior-to-  
test in cold condition

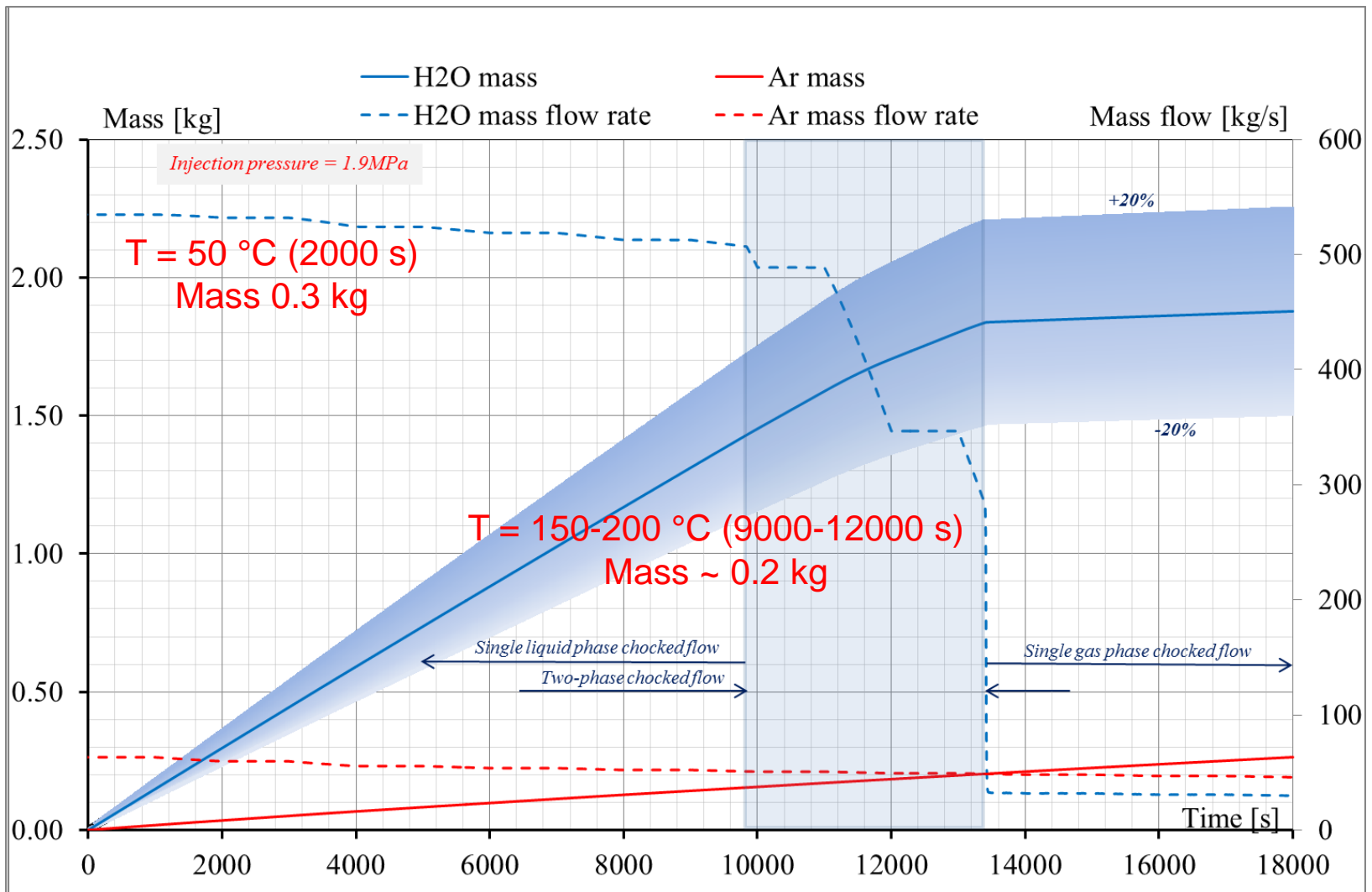
- Water @ 19 bar, 40°C
- Mass flow rate of 1500 g/h not reliable
- Signal LV is stable from 2000 to 7000 s
- Average mass flow rate of 667 g/h
- Total mass of injected water in 5000 s is 0.93 kg



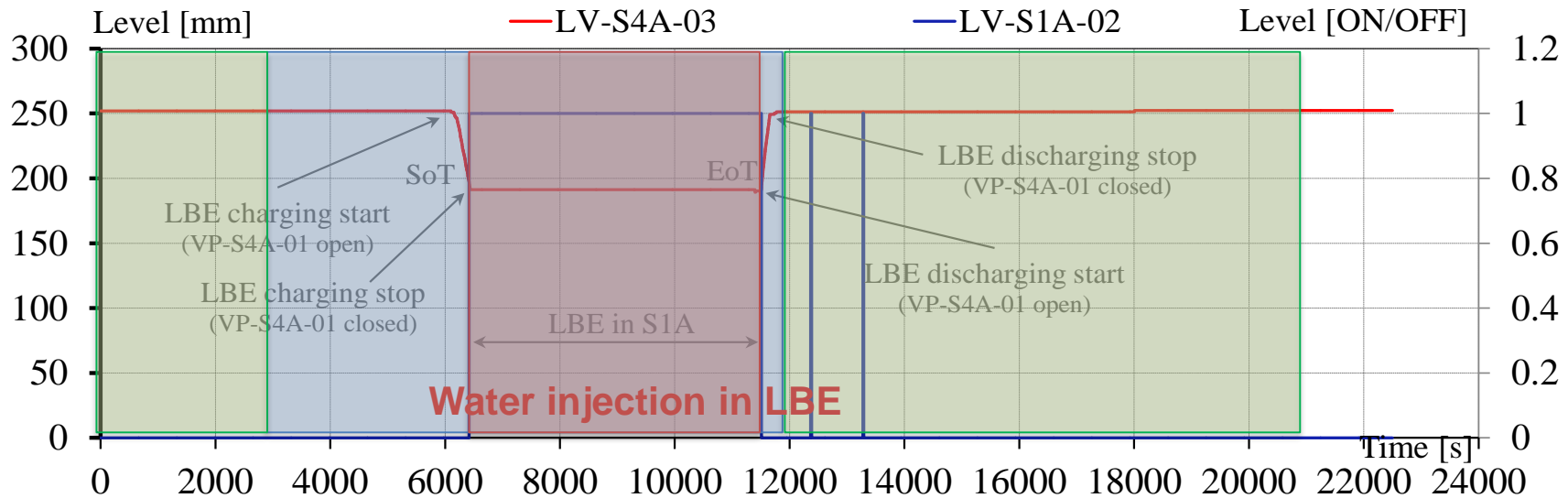
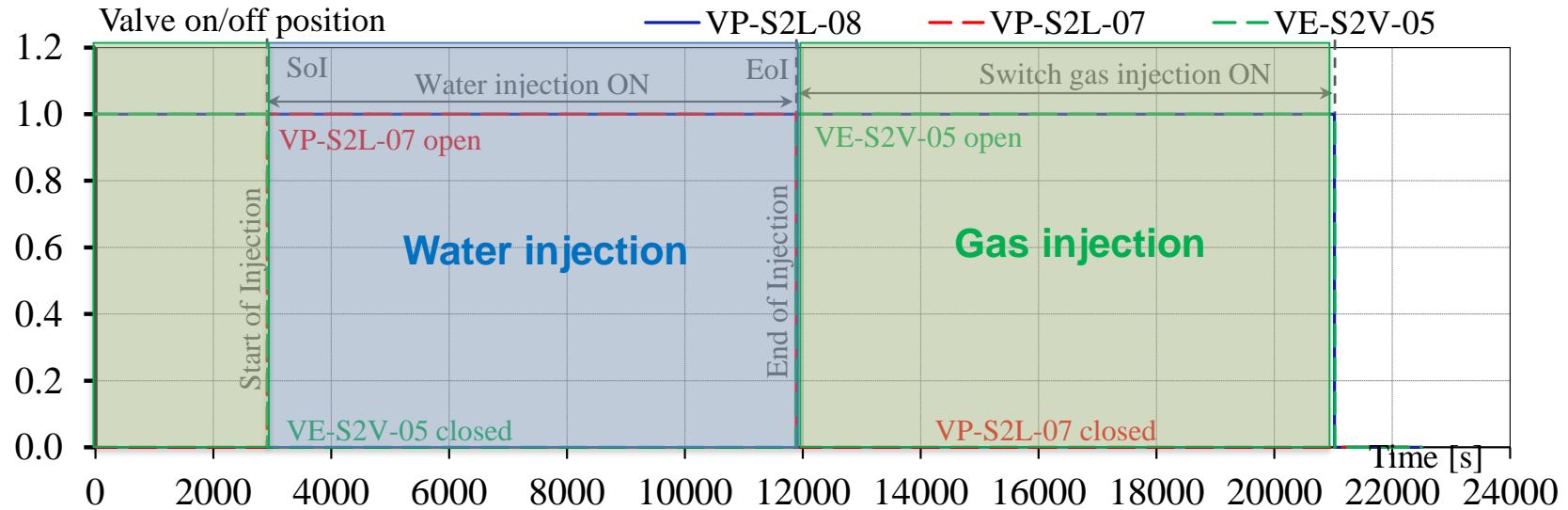




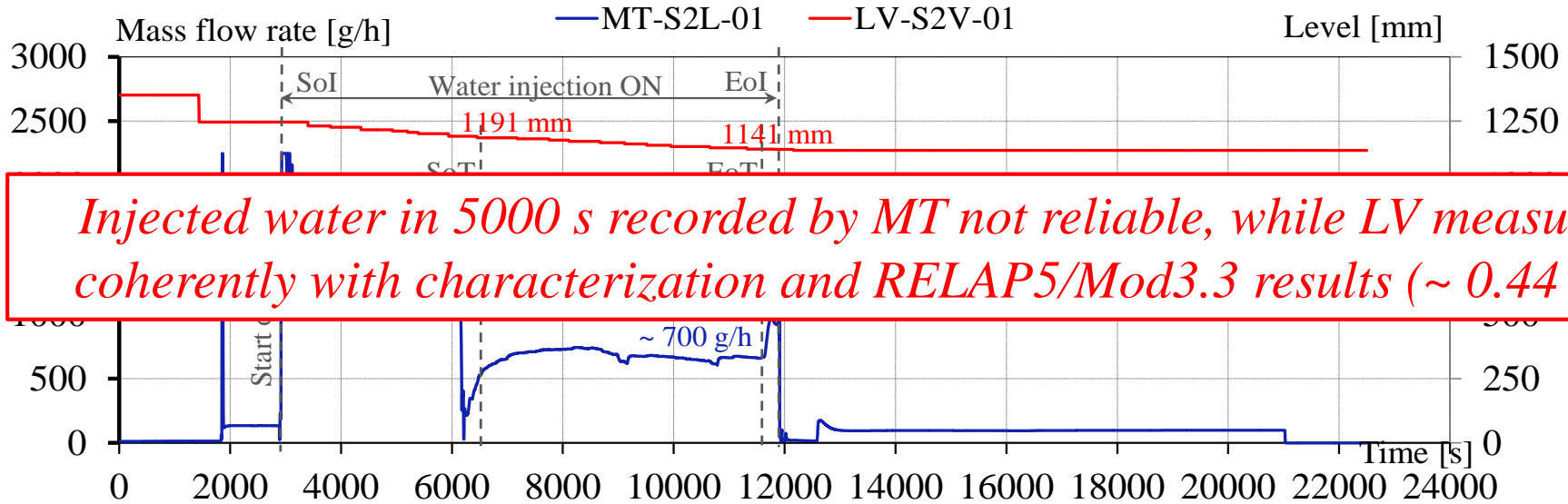
# Test C.1.1\_60 : RELAP5/Mod3.3 analyses



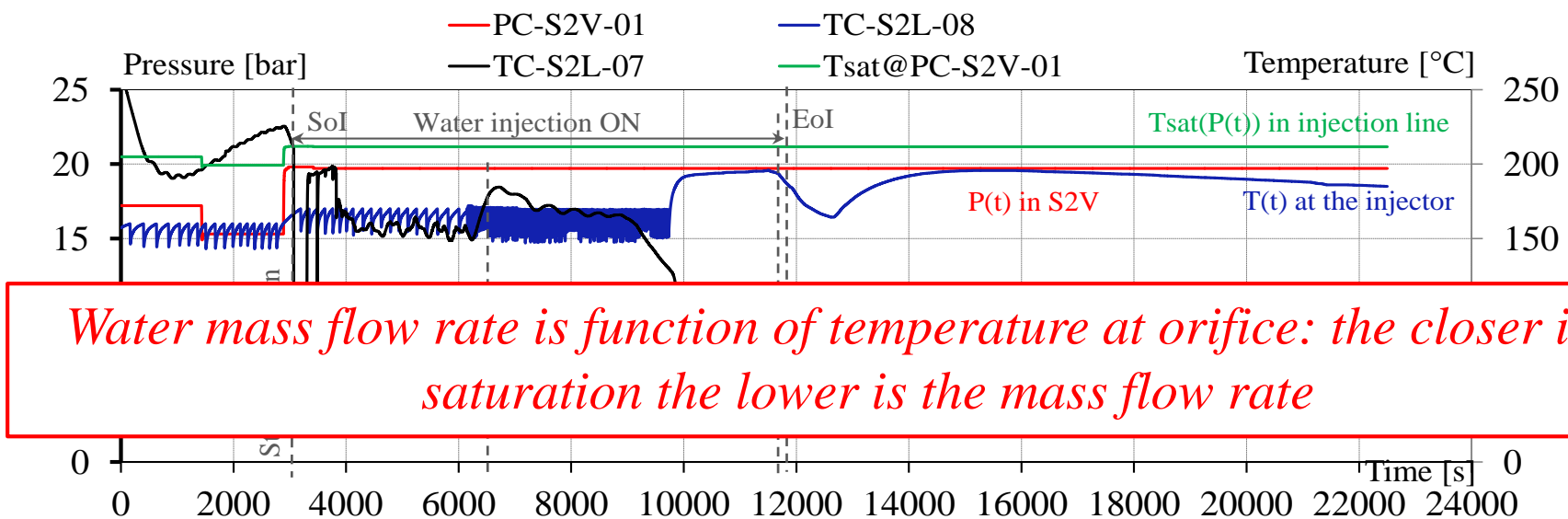
# Test C.1.1\_60 : EDTAR



# Test C.1.1\_60 : EDTAR



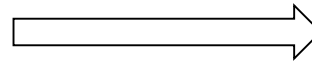
*Injected water in 5000 s recorded by MT not reliable, while LV measured coherently with characterization and RELAP5/Mod3.3 results (~ 0.44 kg)*



*Water mass flow rate is function of temperature at orifice: the closer is the saturation the lower is the mass flow rate*

# Test C.1.1\_60 : EDTAR

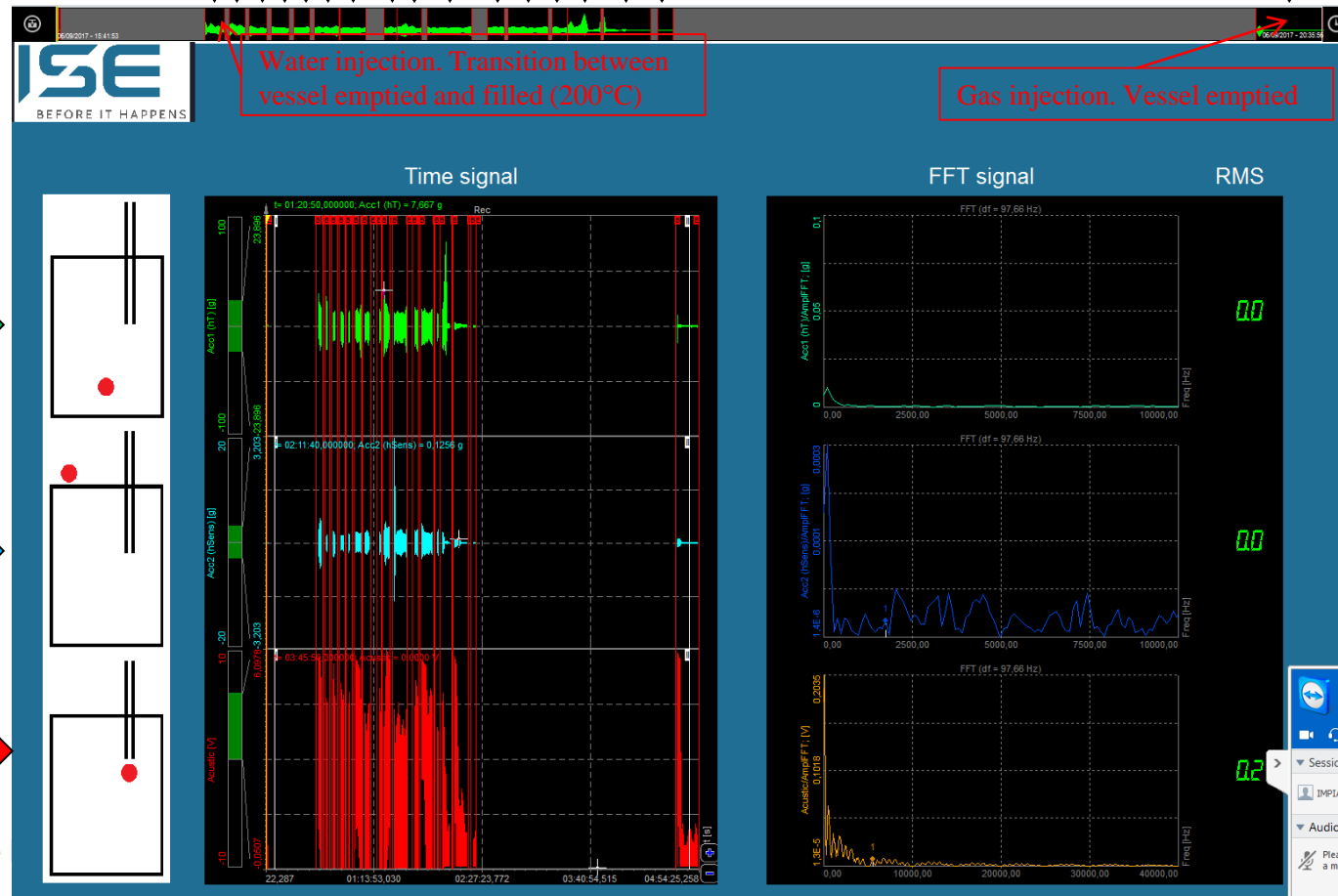
It seems possible to distinguish the phases:



Analyses of data is ongoing

1. Water injection w/o LBE in S1A
2. Water injection w LBE in S1A
3. Gas Injection

Acquisitions in intervals from time 16.31 to 20.35 – about 30GB of compressed data



High Temperature Accelerometer – HTA



High Sensitivity Accelerometer – HSA



Acoustic Emission (AE)

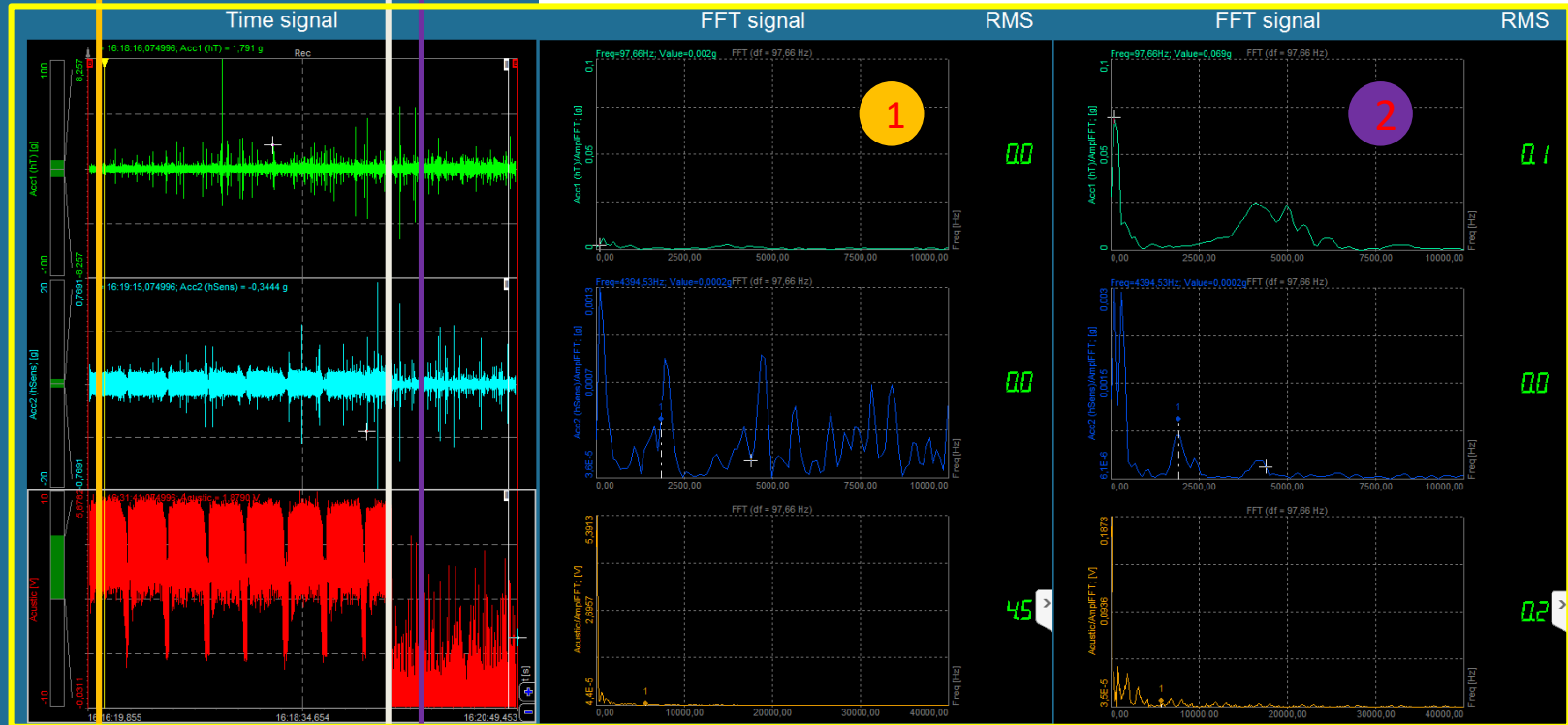
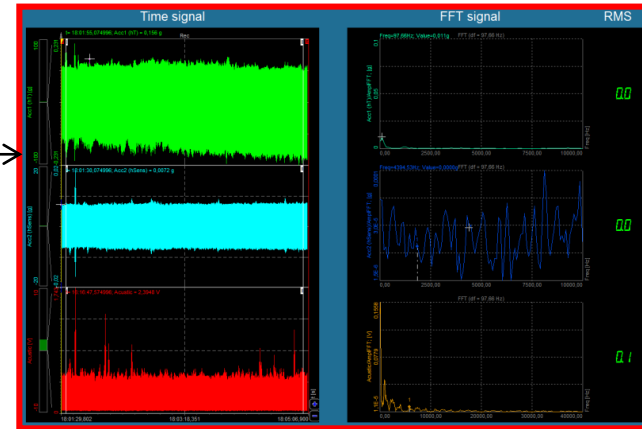
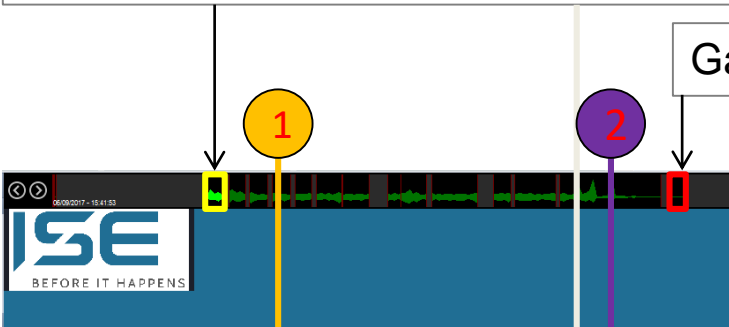


Small Leakage

# Test C.1.1\_60 : EDTAR

Water injection. Transition between vessel emptied and filled

Gas Injection



# Summary and Follow-up

- ❑ An experimental activity for characterizing the leak rate through typical cracks occurring in the pressurized tubes has been designed and implemented
- ❑ 50 laser drilled disks have been manufactured and characterized for simulating the leak
- ❑ A primary detection system – Acoustic Detection (ADS) – has been installed and tested
- ❑ Alternative detection systems, supported by the PAR2016, have been also identified and installed. They are: 1) High Sensitivity Accelerometer HSA; 2) High Temperature Accelerometer HTA; and 3) Acoustic Emission AE
- ❑ The experimental campaign was successfully concluded executing 8 tests (laser micro-holed plate from 40 to 200  $\mu\text{m}$ )
- ❑ Preliminary evaluation of data seems to demonstrate that is possible to distinguish the different phases of the experiment. Analysis of data is in progress
- ❑ Analyses of the experimental data and the preparation of the EDTAR are ongoing

Ing. Marica Eboli, Ph.D.  
marica.eboli@ing.unipi.it







Italian National Agency for New Technologies,  
Energy and Sustainable Economic Development

# Natural circulation experiments in the NACIE-UP loop

*ADP-PAR2017-LP2*

*Università di Roma La Sapienza 14-15/06/2018*

**I. Di Piazza (ENEA FSN-ING-TESP)**

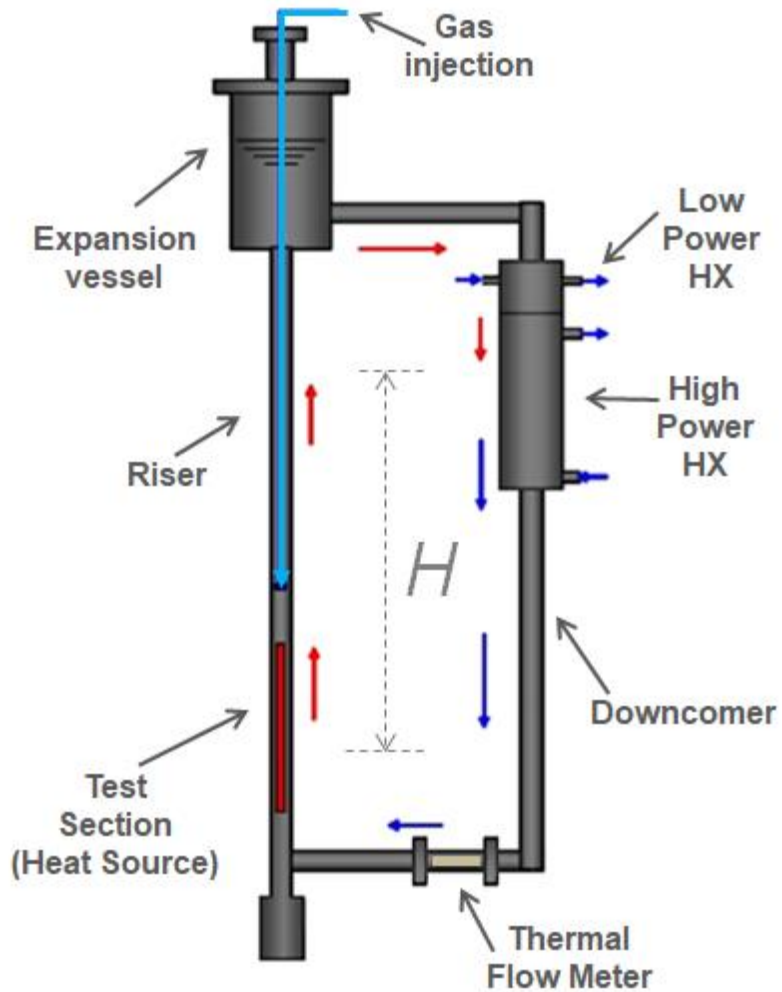


**Workshop tematico ADP MiSE-ENEA (PAR2017-LP2)**

*Generation IV Lead Cooled Fast Reactor: Stato Attuale Della Tecnologia E Prospettive Di Sviluppo*

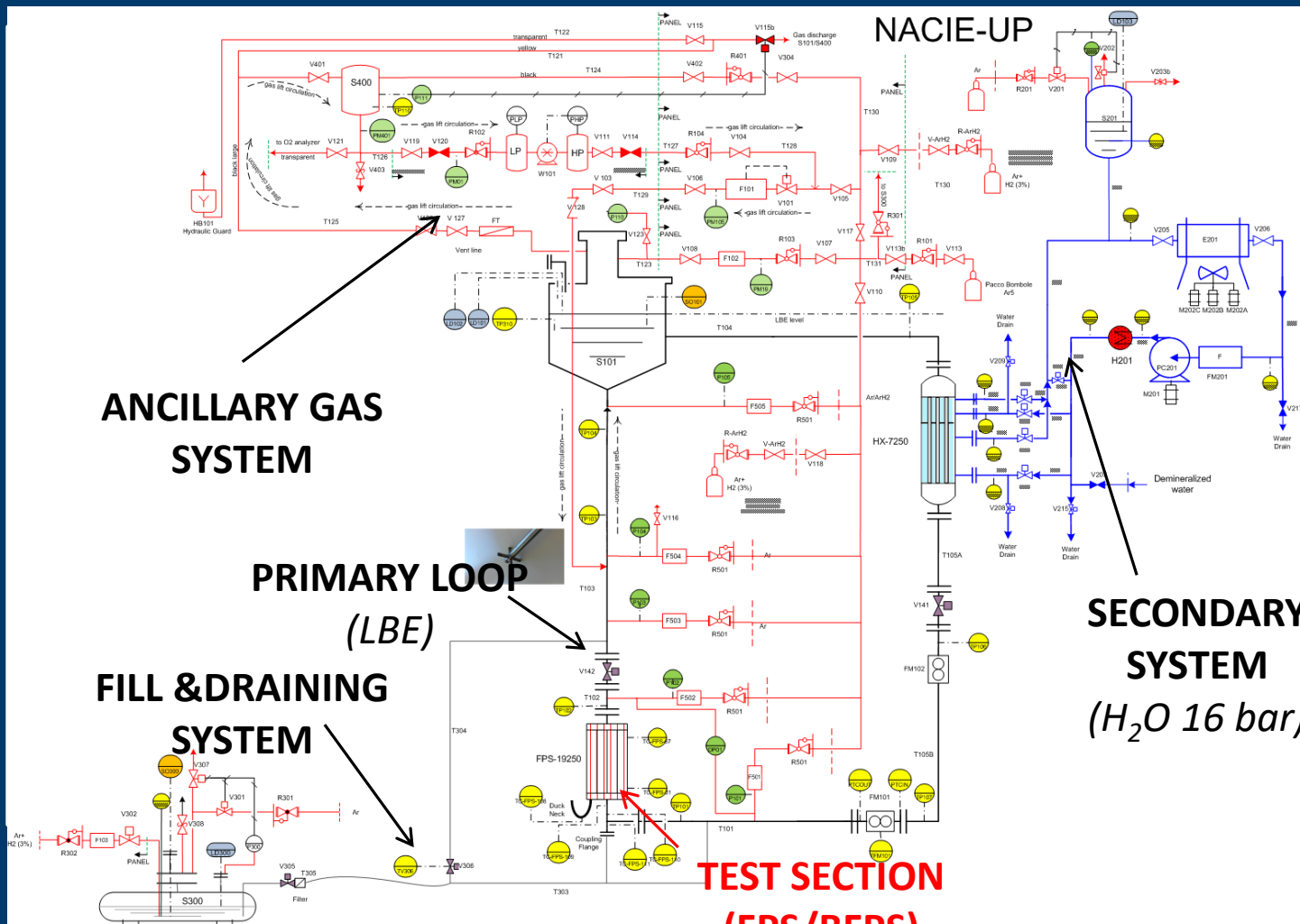
# Summary

- **NACIE-UP facility**
  - **Fuel Pin Bundle Simulator**
- **Experimental test matrix**
- **Experimental results**
  - **Comparison between ADP10 & ADP06**
  - **FPS temperature - Test ADP07**
- **Conclusions**



## NACIE-UP Facility – Primary loop

Composed by heat source (FPS), heat sink ( $H_2O$  Hx), expansion vessel, prototypical thermal flow meter



**ANCILLARY GAS SYSTEM**

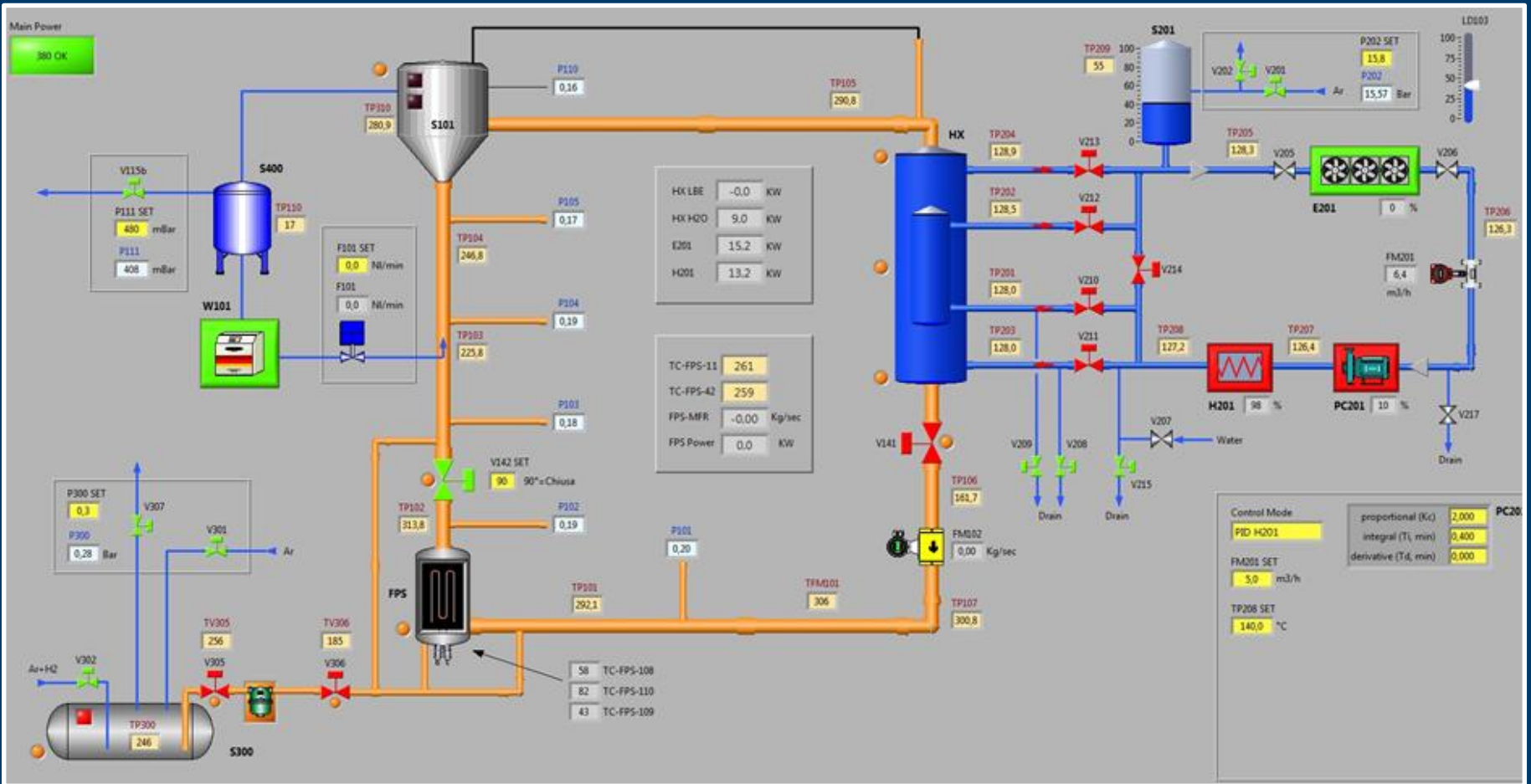
**PRIMARY LOOP (LBE)**

**FILL & DRAINING SYSTEM**

**SECONDARY SYSTEM (H<sub>2</sub>O 16 bar)**

**TEST SECTION (FPS/BFPS)**

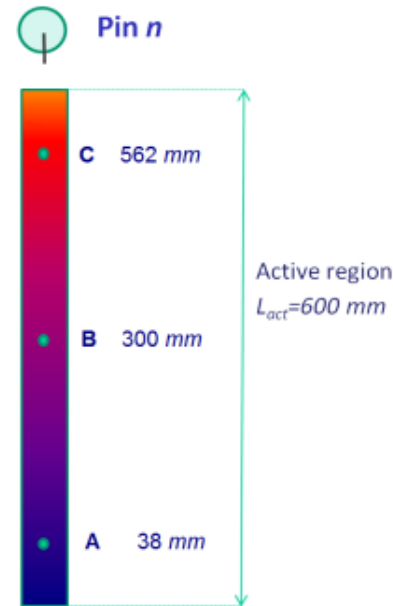
# NACIE-UP Facility – P&ID



# NACIE-UP PLC

Schematic layout of the primary (LBE) and secondary (H<sub>2</sub>O) systems, of the gas system and of the fill & drain system

# The Fuel Pin bundle Simulator



|              |                     |
|--------------|---------------------|
| $D_{pin}$    | 6.55 mm             |
| $P$          | 8.4 mm              |
| $P/D$        | 1.2824              |
| $d$          | 1.75 mm             |
| $P_{wire}$   | 262 mm              |
| $L_{tot}$    | 2000 mm             |
| $L_{active}$ | 600 mm              |
| $D_{H,nom}$  | 3.84 mm             |
| $q''_{max}$  | 1 MW/m <sup>2</sup> |

- **11 instrumented pins**
- **52 TCs** (0.35 mm thick) - **wall embedded thermocouples location**
- **15 TCs** (0.5 mm thick) - **5 instrumented sub-channels**
- Instrumentation distributed along three axial positions (A, B, C):  **$z = 38, 300, 562$  mm** from the beginning of the active length
- Pin 3 instrumented with wall embedded TCs every 43.66 mm (13 TCs)

# Instrumentation

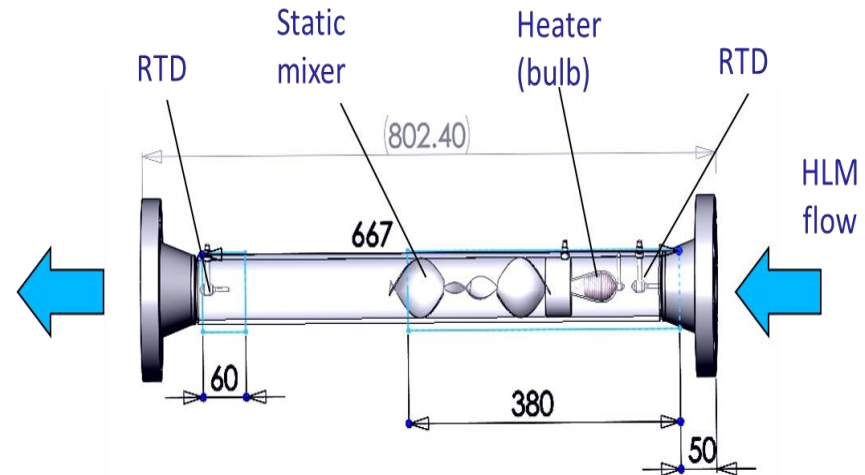
Some instrumentation is installed in the loop:

- Prototypical thermal flow meter
- loop thermocouples
- Test section FPS thermocouples (bulk and wall)

# Thermal Flow Meter



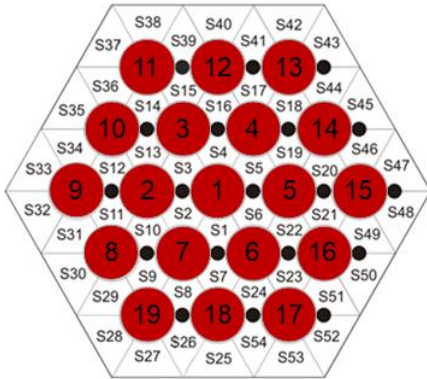
- A prototypical thermal flow meter for liquid metals was developed by ENEA in collaboration with Thermocoax
- **It is made by a flanged pipe (SS) with an heater technological development by THX (a few kW), a static mixer, 2 RTD and an internal RTD in the bulb**
- Low pressure losses
- No limiting working temperature
- Specific DACS developed
- **Accurate at low and medium flow rates (0-15 kg/s)**
- **Range can be easily extended**





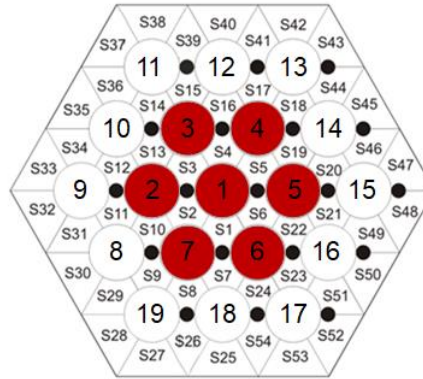
# Experimental test matrix

## TEST ADP 10



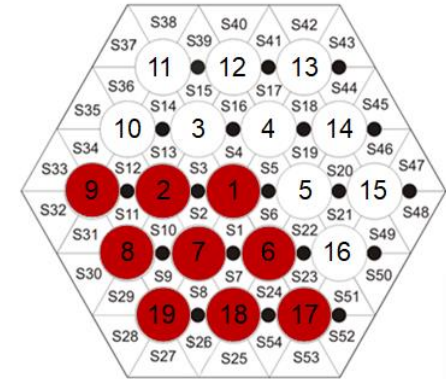
- 19 active pins
- FPS power **30 kW**
- $q_w'' \approx 127.9 \text{ kW/m}^2$
- $\dot{m}_{gas} = 10 \text{ NI/min}$   
→ 0 NI/min
- $\dot{m}_{H_2O} = 10 \text{ m}^3/\text{h}$
- $T_{in, H_2O} = 170 \text{ }^\circ\text{C}$

## TEST ADP 06



- 7 active pins
- FPS power **30 kW**
- $q_w'' \approx 347.1 \text{ kW/m}^2$
- $\dot{m}_{gas} = 10 \text{ NI/min}$   
→ 0 NI/min
- $\dot{m}_{H_2O} = 10 \text{ m}^3/\text{h}$
- $T_{in, H_2O} = 170 \text{ }^\circ\text{C}$

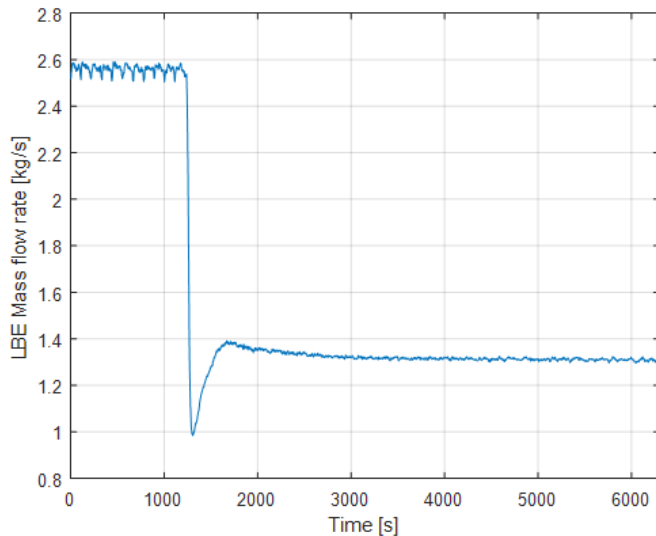
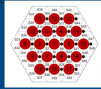
## TEST ADP 07



- 9 active pins
- FPS power **38 kW**
- $q_w'' \approx 342.0 \text{ kW/m}^2$
- $\dot{m}_{gas} = 10 \text{ NI/min}$   
→ 0 NI/min
- $\dot{m}_{H_2O} = 10 \text{ m}^3/\text{h}$
- $T_{in, H_2O} = 170 \text{ }^\circ\text{C}$

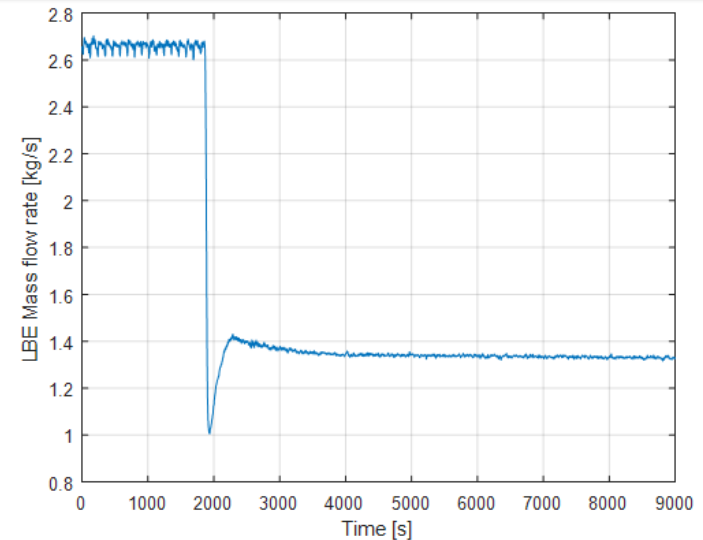
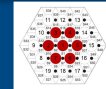
# Experimental results - LBE mass flow rate

## TEST ADP 10



| Test ADP 10                  | Steady state 1 |              | Steady state 2 |              |
|------------------------------|----------------|--------------|----------------|--------------|
| Variable                     | Data           | $\sigma$ [%] | Data           | $\sigma$ [%] |
| $M_{\text{gas}}$ [NI/min]    | 10.0           | 5.0          | 0.1            | 2.8          |
| $M_{\text{lbe}}$ [kg/s]      | 2.56           | 2.9          | 1.31           | 2.9          |
| $\Delta T_{\text{FPS}}$ [°C] | 72.0           | 0.9          | 140.6          | 0.2          |
| $Q_{\text{nom}}$ [W]         | 3.00E+04       | 0.2          | 3.00E+04       | 0.1          |
| $Q_{\text{eff}}$ [W]         | 2.71E+04       | 3.9          | 2.70E+04       | 3.7          |
| $Q_{\text{pre}}$ [W]         | 2236           | 18.0         | 2339           | 9.3          |
| $Q_{\text{tfm}}$ [W]         | 1915           | 0.2          | 1644           | 0.3          |

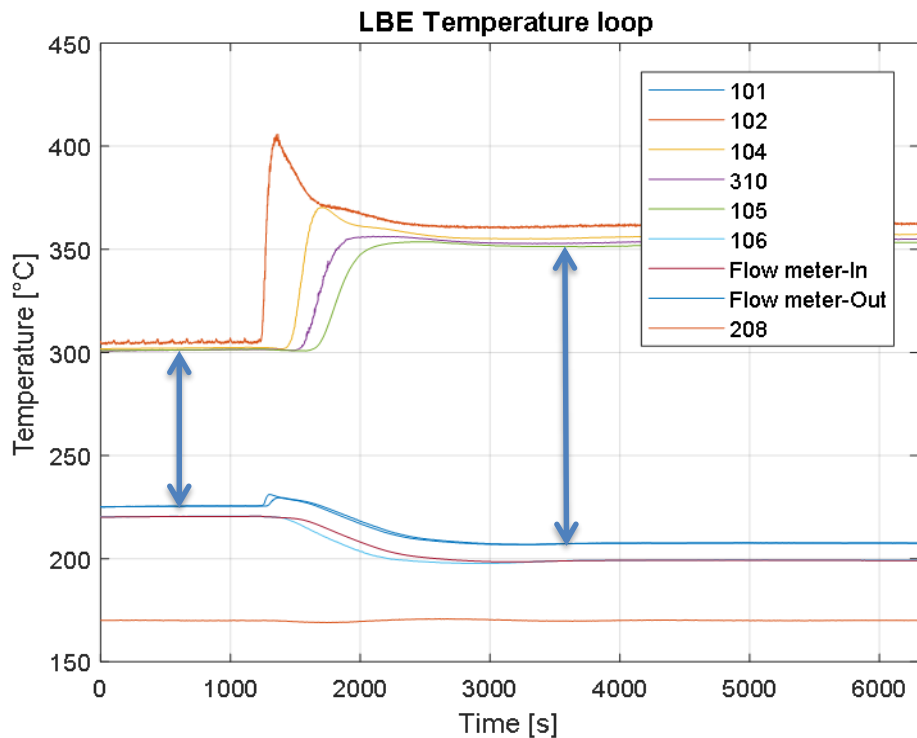
## TEST ADP 06



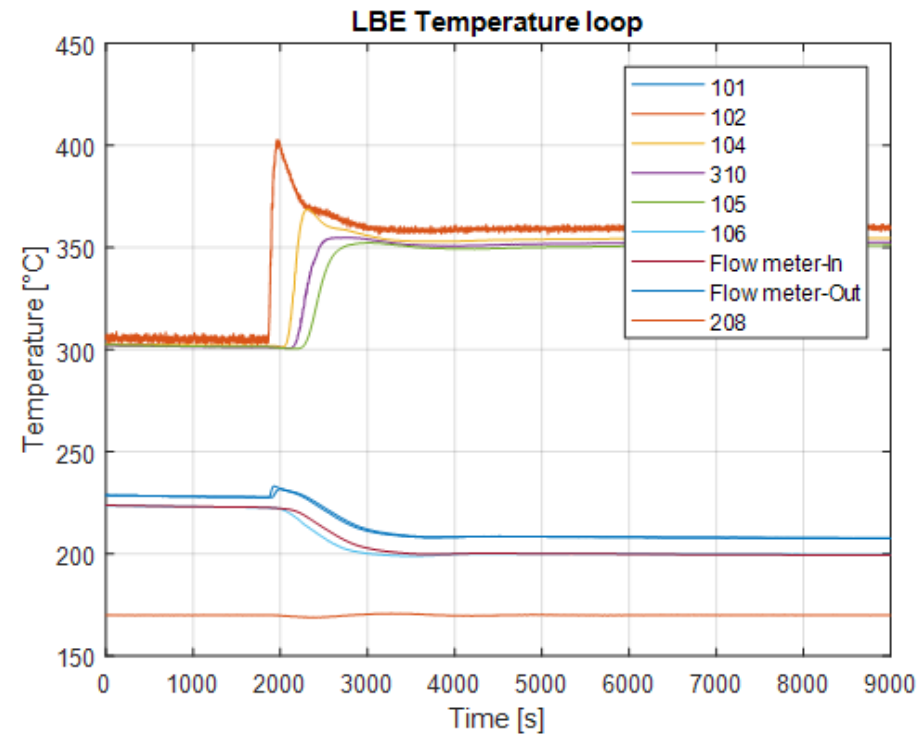
| Test ADP 06                  | Steady state 1 |              | Steady state 2 |              |
|------------------------------|----------------|--------------|----------------|--------------|
| Variable                     | Data           | $\sigma$ [%] | Data           | $\sigma$ [%] |
| $M_{\text{gas}}$ [NI/min]    | 10.0           | 5.0          | 0.0            | 2.8          |
| $M_{\text{lbe}}$ [kg/s]      | 2.66           | 2.9          | 1.33           | 2.9          |
| $\Delta T_{\text{FPS}}$ [°C] | 68.4           | 1.1          | 130.1          | 0.4          |
| $Q_{\text{nom}}$ [W]         | 3.00E+04       | 0.2          | 3.00E+04       | 0.2          |
| $Q_{\text{eff}}$ [W]         | 2.68E+04       | 3.9          | 2.54E+04       | 3.7          |
| $Q_{\text{pre}}$ [W]         | 2508           | 17.5         | 2675           | 8.6          |
| $Q_{\text{tfm}}$ [W]         | 1933           | 0.2          | 1652           | 0.3          |

# Experimental results – LBE temperature

## TEST ADP 10

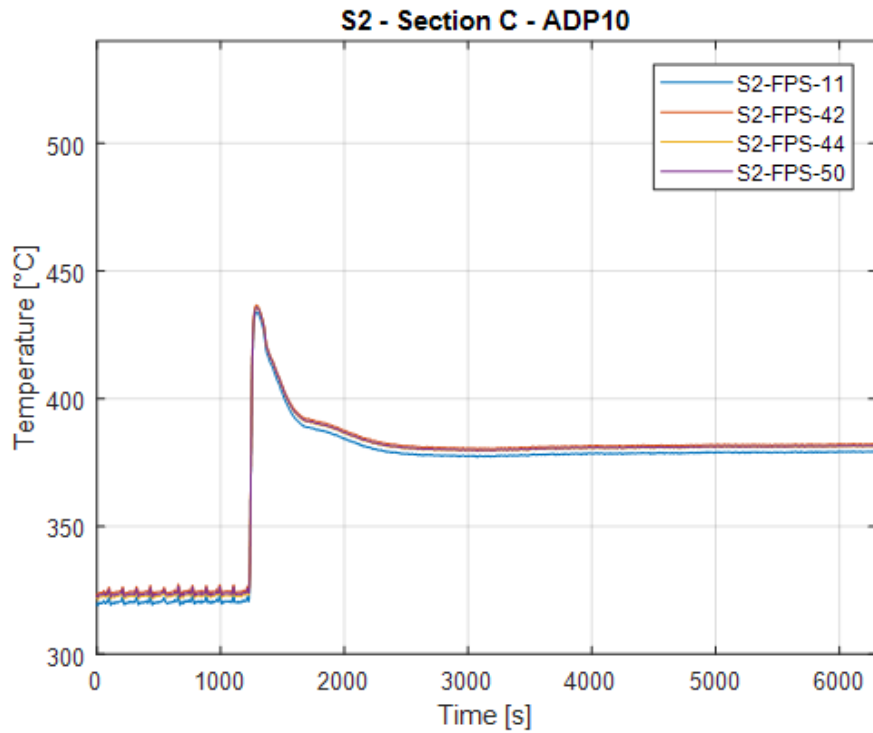


## TEST ADP 06

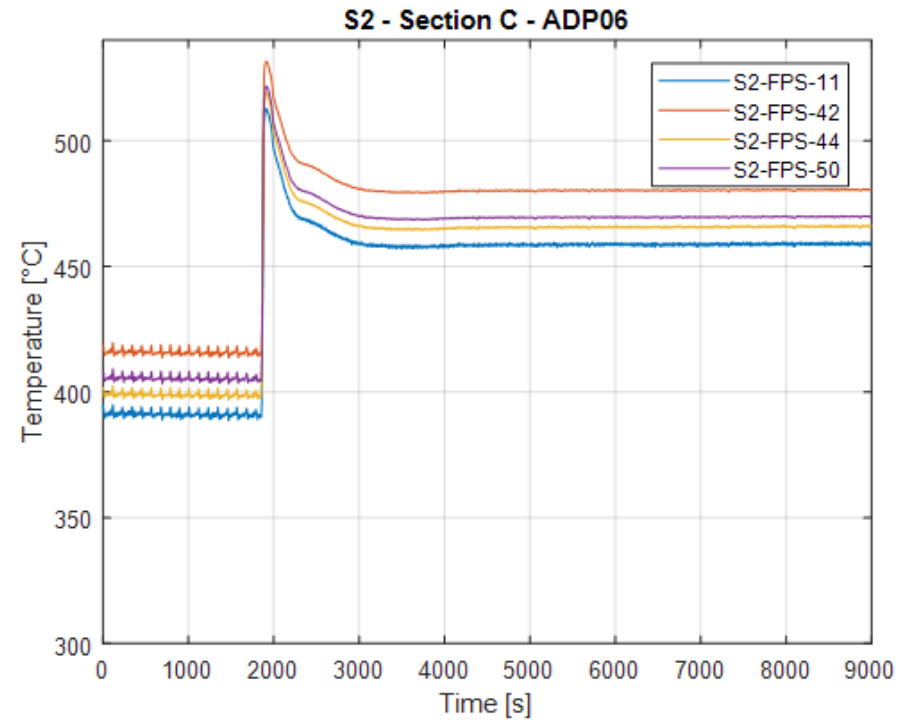


# Experimental results - FPS temperatures S2

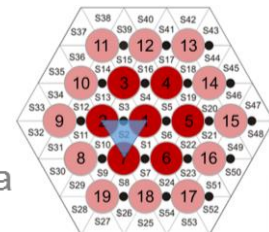
## TEST ADP 10



## TEST ADP 06



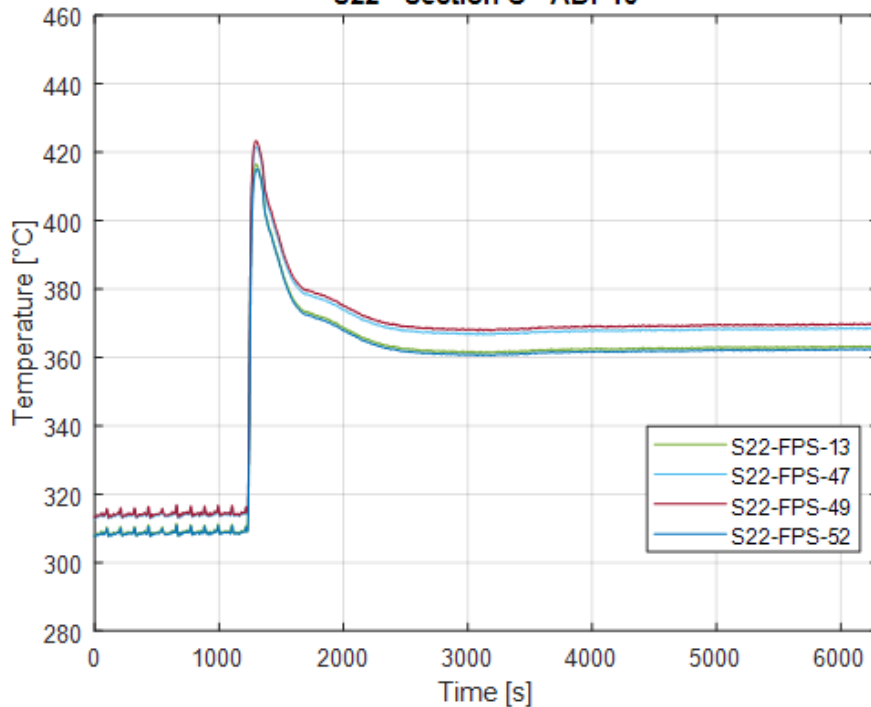
$z = 360 \text{ mm}$



# Experimental results - FPS temperatures S22

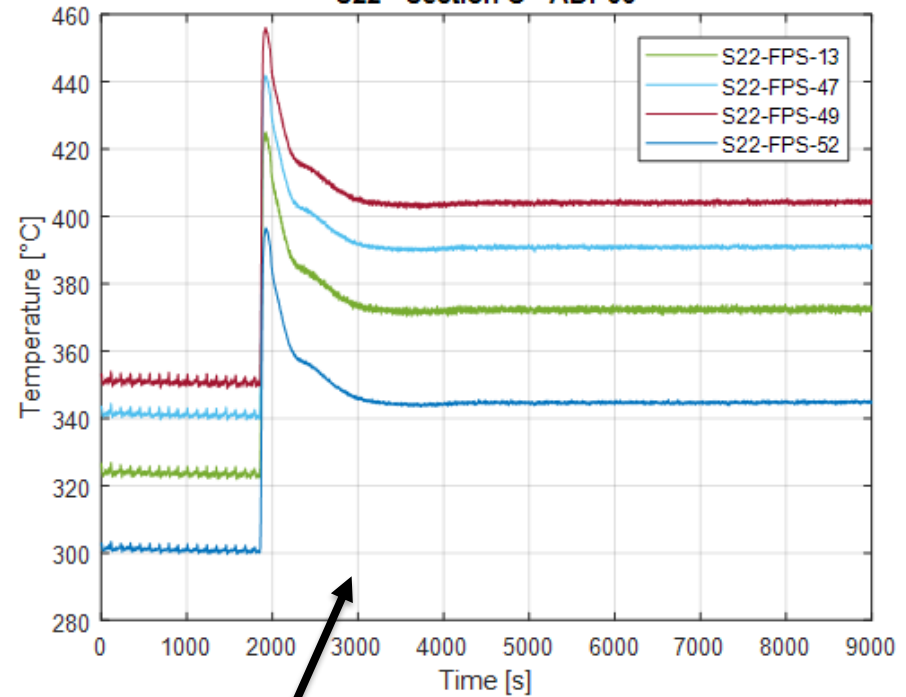
## TEST ADP 10

S22 - Section C - ADP10

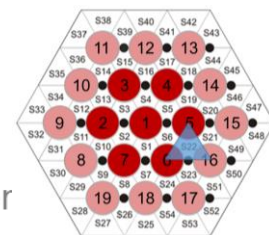


## TEST ADP 06

S22 - Section C - ADP06

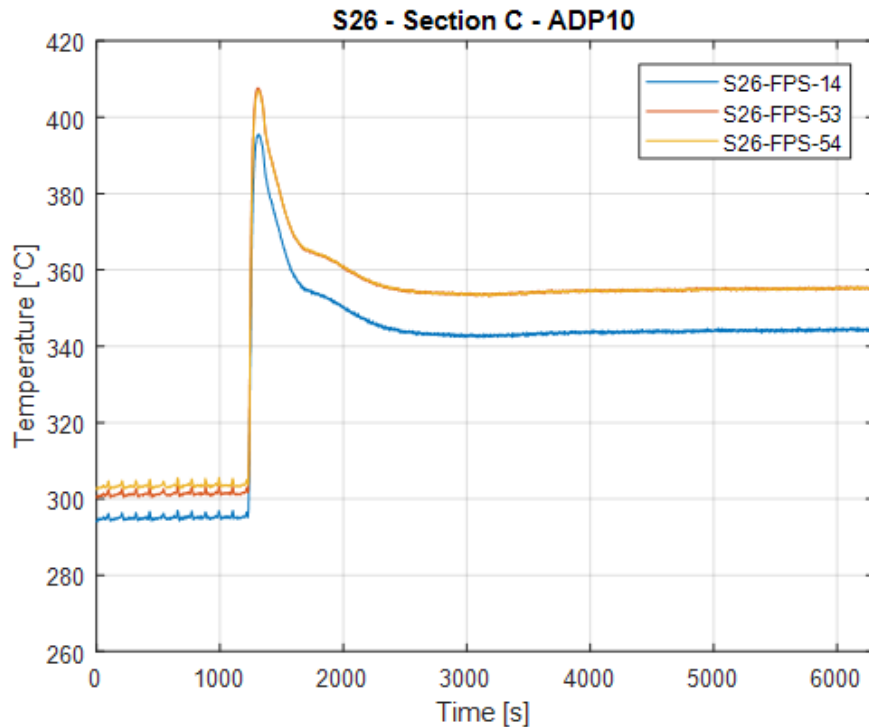


$z = 360\text{mm}$

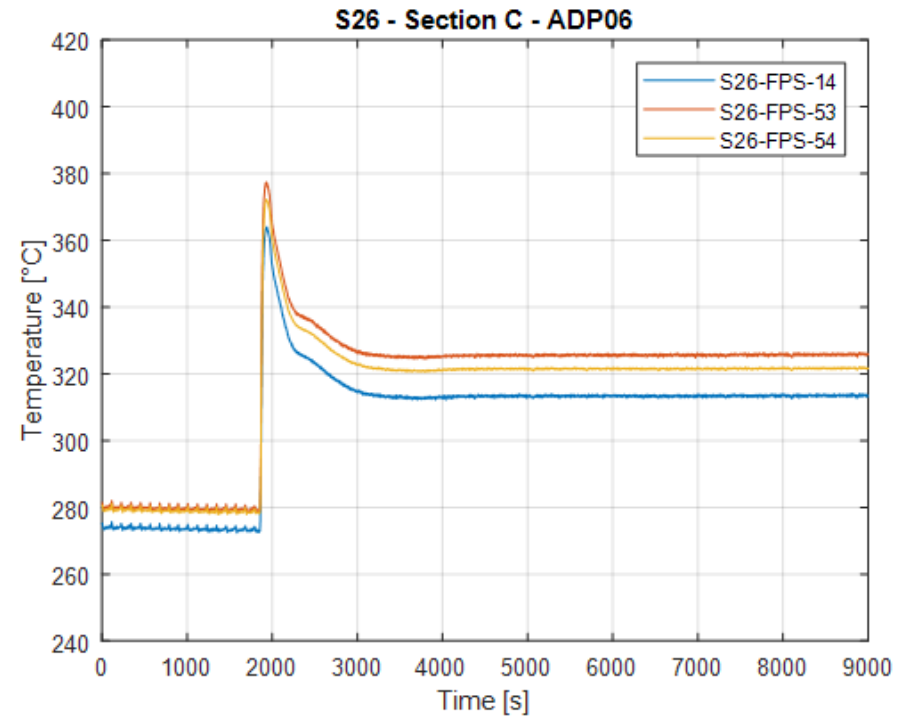


# Experimental results - FPS temperatures S26

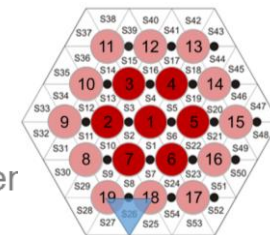
## TEST ADP 10



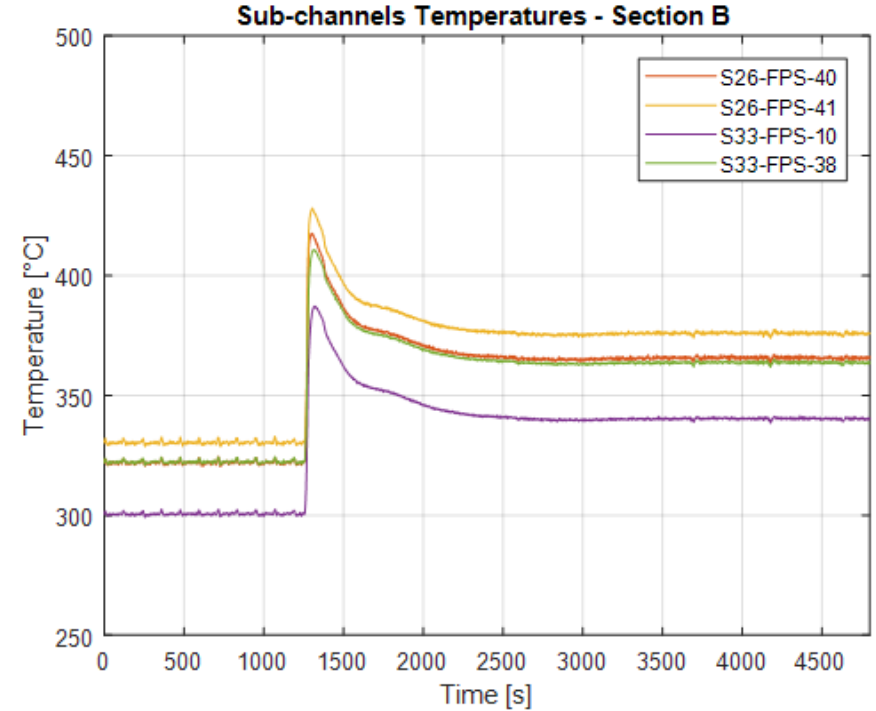
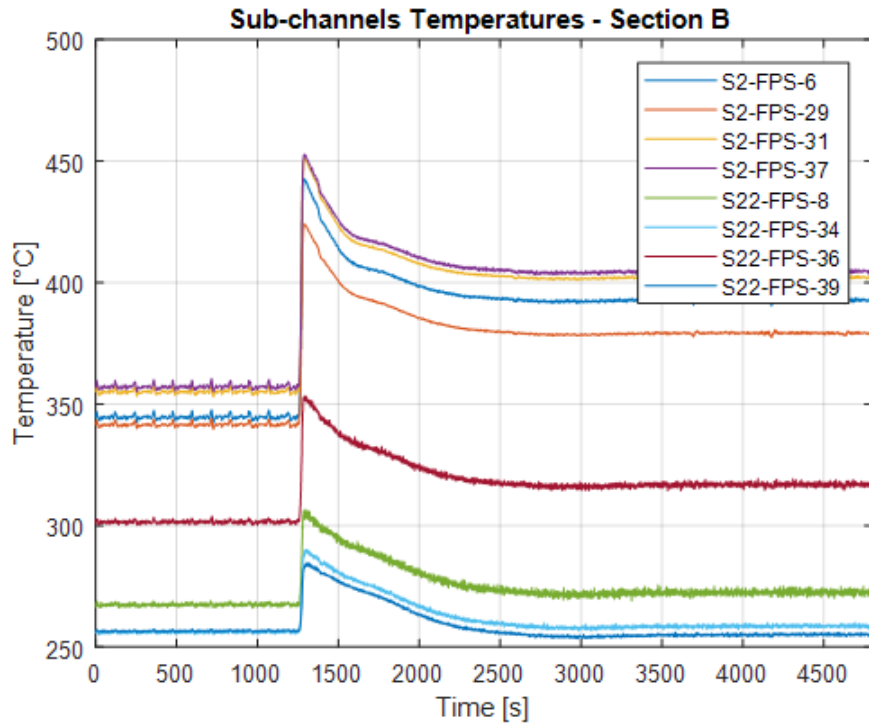
## TEST ADP 06



$z = 360\text{mm}$



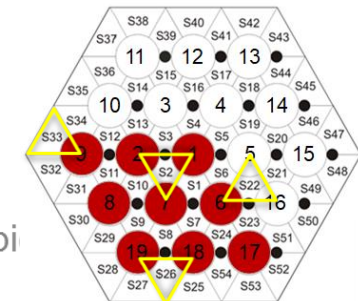
# Experimental results - ADP 07



**Internal sub-channels S2 & S22**

**External sub-channels S26 and S33**

$z = 300 \text{ mm}$



# TESTS PERFORMED

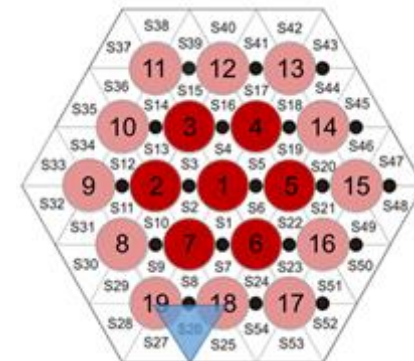


- For all cases non-dimensional numbers were computed according to the definitions and error propagation theory was applied to compute standard deviation

- For a generic function  $Y=f(X_i)$  
$$\sigma_Y^2 = \sum_{i=1}^n \left( \frac{\partial f}{\partial X_i} \cdot \sigma_{X_i} \right)^2$$

- This theory is applied to Re, Pe, Nu numbers error evaluation

- The average Nusselt number is computed as 
$$\text{Nu} = \frac{q''}{(\bar{T}_w - \bar{T}_b)} \cdot \frac{D_{H, \text{nom}}}{k}$$
 by averaging wall and bulk temperatures using weights





# TESTS PERFORMED



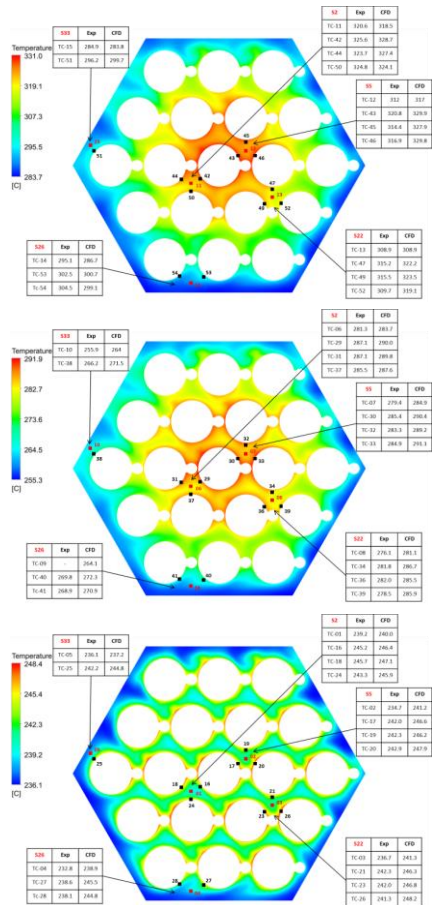
- ADP00: non-dimensional results

| Variable          | Test ADP 00 - Steady state 1 |          |              |           |          |              |           |          |              |
|-------------------|------------------------------|----------|--------------|-----------|----------|--------------|-----------|----------|--------------|
|                   | Section A                    |          |              | Section B |          |              | Section C |          |              |
|                   | Data                         | $\sigma$ | $\sigma$ [%] | Data      | $\sigma$ | $\sigma$ [%] | Data      | $\sigma$ | $\sigma$ [%] |
| Re                | 6897                         | 536      | 7.8          | 7488      | 581.6    | 7.8          | 8117      | 630.5    | 7.8          |
| Pr                | 0.029                        | 0.003    | 9.8          | 0.026     | 0.002549 | 9.8          | 0.023     | 0.0      | 9.8          |
| Pe                | 203                          | 25       | 12.5         | 195       | 24.36    | 12.5         | 186       | 23.3     | 12.5         |
| Nu                | 8.5                          | 0.8      | 8.9          | 5.0       | 0.4716   | 9.3          | 5.1       | 0.6      | 11.2         |
| Nu <sub>K</sub>   | 6.1                          | 0.0      | 0.1          | 6.1       | 0.008901 | 0.1          | 6.0       | 0.0      | 0.1          |
| Nu <sub>U</sub>   | 10.7                         | 0.0      | 0.1          | 10.6      | 0.01065  | 0.1          | 10.6      | 0.0      | 0.1          |
| Nu <sub>S2</sub>  | 9.7                          | 1.0      | 9.9          | 9.4       | 1.598    | 16.9         | 11.6      | 3.2      | 27.8         |
| Nu <sub>S5</sub>  | 6.5                          | 0.5      | 8.4          | 10.0      | 1.723    | 17.2         | 6.3       | 1.1      | 16.6         |
| Nu <sub>S22</sub> | 9.7                          | 0.9      | 9.6          | 8.2       | 1.206    | 14.8         | 7.1       | 1.2      | 17.2         |
| Nu <sub>S26</sub> | 8.7                          | 0.8      | 9.3          | -         | -        | -            | 5.2       | 0.6      | 11.3         |
| Nu <sub>S33</sub> | 7.7                          | 0.7      | 9.6          | 4.2       | 0.3715   | 8.9          | 3.7       | 0.4      | 9.7          |

| Variable          | Test ADP 00 - Steady state 2 |          |              |           |          |              |           |          |              |
|-------------------|------------------------------|----------|--------------|-----------|----------|--------------|-----------|----------|--------------|
|                   | Section A                    |          |              | Section B |          |              | Section C |          |              |
|                   | Data                         | $\sigma$ | $\sigma$ [%] | Data      | $\sigma$ | $\sigma$ [%] | Data      | $\sigma$ | $\sigma$ [%] |
| Re                | 3457                         | 268      | 7.7          | 4060      | 315      | 7.7          | 4647      | 360      | 7.7          |
| Pr                | 0.030                        | 0.003    | 9.8          | 0.024     | 0.002    | 9.8          | 0.019     | 0.002    | 9.8          |
| Pe                | 105                          | 13       | 12.5         | 97        | 12       | 12.5         | 89        | 11       | 12.5         |
| Nu                | 6.9                          | 0.5      | 7.9          | 4.4       | 0.3      | 7.6          | 4.1       | 0.3      | 7.8          |
| Nu <sub>K</sub>   | 5.4                          | 0.0      | 0.2          | 5.4       | 0.0      | 0.2          | 5.3       | 0.0      | 0.2          |
| Nu <sub>U</sub>   | 9.9                          | 0.0      | 0.1          | 9.9       | 0.0      | 0.1          | 9.8       | 0.0      | 0.1          |
| Nu <sub>S2</sub>  | 8.2                          | 0.7      | 8.2          | 9.1       | 0.8      | 8.7          | 13.9      | 1.8      | 12.9         |
| Nu <sub>S5</sub>  | 5.3                          | 0.4      | 7.7          | 9.6       | 0.9      | 9.2          | 5.5       | 0.5      | 8.7          |
| Nu <sub>S22</sub> | 8.7                          | 0.7      | 8.2          | 6.7       | 0.6      | 8.4          | 5.9       | 0.5      | 8.5          |
| Nu <sub>S26</sub> | 5.9                          | 0.5      | 8.1          | -         | -        | -            | 3.3       | 0.3      | 7.8          |
| Nu <sub>S33</sub> | 6.3                          | 0.5      | 8.4          | 3.6       | 0.3      | 7.6          | 3.1       | 0.2      | 7.7          |

- Average Nusselt number close to Kazimi
- Local nusselt number close to Ushakov (infinite lattice)

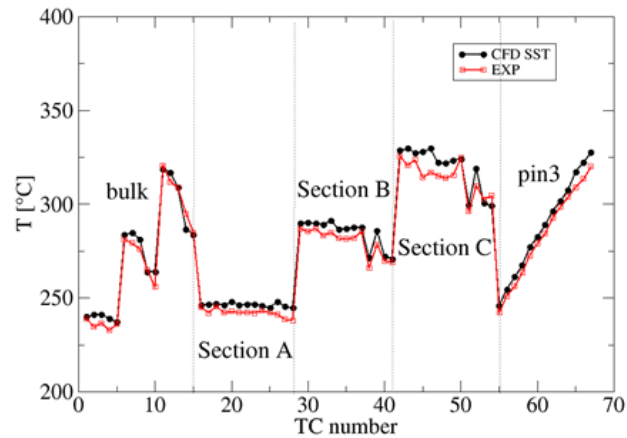
# CFD COMPARISON



Section C

Section B

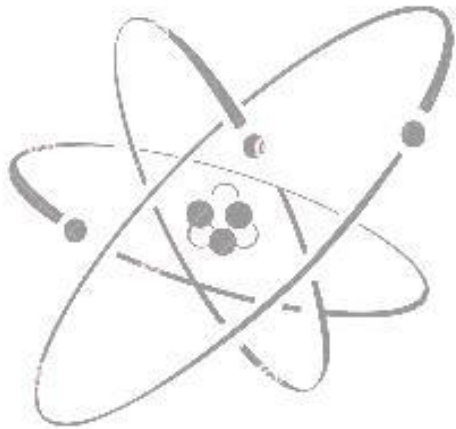
Section A



Results and exp: ICONE papers + NED submission

# Conclusions

- Experimental tests with gas flow rate transition have been performed in NACIE-UP facility;
- A first reference test was characterized by all 19 pins on;
  - Lower local Nu in external sub-channels (S26 and S33)
  - Higher values in the inner sub-channels (S2, S5 and S22)
- A second test, characterized by the same power distributed in among the 7 central pins (higher wall heat flux) was compared to the reference one;
  - Same integral parameters between the two tests
  - S2, S5 and S22 were hotter in the second test, S26 and S33 colder (off during the second test)
- A third test was characterized by power distribution localized in a limited part of the bundle (triangular sections), with pin-wall heat flux comparable with the second test;
  - FPS temperature distribution affected by the power distribution
  - Non-conventional behaviour was noticed in S2
- Obtained experimental data was used to characterize bundle (by computing the heat transfer coefficient). The collected system data can be used to qualify STH codes, whereas the local fuel bundle data (especially the ones from dissymmetric tests) can be useful for the validation of CFD codes and coupled STH/CFD methods for HLM systems.



***Ivan Di Piazza***  
***ENEA C.R. Brasimone***

***Ivan.dipiazza@enea.it***



1101 0110 1100  
0101 0010 1101  
0001 0110 1110  
1101 0010 1101  
1111 1010 0000



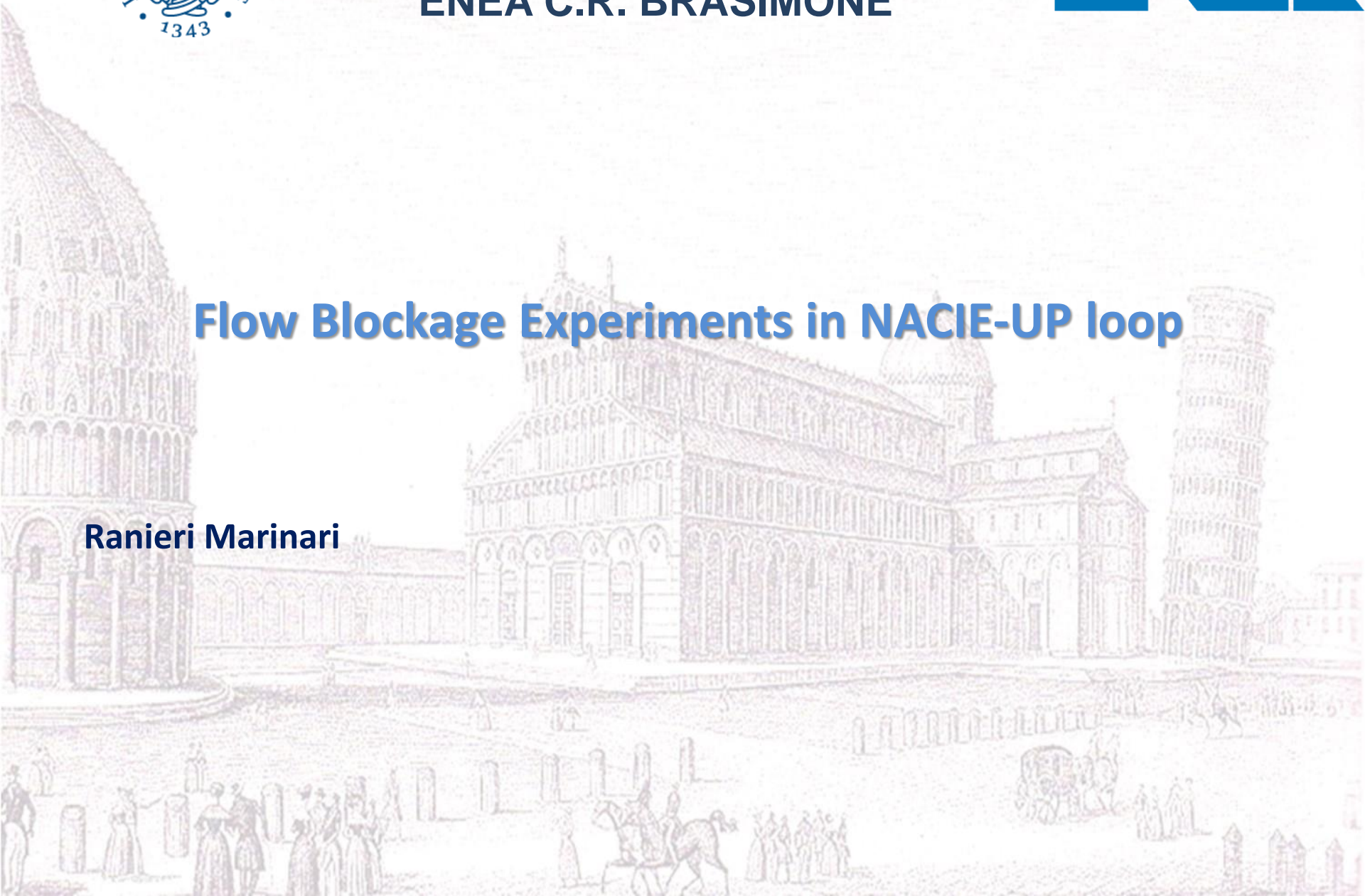


**UNIVERSITA' DEGLI STUDI DI PISA**  
**ENEA C.R. BRASIMONE**



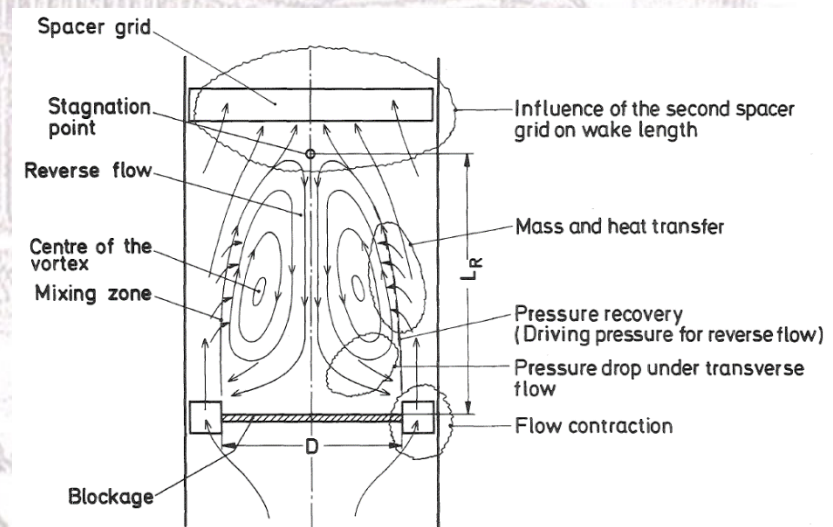
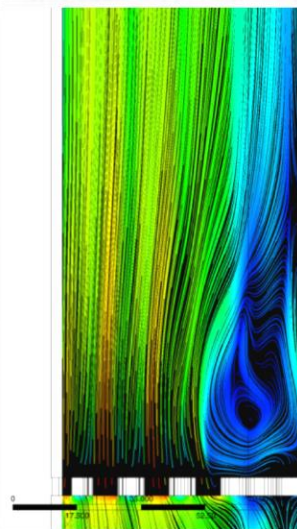
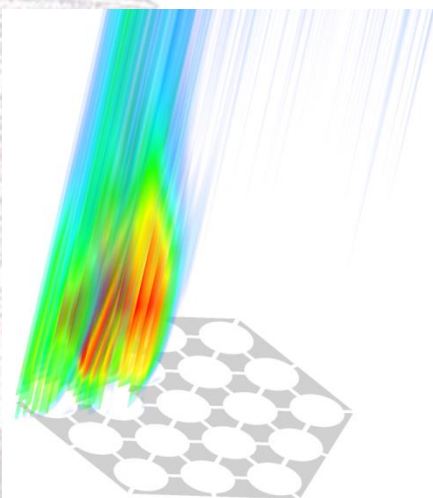
## **Flow Blockage Experiments in NACIE-UP loop**

**Ranieri Marinari**



- Introduction
- NACIE-UP facility
- Pre-test CFD analysis
- Instrumentation & experimental test matrix
- Pre-test Code-to-code CFD comparison
- Ongoing activity: experimental campaign
- Preliminary post-test analysis
- Conclusions

- In the context of GEN-IV heavy liquid metal-cooled reactors safety studies, the flow blockage in a fuel sub-assembly is considered one of the main issues to be addressed and one of the most important and realistic accident for Lead Fast Reactors (LFR) fuel assembly.
- The blockage in a fast reactor Fuel Assembly (FA) may have serious effects on the safety of the reactor leading to the FA damaging or melting. The external or internal blockage of the FA may impair the correct cooling of the fuel pins, be the root cause of anomalous heating of the cladding and of the wrapper and potentially impact also fuel pins not directly located above or around the blocked area.
- Fuel Assembly blockage (total or partial) has been extensively analysed since the early days of fast reactors. While many of these studies refer to Sodium Fast Reactors, the results may be a starting point for LFRs too. The main focus of these analyses is determining the effects of a blockage on the temperature (cladding and coolant) and pressure (coolant) inside the FA as well as at the outlet of the subassembly, and the optimal detection techniques..



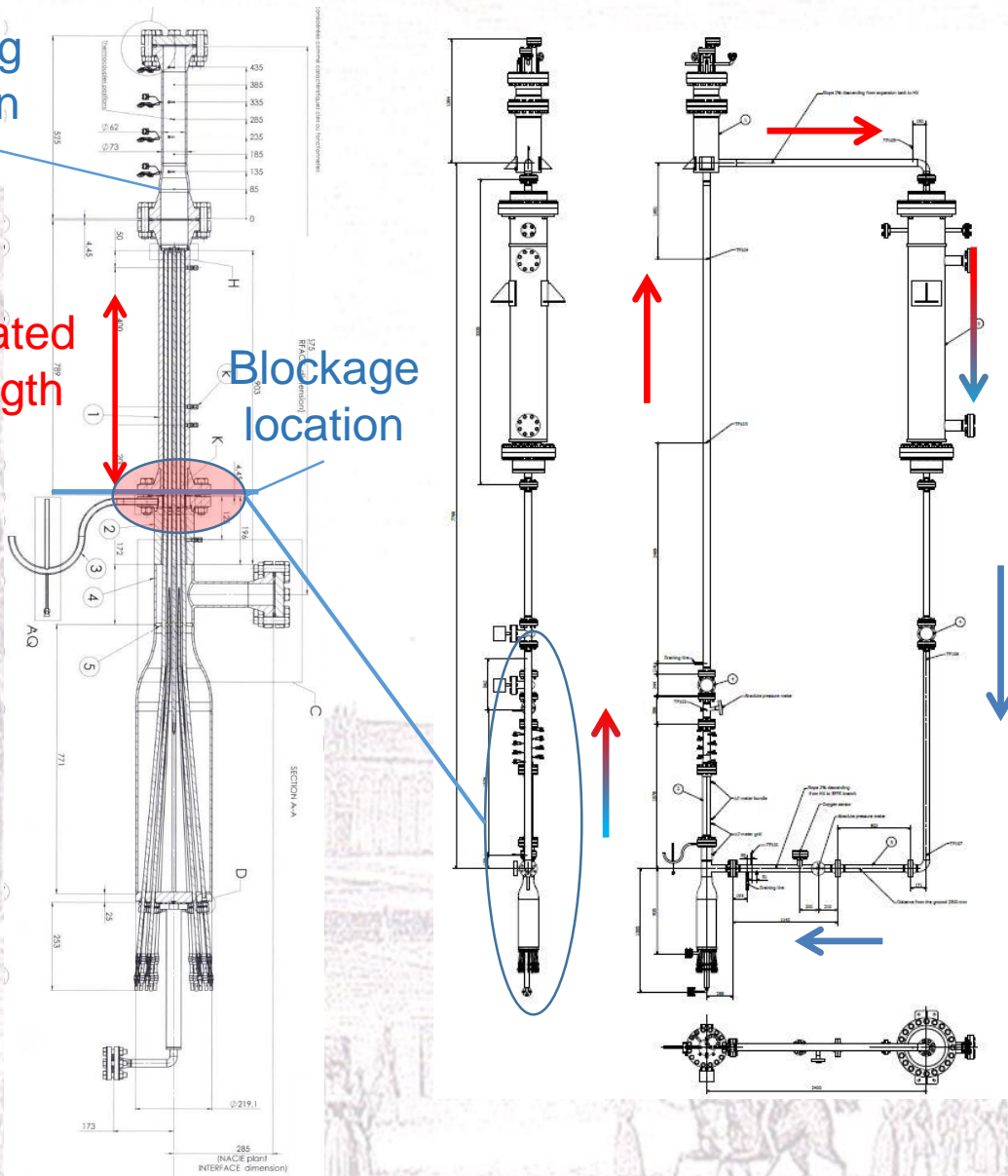
- *Schultheiss (1977)* studied the formation and growth of local blockages in grid spaced fast reactors. Axial growth of blockage is found to be predominant in wire wrapped bundle, whereas radial growth is predominant in grid spaced bundle. The formation of major local blockages in normal fuel element geometries is mainly be caused by fuel expelled after a cladding tube failure.
- Experimental studies of local flow blockage in a LMFBR fuel assembly were carried out by *Nakamura et al. (1980)* using a simulating model in a water test loop. The experiments were conducted in a 61-pin bundle (quadruple scale model of a MONJU core subassembly) containing a planar blockage without leakage flow. The central and edge blockage were used. The wake flow behind the blockage was visualized with dye or air bubble injection to grasp the flow characteristics. Analyzing flow distributions and velocity measurements behind the blockage, it was concluded that the recirculating flow behind the central and edge blockages is stable with no large oscillations discharging vortices. The recirculating flow is similar with those behind a plate or a disk in a free stream.
- Thermal hydraulic features of blocked wire wrapped fuel subassemblies have been investigated through CFD approach by *Raj et al. (2016)*. They found that: the extent of the wake zone behind the blockage increases with blockage radius, Clads partially exposed to blockage are subjected to large circumferential temperature variation and the resulting thermal stress, the total flow reduction is < 2.5% for all blockages that can lead to local sodium boiling. This suggests that global bulk sodium TC at the outlet of the subassembly are unlikely to detect slowly growing internal porous blockages but the wake-induced temperature non-uniformity persists even up to three helical pitch length. This suggests that the sodium temperature non-uniformity at the bundle exit can serve as an efficient blockage indicator. The peak clad temperature is found to be a strong function of porosity (higher clad temperature for lower porosity),



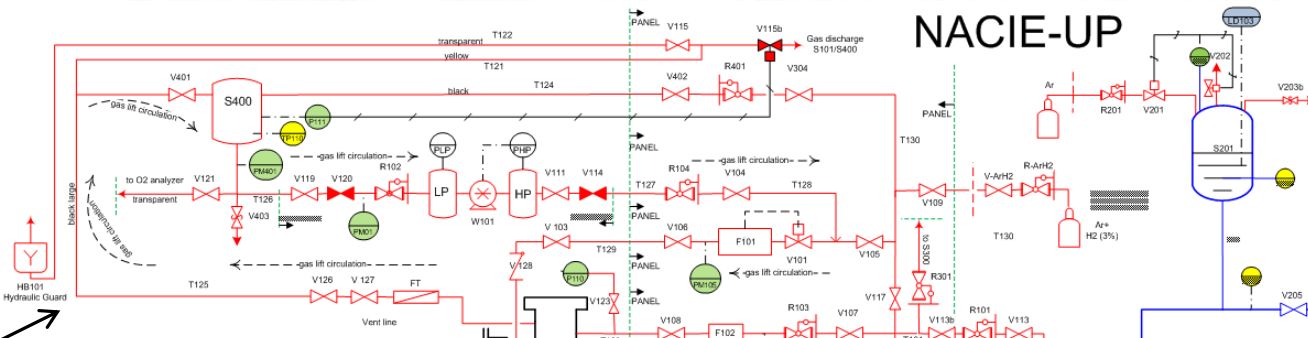
Mixing region

Heated length

Blockage location



| Parameters                 | BFP S | ALFRED FA |
|----------------------------|-------|-----------|
| $d_{pin} [mm]$             | 10    | 10.5      |
| $p/d$                      | 1.4   | 1.32      |
| Wall heat Flux $[MW/m^2]$  | 0.7   | 0.7-1     |
| Max subch velocity $[m/s]$ | 0.8   | 1.1       |
| $N_{pin}$                  | 19    | 127       |
| $L_{active} [mm]$          | 600   | 600       |
| $L_{plenum} [mm]$          | 500   | 500       |

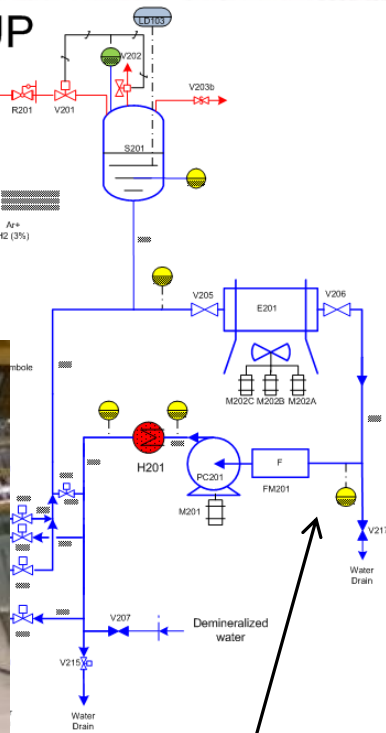
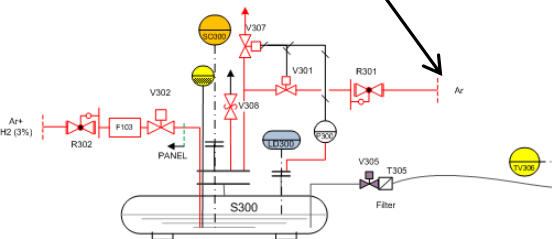


**ANCILLARY GAS SYSTEM**

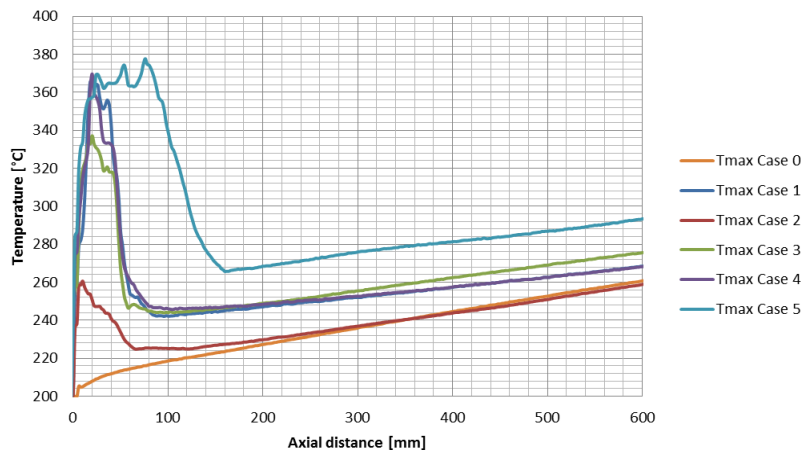
**PRIMARY LOOP (LBE)**

**TEST SECTION (BFPS)**

**FILL & DRAINING SYSTEM**

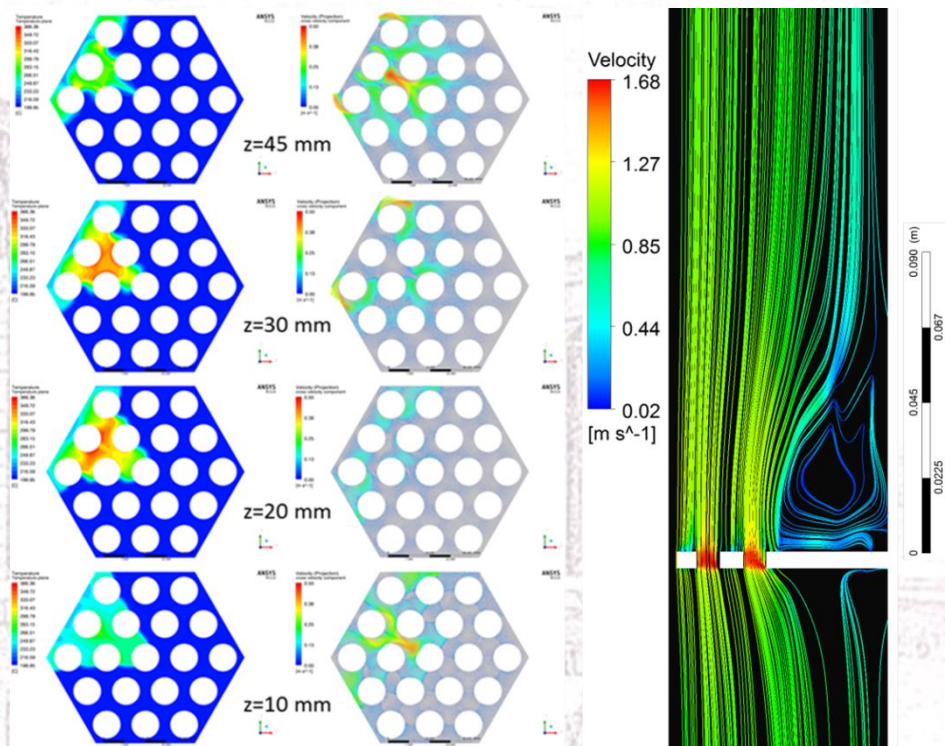
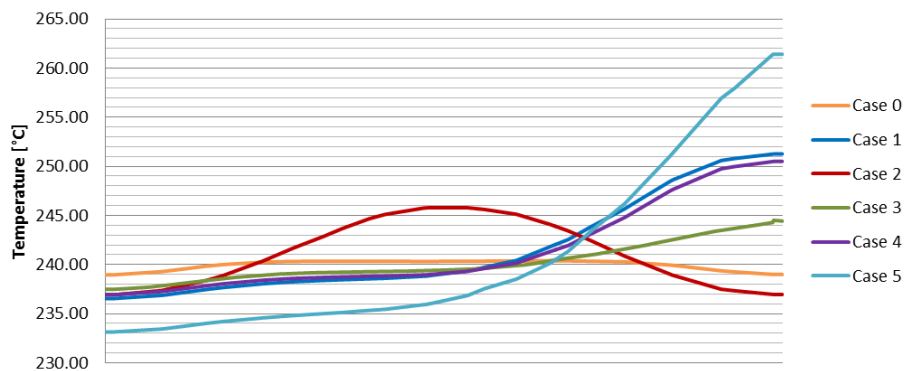


**SECONDARY SYSTEM (H<sub>2</sub>O 16 bar)**

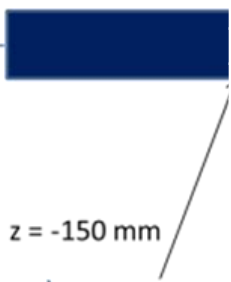
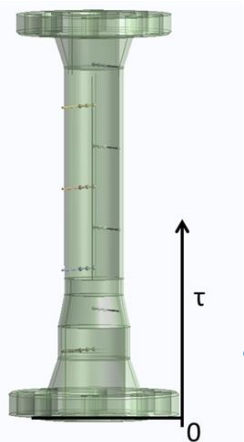


| Mesh     | M nodes [-] | f Darcy [-]    | Nu [-]       | $T_{pin,max}$ [°C] |
|----------|-------------|----------------|--------------|--------------------|
| A        | 10          | 0.01182        | 23.86        | 267.6              |
| B        | 15          | 0.01144        | 17.31        | 269.8              |
| <b>C</b> | <b>19</b>   | <b>0.01130</b> | <b>16.48</b> | <b>272.4</b>       |
| D        | 24          | 0.01131        | 16.52        | 272.6              |

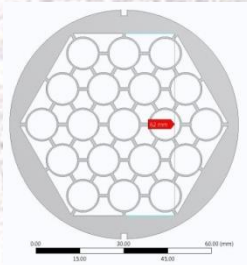
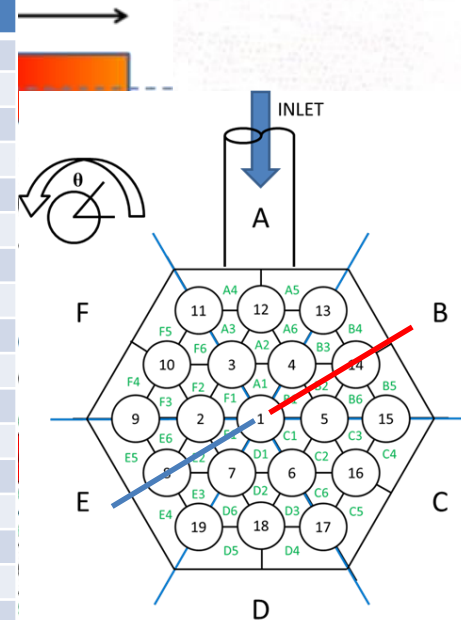
| Case | Blockage type | Mass flow rate [kg/s] | $Re_{BFPS}$ [-] | Power [kW] | Inlet temperature [°C] |
|------|---------------|-----------------------|-----------------|------------|------------------------|
| 0    | 0             | 16                    | 46663           | 94.2       | 200                    |
| 1    | 1             | 16                    | 46663           | 94.2       | 200                    |
| 2    | 2             | 16                    | 46663           | 94.2       | 200                    |
| 3    | 3             | 16                    | 46663           | 94.2       | 200                    |
| 4    | 4             | 16                    | 46663           | 94.2       | 200                    |
| 5    | 5             | 16                    | 46663           | 94.2       | 200                    |



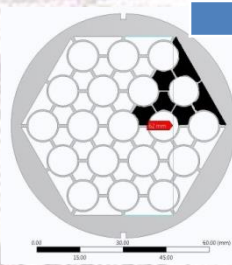
R. Marinari, I. Di Piazza, N. Forgione, F. Magugliani, "Pre-test CFD simulations of the NACIE-UP BFPS test section", Annals of Nuclear Energy 110 (2017), pp. 1060-1072.



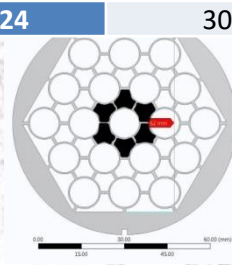
| TC name | r [mm] | τ [mm] | BFPS sector |
|---------|--------|--------|-------------|
| TC-1    | 0      | 85     | E           |
| TC-2    | 15     | 85     | E           |
| TC-3    | 30     | 85     | E           |
| TC-4    | 0      | 135    | B           |
| TC-5    | 15     | 135    | B           |
| TC-6    | 30     | 135    | B           |
| TC-7    | 0      | 185    | E           |
| TC-8    | 15     | 185    | E           |
| TC-9    | 30     | 185    | E           |
| TC-10   | 0      | 235    | B           |
| TC-11   | 15     | 235    | B           |
| TC-12   | 30     | 235    | B           |
| TC-13   | 0      | 285    | E           |
| TC-14   | 15     | 285    | E           |
| TC-15   | 30     | 285    | E           |
| TC-16   | 0      | 335    | B           |
| TC-17   | 15     | 335    | B           |
| TC-18   | 30     | 335    | B           |
| TC-19   | 0      | 385    | E           |
| TC-20   | 15     | 385    | E           |
| TC-21   | 30     | 385    | E           |
| TC-22   | 0      | 435    | B           |
| TC-23   | 15     | 435    | B           |
| TC-24   | 30     | 435    | B           |



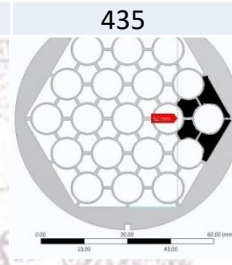
0



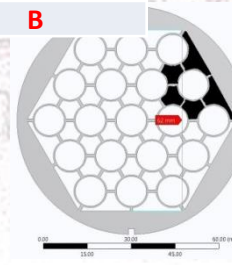
1



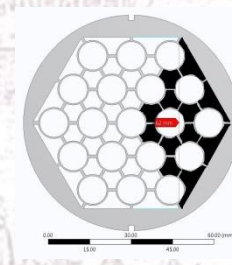
2



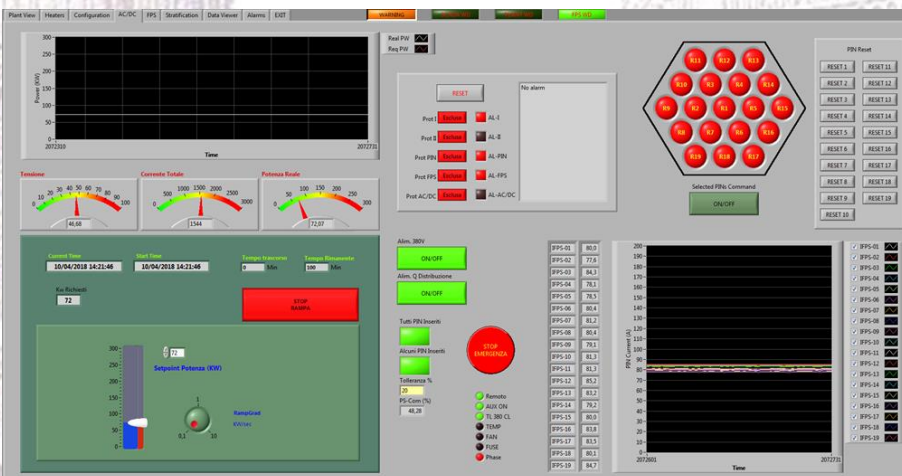
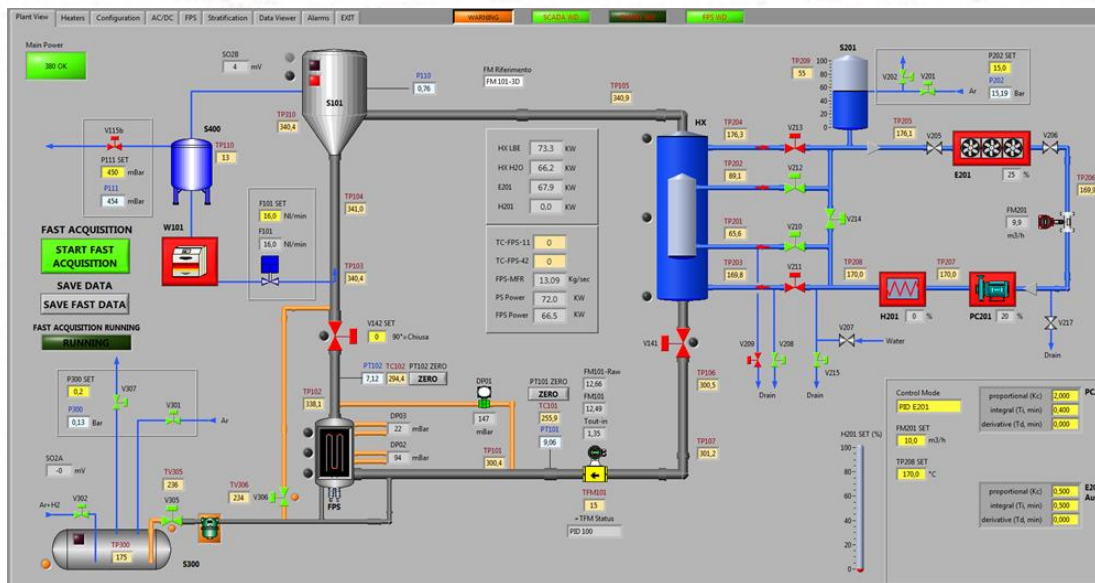
3



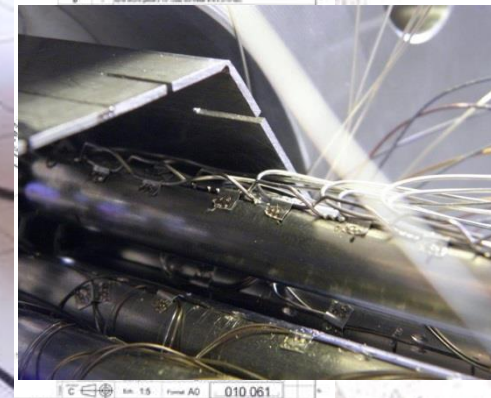
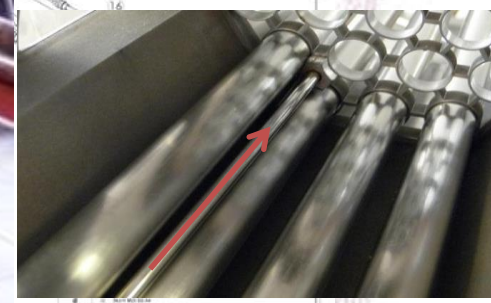
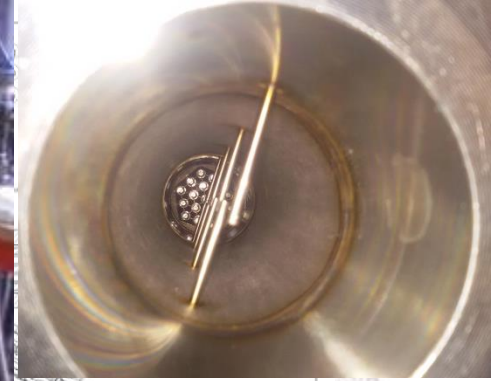
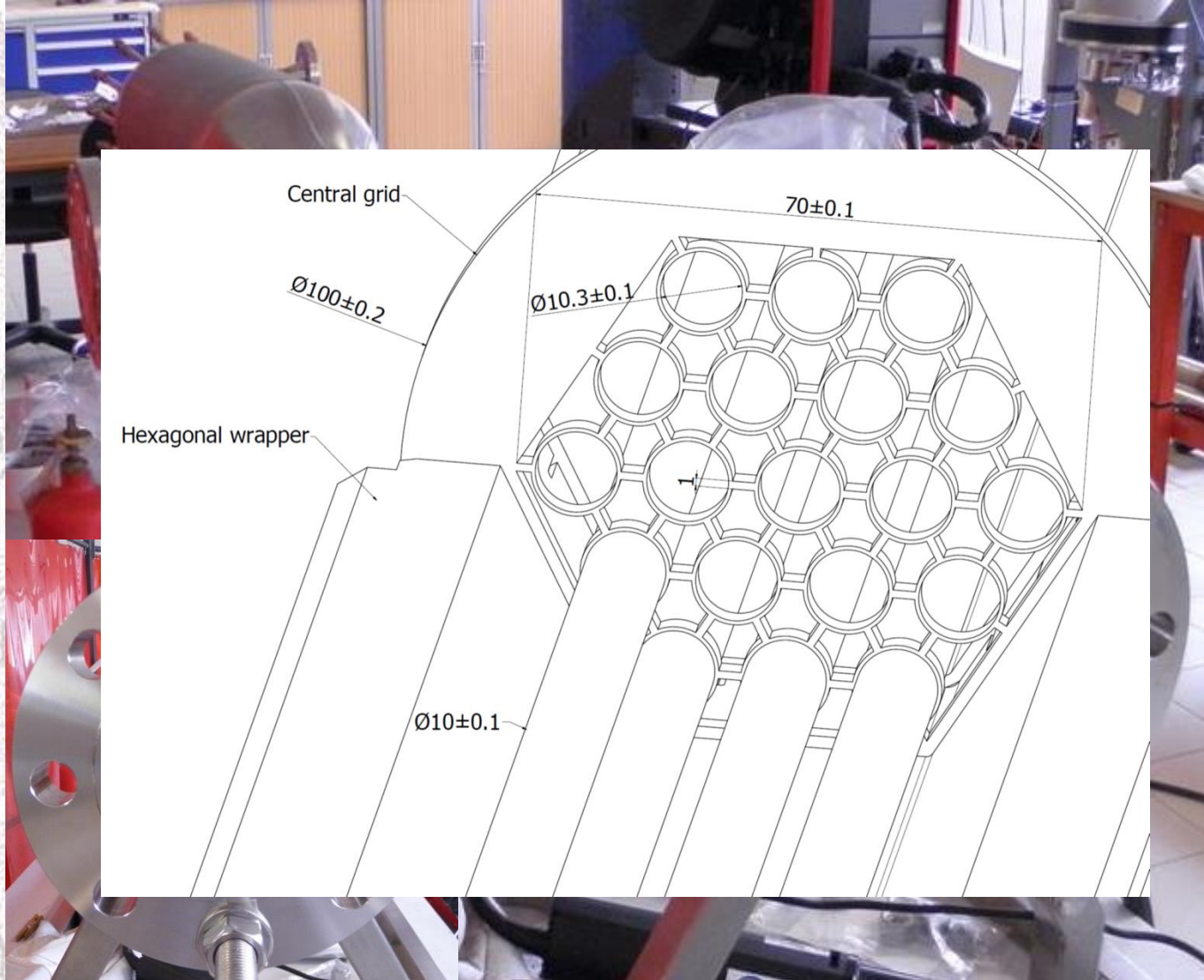
4



5



# Final test section (BFPS)

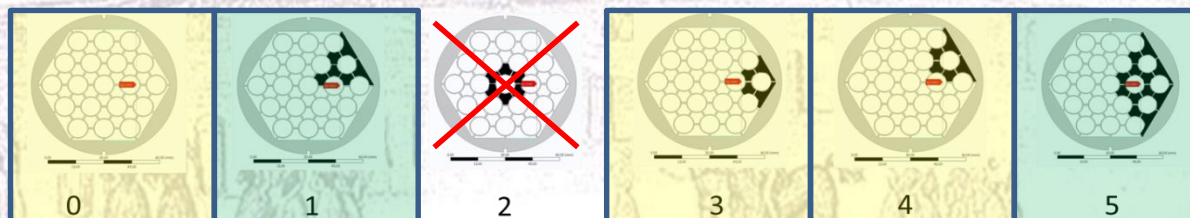


| Test name   | Mass flow rate [kg/s] | Blockage type | Power [kW] | BFPS inlet temperature [°C] |
|-------------|-----------------------|---------------|------------|-----------------------------|
| BFPS-4-0    | 4                     | 0             | 24         | 260                         |
| BFPS-8-0    | 8                     | 0             | 47         | 260                         |
| BFPS-12-0   | 12                    | 0             | 71         | 260                         |
| BFPS-14-0   | 16                    | 0             | 94         | 260                         |
| BFPS-4-3    | 4                     | 3             | 24         | 260                         |
| BFPS-8-3    | 8                     | 3             | 47         | 260                         |
| BFPS-12-3   | 12                    | 3             | 71         | 260                         |
| BFPS-4-4    | 4                     | 4             | 24         | 260                         |
| BFPS-8-4    | 8                     | 4             | 47         | 260                         |
| BFPS-12-4   | 12                    | 4             | 71         | 260                         |
| BFPS-4-4-S  | 4                     | 4             | 47         | 260                         |
| BFPS-12-4-S | 12                    | 4             | 47         | 260                         |
| BFPS-4-1    | 4                     | 1             | 23.55      | 260                         |
| BFPS-8-1    | 8                     | 1             | 47.1       | 260                         |
| BFPS-12-1   | 12                    | 1             | 70.65      | 260                         |
| BFPS-4-5    | 4                     | 5             | 23.55      | 260                         |
| BFPS-8-5    | 8                     | 5             | 47.1       | 260                         |
| BFPS-12-5   | 12                    | 5             | 70.65      | 260                         |

Fundamental tests:

2 fundamental tests at constant power

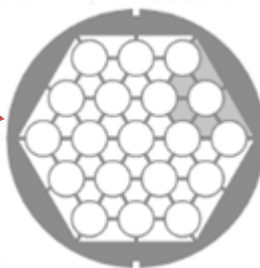
Additional tests



I. Di Piazza, R. Marinari, G. Polazzi, V. Sermenghi, "NACIE-UP experimental setup and test matrix for flow blockage experiment", SESAME WP2, Deliverable 2.5

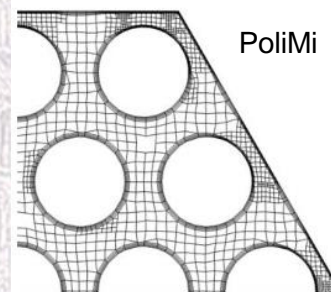
# Code-to-code CFD comparison (pre-test)

- Inlet bend included
- Blockage 4
- LBE: constant properties @220°C (OECD 2007)
- CHT included
- $Pr_t = 2$

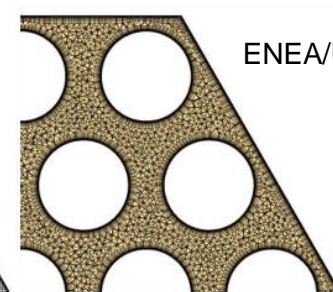


| Boundary | Condizione                    | Valore          |
|----------|-------------------------------|-----------------|
| Inlet    | mfr<br>Temperature            | 8 kg/s<br>200°C |
| Pins     | Heat flux (W/m <sup>2</sup> ) | 156716          |
| Walls    | Velocity                      | No-slip         |
| Outlet   | Relative pressure             | 0 bar           |

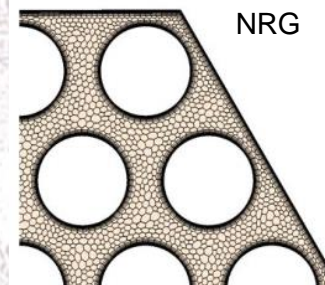
|            | Code        | Mesh  | Type    | Turbulence                  |
|------------|-------------|-------|---------|-----------------------------|
| PoliMi     | Open-FOAM   | 22.3M | Hex     | RANS k-ε                    |
| ENEA/UniPi | CFX 15      | 29.8M | Hex&Tet | RANS k-ε                    |
| NRG        | ★CCM+ 11.06 | 22.4M | Poly    | URANS k-ε                   |
| UniGe/CRS4 | ★CCM+ 11.04 | 14.0M | Poly    | URANS k-ε<br>Prel. LES WALE |



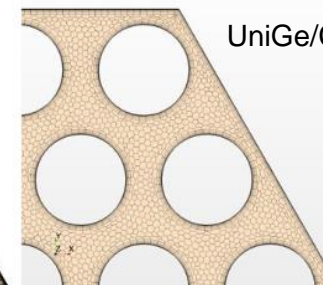
PoliMi



ENEA/UniPi



NRG



UniGe/CRS4



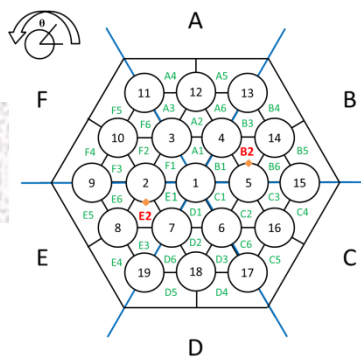
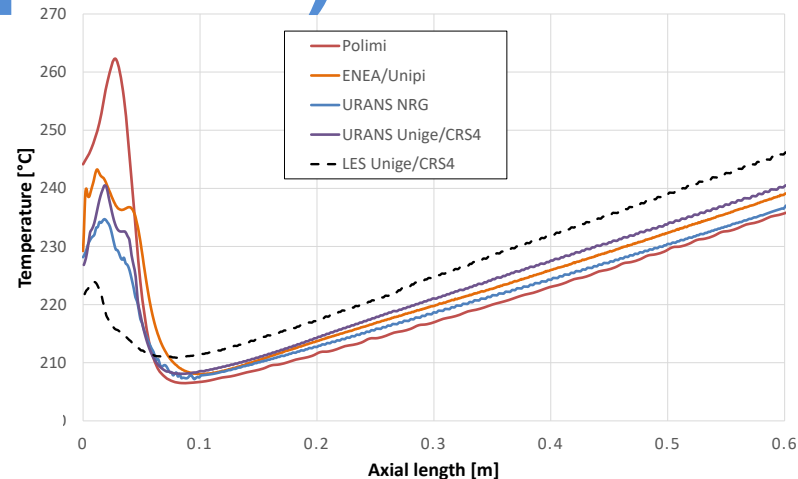
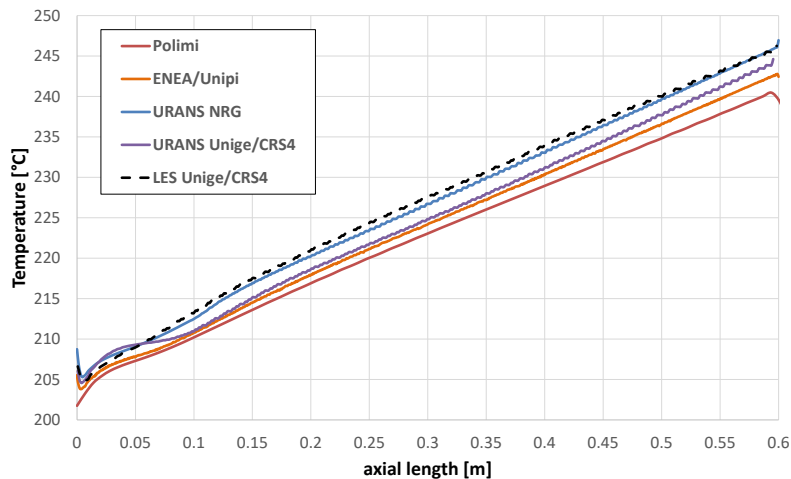


# Code-to-code CFD comparison (pre-test)

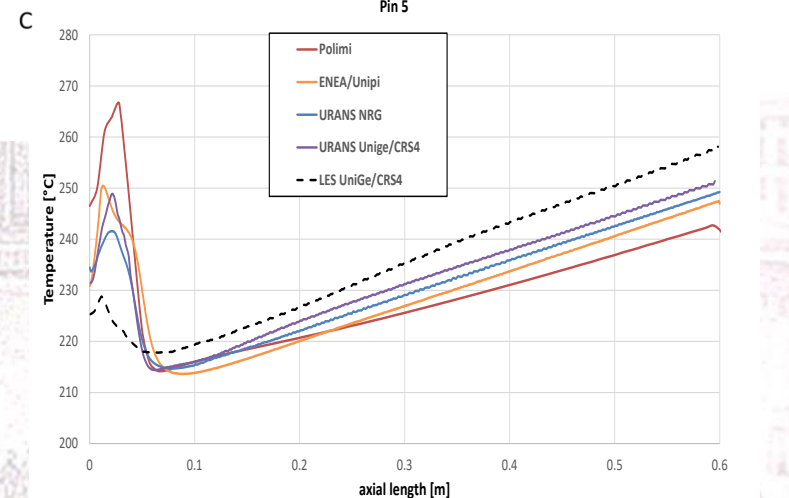
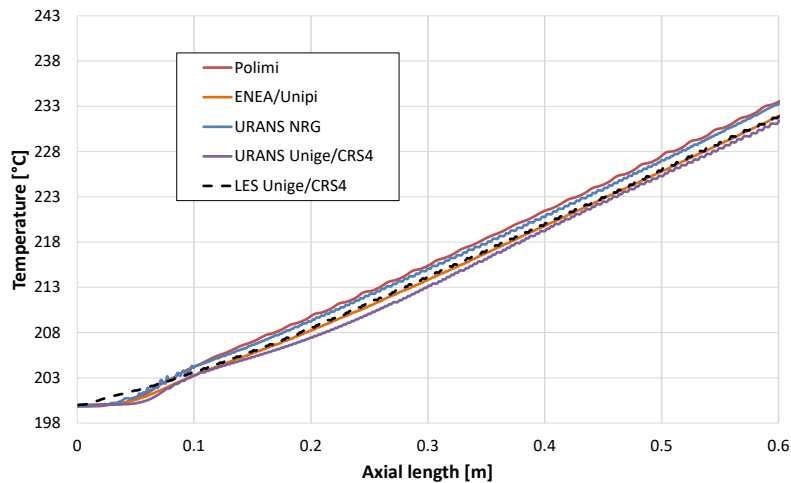


B2

Pin 2

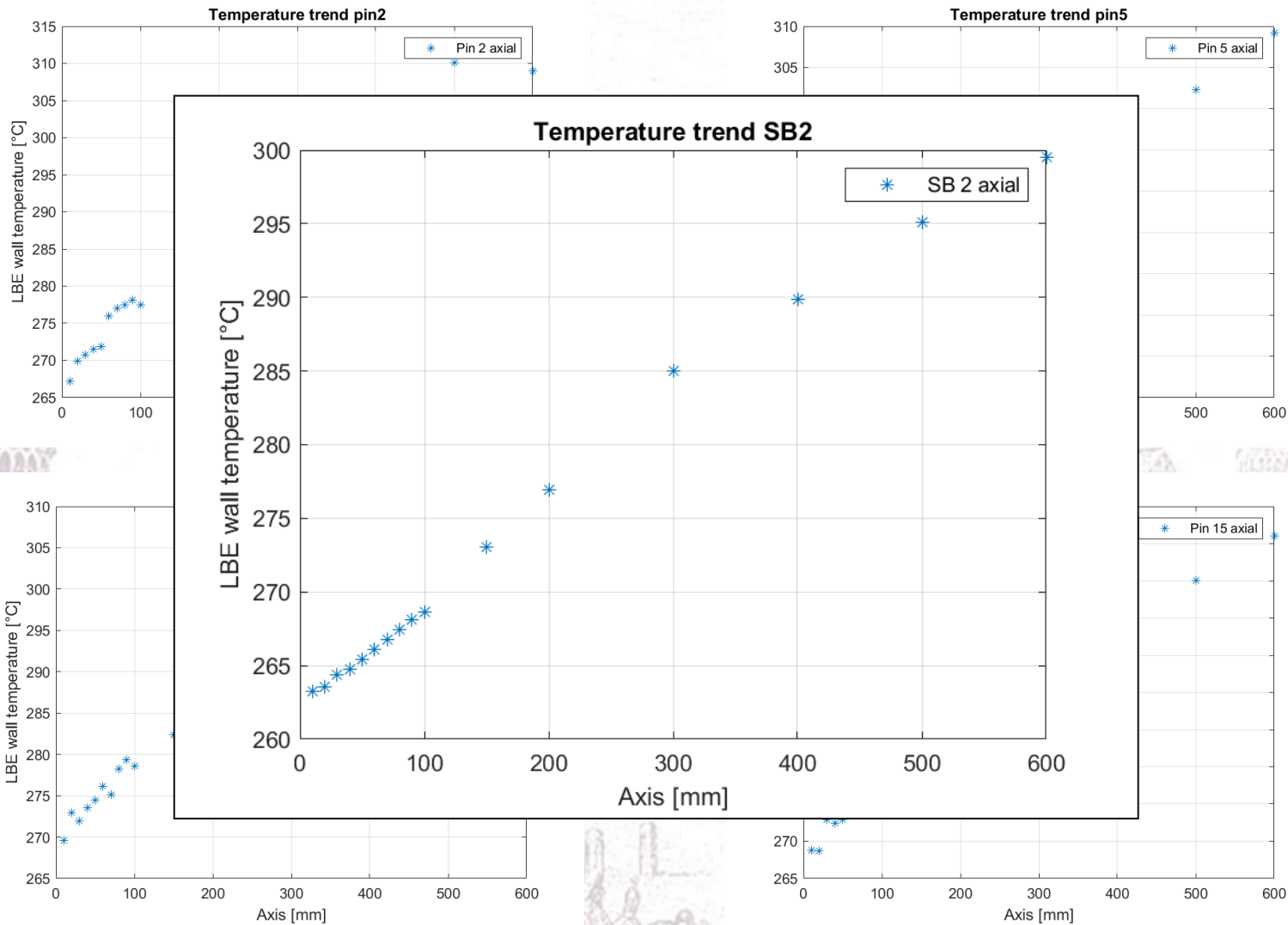


E2



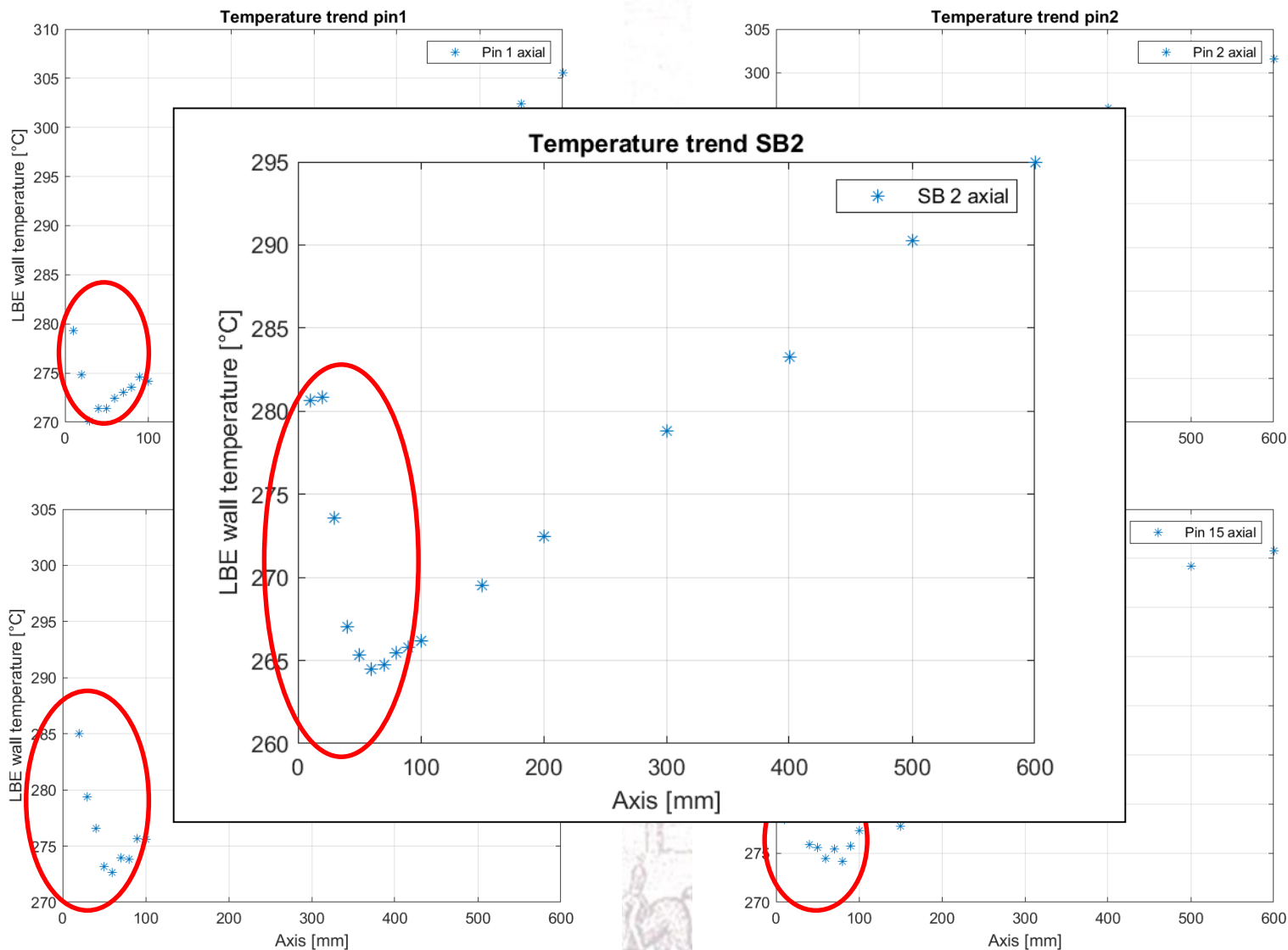
# Experimental campaign

## 8 kg/s - Unblocked case



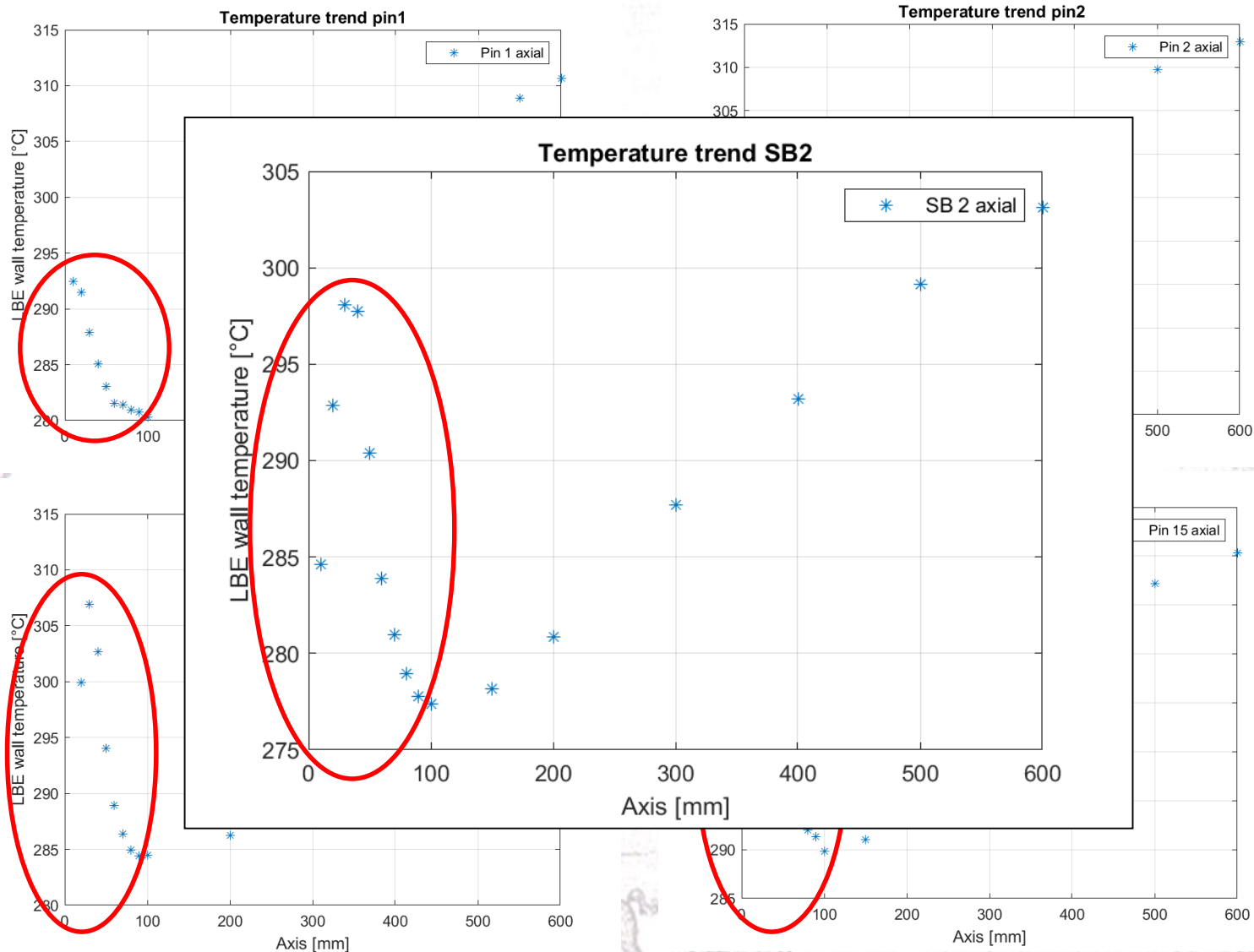
# Experimental campaign

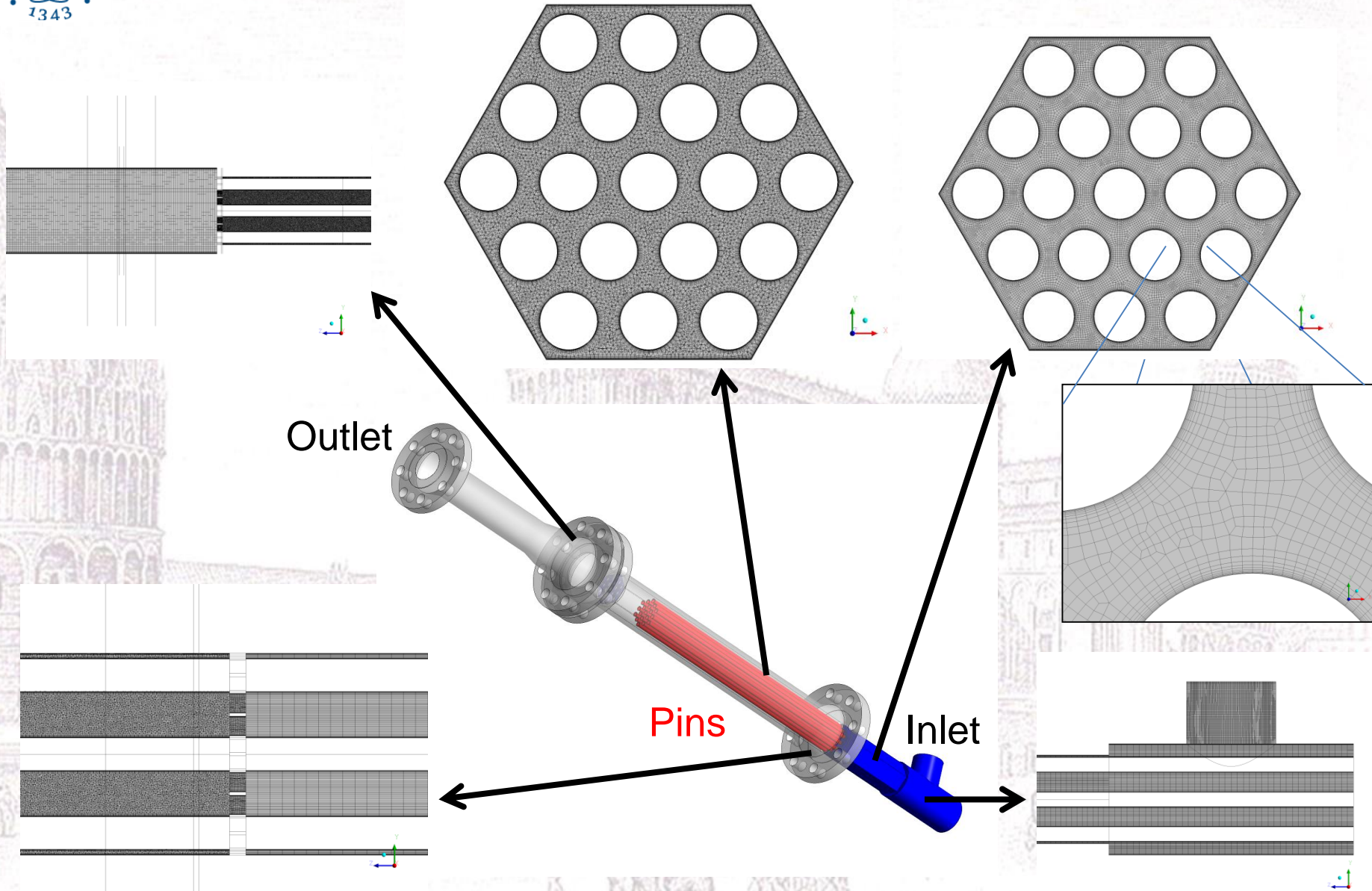
## 8 kg/s – Blockage 1

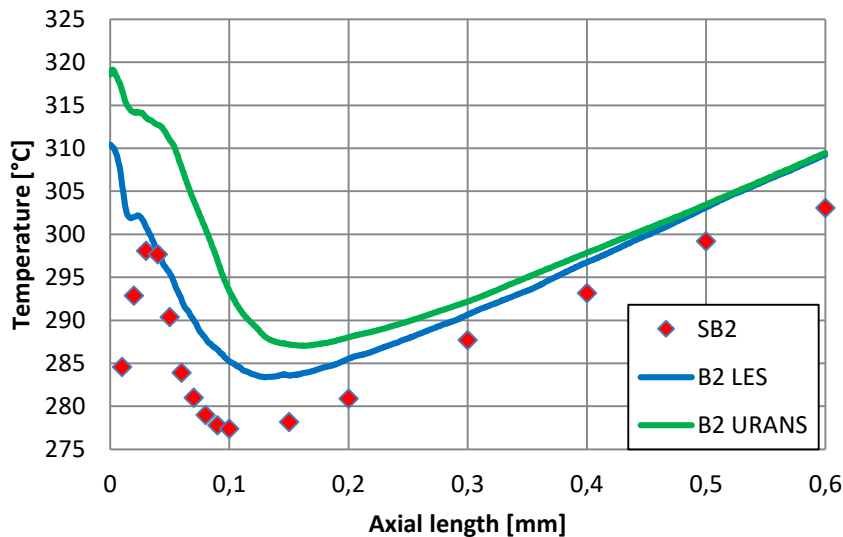
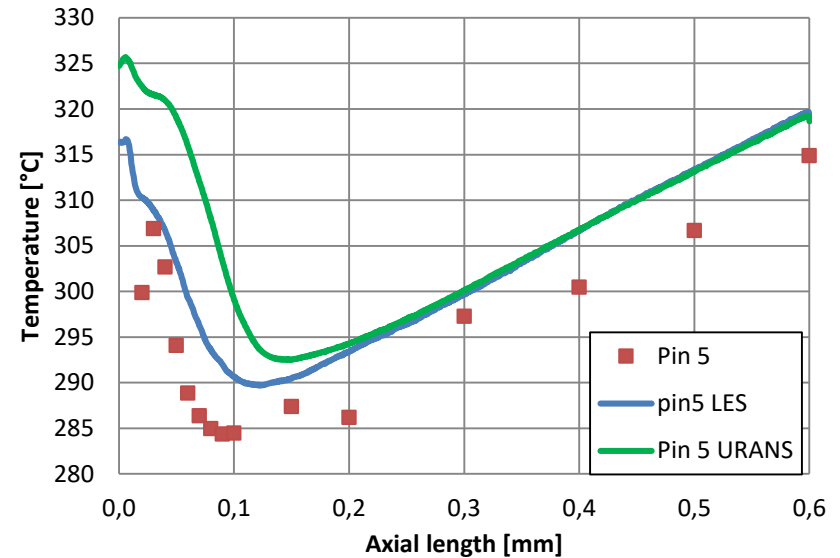
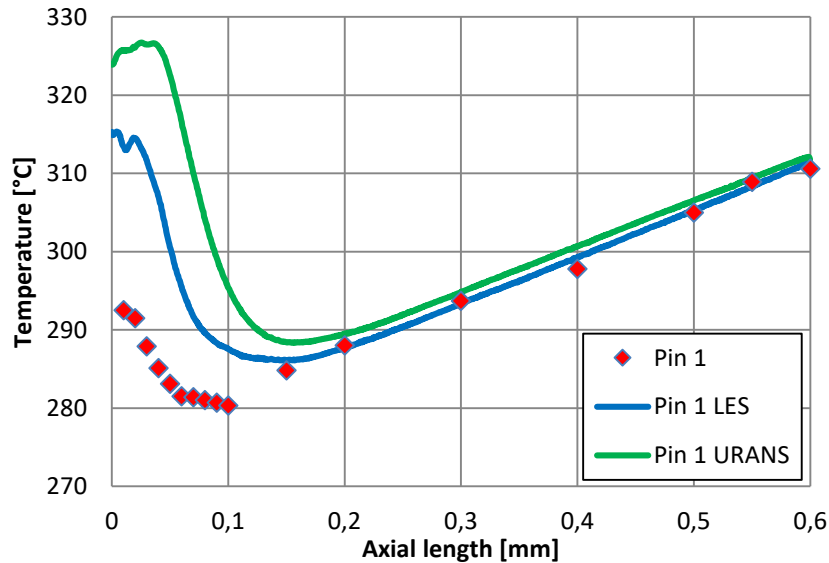


# Experimental campaign

## 8 kg/s – Blockage 5







- The preliminary post test simulations show that CFD results over-predict peak temperature from 15 to 20 °C.
- This behavior will be deeply investigated in the next simulations with other blockages.

- The mechanical design of the test section is finished; the blockage mechanism was fixed; and the instrumentation is fixed according to pre-test CFD studies.
- A CFD benchmark activity (ENEA/UniPi, NRG, PoliMi, UniGe, CRS4) was performed with NURETH paper. The thermal-hydraulics of the new BFPS test section is analyzed for one relevant blockage with different CFD codes and different approaches. All general trends are well captured by RANS and URANS simulations even if there is a remarkable difference between the exact values of these trends (in particular their maxima and minima).
- The experimental campaign is ongoing (2 test blockages were performed).
- The preliminary post test simulations show that CFD results over-predict peak temperature from 15 to 20 °C.
- This behavior will be deeply investigated in the next simulations with other blockages.



**UNIVERSITA' DEGLI STUDI DI PISA**  
**ENEA C.R. BRASIMONE**



**Flow Blockage Experiments in NACIE-UP loop**

**Thank you**





Italian National Agency for New Technologies,  
Energy and Sustainable Economic Development

# GENERATION IV LEAD COOLED FAST REACTOR STATO ATTUALE DELLA TECNOLOGIA E PROSPETTIVE DI SVILUPPO

*Dipartimento di Ingegneria Astronautica, Elettrica ed Energetica*

*Università di Roma "La Sapienza"*

*14-15 Giugno 2018*

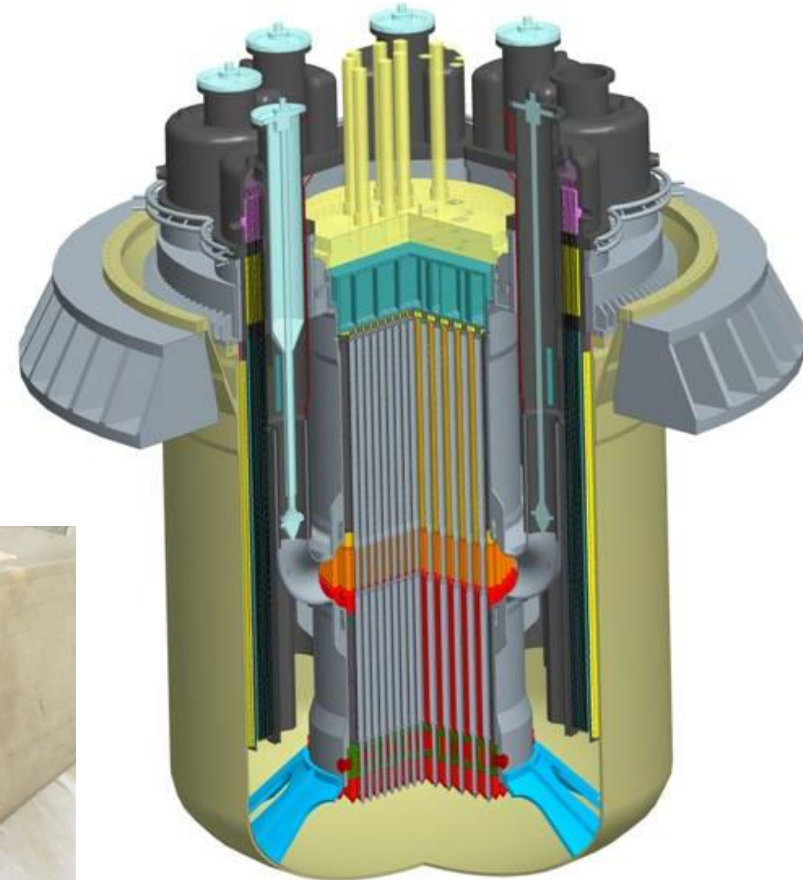
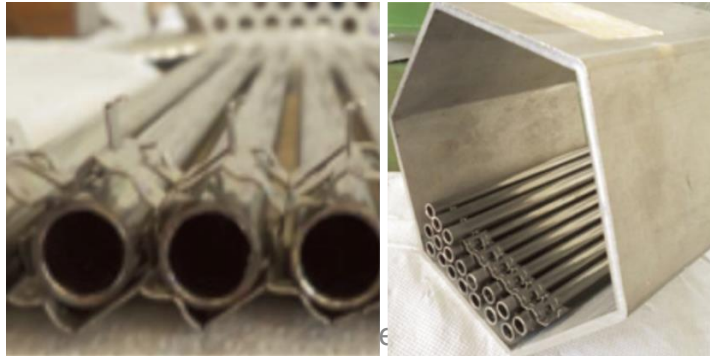
## Structural Material for LFR Application Research Program Overview

Massimo Angiolini



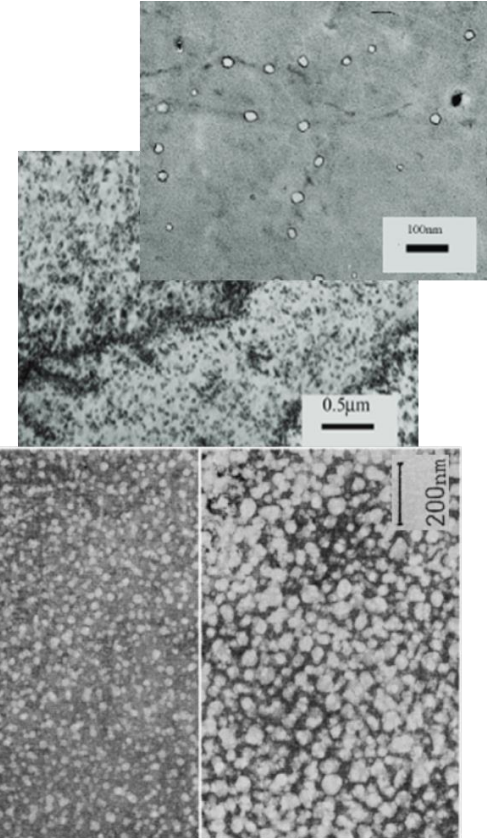
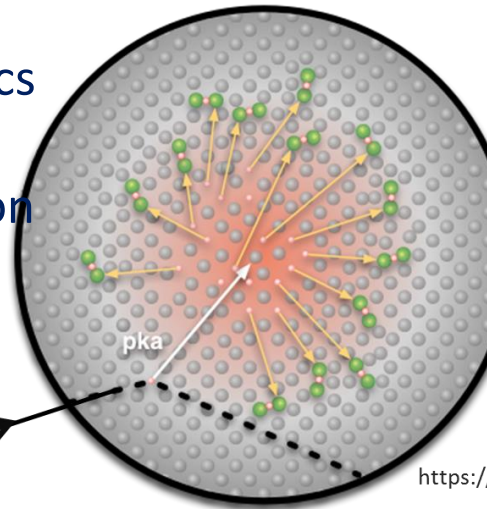
The development of lead cooled fast reactors represents a unique challenge for the materials that are subjected, with different entities, to degradation mechanisms related to:

- Neutron radiation damage
- Exposure to high temperatures
- Exposure to the HLM



# Neutron radiation damage

- Incident neutrons transfers recoil energy to the lattice atoms forming Primary Knock on Atoms (PKA's)
- PKA's displaces neighboring atoms producing atomic displacement cascades, leading to formation of a large population of defects
  - Dislocation loops
  - Voids
- And deviations from thermodynamics
  - Dissolution of precipitates
  - Radiation enhanced precipitation
  - Radiation induced precipitation
  - Radiation induced segregation



# Neutron radiation damage

- The core components and the fuel cladding tubes receive very high irradiation fluences

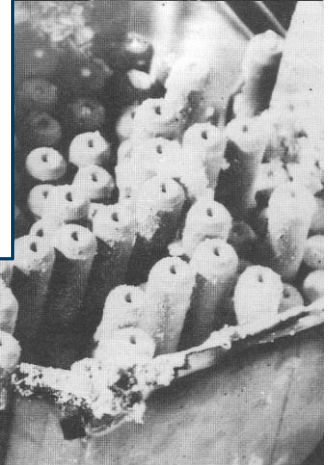
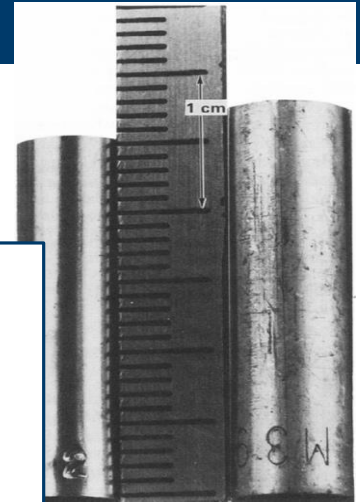
- The enhanced mobility, the several families of precipitates produced lead

**Increasing the life of the cladding more fissile U and plutonium bred from the U is utilized**

**The state of the art is a specification of the 15-15 Ti steel AIM1 able to resist up to about 100 dpa**

**Advanced austenitic steels to reach 150 dpa irradiation for future FR's fuel claddings are under development**

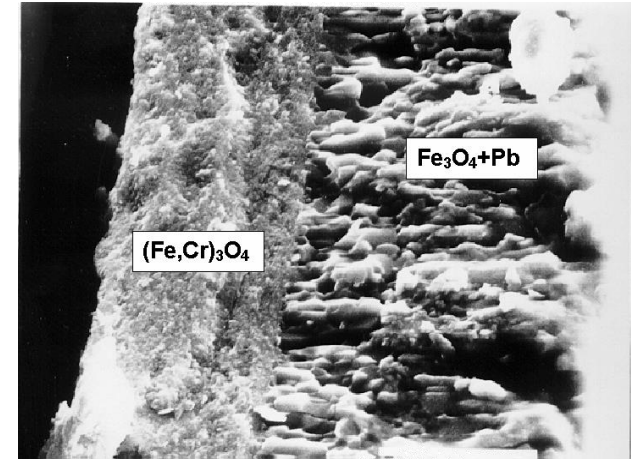
- The increase of the cladding resistance to neutron irradiation is crucial to realize high burnup operation of fast reactors



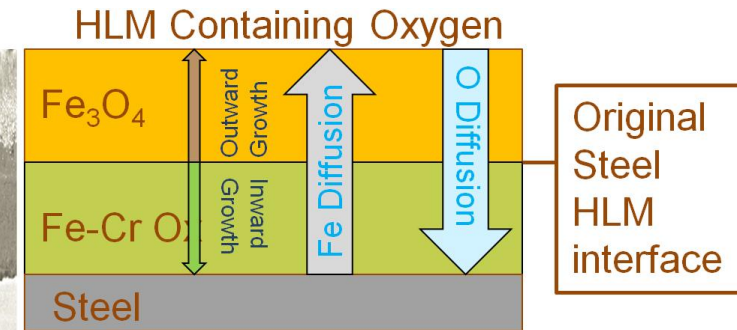
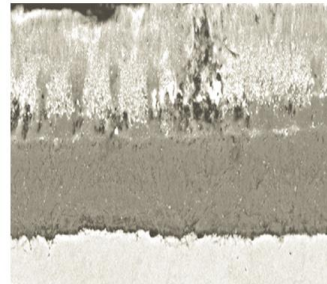
# Corrosion of the steels

The compatibility of steels with lead and LBE represents the main challenge in the development of HLM cooled systems

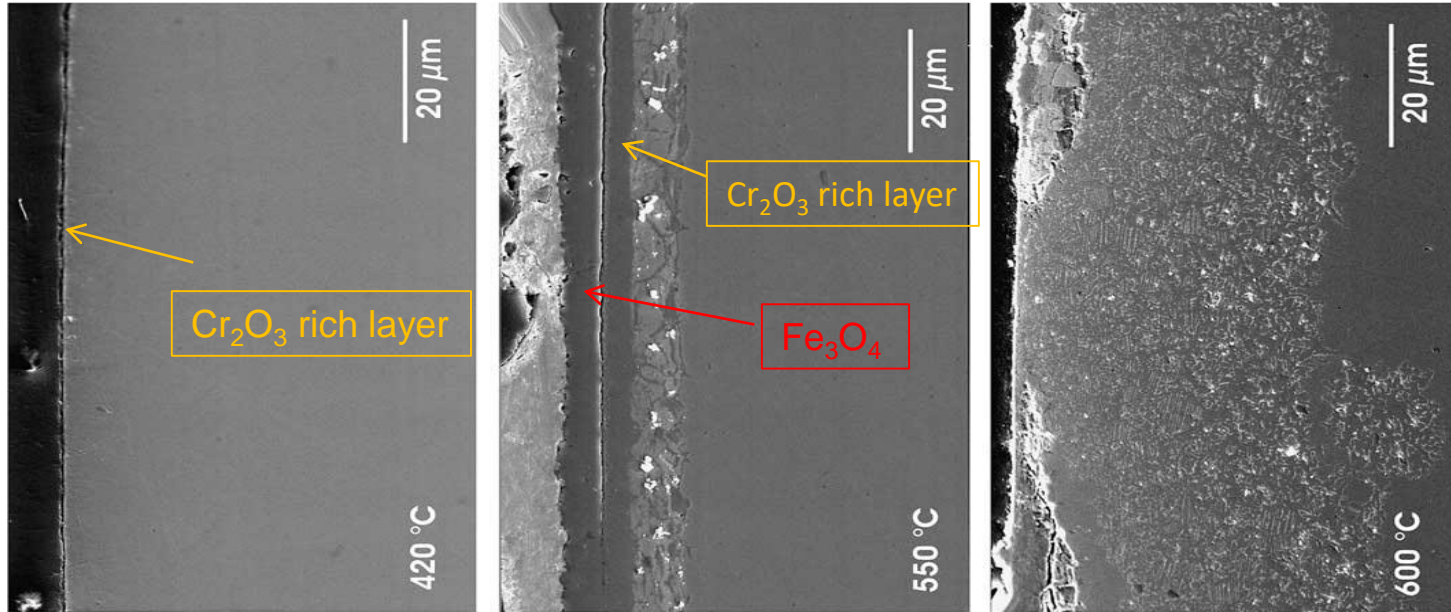
- Not-passivating oxidation leading to thick oxide layers not stable/internal oxidation
- Dissolution of the steel constitutive elements: Ni, Cr and Fe show high solubility in lead-bismuth eutectic
- Liquid metal embrittlement (F/M)



|            | Pure lead<br>T = 550° C | LBE<br>T ≤ 300° C      | LBE<br>T = 460~470° C | LBE<br>T ≥ 550° C       |
|------------|-------------------------|------------------------|-----------------------|-------------------------|
| F/M Steels | Duplex layer            | Very thin Oxide layer  | Duplex oxide layer    | Heavy corrosion         |
| Austenitic | Thin duplex oxide layer | Very thin single layer | Thin single layer     | Thin duplex oxide layer |



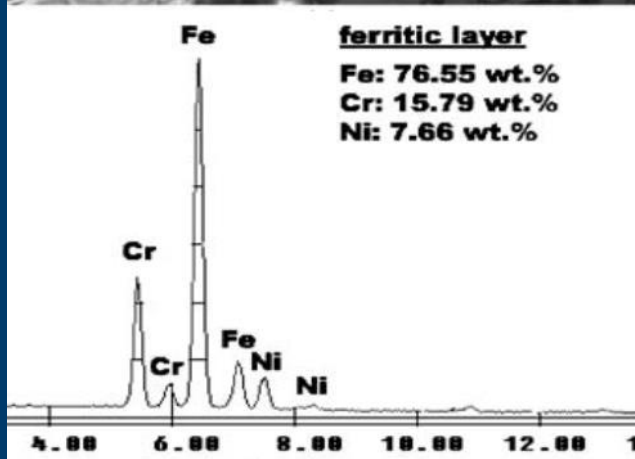
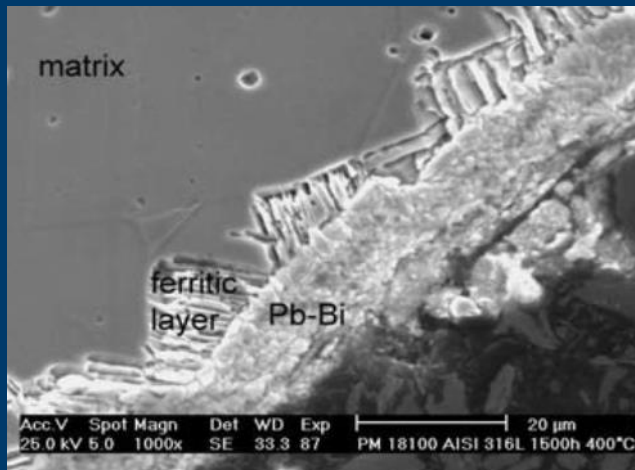
# Corrosion of the steels



DIN1.4970 SS 4000 h (167 d) of exposure flowing LBE  $10^{-6}$  wt% oxygen

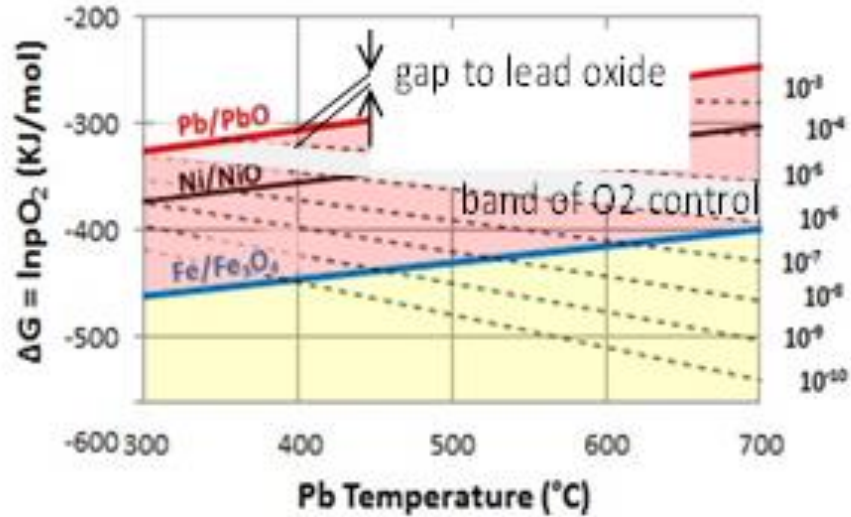
- Thin protective Cr<sub>2</sub>O<sub>3</sub> rich layer @ 420 °C
- Dual magnetite/Cr<sub>2</sub>O<sub>3</sub> rich layer layer partly infiltrated with LBE @ 550 °C
- Severe corrosion/dissolution attack @ 600 °C

bright spots consisting of LBE penetrated the steel matrix.



- The upper temperature limit (450°-470° C) imposed by the corrosion and the relatively high melting temperature of the lead (327,5 °C) pose a limitation to the thermal efficiency attainable by the reactor
- In principle a suitable design and choice of materials (AFA steels, FeCrAl ODS, coatings) would make possible the realization of high temperature HLM cooled systems, all except the core
- At present a material able to resist in high temperature HLM to the fast neutron flux to 100 dpa is missing

# Corrosion protection by AOC



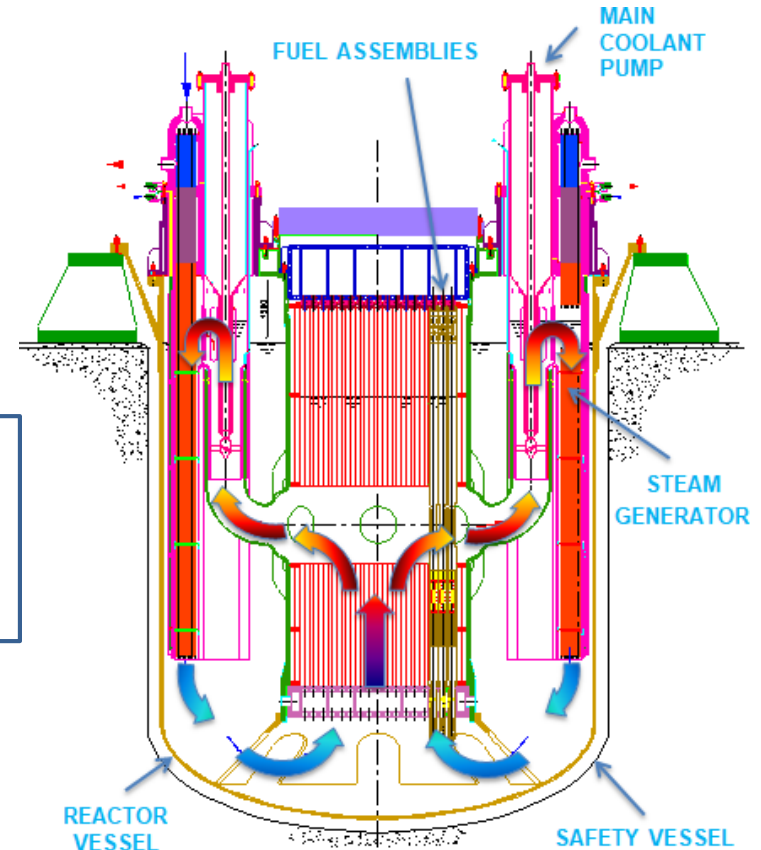
- A possible strategy to handle the corrosion issues is to perform operations under control of the oxygen dissolved in the melt (AOC)
  - Keeping the oxygen content in an interval of concentration below the precipitation of the solid PbO to prevent the formation of solid plugs of lead oxide
  - above that of precipitation of Fe<sub>3</sub>O<sub>4</sub> guarantees the presence of a Fe-Cr oxide layer that protects the steels from the lead
- For tests temperatures higher than the above limits, the formation and protectiveness of oxides is uncertain, and protection usually fails due to dissolution for long times
  - Difficult to control the oxygen content on a large pool with thermal stratification
  - To prevent the dissolution of the steel everywhere, it could be appropriate to maintain oxygen level next to the upper limit with the risk of precipitation of Pb oxide in parts operated at low temperature



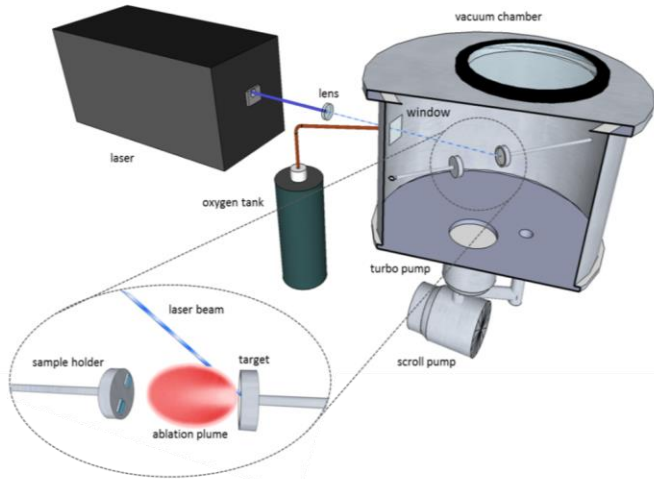
# ALFRED – corrosion protection strategy

- Operate the reactor in “low oxygen conditions”, i.e. [O] below the saturation limit at the coldest temperature of the coolant (400°C), to eliminate the risk of lead oxide precipitation in the whole system
- Use of suitable coatings to achieve the corrosion/erosion resistance in the hottest regions Core, SGP-unit, etc @550°C max

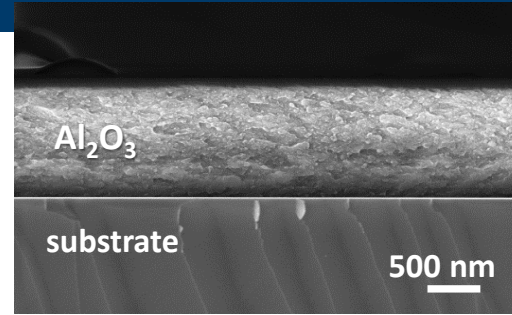
- 15-15 Ti AIM1 Al<sub>2</sub>O<sub>3</sub> PLD coated for the cladding and core components
- Austenitic creep resistant steel with an aluminide diffusion coating for the SG



# Al<sub>2</sub>O<sub>3</sub> PLD nanoceramics



- **high quality coatings**
- custom process: bottom-up approach
- process at **room temperature**
- amorphous films with **nanodispersed crystalline domains**
- **high deposition rate (nm/s)**
- **Line of sight deposition**



F. Garcia Ferré et al. – ACTA MATER – 2013



| Property @RT | Sapphire | PLD Al <sub>2</sub> O <sub>3</sub> | AISI 316L |
|--------------|----------|------------------------------------|-----------|
| $\nu$        | 0,24     | $0,295 \pm 0,025$                  | 0,3       |
| E [GPa]      | 345      | $193,8 \pm 9,9$                    | 200       |
| G [GPa]      | 175      | $75,5 \pm 3,8$                     | 80        |
| B [GPa]      | 240      | $159,2 \pm 11,8$                   | 140       |
| H [GPa]      | 27,8     | $10,3 \pm 1$                       | 4         |
| H/E          | 0,059    | $0,049 \pm 0,007$                  | 0,025     |

**Nanocrystalline oxides have metal like mechanical properties!**



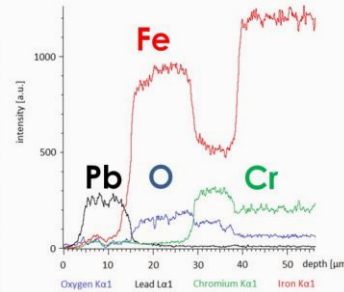
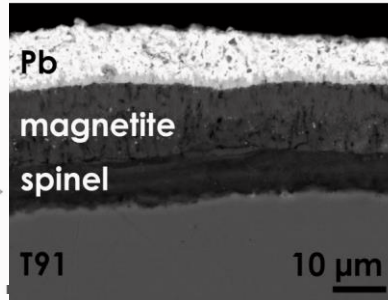
# Al<sub>2</sub>O<sub>3</sub> PLD nanoceramics

## Oxidation in stagnant Pb

uncoated sample



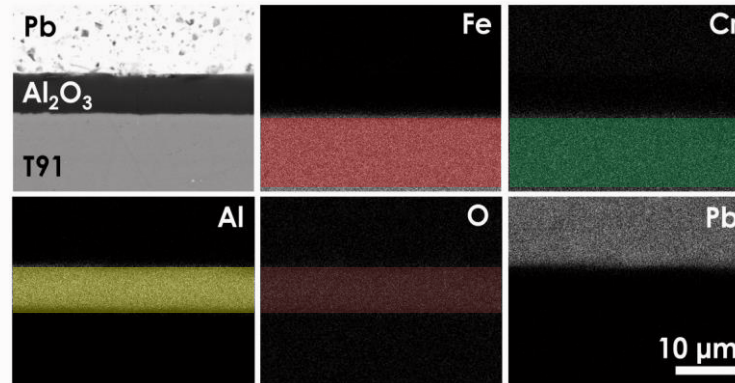
heavy liquid metal corrosion



coated sample

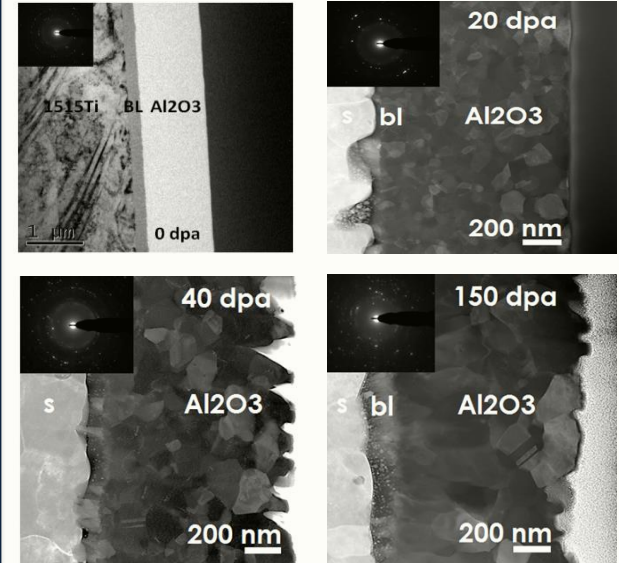


protection



F. Garcia Ferré et al. – CORROS SCI – 2013

## Resistance to n irradiation

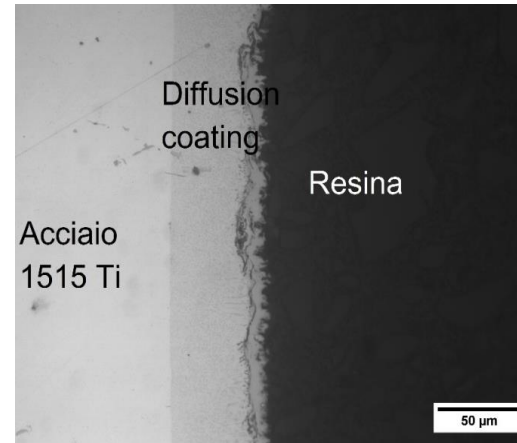
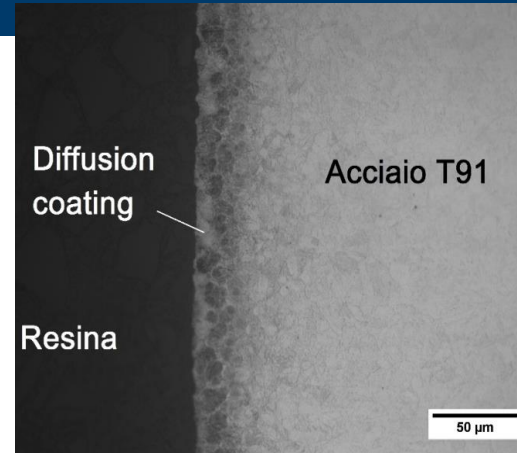


# Al<sub>2</sub>O<sub>3</sub> PLD nanoceramics

- The work on the Al<sub>2</sub>O<sub>3</sub> coatings will be devoted to pre-normative tests aimed at supporting the drafting of design rules for their use as corrosion-resistant coatings for the the LFR core
- The series of corrosion data will be completed with tests in stagnant Pb at 550 ° C at low oxygen (nominal condition, 10-8wt.%) and high oxygen (accidental condition, saturation) started I the last years and devoted to verify the thermodynamic stability of the alumina coating
- In addition, stagnant corrosion tests will be performed at 650 ° C to verify the applicability of the coating to HT LFR systems
- PLD alumina depositions with a chromium buffer-layer will also be tested to verify if the coating passivates in in case of damage or rupture
- Thermal cycling tests will be carried out in an ad hoc device designed and produced by ENEA based on the expected thermal excursions for the component during its life: 25 temperature cycles between RT and 600 ° C.
- Impact tests as well as three-point bending tests will be performed to verify the resistance to the damage by impacts and the tolerance to deformations
- "CREEP-RUPTURE“ tests in lead at the operating conditions of the LFR system
- All the above tests will be followed by electron microscopy observations to characterize and evaluate the damage produced
- In view of the execution of lead fretting tests to evaluate the resistance of the coatings to abrasion, the GIORDI fretting test machine will be updated with a monitor and control system for the [O] and an improved the system for the apply the load to the sample

# FeCrAl diffusion coatings

- The work on diffusion coating started few years ago in collaboration with C.S.M. S.p.A and has been devoted mainly to the optimization of low temperature processes applicable to F/M steels and the austenitics of the 15-15 type for cladding application – activity discontinued/characterizations pending
- The work continues on austenitics of the 15-15 type optimized for high creep resistance for application to the SG of the LFR
- The focus will be on
  - the performance of the coating under the loads typical of this kind of application
    - Creep
    - Fatigue
    - Ratchetting
  - the corrosion behavior vs the oxygen content
    - the Al rich layer if not passive may undergo severe dissolution-corrosion issues
- All the tests will be compared with the analogues performed on uncoated samples
- Samples after testing will be analyzed by electron microscopy in flat and cross-section to characterize and evaluate the damage produced



# Oxygen Control System implementation

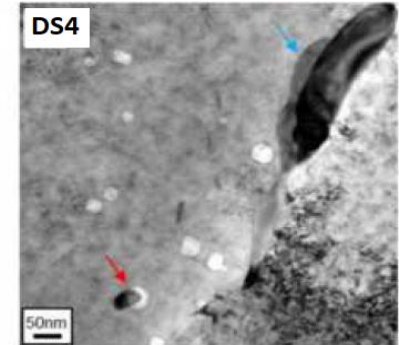
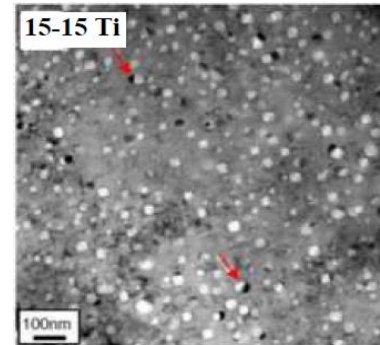
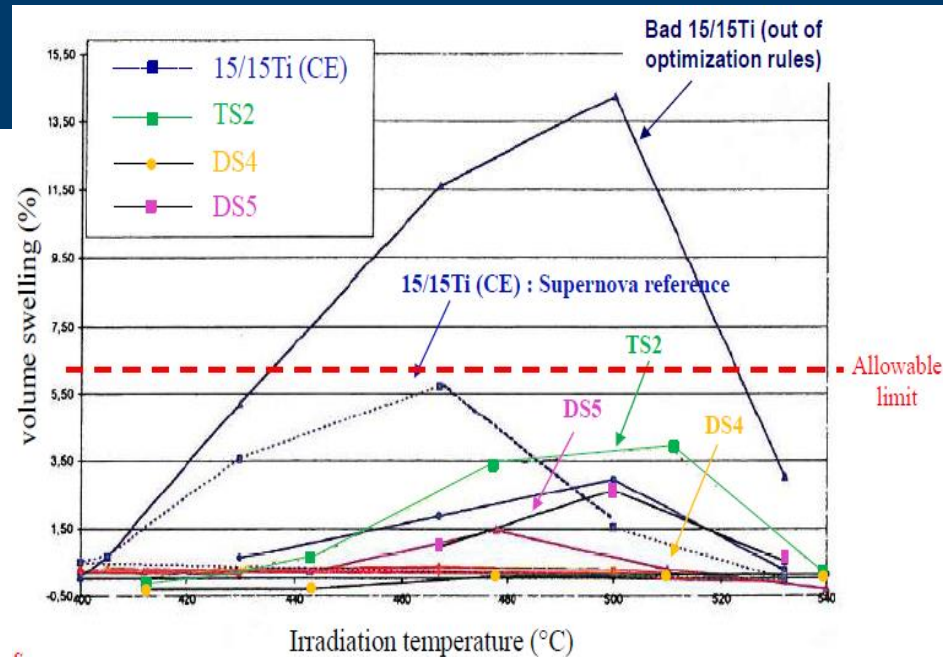
- The final objective of the work will be the demonstration of the feasibility of operations of large HLM plants at low and controlled oxygen concentration, in the range  $10^{-6}$ - $10^{-8}$ % wt
- Development of an oxygen control system in Pb and Pb-Bi for the experimental plants located at C.R. Brasimone
  - HLM pool, loops and storage tanks
- **To this aim the development of monitor and control systems of the [O] is needed**
- development and testing of sensors to in situ monitor the concentration of oxygen in the HLM under typical operating conditions (T and p)
  - new reference air/perovskite and Cu/Cu<sub>2</sub>O electrode systems and new solid electrolyte geometries in Ytria Partially Stabilized Zirconia
- Developments of reliable devices that allow to control the [O]
  - The new oxygen control system based on the injection of Ar-H<sub>2</sub> and Ar-O<sub>2</sub> mixtures will be tested in the LECOR loop system and in the BID1 pool system.

Tests under different operating conditions will be carried out in order to identify the parameters that allow a stable oxygen control



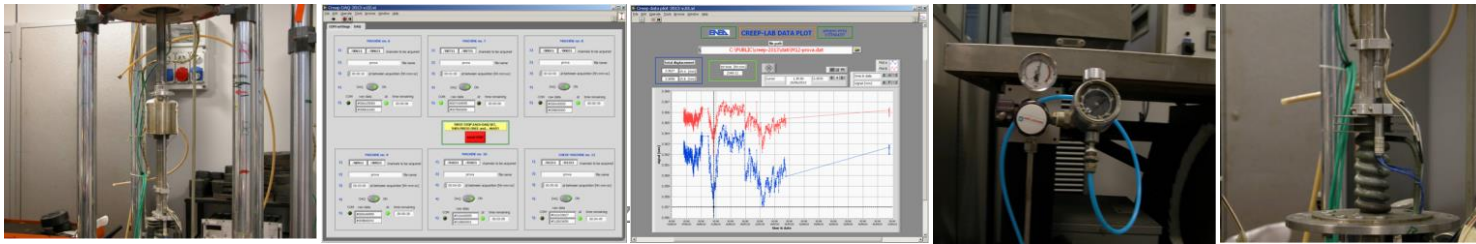
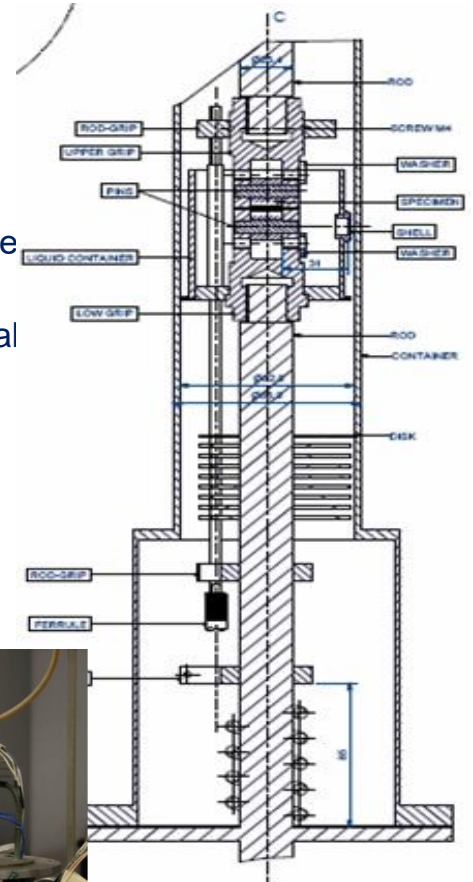
# DS steels development

- Ti and Nb DS steels development started in the 80' in the frame of an ENEA-CEA collaboration
- Among them the DS4 has shown an outstanding performance toward neutron swelling after irradiation in Phénix (SUPERNOVA experiment)
- An evolution of the DS4 is being considered as fuel cladding of the future FR's for the promise to be able to sustain fast neutron irradiation up to 150 dpa with limited swelling and acceptable mechanical properties
- Aim of the work on the DS steels is to re-establish the know-how in the field of the design and manufacturing of special steels and testing the material in the ALFRED conditions
- A new cast (80 Kg) with the DS4 formula has been manufactured by CSM S.p.A. (PAR 2013)
- The DS4 material is being characterized
  - the corrosion behaviour in molten lead
  - mechanical behaviour (tensile, creep)
  - Irradiation with 58 Ni ions @ 110 MeV 550°C presso LNL (in progress)



# Creep tests in HLM

- The experience gained during the last decades has shown that the influence of the molten metal on the mechanical properties is strongly dependent on the chemistry
- The oxide or any other contamination on the surface can mask/protect steel from the contact with the liquid
- Critical issue for creep tests that last months/years
- The “static” system set up during the last years revealed not efficient in maintaining the nominal operating conditions
  - inert / reducing gas lines for each machine for the conditioning of the molten metal
  - modification of the deformation acquisition system
  - designed and implemented a new acquisition system (Hardware / Software)
- Post test characterization revealed in some cases huge oxide deposits
- It has been decided to upgrade the oxygen control system with oxygen sensors and implement a monitor and control system





- PLD coating for LFR application. Status and future developments
- Coating characterization under irradiation.
  - Heavy ions irradiation against neutron irradiation
- Corrosion qualification of materials and coatings in liquid lead for LFR
- Mechanical characterization of coatings
- Coolant chemistry control study for HLM systems
- Double stabilized stainless steels: Status and future developments
- Creep-Rupture tests in HLM environment
- Criticality of manufacturing and advanced processes

F. Di Fonzo

M. Beghi

S. Bassini

M. Bragaglia

S. Bassini

C. Cristalli

A. Coglitore

E. Zanin



UNIVERSITA' degli STUDI di ROMA  
TOR VERGATA



Agenzia nazionale per le nuove tecnologie,  
l'energia e lo sviluppo economico sostenibile



materials, technology & innovation



Structural Material for LFR Application  
15 June 2018 Università di Roma "La Sapienza"

Thanks for your attention  
[massimo.angiolini@enea.it](mailto:massimo.angiolini@enea.it)



1101 0110 1100  
0101 0010 1101  
0001 0110 1110  
1101 0010 1101  
1111 1010 0000





ISTITUTO ITALIANO DI TECNOLOGIA  
CENTER FOR NANOSCIENCE AND TECHNOLOGY

# Nanoceramic Coatings for Advanced Nuclear Systems: status and prospects

M. Vanazzi, D. Iadicicco, B. Paladino, E. Frankberg,  
F. Di Fonzo



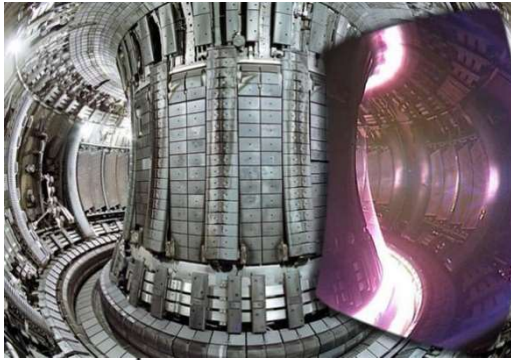
ISTITUTO ITALIANO  
DI TECNOLOGIA

---

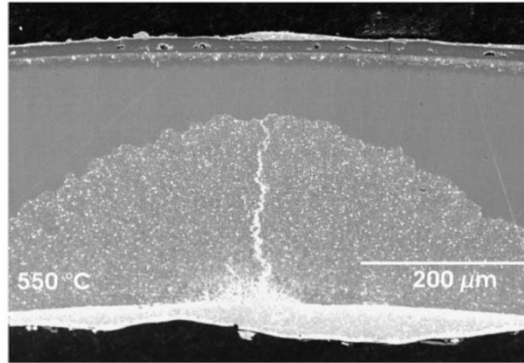
# Introduction

# Future generation nuclear systems (GIV)

## Tritium management

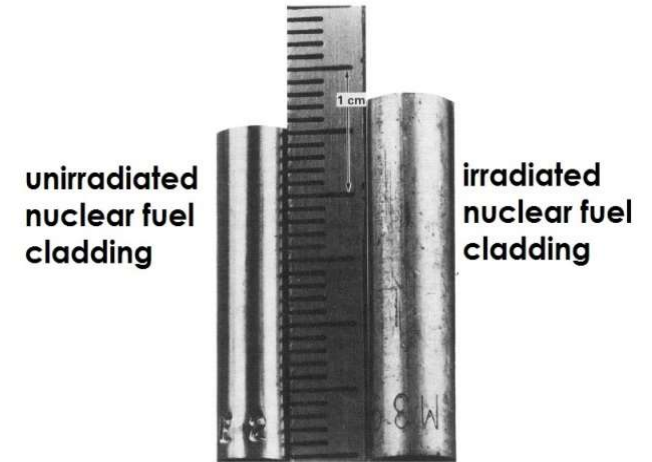


## Corrosion

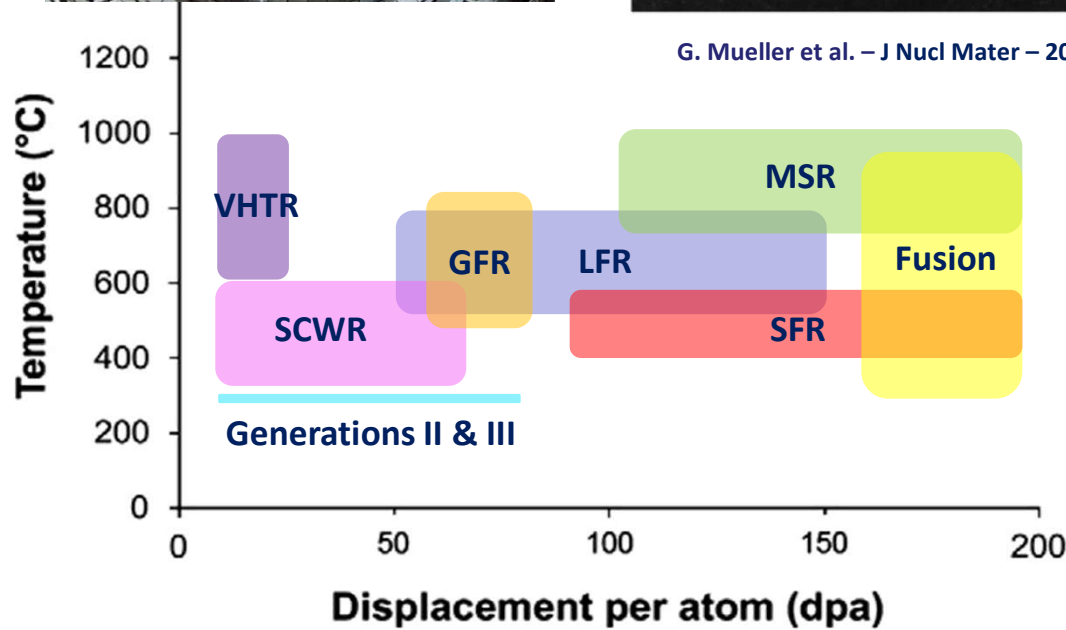


G. Mueller et al. – J Nucl Mater – 2004

## Radiation damage



J.L. Straalsund – Westinghouse Hanford



S.J. Zinkle and G.S. Was – Acta Materialia - 2013

**MAJOR BOTTLENECKS  
FOR ALL SYSTEMS**



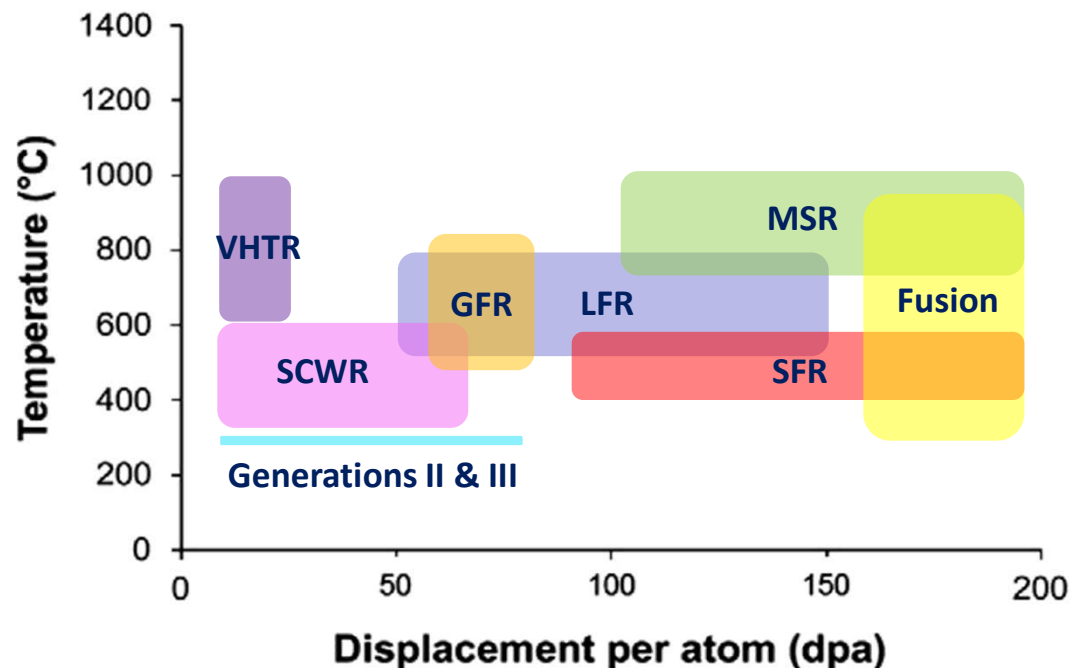
**NEED FOR  
COATINGS**

Future generation nuclear systems aim at:

- Increase efficiency
- Reduce waste generation
- Enhance safety
- Promote non-proliferation

Ultimate goal for LFRs:

- 800 °C
- 150 dpa



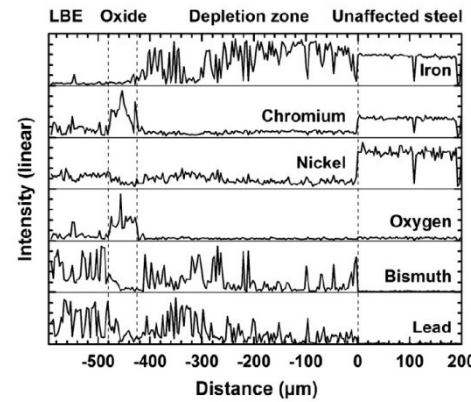
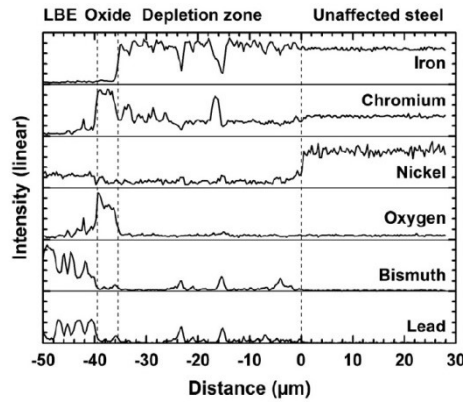
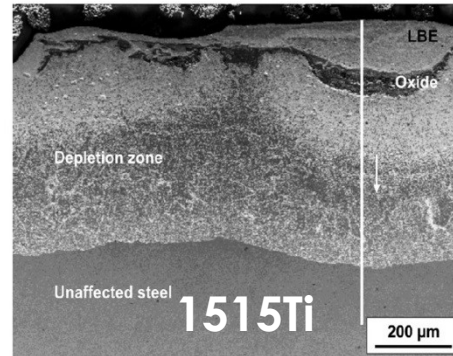
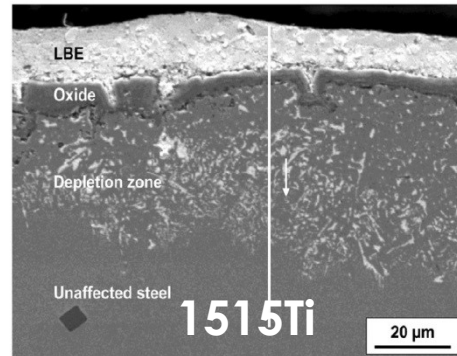
Advantages:

safety  
transmutation of minor  
actinides / fuel breeding

Major issues:

- corrosion
- radiation damage

## Ni leaching in austenitics (23000 h @ 550°C, 10<sup>-6</sup> wt.% O)

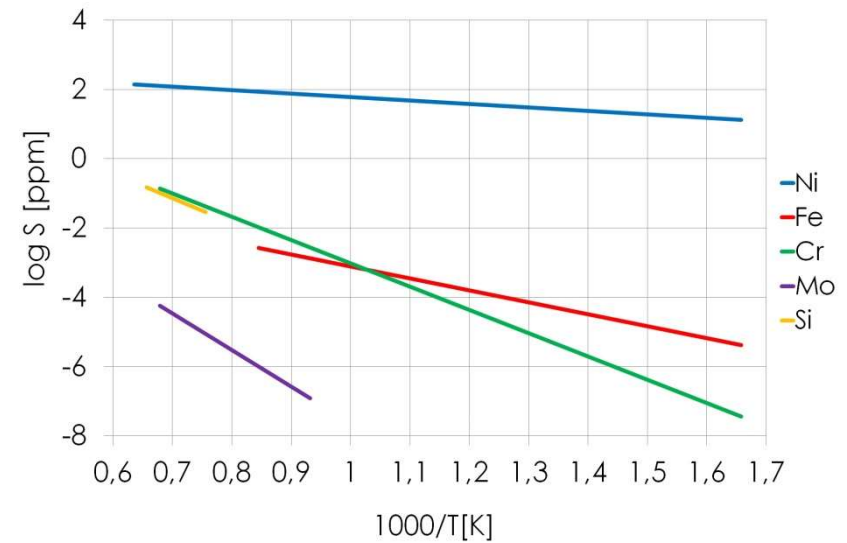


(a)

(b)

C. Schroer et al. - Corros. Sci. - 2014

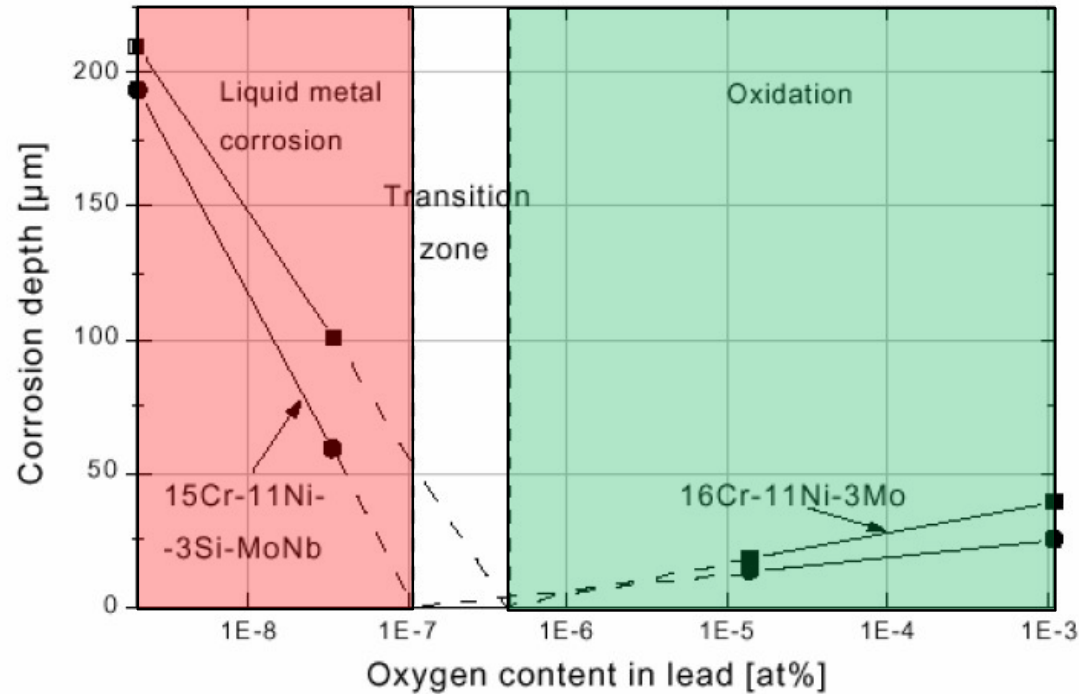
## Solubility of Ni in lead is very high



**In-situ passivation is not viable for T > 500°C-550°C**

(will be exceeded by fuel cladding)

# Heavy liquid metal corrosion

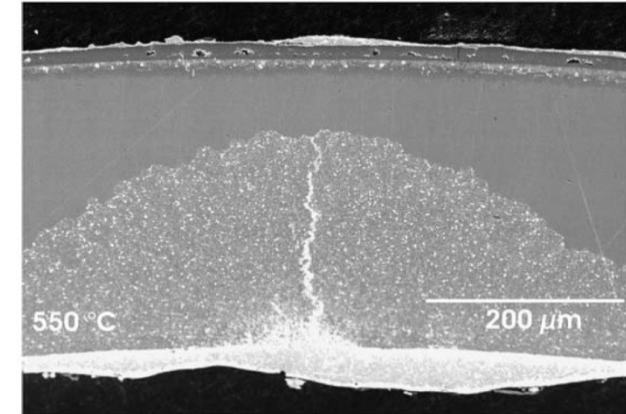


**Austenitic steels exposed to HLM for 3000 hours at 550°C**

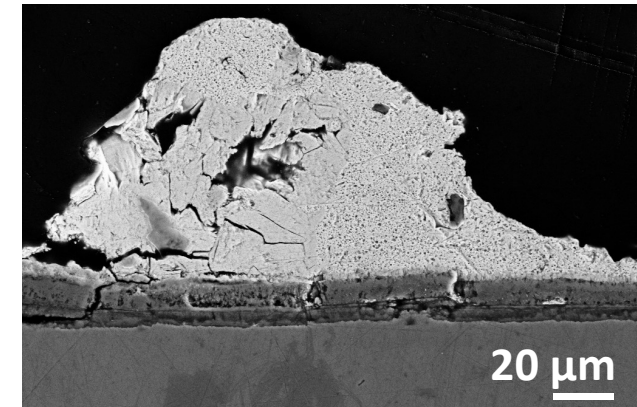
V. Gorynin et al. – Metal Science and Heat Treatment - 1999

**In-situ passivation is not viable for  $T > 500^\circ\text{C}$**   
(will be exceeded by fuel cladding)

G. Mueller et al. – J Nucl Mater – 2004



**Dissolution**

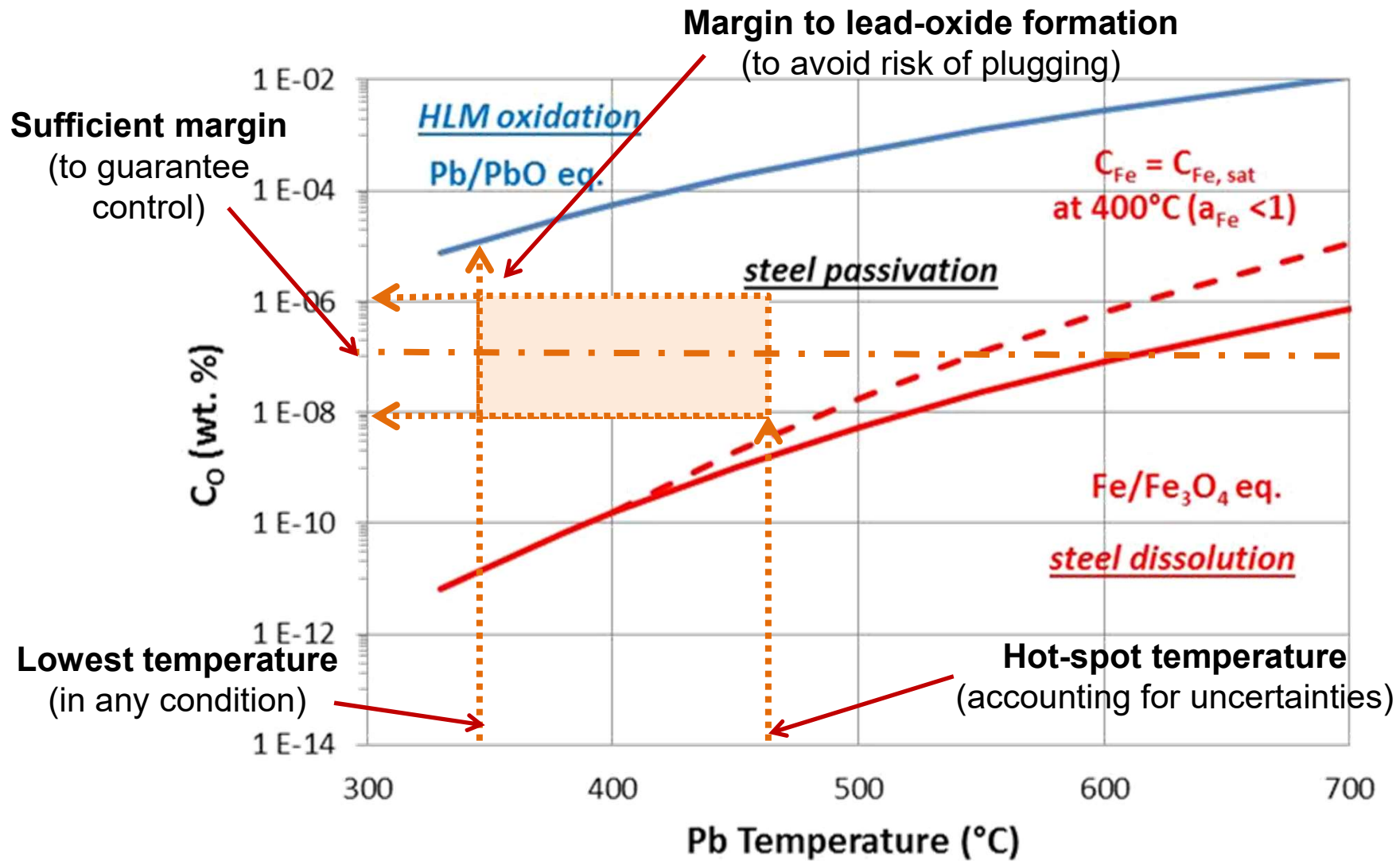


**Oxidation**

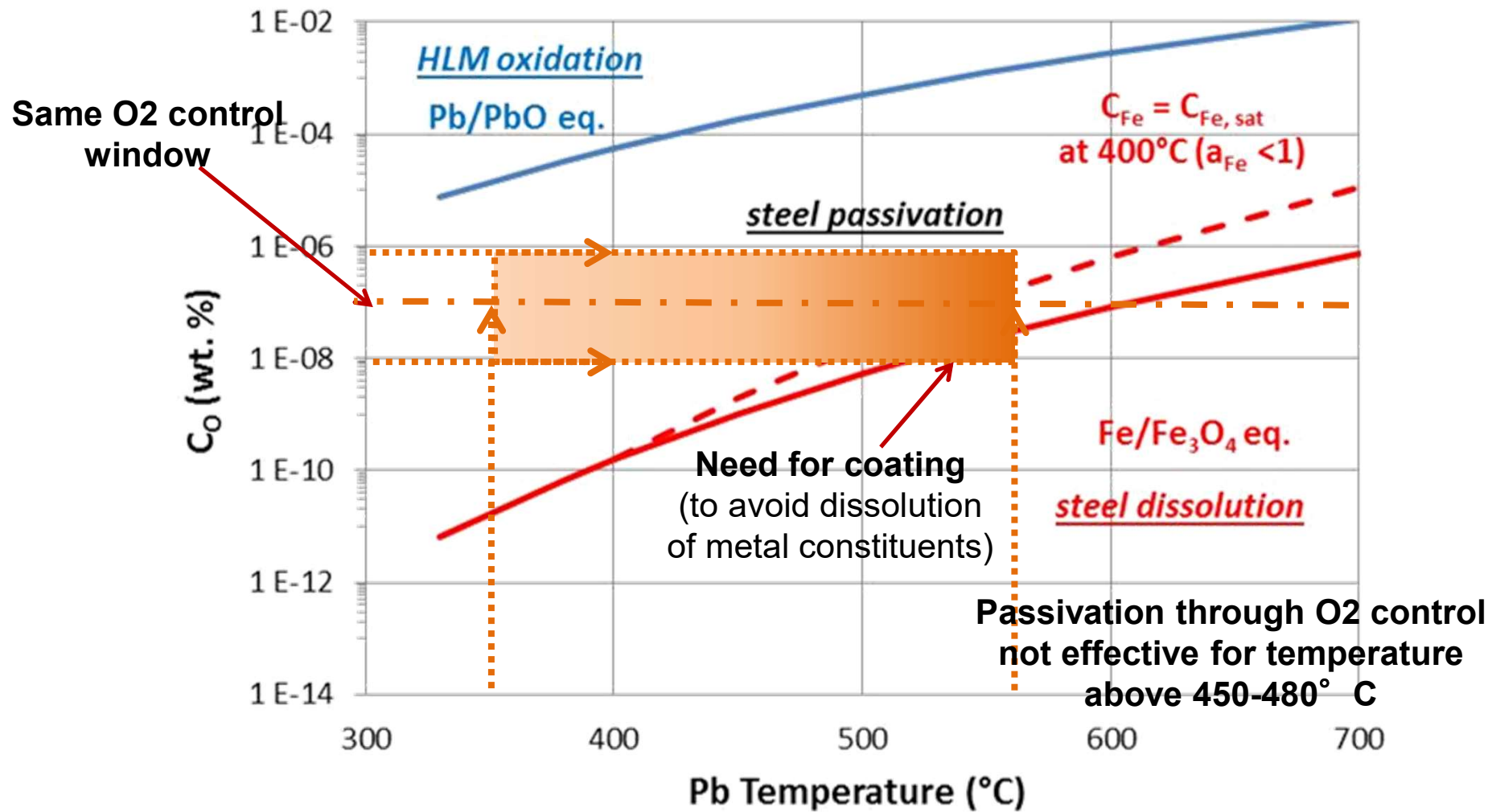




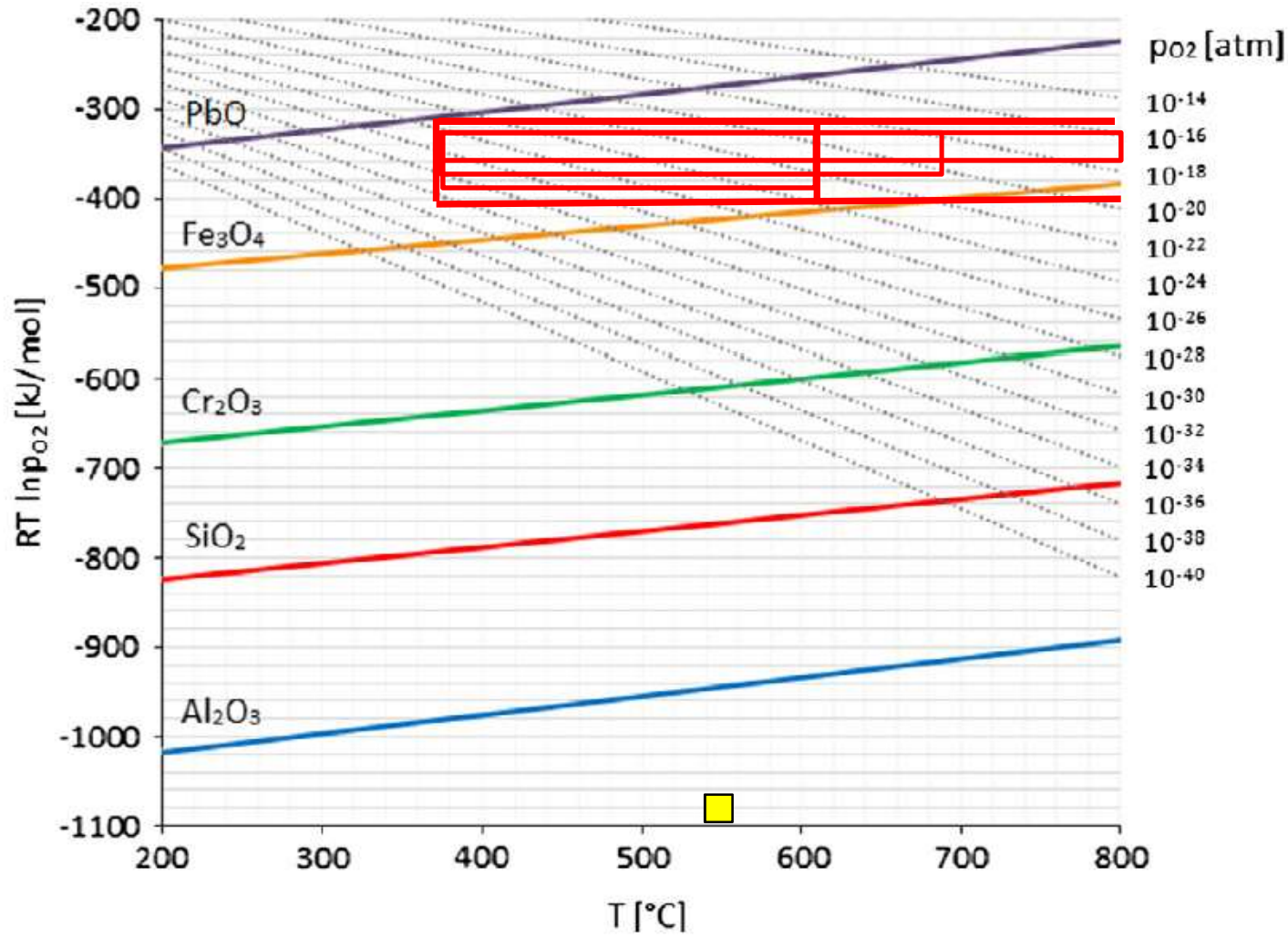
# Impact of temperature (1st stage)



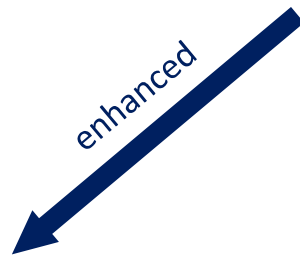
# Impact of temperature (final stage)



# Oxygen Control, fighting with ever narrow operational window!

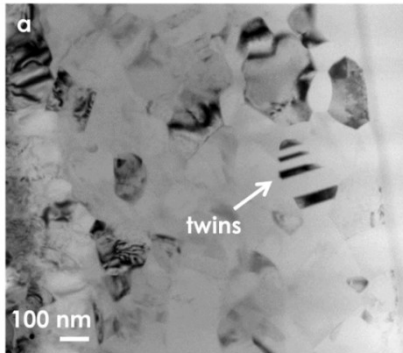


## NANOCERAMICS



**Mechanical  
performance**

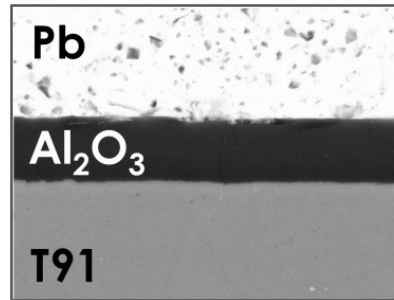
Coble creep, twinning, etc.



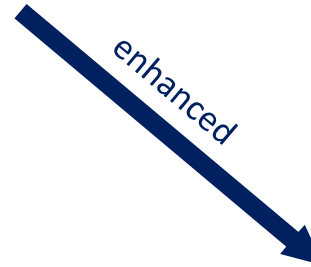
F. Garcia Ferré et al. – SCI REP – 2016



**Corrosion  
resistance**

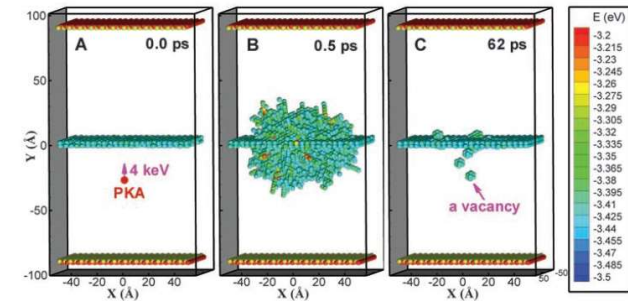


F. Garcia Ferré et al. – CORROS SCI – 2013



**Radiation  
tolerance**

Interstitial emission from GBs

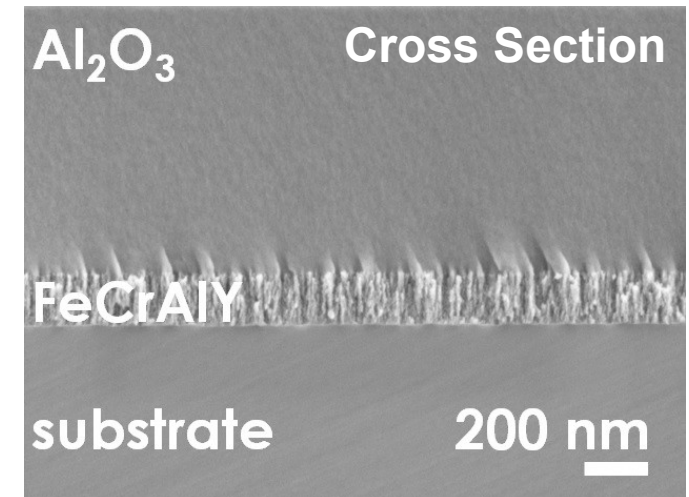
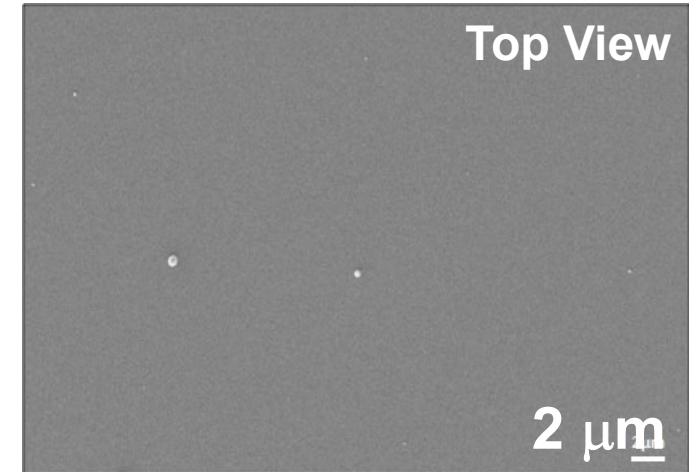
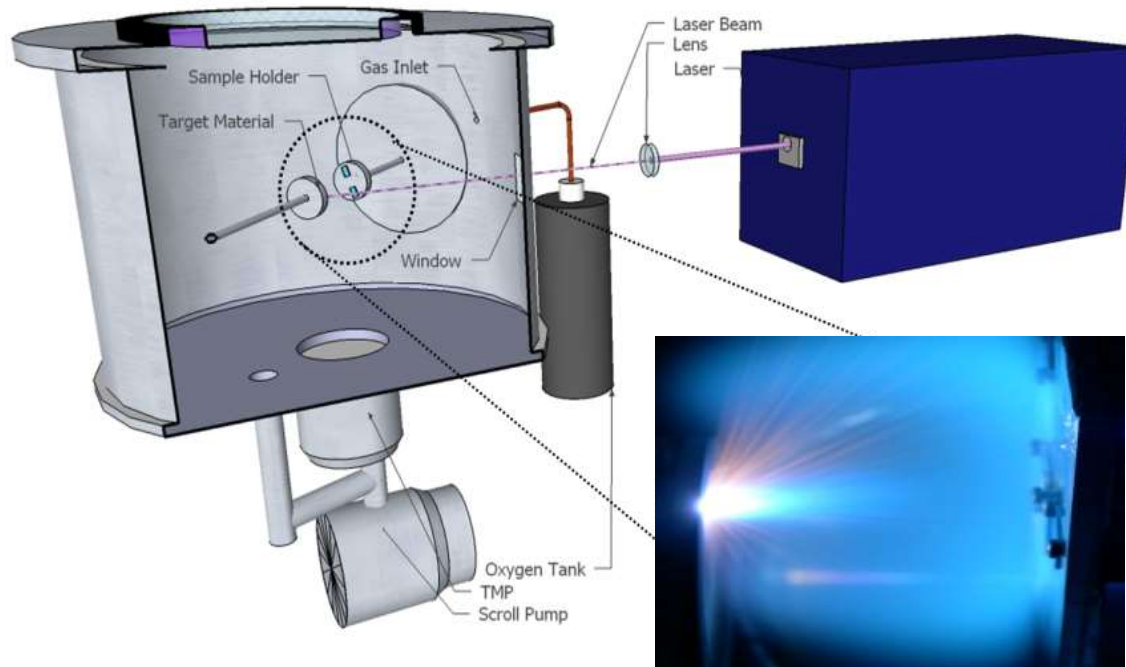


X.M. Bai et al. – Science - 2010

## **Al<sub>2</sub>O<sub>3</sub> films deposited by Pulsed Laser Deposition (PLD)**

Acta Materialia 61, 2662-2670, 2013  
Corrosion Science 77, 375-378, 2013  
Scientific Reports 6, 33478, 2016  
Corrosion Science 124, 80-92, 2017  
Acta Materialia 143, 156-165, 2018

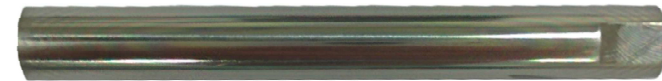
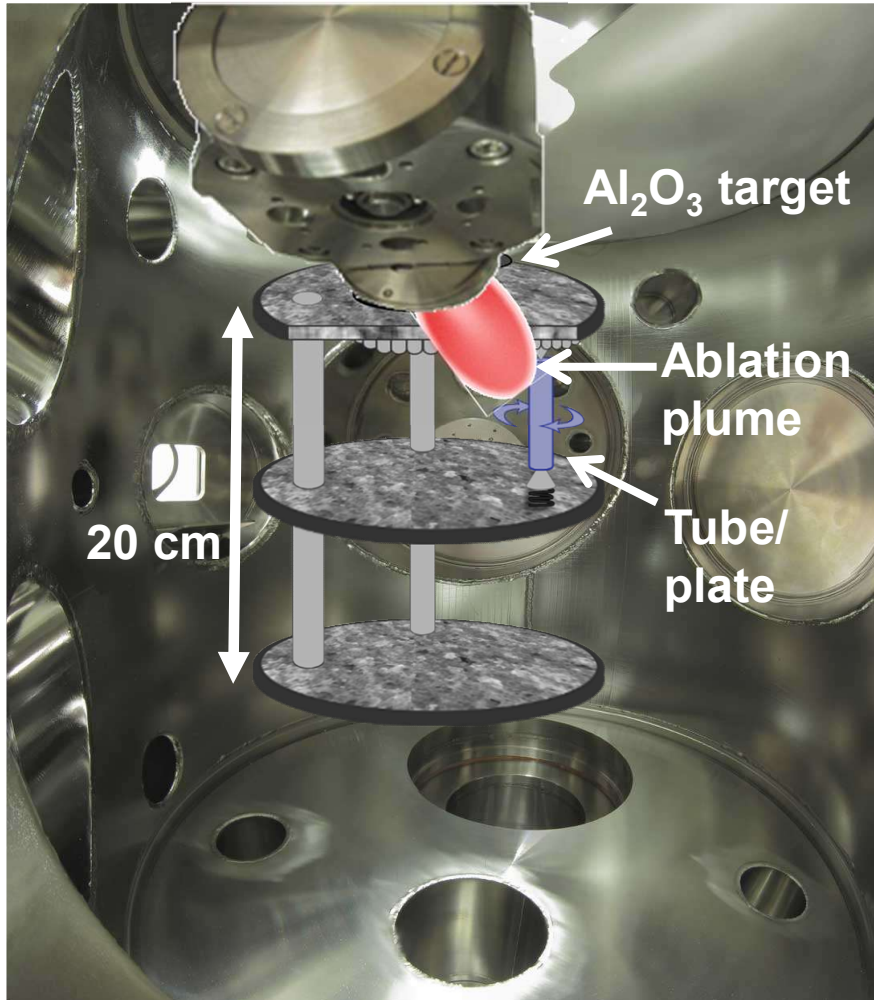
## Pulsed Laser Deposition



- ✓ High quality coatings
- ✓ Custom process: bottom-up approach
- ✓ Process at room temperature

**Al<sub>2</sub>O<sub>3</sub> fully dense coating,  
no pin holes, no defects**

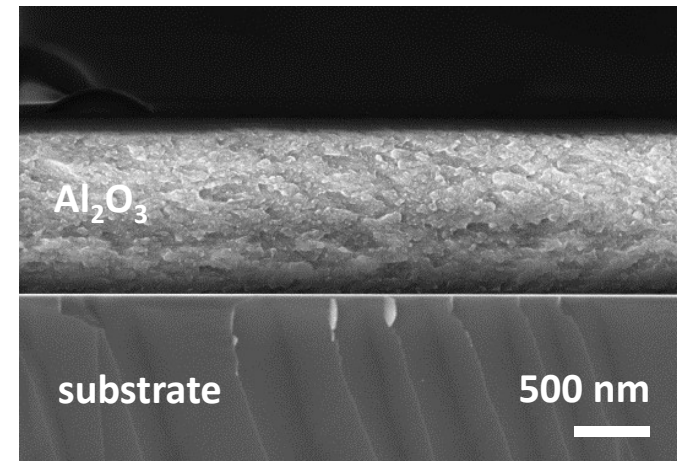
# Processing on tubes & cylinders



1515Ti cylinder + 5  $\mu\text{m}$   $\text{Al}_2\text{O}_3$



AISI 316L tube + 5  $\mu\text{m}$   $\text{Al}_2\text{O}_3$

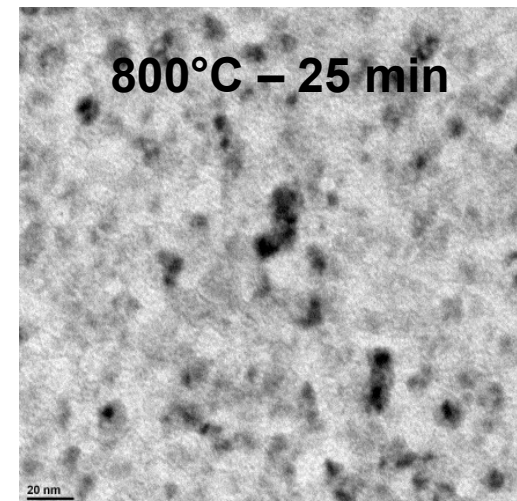
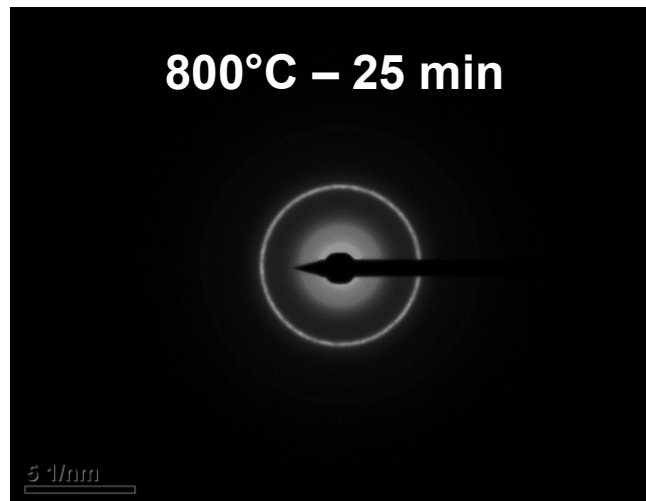
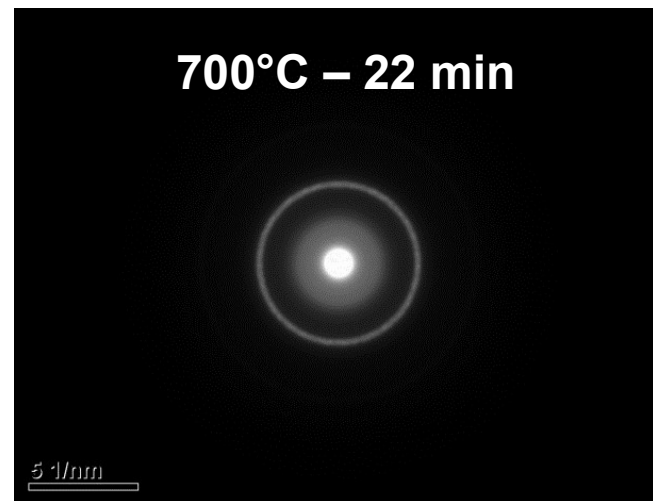
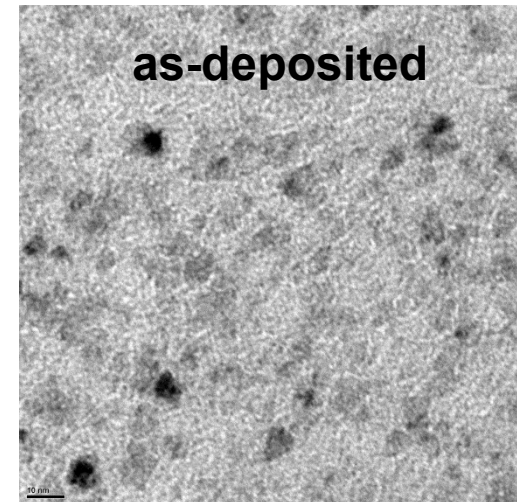
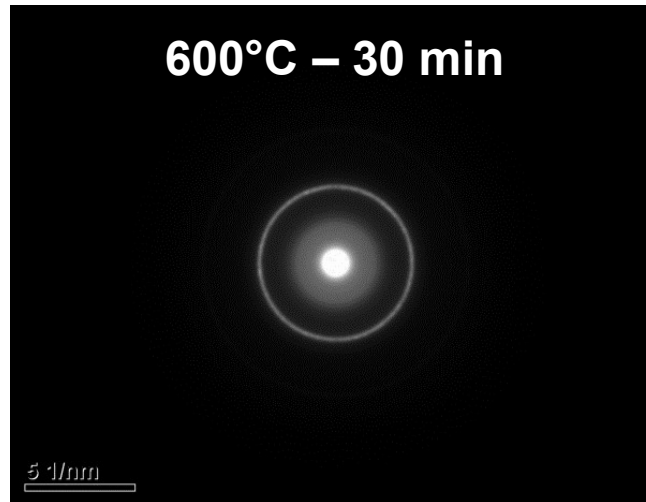
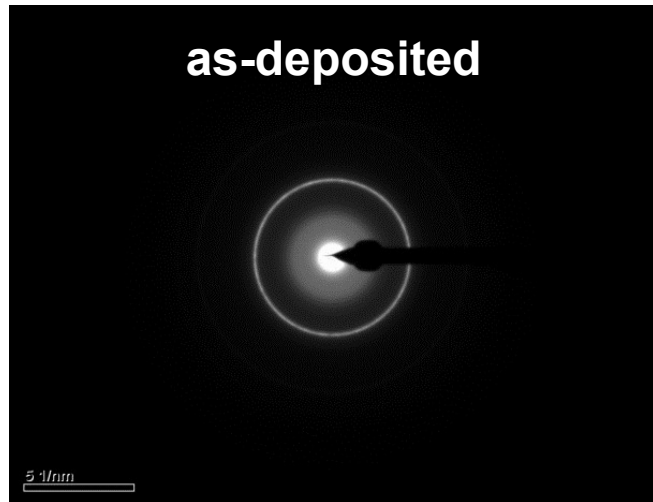


**Fully dense and compact  
ceramic coating**

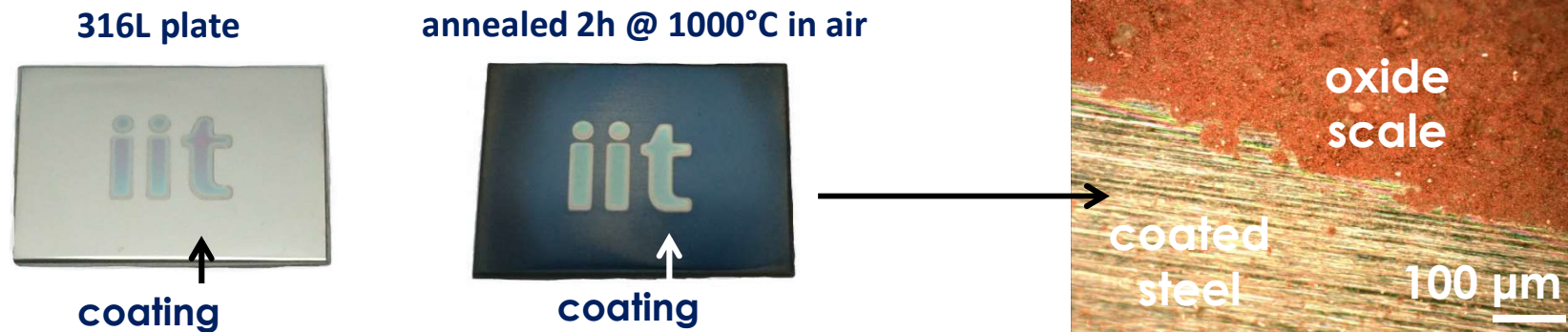


## Thermal stability: in-situ TEM

## BF-HRTEM



# Gas permeation barrier



## **Pb compatibility of $\text{Al}_2\text{O}_3$ barrier coatings**

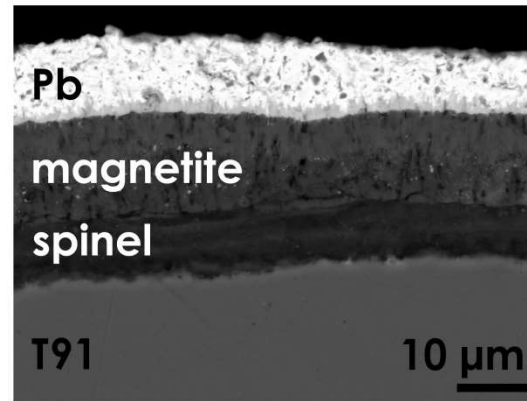
# Corrosion resistance, O<sub>2</sub> saturation

## SS plates

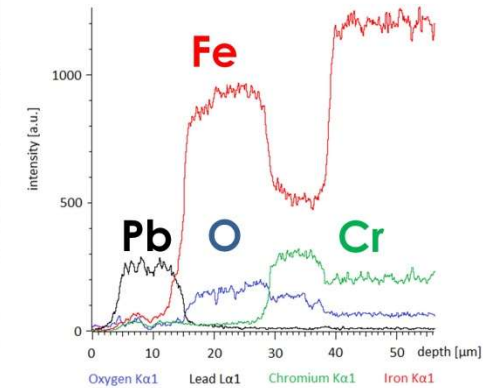
uncoated sample



heavy liquid metal  
corrosion



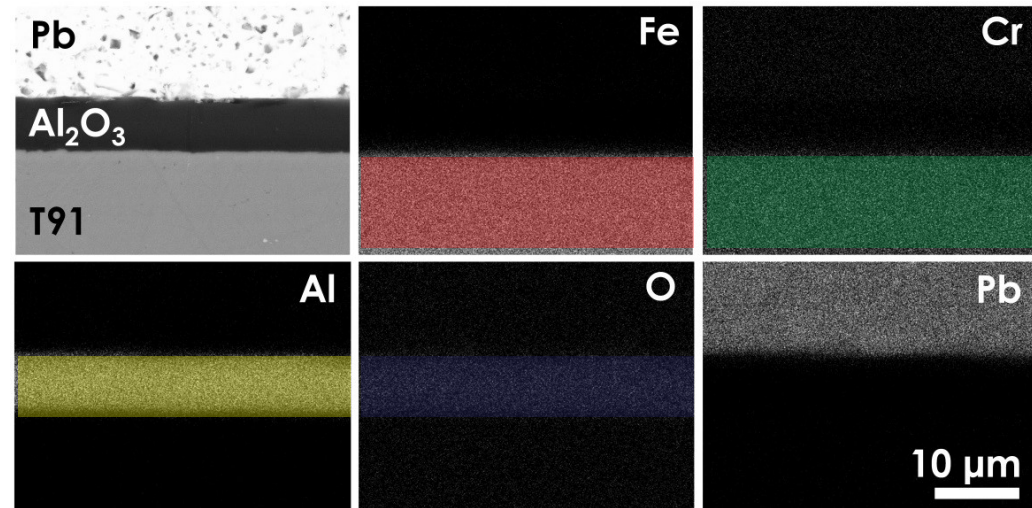
## Oxidizing stagnant Pb test



coated sample



protection



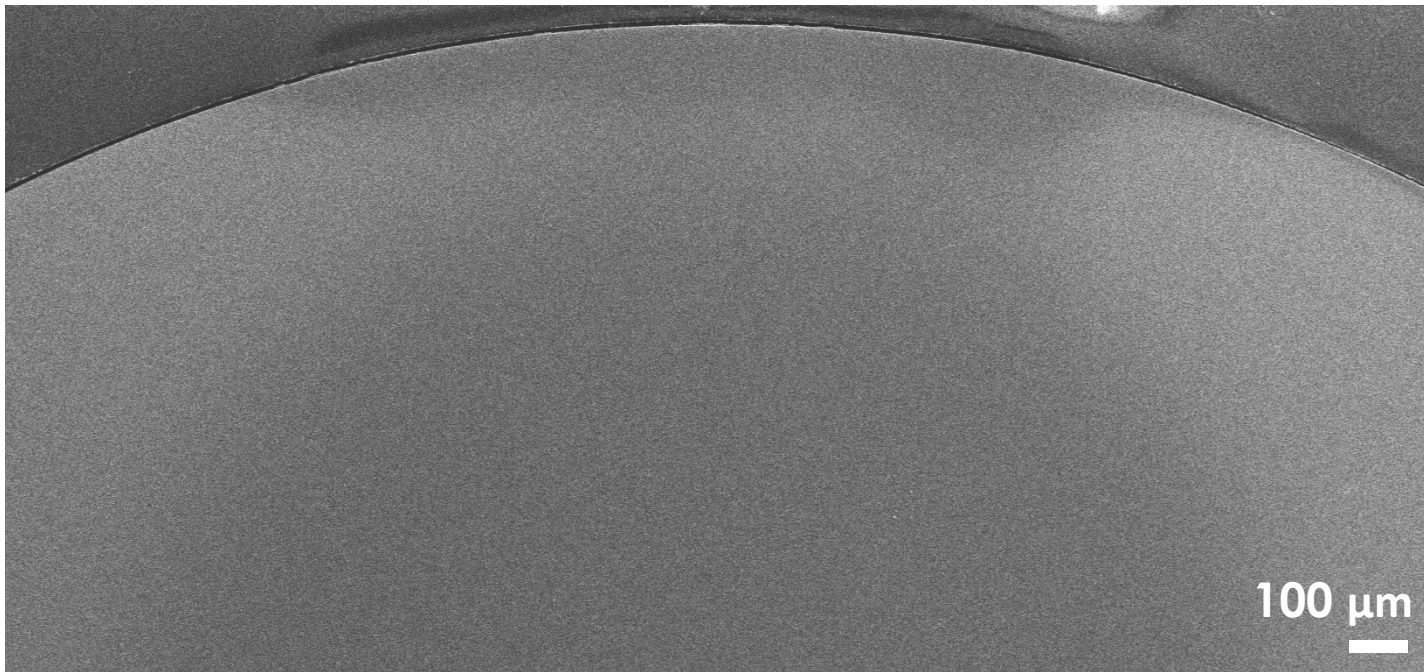
F. Garcia Ferré et al. – CORROS SCI – 2013

**1515Ti cylinder – 5000 h in stagnant Pb @550°C 10<sup>-8</sup> wt.% oxygen**

**1 μm Al<sub>2</sub>O<sub>3</sub> coating**



before



after

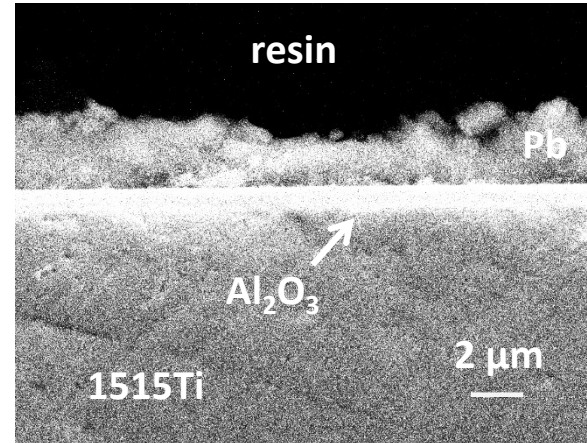
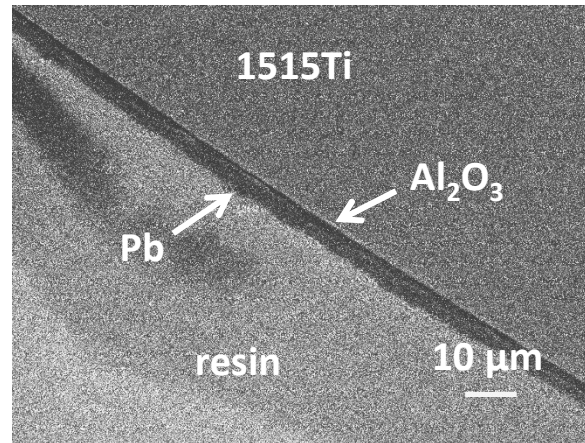
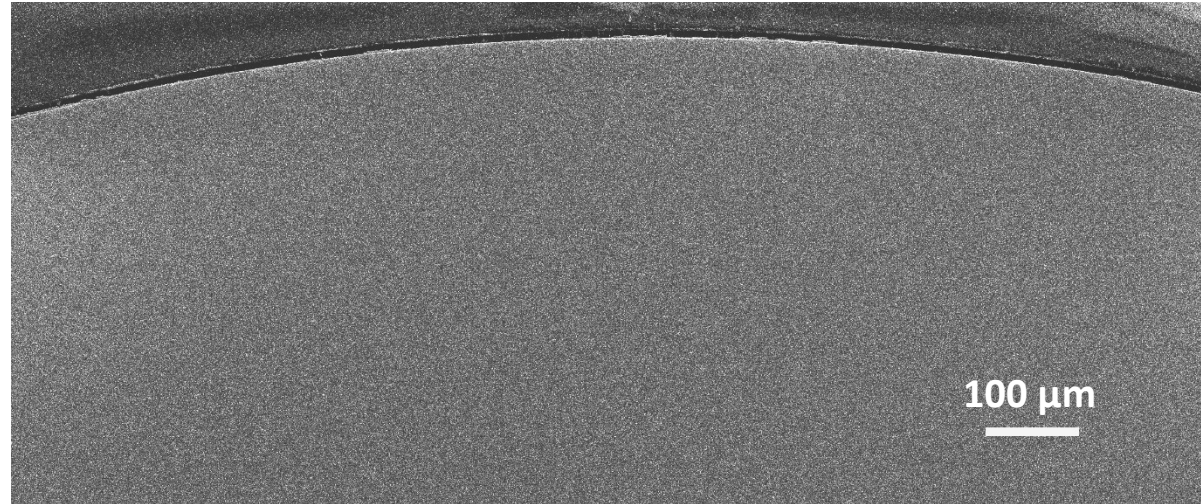
**No solidified lead on the 1515Ti cylinder**  
**NO CORROSION**

# Corrosion resistance, O<sub>2</sub> depletion

NO BL



BEFORE



NO BL



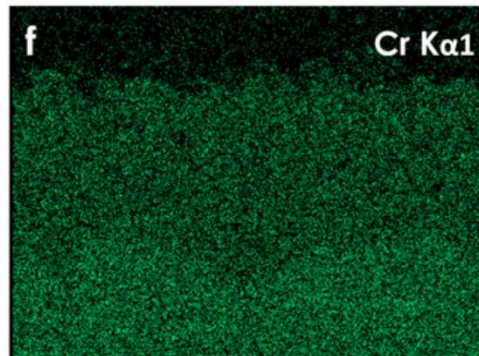
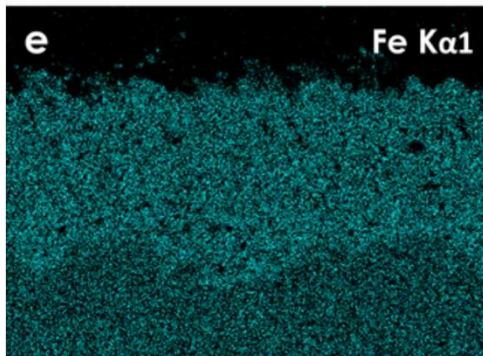
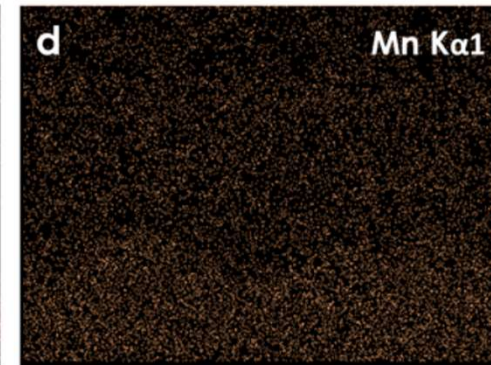
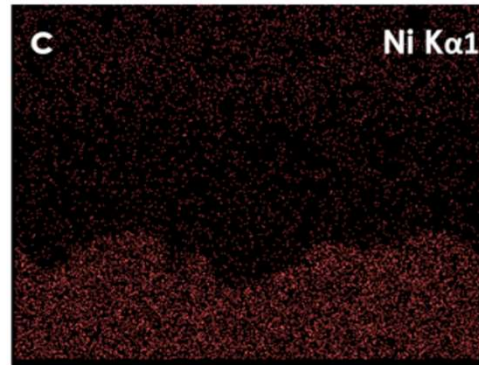
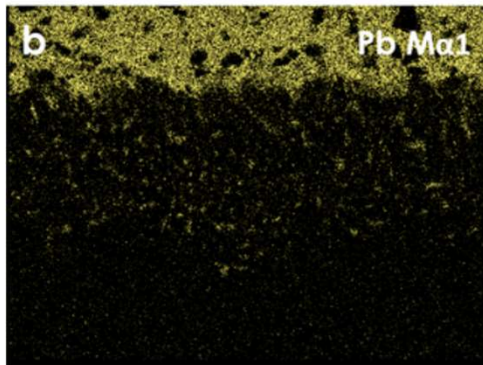
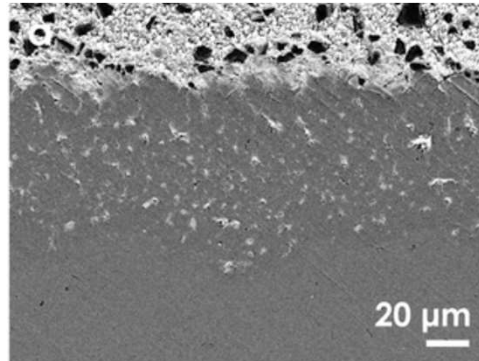
AFTER

**NO corrosion**

# Corrosion resistance, O<sub>2</sub> depletion

5000 h in stagnant Pb

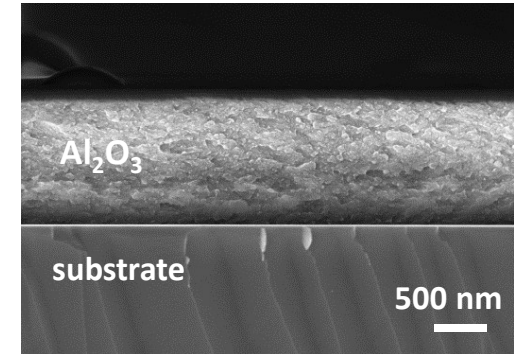
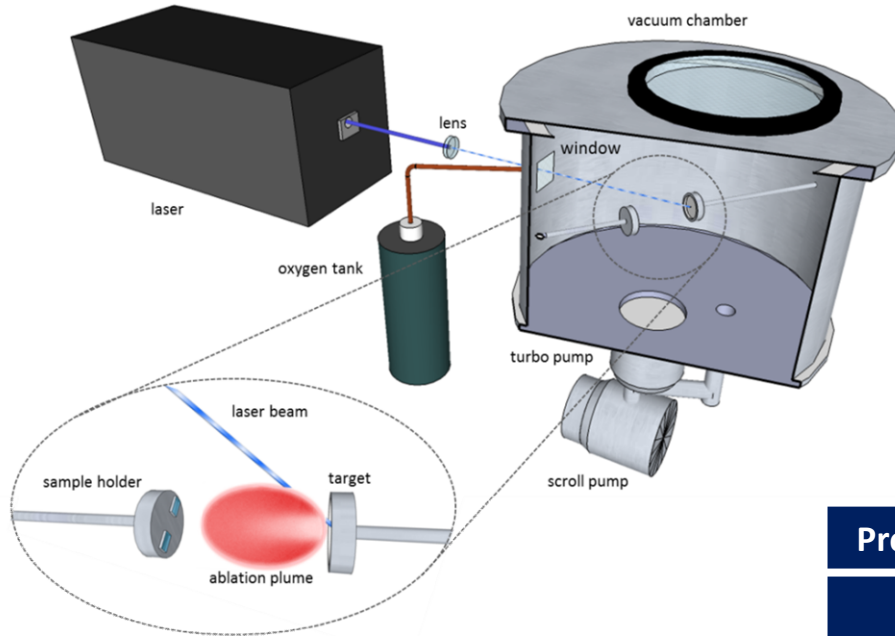
@550°C 10<sup>-8</sup> wt.% oxygen



# Thermomechanical properties



# PLD-grown $\text{Al}_2\text{O}_3$ nanoceramic coatings



F. Garcia Ferré et al. – ACTA MATER – 2013

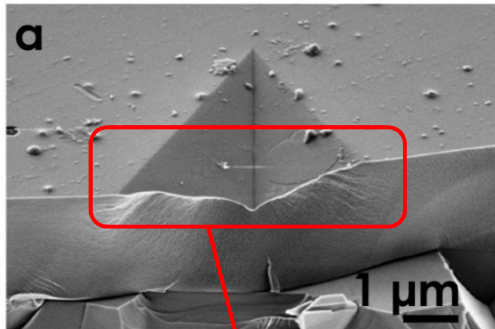
- ✓ high quality coatings
- ✓ custom process: bottom-up approach
- ✓ process at room temperature
- ✓ amorphous films with nanodispersed crystalline domains

| Property @RT | Sapphire | PLD $\text{Al}_2\text{O}_3$ | AISI 316L |
|--------------|----------|-----------------------------|-----------|
| $\nu$        | 0,24     | $0,295 \pm 0,025$           | 0,3       |
| E [GPa]      | 345      | $193,8 \pm 9,9$             | 200       |
| G [GPa]      | 175      | $75,5 \pm 3,8$              | 80        |
| B [GPa]      | 240      | $159,2 \pm 11,8$            | 140       |
| H [GPa]      | 27,8     | $10,3 \pm 1$                | 4         |
| H/E          | 0,059    | $0,049 \pm 0,007$           | 0,025     |

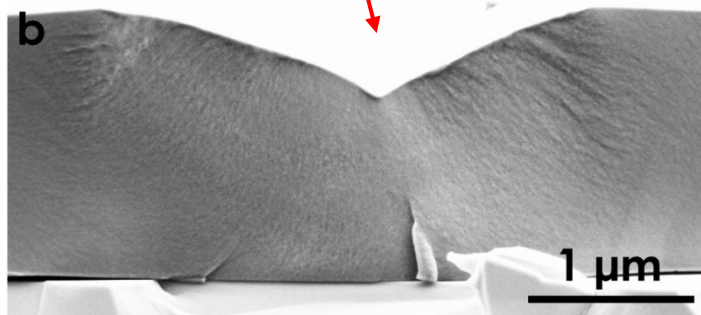
H/E parameter index of wear resistance and fracture toughness

# Mechanical behaviour of PLD-grown $\text{Al}_2\text{O}_3$

- Nanoindentation Tests

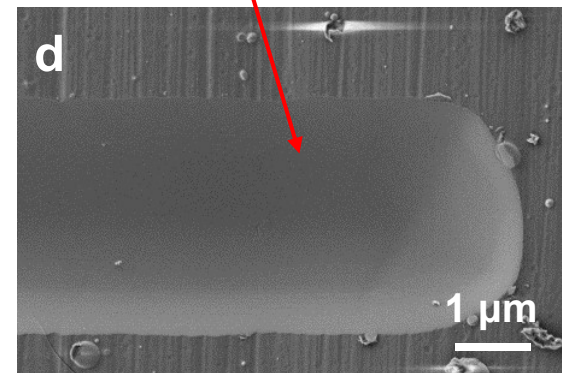
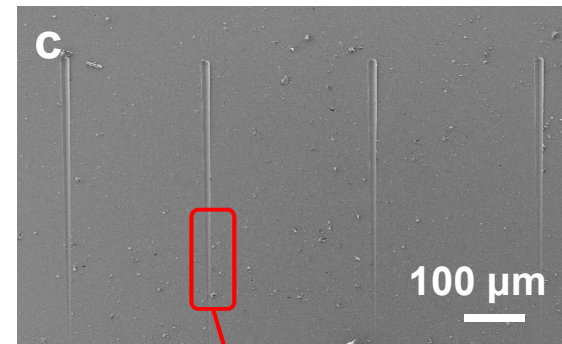


F. Garcia Ferré et al. – ACTA MATER – 2013

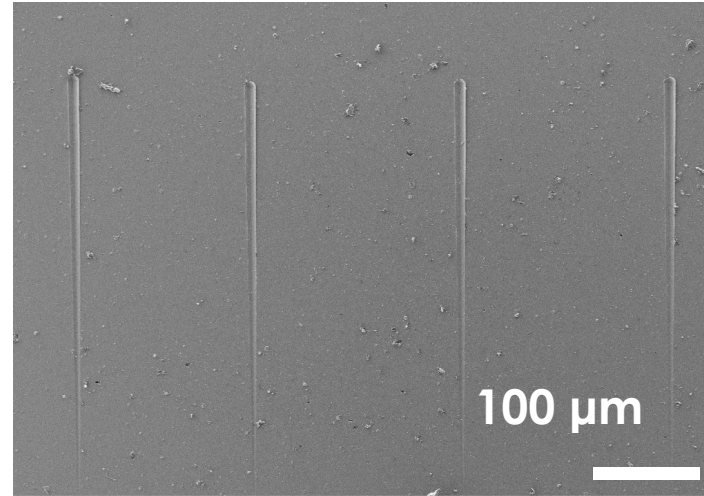
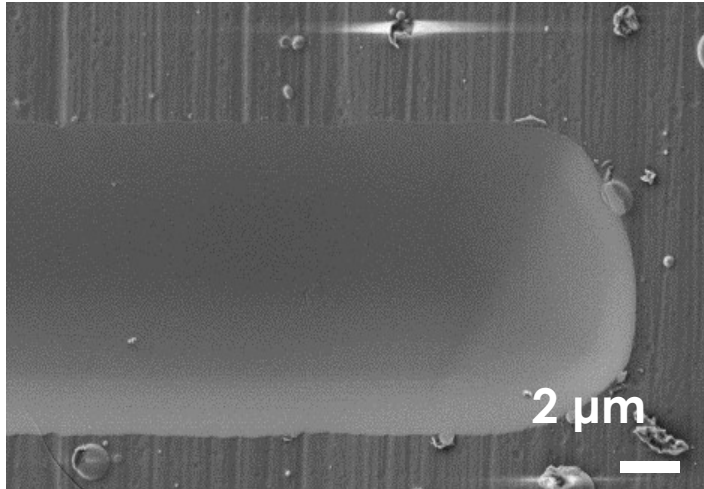


metal-like behavior under plastic strain

- Nanoscratch Tests



strong interfacial bonding



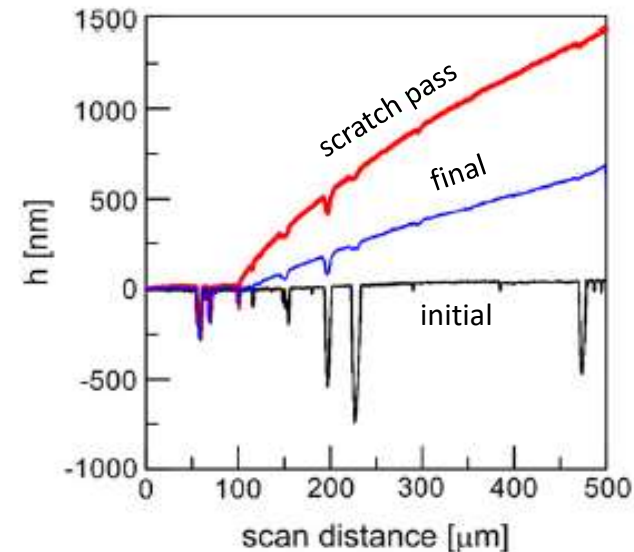
No delamination  
No critical load

Strong interfacial  
bonding

## Nanoscratch tests

- Conical tip ( $r = 10 \mu\text{m}$ )
- Scratch length  $400 \mu\text{m}$
- Maximum load  $500 \text{ mN}$
- $2,5 \text{ mN/s}$  and  $2 \mu\text{m/s}$
- Black line: initial topography at 0 load
- Blue line: final topography at 0 load
- Red line: penetration depth at increasing load

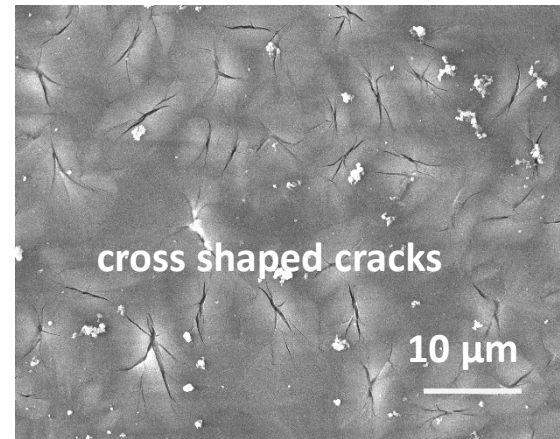
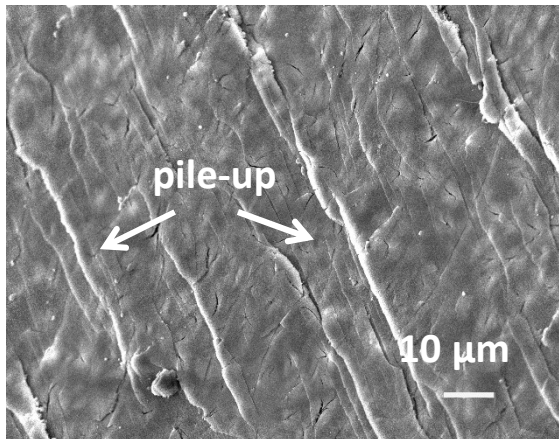
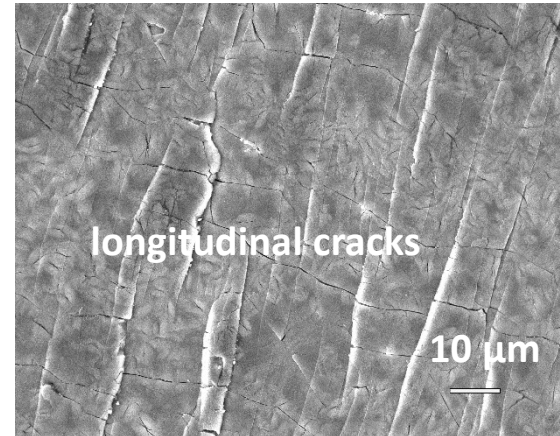
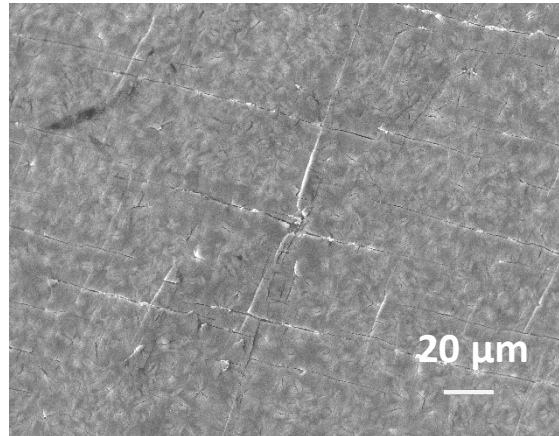
penetration depth vs. scan distance



# Burst test

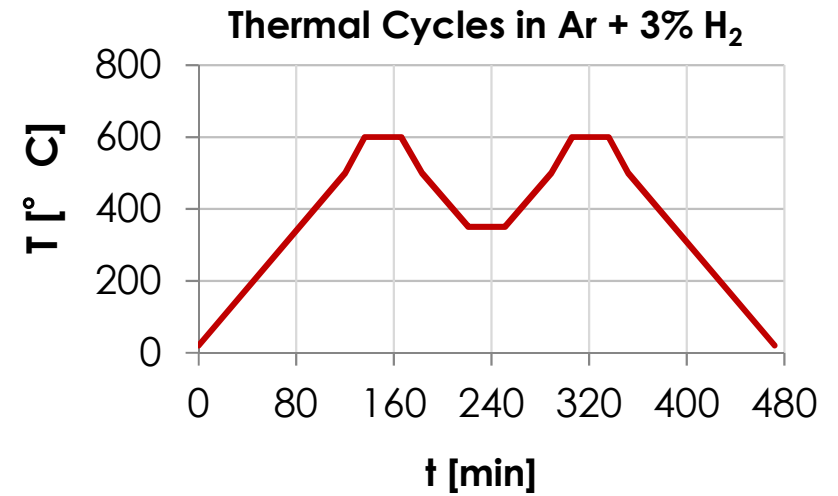


**BEFORE**



**AFTER**

# Thermal cycling



➤ Samples without BUFFER LAYER – after



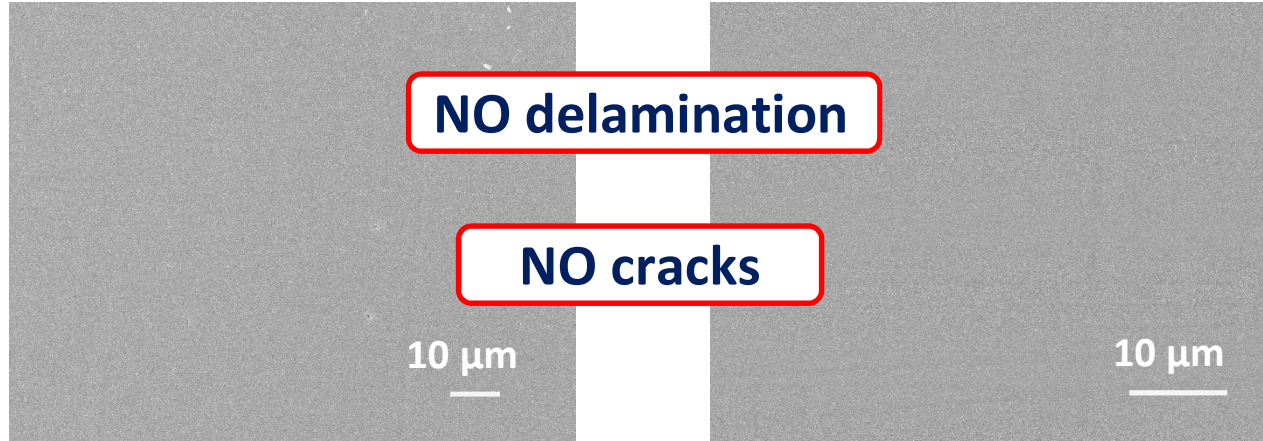
no changes after 12 cycles



# Thermal shock

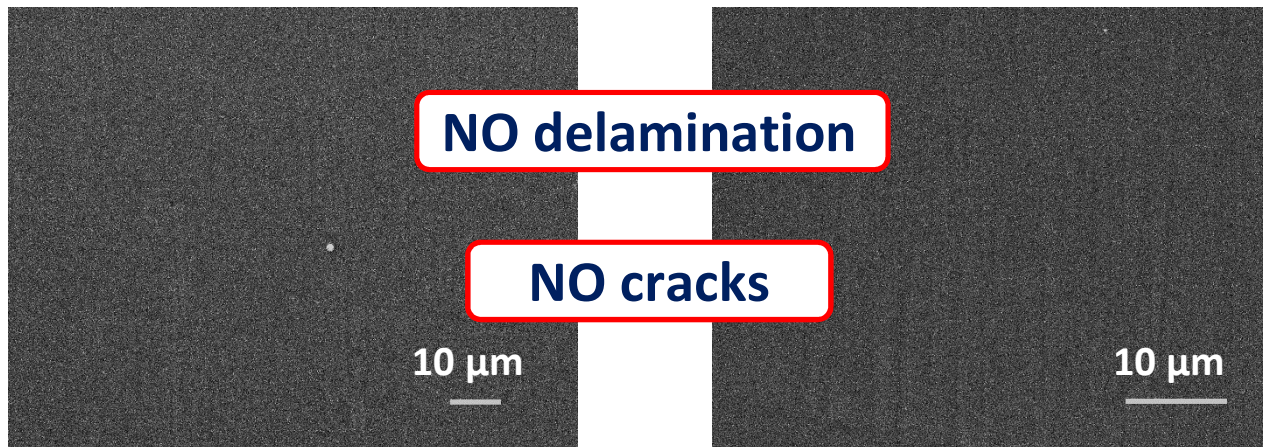
➤ Heated up to 600 °C

➤ Cooled down with N<sub>2</sub> gas flow ( ~10 °C/s)



➤ Heated up to 600 °C

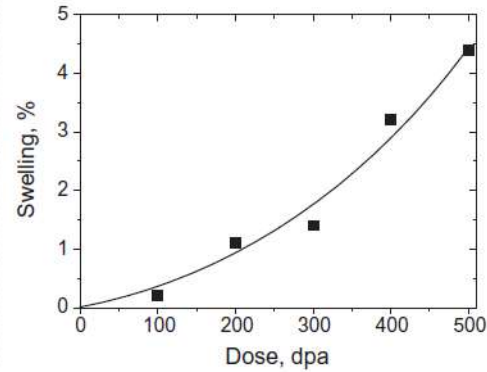
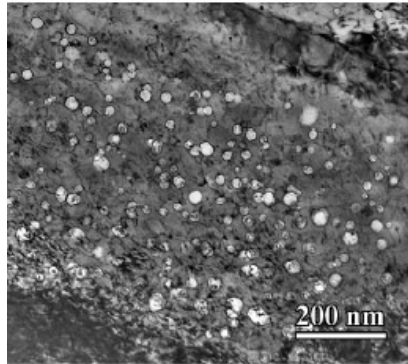
➤ Cooled down in liquid H<sub>2</sub>O ( ~10<sup>2</sup> °C/s)



# Heavy Ion Irradiation of $\text{Al}_2\text{O}_3$ barrier coatings

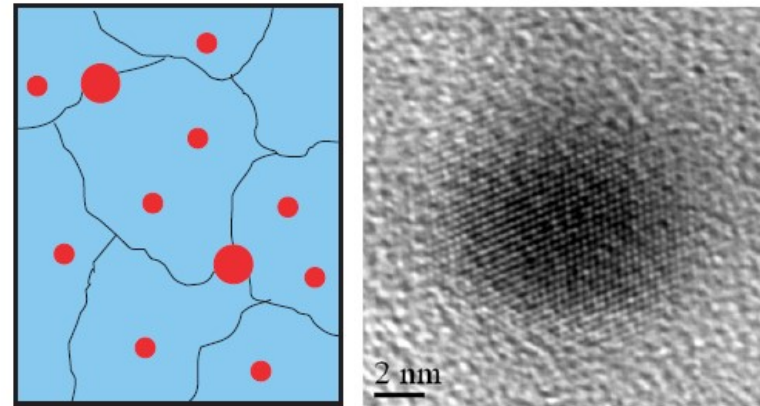
# Radiation tolerant materials

## Low-swelling ferritic martensitic steels



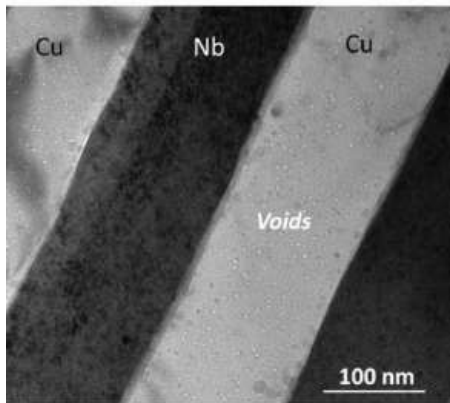
M.B. Toloczko et al. - J. Nucl. Mater. - 2014

## Oxide-dispersion strengthened steels & alloys

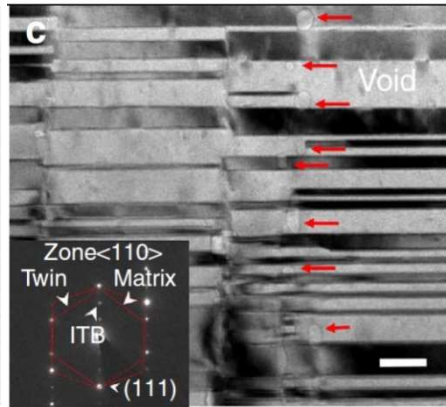


G. Liu et al. - Nature Mater. - 2013 M.L. Lescoat et al. - J. Nucl. Mater. - 2012

## Nanolaminates & nanotwinned metals

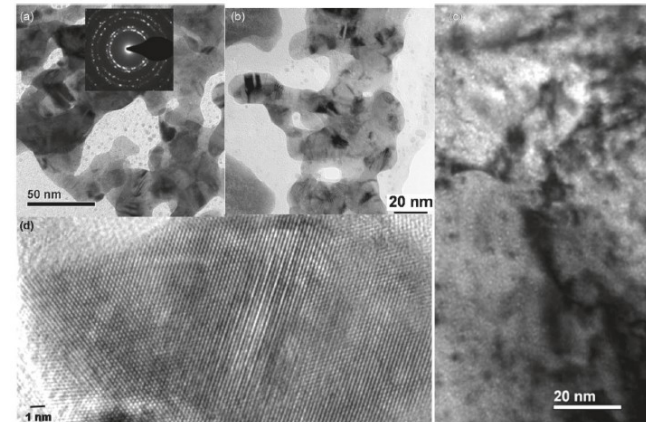


D. Rollet et al. - Adv. Mater. - 2013



Y. Chen et al. - Nature Commun. - 2015

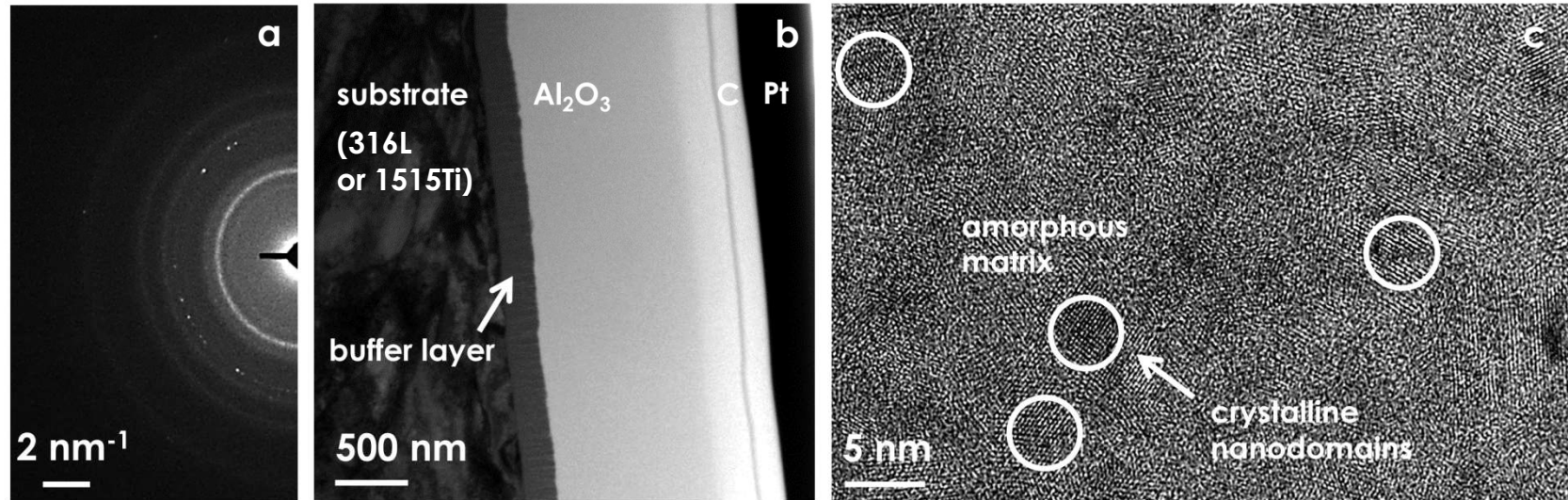
## Nanoporous materials



Y. Chen et al. - Nature Commun. - 2015

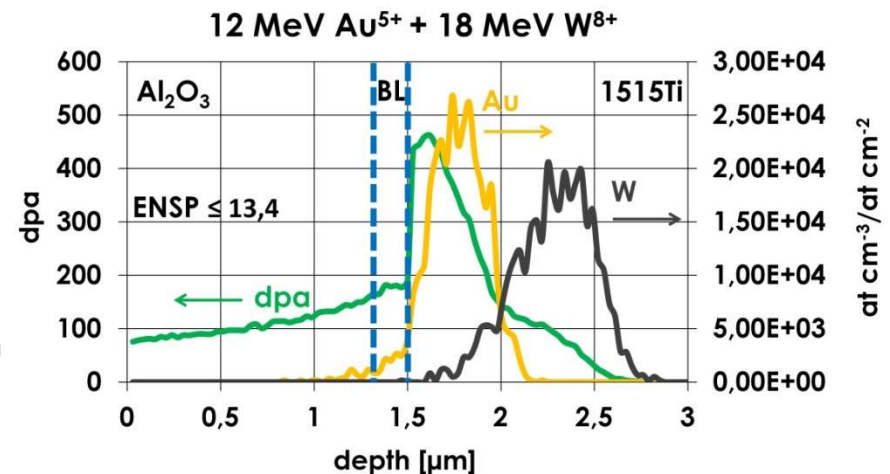


# Heavy ion irradiation (Au + W) of Al<sub>2</sub>O<sub>3</sub>



## Main criteria

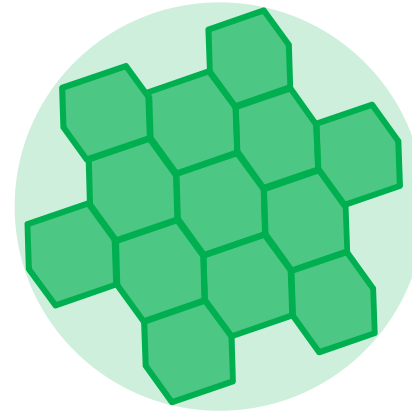
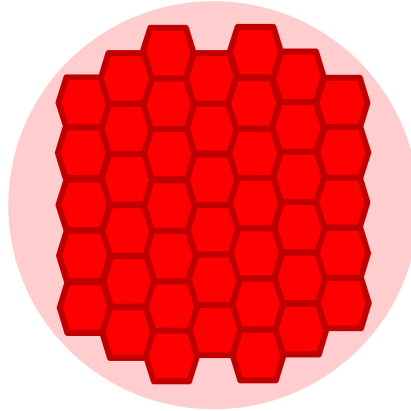
- Minimum coating thickness for nanoindentation: 1  $\mu\text{m}$
- Implantation beyond coating  $\rightarrow$  negligible chemical effects
- Low ENSP ratio to simulate effect of neutrons
- Low enough absolute electronic stopping power to avoid single swift ion track formation (7 keV/nm vs  $\approx$  9,5 keV/nm threshold @RT)
- Different doses, corresponding to **20, 40, 150, 250 and 450 dpa** at the interface between Al<sub>2</sub>O<sub>3</sub> and BL
- dpa calculated using SRIM (Kinchin-Pease)



# Model of evolution

## moderate dpa

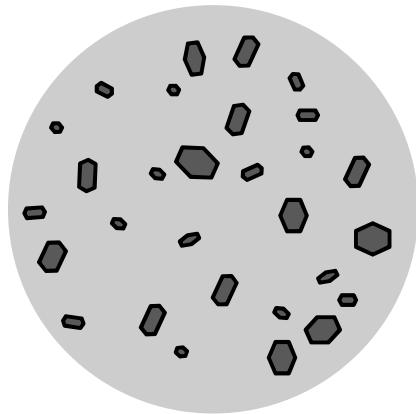
ultra-fine nanoceramic  
GB-driven deformation  
highest fracture toughness



## high dpa

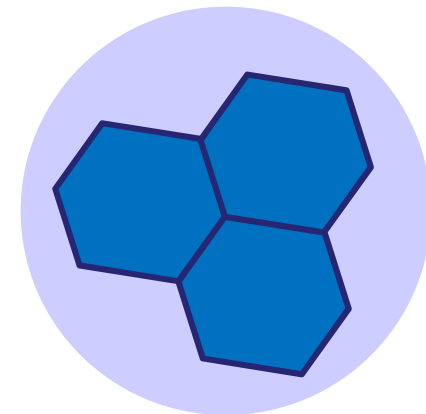
fine nanoceramic  
GB-driven deformation  
sub-linear grain growth

## pristine

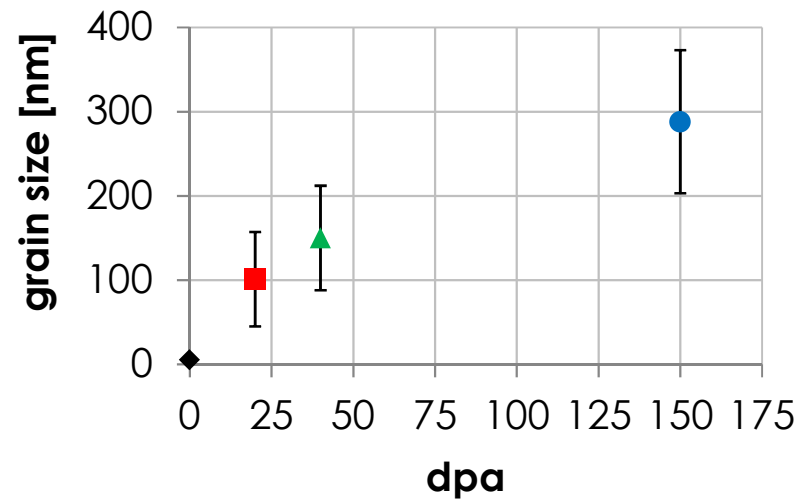


bi-phase nanocomposite  
shear banding  
highest fracture strength

## end-of-life dpa



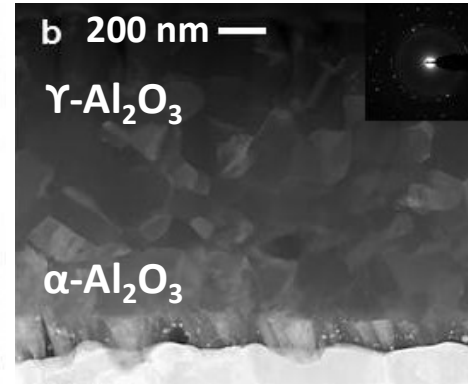
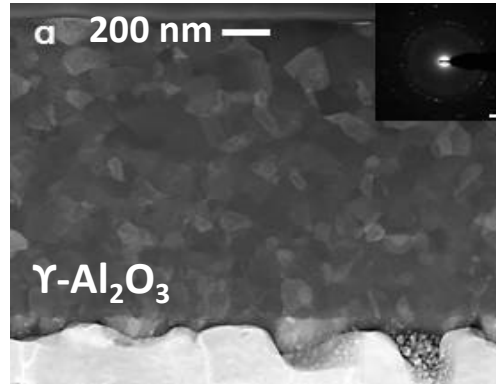
nanoceramic  
GB-driven deformation  
highest stiffness



**Sublinear grain growth**

## moderate dpa

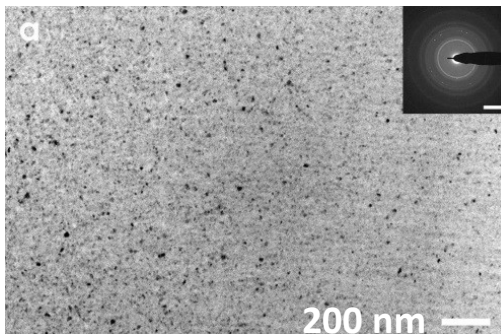
ultra-fine nanoceramic  
GB-driven deformation  
highest fracture toughness



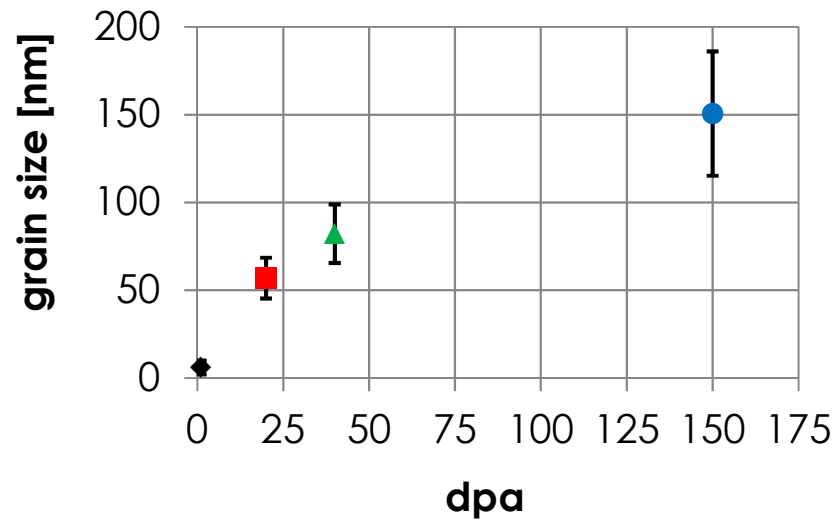
## high dpa

fine nanoceramic  
GB-driven deformation  
sub-linear grain growth

## pristine



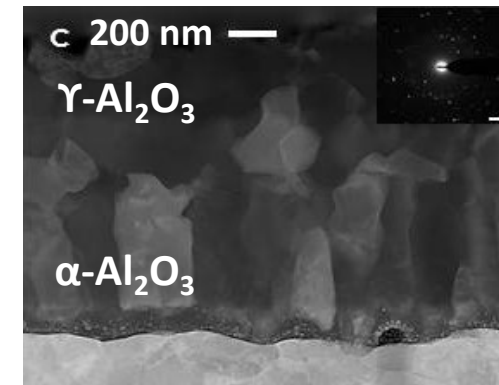
bi-phase nanocomposite  
shear banding  
highest fracture strength



**Sublinear grain growth**

## end-of-life dpa

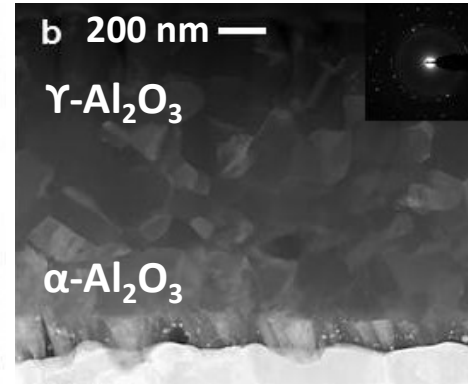
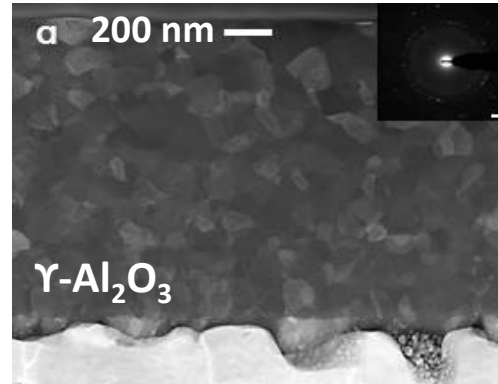
nanoceramic  
GB-driven deformation  
highest stiffness



# Model of evolution

**moderate dpa**

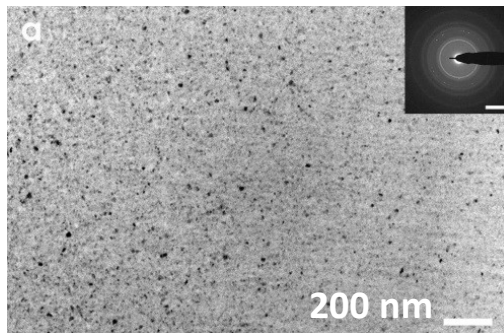
ultra-fine nanoceramic  
GB-driven deformation  
highest fracture toughness



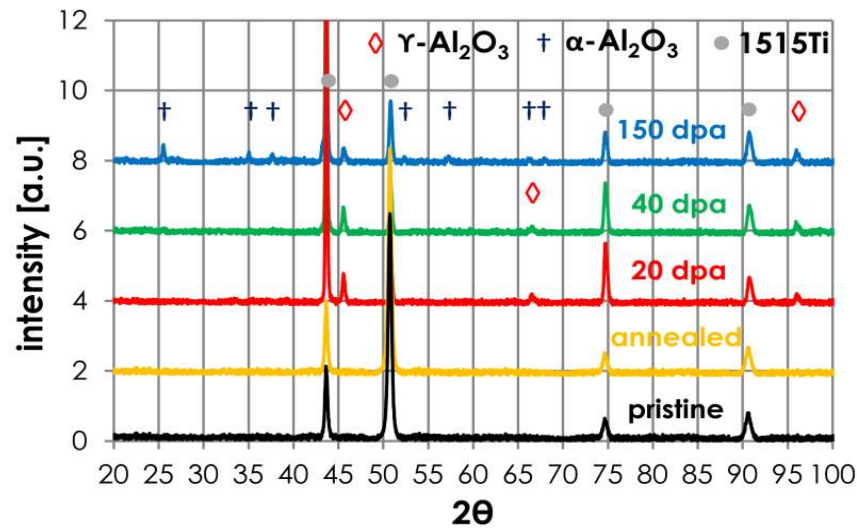
**high dpa**

fine nanoceramic  
GB-driven deformation  
sub-linear grain growth

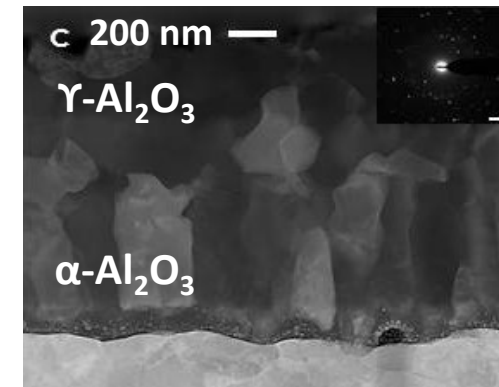
**pristine**



bi-phase nanocomposite  
shear banding  
highest fracture strength



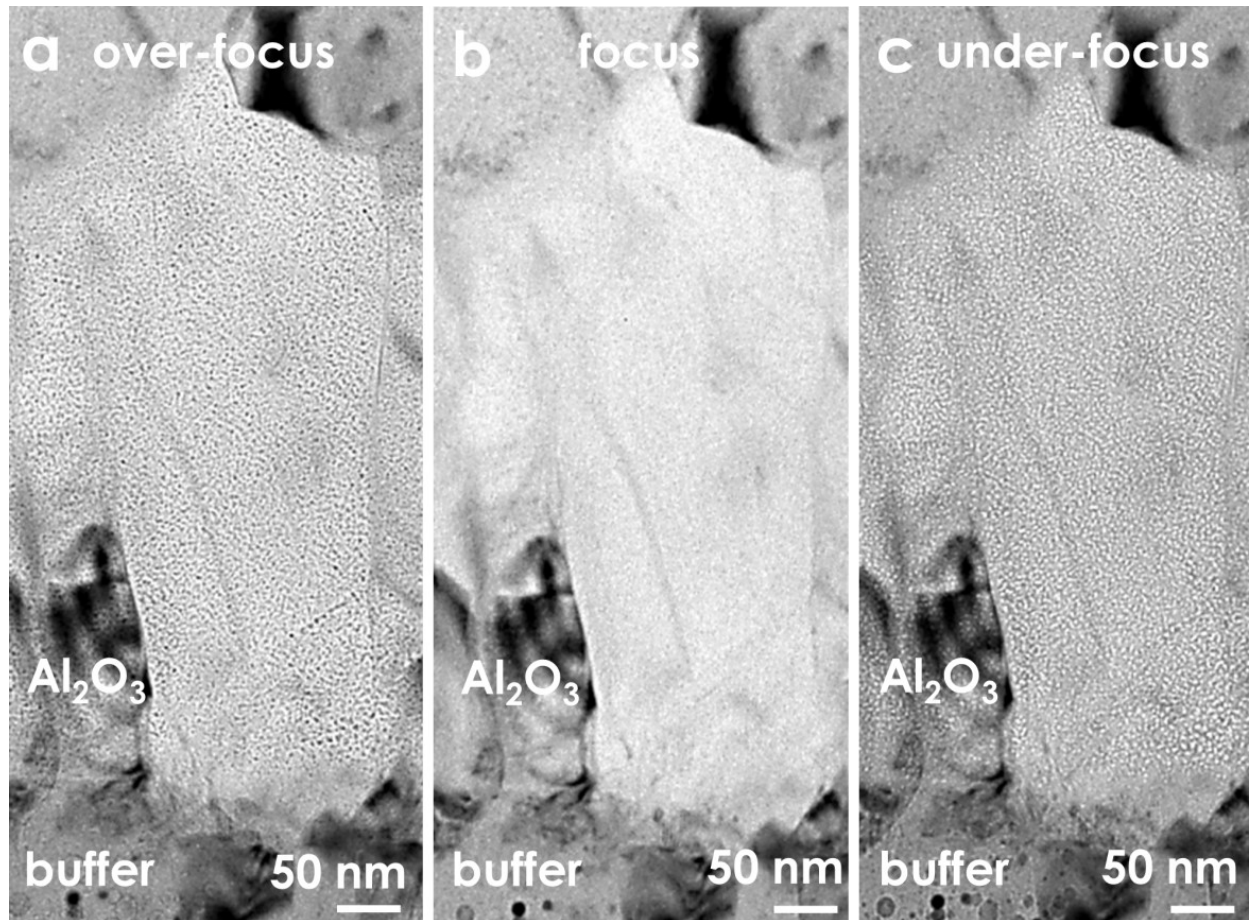
**end-of-life dpa**



nanoceramic  
GB-driven deformation  
highest stiffness

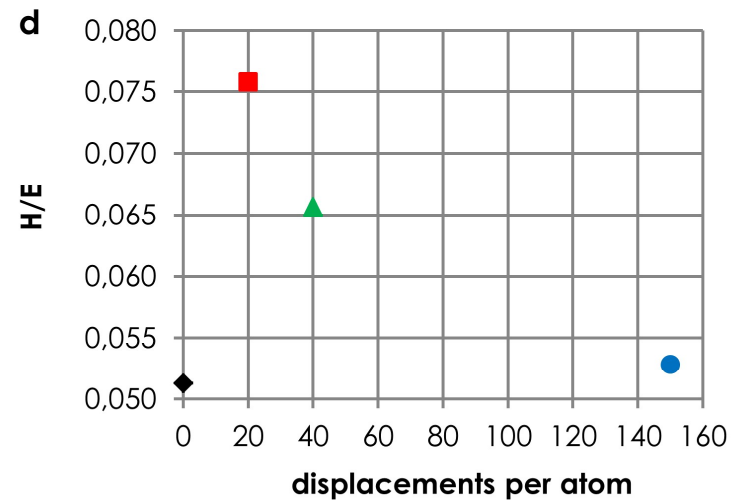
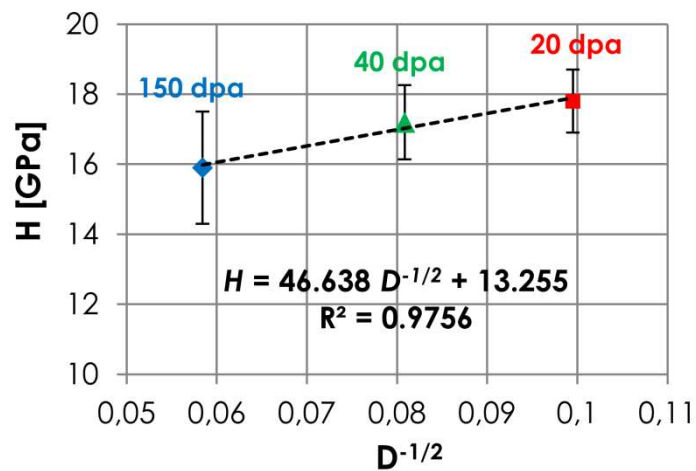
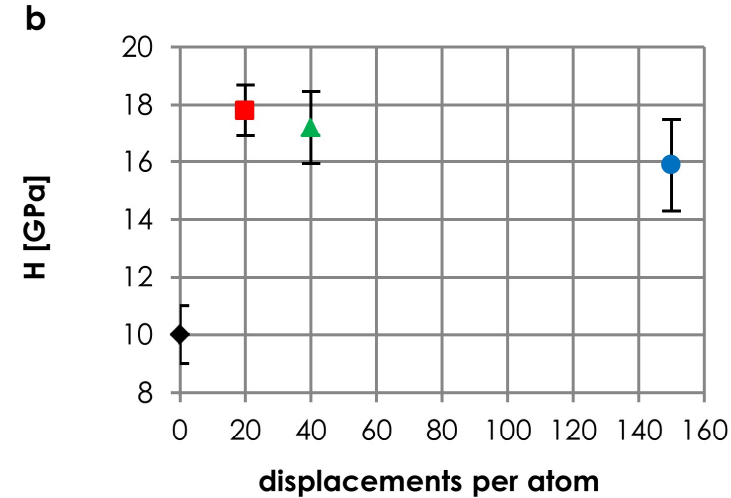
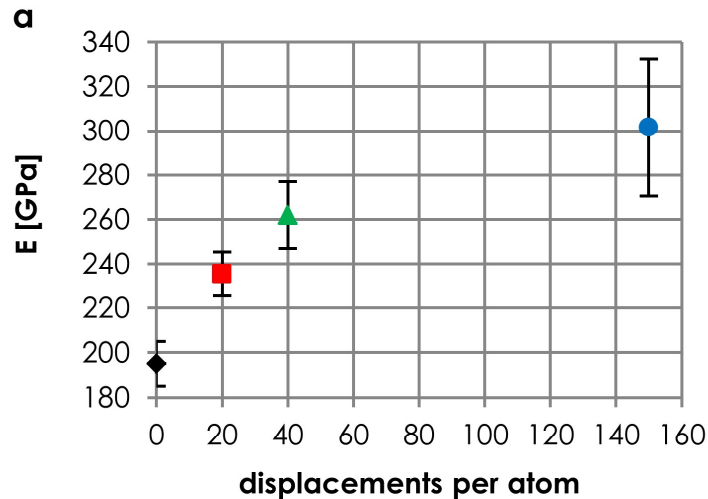
**Phase Transition**

## Heavy ion irradiation (Au + W): structural features



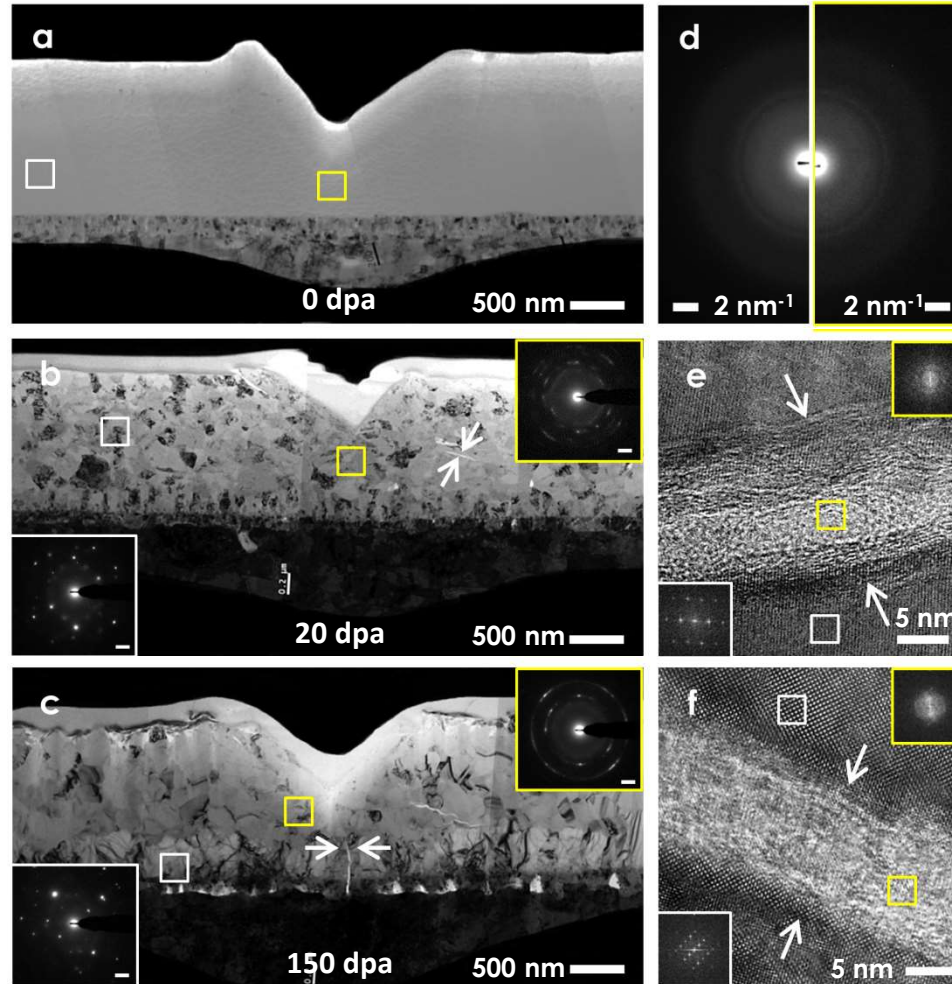
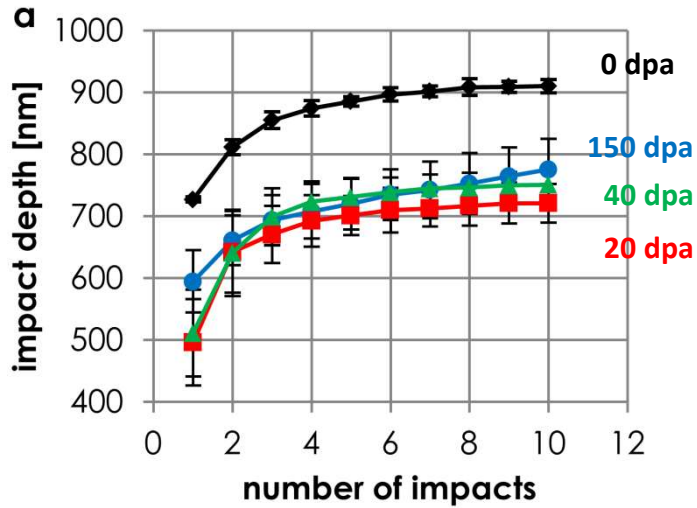
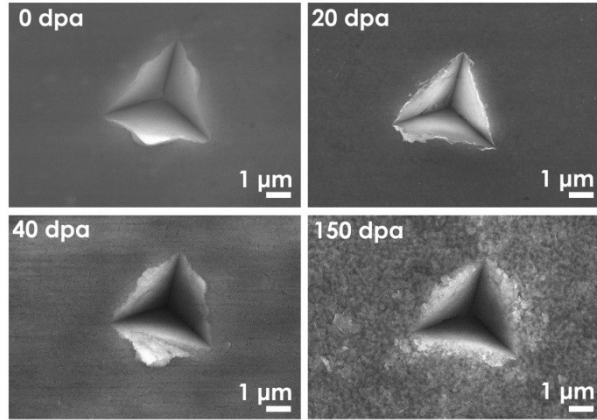
- Large number of small voids, only in a monolayer of grains, at the interface with the buffer layer
- These grains are alpha-alumina. All the other grains are gamma-alumina

# Heavy ion irradiation (Au + W): mechanical properties



- The evolution of the mechanical properties is well fitted by the Hall-Petch relationship
- The structural rearrangements lead to an increase of the H/E ratio in-service (index of fracture toughness)

# Heavy ion irradiation (Au + W): nanoimpact



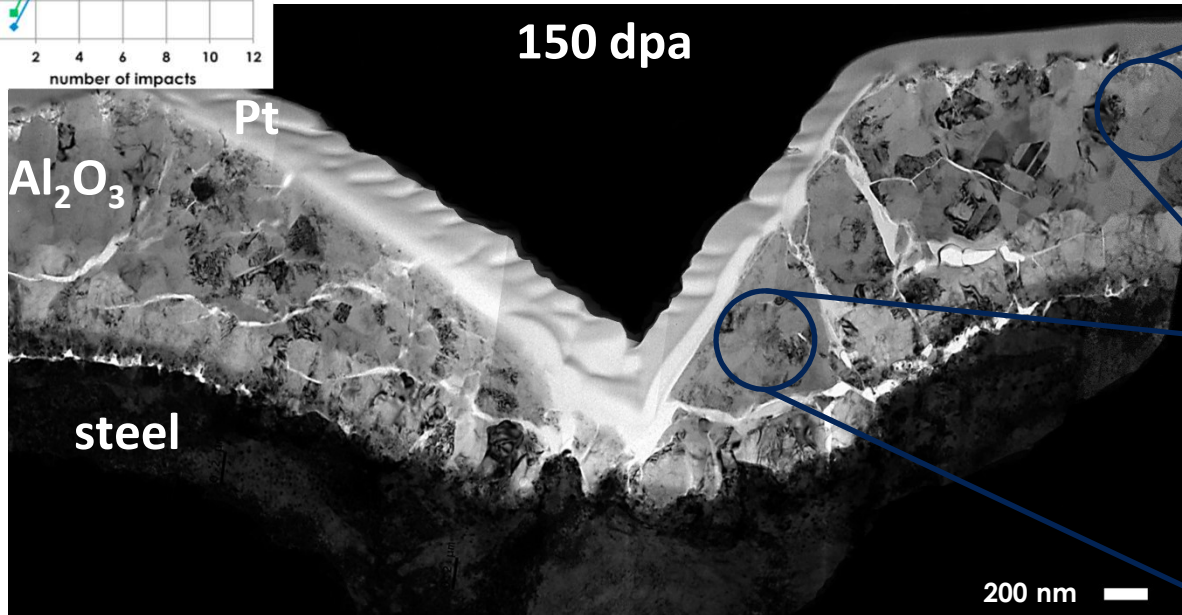
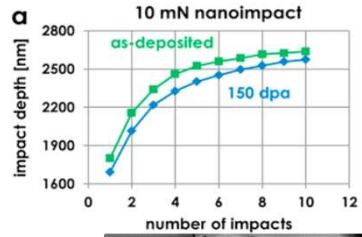
Shear banding

Lattice bending & localized shear amorphization

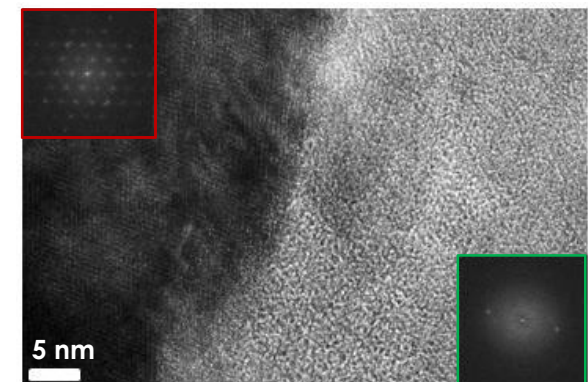
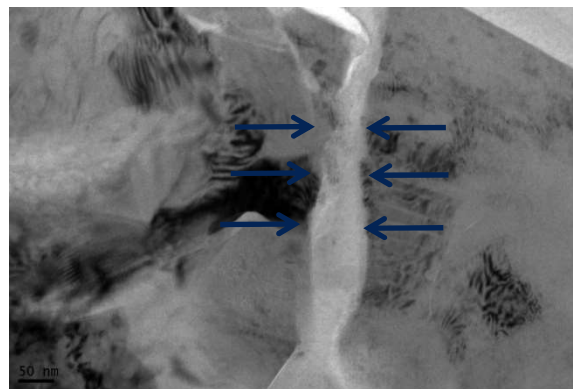
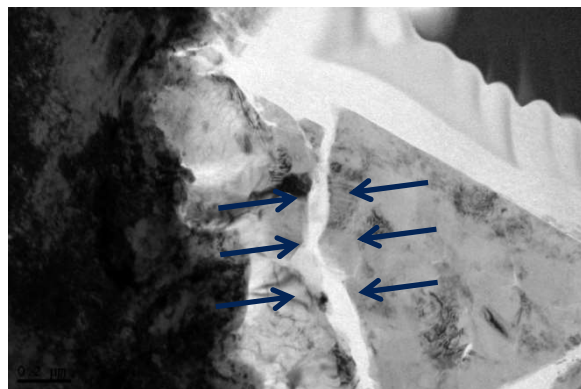
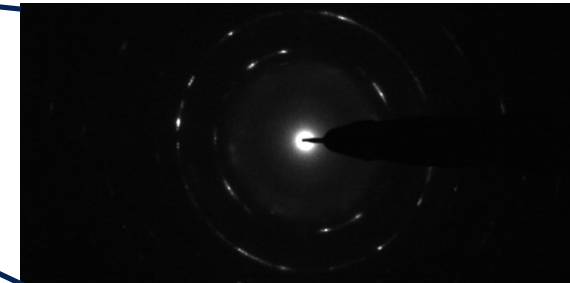
Lattice bending & localized shear amorphization

Impact energy is dissipated more efficiently in irradiated samples

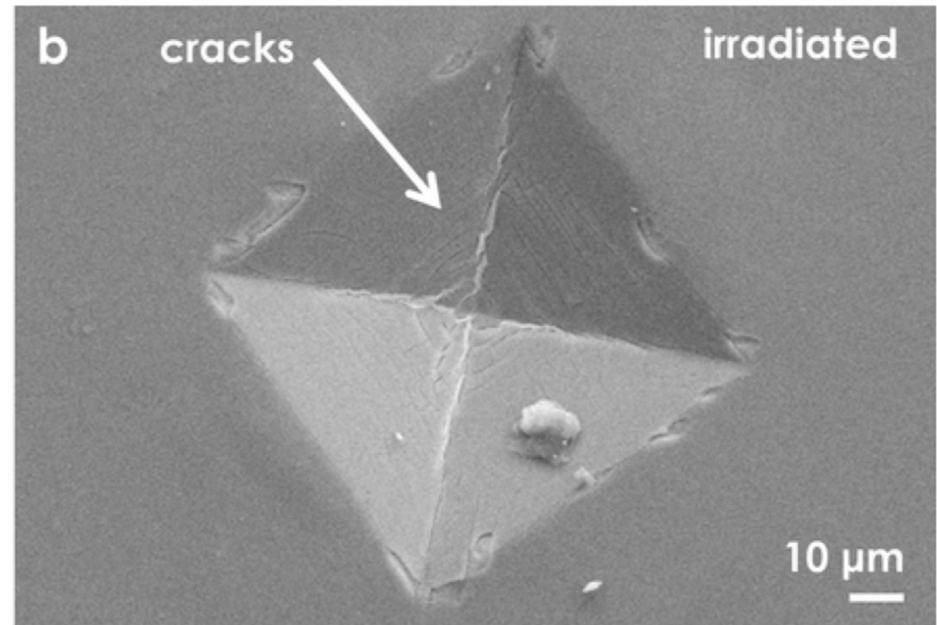
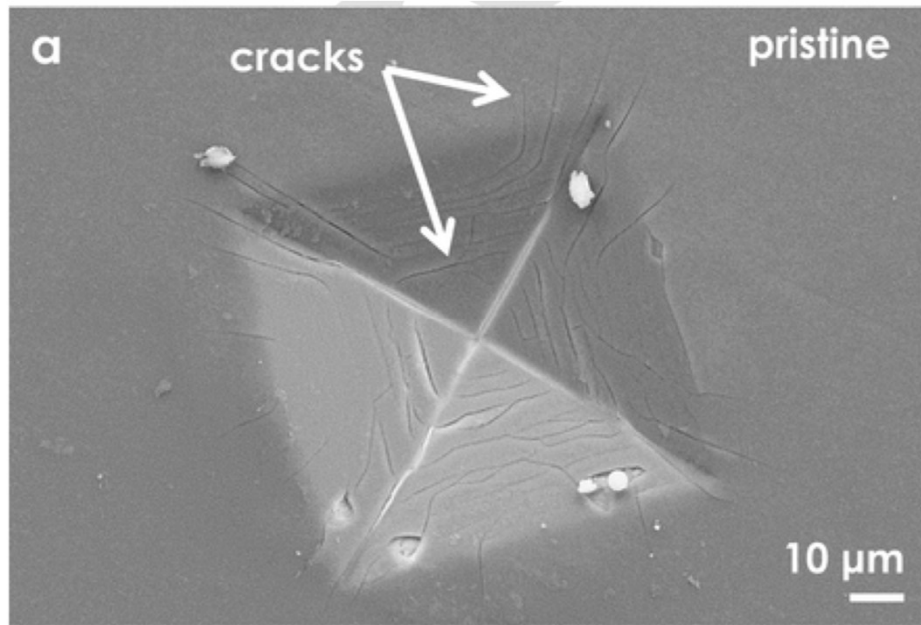
# Heavy ion irradiation (Au + W): nanoimpact – 10 mN



mechanically unloaded



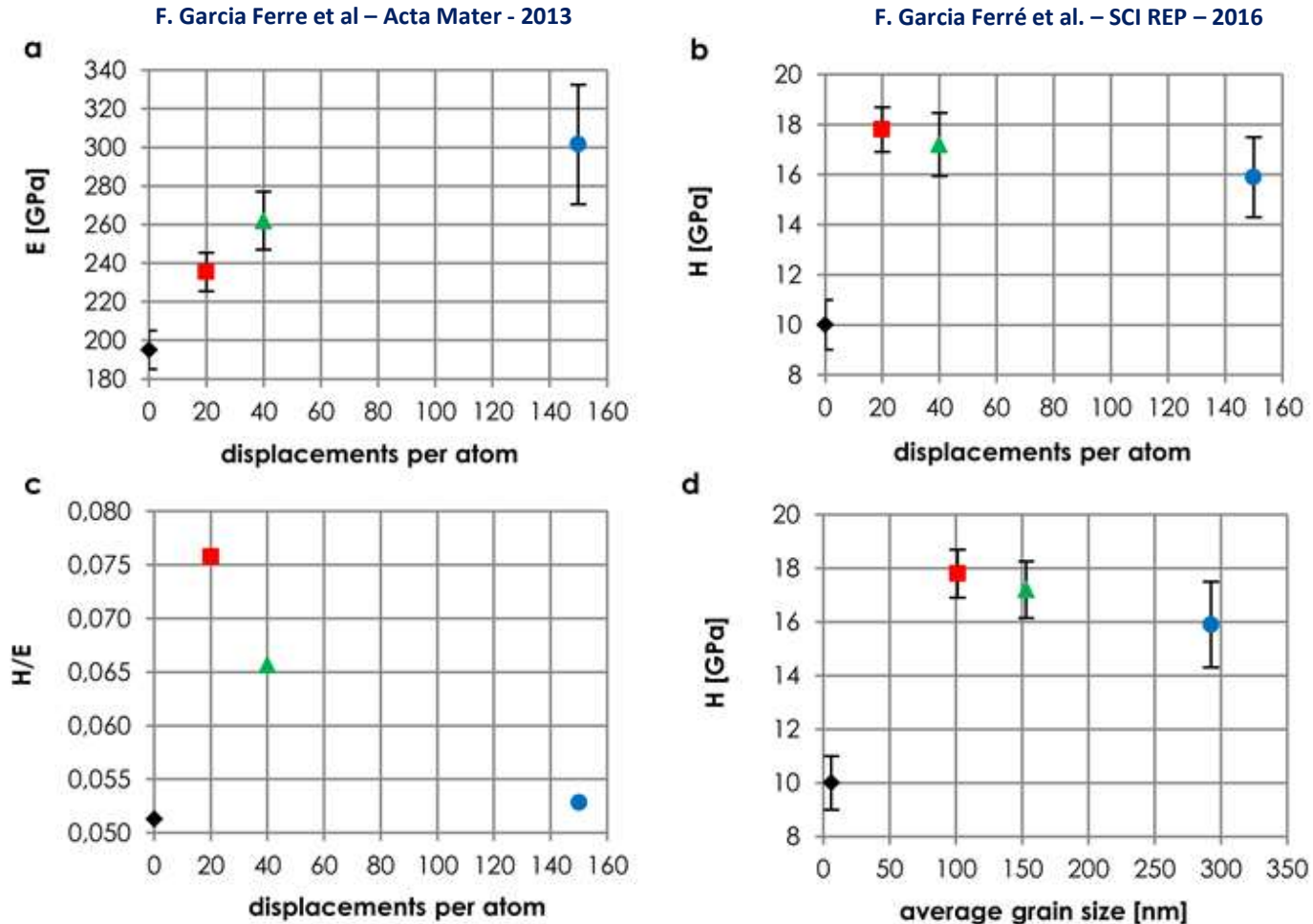




Microindention imprints of the pristine (a) and the irradiated (b) coated  $^{151}\text{Ti}$  plates. The cracks induced are more numerous and longer in the pristine material, suggesting that the fracture toughness is higher after irradiation.

# Evolution of mechanical properties under irradiation: high and low dpa

# Mechanical properties @ high levels of irradiation

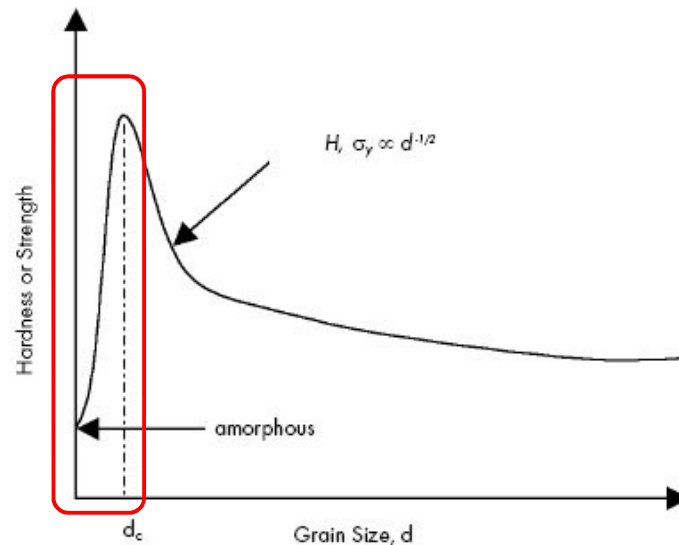


- E and H increase differently under irradiation
- **The Hardness follows the classical Hall-Petch relationship**

➤ Hall-Petch equation:  $H$  ( $\sigma$ ) VS grain size

$$H = H_0 + \frac{k}{\sqrt{D}}$$

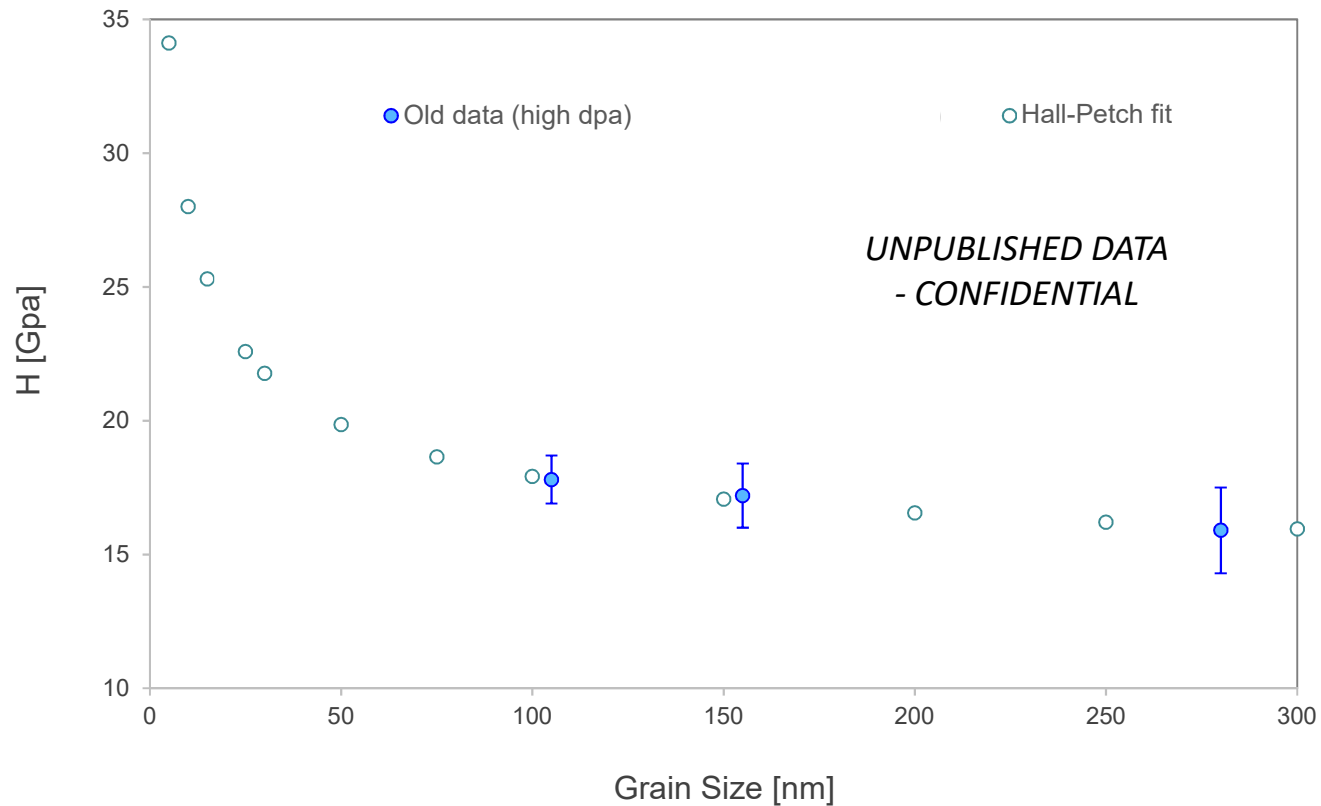
- $D$  grain size (again)
- $H_0$  and  $k$  experimental parameter -  $H_0$  can be related to the perfect mono-crystalline material
- The same equation is valid also for the *Yield Strength*  $\sigma_y$  instead of the Hardness



⇒ The so-called “**Inverse Hall-Petch curve**”:  
from the completely amorphous state  
to maximum hardness

# Hall-Petch fit: old VS new data

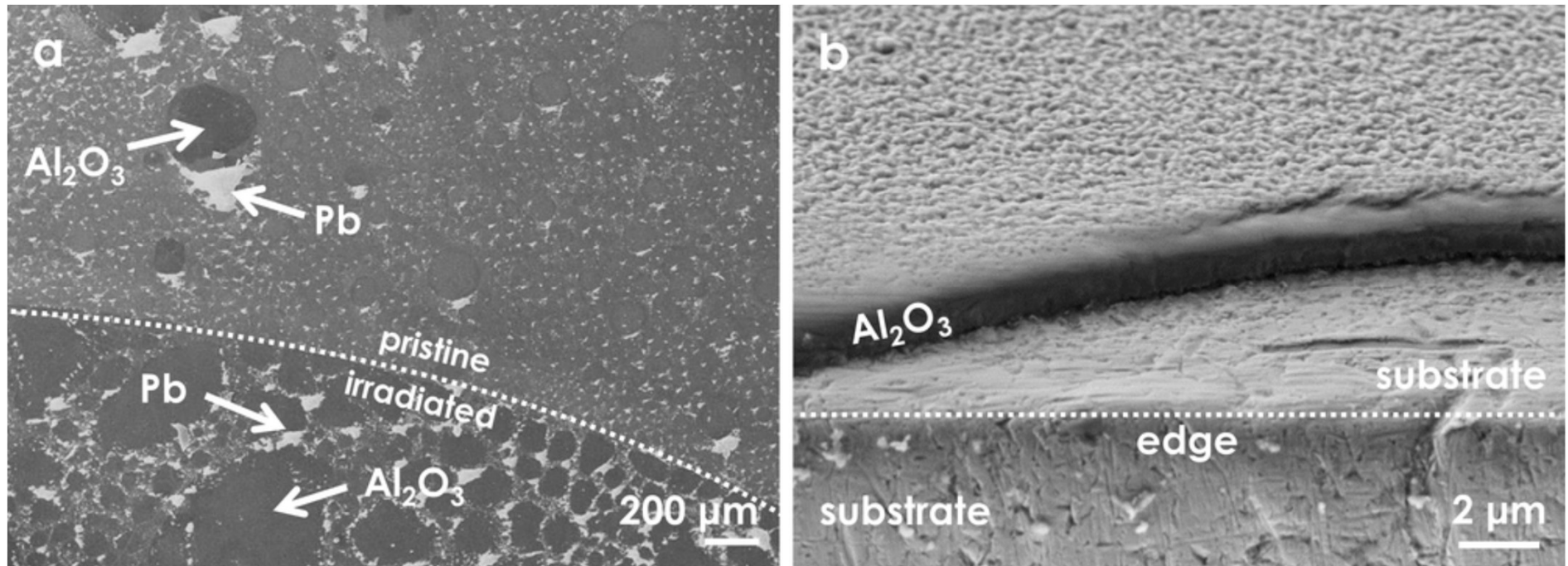
## ➤ Hall-Petch fit: old data (600°C tests)



- Good agreement with previous data

## Corrosion resistance, O<sub>2</sub> depletion

Irradiated sample, 1000 h in stagnant Pb @550°C 10<sup>-8</sup> wt.% oxygen



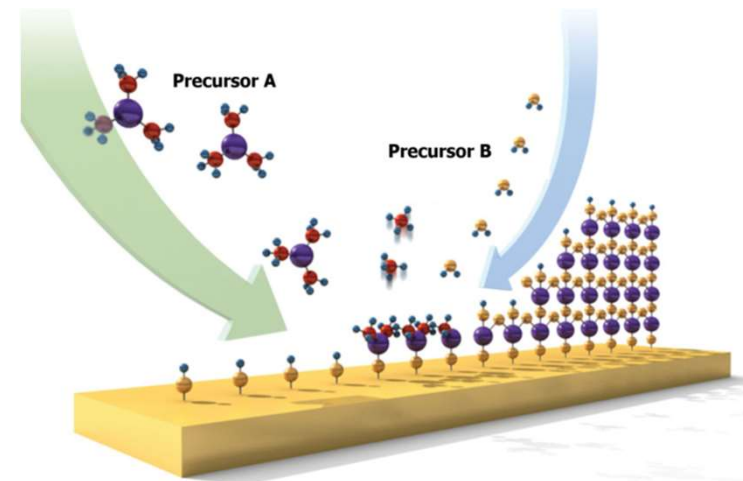
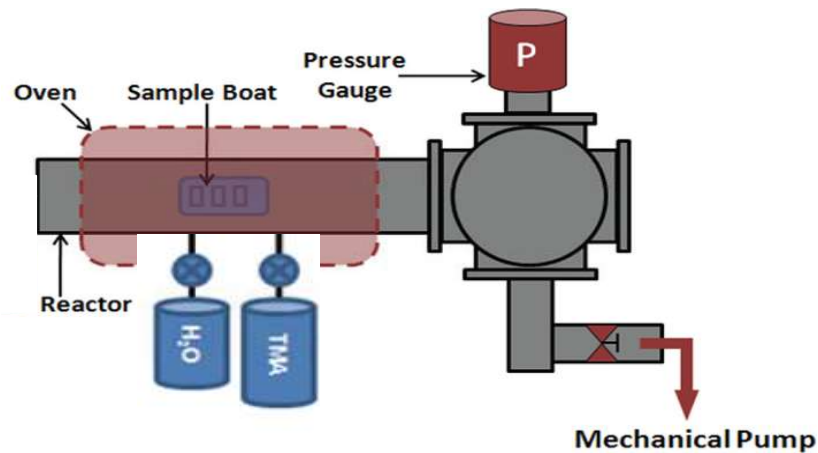
## Complex shapes?





# ALD-grown $\text{Al}_2\text{O}_3$ amorphous coatings

## Atomic Layer Deposition - Set Up

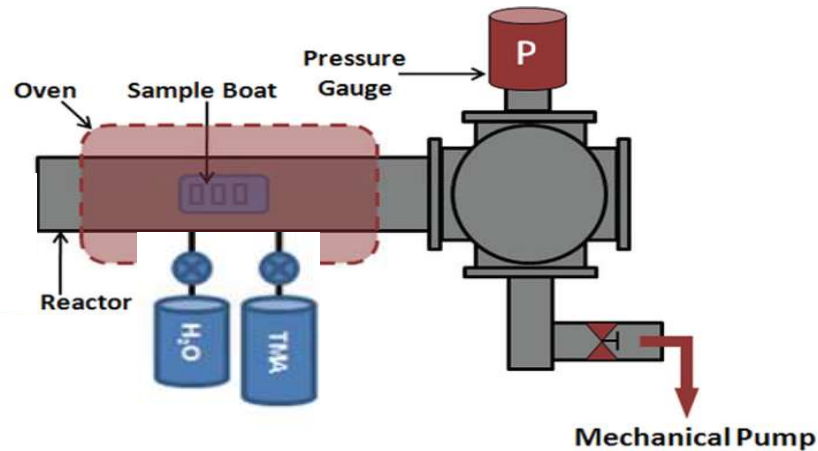


- ✓ **high-grade quality coatings**
- ✓ custom process: bottom-up approach
- ✓ process at **low temperature (i.e. < 200°C)**
- ✓ mainly **amorphous films**

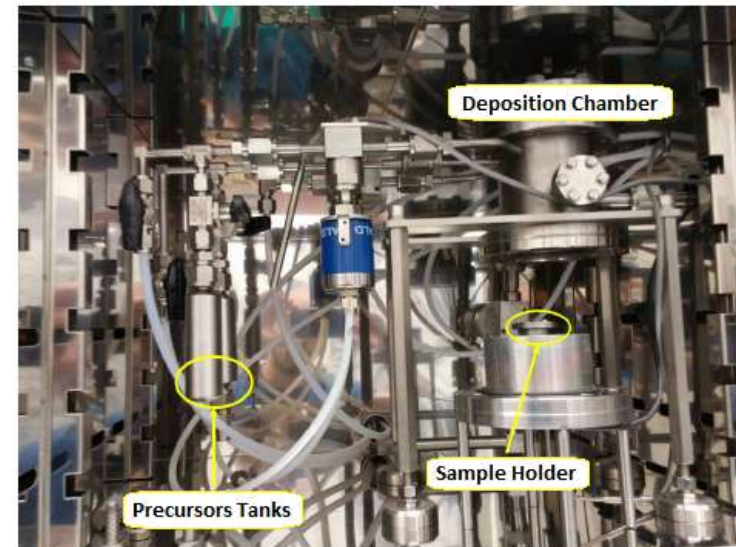
- Chemical Vapor Deposition (CVD)
- Growth at the **atomic scale levels**
- Control through **self-limited reactions**
- **Absence of any defects**
- Maximum **coverage efficiency**

# ALD-grown $\text{Al}_2\text{O}_3$ amorphous coatings

## Atomic Layer Deposition - Set Up



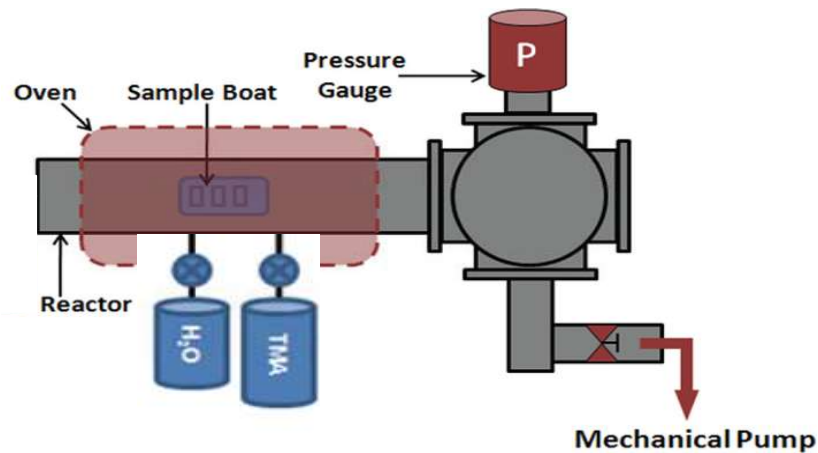
- ✓ high-grade quality coatings
- ✓ custom process: bottom-up approach
- ✓ process at **low temperature** (i.e.  $< 200^\circ\text{C}$ )
- ✓ mainly **amorphous films**



- **Mock-up scale** ALD facility
- Developed by **CNST-IIT**
- Stop Flow Mode ALD
- **Flexible** and **straightforward** set up

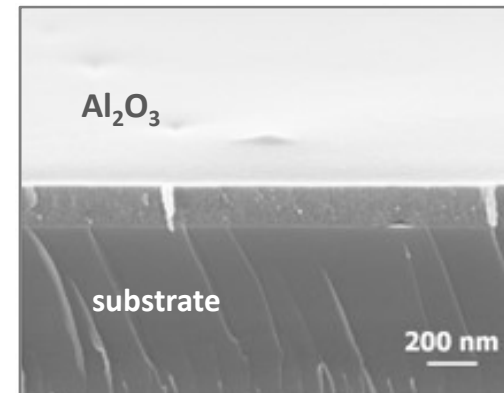
# ALD-grown $\text{Al}_2\text{O}_3$ amorphous coatings

## Atomic Layer Deposition - Set Up



- ✓ high-grade quality coatings
- ✓ custom process: bottom-up approach
- ✓ process at **low temperature** (i.e.  $< 200^\circ\text{C}$ )
- ✓ mainly **amorphous** films

## compact well-adherent ALD films



200nm-thick ALD-grown  $\text{Al}_2\text{O}_3$

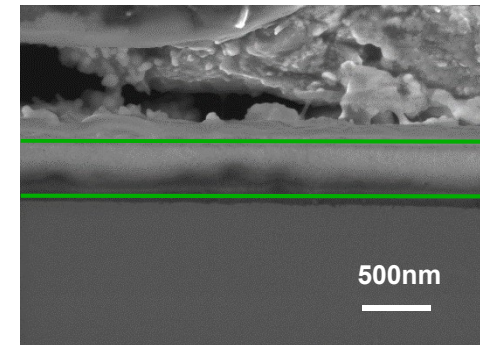
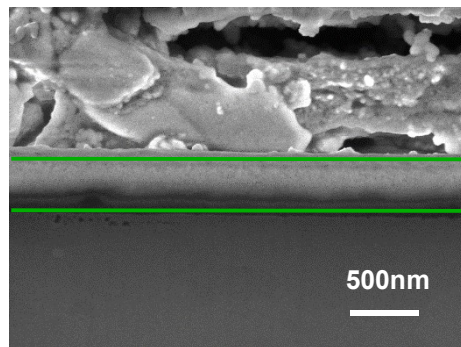
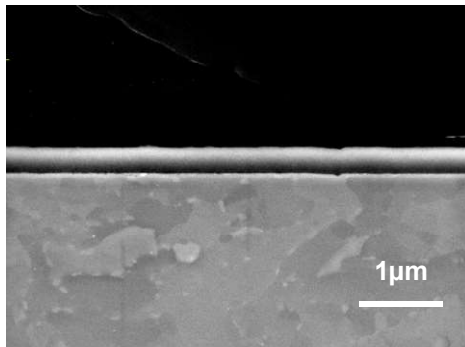
- **Mock-up scale** ALD facility
- Developed by **CNST-IIT**
- Stop Flow Mode ALD
- **Flexible** and **straightforward** set up

# Chemical stability tests on $\text{Al}_2\text{O}_3$ films in Pb-16Li

## Corrosion tests in Pb-16Li on ALD Al<sub>2</sub>O<sub>3</sub>

- Corrosion tests on EUROFER-97 SS substrates with ALD Al<sub>2</sub>O<sub>3</sub> coatings
- Reported results for 1.000 hours exposure tests @ 550°C in static Pb-16Li
  - Ongoing corrosion tests on ALD Al<sub>2</sub>O<sub>3</sub> for longer exposure times

- Sample coated with 500nm-thick ALD Al<sub>2</sub>O<sub>3</sub> -



⇒ No delamination, nor substrate corrosion for the ALD Alumina, too

⇒ Ongoing characterization on surface features

# Acknowledgements & ongoing collaborations



Ente per le Nuove tecnologie, l'Energia e l'Ambiente

## Corrosion tests + financial support

Serena Bassini  
Marco Utili  
Mariano Tarantino  
Pietro Agostini



JANNUS



## heavy ion irradiations

Patrick Trocellier    Cédric Baumier  
Yves Serruys        Odile Kaitasov  
Lucile Beck



WISCONSIN  
UNIVERSITY OF WISCONSIN-MADISON

## TEM + XRD

Alexander Mairov  
Kumar Sridharan



POLITECNICO DI MILANO

## Brillouin & CTE/Res Stress

Edoardo Besozzi  
Marco Beghi



ISTITUTO  
ITALIANO DI  
TECNOLOGIA

## Nanoindentation + nanoimpact

Luca Ceseracciu



EUROfusion



CIRTEN - CONSORZIO INTERUNIVERSITARIO  
PER LA RICERCA TECNOLOGICA NUCLEARE





ISTITUTO ITALIANO DI TECNOLOGIA  
CENTER FOR NANOSCIENCE AND TECHNOLOGY

**Thank You  
for your attention!**



M.G. Beghi

**Coating characterization under irradiation.  
Heavy ions irradiation against  
neutron irradiation.**



**POLITECNICO**  
MILANO 1863

ADP MiSE-ENEA --- PAR2017-LP2 --- 15/06/2018



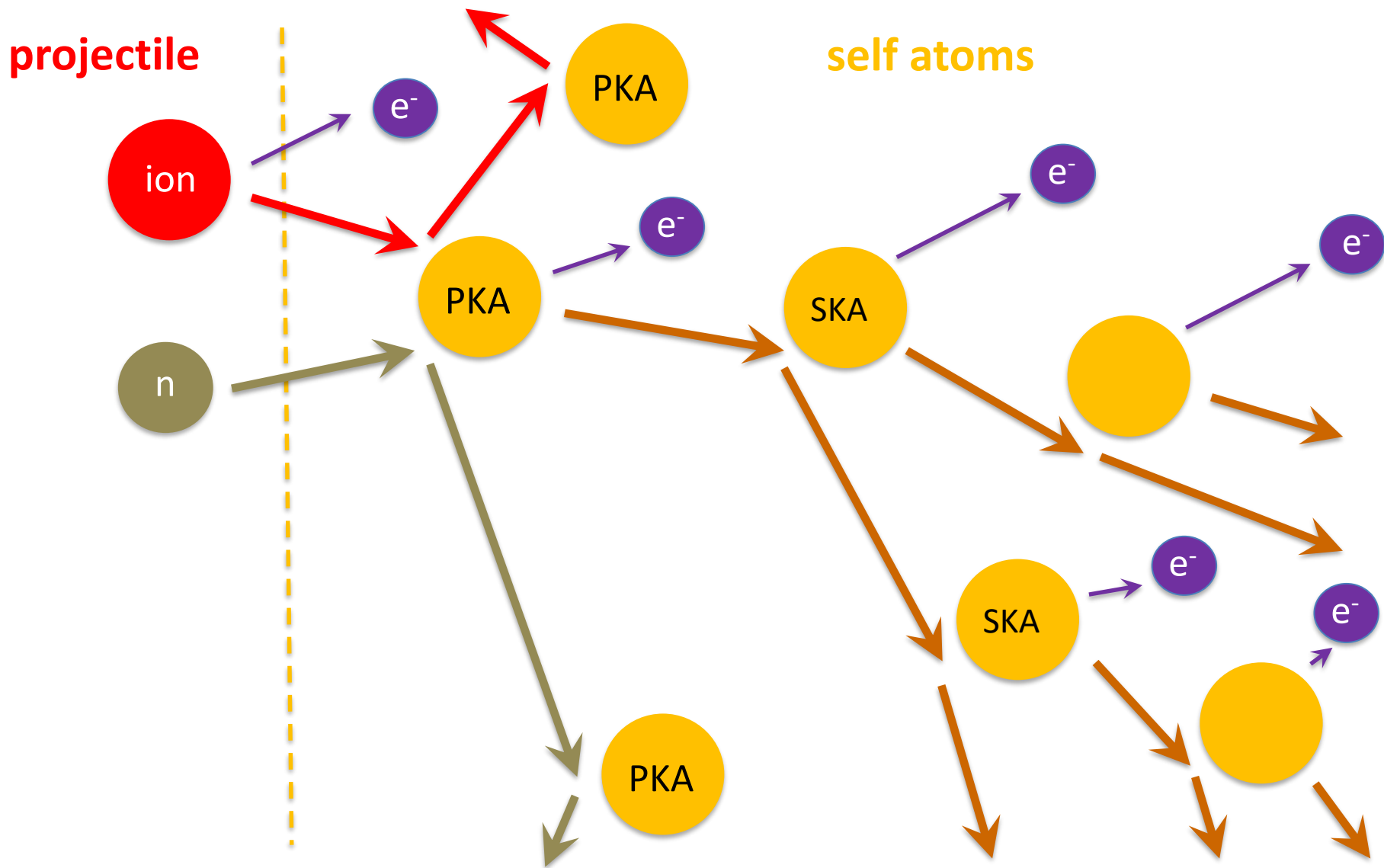
ions irradiation vs. neutron irradiation

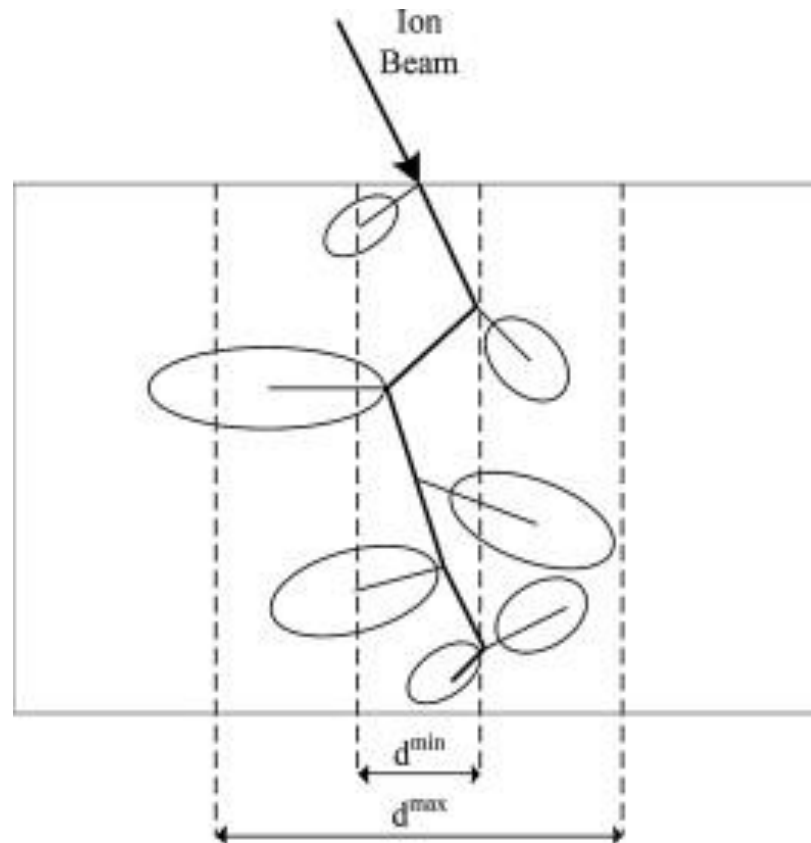
back to basics:

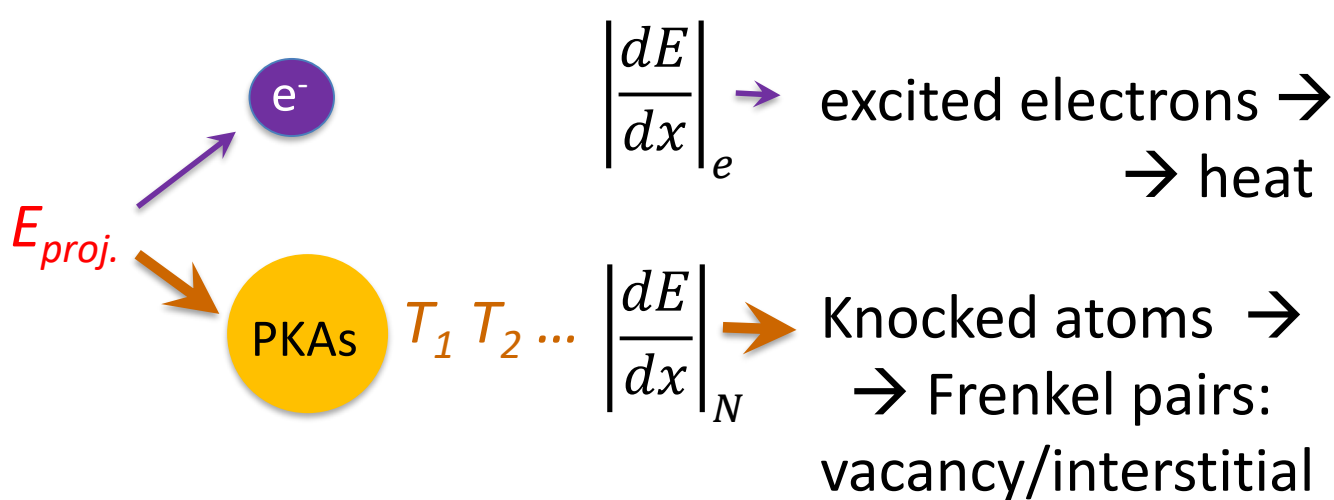
- collisional cascades
- dpa

metals irradiation vs. ceramics irradiation

examples of ceramic coatings under irradiation







$\frac{\left| \frac{dE}{dx} \right|_e}{\left| \frac{dE}{dx} \right|_N}$  Electron to Nuclear Stopping Power ratio

$E_{proj.} \rightarrow T$ 
 $A = \frac{m_{target}}{m_{project}}$ 
 $T_{max} = \delta E$ 
 $\delta = \frac{4A}{(1+A)^2}$

$\delta\left(\frac{1}{A}\right) = \delta(A)$ 
 $\delta(A=1) = 1$ 
 $\delta(A \gg 1) \cong \frac{4}{A}$

isotropic scattering  $\Rightarrow \langle T \rangle = \frac{1}{2} T_{max}$

$$\frac{dn_{pairs}}{dt} = \frac{dn_{casc.}}{dt} \nu \left[ \frac{\#pairs}{\#cascade} \right] = n_{atoms} \phi \sigma_s \nu$$

$$\frac{\int (dn_{pairs}/dt) dt}{n_{atoms}} = \frac{n_{pairs}}{n_{atoms}} = \Phi \sigma_s \nu : \quad \mathbf{dpa}$$

$$\nu \left[ \frac{\#pairs}{\#cascade} \right] = \nu (TPKA)$$

$$E_d = E_{displ.} [\sim 10 \text{ eV}] \gg E_{form.(TD)} [\sim 1 \text{ eV}]$$

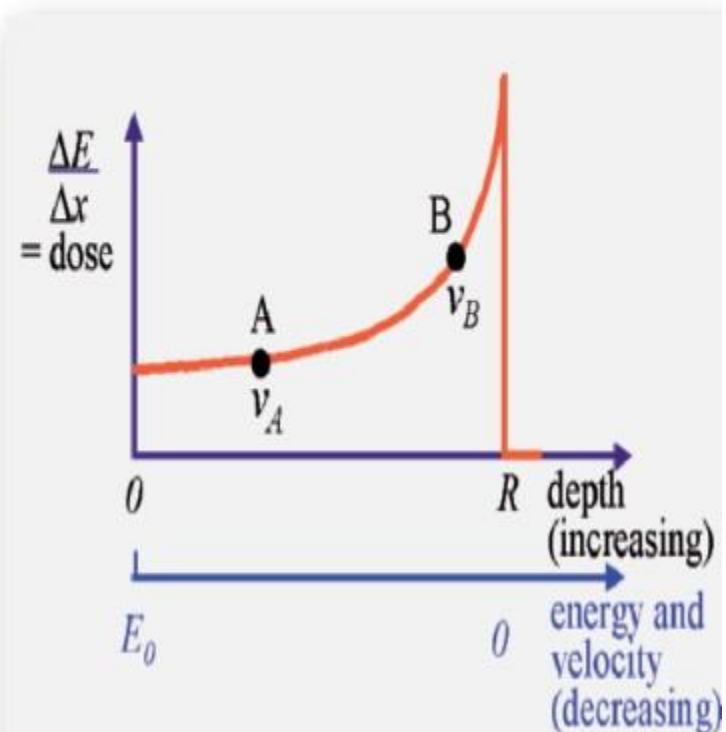
$$\langle \nu \rangle = \frac{T_{PKA}}{2E_d}$$

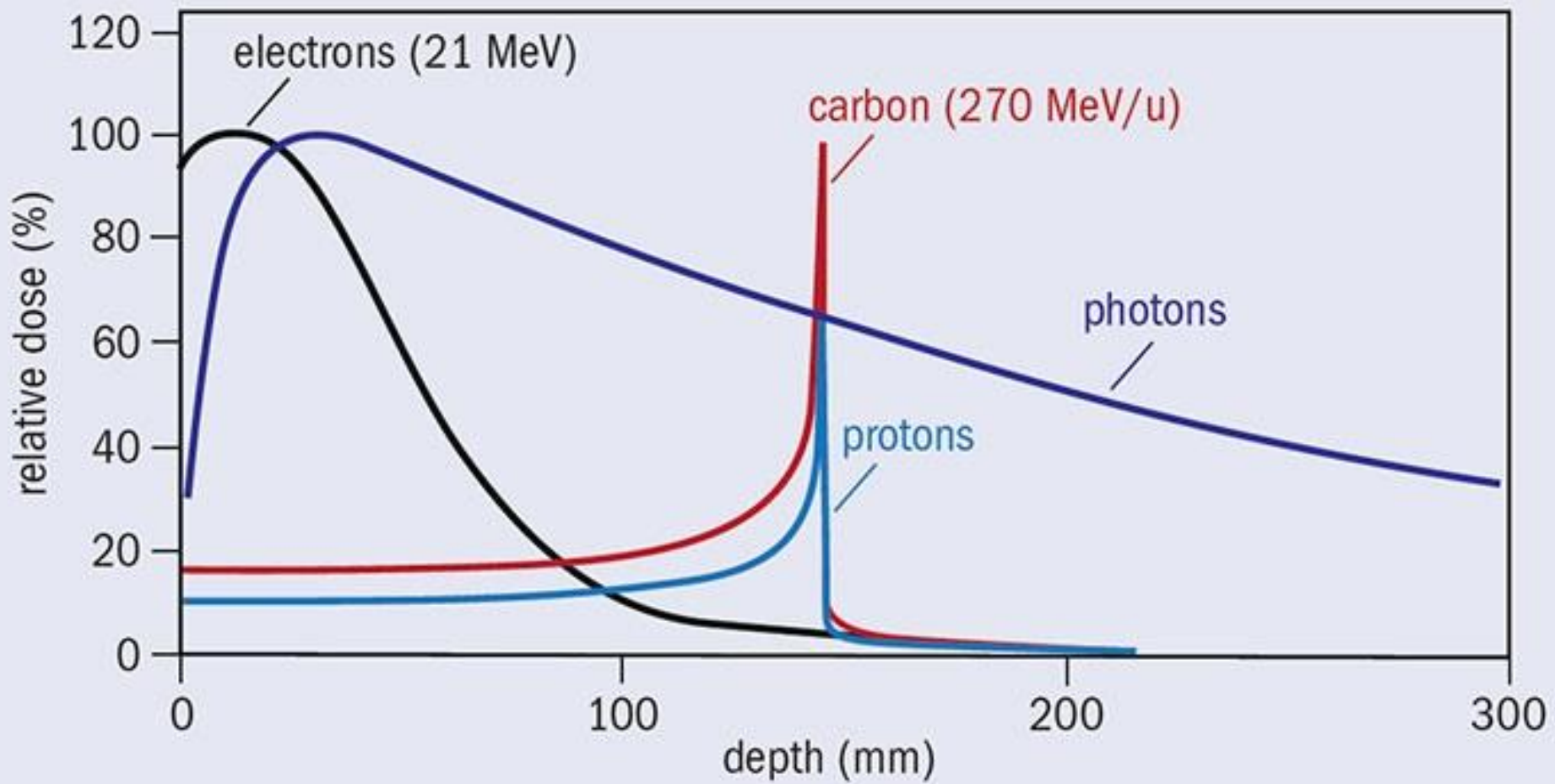
| projectile            | target         | $E_d$ [eV] | $\langle T \rangle = \frac{1}{2} T_{max} = \frac{1}{2} \frac{4A}{(1+A)^2} E_{proj}$ | $\langle v \rangle = \frac{\langle T_{PKA} \rangle}{2E_d}$ |
|-----------------------|----------------|------------|---|--|
| n @1 MeV              | Fe             | ~ 40       | 36 keV  | 900  |
| n @1 keV              | Fe             | ~ 40       | 36 eV   | ~ 1  |
| Fe @36 keV            | e <sup>-</sup> |            | 0.7 eV  |  |
| e <sup>-</sup> @ 1MeV | Fe             | ~ 40       | 20 eV   | > 0  |
| W @18 MeV             | e <sup>-</sup> |            | 106 eV  |  |
| W @18 MeV             | Fe             | ~ 40       | 6.4 MeV   | 80000  |
| Ni @4 MeV             | Fe             | ~ 40       | 2 MeV   | 25000  |

## Energy loss “dE/dx profiles

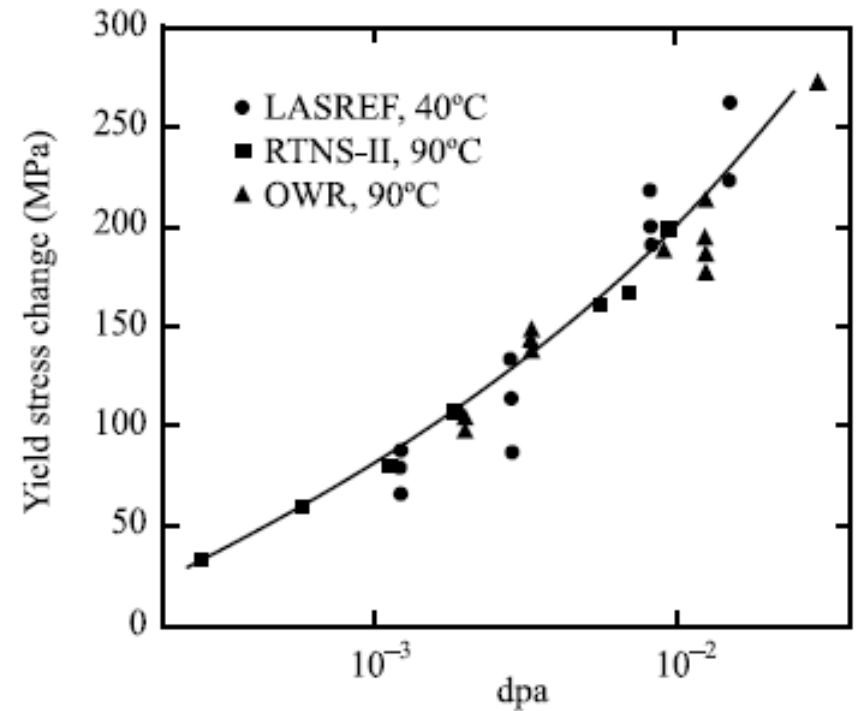
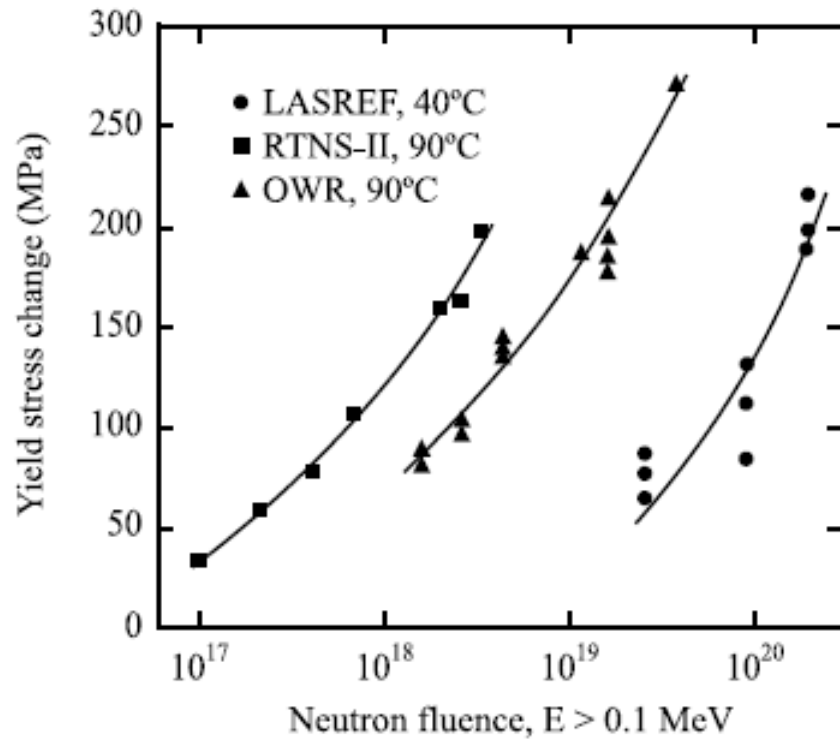
- a proton’s **linear rate of energy loss** “linear energy transfer” (LET)
- is given by the **Bethe-Bloch** formula:

$$\frac{dE}{dx} \propto \frac{1}{v^2} \left( \frac{Z}{A} \right) Z^2$$









## Metals: mono-elemental crystals, unique electron states

evolution of **metals** under **MeV neutrons**, (and  $\sim$  ions):

electrons excitation and de-excitation  $\rightarrow$  heat

injection of Frenkel pairs, concentration  $\gg$  equilibrium conc.

super-saturated solution of vacancies/interstitials evolves (precipitates) according to

- concentration ( $\sim$  dpa)
- Temperature, which determines diffusivity

$\Rightarrow$  (dpa & temperature) good predictor of  
microstructure evolution  $\Rightarrow$  properties evolution

+ He production by  $(n,\alpha)$  reactions

Ion irradiation vs. neutron irradiation

dpa/day instead of dpa/yr  $\Rightarrow$  fast, inexpensive, accessible  
no activation  $\Rightarrow$  post-irradiation analysis much easier  
thin layers vs. bulk

ENSP ratio as low as possible to best simulate neutrons

Possible pre-implantation or co-implantation of He

Ceramics: multi-elemental crystals / amorphous,  
non unique electron states

evolution of **ceramics** under **neutrons & ions**

- covalent bonds: electron localization, excitation, possible relaxation into different state  $\Rightarrow$   
 $\Rightarrow$  possible bonding/chemical evolution
- different elements, chemical environment:  $\langle T \rangle$ ,  $\langle E_d \rangle \Rightarrow \langle v \rangle$  ?
- defect mobility vs. temperature ?

$\Rightarrow$  (dpa & temperature) alone: NOT good predictor of  
microstructure evolution  $\Rightarrow$  properties evolution

also depends on ? spatial correlation of defect birth?

(small / large cascades ?)

## Irradiation:

- Induces disorder (→ amorphization)
- Locally: high energy deposition, promotes order

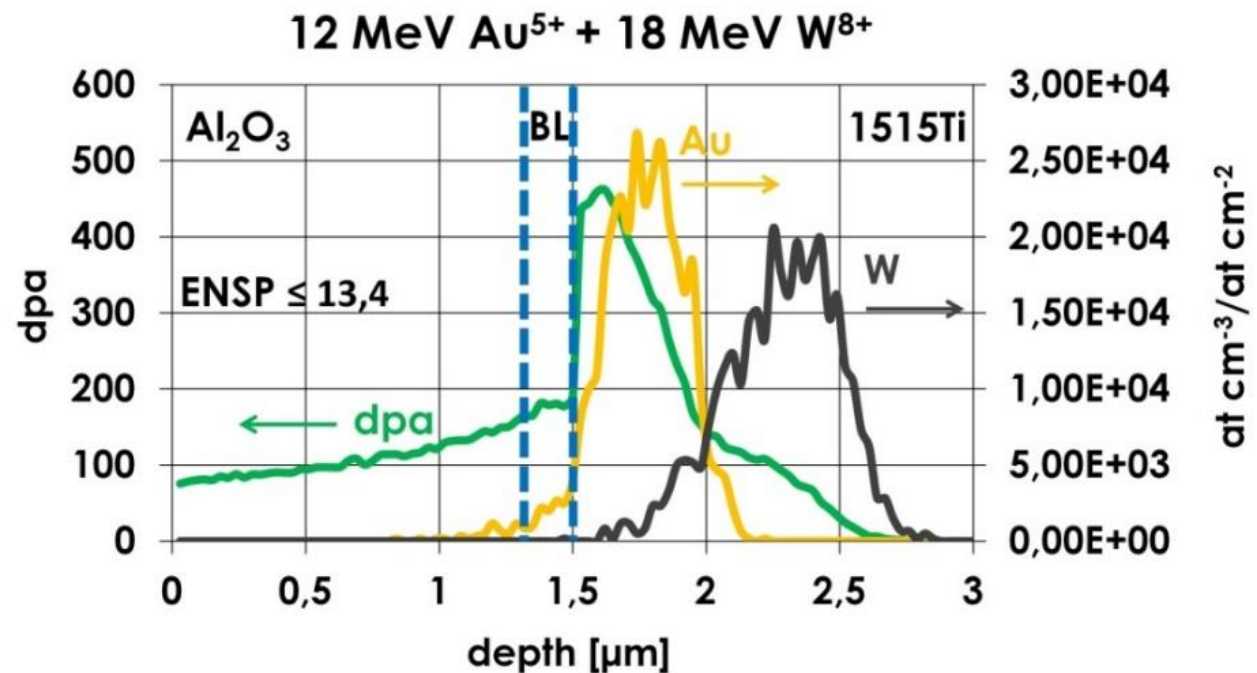
## Crystals (metals and ceramics):

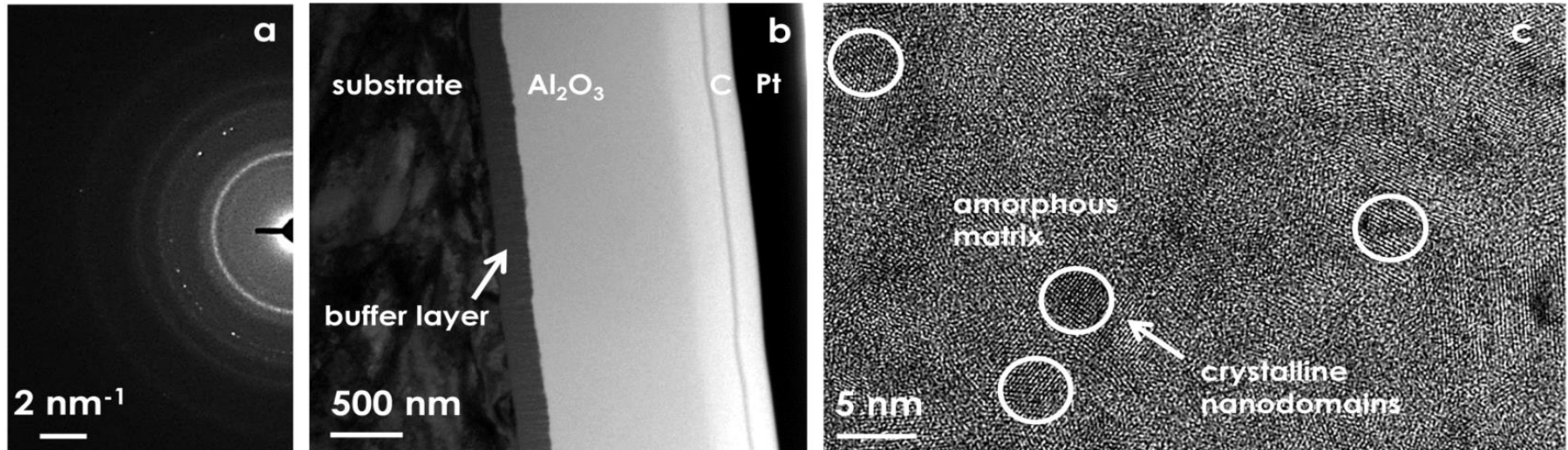
disordering prevails, tends to saturate  
'disordered' regions (grain boundaries, dislocations)  
are sinks for interstitials & vacancies

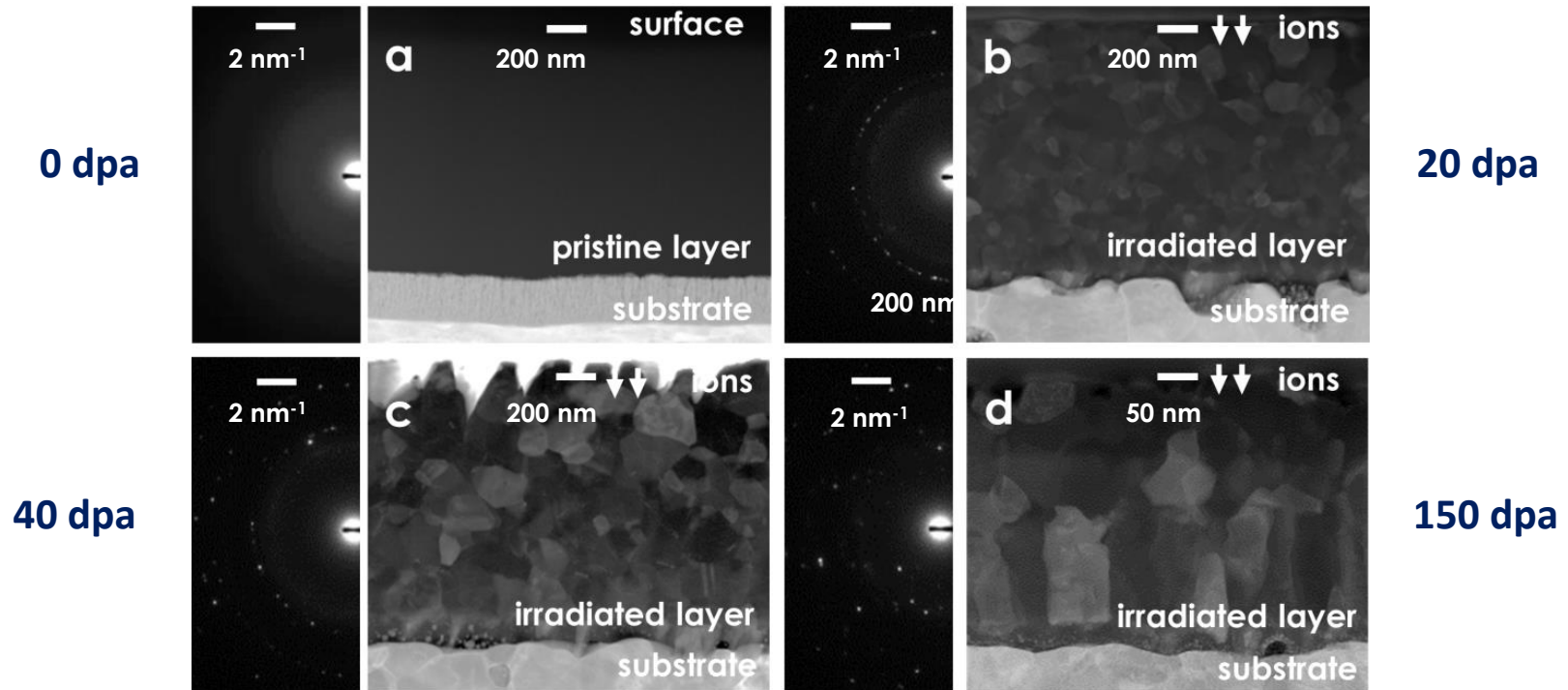
## Amorphous (ceramics)

ordering/disordering compete, ordering can prevail  
interstitials & vacancies no longer well defined  
ultra-nano structures offer sinks for defects

- ❑ Irradiation with **Gold and Tungsten ions @ 600 °C**
- ❑ **Low ENSP** ratio to **simulate effect of Neutrons**
- ❑ Minimum coating thickness for Nanoindentation
- ❑ **Implantation beyond coating** (no chemical effects)
- ❑ Different **damage levels: 0, 20, 40 and 150 dpa** at the interface between  $\text{Al}_2\text{O}_3$  and buffer layer (dpa levels calculated using **SRIM Code**)



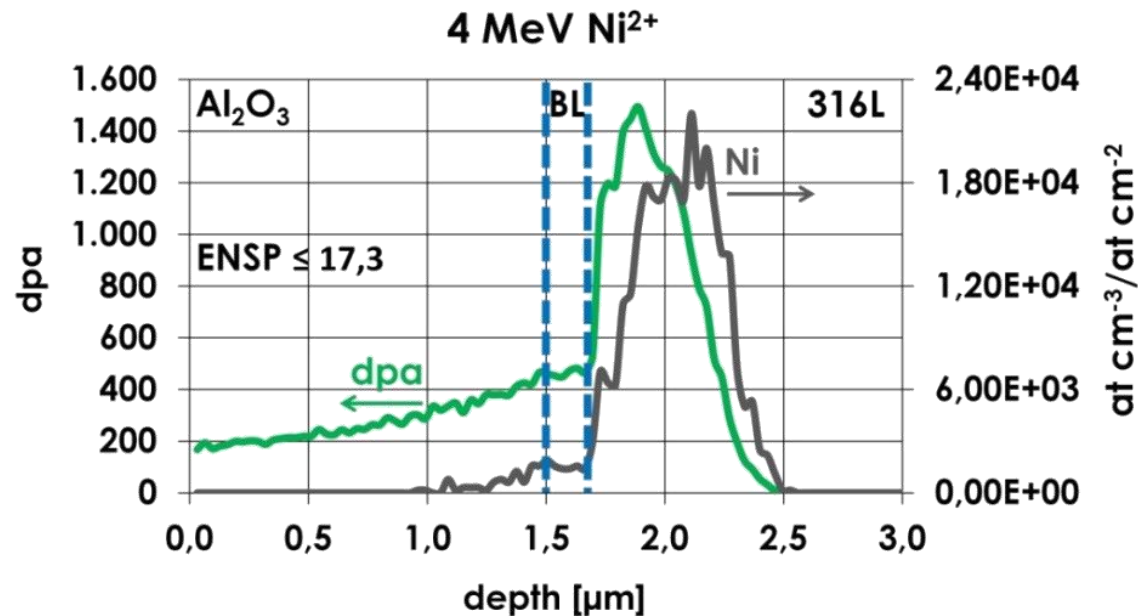


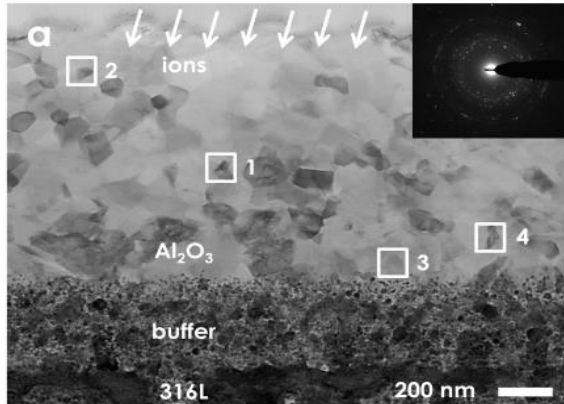


- **Nanocrystallization** followed by **sub-linear grain growth**
- Increase of **crystalline size** and **crystalline fraction**
- $\gamma\text{-Al}_2\text{O}_3$  always present plus **formation of  $\alpha\text{-Al}_2\text{O}_3$  @ 150 dpa**

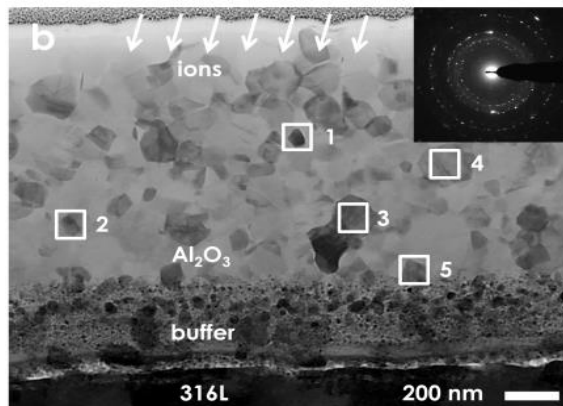


- ❑ Irradiation with **Nickel ions @ 600 °C**
- ❑ **Low ENSP** ratio to **simulate effect of Neutrons**
- ❑ Minimum coating thickness for Nanoindentation
- ❑ **Implantation beyond coating** (no chemical effects)
- ❑ Different **damage levels: 0, 250 and 450 dpa** at the interface between  $\text{Al}_2\text{O}_3$  and buffer layer (dpa levels calculated using **SRIM Code**)



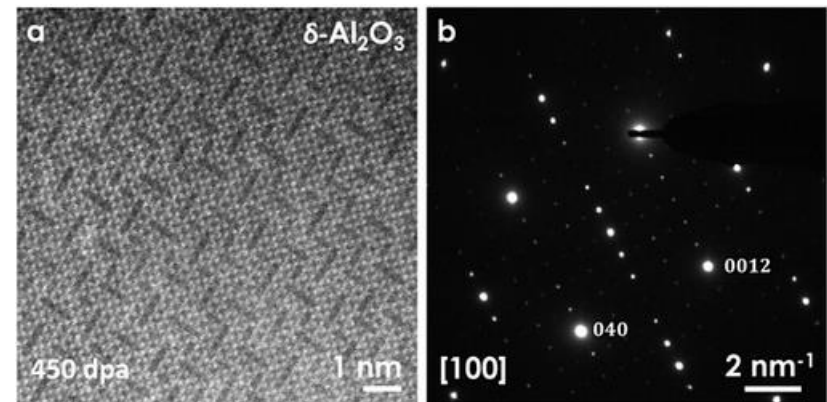


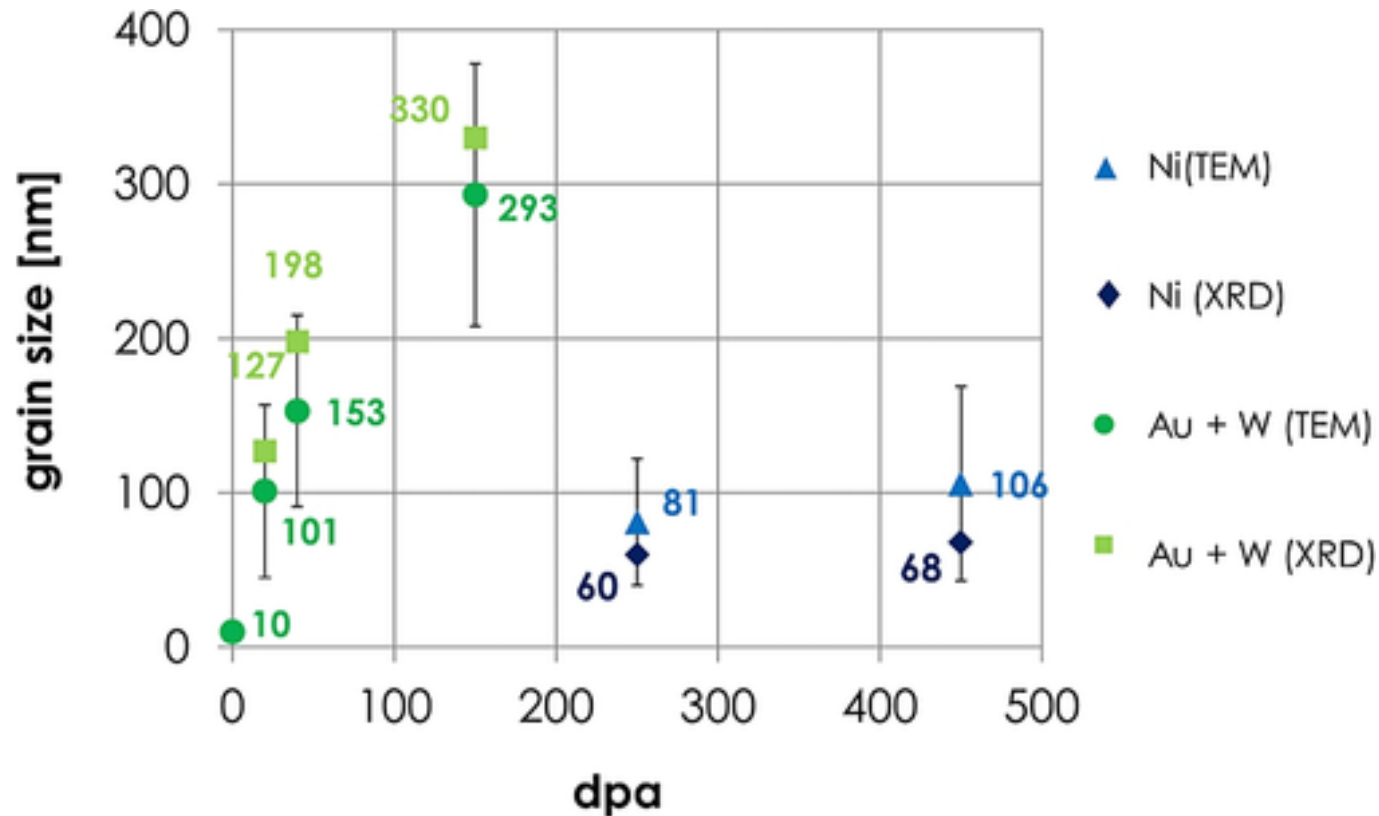
250 dpa



450 dpa

- **Nanocrystallization** and **grain growth** (again)
- No more  $\gamma\text{-Al}_2\text{O}_3$ : **formation of metastable  $\delta\text{-Al}_2\text{O}_3$**
- Increase of **crystalline size** and **crystalline fraction**





Same temperature (600 °C)

- For irradiated ceramics, dpa & temperature are not enough to predict microstructure / properties
- Dependence on
  - space distribution of defect generation (small/large cascades)
  - ... ?



Italian National Agency for New Technologies,  
Energy and Sustainable Economic Development

# Corrosion qualification of materials and coatings in liquid lead for LFR

ADP MiSE-ENEA (PAR2017-LP2)

Dipartimento di Ingegneria Astronautica, Elettrica ed Energetica  
Università di Roma "La Sapienza"

14-15 Giugno 2018

S. Bassini (ENEA FSN-ING-TESP)  
[serena.bassini@enea.it](mailto:serena.bassini@enea.it)



1101 0110 1100  
0101 0010 1101  
0001 0110 1110  
1101 0010 1101  
1111 1010 0000



# MATERIALS & COATINGS FOR ALFRED

$C_o \approx 10^{-6} - 10^{-8} \% \text{ wt.}$

| Component                | Min./Max Temp. Normal Operation (long term) (°C) | Max Temp. Accident Conditions (transient) (°C) | Max. Lead velocity (m/s) | Max. Radiation damage (dpa/y) | Max. Radiation damage (dpa) | Material                                | Coating   | Notes   |
|--------------------------|--|--|--------------------------|-------------------------------|-----------------------------|---|---|---|
| Reactor Vessel           | 380÷430  | 500 (700 <sup>(1)</sup> )                      | 0,1                      | < 10 <sup>-5</sup>            | 0,0002 (40y)                | AISI316LN (ASTM)                        | No  | Back-up<br>Liner of corrosion resistant steel (e.g. AFA)  |
| Inlet                    |  |  |                          |                               | 2,1                         | 316LN (ASTM)                            | No  | Back-up<br>AFA steel  |
|                          |  |  |                          |                               |                             |   | Al diffusion coating by Pack Cementation  |   |
| D                        |  |  |                          |                               |                             | 316LN (ASTM)                            | No  | Al diffusion coating by Pack Cementation  |
| Steam                    |  |  |                          |                               |                             | 316L (ASTM)<br>15Ti (DIN 1.4970)        | No  | Backup: AFA steel; Alloy 800 coated   |
|                          |  |  |                          |                               |                             |   | Al diffusion coating by Pack Cementation  |   |
| Fuel                     |  |  |                          |                               |                             | 15-15Ti (AIM1)                          | Al <sub>2</sub> O <sub>3</sub> by PLD   | No buffer layer (direct coating deposition over the bulk material)  |
| FA                       |  |  |                          |                               | (5y)                        | 15-15Ti (AIM1)                          | Spacer grids & wrapper (outside):<br>Al <sub>2</sub> O <sub>3</sub> by PLD<br>Wrapper (inside): overthickness | Back-up (for wrapper tube): Al <sub>2</sub> O <sub>3</sub> by ALD or PLD (to be developed in-tube deposition) |
| DHR Heat Exchanger       | 380÷430  | 700 <sup>(1)</sup>                             | 0,2                      | < 10 <sup>-3</sup>            | 0,01 (20y)                  | AISI316L (ASTM)<br>15-15Ti (DIN 1.4970) | No  | Backup: AFA steel; Alloy 800 coated   |
|                          |  |  |                          |                               |                             |   | Al diffusion coating by Pack Cementation  |   |
| Primary Pumps (impeller) | 380÷480  | 700 <sup>(1)</sup>                             | 15÷20                    | < 10 <sup>-3</sup>            | 0,01 (20y)                  | AISI300 series                          | Closed impeller: Al diffusion coating by Pack Cementation   | Backup (for open impeller ONLY): AlTiN coating by PVD   |
|                          |  |  |                          |                               |                             |   | Open Impeller: Al <sub>2</sub> O <sub>3</sub> by PLD  |   |

Corrosion qualification of these materials in Pb is mostly missing, especially in the long-term and/or flowing conditions. Some gaps will be covered in the frame of GEMMA EU project

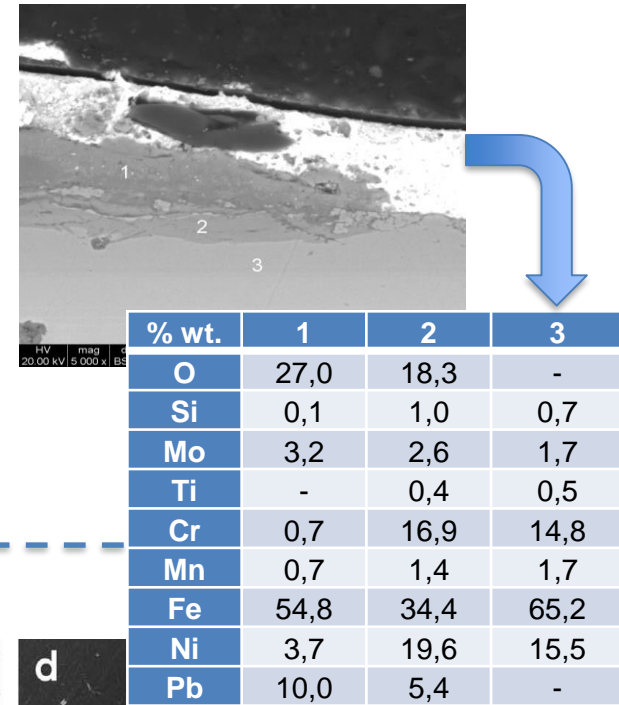
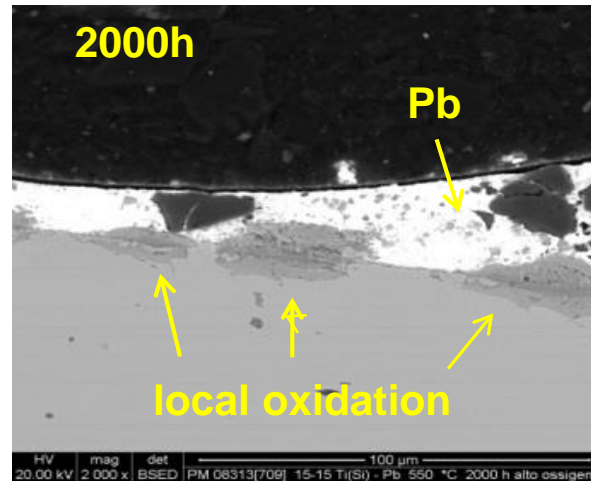
Substrate: 316L(N), 15-15Ti (DIN), 15-15Ti AIM1 (cold worked)  
Back-up: AFA for SG and DHR

# 15-15Ti cold worked, static Pb 550°C

## Fluel cladding & fuel assembly

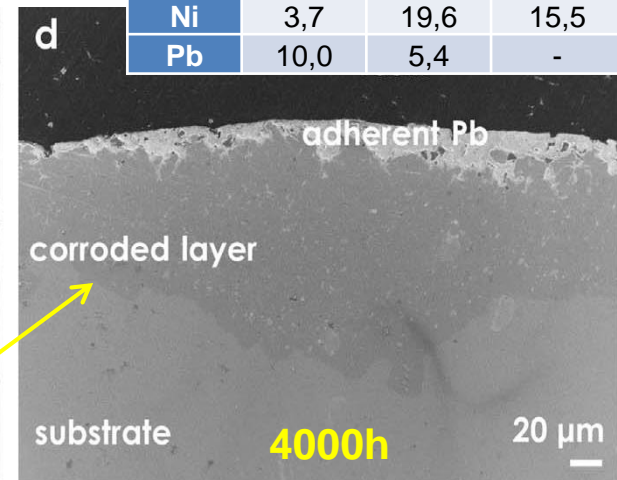
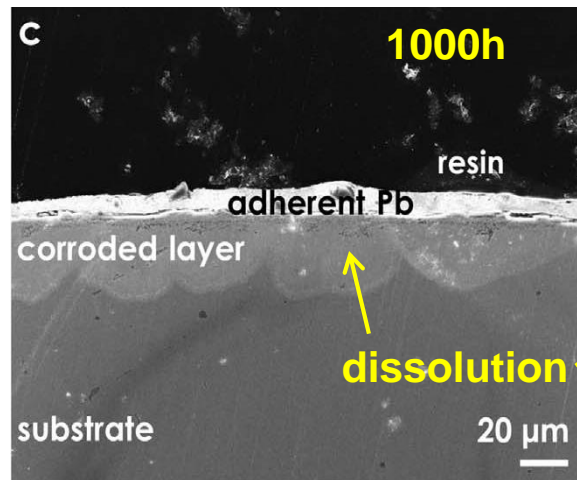
550°C, [O] = 10<sup>-3</sup> % wt.  
(PAR2013)

Local spot of oxidation made of external layer and internal oxidation layer with Ni and Cr diffusion (enrichment).



550°C, [O] = 10<sup>-8</sup> % wt.  
(PAR2016)

Dissolution layer with depth of ≈ 25 μm after 1000h (c).  
Dissolution layer of 85 μm and occasionally 150 μm after 4000h (d). The layers contains Pb (e).



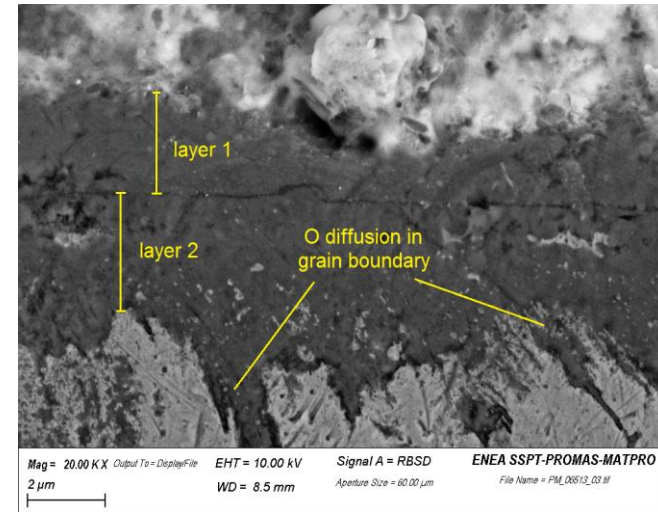
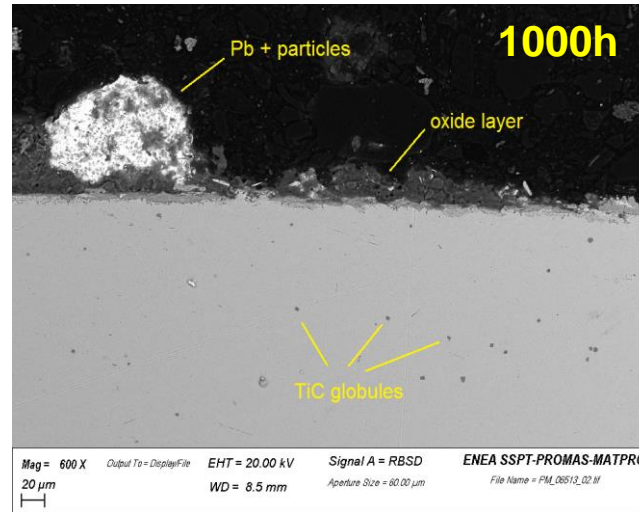
F. García Ferré et al., (2017)

# 15-15Ti and DS4, flowing Pb 550°C

## 15-15Ti, 550°C, [O] = 10<sup>-4</sup> % wt. (flowing) PAR2016

Oxidation (external layer + diffusion) with depth 5-10 μm. No dissolution.

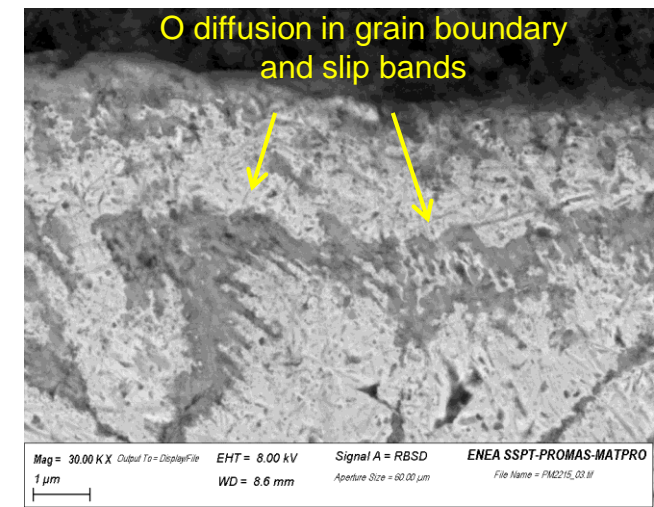
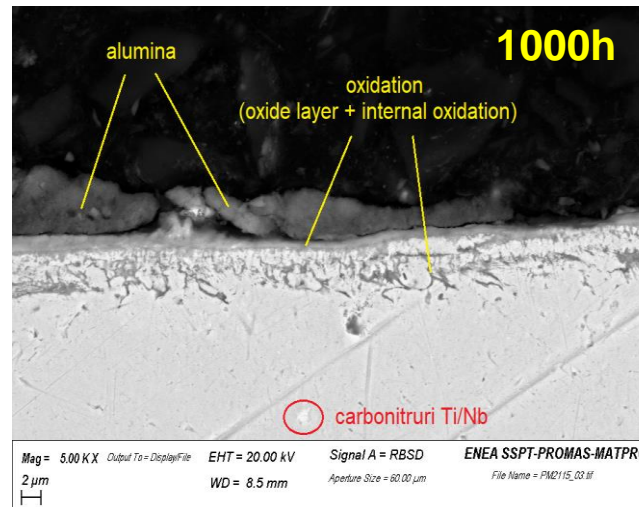
Oxygen penetration in grain boundary and slip bands.



## DS4 (15Cr-25Ni), 550°C, [O] = 10<sup>-4</sup> % wt. (flowing) PAR2016

Oxidation (external layer + diffusion) with depth 4-5 μm. No dissolution.

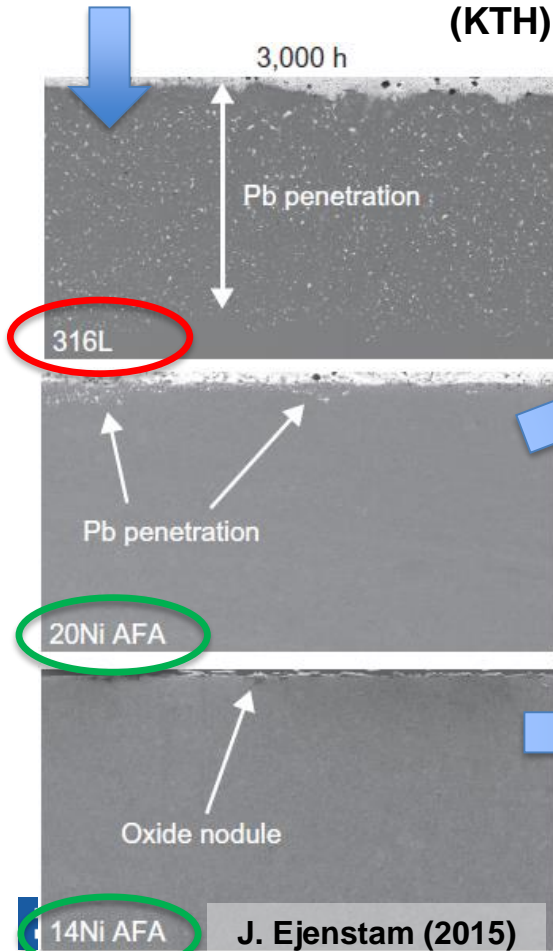
Oxygen penetration in grain boundary and slip bands.



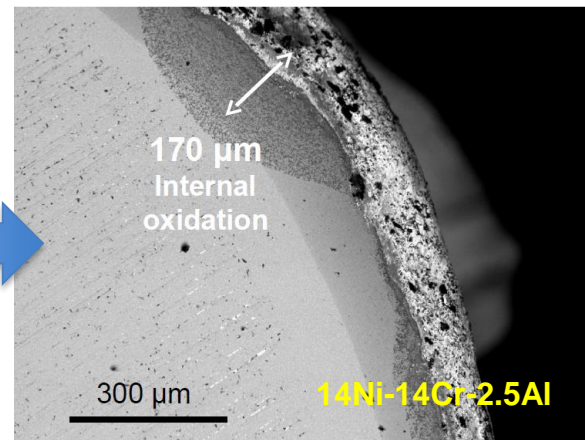
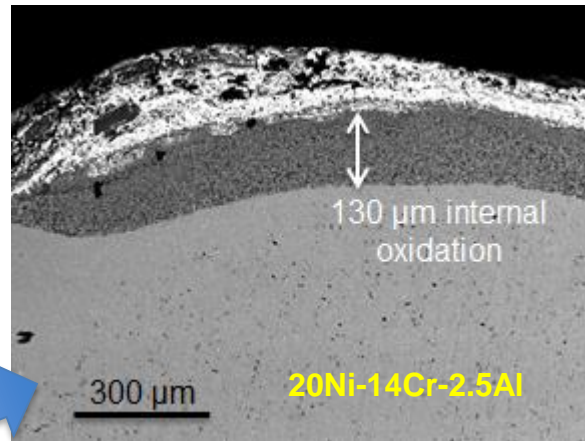


# Alumina Forming Austenitic (AFA) steels

Dissolution for 316L and Pb penetration, better performance for AFA 20Ni and 14Ni at 550°C, [O] = 10<sup>-7</sup>% wt, 3000h (KTH)



AFA at 750°C, 2000h  
[O] = 10<sup>-6</sup>% wt  
internal oxidation observed



**Back-up for SG,  
DHR**

A. Weisenburger, P. Szakálos,  
KOM GEMMA project, 21-22  
June 2017, Rome.

- low % of Al;
- protective Al<sub>2</sub>O<sub>3</sub> layer (better than Fe-Cr oxides at high T);
- austenite structure (no embrittlement, good mech. properties);
- composition will be improved in the frame of GEMMA EU project by KIT and KTH

# AFA by ORNL

## AFA low Ni (OC-Q) – plate 12 x 50 x 64 mm

| Element | C   | Cr | Ni | Mn | Al  | Cu | Nb  | Si   | V    | Ti   | B    | Fe   |
|---------|-----|----|----|----|-----|----|-----|------|------|------|------|------|
| wt. %   | 0.2 | 14 | 12 | 4  | 2.5 | 3  | 0.6 | 0.15 | 0.05 | 0.05 | 0.01 | bal. |

## AFA high Ni (OC-E) – plate 12 x 50 x 64 mm

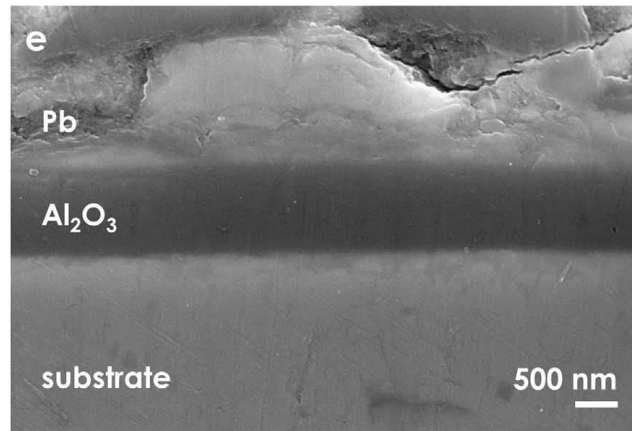
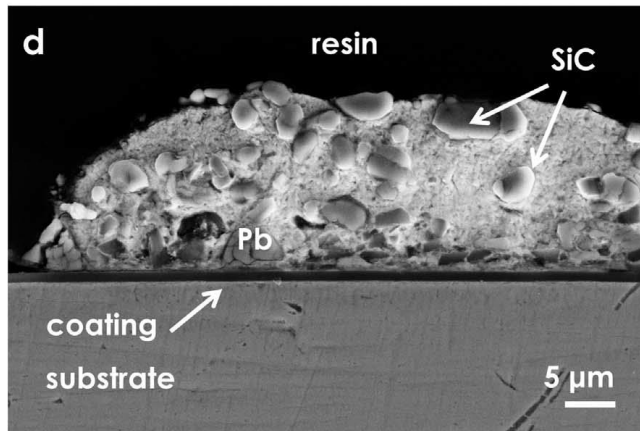
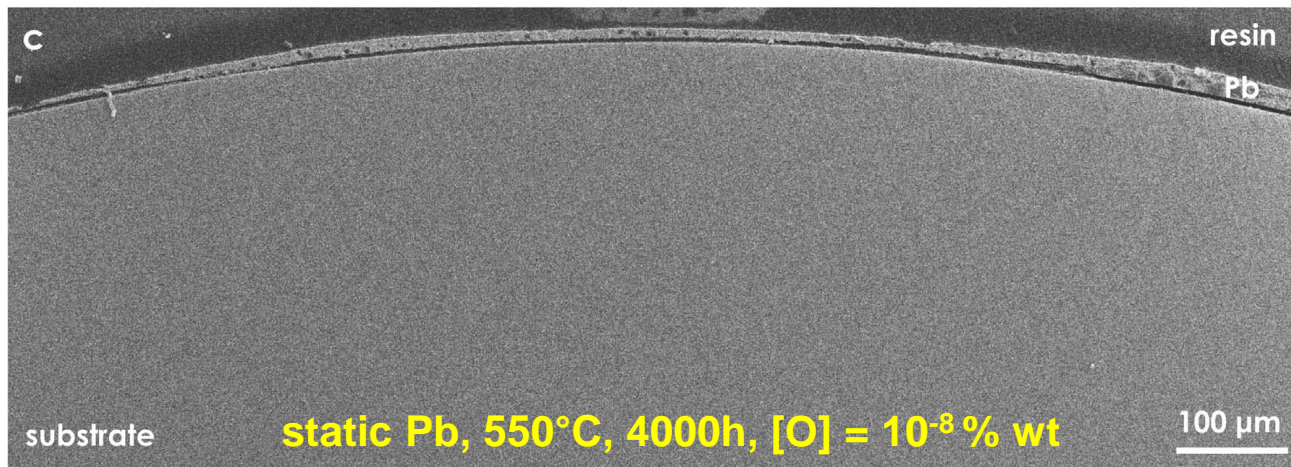
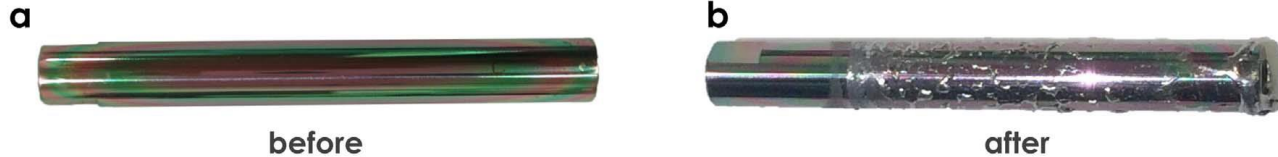
| Element | C   | Cr | Ni | Mn | Al | Cu  | Nb  | Si   | V    | Ti   | B    | Fe   |
|---------|-----|----|----|----|----|-----|-----|------|------|------|------|------|
| wt. %   | 0.2 | 14 | 25 | 2  | 4  | 0.5 | 2.5 | 0.15 | 0.05 | 0.05 | 0.01 | bal. |

- n°7 specimen of AFA 12Ni + n°7 specimen of AFA 25Ni (47x12x6 mm)
- Ra= 0.022-0.037  $\mu\text{m}$  (grinding paper up to 4000P)
- Exposure tests in Pb 550°C, 1000h, high oxygen ( $10^{-3}$  % wt.)
- Exposure tests in Pb 550°C, 1000h, low oxygen ( $10^{-8}$  % wt.)
- Pre- and Post- test characterization to be performed

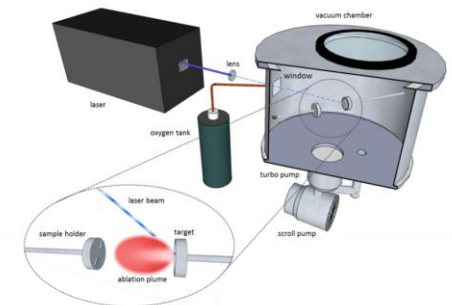


# Al<sub>2</sub>O<sub>3</sub> coating by PLD (IIT)

*amorphous alumina with nano-crystalline inclusions (by IIT)*



coated 15-15Ti with PLD-Al<sub>2</sub>O<sub>3</sub> for fuel cladding & fuel assembly



*Pulsed Laser Deposition*

No evidence of Pb corrosion neither at the macroscopic scale nor at the microscopic scale in tests up to 4000h (PAR2016).

F. García Ferré (2017)

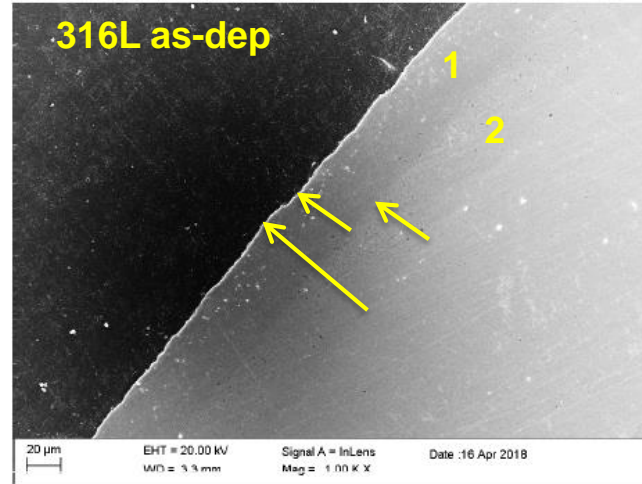
# FeCrAl layer by aluminizing (Diffusion Alloys UK)

For SG, DHR, pumps,  
inner vessels

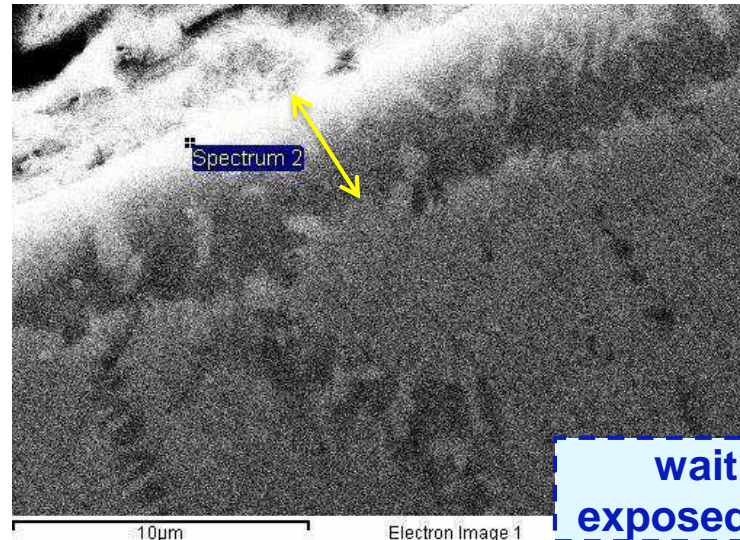
Capability to coat  
complex geometry



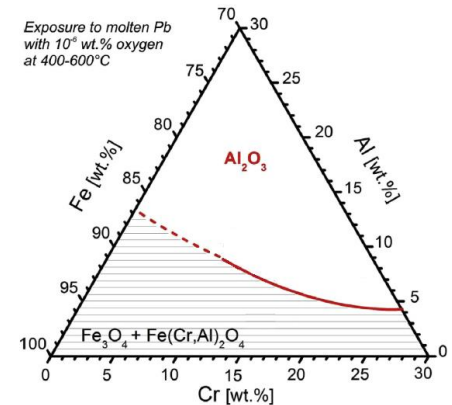
| Element | Weight% | Atomic% |
|---------|---------|---------|
| O K     | 4.06    | 10.87   |
| Al K    | 34.81   | 55.23   |
| Cr K    | 14.66   | 12.07   |
| Fe K    | 27.25   | 20.90   |
| Pb M    | 4.50    | 0.93    |
| Totals  | 85.28   |         |



Pb 550°C 2000h, [O] = 10<sup>-3</sup> % wt.



- 1) diffusion layer 40µm with 40→20 % Al (outer-layer 5µm + inner-layer 35µm)
- 2) further diffusion layer 10→5 % Al between diffusion layer and steel

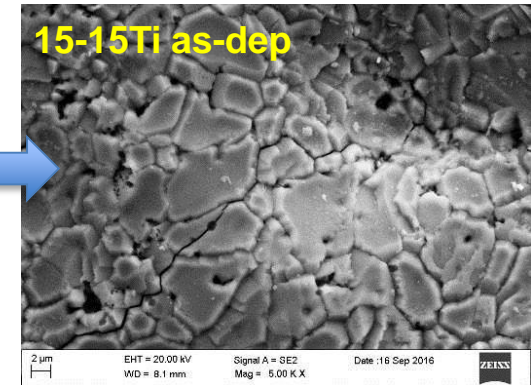
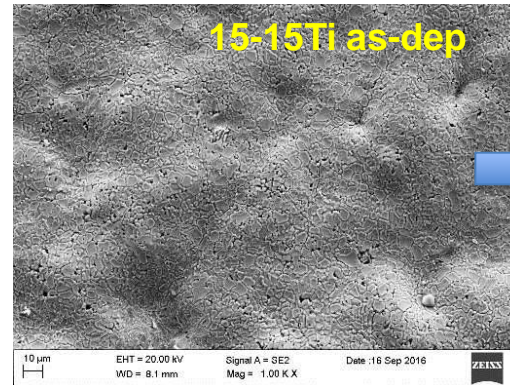
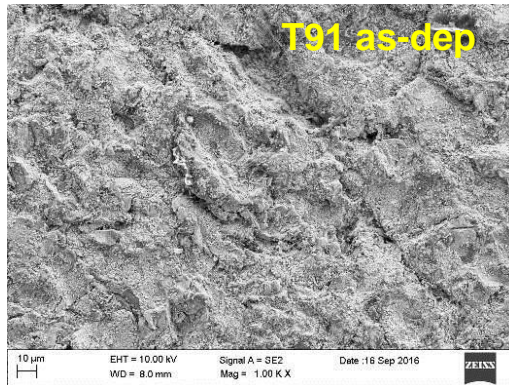


only Pb penetration was observed in the first 5 µm, no formation of Al<sub>2</sub>O<sub>3</sub>.

waiting for specimen  
exposed to low Co for 1000h

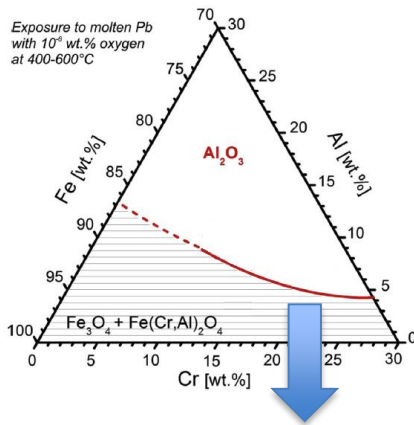
# FeCrAl layer by Pack Cementation (CSM)

FeCrAl layer high Al activity on T91 & 15-15Ti (brittle phases) → need of low Al activity aluminizing

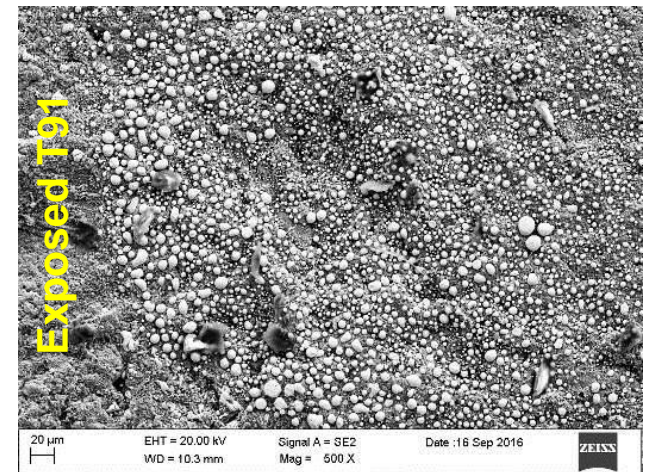
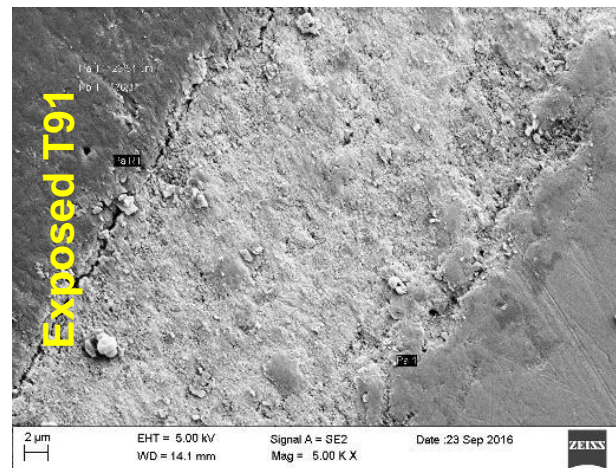


Diffusion coating 20-25 μm + 45-50 μm of further aluminizing, cracks on treated 15-15Ti

Static Pb 550°C, 1500h, low C<sub>0</sub> (PAR2016)



protective and self-healing Al<sub>2</sub>O<sub>3</sub> scale

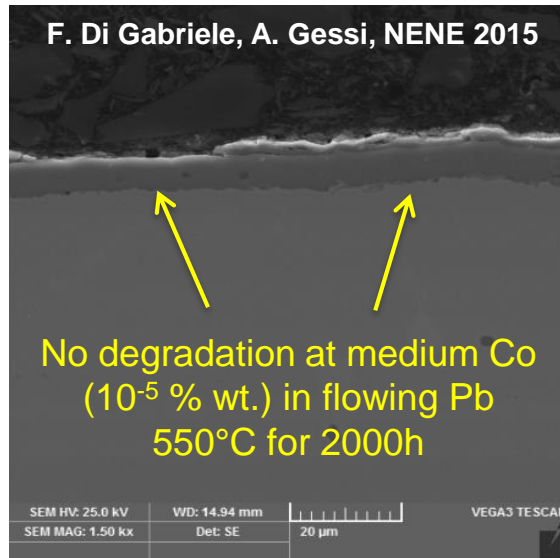


No interaction with Pb (isolated Pb drops on the surface). No thickness reduction after tests.

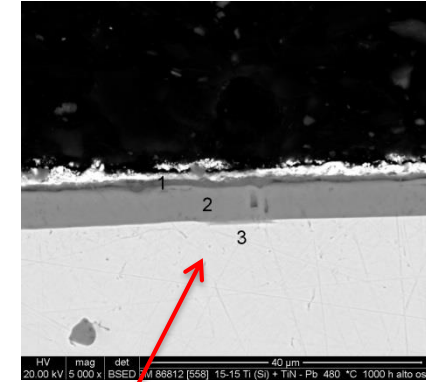
# TiN – AlTiN coatings

**TiN**  
high wear  
resistance

Oxidation  
resistance:  
 $T_{ox} = 450^{\circ}\text{C}$  (air)



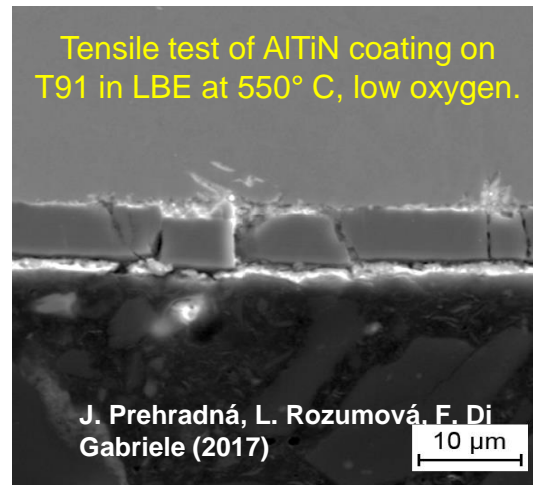
| % wt. | 1    | 2    | 3    |
|-------|------|------|------|
| N     | 13.6 | 31.8 | -    |
| O     | 41.0 | -    | -    |
| Si    | -    | -    | 0.8  |
| Ti    | 42.1 | 67.8 | 1.9  |
| Cr    | -    | -    | 14.1 |
| Mn    | -    | -    | 1.6  |
| Fe    | 0.4  | 0.4  | 64.8 |
| Ni    | -    | -    | 15.1 |
| Mo    | -    | -    | 2.0  |
| Pb    | 2.9  | -    | -    |



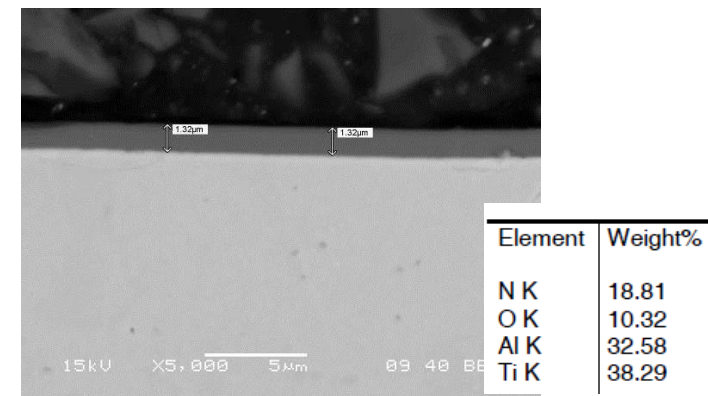
Oxidation of PVD-TiN by CSM in Pb at high Co  
for 1000h ( $10^{-4}$  %  $480^{\circ}\text{C}$  and  $10^{-3}$  % wt.  $550^{\circ}\text{C}$ )  
**PAR2015**

**AlTiN** Back-up for  
impellers in primary  
pumps)

Higher oxidation  
resistance than TiN  
( $T_{ox} = 750^{\circ}\text{C}$  in air)



Cracks in the notch but adhesion  
conserved. No degradation



AlTiN coating as-dep (by CSM),  
some samples exposed in Pb to  
be analysed (**PAR2015**)

# SUMMARY

- 15-15Ti AIM1: corrosion data in liquid Pb are missing, available data are mostly related to LBE
- Qualification in Pb of 15-15Ti AIM1 for ALFRED (+ welding joints) will be performed in GEMMA EU project (static & flowing)
- AFA steels composition will be improved and tested in GEMMA EU project by KTH and KIT
- Screening tests in Pb of AFA from ORNL concluded, pre- and post-test analysis to be performed
- Static tests of Al<sub>2</sub>O<sub>3</sub> by PLD done, tests in flowing condition to be performed in GEMMA EU project
- Aluminizing by Diffusion Alloys UK under study, post-test analysis to be performed on specimen exposed to low Co in Pb
- Exposure tests of AlTiN coatings by CSM performed, post-test analysis to be performed.

# WORKSHOP TEMATICO

ACCORDO DI PROGRAMMA MISE – ENEA  
PAR2017 – PROGETTO B.3 - LP2



## GENERATION IV LEAD COOLED FAST REACTOR STATO ATTUALE DELLA TECNOLOGIA E PROSPETTIVE DI SVILUPPO

ADP MiSE-ENEA (PAR2017-LP2)

Dipartimento di Ingegneria Astronautica, Elettrica ed Energetica Università di Roma "La Sapienza"  
San Pietro in Vincoli, Via Eudossiana 18  
14-15 Giugno 2018

### Coating mechanical characterization

M. Bragaglia, F.R. Lamastra, F. Franceschetti; F. Nanni



**CONTATTI:**

Dipartimento di Ingegneria Impresa  
Università di Roma "Tor Vergata"  
Via del Politecnico, 1, 00133 Roma -Italia  
Tel +39-06.7259.4496 - Fax +39-  
06.7259.4328



# Indice dei contenuti



## **Caratterizzazione microstrutturale e meccanica di diffusion coating in FeCrAl su acciaio AISI 316 L esposti in piombo fuso**

Temperatura 550°C

Tempo 2000h

Concentrazione ossigeno  $10^{-3}$  % wt

### **Caratterizzazione microstrutturale**

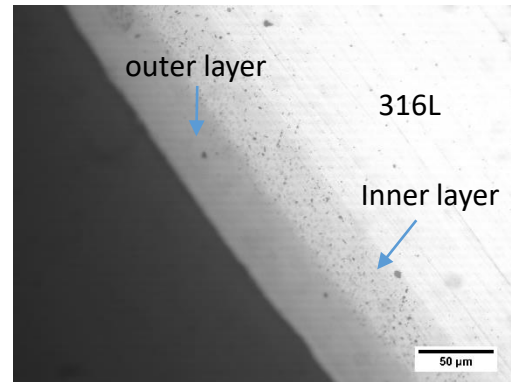
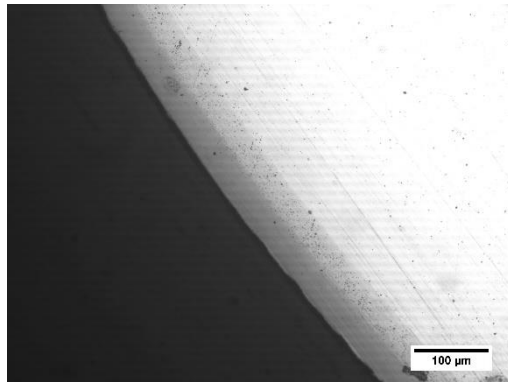
- Microscopia ottica (MO) prima e dopo attacco chimico
- Microscopia a scansione elettronica (SEM)
- Microanalisi EDS

### **Caratterizzazione meccanica**

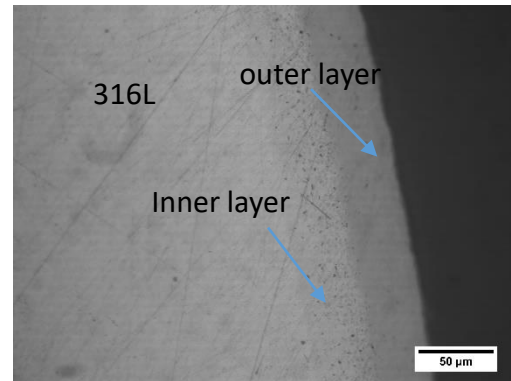
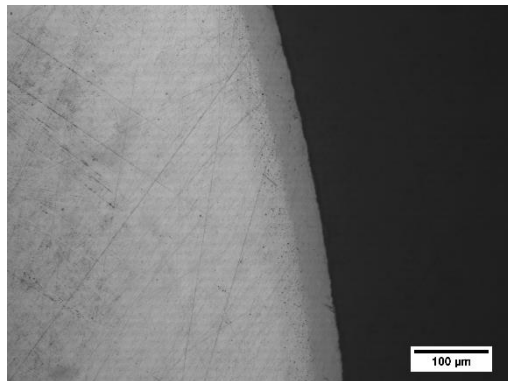
- Test di microdurezza Vickers
- Test di microdurezza Knoop

## Microscopia ottica

Neat



Corroso Pb

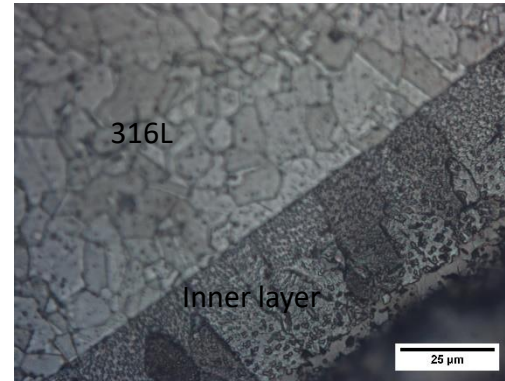
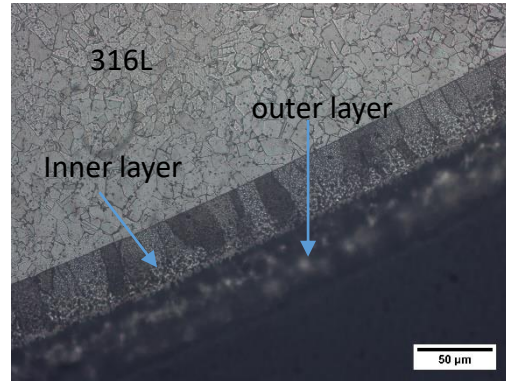
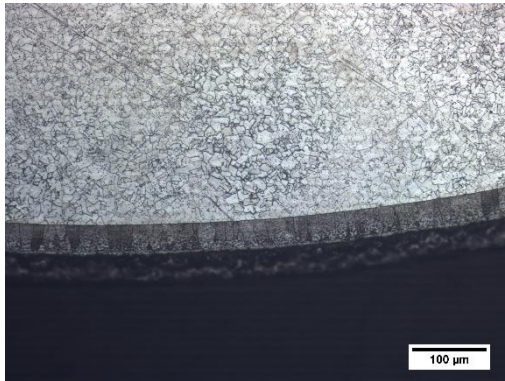


- Rivestimento compatto ed omogeneo buona adesione al substrato
- Presenza di outer layer 30-40 micron
- Presenza di inner layer 30-40 micron
- Inner layer presenza di precipitati
- Non evidenti modifiche dimensionali del coating dopo prove di corrosione in Pb fuso

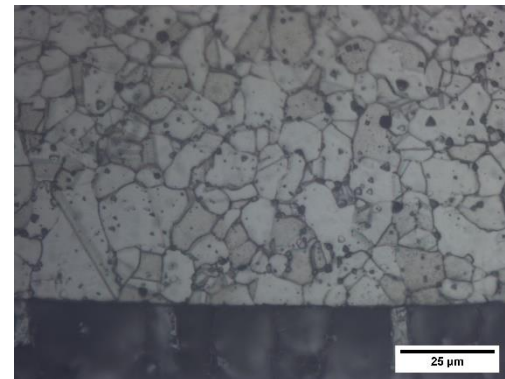
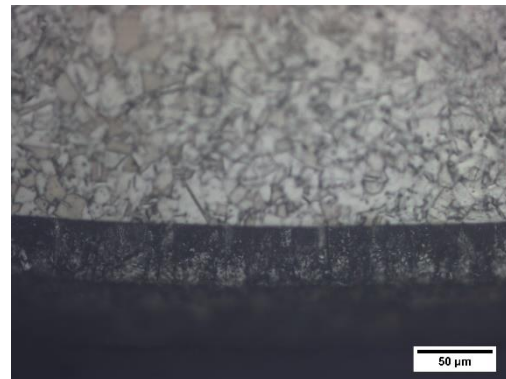
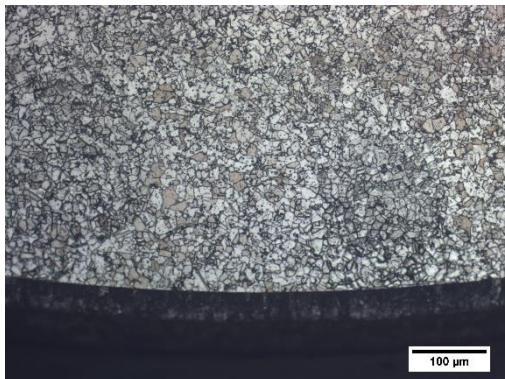
## Microscopia ottica: attacco chimico

Attacco chimico soluzione di acqua regia HCl :  $\text{HNO}_3$  : EtOH per evidenziare la microstruttura

neat



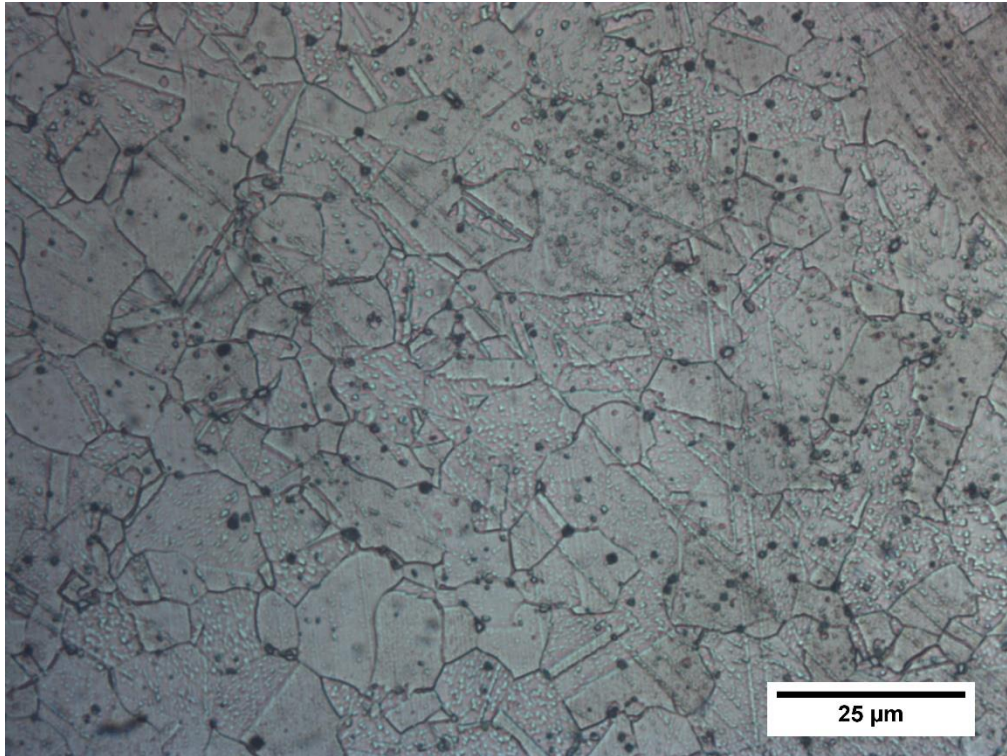
corroso



- Different microstructure outer layer e inner layer
- Inner layer  $\rightarrow$  grana cristallina
- Outer layer  $\rightarrow$  no grana cristallina

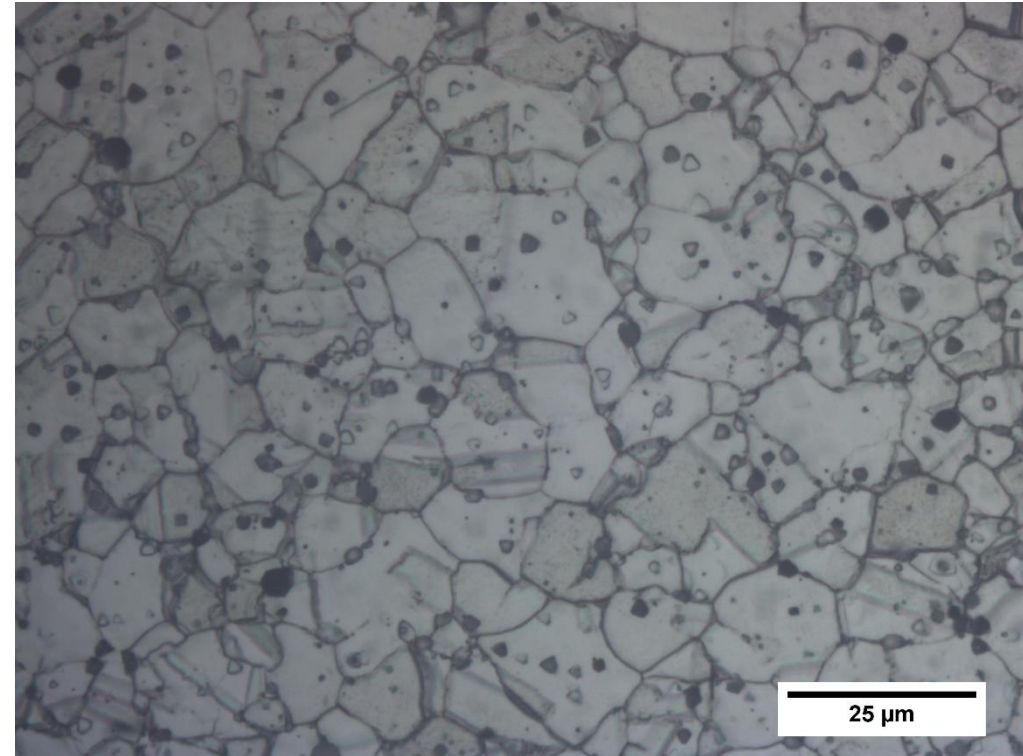
## Microscopia ottica post attacco chimico

Neat



- ASTM grain number 10
- Dm grain 7 um

Corroso Pb



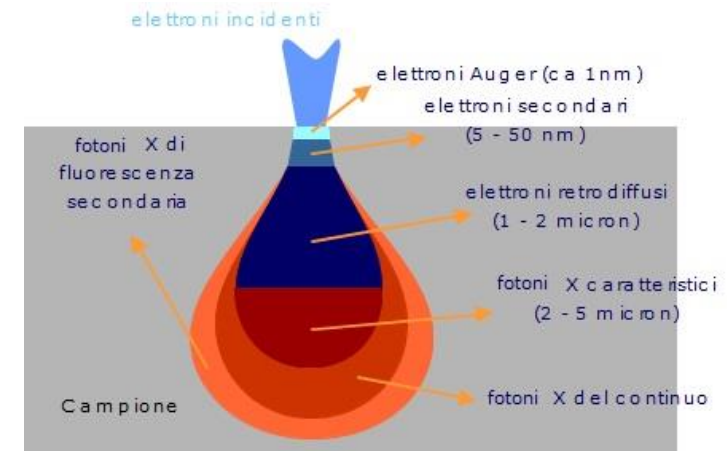
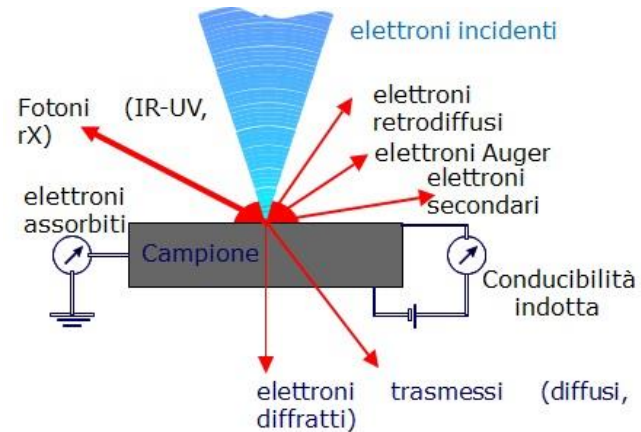
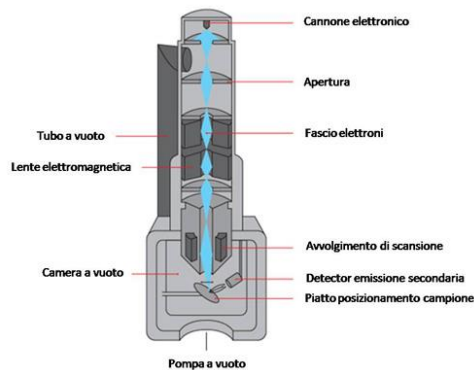
- ASTM grain number 10
- Dm grain 7,5 um

- Post Pb fuso → Leggero aumento dimensioni bordi di grano dell'acciaio, grani più regolari, bordi grano più smussati, assenza di geminati
- Probabili fenomeni di distensione

# Microscopia elettronica a scansione (SEM)

Il **microscopio elettronico a scansione (SEM)** sfrutta la generazione di un fascio elettronico ad alta energia focalizzato e deflesso da un sistema di lenti nel vuoto per scansionare un'area del campione.

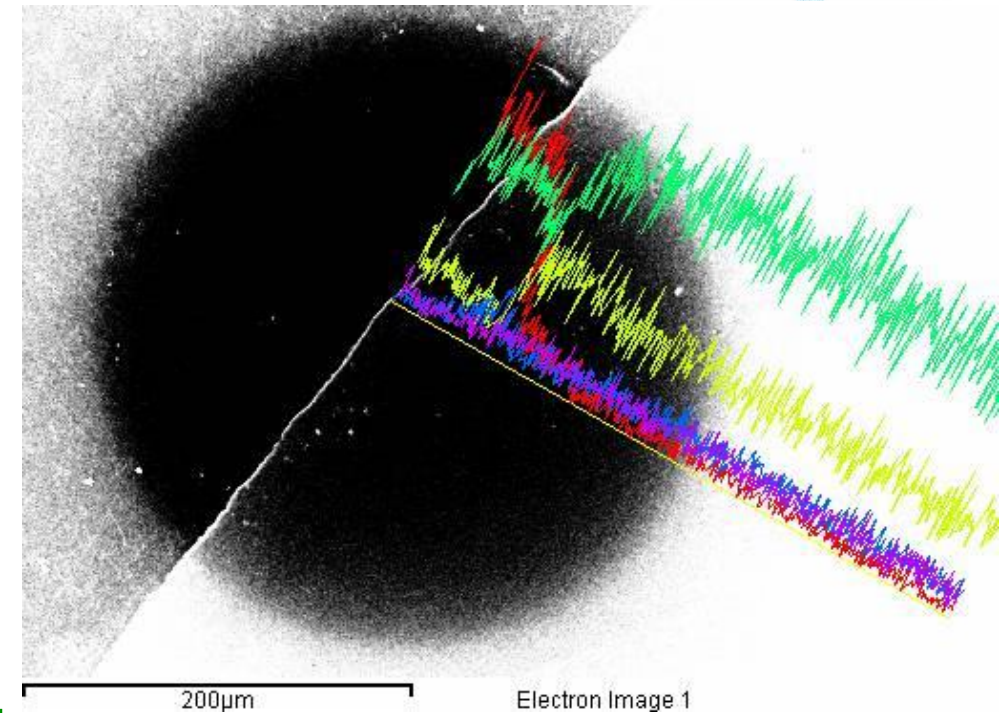
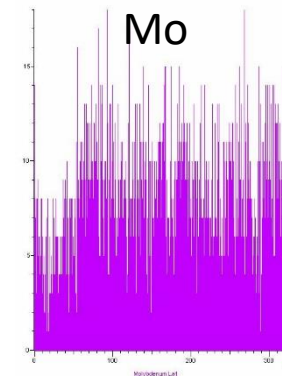
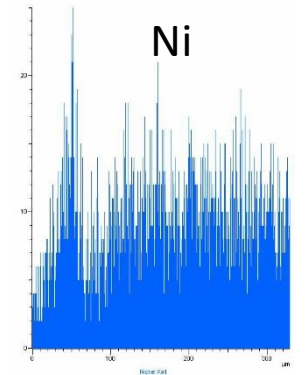
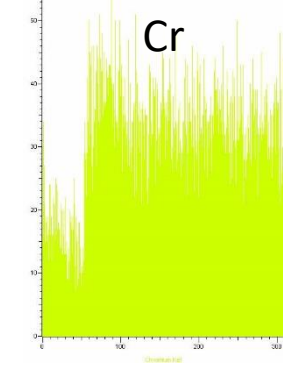
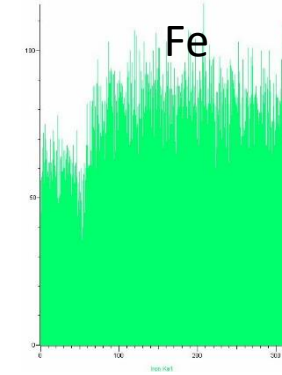
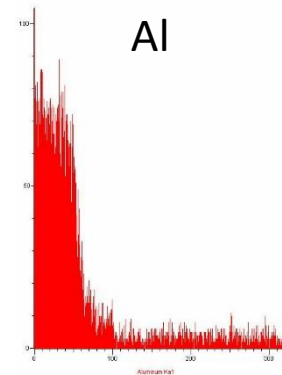
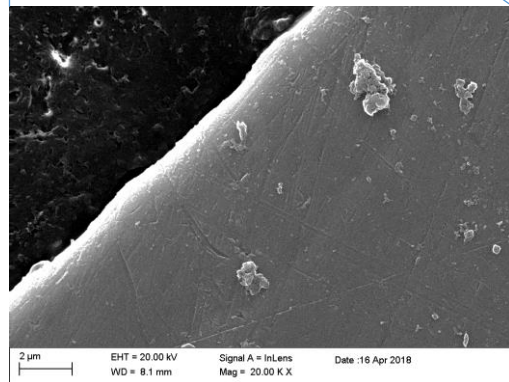
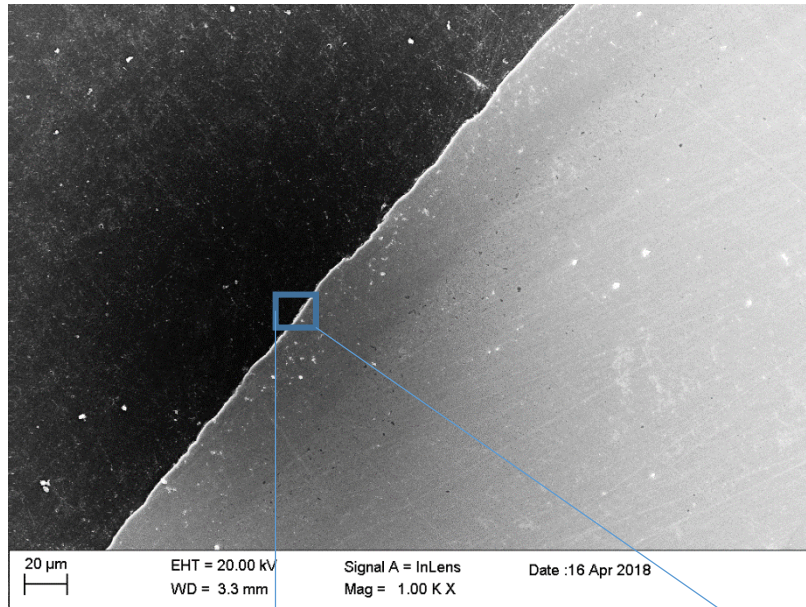
L'interazione fascio-campione genera elettroni secondari e retrodiffusi. Questi sono raccolti da opportuni detectors e convertiti in segnali elettrici. Tali segnali vengono amplificati ed elaborati da un computer fino a formare un'immagine a livelli di grigio.



Permette:

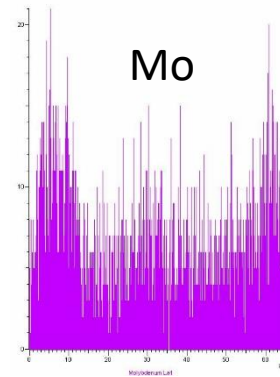
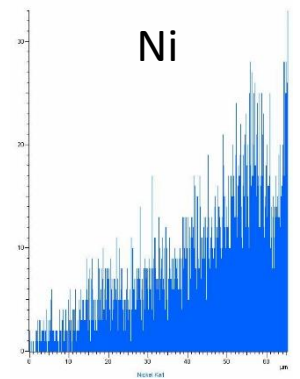
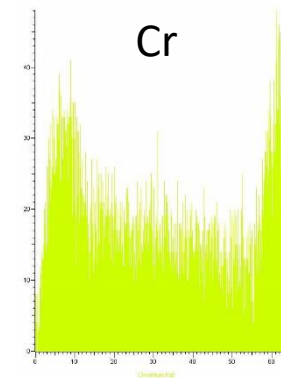
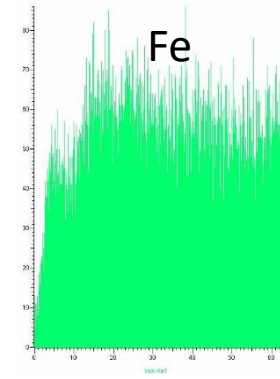
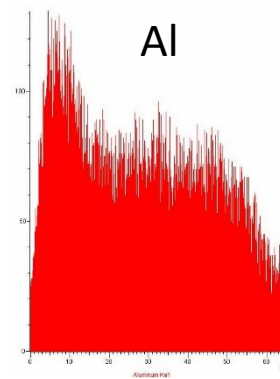
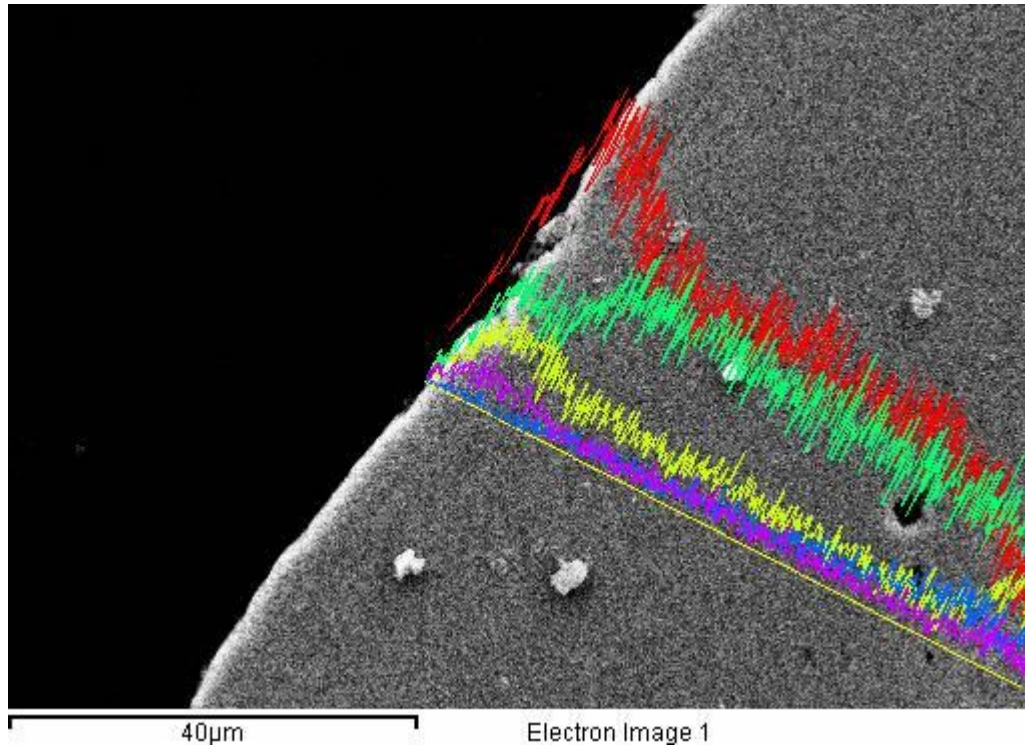
- Analisi morfologica della superficie del campione
- Analisi delle sezioni dei provini (compattezza film dimensioni)
- Analisi Elementare EDS (**Energy Dispersive Spectroscopy**)

# Microscopia SEM Neat



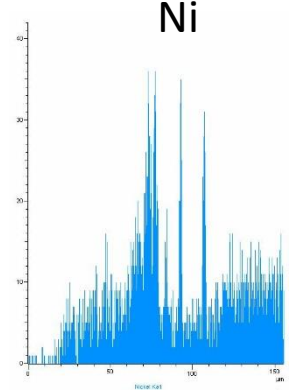
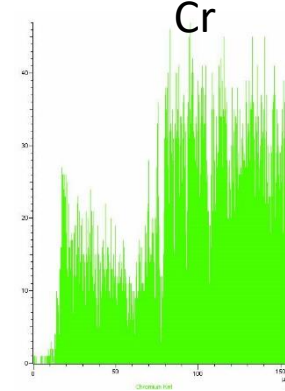
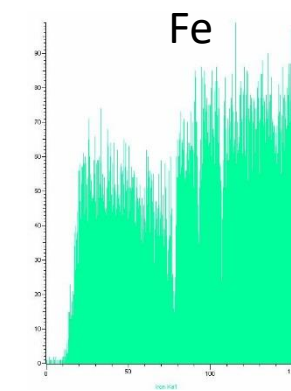
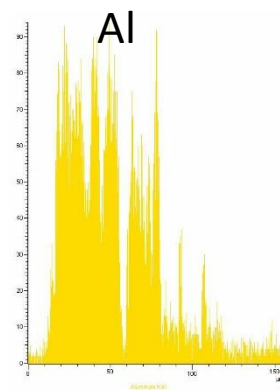
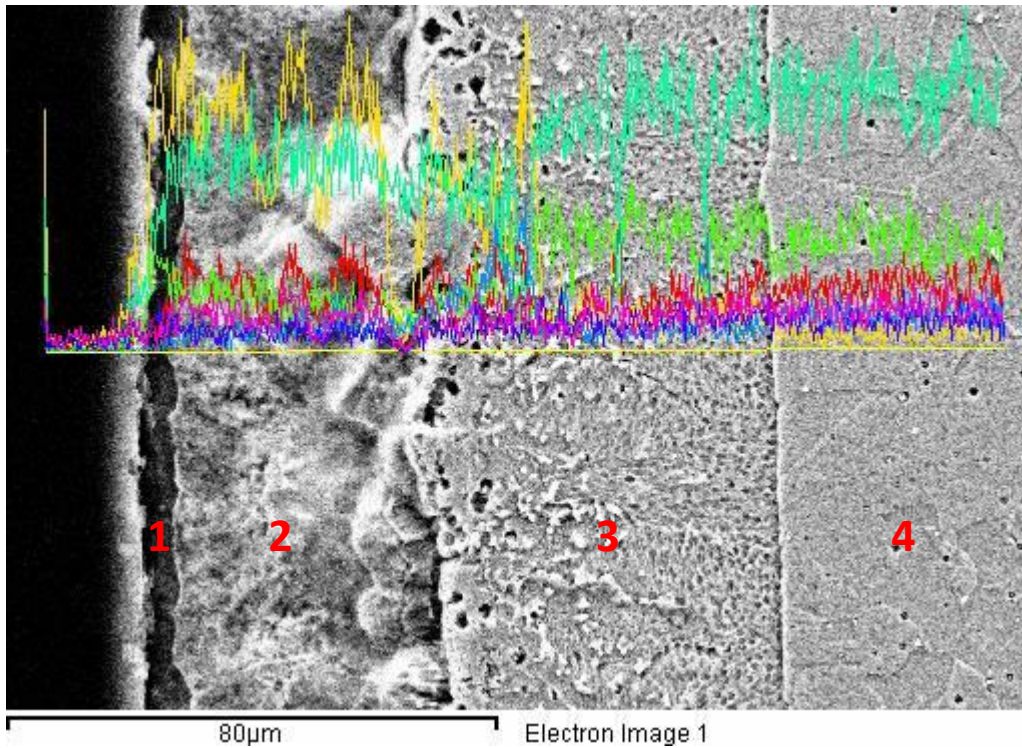
- Diffusion coating in FeCrAl
- Elevato contenuto di Al in outer e inner layer

# Microscopia SEM Neat outer layer



Strato esterno outer layer di circa 3-5 micron molto ricco in alluminio

# Microscopia SEM Neat dopo attacco chimico

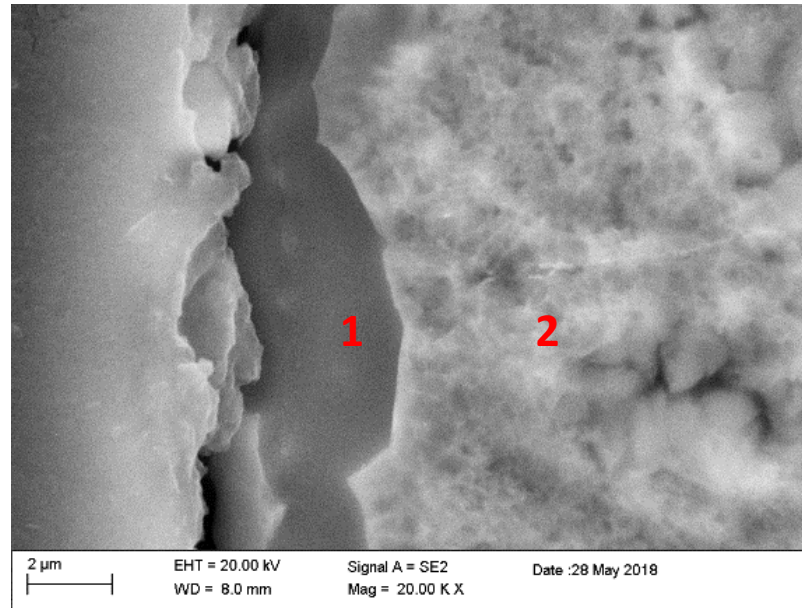
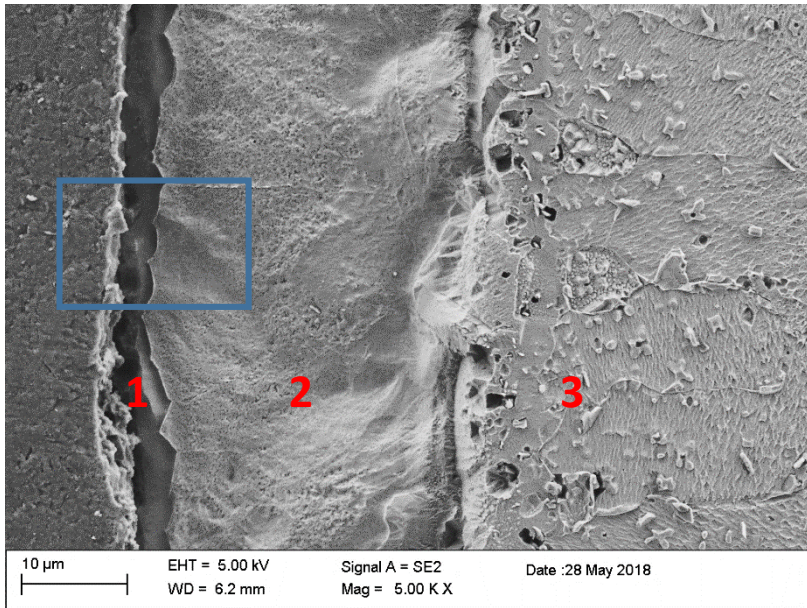


Rivestimento formato da 3 strati

- 1 layer esterno 3-5 micron
- 2 outer layer
- 3 inner layer
- 4 aisi 316 L

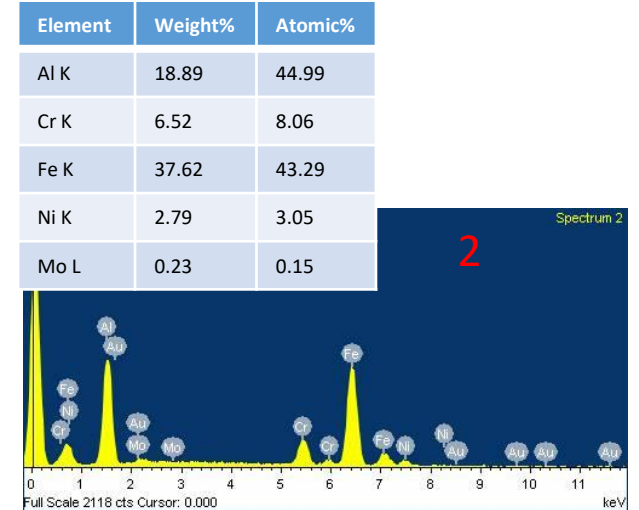
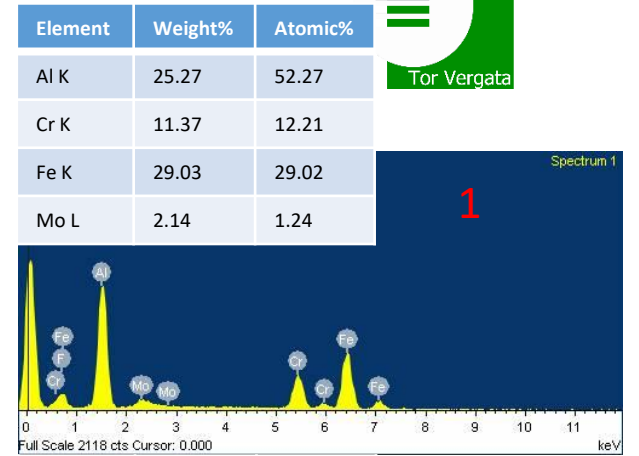


# Microscopia SEM Neat attacco chimico

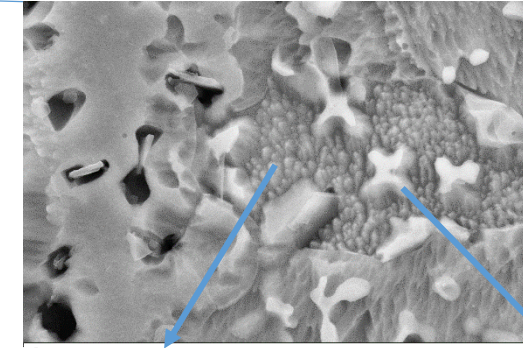
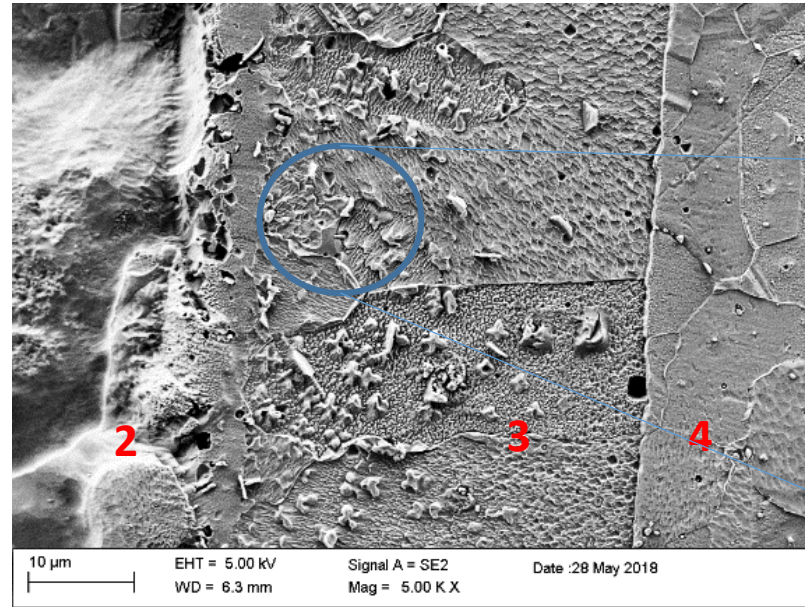
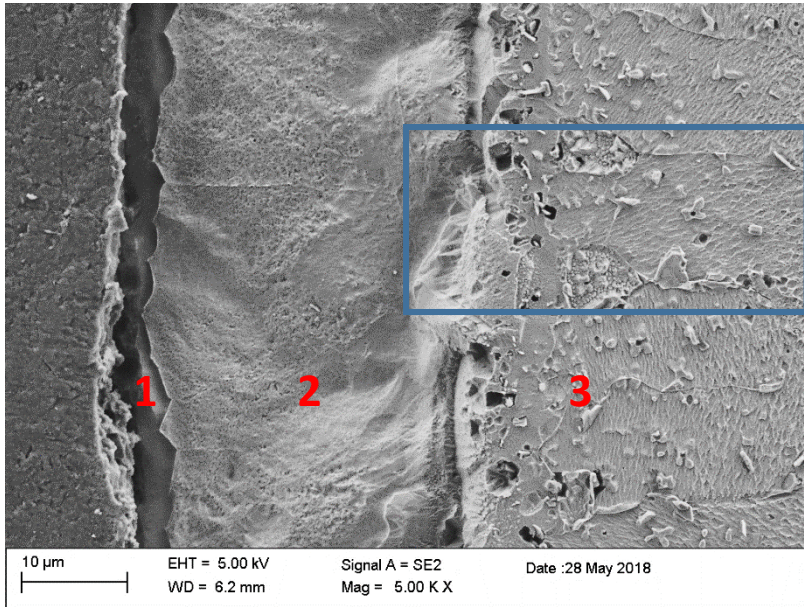


1 spessore 3 micron FeCrAl ad elevato tenore di Al

2 Outer layer FeCrAl spessore 30 micron



# Microscopia SEM neat attacco chimico

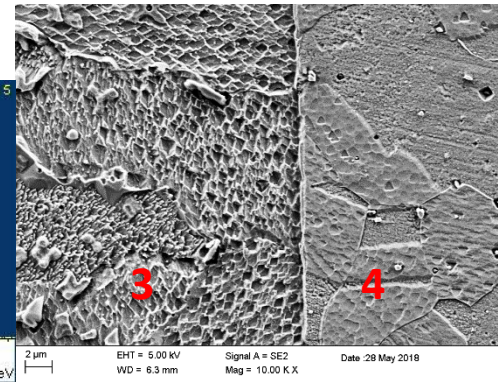
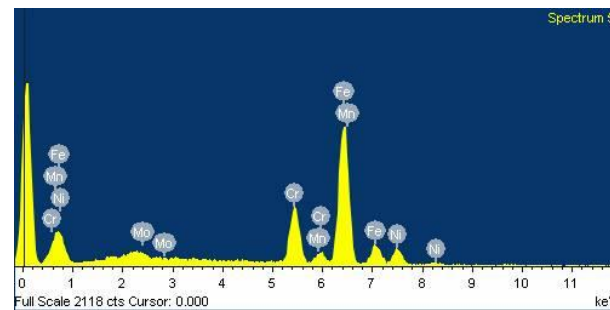


| Element | Weight% | Atomic% | Element | Weight% | Atomic% |
|---------|---------|---------|---------|---------|---------|
| Al K    | 2.27    | 5.57    | Al K    | 24.66   | 49.85   |
| Cr K    | 16.04   | 20.43   | Cr K    | 4.34    | 4.55    |
| Fe K    | 51.19   | 60.68   | Mn K    | 1.27    | 1.26    |
| Ni K    | 2.81    | 3.17    | Fe K    | 17.14   | 16.74   |
| Mo L    | 1.26    | 0.87    | Ni K    | 29.37   | 27.28   |
|         |         |         | Mo L    | 0.56    | 0.32    |

Interfaccia 2-3 zona ricca in NiAl

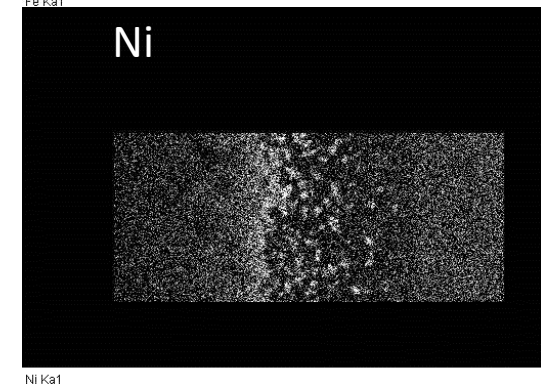
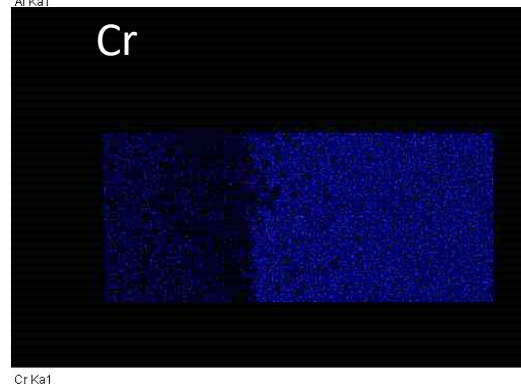
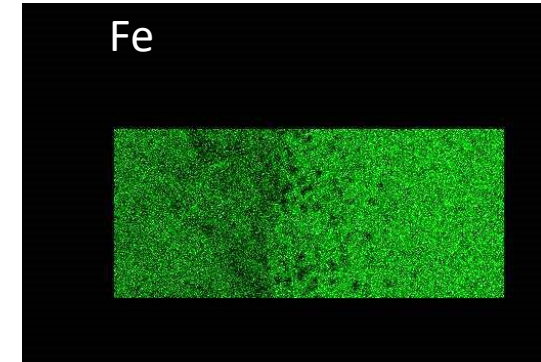
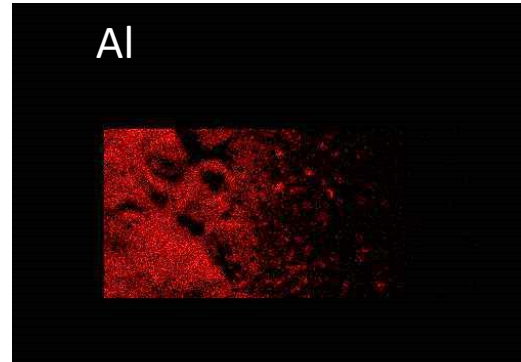
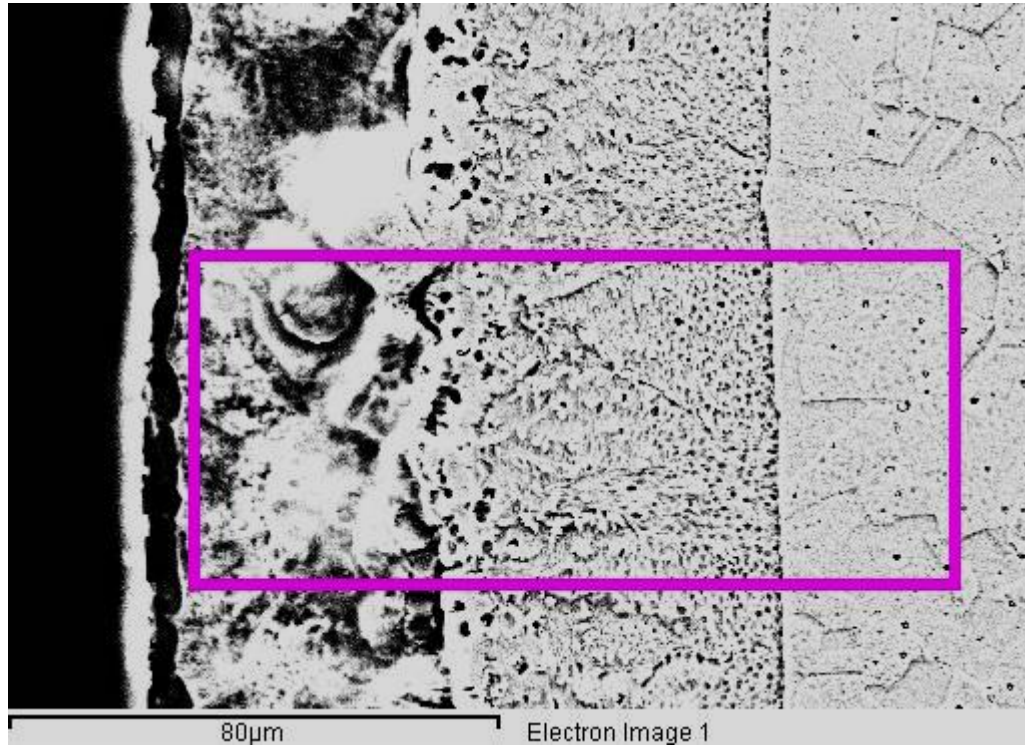
3 inner layer grana cristallina definita spessore 40 micron; precipitati base NiAl immersi in matrice FeCr

4 substrato acciaio 316L



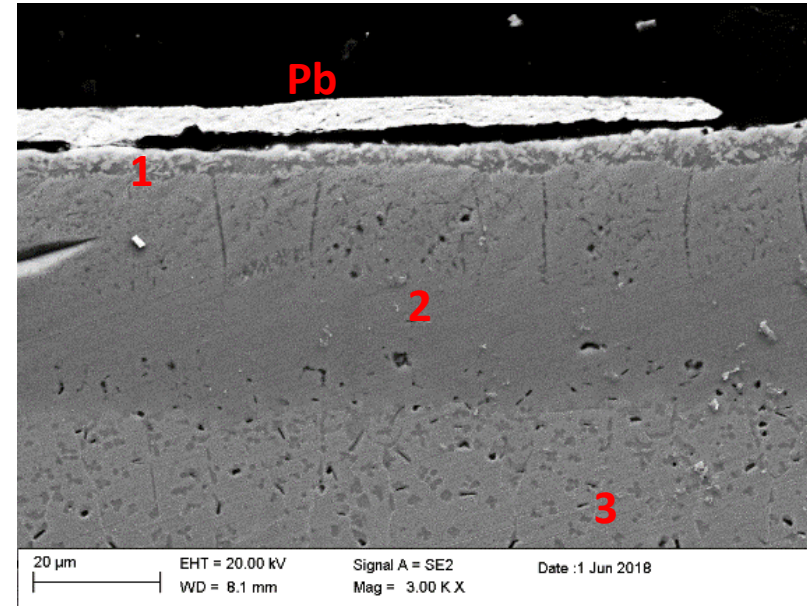
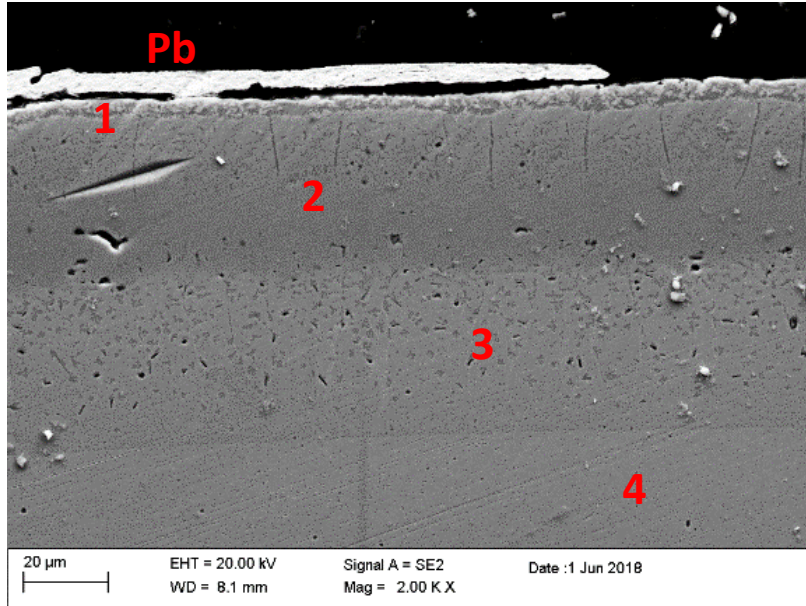
| Element | Weight% | Atomic% |
|---------|---------|---------|
| Cr K    | 12.17   | 18.82   |
| Mn K    | 1.07    | 1.57    |
| Fe K    | 46.96   | 67.61   |
| Ni K    | 8.35    | 11.44   |
| Mo L    | 0.69    | 0.57    |

## Microscopia SEM neat attacco chimico



- Outer layer ricco in alluminio
- interfaccia outer-inner ricca in nickel
- Precipitati NiAl nell'inner layer immersi in matrice FeCr

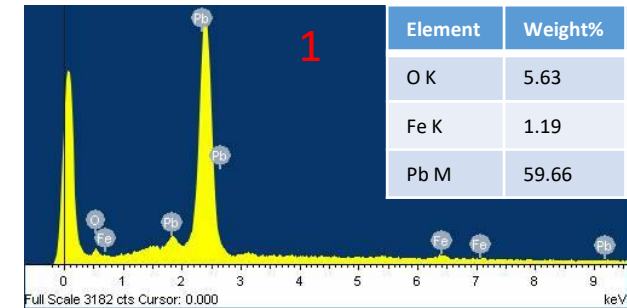
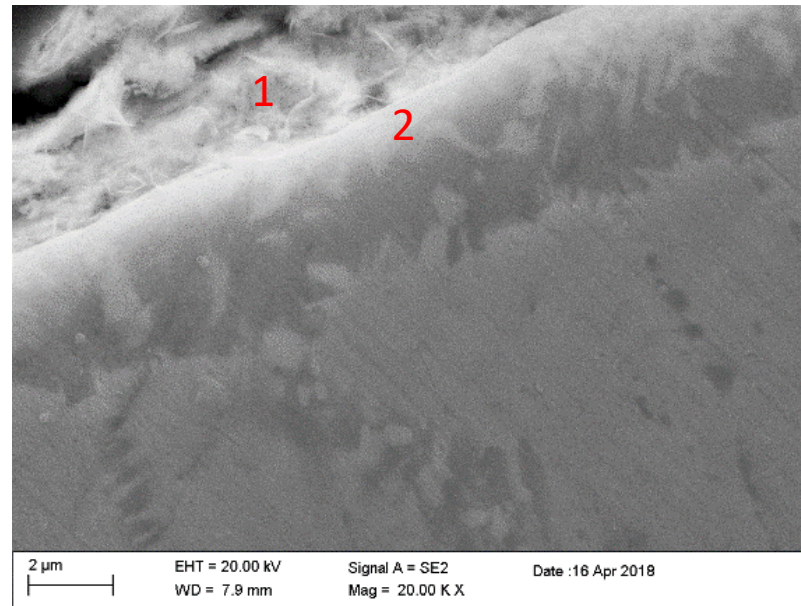
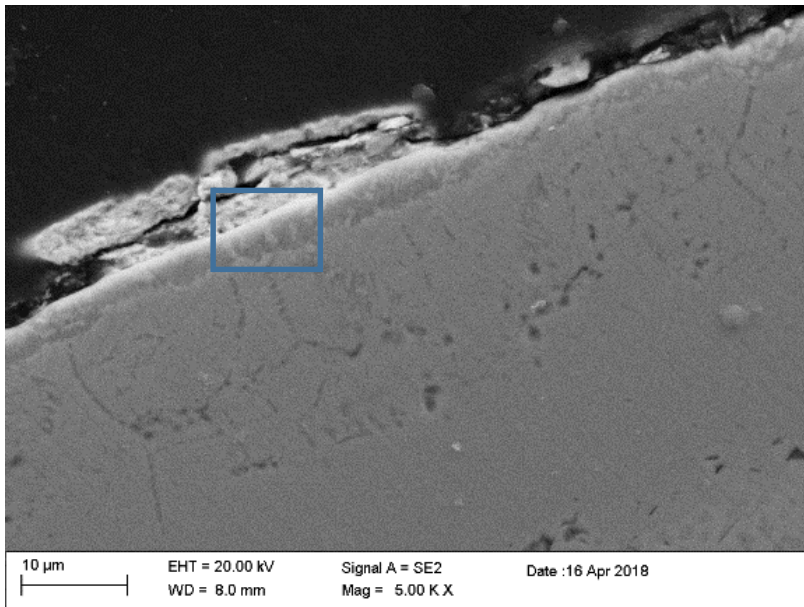
## Microscopia SEM provino corrosivo



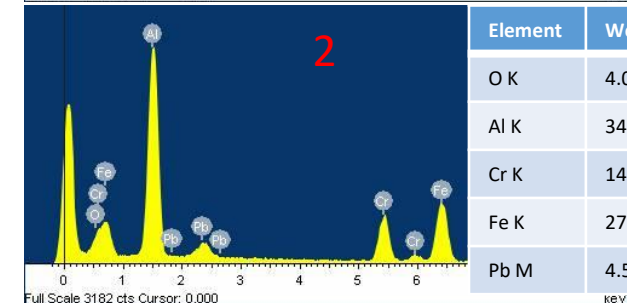
Mantenimento del diffusion coating dopo prove di corrosione in Pb fuso

- 1 layer esterno 3 micron
- 2 outer layer
- 3 inner layer
- 4 aisi 316L

# Microscopia SEM provino corrosivo



| Element | Weight% | Atomic% |
|---------|---------|---------|
| O K     | 5.63    | 53.21   |
| Fe K    | 1.19    | 3.23    |
| Pb M    | 59.66   | 43.56   |

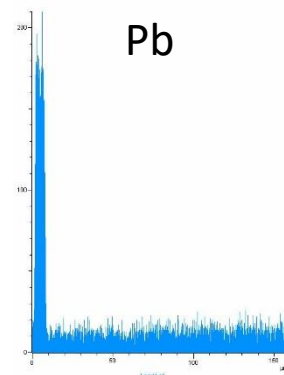
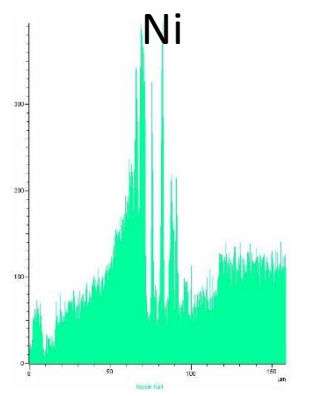
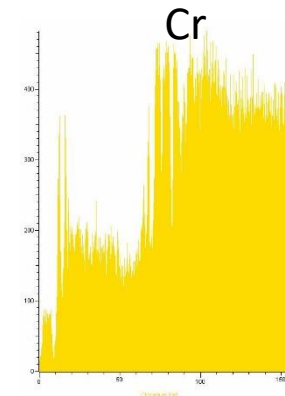
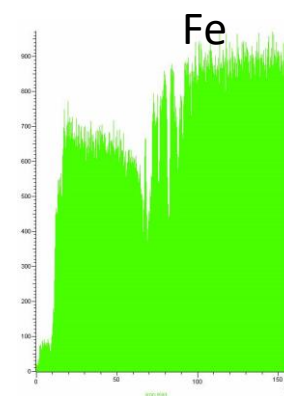
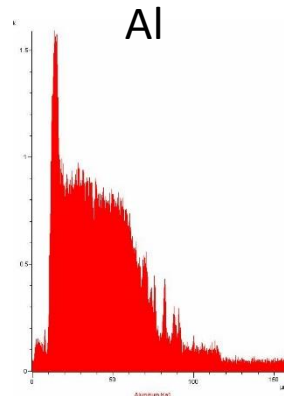
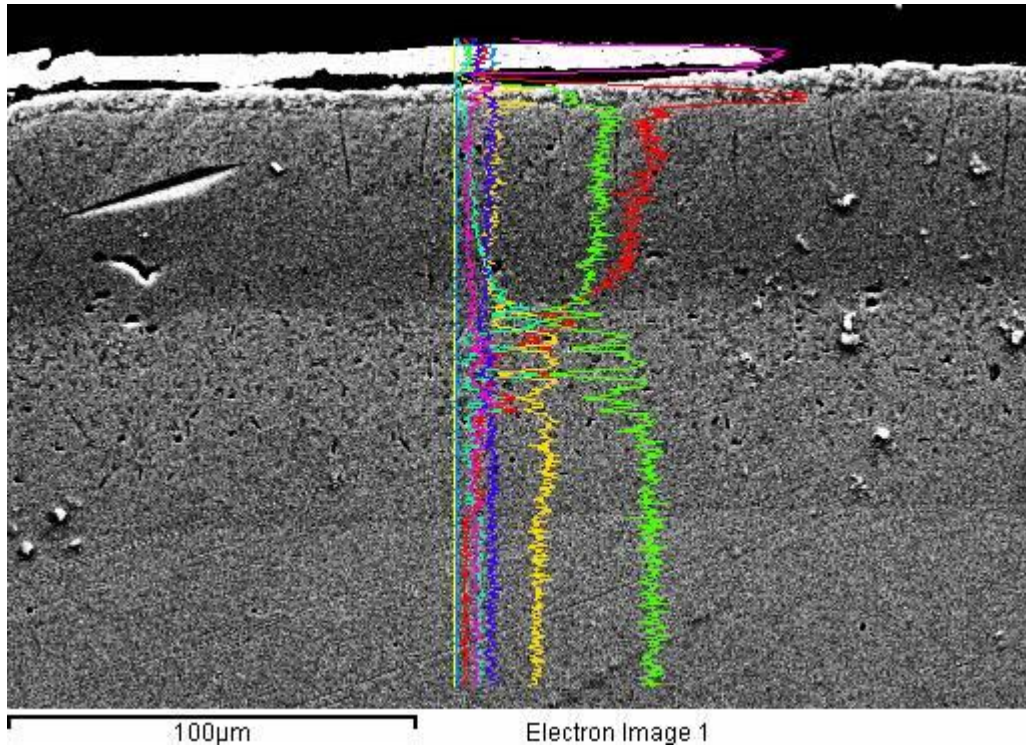
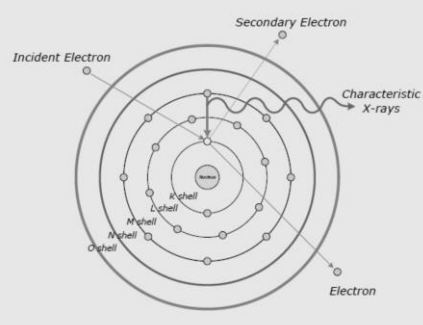


| Element | Weight% | Atomic% |
|---------|---------|---------|
| O K     | 4.06    | 10.87   |
| Al K    | 34.81   | 55.23   |
| Cr K    | 14.66   | 12.07   |
| Fe K    | 27.25   | 20.90   |
| Pb M    | 4.50    | 0.93    |

No formazione scaglia di ossido di alluminio

- 1 Residuo del bagno di piombo (elevato tenore di ossigeno probabile ossido di piombo)
- 2 Tracce di piombo nei primi micron superficiali

# Microscopia SEM provino corroso in Pb

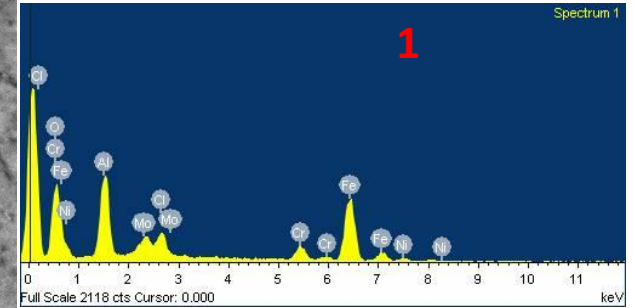
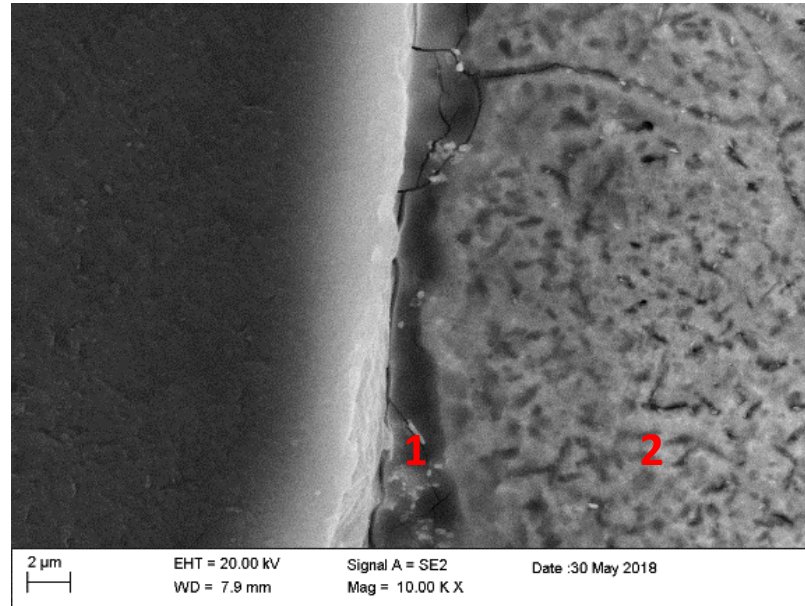
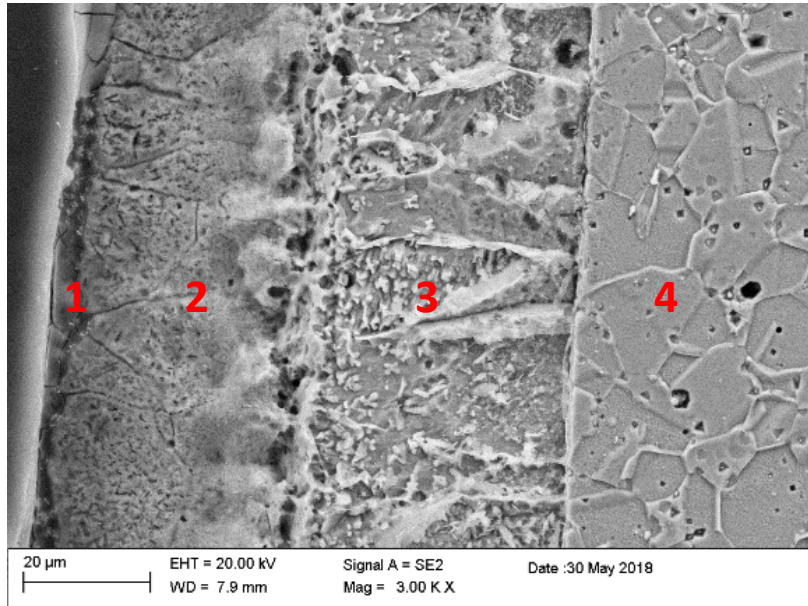
|                   |    |
|-------------------|----|
| Lead              |    |
| 82                | Pb |
| 207.2             |    |
| 11.34             |    |
| L $\alpha$ 10.550 |    |
| M 2.342           |    |

|                   |    |
|-------------------|----|
| Molybdenum        |    |
| 42                | Mo |
| 95.94             |    |
| 9.01              |    |
| K $\alpha$ 17.441 |    |
| L $\alpha$ 2.293  |    |

Rivestimento rimane inalterato in termini compositivi dopo il test in Pb fuso  
 Piombo assente lungo l'intera sezione investigata → no diffusione nel rivestimento

Da notare che il livello energetico L $\alpha$  del Mo è sovrapponibile al livello energetico M del Pb

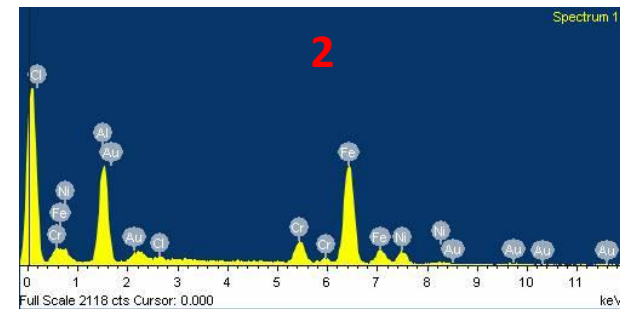
# Microscopia SEM provino corrosivo in Pb, attacco chimico



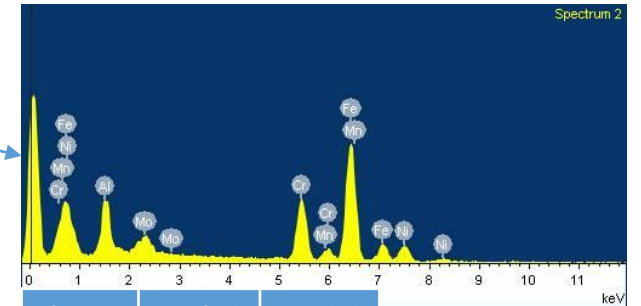
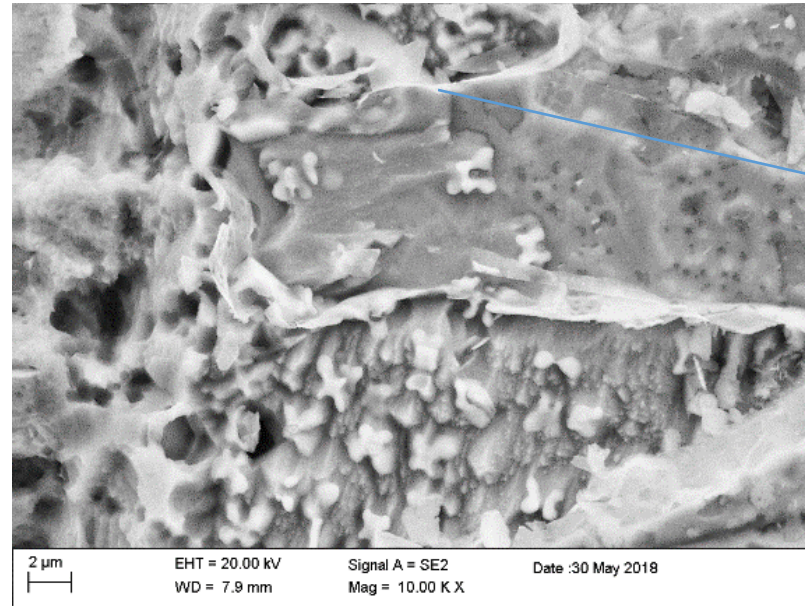
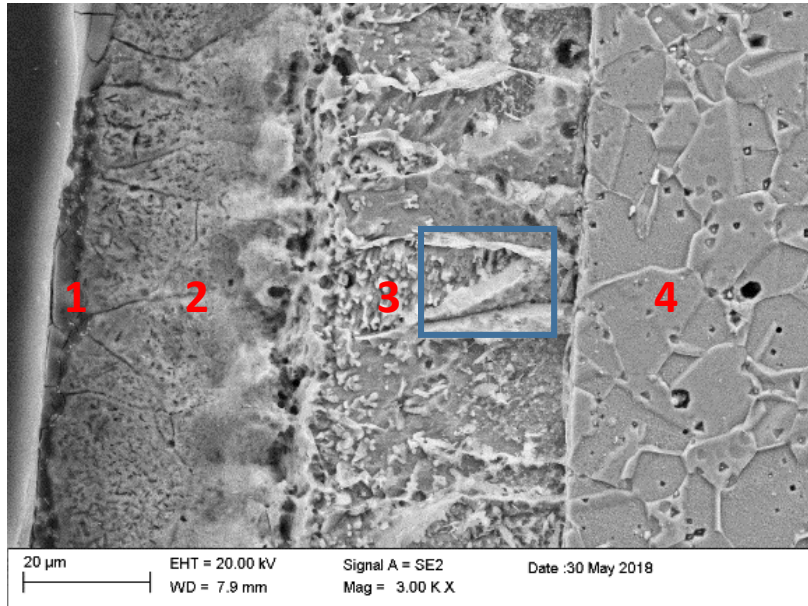
Gli spessori dei layer rimangono inalterati dopo corrosione in Pb

- 1 spessore 3-5 micron
- 2 outer layer 30-35 micron
- 3 inner layer 40-45 micron

No evidenti variazioni composizione chimica dei layer

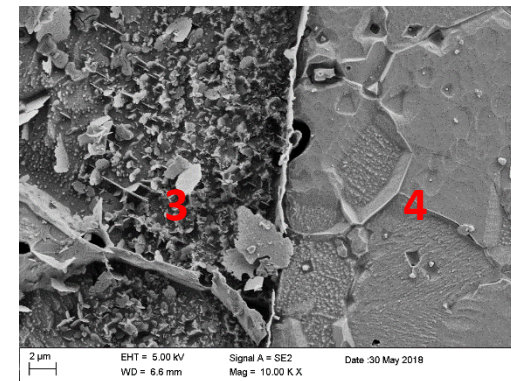


# Microscopia SEM provino corrosivo in Pb, attacco chimico



| Element | Weight% | Atomic% |
|---------|---------|---------|
| Al K    | 8.93    | 22.32   |
| Cr K    | 13.68   | 17.74   |
| Mn K    | 0.94    | 1.15    |
| Fe K    | 39.20   | 47.34   |
| Ni K    | 8.12    | 9.33    |
| Mo L    | 3.01    | 2.12    |

Inner layer stessa morfologia e composizione chimica prima e dopo corrosione in Pb.



| Element | Weight% | Atomic% |
|---------|---------|---------|
| Cr K    | 95.30   | 18.39   |
| Mn K    | 8.63    | 1.58    |
| Fe K    | 374.50  | 67.30   |
| Ni K    | 61.65   | 10.54   |
| Mo L    | 9.72    | 1.02    |



# Microdurezza Vickers e Knoop

**Durezza:** resistenza di un materiale alla deformazione plastica localizzata.

**Microdurezza Vickers/ Knoop:** utilizzata per la caratterizzazione di materiali molto duri e tipicamente per il controllo dei trattamenti superficiali.

Modalità di prova: **ISO 6507-1:2005**

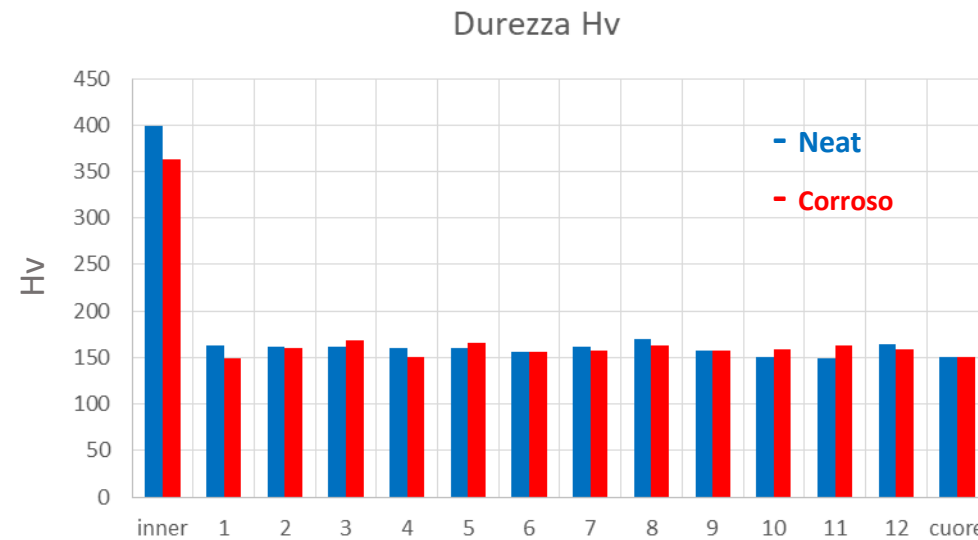
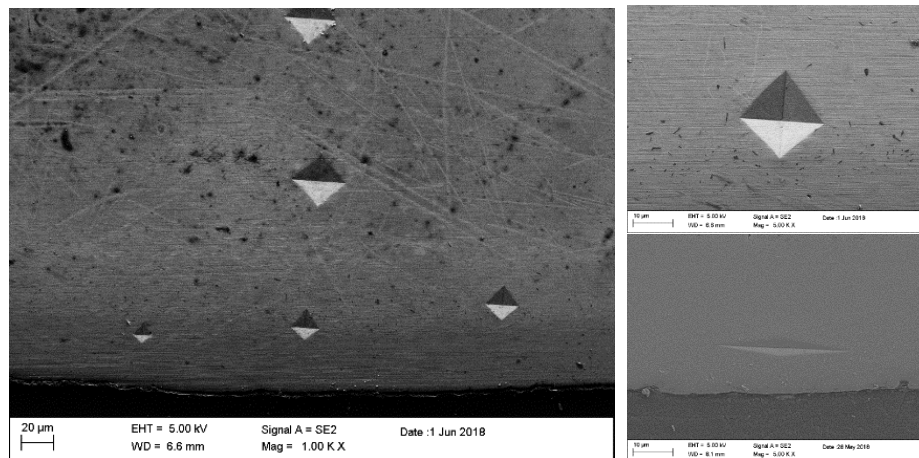
- ✓ Penetratore Vickers/Knoop compresso ortogonalmente contro la superficie del provino applicando un determinato carico per un tempo stabilito.
- ✓ Rimozione dell'indentatore.
- ✓ Misura delle diagonali dell'impronta tramite microscopio ottico.
- ✓ Calcolo della durezza.

**Condizioni di prova:**

- Indentatore Vickers/Knoop
- Carichi: 300 - 50 g
- Tempo: 30 s

$$HV = \frac{P}{S} = 0.102 \frac{P \cdot \sin\left(\frac{136^\circ}{2}\right)}{d^2}$$

$$HK = \frac{P}{A_{PAC}} = \frac{P}{L^2} \frac{2 \cdot \operatorname{tg} \theta}{\operatorname{tg} \varphi} \quad \left( = 14.229 \cdot \frac{P}{L^2} \right)$$



- Durezza knoop outer layer
- Neat : 1150 ± 54Hk
  - Corroso: 1030 ± 60 Hk

No significative variazioni di durezza dopo esposizione Pb

## Conclusioni



Sono stati caratterizzati diffusion coating su AISI 316L esposti in bagno di Pb fuso 550°C con concentrazione di Ossigeno pari a  $10^{-3}$  % wt

- I diffusion coating FeCrAl analizzati risultano uniformi omogenei e compatti
- Tre differenti zone all'interno del diffusion coating
- Lieve modifica delle dimensioni dei grani dopo esposizione Pb
- No alterazioni del rivestimento dopo esposizione a Pb
- No formazione di scaglia ossido di alluminio durante esposizione Pb
- No variazione durezza superficiale e a cuore dopo corrosione

To do:

Analisi XRD ed identificazione delle fasi cristalline che compongono il diffusion coating a convalida dell'ipotesi di non avvenuta corrosione  
Caratterizzazione diffusion coating esposti in Pb (550°C concentrazione ossigeno  $10^{-8}$  % wt)

## Tesi e pubblicazioni



### **Alessandro Merli**

*“Caratterizzazione microstrutturale meccanica e tribologica di rivestimenti PLD in allumina su acciai inox per applicazioni nucleari”*

*Laurea in Ingegneria Meccanica*

### **Fabrizio Mario Ferrarese**

*“Caratterizzazione di film ceramici sottili per applicazioni nei reattori nucleari di quarta generazione”*

*Laurea in Scienza dei Materiali*

### **Emanuele Rossi**

*“Caratterizzazione di rivestimenti FeCrAlY HVOF per applicazioni nei reattori nucleari di quarta generazione”*

*Laurea in Ingegneria Meccanica*

### **Mario Bragaglia**

*“Caratterizzazione di materiali strutturali ricoperti per applicazioni nucleari”*

*Dottorato di Ricerca in Ingegneria Industriale*

### **Paper Corrosion Science 2017**

**Radiation tolerant nanoceramic coatings for lead fast reactor nuclear fuel cladding**

F. García Ferré, A. Mairov, M. Vanazzi, S. Bassini, M. Utili, M. Tarantino, M. Bragaglia, F.R. Lamastra, F. Nanni, L. Ceseracciu, Y. Serruys, P. Trocellier, L. Beck, K. Sridharan, M.G. Beghi and F. Di Fonzo

# WORKSHOP TEMATICO

ACCORDO DI PROGRAMMA MISE – ENEA  
PAR2017 – PROGETTO B.3 - LP2



## GENERATION IV LEAD COOLED FAST REACTOR STATO ATTUALE DELLA TECNOLOGIA E PROSPETTIVE DI SVILUPPO

ADP MiSE-ENEA (PAR2017-LP2)

Dipartimento di Ingegneria Astronautica, Elettrica ed Energetica Università di Roma "La Sapienza"  
San Pietro in Vincoli, Via Eudossiana 18  
14-15 Giugno 2018

### Coating mechanical characterization

M. Bragaglia, F.R. Lamastra, F. Franceschetti; F. Nanni



**CONTATTI:**

Dipartimento di Ingegneria Impresa  
Università di Roma "Tor Vergata"  
Via del Politecnico, 1, 00133 Roma -Italia  
Tel +39-06.7259.4496 - Fax +39-  
06.7259.4328



Italian National Agency for New Technologies,  
Energy and Sustainable Economic Development

# Coolant chemistry control study for HLM systems

ADP MiSE-ENEA (PAR2017-LP2)

Dipartimento di Ingegneria Astronautica, Elettrica ed Energetica  
Università di Roma "La Sapienza"

14-15 Giugno 2018

S. Bassini, A. Antonelli, G. Fasano (ENEA FSN-ING-TESP)  
serena.bassini@enea.it



# CHEMISTRY OF HLM (LEAD AND LBE)



Slag deposit in the circuit during circulation pump tests

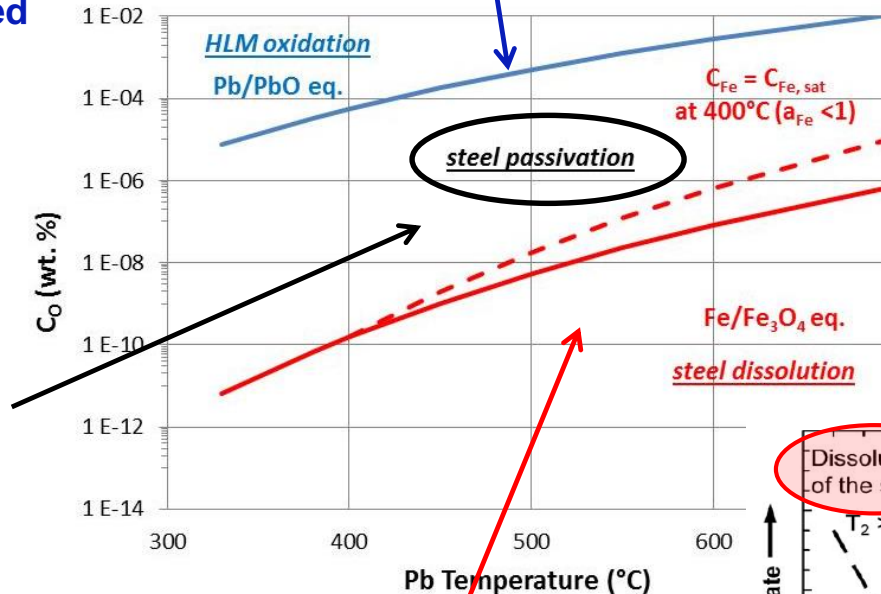
Slag deposit in heat exchanger



**Oxygen saturation and PbO deposition**

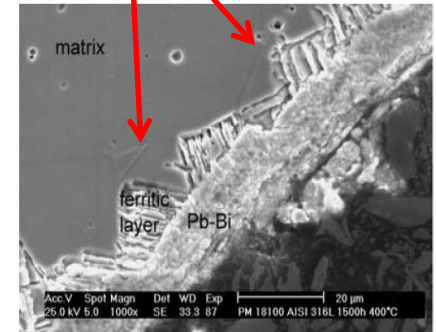
plugging in Pb-Bi cooled K-27 Russian Nuclear Submarine in 1960'

oxygen balancing for steel passivation and to avoid PbO formation: need of oxygen sensors and oxygen control devices



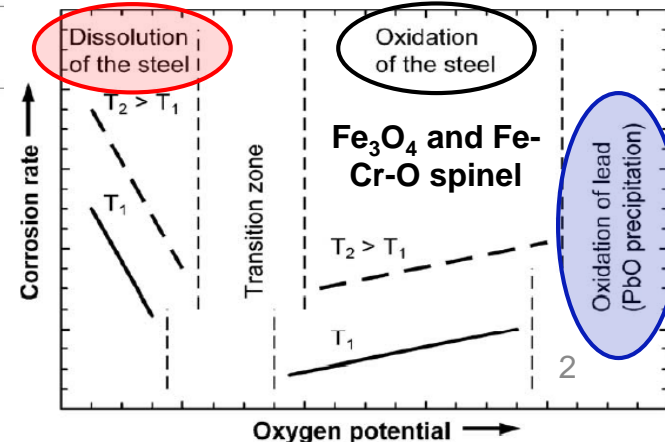
**Steel corrosion at low oxygen content**

Ni and Cr dissolution in 316L steel. Flowing LBE, 400°C, low C<sub>O</sub>, 1500 h.



Benamati et al., J Nucl Mater 335 (2004) 169-173.

C. Schroer, Nucl Eng Des, 241 (2011) 4913-4923.



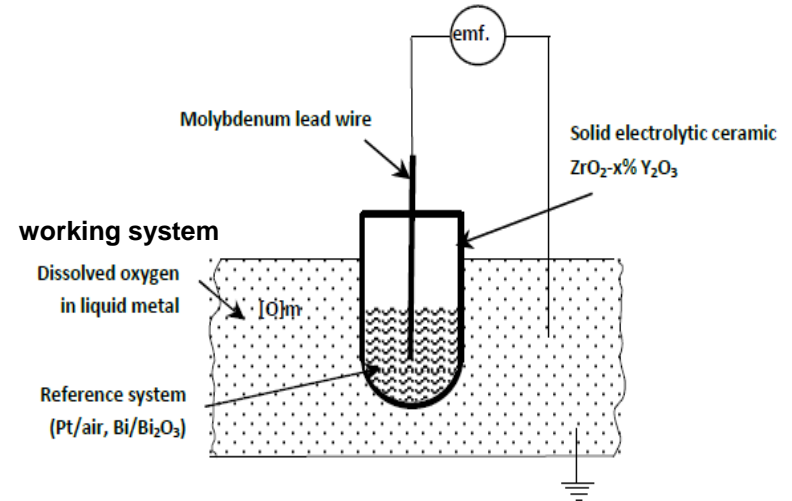
# POTENTIOMETRIC OXYGEN SENSORS FOR HLM (lab scale)

## potentiometric sensor

$$E_{th} = \frac{RT}{4F} \cdot \ln \frac{p_{O_2(ref)}}{p_{O_2(Pb,LBE)}}$$

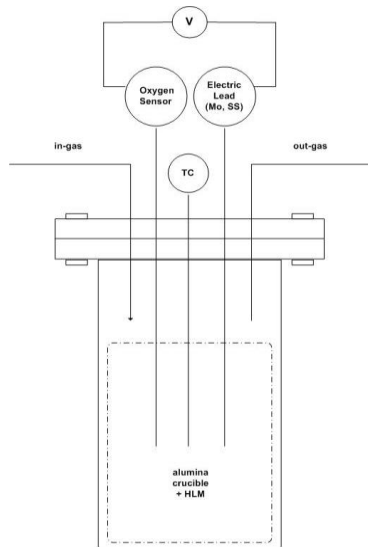
well-known (reference system)  
to be evaluated (working system)

+ ceramic solid electrolyte for O<sup>2-</sup> conduction (Yttria Stabilized Zirconia)



**Reference systems:**  
 Pt-air, Bi/Bi<sub>2</sub>O<sub>3</sub>, Cu/Cu<sub>2</sub>O  
**Solid electrolytes:**  
 YPSZ and YTSZ

set-up for oxygen sensor testing



V = high-impedance voltmeter  
In-gas = flowing argon

### Calibration at oxygen saturation

Comparison of the experimental potential ( $E_{exp}$ ) with the theoretical potential ( $E_{th}$ ) expected in oxygen-saturated HLM at different  $T_{HLM}$ .

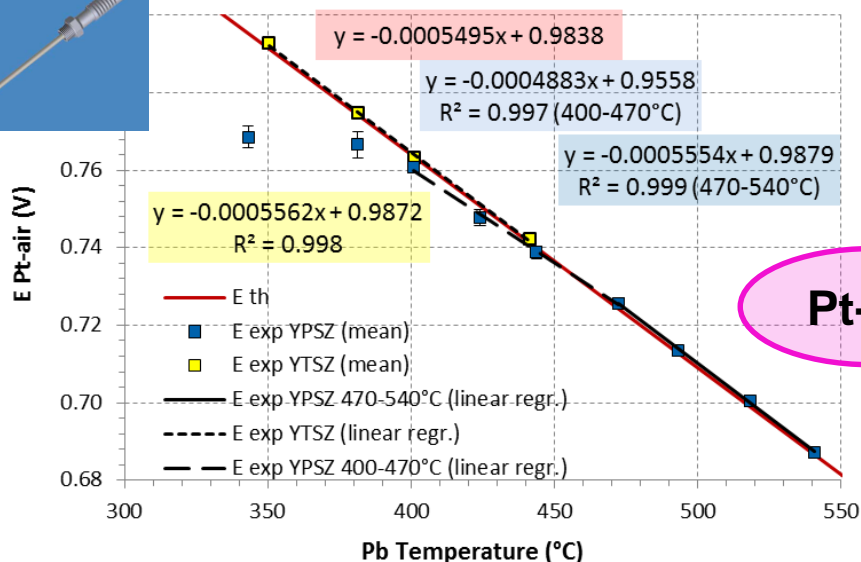
# STUDY OF REFERENCE SYSTEM: AIR + STUDY OF SOLID ELECTROLYTE: YTSZ & YPSZ

RACHEL Lab

REACTIONS AND ADVANCED CHEMISTRY FOR LEAD



## Influence of the reference and solid electrolyte on the min. reading temperature



**Pt-air + YPSZ** sensor reading  
down to 400°C

**Pt-air + YTSZ** sensor reading  
down to 350°C

YPSZ = Yttria Partially Stabilized Zirconia

5 % mol of yttria

YTSZ = Yttria Totally Stabilized Zirconia

8 % mol of yttria

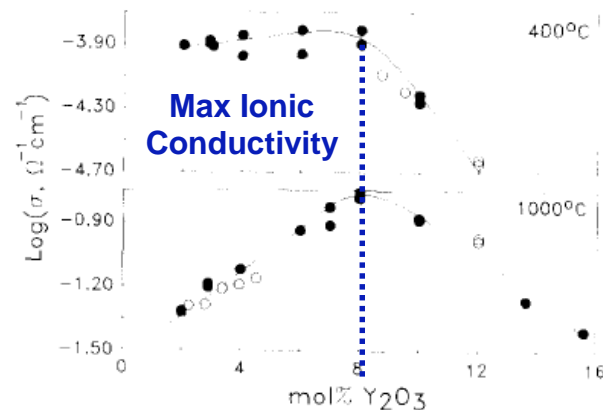


Fig. 2. Conductivity variation as a function of dopant content in Y<sub>2</sub>O<sub>3</sub>-ZrO<sub>2</sub>. (○) single grain, (●) polycrystalline specimens.

ionic conductivity: YTSZ > YPSZ  
but mechanical strength: YTSZ < YPSZ

S.P.S. Badwal, Solid State Ionics 52 (1992) 23-32.



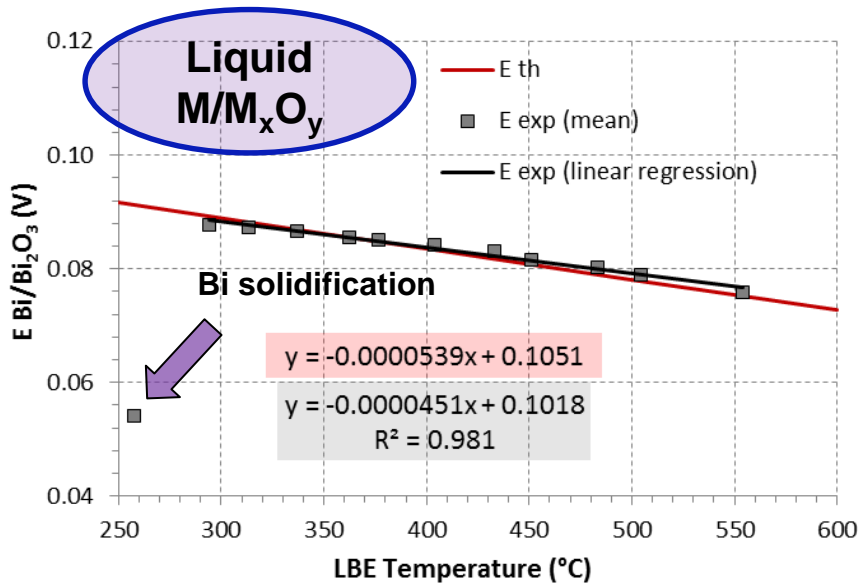


# STUDY OF REFERENCE SYSTEMS: $M/M_xO_y$

## Influence of the reference on the min. reading temperature

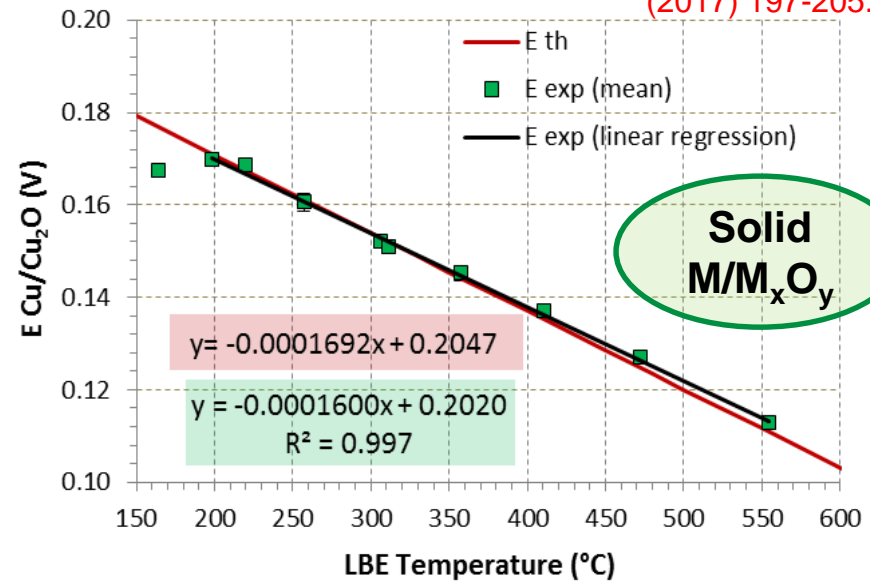


S. Bassini et al., J. Nucl. Mater. 486 (2017) 197-205.



**Bi/Bi<sub>2</sub>O<sub>3</sub>**

Min. reading  $T \approx 290^\circ\text{C}$ ;  
tendency to crack due to Bi  
volume variation ( $T_{m,Bi} = 271^\circ\text{C}$ )

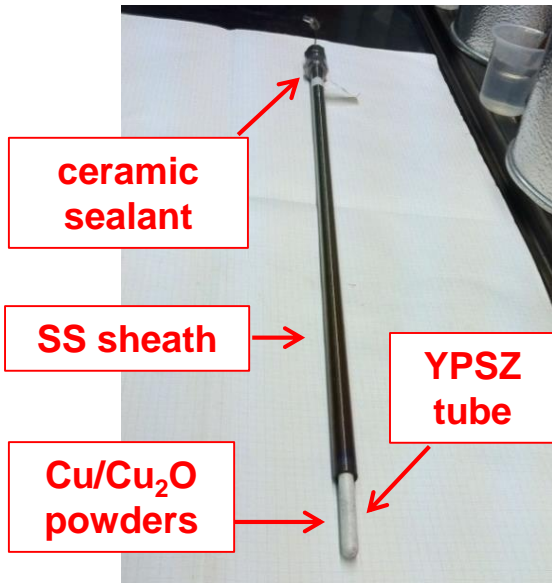


**Cu/Cu<sub>2</sub>O**

Min. reading  $T \approx 200^\circ\text{C}$ ;  
tendency to powders sintering in the  
long-term ( $T_{m,Cu} = 1085^\circ\text{C}$ )

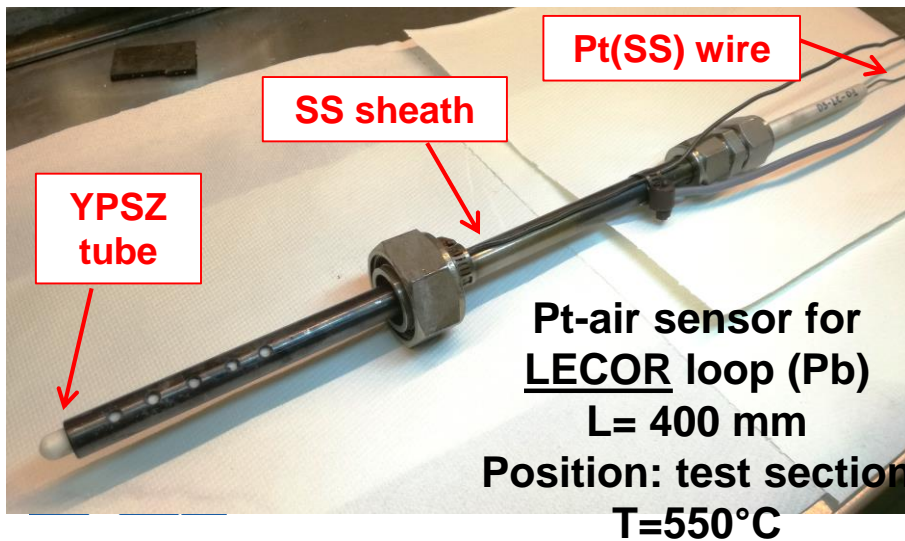
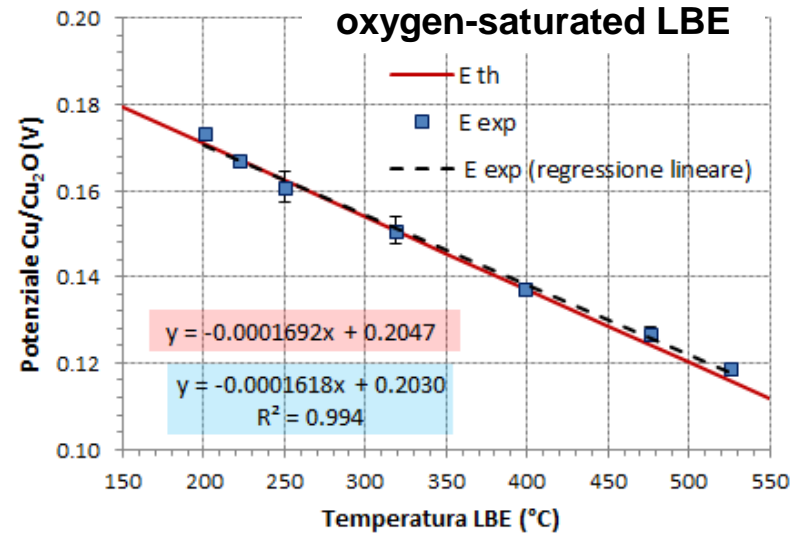


# OXYGEN SENSOR FOR LOOPS

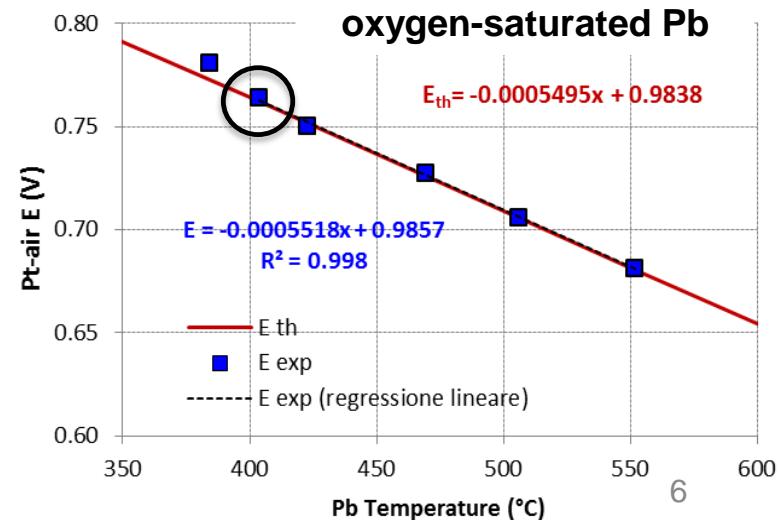


**Cu/Cu<sub>2</sub>O sensor for  
NACIE-UP loop (LBE)**  
L= 600 mm  
Position: expansion  
vessel,  
T=200-400°C

Min. reading T ≈ 200°C  
(but powder sintering)

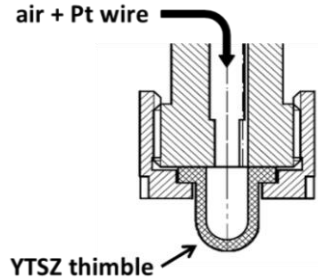


**Pt-air sensor for  
LECOR loop (Pb)**  
L= 400 mm  
Position: test section  
T=550°C



Min. reading T ≈ 400°C

# OXYGEN SENSOR FOR LARGE HLM POOL - Type 1



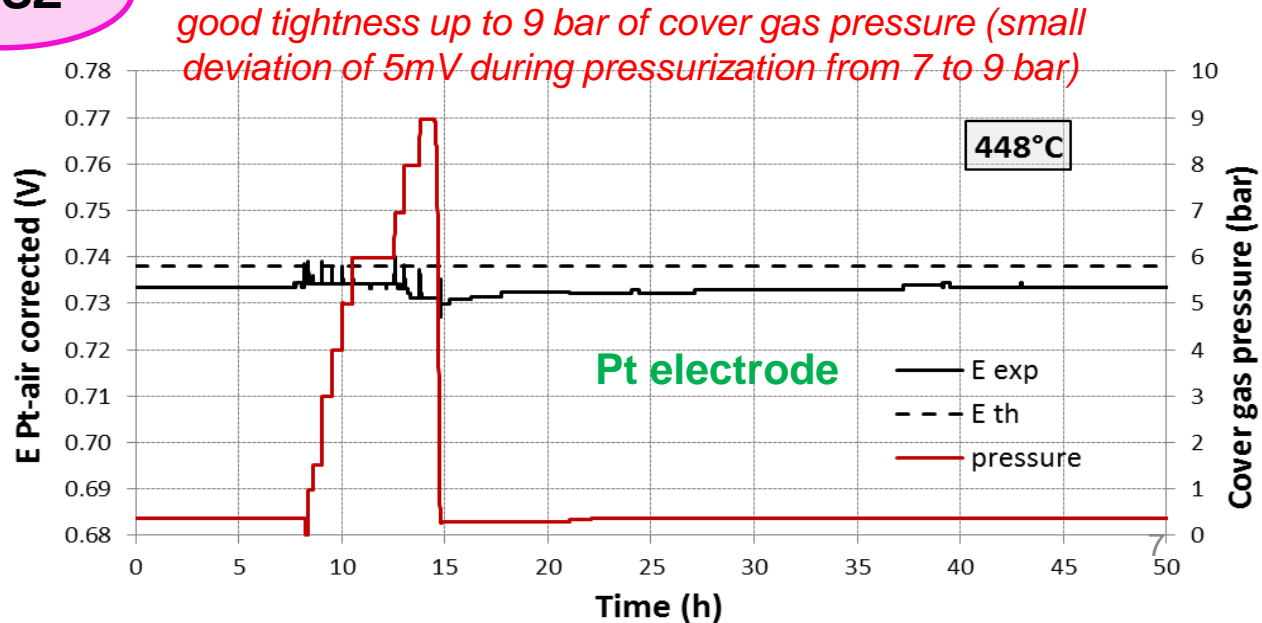
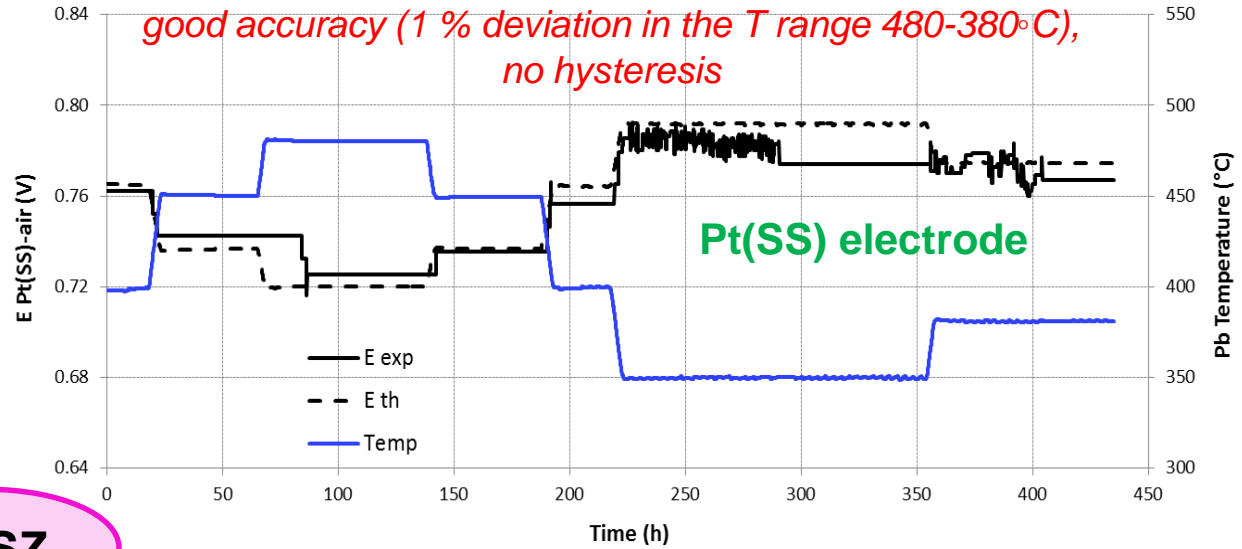
Tot lenght = 1100 mm



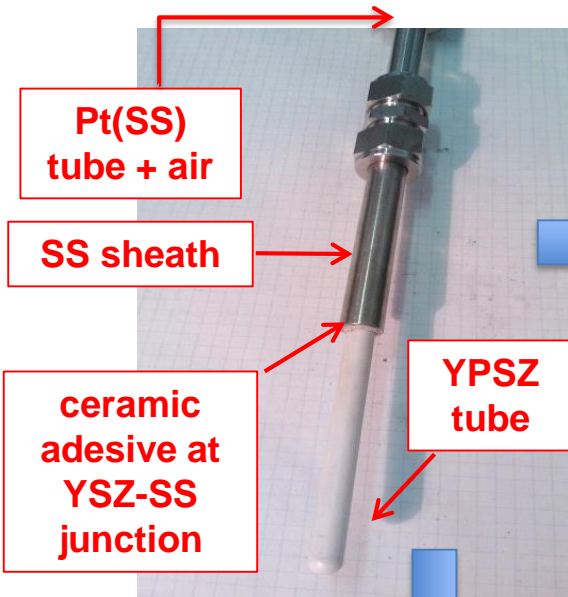
Calibration & Test at High Pressure in Pb storage tank

*Min. reading  $T \approx 380^\circ\text{C}$ , OK for Pb systems. Need of another reference for LBE systems.*

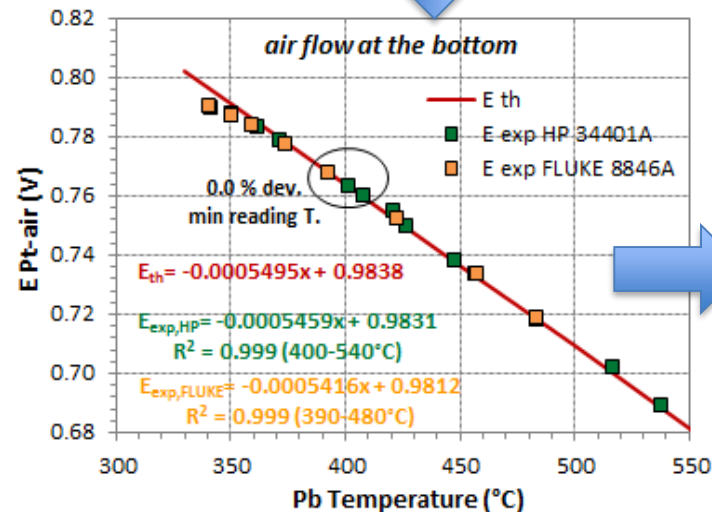
**YTSZ**



# OXYGEN SENSOR FOR LARGE HLM POOL - Type 2



*sensors manufactured for CIRCE (2000 and 4000 mm): too high electric resistance at 390-400°C*



**For small sensor:**  
Min. reading  $T \approx 400^\circ\text{C}$

**For long sensor:**  
Min. reading  $T \gg 400^\circ\text{C}$   
(other technological issues)

**CIRCE facility**  
Main vessel:  $d = 1.2 \text{ m}$ ;  
 $L = 8.5 \text{ m}$ ;  
70-90 ton of LBE,  
 $T_{pool} \approx 400^\circ\text{C}$  (new configuration)

# OXYGEN SENSORS: TESTS ONGOING AND PLANNED

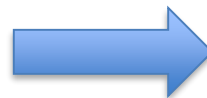
RACHEL Lab

REACTIONS AND ADVANCED CHEMISTRY FOR LEAD



Study of sensitive element of pool type-1 sensor in lab capsules with different:

- zirconia electrolytes (YTSZ, YPSZ);
- improved air-based reference.



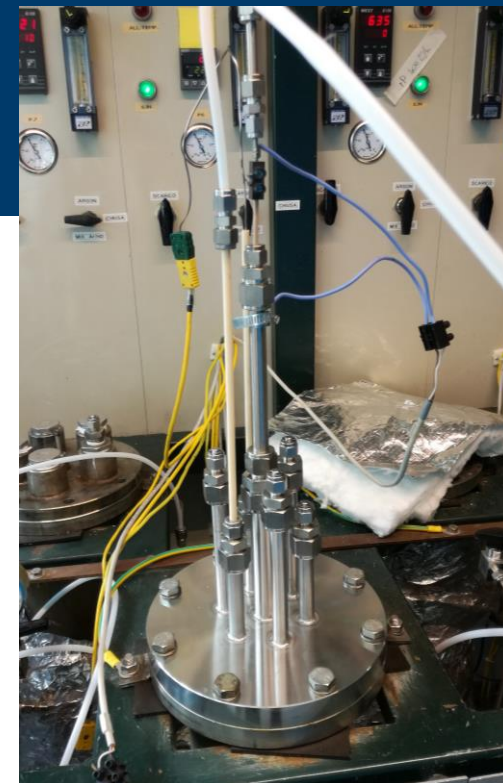
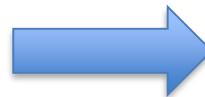
YTSZ



YPSZ

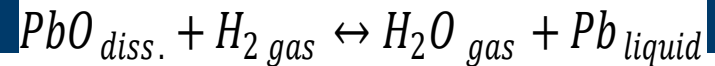
Baseline study of other reference systems with better performance (new device):

- Cu/Cu<sub>2</sub>O mod. (to prevent sintering);
- improved air references (perovskite-air system)



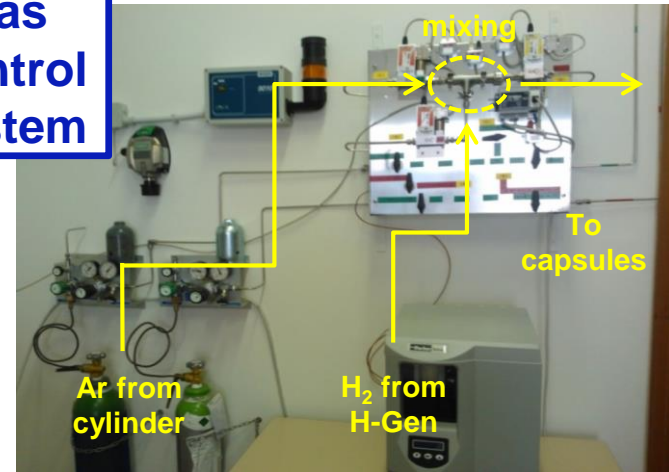
*Capsula Prova Sensori*

# DEOXYGENATION WITH H<sub>2</sub>: STATIC HLM, LAB SCALE

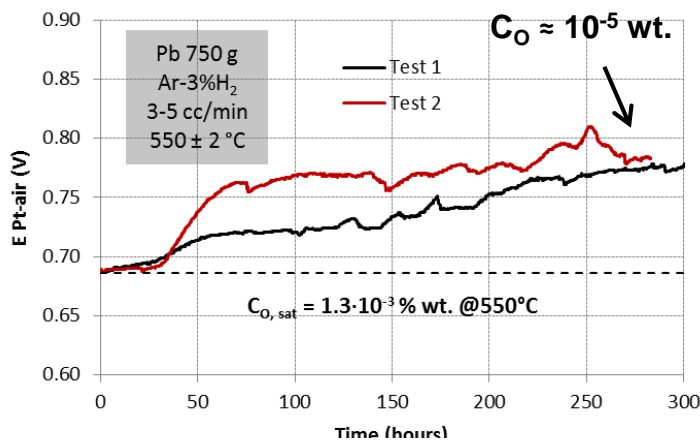


Target C<sub>O</sub> = 10<sup>-7</sup> - 10<sup>-8</sup> % wt.

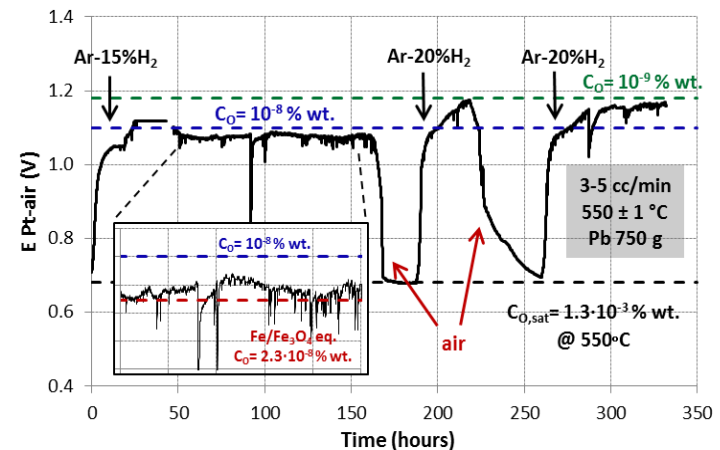
Gas Control System



capsules for HLM chemistry & corrosion tests (750 g liquid Pb)



EMF ↑, C<sub>O</sub> ↓



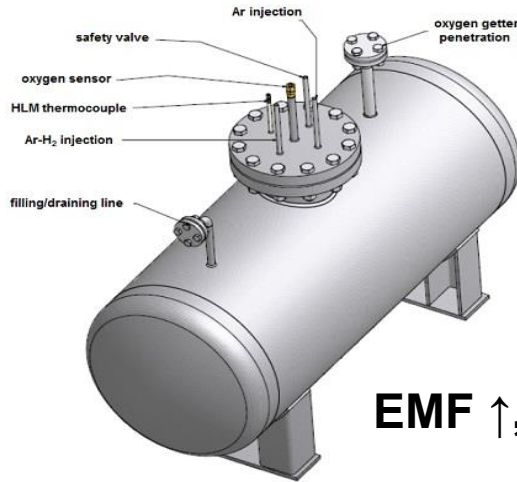
commercial Ar-3%H<sub>2</sub> gas (bubbling) → no efficient Pb deoxygenation in reasonable times → need of a dedicated gas control system

easy and fast Pb deoxygenation using Ar-H<sub>2</sub> gas with H<sub>2</sub> ≥ 10 % vol.

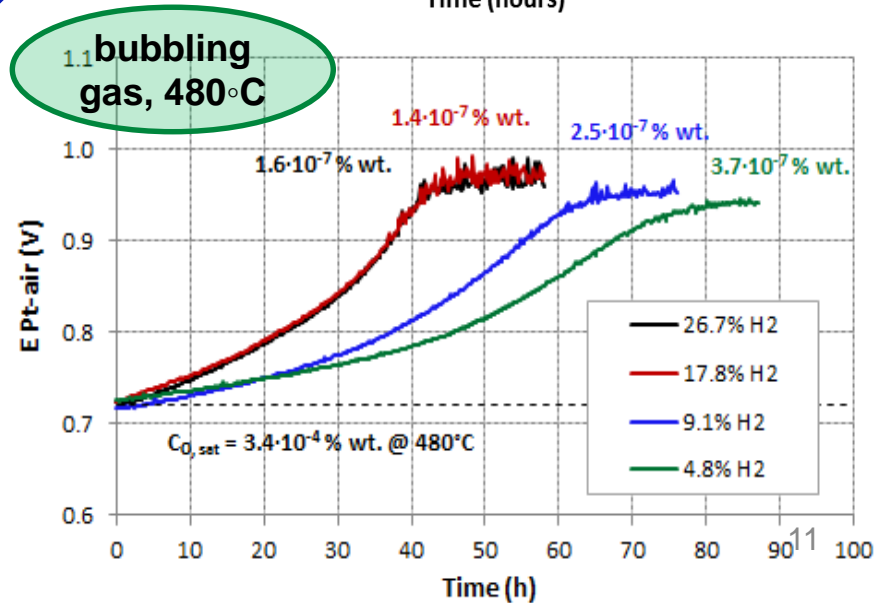
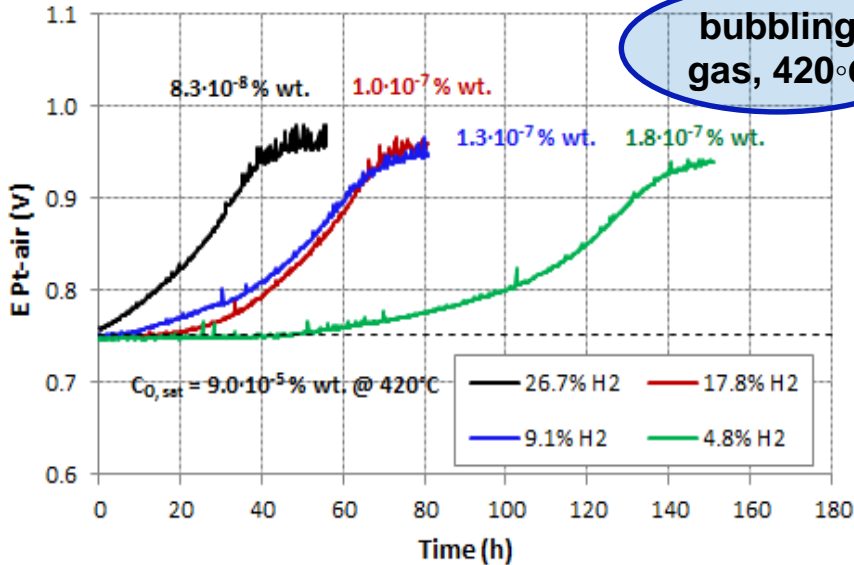
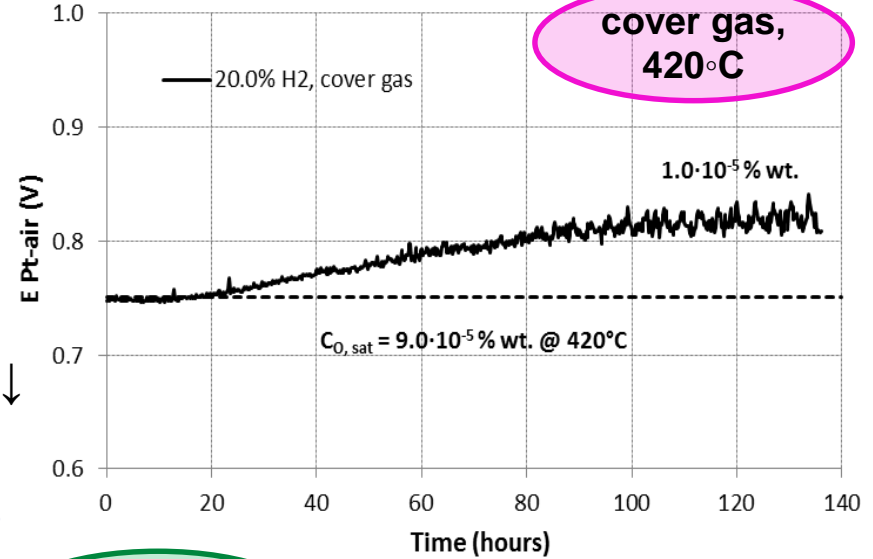
# DEOXYGENATION WITH H<sub>2</sub>: STORAGE TANK



≈ 285 L of liquid Pb,  
gas control system  
implemented

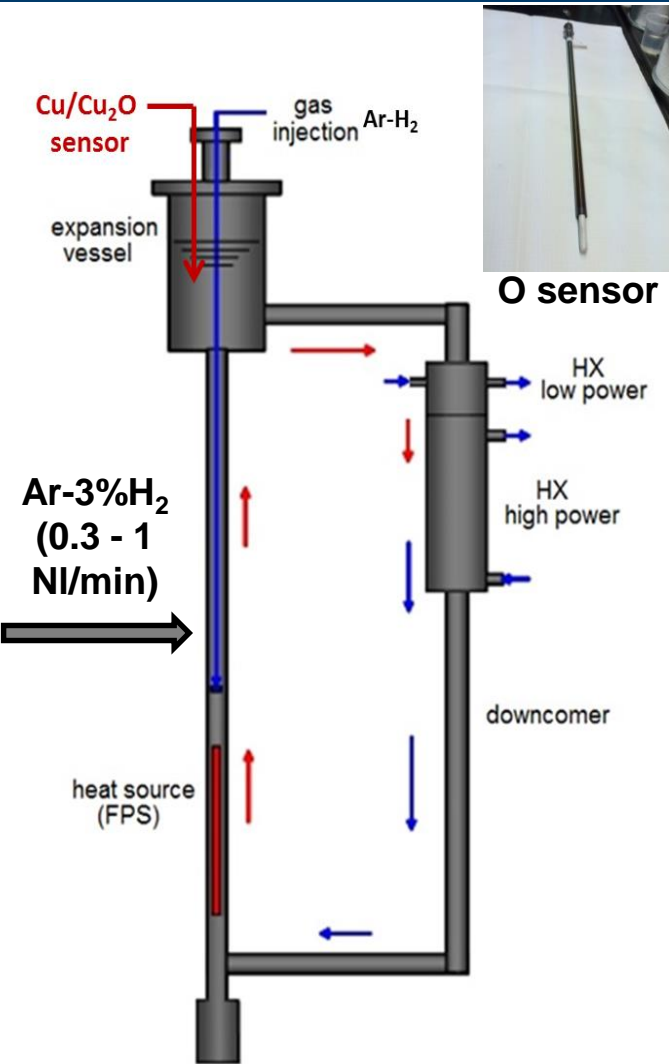


EMF ↑, C<sub>O</sub> ↓



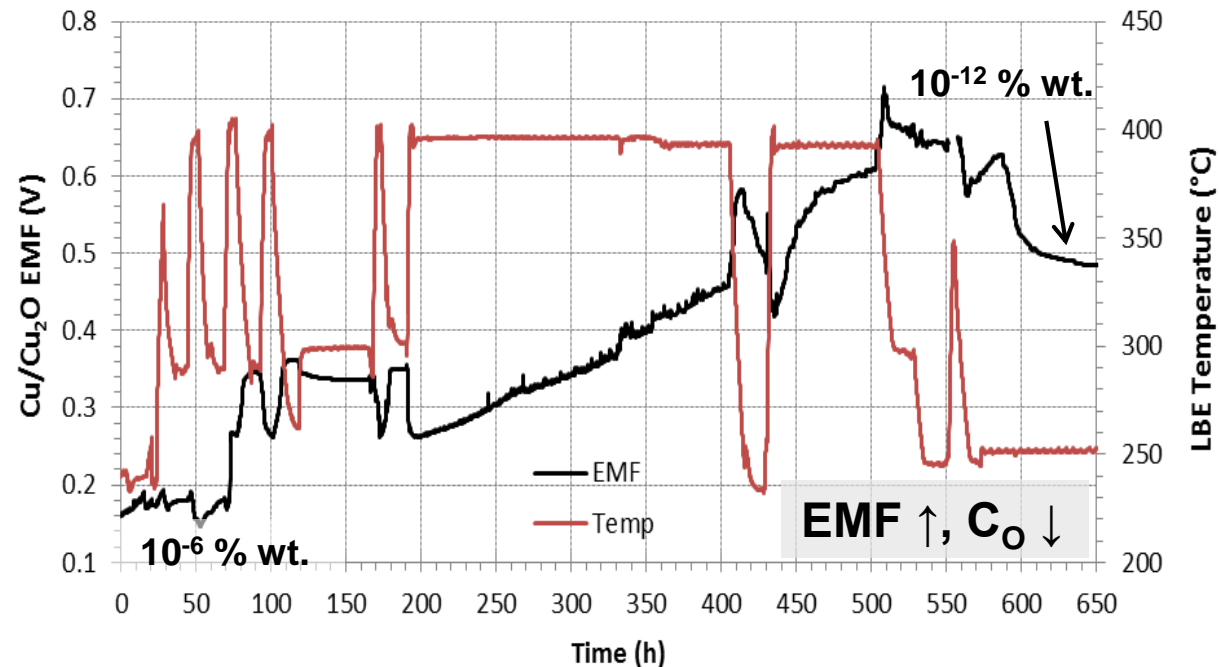
higher deoxygenation efficiency for higher T<sub>HLM</sub>,  
H<sub>2</sub> %, and HLM mixing (i.e. bubbling)

# DEOXYGENATION WITH H<sub>2</sub>: LOOP FACILITY



- 1) Gas washing of the circuit at high T to remove O<sub>2</sub> and H<sub>2</sub>O inside the loop;
- 2) Deoxygenation of HLM with Ar-H<sub>2</sub> to reach low C<sub>O</sub>.

S. Bassini et al., Prog. Nucl. Energ. 105 (2018) 137-145.



NACIE-UP loop  
200L of LBE, 200-400°C

high deoxygenation efficiency even with Ar-3%H<sub>2</sub> thanks to the forced HLM circulation → too low C<sub>O</sub> reached → need for oxygen supply (e.g. Ar-O<sub>2</sub> injection) and/or reduced deoxygenation efficiency



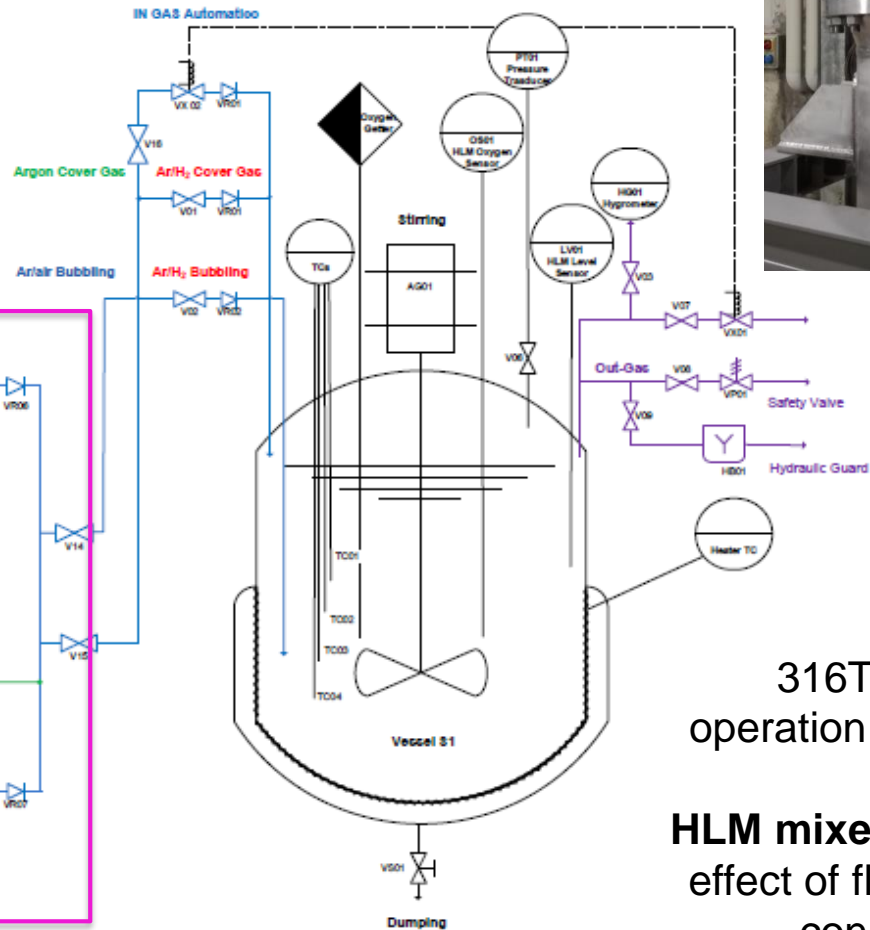
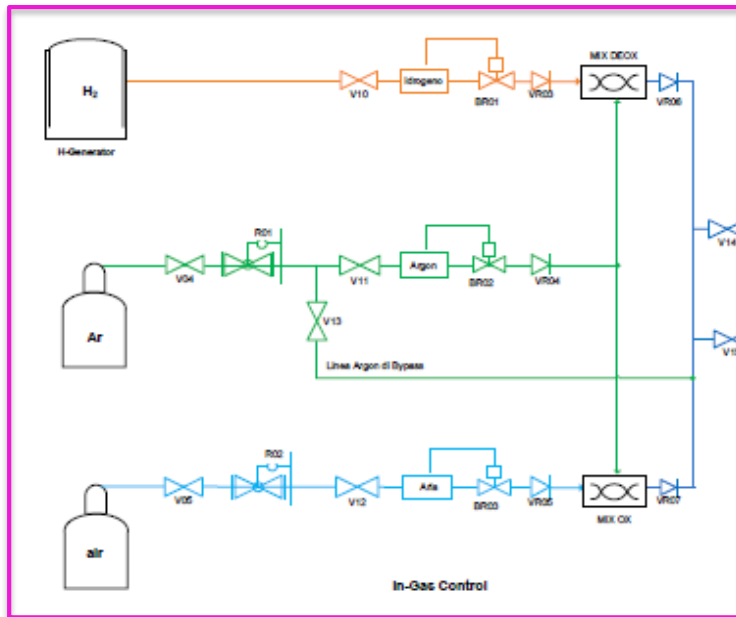
# BID1 SMALL POOL (Pb)

## BID1 “Brasimone gas Injection Device 1”

Small pool (Pb  $\approx$ 150 L) to test oxygen control methods:

- H<sub>2</sub> and O<sub>2</sub>(air) injection
- oxygen getters (Ti, Ta, Zr)
- oxygen sensors performance

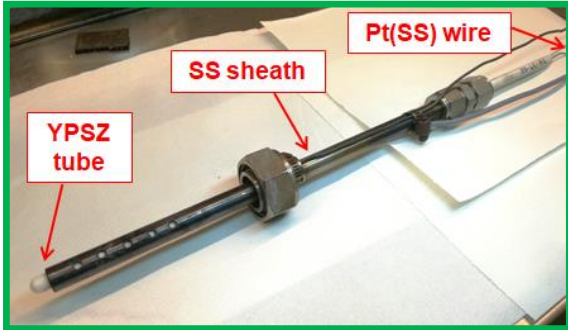
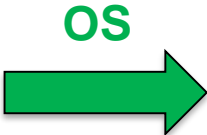
OCS with Ar-H<sub>2</sub> + Ar-O<sub>2</sub>  
also for LECOR Pb loop



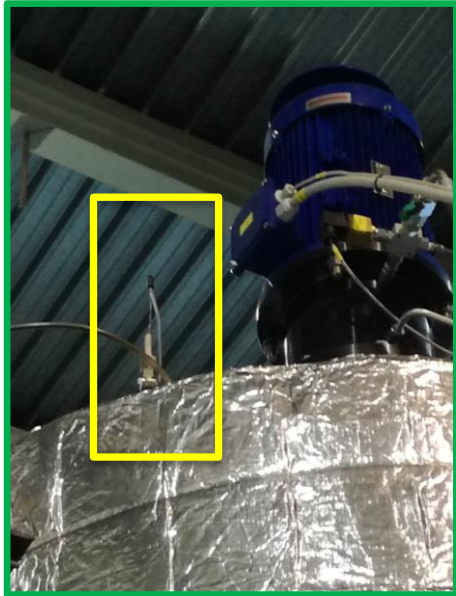
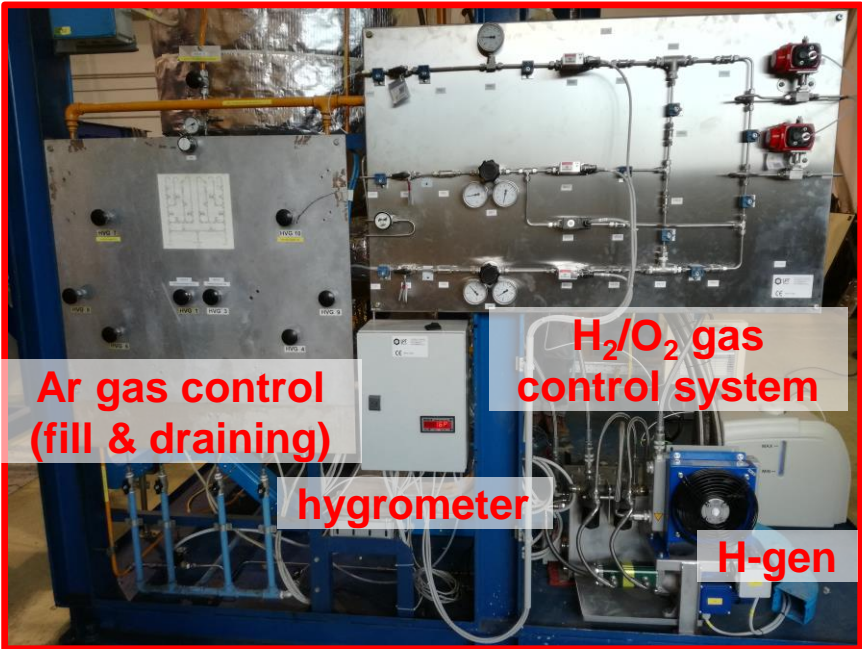
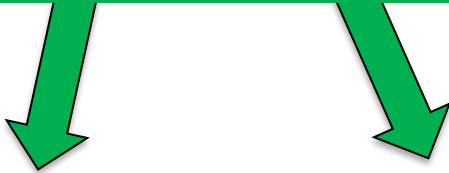
316Ti for the  
operation up to 550°C

**HLM mixer** to study the  
effect of fluid-dynamic  
conditions

# OCS IMPLEMENTATION FOR LECOR LOOP



OCS (storage tank+exp.vessel)



After exp. vessel 430°C



Test section 550°C

# SUMMARY

- Baseline study on different oxygen sensors: the min. reading  $T$  of the sensor is influenced by the reference system (mainly), new reference electrodes will be tested.
- Oxygen sensor prototypes for large HLM pool were developed and tested. Current Pt-air configurations have a min. reading  $T \geq 400^\circ\text{C}$ , different reference should be developed and used to have better detection capability.
- HLM deoxygenation with Ar- $\text{H}_2$  gas was performed in small capsules (lab), storage tank and loop facility exploiting a dedicated gas control system.
- A gas control system based on Ar- $\text{H}_2$  and Ar- $\text{O}_2$  injection is available for BID1 pool and LECOR loop for oxygen control study.

THANK YOU FOR THE ATTENTION

THANK YOU FOR THE ATTENTION

RACHEL Lab

REACTIONS AND ADVANCED CHEMISTRY FOR LEAD





Italian National Agency for New Technologies,  
Energy and Sustainable Economic Development

# *Double stabilized stainless steels Status and future developments*

WORKSHOP TEMATICO ACCORDO DI PROGRAMMA  
MISE – ENEA PAR2017

Università di Roma "La Sapienza" , 15 Giugno 2018

C. Cristalli, L. Pilloni, N. Bettocchi, L. Masotti (ENEA FSN-ING-QMN)



1101 0110 1100  
0101 0010 1101  
0001 0110 1110  
1101 0010 1101  
1111 1010 0000

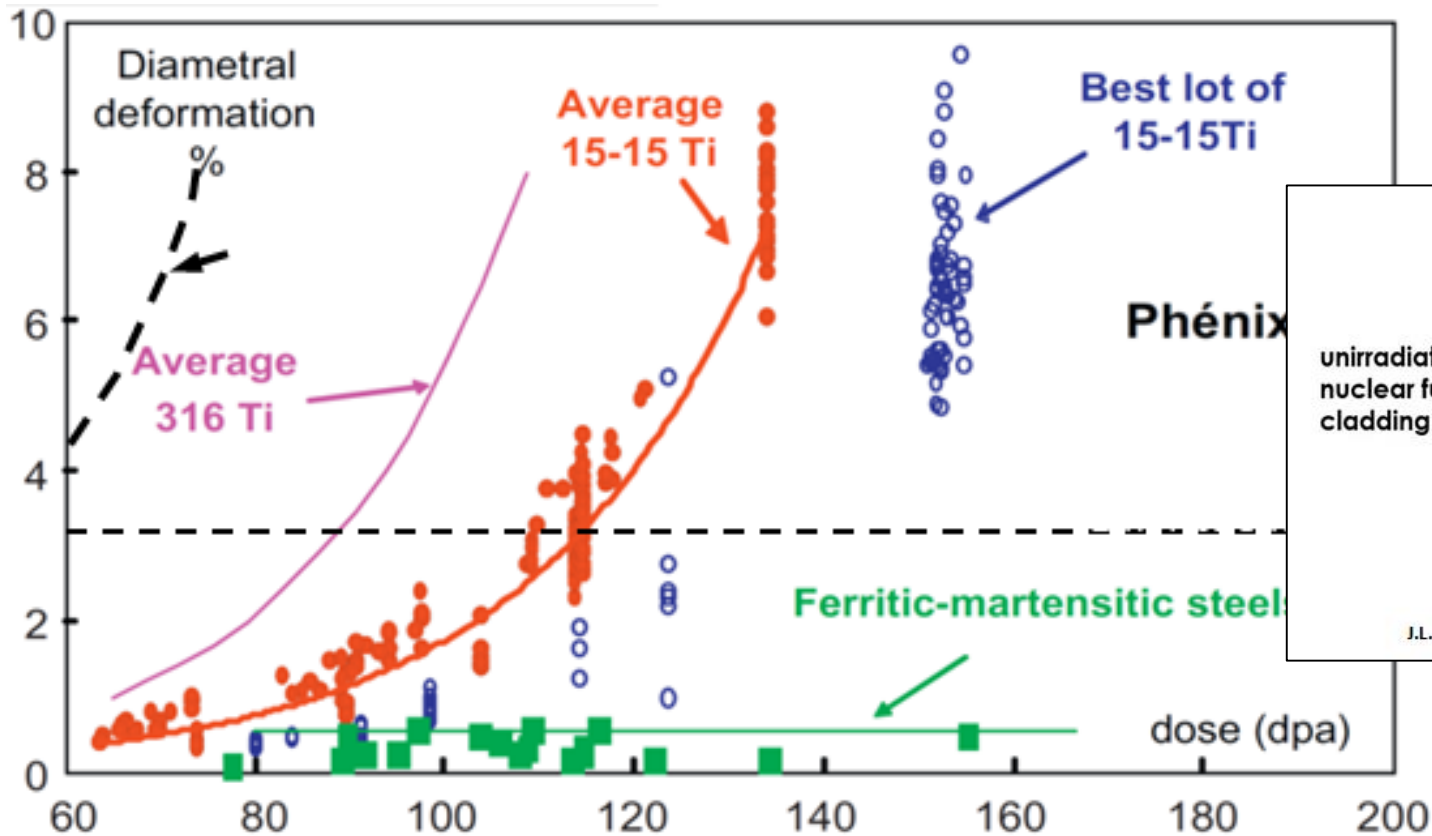


# Contents

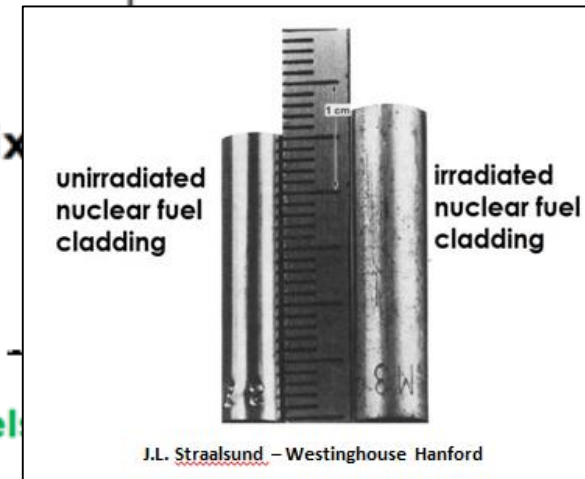
- Introduction about the challenge of swelling reduction and the development of the DS steels
- Neutron irradiation results (1988, Saclay)
- Production of a new DS4 plate(2014, ENEA-CSM)
- Status of the on going characterization of the new plate (ENEA-Brasimone)

# Introduction

## The challenge of swelling reduction; beyond 15-15 ?



[Séran et al.]



# Introduction

At the beginning of the '80s, within an experimental program carried out at the Saclay Center, the under electrons irradiations (1 MeV) have shown the effectiveness of the simultaneous presence of Ti and Nb on the swelling resistance of 316 and 15 Cr-15 Ni matrix.

Development of the **First Generation** of Double Stabilized Steels:

**316DS**

**15-15DS**

In the first generation double stabilized steels the annealing temperature used, 1125° C, didn't result sufficient to obtain a good solubilization of "free" Ti and Nb also because of the high stabilization ratio.



Revision of the composition



Birth of the **2nd Generation** Double Stabilized steels:

**DS3** (15Cr-15Ni)

**DS4** (15Cr-25Ni)

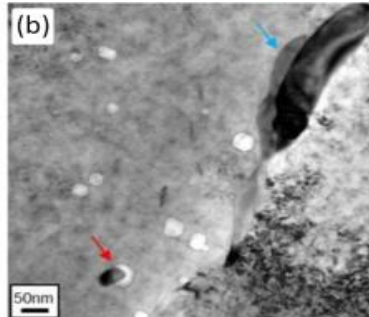
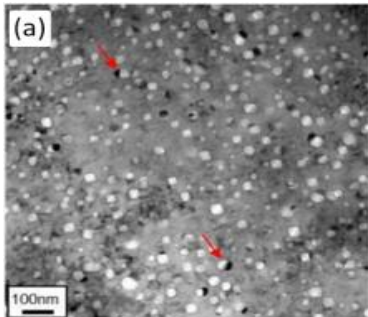
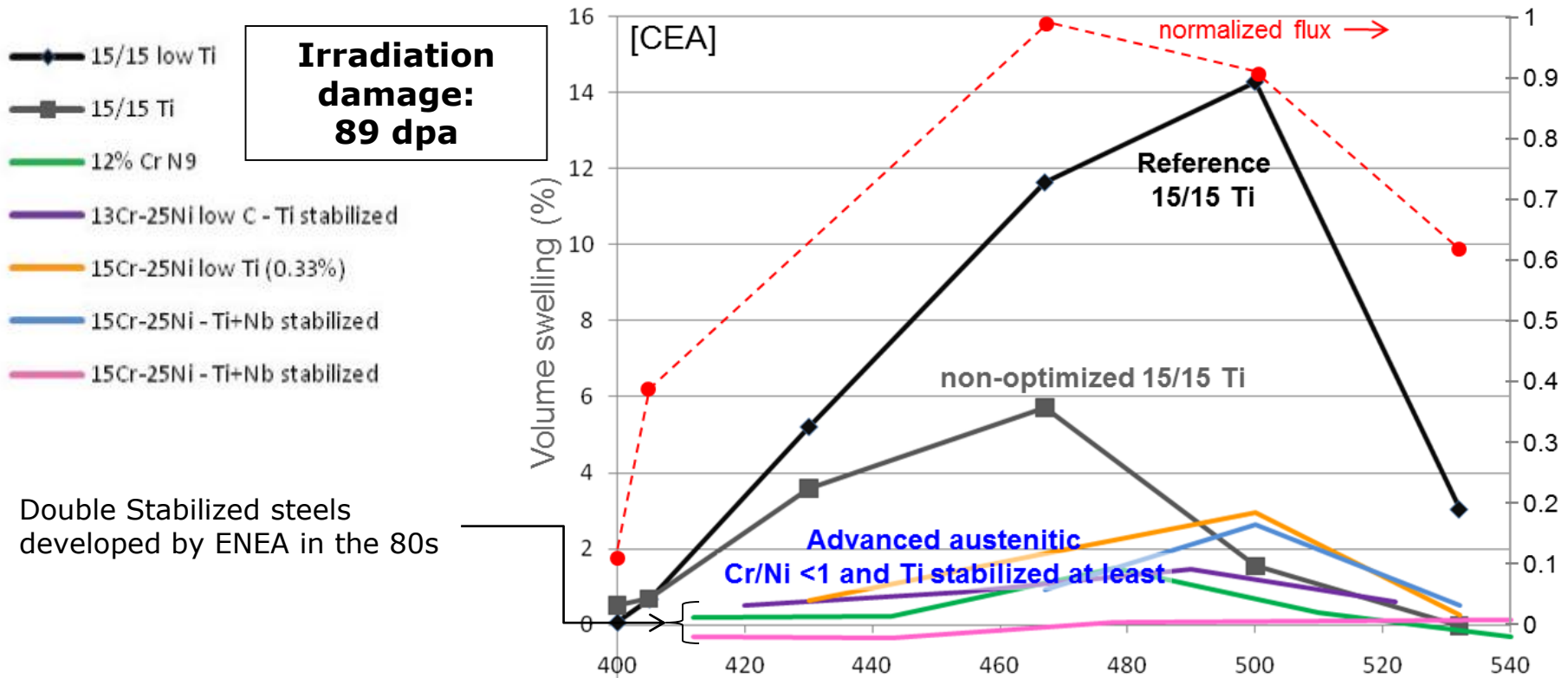
**DS5**(15Cr-25Ni)

Stabilization Ratio :

$$R = \frac{[Ti] + [Nb] - [N]}{[C]}$$

# Factors affecting swelling reduction

## Irradiation Tests at Saclay: the results of the experience « Supernova »



Low amount of cavities in the advanced austenitic stainless steel (b) if compared to the non-optimized 15-15 Ti (a)



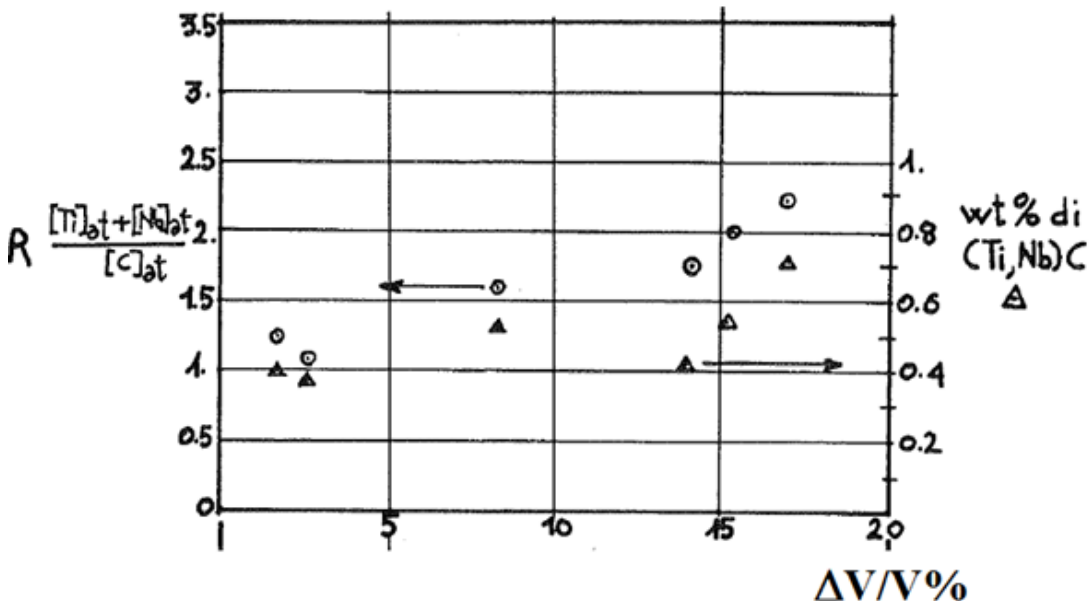


# Factors affecting swelling reduction

## Beneficial effect 3: Double Stabilization; how primary and secondary precipitation of carbides affect swelling

A good high temperature creep resistance for an austenitic steel is essentially due to microprecipitation of carbides which result finely dispersed on the dislocations network;

- Primary precipitation, the one occurring during the annealing heat treatment of the steel. Low primary precipitation means sufficient "free" contents of Carbon, Ti and Nb in solid solution in order to allow a secondary (in service) beneficial precipitation.
- Secondary, so-said "in-service" precipitation, occurring during operation inside the reactor. This sort of "in-service" precipitation is highly effective as movement inhibitor for linear defects..



The precipitation of carbides doesn't only act on the creep resistance of the material; it also has positive effects on the stability under irradiation. Here's a graphical investigation of the first 90's about the dependence of swelling attitude on the primary precipitation and on the stabilization ratio for a 15Cr-15Ni matrix. As long as the primary precipitation is kept low (keeping the stabilization ratio close to 1) the secondary (highly desirable) precipitation is fostered and the limited swelling attitude is a consequence.

# 15-15 Ti; Phase Diagram according to Thermocalc

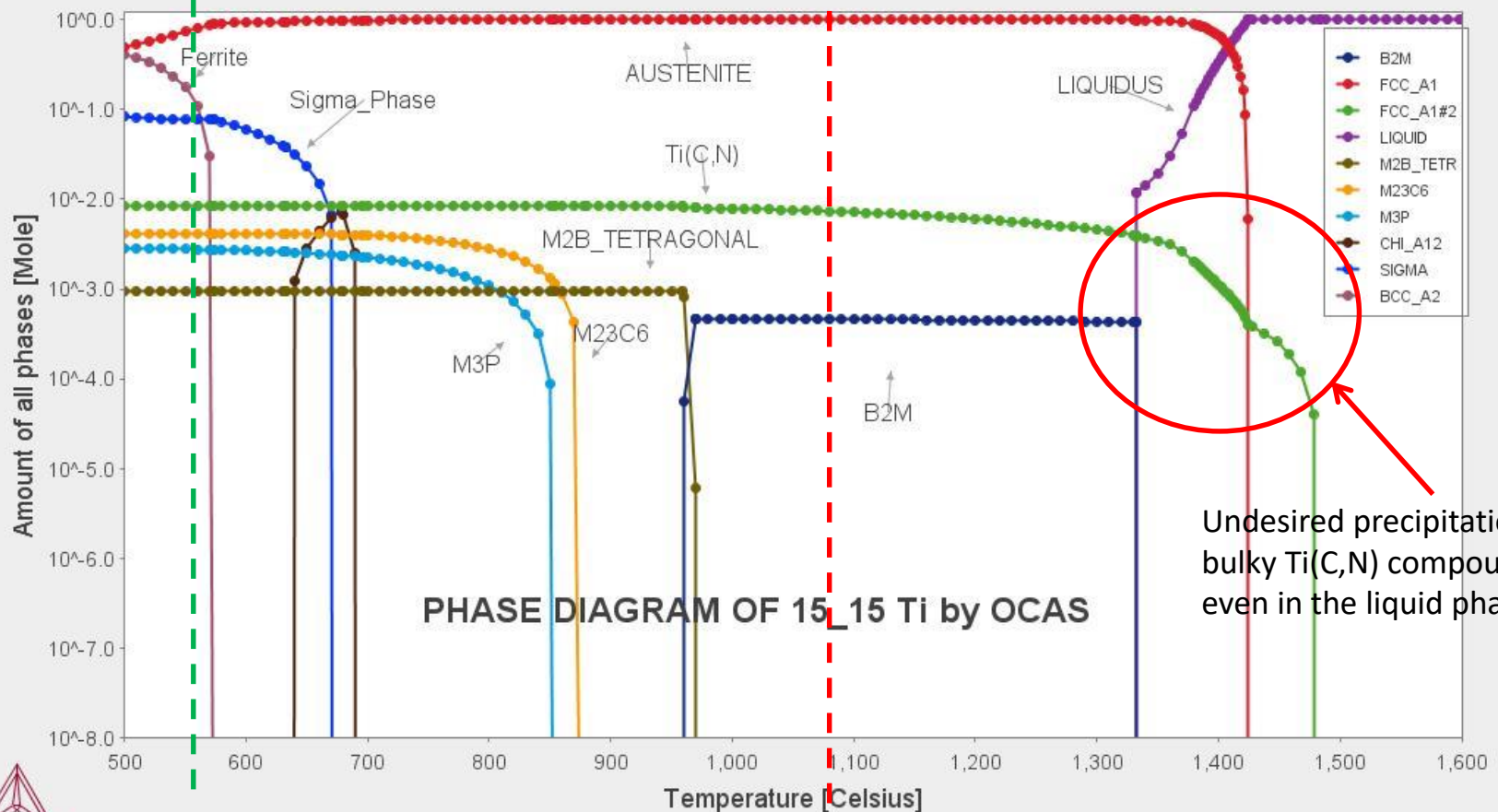
2016.10.31.18.15.25

TCFE7: Fe, Ti, Cr, Mn, Ni, Mo, B, C, N, Si, P

Pressure [Pascal] = 100000.0, System size [Mole] = 1.0, Mass percent Ti = 0.38, Mass percent Cr = 15.03, Mass percent Mn = 1.45, Mass percent Ni = 15.03, Mass percent Mo = 1.5, Mass percent B = 0.0061, Mass percent C = 0.097, Mass percent N = 0.01, Mass percent Si = 0.79, Mass percent P = 0.04

Exercise temperature (secondary precipitation)

Annealing temperature (primary precipitation)



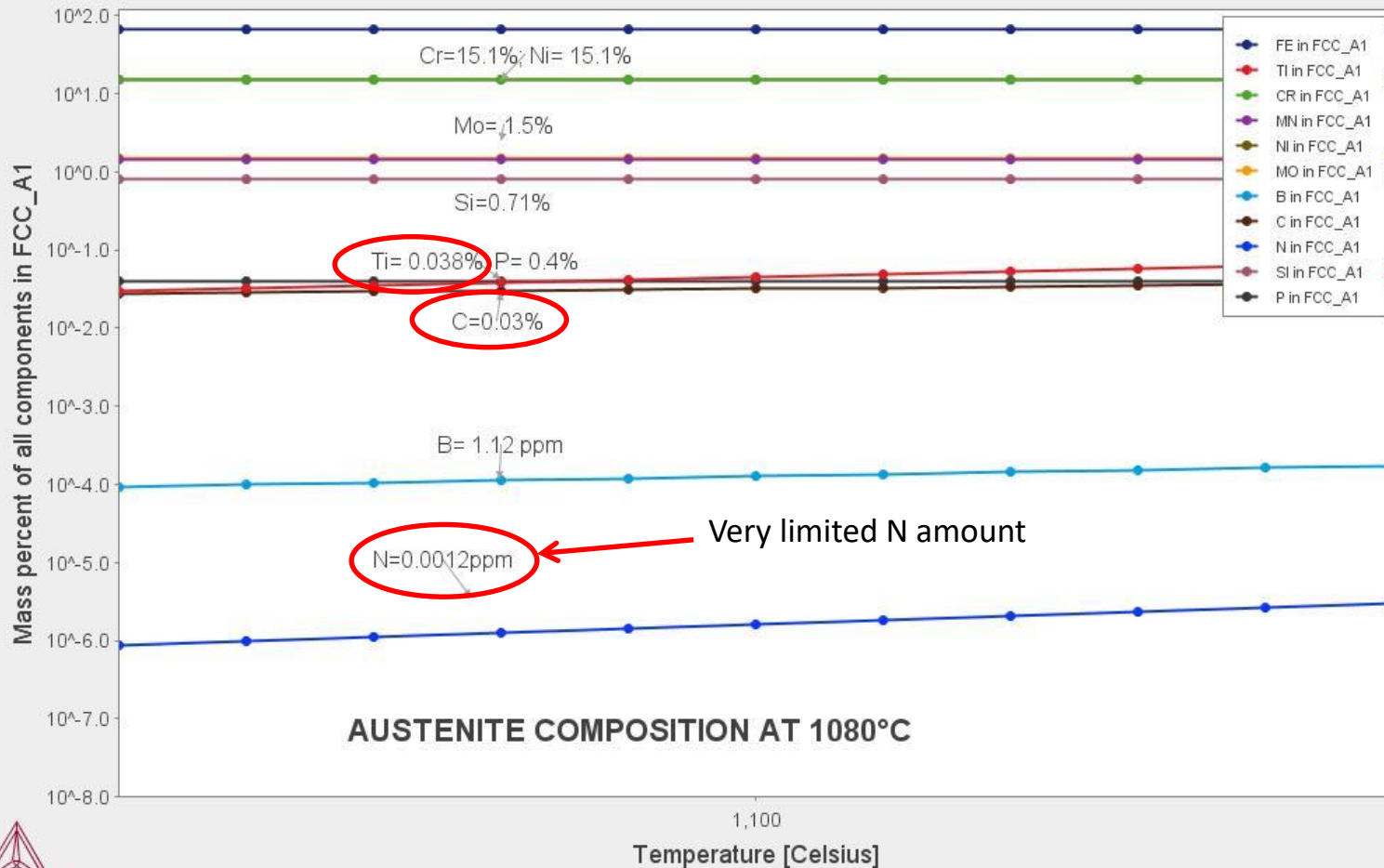
# 15-15 Ti; Phase Diagram according to Thermocalc

Available contents of carbo-nitride forming elements in the Austenite phase at the annealing temperature (1080 ° C)

2016.10.31.18.47.39

TCFE7: Fe, Ti, Cr, Mn, Ni, Mo, B, C, N, Si, P

Pressure [Pascal] = 100000.0, System size [Mole] = 1.0, Mass percent Ti = 0.38, Mass percent Cr = 15.03, Mass percent Mn = 1.45, Mass percent Ni = 15.03, Mass percent Mo = 1.5, Mass percent B = 0.0061, Mass percent C = 0.097, Mass percent N = 0.01, Mass percent Si = 0.79, Mass percent P = 0.04



# DS4; Phase Diagram according to Thermocalc

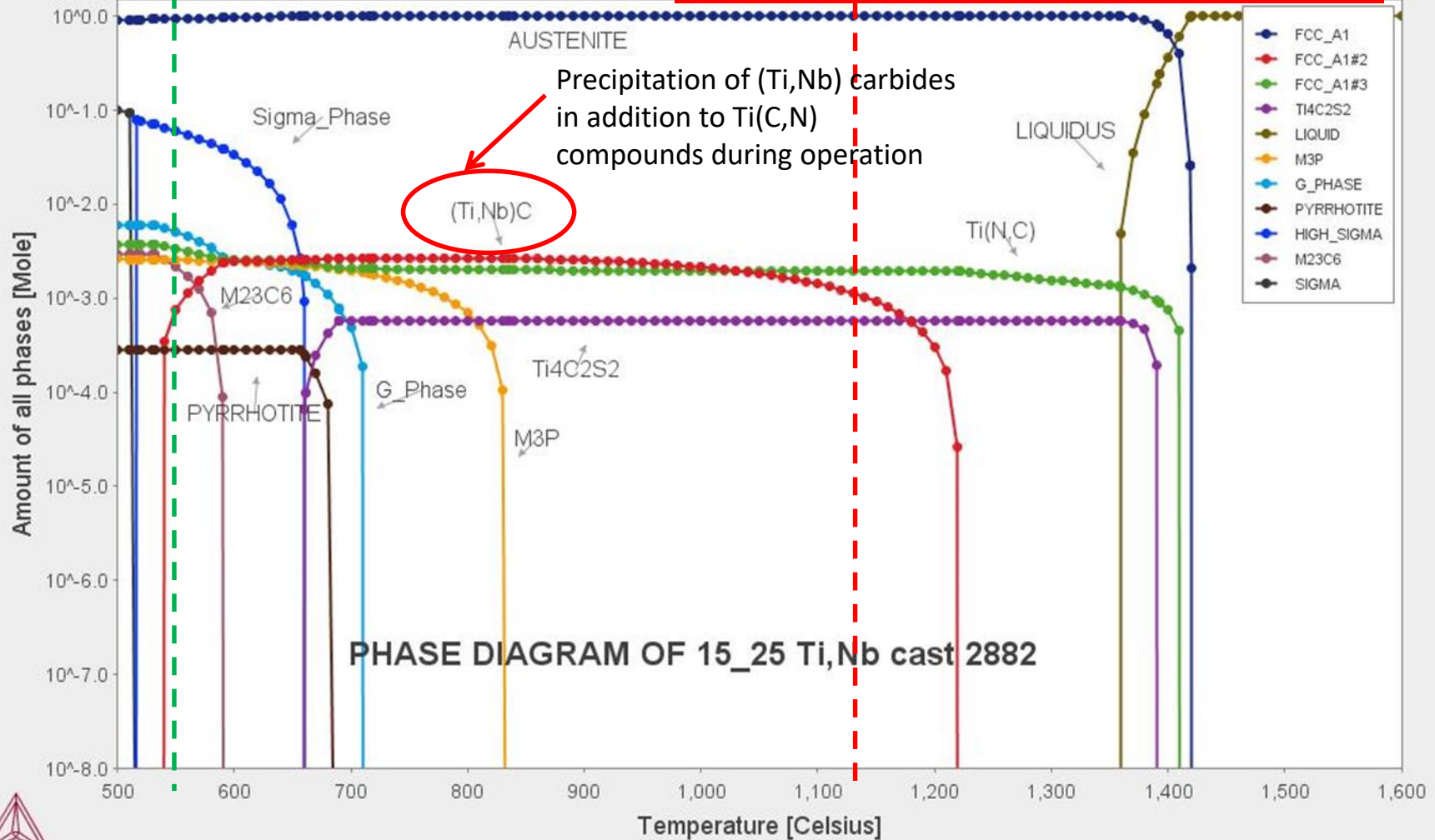
2016.10.31.22.29.39

TCFE7: Fe, Ti, Cr, Ni, Mo, C, N, Si, P, S, Al, Nb

Pressure [Pascal] = 100000.0, System size [Mole] = 1.0, Mass percent Ti = 0.17, Mass percent Cr = 14.8, Mass percent Ni = 24.6, Mass percent Mo = 1.46, Mass percent C = 0.041, Mass

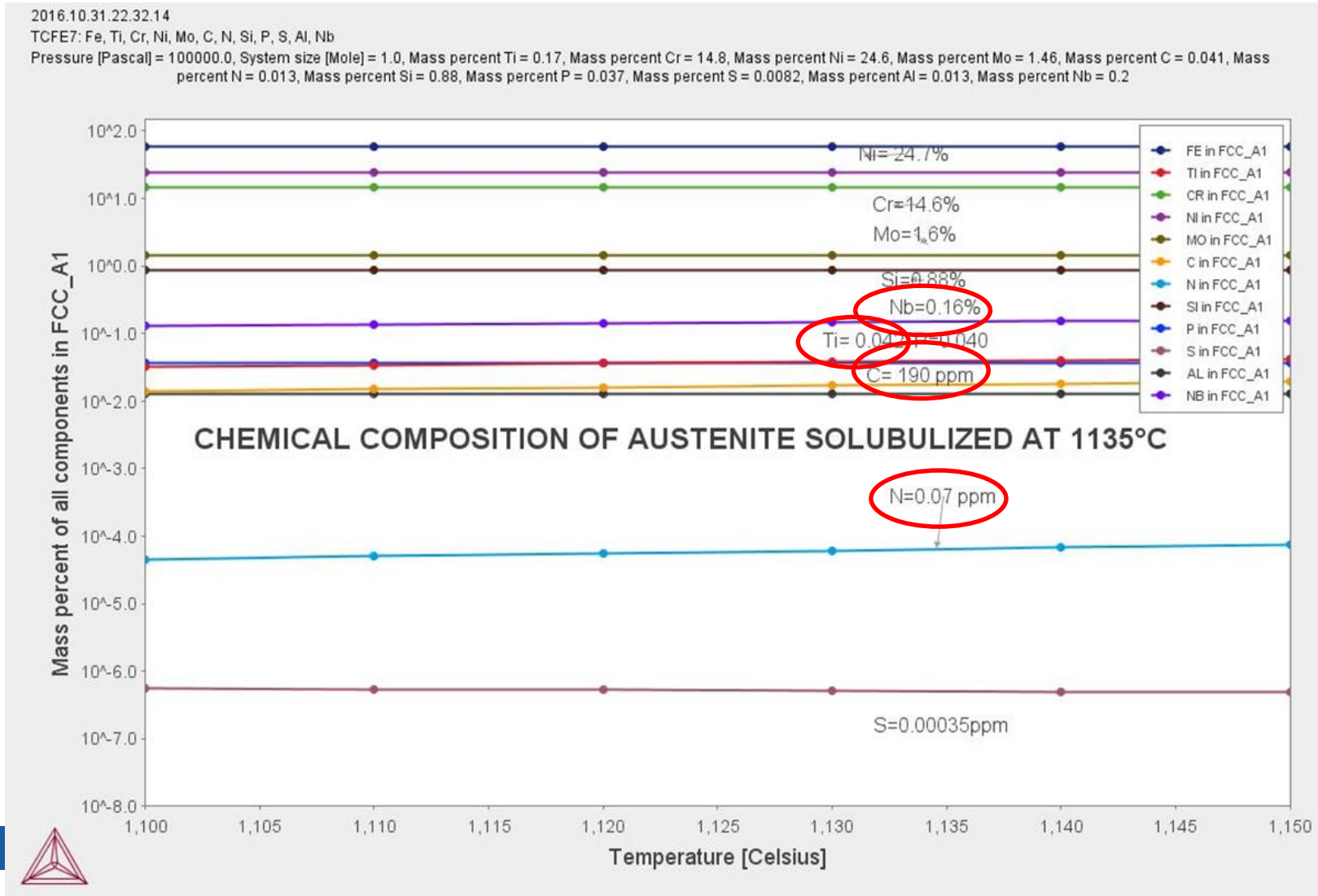
Exercise temperature (secondary precipitation)

Annealing temperature (primary precipitation)



# DS4; Phase Diagram according to Thermocalc

**Increased available contents of carbo-nitride forming elements in the Austenite phase at the annealing temperature (1135 ° C)**



# 2014 - Production DS4 plate



Production of a new DS4 ingot in 2014



Hot rolling of the ingot (Pre-heating  $-1200^{\circ}\text{C}$ )



After last hot rolling stage ( $919^{\circ}\text{C}$ ) 20 mm thickness



Solubilization annealing  $1135^{\circ}\text{C}$

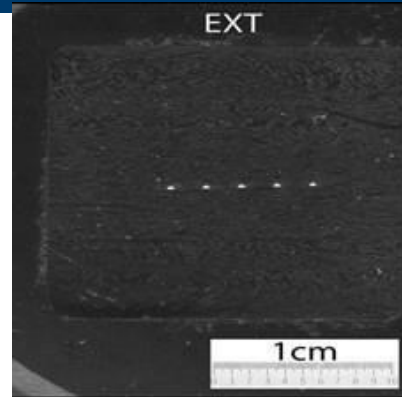
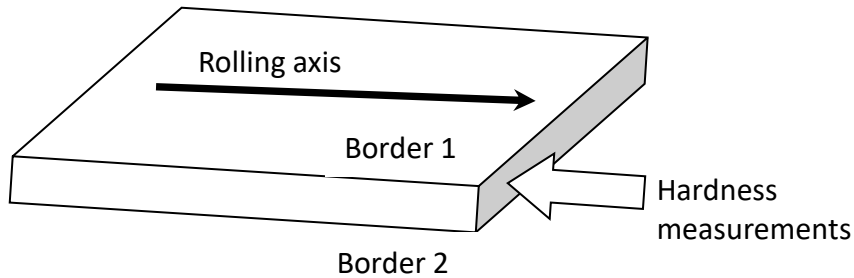


Cold working up to 15 mm thickness

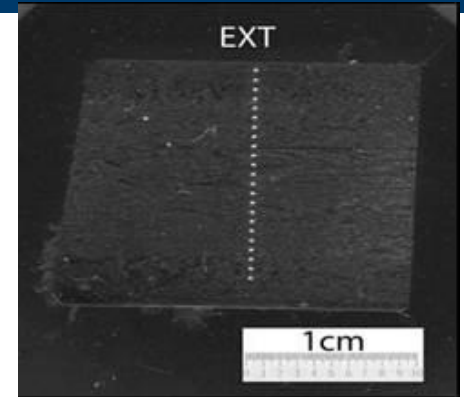


*«waving» on the rolling direction due to 20% c.w.*

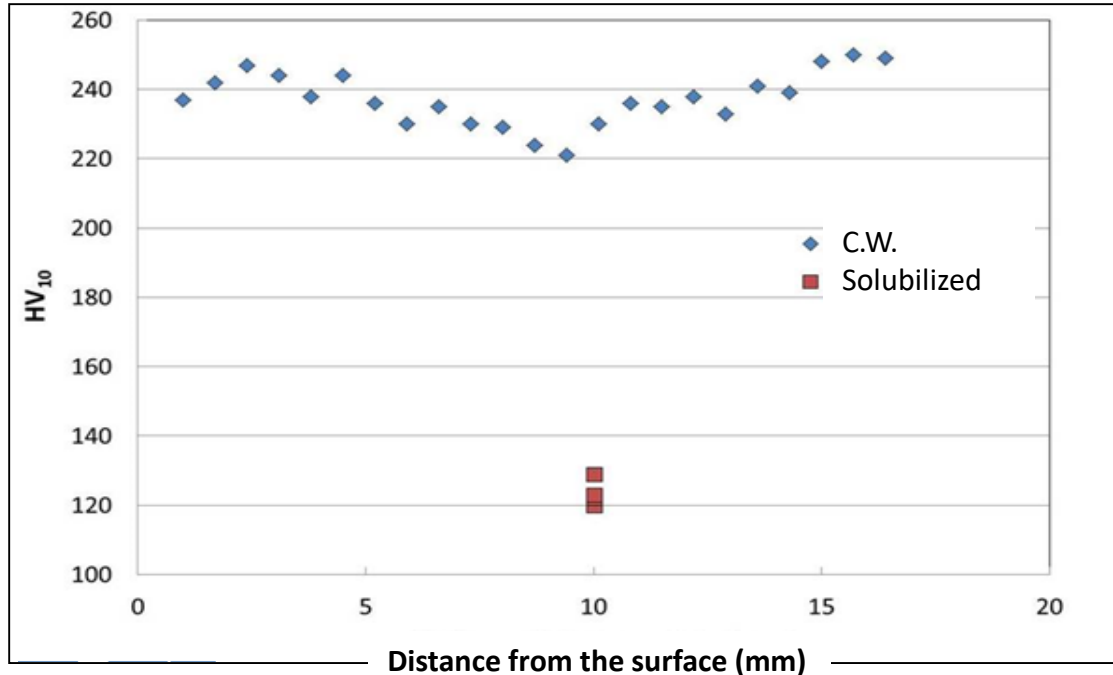
# Production of DS4 plate; Hardness measurements



solubilized  
(T-L direction)



Cold worked  
(L-T direction)



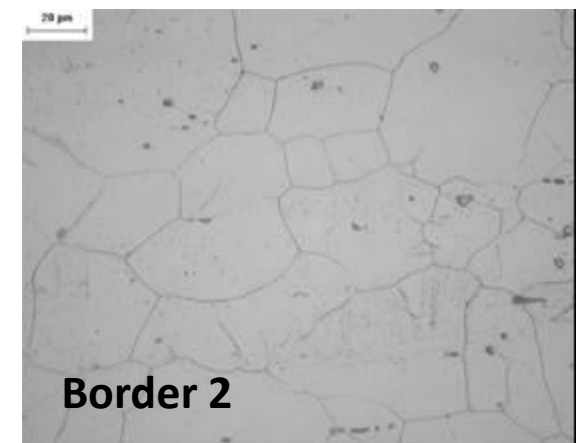
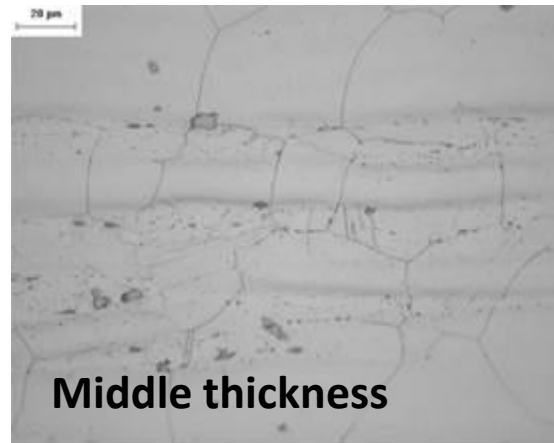
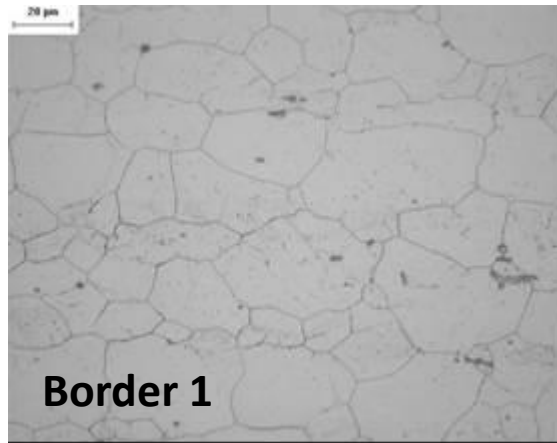
**80s batch (DS4): 260 HV**



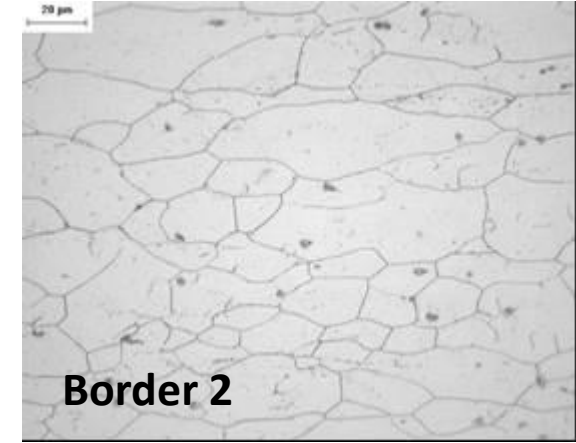
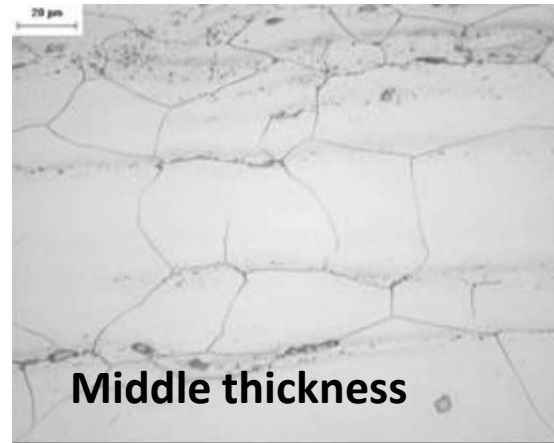
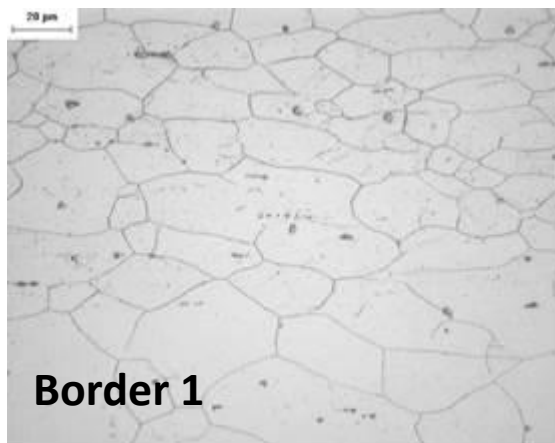
# Grain Size (32-45 mm in the 80s batch)



## After solubilization



## After 20% c.w.

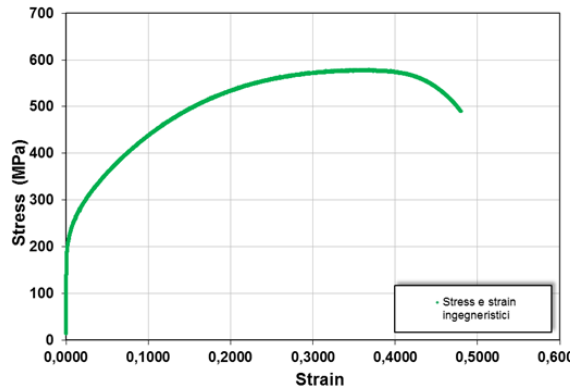


# Tensile Properties; qualitative comparison

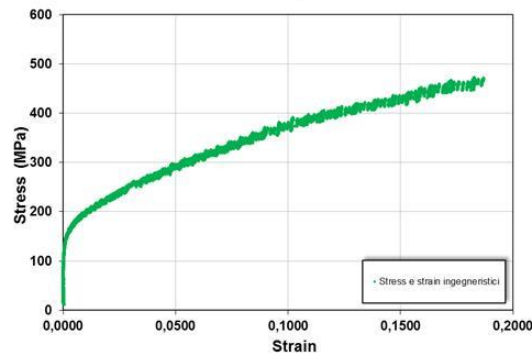


## Solubilized Material (RT, 550° C, 650° C)

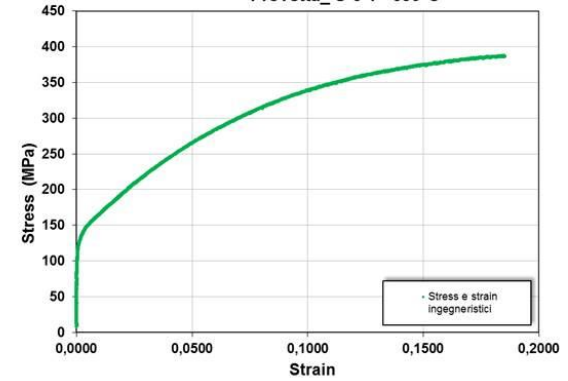
Provetta\_S-1 T= R.T.



Provetta\_ T=550°C

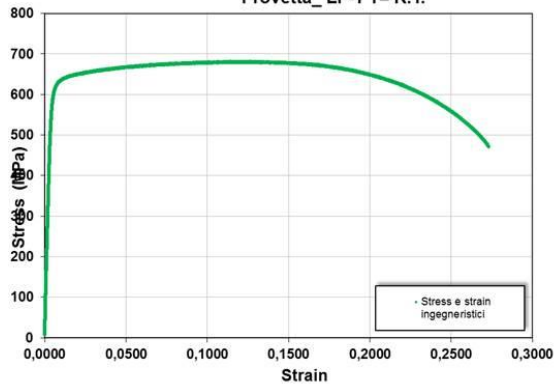


Provetta\_S-6 T= 650°C

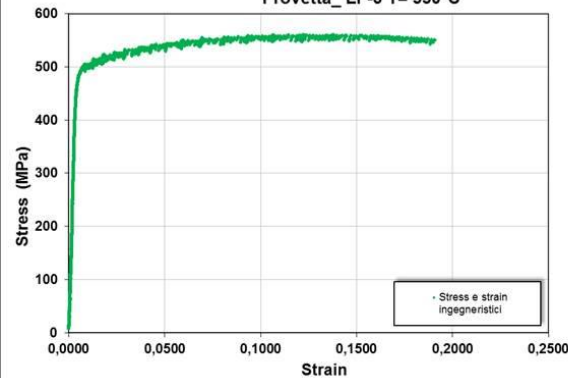


## 20% C.W. material (RT, 550° C, 650° C)

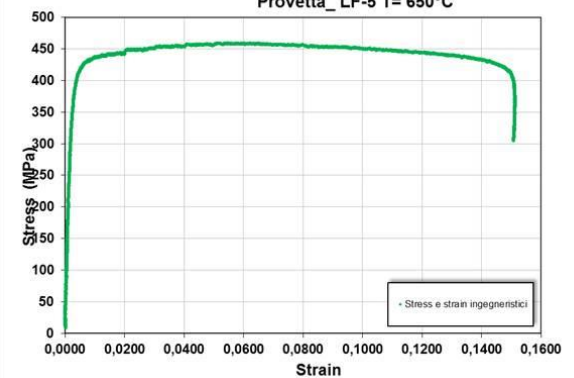
Provetta\_LF-1 T= R.T.



Provetta\_LF-3 T= 550°C

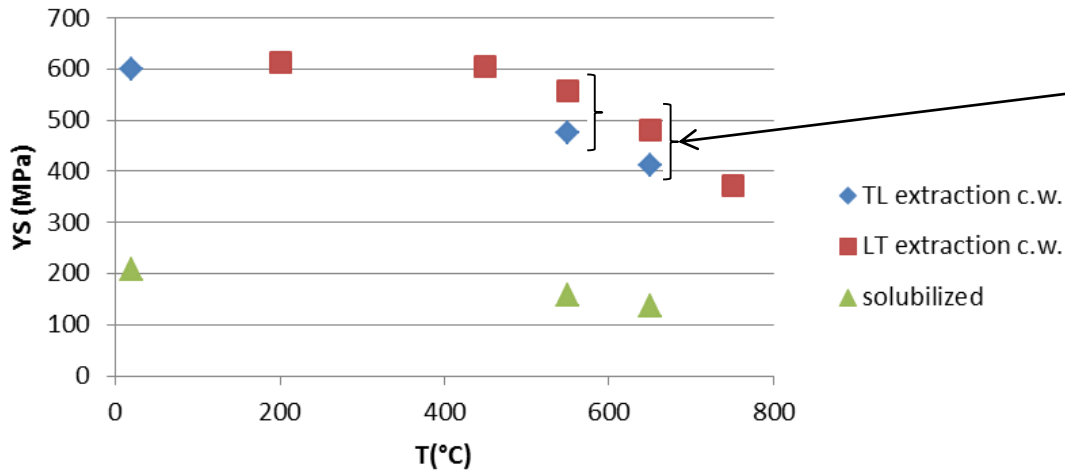


Provetta\_LF-5 T= 650°C



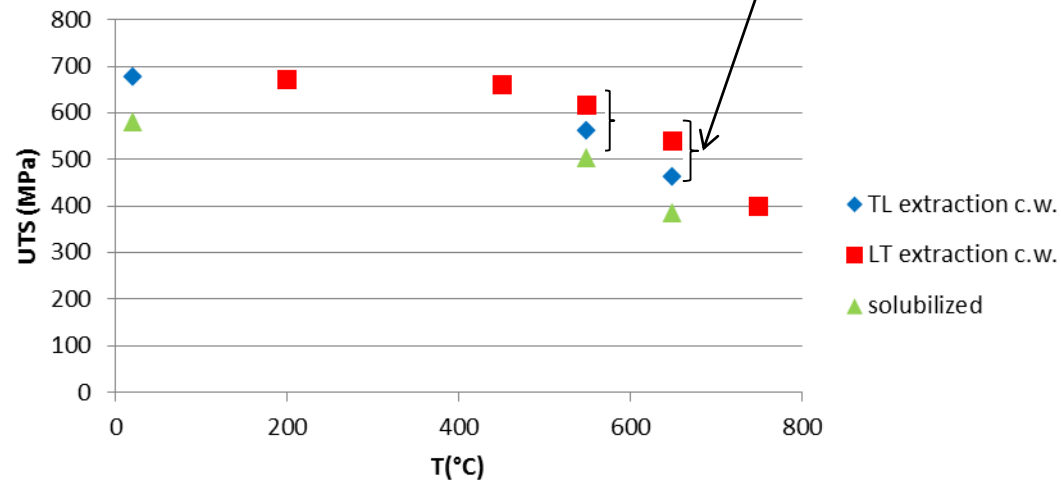
# Anisotropy of the material; comparison between extraction directions

## Yield Strenght (0,2% PL. Def.)



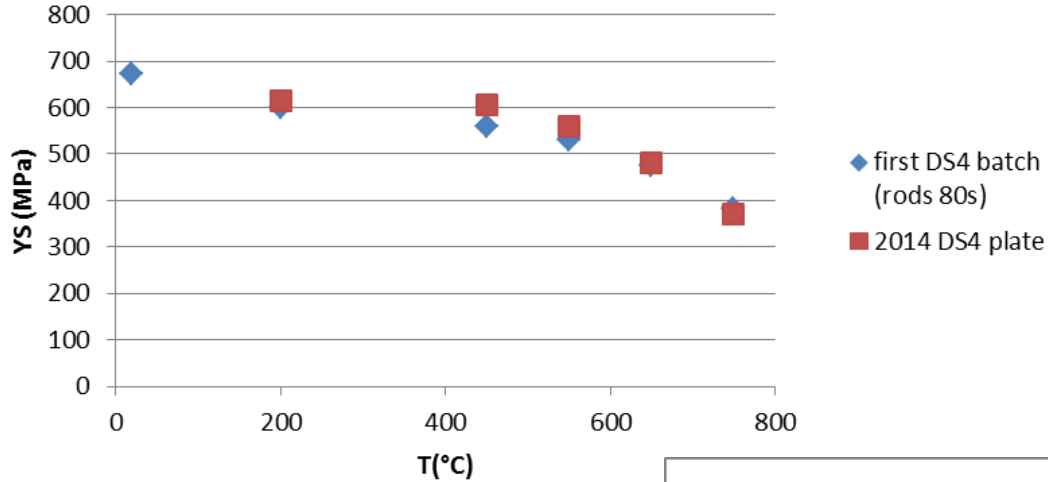
Anisotropy of the produced plate

## Ultimate Tensile Strenght



# Comparison DS4; rods 90s vs 2014 plate

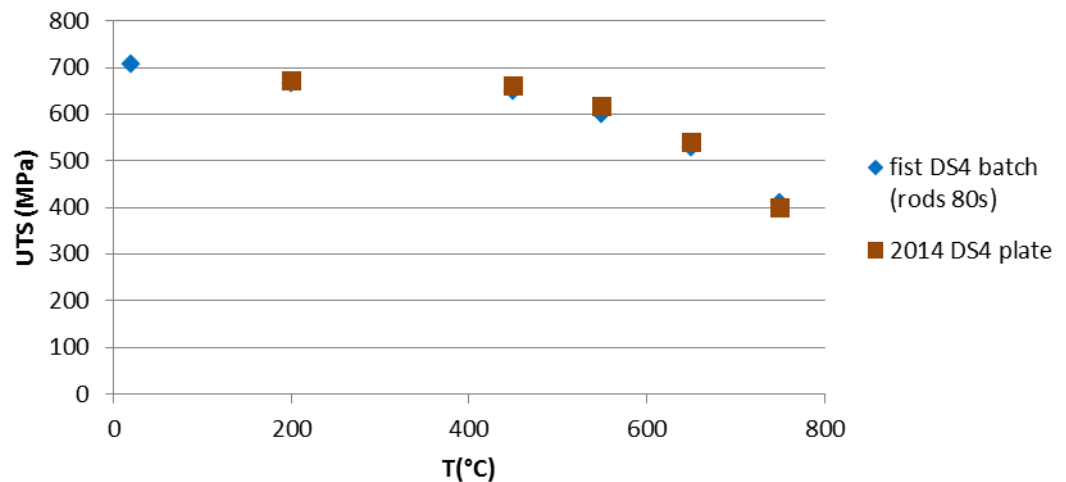
## Yield Strength (0,2% PL. Def.)



Data 90s:

*G. Filacchioni, U. de Angelis, D. Ferrara, L. Pilloni / Proceedings B.N.E.S., London, 1990*

## Ultimate Tensile Strength

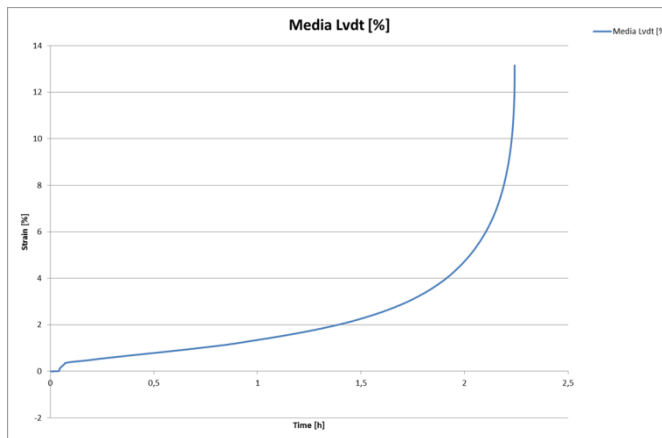


Comparable mechanical properties of the new plate with respect to the rods characterized in the 90s

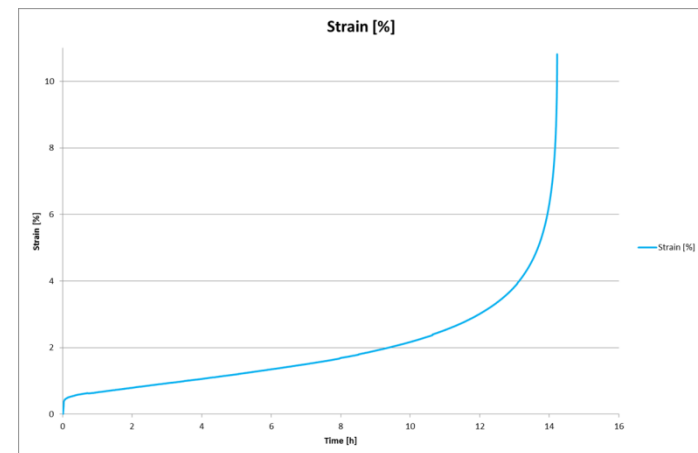
# Experimental activities in progress ...

- **Corrosion Tests (flowing lead)**; 1000 hrs exposure completed (flowing Pb,  $10^{-5}$  wt% O<sub>2</sub>);
- **Ion irradiation**; target: 100 dpa (58 Ni, 110 MeV). In progress (four sessions completed, one additional session to achieve the target dose);
- **Creep tests**; In Progress ...

Test 650° C – 415 Mpa (Yield Stress)

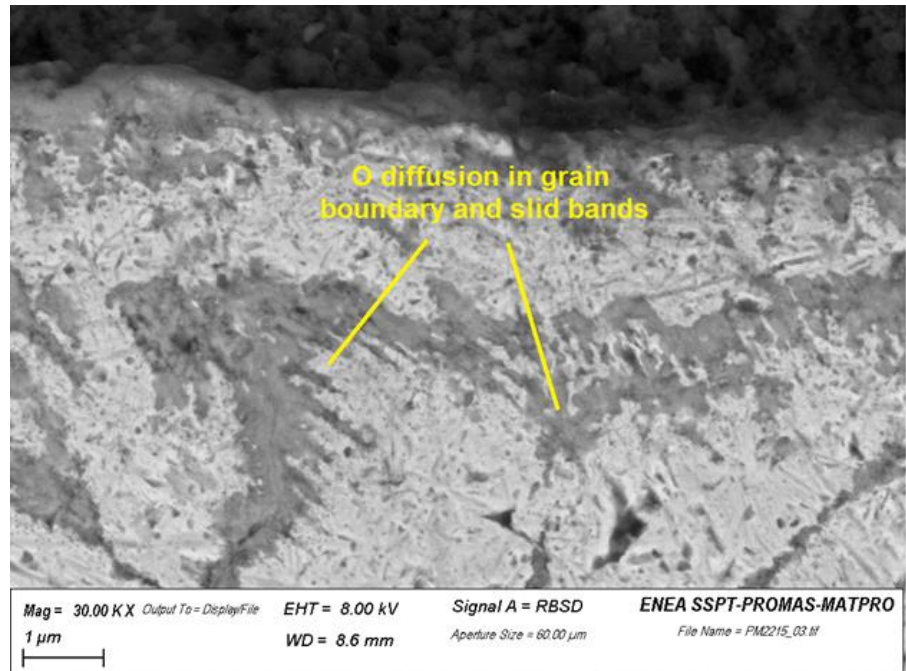
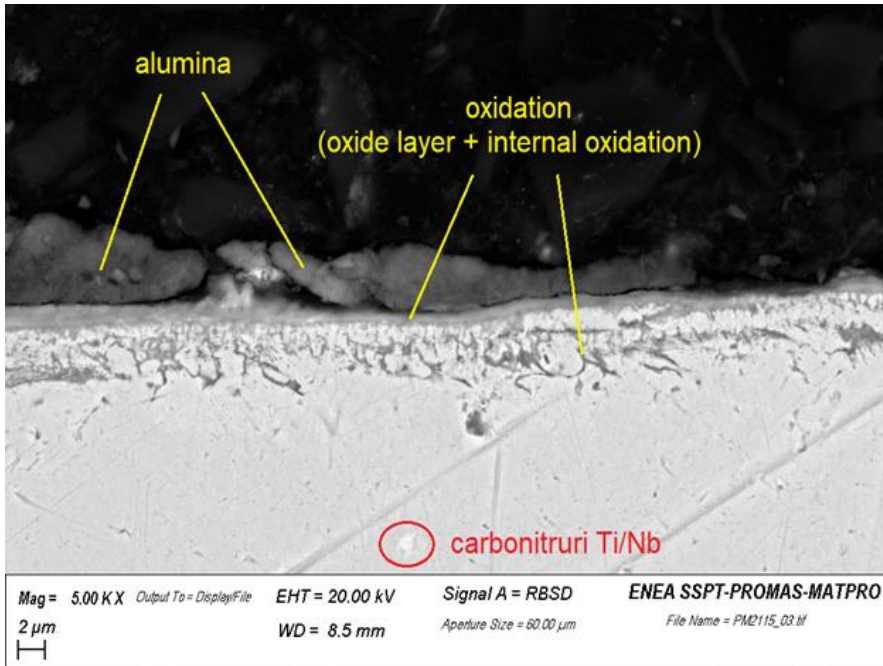


Test 650° C – 390 Mpa



# Corrosion tests

**Experimental;** Exposures in flowing Lead ; 1000 hrs at 550°C, velocity 1.3 m/s, Oxygen content between 10-4 and 10-5 wt % ; carried out in LECOR plant.

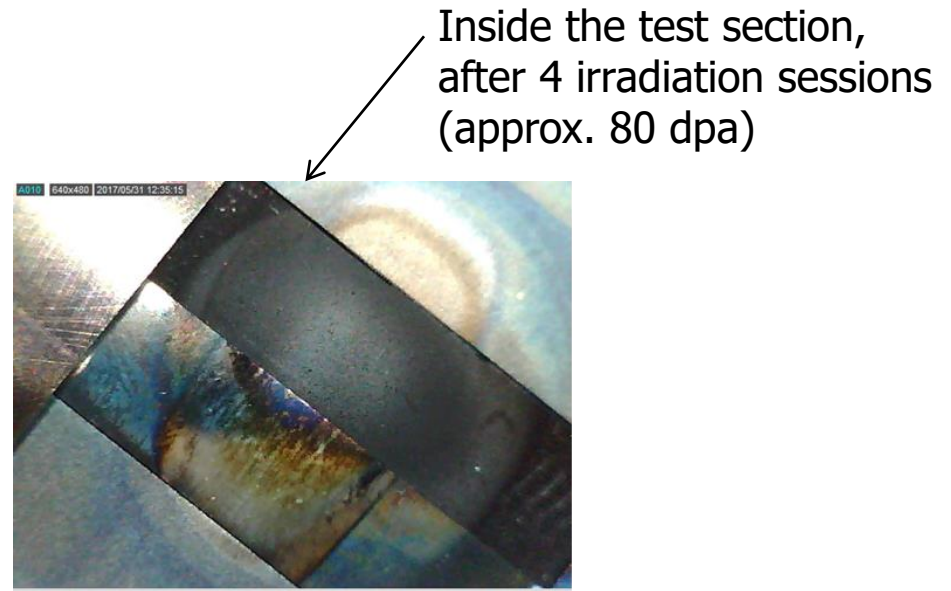


**Results:** after 1000 hrs the prevailing degradation mechanism is Oxidation; thickness of the oxide layer between 5 and 10  $\mu$ m. No dissolution is noticeable . Further analysis on the exposed samples (EDS aimed at the detection of the composition of the corrosion layers) are on-going and will be delivered in the next AdP report.

# Running activities: Ion-Irradiation

Irradiating in LNL (Laboratori Nazionali di Legnaro, INFN, Padova);  
5 irradiation sessions (two days each) in order to achieve the 100 dpa target  
dose; start: July 2015, end: December 2018

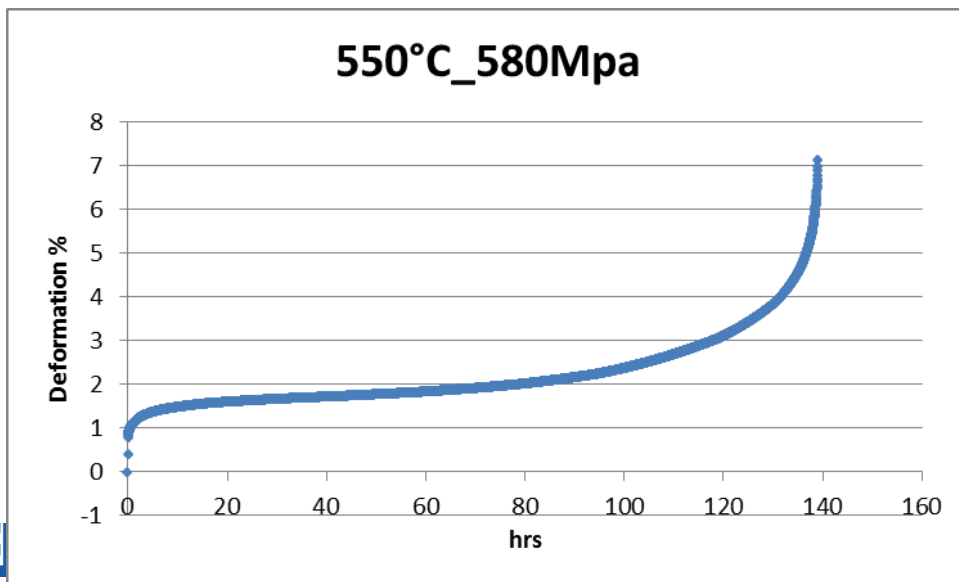
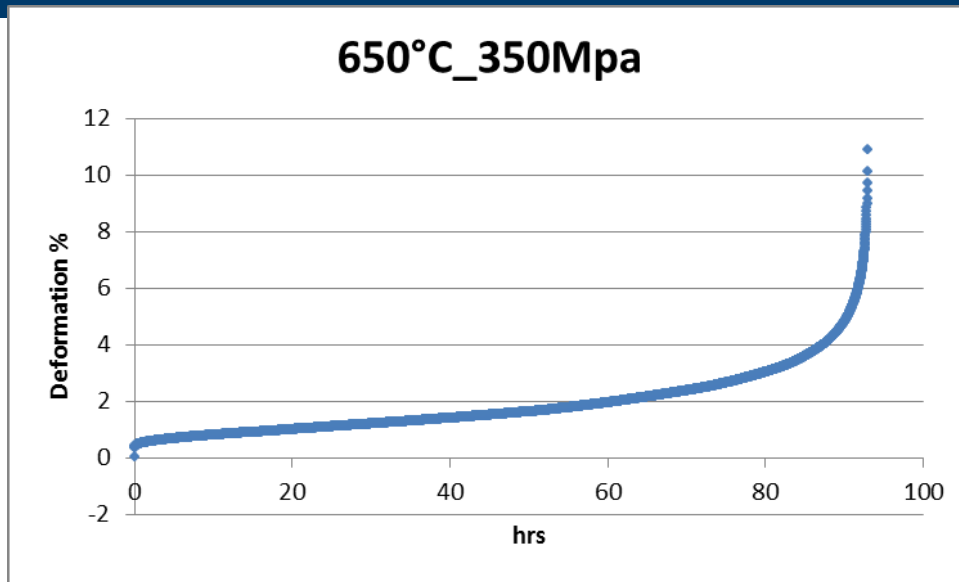
- Geometry of the sample: 20mm x5mm x1,3 mm; polished surfaces



- Target: 100 dpa
- Heavy ions: 58 Ni
- 110 MeV

In progress ... (four sessions completed, last session postponed due to the rupture of the "laddertron" of the TANDEM facility)

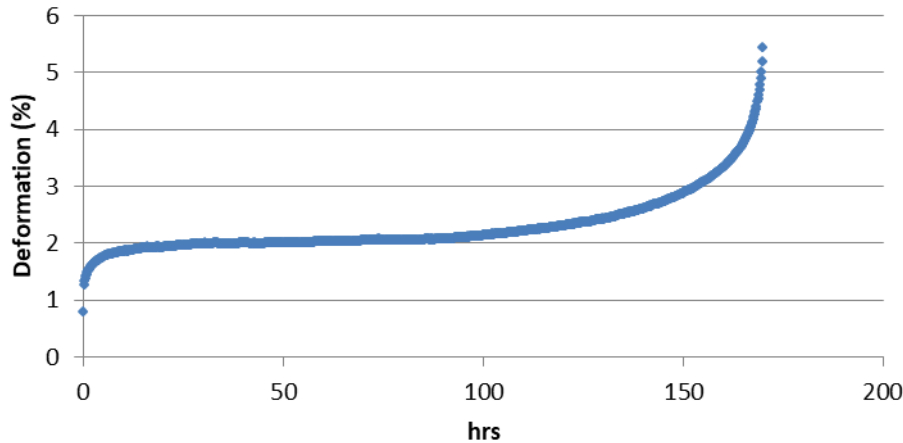
# Creep characterization in progress ; 2017 Results



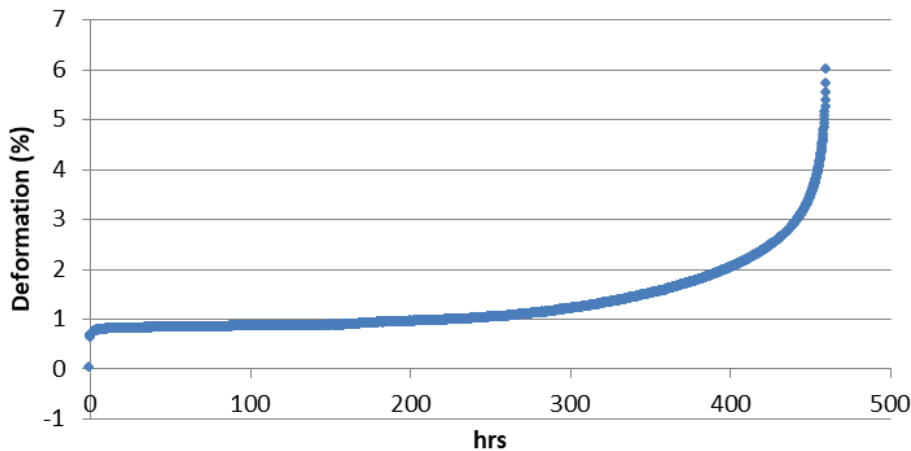


# Creep characterization in progress ; 2018 Results

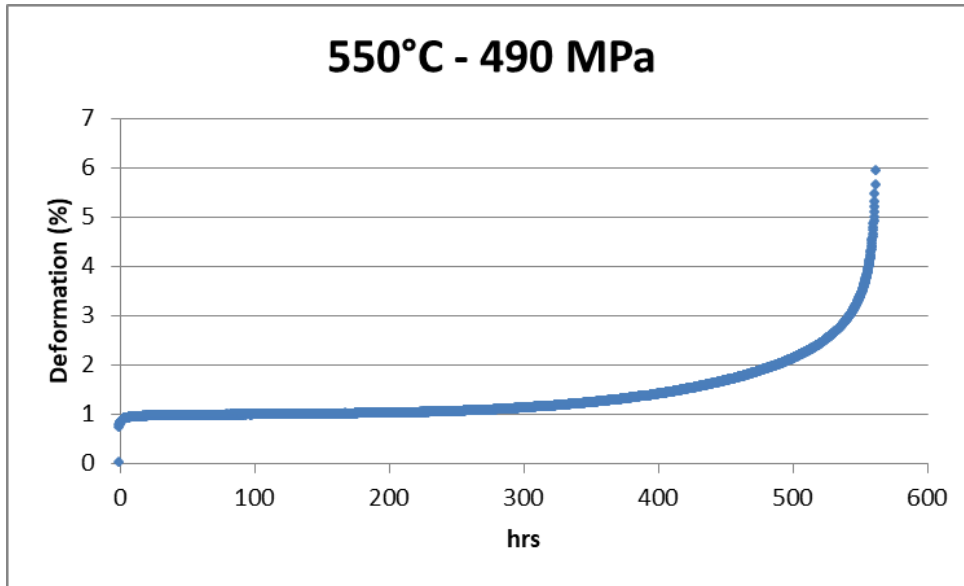
## 550°C\_547MPa



## 550 °C - 519 MPa

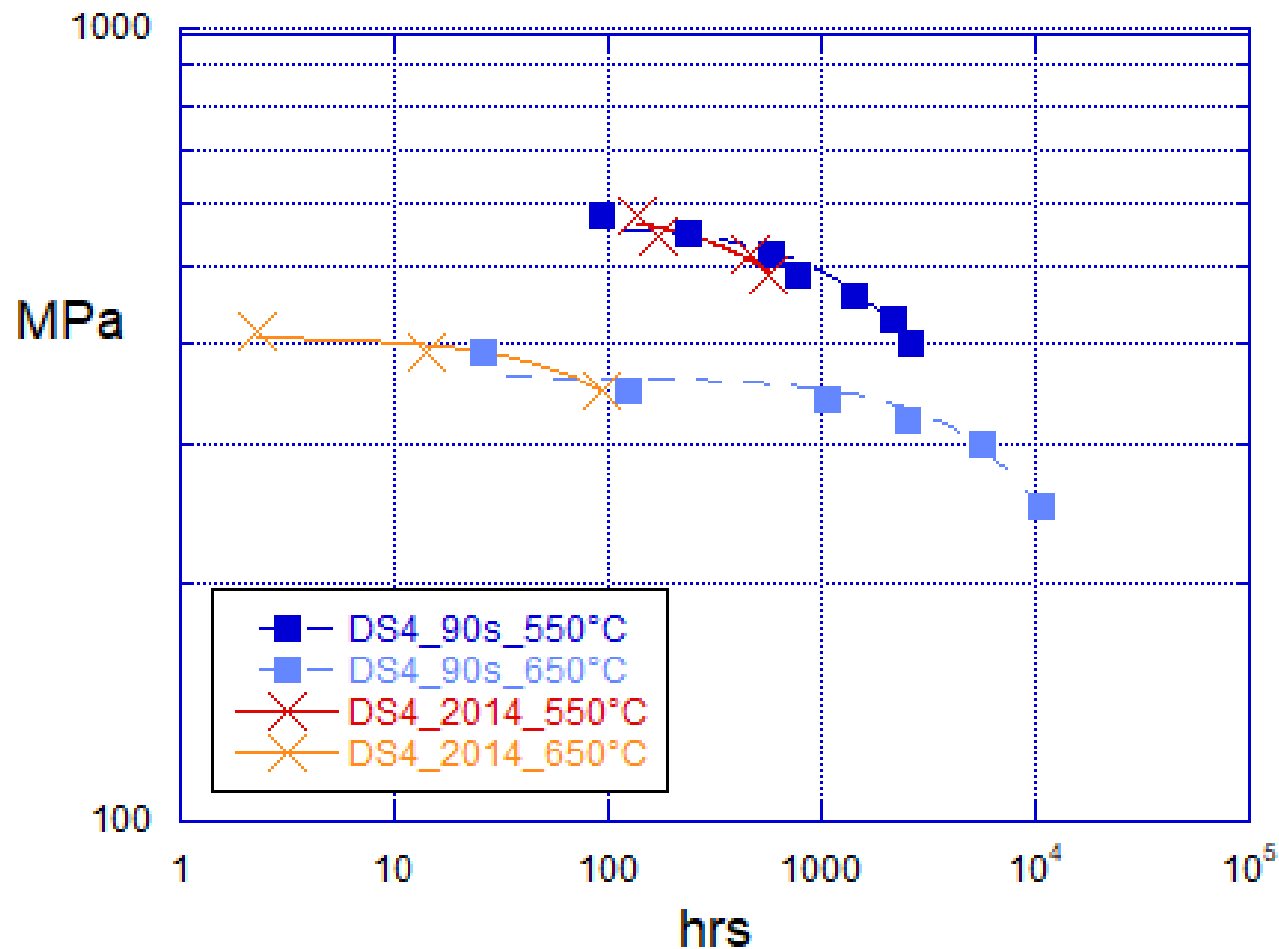


# Creep characterization in progress ; 2018 Results



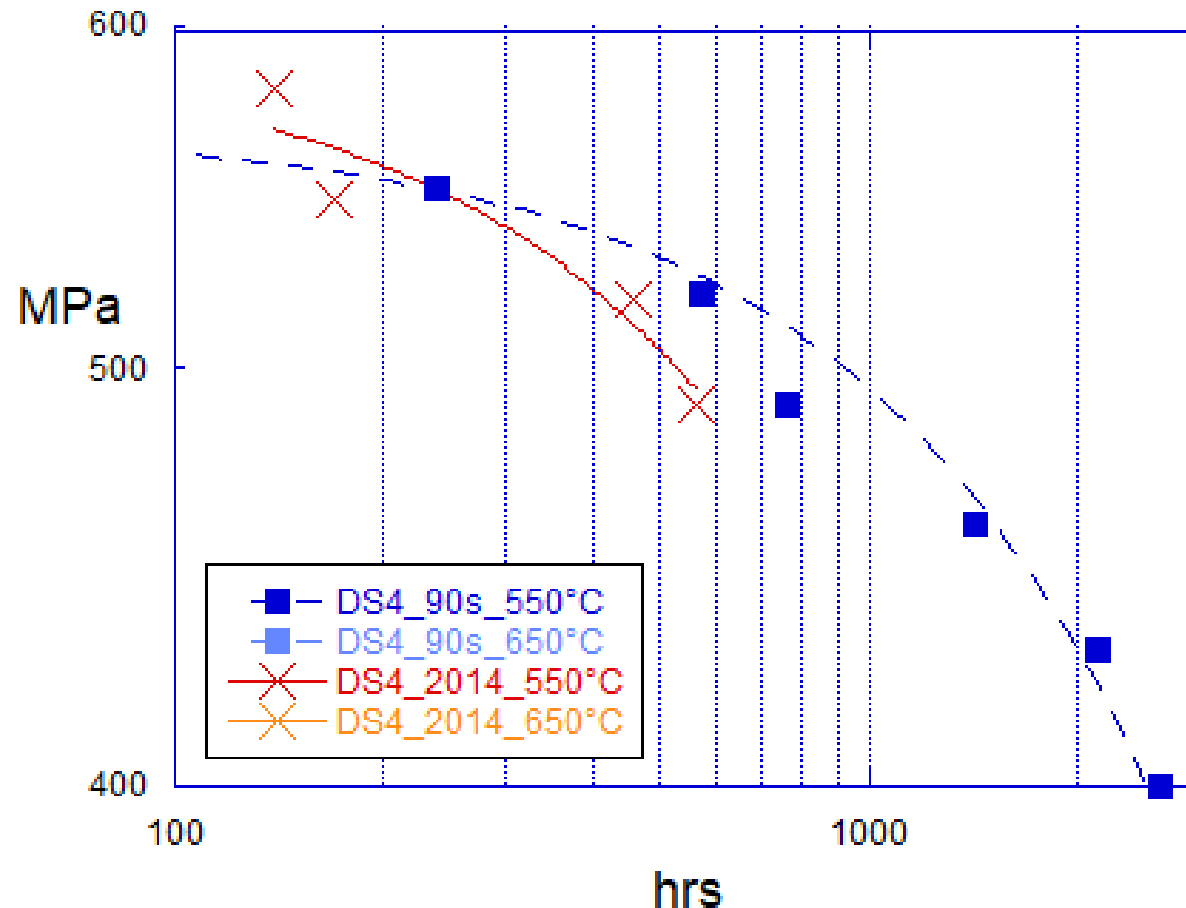
# Partial comparison; 2018 Results

Partial results show poorer creep properties for 2014 batch compared to the former « Supernova » rods ...

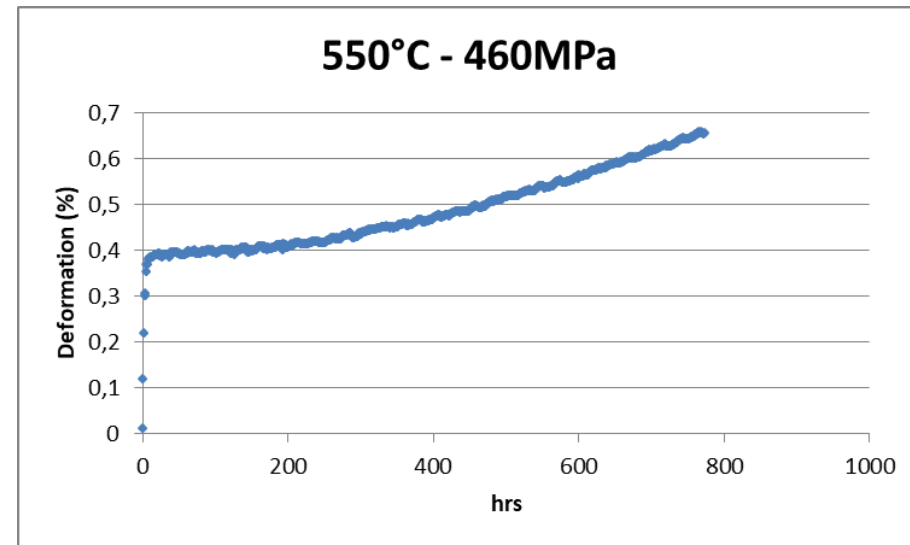
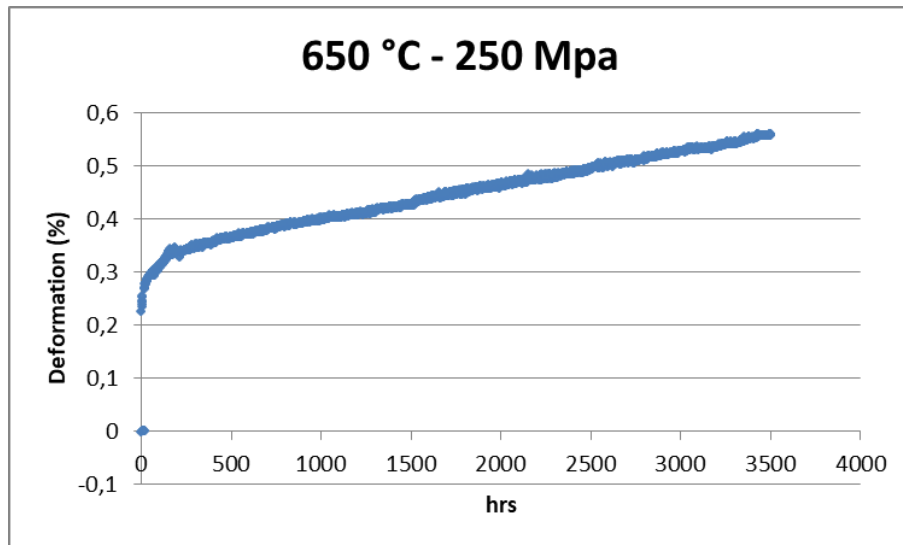
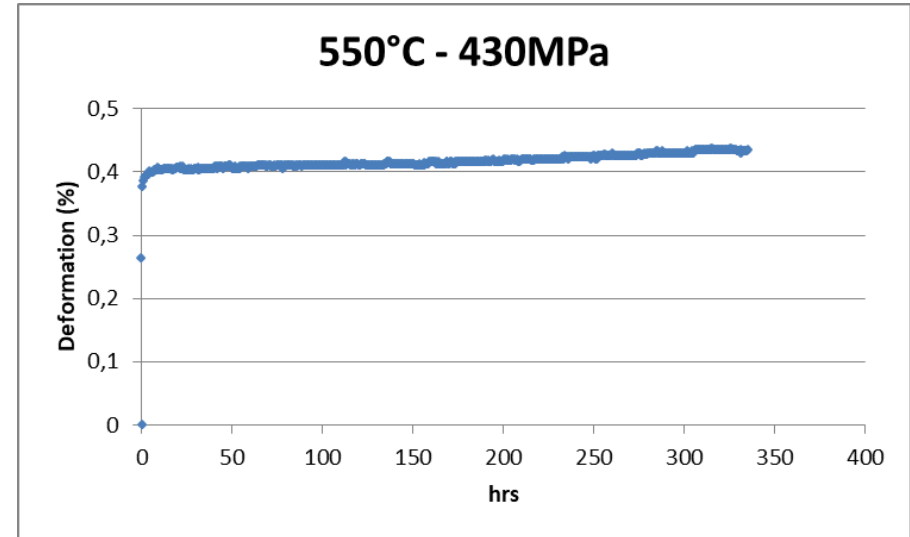
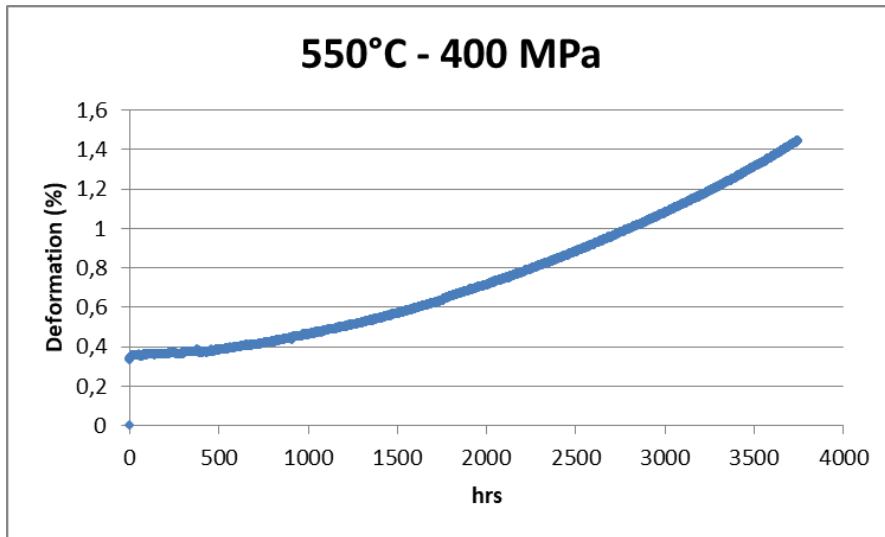


# Partial comparison; 2018 Results

Partial results show poorer creep properties for 2014 batch compared to the former « Supernova » rods ... but ...

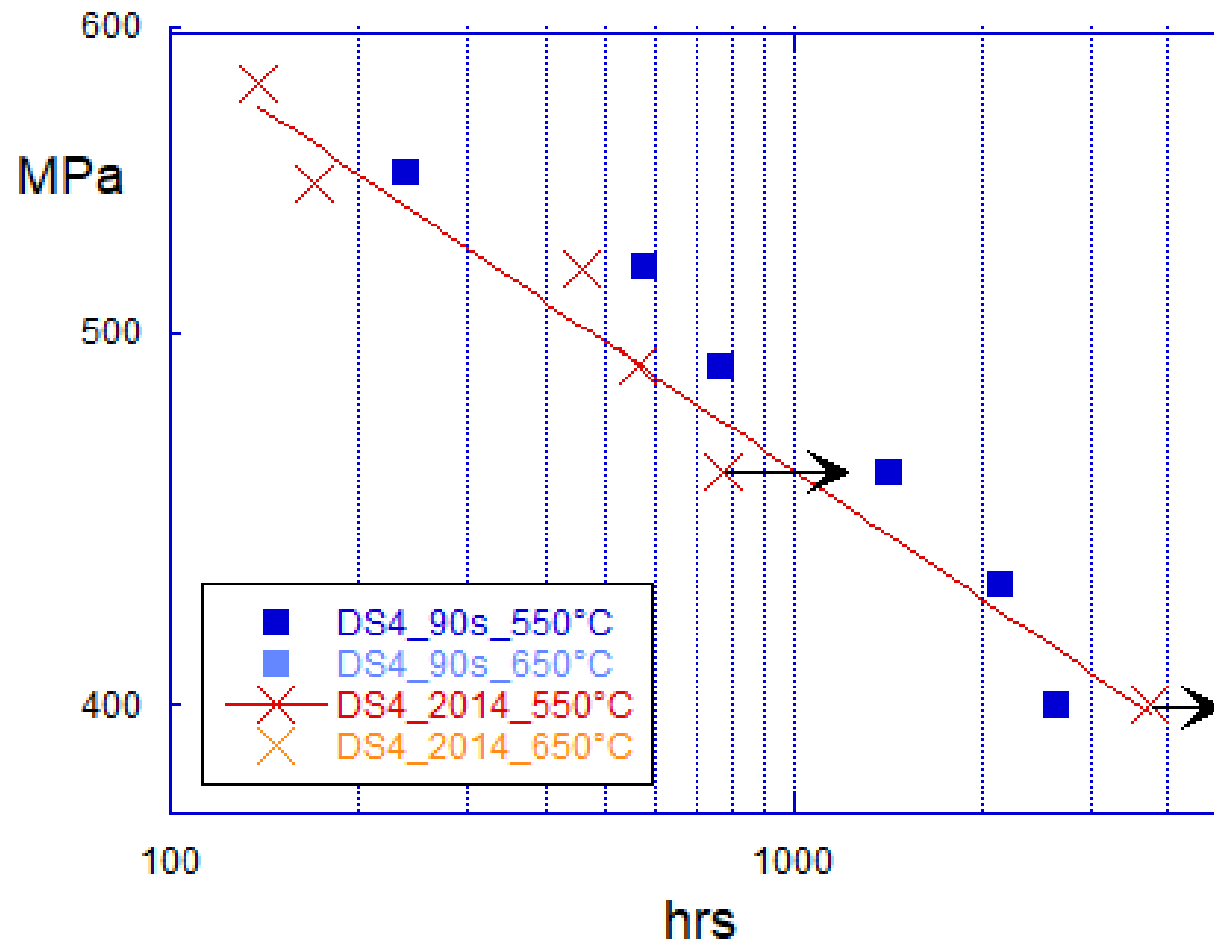


# Creep characterization in progress; running tests



# Partial comparison; 2018 Results

Still running test reveal improved creep performance at the lower loads ...



# Conclusions

Double stabilized steels appear very promising because of the following reasons:

- the long term properties resulted nearly the best among the austenitic stainless steels (improved creep resistance of the former “Supernova” batch);
- the common C.E.A.-E.N.E.A. irradiation programme, the Supernova rig loaded in Phenix FBR at the beginning of May 1988, demonstrated the good swelling resistance;
- The features affecting the good swelling behaviour of these alloys are thought to be the high c.w. rate, the increased Ni content and the double stabilization (addition of Ti and Nb) which grants the possibility to tune up the precipitation of primary and secondary carbides in order to reduce the swelling;
- A new DS4 plate has been produced in 2014 and the tensile properties appear superposed to the ones of the former DS4 batch (namely the “Supernova” rods). Lower values of Uniform and Total Deformations of the new cast when compared to the ones of the former batch (irradiated in Supernova). Less performing creep behaviour of the new batch respect to the former one (according to the short tests) but improved performance at the lower loads according to the still running test (550° C-400MPa). Waiting the results of the ion irradiation programme (expected within the year).

# Dissemination and publications



Logout

## ABSTRACT SUBMISSION

**Title:** Status of the research on swelling resistant double stabilized austenitic steels

**Abstract No.** 0273  
**Title** Status of the research on swelling resistant double stabilized austenitic steels  
**Abstract** [DS\\_Steels.doc](#)  
**Template used** Yes

### Text Abstract

The qualification of the fuel cladding material is one of the most crucial issues in Fast Reactors technology. Historically, the main limiting factor is related to cladding swelling; namely the increase of volume that takes place in materials subjected to intense neutron radiation and due to nucleation and growth of point defects aggregates.

At the beginning of the '80s, within an experimental program carried out at the Saclay Center, the under electrons irradiations (1 MeV) had shown the effectiveness of the simultaneous presence of Ti and Nb on the swelling resistance of 316 and 15 Cr-15 Ni matrix. Then, after a further optimization of the chemical composition, innovative alloys had been realized based on 15 Cr-15 Ni and 15 Cr - 25 Ni matrix. The outcomes of the PIE (Post Irradiation Examination) in the frame of the "Supernova" experiment on these new steels, which took place in the early 90s, appeared extremely promising, particularly concerning the 15 Cr-25 Ni (Ti + Nb) matrix. This led ENEA to start the production of a new batch of DS4 (15 Cr-25 Ni) steel in 2014.

The criteria which led the alloy design will be presented in this paper; the microstructural and compositional features that are expected to control and limit the swelling ratio are the high Ni content, the secondary precipitation of Ti and Nb carbides and the cold working in the range of 20% (section reduction ratio).

The DS4 steel plate has then been characterized in terms of mechanical properties (hardness, tensile and creep), corrosion behaviour in flowing lead and ion irradiation. The status of the material after a 80 dpa damage by means of heavy ions (58 Ni - 110 MeV) will be reported and the outcomes of the mechanical characterization and corrosion tests will be presented.

**App** Yes  
**Approval** Confirm  
**Copyright** Yes  
**Affiliations** (1) ENEA, n/a, Italy  
(2) INFN-LNL, n/a, Italy  
**Authors** C. Cristalli (1) Presenting  
M. Angiolini (1)  
S. Bassini (1)  
A. Candelori (2) (2)  
L. Pilloni (1)



Thank you for your attention

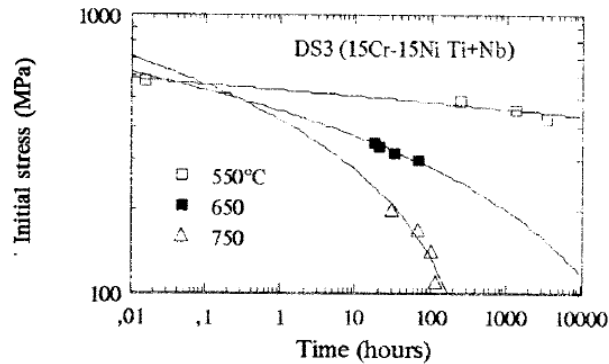
# Mechanical Characterization (1990): tensile & creep

## Fitting of data

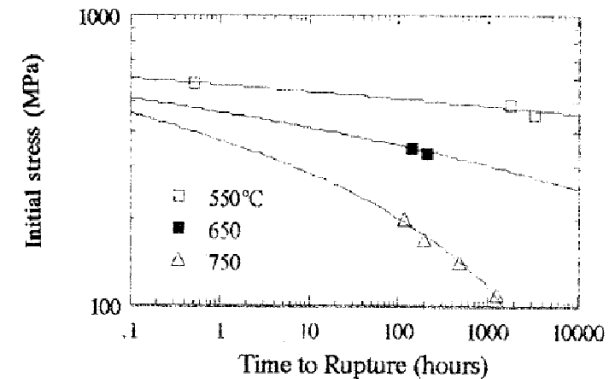
G. Filacchioni, L. Pilloni and oth. «Mechanical and structural behaviour of the second double stabilized steels generation», B.N.E.S. London,1990

Fitting function:  
$$t = K \cdot \exp(-\gamma \cdot \sigma)$$

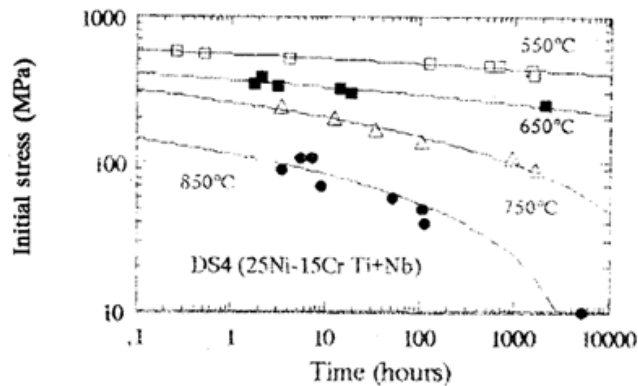
### Time to obtain 0.2% of creep strain; DS3



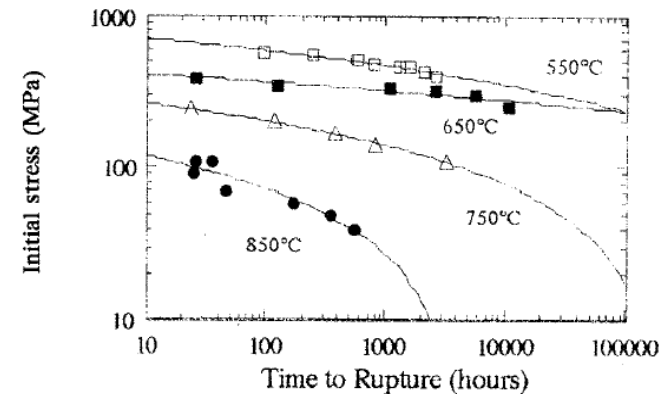
### Time to failure; DS3



### Time to obtain 0.2% of creep strain; DS4



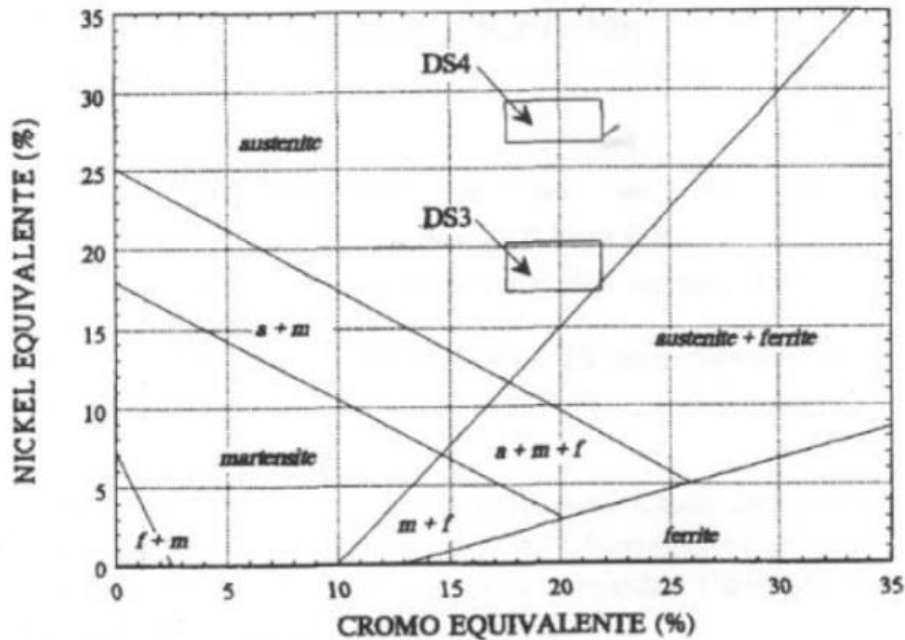
### Time to failure; DS4



# Introduction

## Production of the first batch of DS alloys (2<sup>nd</sup> gen) in the late 80s

### Position into the Shaffler's diagram



### Manufacturing Details

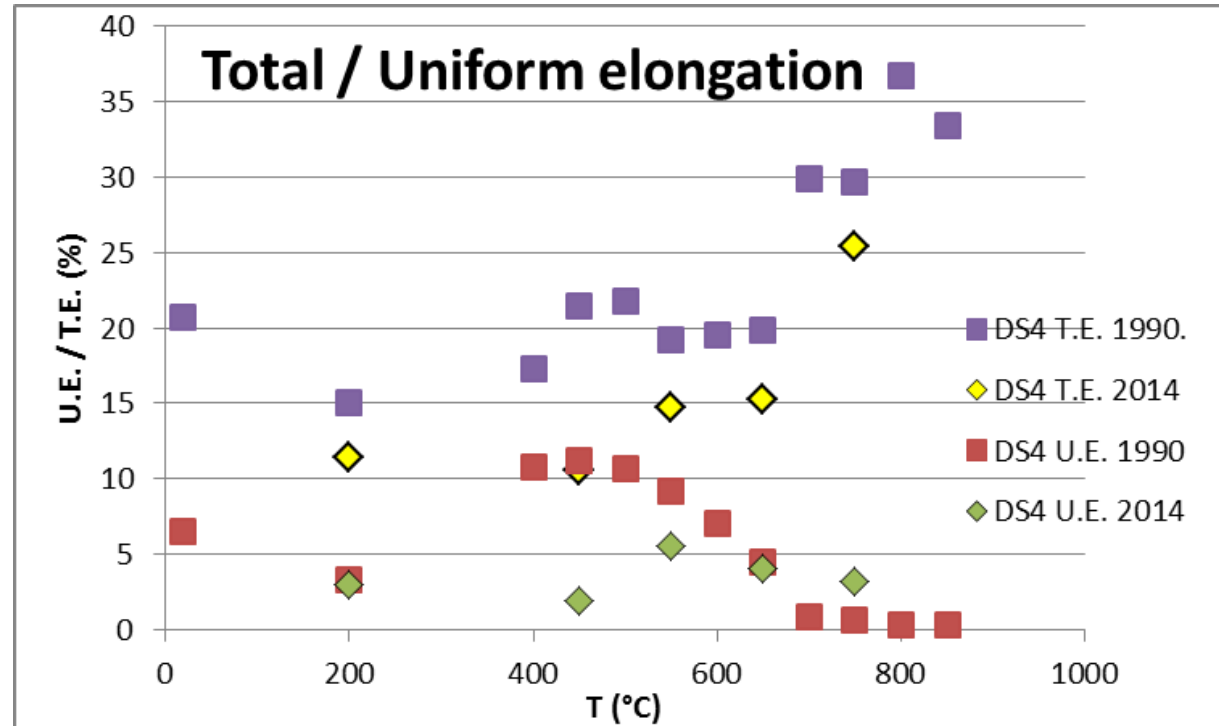
Two kinds of products realized:

- rods (external diameter 8 mm)
- cladding pipes (ext. diam. 6,55 mm, internal 5,65)

The rods and the pipes were **cold-worked** with a final section reduction ratio of **20%**.

**Annealing** temperature before final cold-working : **1100° C** ( 5 minutes in Argon atmosphere ), followed by air cooling.

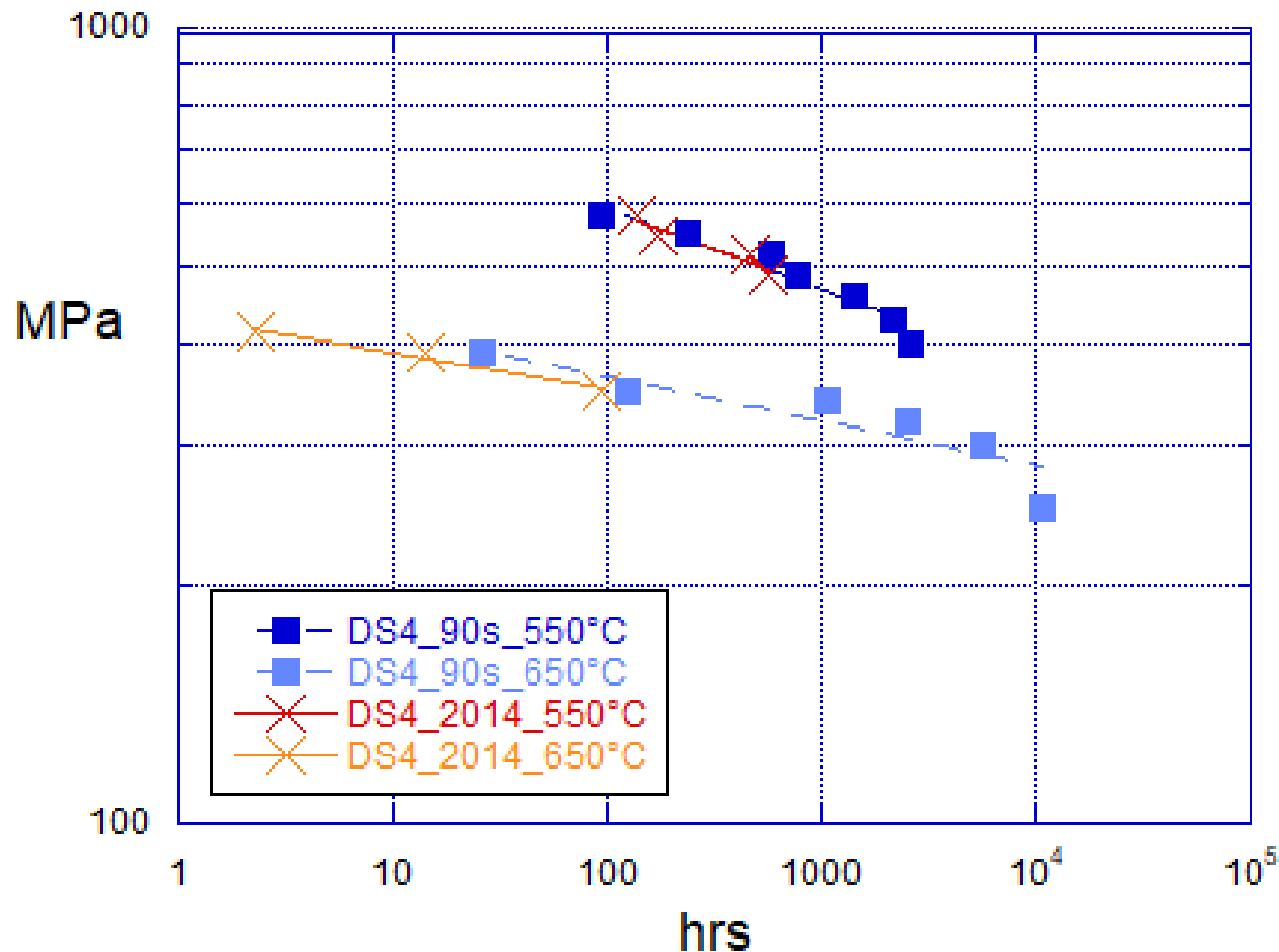
# Total/Uniform Elongation; Comparison



Concerning the uniform elongation DS4 behaviour was excellent. In the interval between 400 and 600-650° C the steel performs values that are almost twice respect to those of the other steels. This behavior, similar to the best ones for the stainless steels with high yield strength, is symptomatic of good characteristics of stretchiness, performing delayed onset of mechanical instability. The values of the deformations, comparing the new batch to the former one, appear averagely less performing.

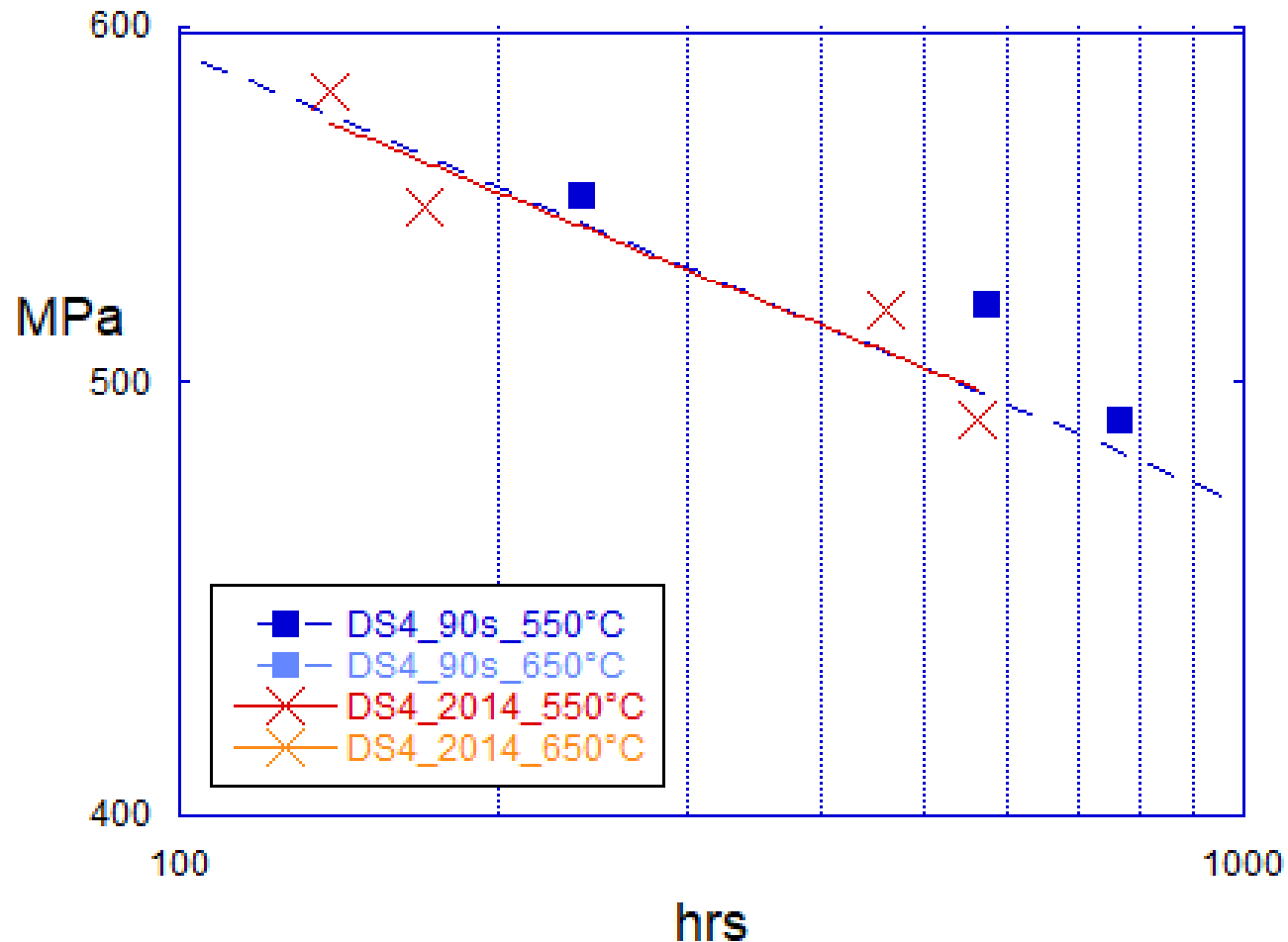
# Creep characterization in progress ...

Partial results show poorer creep properties for 2014 batch compared to the former « Supernova » rods...



# Creep characterization in progress ...

Partial results show poorer creep properties for 2014 batch compared to the former « Supernova » rods...





Advanced steels production  
Austenitic steel AIM1 15Ni15 Cr for fast reactors

250  $\mu\text{m}$

# Processi di produzione

## Primary Melting

VACUUM  
INDUCTION  
MELTING



## Secondary Melting

ELECTRO SLAG  
REMELTING



## Thermo-mechanical transformation

HOT / COLD ROLLING

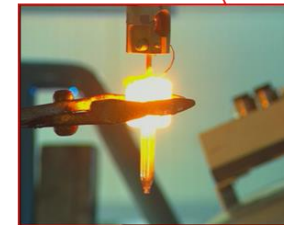
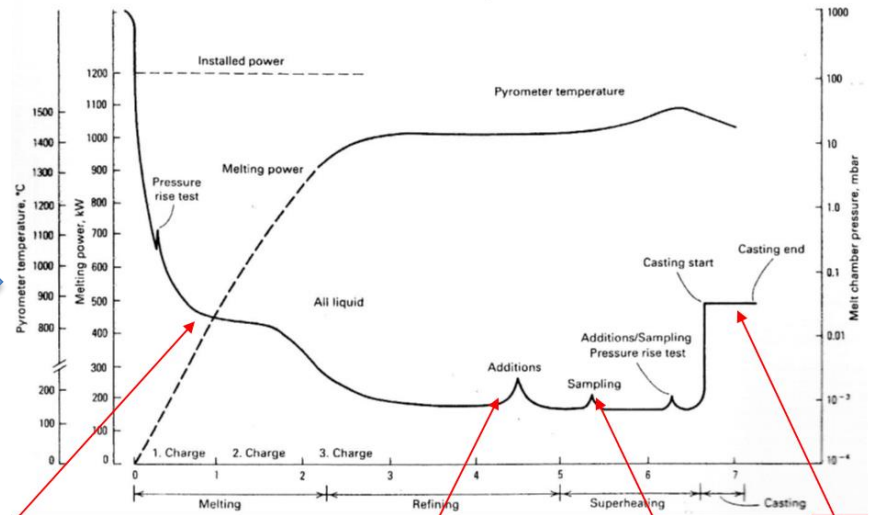
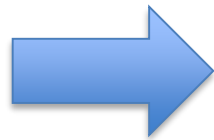




# VIM ingots

VIM ingots produced by using high purity raw materials:

- vacuum/ controlled atmosphere process
- On-line chemical analysis



# Vacuum Arc Remelting



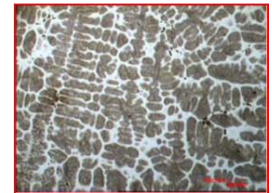
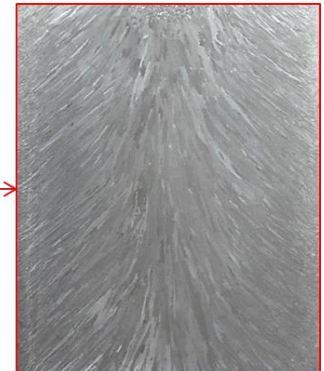
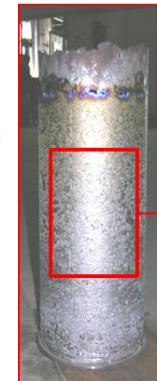
The L 240/PESR is a multi-purpose laboratory furnace for high quality material production and development.

The furnace allows the following processes and features:

- Ingot melting with various mold diameters and lengths, using the consumable electrode technique. Remelting of all materials from copper to high melting point materials.

VIM ingot remelting for:

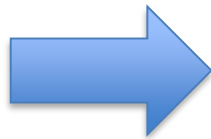
- Desulfuration
- Nitriding
- O<sub>2</sub>, N<sub>2</sub> e H<sub>2</sub> removal
- Inclusion removal
- Directional solidification
- Solidification structure refining
- Homogeneity
- Less segregation



# Hot rolling

VIM + VAR ingots, after mechanical machining and homogenization heat treatment have been subjected to hot rolling.

From 120 mm ( $T > 1000^{\circ}\text{C}$ ) to  $\sim 25$  mm.



\*



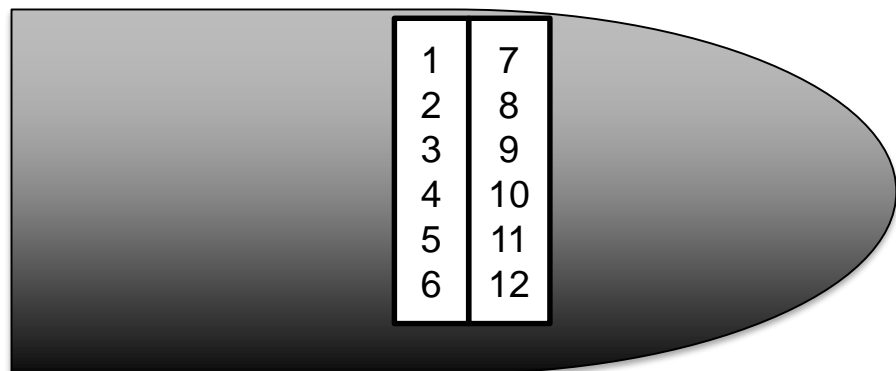
# Cold rolling

Two step lamination :

- 1) ~ 20mm,
- 2) Final 15mm.

Thermal treatment between the two steps.

The thermal treatments have been optimized, by means laboratory trials to obtain the technical requirements



# Specifications



Targets



$620 \leq R_{p0,002} \leq 840 \text{ Mpa}$   
 $R_m \geq 760 \text{ Mpa}$   
 $A_{tot} \geq 18\%$

| Sigla provetta                                  |                      | Specimen ID   | 1515 Ti - A | 1515 Ti - B | 1515 Ti - C | MEDIE    |
|---|----------------------|---|-------------|-------------|-------------|----------|
| Velocità deformazione fino a Rp, ReH, ReL (1/s) |                      | Strain rate up to Rp, ReH, ReL                                    | 2.50E-04    | 2.50E-04    | 2.50E-04    | 2.50E-04 |
| Velocità per Rm (1/s)                           |                      | Strain rate for Rm  | 6.70E-03    | 6.70E-03    | 6.70E-03    | 6.70E-03 |
| T (°C)  | Temperatura di prova | Test temperature  | RT          | RT          | RT          | RT       |
| do (mm)   | Diametro Iniziale    | Original diameter of the parallel length                          | 8.92        | 8.92        | 8.88        | 8.91     |
| So (mm <sup>2</sup> )                           | Sezione Iniziale     | Original cross sectional area of the parallel length              | 62.49       | 62.49       | 61.93       | 62.39    |
| Lo(mm)  | Tratto Utile         | Original gauge length   | 45          | 45          | 45          | 45       |
| Le(mm)  | Base Estensimetro    | Extensometer gauge length   | 50          | 50          | 50          | 50       |
| Fp 0,2 % (N)                                    | Carico Scost. Prop.  | Force corresponding to the proof strength, plastic extension 0.2% | 45780       | 47615       | 45964       | 46233    |
| Fmax (N)  | Carico Massimo       | Maximum force   | 52103       | 52514       | 51946       | 52305    |
| Lu (mm)   | Lunghezza Ultima     | Final gauge length after fracture                                 | 53.19       | 52.82       | 53.19       | 52.81    |
| du (mm)   | Diametro Ultimo      | Minimum diameter after fracture                                   | 5.75        | 5.62        | 5.67        | 5.66     |
| Su (mm <sup>2</sup> )                           | Sezione Ultima       | Minimum cross sectional area after fracture                       | 25.97       | 24.81       | 25.25       | 25.19    |
| <b>Rp 0,2 % (MPa)</b>                           | C. Unit. Sc. Prop.   | Proof Strength, plastic extension 0.2%                            | 733         | 762         | 742         | 746 ✓    |
| <b>Rm (MPa)</b>                                 | C. Unit. A Rottura   | Tensile strength  | 834         | 840         | 839         | 838 ✓    |
| <b>A (%)</b>                                    | Allungamento Perc.   | Percentage elongation after fracture                              | 18          | 18          | 18          | 18,1 ✓   |
| Z (%)   | Strizione Perc.      | Percentage reduction of area after fracture                       | 58          | 60          | 59          | 60       |

# Final result

---



## Material in line with requirements:

1) Grain size: 8,19 G (center)

2) Mechanical properties

✓  $R_{p0,2\%} = 746 \text{ Mpa}$

✓  $R_m = 838 \text{ Mpa}$

✓  $A_{tot} = 18\%$

3) Inclusional state according to ASTM E45 – Method D

# Powder Metallurgy

---



Powder Metallurgy is a continually and rapidly evolving manufacturing technology that includes most metallic and alloy materials, and a wide variety of shapes and dimensions.

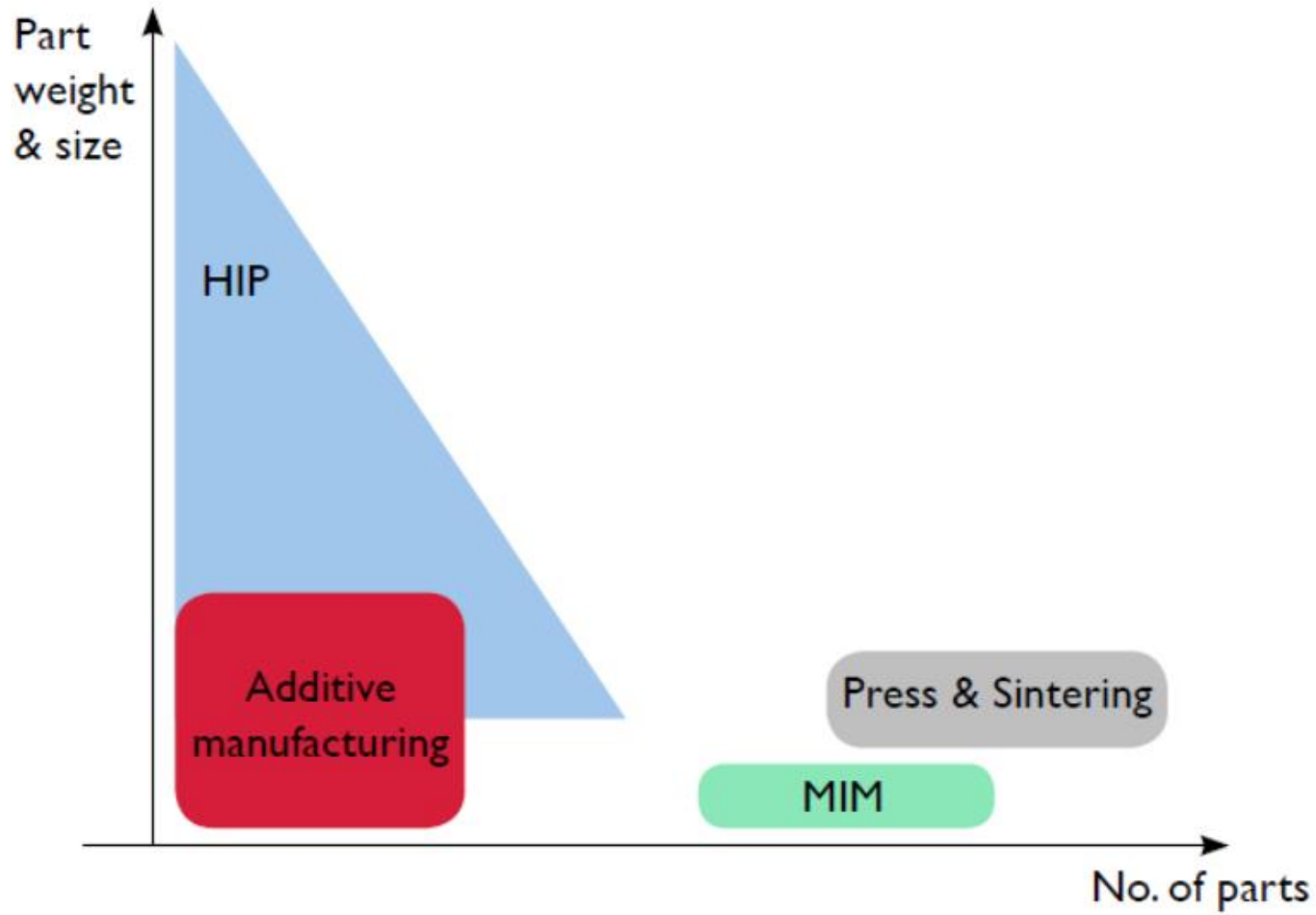
The European Market alone has an annual turnover of over 6,000 M€, with annual worldwide metal powder production exceeding 1 million tonnes.

The mostly PM technologies are:

- Press & Sintering
- Hot Isostatic Pressing (HIP)
- Metal Injection Moulding (MIM)
- Coatings for Surface Engineering
- Additive manufacturing (AM)



# Powder Metallurgy



Positioning map of various PM technologies according to part weight or size and production series



# Metal additive manufacturing

---

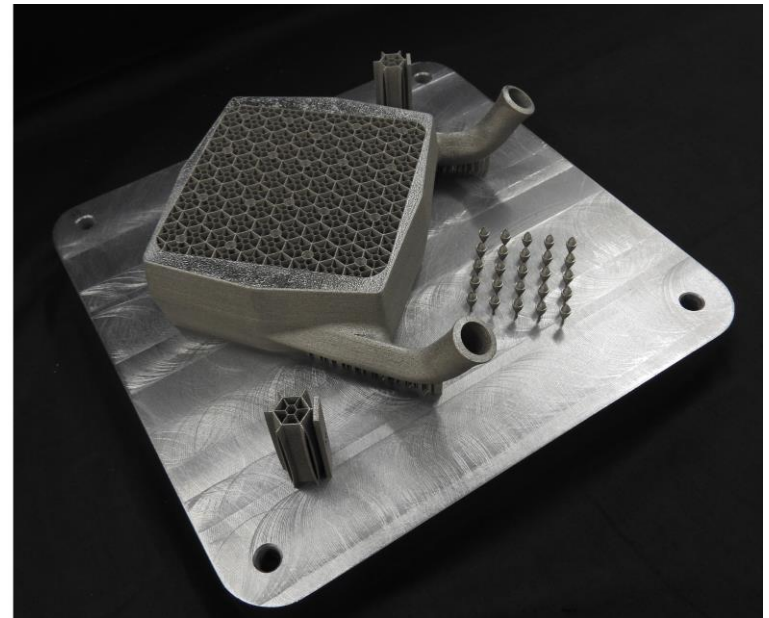


According to the ASTM standard F2792-10 “AM is the process of joining materials to make objects from 3D model data, usually layer upon layer, as opposed to subtractive manufacturing methodologies” such as machining.

# Design for AM



Topological optimization



Designed for SLM  
PoliMi compact motorcycle radiator

- ✓ Morphological freedom – use material where required
- ✓ Use of light-weight structures
- ✓ Less material, shorter process, lower cost

# AM key benefits

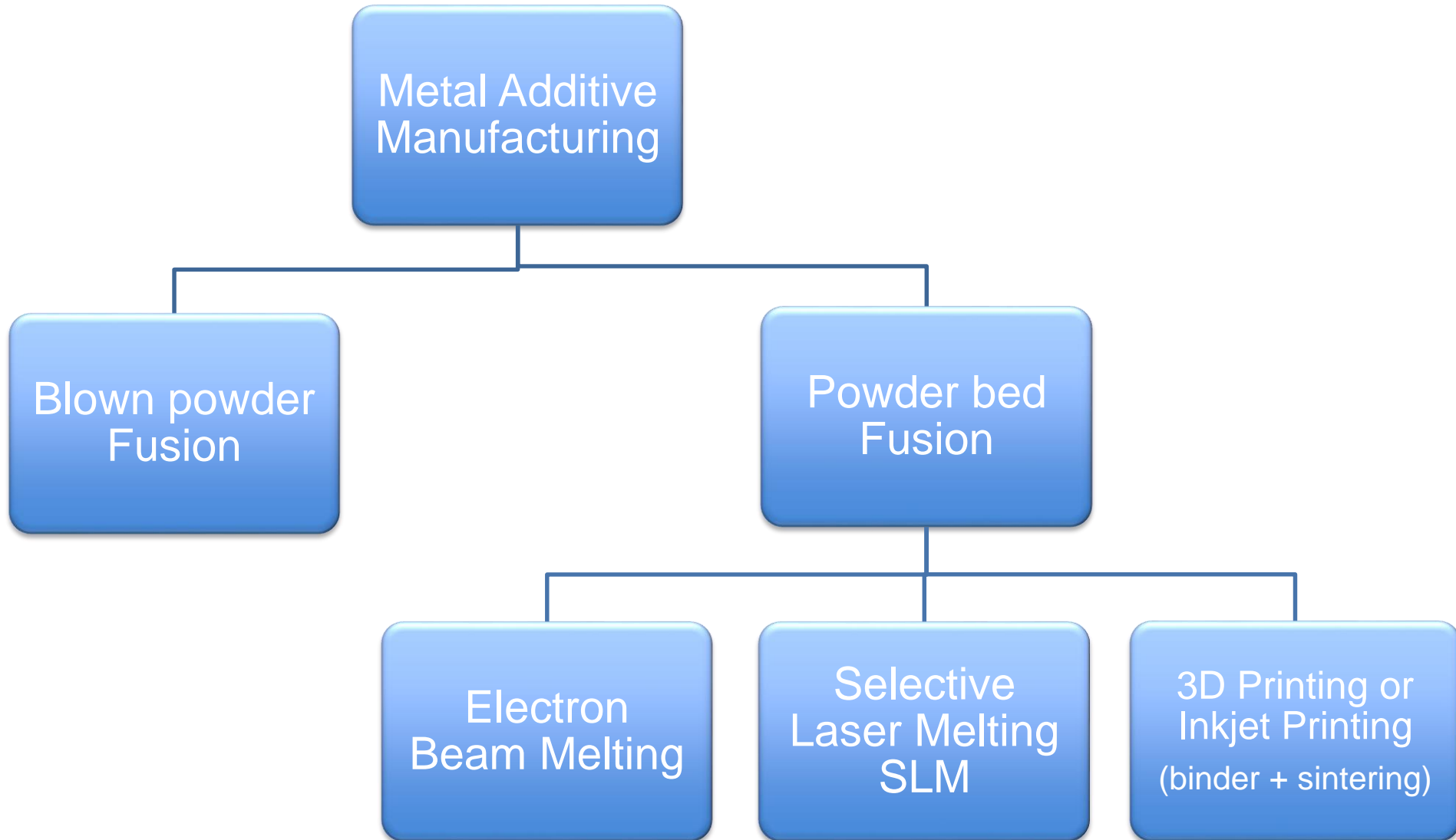
---



1. Increased **design freedom** versus conventional casting and machining;
2. **Light weight** structures, made possible either by the use of lattice design or by designing parts where material is only where it needs to be, without other constraints;
3. **New functions** such as complex internal channels or several parts built in one;
4. Net shape process meaning less raw material consumption, up to 25 times less versus machining, important in the case of expensive or difficult to machine alloys. The net shape capability helps creating complex parts in one step only thus reducing the number of assembly operations such as welding, brazing;
5. **No tools** needed, unlike other conventional metallurgy processes which require molds and metal forming or removal tools;
6. **Short production cycle time**: complex parts can be produced layer by layer in a few hours in additive machines. The total cycle time including post processing usually amounts to a few days or weeks and it is usually much shorter than conventional metallurgy processes which often require production cycles of several months.

# AM technologies

---



# Development of the metal alloy

---



The alloy design and the alloys development is necessary to define the best chemical composition for AM processes.

This will lead to a new proprietary alloy, very suitable for AM technologies.

This alloy design and development will be focused on aluminum alloys.

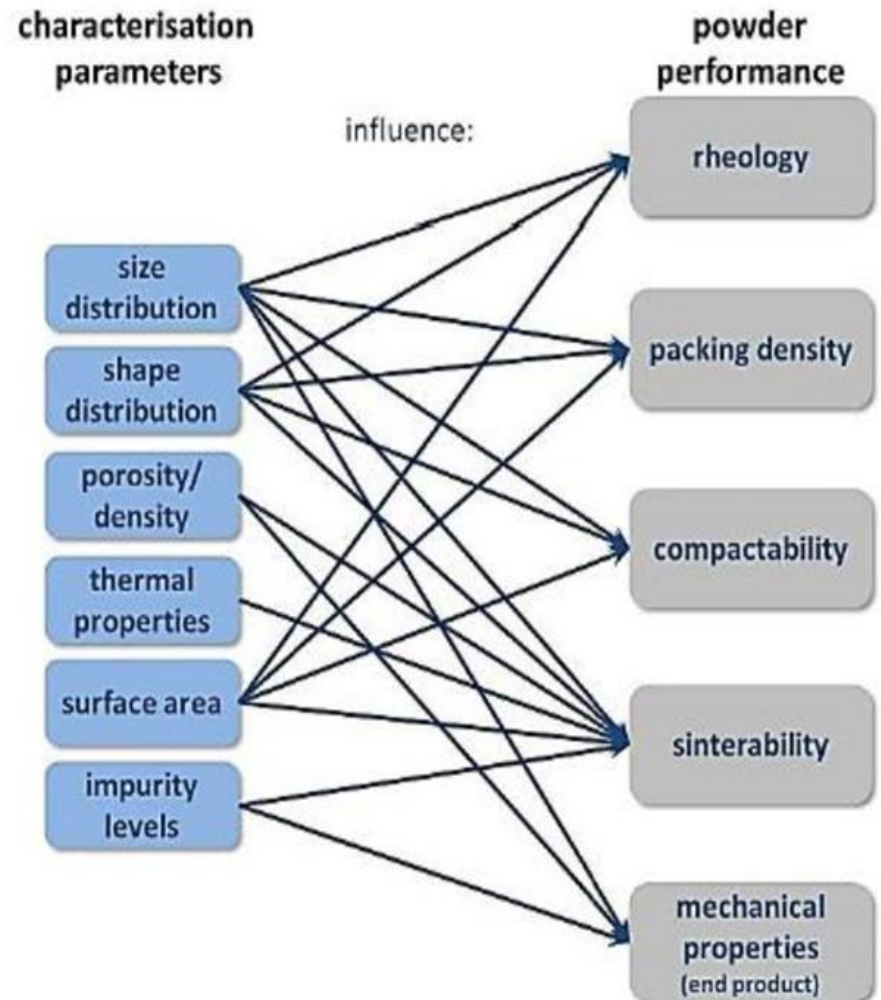
The commercial Al alloys actually available for AM processes have limited mechanical properties as shown in the Figure below (Metal AM - Metal powders – the raw materials). The market needs an increase of mechanical behavior for high demanding applications and this goal can be achieved by a proper new alloy design.



# Metal powder properties

Most relevant factors that play a important role and that have an effect o the finished product are:

- ✓ morphology;
- ✓ particle size distribution;
- ✓ density;
- ✓ porosity;
- ✓ thermal properties;
- ✓ surface properties;
- ✓ impurities.





# RINA for Powder Metallurgy & Additive Manufacturing

12 53 BES

# Expertise on PM & AM

---



In the last fifteen years RINA has developed a specific expertise and know how in the areas of:

- ✓ Coatings for Surface Engineering
- ✓ Additive Manufacturing (AM)
- ✓ Metal Powders production, for various applications including AM itself.



# Expertise on PM & AM

---



Relatively AM, RINA has developed its expertise with the purchase of two 3D printing machines.

Relatively powder production instead RINA with its VIGA plant (Vacuum Inert Gas Atomizer) have been **produced and developed** a significant amount of chemical compositions mainly of **steels**, superalloys, copper and aluminum alloys

# Actual projects

---



Actually RINA is currently supporting various clients in the activities of:

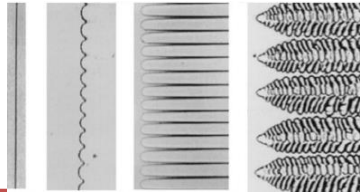
- ✓ alloy design and pilot production for new powders grade
- ✓ feasibility studies for the installation of new atomization plants
- ✓ market analysis
- ✓ roadmap for choice of the best technologies according to material/final application
- ✓ chemical, physical, metallurgical and mechanical characterization of AM products
- ✓ AM process yield optimization
- ✓ Powder Manufacturing process optimization / Expert on site
- ✓ Technical Support during Plant commissioning
- ✓ Training

# RINA activities within the AM value chain



Alloy design

Define new compositions with specific properties (e.g. Ni alloy with high creep resistance) to be processed by ALM

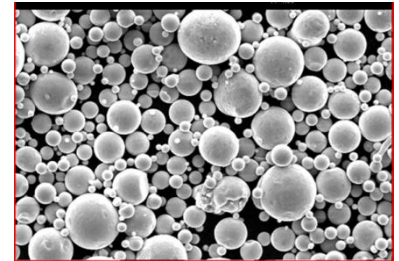


Thermodynamic model

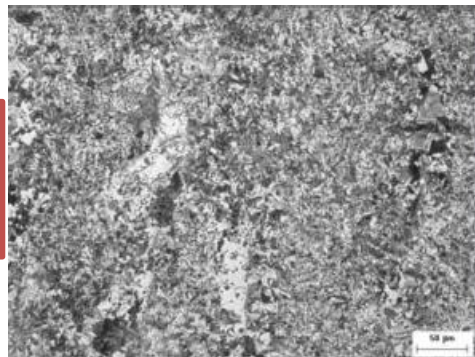
- ALM process conditions similar to welding (rapid solidification)
- Analysis of solidification mechanisms
- Microsegregation mode
- Definition of T solidus



Process Metallurgy (VIM-VIGA)



Heat treatments / post treatments

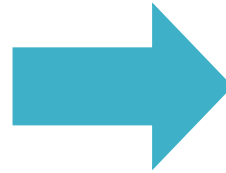


Microstructural and mechanical characterization

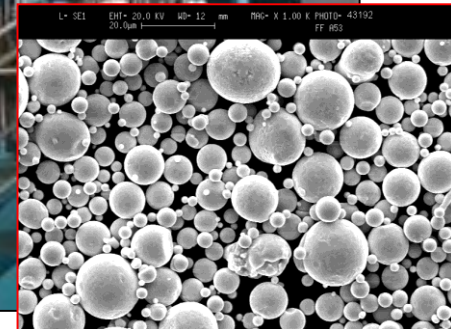
# Pilot Plant for powder manufacturing



## VACUUM INDUCTION MELTING



## VACUUM INDUCTION GAS ATOMISATION



# Metal powder produced at CSM



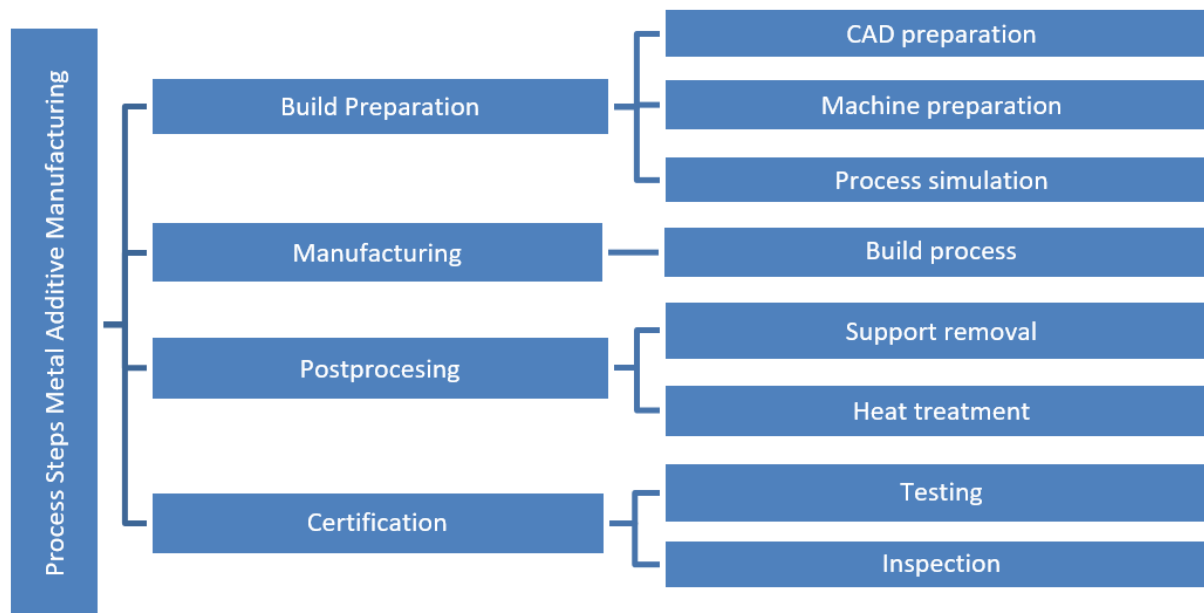
| Alloy Grade    | Tipology            | Applications   | Properties           | Market sector   |
|----------------|---------------------|----------------|----------------------|-----------------|
| Fe 5Al 10Si    | Steel               | Coating        | High conductivity    | Food            |
| Fe 21Cr 6Al    | Steel               | Coating        | Corrosion resistance | Aerospace       |
| Fe 25Cr 5Si    | Steel               | Coating        | Corrosion resistance | Aerospace       |
|                |                     |                |                      | Metal Injection |
| Fe based       | Steel               | Sintering      | Corrosion resistance | Moulding        |
| Fe based       | High Nitrogen Steel | Sintering      | Corrosion resistance | Bio Medical     |
| Fe based       | High Nitrogen Steel | Sintering      | High Temp resistance | Aerospace       |
| PM1000         | ODS Steel           | Sintering      | Mechanical strenght  | Aerospace       |
| PM2000         | ODS Steel           | Sintering      | Mechanical strenght  | Aerospace       |
| NiCoCrAlY      | Superalloys         | Coating        | High Temp resistance | Aerospace       |
| Ni based       | Superalloys         | Coating        | High Temp resistance | Tooling         |
| Inconel 718    | Superalloys         | Coating        | High Temp resistance | Aerospace       |
|                |                     | Additive Layer |                      |                 |
| Ni based       | Superalloys         | Manufacturing  | High Temp resistance | Aerospace       |
| Cu Oxygen free | Copper              | Testing        | High conductivity    | Energy          |
|                |                     | Additive Layer |                      |                 |
| CoCr           | Cobalt Based        | Manufacturing  | Corrosion resistance | Bio Medical     |
|                |                     | Additive Layer |                      |                 |
| Al Sc          | Al alloys           | Manufacturing  | High Temp resistance | Aerospace       |

# Qualification and certification process for AM materials and components



AM is a disruptive technology which has high potential in all the industrial sectors. Anyway it is a «new» technology and standardization as well as qualification and certification processes are still ongoing.

Quality and safety are involved in any step of the manufacturing process, from the design phase to the raw materials acquisition, from processing to finishing, so it needs a specific study of each step.



Example of processing steps for Metal AM manufacturing

# Qualification and certification process for AM materials and components



Qualification is different from certification

|                  | Qualification  | Certification   |
|------------------|--|---|
| Scope            | Process of evaluating a prototype design/material / product during the development/testing phase to determine whether it meets the specified requirements for that phase.      | The process of evaluating a material /product /component during or at the end of the development process / regular production to determine whether it satisfies specified technical requirements. |
| Objective        | To ensure that prototype meet the specified requirements to go to validation phase.  | To demonstrate that the product fulfills its intended use when placed in its intended environment.  |
| Evaluation items | Feasibility reports, requirement specs, design specs, test cases, procedure qualification, process parameters, etc.  | The actual product  |
| Activities       | <ul style="list-style-type: none"><li>— reviews</li><li>— audits / site-visits</li><li>— witness testing</li><li>— compliance statement</li><li>— facility approvals</li></ul> | <ul style="list-style-type: none"><li>— inspections</li><li>— testing</li><li>— product certification</li></ul>   |

# Qualification and certification process for AM materials and components

---



The certification Pathway can be divided in three phases:

## Phase 1: Procedure qualification phase

Manufacturers or end users run qualifications/ the proof of concept to prove that they have feasible technology /products.

## Phase 2: Approval phase

Manufacturer's or end user's design or manufacturing capabilities and process controls are assessed to determine if the manufacturer can produce specific grades or types of materials that conform to the Rules

## Phase 3: Certification phase

Manufacturers/end users require a certification authority to certify material or products from regular production, either as individual parts or in batches, depending on the certification requirement of those parts. Material certification and component /product certification are relevant activities in this phase.







Agenzia nazionale per le nuove tecnologie,  
l'energia e lo sviluppo economico sostenibile

# Termomeccanica di nocciolo

## Analisi vibrazionale della barretta

*Dipartimento di Ingegneria Astronautica, Elettrica ed Energetica  
Università di Roma 'La Sapienza' - San Pietro in Vincoli  
14-15 Giugno, 2018*

**Alessandro Poggianti – ENEA**



1101 0110 1100  
0101 0010 1101  
0001 0110 1110  
1101 0010 1101  
1111 1010 0000



# Contesto del lavoro

## Riferimento

L'intera Linea Progettuale 2 è dedicata all'avanzamento della tecnologia del **LFR**

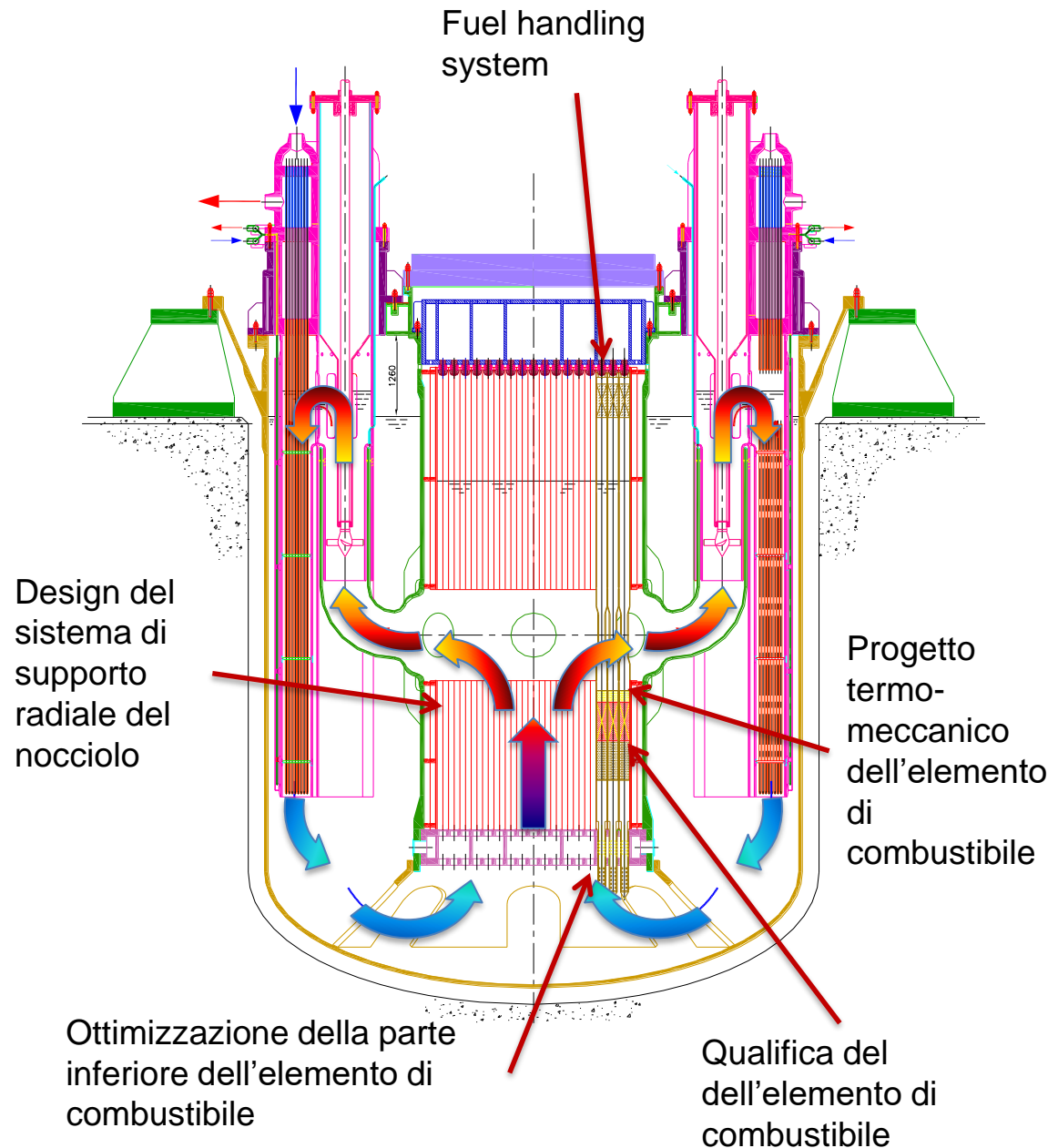
Tutte le attività vertono su **ALFRED**, assunto a riferimento nella sua qualità di **dimostratore** della tecnologia **LFR**.

Fra le attività condotte nell'ambito dell'AdP, un blocco considerevole è dedicato al **progetto di nocciolo**, in particolare:

- sviluppo, revisione e affinamento del progetto;
- sviluppo, validazione ed applicazione di metodologie e strumenti di analisi a supporto della progettazione.

## ALFRED core design: cosa c'è da fare

La maggior parte dei punti aperti sul progetto di nocciolo riguardano il corretto dimensionamento (e, qualora richiesto, la rivisitazione) dei principali componenti del nocciolo, avendo come riferimento ultimo la qualifica dell'elemento di combustibile, del sistema di supporto del nocciolo e del sistema di movimentazione degli elementi freschi ed esausti per e da il nocciolo.



# Analisi vibrazionale

## Corner rod cooling and flow induced vibration in an ALFRED fuel assembly – FALCON doc. NRG-23591/16.140918

- Dati geometrici
- Proprietà fisiche di fluido e barretta
- Temperature del fluido
- Possibili risonanze a 400Hz e 10.2 Hz

### **Ipotesi**

- Spacer posizionato a 100 mm dalla zona attiva

### **Aspetti da investigare**

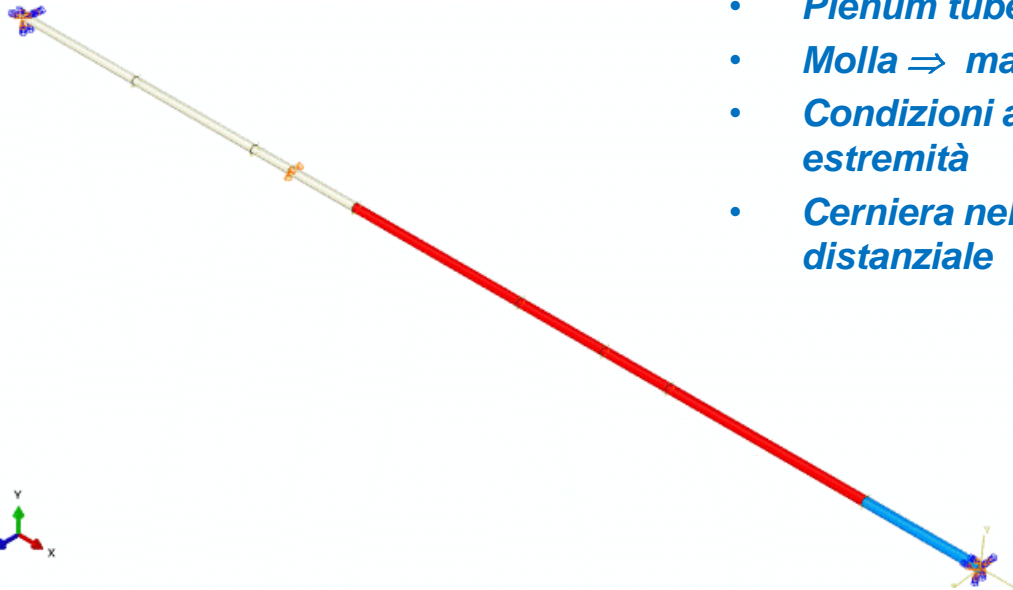
- Frequenze naturali della barretta
- Vibrazione della barretta immersa nel fluido
- Influenza delle barrette vicine
- Valutazione di possibili urti tra le barrette

# Modello Elementi finiti barretta

## Barretta



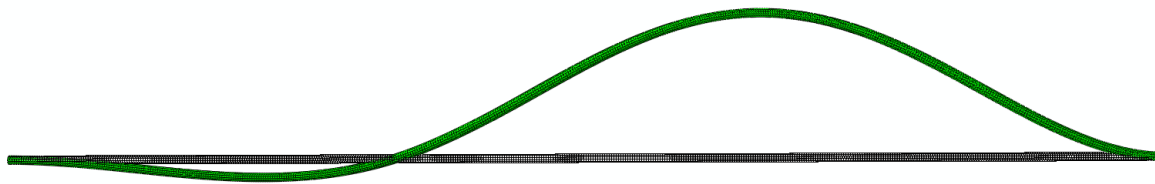
- *Elementi 'Shell' per la guaina*
- *Pastiglie combustibile  $\Rightarrow$  masse*
- *Plenum tube  $\Rightarrow$  massa + rigidezza*
- *Molla  $\Rightarrow$  massa*
- *Condizioni al contorno  $\Rightarrow$  incastro alee estremità*
- *Cerniera nel punto di contatto cn il distanziale*



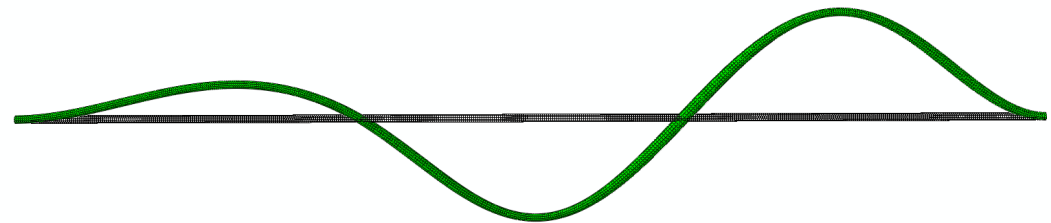
# Analisi modale

## Forme modali e frequenze

| Mode | Hz   |
|------|------|
| 1    | 30.0 |
| 2    | 83.5 |
| 3    | 163  |
| 4    | 220  |
| 5    | 302  |
| 6    | 455  |



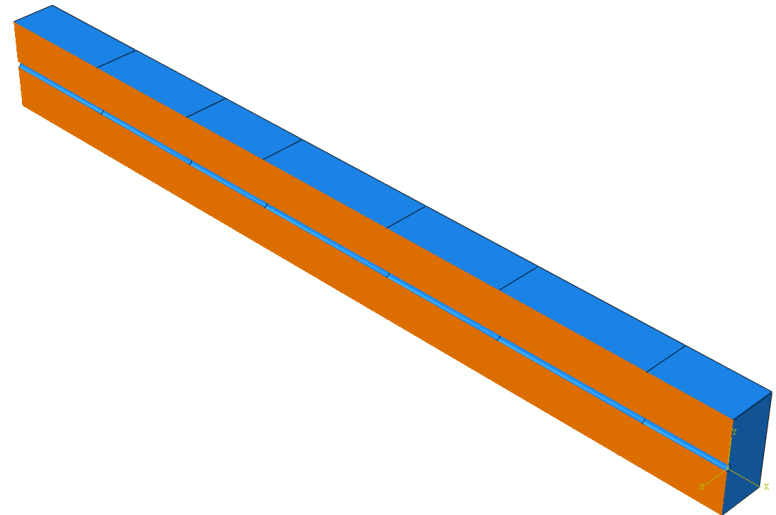
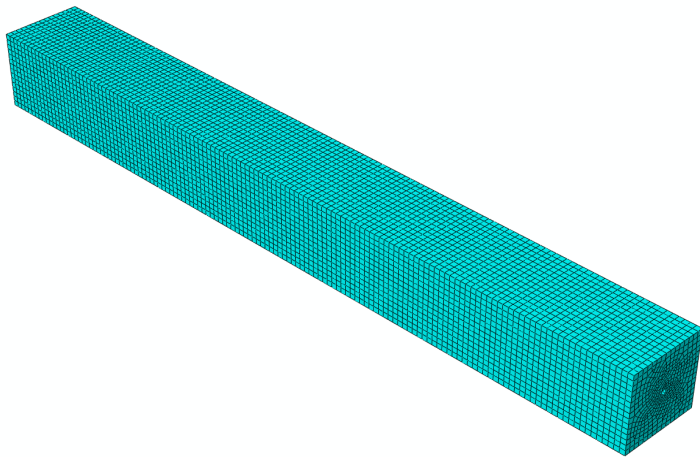
Solo struttura  
ODB: Single-pin-Freq.odb Abaqus/Standard 3DEXPERIENCE R2016x Tue Sep 19 12:13:57  
Step: Freq  
Mode 1: Value = 35505. Freq = 29.989 (cycles/time)  
Deformed Var: U Deformation Scale Factor: +1.370e-01



Solo struttura  
ODB: Single-pin-Freq.odb Abaqus/Standard 3DEXPERIENCE R2016x Tue Sep 19 12:13:57 ora legale Europa occidentale 2017  
Step: Freq  
Mode 3: Value = 2.75286E+05 Freq = 83.505 (cycles/time)  
Deformed Var: U Deformation Scale Factor: +1.370e-01

# Analisi dinamica della barretta immersa nel fluido

- *L'analisi modale non tiene in conto la presenza del fluido attorno alla barretta*
- *E' stato costruito un nuovo modello che riproduce anche una parte del fluido attorno alla barretta.*
- *La zona di fluido modellata ha dimensioni 150x150mm*





# ABAQUS Co-esecuzione

- *Tutte le analisi sono state fatte usando la tecnica di co-simulazione fornita dal codice Abaqus.*
- *La tecnica di co-simulazione di Abaqus consente di risolvere problemi complessi di interazione fluido-struttura (FSI) accoppiando il modulo Abaqus/Standard al modulo Abaqus che è un programma computazionale di analisi fluido dinamica (CFD).*
- *Abaqus/Standard risolve il problema strutturale e Abaqus CFD risolve il dominio del fluido.*

# Vibrazione della barretta immersa in piombo

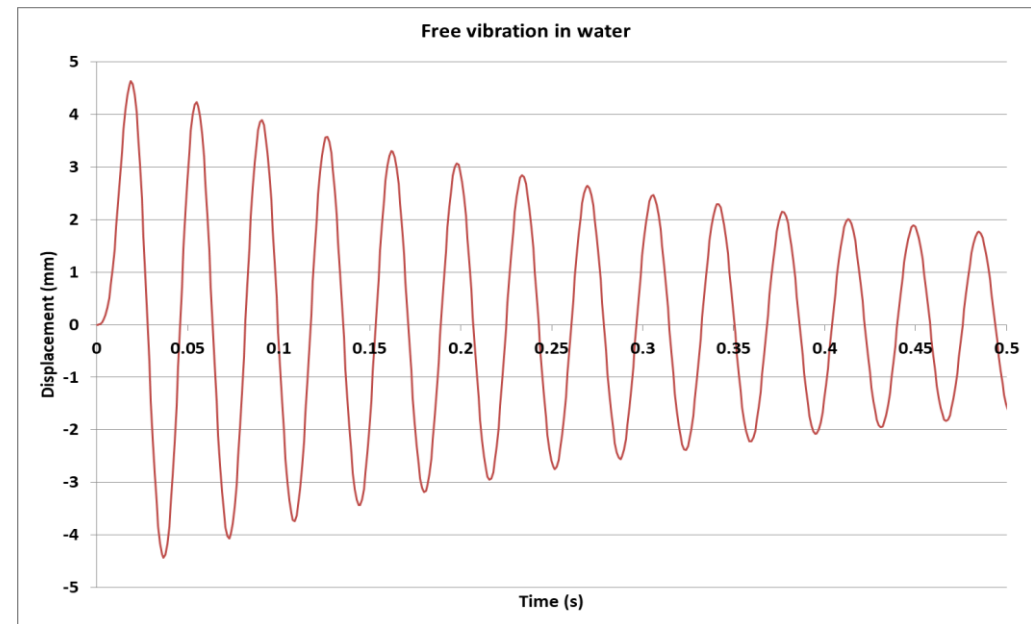
- *Il fluido intorno alla barretta è modellato come piombo fuso*
- *E' stato applicato un impulso di accelerazione all'intera barretta*
- *La barretta viene lasciata libera di vibrare sulla sua prima frequenza naturale*

## **Risultati attesi:**

- *Frequenza più bassa di quella calcolata con analisi modale (30.3 Hz)*
- *Smorzamento non trascurabile*

## **Risultati ottenuti**

- *Frequenza 18.5 Hz*
- *Smorzamento 2.8%*
- *Gli spostamenti non sono realistici perché il carico imposto serve solo per valutare il modello*



**La prima frequenza della barretta immersa in piombo risulta abbastanza lontana dalla possibile risonanza a 10.2 Hz**

# Individuazione delle frequenze dei modi superiori

*Il metodo usato fino a questo punto è in grado di individuare la prima frequenza naturale, ma non riesce ad evidenziare i modi superiori*

- Per questo si è deciso di utilizzare la scomposizione in serie di Fourier dei risultati ottenuti (segnale in uscita) sia in termini di accelerazione sia in termini di spostamento.
- Per ottenere una scansione in frequenza del segnale di uscita, con una definizione tale da evidenziare le frequenze fino a circa 400 Hz, si è deciso di campionare a  $2.5e-4$  s in modo da ottenere 10 punti per ogni periodo, alla frequenza di 400Hz.
- Del segnale in uscita sono stati selezionati 4096 punti che corrispondono a circa 1s di acquisizione.

# Individuazione delle frequenze dei modi superiori

*Prima di iniziare questa fase, il modello della barretta è stato rivisto per migliorare alcuni aspetti.*

*Questo ha causato un piccolo cambiamento nel valore delle frequenze calcolate con l'analisi modale, i cui valori aggiornati sono riportati di seguito*

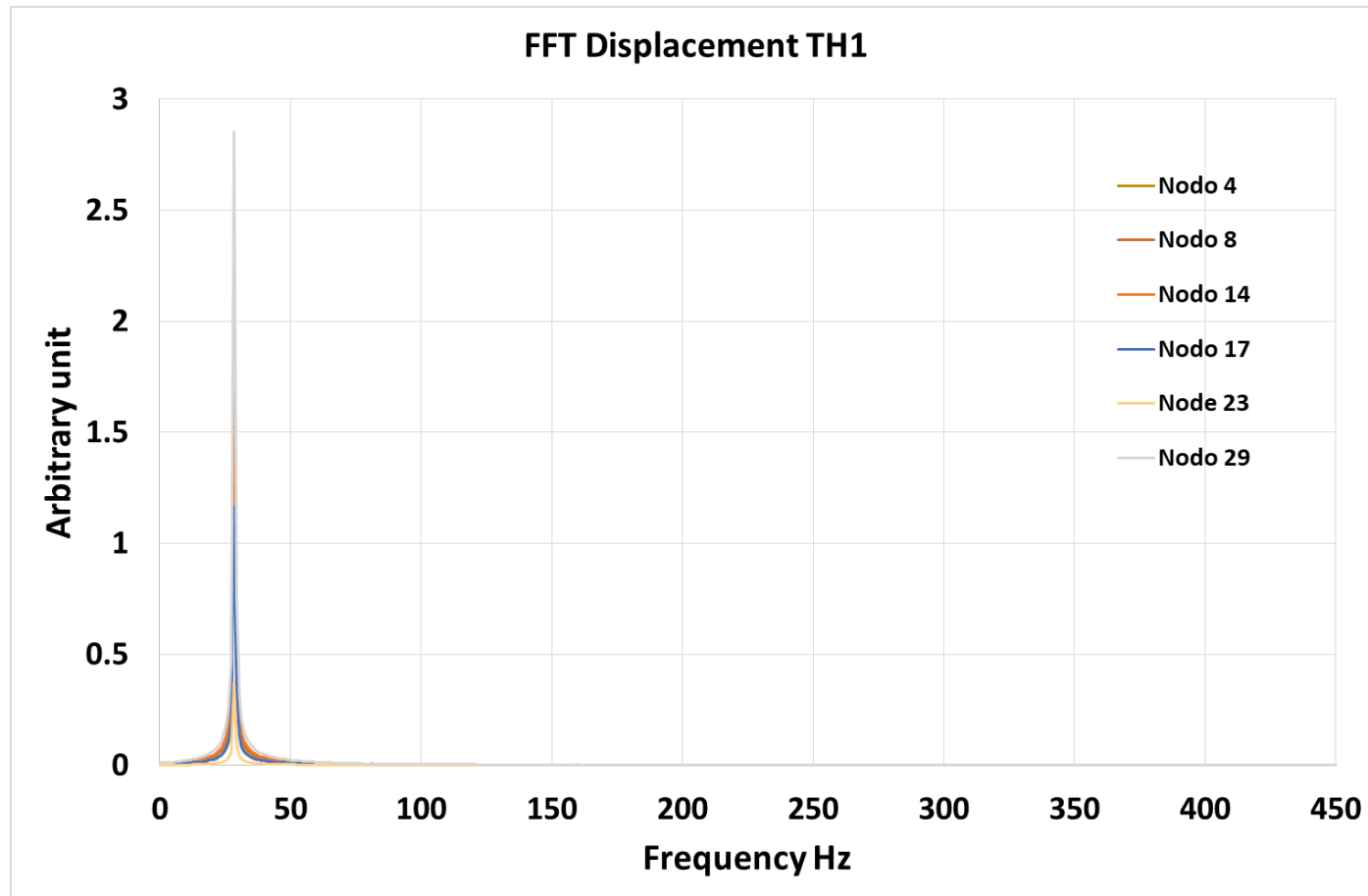
| Frequency (Hz) |
|----------------|
| Modal Analysis |
| 28.5           |
| 81.5           |
| 161            |
| 210            |
| 297            |
| 450            |

# Individuazione delle frequenze dei modi superiori

*Inizialmente sono state ripetute le analisi eseguite negli step precedenti per verificare che la prima frequenza propria, estratta con questo metodo coincida con quella calcolata con l'analisi modale*

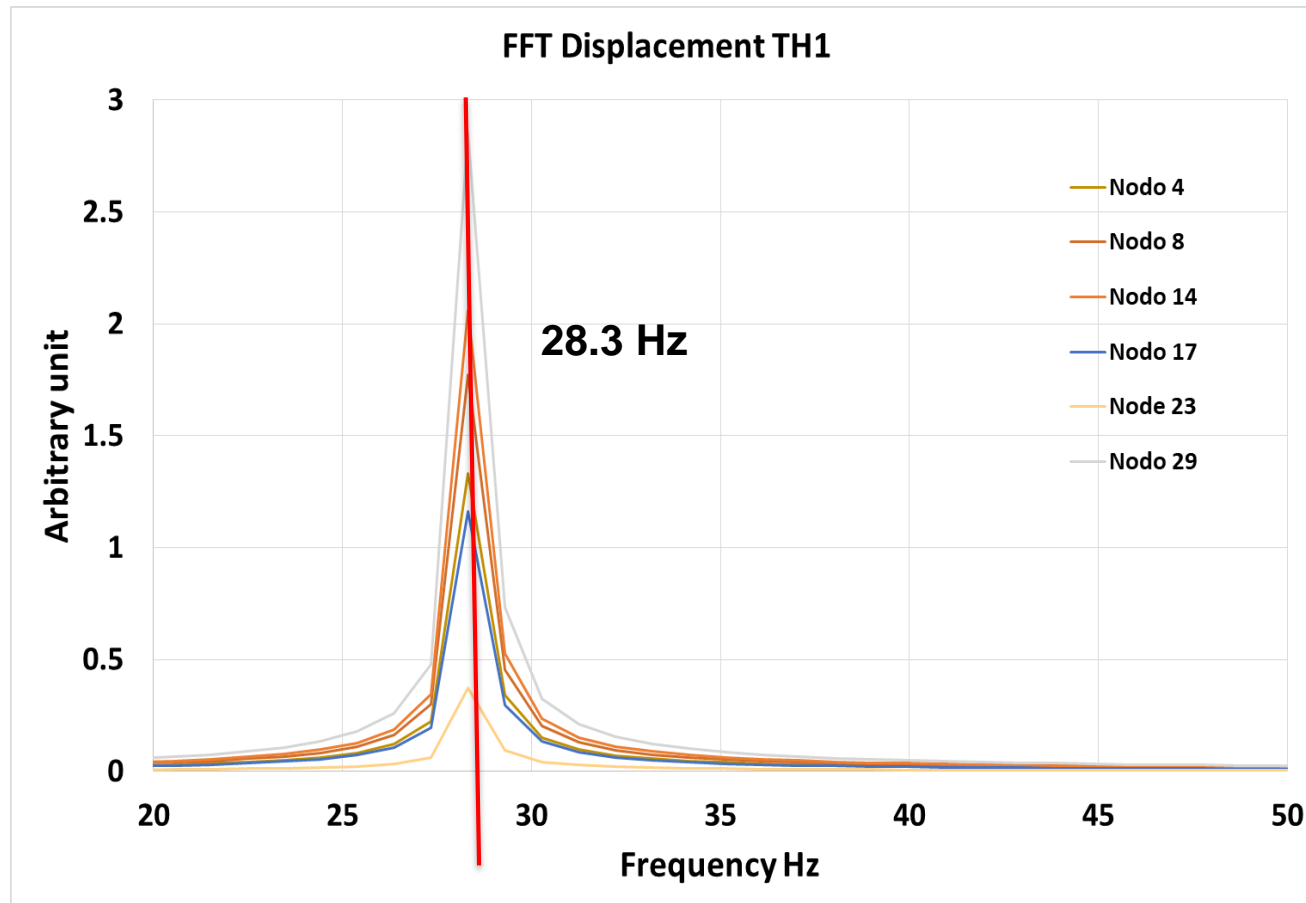
*I risultati usati per la decomposizione sono quelli ottenuti applicando un impulso di accelerazione a tutta la barretta che viene poi lasciata libera di vibrare (eccitazione "kick").*

# Individuazione delle frequenze dei modi superiori



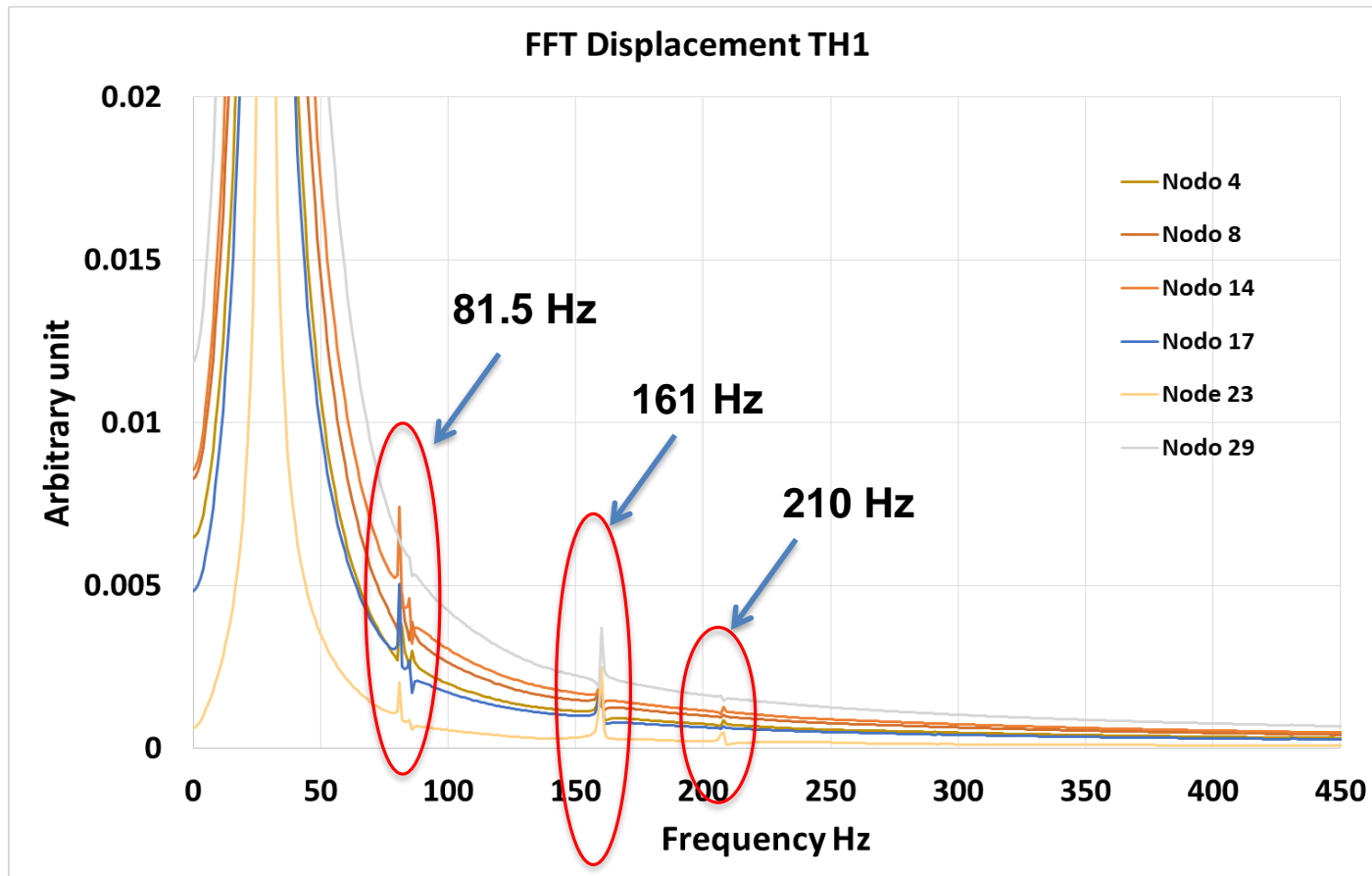
*Decomposizione in serie di Fourier dello spostamento in alcuni punti della barretta  
eccitazione "kick"*

# Individuazione delle frequenze dei modi superiori



*Decomposizione in serie di Fourier dello spostamento in alcuni punti della barretta  
eccitazione "kick"*

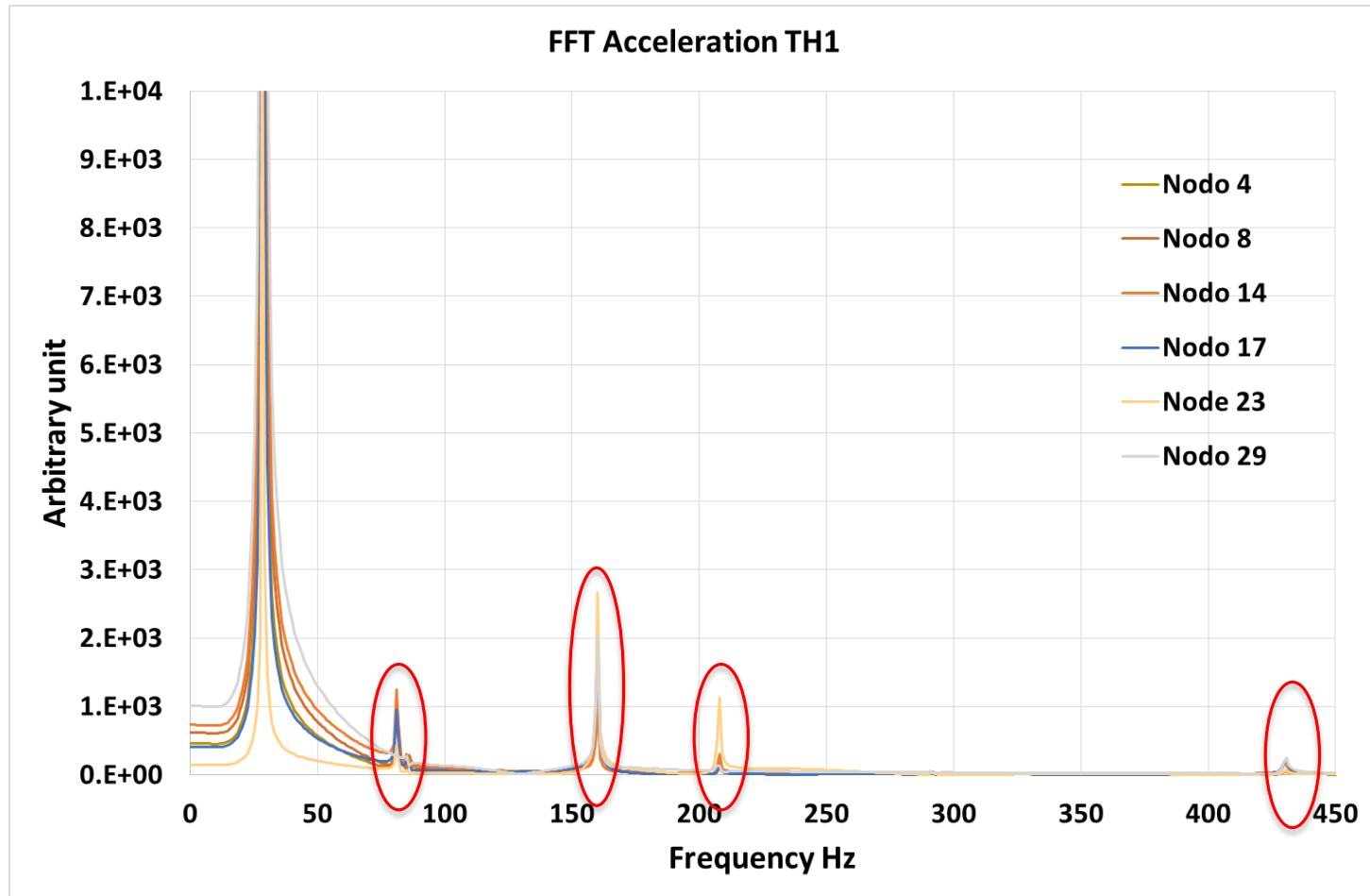
# Individuazione delle frequenze dei modi superiori



*Decomposizione in serie di Fourier dello spostamento in alcuni punti della barretta eccitazione "kick"*



# Individuazione delle frequenze dei modi superiori



*Decomposizione in serie di Fourier dell'accelerazione in alcuni punti della barretta eccitazione "kick"*

# Individuazione delle frequenze dei modi superiori

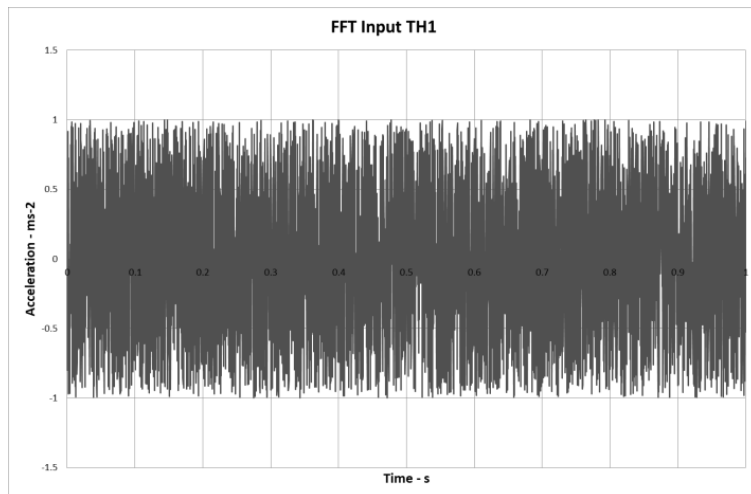
*La prima frequenza, così calcolata risulta 28.3Hz in ottimo accordo con quella calcolata con l'analisi modale.*

*Per mettere ancora più in evidenza le frequenze superiori occorre però un impulso sulla barretta che sia in grado di eccitare tutte le frequenze nel range considerato (0-400 Hz)*

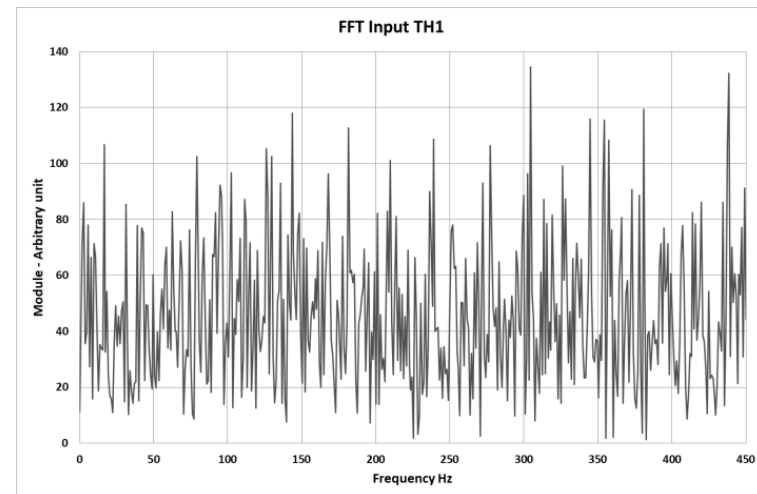
# Individuazione delle frequenze dei modi superiori

*Time history generate con diverse strategie:*

- *Time history di rumore bianco (eccitazione "white noise"), ottenuta tramite la generazione di numeri casuali.*
- *Lo spettro di queste time history contiene tutte le frequenze, ma con ampiezza casuale*
- *Per avere risultati non influenzati dalla forma del singolo spettro, viene utilizzata la media dei risultati ottenuti con tre diverse time history*



Time history rumore bianco

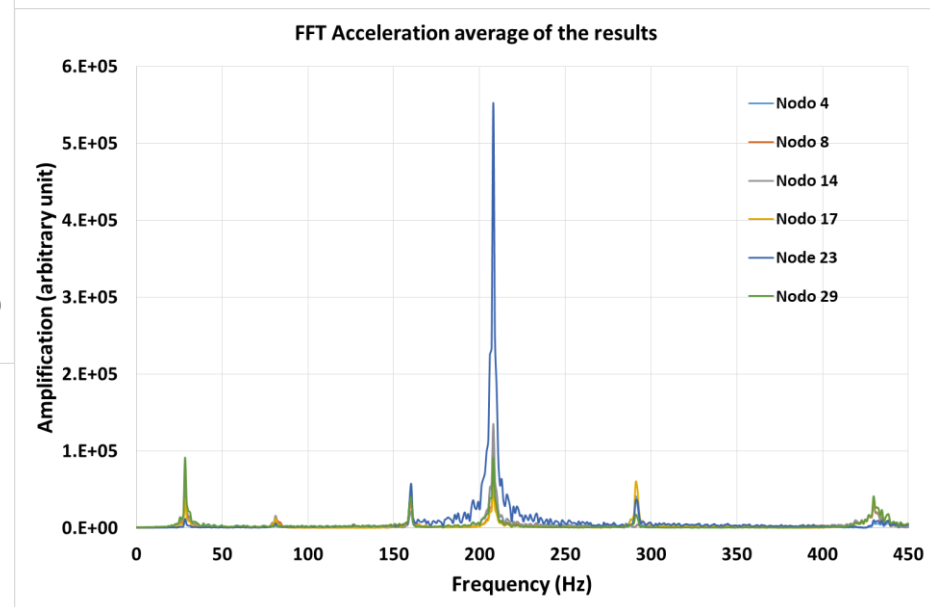
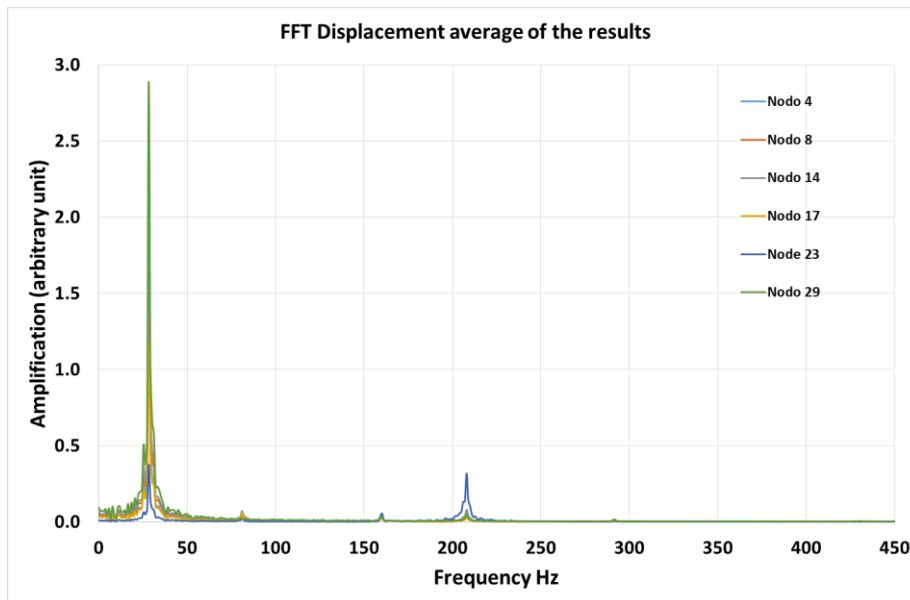


Spettro rumore bianco

# Individuazione delle frequenze dei modi superiori

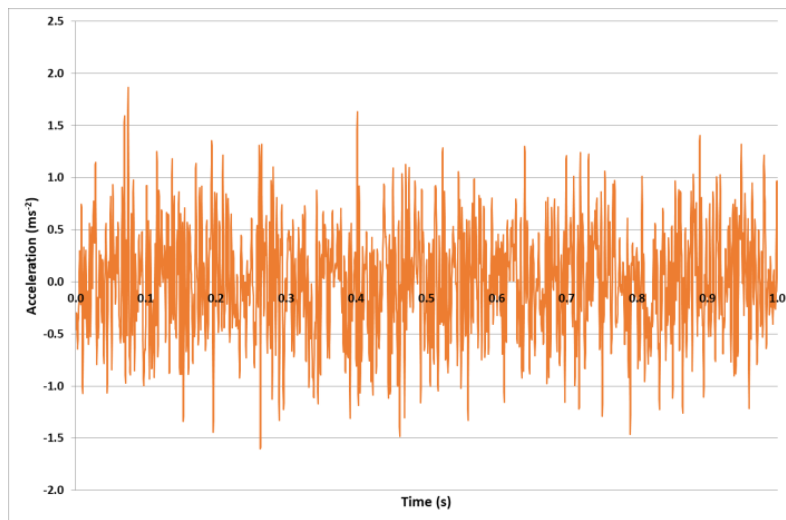
*Risultati time history eccitazione "white noise"*

*Si nota che, l'amplificazione negli spostamenti è meno evidente alle alte frequenze perché, naturalmente vibrazioni ad alta frequenza non consentono spostamenti elevati.*

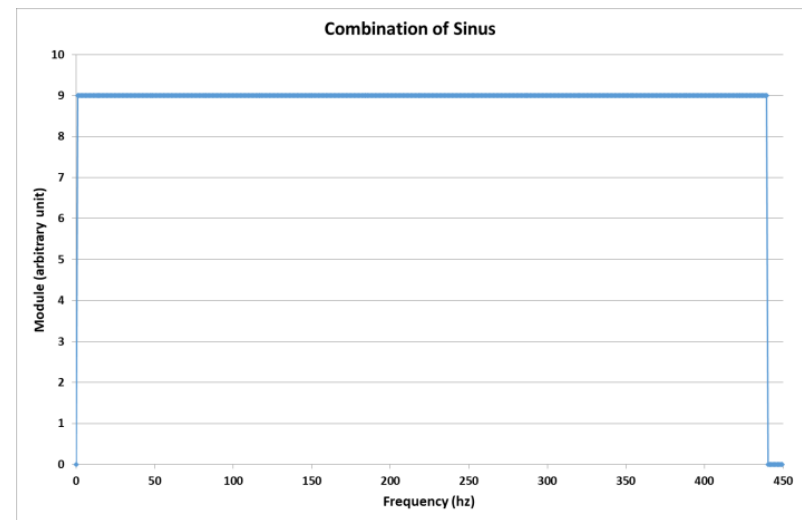


# Individuazione delle frequenze dei modi superiori

*Time history generata come somma di sinusoidi con frequenze diverse, stessa amplificazione ma fase diversa (eccitazione “sinus”). In questo caso lo spettro che si ottiene è uniforme nell’intervallo di frequenze considerato e non occorre generare più time history.*



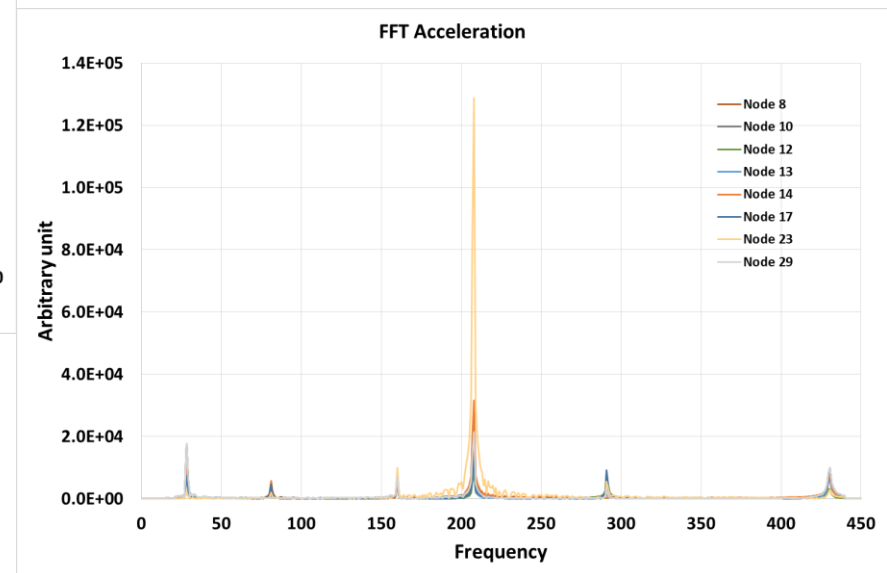
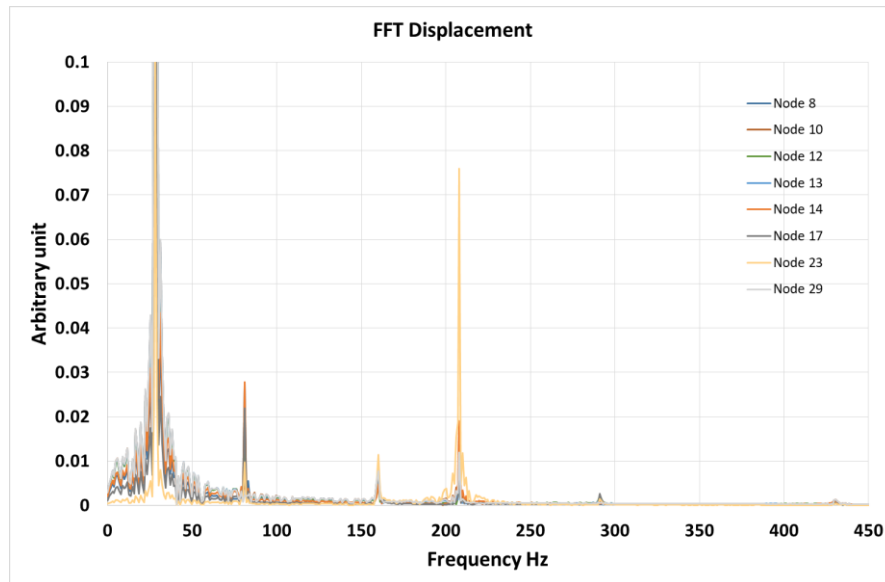
Time history somma di sinusoidi



Spettro somma di sinusoidi

# Individuazione delle frequenze dei modi superiori

## Risultati time history eccitazione "sinus"



# Individuazione delle frequenze dei modi superiori

## *Confronto risultati*

| Frequency (Hz) |                       |
|----------------|-----------------------|
| Modal Analysis | Time history analysis |
| 28.48          | 28.32                 |
| 81.45          | 81.05                 |
| 160.8          | 160.2                 |
| 209.8          | 208.0                 |
| 297.3          | 291.0                 |
| 449.9          | 429.7                 |

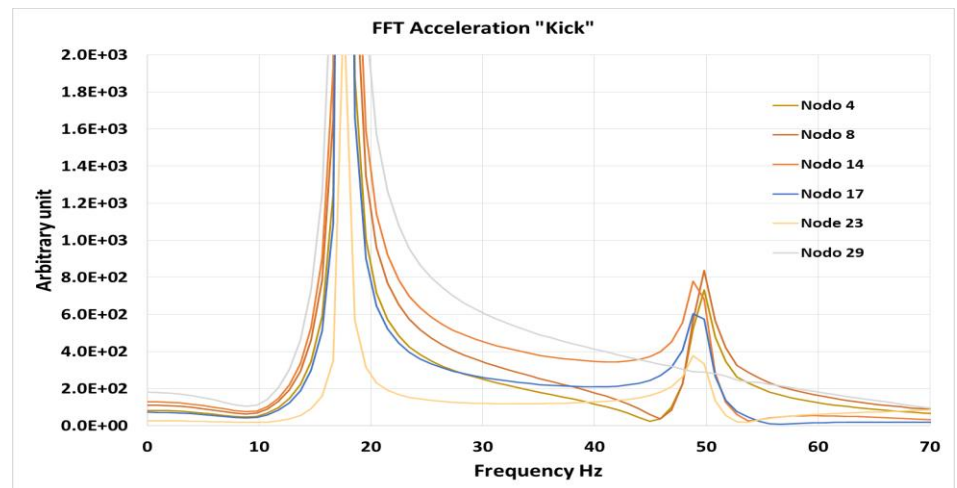
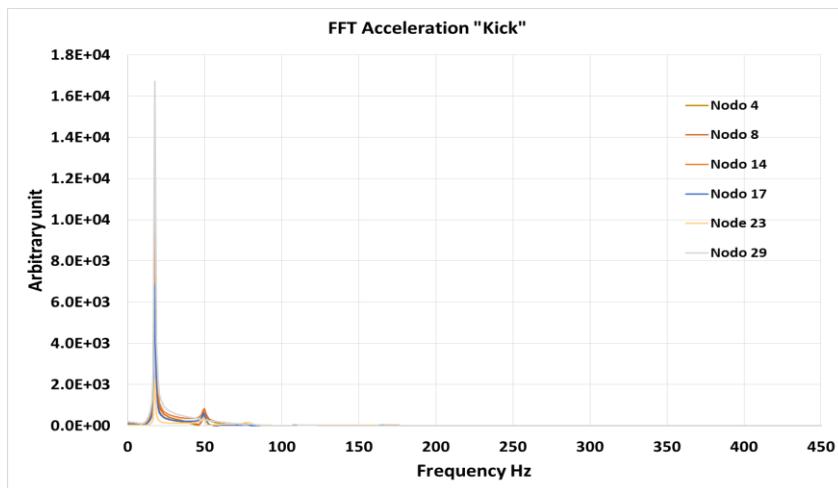
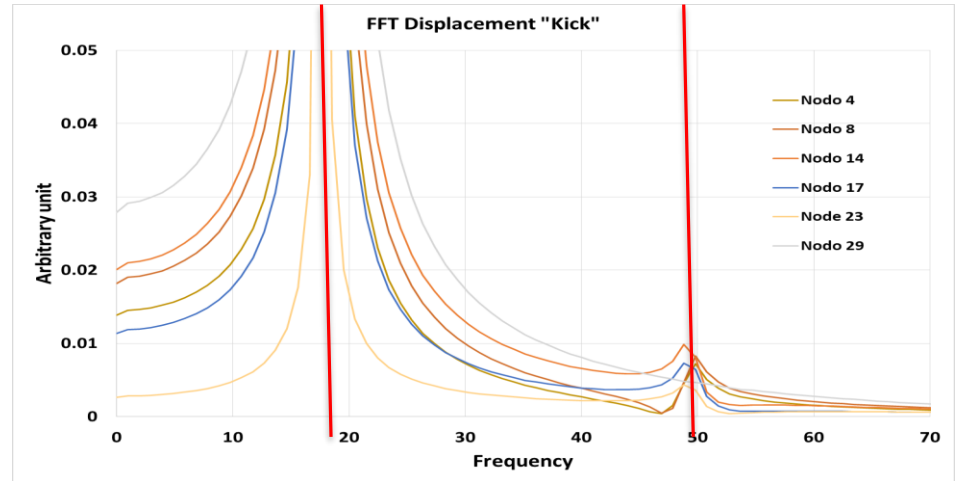
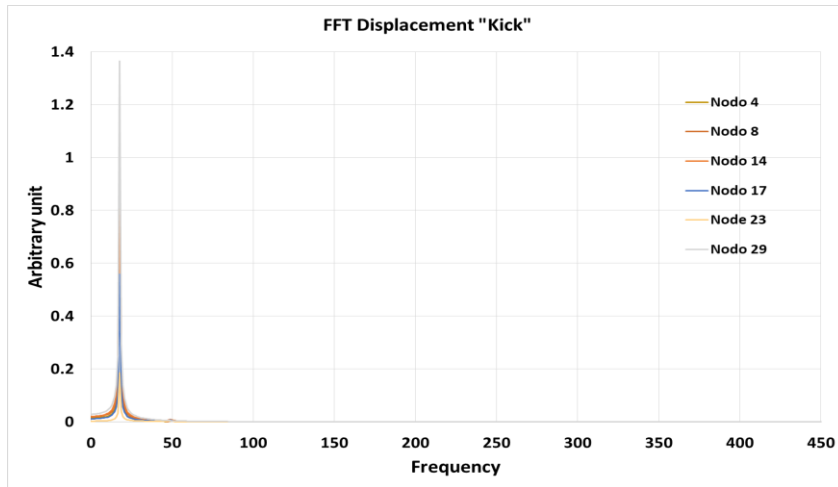
# Individuazione delle frequenze dei modi superiori barretta immersa in piombo

- *Ottenuta la conferma che con questo metodo è possibile evidenziare le frequenze più alte, si applica la stessa procedura alla barretta singola, immersa in piombo.*
- *Oltre alle time history prima specificate si prendono in considerazione anche i risultati ottenuti applicando un impulso di accelerazione.*



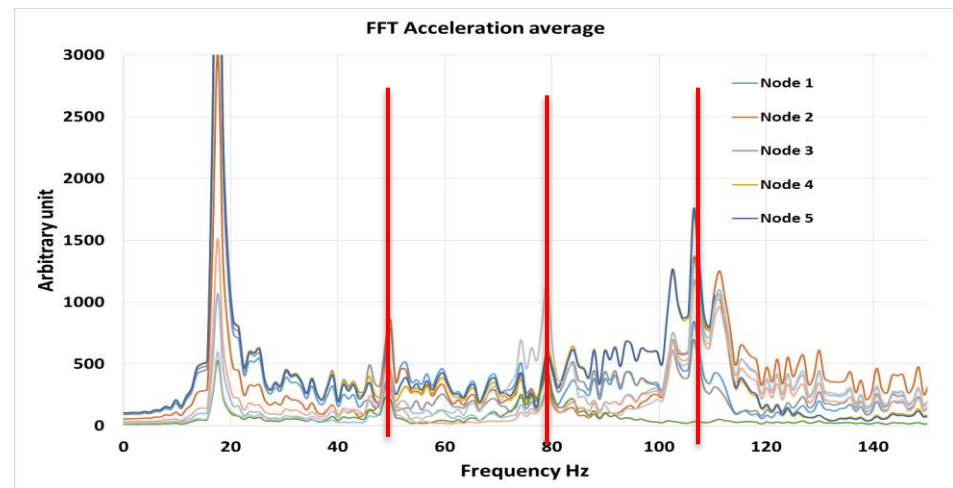
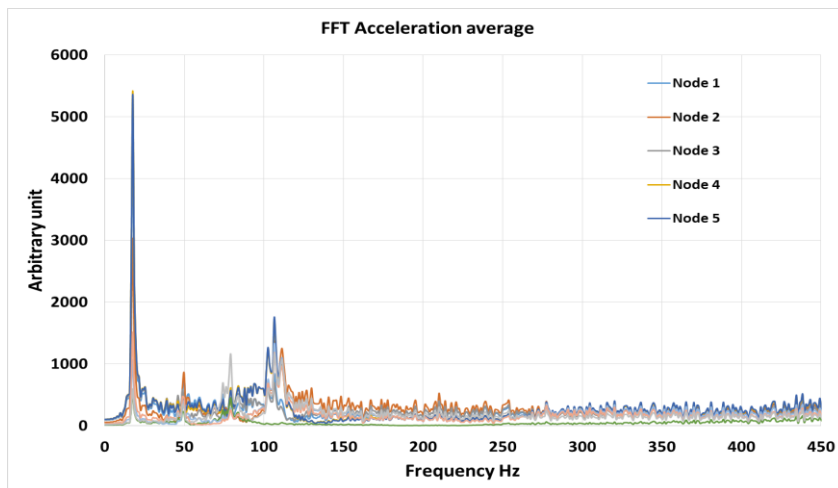
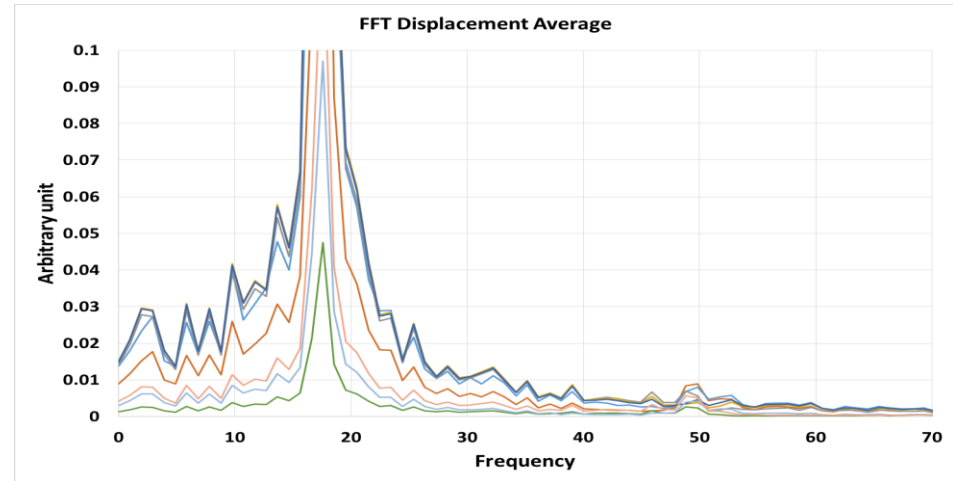
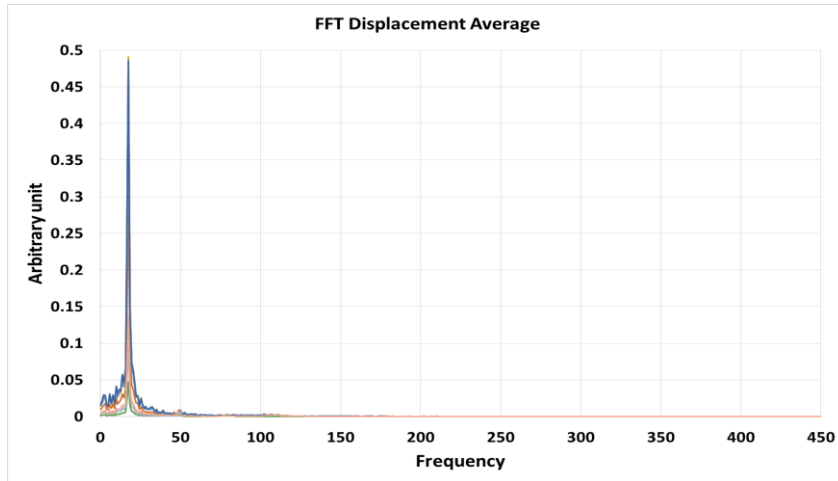
# Individuazione delle frequenze dei modi superiori barretta immersa in piombo

## Risultati time history eccitazione 'kick'



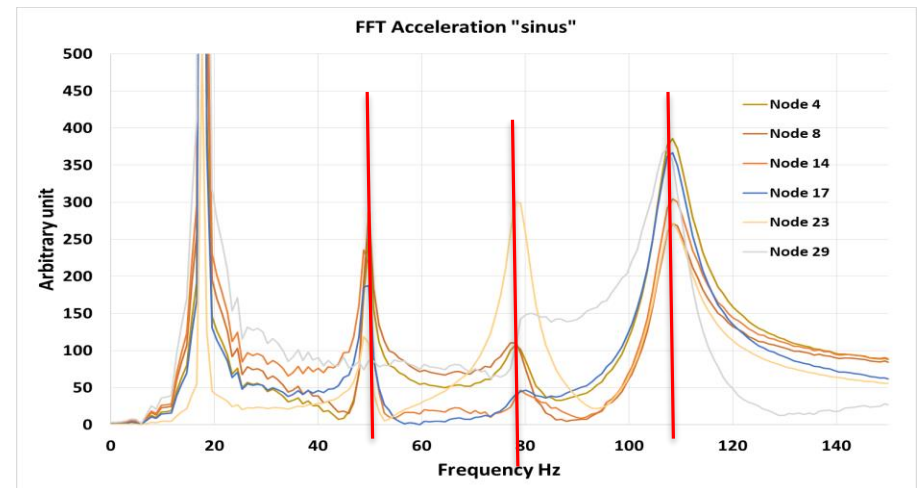
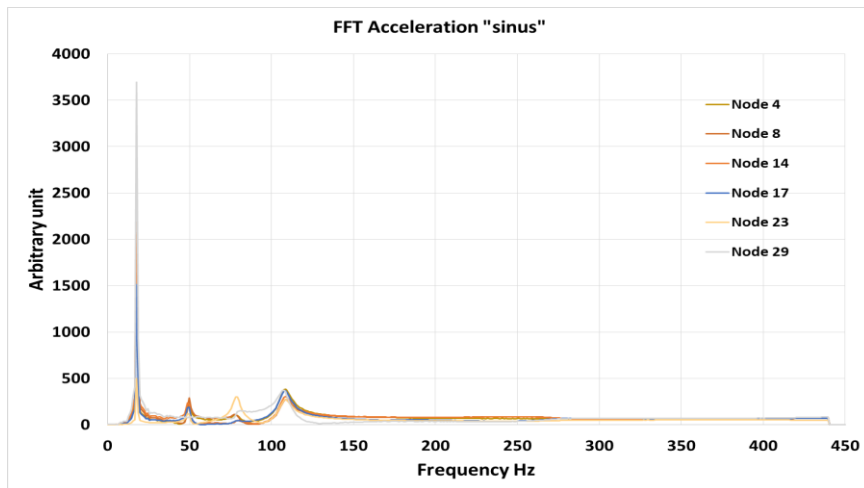
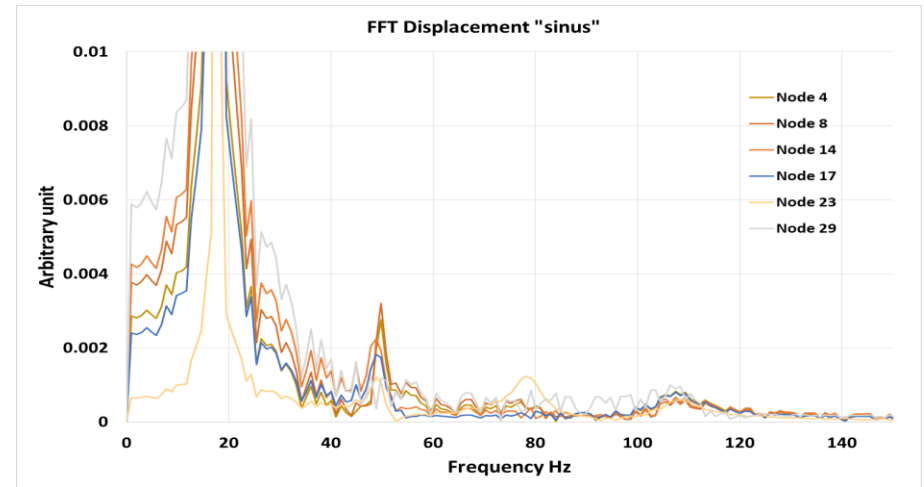
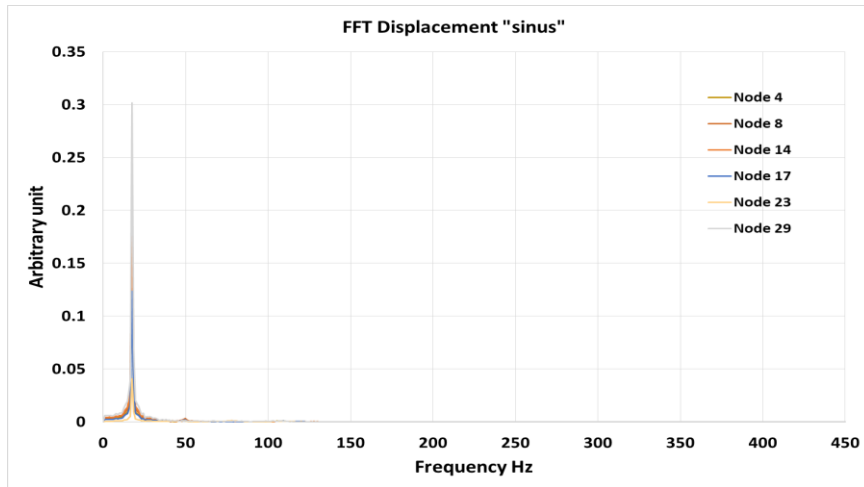
# Individuazione delle frequenze dei modi superiori barretta immersa in piombo

*Risultati time history eccitazione 'with noise'*



# Individuazione delle frequenze dei modi superiori barretta immersa in piombo

## Risultati time history eccitazione 'sinus'



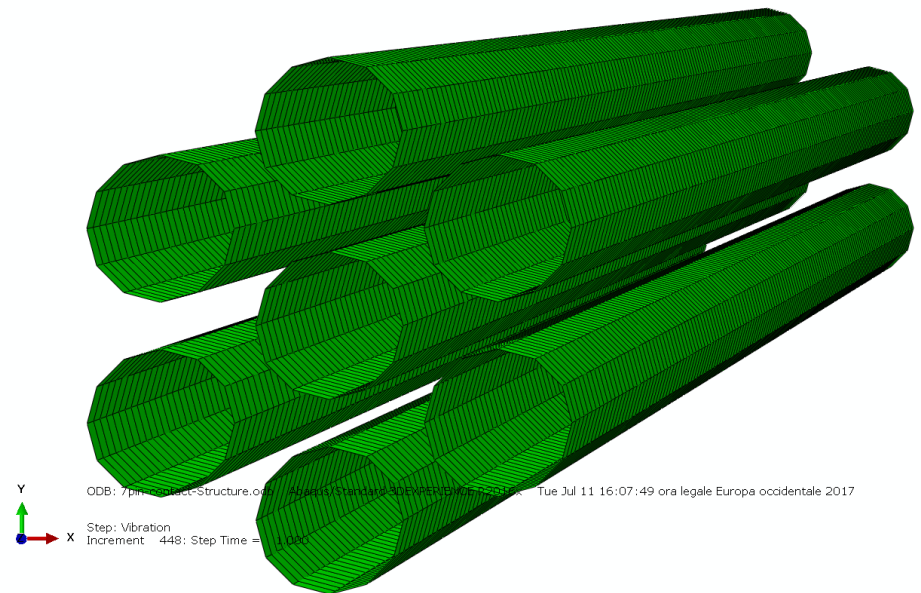
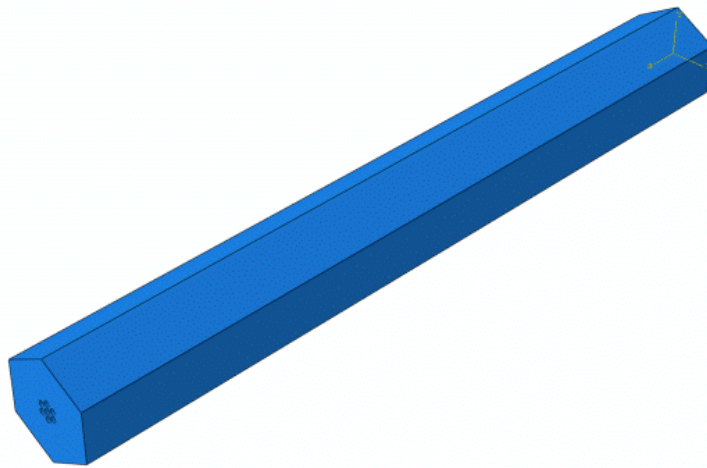
# Individuazione delle frequenze dei modi superiori barretta immersa in piombo

## *Risultati*

| Frequency (Hz)        |
|-----------------------|
| Time history analysis |
| 17.6                  |
| 49.8                  |
| 78.1                  |
| 107.4                 |

# Analisi dinamica di un gruppo di barrette immerse in piombo

- Lo scopo è quello di studiare l'influenza delle prima fila di barrette attorno alla barretta centrale
- Per questo è stato modellato un gruppo di sette barrette
- La porzione di fluido considerata ha le stesse dimensioni della scatola dell'elemento
- Le condizioni al contorno imposte al fluido simulano una scatola rigida

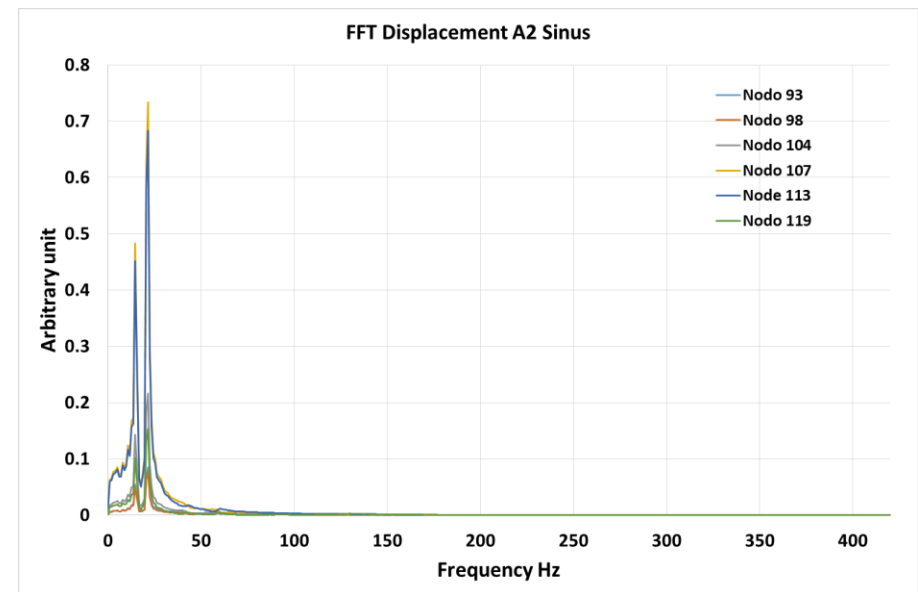
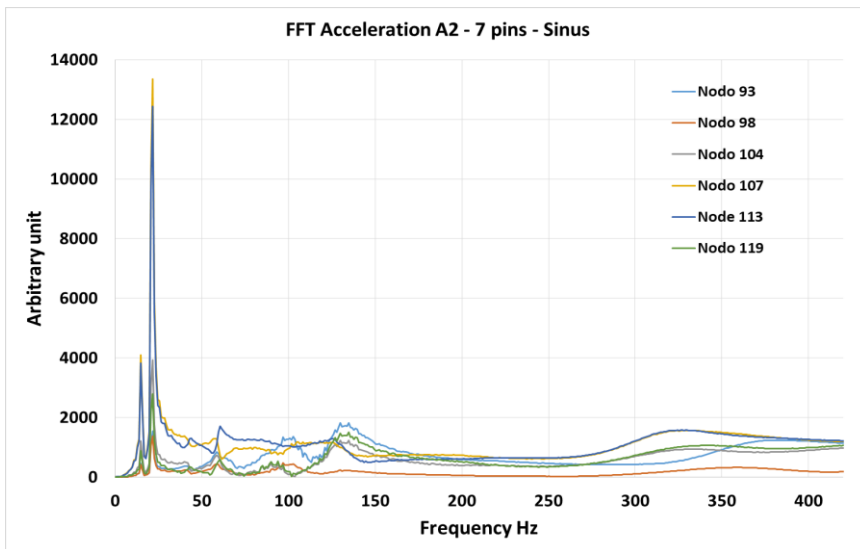




# Individuazione delle frequenze dei modi superiori barretta immersa in piombo

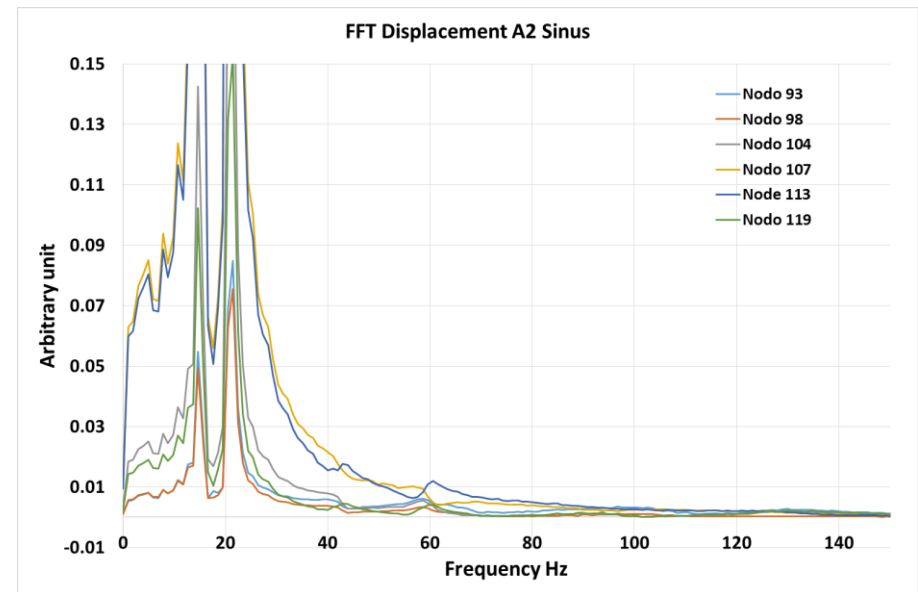
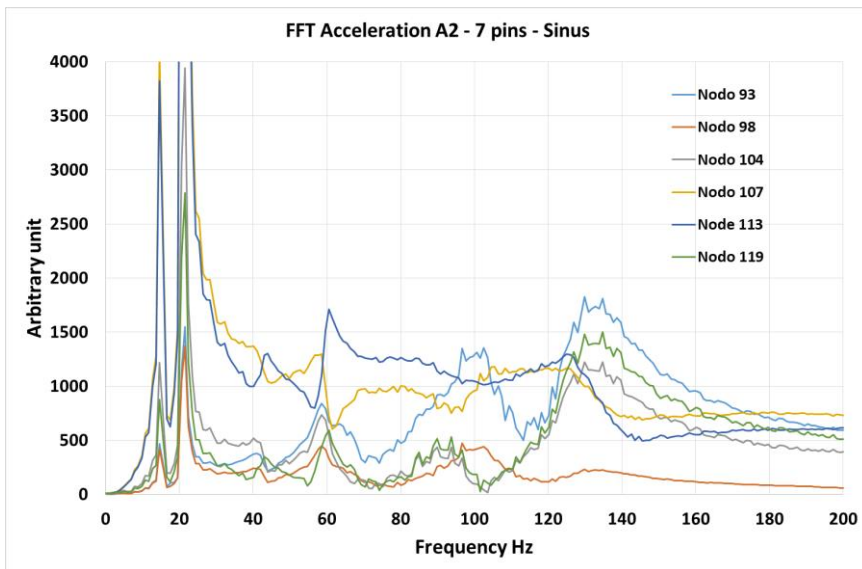
*Risultati time history eccitazione 'sinus' – barretta centrale del gruppo di 7*

- il movimento del fluido innesca un movimento in entrambe le direzioni orizzontali delle barrette circostanti, questo movimento a sua volta genera delle retroazioni sulla barretta centrale rendendo più caotica la risposta*



# Individuazione delle frequenze dei modi superiori barretta immersa in piombo

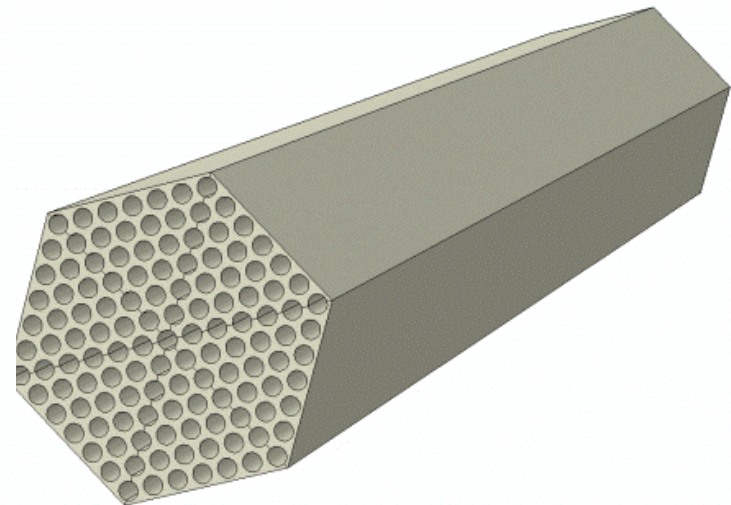
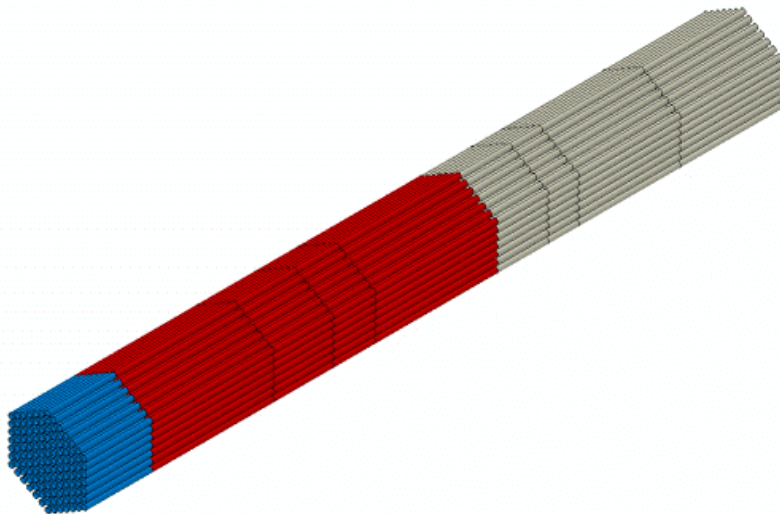
*Neppure ingrandendo la scala si riescono a cogliere bene le frequenze proprie*





# Next steps

- *Approfondire la valutazione del fascio a 7 barrette applicando lo stesso impulso a tutte*
- *Modellare tutte le barrette e il fluido per riprodurre una condizione più realistica*
- *Applicare un'eccitazione il più possibile realistica calcolando l'andamento delle pressioni sulla superficie delle barrette nel tempo*



***GRAZIE PER L'ATTENZIONE***

# ALFRED

## Fuel Assembly design

*«GEN-IV LEAD COOLED FAST REACTOR  
STATO ATTUALE DELLA TECNOLOGIA E PROSPETTIVE DI SVILUPPO»  
Workshop tematico AdP MISE – ENEA PAR2017 – PROGETTO B.3 - LP2  
Università di Roma «La Sapienza», 14-15 Giugno 2018*

**G. Grasso, A. Palumbo, F. Lodi**



1101 0110 1100  
0101 0010 1101  
0001 0110 1110  
1101 0010 1101  
1111 1010 0000



# Problems to be faced

## 1. Irradiation-induced deformations

In **Fast Reactors**, the high burnups imply high irradiation doses to the structural materials. As the former are desired, the latter are to be faced.

In **Lead-cooled Fast Reactors**, presently qualified irradiation-resistant materials (i.e., ferritic-martensitic steels) cannot be used because of environmental issues (mostly, liquid metal embrittlement).

The envisioned austenitic stainless steels, at the doses anticipated for ALFRED, are prone to **swelling**.

# Problems to be faced

## 2. Pressure-induced deformations

In **Fast Reactors**, the differential pressure of the coolant flowing inside vs. outside the sub-assemblies exerts forces on the flat faces of the wrapper.

In **Lead-cooled Fast Reactors**, the differential pressure is anticipated to be much less, and so is the associated force.

Even though moderate, the resulting force expected in ALFRED may lead to **bulging**.

# Problems to be faced

## 3. Temperature-induced deformations

In **Fast Reactors**, the flux and power profiles throughout the core determine also temperature gradients within the fuel assemblies, which result in differential expansions of the structural elements.

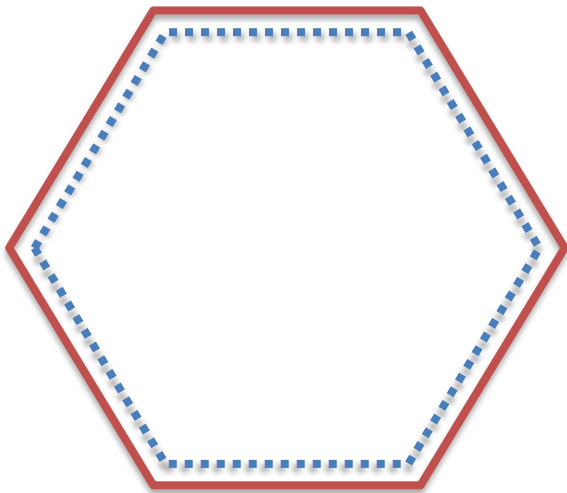
In **Lead-cooled Fast Reactors**, this effect might be reduced or magnified, depending on the adopted inlet-outlet temperatures.

The inlet and outlet temperatures planned in the different phases of ALFRED operation determine progressively increasing **bowing**.

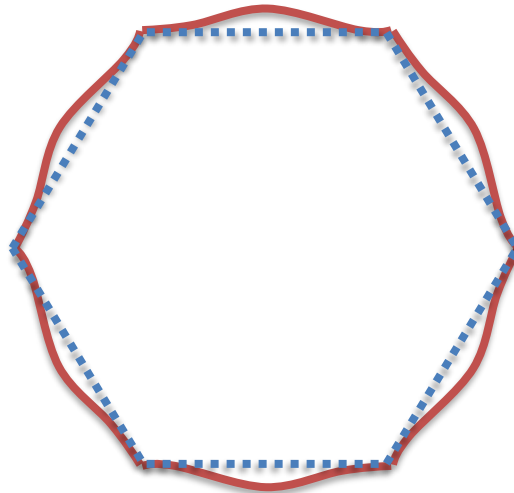
# Problem to be faced

## Summary of anticipated deformations

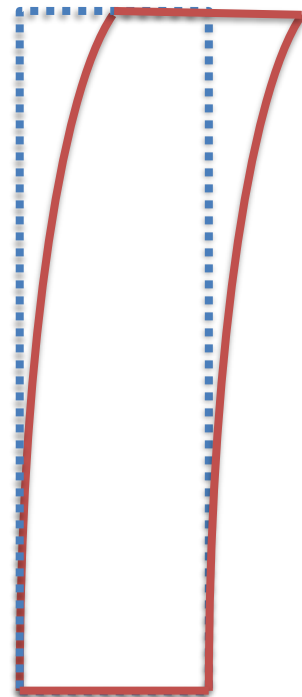
**Swelling**



**Bulging**



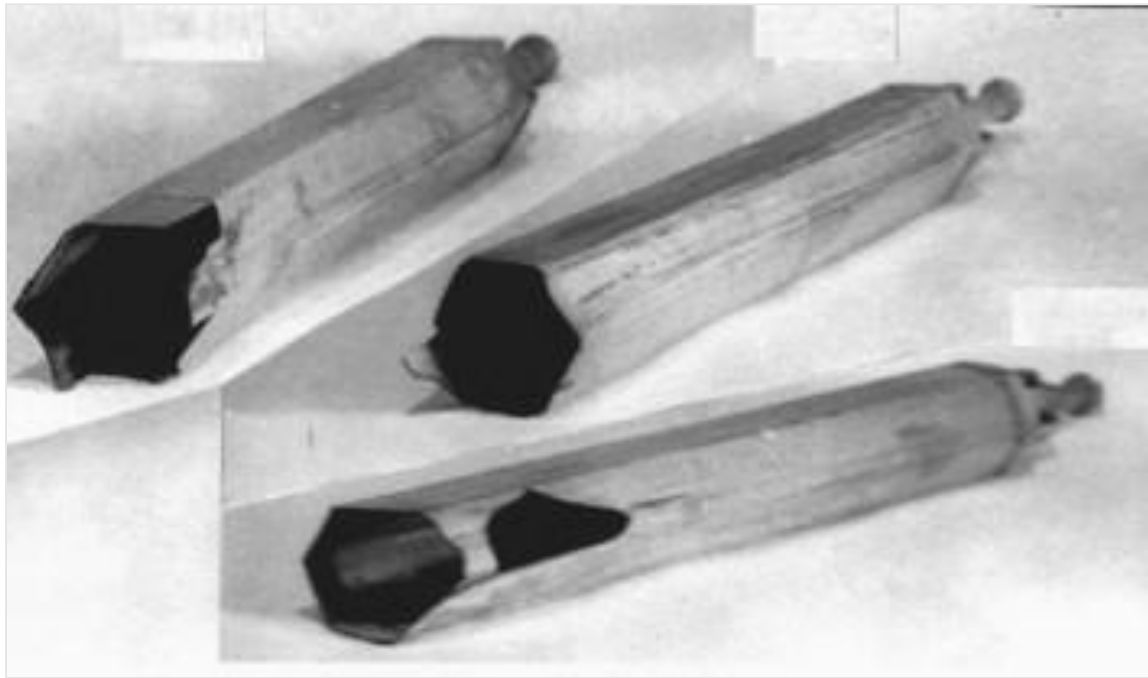
**Bowing**



# Problem to be faced

## Overall effect

Once combined, all these causes can determine severe deformations to the wrapper...





# Requirements to be ensured

## 1. Prevention of accidental reactivity insertions

In **Fast Reactors**, the core is not in its most critical configuration, and moderation ratio is not required – rather detrimental – to criticality, so that any reduction of the coolant volume fraction inserts reactivity.

In **Lead-cooled Fast Reactors**, the high density of the coolant can magnify the effects of earthquakes in terms of solicitations to the core.

The small dimensions of the ALFRED core, making it more sensible to geometrical reactivity effects, require minimizing **compaction** events.

# Requirements to be ensured

## 2. Reactivity feedback

In **Fast Reactors**, the lack of moderator eliminates the largest feedback mechanism, turning the coolant effect positive and counterbalanced by small geometrical feedbacks.

In **Lead-cooled Fast Reactors**, the coolant density effect is much lower (if not negative), but the moderator feedback still misses.

The inherent controllability of the ALFRED (notably in DEC) needs to rely on all available mechanisms, including **flowering**.

# Requirements to be ensured

## 3. Insertion capability of control/shutdown devices

In **Fast Reactors**, control devices are usually massive bundles of rods inserted within fixed structures occupying one full core position.

In **Lead-cooled Fast Reactors**, instead of gravity, buoyancy can be exploited (since the rods are lighter than the coolant they displace), but the overall layout is not changed.

Despite the small sub-assemblies of ALFRED, making tolerances even more tight, ensuring the **clearance** needed for insertion is mandatory.

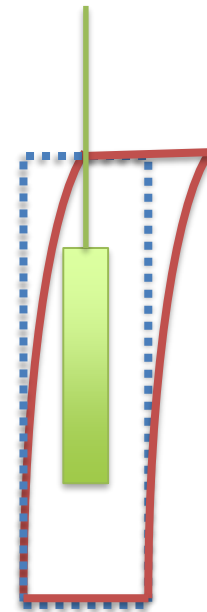
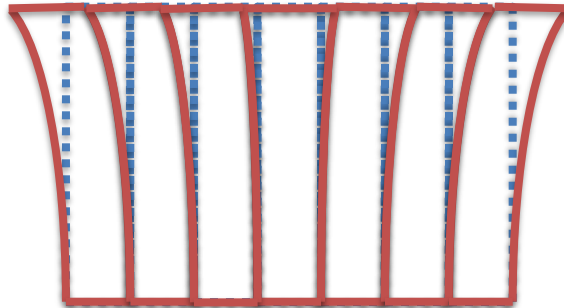
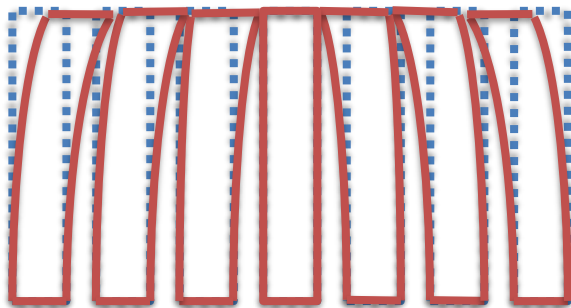
# Requirements to be ensured

## Summary of requirements

**Prevent compaction**

**Allow flowering**

**Ensure clearance**



# Approach to solution

## Object of study

First of all, the study is focused on the Fuel Assemblies only, being easily transferrable to other types of sub-assemblies later on.

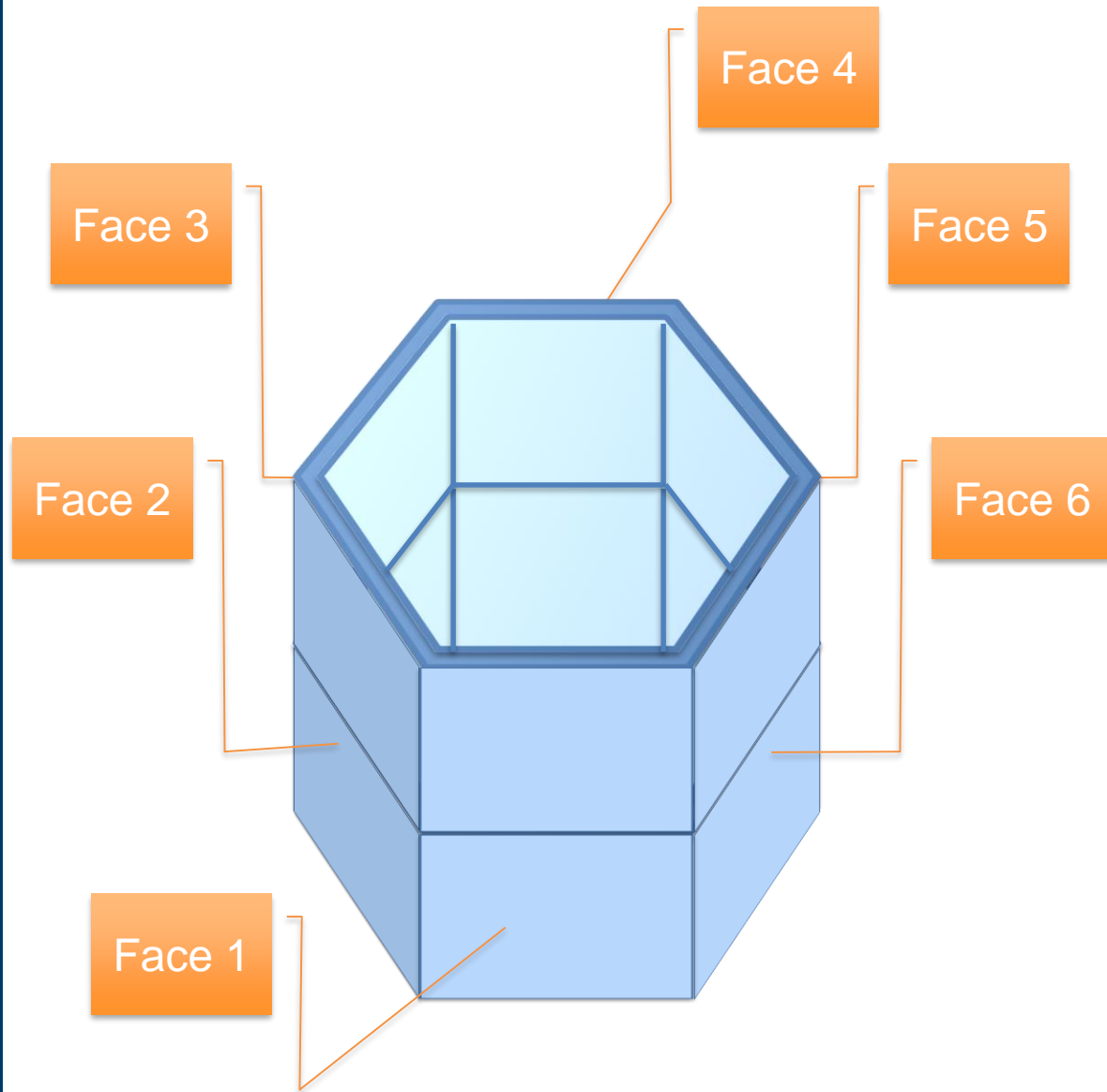
The study is then focused on the wrapper, being the resisting structure of an ALFRED Fuel Assembly.

In this phase, unrestrained deformations are considered.

# Modeling

## Discretization

Each wrapper's face is modeled independently, and all are divided into regular axial slices

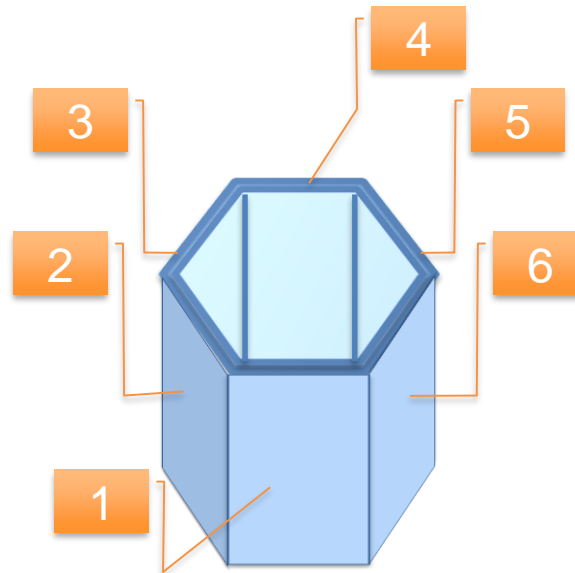


# Modeling

## Lumping

The actual values of the main parameters (temperature and neutron dose), whose distributions on the whole wrapper are known axially and along the perimeter, are lumped by representative values, for each face and at each quote of interest.

| Quote z [cm] | Temperature [°C] |             |             |           | Flux [n/cm <sup>2</sup> s] |             |             |           |
|--------------|------------------|-------------|-------------|-----------|----------------------------|-------------|-------------|-----------|
|              | face 1           | faces 2 & 6 | faces 3 & 5 | face 4    | face 1                     | faces 2 & 6 | faces 3 & 5 | face 4    |
| 0            | 405.7            | 405.7       | 405.7       | 405.7     | 4.653E+14                  | 4.324E+14   | 3.84E+14    | 3.696E+14 |
| 3            | 407.93082        | 407.86667   | 407.74565   | 407.68931 | 5.405E+14                  | 5.052E+14   | 4.51E+14    | 4.335E+14 |
| 6            | 410.43038        | 410.28919   | 410.02283   | 409.89904 | 6.113E+14                  | 5.738E+14   | 5.142E+14   | 4.939E+14 |
| 9            | 413.17967        | 412.94939   | 412.51493   | 412.31334 | 6.774E+14                  | 6.38E+14    | 5.736E+14   | 5.505E+14 |
| 12           | 416.15967        | 415.82909   | 415.20539   | 414.91635 | 7.388E+14                  | 6.978E+14   | 6.289E+14   | 6.034E+14 |
| 15           | 419.35138        | 418.91013   | 418.0776    | 417.69221 | 7.953E+14                  | 7.53E+14    | 6.802E+14   | 6.523E+14 |
| 18           | 422.73579        | 422.17434   | 421.11498   | 420.62505 | 8.469E+14                  | 8.035E+14   | 7.273E+14   | 6.972E+14 |
| 21           | 426.29388        | 425.60353   | 424.30094   | 423.69903 | 8.934E+14                  | 8.493E+14   | 7.7E+14     | 7.38E+14  |
| 24           | 430.00664        | 429.17956   | 427.6189    | 426.89827 | 9.348E+14                  | 8.901E+14   | 8.082E+14   | 7.744E+14 |
| 27           | 433.85506        | 432.88424   | 431.05227   | 430.20692 | 9.709E+14                  | 9.258E+14   | 8.419E+14   | 8.065E+14 |
| 30           | 437.82012        | 436.6994    | 434.58445   | 433.60913 | 1.002E+15                  | 9.564E+14   | 8.708E+14   | 8.34E+14  |
| ...          | ...              | ...         | ...         | ...       | ...                        | ...         | ...         | ...       |



## Modeling

## Analysis

At each quote, the moment generated by the differential thermal dilation and swelling is computed.

This in turn is applied to the solution of the problem of deformation of an unrestrained beam, retrieving the rotation and displacement of each axial segment of the wrapper.

$$M_i = M_i^{Th} + M_i^{Sw}$$

$$M_i^{Th} = \int_i E \alpha T y dA$$

$$M_i^{Sw} = \int_i E \varepsilon y dA$$

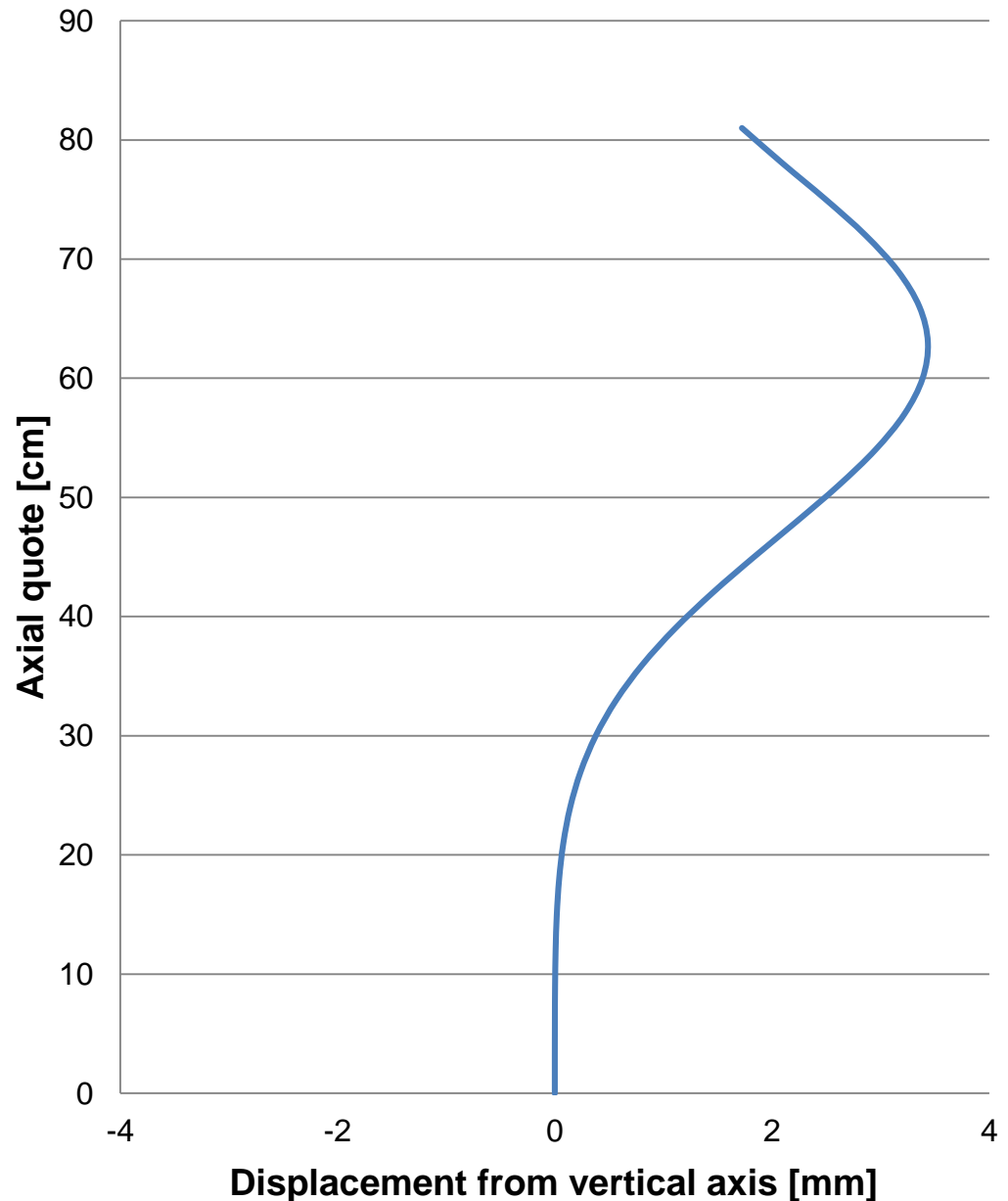
$$\frac{d^2 y_i}{dz_i^2} = \frac{M_i}{E_i I_i}$$



# Results

Figure shows the deformed shape for the fuel assembly mostly subject to bowing (i.e., the one suffering the maximum thermal and flux gradients).

The results – obtained under the hypothesis of unrestrained deformations! – report a maximum displacement from the original axis by 3.44 mm.



# Conclusions

## Summary

- A methodology for computing the unrestrained displacement of a fuel assembly has been developed, cross-checked and applied to the ALFRED case.
- The preliminary results for the most stressed fuel assembly report a peak displacement of 3.4 mm from the axis, which seems acceptable i.e., easily manageable by engineering means.

# Conclusions

## Future work

- The methodology – presently analytical – shall be validated before other, more formal applications.
- The methodology shall be coded, targeting two possible tools:
  - TEIA, which will include also the mechanical interaction with the bundle within the wrapper;
  - FEBE, which will extend the analysis to the whole core, removing the unrestrained hypothesis thereby allowing the evaluation of the mutual interaction among S/As.

Giacomo Grasso  
giacomo.grasso@enea.it



1101 0110 1100  
0101 0010 1101  
0001 0110 1110  
1101 0010 1101  
1111 1010 0000



*Feasibility studies  
of an experimental campaign  
in TAPIRO devoted to the analysis  
of nuclear database for minor actinides*

**Use of new nuclear data libraries  
for the Monte Carlo analysis  
of neutronic measurements  
in the TAPIRO reactor**

C. Di Gesare<sup>1</sup>, D. Caron<sup>1</sup>, S. Dulla<sup>1</sup>, P. Ravetto<sup>1</sup>,  
M. Carta<sup>2</sup>, V. Fabrizio<sup>2</sup>

<sup>1</sup>*Politecnico di Torino, Italy*

<sup>2</sup>*ENEA Casaccia, Italy*

# Outline

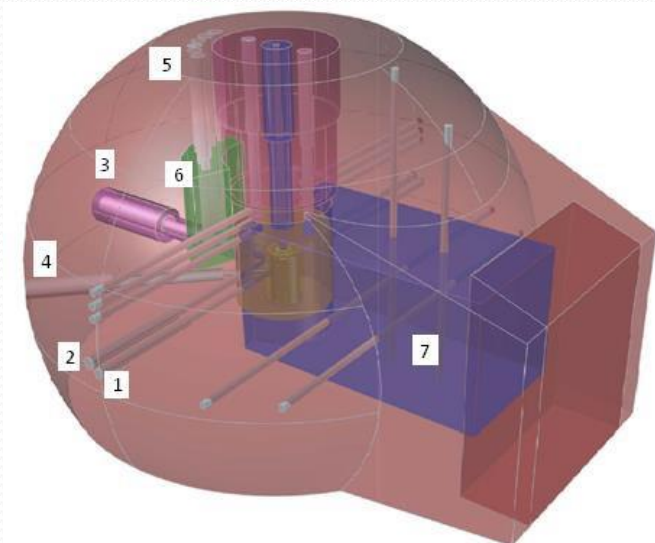
- The TAPIRO reactor
- Aim of the work
- The SERPENT model of TAPIRO
  - Geometrical configuration
  - Nuclear data
- Comparison of nuclear data libraries
  - Reaction rates in radial channel 1 (RC<sub>1</sub>)
  - Neutron currents in RC<sub>1</sub>
  - $k_{\text{eff}}$
- Conclusions and perspectives

# The TAPIRO reactor



- TAPIRO (TAratura Pila Rapida Potenza ZerO)
    - fast spectrum research reactor
    - Located in ENEA laboratories in Casaccia, Italy
    - In operation since 1971
- 
- Square cylinder core (diameter about 12 cm)
  - Fuel made of a uranium-molybdenum alloy (98.5 wt.% U–1.5 wt.% Mo, 93.5% enrichment)
  - Maximum operating power 5 kW
  - Multipurpose facilities
    - Well-characterized neutron spectrum
    - Allows irradiation in various conditions
    - Adopted for analysis of materials under irradiation

# The TAPIRO reactor



- TAPIRO (TAratura Pila Rapida Potenza ZerO)
  - fast spectrum research reactor
  - Located in ENEA laboratories in Casaccia, Italy
  - In operation since 1971

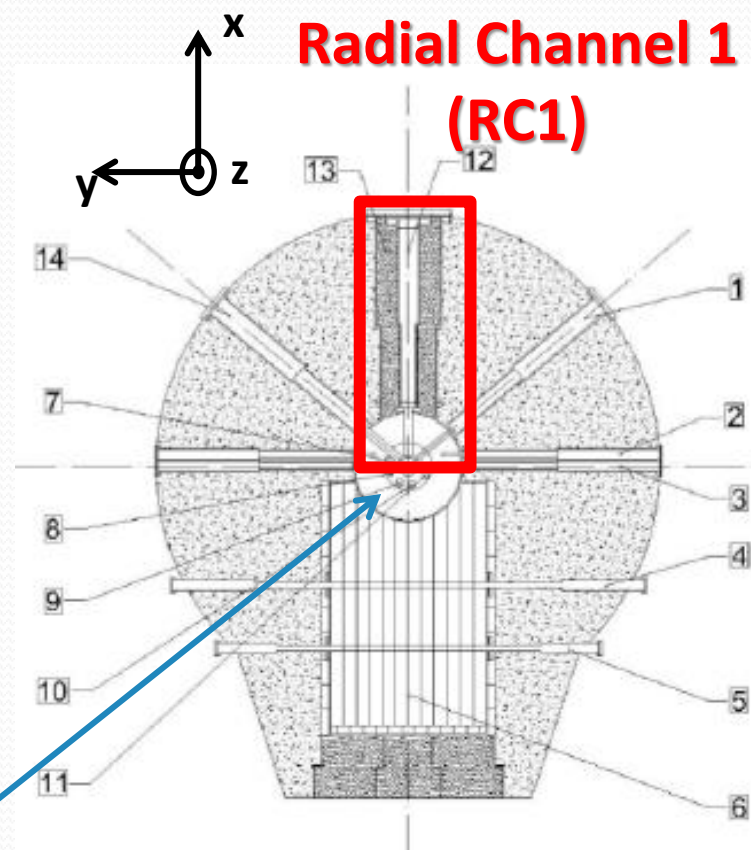
- Square cylinder core (diameter about 12 cm)
- Fuel made of a uranium-molybdenum alloy (98.5 wt.% U–1.5 wt.% Mo, 93.5% enrichment)
- Maximum operating power 5 kW
- Multipurpose facilities
  - Well-characterized neutron spectrum
  - Allows irradiation in various conditions
  - Adopted for analysis of materials under irradiation



# Experimental campaign in TAPIRO

*x-y section of the reactor at  $z=1$  m*

- SCK-CEN/ENEA experimental campaign carried out in 1980-86
- Fission rates of Np-237, U-238 and U-235 measured in RC1
- Previous work
  - Simulation of these experiments with stochastic and deterministic tools (see M&C2017) → **discrepancies**
  - Preliminary sensitivity analysis on the influence of copper nuclear data in simulations



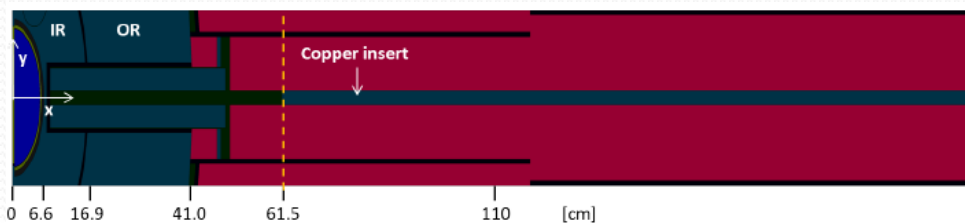
**Copper reflector**

# Objective of the work

- Computational modelling of the TAPIRO reactor with SERPENT Monte Carlo code
- Reconstruction of experimental data performed in the SCK-CEN/ENEA experimental campaign
- **Comparison of different libraries** available
  - the original JEFF-3.1.1 library
  - upgraded version with new nuclear data for copper isotopes based on the new ENDF/B-VIII.beta5 library
  - new library based entirely on ENDF/B-VIII.beta5.
- Discussion of
  - differences among the three different data sets
  - resulting effect of the reaction rates, currents ...

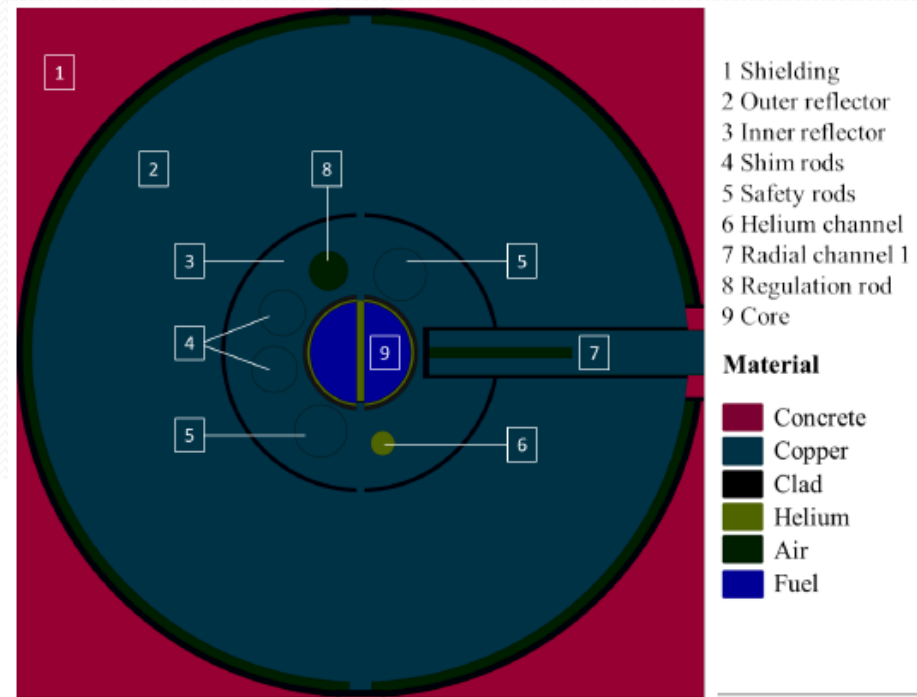
# SERPENT model of TAPIRO

- Serpent version 1.19, with different libraries (as detailed later on)
  - Model including the whole system (biological shield)
  - Focus on the modelling of RC1 (other channels not modelled)
  - Simulated access groove bigger than in reality to improve statistical convergence



*RC1 model (with copper insert up to 61.5 cm)*

*x-y section at z=1 m*



# Nuclear data in Serpent

- The version of Serpent employed has cross-section libraries based on
  - JEF-2.2
  - JEFF-3.1
  - JEFF-3.1.1** *Adopted in previous evaluations of TAPIRO (PAR 2016)*
  - ENDF/BVI.8
  - ENDF/B-VII

- New libraries can be produced from raw ENDF format data using NJOY

**From ENDF/B-VIII.beta5 nuclear data (released 10/2017) a new library has been generated**

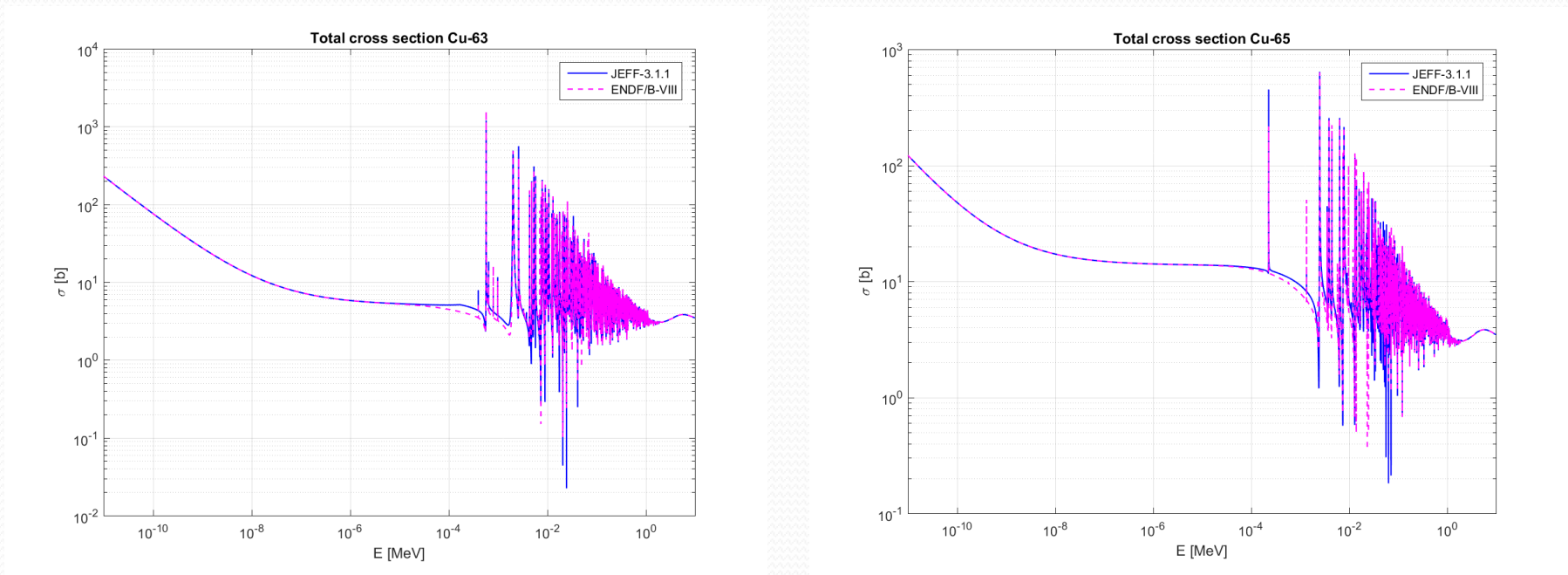
- The effect of the new data has been assessed in two steps
  - Update of Copper X-sections in existing JEF-3.1.1 library
  - Full library based on ENDF/B-VIII.beta5

# Objective

**Compare the experimental fission rates in RC<sub>1</sub> with the results of Monte Carlo simulations, to assess the role of the nuclear data, with a specific focus on the role of copper**

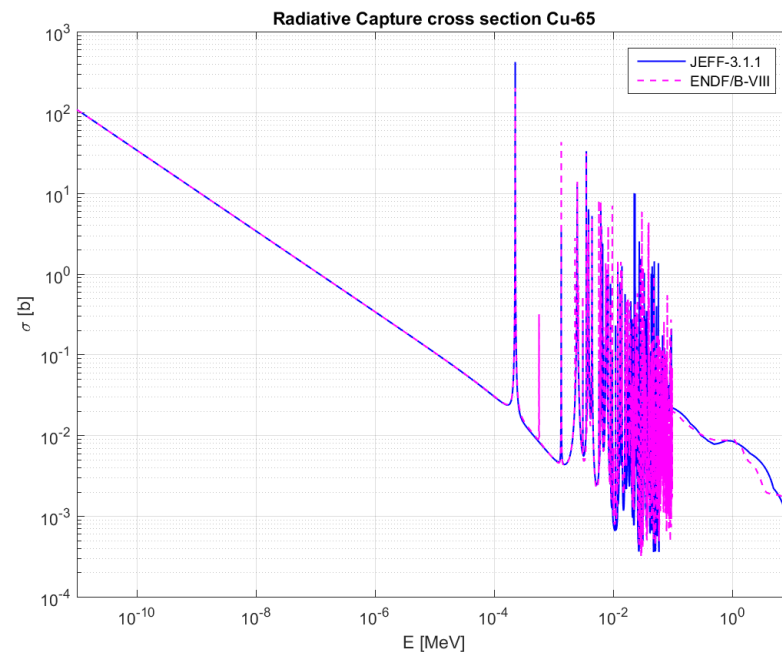
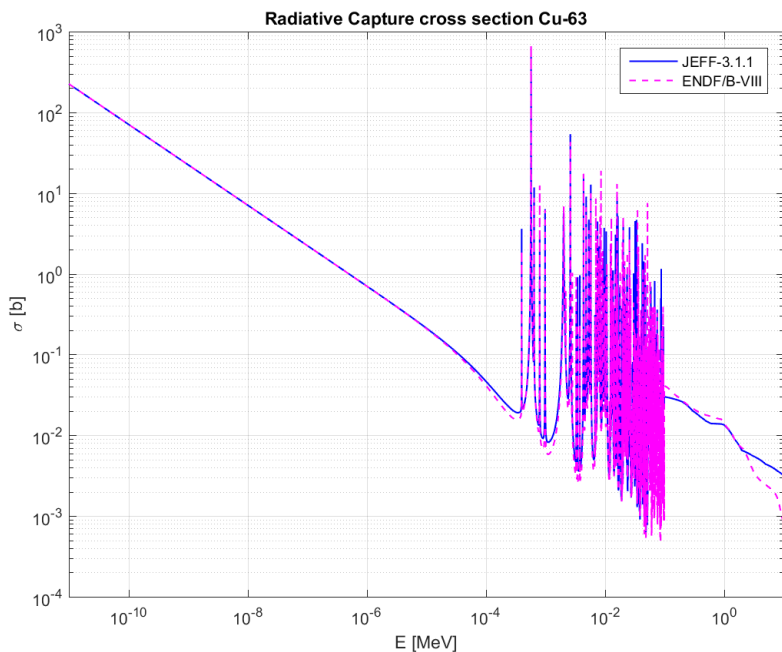
# Copper cross section behavior - I

- Isotopes present in natural copper have been considered (69.2% Cu-63 and 30.8% Cu-65)
- **General comment**: ENDF/B-VIII data lower than JEFF-3.1.1  
 → weaker decay of the neutron flux in the reflector



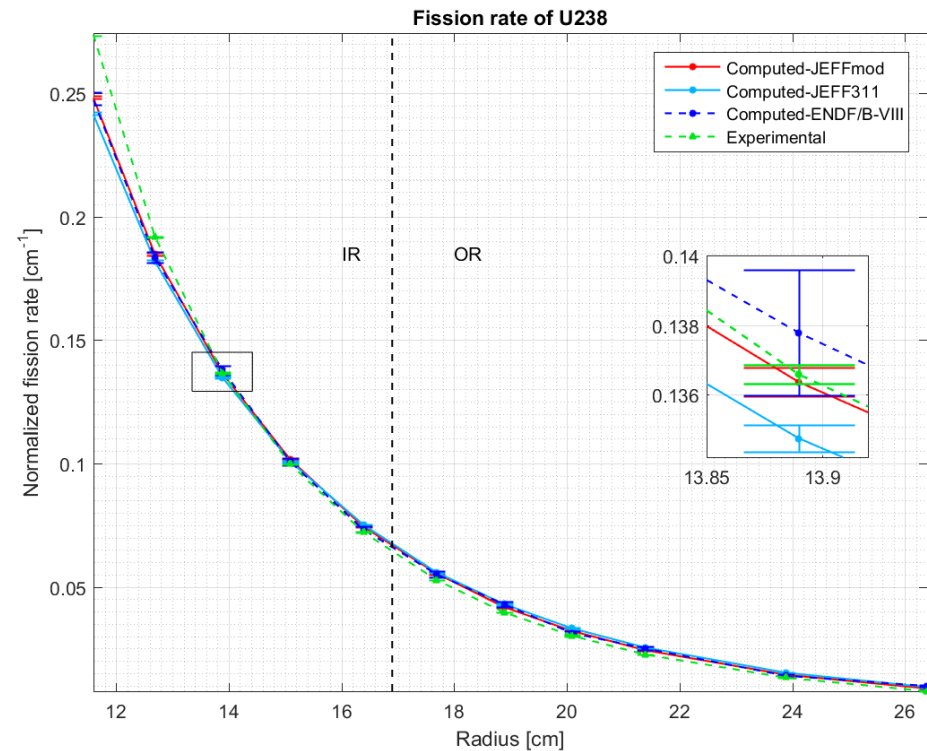
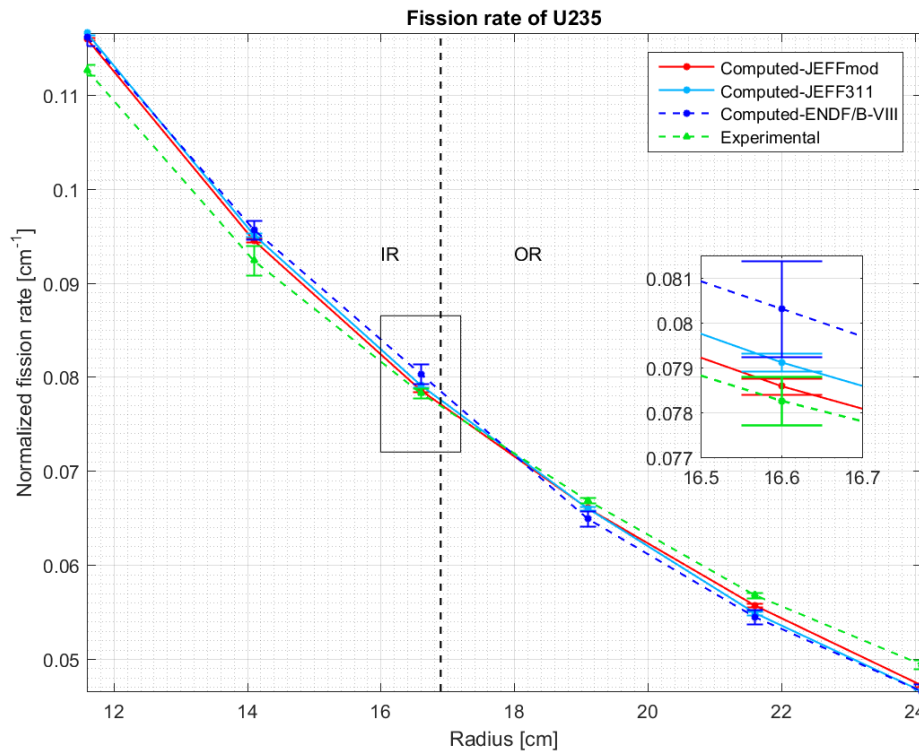
# Copper cross section behavior - I

- Other comparison of copper cross sections performed between ENDF/B-VIIIbeta and new JEFF-3.2 → small discrepancies



# Effect on RC<sub>1</sub> fission rates - I

- Simulations performed for the isotopes considered in the experiments: Np-237, U-235, U-238, Pu-239





# Effect on RC<sub>1</sub> fission rates - II

- All reaction rates are normalized to the same spatial integral along the axis of the channel.
  - Use of new data for copper (JEFFmod results) improves agreement
  - Use of the full new library (ENDF/B-VIII results) gives different performances depending on the isotope

Differences evaluated: sign disagreement is observed in some locations along the radial coordinate

| Np-237        |                 |                 |                   |
|---------------|-----------------|-----------------|-------------------|
| <i>r</i> [cm] | JEFF-3.1.1      | JEFF-3.1.1 mod. | ENDF/B-VIII.beta5 |
| 11.60         | 0.0099 (9E-04)  | 0.0072 (9E-04)  | 0.009 (1E-03)     |
| 12.74         | 0.0020 (5E-04)  | 0.0005 (5E-04)  | 0.001 (1E-03)     |
| 13.94         | -0.0020 (4E-04) | -0.0028 (4E-04) | -0.0027 (9E-04)   |
| 15.14         | -0.0028 (4E-04) | -0.0029 (4E-04) | -0.0024 (8E-04)   |
| 16.40         | -0.0032 (5E-04) | -0.0030 (5E-04) | -0.0025 (8E-04)   |
| 17.74         | -0.0022 (4E-04) | -0.0017 (4E-04) | -0.0022 (7E-04)   |
| 18.94         | -0.0003 (1E-04) | 0.0003 (1E-04)  | 0.0005 (5E-04)    |
| 20.14         | 0.0002 (1E-04)  | 0.0007 (1E-04)  | 0.0004 (5E-04)    |
| 21.44         | 0.0008 (3E-04)  | 0.0014 (3E-04)  | 0.0005 (5E-04)    |
| 23.94         | 0.0014 (1E-04)  | 0.0018 (1E-04)  | 0.0015 (3E-04)    |

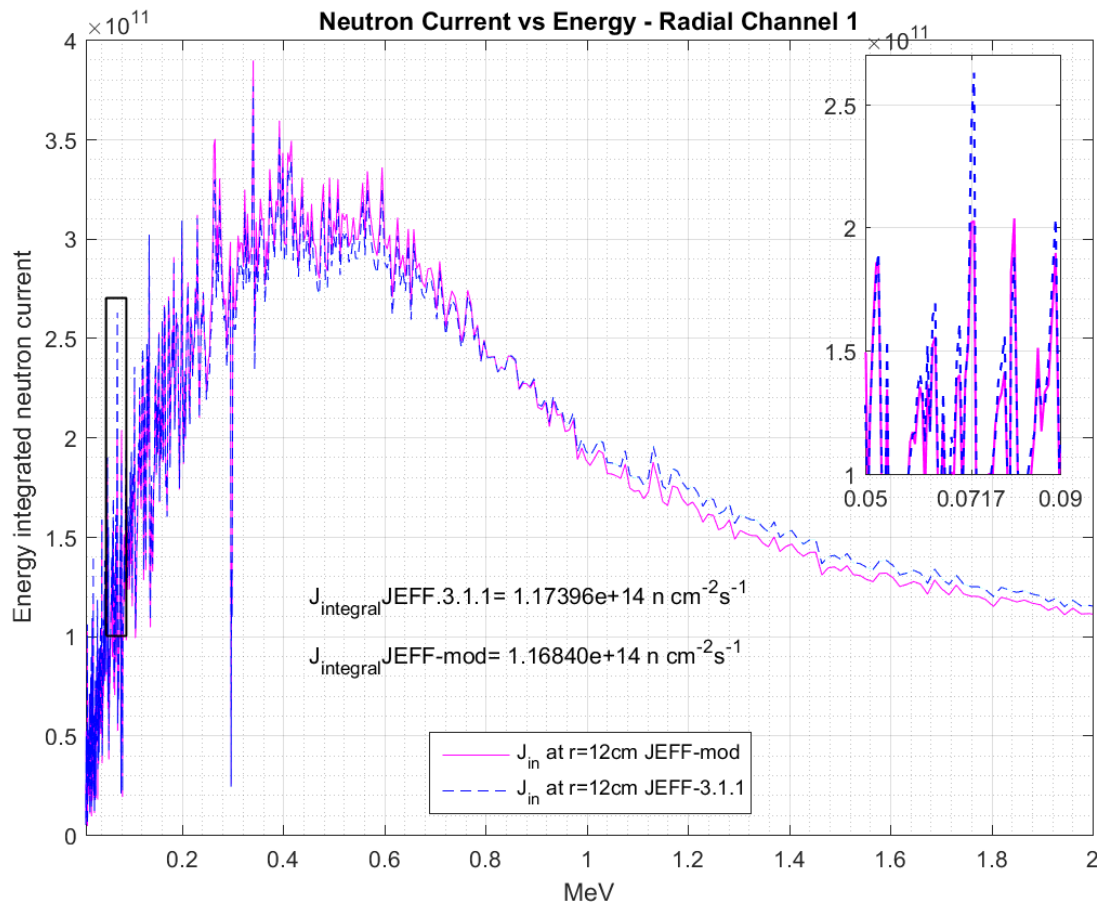
# Effect on relevant neutronic quantities

- Multiplicativity: non-negligible effect, especially when focusing on the modification of copper cross sections only

|           | JEFF-3.1.1                | JEFF-3.1.1 mod.           | ENDF/B-VIII.beta5         |
|-----------|---------------------------|---------------------------|---------------------------|
| $k_{eff}$ | 1.00787 ( $\pm 6.5E-06$ ) | 1.00309 ( $\pm 6.5E-06$ ) | 1.00594 ( $\pm 2.9E-05$ ) |

- Currents: the currents entering RC<sub>1</sub> at different energies have been evaluated
  - Evaluation of the effect of the library change
  - Potential use as source for calculations reduced to RC<sub>1</sub> only

# Neutron current entering RC<sub>1</sub> - I

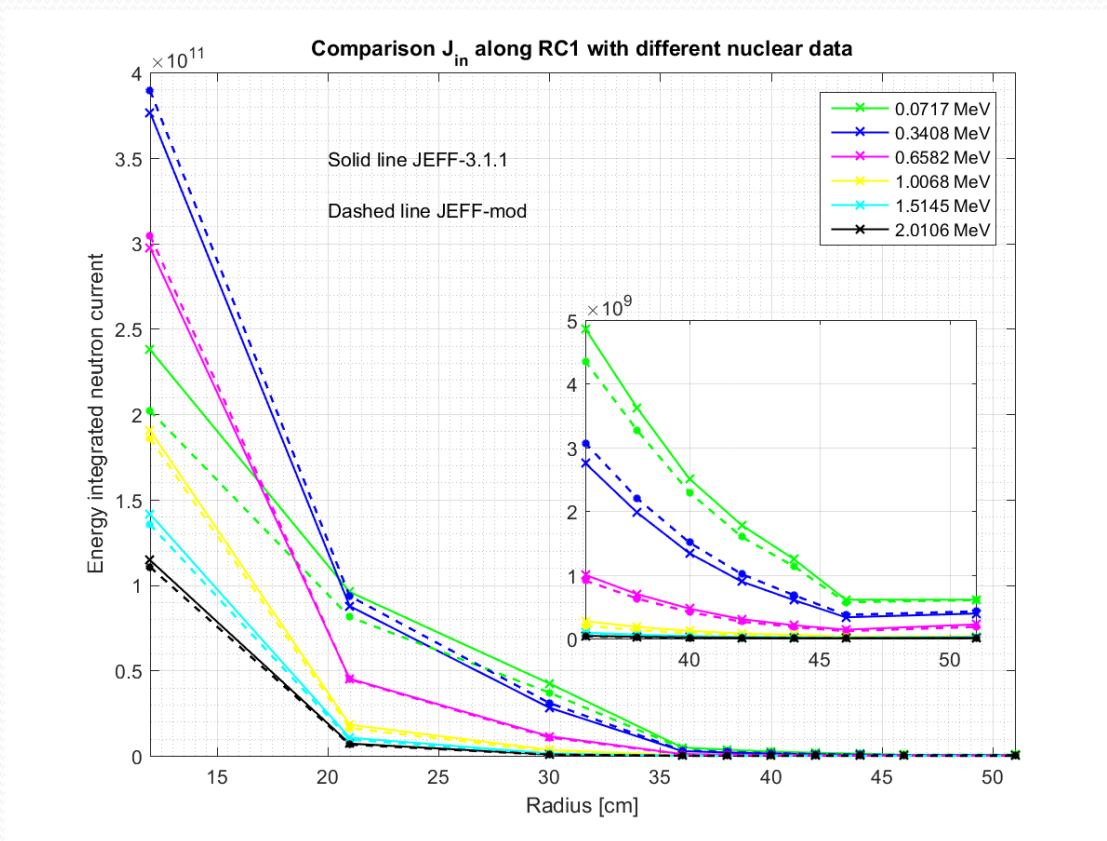


Neutron current entering RC<sub>1</sub> at 12 cm distance from the system center.

Average relative standard deviation 0.0049

Different slowing down effect

# Neutron current entering RC<sub>1</sub> - II



Neutron current entering along RC<sub>1</sub> axis.

Non-negligible effect, especially in some energy ranges

# Conclusions and perspectives

- The effect of nuclear data libraries in the simulation reaction rates in TAPIRO has been assessed
  - Nuclear data for copper play an important role in this experimental facility
  - The adoption of new nuclear data libraries leads to significantly different results
  - The results are not improved in all situations (as compared to experimental data).
  - Further work is needed to draw a definite conclusion on the appropriateness of the new cross section data.
- Perspective work: perform a complete sensitivity analysis of the MA reaction rates as a function of the nuclear data, evidencing the relative role of each components



Thanks for your attention

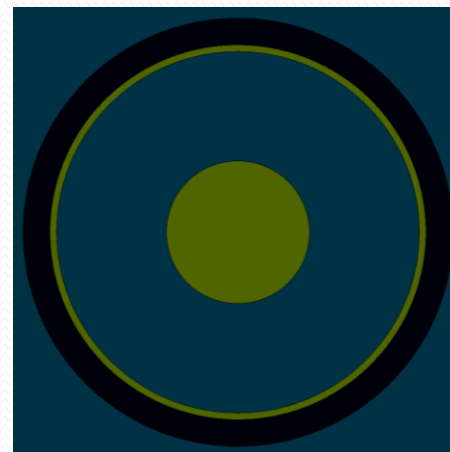
CC BY-SA 3.0, <https://commons.wikimedia.org/w/index.php?curid=531371>  
<https://en.wikipedia.org/wiki/Tapir>  
<https://it.wikipedia.org/wiki/Tapirus>

# Backup slides

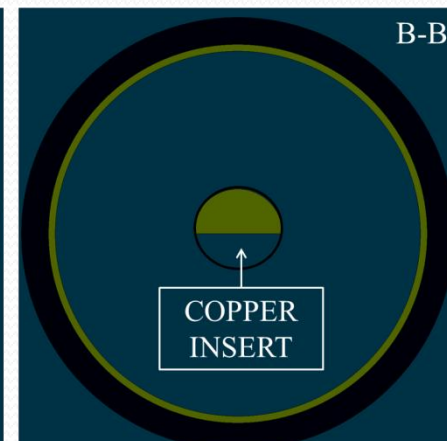
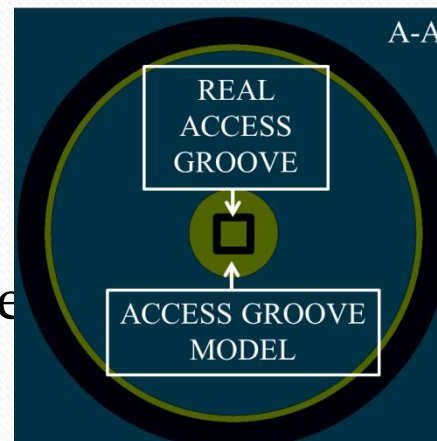
# Model of the access groove

- The dimension of the channel has been modified to get better statistics
  - Large Access Groove (LAG): radius=1.065 cm, detector volume 0.24 cm<sup>3</sup>
  - Small Access Groove (SAG): radius=0.66 cm, detector volume 0.10 cm<sup>3</sup> (for verification)
  - Results show different performance depending on the fission rate observed

LAG

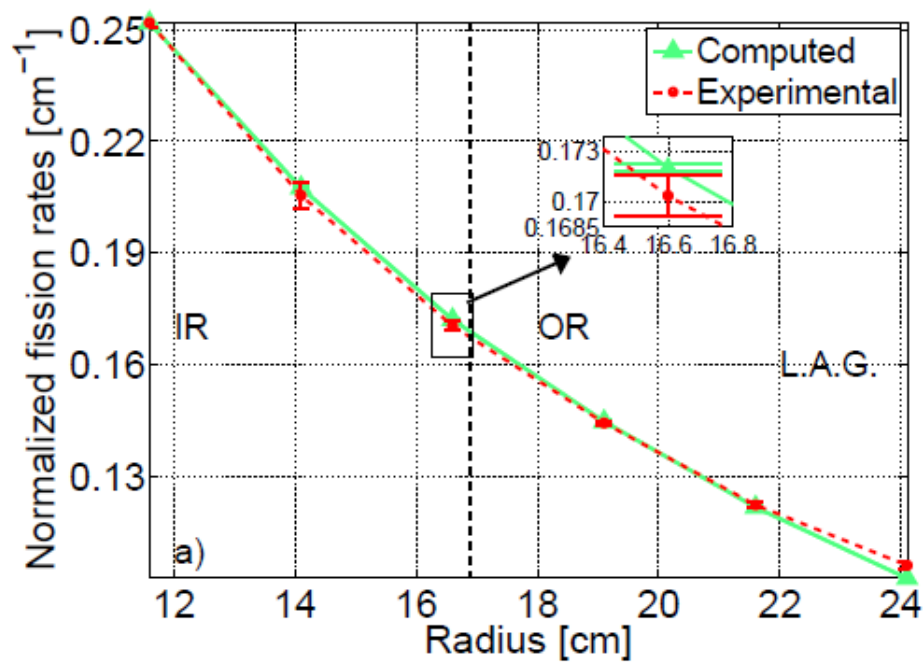
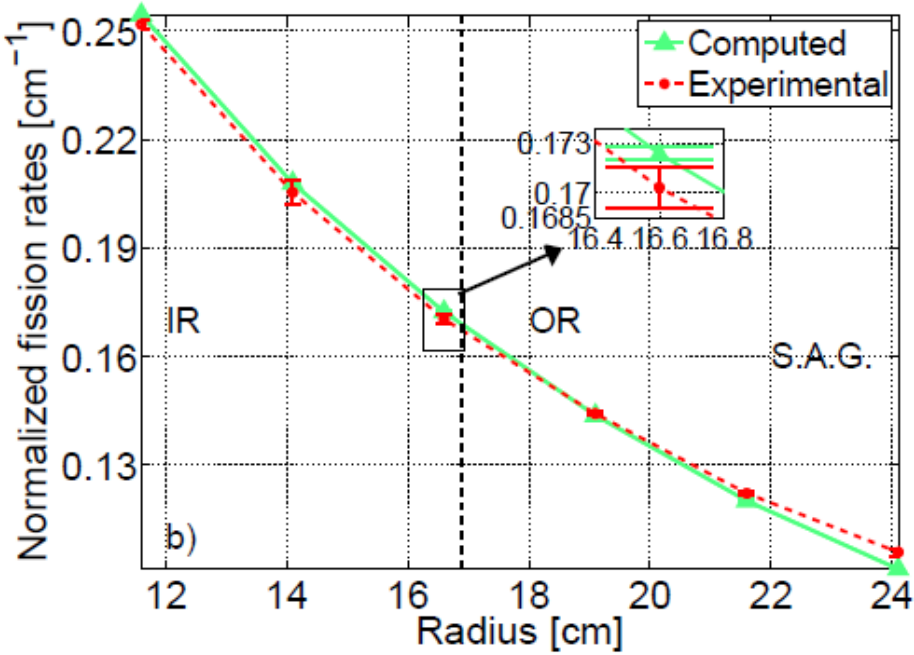


SAG





# Comparison of groove models - I



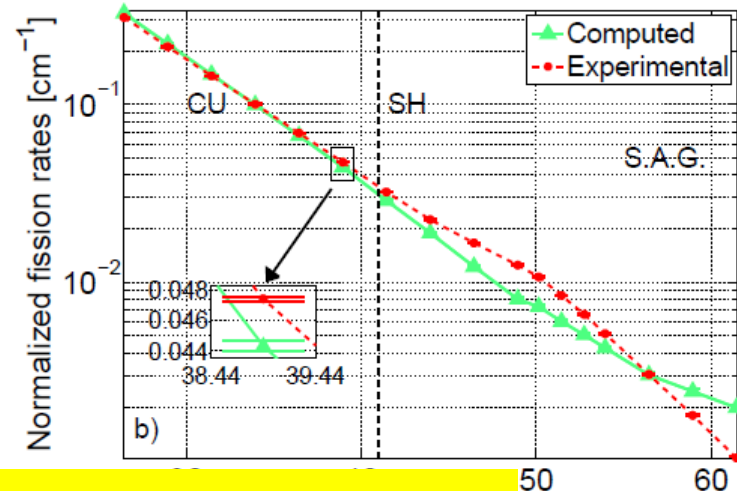
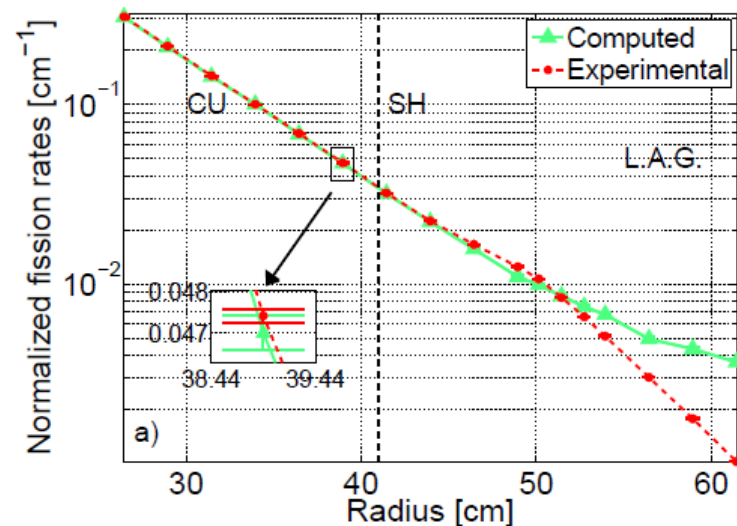
- Fission rate for U-235 shows small discrepancies
- Same results also for further detectors (r>24 cm)
- SAG simulations more computationally intensive

*Localization of detectors*

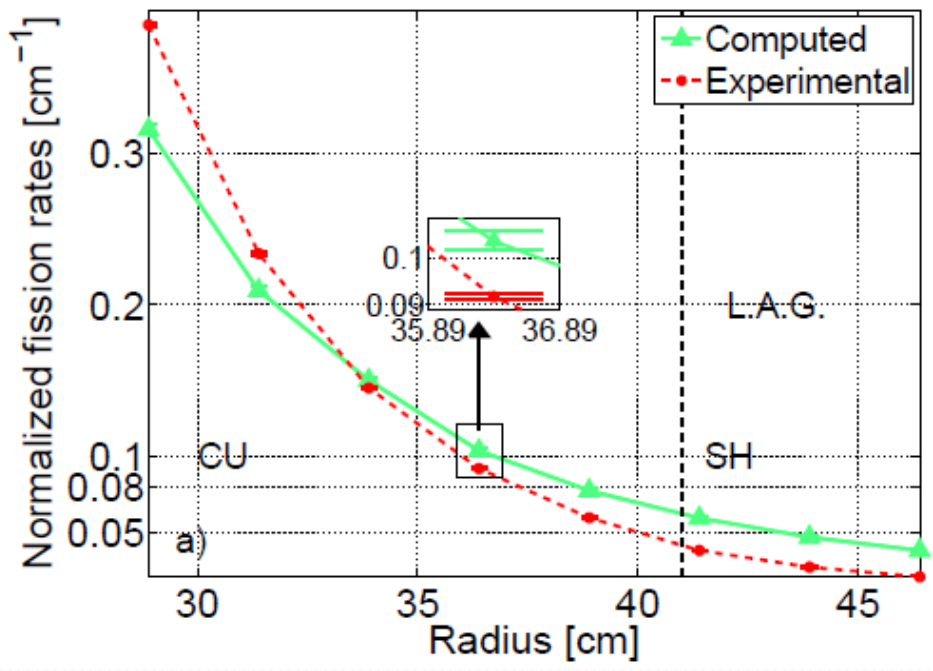
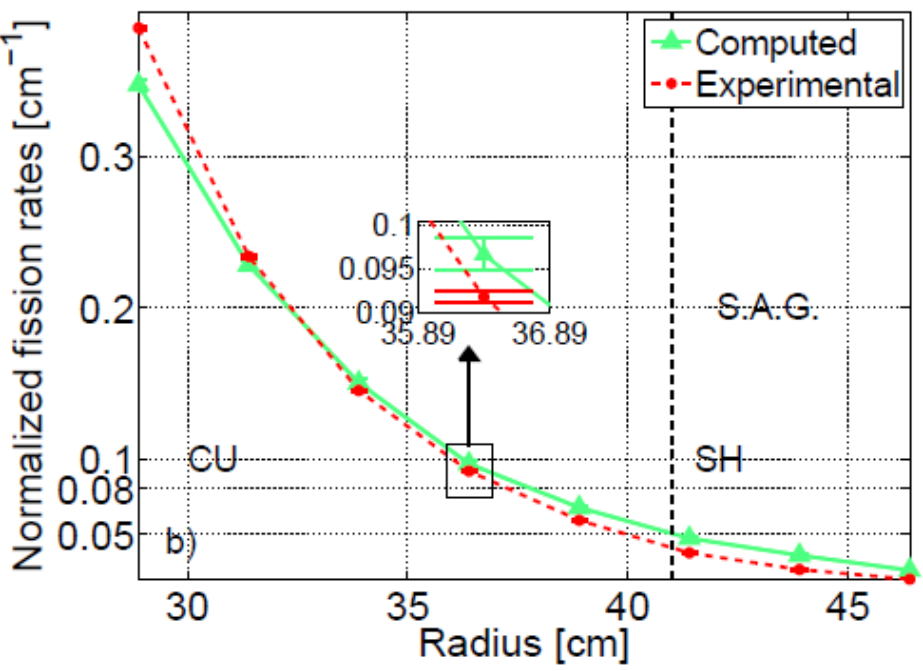


## Comparison of groove models - III

- Fission rate for Np-237 with larger deviations
  - The dimension of the access groove modifies the material composition around the detector
  - SAG case:
    - more copper ( $r < 41$ ) or concrete ( $r > 41$ )
    - Larger absorption in the energy range of fission of Np-237
    - Faster decay of fission rate
    - Still, open issues in the range 50-60 cm



# Comparison of groove models -III



- Fission rate for U-238 shows relevant differences
- Comment on increased absorption by copper/concrete as in previous case is valid
- SAG simulations more computationally intensive

# RECENTI SVILUPPI DELLA METODOLOGIA HGPT

Augusto Gandini, Università Sapienza, Roma  
Vincenzo Peluso, Enea, Bologna

Workshop Tematico  
Accordo di Programma MiSE - ENEA  
***Generation IV - Lead cooled Fast Reactor***  
14-15 Giugno, 2018  
Università Sapienza, Roma

## Introduzione

Partendo da un primo concetto di conservazione dell'importanza definito da Kadomtzev<sup>1</sup> nel campo fotonico, un metodo di calcolo perturbativo su basi euristiche venne successivamente proposto nel campo neutronico da Usachev per studi sui rapporti di tassi di reazione<sup>2</sup>. Il metodo di Usachev venne quindi esteso<sup>3,4,5</sup> per includere una gamma più ampia di funzionali lineari e non lineari.

Questo metodo è denominato HGPT (Heuristical Generalized Perturbation Theory) per distinguerlo da forme successive di derivazione, in particolare quelle basate su tecniche variazionali,<sup>6,7,8,9</sup> generalmente note come metodi GPT.

- 
1. Kadomtzev, B.B., "On the Importance Function in Radiation Transport Theory", Dokl. An. URSS, **113**, N. 3 (1957).
  2. Usachev, L.N., Atomnaya Energiya, **15**, 472 (1963) .
  3. Usachev, L.N., ZARISKI, S.M., Atomizdat, **2**, 242 (1965).
  4. Gandini, A., Journal of Nucl. En., **21**, 755 (1967) .
  5. Gandini, A., "Generalized Perturbation Theory Methods", *Advances Nucl.Sci.Tech.*, Vol.**19.**, Plenum, New York, (1987).
  6. Gandini, A., Annals of Nuclea Energy, **24**, 1241 (1997).
  7. Stacey, W.M., Jr., "Variational Methods in Nuclear Reactor Physics", Academic Press, New York (1974).
  8. Lewins, J., "Importance, the Adjoint Function,pergamon Press, Oxford (1965).
  9. Cacuci, D.G., Weber C.F., Oblow, E.M., Marable, J.M., Nucl. Sci. Eng., **75** 88 (1980).

# ***RECENTI SVILUPPI DELLA METODOLOGIA HGPT***

---

Verranno nel seguito descritti tre recenti sviluppi basati su questa metodologia, relativi agli argomenti:

- monitoraggio della sottocriticità di un sistema ADS;
- rilevamento di potenziali punti caldi;
- analisi del burn-up

## 1. Monitoraggio della sottocriticità

Un problema connesso con l'operazione di un reattore sottocritico (ADS) è posto dalla necessità di valutare online con sufficiente precisione il suo livello di sottocriticità.

Nel seguito illustreremo un approccio generale a questo problema, partendo dalle equazioni della cinetica puntuale relative a questi sistemi.<sup>10,11</sup>

---

10. Gandini, A., "HGPT Based Sensitivity Methods for the Analysis of Subcritical Systems", Ann. Nucl. Energy, **28**, 1193 (2001) .

11. Gandini, A., "ADS Subcriticality Evaluation Based on the Generalized Reactivity Concept", Ann. Nucl. Energy, **31/7**, 813 (2004).

# RECENTI SVILUPPI DELLA METODOLOGIA HGPT

---

## Equazioni della cinetica puntuale

- Nella cinetica puntuale dei sistemi sottocritici sono definite due equazioni:
- una governa l'andamento della potenza (P) a seguito di una perturbazione di uno o più parametri di sistema, tra cui la sorgente esterna
  - l'altra governa le densità effettive dei precursori dei neutroni ritardati ( $\xi_i$ )

$$l_{\text{eff}} \frac{dP}{dt} = (\rho_{\text{gen}} - \alpha \beta_{\text{eff}}) P + \alpha \sum_{i=1}^I \lambda_i \xi_i + \zeta(1-P) + \rho_{\text{source}}$$

$$\frac{d\xi_i}{dt} = \beta_{i,\text{eff}} P - \lambda_i \xi_i$$

Alle condizioni iniziali la potenza P è normalizzata all'unità, mentre le densità effettive dei precursori  $\xi_i$  sono date dal prodotto normalizzato delle densità dei precursori stessi per la loro importanza

$$\xi_i = \frac{\langle m_{s,0}^* m_i \rangle}{\langle \mathbf{n}_{s,0}^*, \bar{\chi} S_{f,0} \phi_0 \rangle} \quad \begin{array}{l} \text{(i'th effective precursor density)} \\ \text{( } \bar{\chi} S_{f,0} \phi_0 = \text{fission source )} \end{array}$$



# RECENTI SVILUPPI DELLA METODOLOGIA HGPT

---

La quantità  $\zeta$  che compare nell'equazione che governa l'andamento della potenza corrisponde ad un termine di normalizzazione

$$\zeta = \frac{1}{\langle \mathbf{n}_{s,o}^*, \bar{\chi} \mathbf{S}_{f,o} \phi_o \rangle}$$

Al denominatore di questo termine compare la funzione importanza neutronica  $\mathbf{n}_{s,o}^*$ . Questa funzione è governata dall'equazione aggiunta associata alla potenza normalizzata

$$\mathbf{B}_o^* \mathbf{n}_{s,o}^* + \frac{\gamma}{W_o} \mathbf{\Sigma}_{f,o} = 0$$

( $\gamma$  = energy units per fission)  
( $W_o$  = Potenza nominale)

# RECENTI SVILUPPI DELLA METODOLOGIA HGPT

---

Nell'equazione che regge la potenza compaiono delle quantità con un significato fisico preciso

$$l_{\text{eff}} = \zeta \langle \mathbf{n}_{s,o}^*, \mathbf{V}^{-1} \boldsymbol{\phi}_o \rangle \quad (\text{vita media effettiva dei neutroni pronti})$$

$$\rho_{\text{gen}} = \zeta \left( \langle \mathbf{n}_{s,o}^*, \delta \mathbf{B} \boldsymbol{\phi}_o \rangle + \frac{\gamma}{W_o} \langle \delta \boldsymbol{\Sigma}_f, \boldsymbol{\phi}_o \rangle \right) \quad (\text{reattività generalizzata relativa alla perturbazione di parametri di sistema})$$

$$\rho_{\text{source}} = \zeta \langle \mathbf{n}_{s,o}^*, \delta \mathbf{s}_n \rangle \quad (\text{reattività generalizzata relativa alla perturbazione della sorgente esterna})$$

# RECENTI SVILUPPI DELLA METODOLOGIA HGPT

---

Il coefficiente di sottocriticità  $K_{\text{sub}}$  è definito da un rapporto in cui compaiono la sorgente di fissione e la sorgente esterna pesate con la loro importanza

$$K_{\text{sub}} = \frac{\langle \mathbf{n}_{s,o}^*, \bar{\chi} S_{f,o} \phi_o \rangle}{\langle \mathbf{n}_{s,o}^*, \mathbf{s}_n \rangle + \langle \mathbf{n}_{s,o}^*, \bar{\chi} S_{f,o} \phi_o \rangle}$$

Il termine di sorgente esterna al denominatore  $\langle \mathbf{n}_{s,o}^*, \mathbf{s}_n \rangle$  risulta eguale al valore della potenza nominale normalizzata, cioè all'unità. L'espressione del coefficiente  $K_{\text{sub}}$  risulta quindi semplificata

$$K_{\text{sub}} = \frac{\langle \mathbf{n}_{s,o}^*, \bar{\chi} S_{f,o} \phi_o \rangle}{1 + \langle \mathbf{n}_{s,o}^*, \bar{\chi} S_{f,o} \phi_o \rangle}$$

# RECENTI SVILUPPI DELLA METODOLOGIA HGPT

---

$$K_{\text{sub}} = \frac{\langle \mathbf{n}_{s,o}^*, \bar{\chi} S_{f,o} \phi_o \rangle}{1 + \langle \mathbf{n}_{s,o}^*, \bar{\chi} S_{f,o} \phi_o \rangle}$$

Ricordando l'espressione del termine di normalizzazione

$$\zeta = 1 / \langle \mathbf{n}_{s,o}^*, \bar{\chi} S_{f,o} \phi_o \rangle$$

si può definire il coefficiente  $K_{\text{sub}}$  come dato da un rapporto in termini di  $\zeta$

$$K_{\text{sub}} = \frac{1}{1 + \zeta}$$

La quantità  $\zeta$  può essere a sua volta definita come un rapporto in termini di  $K_{\text{sub}}$

$$\zeta = \frac{1 - K_{\text{sub}}}{K_{\text{sub}}}$$

Questa espressione consente di poter assumere la quantità  $\zeta$  come un appropriato indice di sottocriticità

## *Il metodo*

Consideriamo una variazione della posizione di una barra di controllo (calibrata) in un reattore sottocritico. Ad essa corrisponderà un valore sperimentale di reattività  $(\delta k_{\text{eff}} / k_{\text{eff}})_{\text{B}}^{\text{exp}}$ .

Il valore della reattività generalizzata associata ad esso può essere assunto come il prodotto del suo valore calcolato per un fattore di bias

$$\rho_{\text{gen},\text{B}}^{\text{exp}} = \rho_{\text{gen},\text{B}}^{\text{cal}} f_{\text{b}}$$

Il fattore di bias  $f_{\text{b}}$  è definito da un rapporto

$$f_{\text{b}} = \frac{(\delta k_{\text{eff}} / k_{\text{eff}})_{\text{B}}^{\text{exp}}}{(\delta k_{\text{eff}} / k_{\text{eff}})_{\text{B}}^{\text{calc}}}$$

dove il numeratore è dato dal valore di calibrazione della barra di controllo mentre il denominatore è dato dalla corrispondente espressione perturbativa standard calcolata.

## RECENTI SVILUPPI DELLA METODOLOGIA HGPT

Analogamente, la reattività generalizzata di sorgente  $\rho_{\text{source}}^{\text{exp}}$ , associata ad una data variazione  $\delta s_n^{\text{exp}}$  della sorgente stessa, può essere rappresentata da un rapporto in termini del coefficiente di sottocriticità  $K_{\text{sub}}$

$$\rho_{\text{source}}^{\text{exp}} = \frac{\langle \mathbf{n}_{s,0}^*, \delta s_n^{\text{exp}} \rangle}{\langle \mathbf{n}_{s,0}^*, \chi S_{f,0} \phi_0 \rangle} \equiv \frac{\delta s_n^{\text{exp}}}{s_n} \frac{1 - K_{\text{sub}}}{K_{\text{sub}}}$$

Consideriamo ora variazioni della posizione della barra di controllo e dell'intensità della sorgente esterna tali da mantenere praticamente inalterato il livello della potenza. Ciò si riflette nella condizione per cui le reattività generalizzate associate a tali variazioni si compensano

$$\rho_{\text{gen},B}^{\text{exp}} + \rho_{\text{source}}^{\text{exp}} = 0$$

Ricordando l'espressione della reattività di sorgente si ottiene facilmente il valore cercato del coefficiente di sottocriticità

$$K_{\text{sub}} = \frac{\delta s_n^{\text{exp}} / s_n}{\delta s_n^{\text{exp}} / s_n - \rho_{\text{gen},B}^{\text{exp}}}$$

## *Conclusione*

Il metodo proposto può essere utilizzato per lo sviluppo di un sistema di misura della sottocriticità di un reattore ADS durante la sua normale operazione sulla base della rilevazione di piccole variazioni della posizione della barra di controllo e dell'intensità della sorgente esterna.

Un esercizio di simulazione numerica<sup>12</sup> è stato considerato in vista di un esperimento su una configurazione sottocritica del reattore TRIGA. L'esercizio ha dimostrato la potenzialità del metodo proposto.

L'esperimento su menzionato è attualmente in corso.

---

12. Carta, M., et al. , "The Power Control Based Subcriticality Monitoring (PCSM) Method for ADS Reactors", RRFM/IGORR Conference, Berlin, March 2016.

## 2. Identificazione di punti caldi

Attraverso l'uso della teoria perturbativa generalizzata<sup>1</sup> e delle tecniche di inferenza probabilistica<sup>2</sup> è stato sviluppato un metodo<sup>3</sup> utilizzabile in un sistema di protezione per la rilevazione di possibili punti caldi (hot spot) durante il normale funzionamento di un reattore.

Il metodo è basato su misurazioni online del flusso neutronico.

Si presume che queste misurazioni siano effettuate da rivelatori autoalimentati (SPND), denominati anche 'collettroni'.

- 
1. Gandini, A., "Generalized Perturbation Theory (GPT) Methods. A Heuristic Approach", in *Advances in Nuclear Science and Technology*, Vol. 19, Plenum Publ.,(1987).
  2. Gandini,A., "Uncertainty Analysis and Experimental Data Transposition Methods", *Handbook Uncertainty Anal.*,CRC(1988).
  3. Gandini, A., "Hot Point Detection Method", *Ann. Nucl. En.*, 38 (2011) 2843.



Il metodo è stato concepito per il suo utilizzo nei reattori termici, in particolare nei PWR.

Il suo utilizzo nei reattori veloci è legato allo sviluppo di tecniche di rilevamento del flusso neutronico sufficientemente precise<sup>4</sup>

---

4. Lepore, L., Remetti, R., Cappelli, M., J. Nucl. Eng. and Rad. Sci., 2(4), NERS-15-1205, doi: 10.1115/1.4033697 (2016).

# ***RECENTI SVILUPPI DELLA METODOLOGIA HGPT***

---

Il metodo tiene conto degli errori associati alle misurazioni.

Esso consente inoltre di valutare l'effetto sulla qualità dei rilevamenti a seguito di possibili guasti degli strumenti di misura.

Tale valutazione può essere utile per definire una strategia di protezione adeguata in termini di qualità, numero e distribuzione dei collettroni.

## *Teoria*

Supponiamo che un numero fisso (N) di collettroni sia posizionato nel nocciolo di un dato reattore. Consideriamo quindi un numero (M) di ipotetiche posizioni di punti caldi.

Per semplicità assumiamo anche che in ogni ipotetica posizione di punto caldo rimanga costante il rapporto

$$r_m \equiv p_m^{\max} / \bar{p}_m$$

tra la densità di potenza lineare massima e quella media.

# RECENTI SVILUPPI DELLA METODOLOGIA HGPT

---

Viene fissata una prima soglia  $p_m^{\text{max},1}$  della densità di potenza lineare massima, oltre la quale si innesca un avviso di attenzione

Viene quindi fissata una seconda soglia  $p_m^{\text{max},2}$  al di sopra della quale si verifica l'arresto dell'impianto.

Dall'analisi dei rilevamenti dei collettroni, la possibilità della presenza di una condizione di punto caldo in una o più delle M posizioni ipotetiche deve essere valutata in relazione alle soglie assegnate.

## ***RECENTI SVILUPPI DELLA METODOLOGIA HGPT***

---

Questa metodologia utilizza dei coefficienti di sensitività ( $w_{n,m}$ ). Essi rappresentano il contributo di una sorgente di fissione unitaria, localizzata in un dato elemento ( $m$ ) di combustibile, al suo rilevamento in ciascuno degli  $N$  collettroni.

Questi coefficienti formano un vettore,  $w_m$ , caratteristico di ciascuna delle possibili posizioni di punti caldi. In un certo senso, questo vettore può essere considerato come una loro 'firma'.

Data una serie di misurazioni  $Q_n^{\text{ex}}$  ( $n = 1, \dots, N$ ), la ricerca di un potenziale punto caldo inizia quando uno o più rilevamenti differiscono significativamente, vale a dire oltre margini di incertezza stabiliti, dai valori nominali.

La posizione, o posizioni, di punto caldo e il valore della relativa intensità sono ottenuti mediante tecniche di inferenza probabilistica.

Viene tenuto in conto il grado di degradazione del sistema di collettroni.

## *Applicazione numerica*

È stata effettuata una simulazione numerica<sup>5</sup> relativa a un progetto di sistema PWR di dimensioni medie<sup>6</sup>. Il sistema è stato semplificato in una geometria x, y.

Per l'analisi è stato utilizzato il codice Eranos<sup>7</sup>.

I calcoli sono stati fatti in approssimazione di diffusione utilizzando una libreria di sezioni d'urto a 15 gruppi.

---

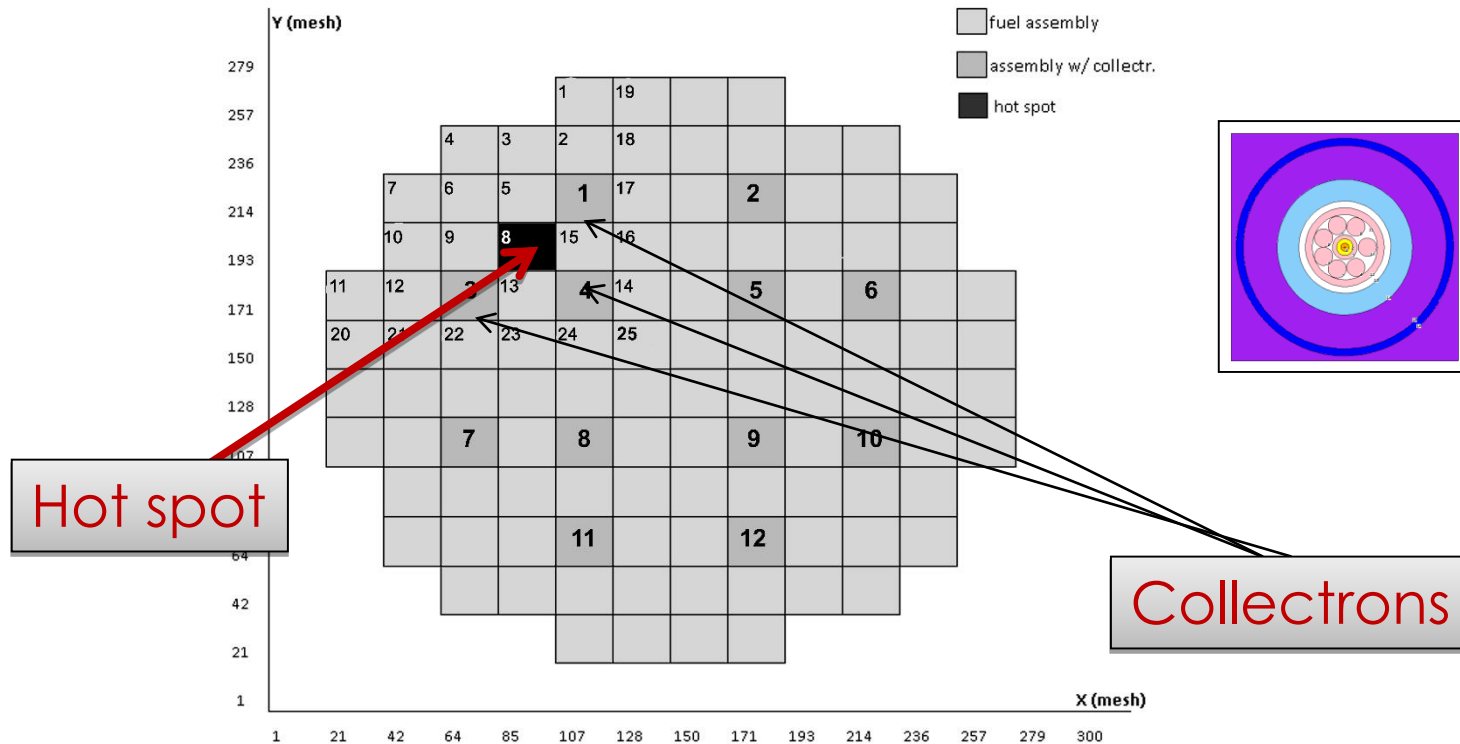
5. Gandini, A., et al., Ann. Nucl. Energy, 50,175 (2012).

6. Cumo, M., Naviglio, A., Sorabella, L., "MARS, 600 MWth Nuclear Power Plant", ANES Symposium, Miami, 2004.

7. Rimpaut, G., et al., "Physics Documentation of the ERANOS. The ECCO Cell Code", CEA Technical Note RT-SPRC-LEPh-97-001 (1997).

# RECENTI SVILUPPI DELLA METODOLOGIA HGPT

Posizioni degli elementi contenenti i collettroni e posizioni degli elementi di combustibile



Per la simulazione del punto caldo è stata scelta la posizione 8

# RECENTI SVILUPPI DELLA METODOLOGIA HGPT

---

Per questo esercizio di simulazione, si è assunto che i 'rilevamenti'  $Q_n^{\text{ex}}$  corrispondano a un insieme di quantità casualmente ordinate secondo una legge di distribuzione gaussiana caratterizzata da determinati valori calcolati  $Q_n^{\text{cal}}$  e una deviazione standard del 5%.



## RECENTI SVILUPPI DELLA METODOLOGIA HGPT

In questa tabella vengono riportati i risultati dell'esercizio di simulazione. Da notare come la posizione e l'intensità del punto caldo rilevato vengano identificate in modo univoco fino al guasto di cinque collettroni.

| Degradation<br>(Failed collectrons) | Hot spot candidates<br>positions | Hot spot  |           |             |
|-------------------------------------|----------------------------------|-----------|-----------|-------------|
|                                     |                                  | Simulated | Estimated | Stand. Dev. |
| 0                                   | 8                                | 1.000     | 1.003     | 0.079       |
| 1                                   | 8                                | 1.000     | 1.003     | 0.094       |
| 1,2                                 | 8                                | 1.000     | 1.004     | 0.095       |
| 1,2,3                               | 8                                | 1.000     | 1.008     | 0.123       |
| 1,2,3,4                             | 8                                | 1.000     | 1.005     | 0.153       |
| 1,2,3,4,5                           | 8                                | 1.000     | 1.007     | 0.162       |
| 1,2,3,4,5,6,7                       | 6,8,9,15                         | 1.000     | 1.006     | 0.176 (min) |

## *Conclusione*

I risultati ottenuti con l'esercizio di simulazione indicano come il metodo proposto possa essere utilizzabile in un sistema di protezione per la rilevazione di possibili punti caldi.

Questo metodo può essere utile anche in una fase di progettazione.

L'analisi approfondita sulla distribuzione dei collettroni e sulle loro sequenze di guasti può infatti consentire di identificare configurazioni ottimali sulla base di criteri dell'ingegneria impiantistica e sulla base di considerazioni economiche.

Un interesse a questa metodologia è stato recentemente manifestato dalla società belga Tractebel. Sono in corso contatti in vista di una possibile collaborazione.

# ***RECENTI SVILUPPI DELLA METODOLOGIA HGPT***

---

L'applicabilità della metodologia potrebbe anche essere presa in considerazione per la rilevazione di un punto caldo prodotto dal blocco di flusso di un canale.

Un blocco di flusso produrrebbe infatti un aumento della temperatura locale, che a sua volta causerebbe un'alterazione (in questo caso riduzione) del tasso di fissione per l'aumento dell'assorbimento neutronico a causa dell'effetto Doppler.

## 3. Metodologia per l'analisi del burn-up

La metodologia per l'analisi perturbativa di funzionali della densità neutronica e di quella dei nuclidi che evolvono durante il burn-up è stata sviluppata secondo la teoria delle perturbazioni generalizzate su base euristica (HGPT).<sup>1,2</sup>

Questa metodologia può essere applicata sia a sistemi critici che sottocritici.

- 
1. A. Gandini, "Generalized Perturbation Theory (GPT) Methods. A Heuristic Approach", in *Advances in Nuclear Science and Technology*, Vol. 19, Plenum Publishing Corporation, New York, 1987.
  2. A. Gandini, "Sensitivity Analysis of Source Driven Subcritical Systems by the HGPT Methodology", *Annals of Nuclear Energy*, 24, 1241 (1997).

# ***RECENTI SVILUPPI DELLA METODOLOGIA HGPT***

---

I funzionali d'interesse possono riguardare, in particolare:

- L'accumulo di isotopi del combustibile a fine ciclo. In questo caso il metodo può essere utilizzato per la ricerca di valori ottimali di parametri di progetto o per la ricerca di strategie ottimali di caricamento del combustibile.
- La fluenza ad un tempo e punto stabiliti. In questo caso il metodo può essere utilizzato per analizzare il danneggiamento sui materiali con la vita del reattore.
- La radiotossicità delle scorie a lungo termine.
- Il parametro di controllo a fine ciclo. L'analisi di questa quantità può essere d'interesse in studi volti ad estendere il ciclo di vita del reattore.

# RECENTI SVILUPPI DELLA METODOLOGIA HGPT

---

## Equazioni

Il campo non-lineare d'interesse per lo studio del burn-up riguarda le funzioni:

- densità neutronica  $\mathbf{n}(\mathbf{r},t)$ ,
- densità dei nuclidi  $\mathbf{c}(\mathbf{r},t)$ ,
- parametro intensivo di controllo sulla potenza  $\rho(t)$ .

Equazioni che le governano:

$$\mathbf{m}_{(n)}(\mathbf{n}, \mathbf{c}, \rho | \mathbf{p}) = -\frac{d\mathbf{n}}{dt} + B(\mathbf{c}, \rho | \mathbf{p})\mathbf{n}_o + \mathbf{s}_n(\mathbf{p}) = \mathbf{0} \quad \begin{array}{l} \text{- Neutron density equation} \\ \text{(at quasi static conditions: } d\mathbf{n}/dt \approx 0) \end{array}$$
$$\mathbf{m}_{(c)}(\mathbf{n}, \mathbf{c} | \mathbf{p}) = -\frac{d\mathbf{c}}{dt} + E(\mathbf{n}, \mathbf{c} | \mathbf{p})\mathbf{c} = \mathbf{0} \quad \text{- Nuclide density equation}$$
$$m_{\rho}(\mathbf{n}, \mathbf{c} | \mathbf{p}) = \langle \mathbf{c}^T \mathbf{S} \mathbf{n} \rangle_{\text{sys}} - W = 0 \quad \text{- Power (W) condition}$$

Il vettore  $\mathbf{p}$  rappresenta i parametri di sistema

Gli operatori  $B$  ed  $E$  dipendono: il primo dalla densità del combustibile ( $\mathbf{c}$ ) e dal parametro di controllo ( $\rho$ ), il secondo dalla densità neutronica ( $\mathbf{n}$ ).

# RECENTI SVILUPPI DELLA METODOLOGIA HGPT

---

Un funzionale d'interesse può essere in generale rappresentato da un'espressione integrale

$$Q = \int_{t_0}^{t_F} dt \left( \langle \mathbf{h}_n^{+T} \mathbf{n} \rangle_{\text{sys}} + \langle \mathbf{h}_c^{+T} \mathbf{c} \rangle_{\text{sys}} + h_\rho^+ \rho \right)$$

dove  $\mathbf{h}_n^+, \mathbf{h}_c^+, h_\rho^+$  sono quantità assegnate.

# RECENTI SVILUPPI DELLA METODOLOGIA HGPT

---

Consideriamo un nocciolo suddiviso in macrozone di combustibile e una schematizzazione a step temporali.

Secondo la metodologia HGPT la variazione prodotta nel funzionale considerato da una perturbazione dei parametri di sistema viene data da una somma

$$\delta Q = \sum_{j=1}^J \delta p_j \sum_{i=1}^I \sum_{z=1}^Z V_z \left( \boldsymbol{\psi}_i^{*T} \frac{\partial \mathbf{m}_{n,z,i}}{\partial p_j} + \left( \int_{\Delta_i} \mathbf{c}_z^{*T} dt \right) \frac{\partial \mathbf{m}_{c,z,i}}{\partial p_j} + \rho_i^* \frac{\partial m_{\rho,z,i}}{\partial p_j} \right)$$

dove compaiono le funzioni importanza associate alle densità dei neutroni e dei nuclidi ed al parametro di controllo.



# ***RECENTI SVILUPPI DELLA METODOLOGIA HGPT***

---

## *Attività previste*

Il lavoro finora svolto in questo campo è consistito nell'implementazione della metodologia perturbativa HGPT nel codice di calcolo Eranos in relazione a casi relativamente semplici.

Futuri sviluppi richiedono la stretta collaborazione con il gruppo francese di Cadarache responsabile di questo codice.

Recentemente, ad una nostra proposta su temi specifici di collaborazione, abbiamo ricevuto un riscontro molto positivo.

E' previsto un incontro per stabilire un programma di attività comune che dovrebbe vedere coinvolti laureandi e/o dottorandi nostri e loro.

**GRAZIE DELLA VOSTRA ATTENZIONE**

# Neutronic codes validation for LFR applications: status and perspectives

ADP MiSE-ENEA PAR2017 B.3-LP2

Gen.IV-LFR: Stato attuale della tecnologia e prospettive di sviluppo

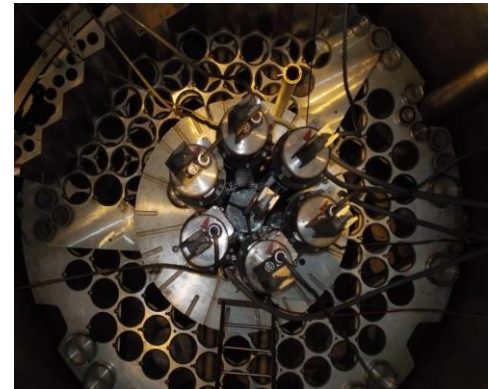
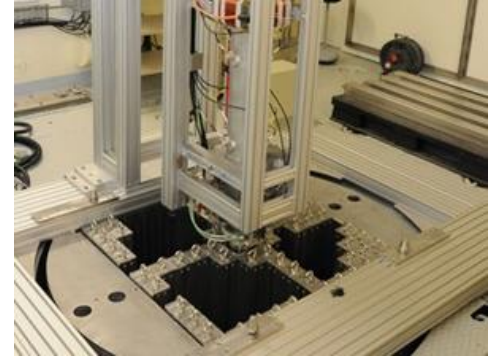
*Università di Roma «La Sapienza», 14-15 giugno 2018*

**M. Sarotto, G. Grasso, P. Console Camprini (ENEA)**



# Contents

- 1) Framework
- 2) Validation process for LFR
- 3) Neutronic parameters
- 4) Experimental campaigns:
  - LR-0 reactor (CVR, Czech Republic)
  - VENUS-F reactor (SCK•CEN, Belgium)
- 5) Codes validation campaign  
(Deterministic and Monte Carlo)
- 6) Some C/E results & analyses
- 7) Conclusions and perspectives



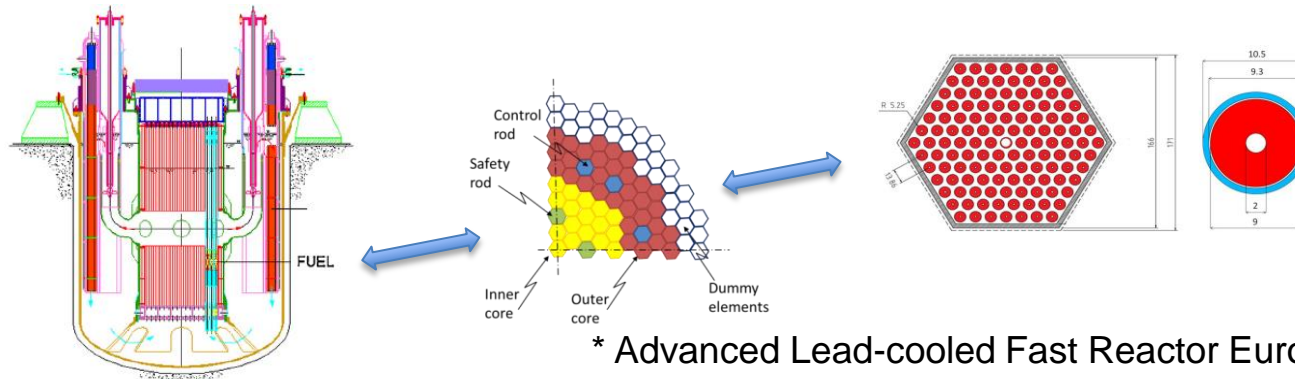
# 1 Framework

The design of the ALFRED\* core/reactor:

- was defined in EURATOM FP7 LEADER project
- has been refined in ADP ENEA-MiSE PAR2015-17 B.3-LP2
- is currently under development by FALCON international consortium



**ENEA was/is responsible for the core design activities**



MOX fuel with  
 $\cong 22 / 27$  wt.%  
Pu mass content

\* Advanced Lead-cooled Fast Reactor European Demonstrator

## 2 Validation process for LFR

### Validation of neutronic codes for LFR

LFR is new reactor concept → **Complete Validation for neutronic codes and nuclear data libraries** is needed for core design & licensing (simulation tools & nuclear data are among the main sources of uncertainties)

Validation activities for TH analyses in Pb/PbBi systems carried out in the past, but a similar effort for neutronic analyses not yet done

→ Necessity of:

- **Representative experiments of predicted LFR conditions**
- **Experimental measurements of relevant parameters**
- **Validation of codes reliability** by calc. vs. measures comparison

# 3.1 Neutronic parameters

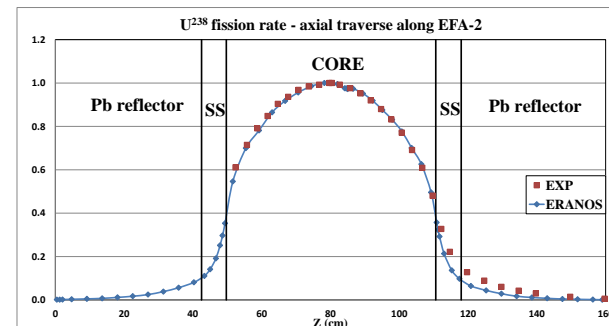
Validation of neutronic codes/libraries requires experimental measurements in LFR representative conditions of:

- \* **integral parameters:** critical mass (i.e.,  $k$  multiplication factor or reactivity  $\rho$ ), reactivity worth of  $n$  absorbers (Control & Safety Rods), delayed neutron fraction and mean generation time ( $\beta$  and  $\Lambda$ ), reactivity feedbacks/coefficients

$$\hat{\beta}_i = \frac{\sum_m \hat{\beta}_i^{(m)} \langle \sum_{g'} v_{g'}^{(m)} \Sigma_{f,g'}^{(m)}(\mathbf{r}) \phi_{g'}(\mathbf{r}) \rangle_{\mathbf{r}}}{\sum_m \langle \sum_{g'} v_{g'}^{(m)} \Sigma_{f,g'}^{(m)}(\mathbf{r}) \phi_{g'}(\mathbf{r}) \rangle_{\mathbf{r}}}$$

- \* **local parameters:** radial and axial traverses (flux and reaction rates), spectrum indexes, void reactivity worth

$$SI^r = \frac{\sum_g \sigma_g^r \phi_g}{\sum_g \sigma_g^{F25} \phi_g}$$



## 3.2 Validation of neutronic codes

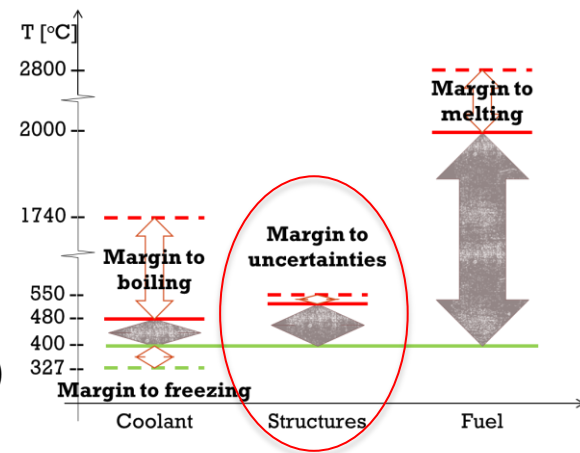
Best-estimate codes (& data) with evaluation of uncertainties.

Validation is inherently associated with the use of **best-estimate codes** and **nuclear data**, by **evaluating the uncertainty** in reproducing exp. results.

Uncertainties may come from:

- materials properties & geometrical tolerances (for e.g. fuel pellets, cladding and wrapper geometries)
- nuclear data (cross sections, delayed n fraction, etc.)
- calculation methods (Monte Carlo & deterministic)

Assessment of confidence in results (i.e., uncertainty) is used to strengthen the ALFRED core design.





# 4.1 Experimental campaigns

Most aimed requirement for **VALIDATION** is the achievement of a “LFR representative spectrum” for the main neutronic parameters

LFR representative experimental results available from:

- 1) **VENUS-F zero-power reactor**, during EURATOM FP7 FREYA\* project
- 2) **LR-0 zero-power reactor**, during PAR2015-17 (ENEA-CVR contract)

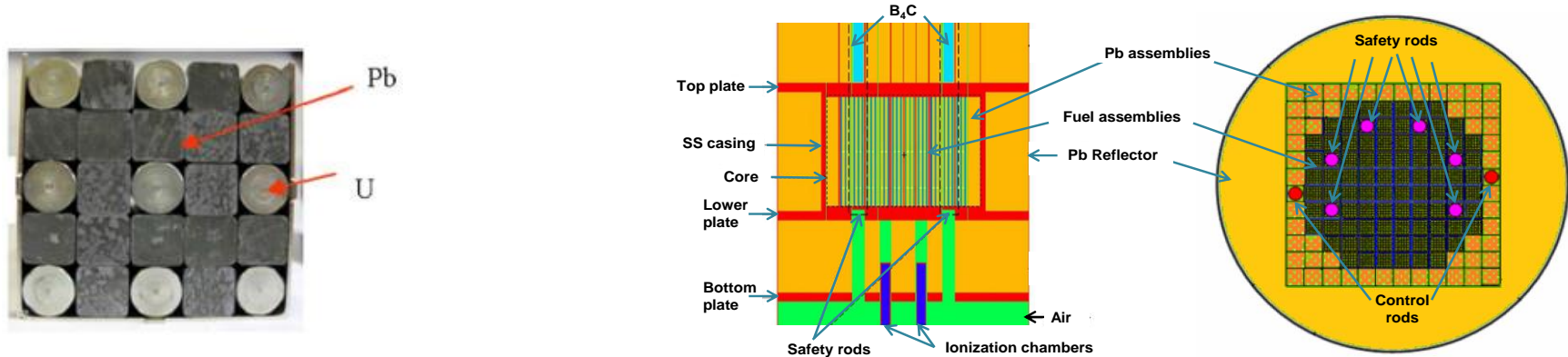
While in LR0 only local parameters were measured, in VENUS-F integral tests and local measures were performed.

| Experiment | Measured n parameters | n codes                     |
|------------|-----------------------|-----------------------------|
| VENUS-F    | Integral & Local      | Monte Carlo & Deterministic |
| LR-0       | Local                 | Monte Carlo                 |

\* Fast Reactor Experiments for hYbrid Applications

## 4.2 VENUS-F facility

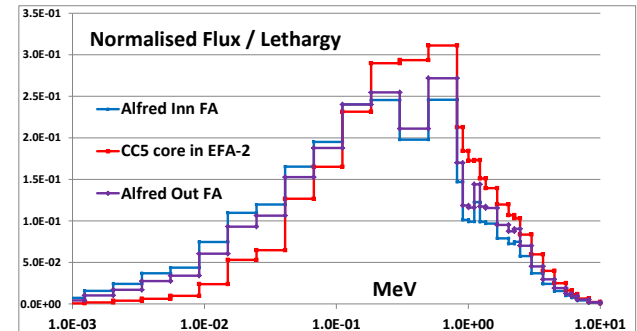
### Core components, radial and axial reflectors in solid lead



Fuel Assembly (FA) is 5x5 square matrix with:

- U metallic rods (30 U<sup>235</sup> wt.%)
- Pb blocks simulating LFR coolant.

→ FA/core spectrum too hard for ALFRED (MOX)



# 4.3 VENUS-F core representative of ALFRED

To reproduce LFR n spectrum ...

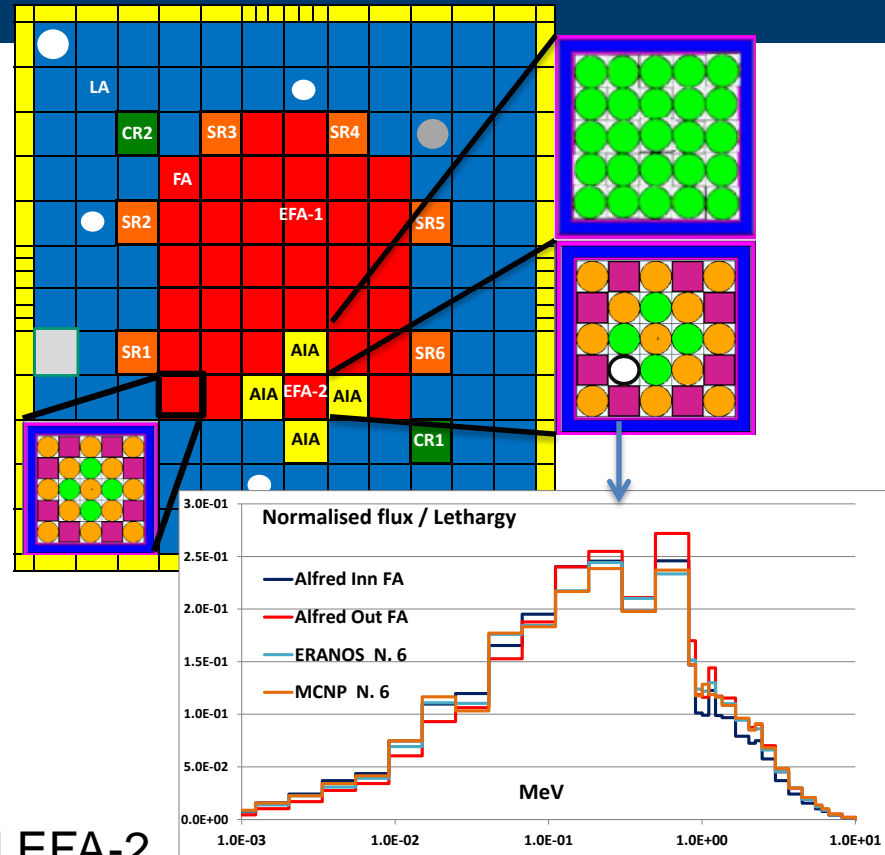
... moderating elements introduced:

- 4 Al Oxide ( $Al_2O_3$ ) rods in FA (green)
- 25  $Al_2O_3$  rods in inert assemblies (AIA\*)

Accurate reproduction of the ALFRED spectrum (> 1 keV) in an EFA\*\* (EFA-2)

**Measured parameters:**

- **integral:** k, Control Rods worth
- **local:** fission rates traverses & spectrum indexes in EFA-2, void reactivity effects in & around EFA-2.



\* Alfred Inert Assembly \*\* Experimental FA



## 4.4 LR-0 facility

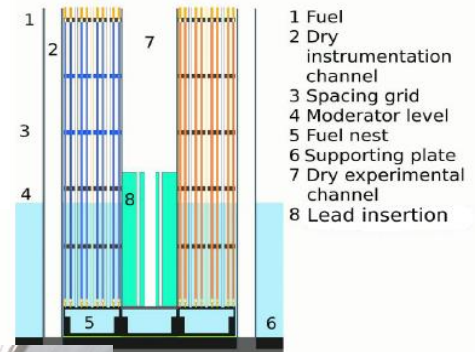
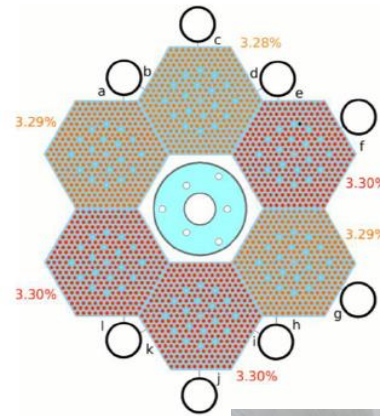
### A dry channel in the centre of six VVER FAs

LR-0 is a zero-power pool-type LWR used to measure the n-physical characteristics of VVER\* reactors.

Driver core is an hexagonal ring made of six FA with  $\text{UO}_2$  fuel ( $\text{U}^{235}$ : 3.28 - 3.3 w.t.%).

Criticality tuned by adjustments of water level

Central dry position free to insert a test section

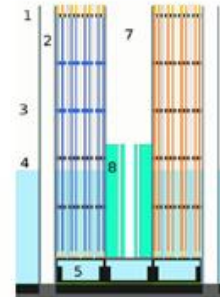


\* Water-Water Energetic Reactor

## 4.5 LR-0 core «representative» of ALFRED

To reproduce n propagation in lead...

... in the dry channel a SS cylindrical shell filled by Pb was introduced, with six fuel pins ( $U^{235}$  3.6 w.t.%) at  $\neq$  distances from the centre.



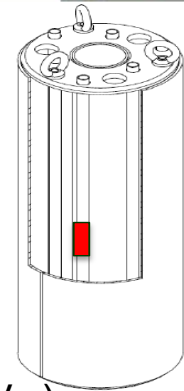
**Measured parameters:**

- **local:** flux and power distributions through **measured  $\gamma$**  (after 2.5 h irradiation) emitted by:

-  **$Np^{239}$** , via  $U^{238}$  capture  $\rightarrow$  **flux**

( $t_{1/2} = 2.35$  d  $\rightarrow$  277 keV  $\gamma$ )

-  **$Sr^{92}$** , via  $U^{235}$  and  $U^{238}$  fission  $\rightarrow$  **power** ( $t_{1/2} = 2.7$  h  $\rightarrow$  1384 keV  $\gamma$ )

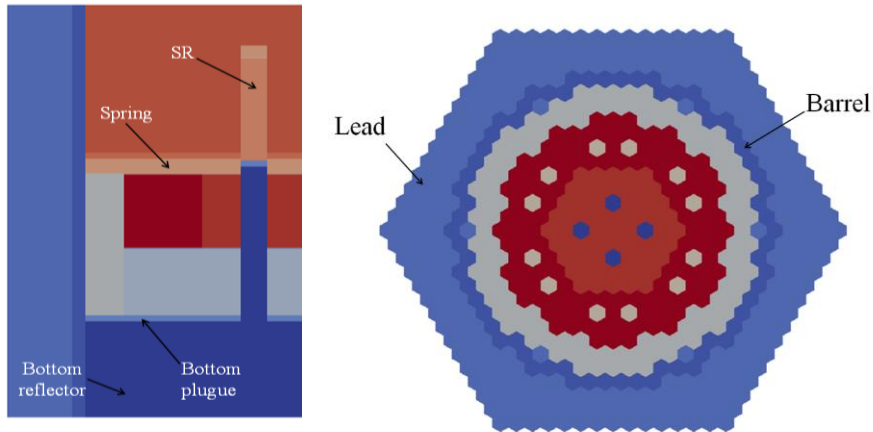


# 5.1 Neutronic codes

## Neutronic codes used at ENEA FSN SICNUC division

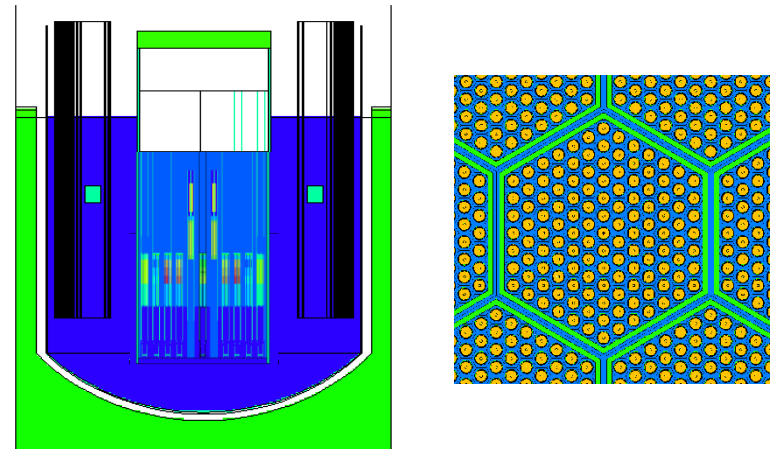
### Deterministic codes

**ERANOS** (CEA), **PHISICS** (INL),  
**Scale suite** (ORNL)



### Monte Carlo codes

**MCNP** (LANL), **Serpent** (VTT),  
**GEANT** (CERN)



## 5.2 Neutronic codes validated

### ERANOS, MCNP and SERPENT

In **LR-0**:

- **MCNP6.1** code (ENEA and CVR)

**Mont Carlo N-Particle**

Continuous treatment of energy dependence

Exact heterogeneous geometry description

**ENDF/B-VII.1** nuclear data library

In **VENUS-F**:

- **ERANOS 2.2n** (ENEA)

**European Reactor ANalysis Optimised System**

Heterogeneous-homogenised cross-sections (ECCO)

Full core calculations with 3D XYZ core geometry model

**JEFF3.1** and **ENDF/B-VI.8** nuclear data libraries

- **MCNP** and **SERPENT**

(other FREYA partners) → Different MCNP versions and nuclear data libraries

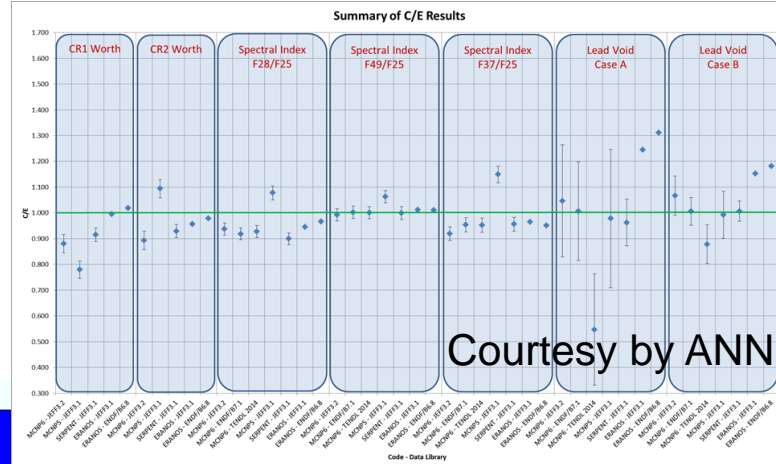
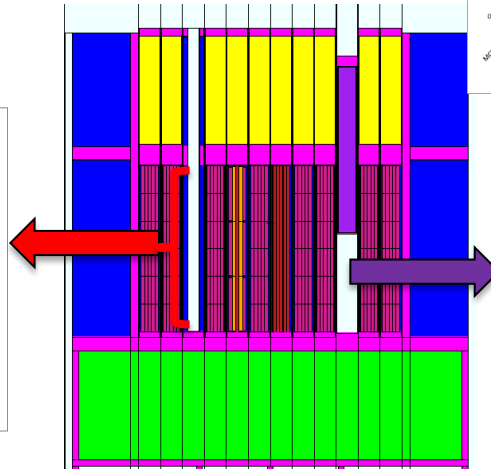
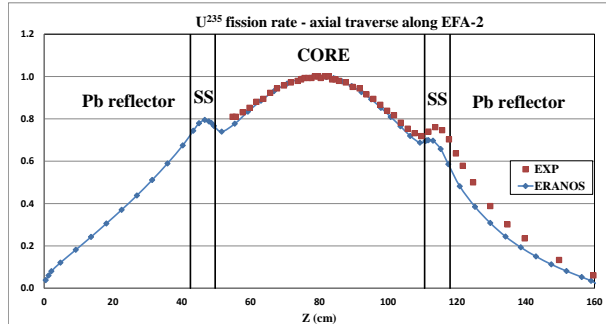
- experimental and calculation results confidential (FREYA partners)

# 5.3 Codes Validation campaign in VENUS-F

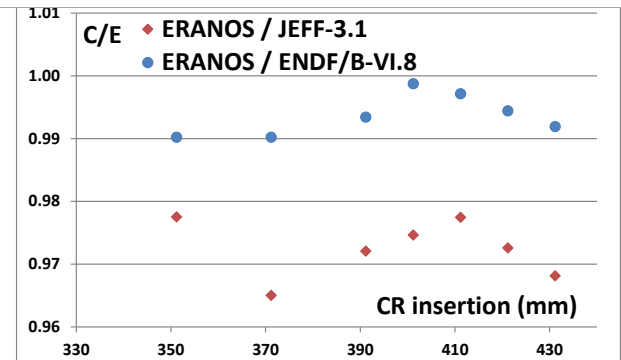
ERANOS, MCNP & SERPENT with  $\neq$  data

All (integral and local) parameters measured compared with calculations obtained by  $\neq$  codes and  $\neq$  data libraries: major part of results\* compatible within 1-3 $\sigma$  uncertainty level

\* here shown as C/E  
(Calculated-to-Experimental ratio)



Courtesy by ANN



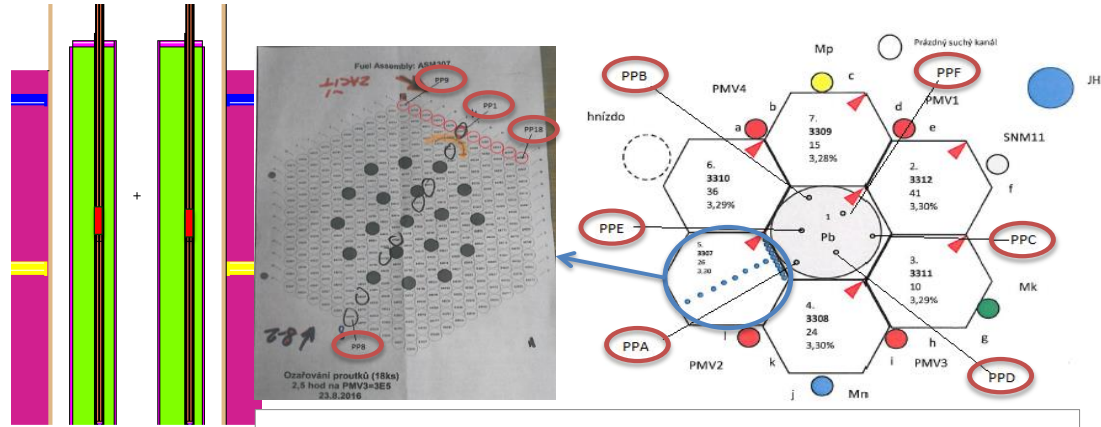


# 5.4 Code validation campaign in LR-0

MCNP with ENDF/BVII.1 data

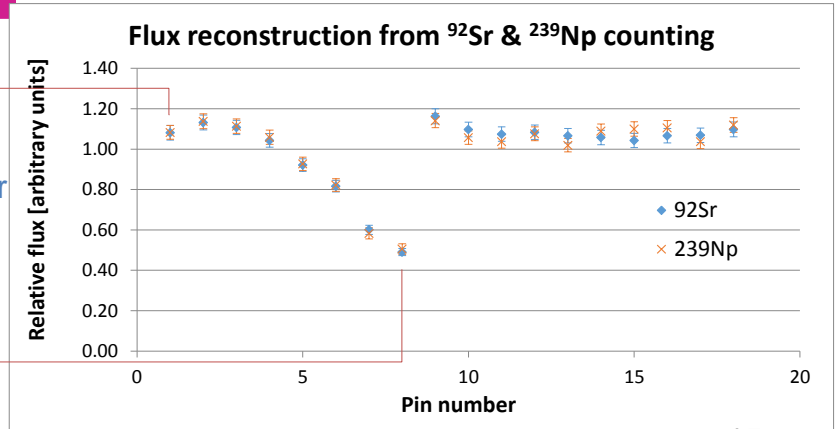
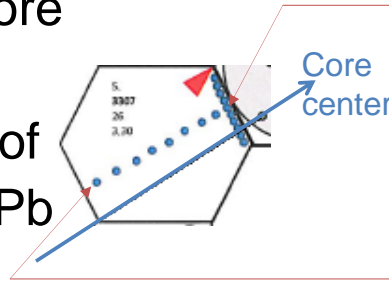
Local flux & power distributions measured & simulated in:

- 6 fuel pins in Pb shell
- 19 fuel pins in one FA



→ 3D flux/power map in core

→ Validation of prediction of n propagation through Pb



# 6.1 Example of results: $k$ , $\beta$ & $\Lambda$ in VENUS-F

During FREYA, 5 critical core layouts were assembled & characterized (CR0, CC5-CC8), where: - CR0 is the start up core  
- CC6\* is «ALFRED representative» core

Kinetic parameters ( $\beta$ ,  $\Lambda$ ) were measured in CR0

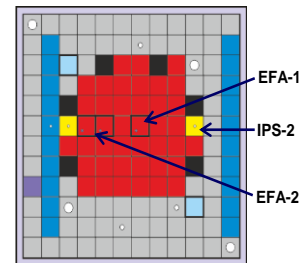
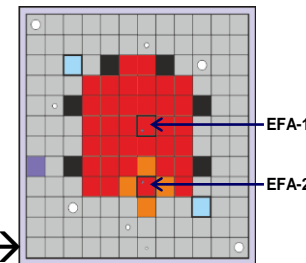
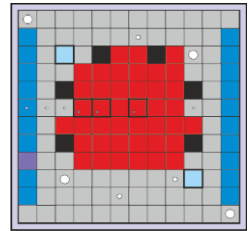
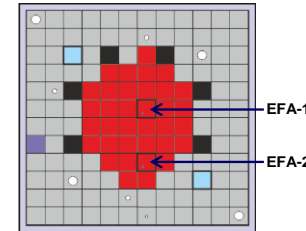
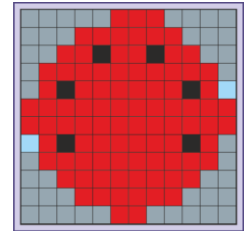
Calculations of  $k$ ,  $\beta$  and  $\Lambda$  were analysed:

- by comparison with experimental measurements
- by code-to-code (& library-to-library)

comparison

| Core       | $\beta_{\text{eff}}$ (pcm) | $\Lambda$ (ns) |
|------------|----------------------------|----------------|
| CR0        | $730 \pm 11$               | $410 \pm 40$   |
| Experiment | $730 \pm 11$               | $410 \pm 40$   |
| ERANOS     | 722.5                      | 498            |

| Core | $\rho$ (pcm, JEFF3.1) |             | $\Delta\rho$ (pcm) |
|------|-----------------------|-------------|--------------------|
|      | ERANOS                | Serpent     |                    |
| CR0  | 419                   | $496 \pm 2$ | -77                |
| CC5  | 214                   | $763 \pm 3$ | -549               |
| CC6  | 405                   | $812 \pm 2$ | -407               |
| CC7  | 205                   |             |                    |
| CC8  | 428                   | $186 \pm 1$ | 242                |



\* Critical Core n. 6 →

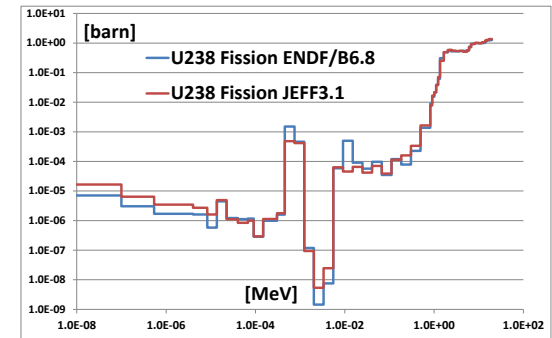
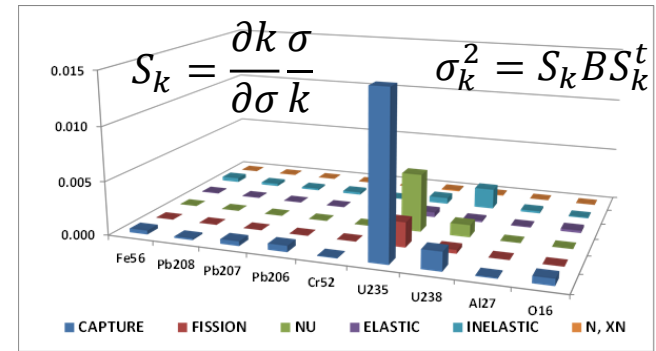
## 6.2 Uncertainty on $k_{\text{eff}}$ value (VENUS-F)

Neutronic codes yield a systematic over-estimation of core reactivity in all 5 core layouts (<1 %). Possible reasons:

- bias in geometry core modelling (negligible)
- materials specifications (e.g., Pb purity)
- **nuclear data uncertainties.**

Further in-depth analyses indicate:

- **2% uncertainty due to cross-sections data** (sum over energy groups, cross-sections & isotopes)
- max 0.6% difference with  $\neq$  code or  $\neq$  data
- main cause of  $k_{\text{eff}}$  over-estimation could be due to actual  $\text{U}^{235}$  wt.% (no variance available)

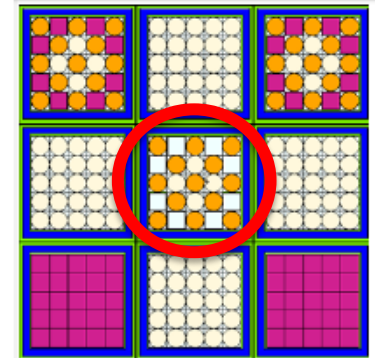


# 6.3 Data base of measures/simulations (VENUS-F)

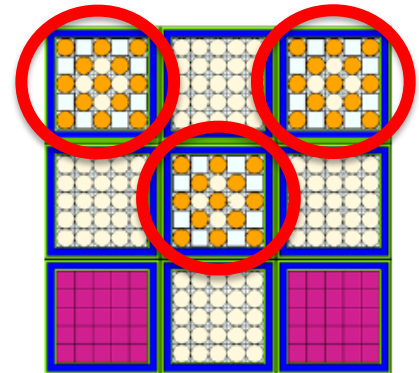
All calculated parameters were compared (C-E) with 1-3 $\sigma$  measurement uncertainty, e.g., data set for CRs worth & void effects

| CR worth | Code    | Library   | C-E          |
|----------|---------|-----------|--------------|
| CR1      | MCNP6.1 | JEFF3.2   | > 3 $\sigma$ |
|          | MCNP5   | JEFF3.1   | > 3 $\sigma$ |
|          | SERPENT | JEFF3.1   | > 3 $\sigma$ |
|          | ERANOS  | JEFF3.1   | < $\sigma$   |
|          |         | ENDF/B6.8 | < $\sigma$   |
| CR2      | MCNP6.1 | JEFF3.2   | < 3 $\sigma$ |
|          | MCNP5   | JEFF3.1   | < 3 $\sigma$ |
|          | SERPENT | JEFF3.1   | < 3 $\sigma$ |
|          | ERANOS  | JEFF3.1   | < 3 $\sigma$ |
|          |         | ENDF/B6.8 | < $\sigma$   |

| Case   | Code    | Library    | C-E          |
|--------|---------|------------|--------------|
| Case A | MCNP6.1 | JEFF3.2    | < $\sigma$   |
|        |         | ENDF/B7.1  | < $\sigma$   |
|        |         | TENDL 2014 | < 3 $\sigma$ |
|        | MCNP5   | MCNP5      | < $\sigma$   |
|        | SERPENT | SERPENT    | < $\sigma$   |
|        | ERANOS  | JEFF3.1    | > 3 $\sigma$ |
| Case B | MCNP6.1 | JEFF3.2    | < $\sigma$   |
|        |         | ENDF/B7.1  | < $\sigma$   |
|        |         | TENDL 2014 | < 3 $\sigma$ |
|        | MCNP5   | MCNP5      | < $\sigma$   |
|        | SERPENT | SERPENT    | < $\sigma$   |
|        | ERANOS  | JEFF3.1    | > 3 $\sigma$ |
|        |         | ENDF/B6.8  | > 3 $\sigma$ |



«Case A»



«Case B» 18

Measurement uncertainty coupled with uncertainty analyses  
 → Assessment of the confidence level of calculation results.


## 6.4 Some significant results in LR-0

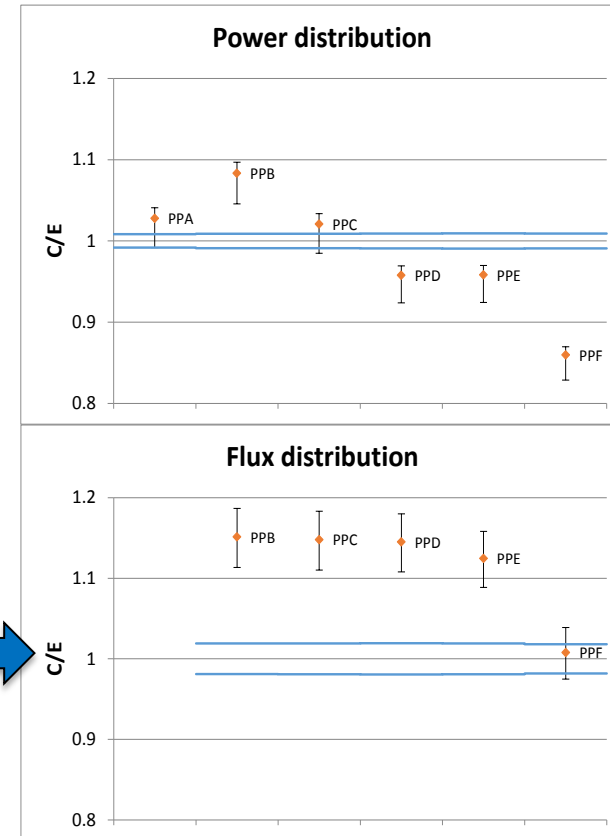
**Initial verification** of reactor model in MCNP:

- $k_{\text{eff}}$  reproduced with 0.4% accuracy
- **Reactor power level**, obtained with good accuracy independently by 2 calculation routes (2.2 & 2.3 mW);

**Validation of n propagation** capability by **local** flux and power distributions:

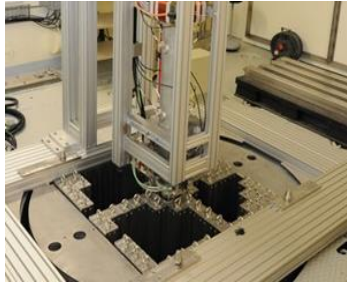
- $\gamma$  **counts** from  $\text{Np}^{239}$  and  $\text{Sr}^{92}$  with 10-15% accuracy

A systematic over-estimation found for  $\text{Np}^{239}$  counts.  Seems to confirm the over-estimation of the  $\text{U}^{238}$  capture cross-section (observed also in LWR case)



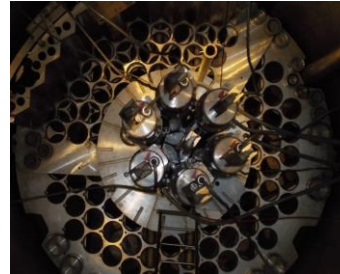
# 7.1 To summarise

Validation activities performed to assess confidence of n codes, based on the access to experimental results in key facilities



**VENUS-F (Mol, BE) for:**

- critical mass
- flux & spectrum traverses
- absorber & lead void worth



**LR-0 (Řež, CZ) for:**

- neutron propagation in Pb, in terms of attenuation and spectral shift (through local flux & power distributions)

**Data-base of measurements & calculation results** available for both experiments.

In VENUS-F, calc. results available for  $\neq$  codes/data libraries, with further uncertainty analyses.

→ Significant feedbacks to neutronic analyst for the correct LFR core modelling

## 7.2 Conclusions and perspectives

### Concluding remarks

- 1) VENUS-F experiments contribute to **Validation of ERANOS, MCNP and SERPENT codes for LFR**
- 2) LR-0 experiments (properly arranged despite the poor integral LFR representativeness) further contribute to **Validation of MCNP code reliability**

### Future perspectives

- Validation activity will proceed by:
- **further in depth-analyses** with different codes/libraries, sensitivity & uncertainty analyses
  - **systematic arrangement of all available data**  
→ Validation dossier to be used for ALFRED pre-licensing phase

massimo.sarotto@enea.it  
ENEA FSN SICNUC PSSN



1101 0110 1100  
0101 0010 1101  
0001 0110 1110  
1101 0010 1101  
1111 1010 0000





# ALFRED Core Design

## Status and future work

*«GEN-IV LEAD COOLED FAST REACTOR  
STATO ATTUALE DELLA TECNOLOGIA E PROSPETTIVE DI SVILUPPO»  
Workshop tematico AdP MISE – ENEA PAR2017 – PROGETTO B.3 - LP2  
Università di Roma «La Sapienza», 14-15 Giugno 2018*

**G. Grasso, F. Lodi, M. Sarotto, D. Castelluccio,  
A. Poggianti, A. Palumbo, S. Barberio, G. Nallo**



|                 | $\Delta K / 2.00$<br>4000 pcm<br>= 4 m                 | 2500 pcm<br>= 14  | AFRONTA                       |
|-----------------|--|---|-------------------------------|
| MW              | 300  | 300   | 300                           |
| %               | 32.04%   | 28.8%   | <del>28</del> 29%             |
| $U - P_0$ (Ton) |  |   | $U + 1.74 P_0 = 6.9t$ (HM)    |
| $r$ (cm)        | 67.4 cm  | 60 cm   | -5000 110 cm <sup>+4000</sup> |
| $z$ (cm)        | 65   | 60  | +2500 pcm 65 cm               |
| VF              | cool 62.73   | 47.95   | 49.04                         |
|                 | stro 13.41   | 15.70   | 17.25                         |
|                 | fuel 23.26   | 26.35   | 33.71                         |
|                 | $CO_2 = 1.52t$<br>$P_{O_2} = 2.62t$<br>$15.4t = 1.103$ | $CO_2 = 5.41t$ (Box)<br>$P_{O_2} = 1.88t$<br>$k_{eff} = 1.08$ | $K = 1.08$                    |

## Conceptualization

# Core systems

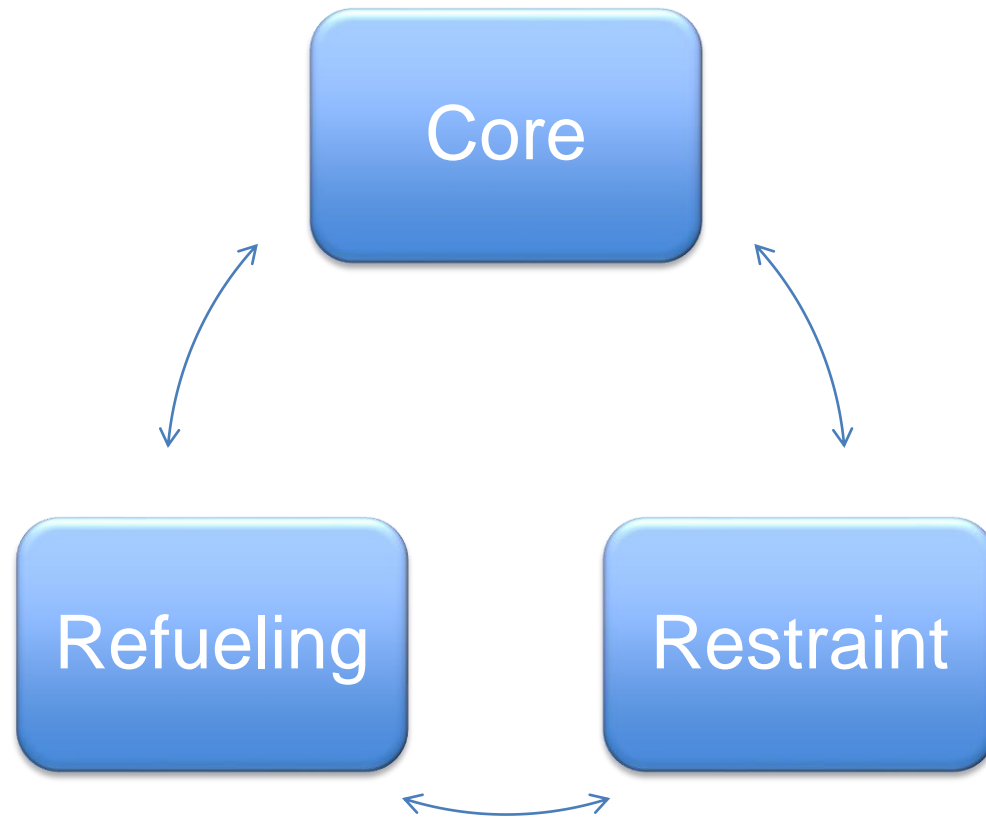
## Technical review

The previous core (i.e., v.1.00 as of LEADER) was already a good one (though a bit too large...).

BUT, the restraint and the refueling systems were completely missing. Even worse: the underlying strategies were missing at all!

# Core systems

## Interfaces



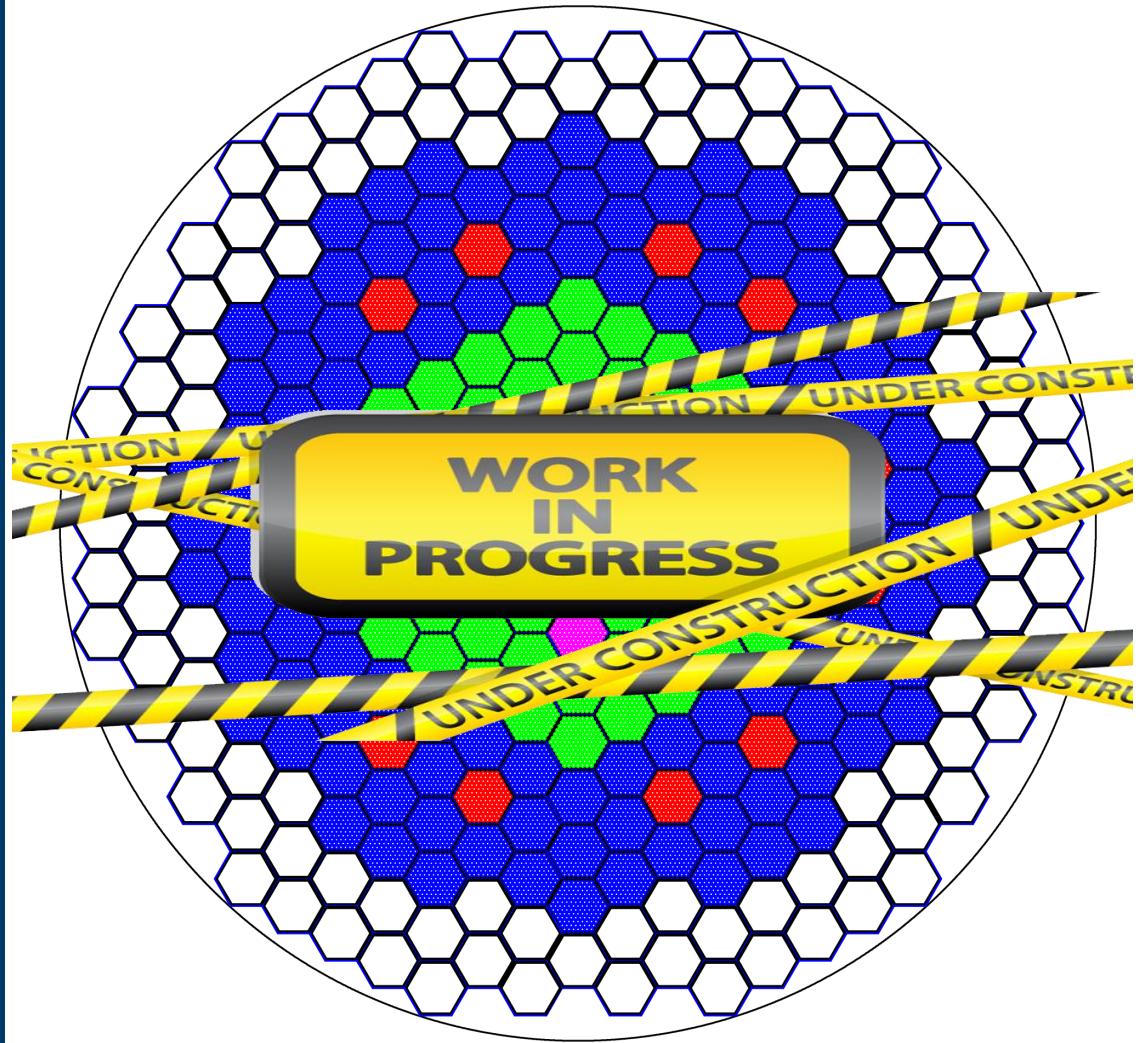
# Core Systems

## Core

### Criteria\*:

- Remove heat with as uniform  $\Delta T$  as possible (including from non-fuel zones)
- Withstand accidents through inherent response (negative feedbacks)

\* Main ones



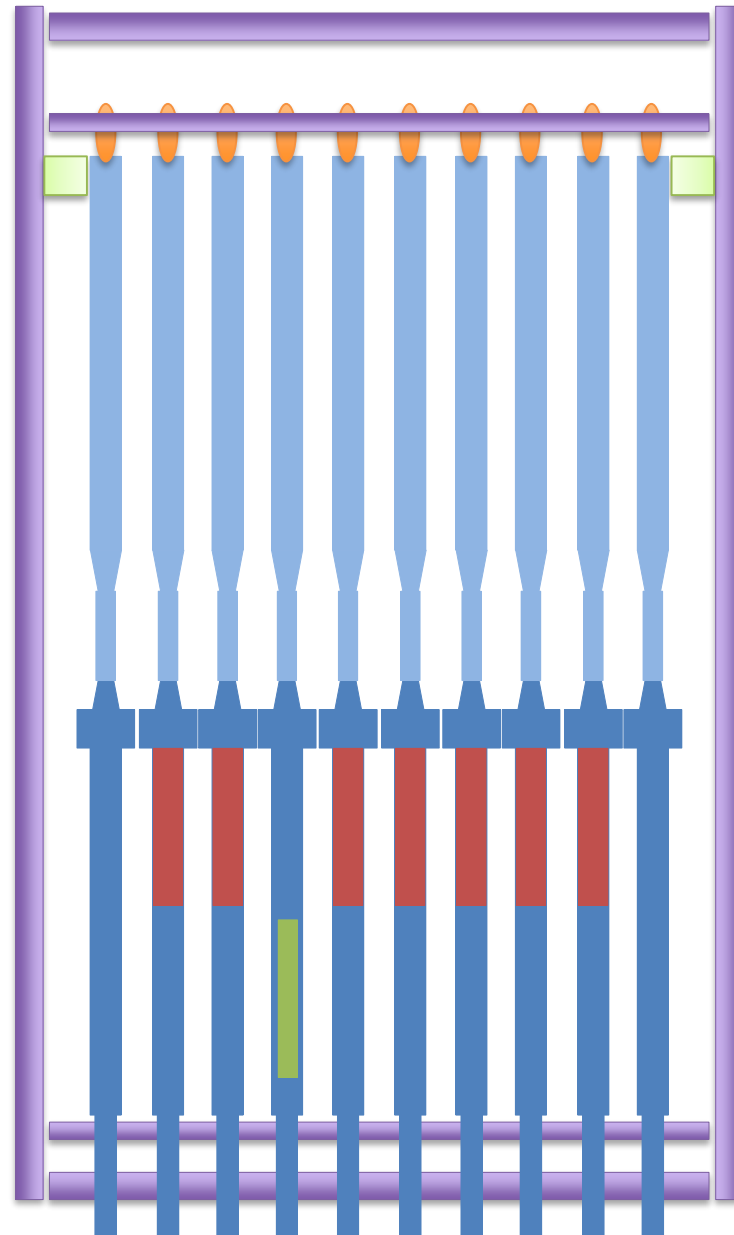
# Core Systems

## Restraint

### Criteria\*:

- Prevent S/As vibration during operation
- Counteract S/As bowing
- Allow core flowering during accidents
- Permit minimal S/As extraction forces during refueling

\* Main ones



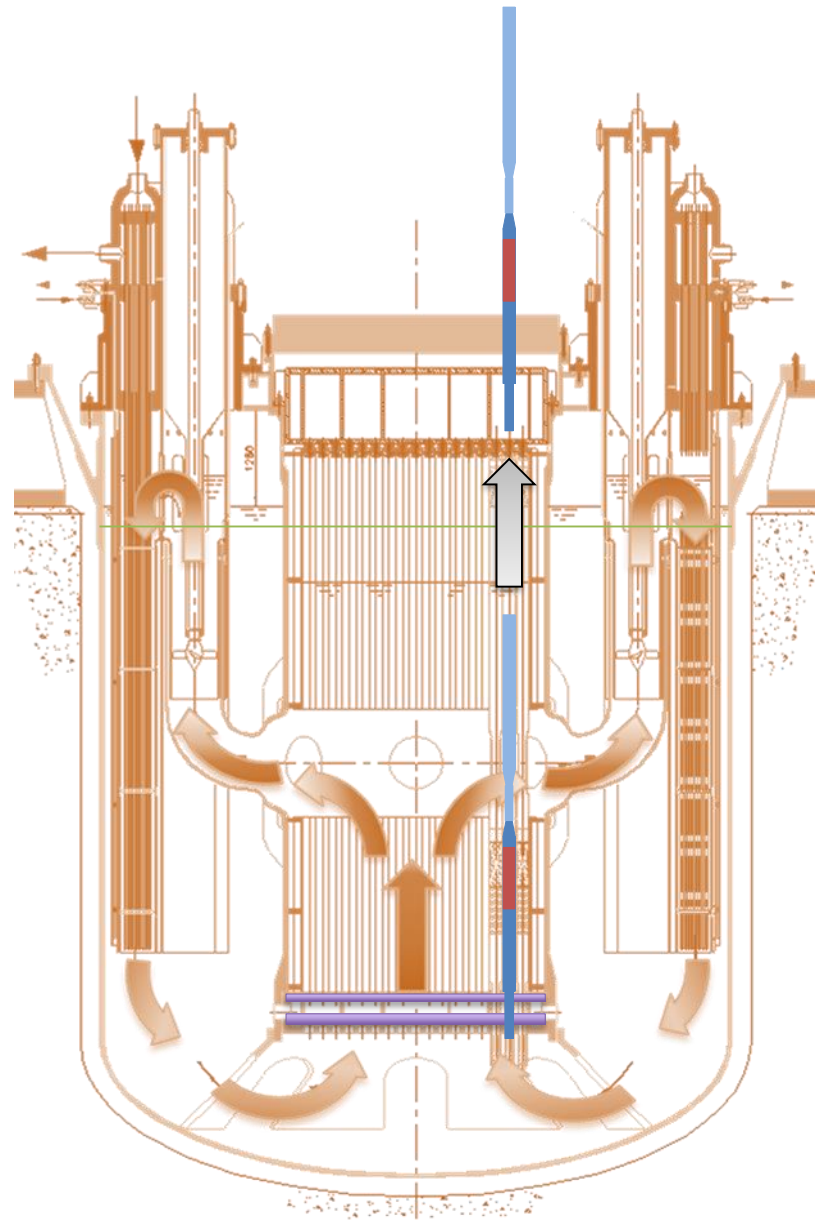
# Core Systems

## Refueling

### Criteria\*:

- Permit passive cooling during all transfer phases
- Permit continuous monitoring of the status of the sub-assemblies
- Permit retrieval of sub-assemblies for post-irradiation examinations

\* Main ones





## Core



# Core system

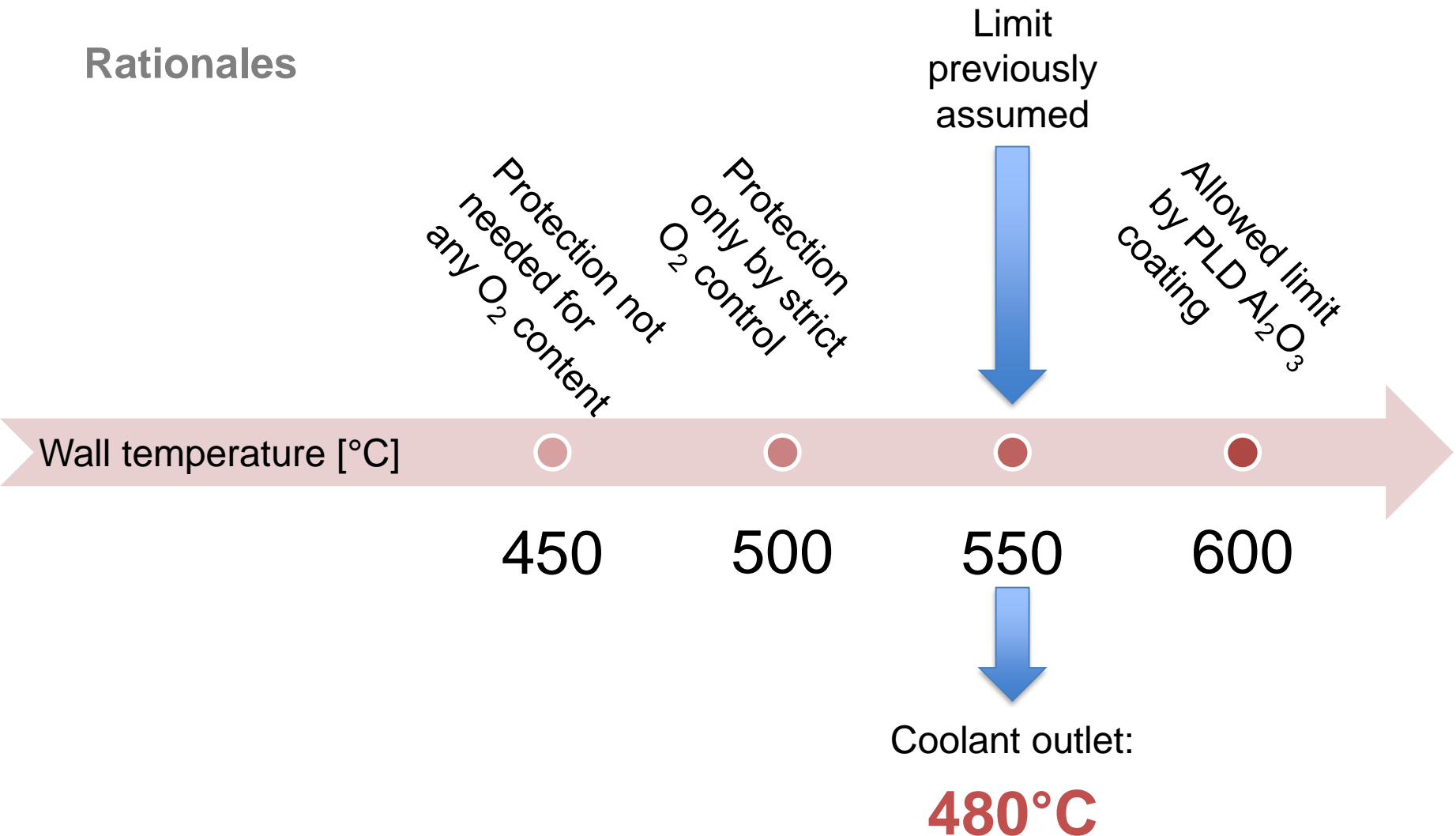
## Needs

“What the hell: squeeze that core!!!”

(Michele, Alex, Mariano, Trump, etc.)

# Core system

## Rationales



# Core system

## Strategy

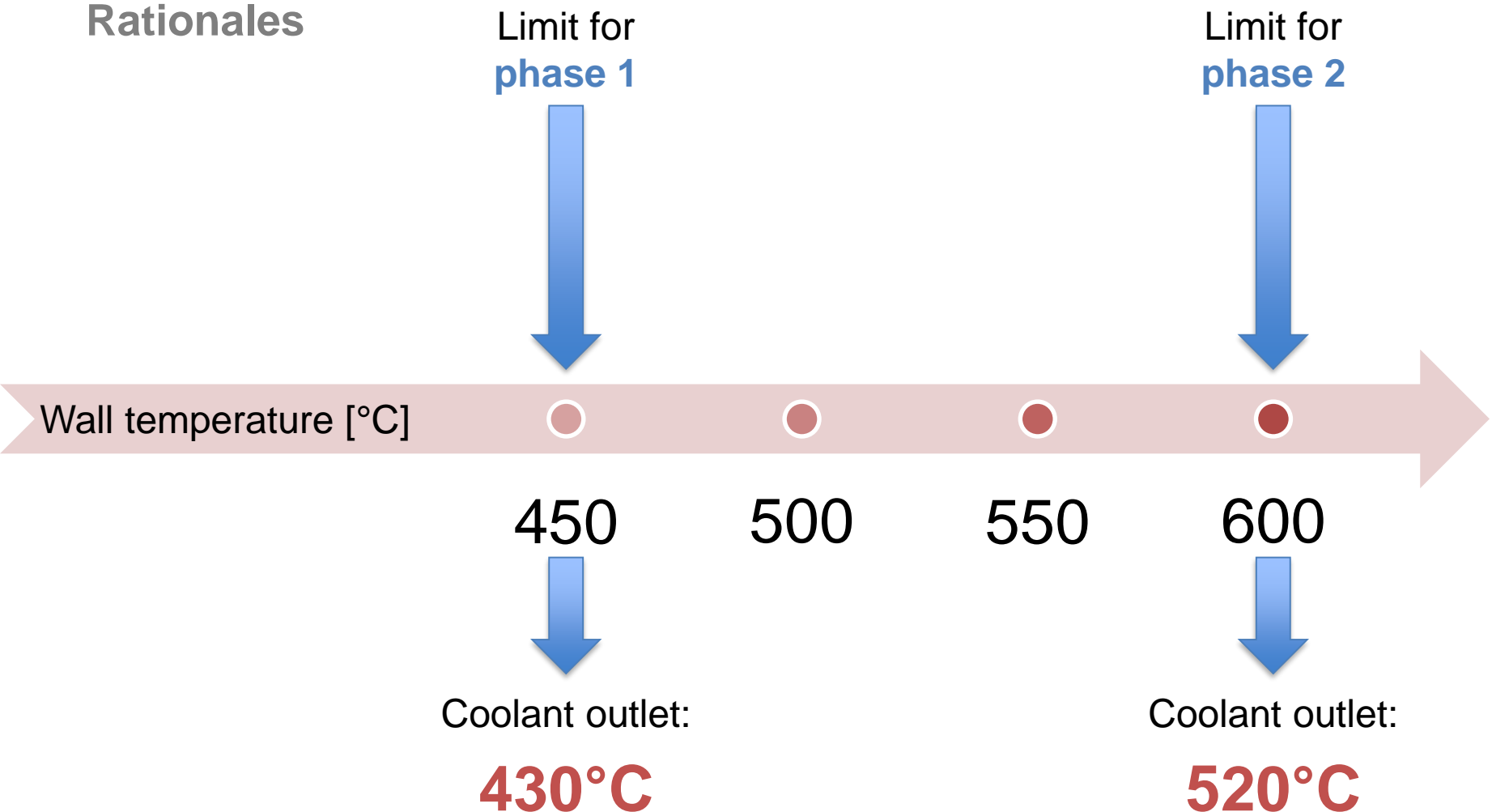


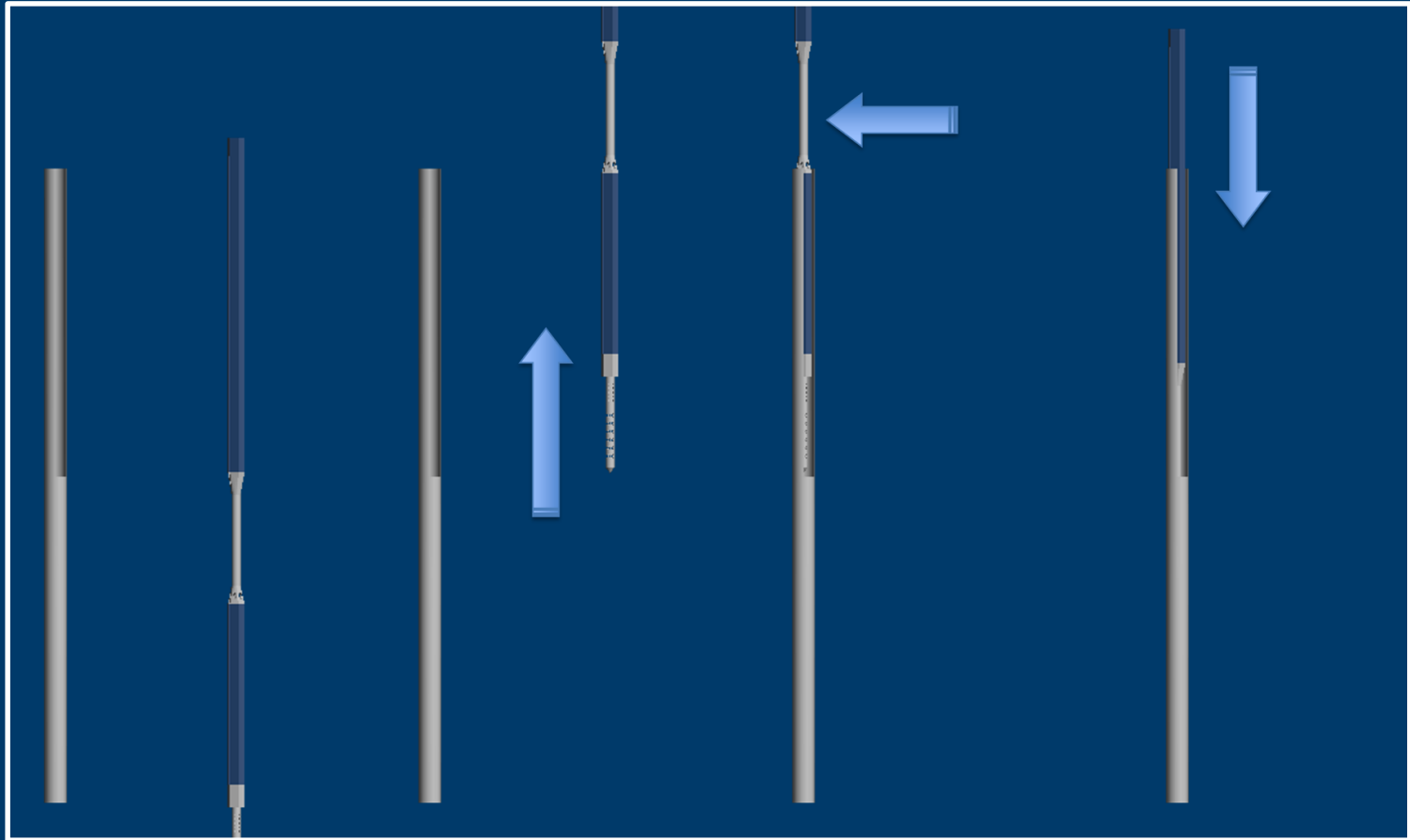
The operation of ALFRED will be based on a stepwise approach:

- **phase 1**: operation at **low power** in **low-temperature** range
  - presently existing proven materials working without corrosion protection
- **phase 2**: operation at **full power** in **high-temperature** range
  - coated materials fully qualified during phase 1

# Core system

## Rationales





## Refueling

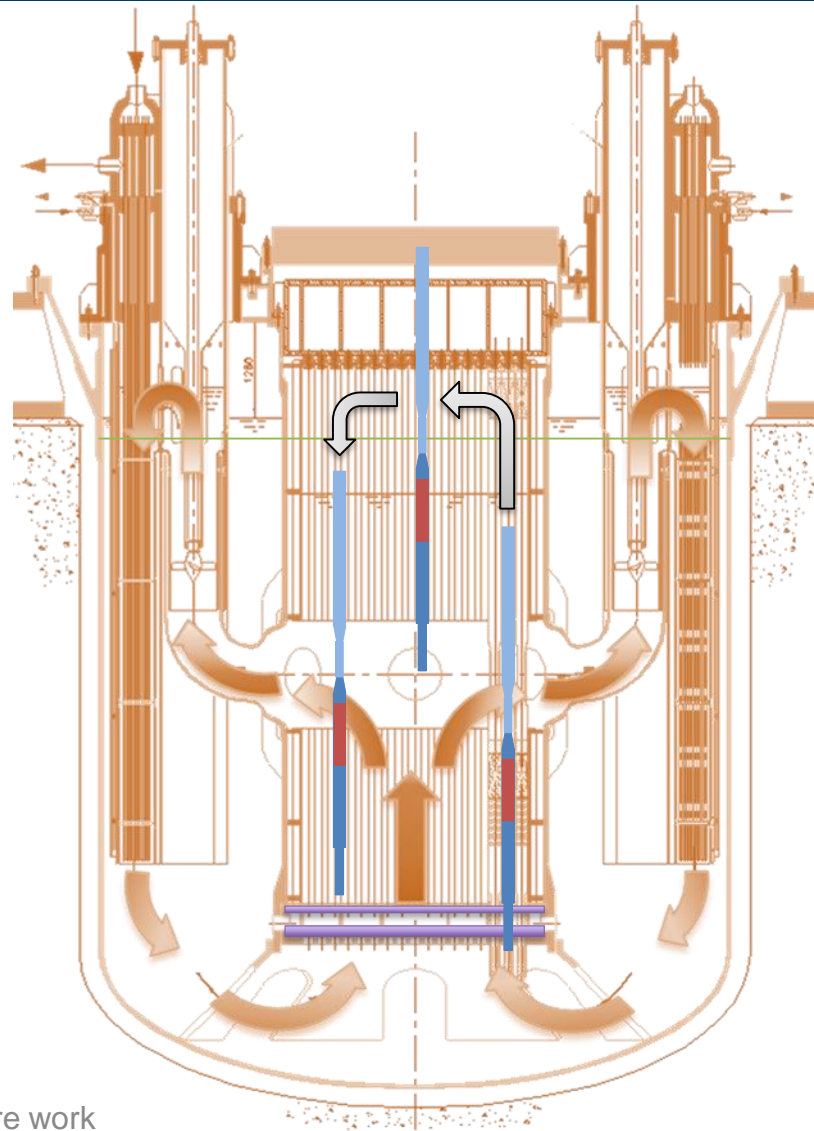
# Refueling system

## Concept

«If the fuel assembly doesn't go to the pool, the pool goes to the fuel assembly»

A transfer flask is used to bring the spent fuel assemblies to the cooling pond.

The transfer flask, filled by lead, maintains the fuel assembly submerged – hence effectively and passively cooled – during the whole transfer.



# Refueling system

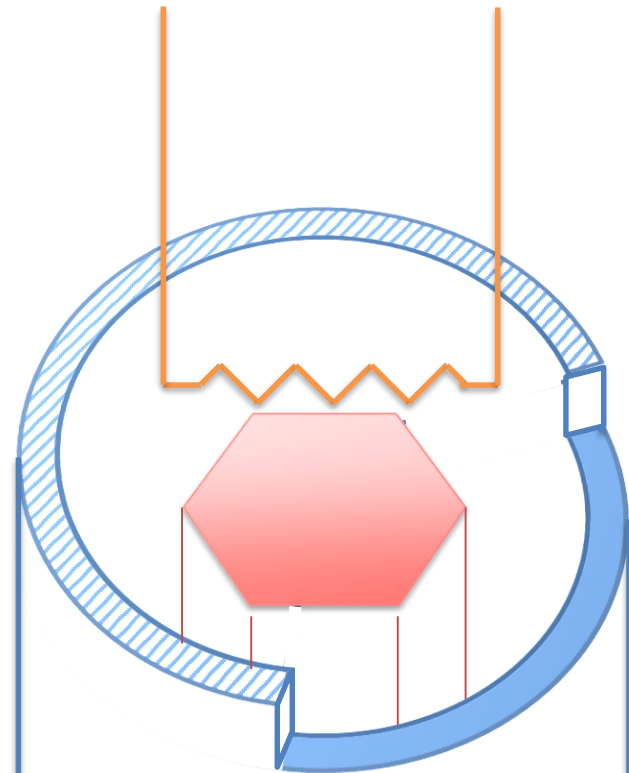
## Solution

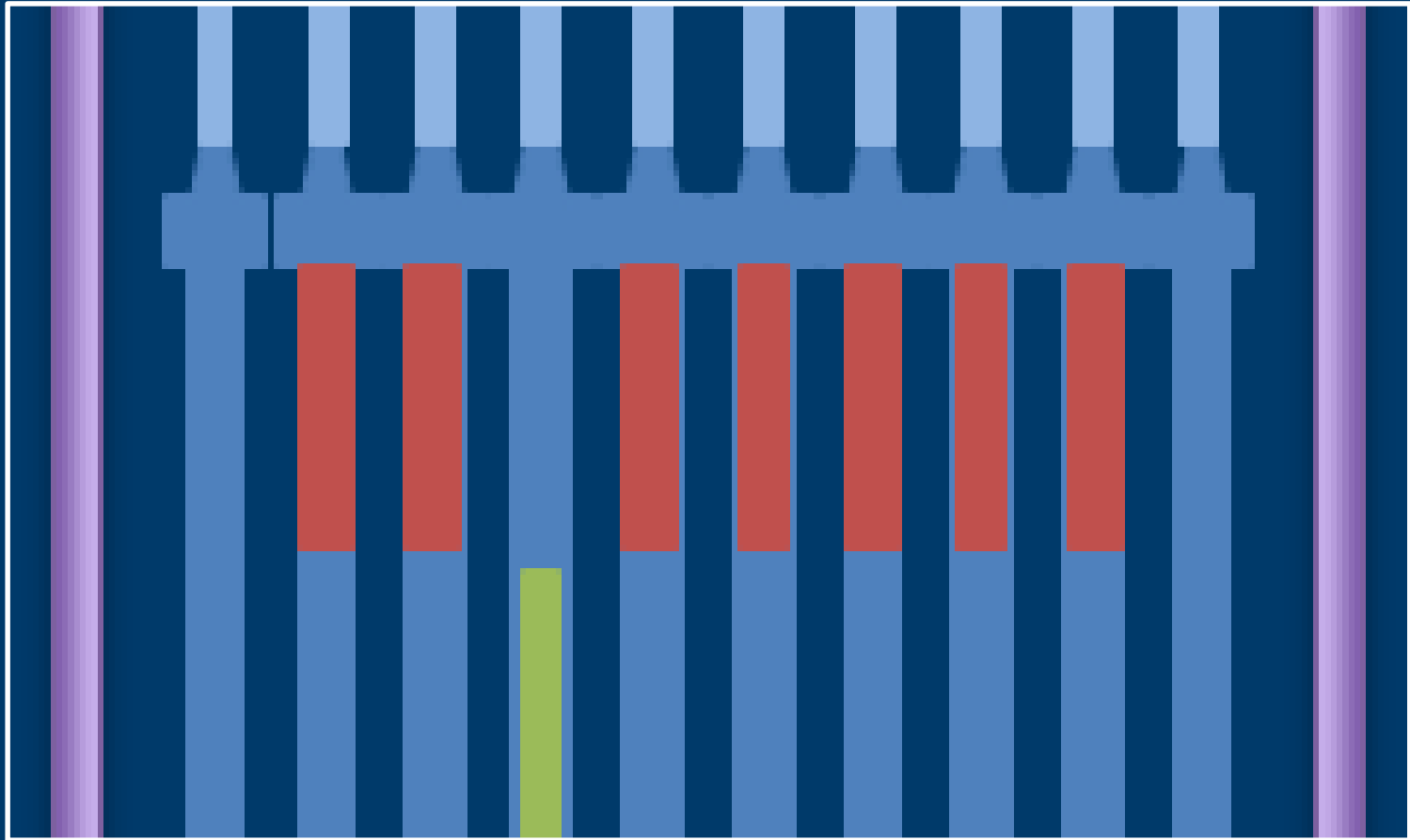
The flask provides passive cooling

- inside, thanks to lead
- outside, through natural circulation of gas

Within the flask, also several auxiliaries can be placed:

- heater
- instrumentation
- fill & drain





## Restraint

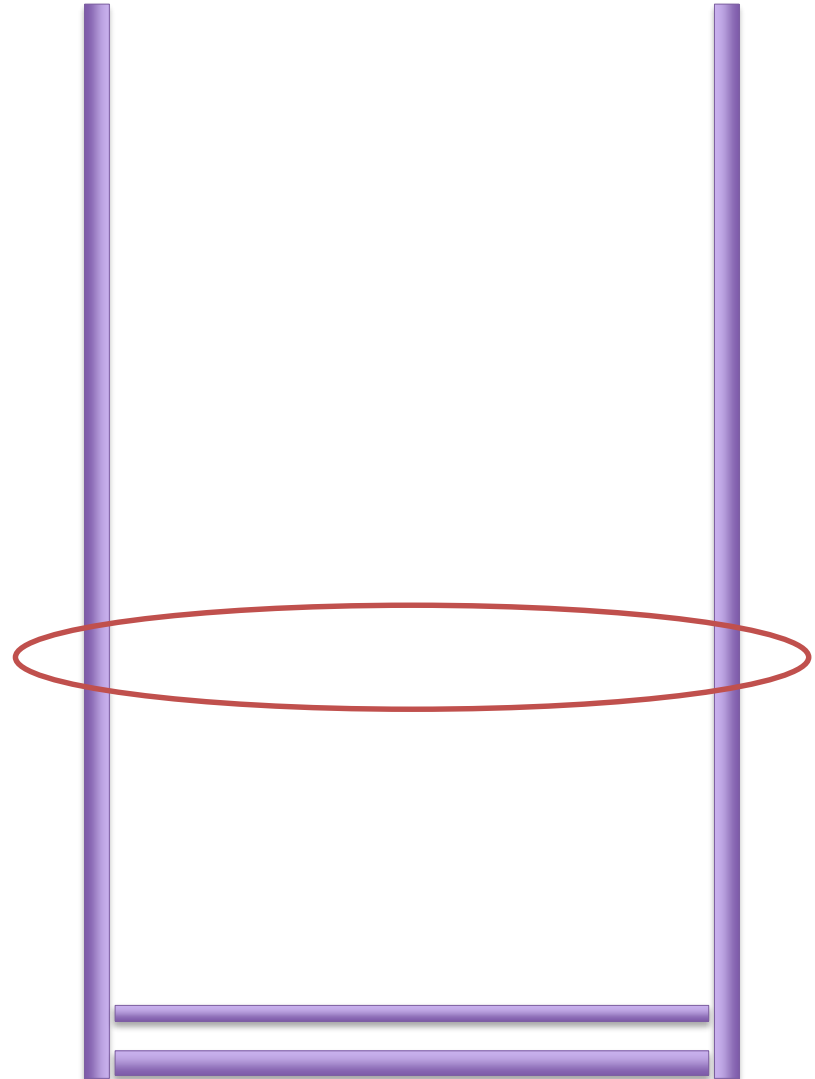


# Restraint system

## Concept

A trade-off between opposing needs: stiffness and freedom

1. All the sub-assemblies (fuel, control/shutdown, dummy) are positioned on a lower core plate
2. An upper core plate, provided of a stiff radial restraint, is brought to engage the heads of the S/As to tighten the lattice
3. A network of pads in contact provides the aimed feedback response mechanism





# Engineering



ALFRED v.2.00 – New Core and Primary System Design

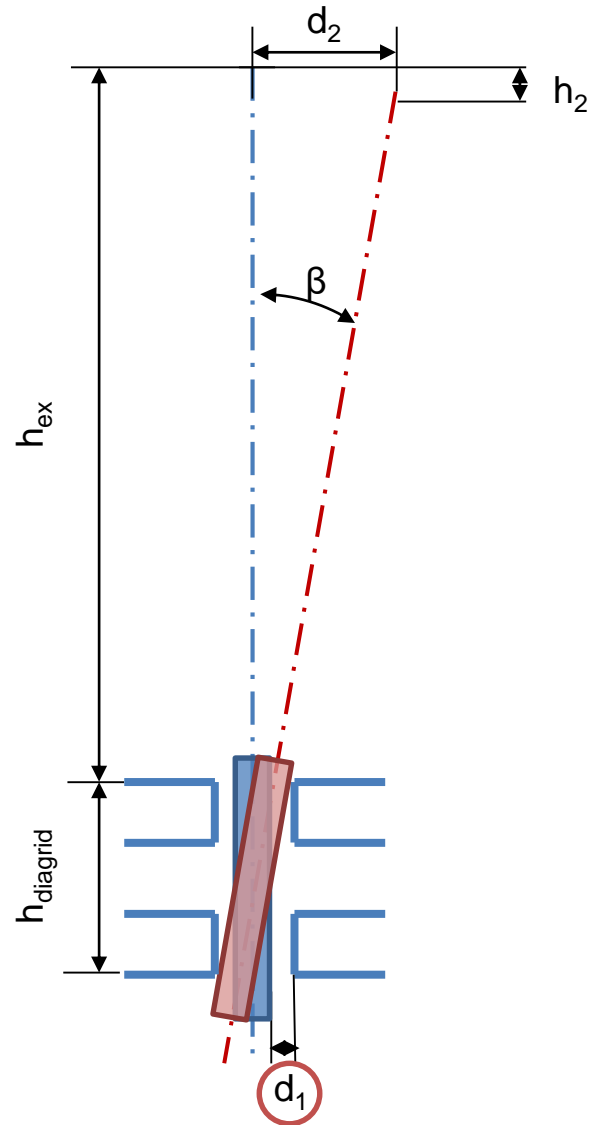
Memorandum of Understanding between ENEC and the Government of the State of Palestine, dated 10/2008

## Example

# Interfaces

Gap in the connection S/As  
Spike-Diagrid:

- Clearance to «tilt» the S/As so as to recover some space, facilitating extraction during refueling despite their bowing

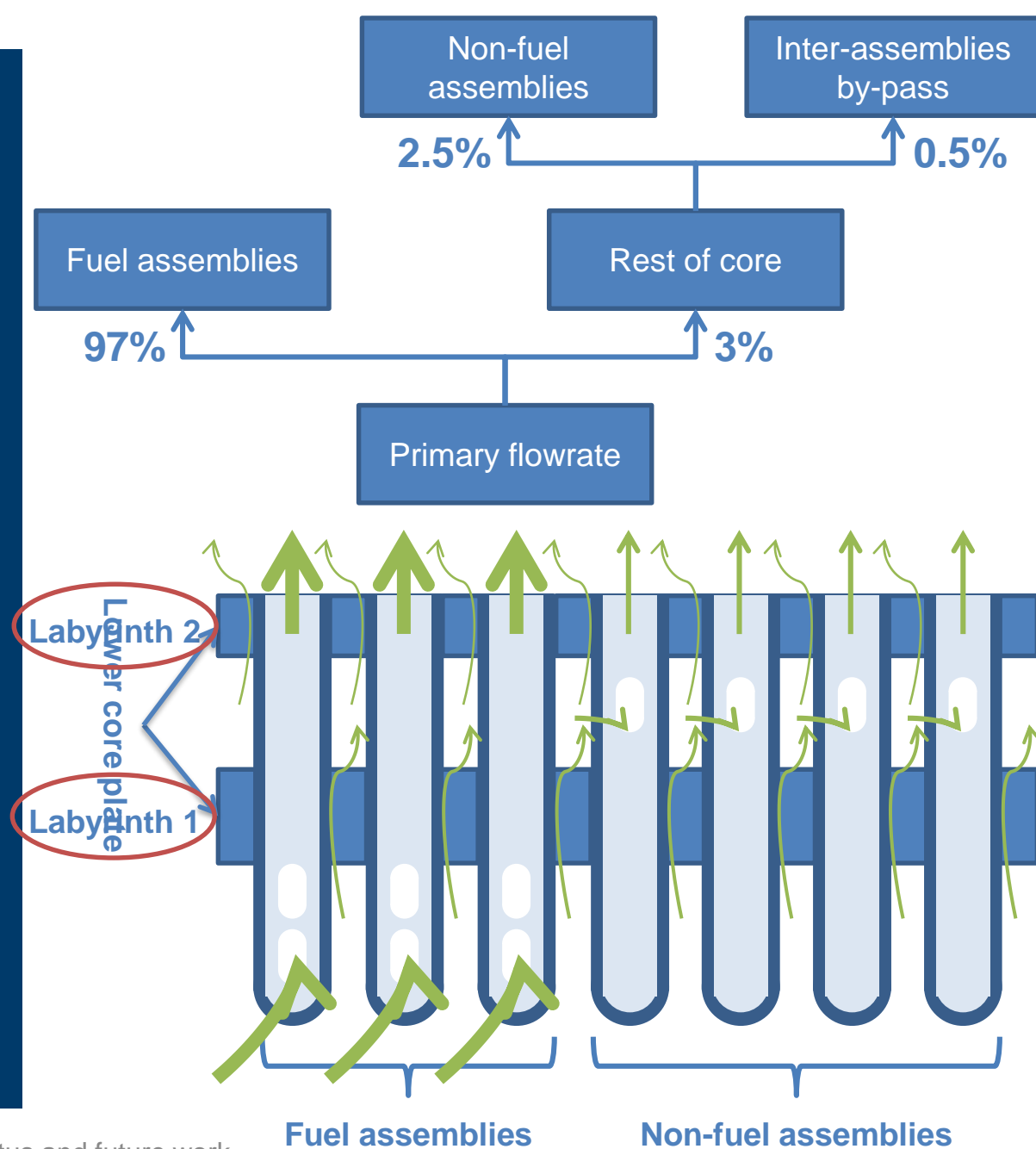


# Example

## Interfaces

Gap in the connection S/As  
Spike-Diagrid:

- Clearance to «tilt» the S/As so as to recover some space, facilitating extraction during refueling despite their bowing
- Clearance exploitable to tune the primary flowrate so as to easily align to the power distribution



## Example

# Engineering

Careful redesign of all components of sub-assemblies:

- Standardizing manufacturing through shared parts
- Avoiding welds wherever possible
- Simplifying assembling
- Enhancing “tolerances-tolerance” as far as practicable.

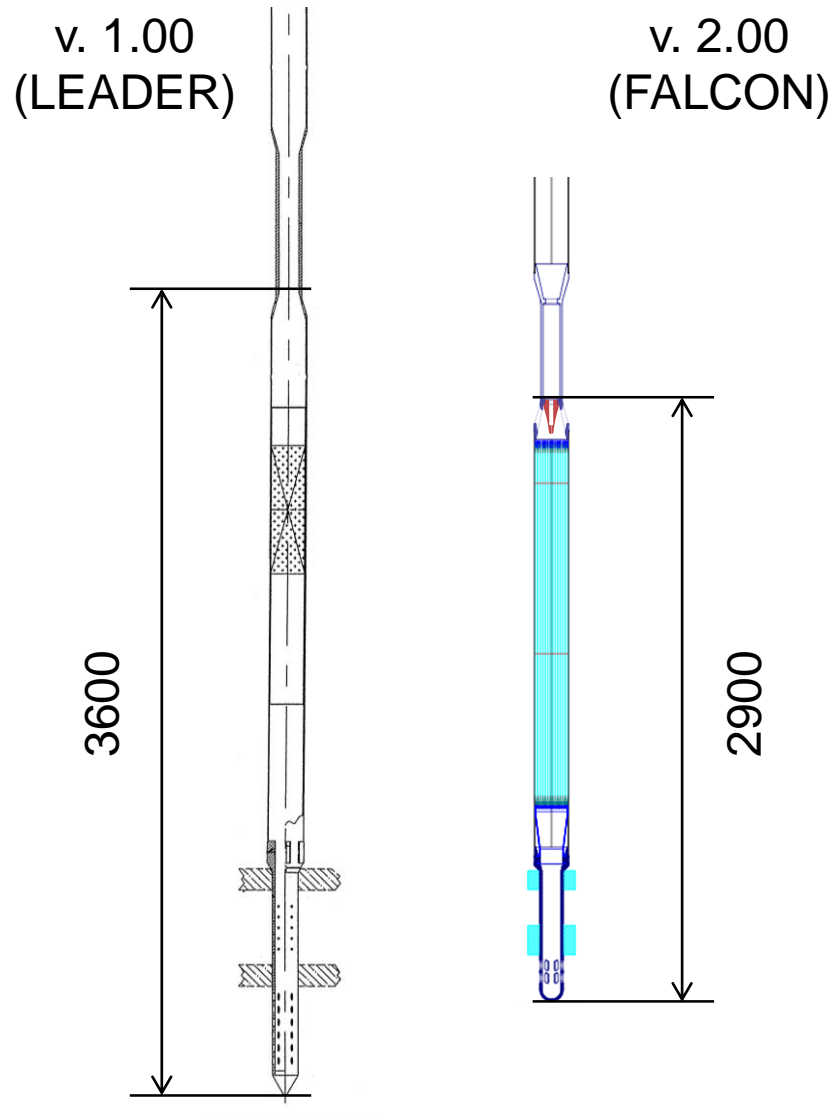


## Example

# Optimization

Reduction of primary system volume:

- Optimization of the length of the cooled part of the fuel assemblies (the rest being stem), now 700 mm shorter overall.
- This also impacts (twice) on the refueling system and vessel length, through the lead level.



## Example

# Innovation

Design of an innovative shutdown system:

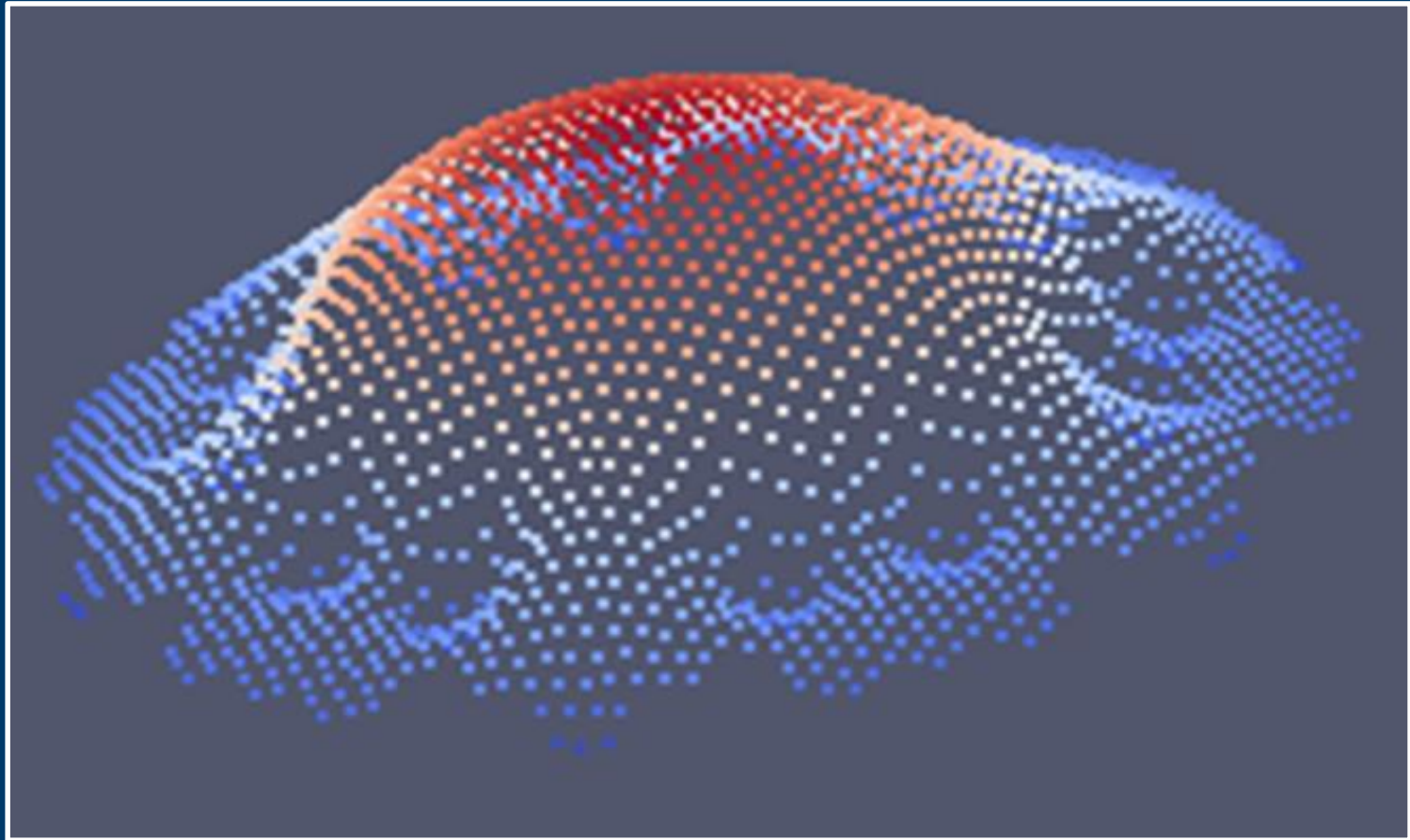
- Capable of operating passively, but both upon command (active) and inherently (passive)
- Resilient to extreme events, hence available in very ultimate conditions
- Diversified from other (more typical) systems





## Simulation capabilities





## Simulation codes

# Simulation Codes Development

Functions:

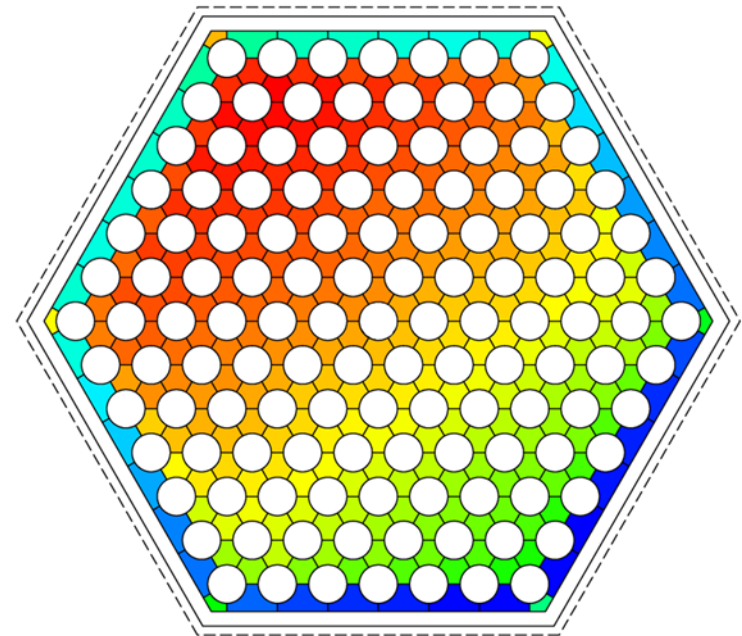
- to support the design of core components/systems
- to address complex phenomena provide orifice for gagging according to (small difference) power regions the FAs have been apportioned into

```
117 if (username != null) {
118     if (!database.userExists(username)) {
119         throwFailedLoginException(
120             "User " + username + " doesn't exist.");
121     }
122     if (!isIdentityAssertion()) {
123         String passwordWant = null;
124         try {
125             passwordWant = database.getUserPassword(username);
126         } catch (NotFoundException shouldNotHappen) {}
127         String passwordHave = getPasswordHave(username, callback);
128         if (passwordWant == null || !passwordWant.equals(passwordHave)) {
129             throwFailedLoginException(
130                 "Authentication Failed: User " + username + " had password " +
131                 "Have " + passwordHave + ". Want " + passwordWant);
132         }
133     }
134     else {
135         // anonymous login - let it through?
136         System.out.println("\tempty username");
137     }
138     loginSucceeded = true;
139     loginSubject.add(new MLUserImpl(username));
140     loginSubject.setName(username);
141 }
```

# Simulation Codes – Development

## ANTEO+

- A thermal-hydraulic code based on the “sub-channel” approach to investigate the FA (plus by-pass) for
  - flow rate distribution among sub-channels
  - temperature distribution among sub-channels (and on the cladding outer surface and FA wrapper)

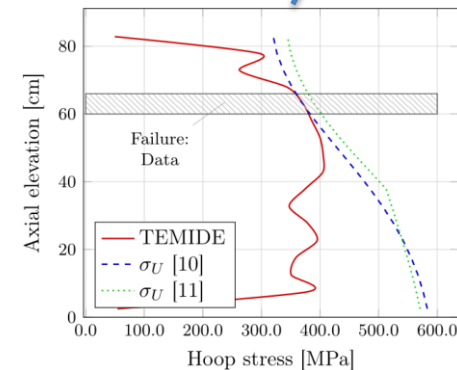
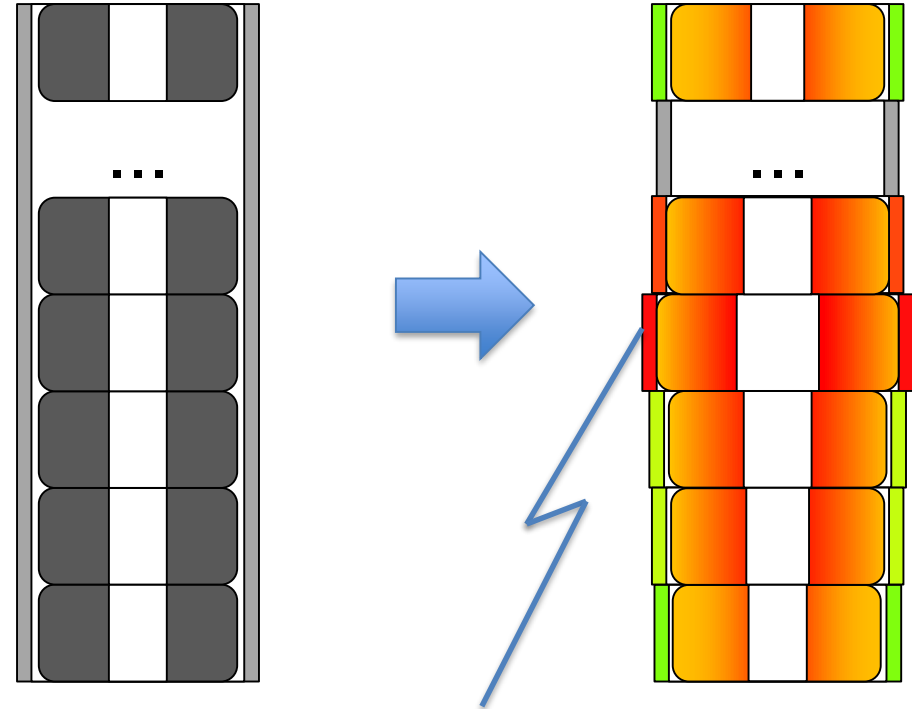


# Simulation Codes – Development

## TEMIDE



- A thermo-mechanic code investigating the fuel pin in terms of
  - dilation, swelling, cracking, creep, gas release, etc. of the fuel pellet
  - dilation, swelling, creep, PCMI, etc. of the cladding

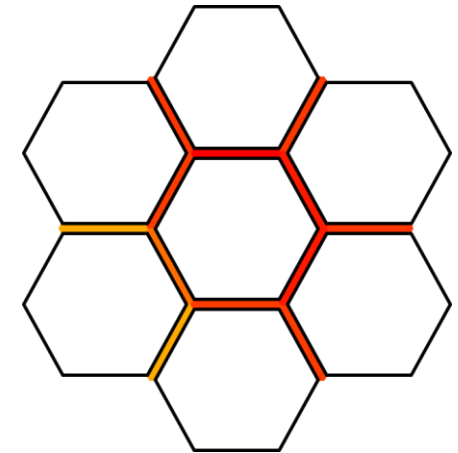
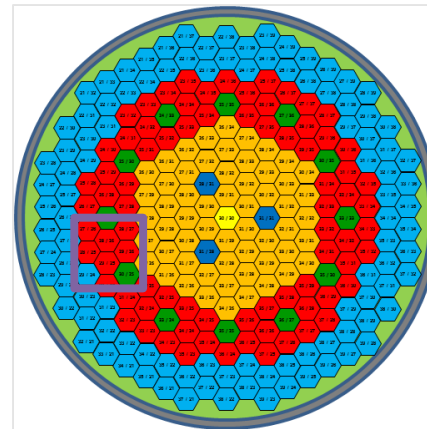


# Simulation Codes – Development

## TIFONE

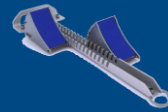


- A thermal-hydraulic code based on the “sub-channel” approach to investigate the by-pass region among the S/As in terms of
  - flow rate distribution among gaps
  - temperature distribution among gaps (including on the S/A wrappers)

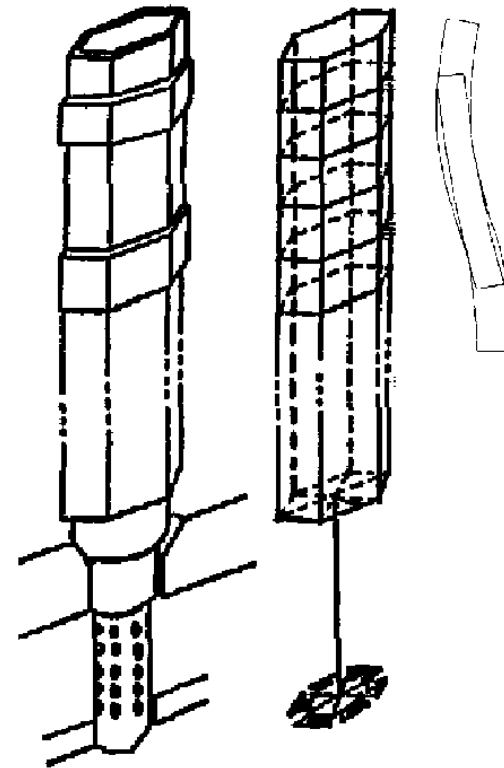


# Simulation Codes – Development

## TEIA

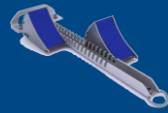


- A thermo-mechanic code investigating – at S/A level – the
  - deformation (dilation/bending) of the wrapper
  - interaction between the wrapper and the inner bundle

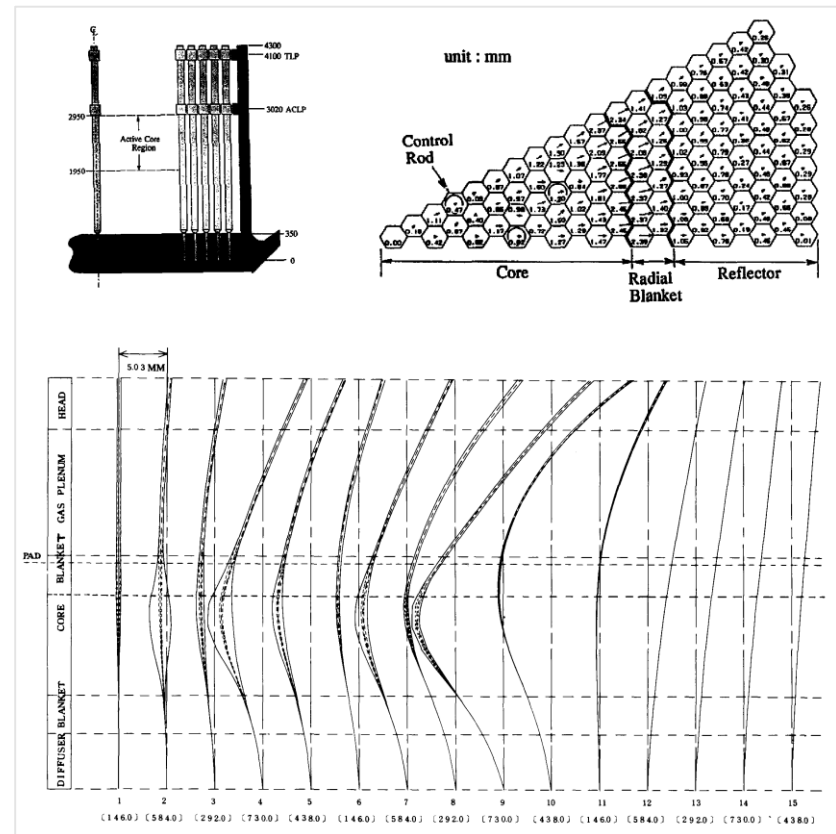


# Simulation Codes – Development

## FEBE



- A thermo-mechanic code investigating – at core level – the
  - collective behavior of deformed S/As
  - interaction between the S/As
  - response of the core restraint system to core deformations (also in terms of reactivity)

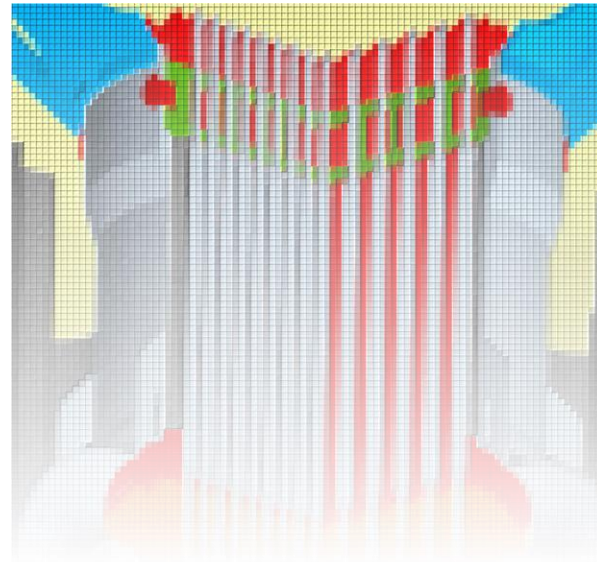
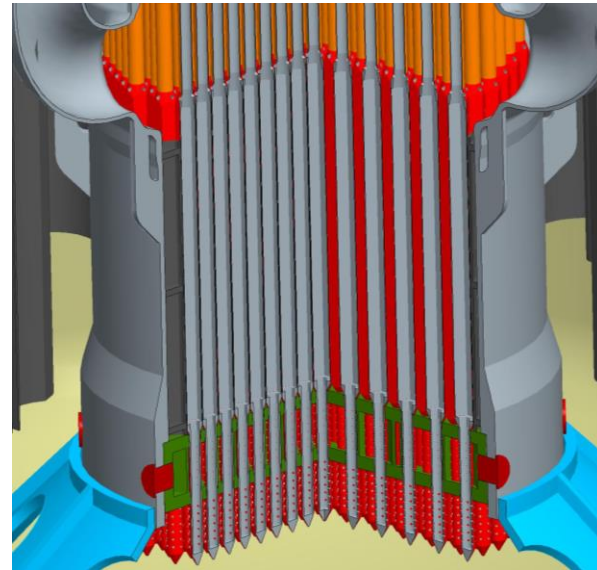


## Simulation Codes

# Validation

Functions:

- to assess confidence in the results of simulations

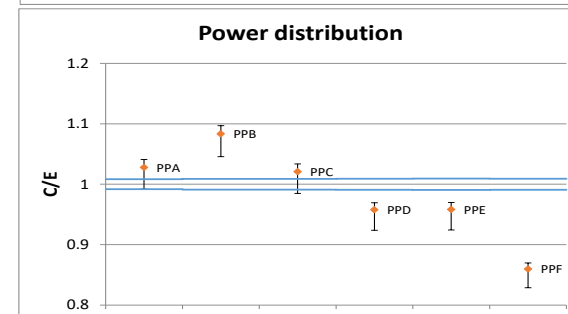
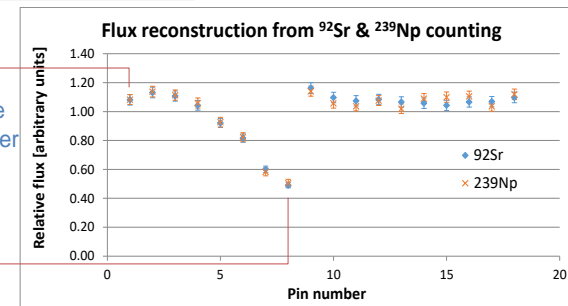
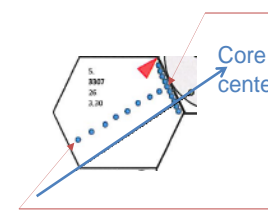
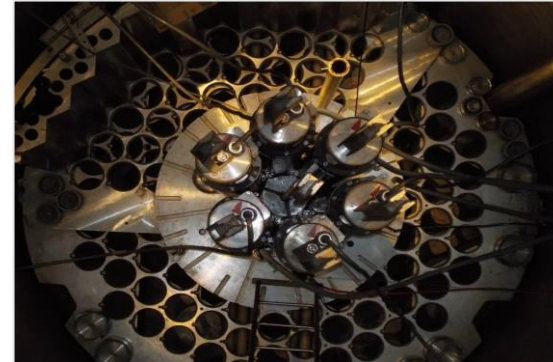




# Simulation Codes – Validation

## Assess confidence

- Precise experiments are reviewed, or designed and conducted, to retrieve relevant information for estimating and assessing the capability to predict the real behavior through simulation:
  - VENUS-F + LR-0 for ERANOS/MCNP;
  - CIRCE-ICE + NACIE-UP + ... for ANTEO+
  - literature databases for TEMIDE



# Simulation Codes – Validation

## Status

- ERANOS & MCNP



Good database, but to be verified whether considered sufficient by CNCAN

- ANTEO+



Very large database

- TEMIDE & Transuranus



Validated against the few publicly available cases; looking for other results



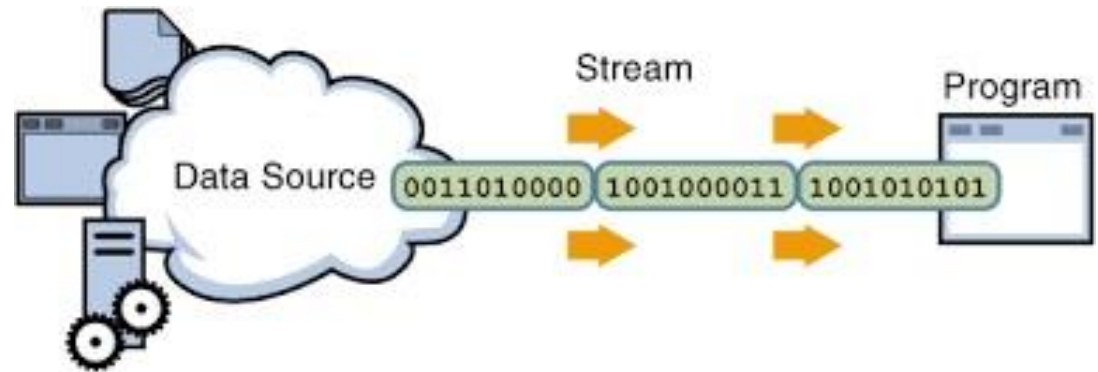
## Supporting tools

## Supporting tools

# Pre-processing

Functions:

- to homogenize the description of material properties
- to standardize the generation of input data
- to avoid human errors in processing large amounts of information (QA)



# Supporting Tools – Pre-processing

## Homogenize material properties

- Tools for extracting specific properties for fuel, coolant, absorber and structural materials
  - single values
  - tables
- Exploitable as stand-alone tools (executables or excel sheets) or embeddable into codes (fortran modules of subroutines and functions)

The screenshot shows an Excel spreadsheet with the following data:

|    | A         | B                        | C | D                            | E         | F    | G           | H    | I         | J | K |
|----|-----------|--------------------------|---|------------------------------|-----------|------|-------------|------|-----------|---|---|
| 1  | INPUT     |                          |   |                              |           |      |             |      |           |   |   |
| 2  | Fuel      |                          |   |                              |           |      |             |      |           |   |   |
| 3  |           | O/M ratio                |   | 1,97                         |           | at.% | wt.%        |      |           |   |   |
| 4  |           | enrichment               |   | 23,2 wt.%                    |           |      | 23,08003206 | 23,2 | 22,429797 |   |   |
| 5  |           | porosity                 |   | 5 %                          |           |      |             |      |           |   |   |
| 6  | Operation |                          |   |                              |           |      |             |      |           |   |   |
| 7  |           | BU                       |   |                              | MWd/kg-HM |      |             |      |           |   |   |
| 8  |           | FADP                     |   |                              |           |      |             |      |           |   |   |
| 9  |           | PDF                      |   |                              |           |      |             |      |           |   |   |
| 10 |           | Fax                      |   |                              |           |      |             |      |           |   |   |
| 11 | Pin       |                          |   |                              |           |      |             |      |           |   |   |
| 12 |           | hollow radius            |   | 1 mm                         |           |      |             |      |           |   |   |
| 13 |           | pellet radius            |   | 4,5 mm                       |           |      |             |      |           |   |   |
| 14 |           | gap thickness            |   | 0,15 mm                      |           |      |             |      |           |   |   |
| 15 |           | clad thickness           |   | 0,6 mm                       |           |      |             |      |           |   |   |
| 16 |           | active height            |   | 45 cm                        |           |      |             |      |           |   |   |
| 17 |           | plenum radius            |   |                              |           |      |             |      |           |   |   |
| 18 | Core      |                          |   |                              |           |      |             |      |           |   |   |
| 19 |           | pins                     |   |                              |           |      |             |      |           |   |   |
| 20 |           |                          |   |                              |           |      |             |      |           |   |   |
| 21 | OUTPUT    |                          |   |                              |           |      |             |      |           |   |   |
| 22 | Fuel      |                          |   |                              |           |      |             |      |           |   |   |
| 23 |           | at. density              |   | 6,9504658968E-02 at./barn cm |           |      |             |      |           |   |   |
| 24 |           | at. HM density           |   | 2,9402342077E-02 at./barn cm |           |      |             |      |           |   |   |
| 25 |           | wt. density              |   | 10,4692927 g/cm3             |           |      |             |      |           |   |   |
| 26 |           | wt. HM density           |   | 5,26491908 g/cm3             |           |      |             |      |           |   |   |
| 27 |           | at. inventory (1 pin)    |   | 4,536876312 mol              |           |      |             |      |           |   |   |
| 28 |           | at. HM inventory (1 pin) |   | 1,527507782 mol              |           |      |             |      |           |   |   |
| 29 |           | wt. inventory (1 pin)    |   | 0,412134555 kg               |           |      |             |      |           |   |   |
| 30 |           | wt. HM inventory (1 pin) |   | 0,364187424 kg               |           |      |             |      |           |   |   |
| 31 | Operation |                          |   |                              |           |      |             |      |           |   |   |
| 32 |           | frac. BU                 |   | %                            |           |      |             |      |           |   |   |
| 33 |           | GFP prod rate            |   | mol/g                        |           |      |             |      |           |   |   |
| 34 |           | GFP produced             |   |                              |           |      |             |      |           |   |   |
| 35 |           | GFP rel rate             |   |                              |           |      |             |      |           |   |   |
| 36 |           | GFP released             |   |                              |           |      |             |      |           |   |   |
| 37 | Design    |                          |   |                              |           |      |             |      |           |   |   |
| 38 |           | minimum gap              |   |                              |           |      |             |      |           |   |   |

```
1 |<code>gpc ->documents\coolant\00 - /coolant00
Please enter the reference coolant Pb

Property | value | unit |
rho*cp (int) | 1553203.08 | J/K m^3 |
.....

Please enter the property to be displayed: rhoCp
Please enter the reference temperatures [°C] 400 400

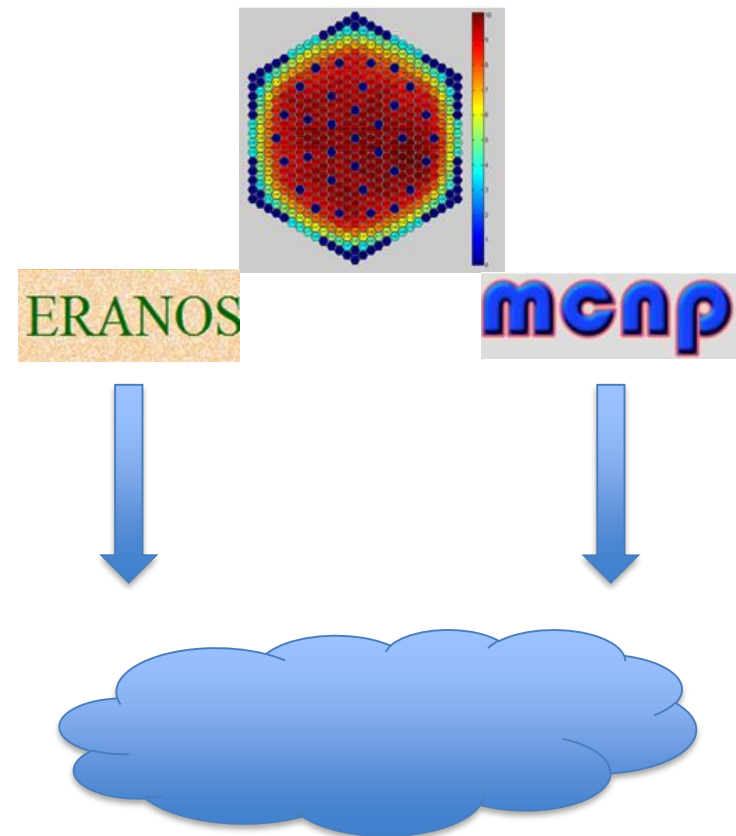
Property | value | unit |
rho*cp (int) | 1534670.14 | J/K m^3 |
.....

Please enter the property to be displayed: |
```

# Supporting Tools – Pre-processing

## Standardize input data

- Tools for extracting information from (huge) output files of “father” codes, and formatting them for use as input to “child” codes
- Stand-alone fortran tools (executables) for direct use, or modules (subroutine and functions) to be embedded in more general coupling platforms

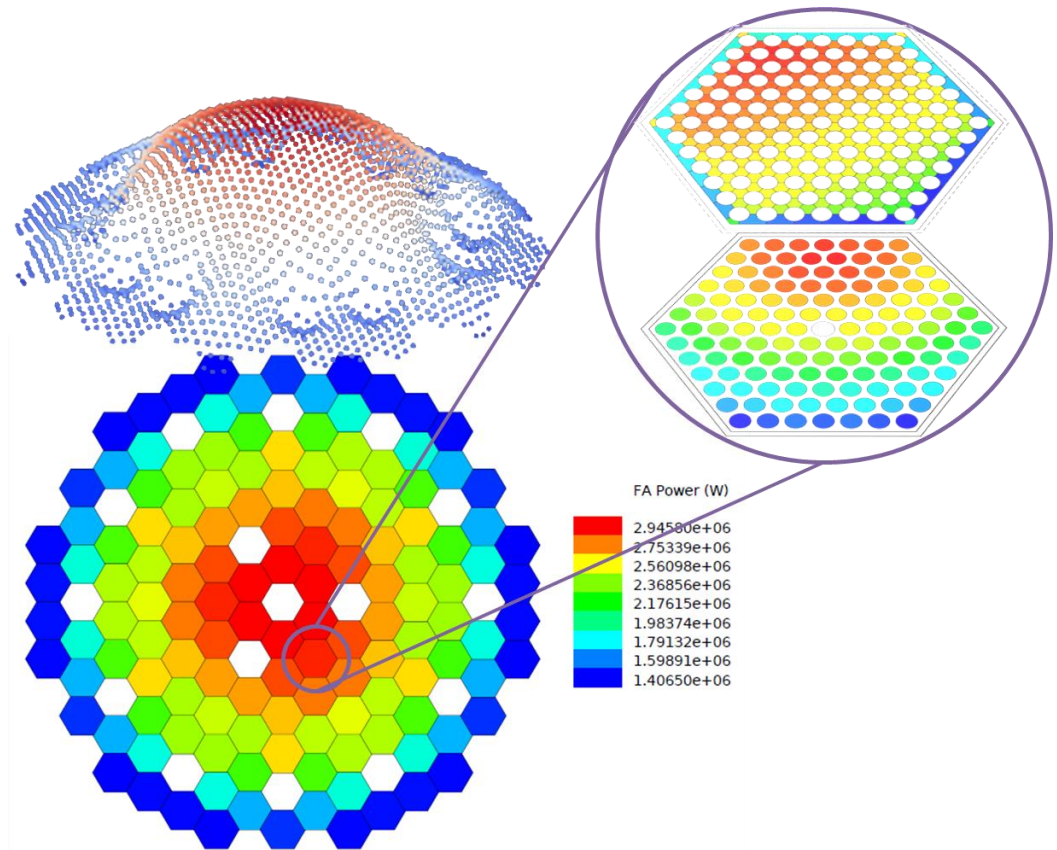


## Supporting tools

# Post-processing

### Functions:

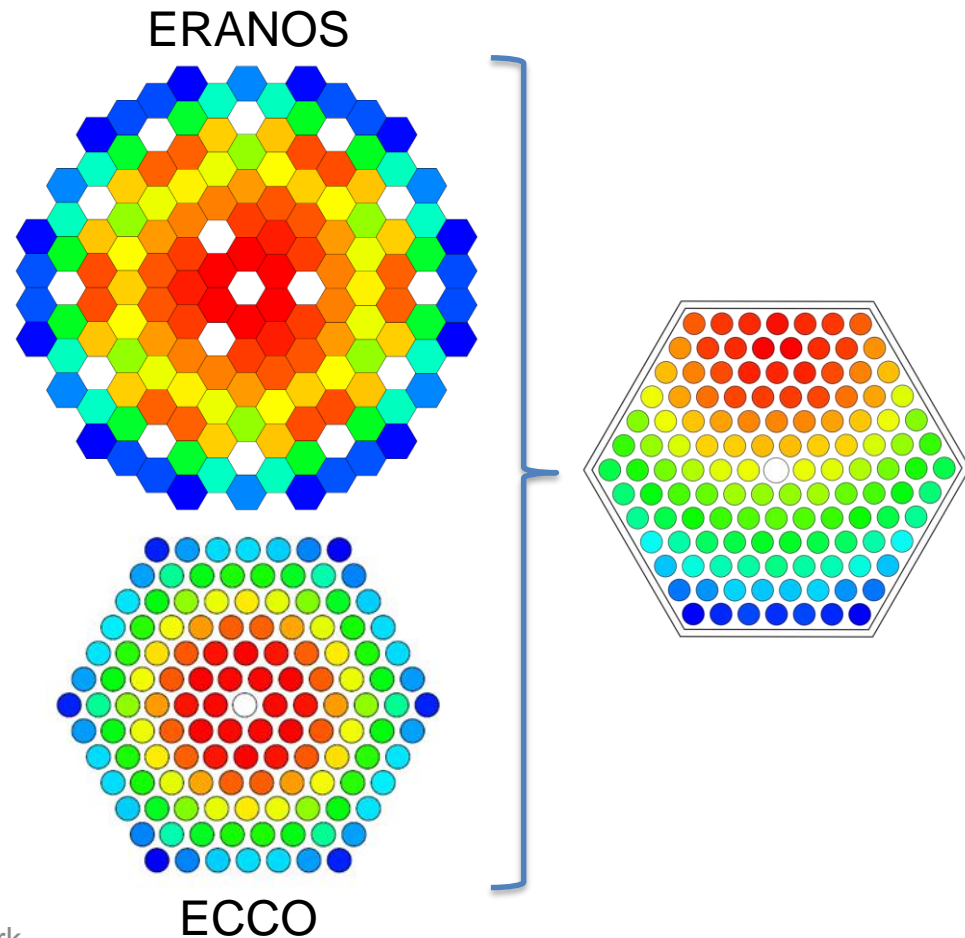
- to extract main results from (huge) output file and make them available (raw or processed) to the user
- to visualize key results into human friendly (graphical) format
- to avoid human errors in processing large amounts of information (QA)



# Supporting Tools – Post-processing

## Extract main results

- Tools for extracting main results from output files of a simulation code and produce tables of values
- Tools for processing main results from output files of more simulation codes and combine them:
  - flux reconstruction (pin by pin)
  - power reconstruction (pin by pin)

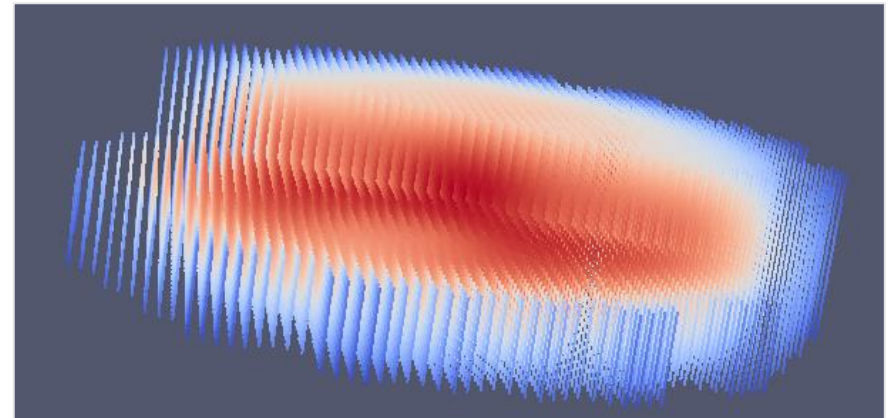




# Supporting Tools – Post-processing

## Visualize key results

- Tools for extracting information from (huge) output files and producing 2D or 3D plots of
  - core flux
  - core power (mesh)
  - core power (FA by FA)
  - FA power (pin by pin)
  - axial power distribution (pin)
  - coolant temperature (FA)
  - axial coolant temperature distribution (sub-channel or pin)



Giacomo Grasso  
giacomo.grasso@enea.it



## **Copyright © 2018 – FALCON**

This presentation contains proprietary and confidential data, information and formats. All rights reserved.

No part of this presentation may be reproduced, distributed, or transmitted in any form or by any means, including photocopying, recording, or other electronic or mechanical methods, without the prior written permission of FALCON.